Forschungszentrum Jülich
in der Helmholtz-Gemeinschaft

50 Jahre / Zukunft

Neutron Scattering at FRJ-2

Experimental Reports 2005/6



Editors: Th. Brückel, D. Richter, R. Zorn

Persistent Identifier: urn:nbn:de:0001-00352
http://nbn-resolving.de/urn/resolver.pl?urn=urn:nbn:de:0001-00352

Published by Forschungszentrum Jülich GmbH
D-52425 Jülich, Germany
Phone: +49 2461 61-0

Editors: T. Brückel, D. Richter, R. Zorn

Forschungszentrum Jülich does not accept any responsibility for loss or damage arising from the use of information contained in this report. Reproduction including extracts is permitted subject to crediting the source.

Summary

2006 marks a major reorientation for research with neutrons at Forschungszentrum Jülich (FZJ): While the facility in Jülich, around the DIDO research reactor FRJ-2, was permanently shut down on May 2nd, Jülich strengthens its activities at external neutron sources. For this purpose the "Jülich Centre for Neutron Science" (JCNS) was founded in February 2006. JCNS encompasses the in-house research with neutrons, the instruments and methods development, and the instrument operation with user programmes at the reactor FRM-II in Munich, the SNS spallation source in Oak Ridge, and the ILL high-flux reactor in Grenoble.

The Research Centre FZ-Jülich has offered its neutron research facilities to a growing national and international user community for the benefit of their research using neutron beams. FZ-Jülich has operated a 23 MW DIDO reactor that delivered a total neutron flux of 2.9×10^{14} n/cm^{2}s (undisturbed) for a comprehensive suite of 17 instruments installed at 5 individual thermal beam tubes and, in addition, 5 external cold neutron guides.

In the year 2005 and 2006 the reactor was in operation for 258 days and we are happy to announce that more than 195 individual experiments (constituting 50 % of the total) were carried out by a large external user community from 91 institutions all over the world. In close collaboration with internal staff the study of soft matter systems took the largest stake. In addition, subjects of biology, magnetism and engineering were among the other main topics of the experimental programme.

We gratefully acknowledge the funding programme "Jülich Neutrons for Europe" under the European initiative NMI3 that enabled numerous external users from the EU and associated countries to come over, visit Jülich and perform their experiments.

This book comprises the report to the research programme "Large Scale Facilities for Research with Photons, Neutrons and Ions" (PNI) of the Helmholtz Society and the scientific reports of the experiments completed in 2005 and 2006. We wish to thank all external users, local applicants, instrument responsibles, and technical staff for their joint efforts and contributions to the success and progress of the Jülich Neutron Research Facility.

Contents

Introduction 1
PNI Report 5
Instrumental Developments 13
Thermal Neutron Experiments 23
Twin Diffractometer (SV-7) 23
Neutron Diffractometer (SV-28) 91
Time-of-Flight Spectrometer (SV-29) 113
Triple-Axis Spectrometer (UNIDAS) 151
Cold Neutron Experiments 167
High Resolution Backscattering Spectrometer (BSS) 167
Double Crystal Diffractometer (DKD) 225
Time-of-Flight Spectrometer for Diffuse Neutron Scattering (DNS) 233
Neutron Reflectometer (HADAS) 267
Small Angle Neutron Scattering (KWS-1) 301
Small Angle Neutron Scattering (KWS-2) 453
Ultra Small Angle Neutron Scattering (KWS-3) 567
Neutron Spin Echo Spectrometer (NSE) 581
Publications 611
Neutron Instruments and Methods 613
Crystallography 620
Excitations 623
Magnetism 628
Soft Condensed Matter, Liquids, Glasses 638
Transport Processes 661
Biology 662
Geology, Archaeology 664
Materials Science, Engineering 669
Theses 672
Training 675

Introduction

With the FRJ-2 research reactor and the ELLA external neutron guide laboratory, the Research Centre Jülich (FZJ) was operating a powerful neutron source with a special priority in the field of cold neutrons. At a thermal power of 23 MW, the FRJ-2 reached a maximum thermal neutron flux of 2.9×10^{14} neutrons/cm^{2}s (undisturbed) in the heavy water moderator. The liquid hydrogen cold source is located close to the reactor's flux maximum and three neutron guides supplied the instruments at the ELLA external neutron guide laboratory with cold neutrons of 3–15 Å wavelength. The reactor and its instruments were open to scientists from Germany, Europe and across the globe for the benefit of their scientific research goals. The FZJ gratefully acknowledges complementary funding support from the EU that helped to fulfil our goals, namely providing large-scale research equipment for a wide range of scientific applications in the university and non-university sector far beyond the Research Centre itself. On May 2nd, 2006 the reactor was shut down. Some of our best instruments are being relocated to the new research reactor FRM-II in Munich. Because of the short running time in 2006 this report combines the results of the years 2005 and 2006.

The total number of reactor operation days was 189 in 2005 and 69 in the four months operation in 2006. In total, 387 individual experiments were completed in 2005 and 2006. Taking into account the longer reporting period, this is still a 16 % rise in comparison to the performance of 2004, when 249 experiments were done. External proposals made up for about 50 % of the experiments. Fig. 1 shows the number chart of the experiments per instrument. Concerning the number of experiments the small-angle scattering machines KWS-1 and -2 clearly stand out. This is mostly due to the fact that SANS experiments are usually shorter. In contrast to 2004 both SANS machines were available with equal performance. This led to an increase of their use by 54 % (adjusted to operation time) showing that there is a clear demand for two such machines by the user community.

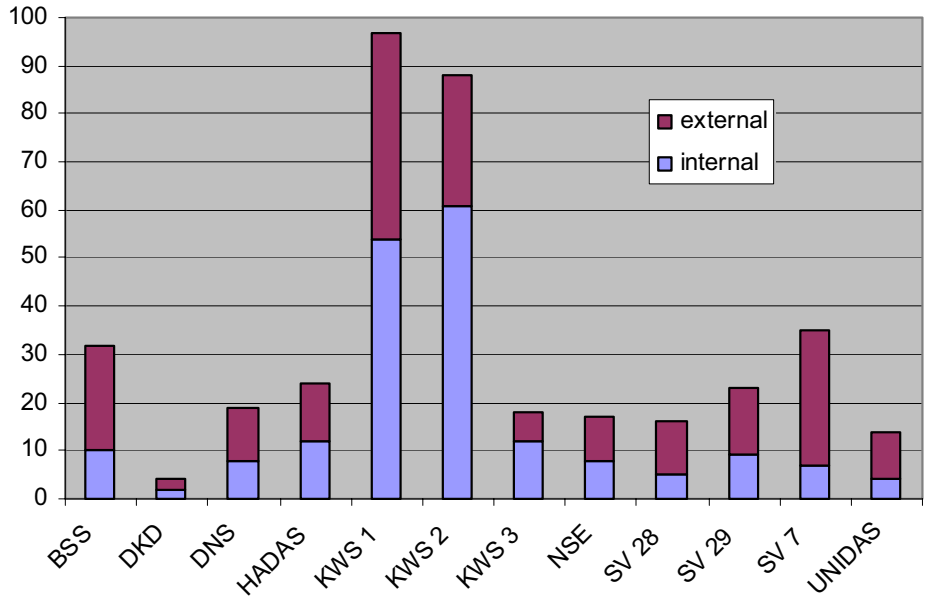


Figure 1: *Experiments performed in the year 2005 and 2006 on the neutron scattering instruments at FRJ-2*

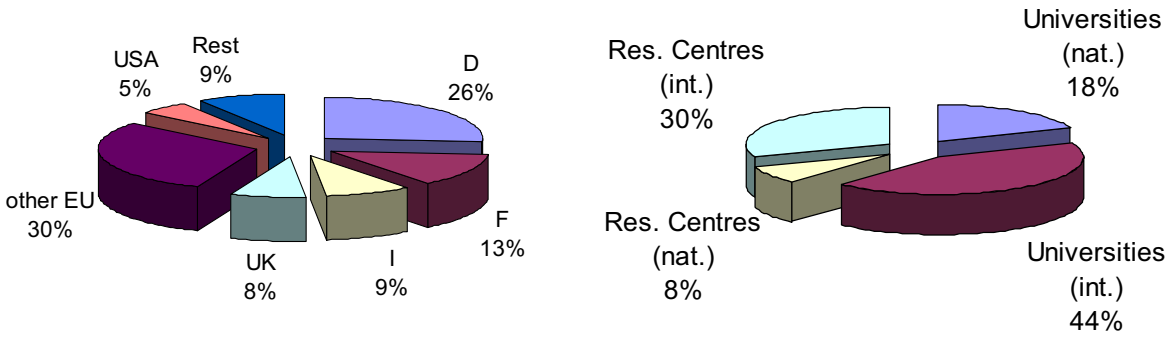


Figure 2: *Geographical pattern of FRJ-2 user groups and type of their home institution in the years 2005 and 2006*

Fig. 2 shows the geographical and institutional distribution of the user groups visiting Jülich. 22 countries were represented in 2005 and 2006, five more than in the year before. Notably, for the first time researchers from Asia (China, Taiwan and Korea) and South/Middle America (Mexico and Uruguay) used the facility. Although the absolute numbers of German institutions remained unchanged their share decreased due to the strongly increased number of non-German European proposers. Among those France, Italy and the United Kingdom were particularly active. The largest number of experimental groups is from universities and its share has increase further from 54 % in 2004 to 62 %. This stresses the importance of the FRJ-2 facility in the academic community and across the European landscape of neutron sources.

The largest share of the experiments was on soft matter systems as in the last years. Nonetheless, structural investigations of hard matter and magnetism are well represented, too.

Since the beginning of the 6th Framework Programme of the EU the European user programme "Jülich Neutrons for Europe" became an activity of NMI3, the Integrated Infrastructure Initiative for Neutron Scattering and Muon Spectroscopy. Proposals accepted under the programme benefit from funding by the European Commission (travel expenses for users). Although the number of beam days requested under this programme decreased to 515 (from 802 in 2004) this still corresponds to an overload factor of more than four compared to the contractual beam time. In order to cope with this situation more time was given as required by the programme (209 days instead of 156). Nevertheless, the selection had to be very strict and many scientifically qualified proposals had to be turned down just because of lack of beam time. In addition to the EU programme, the existing support for German university users was continued.

Last but not least, in autumn 2005 and spring 2006 the 9th and 10th International Neutron Laboratory Course took place in Jülich[1]. These training courses for students were now supported by the NMI3 as the successor of the European Neutron Round Table. As in the year before, the number of students was limited to 55. There were more than double as many applications in both years so that there had to be a strict selection. About half of the accepted students came from foreign countries. Remarkably, for the course in 2006 for the first time in the history of the lab course the number of female participants exceeded that of male students.

[1] Because of the shutdown of the reactor the 10th lab course had to be preponed from its usual autumn date to spring. In this way the continuity of the annual lab course could be preserved because the 11th installation will be held in autumn 2007 using the instruments after their relocation to FRM-II in Munich.

After the start-up of the new FRM-II reactor in Munich, there were four medium flux reactors in Germany: the FRM-II in Garching, FRJ-2 in Jülich, FRG-1 in Geesthacht and BER-II in Berlin. Despite the request from the European user community, the German federal government will only support the operation of two German neutron sources in the long term: FRM-II as the most modern research reactor and BER-II with its specialisation in extreme sample environment, in particular high magnetic fields. Therefore, it had been decided to concentrate the German neutron scattering activities by relocating the best Jülich instruments to Munich and on the other hand permanently shutting-down FRJ-2 on May 2nd, 2006. This closing of a major European facility will have a significant impact on European research activities with neutrons just at a time, when in the USA and Japan new MW spallation sources are starting-up. The former facility, SNS at Oak Ridge, started production of the first neutrons just a few days before the shut-down of FRJ-2.

But does this imply the end of neutron research in Jülich? Not at all!

Jülich is determined to remain a leading centre of research with neutrons even without its own source. The "Jülich Centre for Neutron Science" — founded February 16th, 2006 with an inauguration attended by some 260 scientists from all over the world — comprises the operation of instruments at external sources, instrument development and in-house research. The instrument activities will take place at three geographical locations: Munich/Germany, Oak Ridge/USA, and Grenoble/France.

With the Technical University of Munich TUM, a collaboration agreement was signed in June 2004. With joined forces of TUM and FZJ FRM-II will be the leading German user facility and one of the leading centres for research with neutrons world-wide. An outstation of FZJ with its own personnel housed in a dedicated building is currently being established at FRM-II (JCNS-FRMII).

Some of the best Jülich instruments are currently upgraded and relocated to FRM-II: the SANS machines KWS-1, KWS-2, KWS-3, the cold and thermal TOF-spectrometers DNS and TOPAS (an upgrade of SV-29), the spin echo instrument NSE, a reflectometer (MARIA) with polarisation analysis based on HADAS, and finally SPHERES, a backscattering spectrometer with phase space transformer which is currently being built by FZJ with funding from the federal government for Munich. While 1/3 of the beam time on these instruments will be reserved for in-house research, 2/3 will be allocated to external users through a proposal system.

At SNS (Oak Ridge, USA) we are building a beyond-state-of-the-art neutron spin echo instrument with unprecedented resolution in the μs spin-echo time regime with 6 orders of magnitude in dynamical range. This instrument will open access to the first MW spallation source for German users.

The operation of instruments at Institut Laue-Langevin (Grenoble, France), namely the triple-axis spectrometers IN12 and IN22, the NSE spectrometer IN15, and the single-crystal diffractometer D23 will also be maintained in this context.

To conclude: while the FRJ-2 as an important neutron source in Europe was shut down, Jülich will remain a major centre for research with neutrons due to its dedicated commitment at FRM-II, SNS and ILL.

Because since 2005 the operation of the neutron scattering facility FRJ-2 is part of the research programme "Large Scale Facilities for Research with Photons, Neutrons and Ions"

(PNI) of the Helmholtz Association, this report has a different structure than the preceding reports: As the first part this document contains the PNI report in German language and reports on the main instrumental achievements under this programme. The second part comprises the experimental reports from experiments carried out at FRJ-2 in the years 2005/2006 and publications of the past five years that are related to FRJ-2 experiments. The reports are grouped by instrument[2] and preceded by a tabular description of the instrument parameters. Detailed descriptions of the instruments can be found in the instrument handbook "Neutron Scattering Experiments at the Research Reactor in Jülich" or the web site www.neutronscattering.de .

Reiner Zorn

[2] The SANS proposals are labelled by the instrument they originally applied for. Some experiments were transferred between KWS-1 and KWS-2 because of better feasibility or availability. For experiments involving combinations of instruments often only single reports were submitted. These are then listed under the instrument which is considered the most important for the objective. The instruments β-NMR, SV-30, EKN, LAP-ND are not represented here because they are under construction, only used for test purposes, or not demanded during 2005/6. Nevertheless, their specifications can be found in the instruments handbook and on the web site.

Programmanteil „Großgeräte für die Forschung mit Photonen, Neutronen und Ionen“

Forschungsbereich „Struktur der Materie“ Koordinator: Prof. A. Wagner, DESY
Programm „Großgeräte für die Forschung mit Photonen, Neutronen und Ionen“
Sprecher. Prof. M. Steiner, HMI
FZJ- Ansprechpartner für den Programmanteil: Prof. Th. Brückel, IFF

A Ziele und Einbettung in den Forschungsbereich

Im Forschungsbereich Struktur der Materie kommen eine Vielzahl von Großgeräten zum Einsatz, die Forschungsmöglichkeiten mit Photonen, Neutronen und Ionen für eine breite Palette von Wissenschaftsdisziplinen, angefangen von Physik, Chemie, Biologie und Geowissenschaften, bis hin zu Materialwissenschaften, Ingenieurwissenschaften und Umweltforschung bieten. Der größte Teil der an diesen Großgeräten verfügbaren Strahlzeit wird externen Nutzern zur Verfügung gestellt, die hauptsächlich von Universitäten, aber auch von außeruniversitären Forschungseinrichtungen und der Industrie kommen.

Das Forschungszentrum Jülich FZJ ist im Bereich der Forschung mit Neutronen aktiv. Dabei resultiert die spezielle Rolle Jülichs innerhalb der deutschen Neutronenlandschaft aus:

- einer leistungsstarken Eigenforschung auf dem Gebiet kondensierter Materie mit Schwerpunkten im Bereich weicher Materie und im Magnetismus;
- einem Nutzerbetrieb, der in diesen wissenschaftlichen Schwerpunktsbereichen Unterstützung durch Experten und Laboreinrichtungen bietet;
- einem wissenschaftsmotivierten Methoden- und Instrumententwicklungsprogramm;
- der Nutzung der zukunftsweisenden Möglichkeiten der Neutronenforschung an gepulsten MW- Spallationsquellen.

Die Jülicher Arbeiten sind in das Helmholtz-Programm „Großgeräteforschung mit Photonen, Neutronen und Ionen“ PNI eingebunden, das formal im Jahr 2005 begonnen hat. Forschung mit Neutronen ist zugleich ein Grundpfeiler des Programms "Kondensierte Materie" und liefert wichtige Beiträge auch in anderen Programmen, z. B. "Informationstechnologie mit nanoelektronischen Systemen".
.

B Programmergebnisse

Erreichte Meilensteine und/oder herausragende wissenschaftliche Ergebnisse

Die an den Neutroneninstrumenten des FZJ durchgeführte Eigenforschung ist wesentlicher Bestandteil des HGF- Programms "Kondensierte Materie", siehe den entsprechenden Fortschrittsbericht. Schwerpunkte liegen in den Themenbereichen "Elektronische und magnetische Phänomene" und "Weiche Materie und Biophysik". Die strategische gegenseitige Verzahnung der beiden Programme „Kondensierte Materie“ und „PNI“ führt zu einer von der Wissenschaft getriebenen Methoden- und Instrumentenentwicklung. Dadurch werden auch neue Möglichkeiten für andere HGF- Programme bereitgestellt, etwa für das Programm "Informationstechnik mit nanoelektronischen Systemen" in dem Forschungsbereich "Schlüsseltechnologien".

Der Reaktor einschließlich seiner kalten Neutronenquelle erreichte in 2005 eine Verfügbarkeit von 98,9 %. Damit nimmt der FRJ-2 im Zuverlässigkeitsvergleich einen internationalen

Spitzenplatz ein. Insgesamt wurden 257 Neutronenstreuexperimente an 17 Instrumenten durchgeführt. Die Nachfrage nach Strahlzeit durch die europäischen Nutzer im Rahmen des EU- geförderten "NMI3 Access Programme" war mit einer Überbuchungsquote von 4.4 relativ zur vertraglich vereinbarten Messzeit weiterhin sehr hoch, was die Attraktivität Jülichs auf internationalem Niveau belegt. Europäische Nutzer kamen hauptsächlich aus Frankreich, Spanien, Großbritannien, Italien, Belgien und den Niederlanden.

Im Jahr 2005 wurden innerhalb des Instrument-Entwicklungsprogramms folgende Ziele erreicht:

Auflösungsverbesserung für NSE Spektrometer: Neuartige Korrekturspulen, so genannte Fresnelspulen wurden entwickelt, die eine wesentliche Steigerung der Auflösung von Spinechospektrometern erlauben. Erste Tests am Jülicher Spinechospektrometer ergaben eine Auflösungsverbesserung um annähernd einen Faktor 2. An dem Spektrometer, das für die SNS gebaut wird, können damit in Zukunft auch extrem langsame Bewegungen großer Makromoleküle bis in das Zeitfenster von 1 Microsekunde verfolgt werden.
Fertigstellung des Rückstreuspektrometers SPHERE: Im Rahmen der Verbundforschung wurde in den letzten Jahren am FRM-II ein Rückstreuspektrometer aufgebaut. Das Instrument zeichnet sich durch innovative Elemente, wie einen Phasenraumtransformator und einen Dopplerantrieb mit Linearmotor aus. In 2005 konnten alle wesentlichen Elemente des Instruments aufgebaut werden, so dass in 2006 die Inbetriebnahme erfolgen kann.
Inbetriebnahme des thermischen Dreiachsspektrometers SV30: In den vergangenen Jahren wurde das in die Jahre gekommene Instrument SV4 durch ein thermisches Dreiachsinstrument neuester Bauart (SV-30) ersetzt. Dieses Instrument wurde speziell für die Polarisationsanalyse mit Hilfe von Heliumfilterzellen entwickelt. Die Polarisation des Heliumgases wird mit zwei verschiedenen Techniken erreicht, die beide in Jülich entwickelt werden: das optische Pumpen metastabil angeregter Atome und das optische Pumpen über den Spinaustauschprozeß. Das Spektrometer ist ausgerüstet mit zwei großen doppelt fokussierenden Monochromatoren. Der Neutronenfluß an der Probe ist fast eine Größenordnung höher als der des alten Instruments. Nachdem das Instrument in 2004 fertig gestellt wurde, konnte es in 2005 endgültig in Betrieb genommen werden. Verschiedene Experimente zur Phononenspektroskopie und zur Bestimmung magnetischer Anregungen in korrelierten Elektronensystemen wurden durchgeführt.
Vollständige Vektorpolarisationsanalyse: Eine neuartige, extrem effiziente Methode für die vollständige Vektorpolarisationsanalyse in der Neutronenstreuung wurde am FZJ entwickelt. Im vergangenen Jahr konnten verschiedene Demonstrationsexperimente an komplexen magnetischen Materialien mit der neuen Methode erfolgreich durchgeführt werden. Zum ersten Mal ist es möglich, die volle Polarisationsmatrix für alle zugänglichen Energie- und Impulsüberträge zu bestimmen. Die neue Methode ermöglicht die vollständige Vektorpolarisationsanalyse auch an einem Multidetektor- und Flugzeitinstrument und ist deshalb von besonderem Interesse für Spallationsneutronenquellen. Die Methode erlaubt es, komplexe magnetische Strukturen mit chiralen Komponenten zu lösen und ermöglicht die experimentelle Trennung von Korrelationen zwischen kern- und magnetischen Freiheitsgraden in Festkörpern.
Larmor Kodierung: Im Rahmen des EU- Projekts „Polarized Neutron Techniques“ wurden neuartige Möglichkeiten zur Kodierung von Richtung oder Geschwindigkeit von Neutronen mit Hilfe des Neutronenspins erforscht. Ein Beispiel ist die Kodierung mit Hilfe von rotierenden Magnetfeldern, die eine einfache Möglichkeit zur Auflösungsverbesserung von Dreiachs- oder Flugzeitspektrometern verspricht.
Fokussierende Kleinwinkelanlage KWS-3: Die Kleinwinkelanlage KWS-3 ist ein weltweit einmaliges Instrument, welches mit Hilfe eines fokussierenden Spiegels eine Eintrittsblende auf den Detektor abbildet. Mit dieser Anlage kann eine Auflösung erzielt werden, die eine

Größenordnung über derjenigen konventioneller Lochblendeninstrumente liegt. In 2005 wurden erste Tests mit einem zusätzlichen Replikaspiegel durchgeführt, der prinzipiell eine Intensitätserhöhung um einen Faktor 2 zulässt. Simulationen haben gezeigt, dass das Instrument durch den geplanten Umzug nach München und der damit verbundenen Endposition an einem Neutronenleiter annähernd zwei Größenordnungen an Fluss gewinnen wird, was völlig neue Anwendungsbereiche erschließen kann.

Programmübergreifende Themen (Vernetzung, Nachwuchs, Chancengleichheit)

Forschung mit Neutronen am Forschungszentrum Jülich ist sehr gut eingebunden in nationale und internationale Netzwerke. Die Errichtung der Außenstelle des FZJ am Forschungsreaktor FRM-II der TUM und die Durchführung des Neutronenpraktikums zusammen mit mehreren NRW Universitäten sind besonders gelungene Beispiele für die Vernetzung des FZJ mit universitären Einrichtungen. Nutzerexperimente europäischer Nutzer werden durch das EU FP6 Access Programm unterstützt. Jülich ist außerdem Koordinator des EU-Exzellenznetzwerks "Soft Matter Composites" (SoftComp), das in 2004 gegründet wurde und in dem 19 akademische Institute und 5 Industriefirmen aus mehreren europäischen Ländern im Bereich der Erforschung weicher Materie zusammen arbeiten. Als Beispiel für eine Vernetzung auf dem Gebiet der Methodenentwicklung sei das größte der gemeinsamen Forschungsnetzwerke für Neutronenstreuung innerhalb des EU FP6 Programms erwähnt. Dieses Netzwerk ist der Entwicklung von fortschrittlichen Larmorpräzessionstechniken für Neutronenstreuung gewidmet. Das Forschungszentrum Jülich koordiniert diese Forschung über "Neutronenpolarisationstechniken" PNT, die insgesamt 20 internationale Partner und Beobachter zusammenbringt. Daneben ist das FZJ an weiteren europäischen Netzwerken beteiligt, wie etwa DETNI zur Detektorentwicklung, NSF zur Entwicklung von Neutronenpolarisationsfiltern oder EURISOL zum Transport- und Aktivierungsverhalten von Hochenergieneutronen. Auf nationaler Ebene arbeitet das „Komitee für Forschung mit Neutronen“ (KFN) zusammen mit Nutzern und den Zentrenvertretern, um eine nationale Strategie im Bereich der Neutronenstreuung zu entwickeln und die politischen Entscheidungsträger zu beraten. Ein Wissenschaftler des Forschungszentrums hat in den Jahren 2003 bis 2005 den Vorsitz dieser gewählten Vertretung der Neutronennutze geführt.

Am FRJ-2 werden wesentliche Drittmittelerträge durch ^{99}Mo Produktion – als Vorstufe des wichtigen Radiopharmazeutikums ^{99}Tc – erlöst.

Nachwuchsförderung im Bereich von Großgeräten ist eine Kernaufgabe der HGF Zentren. Vom 12. - 23. September 2005 wurde am FZJ zum neunten Mal die jährliche Neutronenschule abgehalten. Dieses Praktikum ist bei weitem die größte Schule dieser Art in Deutschland und eine der größten weltweit. Sie besteht aus einer Woche Vorlesung und einer Woche Experimente an 11 Neutronenstreuinstrumenten. Die Vorlesungsmanuskripte werden in Buchform verlegt. Die Schule wird in Zusammenarbeit mit der RWTH Aachen und den Universitäten in Münster, Köln und Bonn durchgeführt.

Ergebnisse der Überzeichnungsvorhaben (Additional Funding)

In Oak-Ridge, USA, wird als erste Neutronenquelle der nächsten Generation eine MW Spallationsquelle, die SNS, realisiert. FZJ beteiligt sich an der Instrumentierung dieser Quelle durch den Bau eines Spin-Echo Spektrometers, welches das Beste seiner Art werden wird. Durch diesen Beitrag zur Instrumentierung erhalten deutsche Nutzer Zugang zur SNS und deutsche Wissenschaftler können Erfahrung mit der Instrumentierung einer solchen neuartigen Quelle sammeln. In 2005 konnte die Entwicklung aller wesentlichen Komponenten des Spektrometers weitgehend abgeschlossen werden. Neben den supraleitenden Magneten mussten insbesondere neue „Fresnel“- Korrekturspulen entworfen werden, die es dem

geplanten Spektrometer an der SNS ermöglichen sollen, zu bisher unerreichten Fourierzeiten von 1 Microsekunde (entsprechend der weltbesten Energieauflösung von 0.7 neV) vorzustoßen. Diese Spulen wurden im existierenden Jülicher Spin Echo Instrument erfolgreich getestet. Damit kann nun der Übergang aus der Konstruktions- in die Bauphase des SNS Instruments erfolgen.

Stand der Umsetzung der Senatsempfehlungen

Auflage: *Aufbauend auf einem übergreifenden Helmholtz-Konzept, sollten FZJ und GKSS eine intensive Beteiligung einschließlich des Transfers von Personal und Instrumentierungen am FRMII starten. Ein Konzept hierfür sollte bis Ende 2004 vorgelegt werden.*
Am 30. Juni 2004 wurde die Eckpunktevereinbarung zur Einrichtung einer Außenstelle des FZJ am neuen Forschungsreaktor FRM-II der TUM unterzeichnet. Die Umsetzung ist in vollem Gange: (i) Ein Gebäude für die Außenstelle ist im Bau und soll im November 2006 fertig gestellt werden; (ii) FZJ hat zusätzliches Personal für den Betrieb der Außenstelle eingestellt; (iii) Die notwendigen Infrastrukturmaßnahmen am FRM-II, wie Medienversorgung, Bau der Neutronenleiter etc. werden durchgeführt; (iii) insgesamt 8 Neutronenstreuinstrumente des FZJ werden für den Betrieb in München vorbereitet.

Auflage: *FZJ sollte dem Stilllegungsplan für DIDO für 2006 folgen*.
Der DIDO Reaktor als die leistungsstärkste Neutronenquelle der HGF wird im Jahre 2006 noch für 84 Tage betrieben und dann am 1. Mai endgültig außer Betrieb genommen. Die Antragsunterlagen für die Stilllegungsgenehmigung sowie die Planung für den anschließenden Rückbau der Anlage sind in Arbeit.

Empfehlung*: Die Entwicklung des Spin-Echo-Instruments durch das FZJ, das am SNS in Oak Ridge eingesetzt werden soll, wird dringend unterstützt.*
Die Verhandlungen mit den amerikanischen Partnern sind weit gediehen und haben am 16. Februar 2006 zur Unterzeichnung eines Zusammenarbeitsvertrags geführt. Zum Stand der technisch- methodischen Arbeiten siehe Punkt „Ergebnisse der Überzeichnungsvorhaben“.

C Weitere Programmentwicklung

Aufgrund der 2004 durch den Aufsichtsrat des Forschungszentrums getroffenen Entscheidung, den Reaktor FRJ-2 im Jahr 2006 stillzulegen und eine Außenstelle auf dem FRM-II Gelände zu errichten, müssen große Teile des Jülicher Anteils an dem Programm geändert werden. Nach der Außerbetriebnahme des DIDO Reaktors wird das FZJ seine Aktivitäten auf dem Gebiet der Forschung mit Neutronen auf externe Quellen verlagern. Explizit sind dies der weltweit leistungsfähigste Forschungsreaktor am Institut- Laue Langevin ILL in Grenoble / Frankreich, die modernste kontinuierliche Neutronenquelle FRM-II bei München und die erste Megawatt Spallationsquelle SNS in Oak Ridge / USA. Im „Jülich Centre for Neutron Science“ wird der Nutzerbetrieb an den FZJ- eigenen Instrumenten an diesen Quellen, die Instrument- und Methodenentwicklung, sowie die Eigenforschung des FZJ im Bereich der Neutronenstreuung zusammengefasst werden.

Methodenentwicklung wird an allen Instrumenten konsequent weitergeführt. Das Spinechoinstrument an der SNS soll 2008 in Betrieb gehen – siehe die Beschreibung des Überzeichnungsprojekts. Das Dreiachsspektrometer IN12 am ILL wird in 2006 eine neue Multianalysatoroption „UFO“ erhalten. Den Schwerpunkt der Instrumententwicklung werden jedoch diejenigen Instrumente bilden, die nach München transferiert und dort an dem FRM-II betrieben werden sollen. Im Jahr 2004 wurde ein Eckpunktepapier zwischen dem Forschungszentrum Jülich und der Technischen Universität München (TUM) unterzeichnet, wel-

ches den Betrieb von 8 Instrumenten am FRM-II durch ein Team von Wissenschaftlern und Technikern des Forschungszentrums vorsieht. Im Einzelnen:

Hochauflösendes Rückstreuspektrometer (SPHERE): Dieses Instrument wurde durch das Forschungszentrum Jülich mit der finanziellen Förderung durch das BMBF im Rahmen der Verbundforschung für den FRM-II Reaktor errichtet. Das Instrument zeichnet sich durch innovative Komponenten aus, wie den Phasenraumtransformations- Chopper und einem schnellen Dopplerantrieb. Die Phase der Inbetriebnahme beginnt Anfang 2006, gefolgt vom regulären Nutzerbetrieb.
Neutronenspinechospektrometer (NSE): Dieses Instrument wird als erstes vom FRJ-2 zum FRM-II transferiert werden. Das Instrument hat den Nutzerbetrieb am FRJ-2 bereits im letzten Zyklus 2005 eingestellt und wird momentan umgebaut. Es soll Ende 2006 am FRM-II betriebsbereit sein. Aufgrund der optimalen Position am Ende eines Neutronenleiters wird ein merklicher Gewinn, sowohl in Intensität als auch in Auflösung, erwartet. Durch neue Fresnelkorrekturspulen kann die Auflösung weiter verbessert werden. Die Instrumentansteuerungs- und Datenaufnahme- Hard- und Software werden vollständig erneuert.
Spektrometer für diffuse Neutronenstreuung (DNS): Für dieses Instrument werden wesentliche Änderungen an Abschirmung, Monochromator und Detektorbank erforderlich. Diese Umbauarbeiten werden sofort nach Außerbetriebnahme des FRJ-2 beginnen. Die Zählraten für die Polarisationsanalyse werden durch eine zweite Detektor- und Analysatorbank verbessert werden. Der zugängliche Raumwinkel wird durch linear ortsauflösende Heliumzählrohre wesentlich vergrößert und die Energieauflösung durch einen schnell drehenden Chopper neuester Bauart verbessert. Erste Tests mit Neutronen am FRM-II sind für Ende 2006 / Anfang 2007 vorgesehen.
Kleinwinkelstreuinstrumente (KWS-1, KWS-2): Beide Instrumente sind Lochblenden-Neutronenkameras neuester Bauart mit einem 20 m langen Detektorflugrohr. Beide sollen direkt nach Außerbetriebnahme des FRJ-2 an den FRM-II transferiert werden. In München wird eines der beiden Instrumente ausgelegt für Experimente mit höchster Intensität (20 % Geschwindigkeitsselektor). Das andere Instrument wird optimiert für hohe relative Impulsraumauflösung mit einem einstellbaren Choppersystem. Es wird eine Option für Kleinwinkelstreuung unter streifendem Einfall erhalten und mit Neutronenpolarisationsanalyse ausgerüstet werden. Beide Instrumente werden Neutronenlinsen erhalten, um Zählraten und Auflösung zu verbessern. Während eines der beiden Instrumente bereits Ende 2006 betriebsbereit aufgebaut sein soll, wird das zweite Instrument in 2007 folgen.
Fokussierende Kleinwinkelanlage KWS-3: Diese weltweit einmalige Anlage setzt einen fokussierenden Spiegel ein, um eine Eintrittsblende auf den Detektor abzubilden. Damit wird eine Auflösung erzielt, die etwa eine Größenordnung besser ist, als bei den Lochblendeninstrumenten. Da das Instrument von einer Neutronenweiche am FRJ-2 an eine echte Neutronenleiterendposition am FRM-II transferiert werden wird, erwarten wir eine Intensitätserhöhung von fast zwei Größenordnungen. Auch dieses Instrument soll Ende 2006 am FRM-II betriebsbereit sein.
Reflektometer für magnetische Nanostrukturen (MARIA): Ein Instrument für Neutronenstreuung unter streifendem Einfall, welches auf dem existierenden HADAS-Reflektometer des FRJ-2 basiert, wird am FRM-II aufgebaut werden. Das Instrument wird für Polarisationsanalyse der diffusen Streuung über einen großen Winkelbereich ausgelegt werden. Es wird in zwei verschiedenen Betriebsmoden arbeiten können: als ein Reflektometer mit vertikaler Fokussierung und als Kleinwinkelinstrument zur Streuung unter streifendem Einfall mit einem kollimierten einfallenden Strahl. Das Instrument wird optimiert für die Untersuchung magnetisch dünner Filme bis herab in den Monolagenbereich und zur Untersuchung von lateral strukturierten magnetischen Nanostrukturen und soll auf diesem Gebiet eine weltweite Spitzenstellung einnehmen.
Thermisches Flugzeitspektrometer mit Polarisationsanalyse TOPAS: Dieses Instrument basiert auf dem existierenden SV-29 Spektrometer des FRJ-2. Es wird ausgelegt für einen

mittleren Bereich von Energieüberträgen bis zu etwa 110 meV, wo Instrumente an kontinuierlichen Quellen aufgrund der höheren Repetitionsrate gut mit Instrumenten an Spallationsneutronenquellen konkurrieren können. Das Instrument wird für die Untersuchung von magnetischen Anregungen optimiert. Es wird eine Option zur Polarisationsanalyse erhalten, die auf Heliumfilterzellen basiert. Dadurch wird es möglich werden, magnetische und Gitteranregungen in korrelierten Elektronensystemen zu trennen.

- Publikationen und Patente sind im Internet nachlesbar unter: www.fz-juelich.de/FB-2005
- Ein Abkürzungsverzeichnis befindet sich in Kapitel A.6

A.1.1.1 Großgerät FRJ-2

Leistungskategorie II
Forschungsbereich „Struktur der Materie“ Koordinator: Prof. Dr. A. Wagner, DESY
Programm „Großgeräte für die Forschung mit Photonen, Neutronen und Ionen“
Sprecher: Prof. Dr. M. Steiner, HMI
FZJ-Ansprechpartner: Prof. Dr. T. Brückel, IFF

Einsatz des Großgeräts

Der FRJ-2 ist nach dem FRM-II die mit Abstand leistungsstärkste Neutronenquelle in Deutschland und eine der leistungsfähigsten Mittelflussquellen im internationalen Vergleich. Einschließlich seiner kalten Quelle und mit seiner hochmodernen Instrumentierung steht der FRJ-2 sowohl Helmholtz-internen als auch externen Wissenschaftlern als leistungsfähiges Großgerät zur Neutronenstreuung zur Verfügung. Neben der Neutronenstreuung wird der FRJ-2 als einer von vier europäischen Forschungsreaktoren und als einziger in Deutschland zur Produktion von Mo-99 im industriellen Maßstab genutzt. Mo-99 ist das Ausgangsprodukt für die Herstellung des in der Medizin nicht mehr verzichtbaren Radiopharmakums Tc-99.

Analyse der Zielerreichung

Wesentliche Ziele zur Weiterentwicklung des FRJ-2 im Jahr 2005 waren die Erhöhung der passiven Sicherheit des Reaktors durch Ertüchtigungen im Bereich der Notstromversorgung und die Installation neuer Pegelstandsgeber und eines neuen Prozessleitsystems für die Beckenanlage.

Planung des Berichtsjahres:

Im Betriebsplan des FRJ-2 wurden für 2005 insgesamt 189 Betriebstage geplant. Gemäß der vertraglichen Vereinbarung zur Mo-99-Produktion war eine Bestrahlung von 160 Targets zur Produktion des Isotops Mo-99 zu erwarten.

Planerreichung des Berichtsjahres:

Der Reaktor einschließlich seiner kalten Neutronenquelle wurde in 2005 an 187 Tagen im Leistungsbetrieb gefahren und erreichte damit eine Verfügbarkeit von 98,9 %, bezogen auf die geplante Betriebszeit. Damit nimmt der FRJ-2 auch im Zuverlässigkeitsvergleich 2005 einen internationalen Spitzenplatz ein. Die durchgeführten Modernisierungen konnten im Rahmen des geplanten Budgets abgewickelt werden. Ungeplante budgetrelevante Ertüchtigungsmaßnahmen wurden 2005 nicht erforderlich.

Die Nachfrage nach Strahlzeit durch die europäischen Nutzer im Rahmen des EU- geförderten "NMI3 Access Programme" war weiterhin sehr hoch, was die Attraktivität Jülichs auf internationalem Niveau belegt. Insgesamt wurden innerhalb dieses Programms 515 Instrumentetage nachgefragt. Dies übersteigt die vertragliche Verpflichtung von 117 Instrumenttagen pro Jahr um das 4.4-fache. Um zumindest diejenigen Messzeitanträge zum Zuge kommen zu lassen, die eine ausgezeichnete Beurteilung durch das international besetzte Strahlzeitkomitee erhielten, wurde die Messzeitvergabe im EU-Programm auf 209 Tage erhöht. Es mussten trotzdem immer noch 60 % aller Anträge aus Mangel an Messzeit zurückgewiesen werden.

Insgesamt wurden 257 Neutronenstreuexperimente an 17 Instrumenten durchgeführt. Die institutionelle Zugehörigkeit dieser Nutzergruppen ergibt sich wie folgt (in jedem Fall ist nur

die Anzahl von unterschiedlichen Gruppen angegeben, wobei natürlich einige Gruppen – insbesondere von nationalen Einrichtungen - mehrere Experimente am FRJ-2 ausgeführt haben): 14 Gruppen von deutschen Universitäten, 36 Gruppen von ausländischen Universitäten, 6 Gruppen von nationalen Forschungszentren und 23 Gruppen von internationalen Forschungszentren. Europäische Nutzer kamen hauptsächlich aus Frankreich, Spanien, Großbritannien, Italien, Belgien und den Niederlanden.

Maßgebliche Abweichungen:

Der Verlust von 2 Betriebstagen im Vergleich zu den für 2005 geplanten 189 Betriebstagen wurde verursacht durch zwei unplanmäßige automatische Reaktorabschaltungen durch Ausfälle im Bereich der Thermoelemente der Brennelementdifferenztemperaturüberwachung. Diese Ausfälle sind bedingt durch die genehmigte Bauart der Brennelemente und auch durch die neue Brennelementdifferenztemperaturüberwachung nicht vollständig zu verhindern, da in jedes Brennelement nur ein einziges Thermoelement eingesetzt werden kann und in diesem Bereich somit auch durch die in 2004 durchgeführten Ertüchtigungsmaßnahmen keine Redundanz aufgebaut werden konnte.
Weiterhin erfreulich entwickelte sich die Produktion von Mo-99. Nicht zuletzt wegen der hohen Anlagenverfügbarkeit konnten in den drei Bestrahlungseinschüben statt der vertraglich vereinbarten 160 Targets insgesamt 174 Targets bestrahlt und an den Kunden ausgeliefert werden.

Besondere Vorkommnisse:

Im Jahr 2005 kam es zu insgesamt 6 unplanmäßigen automatischen Reaktorabschaltungen auf Grund verschiedener Ursachen. Lediglich in 2 Fällen konnte der Reaktor nicht unmittelbar wieder angefahren werden, sondern es musste nach Behebung der jeweiligen Störung das Abklingen der Xenon-Vergiftung abgewartet werden, um den Reaktor wieder auf Nennleistung anfahren zu können. In den anderen Fällen wurde der Reaktor unmittelbar nach Beseitigung der Störung wieder angefahren.
Es sind hierbei keine Erkenntnisse aufgetreten, die den Einsatz von finanziellen Mitteln oberhalb des geplanten Budgets zukünftig erwarten lassen würden.

Gesamteinschätzung der Entwicklung und Vorausschau

Entsprechend dem Beschluss des FZJ- Aufsichtsrates wird der FRJ-2 im Mai 2006 endgültig außer Betrieb genommen. Für den restlichen Betrieb sind in 2006 84 Betriebstage geplant. Es ist davon auszugehen, dass die sehr hohe Verfügbarkeit und Terminzuverlässigkeit der Anlage bis zuletzt auf dem erreichten Niveau gehalten werden kann.
Die vorbereitenden Maßnahmen zur Außerbetriebnahme des FRJ-2, Erstellung der für die Stilllegungsgenehmigung erforderlichen Antragsunterlagen und zur Planung des anschließenden Rückbaus der Anlage wurden vom Betreiber, der Zentralabteilung Forschungsreaktoren des Forschungszentrums Jülich, bereits begonnen.

Larmor labelling by spin flippers with rotating magnetic field

A. Ioffe
Forschungszentrum Jülich GmbH, Institut für Festkörperforschung, 52425 Jülich, Germany

The neutron spin-echo (NSE) method, which is the most powerful tool of high-resolution neutron spectroscopy, is known in two versions: either with the long solenoids or short alternating fields. Here we consider an alternative version that makes use of spin flippers with an in-plane rotating magnetic field vector. Some possible applications of such technique are discussed. This approach can be considered as an alternative to the present-day NSE techniques.

Neutron inelastic scattering provides extremely valuable information about the atomic collective motions with the microscopic length scale from the nearest neighbor distances to a few nanometers and the time scale that ranges from characteristic microscopic times as picoseconds up to microseconds in the case of slow motions as e.g. critical fluctuations in phase transitions, dynamic behavior of disordered systems (structural and spin glasses), etc. The change in neutron energy, ΔE, corresponding to these slow motions is extremely small (in the order of 1 neV) and requires extremely high energy resolution methods. Conventional methods of inelastic spectroscopy, time-of-flight or triple-axis, are relying on a differential approach, when the energy exchange is determined as the difference of two well-defined energies of incident and scattered neutrons. Therefore, any attempt to reach a very high, better than $\Delta E/E=10^{-4}$, energy resolution by conventional neutron spectroscopy methods will require extremely high monochromatization of the incident beam thus resulting in intolerable intensity losses. Indeed, the studies of slow dynamical process required a new non-traditional approach, the so-called neutron spin-echo (NSE) technique [1]. It provides few orders of magnitude higher energy resolution than any other technique of inelastic (quasielastic) neutron scattering.

The NSE technique is based on the phenomenon of Larmor precession of the neutron spin in a transverse magnetic field. When the neutron propagates across a region of magnetic field of strength B, the neutron spin undergoes a precession with the Larmor frequency $\omega_L = \gamma_n B$ (γ_n - the gyromagnetic ratio). The total precession angle φ_L, is defined by this frequency and the time τ of propagation of the neutron through the magnetic field region of length L:

$$\varphi_L = \omega_L \tau = \frac{\gamma_n}{v_n \cdot \cos(\psi)} \int_L B dl \qquad (1)$$

where ψ is the inclination of the neutron trajectory and v_n is the neutron velocity along it.

In this case, the orientation of the neutron spin can be considered as the arrow of a "Larmor clock" that is attached to every neutron. Indeed, the "time" shown by the clock is defined by the field integral (Eq. (1) seen by each neutron. Such a Larmor labelling opens the unique possibility for the development of "unusual" neutron scattering techniques, where the energy (momentum) resolution does not require the initial and final states to be well selected.

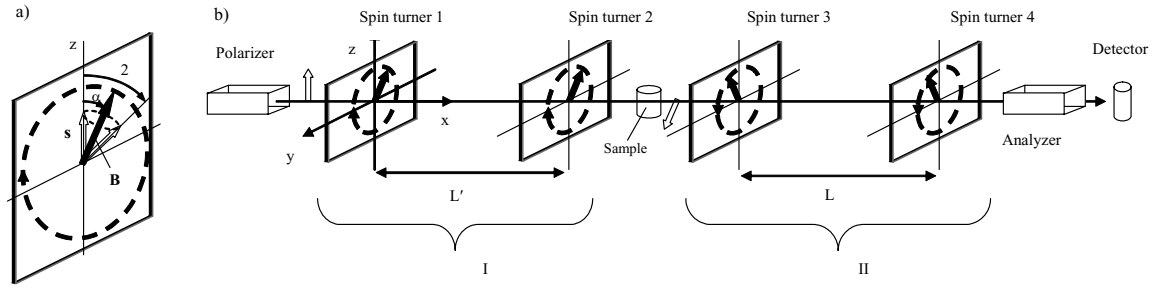


Figure 1. a) The spin flipper with rotating magnetic field (RMF). In-plane rotation of the neutron spin vector is achieved by the Larmor precession of neutron spin by angle π around the magnetic field vector **B**. b) Layout of the NSE spectrometer built by two pairs of the RMF flippers

At present there are two well developed practical realizations of NSE principle: generic NSE technique [1] and neutron resonance spin echo technique (NRSE) [2].

Recently, we proposed a new kind of NSE technique, which is based upon the use of thin magnetic spin flippers with an in-plane rotating magnetic field vector (RFNSE) [3]. The main element of such a NSE spectrometer is the spin turner that provides the in-plane rotation of the neutron spin vector with a constant angular velocity ω, so that the angle of neutron spin rotation will be proportional to time t (Fig. 1a). Practically it is achieved by the Larmor preces-

sion of neutron spin around the magnetic field vector B that rotates in the plane *yz* with the angular velocity ω_B. If the Larmor precession angle is π, then the neutron spin will be mirror- reflected relative to the field vector, thus rotating in the plane *yz* with the angular velocity $\omega = 2\omega_B$.

A pair of such spin turners separated by a field-free area of length *L* (cascade I in Fig. 1b) is acting like a Larmor clock that shows the time $\alpha = 2\omega_B T = 2\omega_B L'/V_n$ of propagation of neutron with velocity V_n between the turners. This time depends both on the neutron velocity V_n and the length L' of its trajectory between flippers, but not on the arrival time. Indeed, the neutron velocity is coded by the angle α, so that the beam polarization at the sample spectrometer is a sinusoidal function of the neutron wavelength λ, $P_z = \cos(2\omega h\lambda L/m_n)$ (here *h* is the Plank constant and m_n is the neutron mass). For a wide spectrum neutron illumination, the neutron beam at the sample is an overlap of such functions with different periods and is completely depolarized.

The NSE principle is to apply a decoding operation to such beam. This decoding operation is essentially the time inversion and is practically achieved either by the change of the field direction (generic NSE) or the change of the sense of the RF-fields rotation (NRSE). The suggested NSE spectrometer is in a way analogue to NRSE spectrometer, so that it contains cascade II (Fig. 1b) with the opposite sense of magnetic field vector rotation. Then the final orientation of the spin vector relative to z-axis is

$$\beta = 2\omega\left[\frac{L_1}{v_n} - \frac{L_2}{v_n + \Delta v_n}\right] \qquad (2)$$

where Δv_n is the change of the neutron velocity at the sample. As it follows from Eq. (2), changing the distance between foils in the cascade II, one can change β in rather wide range, thus providing a sinusoidal modulation of the outgoing neutron beam, the so-called NSE signal.

This novel RFNSE technique can be applied in all cases, when the use of Larmor precession devices may result in an improvement either in energy or momentum resolution of neutron scattering instruments, particularly for an improvement in the resolution of triple-axis spectrometers [4] In this case, the momentum resolution is defined by the triple-axis spectrometer, while the energy resolution is defined by the NSE setup and may be increased up to 1 μeV without significant intensity loss.

Another application of the RFNSE technique is high resolution measurements of the neutron momentum transfer in small-angle scattering, diffraction and reflectometry [5]. In this case the Larmor precession is used to label the angle ψ rather than wavelength as in NSE spectroscopy (Eq. (1)) and, in complete analogy with the abovementioned, a high angular resolution can be obtained when using practically uncollimated incident neutron beams. If a sample is placed in the RFNSE spectrometer with tilted spin turners (Fig. 2), then scattering at the sample results in different path lengths between turners 3 and 4. The NSE signal is recorded by the change of distance L_2. Recalling that the effective field integral is $2\omega_B L'$, one may conclude that the recorded signal is a superposition of NSE signals of different frequencies resulting from different effective field integrals over the neutron trajectories. The scattering profile can be restored by the Fourier transform of the recorded intensity.

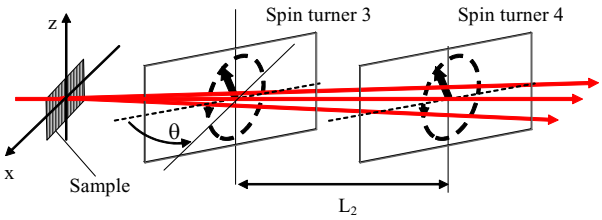


Figure 3. SERGIS configuration. F1- F4 are RMF flippers. Sample is scattering in *xy* plane, where there is no incident beam collimation

The result of Monte-Carlo simulations of a corresponding experiment is shown in Fig. 3. NSE signals corresponding to small beam deviations ψ in the plane *ZX* are well resolved in spite of the use of an only weakly collimated, ± 1°, incident neutron beam [6].

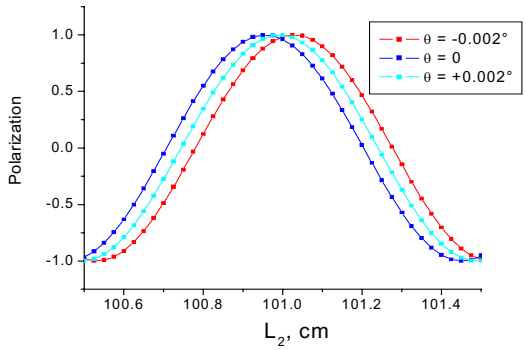


Figure 3. Shift of the NSE signal caused by the deviation of a practically uncollimated (±1°) neutron beam in ZX plane. RMF spin turners driving frequency of 50 kHz, L_1 = 1 m and θ_0= 45°.

It is a pleasure to thank the VITESS team - S. Manoshin, K.Lieutenant and G. Zgismond for their permanent support.

[1]. F. Mezei, Z.Phyzik 255, 146, 1972.
[2]. R. Gähler, R. Golub, J. de Physique, C3-229, 45, 1984.
[3]. A. Ioffe, Physica B 335 (2003) 169; A. Ioffe, Nucl. Instrum. Meth. A529, 2004, p. 39.
[4]. Th.Keller et al. *Physica B*, 241-243 (1997) 101.
[5]. M.Th. Rekveldt, *Physica B*, 234-236 (1997) 1135; J.Major et al., *Physica B:*336,(2003), 8.
[6]. A. Ioffe, S. Manoshin. Nucl. Instrum. Meth. A529, 2004, p. 45.

The New Very Small Angle Neutron Scattering Instrument KWS-3

E. Kentzinger, A. Radulescu, J. Stellbrink, D. Richter and Th. Brückel
Institut für Festkörperforschung, Forschungszentrum Jülich

The newly built very small angle neutron scattering instrument KWS3 is the worldwide unique SANS instrument running on the focusing mirror principle. It allows performing scattering experiments with a wave vector transfer resolution between 10^{-4} and 10^{-3} Å^{-1}, bridging a gap between Bonse-Hart and pinhole cameras. This instrument will be transferred to FRMII, which should lead to an increase in wave vector transfer resolution by one order of magnitude and to an increase in flux by two orders of magnitude.

Ultra-small angle (U-SANS) and small angle neutron scattering (SANS) experiments are performed by two different types of instruments to cover a combined Q-range from ≈10^{-5}Å^{-1} up to ≈1Å^{-1}. Bonse-Hart cameras (Double Crystal diffractometers) are used for U-SANS experiments, whereas the "standard" SANS experiment is performed using a pinhole camera. In principle, the Q-range of both instrument classes overlaps. Typical U-SANS instruments like S18 (ILL), PCD (NIST) or DKD (FZJ) may reach maximum Q-vectors of ≈5x10^{-3}Å^{-1}. The disadvantage of these instruments is that they do not allow taking a full area image on a 2D position sensitive detector. On the other hand, the well-known pinhole instrument D11 at Institut Laue-Langevin (France) reaches a minimum Q-vector of 5x10^{-4} Å^{-1} by use of large wavelengths and sample-to-detector distances (≈40m). But the required instrumental setting pushes both types of instruments to its limits, mainly due to signal-to-noise level and the reduced flux at sample position.

Recently the use of neutron lenses as additional elements of a pinhole SANS instrument has been tested to overcome this intensity problem [1]. The design and concept of the KWS3 instrument at FZ Jülich (Germany) is even more advanced [2]. The principle of this instrument is a one-to-one image of an entrance aperture on a 2D position-sensitive detector by neutron reflection from a double-focusing elliptical mirror. To date, KWS-3 is the worldwide unique SANS instrument running on this principle. It permits to perform SANS studies with a scattering wave vector resolution between 10^{-4} and 10^{-3} Å^{-1} with considerable intensity advantages over conventional pinhole-SANS instruments. Therefore it perfectly bridges the "Q-gap" between U-SANS and SANS: Very Small Angle Scattering (V-SANS). The increasing need for these intermediate Q-vectors arises from the growing interest in biological and colloidal samples, which typically have characteristic length scales in the μm range. In this report we will give a short survey on the instrument concept and its actual realization and present some first results obtained from "real" samples. We will then detail the expected improvements related to the move of KWS-3 to FRMII.

A detailed description of the instrument has already been given in Ref. [2]. Figure 1 shows a sketch of the instrument. The main innovation and challenge in building this instrument was to build a large mirror having a shape as close as possible to an ellipsoid and with a surface roughness less than 5 Å (rms). The mirror is a 1.2 m long, 0.1 m wide and 0.05 m thick toroidal double focusing Zerodur mirror of 11 m focal length, and coated with 1000 Å ^{65}Cu and 100 Å Al as a protection layer. At such a short mirror length with respect to the focal length, the toroidal shape is a good enough approximation to an elliptical shape. The reflection plane has been chosen to be horizontal, reducing the deterioration of the image due to gravity. The entrance pinhole is at one focus of the mirror, the other focus is in the detection plane of a 2D position-sensitive detector. The contrast ratio of the image on the detector was determined to be 10^{-4}.

Very recently a new elliptical mirror, built using the replica technology [3] has been installed concentrically to the toroidal mirror (Fig. 1). First tests with neutrons were performed which indicate that further improvements of the setup are required.

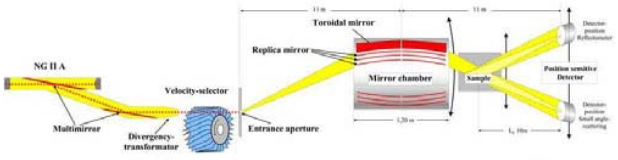


Figure 1 KWS3 experimental setup

At KWS3 the effect of multiple scattering requires special attention. An example of how this effect influences the evaluation of the geometrical and density parameters is presented in Figure 2. There the scattering patterns from a mixed solution of 1% PEB-7.5 random copolymer (M_W=30K) and 4% hexatriacontane paraffin in d-22 are shown for different sample thickness in polymer contrast. The inset of the figure shows the raw data together with the empty beam measurement. Comparison of the intensity in forward direction for the sample and empty beam provided a sample transmission of 10%, 20% and 70% in case of 2mm, 1mm and 0.2mm sample thickness, respectively. Multiple scattering is dominant in the case of the thickest sample while for the 0.2 mm sample thickness it is a minor contribution. Data analysis in terms of Beaucage model [4] revealed a significant variation of the power law behaviour and R_g with sample thickness. We can conclude that in order to have a reasonable sample transmission and to avoid

contribution from multiple scattering very thin samples are required. Recently we developed cells with large radius and variable thickness, covering the full cross section of the incoming beam. This allows to perform a systematic investigation of the multiple scattering effect as a function of cell thickness and thus to avoid misinterpretations. Another way to get the same result is to vary the sample contrast but, for certain samples, this is a much more difficult approach.

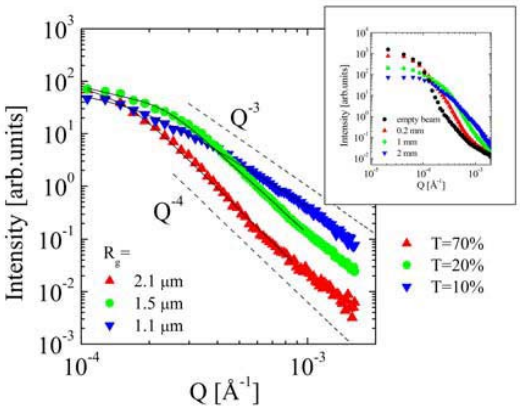


Figure 2 Scattering patterns from a mixed solution of 1% PEB-7.5 random copolymer (MW=30K) and 4% hexatriacontane paraffin in d-22 in polymer contrast. Results obtained for different sample thickness (as denoted by symbols explained within the inset together with the empty beam measurement) reveal how the multiple scattering influences the interpretation of the data.

We present in figure 3 the scattering pattern from a crystalline-amorphous poly(co-olefins) diblock copolymer in dilute solution over the whole Q range accessed by combining all three kinds of small-angle neutron scattering instruments in Jülich: The classical pin-hole instrument KWS2, the focusing-mirror KWS3 instrument and the double crystal diffractometer DKD [5]. The data allow a semi quantitative evaluation of structures of size scales between 10Å and 10 µm and reveal the multilevel morphology of copolymer aggregates, being consistent with the microscope observations (up-right inset of figure 4). By the aggregating *s*PP and amorphous P(E-*co*-P) blocks at small scale a 2-d structure seems to be formed (Q^{-2} power law at larger Q). This structure evolves at intermediate scale into a rod-like structure (Q^{-1} power law at intermediate Q). The rods associate in bundles and the correlation effects between them result in the "shoulder"-like structure at around $Q^* \cong 3.5\text{-}4x10^{-3}$ Å^{-1} (bottom-left inset of figure 3). At much larger scale (micrometer order) the rod bundles form network-like structures with mass fractal aspects (Q^{-3} power law) which associate in very large aggregates resembling snowflakes. The sharp intensity drop at around $7x10^{-5}$ Å^{-1} may reveal an additional contribution from the correlations between lateral branches of these aggregates over a characteristic length of about 10 µm.

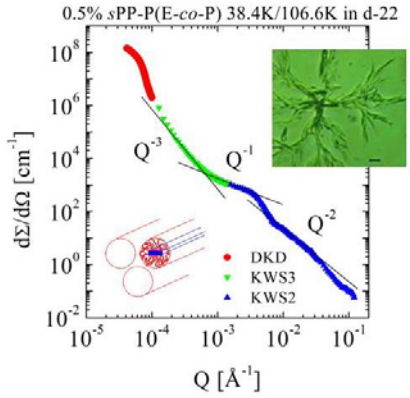


Figure 3 Scattering from a crystalline-amorphous diblock copolymer [4]. The lines indicate power law behaviour in different Q ranges. KWS2: conventional pinhole SANS; KWS3: VSANS; DKD: Double Crystal diffractometer ("U-SANS").

In 2006, KWS3 will be transferred to the new FRMII reactor. A special cold neutron guide will be built, permitting an access to larger wavelengths, leading to an increase in the range of Q-resolutions down to 10^{-5}Å^{-1}. Also, this transfer will result in an increase of the neutron flux at sample position by two orders of magnitudes, permitting the use of small material amounts, which is often the case with biological substances. This dramatic increase in flux will permit to optimally use the reflectometry mode of KWS-3. In this mode, performing SANS on thin film systems under grazing incidence (GISANS) will permit the access to in-plane correlation lengths around the µm, a length scale hardly accessible to off-specular scattering at a reflectometer or to GISANS at a pinhole camera. Also, the implementation of polarized neutrons and a polarization analysis covering the whole detector area will permit the investigation of magnetic correlations.

[1] M.R. Eskilden et al., Nature, **391**, 563, 2000; S.-M. Choi et al., J. Appl. Cryst., **33**, 793 (2000)

[2] B. Alefeld et al., Physica B, **283** 330 (2000), E. Kentzinger et al., Physica B **350** e779–e781 (2004)

[3] http://wave.xray.mpe.mpg.de/rosat/

[4] G. Beaucage and D.W. Schaefer, J.Non-Cryst.Solids 172-**174**, 797 (1994)

[5] A. Radulescu et al., Neutron News, **16-2**, 18 (2005)

High resolution neutron spin-echo spectroscopy facilities of JCNS: status of NSE at FRMII and the new NSE instrument at the SNS, ORNL

M. Ohl [1], O. Holderer [1] , R. Schaetzler [1], T. Kozielewski [1], M. Monkenbusch [1], M. Butzek [2], U. Giessen [2] , Ch. Tiemann[2], R. Achten[2], B. Laatsch[2] , W. Westerhausen [2], H. Kleines [3], M. Drochner [3], P. Suxdorf [3]

[1] *Institut für Neutronenstreuung*
[2] *ZAT, FZ-Jülich*
[3] *ZEL, FZ- Jülich*

Two ultra-high resolution spectrometers will be operated by the Jülich centre of neutron science JCNS. One at the FRMII reactor and the other at the new MW-spallation source SNS in Oak Ridge. The FRMII instrument emerges from the FRJ2-NSE. Fourier times beyond 200ns will be accessible at 13 Å wavelength. Also under construction is a "best-of-class" NSE instrument to be located at the MW spallation source in Oak Ridge. Using superconducting precession coils it shall cover the time range from 1ps to 1μs. A major development issue for both instruments is the development of a new generation of field integral correction elements necessary to achieve a sufficient resolution the high Fourier times.

The two neutron-spin echo spectrometers, the enhanced FRJ2-NSE that is currently being prepared to move to the FRMII in Munich and the newly build SNS-NSE spectrometer will supply the neutron user community with facilities of ultra high resolution spectroscopy. In terms of Fourier times (of the intermediate scattering function S(Q,t)) this means that the FRMII instrument will go beyond 200 ns and the "best-of-class" SNS-NSE will reach 1000 ns. Expressed as energy resolution this may be translated to resolutions of 3.5 respectively 0.7 neV. Utilizing a large available wavelength range a dynamical range of $1{:}10^5$ or $1{:}10^6$ respectively can be realized. The FRMII spectrometer shall become operational at the end of 2006. The SNS-NSE is planned for 2008. Besides the direct execution of NSE experiments the SNS installation will also serve as gateway to other neutron instruments (in particular backscattering and diffractometer) at this new and most powerful spallation source.

Technical improvements to be mentioned for the moving FRJ2-NSE consist of a modernization of the control electronics that is designed according to the Jülich-Munich standard based on the TACO experiment control. New mainly bipolar current sources replace the previous system to improve reliability and accuracy. Software and electronics layout work for the FRMII installation are also the template for the SNS spectrometer. Computer controllable mechanical adjustment stages have been developed for the positioning of the 3 radial field integral correction elements inside each of the two main solenoids. A nonmagnetic sample stage lift has bee build that enables a 2-3 position vertical sample change to be performed by the control program.

A bend guide with polarizing FeSi-multilayer including guide magnetic field and Ni^{58} guide until the velocity selector position has already been installed by the FRMII department at their NL2. To achieve sufficient polarization at longer wavelength also an additional FeSi-polarizer at the entrance of the proper NSE spectrometer is foreseen. The special floor (Tanzboden) for the air cushions is currently being laid.

The SNS spectrometer is just moving from the pure design phase to the construction phase. A SNS beam line BL16 has been assigned and the instrument concept has been approved by the SNS. A number of beam transport and preparation devices have been ordered or are constructed at the FZJ. The neutron guide system, polarizing benders and choppers have been ordered. The parts of the secondary (the proper) spectrometer including a novel magnetic shielding enclosure are in the process of waiting for bids. Development of nonmagnetic, computer adjustable high precision mounting platforms (Hexapods) for the correction elements has been completed by the manufacturer.

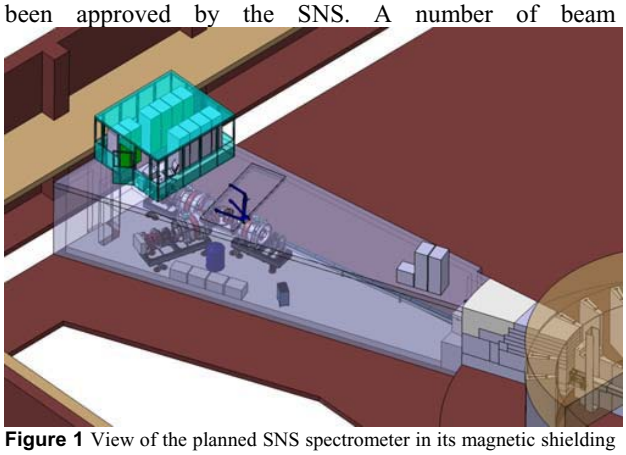


Figure 1 View of the planned SNS spectrometer in its magnetic shielding enclosure, which also serves as radiation shield. The moderator distance of the instrument can be changed by inserting optional neutron guide pieces. Shown is the outermost position which offers the highest possible scattering angle but also the smallest wavelength frame. A better neutron usage is achieved in the close position (the source/moderator is close to the bottom right edge of the picture).

The key technology needed to extend the NSE instrument resolution to the desired high Fourier times and keeping at the same time reasonably large solid angle for sample illumination and –in particular– scattered neutron detection consist in design and manufacturing of the field integral homogenizing correction elements. The problem consist in realization of a radial current density distribution that follows a given radial function j(r) up to a high degree of

accuracy. At the outer radius the needed current density may reach 150A/mm and more. Which for the largest element this means that up to 800W dissipated heat must be removed such that the element stays at temperatures not higher than 60^0C. Since the elements have to be placed into the beam path they must be transparent to neutrons. Whereas the biggest challenge is placed by the correction coils for the SNS spectrometer also the FRMII installation will benefit from the recent and coming improvements. The correction coil development has been supported by the TECHNI program and now by its successor in the EU NMI3 initiative.

After a model calculation which includes the full magnetic field of the "ideal" current density distribution of the chosen design proved that there are no principal physical effects that limit the correction efficiency a manufacturing scheme that enables the maintaining of the high mechanical accuracy of the numerically controlled machines up to the final stage has been devolved and tested. This scheme employing an Al-ground plate that is attached in two steps also enables effective heat extraction via heat conduction in the back plate, see fig 2.

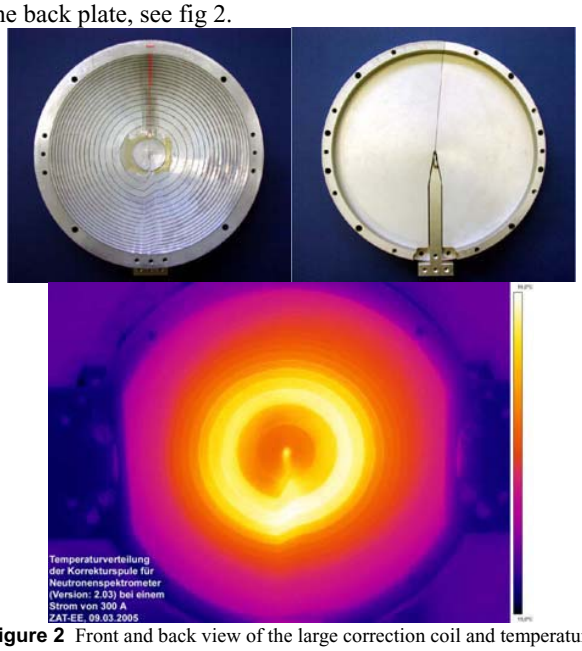


Figure 2 Front and back view of the large correction coil and temperature distribution on the front side with water cooling at the periphery at an operation current corresponding to 1µs Fourier time at the SNS spectrometer. The highest temperature is 55^0C. The active diameter is 20cm.

To assess the function a full set of 3 pairs of correction coils with active diameters 10cm, 15cm and 20cm were computationally optimized to the parameters of the FRJ2-NSE which served in its last operation cycle before the move to Munich as test bed for these novel correctors. We still had not yet (a posterior) mechanical adjustments such that these degrees of freedom had to be approximately be taken into account by "current shifters" that belonged to the original installation of the spectrometer. After appropriate adjustments which corroborated the computed correction coil currents within 1-2% and optimizing the shifters the measurement range could be extended from 22ns to 40ns at λ =8Å (see fig. 3).

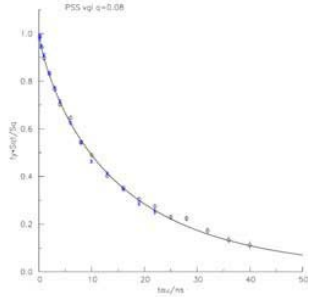


Figure 3 NSE Relaxation curve of a polymer solution in toluene, data extend up to 40ns.

However, phase maps over the large element close to the detector reveal the points that have to be addressed in a next step in order to achieve optimum performance. Figure 4 left side shows the variation of the echo-phase over the detector area (maps the cross section of the correction element) which is a measure for the field integral. The right side of the figure displays the resolution.

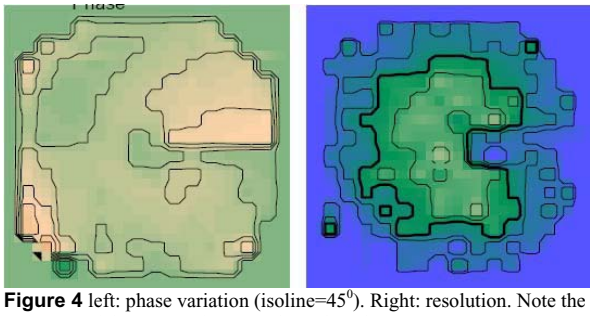


Figure 4 left: phase variation (isoline=45^0). Right: resolution. Note the influence of the current finger at the right side!

The results indicate that 1. the influence of the current finger becomes disturbing at higher Fourier times but is locally restricted and 2. despite the very flat phase map the resolution is unexpectedly low. The latter effect has then been identified to be a consequence of the finite width of the cuts between concentric zones. This could be corroborated computationally and led to a modified cutting scheme that should remove the effect. The other consequence is that measures have to be devised to reduce the influence of the finger, i.e. reduction of the current by more cuts (now possible using the improved cutting scheme) and distributing the correction onto a "stack" of more than one coil.

Acknowledgement: Part of the correction coil development has been supported by the European Commission under the 6th Framework Programme through the Key Action: Strengthening the European Research Area, Research Infrastructures. Contract no: HII3-CT-2003-505925.

Commissioning of the Backscattering Spectrometer SPHERES

Peter Rottländer, Joachim Wuttke, and Wilhelm Bünten
Jülich Center for Neutron Science, FRM–II, 85747 Garching
and
Institut für Festkörperforschung, FZ Jülich, 52425 Jülich

Michael Prager and Dieter Richter
Institut für Festkörperforschung, FZ Jülich, 52425 Jülich

Hans Kämmerling and Heidi Straatmann
Zentralabteilung Technologie, FZ Jülich, 52425 Jülich

Matthias Drochner, Franz-Josef Kayser, Harald Kleines, and Frank Suxdorf
Zentralinstitut für Elektronik, FZ Jülich, 52425 Jülich

The backscattering spectrometer SPHERES (SPectrometer with High Energy RESolution) was initiated by the IFF (Institut für Festkörperforschung) as part of the starting instrumentation of FRM-II (original project name: RSSM) It is now the first instrument at the Garching site of the JCNS (Jülich Centre for Neutron Science).

In the course of the year 2005, all major components were assembled, and commissioning of the instrument started. Figure 1 shows the gas-tight instrument housing. Inside, the walls are covered with polyethylene and cadmium shielding.

Neutrons reach the instrument through a convergent guide that turned out to require additional shielding. Between the primary neutron guide NL6 and the instrument-specific convergent neutron guide, we have a temporary beam shutter and selector assembly which shall be improved in summer 2006 when another instrument will be inserted upstream in NL6.

A gold foil activation analysis has shown an integral neutron intensity of about $1 \cdot 10^{10}$ neutrons per second at the end of the convergent neutron guide, just in front of the chopper. The spatial distribution is reasonably homogeneous; the flux density is $1.8 \cdot 10^9/s/\mathrm{cm}^2$.



FIG. 1: The instrument housing.



FIG. 2: The chopper wheel.

A central component of the spectrometer is the phase-space transformation (PST) chopper. The incoming beam is deflected by rapidly moving pyrolytic graphite (PG) crystals with high mosaicity. This leads to a reduction of the energy spread of the incoming neutrons, on the expense of an increase in angular spread (transformation "from white to wide"). The PG crystals, however, cover only half of the circumference of the chopper wheel, the other half being transparent. Thereby, the PST chopper also provides a time-of-flight discrimination against neutrons that are scattered directly from the sample into the detectors without passing through the analyzers.

The speed requirement of 300 m/s for the PG crystals, and the time-of-flight considerations for the entire instrument led to the conception of a PST chopper with a diameter of 1.2 m and a rotation frequency of 4800 rpm. This is a considerable technological challenge. A carbon fiber wheel failed the tests. We had to give up the idea of a magnetic bearing because of unsolved resonance problems. By now, we use an alumold wheel (Fig. 2) with conventional bearings. For a short time, it is pos-

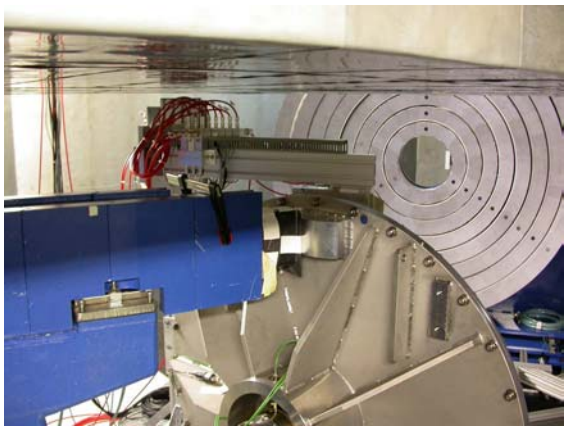


FIG. 3: Inside the instrument housing. On top, cadmium shielding of the ceiling. On the left, in blue: lead shielding of the neutron guide. On the bottom: chopper housing. Above the chopper: a horizontal arm which bears the small-angle detectors. In the rear, ring-shaped: small-angle crystal analyzers.

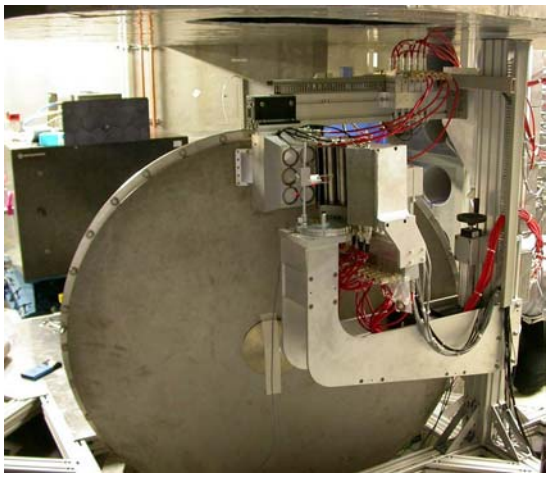


FIG. 4: View from the opposite side. In the middle: sample position, with a laser and a mirror used for optical alignement of monochromator and analyzer crystals. Close to the sample are the detectors. In the rear: the crystal monochromator, mounted on a Doppler drive, on top of a granite block.

sible to operate the wheel at nominal speed. After some hours, however, resonances build up and cause an emergency braking. Therefore, for the time being we operate the PST chopper with one-third of the ideal speed (1600 rmp). This is the only solution that is compatible with the time-of-flight kinematics; it will yield an intensity increase by a factor of two instead of four. In the long term, we will need to replace the chopper wheel by a newly designed one.

Energy scans are performed via Doppler shift in backscattering from moving monochromator crystals. The Doppler drive has now been successfully tested over

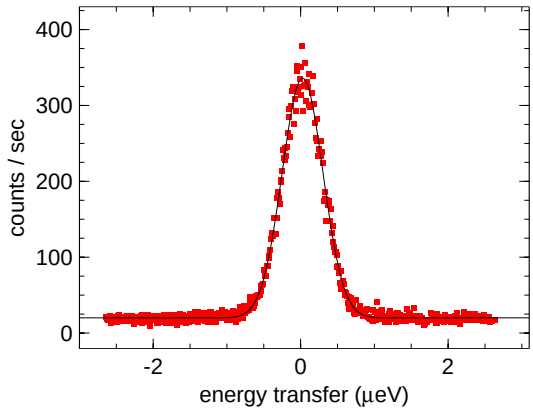


FIG. 5: A resolution scan, measured on a 1.2 mm thick polypropylene sample. Average over all large-angle detectors. Measuring time about 4 minutes. The fitted Gaussian yields a FWHM of 0.65 μeV.

some 20 days of operation; vibrations were minimal even at the maximum velocity amplitude of 4.7 m/s. All components being installed, the entire spectrometer was optically aligned to about a tenth of a degree with help of a laser beam and mirrors.

Wiring of the instrument and installation of media supply has been partly done and will be completed in 2006, together with the installation of the remaining parts of the safety instrumentation and other components. The detector banks are installed, wired, and connected with the data acquisition electronics. Figures 3 and 4 show main components of the instrument before the flight path between chopper and monochromator was encapsulated with boron rubber shielding.

The kernel of the data acquisition software has been written. During each period of the Doppler drive, detector counts are written into a buffer. After each period, a sine is fitted to the Doppler position log. Then, for each buffered time frame, the Doppler velocity is calculated, taking into account the time lag due to neutron flight paths, and the corresponding energy bins are incremented by the buffered detector counts. Figure 5 shows the best resolution scan measured so far. The full width at half maximum is 0.65 μeV.

The γ radiation outside the instrument housing is currently of the order of 4–5 μSv/h, with local peaks of about 15 μSv/h. To fulfill the FRM-II requirement of less than 3 μSv/h just outside the housing, considerable amounts of lead will have to be assembled around the chopper. Along with improving the γ shielding, we strive for reducing the neutron background in the scattering signal.

Neutron Scattering with Vector Polarisation Analysis on $U_{14}Au_{51}$

Werner Schweika,[1] S. Easton,[1,2] and K.-U. Neumann[2]

[1] *Institut für Festkörperforschung, Forschungszentrum Jülich, D-52425 Jülich, Germany*
[2] *Loughborough University, Great Britain*

(Dated: January 19, 2006)

We have developed a new technique of vector polarisation analysis for neutron scattering experiments using an initially precessing neutron polarisation.[1] Different to existing zero-field techniques this method has a much larger potential for applications, since it can be used also on multi-detector and time-of-flight instruments, typical instruments at the new neutron spallation sources. We compare results on the complex magnetic structure of $U_{14}Au_{51}$, with previous findings.[2]

In addition to nuclear coherent scattering, one distinguishes two further scattering cross-sections that are related to the spin properties of the neutron probe. First, the scattering amplitude depends on the spins of the nuclei in a sample, which leads to the so-called spin-incoherent scattering and hydrogen serves as a well-known important example. Second, the neutron's magnetic moment is an ideal probe to study magnetic structures and excitations in condensed matter physics.

Using polarised neutrons and polarisation analysis one can separate experimentally all three distinct contributions. The simplest version of polarisation analysis has an important potential for studies of soft matter.[3] The ability to discern spin-flip (sf) scattering from non-spin flip (nsf) scattering, independent of the direction of the polarisation of the incident beam, allows one to separate coherent from incoherent scattering, *i. e.* to separate self- and pair-correlation functions.

The directional dependence of sf and nsf scattering is of interest for studies of magnetic structures and correlations. In general, scattering cross-sections for magnetic scattering depend on the direction of the polarisation of the incident neutron beam with respect to (i) the scattering vector **Q** and (ii) the direction of the magnetic moments in the sample. Two simple rules can be established: First, only the component of the magnetic moments which is perpendicular to **Q** contributes to scattering of neutrons. Second, the component of the initial neutron polarization, which is perpendicular to the magnetic moments in the sample, changes sign upon scattering. The most common and conventional approach is based on the classical work of Moon, Riste and Koehler[4], where one applies a guide field to turn the polarisation parallel and perpendicular to **Q** for the measurements. This will enable to separate and to analyse the magnetic scattering for many cases: in general this applies for paramagnetic samples, and in case of ordered magnetic structures with collinear spins.

There are many interesting materials, for instance multi-ferroics, with complex magnetic structures which cannot be unambiguously examined by such a conventional technique of polarisation analysis. Another topic is in in the field of highly correlated electrons with unresolved questions concerning possible static and dynamic spin-lattice couplings; these may cause unique non-trivial rotations of the neutron polarisation upon scattering. For solving all these problems it is of high interest to unravel all possible arbitrary rotations of the neutron polarisation.

All previously existing methods for vector polarisation analysis need a zero magnetic field around the sample. The principle to prepare an incident polarisation and measure an arbitrary rotated final polarisation can be realised only for a single specific momentum and energy transfer.

Our method is based on the idea to include and work with precessing neutron polarisation as known from spin-echo techniques.

In the conventional set-up of the DNS instrument at the Jülich research reactor, see Fig. 1, the monochromatic beam will be polarised by the initial polariser, (optionally for inelastic studies the beam will be chopped), then the neutron polarisation may be switched with respect to the guide field by a pi-rotation inside the flipper coil, next the polarisation will enter the field around the sample that can turn the polarisation in x,y,z (or any) direction.

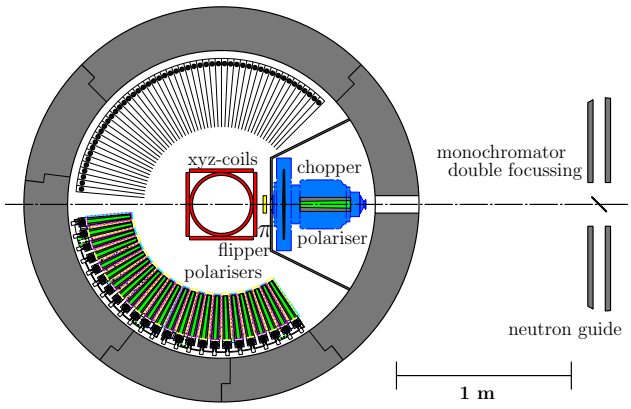


FIG. 1: Scheme of the DNS instrument.

This allows one to measure sf or nsf scattering for all directions, *i. e.* the trace of the polarisation matrix of the initial and final polarisation vector. For polarisation

changes other than 0 oder 180 degrees, which contribute to off-diagonal elements of the polarisation matrix, the final polarisation will start to precess in the applied field and appear as a reduced polarisation in the analyser system.

Instead of attempting to realign the precessing scattered neutrons to determine the changes by the sample, thinking of time reversal gives us an elegant key to a simple solution: We may start with an precessing polarisation in the initial path and we may tune the precession angle for a desired polarisation at the sample. Scattering with polarisation changes from a precessing into a non-precessing state will provide us with the off-diagonal elements of the polarisation matrix.

Surprisingly, we do not need any additional sophisticated equipment for full vector polarisation analysis. We only need to induce a $\pi/2$ rotation (instead of 0 or π) by the flipper and to control the precessing phase by a variation of the applied magnetic field.

Previous vector polarisation studies (polarimetry) on $U_{14}Au_{51}$ using the Cryopad device at the ILL revealed a complex chiral magnetic structure, a so-called q=0 structure, for which AF-magnetic Bragg peaks coincide with nuclear structural Bragg peaks.[5] As an example a measured polarisation stereogram for the (201) peak is shown.

We repeated the experiment on DNS with the new precession technique for VPA. Part of the results are shown in Fig. 3, for the (201) Bragg peak. The crystal is oriented with its b-axis parallel to the vertical z-axis. The spins are ordered within the a-b plane with a hexagonal star-like structure. The nuclear scattering is confirmed by a measurement above the Neel temperature at 30K and remains independent of the polarisation. At lower temperatures two oscillating curves are measured by turning the flipper in $+\pi/2$ and $-\pi/2$ mode. Maxima are found for a rotation of the polarisation from the z to the y direction. For an initial polarisation along x (which is set parallel to the scattering vector) only spin-flip scattering is observed for the magnetic scattering, excluding a rotation to y or z. For all cases, and taking nuclear scattering into account, an effective depolarisation is observed. These results are in excellent agreement with the pol-figures 6b of Ref.5.

In principle this new precession technique is possible on any neutron scattering instrument which allows for conventional polarisation analysis a la Moon, Riste and Koehler[4]. Different to existing zero-field techniques this method has a unique property which gives a much larger potential for applications, since it can be used also on multi-detector and time-of-flight instruments, typical instruments at the new neutron spallation sources.

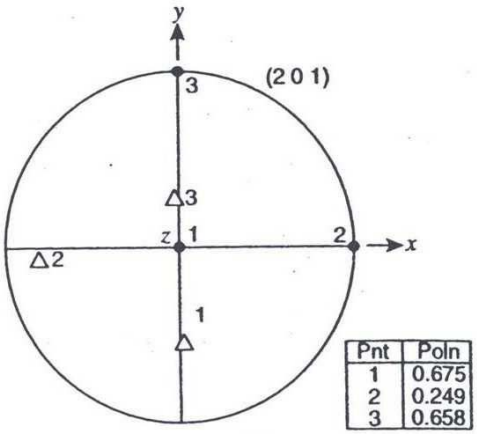


FIG. 2: Stereogram for (201) of $U_{14}Au_{51}$ at 15 K. Full (open) symbols indicate the direction of initial (final) polarisation taken from Brown *et al.*[5]

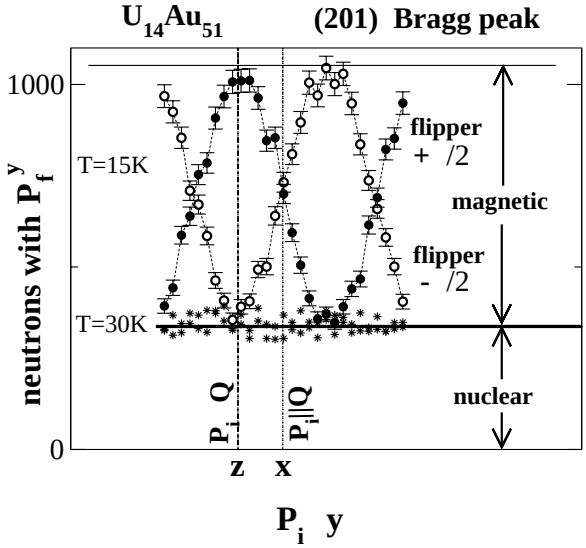


FIG. 3: Vector polarisation analysis on the (201) Bragg peak of $U_{14}Au_{51}$. Initially the polarisation is perpendicular to the applied field in y-direction. At lower temperatures, T=15K, there is an additional magnetic contribution for which the neutron polarisation changes from P_i ‖z to P_f ‖y. At 30K there is only a nuclear Bragg component which continues to precess after the scattering event.

[1] W. Schweika, Physica B **335** (1-4), pp.157-163 (2003).
[2] W. Schweika, S. Easton, K.-U. Neumann, Neutron News **16** (2), 14-17 (2005).
[3] A. Narros, A. Arbe, F. Alvarez, J. Colmenero, R. Zorn, W. Schweika, D. Richter Macromolecules **38**, 9847 (2005).
[4] R.M. Moon, T. Riste, W.C. Koehler, Phys. Rev. **181**, 920 (1969).
[5] P. J. Brown et al. J. Phys.: Cond. Matter 1997.

Twin Diffractometer (SV7)



Instrument Parameters

Monochromators ***- standard:*** ***- optional:***	 Ni (220), PG (002) Ni (200), Cu (111), Pb (311), Ge (111)/(311)
Monochromator angles:	52° and 40°
Wavelengths:	1.0 Å $\leq \lambda \leq$ 2.3 Å
Collimators ***- primary beam:*** ***- scattered beam (optional):***	 Soller: 12 min radially oscillating
Max. beam size:	25 × 40 mm^2
Mean sample volume (cylinder):	10 mm ∅, 30 mm high
Scattering region:	$0° \leq 2\Theta \leq 90°$
Detectors:	linear JULIOS units
Max. neutron flux at sample:	10^6 n/cm^2 s
d-spacings:	0.7 Å $\leq d \leq$ 35 Å
Mean resolution Δd/d:	10^{-2}
Sample environment:	Closed cycle He-cryostat: 4 ... 293 K; He-bath cryostat: 1.5 ... 4.2 K; He-3 cryostat: 0.3 ... 293 K; Split coil magnet cryostat: 0 ... 7 T, 4 … 293 K; cryofurnace 4 ... 400 K; Full circle goniometer with external ω-rotation: 293 K; Flow cryostat containing full circle goniometer: 4 ... 293 K

Instrument Responsible

Dr. Jens Walter	Tel. +49-(0)2461-61-6024	Email: j.walter@fz-juelich.de
Rolf Skowronek	Tel. +49-(0)2461-61-3639	Email: r.skowronek@fz-juelich.de

Institut für Festkörperforschung
Forschungszentrum Jülich GmbH
D-52425 Jülich

Experimental Report
of Neutron Scattering Experiments
at the FRJ-2 Reactor

Proposal number:	SV7-04-001		
Experiment title:	**Texture analysis of antique Dutch tin spoons from Amsterdam: 1350-1750 AD**		
Dates of experiment:	30.01.05-03.02.05 03.03.05-04.03.05	Date of report:	14.06.2006
Experimental team: Names	Addresses		
Visser, Dirk Hallebeek, Peter Kockelmann, Winfried Veerkamp, Jorgen	Department of Physics, University of Warwick, Gibbet Hill Road, Coventry CV4 7 AL, UK and NWO-Physics, ISIS Facility, RAL, Chilton, Didcot OX11 0QX, UK Netherlands Institut for cultural Heritage (ICN) Gabriel Metsustraat 8, Postbus 76709 1070 KA Amsterdam, NL Mineralogisch-Petrologisches Institut , Universität Bonn, Poppelsdorfer Schloss, D-53115 Bonn Archeology Amsterdam, Noordermarkt 45, 1015NA Amsterdam, NL.		
Local Contact:	J. M. Walter		

Experimental report text body

Introduction

The Department of Archeology of Amsterdam has a collection of 861 tin spoons of which the earliest examples are dated around 1350 and the last ones around 1750. At this time the production of tin spoons in Amsterdam ceased. In order to make tin (Sn) usefull for appliances, it has to be alloyed with another material to make it harder. Often used alloying metals are lead (Pb) or copper (Cu). At that time it was already known that a too high percentage of Pb caused a public health hazard. A safe percentage should not be higher than 10%. It is known that in the early period one often did not adhere to this rule due to the fact that lead was much cheaper than tin. After 1530, the production of tin spoons in Amsterdam was regulated and overseen by the Guild. Also other alloying metals were used, e.g. Cu or even Cd. The amount of Cu in Sn should be determined by its solubility, in general only a few percent. However, objects have been found with much higher Cu-concentrations, up to 20% (15th century Coventry [1]). The alloying with Pb shows, however, a much larger distribution.

Measurements and Results

Apart from the main phase composition of the spoons, obtained on ROTAX, we obtained more information on the production methods provided by texture analysis. Complementary to measurements on ROTAX, where we could obtain semi-quantitative texture information on some of the spoons, we in these measurements confirm these results and obtained more quantitative information on the crystallographic orientation distributions of more objects. We conducted texture measurements of fourteen spoons, distinguishing between different parts of the spoons as some of the spoons have also an iron core in the handle. Additionally production methods may vary for different parts of the spoons. For all the spoons we related the existing metallurgy data of the objects. Due to the form anisotropy of the spoons, it was not possible to measure complete pole figures of the spoons,

which would in this case also show form texture. Therefore only distinct φ-rotations in certain χ-tilts were selected for the measurements. From the resulting cascading diffraction patterns as a function of the orientation, it is possible to obtain qualitatively by the comparison of the different peak heights, whether the spoon was casted in a mould from molten material or worked by mechanical force. Spoon parts that were casted in a mould show only distinct singular peak heights of single crystallites (see Fig. 1), whereas mechanically worked spoon parts show a classical bulk texture distribution, which varies in a wavy distribution depending on the measured angle (see Fig. 2).

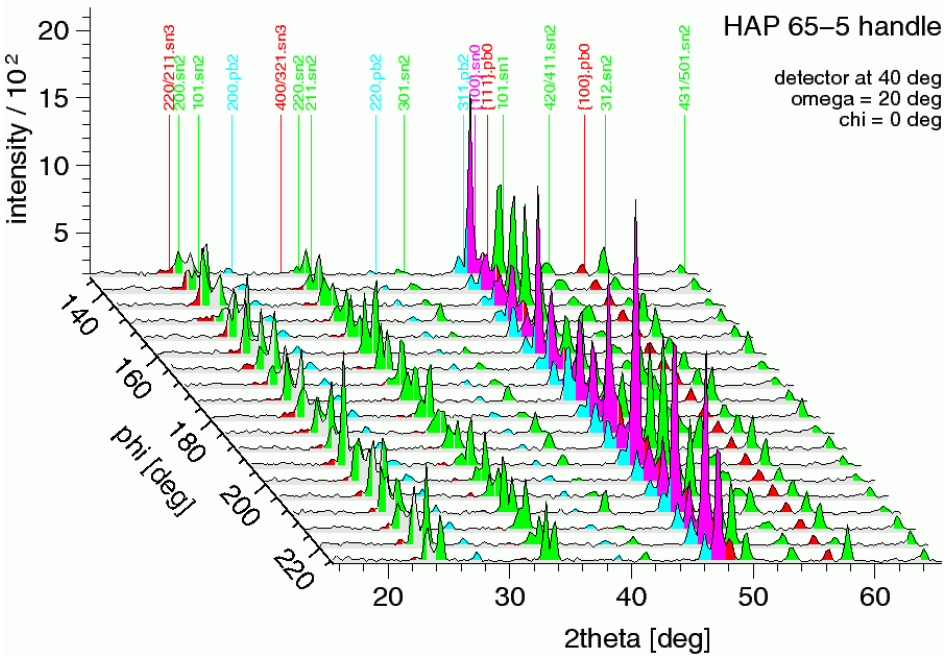


Fig.1: Casted spoon handle shows single crystals not in preferred orientation

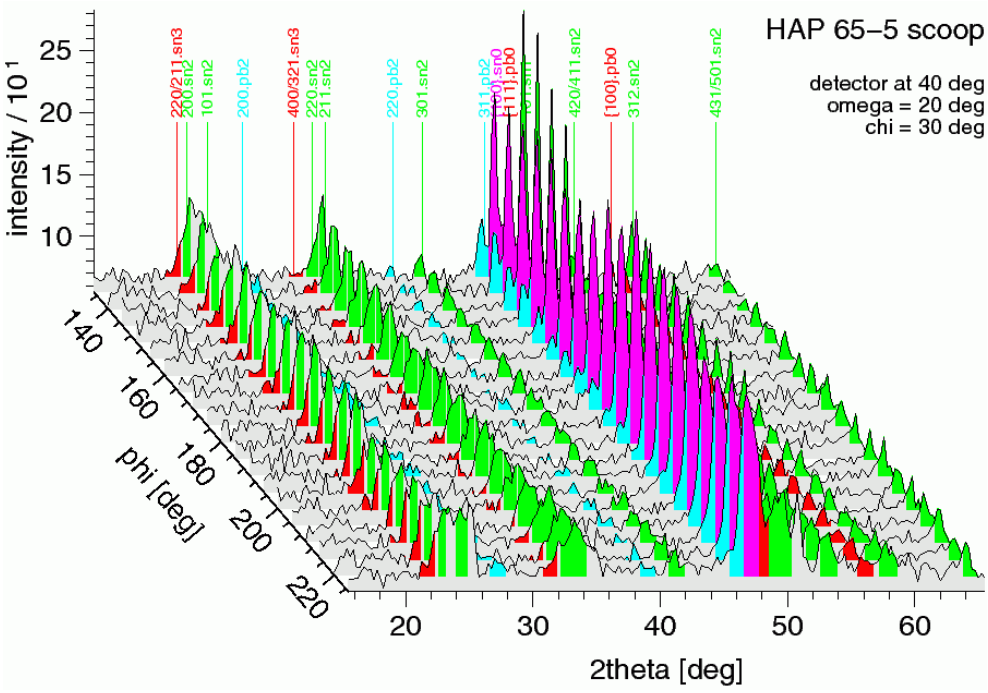


Fig. 2: Mechanically worked spoon scoop shows crystallographic preferred orientation

Institut für Festkörperforschung
Forschungszentrum Jülich GmbH
D-52425 Jülich

Experimental Report
of Neutron Scattering Experiments
at the FRJ-2 Reactor

Proposal number:	SV7-04-007		
Experiment title:	**Neutron diffraction studies of magnetic transitions in $TmNi_4Al$ - continuation**		
Dates of experiment:	2005	Date of report:	23.03.2006
Experimental team: Names	Addresses		
T. Toliński, A. Kowalczyk	Institute of Molecular Physics Polish Academy of Sciences Smoluchowskiego 17 60-179 Poznań, Poland		
A. Hoser R. Skowronek	Institut fuer Krystallography, Aachen MIN/ZFR (Univ. of Bonn)		
Local Contact:	Dr. A. Hoser		

Experimental report text body

The RNi_4Al compounds (R = rare earth or Y) crystallize in the hexagonal $CaCu_5$-type of structure (Fig. 1), point group *P6/mmm*. Ce occupies the 1a site (0,0,0) and Ni(1) the 2c site (1/3,2/3,0). Ni(2) and Al are statistically distributed over the 3g site (1/2,0,1/2) [1].

In the year 2005 we performed the second part of the measurements on the $TmNi_4Al$ compound using the SV7 instrument. The polycrystalline $TmNi_4Al$ compounds were synthesized by induction melting under an argon atmosphere. As the ingot a stoichiometric amounts of the constituent elements were used. The neutron wavelength was equal to 1.096 Å. The sample was contained in a cylindrical vanadium can mounted (1) in a refrigerator cryostat and (2) in a cryomagnet with external magnetic fields up to 5 T perpendicular to the horizontal diffraction plane. The magnetometric measurements were performed using a MagLab 2000 System (Oxford Instruments Ltd.).

Magnetometric measurements for $TmNi_4Al$ have shown a double peak in the ac magnetic susceptibility at 5.8 K and 2.8 K (Fig. 2), contrary to the other RNi_4Al members (R = rare earth) showing a single phase transition. The first part of the neutron diffraction experiments revealed only an increase of the low angle peaks' intensities between 4.2 K and 1.8 K. Therefore, the two peaks in the ac susceptibility may be due to a switch between two different slightly non-collinear orders of the magnetic moments. Tm and its alloys are known to create non-collinear magnetic phases, therefore this same can be expected in the case of $TmNi_4Al$.

The second part of the neutron diffraction experiment have shown that, alternatively, the two peaks in the ac magnetic susceptibility may be due to a small distortion of the crystallographic structure. The latter possibility results from the observed broadening of the diffraction peaks (Fig. 3). Besides, the effect of the magnetic field has been studied in more details. It appears that numerous reflections disappear after application of the magnetic field - this behavior is still not fully explained.

The analysis of the magnetic structure shows the magnetic moments ordering in the ***c*** – direction, whereas in the case of RNi_4Al for R = Nd, Tb, and Dy the magnetic moments have ordered within the hexagonal plane [1-3]. It can be explained by the crystalline electric field (CEF) effect and the change of the sign of the related second order Stevens factor [4].

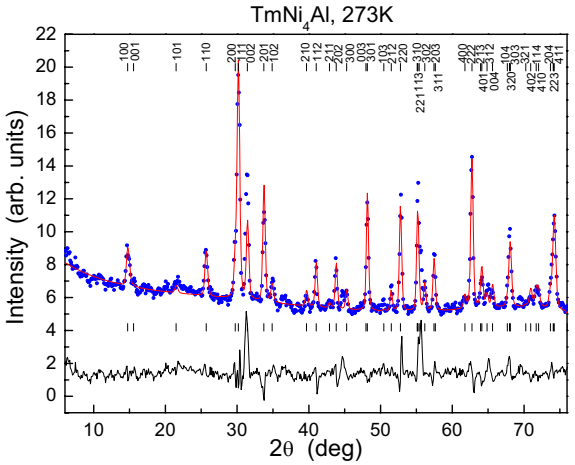


Fig. 1. The neutron diffraction pattern at 273K refined by FULLPROF assuming the $CaCu_5$ - type of structure.

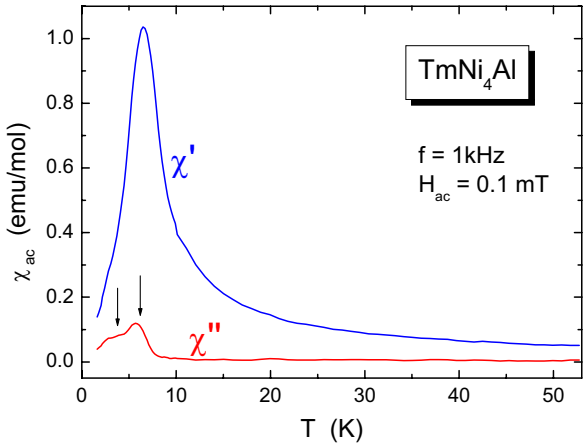


Fig. 2. Magnetic ac susceptibility showing two peaks in the absorption component.

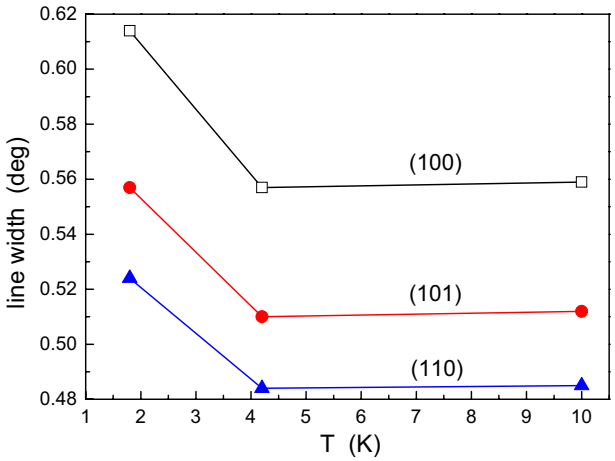


Fig. 3. Temperature dependence of the linewidth for the low angle reflections. The broadening below 4 K is clearly visible.

References:

[1] T. Toliński, W. Schäfer, W. Kockelmann, A. Kowalczyk and A. Hoser, Phys. Rev. B **68**, 144403 (2003).
[2] T. Toliński, W. Schäfer, G. Chełkowska, W. Kockelmann, A. Hoser, B. Andrzejewski, A. Szlaferek, A. Kowalczyk, Mol. Phys. Rep. **38**, 134 (2003).
[3] T. Toliński, W. Schäfer, A. Kowalczyk, B. Andrzejewski, A. Hoser, A. Szlaferek, J. Alloys Compd. 385, 28 (2004).
[4] submitted to phys. stat. sol. (b).

Institut für Festkörperforschung
Forschungszentrum Jülich GmbH
D-52425 Jülich

Experimental Report
of Neutron Scattering Experiments
at the FRJ-2 Reactor

Proposal number:	SV7-04-013		
Experiment title:	**Study of the stress on 16NiCrMo quenched steel**		
Dates of experiment:	28.01.2005-1.02.2005	Date of report:	15.02.2006
Experimental team: Names	Addresses		
Salvatore Magazù	Dipartimento di Fisica Universita' di Messina C.da Papardo Sperone S. Agata 98166 Messina Italy phone: 0039-090-6765025 fax: 0039-090-395004		
Local Contact:	Dr. Jens M. Walter		

Experimental report text body

Turning is one of the most employed processing technologies for mechanical components production. Continuous efforts of the manufacturers have always been oriented on the study and research of cutting tools production to allow a higher costs-saving preserving product quality. In these last years the research has been involved on the development of stronger tool materials, able to resist to the thermo-mechanical stresses that are present during machining, with the aim to increase the tool-life. The new design of the tool corner radius has allowed preserving the same product quality due to the "wiper effect" generated during the cut.

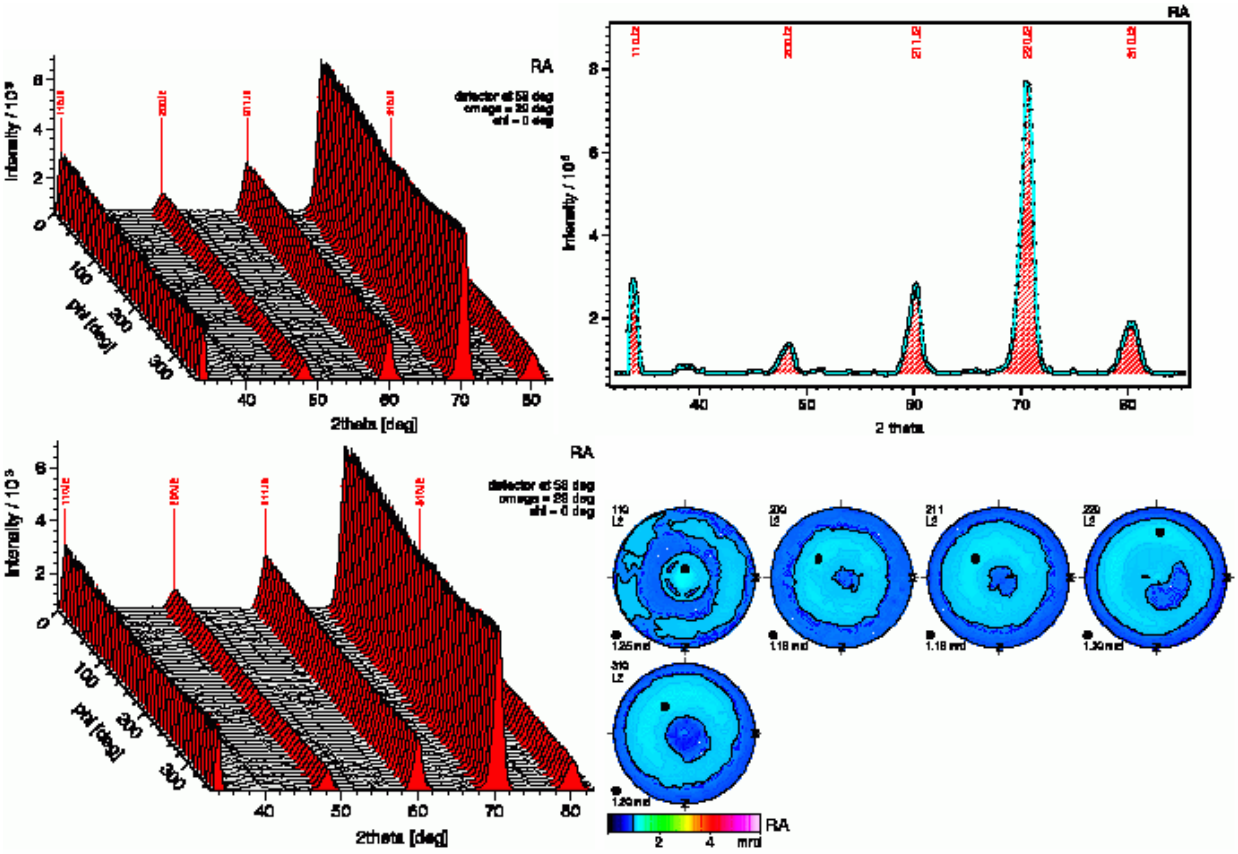
In recent times different tools that can exploit the wiper effect have been produced. They allow substantial productivity improvements or, which is the same, to reduce the time of cut and then to reduce production costs. In particular, if the feed can be increased to double, the cutting time is halved and almost twice as many components are made in the same time maintaining the same surface finish. Otherwise by employing the same feed rate it is possible to achieve excellent surface finish and eliminate, in such cases, the grinding operation.

With the aim to verify the possibility to realize good finishing on hardened materials with the above mentioned new tool-manufacturing technology we used SV7 to perform a set of measurements on 16NiCrMo quenched steel. The main aim is to compare the quality of the manufactured product with the one of the same workpiece obtained by turning with traditional tools and grinding and to completely determine the mechanical performances of such products.
The samples were cementation steels 16NiCr4 which have been submitted to carbo-cementation treatment and therefore they present an external layer rich of carbon which has been transformed in martensite after hardening treatment.

Before the neutron measurements, the samples have been treated by machine-tools with wiper tools, by varying the treatment parameters. One of the samples has been ground for having the opportunity to do the comparison. We measured the hardness of the samples, before other treatments, obtaining for the cemented external layer the value of 58 HRc or 1050HV, for the intermediate un-cemented layer the value of 38 HRc or 750 HV and for the core the value of 20 HRc or 500 HV.
The samples are of three different kinds:

- Sample 1: it has been turned with wiper tools (tool covered by CBN; Radius=0,8mm; V=150 m/1'; a=0,1mm/rev; final ruggedness Ra=0,4micron);
- Sample 2: it has been turned with wiper tools (ceramic tool 6050; Radius=0,8mm; V=250 m/1'; a=0,1mm/rev; final ruggedness Ra=0,6micron);
- Sample RA: it has been ground (Ra = 1micron).

In Figure the results concerning Sample RA are shown. For iron we calculated the pole figures from the diffraction data. The orientation of the pole figures is the direction of view into the pole figure is parallel to the long axis of the cylindrical core samples.



The comparison among the three samples has been performed. At the present we are performing other measurements by using complementary techniques. The production of other samples obtained by using the two methods is also in progress.

Institut für Festkörperforschung
Forschungszentrum Jülich GmbH
D-52425 Jülich

Experimental Report
of Neutron Scattering Experiments
at the FRJ-2 Reactor

Proposal number:	SV7-04-015		
Experiment title:	**Correlation between structural and magnetic properties of $La_{7/8}Sr_{1/8}Mn_{1-\gamma}O_{3+\delta}$ with controlled nonstoichiometry**		
Dates of experiment:	09.03.05-11.03.05 14.06.05-26.06.05	Date of report:	28.03.06
Experimental team: Names	Addresses		
Mr. H. F. Li Dr. Y. Su Mr. J. Persson Dr. P. Meuffels Prof. Dr. Th. Brueckel	Institute of Solid State Research, Research Center Juelich, D-52425 Juelich, Germany		
Local Contact:	Mr. R. Skowronek, Dr. J. Walter		

Experimental report text body

Introduction

The defect chemistry such as cation nonstoichiometry and excess oxygen is a crucial issue for the understanding of manganites. It determines e.g. the orthorhombic-rhombohedral phase transition and the value of the Curie temperature T_c. Moreover, nonstoichiometric manganites are of extremely interest in application to the solid oxide fuel cells. Structural as well as physical properties are very sensitive to the synthesis conditions that can control the relative amount of Mn^{3+} and Mn^{4+} ions. In this report, We performed simultaneous Rietveld refinement combining both neutron and X-ray powder diffraction data of air sintered, Ar and O_2 annealed (1 atm pressure) $La_{0.875}Sr_{0.125}Mn_{1-\gamma}O_{3+\delta}$ samples.

Results

In order to explore the effect of Ar and O_2 annealings on the magnetic properties, the zero-field-cooling (ZFC) and field-cooling (FC) magnetizations as a function of temperature at an applied field of 20 Oe for the three samples were measured (Fig. 1(a)). Structural parameters were determined by the Rietveld method using the FULLPROF program. For each sample, scale factors, zero shifts, lattice constants, atomic positions, isotropic thermal parameters and the occupancies of Mn and oxygen were refined. From Figs. 2(A) and 2(B), one may observe three Bragg reflections, i.e. [400], [224] and [040] in NPD pattern [Fig. 2(a)] and one [111] in XPD pattern [Fig. 2(a')] of the Ar annealed sample. For the air sintered sample, the three reflections degenerate into two reflections [220] and [208] [Fig. 2(b)] and the [111] reflection disappears [Fig. 2(b')]. This shows that the Ar annealed sample has an orthorhombic structure (*Pbnm*, $Z = 4$; *O*), while the air and O_2 annealed samples belong to the rhombohedral space group (R-3c, $Z = 2$; R). The refined formulas of Ar annealed, air sintered and O_2 annealed samples are $La_{0.875}Sr_{0.125}Mn_{0.960(8)}O_{3.024(4)}$ (Ar), $La_{0.875}Sr_{0.125}Mn_{0.986(8)}O_{3.090(2)}$ (Air) and $La_{0.875}Sr_{0.125}Mn_{0.985(8)}O_{3.144(8)}$ (O_2), and they can be expressed as $La_{0.868(1)}Sr_{0.124(1)}Mn_{0.952(8)}O_3$ (Ar),

$La_{0.850(1)}Sr_{0.121(1)}Mn_{0.957(8)}O_3$ (Air) and $La_{0.835(2)}Sr_{0.119(1)}Mn_{0.940(8)}O_3$ (O_2), respectively. At the *O-R* structural transition, the averaged Mn-O-Mn bond angle increases from 161.08(4) º (Ar) to 163.38(1) º (O_2) and 163.64(1) º (Air), respectively. Moreover, the tolerance factor *t* calculated from the averaged La(Sr)-O and Mn-O bond lengths increases from 0.990(1) (Ar) to 0.992(1) (O_2) and 0.993(1) (Air), respectively. Ar and O_2 annealings cause a decrease of the Curie temperature T_c from 240(1) K (Air) via 237(1) K (O_2) to 192(1) K (Ar). The Curie temperature is reduced by ~20% for the sample with orthorhombic structure (Ar) as compared to the samples with rhombohedral structure (Air and O_2). This is explained by a decrease of the total strength of magnetic interactions, due to the changed Mn-O-Mn bond angle, the decrease of the numbers of nearest magnetic neighbors (Fig. 1(b)).

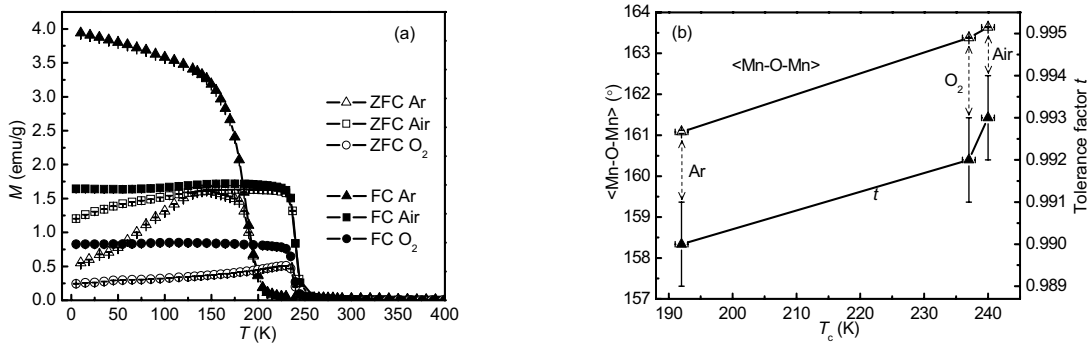


Fig. 1. ZFC and FC magnetization *M* vs. temperature measured at $H = 20$ Oe (a), and mean <Mn-O-Mn> bond angle and tolerance factor *t* vs. the Curie temperature T_c (b) for the three samples.

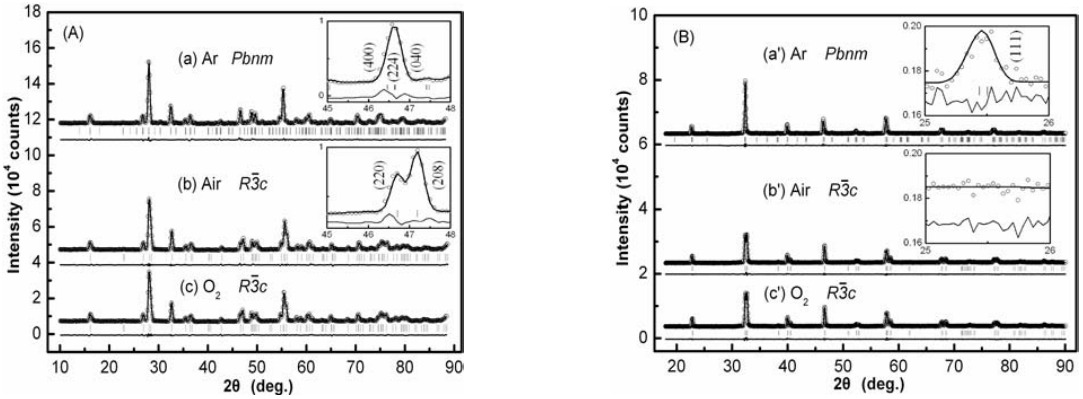


Fig. 2. The observed (circles) and calculated (solid lines) patterns of neutron [(A)] and X-ray [(B)] powder diffraction diagrams for Ar annealed [(a) and (a')], air sintered [(b) and (b')] and oxygen annealed [(c) and (c')] $La_{0.875}Sr_{0.125}Mn_{1-\gamma}O_{3+\delta}$ samples at ambient conditions. The bars mark the positions of Bragg reflections. The lower curve in each panel represents the difference between the observed and calculated patterns. The inset shows magnified patterns in certain 2θ regions.

Conclusions

We have systematically studied the effect of Ar and O_2 annealings on $La_{0.875}Sr_{0.125}Mn_{1-\gamma}O_{3+\delta}$ manganites with a fixed Sr doping. Our results clearly demonstrate that how extremely small change in the stoichiometry can have huge effects on structural and magnetic properties in these compounds based on the perovskite structure. Only ~2.2% relative decrease of oxygen content can lead to a structural transition from rhombohedral to orthorhombic and to a decrease of the transition temperature by ~20%. Such a huge response on small changes of parameters is characteristic of this complex system. To our knowledge, only a combined refinement of X-ray and neutron diffraction data allows one to determine the stoichiometry with the required precision to be able to compare results from different samples.

Institut für Festkörperforschung
Forschungszentrum Jülich GmbH
D-52425 Jülich

Experimental Report
of Neutron Scattering Experiments
at the FRJ-2 Reactor

Proposal number:	SV7-04-020		
Experiment title:	**Magnetic ordering and superstructure in bornite Cu_5FeS_4 polymorphs**		
Dates of experiment:	11.10.04-20.10.04 08.11.04-10.11.04 25.11.04-28.11.04	Date of report:	13.02.2006
Experimental team: Names	Addresses		
M. Romanelli A. Caneschi	University of Florence, Dept. of Chemistry, via della Lastruccia 3 – I50019 Sesto Fiorentino, Italy		
M. Borgheresi	University of Florence, Dept. Earth Sciences, via La Pira 4 - I50121 Firenze, Italy		
F. Di Benedetto G. Pratesi C. Cipriani	Museo di Storia Naturale, Università di Firenze, via La Pira, 4, I50121, Firenze (Italy)		
Local Contact:	J. M. Walter		

Experimental report text body

Introduction

Bornite has three temperature-dependent polymorphs, termed high, intermediate, and low. The intermediate (I-bornite) and low (L-bornite) forms can be described as superstructures of the high-temperature cubic form (H-bornite), the various superstructures arising from an increase in the ordering of vacancies and metal atoms with reducing temperature (Koto and Morimoto 1975; Putnis and Grace 1976; Pierce and Buseck 1978). The L-bornite crystallises in the orthorombic (pseudo-tetragonal) space group *Pbca* where the metals ions hosted in the tetrahedral site of two different sub cells: sphalerite- and antifluorite-type (Kanazawa et al., 1978). The metals locations proposed by Koto & Morimoto (1975) are, according to Collins *et al*. (1981), conceivable but not certain, because the scattering of Cu and Fe is too similar in the X-ray measurements. Moreover, the neutron diffraction data obtained from Collins *et al*. (1981) can be interpreted on the basis of different metals distributions. The problem of discerning between Cu and Fe positions and distributions become very important for the magnetic data interpretation which are directly related to the short-range ions interactions.

Measurements and Results

The measurements were planed at the SV-7 powder diffractometer in order to study the lattice constants variation in the high temperature but also to investigate the magnetic ordering phenomena (long- and short-range ordered magnetic structures) that appear at 70 K.

The bornite sample, from the Natural History Museum, was previously studied using micro analytical

(XRD, EMPA) and advanced spectroscopic and magnetic techniques (EPR, HF^2EPR, ESE, SQUID magnetometry). The measurements were taken on 1 g of powdered sample placed in a cylindrical vanadium can of 7.6 mm diameter and 30 mm height by using the closed cycle He-cryostat (4-293K) and the furnace (293-1500K) for the temperature excursions. The neutron diffraction measurements were obtained, in fact, in the high temperature range (at 200°C, 300°C and from 220°C to 250°C every 5°C), at room temperature and finally in the low temperature range (at 4 K and from 10 to 115 every 5 K) in order to assess and describe the magnetic polymorphs.

The neutron diffraction data (Figg. 1,2) collected in the low temperature region, which reveal at least 4 extra peak, confirmed the presence of an antiferromagnetic structure formed below 70 K and associable with an ordered distribution of the iron cations. No evidence of further magnetic discontinuity, as suggested in literature, has been proved from this diffraction data. The refinement of all the obtained data will carry out some other relevant information, in particular the distribution of Fe ions and their reciprocal interaction.

References

- Collins, M. F.; Longworth, G., Townsend, M. G. (1981); Can. J. Phys.; **59**(4), 535-9
- Kanazawa, Y., Koto, K., and Morimoto, N. (1978) Bornite (Cu5FeS4): stability and crystal structure of the intermediate form. Canadian Mineralogist, **16**, 397–404.
- Koto, K. & Morimoto, N. (1975); Acta Cryst., B**31**, 2268-73.
- Pierce, L. & Buseck, P.R. (1978); Am Mineral., **63**, 1-16
- Putnis, A. and Grace, J. (1976) The transformation behaviour of bornite. Contributions to Mineralogy and Petrology, **55**, 311–315.

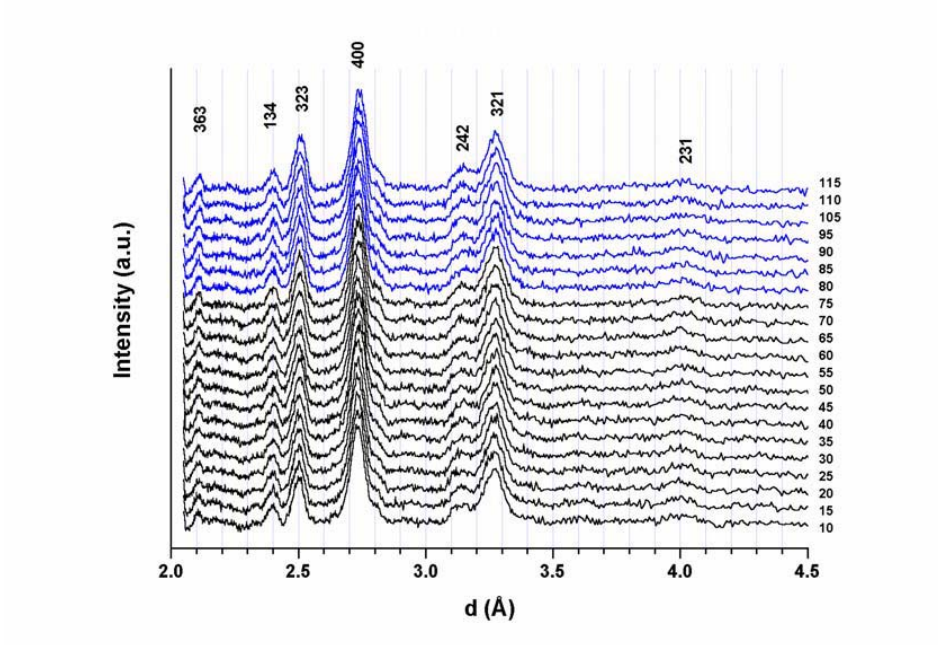


Figure 1

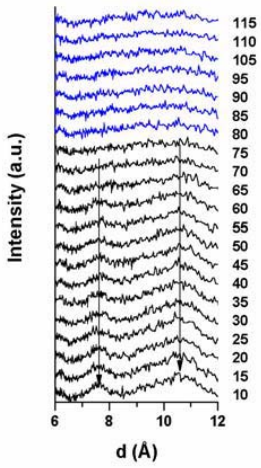


Figure 2

Institut für Festkörperforschung
Forschungszentrum Jülich GmbH
D-52425 Jülich

Experimental Report
of Neutron Scattering Experiments
at the FRJ-2 Reactor

Proposal number:	SV7-04-021		
Experiment title:	**Polyphase deformation of quartzitic mylonites of the Monte Rosa nappe (Southern Switzerland/Northern Italy)**		
Dates of experiment:	20 days	Date of report:	12.02.2006
Experimental team: Names	Addresses		
Pleuger, Jan Froitzheim, Nikolaus	Geologisches Institut der Universität Bonn, Nußallee 8, 53115 Bonn		
Local Contact:	J.M. Walter, E. Jansen, R. Skowronek		

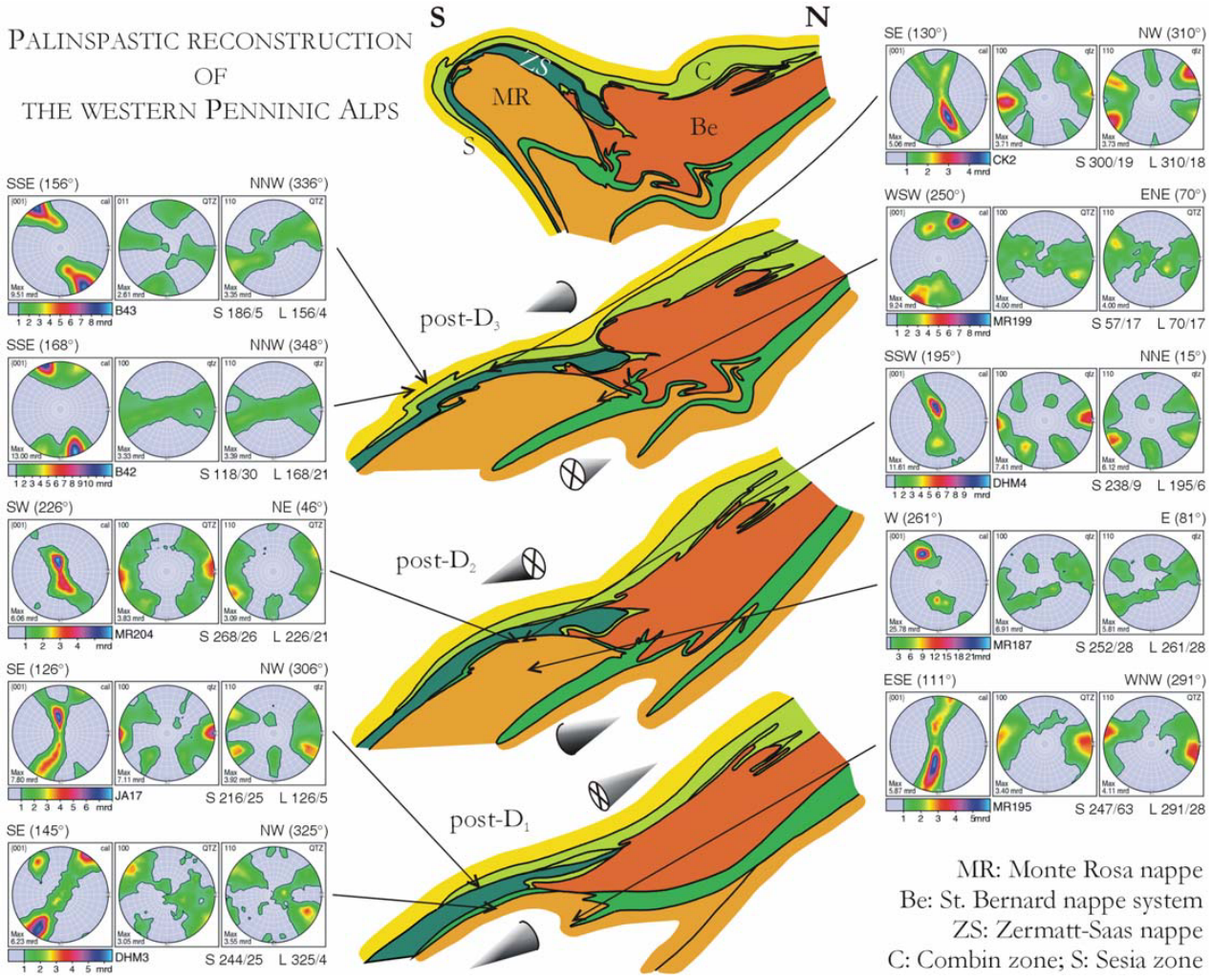
Experimental report text body

The present textures of quartzitic mylonites from the Monte Rosa nappe and adjacent units supplement those obtained earlier in the course of the project and shown in the experimental reports for 2003 (SV7-03-004 & SV7-03-009) and 2004 (SV7-04-005 & SV7-04-006). They provided most useful information about strain during certain stages of deformation while the high-pressure Zermatt-Saas and Monte Rosa nappes were tectonically exhumed. The first deformation phase D_1 led to nappe stacking. The nappes can be viewed as large-scale isoclinal recumbent folds that accommodated intense rotational strain (thrusting) within their strongly thinned overturned limbs. The {c} pole figure of JA17 is an incomplete type I crossed girdle. In terms of flow type, this can be interpreted to result from a weak rotational shear component. The thin section of JA17 shows that strain is strongly partitioned into almost equally large sets of domains of NW-vergent and opposite shear. Other quartz textures also indicate that D_1 strain between the main thrusts had only a small rotational component. It is most probable that larger displacements occurred only along the main thrusts while the nappe stack was otherwise shortened perpendicular to the axial planes of the then developing large nappe folds. Contrarily, the {c} pole figures of samples from the Monte Rosa nappe (DHM3 & MR195) are almost flawless single girdles, the {a} pole figures show one dominant maximum perpendicular to the {c} girdle. These samples with D_1 textures from the Monte Rosa nappe thus yield a stronger rotational component. They originate from levels of intense thrusting, i.e. from the very roof (DHM3) and the base (MR195) of the Monte Rosa nappe.

D_2 is characterized by SW-vergent shearing and intense large-scale folding. D_2 textures from the Monte Rosa nappe (DHM4 & MR204) yield incomplete single girdles of {c} which carry absolute maxima close to y indicating dominant prism <a> slip. Generally, prism <a> slip becomes dominant over basal <a> and rhomb <a> slip at temperatures roughly of upper greenschist- to amphibolite-facies conditions. Comparison of the D_2 textures and those developed in the Monte Rosa nappe during D_1 adumbrates that temperatures may have increased between D_1 and D_2. Other D_2 textures, however, yield different geometries, some of them triclinic and

therefore difficult to interpret in a straightforward manner, such as MR187. The fact that D_2 textures are ambiguous is best accounted for by the strong heterogeneity of D_2 strain.

D_3 effected the SE-vergent shearing and again large-scale folding. Sample CK2 from the base of the Combin zone yields a D_3 texture with a {c} pattern intermediate between type I and II crossed girdles. This and the tendency of {a} to array around the stretching lineation testifies constriction. Two samples (B42 & B43) stem from the base of the Sesia zone. B42 reveals two {c} maxima close to z. The stronger and the weaker one are rotated by about 20° towards x in a counter-clockwise and clockwise sense, respectively. {m} and {a} are almost evenly disposed each on two girdles perpendicular to the {c} maxima. This texture corresponds well with thin section observations that ribbon domains of quartz display opposite but internally consistent senses of shear. By total volume, ribbons with geographically SE-vergent shear sense, corresponding to the stronger {c} maximum, dominate over those with NW-vergent shear sense. The bulk strain of the conjugate ribbon sets was therefore flattening and had a weak rotational component. B43 is dominated by strong single maxima of {c} and {a} at the periphery of the respective pole figures indicative of basal <a> slip. Appendices of the {c} maximum extend towards the interior of the pole figure and document some additional influence of rhomb <a> slip which acted into the opposite direction than basal <a> slip as a conjugate slip system. Consequently, for B43 the same interpretation in regard of strain applies as for B42. A D_3 texture from the Monte Rosa nappe (MR199) has a similar {c} pattern as B42 but {a} and {m} are not that properly arranged on girdles. Variable strain geometries for D_3 must be concluded from D_3 textures from different levels of the nappe stack. CK2 testifies that the rocks along the base of the Combin zone accomodated substantial SE-vergent faulting while elsewhere the strain was rather flattening and only slightly rotational.



Institut für Festkörperforschung
Forschungszentrum Jülich GmbH
D-52425 Jülich

Experimental Report
of Neutron Scattering Experiments
at the FRJ-2 Reactor

Proposal number:	SV7-04-022		
Experiment title:	**Characterisation of ancient pottery of different periods from the excavation of Neos Scopos, Serres in North Greece**		
Dates of experiment:	04.04.2005 – 10.04. 2005	Date of report:	12.12.2005
Experimental team: Names	Addresses		
I. M. Siouris V. Moumtzi	SimLab, Department of Informatics and Communication, TEI of Serres Terma Magnisias 62000 Serres, Greece		
Local Contact:	J. M. Walter, R. Skowronek		

Experimental report text body

Introduction

The present study was the first part of a proposed systematic investigation, using non-destructive neutron diffraction for the characterization of ancient pottery from different periods ranging from 8th to 1st century BC, found at the excavation site of Neos Scopos Serres in North Greece. This is the first comprehensive attempt to study ancient Greek pottery using non-destructive neutron diffraction. The aim of this project is to provide a ceramic/pottery data base of the constituent minerals, firing conditions, weathering and trading patterns, available to both archaeologist and scientists in the field.

Measurements

At the present experiment 10 articles of pottery fragments with approximate dimensions 10 cm^2, 0.2-0.4 cm thick were investigated. The measured samples consisted of various types of potshards from three different ancient periods: Archaic 8th BC (4 samples), Classical (2 samples) and Hellenistic 2nd BC (4 samples). The work is focused on determining the mineral phase compositions (fingerprinting), the thermal profiles develop during manufacturing, and the element distribution, of carefully selected ceramic items discovered in a single localized pit. Neutron data were collected for about 5 hours/sample. The neutron diffraction patterns were analyzed and structure refinements on the mineral phases were carried out using the program AMPhOrAe (Archeometric Multi Phase Ornament & Artifacts analyses). This program is a new extended windows version of the IC-POWLS, developed to serve the multiphase modeling requirements for the analysis of the data collected from neutron diffraction measurements. The measured diffraction patterns of three samples at 273 K are depicted in (Fig.1), along with the corresponding fitted profile calculated intensities from the theoretical

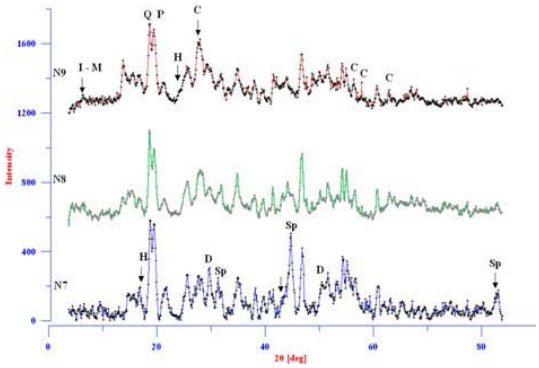


Fig.1: Observed diffraction patterns collected at 273 K of three 2nd century BC samples.

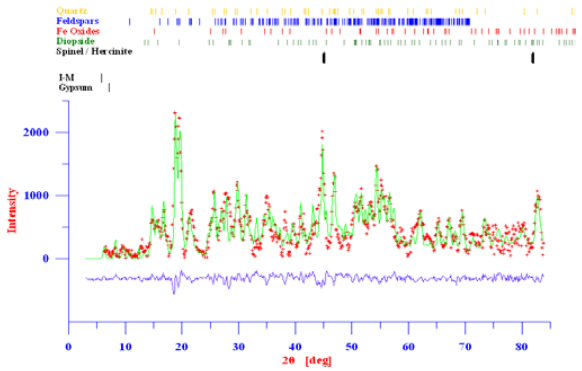


Fig.2: Observed, calculated and difference diagram of sample N7

to final model mineral compositions. Initial modeling of the observed data during the refinement process adopted a quartz, feldspar, plagioclase, hematite and diopside mineral synthesis (see Fig. 3), according to earlier neutron diffraction studies on comparable Greek pottery from Athenian Agora, Krania and Karabournaki.

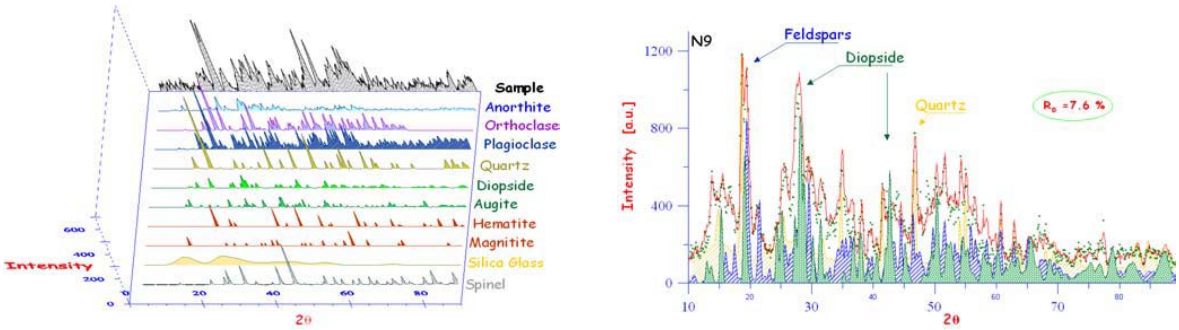


Fig.3: Initial modelling of the observed data at 273 K (left). Final model mineral compositions of N9 (right)

Results and Conclusions

Inspection of the analyzed diffraction patterns reveals the following similarities. All the patterns are dominated by pronounced quartz and feldspar peaks. Additionally, intense Bragg reflections corresponding to diopside (D) and spinel (Sp)/hercynite (Hr) minerals are clearly observed in sample N7 and with lower intensity in samples N8 and N9. Further more, the weak Bragg peaks observed at lower angles may be attributed to the (001) reflection of an illite/muscovite (I-M) phase. The absence of extensive broad humps in the diffraction spectra shows no significant vitreous silica phase, indicating that the firing of the clay could not have exceeded the 1000 ˚C. The firing temperatures were estimated to be within 900 and 1000 ˚C. In the table below the relative weight fractions w (in percent) of Quartz (Q), Feldspar (F), Diopside (D), K-Spinel/ Hercynite (Sp/Hr) and Hematite (H) are given. Strength of reflection intensities at 2θ= 13.8° for (I-M: illite/muscovite) are indicated by (0), (+), (++), (+++) in this table. R_{wp} are the weight percentages for the different samples.

A/A	w(Q)	w(F)	w(D)	w(Sp/Hr)	w(H)	Q/F	I-M	R_{wp}
N7	18.6	67	11.8	11.5	1.6	0.28	+	6.8
N8	26	58	11	++	5	0.45	++	7.8
N9	42	25	28	+	5	1.68	++	7.6

Full paper: I.M.Siouris, J.Walter to appear in Physica B; **Results presented** at ICNS 2005, in Sydney.

Institut für Festkörperforschung
Forschungszentrum Jülich GmbH
D-52425 Jülich

Experimental Report
of Neutron Scattering Experiments
at the FRJ-2 Reactor

Proposal number:	SV7-04-024		
Experiment title:	**Neutron diffraction on $PrNi_4Cu$, $NdNi_4Cu$ and $DyNi_4Cu$**		
Dates of experiment:	36 days	Date of report:	18.05.2006
Experimental team: Names	Addresses		
Dr. T Toliński, Dr. A. Kowalczyk Dr. A. Hoser	Institute of Molecular Physics, PAS, Smoluchowskiego 17, 60-179 Poznań, Poland Institute of Molecular Physics, PAS, Smoluchowskiego 17, 60-179 Poznań, Poland Institut für Kristallographie, RWTH-Aachen, Germany		
Local Contact:	Dr. J. M. Walter, R. Skowronek		

Experimental report text body

Recently, we have intensively studied the RNi_4M (M = B, Al, Si, Ga, Cu) [1-4] compounds, which originate from the RNi_5 type of compounds (R= rare earth) [5]. The RNi_4Cu series differs from the remaining M substitutions by the reason of the Cu(3d) states being close both to the Fermi level (0eV) and the Ni(3d) (-0.7eV) states. Hence, one can suppose that the Cu(3d) peak, which appears at about -3eV in the valence band can hybridize with the Ni(3d) one, influencing the magnetism of nickel by the electron transfer. However, we know, based also on our previous neutron diffraction studies for M = Al [1], that the magnetism of nickel is already cancelled out due to the other atoms contributing to the valence band, especially the rare earth. Therefore, one of the reasons of the present studies has been a comparison of RNi_4Cu with the other RNi_4M compounds.

The polycrystalline RNi_4Cu compounds were prepared by induction melting of the constituent elements under a protective argon atmosphere. The RNi_4Cu compounds (R = rare earth or Y) crystallize in the hexagonal $CaCu_5$-type of structure, point group *P6/mmm*. R ions occupy the 1a site (0,0,0) and Ni(1) the 2c site (1/3,2/3,0). Ni(2) and Cu are statistically distributed over the 3g site (1/2,0,1/2). To verify the electronic structure of RNi_4Cu we have carried out the X-ray photoemission spectroscopy (XPS). The magnetometric measurements were performed using a MagLab 2000 System (Oxford Instruments Ltd.).

The neutron diffraction has been performed using the SV7 instrument and the wavelength was equal to 1.096 Å. The sample was contained in a cylindrical vanadium can mounted (1) in a refrigerator cryostat and (2) in a cryomagnet with external magnetic fields up to 5 T perpendicular to the horizontal diffraction plane. In 2005 the studies have been carried out for R = Nd and Pr [6]. The example of the more advanced data of R = Nd is presented below.

$PrNi_4Cu$ and $NdNi_4Cu$ are characterized by the Curie temperatures of 3.7 K and 11 K, respectively. The magnetic moments in $H = 9$ T were equal to $1.5\mu_B$/f.u. at 1.8 K for $PrNi_4Cu$ and $2.25\mu_B$/f.u. at 4.2 K for $NdNi_4Cu$ [4].

The lattice parameters derived from the neutron diffraction are in good agreement with the X-ray diffraction results. The diffraction patterns have been fitted with the program FULLPROF, by the full-pattern Rietveld refinement.

Fig.1a,b presents the neutron diffraction pattern for $NdNi_4Cu$ obtained at 50 K and 4 K. Below the transition temperature of 11 K [4] only a change in the structural intensities is visible, like in the case of the previously studied $NdNi_4Al$ [1]. It allows one to exclude any antiferromagnetic ordering, for which new reflections would appear. Following the case of $NdNi_4Al$, it is assumed that the magnetic moments of the Nd ions are aligned within the hexagonal plane. The magnetic moment at 4.2 K extracted from the FULLPROF analysis is $1.75\mu_B$, in good agreement with the magnetic moment determined from the magnetization measurements [4], where it was $1.77\mu_B$/f.u. from the extrapolation of the high field part of the *M(H)* curve to $H = 0$. Previously, in the case of $NdNi_4Al$ we have observed a significant discrepancy between the neutron ($1.85\mu_B$) and magnetometric ($1.52\mu_B$/f.u) result. A comparison of the calculated (LMTO) and measured (XPS) electronic structures is being carried out to explain these differences.

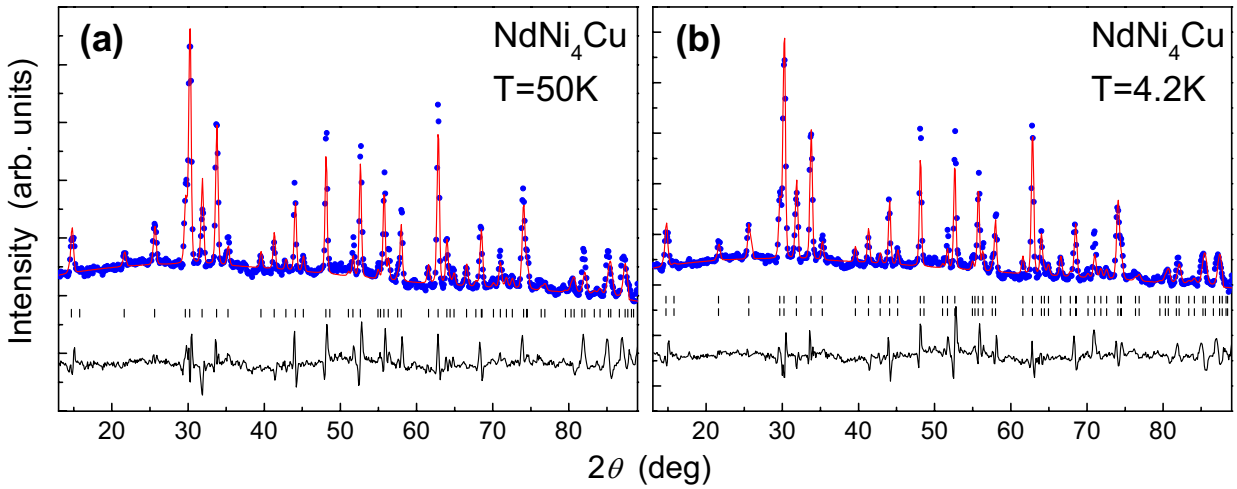


Fig.1. Neutron diffraction pattern of $NdNi_4Cu$ at 50 K (a) and 4.2 K (b). The experimental data and the refinement are represented by dots and a line, respectively. The bottom curve represents the difference between measurements and calculations. For (b) the fit includes both the structural and magnetic contribution.

References

[1] T. Toliński, W. Schaefer, W. Kockelmann, A. Kowalczyk, A. Hoser, Phys. Rev. B 68 (2003) 144403.
[2] T. Toliński, A. Kowalczyk, A. Szlaferek, B. Andrzejewski, J. Kovac, M. Timko, J. Alloys Compd. 347 (2002) 31.
[3] M. Pugaczowa-Michalska, G. Chełkowska, T. Toliński, A. Kowalczyk, phys. stat. sol. (c) 243 (2005) 309.
[4] A. Kowalczyk, T. Toliński, B. Andrzejewski, A. Szlaferek, J. Alloys Compd. 413 (2006) 1.
[5] W.E. Wallace, Rare Earth Intermetallics, ed. A.M. Alper, J.L. Margrave, A.S. Nowick, Academic Press, New York and London 1973, p.266.
[6] T. Toliński et al., submitted to J. Alloys Compd.

Institut für Festkörperforschung
Forschungszentrum Jülich GmbH
D-52425 Jülich

Experimental Report
of Neutron Scattering Experiments
at the FRJ-2 Reactor

Proposal number:	SV7-04-025		
Experiment title:	**Antiferromagnetic correlations in some Ce-based intermetallic compounds**		
Dates of experiment:	06.04.06-09.04.06	Date of report:	18.05.2006
Experimental team: Names	Addresses		
Dr. T Toliński, Dr. A. Kowalczyk Dr. A. Hoser	Institute of Molecular Physics, PAS, Smoluchowskiego 17, 60-179 Poznań, Poland Institute of Molecular Physics, PAS, Smoluchowskiego 17, 60-179 Poznań, Poland Institut fuer Kristallographie, RWTH-Aachen, Germany		
Local Contact:	Dr. J. Walter, R. Skowronek		

Experimental report text body

Our recent investigations of the $CeNi_4M$ compounds for M = B [1], Al [2], Ga [3] and Cu [4] have revealed a contradictory behavior. From one side, the reduced effective moment extracted from the magnetic susceptibility and satellites observed in the X-ray photoemission 3d spectra suggest a strongly mixed valence behavior. Simultaneously, a low temperature minimum in resistivity and an anomaly in specific heat indicate the possibility of a Kondo system, which would exclude the mixed-valency. We have ascribed the anomalies to a Kondo impurity-like behavior, i.e. a small amount of Ce ions in incorrect crystallographic positions mimicking the classical Kondo effect for diluted systems. However, the specific heat anomaly at 6 K can be alternatively explained by a small contribution of an antiferromagnetic impurity phase - a possibility supported by a small negative paramagnetic Curie temperature (-10 K). The purpose of the neutron diffraction studies has been to confirm or to exclude the existence of any antiferromagnetic correlations.

The neutron diffraction experiment has been carried out using the SV7 instrument and the wavelength of 1.096 Å. The polycrystalline $CeNi_4Cu$ compounds crystallize in the hexagonal $CaCu_5$-type of structure, point group *P6/mmm*.

The preliminary neutron diffraction measurements were realized for temperatures of 4, 50 and 300 K. At the accessible accuracy no additional - in respect to the crystallographic - reflections could be observed going down from room temperature to 4 K, i.e. below the anomaly at 6 K for specific heat [4]. Therefore, at this stage of investigations the neutron diffraction does not support the possibility of an antiferromagnetic contribution. However, more accurate and covering temperatures below 4 K measurements are necessary.

In spite of the lack of any extra peaks, two other effects of the temperature decrease are found. First, the expected contraction of the lattice constants and, consequently, the unit cell volume is observed. The lattice constants are collected in Table 1.

Temperature	*a* (Å)	*c* (Å)
300 K	4.92197	4.01718
50 K	4.90790	4.00997
4 K	4.90696	4.01021

Table 1: Temperature dependence of the lattice parameters for the $CeNi_4Cu$ compound.

Second, an increase of some intensities occurs, mainly for the (111), (201), (210), (301), (221) and (222) reflections. Opposite to our previous studies on RNi_4M the low angle peaks are not affected by lowering temperature. The growth of the structural intensities can be explained by a ferromagnetic ordering of the rare earth ions. The corresponding fit with FULLPROF program is displayed in Fig. 1. The obtained magnetic moment of $2.01\mu_B$ (assumed to lie in the hexagonal plane) is close to the free ion value ($2.14\mu_B$). However, the ordering would have to start already in the range 50-300 K, whereas the magnetic susceptibility indicates a paramagnetic behavior in the whole temperature range. Similar quality fit can be obtained assuming that the magnetic moment is due to Ni (usually magnetic contribution of Ni is negligible in RNi_4M compounds). It would explain a high ordering temperature, however the estimated value ($>0.8\mu_B$) of magnetic moment exceeds the saturation moment of Ni ($0.6\mu_B$). Further, higher accuracy and magnetic field assisted measurements should provide more answers to these questions.

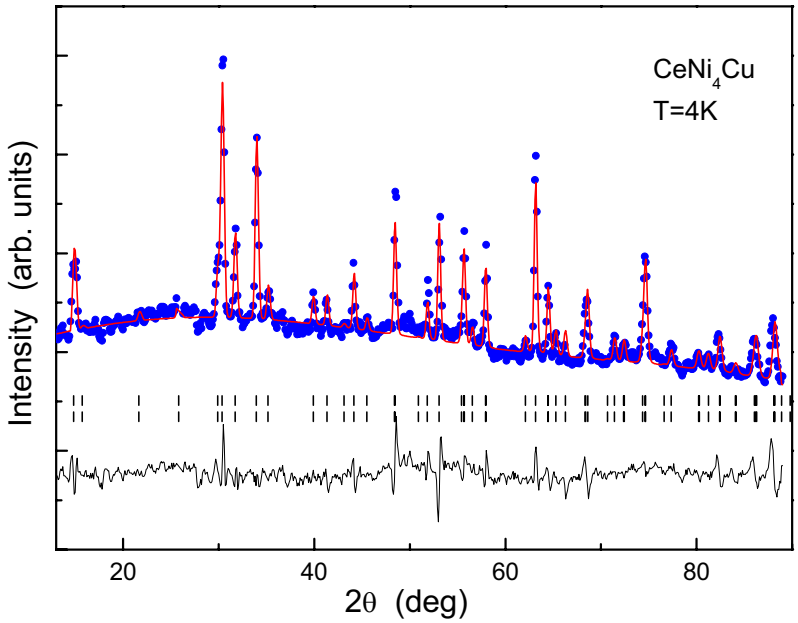


Fig.1. Neutron diffraction pattern of $CeNi_4Cu$ at 4.2 K fitted assuming the structural and the magnetic phase with magnetic moments on the Ce ions.

References

[1] T. Toliński, A. Kowalczyk, M. Pugaczowa-Michalska, G. Chelkowska, J. Phys.: Condens. Matter **15**, 1397 (2003).

[2] T. Toliński, A. Kowalczyk G. Chełkowska, M. Pugaczowa-Michalska, B. Andrzejewski, V. Ivanov, A. Szewczyk, M. Gutowska, Phys. Rev. B **70**, 064413 (2004).

[3] T. Toliński, A. Kowalczyk, V. Ivanov, G. Chełkowska, M. Timko, Czech. J. Phys. **54**, D287 (2004).

[4] T. Toliński, A. Kowalczyk, G. Chełkowska, A. Szewczyk, M. Gutowska, J. Phys.: Condens. Matter **18**, 3435 (2006).

Institut für Festkörperforschung
Forschungszentrum Jülich GmbH
D-52425 Jülich

Experimental Report
of Neutron Scattering Experiments
at the FRJ-2 Reactor

Proposal number:	SV7-04-026		
Experiment title:	**Erfassung und Bewertung ausgewählter Vorkommen von Natursteinen und ihrer gesteinstechnischen Eigenschaften**		
Dates of experiment:	20.09.05-27.09.05	Date of report:	19.06.2006
Experimental team: Names	Addresses		
Hoffmann, Andreas Siegesmund, Siegfried	Geowissenschaftliches Zentrum der Universität Göttingen (GZG) Abteilung für Strukturgeologie und Geodynamik Goldschmidt Str. 3 D-37077 Göttingen		
Local Contact:	J. M. Walter, E. Jansen		

Experimental report text body

Grundlegende Voraussetzung für die Erfassung und Bewertung der gesteinstechnischen Eigenschaften der Naturwerksteine ist die fundierte Zustandsbeschreibung durch petrographische, gefügekundliche und technische Kenngrößen. Durch Texturuntersuchungen, als wohl wichtigstes Gefügeelement zur Materialprognose, wurde an ausgewählten Naturwerksteinen gezeigt, ob vorhandene kristallographische Vorzugsorientierungen existieren. An dem Probenmaterial sollten Homogenitätsbereiche bestimmt werden, d.h. ob die Texturen in Intensität, Symmetrie bzw. bezüglich eines externen Referenzsystems übereinstimmen oder vollständig variabel sind.
Die Texturmessungen der Marmore zeigen insgesamt eine deutliche Orientierung der kristallographischen Achsen. Die c-Achsen sind dabei überwiegend parallel zur z-Richtung angeordnet und demonstrieren mehrheitlich ein einfaches Polpunktmaximum. Da alle Gesteine mit dieser Verteilung der Achsen eine makroskopisch deutlich erkennbare Foliation aufweisen, die in der x- und y-Richtung aufgespannt wird, sind die c-Achsen senkrecht zur Foliation der Gesteine ausgerichtet. Die Verteilung der c-Achsen in der Probe 29AH ist ebenfalls einfach ausgebildet. Die Achsen sind dabei jedoch nicht parallel zur z-Richtung angeordnet, was sich vermutlich aus der aus dem Umstand ergibt, dass das Gestein makroskopisch keinerlei erkennbare Vorzugsorientierungen aufweist. Die Probenahme konnte daher nicht unter vollständiger Berücksichtigung des externen Referenzsystems erfolgen. Das Doppelmaximum der c-Achsen bei der Probe 14AH ist eventuell auf tektonische Bewegungen zurückzuführen, da die Lagerstätte lokal durch eine intensiv ausgeprägte Scherzone beeinflusst wird.

Texturmessungen und thermische Dehnung der Marmore
An der Universität Göttingen wurden an dem Probenmaterial zentrale Elemente der Verwitterungsprozesse simuliert, wie z.B. das thermische Dehnungsverhalten der Marmore mittels eines Dilatometers.

Die Ergebnisse der thermischen Dehnung demonstrieren deutlich, dass die jeweiligen Längenänderungen von der Textur des Materials abhängen. In diesem Zusammenhang zeigt beispielsweise die Probe 01AH eine ausgeprägte Ansiotropie des Dehnungsverhaltens, wobei die größten Änderungen parallel zur z-Richtung, also parallel zur bevorzugten Orientierung der c-Achsen auftreten (Abb.1a, b). Das anisotrope thermische Dehnungsverhalten ergibt sich aus den Einkristalleigenschaften des Calcits, der sich unter dem Einfluss von Temperatur in Richtung der kristallographischen c-Achse ausdehnt und parallel zur a-Achse kontrahiert. Das gleiche gilt auch für den zweiten gemessenen Texturtyp in Abb. 2.

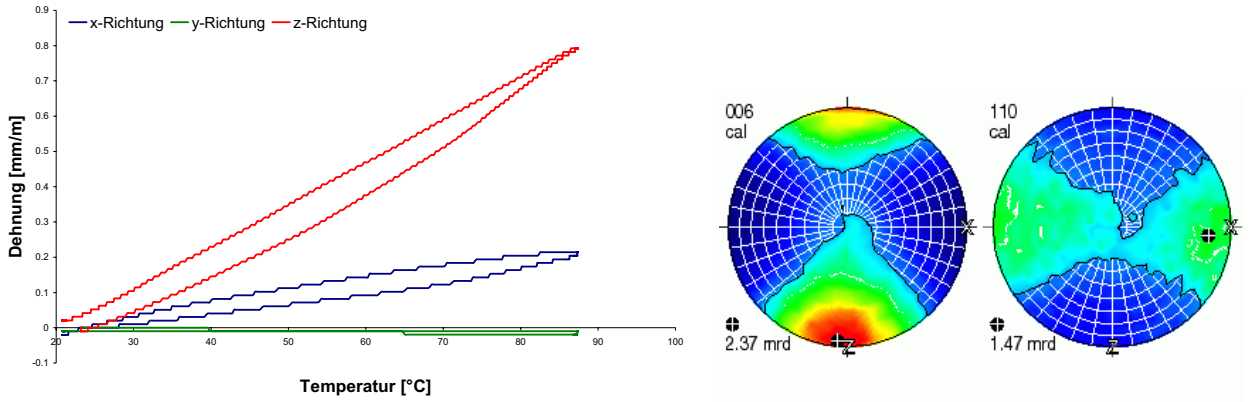


Abb. 1: Thermische Längenänderung der Probe 01AH mit maximaler Ausdehnung in z-Richtung (links). Die Richtung der maximalen Ausdehnung korrespondiert dabei mit der bevorzugten Orientierung der kristallographischen c-Achen (rechts).

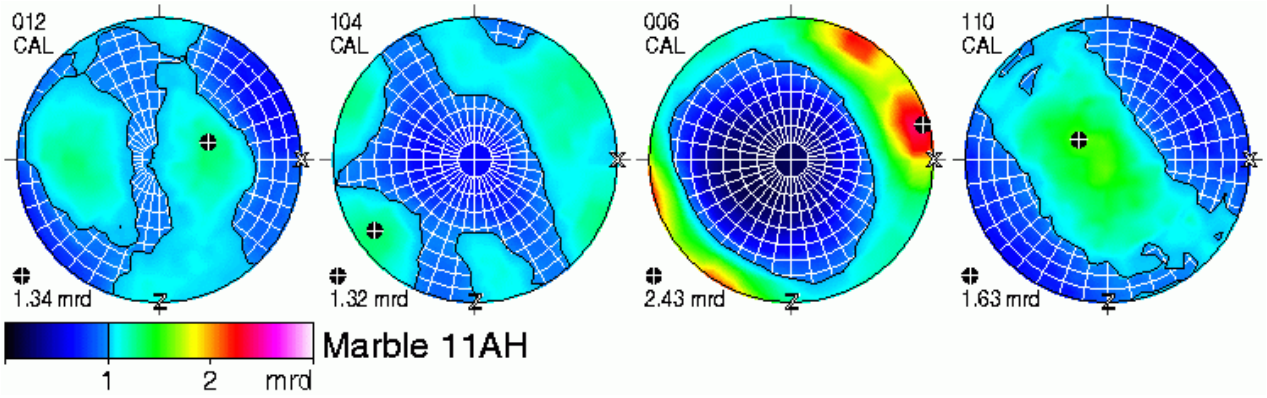


Abb. 2: Texturtyp eines Doppelmaximums eines Marmor-Naturwerksteins

Institut für Festkörperforschung
Forschungszentrum Jülich GmbH
D-52425 Jülich

Experimental Report
of Neutron Scattering Experiments
at the FRJ-2 Reactor

Proposal number:	SV7-04-027		
Experiment title:	**Kinematic analysis of the Sierra Ballena Shear Zone and their meaning in the structure of the Precambrian of SE Uruguay**		
Dates of experiment:	04.10.04-07.10.04 10.10.04-11.10.04 22.11.04-28.11.04	Date of report:	12.04.2006
Experimental team: Names	Addresses		
Oyhantcabal, Pedro Siegesmund, Siegfried	Departamento de Geologia, Facultad de Ciencias Universidad de la Republica Igua 4225 CP 11400 Montevideo, URUGUAY Abteilung für Strukturgeologie und Geodynamik Geowissenschaftliches Zentrum der Georg-August-Universität Göttingen (GZG) Goldschmidtstrasse 3 D - 37077 Göttingen		
Local Contact:	Dr. Jens M. Walter, R. Skowronek, E. Jansen		

Experimental report text body

Einleitung

Die „Sierra Ballena Scherzone" ist eine horizontale Scherzone, die den Neoproterozoischen Gürtel „Dom Feliciano" in Südamerika in zwei unterschiedliche Domänen unterteilt. Die Deformation in der Sierra Ballena Scherzone fand unter regionalen grünschieferfaziellen Bedingungen statt. Die Hauptdeformationsphase war transpressiv, in der reine Scherung vorherrschend war. Die Deformation führte sowohl zur Ausbildung von dextralen als auch von sinistralen Scherzonen und zu der Platznahme von synkinematischen Graniten. Altersdatierungen dieser granitischen Intrusionen ergeben daher ein Deformationsalter von 600 bis 580 Ma. Die Korrelation dieser Scherzone mit der Purros Scherzone des Kaoko Belts im Damara Orogen in Namibia ist derzeit gegenstand wissenschaftlicher Disskussion.

Messungen und Korrelationen

Zur Charakterisierung der Scherzonen und ihrer Deformationsmechanismen und –bedingungen, muß eine detaillierte Untersuchung der Mikrogefüge herangezogen werden. Die Mikrostrukturen im Quarz, die an granitischen Myloniten dieses Stadiums beobachtet werden können, sind charakteristisch für „dislocation creep Regime 2". Die Polfiguren von Quarz der am SV7 gemessenen Neutronentexturen sind asymmetrische gekreuzte Gürtel und asymmetrisch einfache Gürtel mit Rhomb-*a* als aktivem Gleitsystem. Sowohl die beobachteten Mikrostrukturen als auch die Polfiguren deuten auf mittlere grünschieferfazielle Bedingungen während der transpressiven Verformung.

Eine zweite Deformationsphase war „strike-slip" artig mit sinistraler, dominanter einfacher Scherung. Ar/Ar Alterbestimungen an Muskovit der mylonitschen Quarzite zeigen dieses zweite Ereignis in zwei verschiedenen

Altersgenerationen an. Das Alter dieser zweiten Deformationsphase liegt zwischen 579 und 581 Ma. Die Mikrostrukturen des Quarz zeigen den Übergang von „dislocation creep Regime 2" zu „dislocation creep Regime" 3 an. Die Textur Polfiguren zeigen ein *c*-Achsen Maximum in Y-Richtung, mit Prismen-a als Hauptgleitsystem (siehe Abb. 3). Diese Charakteristika zeigen eine Deformation bei oberen grünschiefer- bis unterern amphibolitefazieller Metamorphosebedingungen an (~500 °C). Die schiefe Lage der *c* und *a* Achsen Maxima in den Polfiguren relativ zur Scherebene im Gelände, kann als ein Nachweis für transpressive Verformung betrachtet werden (Abb. 1).

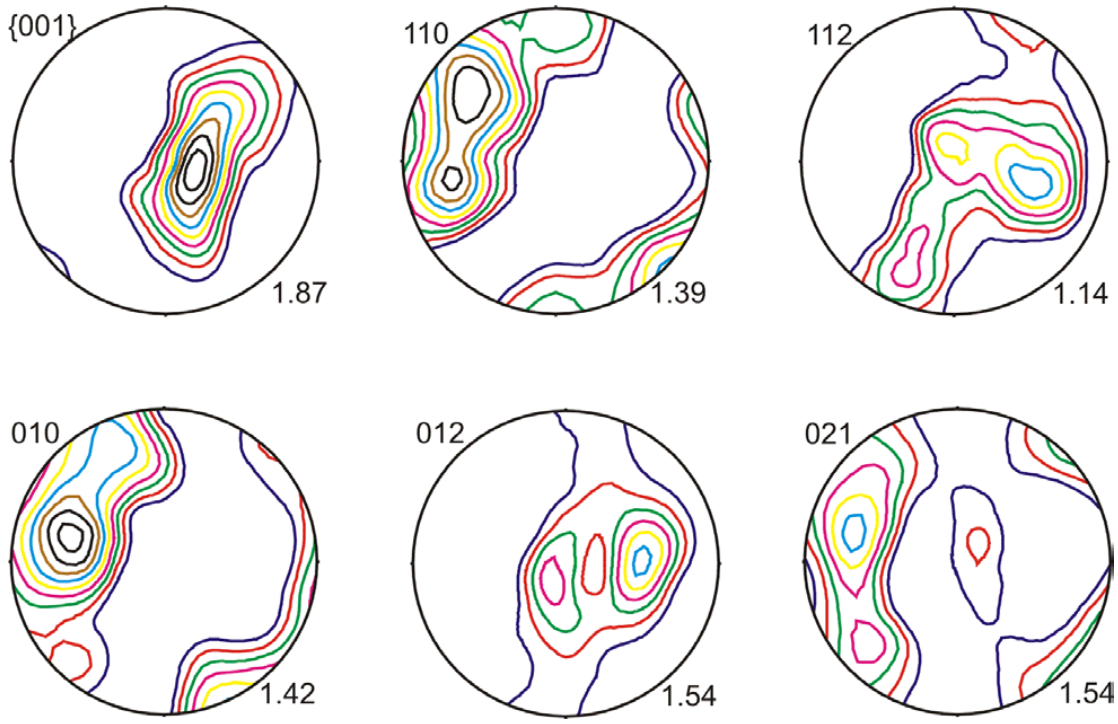


Abb 1: Quarzpolfiguren zeigen transpressive Deformationsgeometrien durch die schiefe Lage der c- und a-Achsen relativ zur horizontalen Scherebene. Das c-Achsen Maximum in Y-Richtung zeigt das Prismen-a Hauptgleitsystem bei oberen grünschiefer- bis untere amphibolitfaziellen Bedingungen

Institut für Festkörperforschung
Forschungszentrum Jülich GmbH
D-52425 Jülich

Experimental Report
of Neutron Scattering Experiments
at the FRJ-2 Reactor

Proposal number:	SV7-04-028		
Experiment title:	**Texturen dolomitischer Itabirite**		
Dates of experiment:	10 days	Date of report:	26.06.2006
Experimental team: Names	Addresses		
H. Siemes C. Rosière	Institut für Mineralogie und Lagerstättenlehre RWTH Aachen Bunsenstr. 8, 52056 Aachen Instituto de Geosciencas Universidade Federal de Minas Gerais Av. Antonio Carlos, 6627 CEP 31270-901 Belo Horizonte, MG, Brasilien		
Local Contact:	J.M. Walter, E. Jansen, R. Skowronek		

Experimental report text body

Itabirite is a metamorphic variety of iron formations from the Itabira group that is a iron-rich stratigraphic unit from the Paleoproterozoic Minas supergroup in the Quadrilátero Ferrífero Mineral District. The itabira Group contains two units: i) the lower Cauê Formation characterized by the predominance of quartz itabirite, composed mainly of quartz and iron oxides (hematite and magnetite/martite) with local compositional varieties comprising silicates (chlorite/clinochlore, talk and amphiboles) and carbonates (mainly dolomite), and ii) the upper Gandarela formation comprising mainly dolomite which grades into the Cauê formation with the development of Fe-rich dolomite and dolomitic itabirite. The units of the Itabira Group may also grade into the underlying Batatal Formation. This unit comprises mainly phyllites of variable compositions but also dolomites and volcanic/volcanoclastic rocks.

Three main compositional types of itabirite could be discriminated in the in the Itabira group:

Quartz- Itabirite - quartz and iron oxides

Dolomitic Itabirite - dolomite, quartz, iron oxides and minor silicates

Silicate-rich/Amphibolitic Itabirite - silicates (chlorite/clinochlore, talk, amphiboles), iron oxides, some quartz and dolomite.

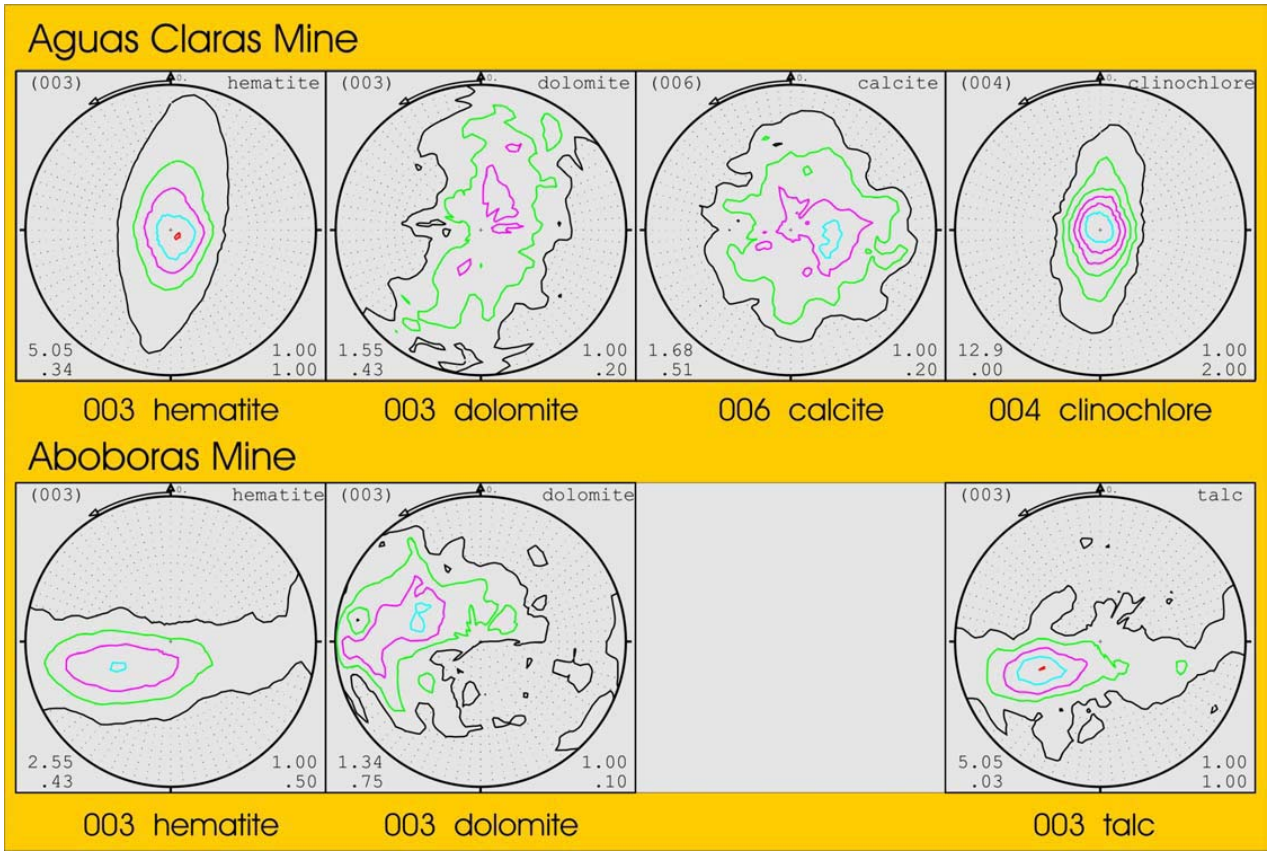
The present lithological varieties in the Itabira group are product of metamorphic mineral changes so it is not possible to find a direct relation to sedimentary facies, such as in anchimetamorphic sequences in several basins as the Transvaal-Griqualand West in South Africa and the Hamersley basin in Australia. Iron formations present a more or less regular banding due to primary variations in the composition related to sedimentation and diagenetic transformations and this structure remain more or less well preserved during metamorphism or may be transposed by deformation. Mineralogy and fabric, otherwise, reflect changing conditions during diagenesis, hydrothermal mineralization, metamorphism and deformation.

In the itabirites most hematite crystals are product of metamorphic recrystallization, dolomite is considered to be a product of diagenetic change of sedimentary carbonates and silicates which are probably always formed by metamorphic (solid state) reactions.

The metamorphic grade and intensity of deformation in the Quadrilátero Ferrífero increases eastwards and the degree of preferred orientation of hematite also increases with the development of oriented hematite platelets named specularite which texture changes according to the characteristics in intensity of deformation undergone by the rock.

The first attempt to understand the deformation behavior of hematite and the types of texture developed was accomplished in monomineralic (hematitic) high-grade ores where gangue minerals were leached out or substituted by hydrothermal fluids during the mineralization processes.

The determination of the partial texture of several mineralogical components from dolomitic itabirite, namely, hematite, dolomite, chlorite (clinochlore) and talk indicate that they were deformed under the effect of a single deformation plan, but with the development of entirely different degrees of preferred orientation. Hematite presents similar texture as phyllosilicates but carbonates present a weaker texture.



For details see references e.g.:

Bascou, J., Raposo, M.I.B., Vauchez, A., Egydio-Silva, M., (2002) Titanohematite lattice preferred orientation and magnetic anisotropy in high-temperature mylonites. Earth and Planetary Science Letters 198, 77-92.

Jansen, E., Schäfer, W., Kirfel, A. (2000) The Jülich neutron diffractometer and data processing in rock texture processing. Journal of Structural Geology 22, 1559-1564.

Rosière, C.A., Siemes, H., Quade, H., Brokmeier, H.-G., Jansen, E.M. (2001) Microstructures, textures and deformation mechanisms in hematite. Journal of Structural Geology 23, 1429-1440.

Siemes, H., Klingenberg, B., Rybacki, E., Naumann, M., Schäfer, W., Jansen, E., Rosière, C.A. (2003) Texture, microstructure, and strength of hematite ores experimentally deformed in the temperature range 600° to 1100°C and at strain rates between 10^{-4} and 10^{-6} s^{-1}. Journal of Structural Geology 25, 1371-1391.

Institut für Festkörperforschung
Forschungszentrum Jülich GmbH
D-52425 Jülich

Experimental Report
of Neutron Scattering Experiments
at the FRJ-2 Reactor

Proposal number:	SV7-04-029		
Experiment title:	**Low and high-temperature behaviour of kyanite. Thermoelastic constants and structural evolution**		
Dates of experiment:	24.01.05-30.01.05 12.04.05-14.04.05 10.06.05-27.06.05	Date of report:	12.04.2006
Experimental team: Names	Addresses		
Gatta, Giacomo Diego Nestola, Fabrizio	Bayerisches Geoinstitut Universität Bayreuth Universität Str. 30 D-95447 Bayreuth Germany		
Local Contact:	Dr. Jens M. Walter, R. Skowronek		

Experimental report text body

Introduction

Kyanite is one of the three Al_2SiO_5 polymorphs (with andalusite and sillimanite). The fields of stability and the thermodynamic properties of the Al_2SiO_5 polymorphs play a crucial role of these minerals in the fields of the metamorphic petrology. In addition, the Al_2SiO_5 polymorphs are object of interest in the industrial applications of refractory materials. By calcinations, these minerals convert to mullite ($Al_6Si_2O_{13}$) and silica (SiO_2) at temperatures in excess of 1200-1400°C at ambient pressure, (Harben, 1999). Refractory materials that contain the Al_2SiO_5 polymorphs and/or synthetic mullite include e.g. insulating brick, firebrick and kiln furniture. In addition, the interlocking grain structure of kyanite and mullite applies ancillary mechanical strength to refractory and other non-refractory ceramic materials. Other end uses of kyanite and related materials include electrical porcelain, floor and wall tiles, foundry use, sanitary ware, and other related products. Despite the petrologic importance and the industrial use of kyanite, sillimanite and andalusite, the relative fields of stability of the Al_2SiO_5 polymorphs are not completely clear because of the small change in thermodynamic properties associated to the polymorphic phase transition (Winter and Ghose, 1979; Kerrick, 1990; Bohlen et al., 1991).

Measurements and Results

The high-temperature (H*T*) behaviour of kyanite (Al_2SiO_5) was investigated by means of *in-situ* neutron powder diffraction at the powder diffractometer SV7 in Jülich in a temperature range of room temperature up to 1200°C. Within the investigated *T*-range, no phase transition has been observed. The axial and volume thermal expansion coefficient ($\alpha_j=l_j^{-1}\cdot\partial l_j/\partial T$, $\alpha_V=V^{-1}\cdot\partial V/\partial T$), calculated by weighted linear regression through the data points, are: $\alpha_a = 5.5(2)\cdot10^{-5}$, $\alpha_b = 5.9(2)\cdot10^{-5}$, $\alpha_c = 5.18(8)\cdot10^{-6}$, $\alpha_V = 7.4(1)\cdot10^{-3}$ °C^{-1}, with $\alpha_a:\alpha_b:\alpha_c =$ 1.06 : 1.14 : 1.00. All the three angles of the kyanite lattice show a slight decrease with *T*, with $\partial\alpha/\partial T = -2(2)\cdot10^{-5}$, $\partial\beta/\partial T = -4(1)\cdot10^{-5}$, $\partial\gamma/\partial T = -10(2)\cdot10^{-5}$ °/°C. The magnitudes of the principal unit-strain coefficients (ε_1, ε_2, ε_3) and the

orientations of the thermal strain-ellipsoids, between the ambient temperature and each measured *T*, were calculated. The magnitude and the orientation of all the three unit-strain coefficients are almost maintained constant with *T*. At T-T_0=1177 °C , ε1^*a* = 76(2)°, ε1^*b*=70(2)°, ε1^*c*= 38(3)°, ε2^*a*= 49(3)°, ε2^*b*= 66(3)°, ε2^*c*= 127(4)°, ε3^*a*= 135(3)°, ε3^*b*= 31(3)°, ε3^*c*= 91(2)° with $\varepsilon_1:\varepsilon_2:\varepsilon_3$ =1.57:1.29:1.00. The structural refinements, performed at 23, 600, 650, 700, 750, 800, 850, 900, 950, 1050 and 1200°C allowed the description of the structural evolution and the main *T*-induced deformation mechanisms.

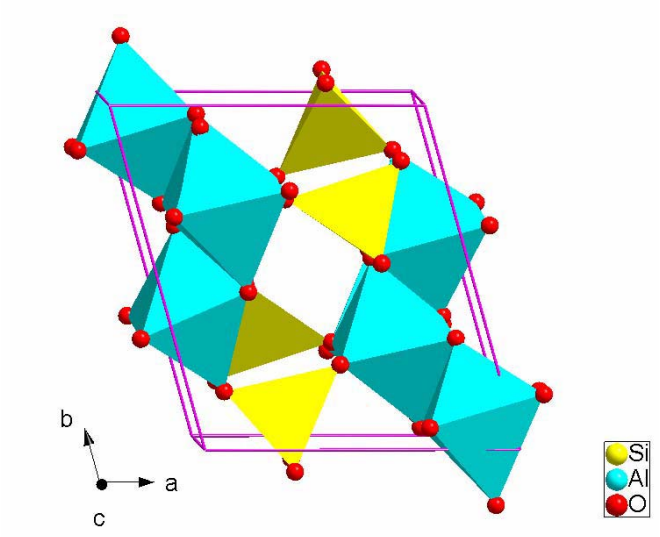


Fig. 1. The crystal structure of kyanite

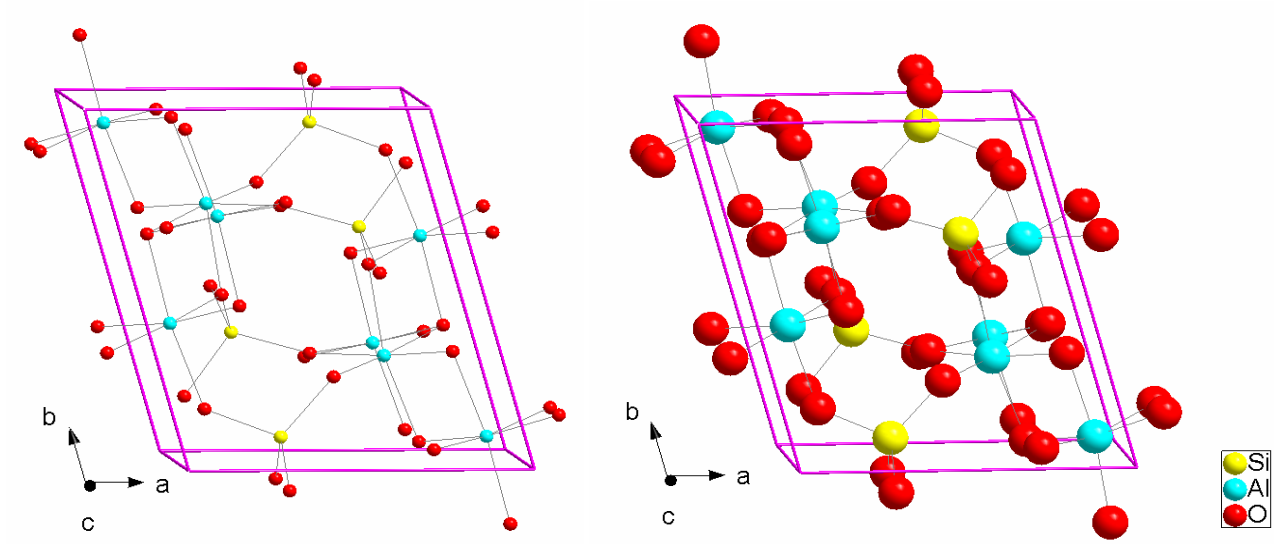


Fig. 2 . Clinographic view of the crystal strutture of kyanite based on the structure refinements at room and 1200°C

References

[1] Winter, J.K and Ghose, S. (1979) *American Mineralogist*, **64**, 573-586.
[2] Kerrick, D.M. (1990) Reviews in Mineralogy, Volume 22, *Mineralogical Society of America*, Washington, D.C., pp. 406.
[3] Bohlen, S.R., Montana, A. and Kerrick, D.M. (1991) *American Mineralogist*, **76**, 677-680.

Institut für Festkörperforschung
Forschungszentrum Jülich GmbH
D-52425 Jülich

Experimental Report
of Neutron Scattering Experiments
at the FRJ-2 Reactor

Proposal number:	SV7-05-001		
Experiment title:	**Texture of hematite ore deformed to high strains in torsion**		
Dates of experiment:	12 days	Date of report:	16.02.2006
Experimental team: Names	Addresses		
H. Siemes * B. Klingenberg	Institut für Mineralogie und Lagerstättenlehre RWTH-Aachen, D-52056 Aachen	* Förderung DFG Si209/36-1	
E. Rybacki M. Naumann	Geoforschungszentrum Potsdam Projektbereich 3.2: Rheology and Tectonophysics D-14474 Potsdam		
K. Kunze	Geologisches Institut, ETH-Zürich CH-8092 Zürich		
Local Contact:	J.M. Walter, E. Jansen		

Experimental report text body

Einführung

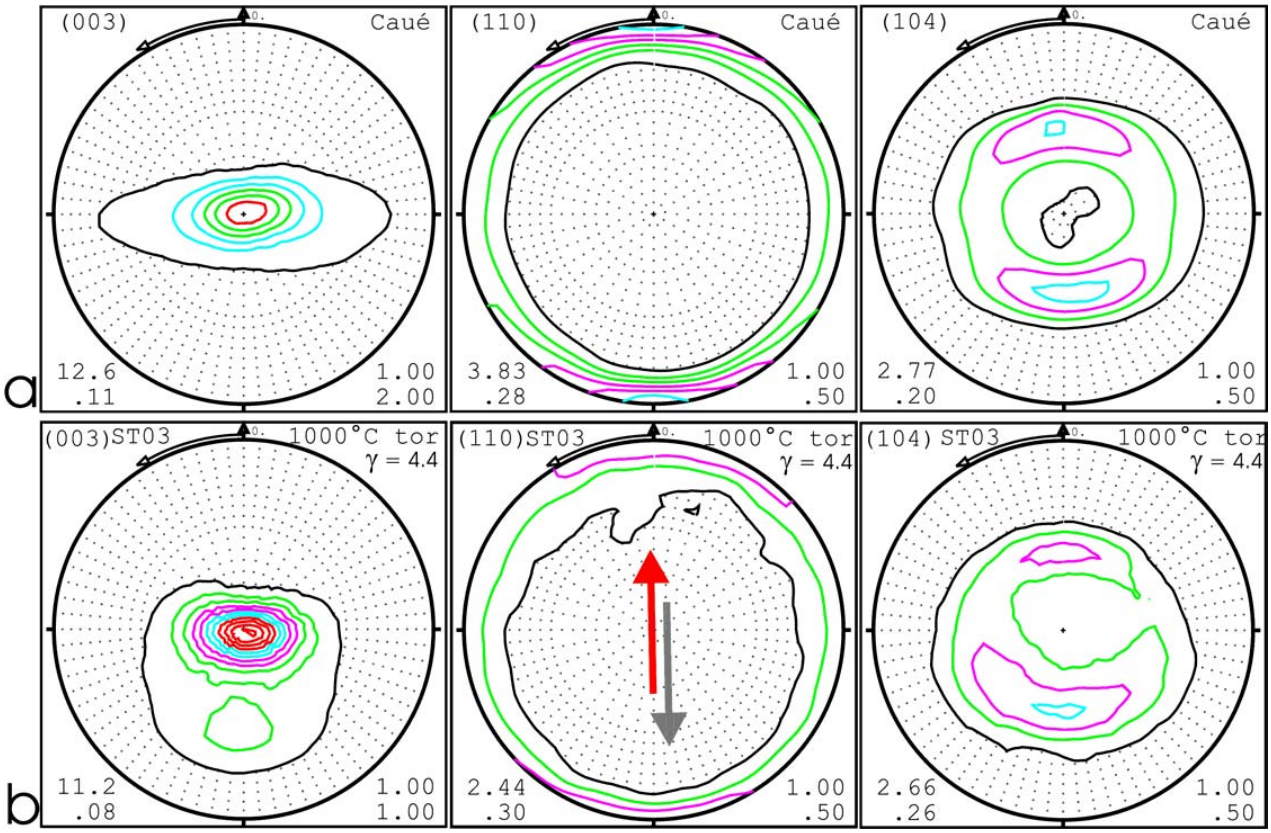
Die Beziehungen zwischen der Mikrostruktur und der kristallografischen Vorzugsorientierung (Textur) von Hämatiterzen des Eisernen Vierecks in Brasilien und von anderen Lokalitäten wurden in vielen Veröffentlichungen behandelt, z.B. Quade et. al. 2000, Rosière et al. 2001, Bascou et al. 2002. Polfiguren dieser Hämatiterze zeigen kreisförmige bis elliptische c-Achsen-Maxima, die um den Pol der Foliation liegen. Die Pole der Prismenflächen liegen auf Großkreisen in der Foliationsebene und die Maxima auf diesen fallen mit der Lineation zusammen (Abb. a). Die Entstehung dieser Regelung wird auf Scherverformungprozesse zurückgeführt. Bei experimentellen Stauchversuchen an polykristallinem Hämatit gab es Anzeichen der Bildung eines c-Achsenmaximums senkrecht zur Kompressionsrichtung (Siemes et al. 2003). Da jedoch zu vermuten war, dass Gleiten parallel zur Basis des Hämatits Ursache der Regelung ist, wurden Scherexperimente an polykristallinen Hämatitaggregaten konzipiert.

Konzeption der Versuche

Zunächst wurden drei Torsionsversuche in einer Hochdruck-Hochtemperatur-Apparatur (Paterson & Olgaard, 2000) konzipiert, um zu prüfen, ob und wie diese Versuche sich mit Hämatiterz realisieren lassen. Als Versuchsmaterial wurde ein Hämatiterz von Sishen, Südafrika, gewählt, das fast ungeregelt ist und eine Kristallitgröße von 5-60 Mikrometer aufweist (Siemes et al. 2003). Proben mit 14 mm Durchmesser und 10 mm Länge wurden für die Torsionsversuche hergestellt. Eine Schutzhülle aus Silber-Palladium in einem Eisenjacket, das die Probe vom Druckmedium Argon trennt, erwies sich als die geeignete Versuchsanordnung, um Hämatit mit nur geringer Magnetitbildung zu verformen. Bei Temperaturen von 1000°C bis 800°C wurden bei 400 MPa allseitigem Druck, mit einer Torsionsrate von $6*10^{-5}s^{-1}$ in 30-Stunden-Versuchen Scherverformungen von 3,8 bis 4,4 erreicht.

Erste Ergebnisse der Versuche bei 1000°C

Der Hämatit ist bei 1000°C zu einem gleichförmigen polygonalen Korngefüge rekristallisiert, das sich auch bei natürlich verformten Erzen findet. Die Korngrößen weisen dabei keine Unterschiede über die Probenquerschnitte auf, obwohl die finite Scherverformung von Null im Zentrum der Probe bis zum maximalen Wert an der Peripherie variiert. Neutronentexturmessungen (Jansen et al. 2000) im Probenbereich mit der stärksten Verformung ergaben für die (0003)-Polfigur ein zentrales, elliptisches Maximum im Pol der Scherebene. In der (11-20)-Polfigur befindet sich auf dem Grundkreis ein Maximum, das die Orientierung der Scherrichtung angibt. Die (10-14)-Polfigur, die zwei bananenförmige Maxima (Quade 1988) unterschiedlicher Höhe aufweist, lässt auf den Schersinn schließen (Abb. b). Diese Polfiguren stimmen weitgehend mit Polfiguren natürlich verformter Hämatiterze überein. Im Gegensatz zum homogenen Korngefüge besitzt die Textur einen grossen Gradienten von nahezu regellos im Zentrum (undeformiert) zu stark geregelt am Rand (maximaler Shear-Strain) wie EBSD-Messungen (Kunze et al. 1993) zeigen. Die Beobachtungen unterstützen die Vermutung, dass Hämatiterz bevorzugt durch Versetzungsgleiten auf {0001}<11-20> mit simultaner dynamischer Rekristallisation deformiert.



(0003)-, (11-20)- und (10-14)-Polfiguren a) natürlich verformtes Hämatiterz, Caué, Minas Gerais, Brasilien, b) experimentell verformtes Hämatiterz aus dem Randbereich der tordierten Probe, Polfiguren parallel zur Scherebene, Scherrichtung etwa NS, Schersinn N.

Danksagung

Die Autoren danken der Deutschen Forschungsgemeinschaft und den Mitarbeitern der beteiligten Institute.

Literatur

Bascou, J., Raposo, M.I.B., Vauchez, A., Egydio-Silva, M., 2002. Earth and Planetary Science Letters 198, 77-92.
Jansen, E., Schäfer, W., Kirfel, A., 2000. Journal of Structural Geology 22, 1559-1564.
Kunze, K., Wright, S.I., Adams B.L. and Dingley D.J., 1993. Textures and Microstructures 20, 41-54.
Paterson, M.S., Olgaard, D.L. 2000. Journal of Structural Geology 22, 1341-1358.
Quade, H., 1988. Textures and Microstructures, 8-9, 719-736
Quade, H., Rosière, C.A., Siemes, H., Brokmeier, H.-G., 2000. Zeitschrift für angewandte Geologie, Sonderheft 1, 155-162.
Rosière, C.A., Siemes, H., Quade, H., Brokmeier, H.-G., Jansen, E.M., 2001. Journal of Structural Geology 23, 1429-1440.
Siemes, H., Klingenberg, B., Rybacki, E., Naumann, M., Schäfer, W., Jansen, E., Rosière, C.A., 2003. J. Struct. Geol. 25, 1371-1391.

Institut für Festkörperforschung
Forschungszentrum Jülich GmbH
D-52425 Jülich

Experimental Report
of Neutron Scattering Experiments
at the FRJ-2 Reactor

Proposal number:	SV7-05-002		
Experiment title:	**Magnetic and Mineral Fabrics in Synthetic Marbles**		
Dates of experiment:	72 days	Date of report:	16.05.2006
Experimental team: Names	Addresses		
Leiss, Bernd Hirt, Ann Schmidt, Volkmar Piguet, P. Burlini, Luigi	Geowissenschaftliches Zentrum der Universität Göttingen (GZG) Abteilung Strukturgeologie und Geodynamik Goldschmidt Str. 3 D-37077 Göttingen Institut für Geophysik, ETH-Hoenggerberg, CH-8093 Zürich, Switzerland Geologisches Institut, ETH Zurich, CH-8092 Zürich, Switzerland		
Local Contact:	Jens M. Walter		

Experimental report text body

Introduction

The anisotropy of magnetic susceptibility (AMS) of rocks reflects the preferred orientations of minerals. Therefore AMS is a quick and easy way to characterize rock fabrics (Hrouda 1982, Borradaile 1988); the obtained result is also called the magnetic fabric of the rock. The method has been often used to measure the orientation of ferromagnetic minerals, mainly magnetite, but in recent studies it has been increasingly used to measure textures of paramagnetic minerals as phyllosilicates (Lüneburg et al. 1999, Cifelli et al. 2004). AMS of calcite textures A further application is the measurement of diamagnetic textures, especially calcite textures. Calcite is suitable for the AMS method, because it has a high magnetic anisotropy with the minimum susceptibility along the crystallographic c-axis. Therefore a preferred orientation of the c-axes, which can be induced by deformation, generates a magnetic fabric. The relationship between AMS and deformation of marbles has been investi- gated in laboratory (Owens & Bamford 1976) and field studies (de Wall et al. 2000). However, the diamagnetic fabric of calcite is relatively weak and easily overprinted by paramagnetic and ferromagnetic phases. In natural carbonate rocks the ferromagnetic and the paramagnetic subfabrics should be separated to assure a correct interpretation of the AMS. This separation can be made by torque measurements in high fields at different temperatures

Textures of artificial calcite-muscovite aggregates

To test how well AMS reflects the actual mineral texture, we produced a series of artificial calcite-muscovite aggregates. Powders made from Carrara marble and muscovite single crystals were mixed in different proportions and compacted uniaxially at room temperature to obtain a texture. The samples were further compacted hydrostatically to reduce the porosity and to improve the mechanical properties. The samples show a c-axis preferred orientation of the calcite and muscovite along the compaction direction (Fig. 1). The textures

were measured with different methods as AMS, X-ray diffraction and neutron diffraction and the results are compared. Sample volumes of more than 11 cm^3 were used to measure AMS as well as neutron diffraction; the same specimens could be used for both methods. Low- and high-field AMS measurements were made on all samples. The high-field measurements reflect more accurately the weak dia/paramagnetic fabrics. A nearly perfectly oblate AMS ellipsoid with minimum susceptibility axis sub-parallel to the compression direction developed even at very low pressures, and the principle axes of the AMS ellipsoid are co-axial with the calcite fabric ellipsoids. A general increase in AMS is observed with an increase in compaction. The quantitative correlation between the strength of the texture and the AMS will be investigated in the future. Moreover the separation of magnetic sub-fabrics will be tested on these artificial samples. The first results show that AMS can reflect the textures of the individual phases in a multiphase rock.

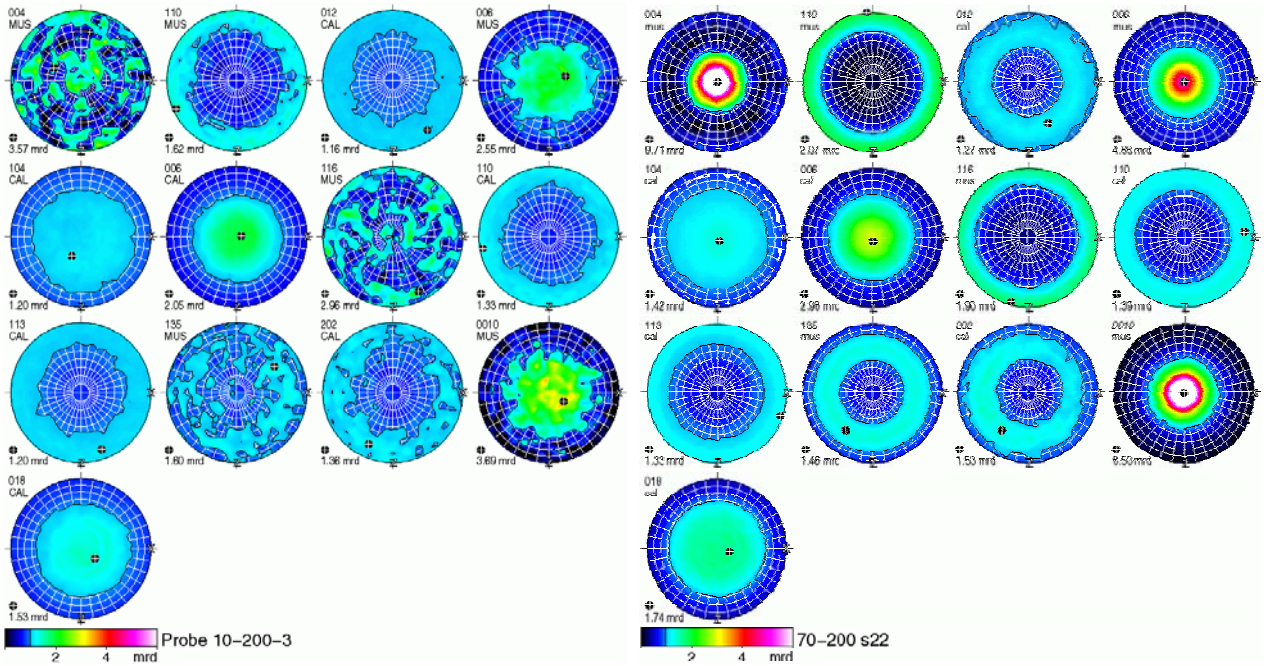


Figure 1: Examples of neutron diffraction pole figures (equal-area, lower hemisphere projection). Compaction direction is normal to the pole figure. Left: 10 % muscovite content, right: 70 % muscovite content

References:

Borradaile GJ (1988) Magnetic-susceptibility, petrofabrics and strain. Tectonophysics 156:1–20

Cifelli F, Mattei M, Hirt AM & Gunther A (2004) The origin of tectonic fabrics in 'undeformed' clays: The early stages of deformation in extensional sedimentary basins. Geophys Res Lett 31: Art. No. L09604

De Wall H, Bestmann M & Ullemeyer K (2000) Anisotropy of diamagnetic susceptibility in Thassos marble: A comparison between measured and modeled data. J Struct Geol 22:1761–1771

Hrouda F (1982) Magnetic-anisotropy of rocks and its application in geology and geophysics. Geophysical Surveys 5:37–82

Lüneburg CM, Lampert SA, Lebit HD, Hirt AM, Casey M & Lowrie W (1999) Magnetic anisotropy, rock fabrics and finite strain in deformed sediments of SW Sardinia (Italy). Tectonophysics 307:51–74

Owens BH & Bamford D (1976) Magnetic, seismic, and other anisotropic properties of rock fabrics. Phil Trans R Soc Lond Ser A 283:55–68

Institut für Festkörperforschung
Forschungszentrum Jülich GmbH
D-52425 Jülich

Experimental Report
of Neutron Scattering Experiments
at the FRJ-2 Reactor

Proposal number:	SV7-05-003		
Experiment title:	**Investigation of $La_{1-x}Sr_xMnO_3$ samples by powder diffractometer**		
Dates of experiment:	14.03.05-20.03.05	Date of report:	22.06.2006
Experimental team: Names	Addresses		
Eugene A. Gorelik	ISM, IFF, Forschungszentrum Jülich		
Local Contact:	Dr. Jens M. Walter		

Experimental report text body

Introduction

The aim of experiment was to check the results of preliminary measurements of LSMO samples made by SV7 and D20 (ILL) powder diffractometer. The strange behaviour of the temperature dependences of integral intensity were found in diffraction experiments made by D20 in Grenoble (see fig.1)

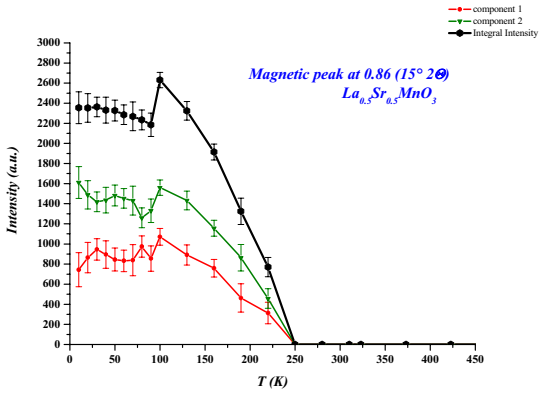


Fig. 1 Temperature dependence of integral intensity of peak (001)

Measurements and Results

Result from that it was interesting to make some new experiment to obtain answers to following questions:

1. Is this the real effect (visualisation of Jan-Teller effect) or it is an artefact of D20 powder diffraction machine (ILL)?
2. What are the exact temperatures of start and end points of effect?
3. How the curves behave around critical temperatures?

To find that information was decided to make neutron powder diffraction measurement of $La_{1-x}Sr_xMnO_3$ samples with x equally 50, 52.5, 55, 57.5 and 60% in a q-range from 0 to 3.5 and in the following temperature areas: 90 – 120 K (step 5 K), 190 – 280 K (step 10 K), 300 – 400 K (step 10 K). Also it was interesting to make preliminary measurements of two new samples with x equally 80 and 90% in a full range of q-values and temperatures.

We had some serious problems with the instrument during the measurements. It was not perfectly calibrate after re-equipment. As a result we had an extremely high background and some additional peaks on the pattern (see fig.2)

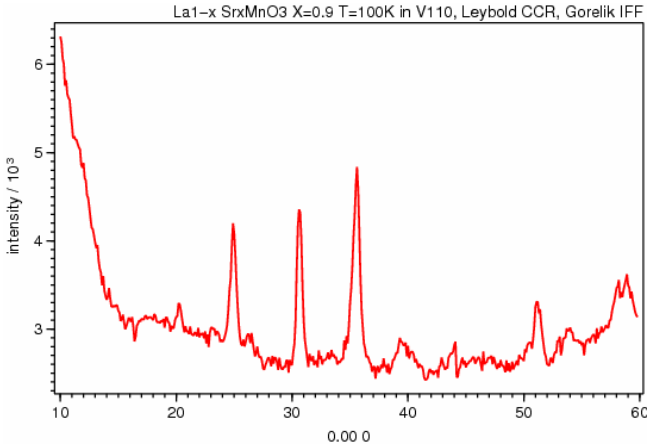


Fig.2 Neutron diffraction of LSMO sample x = 90%. T = 100 K duration of measurements 3 h.

At least only one sample (x = 90%) was measured. The results of this powder diffraction can not be used for following modelling and answers for the questions of experiment also could not be found. To obtain that answers was made another one experiment by DNS instrument. It shows that the gap in temperature dependence of integral intensity of LSMO samples is an instrumental artefact of D20 and does not connected with anyone physical effect.

Institut für Festkörperforschung
Forschungszentrum Jülich GmbH
D-52425 Jülich

Experimental Report
of Neutron Scattering Experiments
at the FRJ-2 Reactor

Proposal number:	SV7-05-004		
Experiment title:	**Neutron diffraction analysis of silver coins from the Himyarite-Sabean Empire**		
Dates of experiment:	34 days	Date of report:	17.05.2006
Experimental team: Names	Addresses		
Kirfel, Armin Kockelmann, Winfried, Yule, Paul	Mineralogisch-Petrologisches Institut der Universität Bonn Poppelsdorfer Schloss D-53115 Bonn Rutherford Appleton Laboratory, ISIS Facility, ROTAX, Chilton, Didcot, Oxon, OX11 0QX United Kingdom Völkerkundemuseum München		
Local Contact:	Jens M. Wa.lter, R. Skowronek		

Experimental report text body

Introduction

The Himyarite, later Himyarite-Sabean empire in the southern part of the Arabic peninsula lasted from about the first century A.D. till the end of the sixth century when it fell under the control of the caliphate of Medina. During the period of its existence coins were issued typically of 10 - 15 mm diameter and carrying heads as motifs on both sides. These coins are expected to consist of pure silver, and the peculiar shape of them, i.e. their irregular and concave (scaphate) appearance (Fig. 1), implies that their patterns were not prepared by casting in a mould, but rather by striking or deep-drawing with mechanical force. Other coins are flat and exhibit bubbles which indicate casting. Although the coins significantly testify to a period during which little real historic information is available, surprisingly they have never been studied fully so far, e.g. by means of physical methods. It is the aim of our study to non-destructively determine the metallurgical composition, e.g. the phase abundance of Ag and eventually other metals like Cu, and to obtain information about the manufacturing methods, both also as a function of age.



Fig. 1) Examples of himyarite silver coins: flat with bubbles (left) and concave (right)

Measurements and Results

In order to assess these questions, 10 coins of different ages and locations have been selected from the collection held by the Staatliche Museum für Völkerkunde in Munich in order to determine their phase compositions by neutron diffraction. This is the only appropriate technique if the object(s) of interest are not to be damaged at all by the very method of investigation. Furthermore neutron diffraction was chosen as the appropriate method to obtain data from the complete sample volume. Additionally density measurements have been conducted and correlated to the phase refinements from the neutron powder diffraction data.

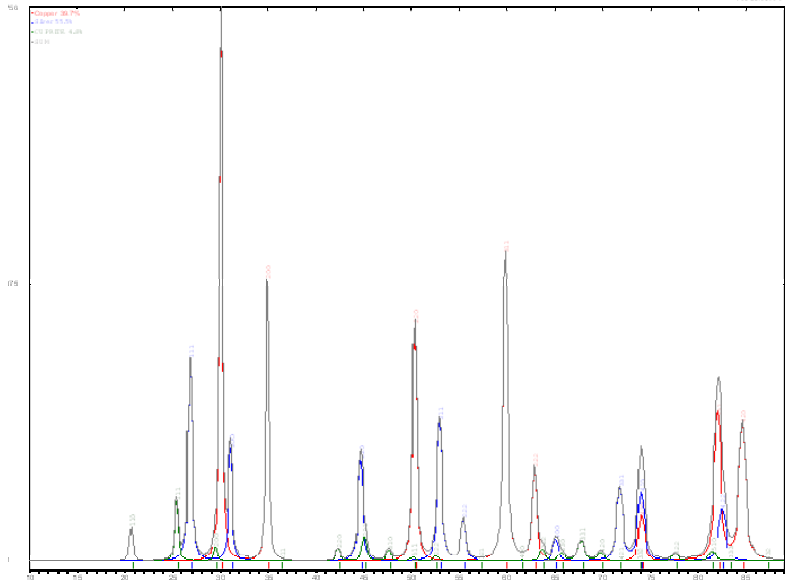


Fig. 1: Rietfeld refinement of silver coin for phase compositions

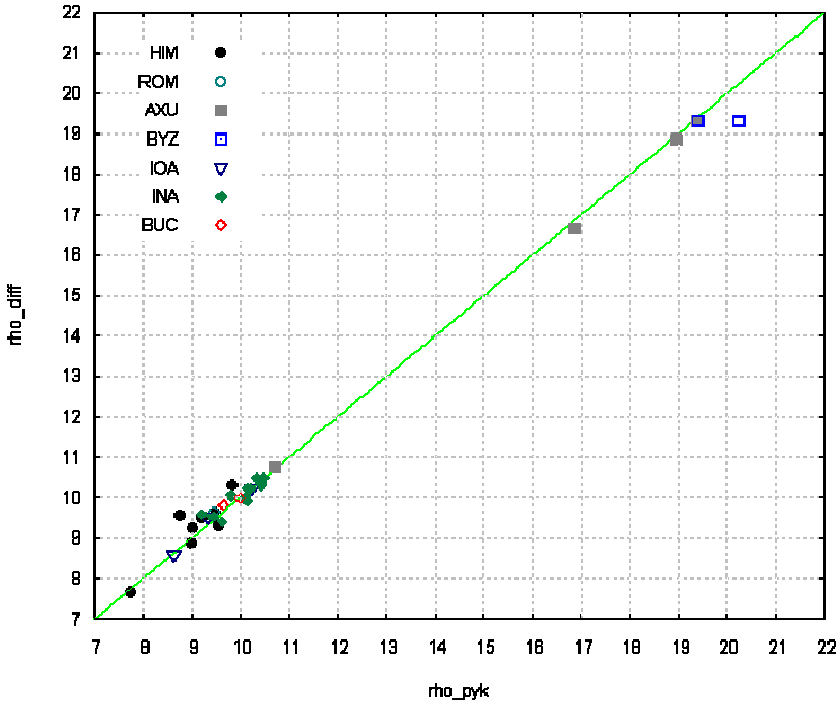


Fig. 2: Density measurements correlated with phase analysis

Institut für Festkörperforschung
Forschungszentrum Jülich GmbH
D-52425 Jülich

Experimental Report
of Neutron Scattering Experiments
at the FRJ-2 Reactor

Proposal number:	SV7-05-005		
Experiment title:	**Crystal fabric of lava flows and domes by textural neutron diffraction analysis**		
Dates of experiment:	30.08.05, 12.01.06 18.04.06-26.04.06	Date of report:	12.04.2006
Experimental team: Names	Addresses		
Fiori, Fabrizio Albertini, Gianni Iezzi, Gianluca Ventura, Guido	Dipartimento di Scienze Applicate ai Sistemi Complessi, Sez. Scienze Fisiche – Università Politecnica delle Marche, Via Brecce Bianche, 60131 Ancona (Italy) Dipartimento di Fisica e Ingegneria dei Materiali e del Territorio – Università Politecnica delle Marche, Via Brecce Bianche, 60131 Ancona (Italy) Dip. Scienze della Terra, Università di Chieti (Italy) Osservatorio Vesuviano, Ercolano, Napoli (Italy)		
Local Contact:	Dr. Jens M. Walter, E. Jansen R. Skowronek		

Experimental report text body

Introduction

For the fabric determination and its variation on different volcanic rocks it is important to obtain important insights on the kinematical processes underwent by both lavas and pyroclastic flows, during their ascent and emplacement processes across and on the Earth (Smith, 2002). Basically crystals can be regarded as passive strain markers for both diluite (not-interacting) crystal-poor bearing lavas (Manga, 1998; Castro et al., 2002; Iezzi and Ventura, 2002; Canon-Tapia and Castro, 2004) or (small to strong) interacting crystal-bearing lavas (Shelley, 1985; Wada, 1992; Ventura et al., 1996). The theoretical assumption to use crystals as passive strain markers implies, that they must be undeformable and not-growing solid particles during magma deformation. The spatial alignment of crystals can therefore to be used such to reconstruct the strain path underwent by a lava and/or pyroclastic rocks during their emplacement.

Measurements and results

Since long time the determination of volcanic crystal fabric has been mainly carried out using microscopic (optical and electronic) observations and AMS measurements. Taking in account that, we have carried out several neutron texture diffraction experiments at the SV-7 diffractometer, with twofold aims: a) introduce a new and completely independent analytical tool for crystal fabric determination in the modern volcanology science and b) to elucidate the crystal fabric parameters of several (mainly effusive) volcanic rocks.

Thus crystal fabric analysis allows to constraint and in principle also to reconstruct the deformation path suffered by a lava or by a smaller portion of it. Anyway despite its potential applications, its use have been relatively poor adopted for volcanic rocks. The few studies which report crystal fabric analyses for effusive magmatic rocks have been carried out using optical thin section observations or AMS measurements. However

all these studies take advantages from particular and extreme favourable situation of cropping exposure, such as the possibility to determine the section containing the shear direction or the shear plane (Ventura et al., 1996) or the situation on which is possible to reconstruct the crystal orientation in space due to the extremely low crystallinity of the rocks and also to their smaller dimensions (tens of μm) (Manga, 1998; Castro et al., 2002; Canon-Tapia and Castro, 2004). Moreover AMS data can be used only for certain mineral association, as a function of their chemistry and their spatial arrangements (continuous *vs.* not-continuous network Fe-bearing phases).

By contrast, neutron diffraction crystal textural analysis can be used for most types of volcanic rocks. It has the advantage to analyse a large rock volume (order of cm^3 units) directly in 3D and to be selective for any mineral phase hosted in the rock specimen under investigation (Schäfer, 2002). For the fabric determination is it is of capital importance to constraint and link the measured crystallographic orientation (CPO) for each mineral phase (see Fig. 1) with the crystal shape orientation in the rock. In any case is important to stress that the majority of silicate magmatic minerals have crystal shapes currently from medium to high anisotropic. Thus is generally rather easy to determine which crystal direction correspond to a well determined crystallographic direction.

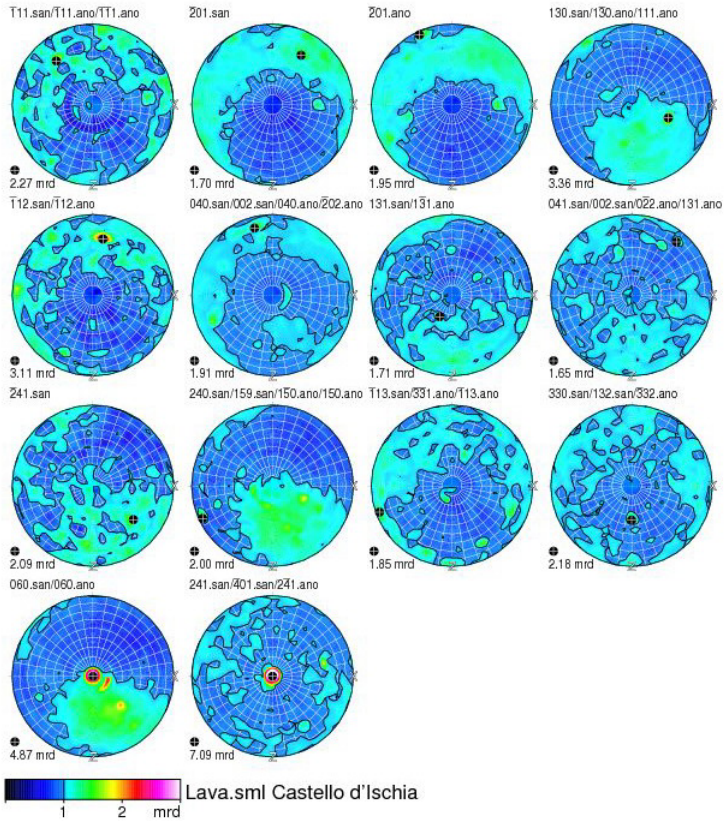


Fig.1 Texture measurement of a lava from Castello d'Ischia

References

[1]Canon-Tapia E., Castro J. (2004). Journal of Volcanology and Geothermal Research, 134: 169-182.
[2]Castro J., Manga M., Cashman K. (2002). Earth and Planetary Science Letters, 199: 211-226.
[3]Iezzi G., Ventura G. (2002). Earth and Planetary Science Letters, 200: 33-46.
[4]Manga M. (1998). Journal of Volcanology and Geothermal Research, 86: 107-115.
[5]Schäfer W. (2002). European Journal of Mineralogy, 14: 263-290.
[6]Shelley D. (1985). Journal of Volcanology and Geothermal Research, 25: 69-79.
[7]Smith J.V. (2002). Earth-Science Reviews, 57: 279-297.
[8]Ventura G., De Rosa R., Colletta E., Mazzuoli R. (1996). Bulletin of Volcanology, 57: 555-562.
[9]Wada Y. (1992). Journal of Volcanology and Geothermal Research, 49: 119-126.

Institut für Festkörperforschung
Forschungszentrum Jülich GmbH
D-52425 Jülich

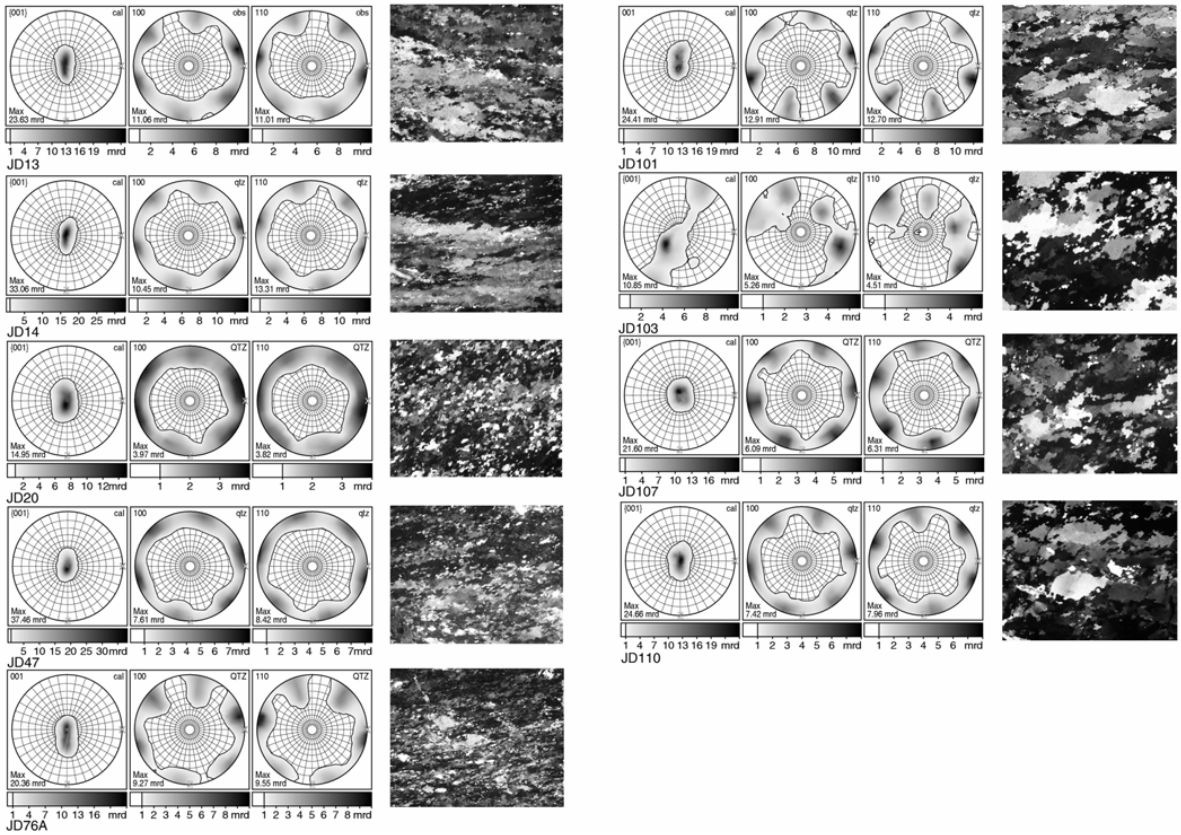
Experimental Report
of Neutron Scattering Experiments
at the FRJ-2 Reactor

Proposal number:	SV7-05-006		
Experiment title:	**Neutron texture goniometry on quartzitic mylonites of a Permian detachment fault at the base of the Collio basin, northern Italy**		
Dates of experiment:	04.03.05-07.03.05 23.06.05-27.06.05 19.08.05-20.08.05	Date of report:	14.06.2006
Experimental team: Names	Addresses		
N. Froitzheim J.F. Derks	Geologisches Institut der Universität Bonn, Nußallee 8, D-53115 Bonn		
Local Contact:	J.M. Walter		

Experimental report text body

In the area of the Alpine Orobic anticline (Southern Alps), a large-scale extensional detachment fault was identified that separates Hercynian basement in the core of the anticline from overlying Permian clastic sediments and volcanic rocks (Collio Formation). The basement consists mainly of paragneiss (Morbegno gneiss) which is intruded by plutons, known as Val Biandino Granodiorite and Valle Biagio Granite. The emplacement of plutons was probably coeval with and genetically related to deposition of volcanics in the Collio Formation in the late Sakmarian to middle Artinskian, c. 287-280 Ma ago.The Collio Formation is everywhere in the study area separated from the basement by a layer of cataclasite. The Morbegno Gneiss underlying the cataclasite is a mylonite with a strong foliation and lineaton. The foliation is parallel to the cataclasite layer and therefore also to the basement/Collio contact. The intensity of the mylonitic deformation is strongest near the top and decreasing downward. The thickness of the mylonitic zone is about 100 metres. The Val Biandino Granodiorite is partly affected by the same mylonitisation as the Morbegno Gneiss, but also contains locally mylonite xenoliths. These observations indicate overall contemporaneity between mylonitisation and granodiorite intrusion.
Mylonitisation happened under higher greenschist-facies conditions near the intrusions, and under lower greenschist-facies conditions away from them (biotite and chlorite zone, respectively). While plagioclase is only brittlely deformed, quartz is always dynamically recrystallised. In some samples, quartz grain shapes suggest recrystallisation by grain-boundary migration (e.g., sample JD 103). Other samples have a uniform, very small grain size, suggesting subgrain rotation as the dominant recrystallisation mechanism (e.g., sample JD 20). In thin sections parallel to the X-Z plane of the finite strain, abundant shear-sense criteria indicate top-to-the-SE shearing, both in the biotite zone and the chlorite zone mylonites. Textures of nine almost monomineralic quartz mylonites have been analysed. All diagrams are upper-hemisphere Wulff projections. All textures except one (JD 103) are very similar and surprisingly clear and regular. {c} forms a single

maximum parallel to the foliation and perpendicular to the stretching lineation, i.e. parallel to the strain Y axis. This maximum is strong and partly round, partly slightly elongated in the plane perpendicular to the stretching lineation. The shear sense is given by the {m} and {a} pole figures. Both {m} and {a} pole figures show three maxima distributed on a great circle parallel to the X-Z plane. These maxima are not symmetric with respect to the foliation trace, but rotated anticlockwise in the case of {m} and clockwise in the case of {a}. The strongest of the {a} maxima, representing the dominant slip direction, is rotated about 10° to 20° clockwise from the stretching direction. The textures are clear evidence for predominant prism <a> slip. The obliquity indicates dextral (top-to-the-SE) shear sense. Prism <a> slip becomes dominant in quartz mylonites under temperatures above c. 500° C. Temperatures above 500° C during the mylonitisation of the Morbegno gneiss are in line with the observed stability of biotite. As demonstrated above, the mylonitic shearing was broadly synintrusive. Therefore, heat from the rising melt body may have caused the elevated temperatures. JD 103 is the only sample with a different texture. The thin section shows strongly sutured and interlocking quartz grain boundaries suggestive of grain-boundary migration recrystallisation. Biotite is completely replaced by chlorite, whereas it was stable during deformation in the other samples. In JD 103, {c} is distributed on an oblique single girdle suggesting top-to-the-SE shearing. Two maxima are on this girdle, one near the periphery, and a stronger one about 40° away from the centre of the pole figure. The weaker {c} maximum close to the periphery may result from the activity of basal <a> slip. In this case, the texture may represent deformation under lower temperatures than for the other samples, which is in line with the observed replacement of biotite by chlorite.
The fault marked by the cataclasite layer at the basement/Collio contact accommodated strong exhumation of the footwall: It juxtaposes footwall mylonites initially deformed under high temperatures (above c. 500° C) against hanging-wall volcanics erupted at Earth's surface. We therefore interpret the fault as an extensional detachment fault and call it "Grassi detachment fault". The mylonites formed during an early stage of its activity. They were transported upward by the continuing tectonic unroofing of the footwall as a metamorphic core complex. Therefore we assume that the brittle Grassi detachment fault had the same kinematics, top-to-the-SE, as the mylonites.



Institut für Festkörperforschung
Forschungszentrum Jülich GmbH
D-52425 Jülich

Experimental Report
of Neutron Scattering Experiments
at the FRJ-2 Reactor

Proposal number:	SV7-05-007		
Experiment title:	**Pilot-Studie für Neutronentexturgoniometrie-Messungen an ultramafischen Gesteinen**		
Dates of experiment:	08.03.05-09.03.05	Date of report:	11.05.2006
Experimental team: Names	Addresses		
Grimmer, Jens Leiss, Bernd	Geologisch-Paläontologisches Institut, Ruprecht-Karls-Universität Heidelberg, Im Neuenheimer Feld 234, D-69120 Heidelberg Geowissenschaftliches Zentrum der Universität Göttingen (GZG) Abteilung Strukturgeologie und Geodynamik Goldschmidt Str. 3 D-37077 Göttingen		
Local Contact:			

Experimental report text body

Einleitung und Fragestellung

Ultramafische Gesteine in hochgradig metamorphen Kristallindecken von Kollisionsorogenen sind wichtige Indikatoren dafür, dass die Versenkung kontinentaler Krustengesteine bis in den oberen Mantel erfolgte. Diese ultramafischen Gesteine wurden vermutlich während der Subduktion bzw. der Exhumierung tektonisch in die Krustengesteine eingeschuppt. Die wahrscheinlich auftriebsgesteuerte Exhumierung dieser Kristallingesteine bringt dabei Fragmente des lithosphärischen Mantels in krustale Niveaus. Texturelle Untersuchungen an diesen Mantelgesteinen geben wesentliche Aufschlüsse über Deformationsmechanismen, -richtungen und -temperaturen, die wiederum wichtige Informationen über die orogenen Prozesse liefern.

Die untersuchte Probe 005b stammt aus einem dunitischen Bereich des Kittelfjäll-Peridotit, der linsenförmig in einer Kristallindecke aus Gneisen, Glimmerschiefern und Amphiboliten Platz genommen hat. Diese Kristallindecke gehört zur Seve-Einheit der schwedischen Zentralkaledoniden. Die Kristallingesteine der Seve-Einheit repräsentieren den ehemaligen distalen passiven Kontinentalrand Balticas, der im frühen Paläozoikum subduziert und nachfolgend exhumiert wurde.

Die Analyse der kristallographischen Vorzugsorientierung der Probe 005b mit der Neutronentexturgoniometrie dient einerseits der Quantifizierung der Olivin-Textur sowie andererseits dem Vergleich mit AMS-Messungen. Der Zusammenhang zwischen dem gesteinsmagnetischen Gefüge und kristallographischen Vorzugsorientierungen ist weder qualitativ noch quantitativ verstanden und ein wesentliches methodisches Ziel. Die Anwendung der Neutronenbeugung ist bei dieser Probe Voraussetzung, da sie Korngrößen bis zu 1 mm aufweist.

Ergebnisse

Die Ergebnisse der Neutronentexturgoniometrie-Messungen und der Gesteinsmagnetik sind in Abb. 1, 2 und 3 dargestellt. Die Neutronentexturgonio-metrie-Messungen ergeben eine deutliche kristallographische

Vorzugsorientierung (Abb. 1). Es zeigt sich eine sehr gute Übereinstimmung der (100)-Richtung mit der Richtung der größten Hauptsuszeptibilität (k_{max}) bzw. der (001)-Richtung mit der Richtung der kleinsten Hauptsuszeptibilität (k_{min}). Die Ergebnisse zeigen eine signifikante kristallplastische Deformation, die sich durch Neutronentextur-goniometrie-Messungen und gesteinsmagnetische Methoden quantifizieren lassen. Für weitere und tiefer gehende quantitative Vergleiche zwischen beiden Methoden sowie eine regionalgeologisch-tektonische Interpretation ist allerdings ein wesentlich umfangreicherer Datensatz notwendig.

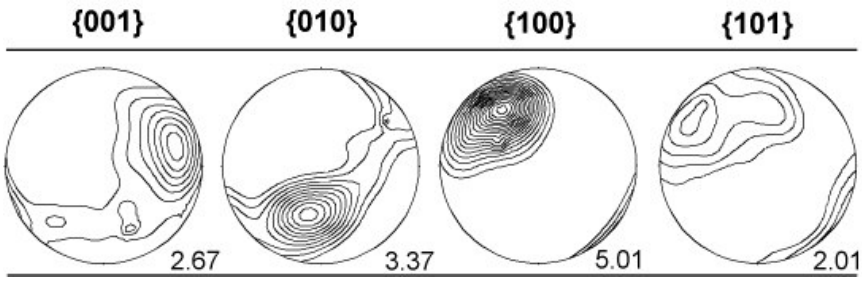


Abb. 1: Polfiguren der Probe 005b. Die quantitative Textur wurde auf Basis der experimentellen Polfiguren mit Hilfe der Texturkomponentenmethode bestimmt.

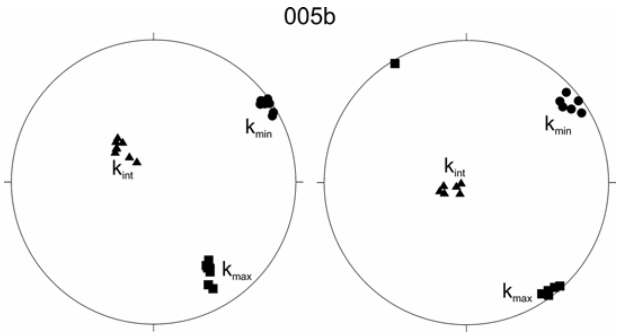


Abb. 2: Die Hauptsuszeptibilitäten (k_{max}, k_{int}, k_{min}) der Probe 005b wurden bei Raumtemperatur (links) und bei niedrigen Temperaturen (rechts), d.h. Temperaturen unterhalb des Verwey-Übergangs (<-155°C) gemessen. Die Tieftemperaturmessung diente zur Hervorhebung des paramagnetischen Olivin-Gefüges, da aufgrund geringer retrograder Überprägung Magnetit gebildet wurde, dessen Einfluss auf das Gesamtgefüge (links) hierdurch nahezu eliminiert werden konnte.

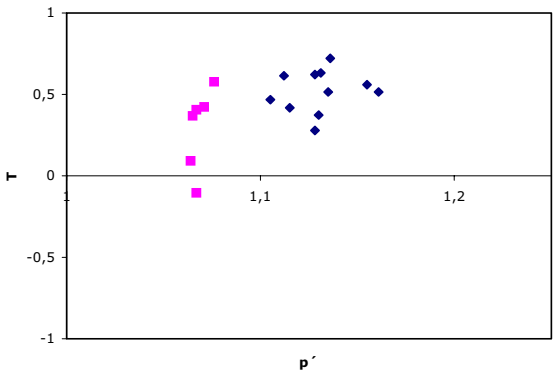


Abb. 3: Jelinek-Diagramm der Probe 005b mit Angabe von Formfaktor T und dem korrigierten Grad der Anisotropie der magnetischen Suszeptibilität P´. P´ streut wesentlich geringer, wenn der Einfluss des ferrimagnetischen Magnetits unter niedrigen Temperaturen (<-155°C) nahezu eliminiert ist. Insgesamt ist P´ mit Werten von 1,064 bis 1,076 relativ gering.

Institut für Festkörperforschung
Forschungszentrum Jülich GmbH
D-52425 Jülich

Experimental Report
of Neutron Scattering Experiments
at the FRJ-2 Reactor

Proposal number:	SV7-05-008:		
Experiment title:	Neutron Diffraction on new Carbodiimides		
Dates of experiment:	21.04.05-25.04.05 09.05.05-12.05.05 25.10.05-01.11.05 12.12.05-13.12.05 13.02.06-16.02.06	Date of report:	28.6.2006
Experimental team: Names	Addresses		
Dr. Müller, Paul Prof. Dr. R. Dronskowski, Dr. Liu, Xiaohui	Institut für Anorganische Chemie der RWTH Aachen Landoltweg 1, 52056 Aachen		
Local Contact:	Dr. Jens M. Walter		

Experimental report text body

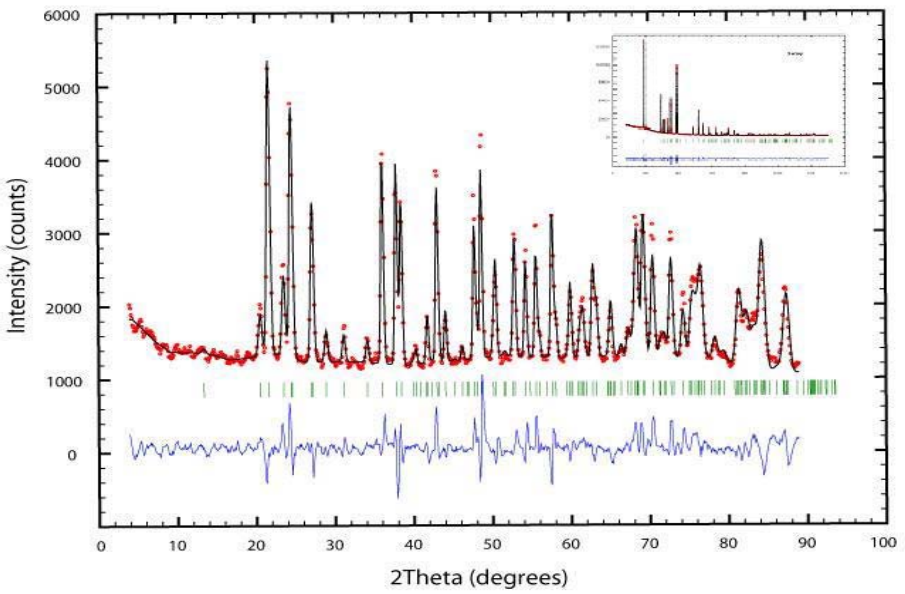
Neutron data on a powdered sample of CuNCN were collected using the SV7 diffractometer with λ = 1.09590 Å radiation. The crystal structure eventually arrived at is based on a Rietveld refinement with a data set of 138 reflections using a Gaussian profile for temperatures of 293 and 4 K. The residual values referring to the data from 4 K and 293 K arrive at 0.050/0.044 (R_p), 0.068/0.063 (R_{wp}), and 0.11/0.13 (R_{Bragg}) for a total of 14 variables. The final structural parameters are given in Table 1 while an overview of the Rietveld refinement at 4 K is shown in Figure 1.

The crystal structure of CuNCN derived from neutron diffraction corroborates the earlier X-ray diffraction analysis [1]. The Cu^{2+} ions form cationic sheets parallel to the *ab* face. Each Cu^{2+} ion is coordinated by six nitrogen atoms in the spirit of a typical first-order Jahn–Teller effect. The NCN^{2-} units run parallel with the *c* axis. The volume of the unit cell decreases slightly with temperature, which indicates that no structural phase transition happens down to 4 K. The complex anion is practically linear (N–C–N = 177.4(9)°) with approximate $D_{\infty h}$ symmetry at 4 K but slightly more bend (N–C–N = 173.2(9)°) at 293 K which stands for C_{2v} symmetry but is still very close to $D_{\infty h}$. All bond lengths and angles are apparently unaffected by changes in temperature.

Table 1. Structural parameters and conventional reliability factors for CuNCN at temperatures of 4 K and 293 K obtained from the Rietveld refinement of the neutron powder diffraction data.

	$T = 4$ K	$T = 293$ K
Space group	*Cmcm*	*Cmcm*
a (Å)	2.9916(5)	2.9915(5)
b (Å)	6.1482(9)	6.191(1)
c (Å)	9.406(1)	9.411(1)
V (Å^3)	173.01(4)	174.27(5)
Cu on 4*a* (0, 0, 0)		
B_{iso} (Å^2)	0.58(7)	1.63(9)
N on 8*b* (0, *y*, *z*)		
y	0.3802(7)	0.3806(7)
z	0.3810(4)	0.3808(4)
B_{iso} (Å^2)	1.02(5)	1.79(6)
C on 4*c* (0, *y*, 1/4)		
y	0.3847(15)	0.3925(14)
B_{iso} (Å^2)	0.80(9)	1.4(1)
R_p, R_{wp}, R_{Bragg}:	0.050, 0.068, 0.11	0.044, 0.063, 0.13

Fig. 1. Observed, calculated, and difference intensities for the neutron-diffraction Rietveld refinement of CuNCN at 4 K. The vertical markers show the positions of the Bragg reflections used to simulate the pattern and right above is the XPD refinement.



References

[1] X. Liu, M. Wankeu, H. Lueken, R. Dronskowski, Z. Naturforsch. **60b**, 593-596 (2005).

Institut für Festkörperforschung
Forschungszentrum Jülich GmbH
D-52425 Jülich

Experimental Report
of Neutron Scattering Experiments
at the FRJ-2 Reactor

Proposal number:	SV7-05-010		
Experiment title:	**Extinction measurements on high purity copper**		
Dates of experiment:	15.08.05-28.08.05 02.09.05-03.09.05 05.10.05	Dates of experiment:	14.12.2005
Experimental team: Names	Addresses:		
Jesús Palacios G.	Escuela Superior de Física y Matemáticas Instituto Politécnico Nacional Edif.. 9 de la UP ALM Av. Instituto Politécnico Nacional S/N 07739 México City		
Local Contact:	Dr. Jens Walter, Ekkehard Jansen, Rolf Skowronek		

Experimental report text body

Introduction

Primary and secondary extinction in X-ray and neutron diffraction of crystals has been widely investigated since it affects measurements intended to determine crystal structures, including charge densities and thermal parameters. Extinction is present also in diffraction of polycrystals, especially when annealed and with high texture intensity. However, there have been only a few systematic studies aimed to determine the extent of its influence. For the quantitative texture analysis this is important. Thus, the aim of this investigation is to quantify the influence of this phenomenon for the special case of pure cold rolled and also recrystallized copper samples. Here the results of 96% cold rolled and annealed high purity copper samples are reported.

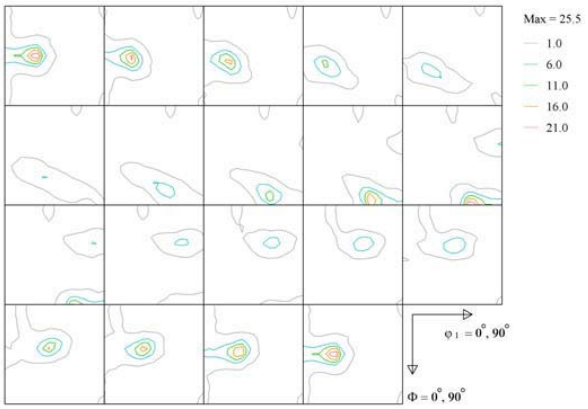
Measurements and Results

In the first sample, due to its deformed condition, coherent domains are small and do not contribute to primary extinction and thus we expect mainly secondary extinction. In the annealed sample primary extinction could also be present.

As well known, primary and secondary extinction affect strong reflections more strongly, and so, a difference should be observed when the Orientation Distribution Function (ODF) obtained through strong reflections ((111), (200) and (311)) and that obtained from weaker reflections ((220), (222) and (331)) are compared. Extinction also depends on wavelength and here it is also intended to search if this effect is also observable. Pole figures (111), (200), (220), (222), (311), (331), (400), (420), (422), (440), (531) and (620) were measured with wavelength $\lambda_1 = 2.332$ Å, $\lambda_2 = 1.166$ Å and $\lambda_3 = 0.777$ Å. Unfortunately intensities for the latter were small and statistically not relevant for high Miller index reflections, i.e. from reflection (331) on. Partial or total peak overlapping also prevented the use of large Miller index reflections with λ_2 for ODF evaluation. With the first wavelength only the first two reflections could be measured. Overlapping of reflections could be partially

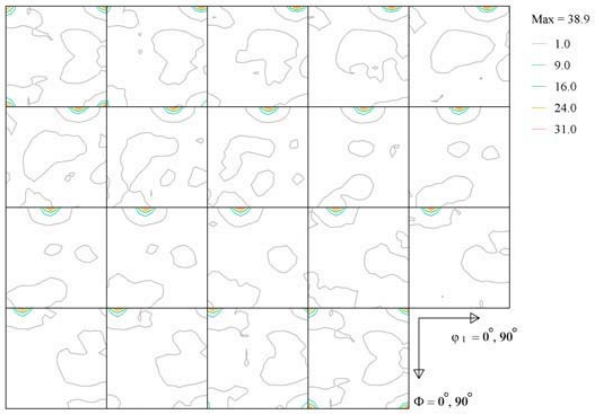
avoided by the use of a graphite filter.
According to the value of the position angle Ω of the Eulerian Cradle, a given reflection angle 2θ can appear at a lower or at a higher angle than Ω, or coincide with it. A comparison of these equivalent ODFs obtained by pole figures measured with λ_2 from reflections (111), (200) and (311), allow a consistency test and a measure of the accuracy of our measurements. In our case this was of the order of 5%. A comparison of these ODFs with the one obtained with λ_3 for the deformed sample gave a difference of 6%, which is actually within the measuring error range. An ODF from high Miller indexes however could not be obtained for the cold rolled sample, due to the low available intensities. The annealed sample shows a strong cubic texture, and when measured with λ_3, a 30% increment of pole density could be observed between the ODFs determined from low intensity reflections and strong reflections. Such a large increase in pole density is not likely to be caused by secondary extinction alone. Also an increase of 11% could be observed when compared with corresponding λ_2 values. Fig. 1 shows the ODF measured with λ_2 when each used reflection coincided with Ω. Figs. 2 show the ODFs with λ_3 for the annealed sample, from strong reflections (Fig. 2a), and from weak reflections (Fig. 2b). Fig.3 shows the ODFs with λ_2 for the annealed sample, from strong reflections.
Although further evaluations are needed, it can be concluded that:

a) For low or moderate texture, wavelength dependence lies within error range. For strong texture, it amounts to 11%.
b) Due to the large pole density values obtained from weak reflections, as compared with those obtained from strong reflections, primary, as well as secondary extinction are present in the strong reflections.



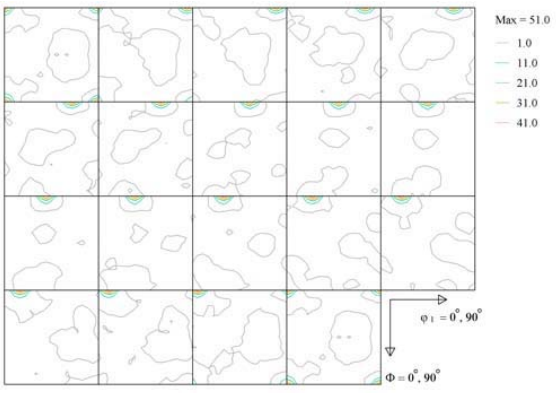
2EQ

Fig. 1. ODF of 96% cold rolled sample obtained with λ_2 from reflections (111), (200) and (311).



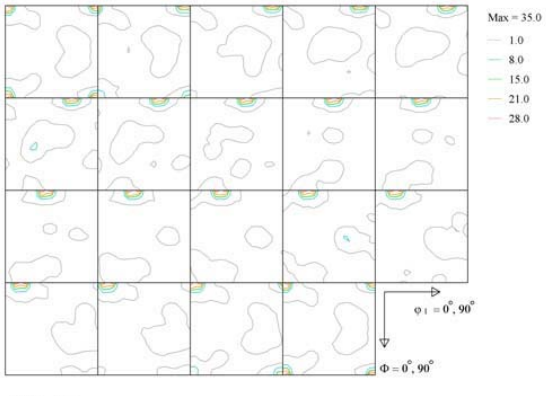
3NE_AN

Fig.2 a) ODF of annealed sample obtained with λ_3 from strong reflections



3NE_HI_AN

Fig. 2 b). ODF of annealed sample obtained with λ_3 from weak reflections



2EQ_AN

Fig. 3. ODF of annealed sample obtained with λ_2 from strong reflections

Institut für Festkörperforschung
Forschungszentrum Jülich GmbH
D-52425 Jülich

Experimental Report
of Neutron Scattering Experiments
at the FRJ-2 Reactor

Proposal number:	SV7-05-011		
Experiment title:	**Neutron diffraction study of the NaNbO3 submicron powder**		
Dates of experiment:	29.08.05-02.09.05 27.09.05-06.10.05	Date of report:	29.06.2006
Experimental team: Names	Addresses		
Pithan, Christian Shiratori, Yosuke Magrez, Arnauld	IFF, Forschungszentrum Jülich Laboratory for Nanostructures and Novel Electronic Materials Institute of Physics and Complex Matter École Polytechnique de Lausanne		
Local Contact:	Dr. J. M. Walter		

Experimental report text body

As indicated in the original proposal, particle size-induced phase transitions in the $(K_xNa_{1-x})NbO_3$ powders have to be clarified. So far size-induced phase transitions in $(K_{0.5}Na_{0.5})NbO_3$ and $NaNbO_3$ powders have been reported, respectively [1,2].

1. Temperature tuning neutron diffraction study for $(K_{0.5}Na_{0.5})NbO_3$

$(K_{0.5}Na_{0.5})NbO_3$ transforms from a monoclinic symmetry (M type structure) towards a triclinic one (T type structure) by reducing the particle size below a critical size of 100nm. This feature is surprisingly accompanied by an expansion of the lattice. From XRPD refinements, several space groups are possible for both symmetries (P2 or Pm for M type and P1 or P-1 for T type) when refining the crystal structure. Raman spectroscopy and nuclear site group analysis of the Raman active normal modes supported P1 as possible space group for fine powders while this method was not sufficient to extract the true space group for the coarse powder, M type structure [1]. As reported in the FRJ-2 Experimental Reports 2004 [3], refinements of the neutron diffractions concluded Pm and P1 to be the more suitable space groups for the M and T type structures, respectively.
Results: Neutron diffraction patterns, which have been recorded for both types of powders at various temperatures (-150 – 800 °C), were analyzed. We could see successive structural phase transitions for both powders. For the coarse powder (particle size > 200 nm), a drastic spectral change corresponding to the transition from monoclinic to cubic phases was confirmed at around 450 °C. On the other hand, phase transition behavior for the fine powder (particle size < 200) was more diffused.

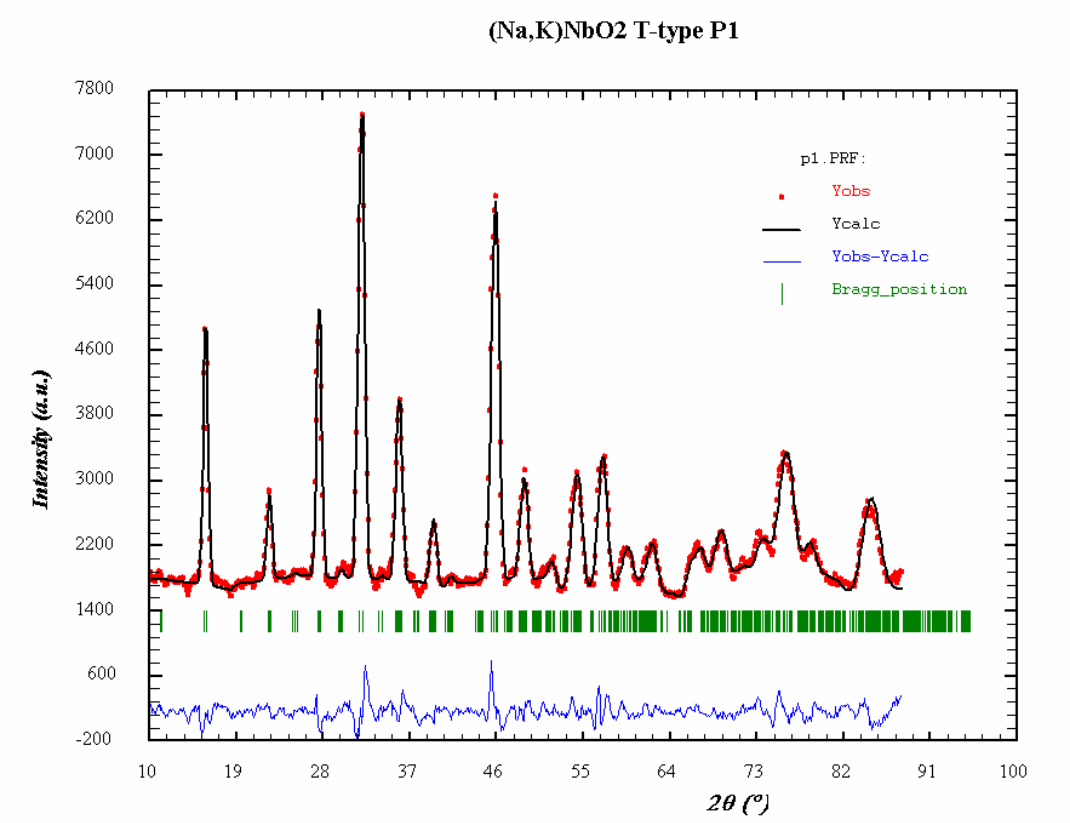
2. Neutron diffraction study for the $NaNbO_3$ submicron powder at various temperatures

$NaNbO_3$ showed a unique phase transition behavior [2]. Coarse powders take an orthorhombic Pbcm structure. At an averaged particle size of around 600 nm, the space group transforms to $Pmc2_1$, which shows an enhanced

piezoelectric property, accompanied by lattice expansion. In the intermediate particle size range (200 – 400 nm), the $Pmc2_1$ symmetry still holds but the lattice volume decreases with decreasing particle size. Finally, fine powders consisting of particles with an average diameter of 70 nm present a structure described in a Pmma space group, which has a centrosymmetric structure. This structure assigned for the fine powders has the most compact reduced cell.

Recent temperature tuning Raman spectroscopy revealed that the piezoelectric submicron powder undergoes successive phase transitions toward a more symmetric phase on heating from -150 °C up to 450 °C and takes at least four polymorphs within this range. Transition points seem to be about -100, 120 and 340 °C from the overview of Raman spectra and these phases are new. In order to elucidate the crystallographic structures of these different phases, neutron diffraction measurements at various temperatures (-150, -50, 20, 50, 100, 150, 200, 300 and 400 °C) and their refinements are necessary. We believe that the mechanisms of the successive phase transitions and the Curie temperature for the piezoelectric phase can be revealed by the combination of temperature tuning Raman spectroscopy and neutron diffraction.

Results: Neutron diffraction patterns for the submicron $NaNbO_3$ powder indicated that at least three types of phases exist within the measuring temperature region.



References

[1] Y. Shiratori, A. Magrez, C. Pithan, "Phase transformation of $KNaNb_2O_6$ induced by size effect", Chem. Phys. Lett. 391 (2004) 288.

[2] Y. Shiratori, A. Magrez, J. Dornseiffer, F.-H. Haegel, C. Pithan, R. Waser, "Polymorphism in micro-, submicro- and nano-crystalline $NaNbO_3$", J. Phys. Chem. B (2005) in press.

[3] R. Skowronek, J. Walter, C. Pithan, Y. Shiratori, A. Magrez, "Neutron diffraction study of nanocrystalline and microcrystalline $(K_{0.5}Na_{0.5})NbO_3$ powders", in The FRJ-2 Experimental Reports 2004, ed. T. Brückel, D. Richter, R. Zorn, Forschungszentrum Jülich GmbH, p. 33.

[4] C. Pithan, Y. Shiratori, J. Dornseiffer, F.-H. Haegel, A. Magrez, R. Waser, "Microemulsion mediated synthesis of nanocrystalline $(K_x,Na_{1-x})NbO_3$ powders", J. Cryst. Growth. 280 (2005) 191.

Institut für Festkörperforschung
Forschungszentrum Jülich GmbH
D-52425 Jülich

Experimental Report
of Neutron Scattering Experiments
at the FRJ-2 Reactor

Proposal number:	SV7-05-012		
Experiment title:	**High-temperature/Low-temperature structural behavior of phosgenite, $Pb_2CO_3Cl_2$**		
Dates of experiment:	09.12.05-12.12.05 18.02.06-26.02.06 06.03-06-12.03.06	Date of report:	10.05.2006
Experimental team: Names	Addresses		
Gatta, G. Diego	Dipartimento di Scienze della Terra Università degli Studi di Milano I-20133 Milano Italy		
Local Contact:	Dr. J. Walter, R. Skowronek		

Experimental report text body

Phosgenite is a rare mineral consisting of lead chlorocarbonate [$Pb_2Cl_2(CO_3)$]. It forms from the oxidation of lead bearing minerals, such as when galena (PbS) comes in contact with carbonated and chlorinated waters. Usually natural phosgenite is found associated with cerussite ($PbCO_3$), anglesite ($PbSO_4$), galena and limonite ($Fe_2O_3 \cdot nH_2O$). The crystal structure of phosgenite was first refined by Gruseppetti and Tadini (1974). The structure (unit-cell: a = 8.1600 Å, c = 8.8830Å, Z=4; space group: $P4/mbm$) consists of continuos layers parallel to the c-axis where large Pb-polyhedra lie, which are bridged by CO_3^{2-} units, see Fig. 1.

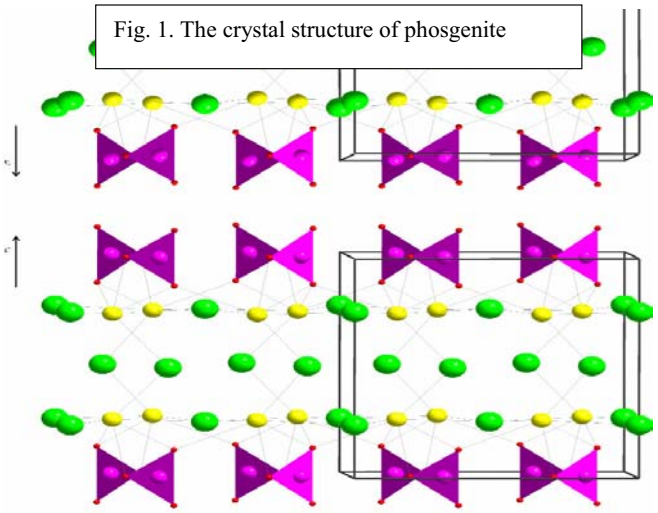


Fig. 1. The crystal structure of phosgenite

The structural arrangement in parallel planes is in fact reflected by the good cleavage parallel to (001). The coordination number of the Pb-site in the crystal structure of phosgenite is 7:3 chlorines and 4 oxygens belonging to the CO_3 groups (Fig. 1). The interest in the stabilities of carbonate minerals within the Earth, considered as a buffer for the long-term cycling of CO_2 between the atmosphere, oceans and the solid Earth, gave rise to a relevant number of high-pressure and high-temperature experiments on natural C-bearing phases as calcite (low pressure-CaCO3), aragonite (high pressure-$CaCO_3$), dolomite [$MgCa(CO_3)_2$], strontianite ($SrCO_3$), witherite ($BaCO_3$), otavite ($CdCO_3$),

rhodochrosite ($MnCO_3$) and cerussite ($PbCO_3$) (Redfern, 2000). However, a few studies have been devoted to Cl, F and OH-bearing carbonates. In particular, no study was devoted to the low and high temperatures and high pressure behaviour of phosgenite and, as a consequence, the main thermodynamic parameters of this mineral are still completely unknown.

In this study, we proposed to investigate the high/low-temperature crystal chemistry of a natural phosgenite using neutron diffraction. Neutron experiment was required because of the crystal chemistry of this material consists of heavy element (*i.e.* Pb) and light element (*i.e.* C) which makes any high pressure X-ray powder diffraction data not useful for reliable structural refinements.

We performed a data collection at room condition (295K), at low-temperature (down to 4K) and at high-temperature (up to 473K) by neutron powder diffraction. The structural refinement of phosgenite at room condition confirms the topological asset described by Gruseppetti and Tadini (1974) with a tetragonal lattice. In Fig. 2 is reported the Rietveld full-profile fit. However, at between 295 and 433K the structure appear undergoes to a phase transition and the new high-temperature phase appear to be better described with a triclinic lattice with : a=8.305389 Å, b= 8.016596 Å, c= 9.941740 Å, α =83.036°, β=106.055°, γ=91.315° and V=631.381 $Å^3$. In Fig. 3 is shown the LeBail full-profile fit of the H*T*-phosgenite at 433K. The work is in progress to refine the crystal structure of the triclinic H*T*-phase.

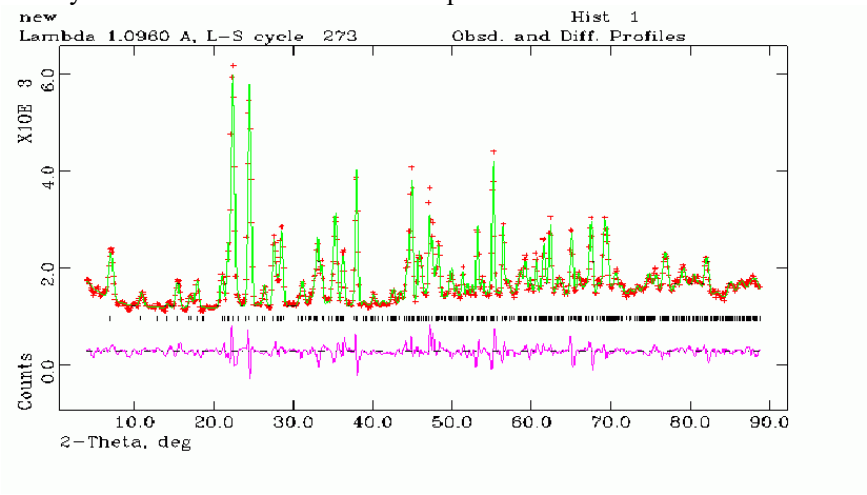


Fig. 2 Rietveld full-profile fit of phosgenite at 295K

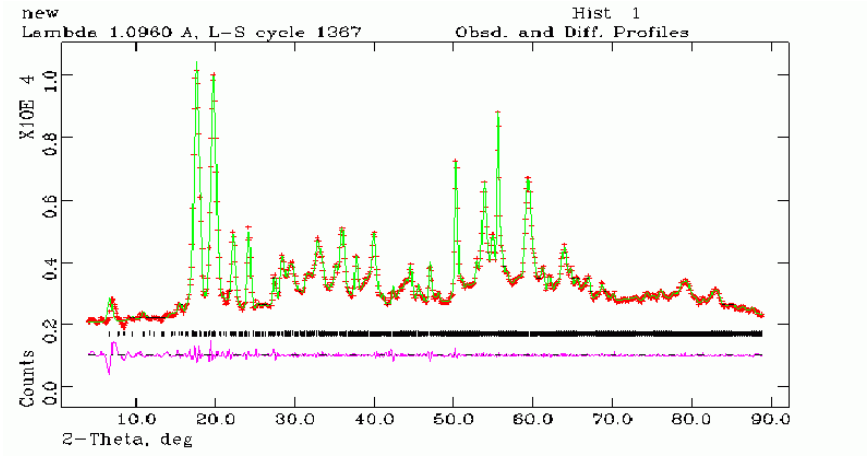


Fig. 3 LeBail full-profile fit of phosgenite at 433K

References

Gruseppeti, G. & Tadini, C. (1974). *Tshermarks Min. Petr. Mitt.*, **21**, 101-109.
Redfern, S.A.T. (2000). *Rev. In Min. Geoch.,* **41**, 289-308.

Institut für Festkörperforschung
Forschungszentrum Jülich GmbH
D-52425 Jülich

Experimental Report
of Neutron Scattering Experiments
at the FRJ-2 Reactor

Proposal number:	SV7-05-013		
Experiment title:	Neutron Diffraction on Ni-Carbodiimides		
Dates of experiment:	25.10.05-01.11.05	Date of report:	28.6.2006
Experimental team: Names	Addresses		
Dr. Müller, Paul Krott, Manuel Prof. Dr. R. Dronskowski, Dr. Liu, Xiaohui	Institut für Anorganische Chemie der RWTH Aachen Landoltweg 1, 52056 Aachen		
Local Contact:	Dr. Jens M. Walter		

Experimental report text body

$Ni(HNCN)_2$, is a fine green, air stable powder. X- Ray diffraction experiments on powdered samples led to space group *Pnnm*, crystallographic data are given in tables 1 and 2.

Table 1. Crystallographic data for $Ni(HNCN)_2$.

Formula:	$Ni(HNCN)_2$
Crystal system, color and form:	Orthorhombic, green powder
Lattice parameters:	a = 6.468 Å
	b = 8.768Å
	c = 3.236Å

Table 2. Positional parameters parameter for $Ni(HNCN)_2$.

atom	Wyckoff-site	x	y	z
Ni	2*a*	0	0	0
N1	4g	0.708	0.48	0
C	4g	0.185	0.639	0
N2	4g	0.087	0.768	0

Although our earlier experiments on $Cu_4(NCN)_2NH_3$ had shown, that it is possible to determine the H-positions with a powder sample without the use of deuterated samples, we now realized that the use of non-deuterated compounds results in a rather poor powder pattern (cf. fig.1) with the typical background of a hydrogen- containing sample.

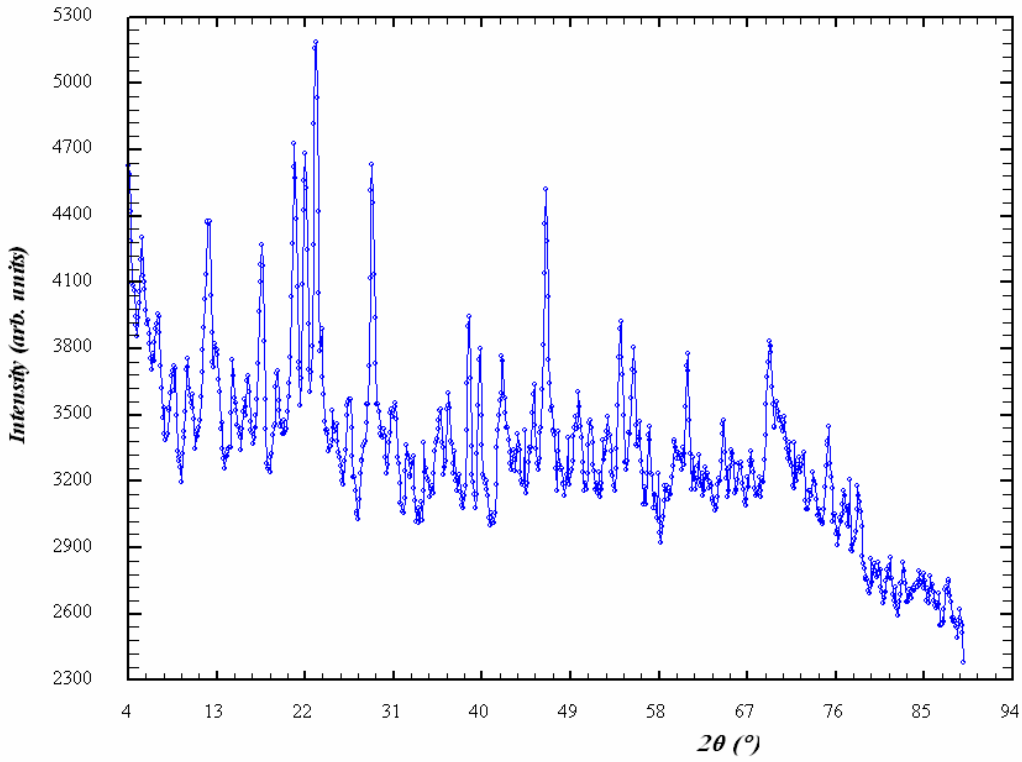


Fig. 1 Neutron powder diagram of $Ni(HNCN)_2$ at 298K

The reflections of the powder pattern can be indexed by the orthorhombic cell, but the intensities are to poor to allow the determination of the hydrogen position with profile refinement calculations. Therefore we started additional experiments to grow single crystals for X-ray diffraction experiments to get more information about the crystal structure.

Institut für Festkörperforschung
Forschungszentrum Jülich GmbH
D-52425 Jülich

Experimental Report
of Neutron Scattering Experiments
at the FRJ-2 Reactor

Proposal number:	SV7-05-14		
Experiment title:	**Neutron diffraction analysis of silver coins from the Himyarite-Sabean Empire**		
Dates of experiment:	51 days	Date of report:	17.05.2006
Experimental team: Names	Addresses		
Kirfel, Armin, Kockelmann, Winfried Yule, Paul	Mineralogisch-Petrologisches Institut der Universität Bonn Poppelsdorfer Schloss 53115 Bonn Rutherford Appleton Laboratory, ISIS Facility, ROTAX, Chilton, Didcot, Oxon, OX11 0QX United Kingdom Völkerkundemuseum München		
Local Contact:	Dr. Jens M. Walter, Rolf Skowronek		

Experimental report text body

1. Introduction

This investigation is a follow-up project from the proposal SV7-05-004, where silver coins from the Himyarite and later Himyarite-Sabean empire in the southern part of the Arabic peninsula were investigated. In these first measurements 10 coins have been measured by neutron diffraction to determine the phase compositions and to correlate these with density measurements. Due to the auspicious results from the first measurements we measured another set of 40 coins with the same aim as in the last campaign. The peculiar shape of the coins, i.e. their irregular and concave (scaphate) appearance, implies that their patterns were not prepared only by casting in a mould, but rather by striking or deep-drawing with mechanical force. However, other coins are flat and exhibit bubbles which indicate casting.

Measurements and results

The coins were selected to cover a broader range over time and locations to determine their variation in composition in more detail. Furthermore selected coins were also measured in the texture diffractometer SV7 to enlighten the manufacturing techniques further more. For these measurements flat and concave coins were selected to gain information about the technique used to obtain concave coins as describe above. Another question addressed by the selection of sample coins for texture analysis was, whether the manufacturing technique had changed over time and may it possible to identify counterfeited coins in the variation of manufacturing techniques in the same period of time.
Due to the form anisotropy of the coins, it was not possible to measure complete pole figures of the coins, which would in this case also show form texture. Therefore only distinct φ-rotations in certain χ-tilts were selected for the measurements. From the resulting cascading diffraction patterns as a function of the orientation,

it is possible to obtain qualitatively by the comparison of the different peak heights, whether the coin was casted into a mould from molten material or worked by mechanical force. Casted coins show only distinct singular peak heights of single crystallites (see Fig. 1, 3), whereas mechanically worked coins show a classical bulk texture distribution, which varies in a wavy distribution depending on the measured angle (see Fig. 2).

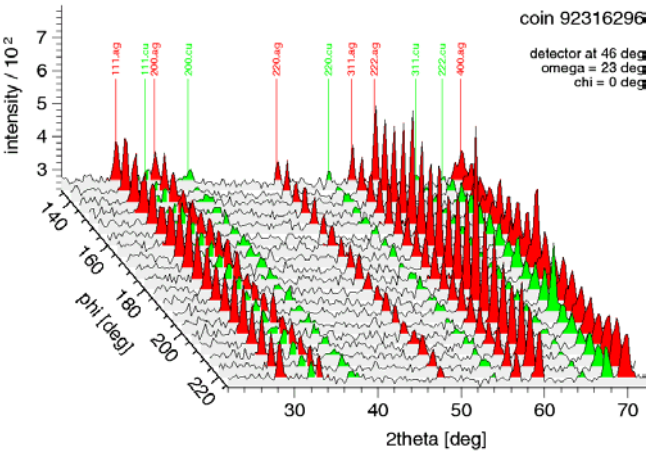


Fig. 1: Casted hymeriade silver coin with single crystal peaks

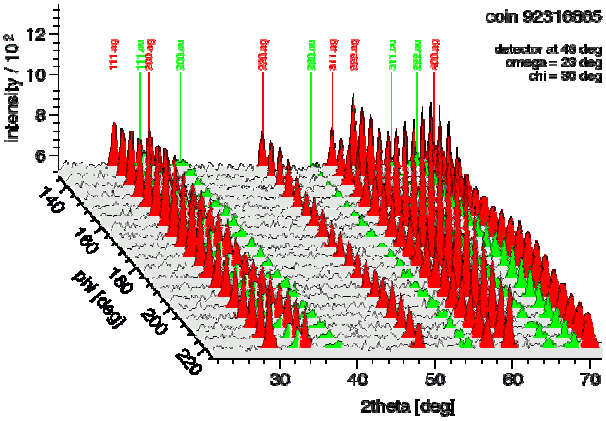


Fig. 2: mechanically worked flat silver coin

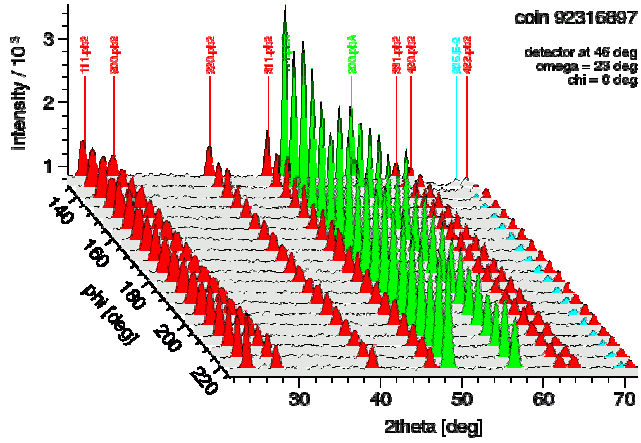


Fig. 3: Casted flat silver coin with single crystal peaks

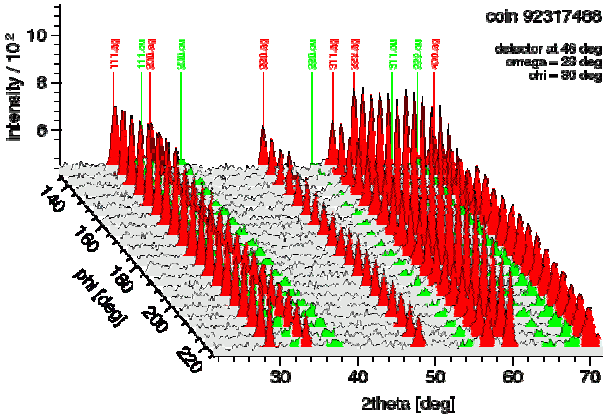


Fig. 4: mechanically worked concave silver coin

Institut für Festkörperforschung
Forschungszentrum Jülich GmbH
D-52425 Jülich

Experimental Report
of Neutron Scattering Experiments
at the FRJ-2 Reactor

Proposal number:	SV7-05-015		
Experiment title:	**Low-and high field magnetic and mineral fabrics of carrara marbles**		
Dates of experiment:	29.11.05-18.12.05 14.04.06 27.04.06-28.04.06	Date of report:	18.05.2006
Experimental team: Names	Addresses		
Otto, Michael Leiss, Bernd	Geowissenschaftliches Zentrum der Universität Göttingen Abteilung Strukturgeologie und Geodynamik Goldschmidt Str. 3 D-37077 Göttingen		
Local Contact:	Jens Walter, Ekkehard Jansen		

Experimental report text body

Introduction

The anisotropy of magnetic susceptibility (AMS) is a time-efficient method to describe crystallographic preferred orientations of rocks and has been applied in a wide field of sedimentary, metamorphic and magmatic geology. The method, however, suffers from limitations which mainly result from the interference of diamagnetic, paramagnetic and ferromagnetic fabrics (de Wall 2005) — the term ferromagnetism is used in a wider sense here, including e.g. ferrimagnetism. The AMS is an integral parameter which describes a crystallographic preferred orientation as an ellipsoid. The quantitative correlation of the AMS with the crystallographic preferred orientations should help to allow a closer view at the applicability and the limitations of the AMS analysis (see also Schmidt et al. 2006 a, b).

Measurements

Schmidt et al. (2005, 2006 a,b) developed a method for the separation of paramagnetic from diamagnetic fabric. It is achieved by the comparison of room-temperature and low-temperature (77 K) measurements using the high-field torque method. This method was applied and compared to neutron textures on synthetically-deformed calcite-mica samples. To test the application of the new methods on naturally deformed rocks, mica-bearing calcite marbles and mylonites from the Alpi Apuane in Italy and dolomite mylonites from the Damara Orogen in Namibia were selected. Selection criteria were varying mica contents and varying intensities/types of their crystallographic-preferred orientations (CPOs). Quantitative texture analyses were carried out by means of the ‘powder and texture diffractometer SV7’ at the research reactor Jülich 2 of the Research Center Jülich (FRJ-2) in Germany. Due to a low absorption coefficient of neutrons in condensed matter, neutron diffraction allows a volume related quantitative texture analysis of the sample cylinders which were also used for AMS measurements. Only this strategy allows a direct correlation of CPOs with the AMS. The 30 samples analysed cover a large variety of texture types. The carbonate phases show single c-axis maxima (Fig.1), covering a

range from weak to very strong intensity maxima. Other samples show distinct to weak c-axis double maxima (Fig. 2). Furthermore, some samples show partially developed girdle distributions with moderate to weak intensity. In one case, dolomite displays a completely developed girdle distribution. The mica phases show c-axis preferred orientations covering a range of very weak to very strong single maxima.

Results

The results of this study are based on a large variety of fabric types of carbonate-mica marbles and mylonites, i.e. varying mica content, grain sizes, grain shapes, types and intensities of the crystallographic preferred orientation. The presented first correlations of the AMS and CPO for the single mineral phases in general demonstrate a good matching. Regarding the comparison of texture types and the AMS, limitations are possible. While single c-axis maxima and girdle-like c-axis distributions can be also distinguished by the AMS, it is obvious that distinguishing between these types and the double c-axis type is not possible at the present stage.

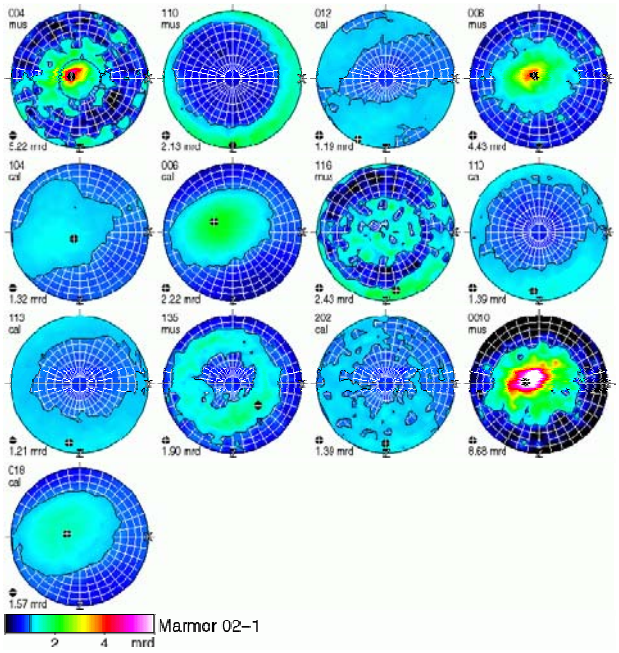


Fig. 1 Single c-axis maxima of calcite and muscovite

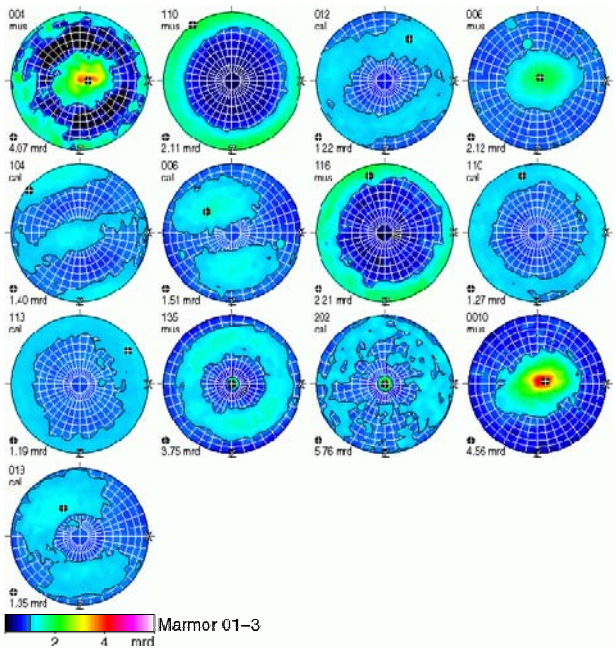


Fig. 2 Double calcite c-axis maximum and single mica c-axis maximum

References

De Wall, H (2005) Die Anisotropie der magnetischen Suszeptibilität — eine Methode zur Gefügeanalyse. Z. d. dt. Geol. Ges. 155, 287–298

Martin-Hernandez F & Hirt AM (2001) Separation of ferrimagnetic and paramagnetic anisotropies using a high-field torsion magnetometer. Tectonophysics 337, 209–221

Hrouda F (1982) Magnetic-anisotropy of rocks and its application in geology and geophysics. Geophysical Surveys 5, 37–82

Lowrie W (1989) Magnetic Analysis of Rock Fabric. In: James, DE The Encyclopedia of Solid Earth Geophysics, 698–706

Schmidt, V, Hirt, AM, Burlini, L & Leiss, B (2005) Crystallographic-Preferred Orientations and Anisotropic Magnetic Susceptibilities in Experimentally Produced Calcite Samples: Deformation Mechanics, Rheology and Tectonics 2005, Zürich, pp 190

Schmidt V, Hirt AM & Rosselli P (2006a) Separation of magnetic subfabrics by high-field, low-temperature torsion measurements. 11. Symposium “Tektonik, Struktur- und Kristallingeologie”

Schmidt V, Hirt AM, Burlini L, Leiss B & Walter JM (2006b) Measurement of calcite crystallographic preferred orientations by magnetic anisotropy and comparison to diffraction methods. 11. Symposium “Tektonik, Struktur- und Kristallingeologie”

Institut für Festkörperforschung
Forschungszentrum Jülich GmbH
D-52425 Jülich

Experimental Report
of Neutron Scattering Experiments
at the FRJ-2 Reactor

Proposal number:	SV7-05-016		
Experiment title:	**The crystal structure of methyl bromide clathrate at T=4K**		
Dates of experiment:	27.01.06-29.01.06	Date of report:	20.5.2006
Experimental team: Names	Addresses		
M. Prager R. Skowronek	Forschungszentrum Jülich Inst. F. Mineralogie, Universität Bonn		
Local Contact:	E. Jansen, J. Walter		

Experimental report text body

Clathrates are a fascinating class of materials: a framework of matrix molecules forms cages which allow incorporating simple molecules in identical environments which thus experience the same matrix effect. The combination of different host and guest molecules allows a huge variety of clathrates to be produced. Water clathrates with water soluble guest molecules like tetrahydrofuran can be prepared easily. A recently grown interest concentrates on the methane water clathrates [1] which are only stable in a certain pressure-temperature regime. This 'burnable ice' exists in nature and may form one of the largest energy reservoirs on earth.

From a fundamental point of view methane represents a prototype of a non polar guest molecule. Methyl halides are interesting and different probes of the clathrate cages compared to methane because it interacts with the host surface via dipolar interaction. We already studied the methyl iodide clathrate. To incorporate this non water-soluble molecule to form the clathrate CH_3I x $17H_2O$ a special preparation technique [2] was developed. The formation of the clathrate becomes evident by the transformation into a transition gel state and an increase of the melting point to T_m~4C. The system crystallizes in the cubic II structure [3]. On this basis very detailed high resolution spectra gave much very important information [4]. Here we extend these studies to methyl bromide clathrate, which is reported to crystallize in the cubic I structure [5]. The prepared CH_3Br x $5.75D_2O$ had a melting point T_m=11°C.

A sample with deuterated matrix was prepared in an analogous way as methyl iodide clathrate. Neutron diffraction was applied using the single crystal side of SV7. The wavelength used was λ=2.332Å. According to literature CH_3Br x $5.75H_2O$ should be of the cubic I structure with a lattice parameter of ~11.8Å. The sample was mounted cold on the precooled head of a CCR cryostat and cooled to the required temperatures. Fig. 1 shows a typical diffraction pattern. All observed Bragg peaks can be indexed within the cubic I structure. A lattice parameter of a=11.9045Å is found at a sample temperature T=10K in agreement with the cubic I structure.

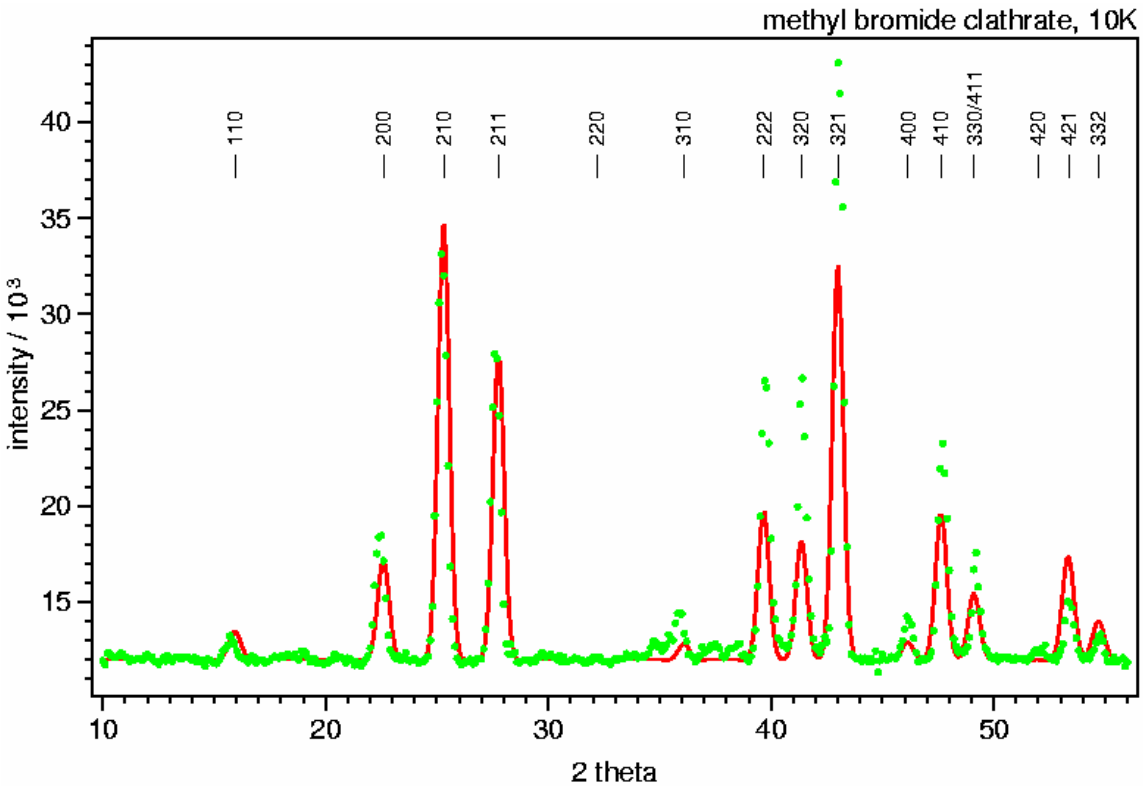


Fig. 1 Diffractogram of $CH_3Br*5.75D_2O$. Sample temperature T=10K. Miller indices characterize each peak.

[1] C. Gutt, W. Press, A. Hüller, J. Tse, H. Casalta, J. Chem. Phys. **114**,4160(2001)
[2] C. Albayrak, Dissertation, Aachen 1988
[3] Experimental reports 2003 of FRJ2, report SV7-02-016
[4] M. Prager, J. Pieper, A. Buchsteiner, A. Desmedt, J. Phys.: Condens. Matter 16,7045(2004)
[5] G.A. Jeffrey in „Inclusion compounds". Vol. 1, p. 135ff, J.L. Atwood et al editors, Academic Press, London, 1984

Institut für Festkörperforschung
Forschungszentrum Jülich GmbH
D-52425 Jülich

Experimental Report
of Neutron Scattering Experiments
at the FRJ-2 Reactor

Proposal number:	SV7-06-001		
Experiment title:	**Investigations on the magnetic structure of MnNCN**		
Dates of experiment:	11.02.06-15.02.06	Date of report:	13.06.2006
Experimental team: Names	Addresses		
Dr. Müller, Paul Krott, Manuel Prof. Dr. R. Dronskowski, Dr. Liu, Xiaohui	Institut für Anorganische Chemie der RWTH Aachen Landoltweg 1, 52056 Aachen		
Local Contact:	Dr. Jens M. Walter		

Experimental report text body

MnNCN, the first carbodiimide of a magnetic transition metal, has been synthesised and characterized by X-Ray diffraction. Lattice constants are $a = b = 3.357(1)$Å, $c = 14.339(2)$Å Spacegroup $R\bar{3}m$.

Table 1. Positional parameters and isotropic displacement parameters for MnNCN with standard deviations in parentheses.

Atom	Lage	*x*	*y*	*z*	*B* (Å^2)
Mn	3*a*	0	0	0	0.1(1)
C	3*b*	0	0	½	1.5(7)
N	6*c*	0	0	0.589(3)	0.4(4)

Magnetic measurements show Curie-Weiss behaviour above 150 K and a Néelpoint about 28 K. We performed neutron diffraction at RT and below the transition point and could prove the existence of a magnetic ordering. Fig 1 shows the experimental results.

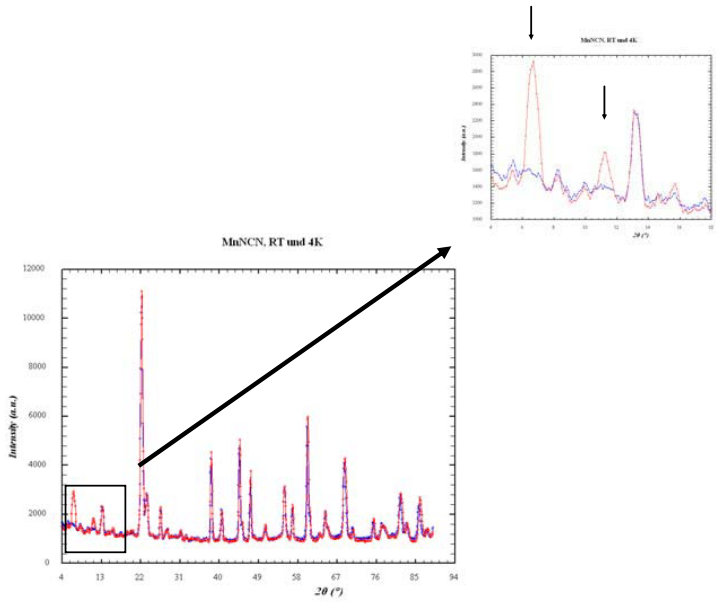


Fig. 1 Neutron diffraction diagrams of MnNCN at RT and 4K.

Due to the weak magnetic reflections we were not able up to now to present the complete magnetic structure. Fig 2 shows a profile fitting that results from a doubling of the c-axis and an orientation of the magnetic moments perpendicular to the c-axis. In consecutive manganese layers the spins are rotated by 60° in the a-b plane.

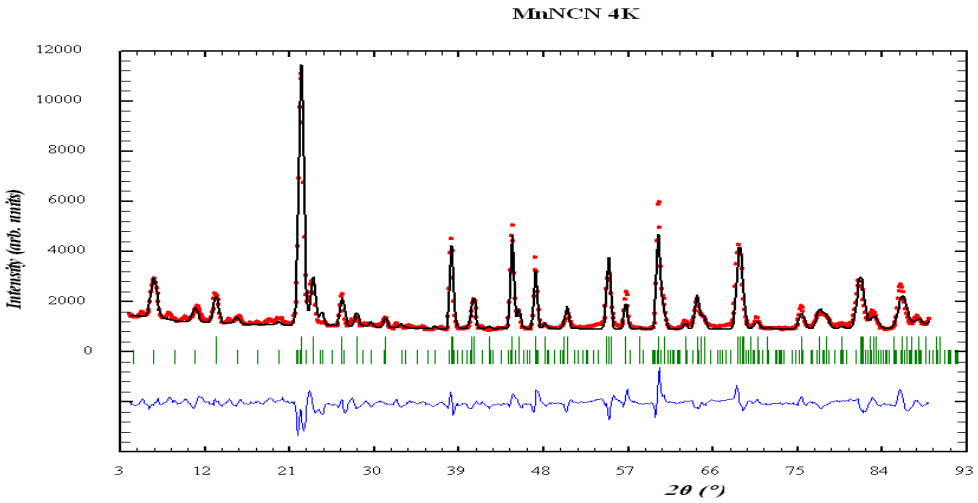


Fig. 2 Rietveld refinement of MnNCN at 4.2K

Institut für Festkörperforschung
Forschungszentrum Jülich GmbH
D-52425 Jülich

Experimental Report
of Neutron Scattering Experiments
at the FRJ-2 Reactor

Proposal number:	SV7-06-002		
Experiment title:	**Textural development of quartzitic mylonites from the Pohorje ultrahigh-pressure unit (Slovenia)**		
Dates of experiment:	06.01.06-13.01.06	Date of report:	14.06.2006
Experimental team: Names	Addresses		
N. Froitzheim J. Pleuger	Geologisches Institut der Universität Bonn, Nußallee 8, 53115 Bonn		
Local Contact:	J.M. Walter		

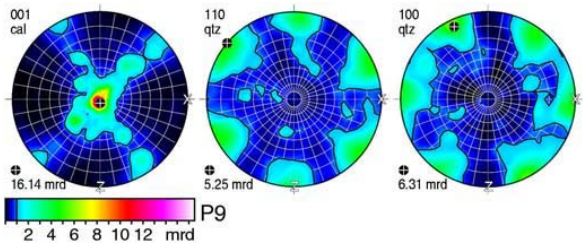
Experimental report text body

Two samples of mylonitised quartzite from the Pohorje mountains in northeastern Slovenia have been analysed in the present project. The Pohorje mountains are the southeasternmost extension of the Alps and expose nappes of the Lower and Upper Central Austroalpine units. The Lower Central Austroalpine complex experienced Cretaceous (c. 90 Ma) high-pressure metamorphism as testifyed e.g. by the well-known eclogites of Koralpe and Saualpe in southeastern Austria. In the Lower Central Austroalpine unit of Pohorje (Pohorje nappe), evidence for ultrahigh-pressure metamorphism, reaching conditions of c. 40 kbar and 900° C (Janák et al., 2006), has recently been discovered in metabasic and metaultrabasic rocks. The metabasic and metaultrabasic rocks are contained as lenses within medium- to high-grade micaschists, gneisses and amphibolites of the Pohorje nappe. Probably in the Early Miocene, a mostly granodioritic to tonalitic pluton intruded into the Pohorje nappe and is now exposed in central parts of the Pohorje mountains. In the Koralpe, most of the exhumation of high-pressure rocks occurred until the end of Cretaceous and was accompanied by strong deformation and retrograde metamorphic reequilibration in the surrounding rocks. In the Pohorje nappe, much deformation in the country rocks of the (ultra)high-pressure rocks probably also happened during the Upper Cretaceous. However, there is also evidence for east- to northeast-vergent extensional shearing during the Miocene which led to the final exhumation of the Pohorje nappe as a metamorphic core complex.

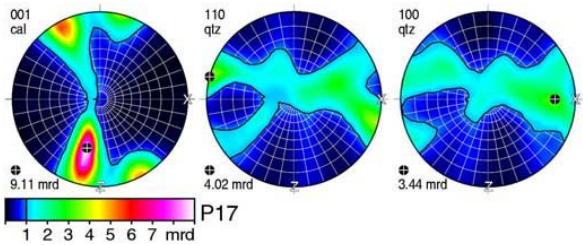
For the samples P9 and P17, the textures do not correspond to the macroscopically visible mineral lineations. Therefore, we rotated the textures around the strain Z axis, i.e. the normal to the mylonitic foliation, so that the strongest {a} maximum fell onto the periphery of the pole figure and the {c} maximum within the foliation plane parallels Y. These rotations are based on two assumptions. First, <a> was the only important slip direction in slip systems that acted during the formation of our textures. One of the {a} maxima should then align with the direction of shear, i.e. normal to Y and near to X. Second, in the case of initially randomly distributed crystallographic axes, homogeneous deformation should, irrespective of the flow type, produce

textures with twofold internal symmetry, either rotational with respect to Y (P9) or with the shear plane as a mirror plane (P17). The resulting texture of P9 yields an incomplete cross girdle distribution of {c} with a strong absolute maximum in the centre of the pole figure. Both {m} and {a} pole figures show three almost equally strong maxima distributed on a great circle parallel to the X-Z plane. The texture is only slightly asymmetric with respect to the strain axes, indicating only a weak component of rotational shear. The shear sense is dextral, i.e. top-to-the-SE (155°) in geographic coordinates. The P9 texture suggests intracrystalline deformation of quartz by dominant prism <a> slip. This slip system becomes dominant in quartz mylonites under temperatures above c. 500° C (Stipp et al., 2002), i.e. in the amphibolite facies. P17 shows two {c} maxima close to Z. The stronger and the weaker one are rotated by about 15° and 25° towards X in a clockwise and anticlockwise sense, respectively. {m} and {a} are unequally strong disposed each on two girdles perpendicular to the {c} maxima. Both {c} maxima and related {m} and {a} orientations would indicate opposite shear senses, which may be conjugate. The net shear sense is dextral (306° in geographic coordinates) as most obviously visible from the inclination of the main {m} and {a} girdles with respect to X. However, also in this case the rotational component of strain was quite weak. The position of the {c} maxima close to the periphery of the pole figure indicate basal <a> slip, possibly with some additional influence of rhomb <a> slip. These slip systems are active under lower temperatures than prism <a> slip, i.e. below 500° C.

In the present state of our study, more structural fieldwork has to be carried out to understand the kinematics of the Pohorje nappe and to interpret the textures in terms of this history. In a mapping project which will be carried out this summer, the large-scale structural history will be investigated and more samples for the comparison of textures with petrological P-T estimates will be collected. So far, we conclude that the shear senses deduced from P9 and P17 are not compatible with the reported kinematics of Miocene extension but rather with Cretaceous deformation. The fact that the shear senses of P9 and P17 are nearly opposite and that the textures formed under amphibolite- and greenschist-facies deformation, respectively, suggests a polyphase Cretaceous deformation history of the Pohorje nappe.



Texture of P9: mylonitic foliation is oriented S225/28, the reconstructed strain X direction is L155/10 (to the right).



Texture of P17: mylonitic foliation is oriented S345/44, the reconstructed strain X direction is L306/37 (to the right).

References:

Janák, M., Froitzheim, N., Vrabec, M., Krogh Ravna, E.J. & de Hoog, J.C.M. (2006): Ultrahigh-pressure metamorphism and exhumation of garnet peridotite in Pohorje, Eastern Alps. - Journal of metamorphic Geology 24, 19-31.

Stipp, M., Stünitz, H., Heilbronner, R. & Schmid, S.M. (2002): The eastern Tonale fault zone: a „natural laboratory“ for crystal plastic deformation of quartz over a temperature range from 250 to 700 °C. - Journal of structural Geology 24, 1861-1884.

Institut für Festkörperforschung
Forschungszentrum Jülich GmbH
D-52425 Jülich

Experimental Report
of Neutron Scattering Experiments
at the FRJ-2 Reactor

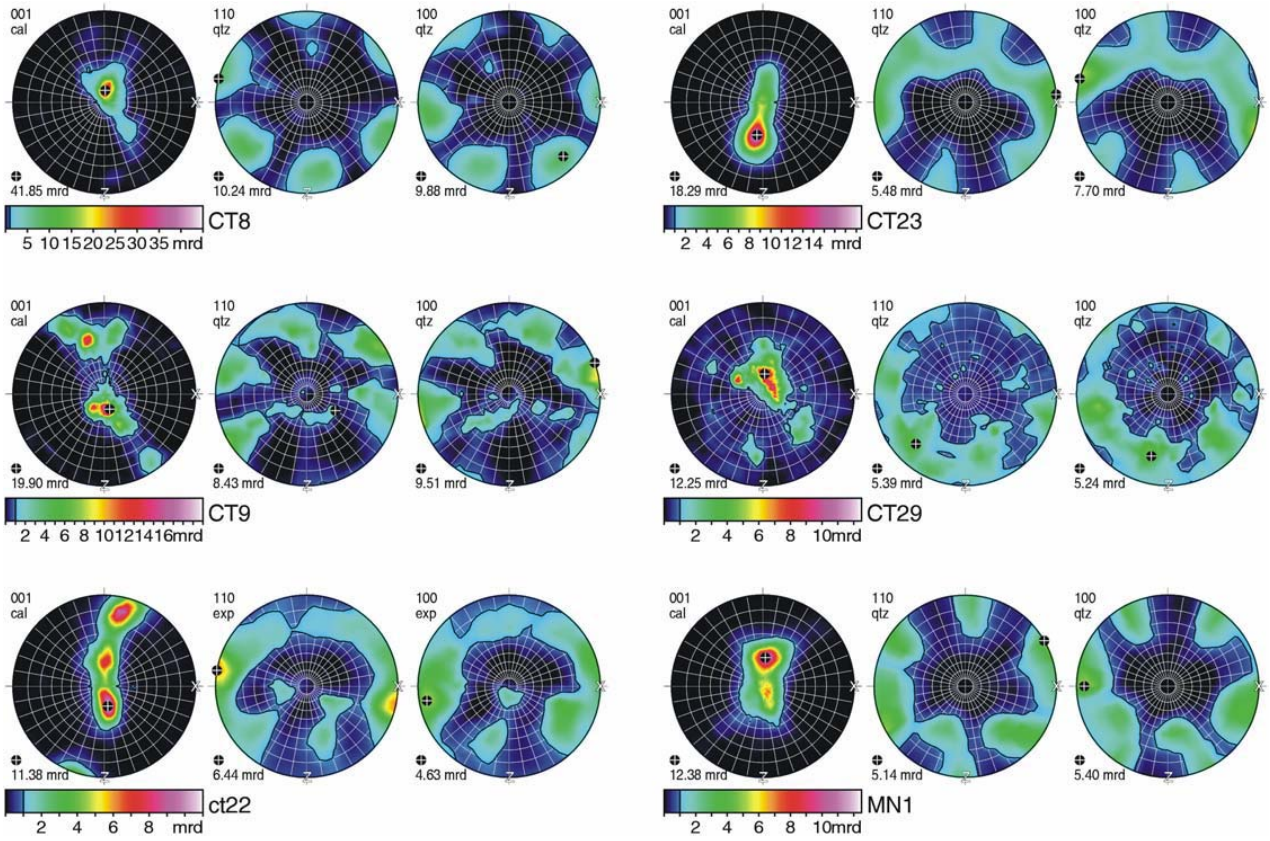
Proposal number:	SV7-06-003		
Experiment title:	**Textural development of quartzitic mylonites of the western Rila Massif, western Bulgaria**		
Dates of experiment:	13.01.06-15.01.06 17.02.06-18.02.06	Date of report:	14.06.2006
Experimental team: Names	Addresses		
N. Froitzheim J. Pleuger C. Tückmantel M. Neisen	Geologisches Institut der Universität Bonn, Nußallee 8, D-53115 Bonn		
Local Contact:	J.M. Walter		

Experimental report text body

The Rhodope complex is part of the Alpine orogen and formed by metamorphic and magmatic rocks representing the deep levels of a collisional orogen. Structural and geochronological work has shown that the Rhodope complex is a stack of nappes, including Hercynian basement, assembled and metamorphosed during the Alpine orogeny. The metamorphic rocks include orthogneiss, paragneiss and schist, metabasic and ultrabasic rocks, calcsilicates, and marble. Recently, evidence for ultrahigh-pressure metamorphism was found in the Central and Eastern Rhodopes. The most widespread regional (Alpine) metamorphism is amphibolite-facies to locally granulite-facies with anatexis. Pelitic schists in the Rila Mountains give evidence that the amphibolite facies was reached during decompression. The complex is the site of voluminous Eocene to Early Miocene syn- and postcollisional magmatism and of postcollisional extension leading to the formation of detachment faults, metamorphic core complexes, and rift basins. Cenozoic sedimentary rocks of the western Rhodope complex occur in rift structures and are interfingered with volcanic rocks related to the Tertiary plutonism.
A most prominent extensional structure is the Gabrov Dol detachment fault that separates the greenschist-facies ophiolitic Frolosh unit in the hanging wall from the mostly amphibolite-facies and gneissic Ograzhden unit in the footwall. In the course of two diploma mapping works in the Rila Massif, six mylonitised quartzites (among many other specimens) have been sampled from three shear zones within the Ograzhden unit in order to gain information about strain geometry, temperature, and shear senses from their textures. This information shall contribute to a better understanding of the complex extensional deformation history and a possible thermal influence by syntectonic plutonism.
In three of the textures, CT8, CT29, and MN1, {c} forms a single maximum close to the strain Y axis which is parallel to the foliation and perpendicular to the stretching lineation. In these cases, {a} forms three maxima in the X-Z plane the strongest of which lies more or less close to X. These textures are evidence for prism <a> slip

which operates in the amphibolite facies above 500 °C. The other three textures also show influence of prism <a> slip in that the {c} maximum extends though the centre of the diagram. In CT23, the position of the absolute {c} maximum between the centre and the periphery of the pole figure probably indicates strong additional rhomb <a> slip. In CT9 and CT22, {c} is distributed over incomplete single girdles. Such textures are commonly interpreted to be formed by the combined activity of basal <a>, rhomb <a>, and prism <a> slip under greenschist-facies conditions. The inclination of the single girdles with respect to the foliation plane (X-Y) indicates a strong rotational component of shear which is sinistral for CT9 and dextral for CT22. For CT9, the same shear sense is also displayed by the position of the strongest {m} maximum c. 20° away from X on the periphery in an anticlockwise sense, and for CT22 by the strongest {a} maximum c. 10° away from X in a clockwise direction.

In the further course of the study, the textures will be compared to grain-shape analyses of the same samples and petrological observations on other rock types. Our preliminary interpretations of the neutron textures are in line with field observations that in higher parts of the Ograzhden unit extensional faults with considerable displacement led to significant exhumation of the units below. The textures and petrological observations on thin sections indepently show that faulting in the investigated shear zones took place partly under amphibolite-, partly under greenschist-facies conditions, while final stages of exhumation were accommodated by brittle faulting.



Institut für Festkörperforschung
Forschungszentrum Jülich GmbH
D-52425 Jülich

Experimental Report of Neutron Scattering Experiments at the FRJ-2 Reactor

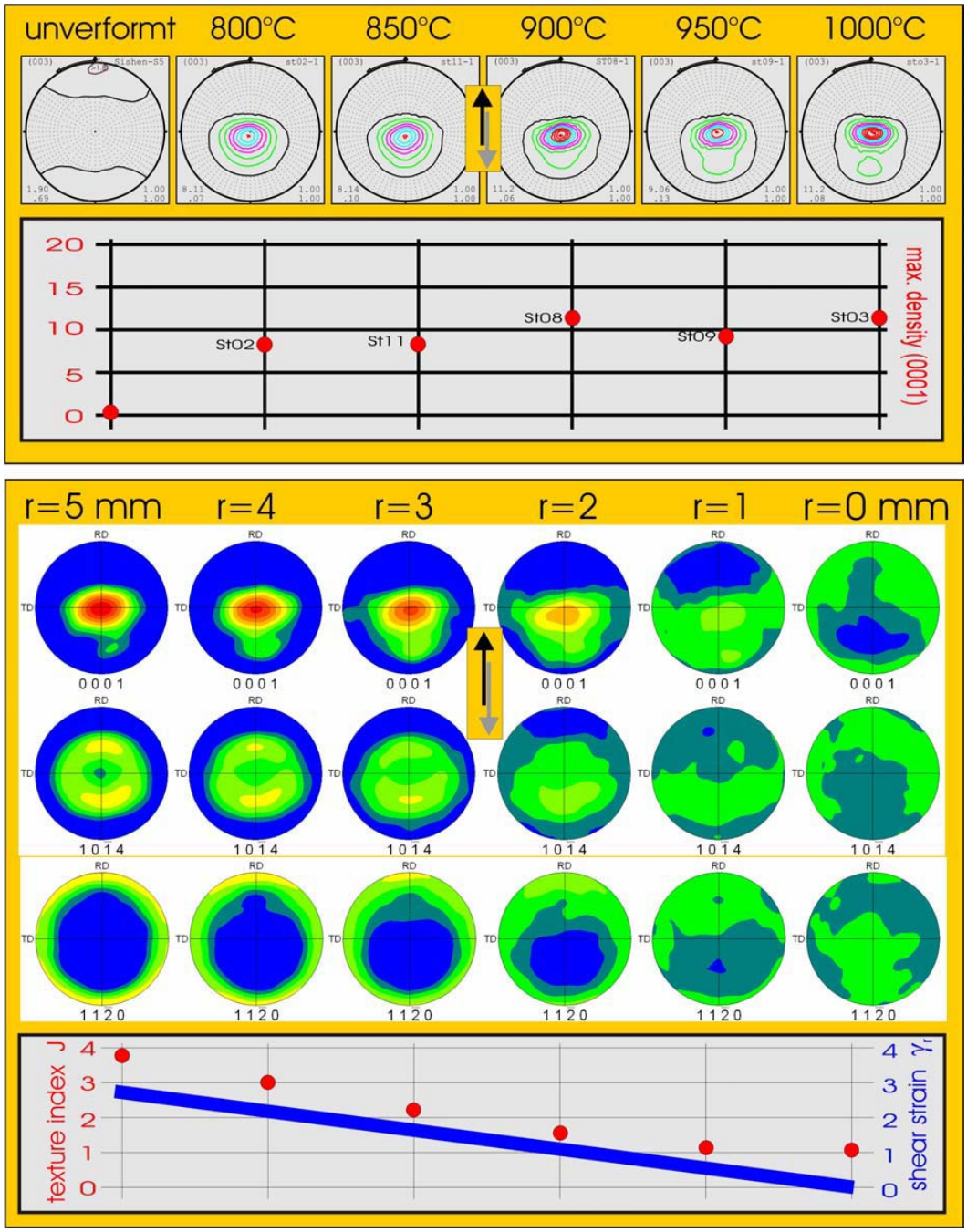
Proposal number:	SV7-06-004		
Experiment title:	**Texture of hematite ore deformed to high strains in torsion**		
Dates of experiment:	17 days	Dates of experiment:	26.06.2006
Experimental team: Names	Addresses		
H. Siemes * B. Klingenberg	Institut für Mineralogie und Lagerstättenlehre RWTH-Aachen, D-52056 Aachen	* Förderung DFG Si209/36-1	
E. Rybacki M. Naumann	Geoforschungszentrum Potsdam Projektbereich 3.2: Rheology and Tectonophysics D-14474 Potsdam		
K. Kunze	Geologisches Institut, ETH-Zürich CH-8092 Zürich		
Local Contact:	J.M. Walter, E. Jansen, R. Skowronek		

Experimental report text body

Dieser Bericht ist eine Ergänzung zu SV7-05-001

Verformungsversuche an feinkörnigem Hämatit (Fe_2O_3) wurden in einer Paterson-Apparatur mit Torsionseinrichtung (Paterson & Olgaard, 2000) bei Temperaturen zwischen 800 und 1000°C gefahren. Die Scherverformungen lagen bei allen Versuchen zwischen γ=4,4 und γ=4,6 und die dabei ereichten maximalen Festigkeiten zwischen 81 und 38 MPa. Der Hämatit ist bei allen Temperaturen zu einem gleichförmigen polygonalen Korngefüge rekristallisiert, das sich auch bei natürlich verformten Erzen findet. Die Korngrößen, die mit steigender Temperatur zunehmen, weisen dabei keine Unterschiede über die Probenquerschnitte auf, obwohl die finite Scherverformung von Null im Zentrum der Probe bis zum maximalen Wert an der Peripherie variiert. Neutronentexturmessungen (Jansen et al. 2000) im Probenbereich mit der stärksten Verformung und EBSD-Messungen (Kunze et. al. 1993) ergaben für die Polfigur des 0003-Reflexes ein zentrales, elliptisches Maximum nahe dem Pol der Scherebene. Die Höhe des 0003-Maximums nimmt dabei von 8,1 bis 11,2 [m.u.d.] (siehe obere Abbildung) mit steigender Temperatur zu. Der Texturindex bei der 1000°C-Probe steigt im Probenquerschnitt von 1,1 im Zentrum auf 3,8 an der Peripherie (siehe untere Abbildung) an. Auf dem peripheren Gürtel der $\{11\bar{2}0\}$-Polfigur befindet sich ein Maximum, das die Orientierung der Scherrichtung angibt. Die $\{10\bar{1}4\}$-Polfigur, die zwei bananenförmige Maxima (Quade, 1988) unterschiedlicher Dichte und Ausdehnung aufweist, lässt auf den Schersinn schließen. Diese Polfiguren stimmen weitgehend mit Polfiguren natürlich verformter Hämatiterze überein.

Danksagung
Die Autoren danken der Deutschen Forschungsgemeinschaft und den Mitarbeitern der beteiligten Institute sowie den Geologen der Sishen Mine (Kumba Resources) für die Bereitstellung des Probenmaterials.



Literatur

Bascou, J., Raposo, M.I.B., Vauchez, A., Egydio-Silva, M., 2002. Earth and Planetary Science Letters 198, 77-92.

Jansen, E., Schäfer, W., Kirfel, A., 2000. Journal of Structural Geology 22, 1559-1564.

Kunze, K., Wright, S.I., Adams B.L. and Dingley D.J., 1993. Textures and Microstructures 20, 41-54.

Paterson, M.S., Olgaard, D.L. 2000. Journal of Structural Geology 22, 1341-1358.

Quade, H., 1988. Textures and Microstructures, 8-9, 719-736

Quade, H., Rosière, C.A., Siemes, H., Brokmeier, H.-G., 2000. Zeitschrift für angew. Geologie, Sonderheft 1, 155-162.

Rosière, C.A., Siemes, H., Quade, H., Brokmeier, H.-G., Jansen, E.M., 2001. J. Structural Geology 23, 1429-1440.

Siemes, H., Klingenberg, B., Rybacki, E., Naumann, M., Schäfer, W., Jansen, E., Rosière, C.A., 2003. J. Struct. Geol. 25, 1371-1391.

Institut für Festkörperforschung
Forschungszentrum Jülich GmbH
D-52425 Jülich

Experimental Report
of Neutron Scattering Experiments
at the FRJ-2 Reactor

Proposal number:	SV7-06-005		
Experiment title:	**The crystal structure of methyl chloride clathrate at T=200K**		
Dates of experiment:	30.04.06-01.05.06	Date of report:	20.5.2006
Experimental team: Names	Addresses		
M. Prager R. Skowronek	Forschungszentrum Jülich Inst. F. Mineralogie, Universität Bonn		
Local Contact:	E. Jansen, J. Walter		

Experimental report text body

We have continued our study of methyl halide clathrates. Methyl halides are interesting and different probes of the clathrate cages compared to methane clathrate [1] because it interacts with the host surface via dipolar interaction. To incorporate the non water-soluble methyl halide molecules into water a special preparation technique was developed for CH_3I x $17H_2O$ [2]. In this case the formation of the clathrate becomes evident by the transformation into a transition gel state and an increase of the melting point to T_m~4C. The preparation technique was applied by us in analogue manner to the chloride compound. The crystal structures cited in the literature [3] were confirmed for the methyl iodide and bromide clathrates [4,5]. So far high resolution neutron scattering tunneling spectra and the densities of states were obtained for the methyl iodide [6] and methyl fluoride [7] clathrates. Based on the structures the detailed high resolution spectra gave important information on the potential surfaces of the cages[6,7]. Here we finish the structural work by investigating methyl chloride clathrate, which is in the literature is reported to crystallize either in the cubic I or cubic II structure [3].

A stoichiometric mixture of 1 CH_3Cl and 5.75 D_2O was used. The two-phase liquid was mixed mechanically and solidified with a new melting point T_m~19°C. The sample was mounted cold on the head of a CCR cryostat precooled to 275K and cooled to the required temperatures. Neutron diffraction was applied using the single crystal side of SV7. The wavelength was λ=2.332Å. Sample temperatures T_S=10K and 200K were used. For the predicted cubic I structure a lattice parameter is ~11.8Å. Fig. 1 shows the diffraction pattern measured at T_S=200K. Compared to the diffraction pattern of methyl bromide clathrate which is cubic I [5] the rather empty spectrum begins with lines at much higher scattering angles only and cannot represent a classical clathrate structure. A search for the unit cell lead to a indexing in the hexagonal space group $P6_3mc$ with lattice parameters a=4.504A and c=7.333A. These are the lattice parameters of hexagonal ice Ih. It was confirmed in an experiment on V3 of HMI that the methyl chloride is pumped off in the present experiment and we were left with pure hexagonal ice.

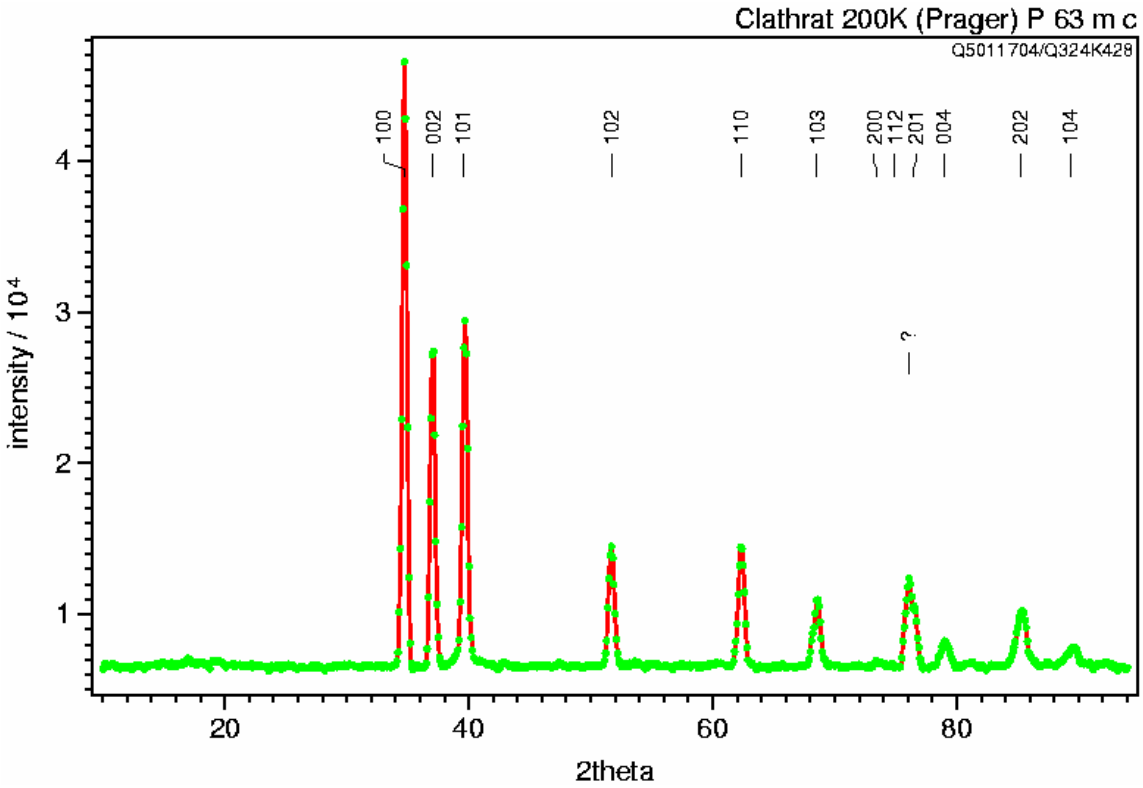


Fig. 1 Diffractogram of D_2O. Sample temperature T=200K. Miller indices characterize each peak. A minor uncertainty represents the doublet line deforming the 201 peak.

[1] C. Gutt, W. Press, A. Hüller, J. Tse, H. Casalta, J. Chem. Phys. **114**,4160(2001)
[2] C. Albayrak, Dissertation, Aachen 1988
[3] G.A. Jeffrey in „Inclusion compounds". Vol. 1, p. 135ff, J.L. Atwood et al editors, Academic Press, London, 1984
[4] Experimental reports 2003 of FRJ2, report SV7-02-016
[5] This volume, report SV7-05-016
[6] M. Prager, J. Pieper, A. Buchsteiner, A. Desmedt, J. Phys.: Condens. Matter 16,7045(2004)
[7] M. Prager, J. Baumert, W. Press, M. Plazanet, J.S. Tse, D.D. Klug, Phys. Chem. Chem. Phys.7,1228(2005)

Neutron Diffractometer (SV28)



Instrument Parameters

	Diffractometer 1	*Diffractometer 2*
Monochromator (reflection):	Cu (220)	Cu (200)
Wavelength:	0.087 nm	0.124 nm
Neutron flux density:	2.5×10^6 n/cm^{2}s	2.55×10^6 n/cm^{2}s
Mean FWHM of the Bragg reflections:	0.5°	0.5°
Detector, monitor:	^{3}He tubes, fission chambers	
Inner diameter of the Eulerian cradle:	40 cm	25 cm
Diffractometer control:	PC 486 Linux, interface type Stoe, stepping motor drive (steps of 0.005°), angle encoders with a resolution of 0.005°.	

Instrument Responsible

Dr. Anja Loose Tel. +49-(0)-2461-61-3140 Email: a.loose@fz-juelich.de

Institut für Festkörperforschung
Forschungszentrum Jülich GmbH
D-52425 Jülich

Experimental Report
of Neutron Scattering Experiments
at the FRJ-2 Reactor

Proposal number:	S28-04-013		
Experiment title:	**Precursor effects at the paraelectric ferroelectric phase transition of RDP**		
Dates of experiment:	06.06-28.06.2005	Date of report:	06.06.2006
Experimental team: Names	Addresses		
A. Loose St. Mattauch	Institut für Festkörperforschung, Forschungszentrum Jülich Institut für Festkörperforschung, Forschungszentrum Jülich		
Local Contact:	Anja Loose		

Experimental report text body

Potassium dihydrogen phosphate [KDP] is the most prominent member of an important group of hydrogen bonded ferroelectric crystals [1] of the composition $A(H,D)_2XO_4$ (A=K, Rb, Cs, Tl, NH_4; X=P, As). RDP, isomorphous to KDP and undergoes at 147(1) K a phase transition from the paraelectric phase with the tetragonal space group I-42d (F-4d2) to the ferroelectric phase with the orthorhombic space group Fdd2. The localisation of the protons is specifically connected with the ferroelectricity. Most spectacular is the isotope effect, where upon replacement of H by D (deuteration), the transition temperature Tc increases from 123 K in KDP to 220 K in DKDP. To account for the isotope effect, Blinc has introduced the quantum-tunneling model of the protons in a double minimum potential.
In [1] it was shown that already in the paraelectric phase the tetragonal structure is a superposition in time and space of the two possible ferroelectric orthorhombic structures (see figure 1). Therefor the double well potential is just a superposition of two adjacent in $[PO_4H_2]^-$-groups in time and space.

To investigate the evolution of the structure at the ferroelectric paraelectric phase transition we have measured a set of integral Bragg reflections of a single crystal of RDP at the SV28. The quality of the crystal is of the same kind like the one used in [1] for the high resolution X-ray measurements and so far beyond the instrument resolution of the SV28. We have measured above 2500 reflections of which 301 are unique. The R(int) of these reflections, averaged in the tetragonal space group is 5.4% and the R(sigma) 3.18%. In figure 2 the typical parameters of the standard reflections (3 3 2), (4 0 4) and (4 4 0) are shown. A small change in the integral intensity is visible at longer times (higher index numbers) but no significant change in the FWHM/omega scan is visible.

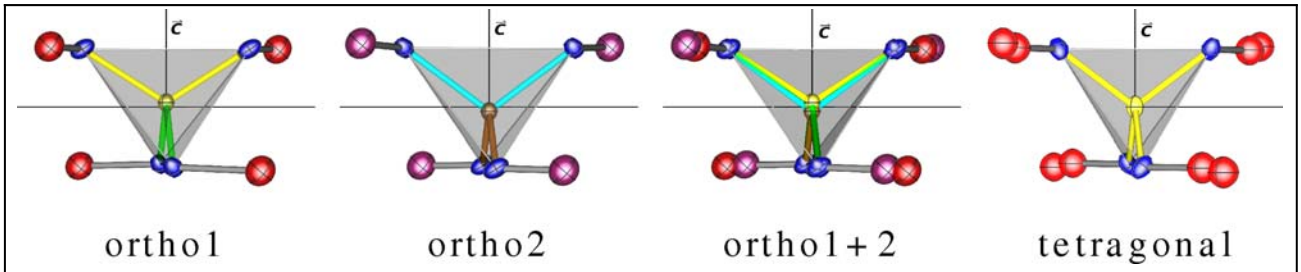


Illustration 1: $[PO_4H_2]^-$-groups in RDP. Left to right: Ferroelectric orthorhombic phase, dipole down antiparallel c (state II); Ferroelectric orthorhombic pahse, dipole up parallel c (state I); Superimposed state I and II; Paraelectric tetragonal phase

In the case of larger temperature fluctuations these values should change dramatically (splitting of reflections). Even the integral reflection should change dramatically due to a change in the extinction parameters (precursor effect [1]).

Now to make a long story short, we were not able to refine the structure successfully in the paraelectric phase. The refinement of the structure in the orthorhombic phase as well as a refinement of mixed structure is still in work.

[1] High resolution neutron and X-ray diffraction studies as a function of temperature and electrical field of the ferroelectric phase transition of RDP

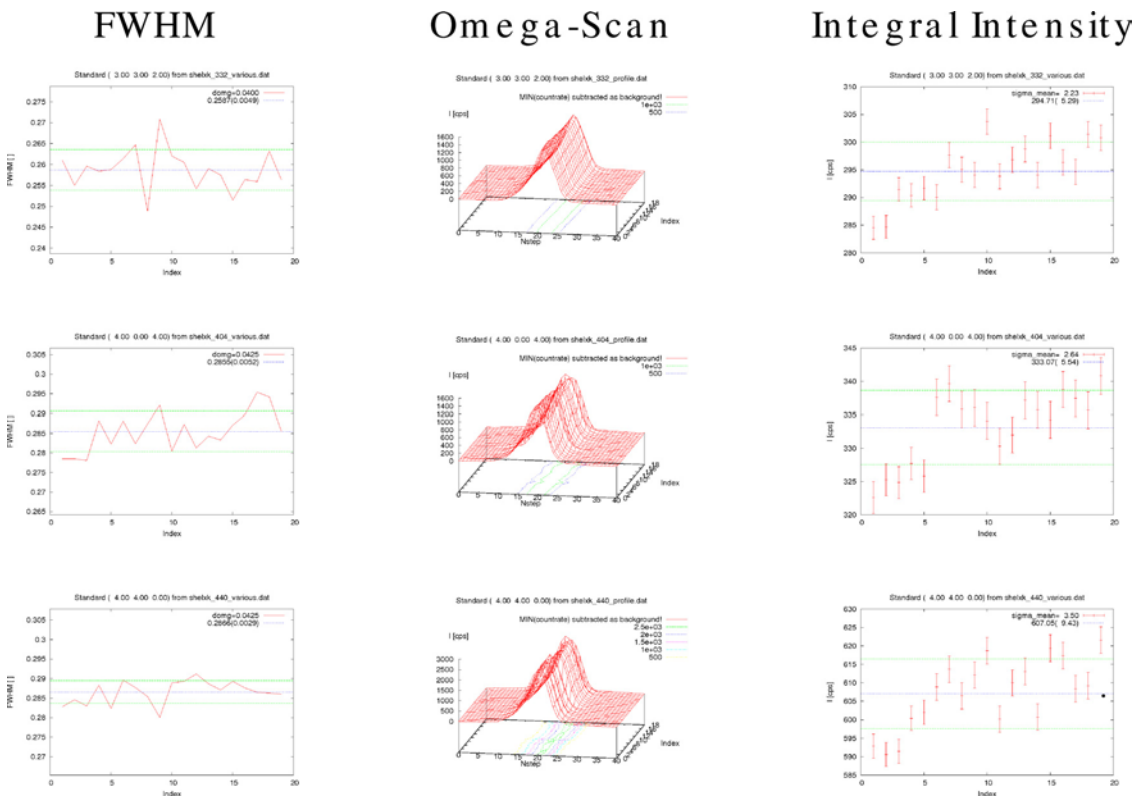


Illustration 2: FWHM, scan profile and integral intensity of standard reflections during the measurement of Bragg reflections 1.5K above Tc.

Institut für Festkörperforschung
Forschungszentrum Jülich GmbH
D-52425 Jülich

Experimental Report
of Neutron Scattering Experiments
at the FRJ-2 Reactor

Proposal number:	S28-04-015		
Experiment title:	$SrTiO_3$ – differences in the oxidised and reduced state		
Dates of experiment:	17.01.-30.01.2005 16.05.-22.05.2005	Date of report:	10.03.2006
Experimental team: Names	Addresses		
TIETZ, Frank	Forschungszentrum Jülich IWV-1		
Local Contact:	Dr. Anja Loose		

Experimental report text body

Strontium titanate ($SrTiO_3$) was selected as a model system for investigating the dimensional change after reduction and re-oxidation due to the valence changes of titanium. The interesting phenomenon in titanium-rich materials is the small shrinkage during reduction although an expansion is expected because of the increased cation radius like it is observed for lanthanum chromites ($Cr^{4+} \rightarrow Cr^{3+}$) or ceria materials ($Ce^{4+} \rightarrow Ce^{3+}$).
In this study the compound $SrTiO_3$ was therefore investigated in more detail by single-crystal neutron diffraction (and XRD).The experiments should clarify a) any atomic displacement in the perovskite lattice and b) where the highest remaining electron density is located after subtracting the atoms from the structure refinement and c) if any additional interactions (bonds) can be deduced from the structure analysis.

For the measurement of the $SrTiO_3$ crystal in the oxidized state, a transparent colorless crystal with dimensions of about 2 x 4 x 0.5 mm was used. After the neutron scattering experiment the same crystal was exposed to a reducing atmosphere (Ar/4% H2) at 1200°C to induce the reduction of Ti^{4+} to Ti^{3+} and the release of oxygen from the lattice compensating the reduction of the Ti ions. The crystal was heat treated for 100 h. Afterwards the sample had a deep black color and was used again for a second neutron scattering measurement.

The results of the neutron scattering experiments are summarized in Table 1.

Table 1: Results of the crystal structure determination before and after reduction

	$SrTiO_3$ oxidised, RT,	$SrTiO_3$ reduced, RT
Space group	Pm-3m	Pm-3m
Lattice parameter (Å)	3.922(5)	3.904(5)
Atomic position (x,y,z), Sr	0.500, 0.500, 0.500	0.500, 0.500, 0.500
Temp.factors (u_{11}, u_{22}, u_{33})	0.005(1), 0.005(1), 0.005(1),	0.003(2), 0.003(2), 0.003(2),
Atomic position (x,y,z), Ti	0.000, 0.000, 0.000	000, 0.000, 0.000
Temp.factors (u_{11}, u_{22}, u_{33})	0.0084(7), 0.0084(7), 0.0084(7)	0.0078(9), 0.0078(9), 0.0078(9)
Atomic positions (x,y,z), O	0.500, 0.000, 0.000	0.500, 0.000, 0.000
Temp.factors (u_{11}, u_{22}, u_{33})	0.002(1), 0.007(1), 0.007(1),	0.000(2), 0.005(2), 0.005(2),
wR^2	2,99 %	3,56 %
R_1	1,74 %	1,77 %
Bond lengths (Å), Sr-O	2.773(4)	2.761(4)
Ti-O1	1.961(3)	1.952(3)
Ti-O2	3.397(4)	3.381(4)

The table clearly shows that no significant atomic displacement can be observed. By fixing the occupation factor of oxygen (full occupation) also no significant differences in the structure analysis appeared. This indicates that the amount of reduced Ti ions and released oxide ions are too small to be detected by neutron scattering. The only small but significant change of the crystal structure is the decrease of the lattice parameter by about 0.5 % and hence resulting in a small decrease of the bond lengths.
This result agrees very well with a dilatometry experiment in which a similar crystal was reduced and re-oxidised *in-situ* giving a length change of 0.3 % at 1000°C. The subsequent investigations performed on single crystals (electrical conductivity, thermogravimetry, dilatometry) have shown that the changes of the properties during redox cycling are much smaller for a single crystal than for polycrystalline ceramics. Therefore the results of the neutron experiments fit very well with the other observations. However, the major aim of these investigations, i. e. the explanation of the shrinkage after reduction of the material, could not be obtained.

Institut für Festkörperforschung
Forschungszentrum Jülich GmbH
D-52425 Jülich

Experimental Report
of Neutron Scattering Experiments
at the FRJ-2 Reactor

Proposal number:	S28-05-002		
Experiment title:	Structural behaviour of topaz at low temperature		
Dates of experiment:	04.04.-24.04.05 and 09.05.-22.05.05	Date of report:	06.02.06
Experimental team: Names	Addresses		
1) G. Diego Gatta 2) F. Nestola 3) G. D. Bromiley	1) Dipartimento di Scienze della Terra, Università degli Studi di Milano, I-20133 Milano, Italy 2) Bayerisches Geoinstitut, Universität Bayreuth, D-95440, Bayreuth, Germany 3) Department of Earth Sciences, Cambridge University, Downing Street, Cambridge CB2 3EQ, UK		
Local Contact:	Dr. Anja Loose		

Experimental report text body

The crystal structure of a natural topaz (ideal formula $Al_2SiO_4(F,OH)_2$) was reinvestigated by means of single-crystal X-ray diffraction (at 298K) and neutron diffraction (at 298 and 10K) and polarized infrared spectroscopy in order to define unambiguously the real symmetry of topaz, the location of the proton and its thermal displacement parameters at room and low-temperature, the hydrogen-bonding and the vibration modes (stretching and bending) of the OH dipole. A single-crystal of natural topaz [$Al_{2.00}Si_{1.05}O_{4.00}(OH_{0.26}F_{1.75})$, 2 x 3 x 13 mm^3] from Ouro Preto, Minas Gerias**,** Brasil was used for the neutron diffraction experiments at 298 and 10K with a Huber four-circle diffractometer (SV28/1) installed at the DIDO reactor – FZJ. A He-cryostat was used for the low-*T* experiment. The incident radiation (obtained using a Cu(200) single-crystal monochromator) with a constant wavelength of 0.87238(1)Å was used for the room and low-*T* experiments. The neutron flux density was about $2.5 \cdot 10^6$ $n \cdot s^{-1} \cdot cm^{-2}$ and the tangential beam tube gave rise to a very small background count rate (~5 s^{-1}). A total of 4446 reflections (of which 988 unique) were recorded at 298K (maximum $2\theta = 99.93^\circ$) and 4049 reflections (of which 632 unique) at 10K (maximum $2\theta = 82.26^\circ$). The systematic extinction rules in general agreed with the space group *Pbnm*. However, we observed 6 and 14 violating reflections for the data collections at 298 and 19 K respectively, belonging to the classes 00*l* (with $l=2n+1$), 0*kl* (with $k=2n+1$) and *h*0*l*.

Intensity of the diffraction data was corrected for Lorentz effect and no absorption correction was applied because of the composition and the dimensions of the sample. The discrepancy factors for the symmetry related reflections were R_{int} = 0.0229 and R_{int} = 0.0251 at 298 and 10 K respectively. The neutron diffraction data were first processed with the program E-STATISTICS, implemented in the WinGX package (Farrugia 1999). The structure of topaz was found to be centrosymmetric at 92.6%. Then, the diffraction data were processed with the program ASSIGN-SPACEGROUP (in WinGX, Farrugia 1999). Two possible space groups (both belonging to the *mmm* Laue class) were selected by the program: *Pbmn* and $Pbn2_1$. However, the Combined Figure of Merit (CFOM) showed unambiguously that the space group *Pbnm* is highly likely (CFOM -*Pbnm*= 0.729, CFOM-$Pbn2_1$ =9.178). The crystal structure refinement was then performed in the space group *Pbnm* using the SHELX-97 software (Sheldrick 1997) with anisotropic thermal displacement parameters and starting from the atomic coordinates of Alberico et al. (2003).

X-ray and neutron structural refinements allow us to infer that the crystal structure of natural topaz with OH/(OH+F)<0.5 can be described with the *Pbnm* space group. Violating reflections, found in the previous investigations and in this study, are likely due to Renninger effect (double diffraction phenomenon). The nuclear density Fourier map shows that the proton is located at Wyckoff 8*d* position and the refined coordinates are: *x*=0.495(2), *y*=0.252(1), *z*=0.1629(7) (Fig. 1). The O-H bond lies on the (010)-plane and forms an angle of about 28.9° with the *c*-axis. Neutron structural refinements at 298 and 10K show that the displacement ellipsoid of the proton is highly anisotropic. The H-bonding arrangement appears to be much more complex than that reported in previous studies, with at least four potential H···O or H···F interactions (distances < 2.38Å).

References

Alberico, A., Ferrando, S., Ivaldi, G., and Ferraris, G. (2003) European Journal of Mineralogy, 15, 875-881.

Farrugia, L.J. (1999) Journal of Applied Crystallography, 32, 837-838.

Sheldrick, G.M. (1997) SHELX-97. Programs for crystal structure determination and refinement. Institute of Inorganic Chemistry, University of Göttingen, Germany.

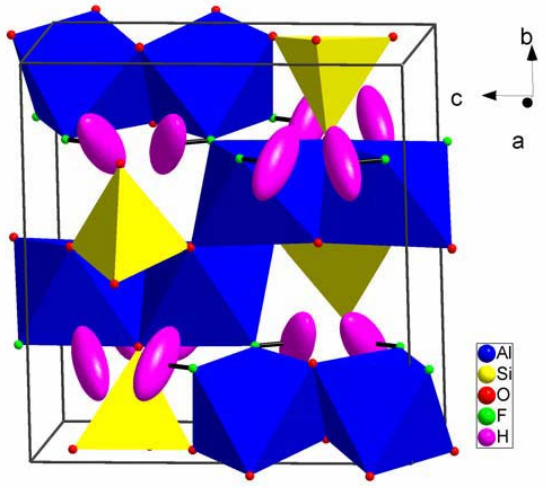


Fig. 1. Clinographic view of the crystal structure of topaz

Institut für Festkörperforschung
Forschungszentrum Jülich GmbH
D-52425 Jülich

Experimental Report
of Neutron Scattering Experiments
at the FRJ-2 Reactor

Proposal number:	S28-05-003		
Experiment title:	**Structure refinement and location of protons in natural cancrinite $Na_8[Si_6Al_6O_{24}]*CO_3*2H_2O$**		
Dates of experiment:	23.05.-29.05.2005 06.06.-15.06.2005	Date of report:	09.03.2006
Experimental team: Names	Addresses		
Dr. G. Redhammer	FB Materialwissenschaften, Abteilung Mineralogie, Universität Salzburg, Hellbrunnerstr. 34, A-5020 Salzburg, Österreich.		
Prof. Dr. G. Roth	Institut für Kristallographie, RWTH Aachen, Jägerstr. 17/19, D-52056 Aachen, Deutschland		
Prof. Dr. G. DellaVentura	Dipartimento di Szienze Geologiche, Università di Roma Tre, Largo S. Leonardo Murialdo 1, I-00146 Roma, Italy		
Local Contact:	Dr. Anja Loose (IFF)		

Experimental report text body

Cancrinite belongs to the group of feldspathoids, which are framework aluminosilicates comprising at least three distinct groups: the leucite, nepheline-kalsilite and cancrinite-sodalite groups. The cancrinite-sodalite group in particular, comprises all phases characterized by three-dimensional connection of six-member rings of silicon and aluminium tetrahedra; each ring is linked to three rings in a preceding layer and to three rings in the succeeding one, such as to form a three dimensional framework. In cancrinite the stacking sequence of these tetrahedral rings gives rise to channels and cavities filled by extra-framework anions and cations. Typical anions within the structural channels are H_2O, OH, and CO_3^{2-}. Also Na^+ and Ca^{2+} are located within these channels and pores. To try to locate hydrogen within the channel, two natural cancrinite samples, one from Kameron, #29509, and one from Kanada, Bancroft #38834 were analysed. Preliminary X-ray diffraction experiments showed both samples to be commensurate, while a second sample of Kanada (# 38855) revealed incommensurate superstructure reflections.

Both cancrinite samples are trigonal, space group $P6_3$, lattice parameters are a = 12.595(5) Å, c = 5.121(5) Å (#29509) and a = 12.60(2) Å, c = 5.121(5) (#38834) respectively. Data sets for both samples were refined R = 2.18 % and 4.17 % respectively. The samples show perfectly ordered Al, Si distribution with average Si-O and average Al-O bond lengths of 1.613(3) Å and 1.732(3) Å. Two positions for the alkali cations are present in the structure, one is located within the cancrinite cage (Na1), and the other one is within the large channel. It was found that the cage position is occupied by sodium only, while both Na and Ca are hosted at the channel site. The (Na,Ca) cations are bonded to three oxygen atoms of the Al-Si framework at a distance of ~ 2.40 Å and to oxygen atoms of a CO_3 groups. The two non-equivalent CO_3 groups show large anisotropic displacements in channel direction and have occupancy of ~ 1/3. Because of the close proximity of the positions, only one can be occupied at any one time.

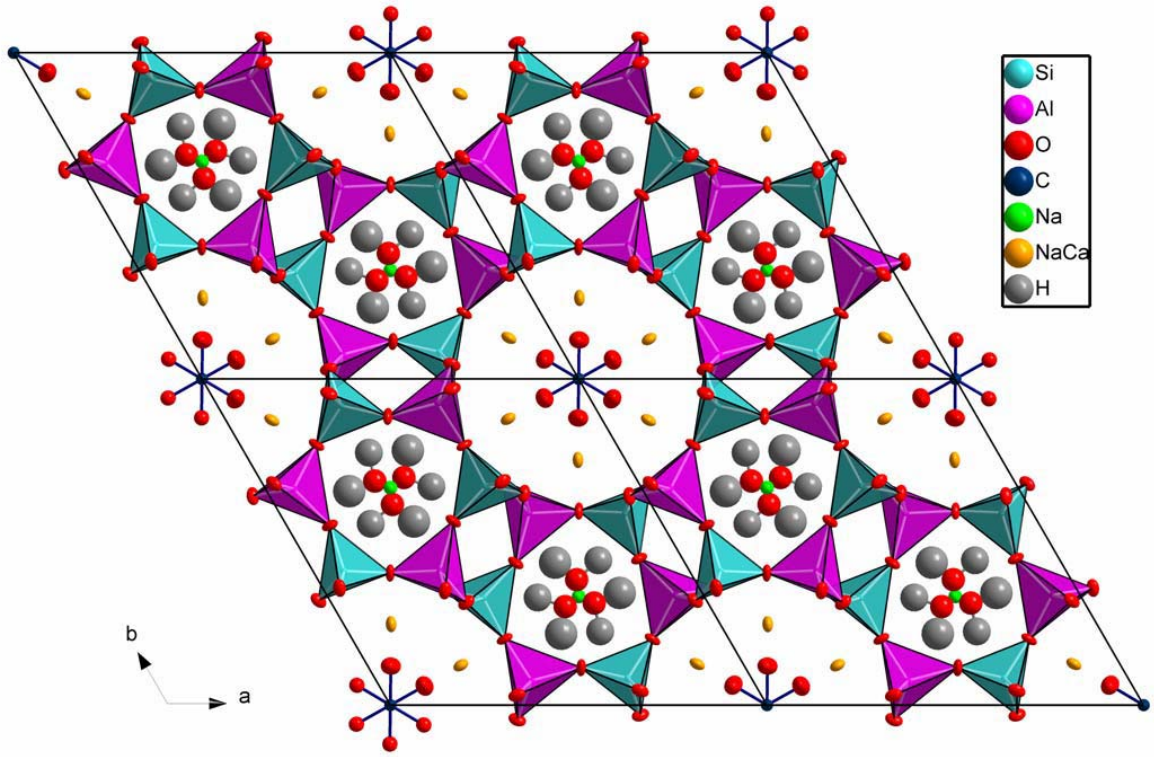
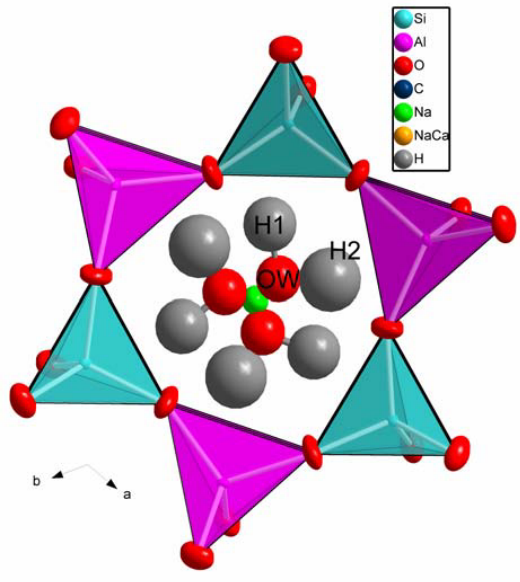


Figure 1: View of the cancrinite structure along the *c* - axis, showing CO_3 groups and NaCa sites within the large channels and Na-sites and H_2O molecules within the cancinite cage.

Detailed inspection of the CO_3 groups show that they are not perfectly coplanar with C-O bond lengths of 1.308(3) Å and 1.293(3) Å for theC1 and the C2 site respectively.



The cancrinite cage hosts sodium at the Na1 site. Thereby sodium is planar coordinated by 6 oxygen atoms of the Al-Si framework at distances of 2.436(3) Å and 2.859(3) Å. Additionally there are two bonds to the oxygen atom of the water molecule at distances of 2.379(7) and 2.874(7) Å. This oxygen atom is located at a general position near to the triad axis. Due to short O-O distances of 0.98(1) Å only one of the three possible positions can be occupied at one time and the maximum occupation of this general site is 0.33. This is actually the case as shown by refinements of the X-ray diffraction data, while the neutron data show a somewhat higher occupation of 0.42. Inspection of difference electron density maps revealed some residuals close to this oxygen atom at distances of ~ 1 Å. Putting hydrogen atoms to these residuals and allowing to refine the occupation of these sites gave reliable O-H distances of 0.95(2) Å and 0.98(2) Å with an occupancy close to 0.4; the H1-Ow-H2 angle amounts 99.3(9)°. The isotropic atomic displacement of the hydrogen atoms is quite large, and in detailed inspection it may be followed that there is a splitting of the H1 and H2 positions and there are a total of four quite well defined hydrogen positions around Ow. The occupancies are between 0.12 and 0.18, the isotropic atomic displacement parameters are similar for all for H with U ~ 0.05 - 0.06.

Institut für Festkörperforschung
Forschungszentrum Jülich GmbH
D-52425 Jülich

Experimental Report
of Neutron Scattering Experiments
at the FRJ-2 Reactor

Proposal number:	S28-05-003/2		
Experiment title:	**Structure refinement on natural Hauyne, ideally $Na_6Ca_2[Al_6Si_6O_{24}](SO_4)_2$**		
Dates of experiment:	15.06.-28.06.2005	Date of report:	30.03.2006
Experimental team: Names	Addresses		
Dr. G. Redhammer	FB Materialwissenschaften, Abteilung Mineralogie, Universität Salzburg, Hellbrunnerstr. 34, A-5020 Salzburg, Österreich.		
Prof. Dr. G. Roth	Institut für Kristallographie, RWTH Aachen, Jägerstr. 17/19, D-52056 Aachen, Deutschland		
Prof. Dr. G. DellaVentura	Dipartimento di Szienze Geologiche, Università di Roma Tre, Largo S. Leonardo Murialdo 1, I-00146 Roma, Italy		
Local Contact:	Dr. Anja Loose (IFF)		

Experimental report text body

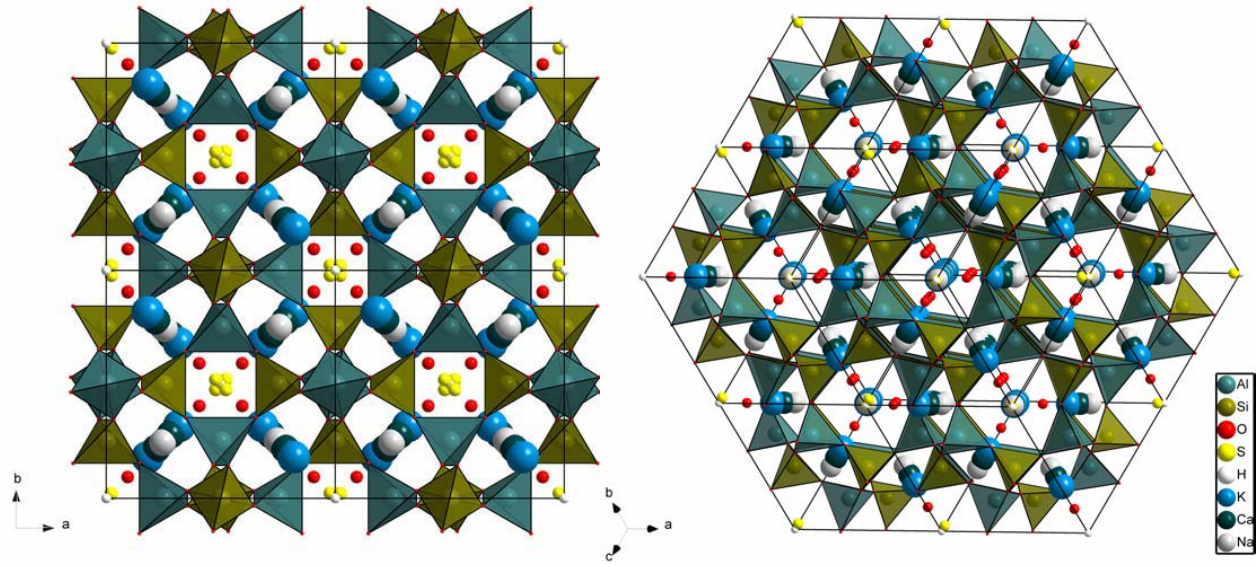
1. Introduction

Hauyne, ideally $Na_6Ca_2[Al_6Si_6O_{24}](SO_4)_2$ is a sulphatic sodalite - group mineral. The structure has 4-membered rings of AlO_4 and SiO_4 tetrahedra that are parallel to the {1 0 0} direction. These rings are connected to form a 3-dimensional framework with 6-membered rings parallel to the {1 1 1} direction giving rise to to cube-octahedral cages. According to literature, the alumino-silicate framework of hauyne has a 1 : 1 Al : Si ratio and these atoms are fully ordered (Hassan & Grundy 1991).The cages can accommodate a large variety of cations such as K^+, Na^+ and Ca^{2+}, with SO_4^{2-} groups as the dominant interstitial anions. Members of this mineral group may also show complex satellite reflections. However, the sample of blue hauyne from Alban Hills, Italy, we have studied, does not show any satellite reflections as proven by preliminary X-ray diffraction experiments. Polarized infra-red experiments hint the presence of a small amount of OH- within the cages.

2. Results and Discussion

The sample of blue hauyne is cubic, space group *P*-43*n*, a = 9.116(5) Å, Z = 1. Structure solution using direct methods revealed the positions of Al, Si and oxygen, building up the alumino-silicate framework. Interstitial cations and anions were located from difference density maps. The final refinement using full anisotropic atomic displacement parameters for the framework atoms converged to final agreement factors R_1 = 2.28 % and wR_2 = 6.43 % for all 186 unique reflections. During refinements a mixed occupation of Al and Si position was tested, however, Al and Si indeed appeared to be fully ordered on the two tetrahedral coordinated framework sites. Figure 1 displays the topology of the structure view in 2 different directions.

Within the channels in {1 1 1}, possible positions for cations Na^+, K^+ and Ca^{2+} were easily located x = 0.681(2), 0.719(2) and 0.754(2) respectively. These positions are only partly filled, giving rise to occupancy of 0.46 for K, 0.28 for Ca and 0.263 for Na respectively. These values correspond well to the chemical composition of the compound as determined from electron microprobe analysis.



(A) **(B)**

Figure 1: Structure of blue Hauyne, **(A)** viewed along the crystallographic a-axis and displaying the four-member rings of edge-sharing AlO_4 and SiO_4 tetrahedra. **(B)** viewed almost along the {1 1 1} direction showing the channels formed by the arrangement of alumino-silicate framework. Cations Na^+, K^+ and Ca^{2+} alternate with SO_4 groups within the channels.

Interpretation of differenced densities arising from SO_4 groups appeared to be difficult. The sulfur atom is displaced from 2(a) position at $^1/_2$, $^1/_2$, $^1/_2$ to a 8(e) position with (x, x, x), x = 0.479(2), the occupancy was fixed to 0.25 as due to the closeness of S-atoms due to fourfold axis the site can only be occupied by $^1/_4$. Oxygen atoms (O2) coordinating the S-atom(s) were found at (x, x, x) x = 0.594(2) giving rise to three reasonable S-O bond lengths of 1.45(4) Å, while one is 1.70(4) Å. However, isotropic displacements especially for the oxygen are very large and some residual density appears in Fourier maps which might be interpreted as oxygen atoms. One of these peaks could be interpreted as oxygen atom (O3) belonging to the SO_4 group with S-O bond length of 1.38(2) Å. A negative difference peak at $^1/_2$, $^1/_2$, $^1/_2$ may be interpreted as an H atom with an oxygen atom (O4) being away 1.07(6) Å with almost the same occupancy of ~ 1/3.

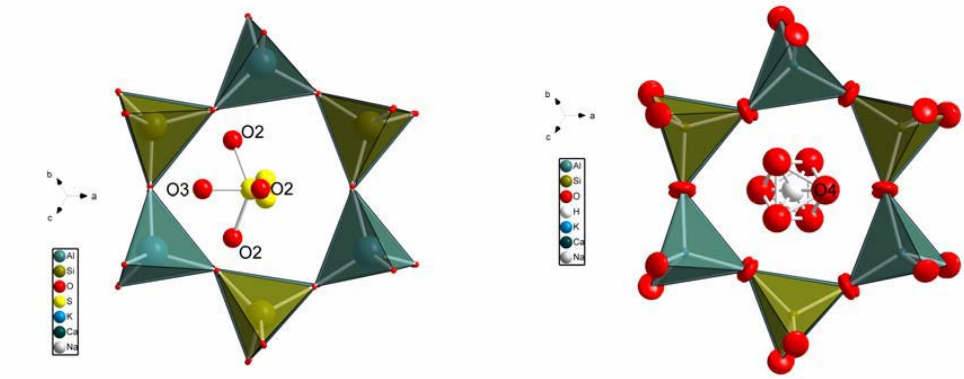


Figure 2: Possible arrangement of SO_4 and OH^- groups in hauyne {1 1 1} channels.

References cited:
Hassan, I., Grundy, H.D. (1991) Canadian Mineralogist 29, 123 - 130.

Institut für Festkörperforschung
Forschungszentrum Jülich GmbH
D-52425 Jülich

Experimental Report
of Neutron Scattering Experiments
at the FRJ-2 Reactor

Proposal number:	S28-05-007		
Experiment title:	High-temperature structural behavior of epidote, $Ca_2(Al, Fe)_3(SiO_4)_3(OH)$		
Dates of experiment:	24.10.-13.11. and 28.11.-18.12.2005	Date of report:	06.02.06
Experimental team: Names	Addresses		
1) G. Diego Gatta	Dipartimento di Scienze della Terra, Università degli Studi di Milano, I-20133 Milano, Italy		
Local Contact:	Dr. Anja Loose		

Experimental report text body

Epidote group of minerals are monoclinic sorosilicates (with mixed SiO_4 tetrahedra and Si_2O_7 groups) with general formula $A_1A_2M_1M_2M_3(SiO_4)(Si_2O_7)O(OH)$, M represent trivalent cations in octahedral sites and A represent divalent cations in larger coordination (Fig. 1). The crystal structure of epidote is built up by two types of endless octahedral chains, parallel to [010], consisting of three non equivalent M1, M2 and M3 octahedra. The proton is bonded to the oxygen site O10 of the M2 polyhedron, with a hydrogen bridge to the O4 site of the neighboring M1 octahedron (following the site notation of Kvick et al. 1988) (Fig. 1). The monoclinic epidote minerals have space group $P2_1/m$. However, on the basis of some spectroscopic investigations, a possible reduction of the symmetry to *Pm* or *P*-1 space group due to "Al/Fe convergent ordering" on M3 was suggested (Franz & Liebscher 2004). Despite the crucial role of natural epidotes in high-pressure/high-temperature metamorphism, no structural investigation of epidotes under non-ambient conditions has been performed. Therefore, the high-*T* structural evolution of a natural epidote $[Ca_2(Al, Fe)_3(SiO_4)_3(OH)]$ from the intrusive/metamorphic complex of Val Sissone, (Rhetic Alps, Italy) was investigated by means of single-crystal neutron diffraction at 23 and 700°C in order to define unambiguously the real symmetry of epidote at high-*T*, the location of the proton and its thermal displacement parameters at room and high-*T*, the hydrogen-bonding evolution with *T* and/or any potential dehydration (deoxydrilation) effect. The diffraction experiments at room and high-*T* were performed with a Huber four-circle diffractometer (SV28/1) installed at the DIDO reactor – FZJ. A furnace designed at the FZJ was used for the high-*T* experiment. The incident radiation (obtained using a Cu(200) single-crystal monochromator) with a constant wavelength of 0.87238(1)Å was used for the room and high-*T* experiments.

A total of 2228 unique reflections were recorded at 23°C ($2\theta_{max}$ = 95.04˚) and 1721 reflections at 700°C ($2\theta_{max}$ = 82.24˚). The systematic extinction rules agreed with the space group $P2_1/m$. The structural refinement with the diffraction data collected at room and high-T was performed in space group $P2_1/m$ at first with isotropic displacement parameters using the SHELXL-97 package (Sheldrick 1997), starting with the atomic coordinates of Kvick et al. (1988). The final least-square cycles were conducted with anisotropic thermal parameters and all the principal mean square atomic displacement parameters were positively defined. The Al/Fe fraction at the M1, M2 and M3 octahedral sites was refined. At the end of the refinements, no peak larger than ±0.68 fm/Å^3 and ±1.20 fm/Å^3 were found in the difference-Fourier map of the nuclear density at 23 and 700°C respectively. The final agreement indexes (R_1) were R_1(23°C)=0.0309 and R_1(700°C)= 0.0562 for 127 refined parameters.
Neutron structural refinements allowed us to infer that the crystal structure of natural epidote is stable at least up to 700°C and no deoxydrilation effect occurs. We can also infer that at room-T the octahedral M1 site shows a low amount of iron [%Fe=2.2(4)%], which is absent at the M2 site. In contrast, a high content of Fe is observed at the M3 site [%Fe=71.6(5)%)]. At 700°C, we do not observe any statistically relevant difference of the cations distribution in the octahedral sites with respect to that observed at room-T [%Fe_{M1}=0.6(12)% and %Fe_{M3}=70.4(14)%]. At present, we have no evidence of any T-induced order-disorder phenomena concerning the Al/Fe distribution in the M1-M2-M3 octahedral sites (the so called "non-convergent ordering") or any high-T phase transition to lower symmetry due to Al/Fe "convergent ordering" on M3 (with a splitting of M3 into two sites: M3 and M3', Franz & Liebscher 2004).

References

Kvick Å, Pluth JJ, Richardson JrJW, Smith JV (1988) Acta Cryst B, 44, 351-355.
Franz G, Liebscher A (2004) Rev. Min. Geoch., 56, 1-80.
Sheldrick, G.M. (1997) SHELX-97. Programs for crystal structure determination and refinement. Institute of Inorganic Chemistry, University of Göttingen, Germany.

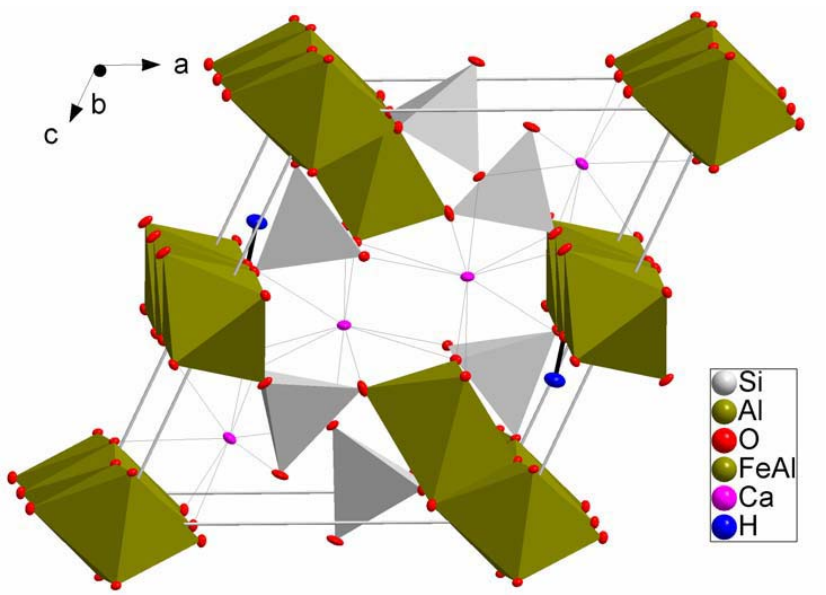


Fig. 1. Clinographic view of the crystal structure of epidote

Institut für Festkörperforschung
Forschungszentrum Jülich GmbH
D-52425 Jülich

Experimental Report of Neutron Scattering Experiments at the FRJ-2 Reactor

Proposal number:	S28-05-008		
Experiment title:	Crystal structure analysis of (1-x)PZN-xNBT		
Dates of experiment:	10.12.-18.12.2005 09.01.-22.01.2006	Date of report:	05.06.2006
Experimental team: Names	Addresses		
Dr. Loose, Anja Prof. Dr. Heger, Gernot Dr. Park, Hyun Min	IFF,FZ-Jülich and Institut für Kristallographie, RWTH Aachen Jägerstr.17-19, D-52056 Aachen Korea Research Institute of Standards and Science (KRISS) Materials Evaluation Center, P.O.Box 102, Yusong, 305-600, Korea		
Local Contact:	Dr. Loose, Anja		

Experimental report text body

The new ferroelectric material (1-x)·Pb(Zn1/3Nb2/3)O3 - x·($Na_{1/2}Bi_{1/2}$)TiO_3, abbreviated as PZN-NBT, has been developed for piezoelectric application. Large single crystals of PZN-NBT up to several cm diameter were grown by the flux method at about 700°C in the cubic Perowskite-structure.
In order to investigate the phase diagram of PZN-NBT as function of temperature and NBT content x, neutron diffraction measurements were performed at the single crystal diffractometer SV28(left) for compositions x = 0.05, 0.10, and 0.15.
Rietveld profile refinements on synchrotron X-ray powder patterns obtained at room temperature with samples of the same nominal compositions yield the polar space group P 4mm. According to the symmetry relation between the cubic high-temperature phase of space group P m-3m and the tetragonal modification of space group P 4mm, there exists 3 twin states with 6 differently oriented ferroelectic domains which may occur at room temperature.
The Bragg-reflections of the multi-twinned crystals are split leading to a broad mountain-like ω-scan profile of typically 1.6° FWHM for a sample of x = 0.15. On heating the reflection splitting is lowered more or less linearly with increased temperature up to about 400 K, where there occurs a jump-like reduction to FWHM = 0.27° which corresponds to the instrumental resolution for high quality single crystals (Fig.2). The discontinuous behaviour of the tetragonal to cubic phase transition (of 1st order) is even more pronounced in case of the intensity data (Fig. 3). The integrated intensity of the sum of the domains remains almost constant up to about 400 K. The small intensity reduction in this range may be attributed to a normal increase of temperature Factors (Debye-Waller). The giant fall from 3700 to 1400 is a signature of the disappearance of the ferroelectric domains: the crystal recovers and according to its good quality extinction effects lead to an important reduction of Bragg-intensities in the cubic high temperature phase. Both observations (integrated intensity and FWHM) are completely reversible on cooling with a hysteresis of about 5.8 K.

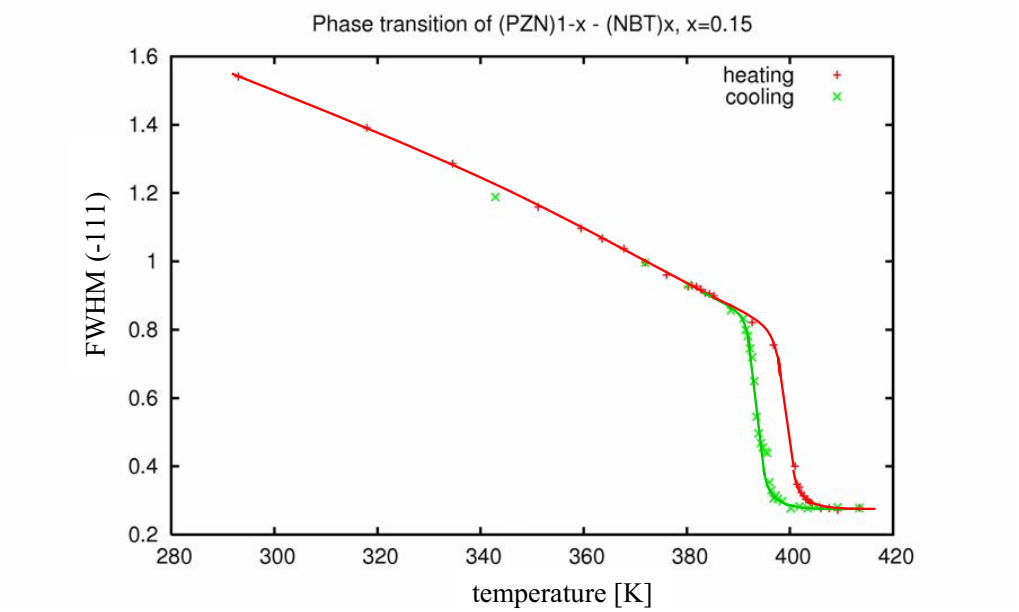


Fig. 1

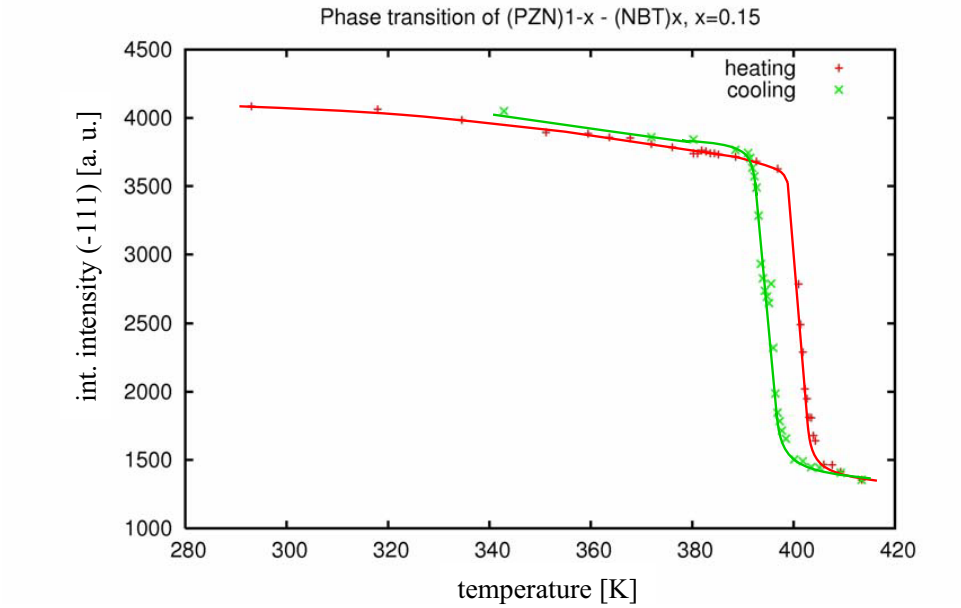


Fig. 2

For the structure refinement of the crystal with composition x = 0.15, based on a complete data set obtained at 420 K, the effective neutron scattering lengths for the A- and B- sites of the ABO_3 Perowskite-structure were calculated according to the nominal composition. The resulting R-factor of 2.6% is very good. It seems that the oxygen sublattice is fully occupied whereas there might be indication for either some vacancies on the B-site or a smaller modification of composition.
For the x = 0.10 crystal the ferroelectric phase transition occurs at about 394 K on heating. A complete data set of Bragg-intensities was measured at 413 K. The results of the structure refinement correspond to those of x = 0.15. The x = 0.05 crystal showed at room temperature no splitting of reflections or even significant increased widths (FWHM). Therefore, a complete set of intensity data was measured at room temperature and also refined in the cubic Perowskite structure type. For all compositions there is an important difference between the mean-square displacements of sites A and B. The octahedron-coordinated B-sites show small U_{ij} values, whereas those of the cubeoctahedron-coordinated A-sites are very large. It seems that the localisation of $Pb^{2+}/Na^{1+}/Bi^{3+}$ with its different ionic radii may give rise to static contributions in the O_{12}-cubeoctahedron.

Institut für Festkörperforschung
Forschungszentrum Jülich GmbH
D-52425 Jülich

Experimental Report of Neutron Scattering Experiments at the FRJ-2 Reactor

Proposal number:	S28-05-009		
Experiment title:	Crystal structure and proton ordering of $(NH_4)_3H(SO_4)_2$		
Dates of experiment:	23.01.06-27.01.06 06.02.06-18.02.06 26.04.06-28.04.06	Date of report:	02.06.06
Experimental team: Names	Addresses		
Prof. Dr. Heger, Gernot Sohn, Yoo Jung Dr. Loose, Anja	Institut für Kristallographie, RWTH Aachen Jägerstr. 17-19, D-52056 Aachen IFF, FZ-Jülich		
Local Contact:	Dr. Loose, Anja		

Experimental report text body

$(NH_4)_3H(SO_4)_2$ (TAHS) is a representative of the ferroelastic $M_3(H/D)(AO_4)_2$-structure family with monovalent M^+-ions (M^+=K^+,Rb^+,Cs^+,NH_4^+/ND_4^+) and A=S, Se which is characterized by strong hydrogen bonds between the AO_4-groups forming AO_4-H/D-AO_4-dimers. The $M_3(H/D)(AO_4)_2$-compounds show a rich variety of polymorphic phases where the phase transitions are related to ordering phenomena of the AO_4/$N(H/D)_4$-groups and the H/D-atoms in the O-(H/D)-O hydrogen bonds. Neutron diffraction studies on single crystals are needed to determine the hydrogen distributions in the crystal structures of the TAHS-phases in detail. This information is essential for to clarify the mechanisms of phase transitions driven by H-ordering.
Large perfect single crystals of TAHS were grown from aqueous solution in the room temperature phase II. A sample of 3x3x3 mm^3 was used for the measurement of a complete set of reflection intensities at the SV28l-diffractometer (λ=0,87238Å) up to $(\sin\theta/\lambda)_{max}$= 0,7 $Å^{-1}$ at room temperature. In order to reduce extinction effects the sample crystal was quenched in liquid nitrogen. A careful analysis of systematic extinctions confirmed that h0l reflections with l=2n+1 are absent in accordance with the monoclinic space group C 12/c1, proposed by X-ray diffraction studies [1, 2]. An additional investigation by ψ-scan technique on h0l reflections with l=2n+1 using a much larger crystal (6x7x8 mm^3) confirmed this result. Even with much increased statistics there was no indication of these “forbidden” reflections. The results of the crystal structure refinement on neutron diffraction data of TAHS II are in agreement with those of the X-ray analyses [1, 2]. The additional new findings consist in
- the dynamical hydrogen-disorder with a double-minimum-potential in the O1-H1···H1-O1 bridge of the (SO_4-H-SO_4) dimers. This is clearly visible from the anisotropic mean square displacements of H1 in Fig. 1.
- the pronounced librations of the $(NH_4)^+$-cations around their well defined N1/N2 positions (see Fig. 2.). This can be interpreted as a consequence of competing N-H···O hydrogen bonds leading to a dynamical disorder. A structure refinement including rigid body rotations of the NH_4 groups is in preparation.

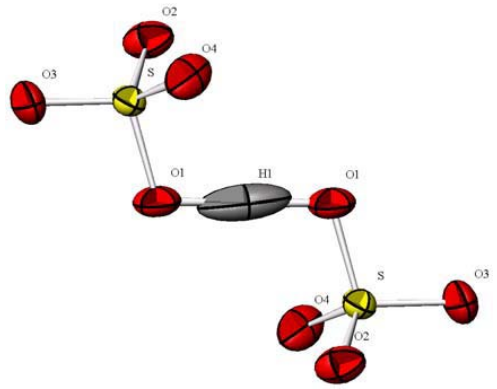


Fig. 1. Two SO_4-tetrahedra connected by an H-bond forming a dimer.

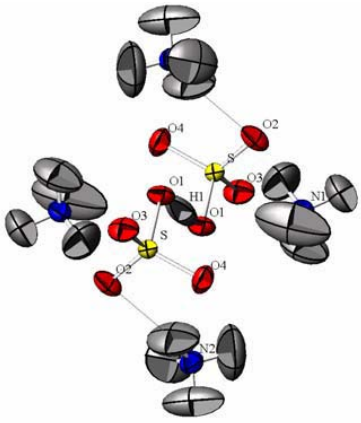


Fig. 2. SO4-H1-SO_4 dimer with surrounding NH_4-groups.

The phase transition between the room temperature phase II and the high temperature phase I was studied by measurements of the integrated intensity of a reflection which does not exist in the high temperature phase I (space group $R\bar{3}m$ or $R\bar{3}$). Fig. 3. shows the temperature dependent intensity of the -2 2 1-reflection. The phase transition temperature determined at 140±2°C corresponds very well to the literature data (140°C).

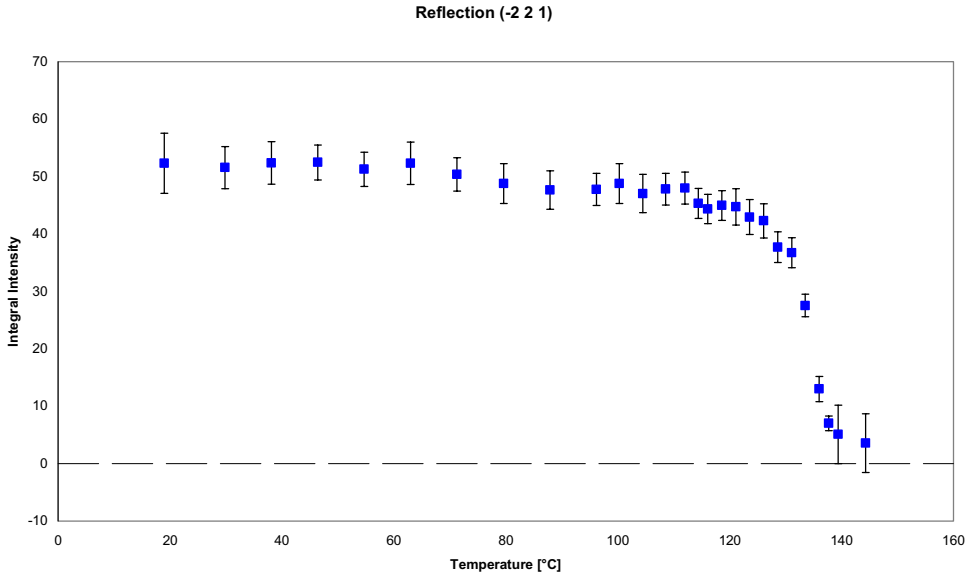


Fig. 3. Temperature dependency of integral intensity of the -2 2 1-reflection.

The reflection profiles at high temperature for $T>T_c$ (II-I) are considerably enlarged. Therefore, it was impossible to obtain reliable integrated reflection intensities in the high temperature phase I of TAHS up to now. We plan to repeat this experiment at high temperature with an unquenched crystal, where we expect better defined reflection profiles.
Temperature dependent X-ray powder diffraction measurements on the II-I phase transition of TAHS confirm the neutron results very well.

[1] K.Friese, M.I.Aroyo, L.Schwalowsky, G.Adiwidjaja, U.Bismayer, Solid State Chem. **165**, 136 (2002)
[2] P.M. Dominiak, J.Herold, W.Kolodziejski, K Wozniak, Inorg.Chem. **42**, 1590 (2003)

Institut für Festkörperforschung Forschungszentrum Jülich GmbH D-52425 Jülich	

Experimental Report
of Neutron Scattering Experiments
at the FRJ-2 Reactor

Proposal number:	S28-05-007/2		
Experiment title:	High-temperature structural behavior of epidote, $Ca_2(Al, Fe)_3(SiO_4)_3(OH)$ (Second Experiment)		
Dates of experiment:	07.-20. April 2006	Date of report:	10.05.2006
Experimental team: Names	Addresses		
G. Diego Gatta	Dipartimento di Scienze della Terra, Università degli Studi di Milano, I-20133 Milano, Italy		
Local Contact:	Dr. Anja Loose		

Experimental report text body

Epidotes are monoclinic sorosilicates (with mixed SiO_4 tetrahedra and Si_2O_7 groups) with general formula $A_1A_2M_1M_2M_3(SiO_4)(Si_2O_7)O(OH)$, M represent trivalent cations in octahedral sites and A represent divalent cations in larger coordination (Fig. 1). The crystal structure of epidote is built up by two types of endless octahedral chains, parallel to [010], consisting of three non equivalent M1, M2 and M3 octahedra. The proton is bonded to the oxygen site O10 of the M2 polyhedron, with a hydrogen bridge to the O4 site of the neighboring M1 octahedron (following the site notation of Kvick et al. 1988) (Fig. 1). The monoclinic epidote minerals have space group $P2_1/m$.

In the first experiment performed by us at the FZJ on the high-T structural behaviour of epidote, $Ca_2(Al, Fe)_3(SiO_4)_3(OH)$, we investigated the T-induced structural evolution of this sorosilicate and the main deformation mechanism on the basis of two data collection and structural refinements at room conditions and at 700°C, respectively. However, the high-T data at 700°C were not suitable for a profound description of the changes in the proton environment and for a TLS-analysis.

We performed a further diffraction experiments at high-T (660°C) with a Huber four-circle diffractometer (SV28/1) installed at the DIDO reactor – FZJ, with a furnace designed at the FZJ, using a crystal of natural epidote from the sample previously used (from the intrusive/metamorphic complex of Val Sissone, Rhetic Alps, Italy). A incident radiation (obtained using a Cu(200) single-crystal monochromator) with a constant wavelength of 0.87238(1)Å was used. A total of 1230 unique reflections were recorded ($2\theta_{max}$ = 70˚). The systematic extinction rules agreed with the space group $P2_1/m$. The structural refinement with the diffraction was performed in space group $P2_1/m$ at first with isotropic displacement parameters using the SHELXL-97 package (Sheldrick 1997), starting with the atomic coordinates of Kvick et al. (1988). The final least-square cycles were conducted with anisotropic thermal parameters and all the principal mean square atomic displacement parameters were positively defined.

The Al/Fe fraction at the M1, M2 and M3 octahedral sites was refined. At the end of the refinements, no peak larger than ±0.90 fm/Å^3 were found in the difference-Fourier map of the nuclear density. The final agreement index was R_1(660°C)= 0.0484for 126 refined parameters.
Neutron structural refinements allowed us to infer that the crystal structure of natural epidote is stable at least up to 660°C and no deoxydrilation effect occurs. At high-*T* we do not observe any statistically relevant difference of the cations distribution in the octahedral sites with respect to that observed at room-*T* . At present, we have no evidence of any *T*-induced order-disorder phenomena concerning the Al/Fe distribution in the M1-M2-M3 octahedral sites (the so called "non-convergent ordering") or any high-*T* phase transition to lower symmetry due to Al/Fe "convergent ordering" on M3 (with a splitting of M3 into two sites: M3 and M3', Franz & Liebscher 2004). The Fig.1 shows the major *T*-induced changes into the crystal structure of epidote on the basis of the structural refinements performed at room-*T* and at 660°C.

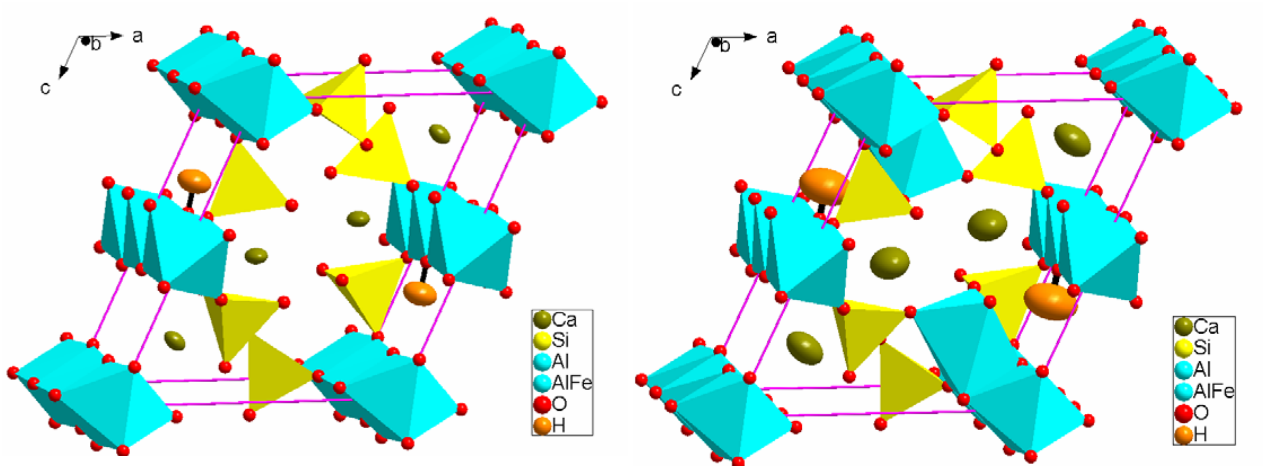


Fig. 1. Clinographic view of the crystal structure of topaz refined at room-*T* (left side) and at 660°C (right-side). Thermal ellipsoid probability: 99%.

References
Kvick Å, Pluth JJ, Richardson JrJW, Smith JV (1988) Acta Cryst B, 44, 351-355.
Franz G, Liebscher A (2004) Rev. Min. Geoch., 56, 1-80.
Sheldrick, G.M. (1997) SHELX-97. Programs for crystal structure determination and refinement. Institute of Inorganic Chemistry, University of Göttingen, Germany.

Institut für Festkörperforschung
Forschungszentrum Jülich GmbH
D-52425 Jülich

Experimental Report of Neutron Scattering Experiments at the FRJ-2 Reactor

Proposal number:	S28-06-002		
Experiment title:	Magnetic structure of TbMnO3		
Dates of experiment:	10.3.2006-13.3.2006	Date of report:	24.5.2006
Experimental team: Names:	Addresses:		
J. Voigt	Institut für Festkörperforschung, Forschungszentrum Jülich		
Local contact:	A. Loose		

We have studied the magnetic structure of a $TbMnO_3$ single crystal by neutron diffraction. The compound has attracted considerable interest because it exhibits multiferroic behaviour. Antiferromagnetic order and the ferroelectric polarization are intimately connected as evidenced by the polarization flop from the *c*-direction to the *b*-direction in an applied magnetic field of several Tesla [1]. The formation of the ferroelectric polarization at $T_c = 28$ K seems to be coupled to a magnetic reorientation transition from a collinear incommensurate (IC) magnetic structure to a non-collinear. This transitions involves also a long range ordering of the Tb^{3+} ions according to a recent neutron diffraction study [2]. The transition temperature is significantly higher than temperature $T_{N,Tb} = 8$ K, at which the Tb moments order with a different propagation vector as compared to the ordering of the Mn subsystem.
Our recent resonant x-ray diffraction raised some doubt on the orientation of the Tb moment in the non collinear phase. According to Kenzelmann et al [2] the moment should be oriented along the crystallographic *a*-direction. The x-ray data gave some hints for an orientation along the *b*-direction, but the data were ambiguous. Hence we performed a single crystal study at temperatures $T = 10$ K, $T = 35K$ and $T = 50$ K using SV28 at a wavelength $\lambda = 0.87$ Å. The sample was mounted in a closed cycle refrigerator with a temperature range from 10 K to room temperature.
Fig 1 shows the integrated intensities for two series of reflections, normalised to the intensity of the (0 Δ 1) reflection. The full *a* component contributes to all reflections of type (0 Δ l). For reflections of type (h Δ 1), the scattering vector becomes more parallel to the *a* component with increasing h.

The same holds for the (0 Δ l) reflections considering the c component of the magnetic moment. The intensity should therefore decrease faster with respect to the (0 Δ 1) reflection at the respective temperature for both series of reflections, if either the a component or the c component is ordered. We observe the expected behaviour for the (0 Δ l) series, but not for the (h Δ 1) series. However, since a scattering vector (h Δ 1) leads to an increased scattering from the c component (the scattering vector becomes more perpendicular to the c direction), the result is still not conclusive. The reflection (0 1 − Δ 1) was not observed, which could be due to the large background. It is particularly sensitive to the Tb moment [2]. Further data analysis is needed to test the published magnetic structure.

References

[1] T. Kimura *et al.*, PHYSICAL REVIEW B **71**, 224425 (2005).

[2] M. Kenzelmann *et al.*, PHYSICAL REVIEW LETTERS **95**, 087206 (2005).

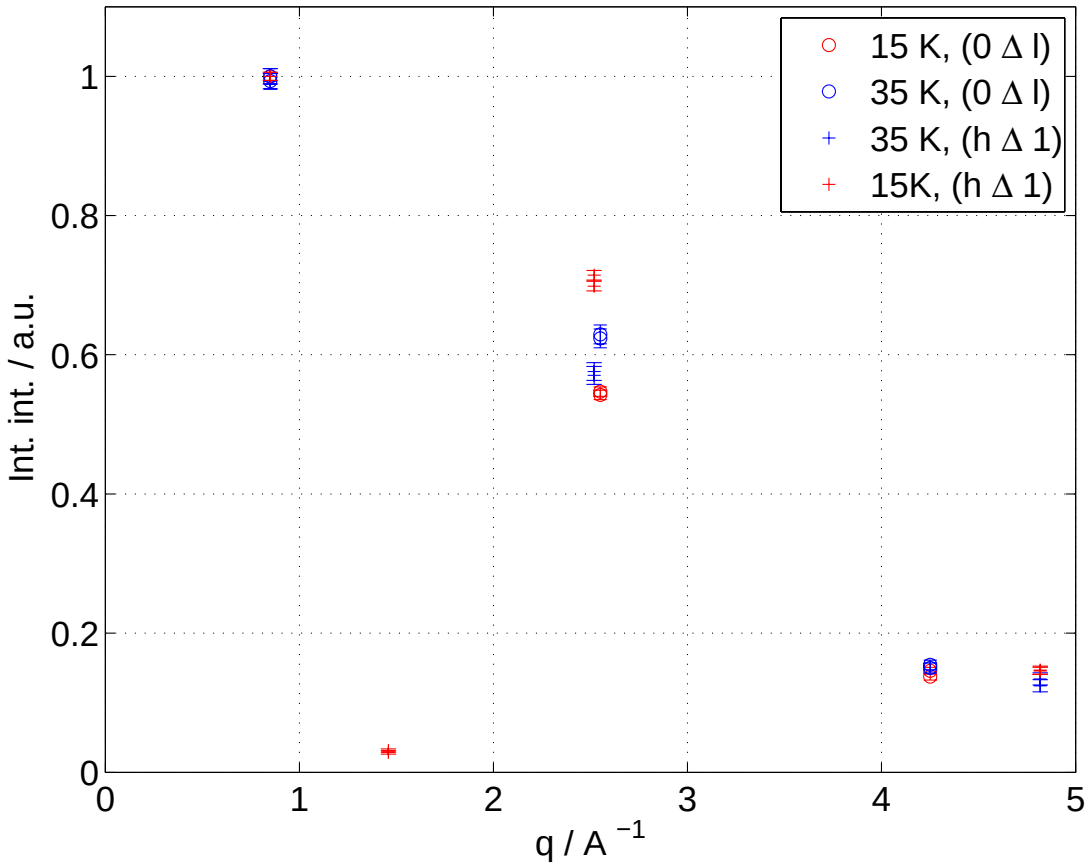
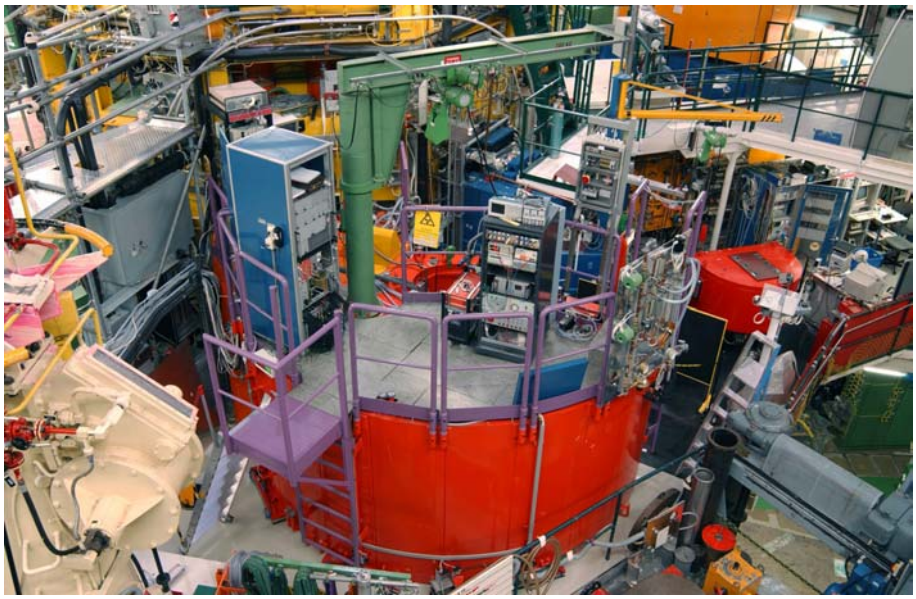


Fig. 1: Integrated intensities of reflections (0 Δ 1), (0 Δ 3), (0 Δ 5), (0 Δ 1), (2 Δ 1), (4 Δ 1), normalised to the intensity of the (0 Δ 1) reflection at the respective temperature.

Time-of-Flight Spectrometer (SV29)



Instrument Parameters

Beam line:	4H2 (radial beam tube)
Monochromator:	matrix of 75 PG002/PG004, vertical+horizontal focusing
Incident wavelengths:	$1.0 \le \lambda \le 4.0$ Å
Take-off angle:	$35 \le 2\Phi_M \le 75°$
Momentum transfer:	$\approx 1 \ldots 10$ Å^{-1}
Energy resolution:	$3\% \le \Delta E/E \le 8\%$
2 phased choppers:	≤ 21000 rpm
Collimation:	0.8°
Duty cycle:	4×10^{-3}
Neutron flux at sample:	$\approx 10^5$ n/cm^2 s
Beam size at sample:	3×8 cm^2
Flight path:	1.91 m
Detectors:	500 ^{3}He counters in 90 units
Solid angle covered:	≈ 0.05 srad
Range of scattering angles:	$10° \le \Theta_S \le 130°$
Sample environment:	
- Cryostats:	$1.5 \le T \le 310$ K
- Top-loading cryofurnace:	$1.5 \le T \le 600$ K
- Furnaces:	$50 \le T \le 1400$ °C
- Low-T pressure cell:	$p \le 3.5$ kbar at $T \ge 4.5$ K

Instrument Responsible

Dr. Michael Prager Tel. +49-(0)-2461-61-6759 Email: m.prager@fz-juelich.de

Institut für Festkörperforschung
Forschungszentrum Jülich GmbH
D-52425 Jülich

Experimental Report
of Neutron Scattering Experiments
at the FRJ-2 Reactor

Proposal number:	S29-05-002		
Experiment title:	Rotational dynamics of methyl groups in the teracyanoquinodimethane plus hexamethylbenzene complex		
Dates of experiment:	4.3.2005, 9 days	Date of report:	25.2.2006
Experimental team: Names	 Addresses		
A. Pawlukojc M. Prager	Institute of Nuclear Chemistry and Technology, Warsaw, Poland Forschungszentrum Jülich		
Local Contact:	M. Prager		

Experimental report text body

Results of this experiment are published in the paper

Titel: Elastic, quasielastic, and inelastic neutron-scattering studies on the charge-transfer hexamethylbenzene-tetracyanoquinodimethane complex

Authors: W. Sawka-Dobrowolska, G. Bator, L. Sobczyk, A. Pawlukojc, H. Ptsiewicz-Bak, H. Rundlöf, J. Krawczyk, M. Nowina-Konopka, P. Jagielski, J.J. Janik, M. Prager, O. Steinsvoll, E. Grech, J. Nowicka-Scheibe

Journal: J. Chem. Phys. 123, 124305(2005)

Abstract: The 1:1 hexamethylbenzene (HMB)-tetracyanoquinodimethane (TCNQ) complex shows a first-order phase transition at 230/218K (heating/cooling) with no change of the space group. The neutron-diffraction studies reveal that this transition is related to a freezing of the rotation of methyl groups. The result for 100K enabled precise determination of configuration of HMB.TCNQ complexes. The planes of HMB and TCNQ molecules form small angle (6°) so that the dicyanomethylene group approaches the HMB molecule to a distance of 3.34A. The conformation of methyl group was exactly determined. The quasielastic neutron-scattering spectra can be interpreted in terms of 120° jumps with different activation barrier in low and high temperature phases, equal to 3.7 and 1.8 kJ/mol, respectively. These values are lower than that for neat HMB (6kJ/mol). The conclusion can be drawn that the methyl groups can reorient more freely in the complex. This conclusion is in agreement with the results of inelastic neutron-scattering studies of low-frequency modes assigned to torsional vibrations of methyl groups. These frequencies are lower than those in neat HMB. The analysed increase of frequencies of these modes as compared with free molecules can be interpreted as due to formation of unconventional C-H…Y bonds which are more pronounced in crystals of neat HMB than in those of HMB.TCNQ. The low-frequency librational modes can be treated as sensitive measure of unconventional hydrogen bonds formed by the CH_3 groups.

Institut für Festkörperforschung
Forschungszentrum Jülich GmbH
D-52425 Jülich

Experimental Report of Neutron Scattering Experiments at the FRJ-2 Reactor

Proposal number:	S29-05-003		
Experiment title:	Studies on the crystalline electric field in $RE_2Ru_2O_7$		
Dates of experiment:	15.3.2005-21.3.2005 6.4.2005-10.4.2005	Date of report:	13.6.2006
Experimental team: Names:	Addresses:		
J. Voigt L. J. Chang	Forschungszentrum Jülich Nuclear science and Technology Development Center Hsinchu 30013, Taiwan		
Local contact:	M.Prager		

Introduction

Pyrochlore oxides of the chemical formula $A_2B_2O_7$, where A is a rare-earth ion and B is a transition-metal ion, have the face-centered-cubic structure with space group *Fd3m* and eight molecules of its general formula in a unit cell. In the $RE_2Ru_2O_7$ (RE= rare earth and Y), Ru has a partially filled 4d shell and possesses a magnetic moment. RE and Ru form two individual networks of corner sharing tetrahedrons [1,2]. It was reported that all the $RE_2Ru_2O_7$ show a specific heat jump in the temperature range 75 -160 K, which is correlated with the rare-earth ion size. In $Tb_2Ru_2O_7$, the specific heat jump was reported at 110 K. An additional magnetic transition was observed at 3.4 K by magnetisation measurement[3]. This magnetic transition was considered to be associated with the magnetic interaction between Tb^{3+} ions. A former inelastic neutron study showed an intensity shift from a distinct crystal field level into quasielastic scattering between 90 and 120 K.

Experimental

15 g of $Tb_2Ru_2O_7$ powder were prepared and characterised by powder x-ray diffraction. The sample is single phase within the accuracy limit of a few percent. Experiments have been performed at SV29 between 2.5 K and room temperature, using a closed cycle cryostat. High resolution data was taken using a neutron wavelength of 3.62 Å. For a wider energy range, a neutron wavelength of 1.81 Å was chosen.

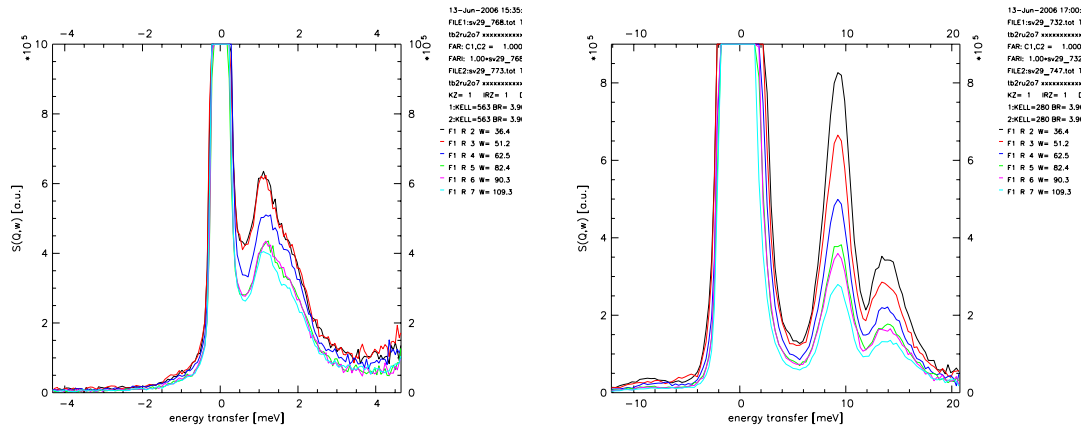


Fig 1: S(Q, ω) for $T < 10$ K. 16 detectors have been integrated, the average 2θ angle is given in the figures. The background was deduced from a measurement with empty sample container. The detectors were calibrated by a vanadium measurement. **Left)** $E_i = 6.2$ meV, **right)** $E_i = 25$ meV.

Results

In Fig 1 we present low temperature spectra measured with different incoming energy E_i. Distinct energy levels are found at 1.1 meV, 1.9 meV, 9.3 meV and 13.7 meV. The intensity of the observed features decreases with increasing scattering angle 2θ, indicative of magnetic excitations following the magnetic form factor. Fig 2 shows the temperature dependence of the low energy spectra at an averaged scattering angle $2\theta = 36.4°$. The excitation at 1.9 meV decreases strongly with increasing temperature. Between 70 K and 100 K the intensity is shifted from the distinct level at 1.1 meV into quasielastic scattering, which may correspond local fluctuations at the Ru site prior to the phase transition.

References

[1] M.Ito et al., J. Phys. Chem. Solids **62**, 337(2001).
[2] C.Bansal et al., Phys. Rev. B **66**, 52406 (2002).
[3] N. Taira et al., J. Mater. Chem **12**, 1475 (2002).

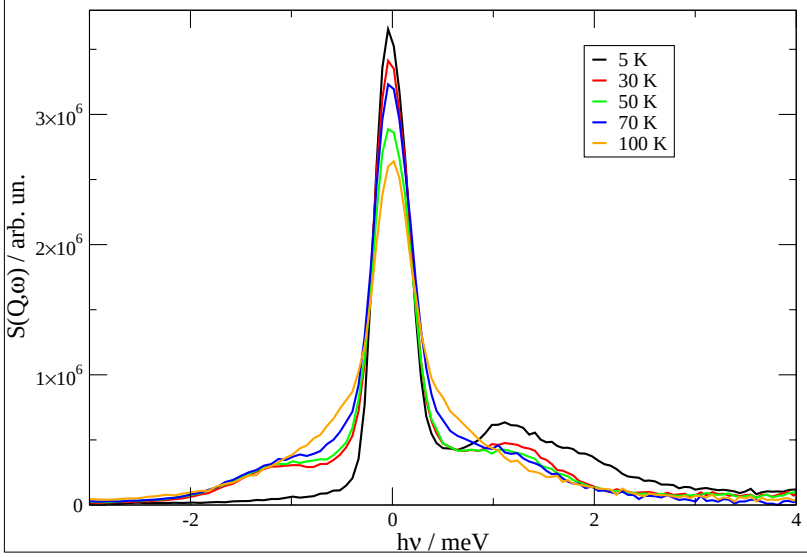


Fig 2: S(Q, ω) as a function of temperature. $E_i = 6.2$ meV, $2\theta = 36,4°$.

Institut für Festkörperforschung
Forschungszentrum Jülich GmbH
D-52425 Jülich

Experimental Report
of Neutron Scattering Experiments
at the FRJ-2 Reactor

Proposal number:	S29-05-004		
Experiment title:	The isotope effect in acetone clathrates		
Dates of experiment:	14 days after 02.03.2005	Date of report:	02.06.2006
Experimental team: Names	Addresses		
M. Prager	Institut für Festkörperforschung, Forschungszentrum Jülich		
Local Contact:	M. Prager		

Experimental report text body

Acetone clathrate could be prepared according to ref [1] with an ingot where some KOH had been added to the stoichiometric mixture of acetone and water. The formation of clathrate requires an annealing step after a first cooling. The clathrate structure has been confirmed earlier by neutron diffraction [2] but the crystal structure – likelyof cubic II structure - is not yet fully solved.
All possible isomers were investigated: h-acetone in H_2O, h-acetone in D2O, d-acetone in H2O and d-acetone in D2O. All samples were annealed after cooling first to 5K at an annealint temperature t=240K for more than 30min. While the spectra of samples with the protonated matrices changed significantly with annealing indicating clearly the transformation in the clathrate structure, those with the deuterated matrix changed little. These samples, however, allow to test a phase change by diffraction. There is even little change of the elastic intensities too, however. Thus it is unclear whether the deuterated host samples are one-phase materials with the expected structure.
The fig. shows the measured spectra of all samples at large scattering angles averaged over 32 of the 125 detectors. The project is going on.

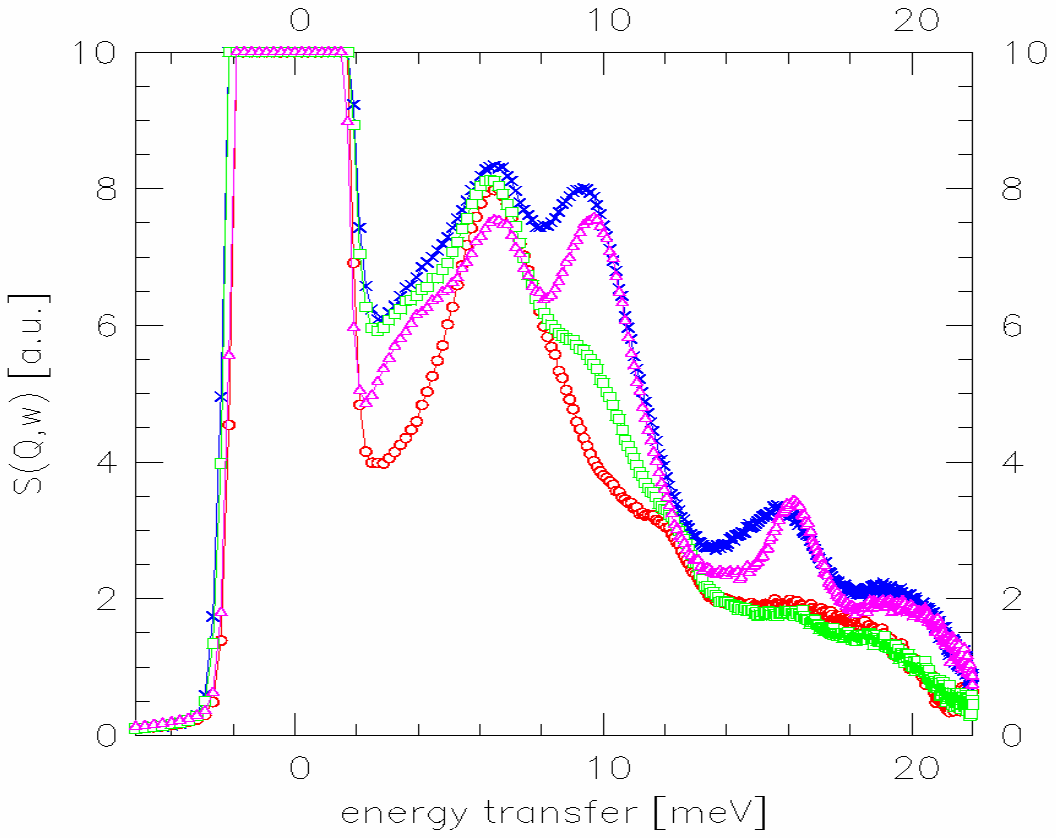


Fig. 1 Spectra of stoichiometric acetone-water mixtures. Sample temperatures T=2.5K.
All samples annealed. oooo: h-aceton:17D_2O; xxxx: d-acetone:17H_2O; square: d-acetone:17D_2O;
Triangle: h-acetone:17H_2O. λ=1.76A.

[1] O. Yamamuro, M. Oguni, T. Matsuo, H. Suga, Solid state commun. **62**,289(1987)
[2] O. Yamamuro, T. Matsuo, H. Suga, W.I.F. David, R.M. Ibberson, A.J. Leadbetter, Physica **B213&214**,405(1995)

Institut für Festkörperforschung
Forschungszentrum Jülich GmbH
D-52425 Jülich

Experimental Report
of Neutron Scattering Experiments
at the FRJ-2 Reactor

Proposal number:	S29-05-005		
Experiment title:	Investigation of choline and acetylcholine neurotransmitter		
Dates of experiment:	24.6.2005, 12 days	Date of report:	25.2.2006
Experimental team: Names	 Addresses		
A. Pawlukojc M. Prager	Institute of Nuclear Chemistry and Technology, Warsaw, Poland Forschungszentrum Jülich		
Local Contact:	M. Prager		

Experimental report text body

Acetylcholine is synthesized in certain neurons by enzyme choline acetyltransferase from the compounds choline and acetyl-CoA. Organic mercurial compounds have a high affinity for sulfhydrol groups, which attributes to its effect on enzyme dysfunction of choline acetyl transferase. This inhibition may lead to acetylcholine deficiency, contributing to the signs and symptoms of motor dysfunction.
Normally, the acetylcholine is quickly removed after having performed its action, this is done by the enzyme acetylcholinesterase which converts acetylcholine into choline and acetate. The devastating effects of nerve agents are due to their inhibition of this enzyme, resulting in continuing stimulation of the muscles, glands and central nervous system.
Acetylcholine and choline were studied as cations in the salts with Cl, Br and I anions. Since the spectra are dominated by the proton dynamics we observe in choline mainly the dynamics of the $N^{+}(CH_3)_3$ group. In acetylcholine the methyl group rotation of the acetyl group will modify the spectrum. Here we observe the superposition of methyl group torsional vibrations of the trimethyl ammonium and the acetyl group. While strong rotational potentials have so far been found for tetramethyl ammonium ions, acetates show low rotational barriers [1].
The TOF spectrometer was used with wavelengths λ=1.76A and λ=1.17A. This gives acces to the lattice modes and low lying internal vibrations. Two typical spectra are shown in the figures. Fig. 1 compares the acetylated sample with the pure choline. Chlorine forms the anion. In fig. 2 we compare two acetylcholine ions with different anions, chlorine and bromine. (Similar spectra are obtained with the iodide compound.)

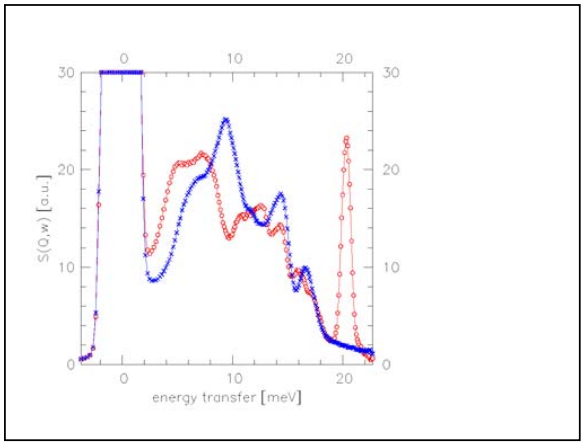


Fig. 1: Acetylcholin chloride (ooo) vs Cholin chloride. T=2.5K.

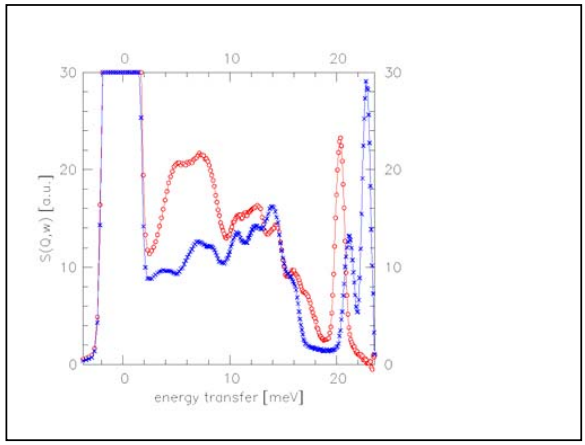


Fig. 2: Acetylcholin chloride (ooo) vs Acetylcholin bromide (xxx). T=2.4K.

In fig. 1 the band at 20meV is obviously related to the acetyl group and represents the librational mode of the methyl group. Its splitting in acetylcholin bromide (fig. 2) must most likely be caused by a symmetry reduction which leads to the presence of inequivalent acetyl environments in this compound. The bands of the trimethyl ammonium group are not such clear. According to the general experience they are more likely found at higher energy transfers. To identify these modes ab-initio calculations at the DFT level using the GAUSSIAN98 program will be well suited. Furthermore the CLIMAX program shall be well used to model the scattering from the different eigenmodes. This program is under way.

Finally, future IR and Raman experiments shall complete the inelastic neutron experiment. Selection rules are expected to contribute to an identification of the character of individual modes.

[1] M. Prager, A. Heidemann, Chem. Rev. **97**,2993(1997)

Institut für Festkörperforschung
Forschungszentrum Jülich GmbH
D-52425 Jülich

Experimental Report
of Neutron Scattering Experiments
at the FRJ-2 Reactor

Proposal number:	S29-05-006		
Experiment title:	Influence of isomerism/substitution on the internal and external modes of various xanthines		
Dates of experiment:	20.9.2005, 17 days	Date of report:	25.2.2006
Experimental team: Names	Addresses		
A. Pawlukojc M. Prager	Institute of Nuclear Chemistry and Technology, Warsaw, Poland Forschungszentrum Jülich		
Local Contact:	M. Prager		

Experimental report text body

The methylxanthines represent a biologically most important class of molecules. These rather simple double ring molecules include the natural drugs caffeine, theobromine and theophylline which are used in daily live and medical application.

Caffeine is an alkaloid found in such foods as coffeefruit, tea etc. Its main pharmacological properties are a stimulant action on the central nervous system with psychotropic effects and stimulation of respiration, a stimulation of the heart rate. By oxidative demethylation caffeine is metabolized in the liver to the dimethylxanthines theobromine, theophylline and paraxanthine. In a second step demethylation leads to monomethylxanthines. Other metabolic steps follow.

Theobromine is an alkaloid found in cocoa and chocolate. Theobromine has an antitussive effect superior to codeine by suppressing vagus nerve activity.

Theophylline is a drug, a phosphodiesterase inhibitor, that is widely used in therapy for respiratory diseases. It is naturally found in black tea and green tea. The main actions of theophylline are relaxation of bronchial smooth muscle, positive inotropic (increases heart muscle contractility and efficiency) and positive chronotropic (increases heart rate) impact. It lowers blood pressure, increases renal blood flow and has some anti-inflammatory effect.

While caffeine, theobromine and theophylline are biologically active, paraxanthin, interestingly, is almost completely inactive and therefore also non toxic.

Theobromine, theophylline and 1,7-dimethylxanthin (paraxanthin) are isomeric molecules. The molecules differ by the positions of the 2 methyl groups on the double ring. The figure shows theophylline as an example

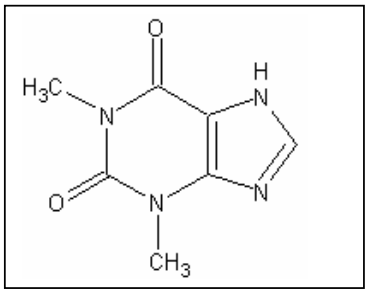


Fig. 1 Molecular structure of theophylline

In theobromine the methyl group between the two oxygens is moved to the upper nitrogen on the 5-ring. In 1,7-dimethylxanthin the bottom CH_3 is moved to this position. In caffeine with its third methyl group all three nitrogen atoms bound by single bonds in the double ring carry a methyl group. This structure allows no isomeric form.

From the spectra measured on SV29 with wavelengths λ=1.76A and λ=1.17A the biologically active theophylline (right) and the inactive 1.7-xanthine (left) are compared in the figures 2 and 3.

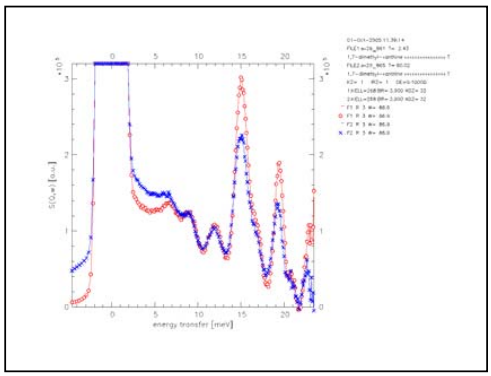


Fig. 2 spectra of 1,7-dimethyl-xanthine at Sample temperatures T=2K and T=60K

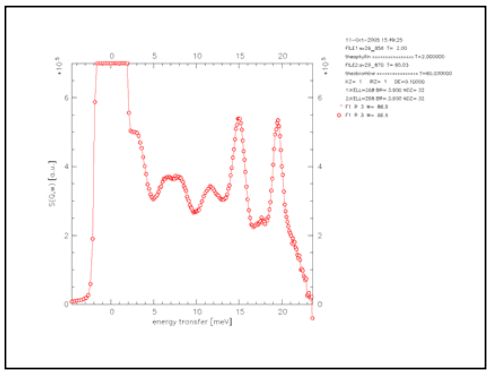


Fig. 3 spectrum of theophylline. sample temperature T=2K

Despite of close similarities – for example finding the two dominant bands at the same energies - there are clear differences especially in the regime of lattice modes. The mode at 3meV in theophylline has possibly to do with the methyl tunnelling mode observed at high energy resolution [1]. It is well known from the halomesitylenes and their derivatives that the hindering potential can strongly and often unexpectedly change with the methyl group position and neighborhood on the ring [2].

The data analysis is under progress. DFT and lattice dynamical calculations are planned.

[1] Experimental Reports FRJ2 2005, Report BSS-05-021
[2]A. del Rio, A. Boucekkine, J. Meinnel, J. Comp. Chem. 24,2093(2003)

Institut für Festkörperforschung
Forschungszentrum Jülich GmbH
D-52425 Jülich

Experimental Report
of Neutron Scattering Experiments
at the FRJ-2 Reactor

Proposal number:	S29-05-007		
Experiment title:	**Magnetic Excitations in nanocrystalline terbium**		
Dates of experiment:	May 2005	Date of report:	May 2006
Experimental team: Names	Addresses		
A. Hoser O. Moze, C. Vecchini A. Michels J. Weissmueller	Institut fuer Festkoerperforschung, Forschungzentrum Juelich, D-52425 Juelich, Germany Università di Modena e Reggio Emilia, Via Campi 213/a, 41100 Modena, Italy Technische Physik, Universitaet des Saarlandes, Saarbrueken, Germany Institut fuer Nanotechnologie, Forschungzentrum Karlsruhe, Karlsruhe, Germany and Technische Physik, Universitaet des Saarlandes, Saarbrueken, Germany		
Local Contact:	M. Prager / A. Hoser		

Experimental report text body

Nanocrystalline composites are attracting attention because of the very different properties they show when compared to their course counterparts. Recent neutron diffraction measurements on a nanocrystalline sample of pure Terbium, with average grain size of 12 nm, gave evidence for the suppression of the antiferromagnetic phase that occurs in the coarse material at 216 K and vanishes at 229 K in the paramagnetic phase. Single crystal Terbium has been widely studied in the past showing the presence of a high energy excitation gap (which correspond to an optical zone center magnon mode) in zero applied field and a lower energy one which corresponds to the acustic magnon mode[1]. No previously reported neutron scattering experiments with the aim to determine the magnetic excitations on this nanocrystalline Rare Earth are known to us. We performed a neutron inelastic scattering experiment on the Time Of Flight Spectrometer SV-29 in order to determine the spin-wave energy gap. A first attempt was done on the Triple Axis Spectrometer UNIDAS and a small inelastic signal was observed at about 8.8 meV at 200K (Fig. 1). Here we report the continuation of this experiment on the TOF SV-29 Spectrometer. These results of these measurements have been just published in J. Appl. Phys[2].
The inelastic neutron scattering measurements were performed on the SV-29 Time of Flight Spectrometer at different temperatures, from 2.5 K to 250 K (T_c=229 K) on a nanocrystalline 1 gm sample of rare earth Terbium. The incident wavelength used was 1.81 Å for determining the high energy magnon mode, and a longer wavelength was used of 2.4 Å. in order to determine the lower energy magnon. A different sample holder has been used with respect to UNIDAS in order to maximaze the scattering intensity vs absorption ratio. It is known that the coarse material shows two inelastic excitations at about 1.5 meV and 9 meV at 90 K. The spectra were collected for long measuring times due to the intrinsic low scattering intensity of the nanosized crystalline sample. The data were corrected for detector sensitivity and for the empty beam. The measurement revealed the presence of two magnetic excitations, one at approximately 10 meV at 2.5 K that decreases with increasing temperature and a very weak one at lower energy at about 2.5 meV.

We think that they correspond respectively to the optical and acoustic magnon modes similar to the magnon modes observed in a single crystal sample. More measurements with the purpose to determine the temperature dependance of the low energy excitation with more accuracy are highly desiderable.

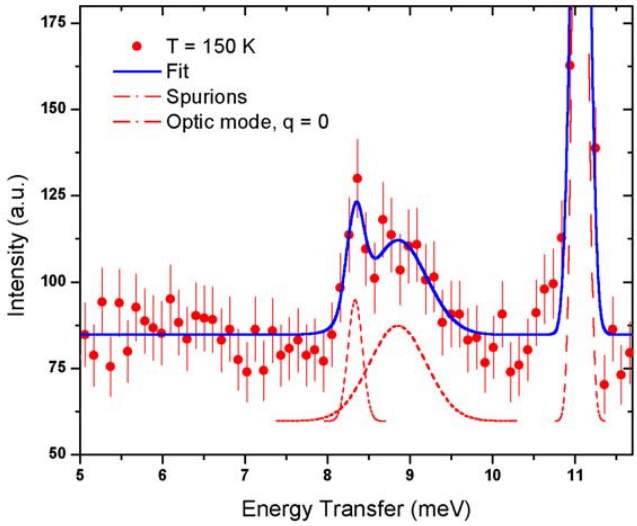


Fig. 1 – Inelastic neutron scattering spectrum for nc Tb at 150 K collected on the triple-axis-spectrometer UNIDAS. The peak at approximately 9 meV is the magnetic excitation that has been attributed to intrinsic optic zone center (q=0) magnon mode. The other two narrow peaks are due to instrumental effects.

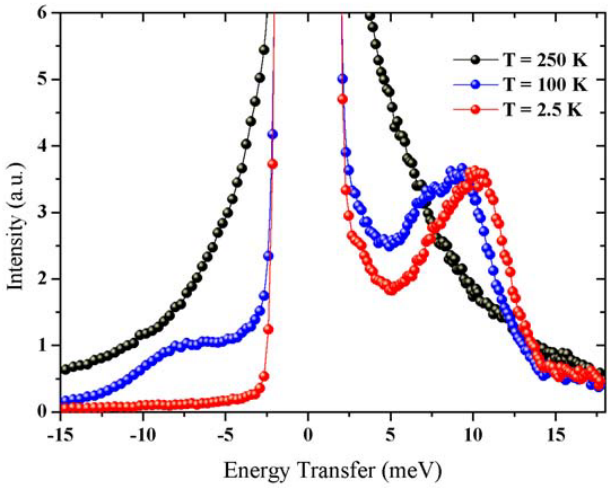


Fig. 2 – Magnetic scattering for nc Tb at 250, 100 and 2.5 K as measured with the TOF spectrometer SV-29. The peak at 10 meV moves with temperature and disappears at 250 K in the paramagnetic state.

Reference:

1) Moeller et al., Phys. Rev. Lett., **16**, 737 (1966.)
2) Vecchini et al., J. Appl. Phys., **99**, 08F502 (2006.)

Institut für Festkörperforschung
Forschungszentrum Jülich GmbH
D-52425 Jülich

Experimental Report
of Neutron Scattering Experiments
at the FRJ-2 Reactor

Proposal number:	S29-05-008		
Experiment title:	Methyl group dynamics in methyl fluoride clathrate: the isotope effect		
Dates of experiment:	19.5.2004, 10 days	Date of report:	22.2.2006
Experimental team: Names	Addresses		
M. Prager	Forschungszentrum Jülich		
Local Contact:	M. Prager		

Experimental report text body

Molecular guest molecules included in water clathrate cages have been recently intensively studied. On the one hand there is the methane clathrate [1,2]. Beside its supposed role as one of the major future fossile energy resources it represents the prototype non polar guest molecule. On the other hand there are the methyl halide guest molecules [3,4] with a strong dipolar moment, varying size and therewith different crystal structures and also varying tendency to form hydrogen bonds with the cage protons. Du to this variability different systems illuminate different aspects of the interaction with the cage in different way. The work on the protonated methyl fluoride clathrate is published [4]. The abstract summarizes:

Neutron spectroscopy in the meV and μeV regime and quasielastic scattering is applied to characterize the dynamics of methyl groups of methyl fluoride guest molecules in cubic I CH_3F-water clathrate. Only above T~60K quasielastic spectra are unaffected by quantum effects. They are well described by two Lorentzians representing the CH_3F species in the small and large cages of the structure. The intensities show that both cages are completely filled. Linear broadenings with temperature follow the model of rotational diffusion. Two clearly separated tunneling bands were observed at T=4.2K and are also assigned to the two types of water cages. Disorder of the environment (H-bonds) is reflected in the shape of the bands. For the less hindered species housing the large cages the tunneling band can be quantitatively converted into a potential distribution function within the model of single particle rotation. Transitions to excited rotational states show the dominance of a sixfold potential term V_6=13meV modified by a weak threefold term distributed around a characteristic value V_3=0.9meV. The potential distribution of V_3 influences the barrier for classical reorientation only weakly in agreement with the results from quasielastic data. Adsorption sites with the guest molecules oriented towards a hydrogen bond along one of twelve local twofold axes of the cage are proposed. Such sites are consistent with the sixfold rotational potential and earlier results from methyl iodide clathrate [3]. Rotation-translation coupling as alternative dynamical process is excluded.

The work is now extended towards the deuterated methyl fluoride clathrate. Diffraction data have been taken on D20 of the ILL, Grenoble, the tunnelling spectrum was measured on IN5 and reproduces a similar broad distribution of tunnelling transitions shifted by the isotope effect of roughly a factor 2. The vibrational density of states of $CD_3F*5.75D_2O$ measured on SV29 is compared to that of the fully protonated material in Fig. 1. Here too a strong isotopic shift is obvious for the peak at ~10meV.

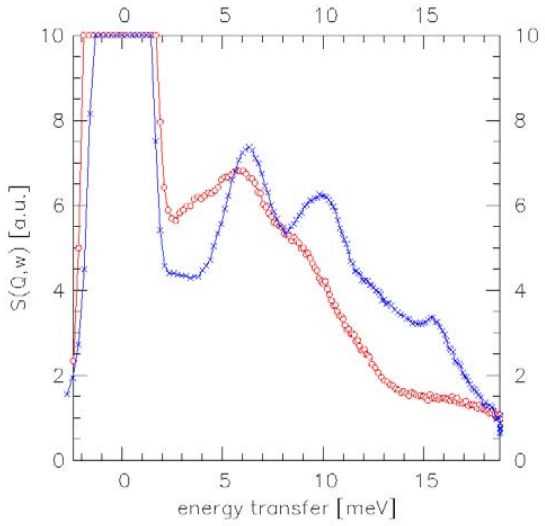


Fig. 1: Spectrum of methyl fluoride clathrate $CD_3F*5.75D_2O$ (ooo). T=4.2K. λ=1.81A. CH_3F*H_2O (xxx) for comparison.

For clarity the cage housing 75% of the molecules is reproduced as fig. 2 below.

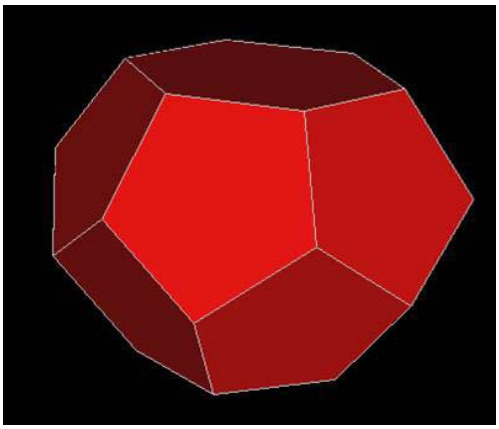


Fig. 2: The large $5^{12}6^2$ cage of the methyl fluoride clathrate $CD_3F*5.75D_2O$, which contains 3/4 of the CD_3F guest molecules. Each corner represent an oxygen of the water shell, each edge a hydrogen bond. There are inequivalent hydrogen bonds: 12 edges connect a pentagon with a hexagon, 12 connect 2 pentagons whith a pentagon on each side of the edge, 12 connect 2 pentagons with a pentagon on one and a hexagon on the other side of the edge.

[1] C. Gutt, B. Asmussen, W. Press, M.R. Johnson, Y.P. Handa, J.S. Tse, J. Chem. Phys. **113**,4713(2000)
[2] C. Gutt, W. Press, A. Hüller, J. Tse, H. Casalta, J. Chem. Phys. **114**,4160(2001)
[3] M. Prager, J. Pieper, A. Buchsteiner, A. Desmedt, J. Phys. Condens. Matter **16**,7045(2004)
[4] M. Prager, J. Baumert, W. Press, M. Plazanet, J.S. Tse, D.D. Klug, PCCP **7**,1228(2005)

Institut für Festkörperforschung
Forschungszentrum Jülich GmbH
D-52425 Jülich

Experimental Report
of Neutron Scattering Experiments
at the FRJ-2 Reactor

Proposal number:	S29-05-009		
Experiment title:	**A systematic search for correlation of hydrogen bonding and lattice dynamics in methyl pyrazines**		
Dates of experiment:	13.6.2005, 11 days	Date of report:	23.2.2006
Experimental team: Names	Addresses		
O. Kirstein M. Prager	ANSTO, Menai, Australien Forschungszentrum Jülich		
Local Contact:	M. Prager		

Experimental report text body

The fundamental quantities that determine the spatial arrangement of the atoms of a molecule and their dynamics are the intermolecular interaction potentials. There are different levels of approximation. In the most fundamental approach the dynamics of molecular crystals is modelled using either ab-initio/molecular mechanics programs e.g. [1,2]. Somewhat more heutistic is the use of semi-empirical interaction potentials. The latter potentials are also known as pair potentials (PP). The most important property of PP's is their transferability, which reduces the number of adjustable parameters and simplifies the theoretical description of atomic interactions within complex molecular systems significantly and would allow in the ideal case to calculate the crystal structure as well as the lattice dynamics of any molecular system. Actually calculations of the properties of molecular crystals using transferable pair potentials (TPP) are essentially limited to systems where accurate crystal structures are known. Transferability is the better the closer the systems are chemically related. Along these lines the interest in the weak hydrogen bond [3] has lanced the systematic X-ray diffraction study of the structures of all methyl pyrazines [4]. Methyl pyrazines are available with 1, 2, 3 and 4 methyl groups. The presence of 2 methyl groups allows the arrangement in 3 isomers. Most materials crystallize in the monoclinic space groups $P2_1/n$ or $P2_1/c$. Only 2-methyl pyrazine assumes a tetragonal lattice with space group I4. The number of molecules in the unit cell varies from 2 to 16. The materials are characterized and classified by their C-H…N hydrogen bonds.

The figure 1 shows the density of states as measured for the so far not investigated 2-methyl-pyridine for energies up to 22 meV . The calculation of the density of states was done *before* the experiment was performed using the local program DYNCAL. The calculation is based on the crystal structure [4] and as in former studies [5] universal force field parameters [6] . The similarity of theoretical and experimental spectra is surprisingly good (fig. 1 bottom). The data evaluation is in progress.

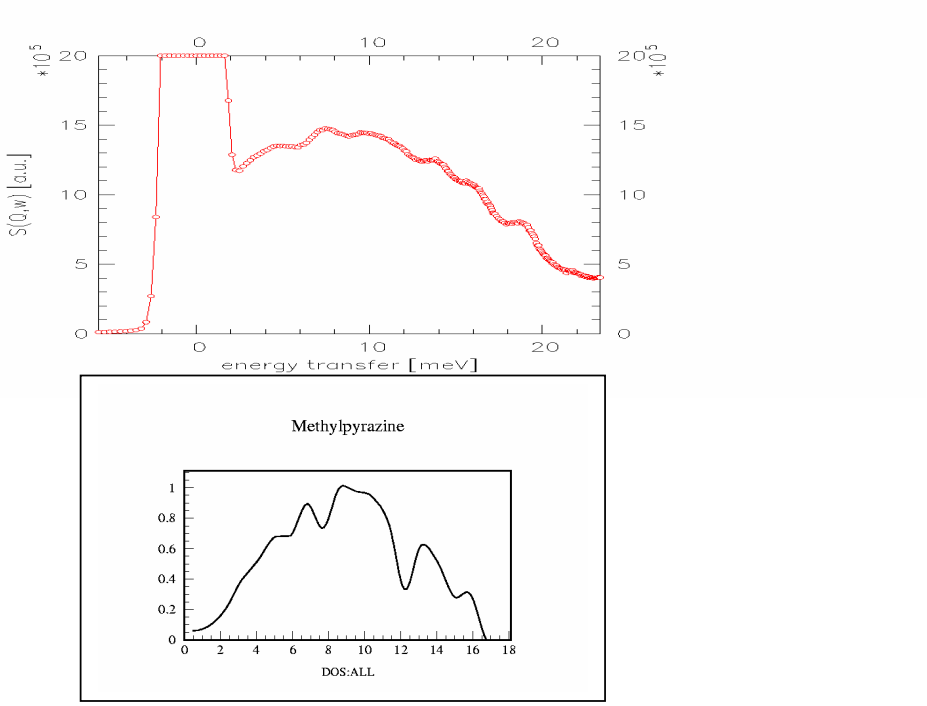


Fig. 1: Comparison of measured spectrum (top) and calculated density of states (bottom).

References

[1] M.R. Johnson, M. Prager, H. Grimm, M.A. Neumann, G.J. Kearley, C.C. Wilson, Chem. Phys. 244 (1999) 49-66

[2] B. Nicolaï, E. Kaiser, F. Fillaux, G.J. Kearley, A. Cousson, W. Paulus, Chem. Phys. 226 (1998) 1-13

[3] G.R. Desiraju, T. Steiner, 'The weak hydrogen bond in structural chemistry and biology', Oxford university press, Oxford, 1999

[4] V.R. Thalladi, A. Gehrke, R. Boese, NJC 24,463(2000)

[5] O. Kirstein, M. Prager, R.M. Dimeo, A. Desmedt, J Chem Phys 122,14502(2005)

[6] A.K. Rappe et al, J. Am. Phys. Soc., Vol 114 No 25, 1992

[7] M.R. Johnson, M. Prager, H. Grimm, M.A. Neumann, G.J. Kearley, C.C. Wilson, Chem. Phys. 244,49(1998)

Institut für Festkörperforschung
Forschungszentrum Jülich GmbH
D-52425 Jülich

Experimental Report
of Neutron Scattering Experiments
at the FRJ-2 Reactor

Proposal number:	S29-05-010		
Experiment title:	INS studies of rotational potentials of methyl groups in complexes of methyl derivatives of pyrazines with chloranilic acid		
Dates of experiment:	07.03.2006, 3 days	Date of report:	02.06.2006
Experimental team: Names	 Addresses		
E. Grech A. Pawlukojc M. Prager	Institut of Chemistry, University of Szczecin, Poland Institute of Nuclear Chemistry and Technology, Warsaw, Poland Institut für Festkörperforschung, Forschungszentrum Jülich		
Local Contact:	M. Prager		

Experimental report text body

The present experiment is part of a broader acces to chargetransfer compounds. Results from a first system studied, tetramethyl pyrazine with chlor anilic acid was published recently [1].
In the framework of this project a new 1:1 charge transfer complex, tetramethylpyrazine (TMP) with squaric acid (SA) is investigated. The complex was synthesized in Szczecin.
Fig. 1 shows the spectrum in the regime of lattice modes at two temperatures. The damping of the strongest lattice mode at an energy of 13meV is taken as fingerprint of its methyl librational origin. The identification of the other bands needs either a lattice dynamical calculation or cross verifications.
The observation of tunnel splittings can help to characterize more convincingly the librational character of a mode of the density of states. Fig. 2 shows the tunnelling spectra of the TMP:SA complex. Two bands at energies 1.55μeV and 4.2μeV are clearly seen. They show equal intensities. The total tunnelling intensity is a factor ~2 lower than expected from the scattering function. This means that 2 tunneling transitions are not resolved. For the crystal structure this means that either there is no symmetry at the site of the TMP molecule or there may be 2 inequivalent TMP molecules in the unit cell with say a mirror plane or a 2-fold axis connecting the two halfs of the TMP molecule.
The 2 measured transition energies, tunnel splitting and first excited librational mode, can be used to determine the rotational potentials of the respective methyl groups. If the shoulder at 15meV is also interpreted as the libration of the methyl group with the smaller tunnel splitting one derives pure $\cos(3\phi)$ potentials with barrier heights of 38meV and 47meV.
Compared to pure TMP these rotational potentials are weaker. Whether there is an influence of charge transfer or whether all changes are solely due to steric effects of the environment requires a mathematical modelling . Such calculations are planed.

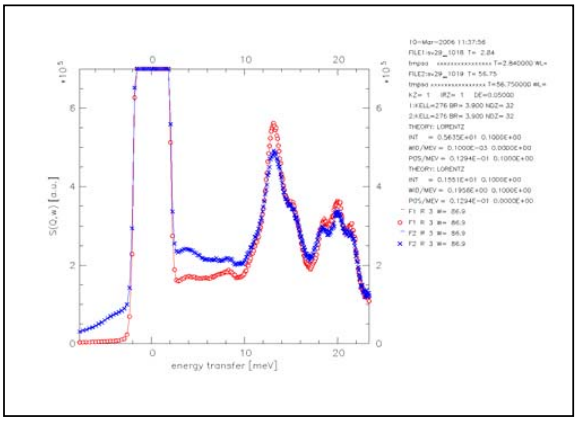


Fig. 1: Spectrum of TMP:SA in the regime of lattice modes. T=2.4K and 50K.

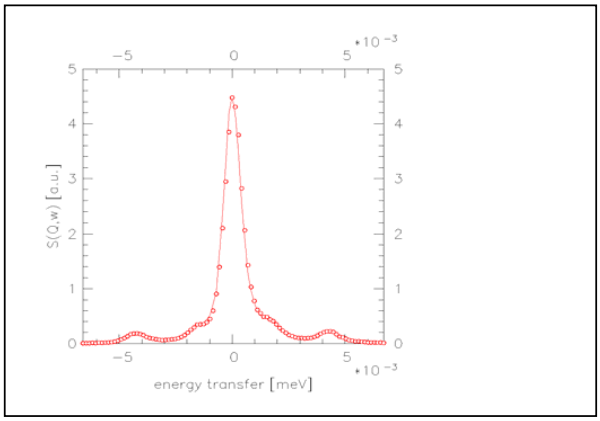


Fig. 2: Spectra of TMP:SA in the regime of tunnel splittings. T=4.5K.

[1] M. Prager, A. Pawlukojc, E. Sobczyk, E. Grech, H. Grimm, J. Phys. Condens. Matter **17**,5275(2005)

Institut für Festkörperforschung
Forschungszentrum Jülich GmbH
D-52425 Jülich

Experimental Report
of Neutron Scattering Experiments
at the FRJ-2 Reactor

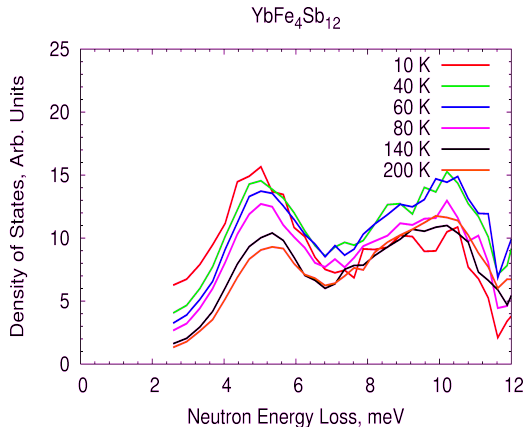
Proposal number:	S29-05-012		
Experiment title:	**P r œr uso fct er ua fhpr e t offuhcr l e fai nqpRfDucfuE x uhofa huci ux ur i ur t uqpRfDue mcr fucr ep t cssofphcur uhl ncr eb dy u$_4$Sd$_{12}$**		
Dates of experiment:	0 ctober 25th- No6ember . th 2885	Date of report:	A arch d1st 288L
Experimental team: Names	ACCresses		
Hermann Rapha1l, GranCjean FernanCe, Keppens Veerle, A anCru Da6iC	Uni6ersité Ce Liège – Dept. Ce Physique – B5 – B4888 Liège – Belgium Uni6ersité Ce Liège – Dept. Ce Physique – B5 – B4888 Liège – Belgium Uni6ersity of Tennessee, Dept A aterial Science anC Engineering, Knox6ille, TN USA 0 ak RiCge National Laboratory, 0 ak RiCge, TN, USA		
Local Contact:	Dr. A . Prager		

mcx uhcE ur fosdhux phfcfuxfcdpi n
s

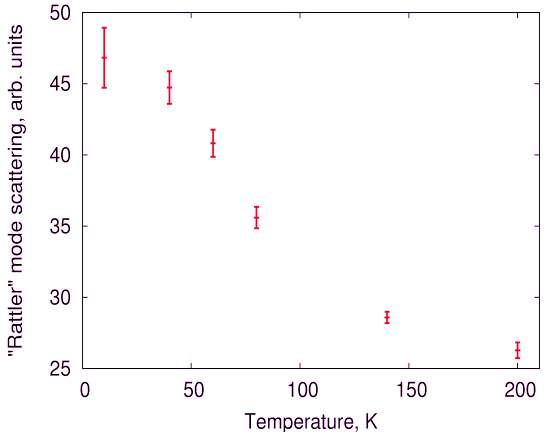
The presence of losely bounC guests, so calleC "rattlers", in the cages of filleC skutteruCites has been shown to yielCa strong reCuction in the lattice thermal conCucti6ity of these materials, with respect to the unfilleC compounCs. Se6eral stuCies of the lattice Cynamics in filleC skutteruCite show that the signature of the "rattler" moCe is that of an Einstein oscillator. In particular this signature is obser6eC through heat capacity measurements anC inelastic neutron scattering. So far the Einstein oscillator peak in the phonon Censity of states has been obser6er in La, Ce, anC Tl filleC skutteruCites by inelastic neutron scattering,[1,2] anC in Eu filleC skutteruCites by nuclear inelastic scattering.[d] The 6alence state of these filler elements Coes not change as function of temperature.

The elastic constants of se6eral skutteruCites ha6e been reporteC [1] anC the signature of the "rattler" is reaCily moCelleC by a two-le6el-system contribution to the free energy, where the two-le6el splitting is the Einstein energy. The shear moCulus, I_{44}, in $LaFe_4Sb_{12}$, show on the left of Fig. 1, can be moCelleC as a the sum, full line, of the Varshni beha6ior, CasheC line, obser6eC in $CoSb_d$ anC a contribution from a two-le6el system[1]. We ha6e measureC the elastic constants of $YbFe_4Sb_{12}$ as function of temperature between 4 K anC d88 K. In $YbFe_4Sb_{12}$, a moCel that supposes that the two-le6el splitting, *lus u* the Einstein energy, exhibits a strong temperature CepenCence, must be useC in orCer to fit the experimental Cata. It has been reporteC that Yb in $YbFe_4Sb_{12}$ may be present in an intermeCiate 6alence state between Yb^{d+} anC Yb^{2+}, which CepenCs on the temperature. With the characteristic temperature for the Yb 6alence fluctuation T* estimateC at ~ 58K [4], the obser6eC feature at 58 K in the elastic constants is likely to be relateC to the intermeCiate 6alence beha6ior of the compounC

The goal of this experiment is to carry out a direct measurement of the Yb Einstein oscillator energy, by a determination of the phonon density of states in $YbFe_4Sb_{12}$ as a function of temperature, between 158 K and 18 K.



t lraison ol : sos [PsilOs4H2]o s4glHpcRDgH2Hsgd4o . Lt sef Lnho2HdHsd4-l12Hs- dsHOPsi2Hdisgu



t lraisch ol : sosHOPsi2Hdiso sPs4-s4IscRDdHs o Fi2HHsicoOR-sogI2HHil4ro2Hd12umOsbu

The inelastic scattering by $YbFe_4Sb_{12}$ has been measured between 18 and 288 K, and the density of states has been calculated, see Figure 1. The prominent feature in the obtained density of states is the peak at ca. 5 meV that is associated with the Yb "rattler". Because of the large Yb scattering cross-section, the peak is clearly 6isible without the subtraction of the acoustic phonon contribution that had to be done in similar experiments.[1,2] It appears that there is no strong dependency of the rattler energy upon temperature and our initial hypothesis is not comforted by this result. The Bose-factor corrected integral inelastic scattering of the "rattler" mode has been obtained from a fit with a single Gaussian contribution of the peak around 5 meV, and is shown in Figure 2. The obser6ed decrease in this figure clearly demonstrates that the phonon density of states of the material is not constant as a function of temperature, and indicates that it is likely an anharmonicity effect that causes the dramatic softening around 58 K that has been obser6ed by elastic constants measurements.

References:

1. V. Keppens, D. Andrus, B. C. Sales, B. C. Chakoumakos, P. Day, R. Coldea, A. B. Maple, D. A. Gajewski, E. J. Freeman and S. Bennington, *, 2Hdisordwr4-R4(* **395**, 8. L (1998).

2. R. P. Hermann, R. Jin, W. Schweika, F. Grandjean, D. Andrus, B. C. Sales and G. J. Long, *) : pgur sSuowsHH* **90**, 1d5585 (288d).

d. Long G. J., Hermann R. P., Grandjean F., Alp E. E., Sturhahn W., Johnson C. E., Brown D. E., Leupold 0 ., and Rüffer R., *) : pgur sSuW7* **1**, 148d82(R) (2885).

4. N. R. Dilley, E. D. Bauer, A. B. Maple, S. Dordevic and D. N. Basov, F. Freibert, T. W. Darling, A. Migliori, B. C. Chakoumakos and B. C. Sales, Phys. Rev. B **61**, 4L88–4L14 (2888); and B. C. Chakoumakos, *PilS2Ho IROOa4lI2HR4*.

Institut für Festkörperforschung
Forschungszentrum Jülich GmbH
D-52425 Jülich

Experimental Report of Neutron Scattering Experiments at the FRJ-2 Reactor

Proposal number:	S29-05-013		
Experiment title:	Crystal field and phonon density of states in REMnO3 (RE=Nd,Pr,Tb,Ho)		
Dates of experiment:	30.11.05-5.12.05 20.1.06-25.1.06	Date of report:	23.5.06
Experimental team: Names:	Addresses:		
J. Voigt	Forschungszentrum Jülich		
Local contact:	M. Prager		

We have studied the inelastic neutron scattering from $TbMnO_3$ powder on the thermal time-of-flight spectrometer SV29. The compound has attracted considerable interest because it exhibits multiferroic behaviour. Antiferromagnetic order and the ferroelectric polarization are intimately connected as evidenced by the polarization flop from the *c*-direction to the *b*-direction in an applied magnetic field of several Tesla [1].

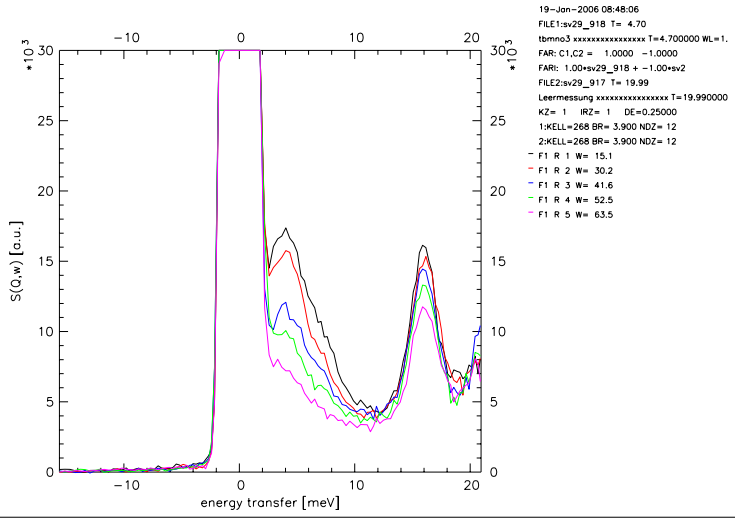


Fig. 1: Spectra integrated over 12 single detectors at 2.5 K as a function of energy transfer. Before S(Q,ω) calculation, the background from an empty sample container was subtracted and the data was corrected for detector efficiency by a vanadium measurement.

The formation of the ferroelectric polarization at $T_c = 28$ K seems to be coupled to a magnetic reorientation transition from a collinear incommensurate (IC) magnetic structure to a non-collinear. This transitions involves also a long range ordering of the Tb^{3+} ions according to a recent neutron diffraction study [2]. The transition temperature is significantly higher than temperature $T_{N,Tb} = 8$ K, at which the Tb moments order with a different propagation vector as compared to the ordering of the Mn subsystem.
The experiment has been performed on the thermal time-of-flight spectrometer SV29, using a wavelength $\lambda = 1.76$ Å, corresponding to an energy $E_i = 26$ meV. The sample was mounted in a closed cycle cryostat, giving a temperature range from 2.5 K to room temperature. In Fig 1 we present the spectra integrating the signal of 12 neighboring detectors for the whole detector array of 125 detectors at a temperature of 2.5 K. We observe two distinct levels at 4.5 and 17.2 meV. S(Q,ω) decreases with increasing scattering angle, indicating the Tb^{3+} form factor. Hence we conclude, that both features are crystal field excitations.
We have recorded spectra at temperatures in the different phases. The temperature evolution is shown in Fig 2. As you go from the low temperature Tb ordered phase into the IC non-collinear and ferroelectric phase, the crystal field levels shift to slightly lower energies. Crossing the transition to the IC collinear magnetic and paraelectric structure doesn't lead to significant changes. Unfortunately the statistics of the 50 K data are too poor to establish any changes on entering the paramagnetic state.

References

[1] T. Kimura *et al.*, PHYSICAL REVIEW B **71**, 224425 (2005).

[2] M. Kenzelmann *et al.*, PHYSICAL REVIEW LETTERS **95**, 087206 (2005).

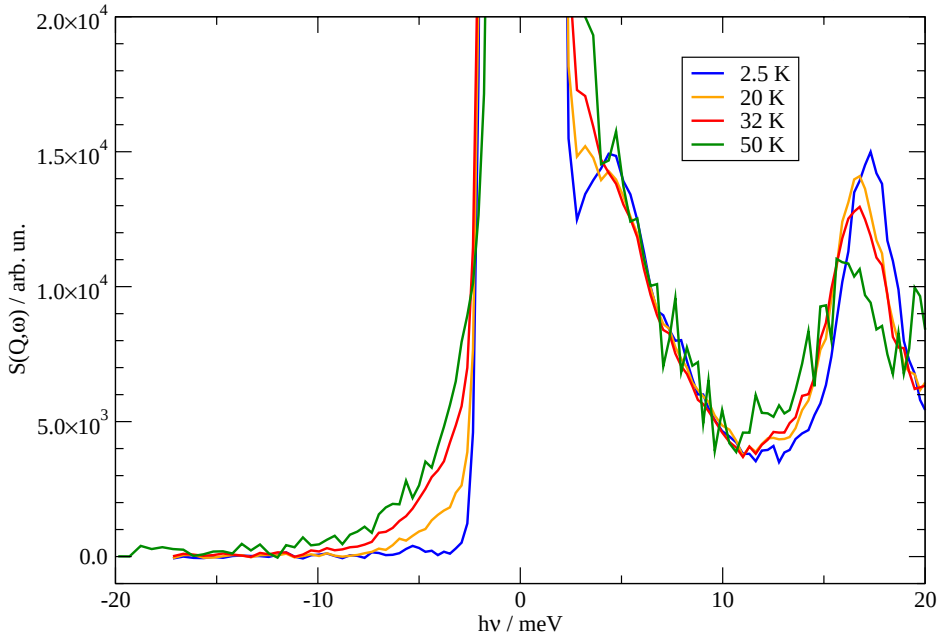


Fig 2: Temperature evolution of S(Q,ω). The spectra are integrated using always 12 detectors out of the sv29 detector array. The centre of the scattering angle is $2\theta = 30.2°$. A vanadium standard was used to calibrate the detectors. The background subtracted from all spectra was measured at $T = 2.5$ K.

Institut für Festkörperforschung
Forschungszentrum Jülich GmbH
D-52425 Jülich

Experimental Report
of Neutron Scattering Experiments
at the FRJ-2 Reactor

Proposal number:	S29-05-014		
Experiment title:	INS studies of rotational potentials of methyl groups in the 2,6-dimethylpyrazine:chloranilic acid complex		
Dates of experiment:	24.06.2005, 6 days	Date of report:	25.02.2006
Experimental team: Names	Addresses		
A. Pawlukojc M. Prager	Institute of Nuclear Chemistry and Technology, Warsaw, Poland Institut für Festkörperforschung, Forschungszentrum Jülich		
Local Contact:	M. Prager		

Experimental report text body

Molecular alloys have attracted wide interest since mixed systems may show properties unexpectedly different from those of the ingot materials. Among many others the complexes of chloranilic acid CLA with electron donor molecules seem to be interesting from the point of view of materials science.
The crystal structure of the 1:1 complex of 2,6-DMP and CLA was determined by X-rays at a sample temperature T=100K. The system is monoclinic $P2_1/c$ with Z=4 dimeric units in the large unit cell [1]. The 4 dimers are related by symmetry. Thus the complex contains just two equally weighted inequivalent methyl groups. A hydrogen bond links the proton of the CLA to the 2,6-DMP constituent via the nitrogen located between its two methyl groups.

The spectra of DMP:h-CLA and DMP:d-CLA were measured in the regime of phonons using wavelengths λ=1.17A and λ=1.76A. The doublet centered around 12meV (fig. 1) is interpreted as methyl libration split by coupling to lattice modes in agreement with a tunnel splitting of 3.3μeV observed with the backscattering spectrometer BSS1 [2]. From the intensity of this tunnelling band it is concluded that the second kind of methyl groups scatters only elastically and must be related with a librational mode at higher energy. The transition at 23meV may be assigned to this mode. Samples to verify the assignment via the isotope effect were not available.
To test whether effects of hydrogen bonding or charge transfer may be visible in the methyl rotational potentials we compare first the rotational potential in the complex to that of pure 2,6-DMP. In this material the rotational potential is found to be much weaker as in the complex [3,4]. Just the opposite happened in the previously studied TMP:CLA where complexation has led to a large reduction of the rotational potentials [5]. This shows that the most important influence must be the geometry of the environment. To identify more subtle effects of charge rearrangement requires a knowledge of the low temperature crystal structure similarly precise as in the case of pure DMP and a similar mathematical treatment of the lattice dynamics.

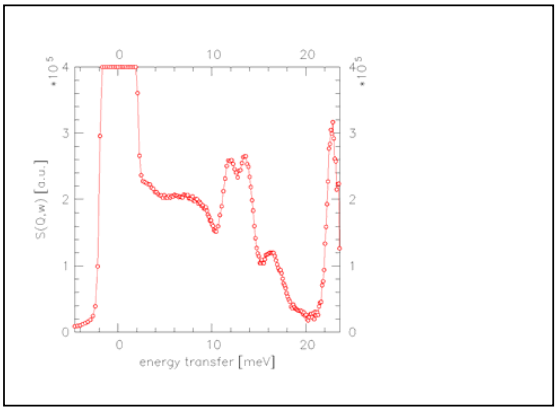


Fig. 1: Spectrum of 2,6-DMP:h-CLA in in the regime of lattice modes

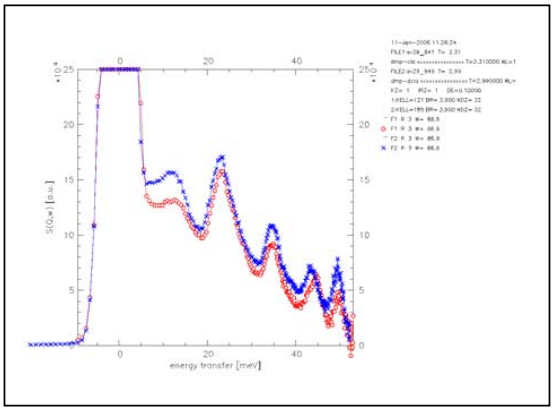


Fig. 2: Spectra of 2,6-DMP:h-CLA (ooo) and 2,6-DMP:d-CLA at energies of internal modes.

While no real changes with deuteration were found at low energy transfers ΔE<20meV fig. 2 shows that also up to 50meV there are only minor differences between the materials with protonated and deuterated hydrogen bonds. Only the band at ~43meV shows a measurable shift to lower energy with deuteration. In analogy to earlier Gaussian98 calculations this mode could be assigned to C-CH_3 wagging or bending modes. It is obvious that a change of the methyl rotational potential can influence such a mode. This observation is consistent with a reduction of the rotational barrier with in 2,6-DMP:d-CLA deduced from a weakly increased tunnel splitting [5].

[1] W. Sawka-Dobrowolska, G. Bator, L. Sobczyk, E. Grech, J. Nowicka-Scheibe, A. Pawlukojc, Struct.Chem., in press
[2] Experimental Report 2005 FRJ2, this volume BSS-05-028
[3] E. Kaiser-Morris, A. Cousson, W. Paulus, F. Fillaux, Acta Cryst. **E57**,o1113(2001)
[4] B. Nicolai, E. Kaiser, F. Fillaux, G.J. Kearley, A. Cousson, W. Paulus,
Chem. Phys. **226**,1(1998)
[5] M. Prager, A. Pawlukojc, E. Sobczyk, E. Grech, H. Grimm,
J. Phys. Condens. Matter **17**,5275(2005)

Institut für Festkörperforschung
Forschungszentrum Jülich GmbH
D-52425 Jülich

Experimental Report
of Neutron Scattering Experiments
at the FRJ-2 Reactor

Proposal number:	S29-05-015		
Experiment title:	Crystal electric field scheme of R_2PdSi_3 (R = Tb, Er, Tm)		
Dates of experiment:	07.12.05-19.12.05 16.01.06-20.01.06	Date of report:	06.06.06
Experimental team: Names	Addresses		
Matthias, Frontzek	TU Dresden, Institut für Festkörperphysik, Zellescher Weg 16; 01062 Dresden		
Local Contact:	Jörg Voigt and Michael Prager		

Experimental report text body

The series R_2PdSi_3 (R = rare earth metal), crystallizing in an AlB_2 derived hexagonal structure, have been found to exhibit strong anisotropic magnetic properties [1] and to show a giant magneto-resistance effect [2]. In the Tb_2PdSi_3 compound low-dimensional magnetism as well as spin-glass like behaviour probably due to geometrical frustration was observed [1]. A spin-glass like transition below the Néel temperature is reported for the Er_2PdSi_3 compound, too [3].
We performed magnetic neutron diffraction studies on R_2PdSi_3 (R = Tb, Er, Tm) single crystals. Due to the crystal electric field (CEF) anisotropy the magnetic moment direction is in the hexagonal plane for Tb_2PdSi_3 ($T_N = 23$ K) and along the hexagonal $\boldsymbol{c}$-axis for Er_2PdSi_3 ($T_N = 7$ K) and Tm_2PdSi_3 ($T_N = 1.8$ K). The modulation of the magnetic moments is along $\boldsymbol{c}^*$ in the case of Tb_2PdSi_3, along $\boldsymbol{a}^*$ for Er_2PdSi_3 and along both directions for Tm_2PdSi_3. The compounds of the isostructual series seem to be strongly influenced by CEF effects and the according magnetocrystalline anisotropy [4]. However, no inelastic neutron scattering experiments have been published so far.
The aim of the experiment was to obtain a first overview of the CEF level scheme of the R_2PdSi_3 compounds. The powder samples ($m \approx 10$ g) of R_2PdSi_3 (R =Y, Tb, Er, Tm) were prepared similar to the single crystal growth process.
The main results for the magnetic ordering compounds are shown in the Figures 1 to 3. For the Tb_2PdSi_3 compound the complete incident energy range of the SV-29 spectrometer was used with additional measurements at incident energies of 6.3 meV and 56.8 meV. Only one CEF transition at around 6.5 meV (Fig. 1) was observed ($T = 2.5$ K). The Er_2PdSi_3 and Tm_2PdSi_3 compounds were only measured with an incident energy of 25.3 meV which provides the highest neutron flux at the sample position. Er_2PdSi_3 features two CEF transitions at 3.35 meV and 8.42 meV ($T = 2.5$ K) in this energy range (Fig. 2).The measurement on the Tm_2PdSi_3 compound was performed in the standard-orange cryostat which allows lower temperatures than the closed cycle cryostat used for the measurement of the other compounds, since Tm_2PdSi_3 orders below $T = 1.8$ K. Similar to Er_2PdSi_3 also in the Tm_2PdSi_3 compound two CEF transitions were observed (Fig. 3). The transition energies are larger with 5.77 meV and 11.28 meV.

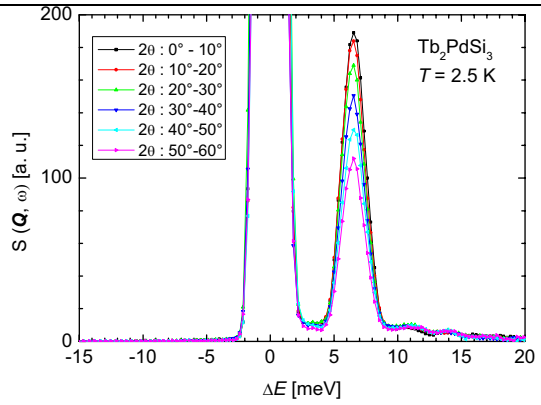


Fig. 1: S(***Q***, ω) of Tb_2PdSi_3 at T = 2.5 K; the incident energy was E = 25.3 meV.

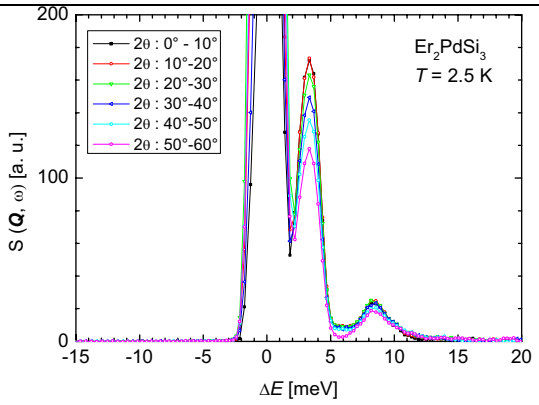


Fig. 2: S(***Q***, ω) of Er_2PdSi_3 at T = 2.5 K; the incident energy was E = 25.3 meV.

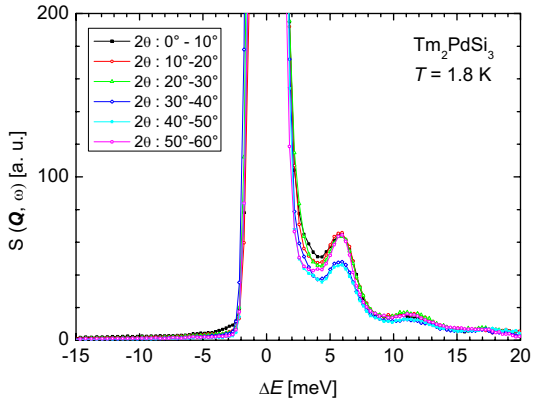


Fig. 3: S(***Q***, ω) of Tm_2PdSi_3 at T = 1.8 K; the incident energy was E = 25.3 meV.

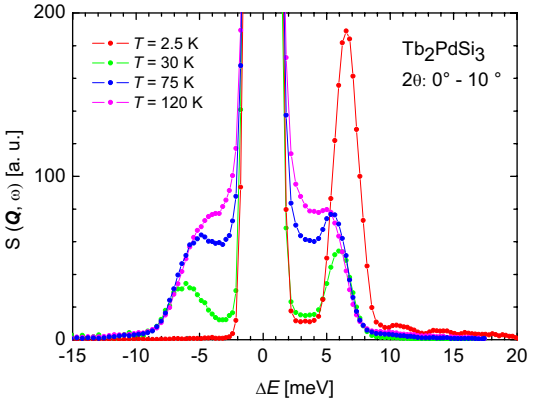


Fig. 4: S(***Q***, ω) of Tb_2PdSi_3 at small scattering angle and at four different temperatures; the data has been modified with the Boltzmann factor (except the T = 2.5 K data); incident energy was E = 25.3 meV.

The measurements were not only performed at lowest temperature but at 4 different temperatures up to 120 K for each of the three magnetic compounds (temperatures were selected according to characteristic temperatures determined from susceptibility measurements). All investigated compounds exhibit a similar temperature dependent behaviour like the Tb_2PdSi_3 compound. A comparison between different temperatures is shown for the Tb_2PdSi_3 compound in Figure 4. The quasi-elastic line broadens strongly with increasing temperature thus making it difficult to determine the exact energy position of the transition. Still, the crystal field levels seem to decrease in energy with increasing temperature. For the Tb_2PdSi_3 compound no additional transition could be observed. In the cases of the Er_2PdSi_3 and Tm_2PdSi_3 compound one expects to observe the additional transition between the two levels measured at lowest temperature. However, this transition can only be observed in the Er_2PdSi_3 compound. For the Tm_2PdSi_3 compound the energy difference between the two measured levels equals the energy of the first level thus making the transition between the two levels undistinguishable from the transition to the first level. The combination of macroscopic data (e. g. susceptibility, magnetisation) and the measured transitions will lead to a first scheme of the CEF for the R_2PdSi_3 compounds.

References:

[1] S. Majumdar, E. V. Sampathkumaran, P. L. Paulose, H. Bitterlich, W. Löser, G. Behr, Phys. Rev. B **62** (2000) 14207
[2] S. Majumdar, H. Bitterlich, G. Behr, W. Löser, P. L. Paulose, E. V. Sampathkumaran, Phys. Rev. B **64** (2001) 012418
[3] K. K. Iyer, P. L. Paulose, E. V. Sampathkumaran, M. Frontzek, A. Kreyssig, M. Doerr, M. Loewenhaupt, I. Mazilu, G. Behr, W. Löser, Physica B **355** (2005) 158-168
[4] M. Frontzek, A. Kreyssig, M. Doerr, M.Rotter, G. Behr, W. Löser, I. Mazilu, M. Loewenhaupt, JMMM *accepted for publication*

Institut für Festkörperforschung
Forschungszentrum Jülich GmbH
D-52425 Jülich

Experimental Report of Neutron Scattering Experiments at the FRJ-2 Reactor

Proposal number:	S29-05-016		
Experiment title:	The study of the quasielastic incoherent neutron scattering from the $K_{1-x}(NH4)_xSCN$ mixed crystals		
Dates of experiment:	13 days between 21.2. – 20.3.2006	Date of report:	20.5.2006
Experimental team: Names	Addresses		
L. Smirnov I. Natkaniec M. Prager	FSUE SSC RF, Institute of theoretical and experimental physics, Russia JINR, Dubna, Russia Forschungszentrum Jülich, Institut für Festkörperforschung		
Local Contact:	M. Prager		

Experimental report text body

KSCN, potassium thiocyanate, undergoes a phase transition at 413 K from orthorhombic phase with space group Pbcm-D_{2h}, Z=4 [1], and lattice parameters a=6.673, b=6.715. c=7.543 Å, into a body-centered tetragonal structure with space group I4/mcm, Z=4 [2] and lattice parameters a=b=6.70, c=7.73 Å. Similarly NH_4SCN, ammonium thiocyanate, undergoes order-disorder phase transition from a high temperature tetragonal phase I with space group I4/mcm-D_{4h}^{18}, Z=4, lattice parameters a=b=6.961, c=8.00Å to antiferro-electric orthorhombic phase II with space group Pbcm-D_{2h}, Z=4, lattice parameters a=6.878, b=6.905, c=7.912 Å at 391K [3-4]. Following transition in NH_4SCN appears at 359K from phase II to phase III with a monoclinic crystal structure with space group C_{2h}^5, Z=4, lattice parameters a=4.247, b=7.146, c=13.022 Å, β=97.8$_o$ [5].

As was shown in [6] KSCN and NH_4SCN can form solid solutions in all concentration region of ammonium. The $K_{1-x}(NH_4)_xSCN$ mixed crystals are obtained in the result of the evaporation of water stoichiometrical solutions of KSCN and NH_4SCN at 323K. KSCN and NH_4SCN are isomorphic at this temperature, ionic radii of these substances are close and this promotes to the formation of solid solutions.

The purpose of the experiment is to determine in the $K_{1-x}(NH_4)_xSCN$ mixed crystals by means of quasielastic incoherent neutron scattering (QENS) the distribution of the barrier to the reorientations of ammonium ions and the energy of the activation in different regimes of concentration. In this first experiment a concentration x=0.1 is chosen to avoid to a large degree the interaction between ammonium ions. The spectrometer was used with a wavelength λ=3.52A and a corresponding energy resolution of δE=0.31meV.
Fig. 1 shows the spectra measured at sample temperatures from 40K to 110K. A clear quasielastic component is visible. It must be assigned to ammonium reorientational jumps. The data wait for a quantitative analysis based on the random rate distribution model (RRDM) [7]. Beside of the quasielastic component we observe a soft inelastic mode around 3.6meV of so far unknown origin. Lattice dynamical calculations will help to identify the character of this mode.

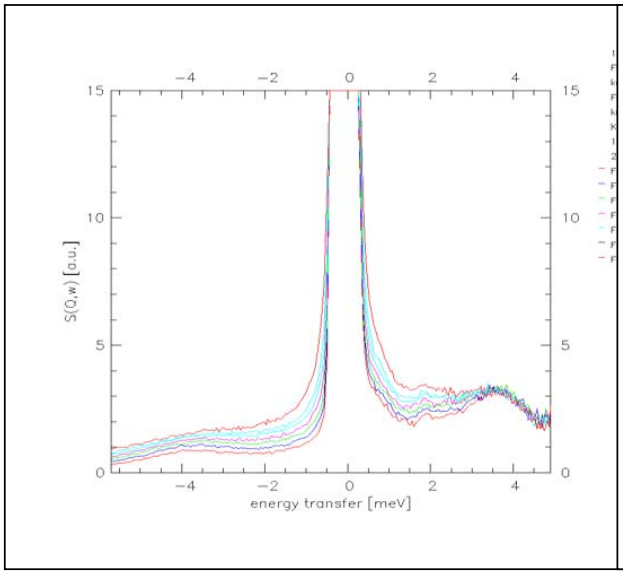


Fig. 1: Spectra of $K_{0.9}(NH_4)_{0.1}SCN$ summed over all Angles. Sample temperature (40-110)K. Data only. Λ=3.52A.

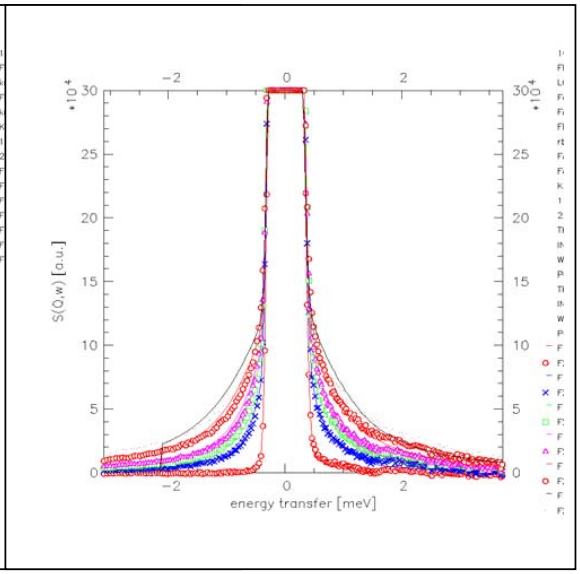


Fig. 2: Spectra of $Rb_{0.9}(NH_4)_{0.1}SCN$ summed over all Angles. Sample temperature (2.4-130)K. Symbols: data, lines: fit. Λ=3.52A.

Fig. 2 shows the similar measurement for the Rb analogous compound of the same ammonium concentration. Again a quasielastic component is visible which is clearly broader as due to weaker rotational potentials. A fit with a single Lorentzian (solid lines of fig. 2) is feasible with reasonable quality. This could mean that only a single time constant exists or, equivalently, that the potential distribution function is very narrow. However, the line intensity depends on temperature. We may attribute this to a much broader distribution of rotational barrier heights where the higher barriers enter the energy window of the spectrometer with increasing temperature. The data analysis is in progress.

References:

1. H.P.Klug, Z.Kristallogr., 85 (1933) 214.
2. Y.Yamada and T.Watanabe, Bull.Chem.Soc.Jpn., 36 (1963) 1032.
3. W.Klement, Jr. and C.W.F.T.Pistorius, Bull. Chem. Soc. Jpn.. 49 (1976) 2148.
4. A.Hamada, S.Yamamoto and Y.Shinnaka, J.Phys.Soc.Jpn., 59 (1990) 954.
5. V.E.Zavodnik, Z.V.Zvonkova, G.S.Zhdanov, E.G.Mirevich, Sov.Phys.-Crystallogr. 17 (1972) 85.
6. I.Natkaniec, L.S.Smirnov, A.I.Solov'ev, Physica B213&214 (1995) 667-668.
7. J. Colmenero, R. Mukhopadhyay, A. Alegria, B. Frick, Phys. Rev. Lett. 80,2350(1998)

Institut für Festkörperforschung
Forschungszentrum Jülich GmbH
D-52425 Jülich

Experimental Report
of Neutron Scattering Experiments
at the FRJ-2 Reactor

Proposal number:	S29-05-017		
Experiment title:	Studies on the Crystal field of $TbMn_2O_5$		
Dates of experiment:	07.02. – 15.02.2006	Date of report:	01.06.2006
Experimental team: Names	Addresses		
Lieh-Jeng Chang	Nuclear Science and Technology Development Center National Tsing Hwa University 101, Sec. 2, Kuang-Fu Road HsinChu, 30013, Taiwan		
Local Contact:	Dr. Jörg Voigt		

Experimental report text body

Introduction

There is currently a great interest in the materials that exhibit interplay between lattice distortions and electrical and magnetic ordering. Among these materials, magnetoelectrics, in which magnetism and ferroelectricity coexist and are mutually coupled, are being investigated extensively. These materials display phenomena such as the control of electrical polarization by the application of an external magnetic field, providing an additional degree of freedom for the design of new devices.[1] However; compounds showing large magnetoelectric effects are extremely rare. The magnetoelectric $TbMn_2O_5$ exhibits a profound interplay between electrical polarization and the applied magnetic field. This is demonstrated by two discoveries: the highly reversible switching of electrical polarization using relatively low magnetic fields of 0-2T; and the combined application of electric and magnetic field, which leaves a permanent imprint in the polarization.[2]

$TbMn_2O_5$ is an insulator and consist of linked $Mn^{4+}O_6$ octahedra and $Mn^{3+}O_5$ pyramids adopting space group *Pbam*. The octahedral share edges to form ribbons parallel to the c axis, adjacent ribbons being linked by pairs of corner-sharing pyramids.[1] The structure at room temperature is orthorhombic. (Fig. 1)[3] The reported neutron diffraction measurements on $TbMn_2O_5$ as a function of temperature and applied field which show unambiguous correlations between dielectric anomalies and changes in the periodicity of the spin structure. First, the onset of ferroelectricity at 38 K is associated with the appearance of incommensurate antiferromagnetic ordering $T_1 = 43$ K. At $T_2 = 33$ K, just above the maximum in spontaneous polarization **P**, propagation vector **k** locks into a commensurate value (1/2, 0, 1/4). Remarkably, at $T_3 = 24$ K, where the dielectric constant **ε** has an upward "jump", **k** becomes suddenly incommensurate again, a rare example of such a transition on cooling. The low temperature transition ($T_4 = 10$ K) coincides with a major increase of the Tb ordered moment. The 43 and 24 K transitions are accompanied by clear anomalies in the lattice parameters, particularly along the *b* "polar" axis, and in the atomic displacement parameters.[4]

Experiments

8 grams of $TbMn_2O_5$ polycrystalline sample have been prepared through conventional solid-state reaction method and characterized by powder x-ray diffraction and magnetization. All the observable peaks on the powder x-ray pattern can be well indexed for showing the sample to be single phase. A broad peak has been observed on the magnetic susceptibility from 50 to 20 K corresponding to the series of transitions mentioned above. Experiments were performed at SV-29, thermal time-of-flight spectrometer, in an orange cryostat for temperature between 2.5 K and 60 K. Neutron wavelength of 1.17 Å and 1.76 Å, which correspond to graphite crystals PG002/PG004 monochromater, were selected for the time-of-flight experiments.

Results

Figure 1(A) shows the experimental results taken at different temperatures at 2 theta ~ 30° by using wavelength 1.76 Å. The Vanadium and empty can had been used to calibrate and normalize each detector. The first peak at ~5 meV shifts to lower energy when the temperatures increase and finally merges to the broad central peak at 60 K. However, no clear shifting was observed for the peaks at ~13, ~16 and ~18 meV. Fig. 1(B) shows the results of different Qs at 2.5 K. All of these four peaks intensity seems to follow the form factor effect to reduce their intensities at high Q. This shows these four peaks correspond to the magnetic moments. A further analysis on the intensity is necessary to prove this magnetic form factor effect. No obvious energy dispersion is observed in the experimental results.

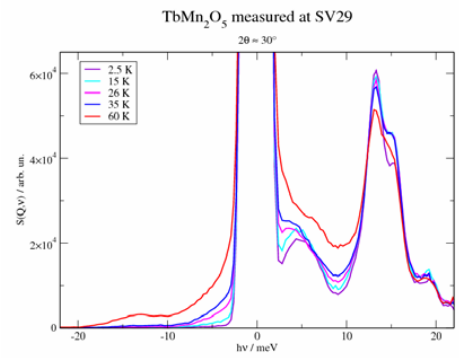


Fig. 1(A) Time-of-flight spectra taken at different temperatures at 2 theta ~ 30° by using wavelength 1.76 Å. The Vanadium and empty can had been used to calibrate and normalize each detector.

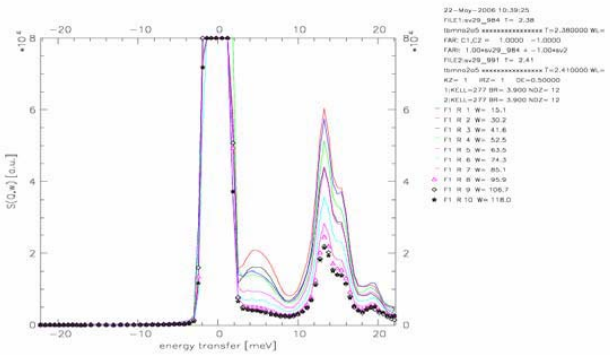


Fig. 1(B) Time-of-flight results of different Qs taken at 2.5 K. All of these four peaks intensity seems to follow the form factor effect to reduce their intensities at high Q.

References:

1. G.R. Blake, et al., Phys. Rev. B **71**, 214402 (1995).
2. N. Hur, et al., Nature (London) **429**, 392 (2004).
3. D. Higashiyama and S. Miyasaka, Phys. Rev. B **72**, 064421 (2005).
4. L.C. Chapon et al., Phys. Rev. Lett **93**, 177402 (2004).

Institut für Festkörperforschung
Forschungszentrum Jülich GmbH
D-52425 Jülich

Experimental Report
of Neutron Scattering Experiments
at the FRJ-2 Reactor

Proposal number:	S29-05-018		
Experiment title:	Methyl group dynamics in methyl bromide clathrate		
Dates of experiment:	12 days between 26.01. – 15.04.2006	Date of report:	20.05.2006
Experimental team: Names	Addresses		
M. Prager	Institut für Festkörperforschung, Forschungszentrum Jülich		
Local Contact:	M. Prager		

Experimental report text body

Clathrates are characterized by a stable framework of host molecules which form cages which allow to incorporate simple guest molecules. The guest molecules experience a matrix effect in **almost identical environments** and thus show in general well defined spectral lines. Cages of water clathrates are distinguished from many other clathrates by the disorder of hydrogen bonds. This makes on the one hand the data analysis more complex but on the other side more interesting since water cages especially with organic guest molecules may represent model systems of H-bonded hydration shells in biology.
We have recently studied water clathrates with methyl iodide [1] and methyl fluoride [2] guest molecules. While CH_3I was found to mirror the potential surface of the water cages in great detail, disorder and eventually the tendency fo form hydrogen bonds mixes such details in case of CH_3F and allows to deduce average potentials and their distribution only.
It can be expected that the other two methyl halide guest molecules with properties in between those of CH_3I and CH_3F may image other details of the clathrate cages. The actual experiment uses methyl bromide as guest molecules. A sample was prepared on site the same way as methyl iodide clathrate by stirring a 1:5.75 molar mixture of CH_3Br and D_2O or H_2O around the final freezing point T_m~9C. According to literature and our own structure determination [3,4,5] methyl bromide clathrate crystallizes in the cubic I phase.
Fig 1 shows the spectra in the regime of phonons. As in the other clathrates the shoulder at energy transfer ~11meV is taken as a sign of clathrate formation. The raw data of the high resolution measurement (fig. 2) reveals unresolved intensity from almost free rotor transitions at T_S=3K and a high rotational mobility of the guest molecules by a quasielastic component. Improved data will be measured at a much better suited cold time-of-flight spectrometer. The isotope effect (figs 3) shows that the strongest vibrational band which shifts by about 1meV to lower energy in the deuterated matrix is likely a host mode. As expected there is almost no change of the methyl rotational dynamics leading to similar high resolution spectra. The data analysis is under work.

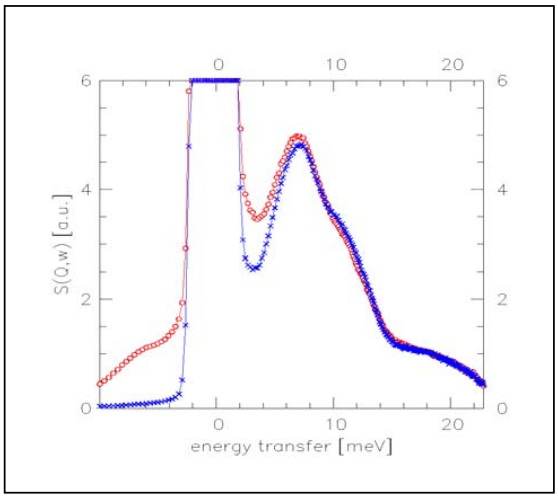


Fig. 1 Spectra of CH3Br*5.75H2O. λ=1.71A.
Sample temperatures T_S=3K (xxx) and 50K(ooo).

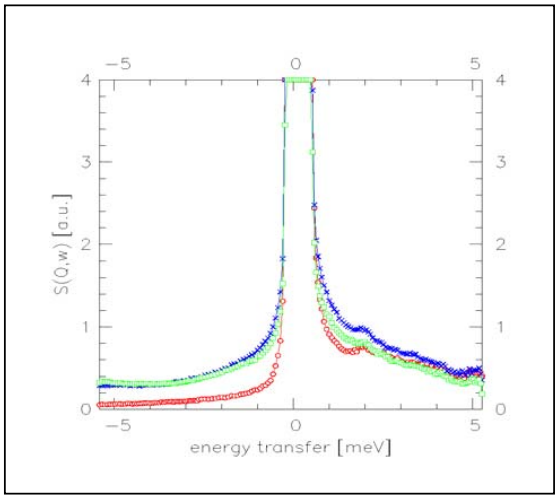


Fig. 2 Spectra of CH3Br*5.75H2O. λ=3.52A.
T_S=3K (ooo), 60K(xxx) and 80K([][][]).

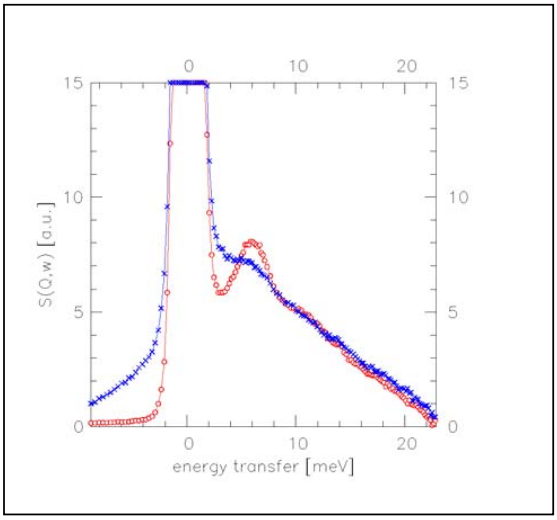


Fig. 3 Spectra of CH3Br*5.75D2O. λ=1.71A.
Sample temperatures T_S=3K (ooo) and 50K(xxx).

[1] M. Prager, A. Desmedt, A. Buchsteiner, J. Pieper, J. Phys., Condens. Matter 16,7045(2004)
[2] M. Prager, J. Baumert, W. Press, M. Plazanet, J. Tse, D.D. Klug, PCCP 7,1228(2005)
[3] A. Jeffryes, in 'Inclusion cmpounds', Vol. 1, p. 1 of 'Inorganic and physical aspects of inclusion', J.L. Atwood et al eds., Oxford University Press, Oxford 1991
[4] J.A. Ripmeester, C.I. Ratcliffe, in 'Inclusion cmpounds', Vol. 4, p. 37 of 'Inorganic and physical aspects of inclusion', J.L. Atwood et al eds., Oxford University Press, Oxford 1991
[5] This volume, report SV7-05-016

Institut für Festkörperforschung
Forschungszentrum Jülich GmbH
D-52425 Jülich

Experimental Report
of Neutron Scattering Experiments
at the FRJ-2 Reactor

Proposal number:	S29-06-001		
Experiment title:	Methyl group dynamics in methyl chloride clathrate		
Dates of experiment:	12 days between 26.01. – 15.04.2004	Date of report:	20.05.2006
Experimental team: Names	Addresses		
M. Prager	Institut für Festkörperforschung, Forschungszentrum Jülich		
Local Contact:	M. Prager		

Experimental report text body

Clathrates are characterized by a stable framework of host molecules which form cages which allow to incorporate simple guest molecules. The guest molecules experience a matrix effect in **almost identical environments** and thus show in general well defined spectral lines. Cages of water clathrates are distinguished from many other clathrates by the disorder of hydrogen bonds. This makes on the one hand the data analysis more complex but on the other side more interesting since water cages especially with organic guest molecules may represent model systems of H-bonded hydration shells in biology.
We studied so far water clathrates with methyl iodide [1] and methyl fluoride [2] guest molecules. CH_3I was found to mirror the potential surface of the water cages in great detail. In case of CH_3F a strong tendency to form H-bonds allows leads to a strong averaging of potentials and allows only potential distributions to be obtained. It is expected that the other two methyl halide guest molecules with properties in between those of CH_3I and CH_3F may image other details of the clathrate cages. The actual experiment deals with methyl chloride guest molecules. A sample was prepared on site the same way as methyl iodide clathrate by stirring a 1:5.75 molar mixture of CH_3Cl and D_2O around the freezing point T_m~19C. According to literature [3,4] methyl chloride clathrate crystallizes in the cubic I phase. Our own structure determination shows, however, that the unit cell is smaller and possibly hexagonal [5]. This has to be confirmed.
Fig 1 shows the inelastic neutron scattering spectra in the regime of phonons. Here the shoulder at energy transfer ~11meV is usually taken as a sign of clathrate formation. A high resolution measurement (fig. 2, xxx) reveals the high rotational mobility of the guest molecules by a broad quasielastic component. Rotation is much faster than for $CH_3Br*5.75H_2O$ [6]. The inelastic band 2.6meV observed at T_S=3K must be attributed to an almost free rotor transition of methyl groups of CH_3Br. Consistent with this assignment there is no isotope effect of this mode with deuteration of the cage. In contrary the strongest vibrational band shifts by about 1meV to lower energy with deuteration of the host matrix and is likely a mode of the ice cage. The data analysis is under work. Further experiment are under way.

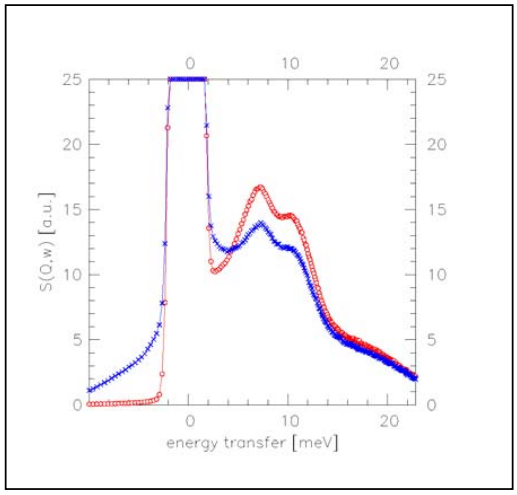


Fig. 1 Spectra of $CH_3Cl*5.75H_2O$. λ=1.71A.
Sample temperatures T_S=3K (ooo) and 50K(xxx).

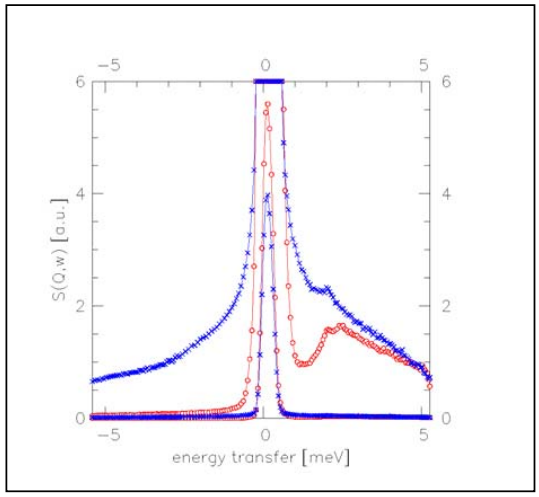


Fig. 2 Spectra of $CH_3Cl*5.75H_2O$. λ=3.52A.
T_S=3K (ooo), 60K(xxx).

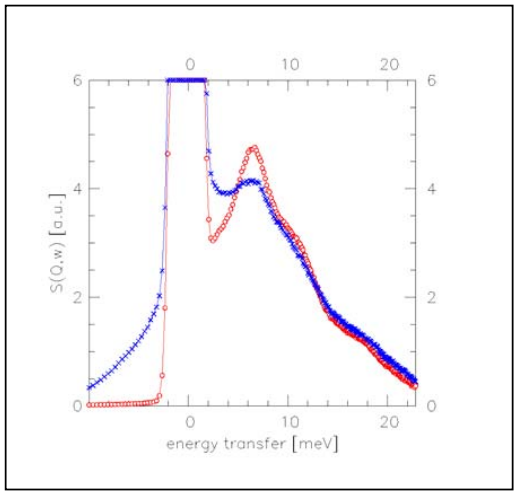


Fig. 3 Spectra of $CH_3BCl*5.75D_2O$. λ=1.71A.
Sample temperatures T_S=3K (ooo) and 50K(xxx).

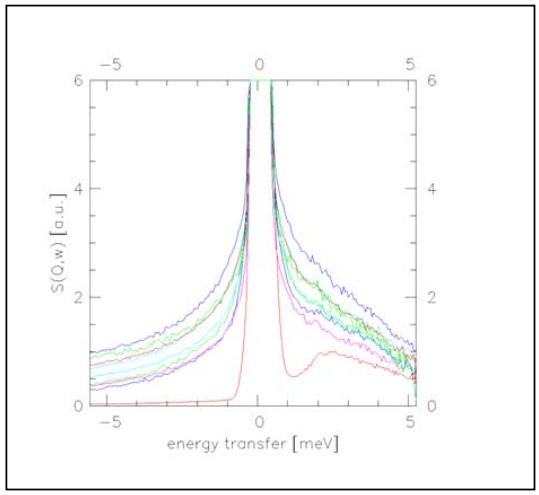


Fig. 4 Spectra of $CH_3Cl*5.75H_2O$. λ=3.52A.
T_S=3K and 40K to 120K, most steps 10K.

[1] M. Prager, A. Desmedt, A. Buchsteiner, J. Pieper, J. Phys.: Condens. Matter 16,7045(2004)
[2] M. Prager, J. Baumert, W. Press, M. Plazanet, J. Tse, D.D. Klug, PCCP 7,1228(2005)
[3] A. Jeffryes, in 'Inclusion cmpounds', Vol. 1, p. 1 of 'Inorganic and physical aspects of inclusion', J.L. Atwood et al eds., Oxford University Press, Oxford 1991
[4] J.A. Ripmeester, C.I. Ratcliffe, in 'Inclusion cmpounds', Vol. 4, p. 37 of 'Inorganic and physical aspects of inclusion', J.L. Atwood et al eds., Oxford University Press, Oxford 1991
[5] This volume, report SV7-06-005
[6] This volume, report S29-05-018

Institut für Festkörperforschung
Forschungszentrum Jülich GmbH
D-52425 Jülich

Experimental Report
of Neutron Scattering Experiments
at the FRJ-2 Reactor

Proposal number:	S29-06-002		
Experiment title:	Phase transformations and excitations in collidin, 2,4,6-trimethyl-pyrazin		
Dates of experiment:	10.03. – 15.03.2006	Date of report:	20.05.2006
Experimental team: Names	 Addresses		
I. Natkaniecz M. Prager	Institut of Nuclear Physics, Krakow, Poland Institut für Festkörperforschung, Forschungszentrum Jülich		
Local Contact:	M. Prager		

Experimental report text body

Collidin, 2,4,6-trimethyl-pyridin, shows an unusual structural behaviour with temperature. At a first cooling from the liquid into the solid phase it becomes disordered and remains so down to the lowest temperatures. Only after annealing below the melting point for some time the system gets long range ordered. The crystal structure was determined by single crystal X-ray diffraction [1]. The crystal was grown from the liquid and thereafter cooled down to 180K. The monoclinic space groups $P2_1/c$ with two molecules in the asymmetric unit was found. One of the methyl groups was thought to be disordered.
We used thermal and high resolution neutron spectroscopy to study the dynamic counterpart of the structure. Fig. 1 shows spectra taken on the thermal TOF spectrometer SV29 at various states of the sample. Circles represent the quenched sample. The broad unstructured intensity distribution of the disordered crystal transforms after annealing into a spectrum with characteristic bands (squares). Their temperature evolution is shown at T=60K (triangles) and T=80K (crosses). The assignment of the bands requires a lattice dynamical calculation.
The high resolution spectra show an analoguous behaviour (fig. 2). The circles represent again the quenched sample at a temperature T=4K. At this temperature quasielastic scattering has died out. The apparent Lorentzian intensity is attributed to rotational tunnelling of methyl groups. Disorder leads to a distribution of rotational potentials and therefore a distribution of tunnel transitions. A model to describe such spectra is available in the literature [2]. It looks that the intensity corresponds to more than 1/3 of the methyl groups found to be disordered in the crystal structure analysis. After annealing a part of the broad intensity distribution has transformed into a clear tunnelling transition (fig. 2, crosses) indicative of the new order. Its low intensity must be related with a symmetry reduction in the ordered phase. At higher temperature (fig. 2, 60K=triangles, 80K=squares) quasielastic scattering is broader than the resolution of the instrument (fig. 2, diamonds) but needs a more elaborate study.

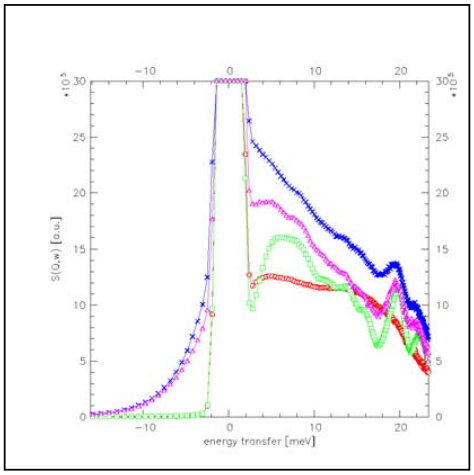


Fig. 1 Spectra of collidin. SV29: λ=1.59A
ooo: quenched, T=3K; square: annealed, T=3K;
triangle: annealed, 60K; xxx: annealed, T =80K

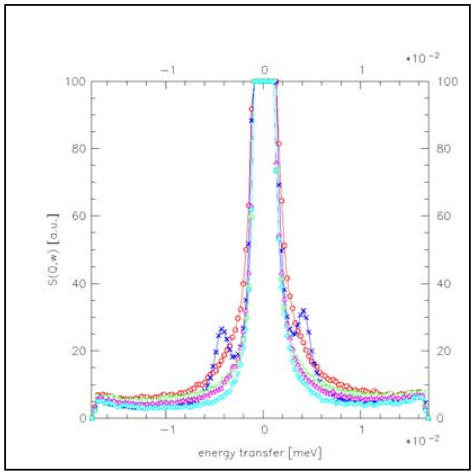
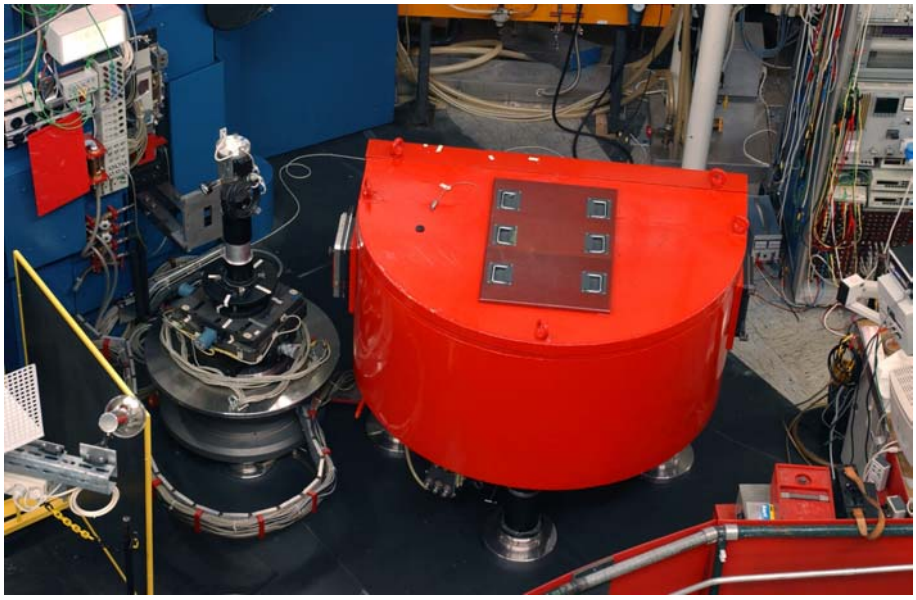


Fig. 1 Spectra of collidin. BSS: λ=6.28A
ooo: quenched, 4.5K; xxx: annealed, 4.5K;
triangle: annealed, 60K; square: annealed, T =80K;
diamond: resolution

Collidin shows some similarities to other cyclic hydrocarbons. With toluene it shares the phase behaviour: disorder at direct cooling – crystallisation after annealing. The way of data analysis used in case of tolene [4] could be applied here too. There is also some analogy with mesitylene. Structurally the two compounds are closely related due to the symmetric arrangement of methyl groups, electrically collidin has a unique tendency of hydrogen bond formation [1]. Some metastable phases exist in both materials. Tunneling spectroscopy is especially suited to resolve the differences [4,5]. These analogies shall be exploited in the ongoing data analysis of collidin.

[1] A.D. Bond, J.E. Davies, Acta Cryst. E57, o1141(2001)
[2] J. Colmenero, R. Mukhopadhyay, A. Alegria, B. Frick, Phys. Rev. Lett. 80,2350(1998)
[3] A. Moreno, J. Colmenero, A. Alegria, B.Frick, M. Prager, J. Chem. Phys. ,(2001) Toluene
[4] I. Natkaniecz
[5] M. Prager, I Natkaniecz, H. Grimm, J. Phys.: Condens. Matter ,(2005)Mesitylene

Triple-Axis Spectrometer (UNIDAS)



Instrument Parameters

Beam tube:	4H4 radial ∅ 4"
Monochromators:	pyrolytic graphite (002), vertical focusing
Analyzers:	pyrolytic graphite (002), focusing germanium (111)
Filter:	pyrolytic graphite, for incident and/or final beam
Collimators:	15' ... 60' (Rutherford collimators)
Angular range ***- Monochromator:*** ***- Scattering angle:*** ***- Analyzer:*** ***- Sample:***	 $12.5° \le \Theta_M \le 60°$ $-90° \le \Phi \le 130°$ $-75 \le \Theta_A \le 75°$ (with different configurations) $-180° \le \psi \le 180°$ $-180° \le \chi \le 180°$ (with $-180° \le \varphi \le 180°$ Eulerian cradle)
Beam size at specimen:	35 x 90 mm^2
Neutron flux at sample position:	typically 5×10^6 n/cm^2 s
Incident:	$0.8 Å \le \lambda \le 4 Å$
Energy transfer:	$0.02 meV \le \hbar\omega \le 80 meV$
Momentum transfer:	$0.05 Å^{-1} \le Q \le 10 Å^{-1}$
Detector:	^{3}He (8 bar)
Background:	≤ 2 cnts/min
Time resolution for stroboscopic experiments:	$2 ms \le \Delta t \le 200 s$
Sample environment:	goniometer, ±20° tilt; Eulerian cradle; 2 closed-cycle cryostats (10 K ≤ *T* ≤ 300 K); 2 bath cryostats (4 K ≤ *T* ≤ 300 K); 2 standard furnaces (300 K ≤ *T* ≤ 1100 K); 1 special furnace (500 K ≤ *T* ≤ 1800 K); 2 four-circle furnaces (300 K ≤ *T* ≤ 1300 K) ; furnace for uniaxial (periodic) pressure; automatic temperature control

Instrument Responsible

Dr. Andreas Hoser Tel. +49-(0)2461-61-4762 Email: a.hoser@fz-juelich.de

Institut für Festkörperforschung
Forschungszentrum Jülich GmbH
D-52425 Jülich

Experimental Report of Neutron Scattering Experiments at the FRJ-2 Reactor

Proposal number:	UDS-04-013		
Experiment title:	Magnetic Excitations in nanocrystalline Tb		
Dates of experiment:	8-18 March 2005	Date of report:	24 May 2005
Experimental team: Names	Addresses		
O. Moze, C. Vecchini Andreas Hoser	Physics Dept, Modena University, Italy Forschungszentrum Juelich, Germany		
Local Contact:	Andreas Hoser		

Experimental report text body

Recent measurements by SANS (Weissműller et al, Phys. Rev. B 69, 054402 [2004]) were performed for the first time on the nanocrystalline hard magnet Tb. Two important parameters used in modelling the magnetic behaviour in this material, and indeed in understanding the nature of the large magnetic anisotropy in nanocrystalline Tb are the spin-wave stiffness constant D and the spin-wave gap Δ, which reflects dipolar and anisotropy contributions.We have recently re-attempted to measure the spin wave excitations in a 1 gm sample of nanocrystalline Tb with a grain size of 13 nm. Inelastic scans were performed at different temperatures in the ferromagnetic region (T_c=226K). Previously performed scans at PSI (Switzerland) on the Triple-Axis Spectrometer TASP, gave evidence of the probable presence of an inelastic peak at about 1.8 THz at 200K. The measurements were performed in the fixed initial energy mode (K_i=2.67 A^{-1}) with energy transfer up to 2.85 THz. Initial diffraction scans were done in order to center scans around the (101) reflection, which is the strongest magnetic and nuclear Bragg peak (Fig. 1). This position was chosen because of the high magnetic scattering intensity and much lower background and small angle scattering than in the forward direction. Due to the low intensity of the inelastic magnetic signal, the measurement time was necessarily very long. Measurements at 200K did not show any intrinsic inelastic peak but showed the presence of 2 Bragg spurion peaks due to analyzer and monocromator reflections at 2 THz and 2.7 Thz. The first one appears to be very broad for a Bragg spurion. Measurements at 150K showed the presence of the 2 spurions, always at 2 THz and 2.7 Thz and of one inelastic peak at 2.1 THz. This peak has an intensity of about 90 counts on top of the background and a width of 0.2 Thz as shown in Fig. 2. Further measurements at 50K evidenced the absence of that peak, that, in our opinion, has moved outside the energy range investigated (Fig. 3) and confirmed the position of the first spurion at 2 THz. In light of the scans at 50K and 150K, we think that the intrinsic inelastic peak at 200K could have moved inside the spurion, broadening it and slightly moving from its original position due to the convolution of the two (Fig. 4).

Further measurements with different temperatures choices and different incoming neutron energies are very desiderable. This will allow tracking of the inelastic signal over a wider temperature range. These measurements are also ***pioneering*** in the sense that they demonstrate what can be done with ***neutrons on rather small nanocrystalline samples***.

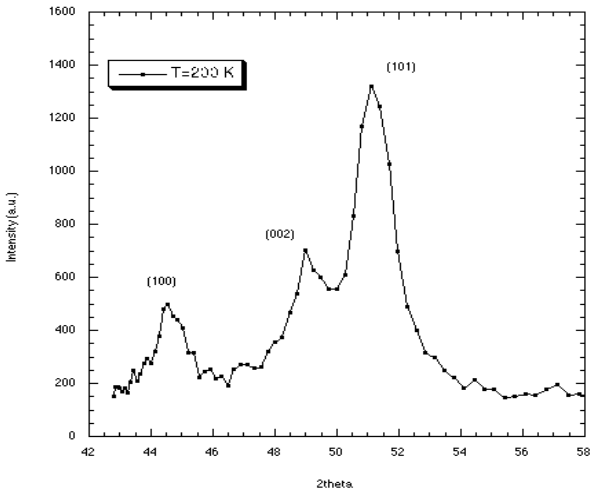


Fig. 1 Elastic scan for nano Tb at T=200K

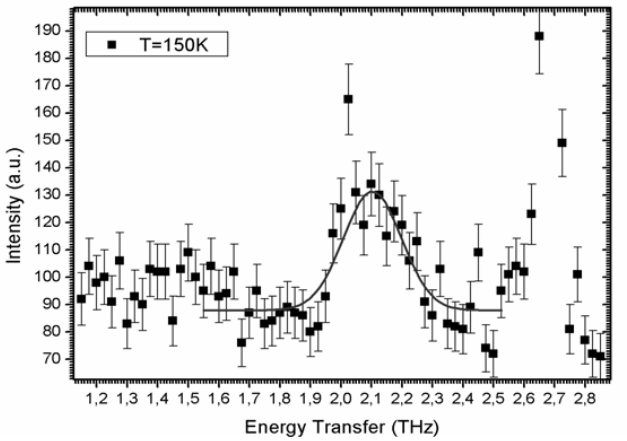


Fig. 2 Zoom of the inelastic peak for nano Tb at T=150K

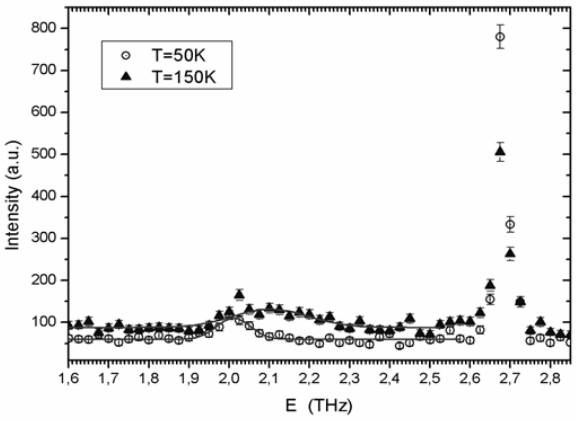


Fig. 3 Inelastic and spurion peaks for nano Tb at T=150K and T=50K

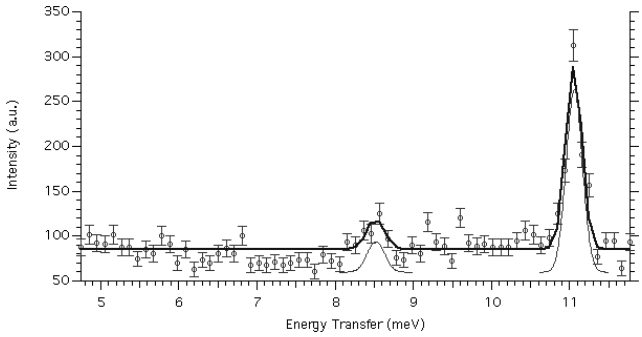


Fig. 4 Inelastic peak convoluted with the spurion at (8.8meV) and

Institut für Festkörperforschung
Forschungszentrum Jülich GmbH
D-52425 Jülich

Experimental Report
of Neutron Scattering Experiments
at the FRJ-2 Reactor

Proposal number:	UDS-05-004		
Experiment title:	**Diffuse scattering in magnetite, and its relationship with anharmonic phonon effects**		
Dates of experiment:	01.11.05 – 14.11.05	Date of report:	06.06.06
Experimental team: Names	Addresses		
Peter Mitchell Joe Hargreaves Geetha Balakrishnan	School of Physics & Astronomy, University of Manchester, M13 9PL, UK School of Physics & Astronomy, University of Manchester, M13 9PL, UK Department of Physics, University of Warwick, CV4 7AL, UK		
Local Contact:	Andreas Hoser		

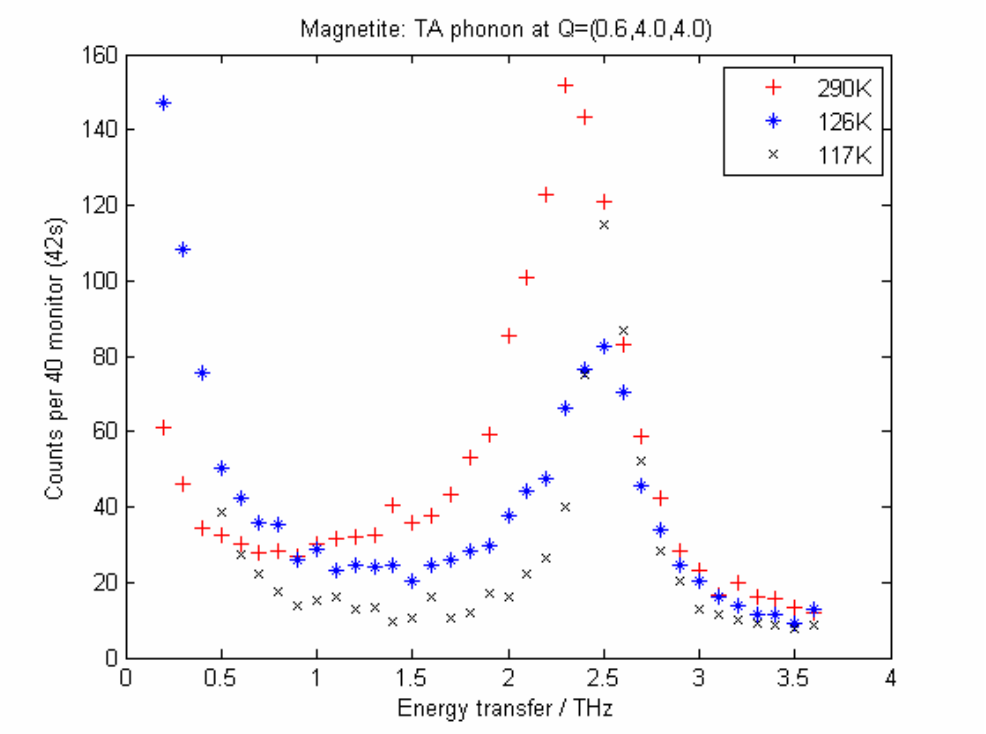
Experimental report text body

Magnetite is perhaps the magnetic material which has been used over the longest period in history. Lodestone, naturally occurring Fe_3O_4, is ferrimagnetic at room temperature, and when magnetised can be used in navigation. However, an understanding of the material in detail still seems elusive. A model, which seemed to explain both the magnetic and other properties, which involved Fe^{2+} and Fe^{3+} ions occupying various sites [1], is now not tenable in the light of a range of evidence [2].

In addition to the paramagnetic to ferrimagnetic transition at 848K, there is a first order structural transition at T_V, which is about 120K, the so-called Verwey transition. The most striking change at this point is that the electrical conductivity falls by a factor of 100 or so. It has been called a metal-insulator transition, but in reality it is a transition between two different semiconducting states. The resistivity decreases as the temperature increases in both phases. Structurally, magnetite is a cubic inverse spinel above T_V, and below T_V the structure is still not completely known, but it is known to be monoclinic [3]. The magnetism is not significantly affected by the transition.

We have grown several large artificial crystals by the floating zone method at Warwick. They show the Verwey transition at about 121K, which indicates both high (metallic) purity and good stoichiometry (i.e. a very low level of oxygen defects). The crystal we have used in this experiment is a single crystal of 3.7cm^3, which is several times larger than crystals used in earlier inelastic scattering studies [4,5,6].

In this experiment, we measured the transverse acoustic phonons at selected wavevectors in the [100], [110] and [111] directions at room temperature, and just above T_V. At room temperature, the phonons become very broad, with a large intensity between the "phonon frequency" and zero, as the zone boundary is approached in the [100] and [110] directions, while they remain good normal modes in the [111]. This is in contrast to the previous phonon measurements [7], where "the observed peak widths could in most cases be accounted for by instrumental widths". This broadening may signal the anharmonicity we seek. It remains down to just above T_V, while the quasi-elastic scattering grows at those wavevectors where the phonons also show anharmonic effects. Below T_V, the phonon becomes sharper again and the intensity between it and zero disappears (see figure).



It was not possible, in the time available for this experiment, to measure the diffuse quasi-elastic scattering as proposed. At all wavevectors where the phonon broadening was seen, there was also strong quasi-elastic diffuse scattering.

The observations of significant phonon broadening achieved in this experiment encouraged the performance of further experiments to characterise these effects in quantitative detail as a function of wavevector and temperature.

References

1 Verwey E J W, Haayman P W and Romeijn C W, J Chem Phys **15** 181, 1947
2 Garcia J and Subias G, J Phys: Condensed Matter **16** R145, 2004
3 Wright J P, Attfield J P and Radaelli P G, Phys Rev **B66** 214422, 2002
4 Fuji Y, Shirane G and Yamada Y, Phys Rev **B11** 2036, 1975
5 Shapiro S M, Iizumi M and Shirane G, Phys Rev **B14** 200, 1976
6 Yamada Y, Wakabayashi N and Nicklow R M, Phys Rev **B21** 4642, 1980
7 Samuelsen E J and Steinsvoll G, Phys Stat Solidi **B61** 615, 1974

Institut für Festkörperforschung
Forschungszentrum Jülich GmbH
D-52425 Jülich

Experimental Report
of Neutron Scattering Experiments
at the FRJ-2 Reactor

Proposal number:	UDS-05-005		
Experiment title:	Magnetic Excitations in nanocrystalline Tb		
Dates of experiment:	08.03. – 18.03.2005	Date of report:	21.06.2006
Experimental team: Names	Addresses		
O. Moze, C. Vecchini Andreas Hoser	Physics Dept, Modena University, Italy Institut für Festkörperforschung, Forschungszentrum Juelich, Germany		
Local Contact:	Andreas Hoser		

Experimental report text body

Recent measurements by SANS (Weissműller et al, Phys. Rev. B 69, 054402 [2004]) were performed for the first time on the nanocrystalline hard magnet Tb. Two important parameters used in modelling the magnetic behaviour in this material, and indeed in understanding the nature of the large magnetic anisotropy in nanocrystalline Tb are the spin-wave stiffness constant D and the spin-wave gap Δ, which reflects dipolar and anisotropy contributions.We have recently re-attempted to measure the spin wave excitations in a 1 gm sample of nanocrystalline Tb with a grain size of 13 nm. Inelastic scans were performed at different temperatures in the ferromagnetic region (T_c=226K). Previously performed scans at PSI (Switzerland) on the Triple-Axis Spectrometer TASP, gave evidence of the probable presence of an inelastic peak at about 1.8 THz at 200K. The measurements were performed in the fixed initial energy mode (K_i=2.67 A^{-1}) with energy transfer up to 2.85 THz. Initial diffraction scans were done in order to center scans around the (101) reflection, which is the strongest magnetic and nuclear Bragg peak (Fig. 1). This position was chosen because of the high magnetic scattering intensity and much lower background and small angle scattering than in the forward direction. Due to the low intensity of the inelastic magnetic signal, the measurement time was necessarily very long. Measurements at 200K did not show any intrinsic inelastic peak but showed the presence of 2 Bragg spurion peaks due to analyzer and monocromator reflections at 2 THz and 2.7 Thz. The first one appears to be very broad for a Bragg spurion. Measurements at 150K showed the presence of the 2 spurions, always at 2 THz and 2.7 Thz and of one inelastic peak at 2.1 THz. This peak has an intensity of about 90 counts on top of the background and a width of 0.2 Thz as shown in Fig. 2. Further measurements at 50K evidenced the absence of that peak, that, in our opinion, has moved outside the energy range investigated (Fig. 3) and confirmed the position of the first spurion at 2 THz. In light of the scans at 50K and 150K, we think that the intrinsic inelastic peak at 200K could have moved inside the spurion, broadening it and slightly moving from its original position due to the convolution of the two (Fig. 4).

Further measurements with different temperatures choices and different incoming neutron energies are very desiderable. This will allow tracking of the inelastic signal over a wider temperature range. These measurements are also ***pioneering*** in the sense that they demonstrate what can be done with ***neutrons on rather small nanocrystalline samples***.

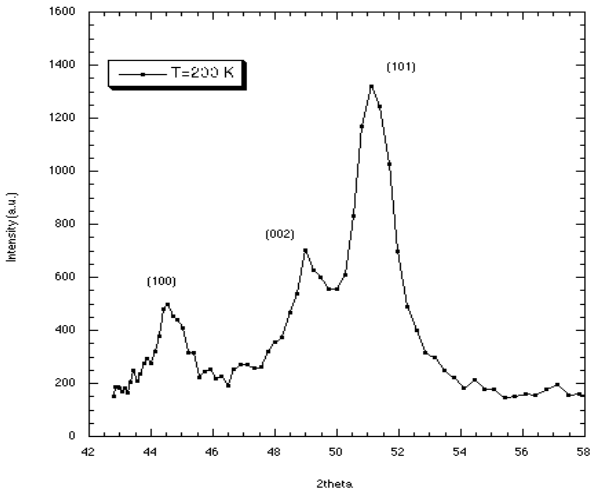


Fig. 1 Elastic scan for nano Tb at T=200K

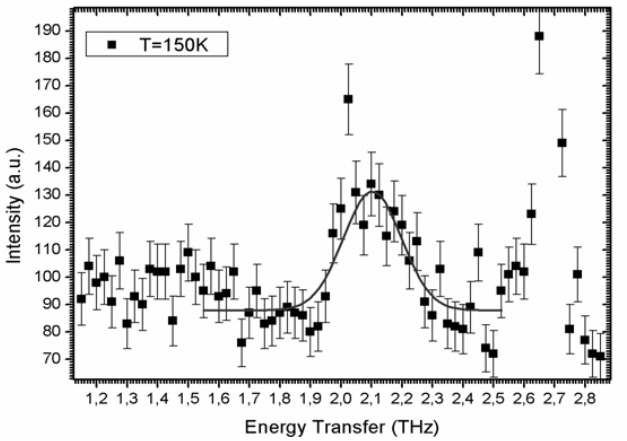


Fig. 2 Zoom of the inelastic peak for nano Tb at T=150K

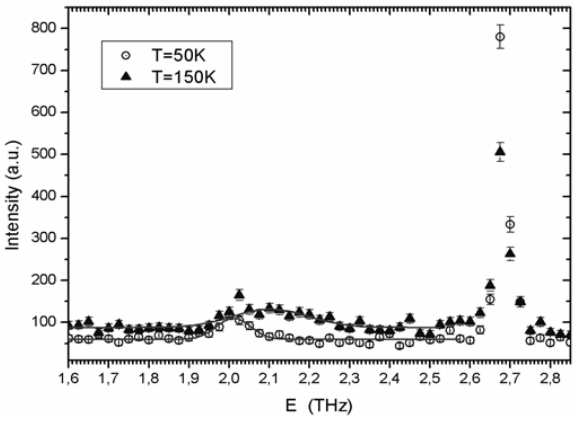


Fig. 3 Inelastic and spurion peaks for nano Tb at T=150K and T=50K

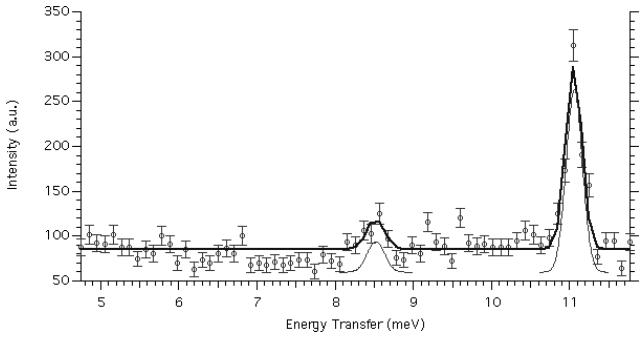


Fig. 4 Inelastic peak convoluted with the spurion at (8.8meV) and

Institut für Festkörperforschung
Forschungszentrum Jülich GmbH
D-52425 Jülich

Experimental Report
of Neutron Scattering Experiments
at the FRJ-2 Reactor

Proposal number:	UDS-05-006		
Experiment title:	Crystal field effects in $ErAl_2$		
Dates of experiment:	30.08. – 04.09.2005 30.10. – 02.11.2005	Date of report:	02.06.2006
Experimental team: Names	Addresses		
U. Köbler A. Hoser	Institut für Festkörperforschung, Forschungszentrum Jülich Institut für Kristallographie , RWTH-Aachen		
Local Contact:	Dr. A. Hoser		

Experimental report text body

$ErAl_2$ is a metallic ferromagnet with cubic $MgCu_2$ structure and a Curie temperature of T_C=13.6 K [1]. The effective Bohr magneton number evaluated from the paramagnetic Curie-Weiss susceptibility is $\mu_{eff}=9.4\mu_B$. This value is consistent with the theoretical value for the free Er^{3+} ion of $\mu_{eff}=9.58\mu_B$.
The observed saturation magnetic moment of $7.4\mu_B$ is considerably smaller than the theoretical free ion value. For the Er^{3+} ion with configuration $^4I_{15/2}$ and g=6/5 a theoretical saturation moment of $9\mu_B$ results. The reduced moment is indicative of crystal field effects.

As we have shown recently [2,3] the dynamics of the magnetic order parameter shows universality at the stable fixed point T=0. This means that saturation of the magnetic order parameter for $T\rightarrow 0$ is according to a single power function of absolute temperature. The universal exponent ε depends on the number of relevant states N=2J+1 per magnetic particle. In isotropic (cubic) magnets ε=9/2 for an odd number of states (J=integer) and ε=2 for an even number of states (J=half-integer). This empirical systematic allows one to determine how many states of the free ion are relevant in the ordered state for $T\rightarrow 0$.
Universality is a consequence of the continuous symmetry of the dynamics in the long range ordered state. Note that the order parameter is located at the Brillouin zone centre. On the other hand, the crystal electric field is a phenomenon on the length scale of the inter-atomic distance. Crystal field effects, therefore, are located at the Brillouin zone boundary. As a consequence, crystal field effects are, in a first approximation, not relevant for the dynamics of the order parameter. This is the case if the crystal field splitting is much smaller than the exchange interaction. A non relevant crystal field is noticed by a saturation moment that conforms to the free ion value. This is realized in the ferromagnetic heavy Rare Earth (RE) elements [3].
In the $REAl_2$ alloys the crystal field is relevant and the saturation moment is reduced with respect to the free ion

value. In contrast to the crystal field splitting of the isolated single ion, reduction of the saturation moment in the ordered state is not a continuous process as a function of decreasing temperature but occurs as discrete crossover events. At a crossover the number of relevant states is reduced by one, i.e. the effective spin is reduced by $\Delta J=1/2$. In other words, at a crossover the universality class changes from $\varepsilon=9/2$ to $\varepsilon=2$ or vice versa.

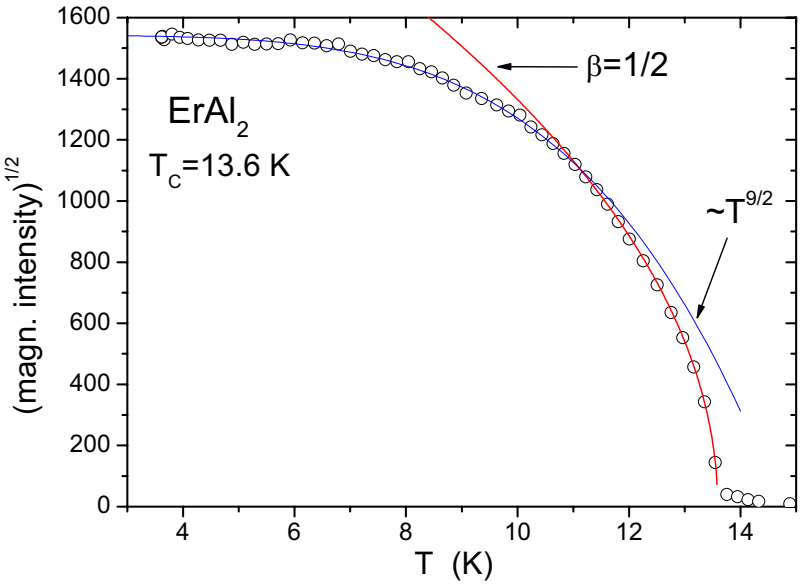
We have performed neutron scattering measurements on an $ErAl_2$ single crystal in zero magnetic field. Note that magnetic saturation, i.e. removal of the magnetic domains can change the universality class. The macroscopic magnetization therefore can give a different result than the zero-field measurement.

Fig. 1 shows the result for the magnetization as a function of temperature. These data are the square root of the (200) diffraction intensity after subtraction of the nuclear intensity. It can be seen that the exponent for $T\rightarrow 0$ is $\varepsilon=9/2$ but the critical exponent β for $T\rightarrow T_c$ is $\beta=1/2$. Note that the two exponents give a fairly complete description of the temperature dependence of the spontaneous magnetization [4].

The exponent $\varepsilon=9/2$ indicates that the spin is integer. Practically the spin can be only J=6 instead of J=15/2. The number of states therefore is reduced from N=16 to N=13, i.e. by $\Delta N=3$. With J=6 and g=6/5 a saturation moment of $7.2\mu_B$ is calculated in good agreement with the observed moment of $7.4\mu_B$.

The fitted mean field exponent $\beta=1/2$ is indicative of a half-integer spin. It is reasonable to assume that the spin has the full value of J=15/2 in the critical range. This assumption is consistent with the large pre-factor of the $(T_c-T)^{1/2}$ power function. Normally the critical power function has an extrapolated value for $T\rightarrow 0$ that is larger by a factor of ~1.3 compared to the saturation value of the order parameter. The fitted critical power function is larger by a factor of ~1.65 for $T\rightarrow 0$ compared to the order parameter. This is consistent with J=15/2.

We consider the result obtained on $ErAl_2$ as consistent with our proposition that in the ordered state the effect of a relevant crystal field is to reduce the number of states, N. A strong crystal field reduces the number of states by more than $\Delta N=1$. On the other hand, a non relevant crystal field leaves the number of states unchanged. Each reduction of the number of states gives rise to a crossover phenomenon, i.e. to a change of the universal exponent ε from $\varepsilon=9/2$ to $\varepsilon=2$ or vice versa. In other words, the crystal electric field has to be treated in a fundamentally different way under the continuous symmetry of the long range ordered state compared to the isolated and non interacting ion.



[1] K.H.J. Buschow, Rep. Prog. Phys. 42 (1979) 1373.
[2] U. Köbler, A. Hoser, Physica B 362 (2005) 295.
[3] U. Köbler, A. Hoser, J. Magn. Magn. Mater. 299 (2006) 145.
[4] U. Köbler, A. Hoser, D. Hupfeld, Physica B 328 (2003) 276.

Institut für Festkörperforschung
Forschungszentrum Jülich GmbH
D-52425 Jülich

Experimental Report
of Neutron Scattering Experiments
at the FRJ-2 Reactor

Proposal number:	UDS-05-007		
Experiment title:	Searching for phonon-like magnetic excitations in $ErAl_2$		
Dates of experiment:	12.01.-14.02.2006 16.02.-26.02.2006	Date of report:	06.06.2006
Experimental team: Names	 Addresses		
A. Hoser U. Köbler	Institut für Kristallographie, RWTH- Aachen Institut für Festkörperforschung, Forschungszentrum Jülich		
Local Contact:	A. Hoser		

Experimental report text body

In recent analyses of the specific heat of magnetic and non magnetic materials we have observed that the universal exponents for $T\rightarrow 0$ are commonly identical for magnetic and non magnetic materials [1]. As is well known, T=0 is a stable fixed point [2]. At those points universality is observed. This means that spontaneous magnetization, specific heat etc. follow exact power functions of absolute temperature over a large temperature range [3]. The standard behaviour for the lattice heat capacity is given by the famous T^3 power function according to the Debye model. Universality is clearly revealed by the fact that the T^3 dependence is confirmed for many solids with different chemical compositions and lattice symmetries. However, two more universality classes represented by T^2 and T^4 functions have also been identified empirically [1].

In order to demonstrate that the Debye T^3 function holds also in magnetic materials we show in Fig.1 heat capacity data for ferromagnetic cobalt. It can be seen, that the T^3 function of the lattice heat capacity holds exactly over a large temperature range. Beyond the T^3 function crossover to a linear temperature dependence follows. This crossover is observed in all magnetic and non magnetic solids [1].
Speaking in terms of renormalization group theory we have to conclude that the magnetic heat capacity is not relevant. This means that the observed universal exponent (ε=3) is defined by the lattice and that the magnetic heat capacity must be contained in the pre-factor of the T^3 function. Note that the zero field spontaneous magnetization of cobalt follows $T^{3/2}$ function for $T\rightarrow 0$ [4]. We should note that the specific heat of ferromagnetic GdMg also shows T^3 function for $T\rightarrow 0$ but the spontaneous magnetization saturates according to T^2 function.

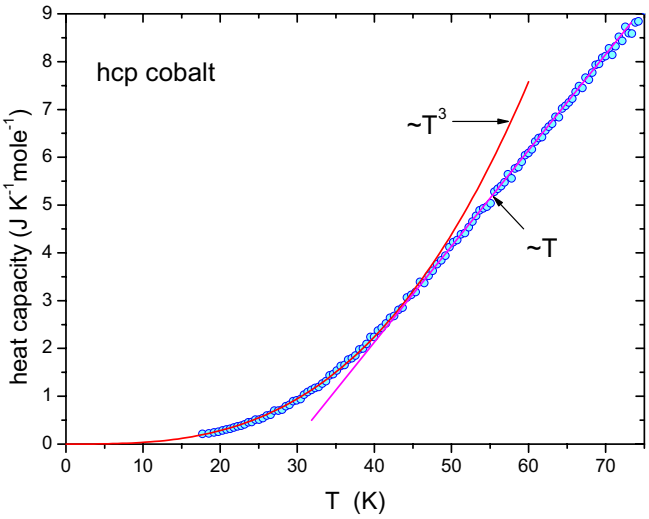


Fig. 1

From the identical exponents for the heat capacity of magnetic and non magnetic solids we have to conclude that phonons are more important than magnons. As a conclusion, it can be expected that the phonon spectra are somehow different above and below the magnetic ordering temperature. Ferromagnetic $ErAl_2$ with T_C=13.6 K is a good candidate to test this. We have measured transversal acoustic phonon modes at 3.4K and at 19K, i.e. below and above Curie temperature. We observe no change in the dispersion curve except reduction of phonon intensities above T_c according to thermal depopulation of ground state.

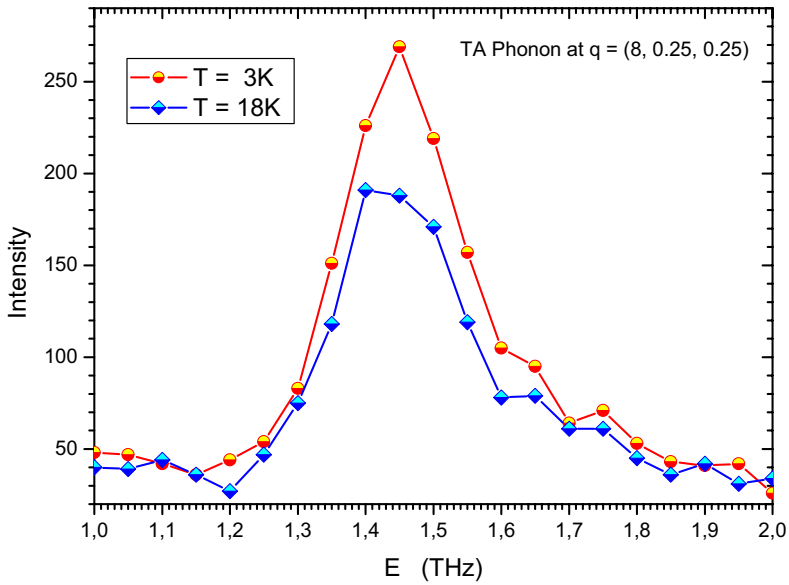


Fig. 2

[1] U. Köbler, M. Kawakami, W. Schnelle, Physica B 367 (2005) 255.
[2] K.G. Wilson, J. Kogut, Phys. Reports 12C (1974) 75.
[3] U. Köbler, A. Hoser, Physica B 362 (2005) 295.
[4] U. Köbler, A. Hoser, J.-U. Hoffmann, C. Thomas, Solid State Commun. 137 (2006) 301.

Institut für Festkörperforschung
Forschungszentrum Jülich GmbH
D-52425 Jülich

Experimental Report
of Neutron Scattering Experiments
at the FRJ-2 Reactor

Proposal number:	UDS-05-008		
Experiment title:	Diffuse scattering in magnetite, and its relationship with anharmonic phonon effects		
Dates of experiment:	05.12.2005 – 19.12.2005	Date of report:	06.06.2006
Experimental team: Names	Addresses		
Peter Mitchell Joe Hargreaves Geetha Balakrishnan	School of Physics & Astronomy, University of Manchester, M13 9PL, UK School of Physics & Astronomy, University of Manchester, M13 9PL, UK Department of Physics, University of Warwick, CV4 7AL, UK		
Local Contact:	Andreas Hoser		

Experimental report text body

Magnetite is perhaps the magnetic material which has been used over the longest period in history. Lodestone, naturally occurring Fe_3O_4, is ferrimagnetic at room temperature, and when magnetised can be used in navigation. However, an understanding of the material in detail still seems elusive. A model, which seemed to explain both the magnetic and other properties, which involved Fe^{2+} and Fe^{3+} ions occupying various sites [1], is now not tenable in the light of a range of evidence [2].

In addition to the paramagnetic to ferrimagnetic transition at 848K, there is a first order structural transition at T_V, which is about 120K, the so-called Verwey transition. The most striking change at this point is that the electrical conductivity falls by a factor of 100 or so. It has been called a metal-insulator transition, but in reality it is a transition between two different semiconducting states. The resistivity decreases as the temperature increases in both phases. Structurally, magnetite is a cubic inverse spinel above T_V, and below T_V the structure is still not completely known, but it is known to be monoclinic [3]. The magnetism is not significantly affected by the transition.

We have grown several large artificial crystals by the floating zone method at Warwick. They show the Verwey transition at about 121K, which indicates both high (metallic) purity and good stoichiometry (i.e. a very low level of oxygen defects). The crystal we have used in this experiment is a single crystal of $3.7cm^3$, which is several times larger than crystals used in earlier inelastic scattering studies [4,5,6]. This experiment was a continuation of experiment UDS-05-004, in which we found significant broadening of the transverse acoustic phonons in both [001] and [110] directions.

We planned to complete this investigation of the various phonon modes near T_V in an attempt to link the quasi-elastic diffuse scattering to specific phonon anharmonic effects. We measured the phonon broadening effects as a function of wavevector (see figures 1 and 2), at room temperature and just above and just below T_V .

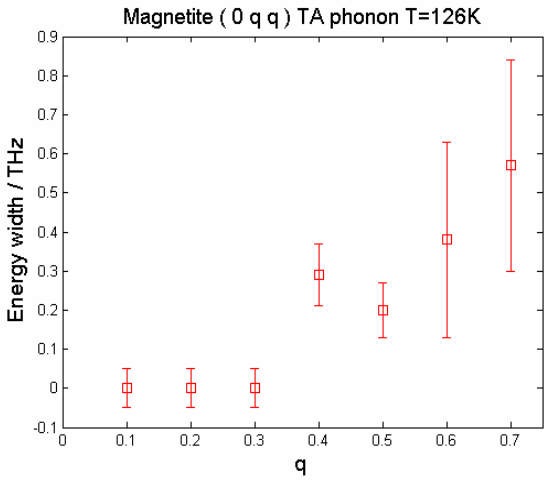


Fig 1: phonon width at 126K in [011]

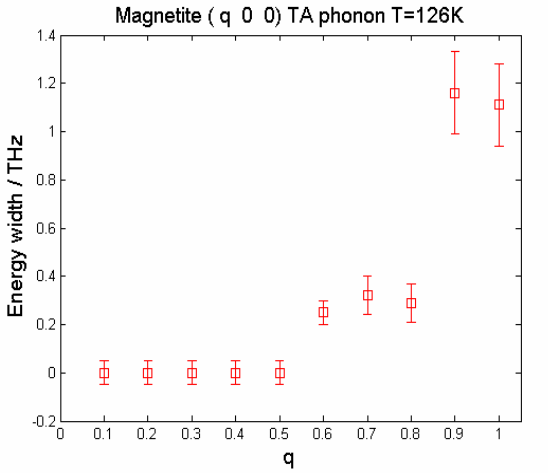


Fig 2 phonon width at 126K in [100]

We also made measurements of the quasi-elastic diffuse scattering in the cubic phase just above, and just below, T_V, in several zones in order to establish the dependence on the magnitude of the wavevector transfer. These measurements are complicated by the appearance of many new Bragg peaks in the low temperature phase. Analysis of the quasi-elastic diffuse scattering is continuing. One early conclusion we arrived at by examining a limited subset of the data, namely that the diffuse quasi-elastic scattering correlates exactly with the wavevectors where significant phonon broadening is observed, is not upheld by more detailed examination of all of the data.

These observations of the phonon linewidths are consistent with the following model for the Verwey transiton. The state above the transition may be considered as a classic semiconductor with a certain band gap (around 200meV estimated from photoemission [7], or 110meV from the gradient of the conductivity-temperature curves [8]). Below it might also be a semiconductor with a wider band gap (around 300meV from photoemission [7], or 270meV from the conductivity-temperature curves [8]). In this case, the structural transition is driven by the gain in electronic energy as the band-gap widens. This model would imply anharmonic vibrational effects which would grow as the temperature is lowered towards the transition, because of the electronic energy gain from the lattice distortion. The reduction in energy which is eventually realised at the transition would gradually favour small distortions from the cubic structure equilibrium atom positions, and so would generate an anharmonic potential. This is observable as the broadening of the phonon modes which has been observed.

References

1 Verwey E J W, Haayman P W and Romeijn C W, J Chem Phys **15** 181, 1947
2 Garcia J and Subias G, J Phys: Condensed Matter **16** R145, 2004
3 Wright J P, Attfield J P and Radaelli P G, Phys Rev **B66** 214422, 2002
4 Fuji Y, Shirane G and Yamada Y, Phys Rev **B11** 2036, 1975
5 Shapiro S M, Iizumi M and Shirane G, Phys Rev **B14** 200, 1976
6 Yamada Y, Wakabayashi N and Nicklow R M, Phys Rev **B21** 4642, 1980
7 Park J-H, Tjeng L H, Allen J W, Metcalf P and Chen C T, Phys Rev **B55** 12813, 1997
8 *Data taken from* Miles P A, Westphal W B and von Hippel A, Rev Mod Phys **29** 279, 1957

Institut für Festkörperforschung
Forschungszentrum Jülich GmbH
D-52425 Jülich

Experimental Report
of Neutron Scattering Experiments
at the FRJ-2 Reactor

Proposal number:	UDS-06-001		
Experiment title:	Influence of hydrogen uptake on spin-density wave magnetism in Cr/V multilayers		
Dates of experiment:	07.04. – 02.05.2006	Date of report:	1 June 2006
Experimental team: Names	Addresses		
Gregor Nowak Arndt Remhof	Institut für Festkörperphysik / Experimentalphysik Ruhr-Universität Bochum 44780 Bochum Germany		
Local Contact:	Dr. Andreas Hoser		

Experimental report text body

The spin-density wave (SDW) state in thin Cr films is known to be under influence of contaminations, dimensionality (film thickness) and proximity effects from neighboring layers [1]. As the SDW is completely suppressed in $Cr_{1-x}V_x$ alloys for x>0.04, we investigated the dependence on the SDW state in thick Cr layers sandwiched between thin V films [2 ,3] and in epitaxial Cr/V multilayers [4]. An unpredicted strong and long-range effect on the polarization, period, and the Néel temperature of the SDW in rather thick Cr films was found. The magnetic phase diagram of the multilayers turned out to be rather complex. For Cr layers thinner than 120 A the samples behave paramagnetic. At this thickness a commensurate SDW originates and as Cr thickness increases further a fraction of incommensurate SDW appears and expands. Finally the SDW becomes completely incommensurate. The Néel temperature of the incommensurate SDW scales with Cr thickness as well. V is known to dissolve considerable amounts of hydrogen, resulting in lattice expansion and in a modified electronic band structure. This ability has been employed to tailor the magnetic properties of H-loaded Fe/V [5,6] heterostructures.

In the present experiment we investigated the influence of H loading in a [Cr(500ML)/V(14ML)]∗4 superlattice. The epitaxial sample was prepared by conventional dc sputtering in ultra high vacuum (UHV) onto polished MgO (001) substrate (20∗20∗0.5mm^3). Details of the sample preparation and the SDW state of the H-free sample may be found in [4]. For the H-loading experiments, the cryostat was connected to a gas loading system, consisting of two capacitance manoscopes to enable gas-independent pressure measurements and a vacuum leak valve to allow precise adjustment of the H pressure. As *in-situ* experiments were not possible, the different loading and unloading kinetics of the sample were exploited. First, the sample was exposed to a hydrogen pressure of 100 mbar up to 1000 mbar. At this pressures H saturation of the sample is reached quite quickly. After a 30 minutes the sample is cooled in the H atmosphere below 230K. At this temperature the unloading is suppressed and the H motion within the sample is frozen. Subsequently the cryostat is evacuated

down to the 10^{-7} mbar regime before the begin of the experiment. From a previous experiment we know that the sample is in the incommensurate SDW state at low temperatures. At 220K the commensurate phase occurs. Both phases coexist than until 250K. Above 250K only the commensurate phase is seen. Figure 1 shows a temperature series of the 100 mbar hydrogen loaded sample. First we notice that even at the lowest measured temperature (20K) we found after H-loading up to 1000mbar enhance intensity around the position of the commensurate SDW.

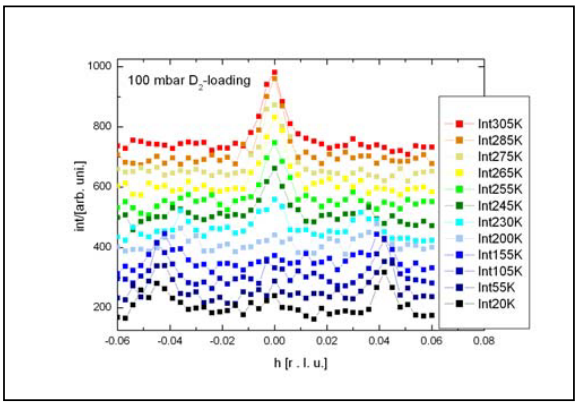


Fig.1

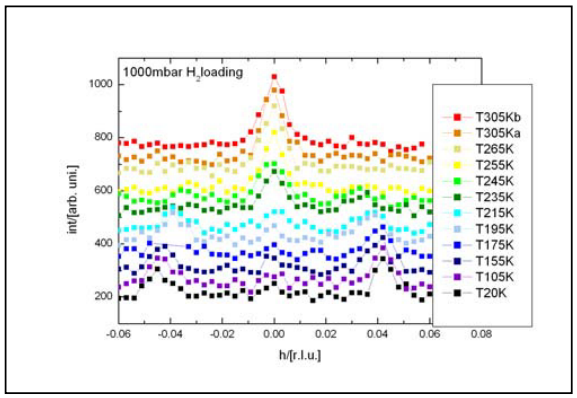


Fig.2

Neutron scattering scans taken in the L direction around the Cr(010) reflection in the H-loaded state (p_{H2}=100mbar (left) and p_{H2}=1000mbar (right)) to explore the SDW polarization. Scans recorded at different temperatures are depicted with an offset in the vertical direction for clarity. The incommensurate phase can be identified by the two satellite reflections at L=±0.04, while the reflection at L=0 is indicative for the commensurate phase.

The temperature at which the incommensurate SDW state is completely suppressed, indicated by the depression of the Bragg-reflection satellites, is 10-20 K lower for the hydrogen loaded state as for the virgin state. Additionally, small volume fractions of the hydrogen loaded sample are in the commensurate phase even at low temperatures (20K). This has not been observed for the pristine sample. Obviously the presence of hydrogen in the V layers favors the commensurate SDW state within the adjacent Cr layers. The differences observed for the 100mbar loading and for the 1000 mbar loading are rather small, suggesting that saturation is already achieved at 100 mbar.

Acknowledgements

We would like to thank B. Hjörvarsson and A. Liebig for the preparation of the sample.
This project was founded by the Sonderforschungsbereich 491, "Magnetic Heterostructures – Spin Structures and Spin Transport" and by the EU INTAS project ref. nr. 03-51-4778.

References

[1] P. Bödeker, A. Schreyer, H. Zabel, Phys. Rev. B **59**, 9408 (1999).
[2] E. Kravtsov, A. Nefedov, F. Radu, A. Remhof, H. Zabel, R. Brucas, B. Hjörvarsson, A. Hoser, S. B. Wilkins, Phys. Rev. B **70** 054425 (2004)
[3] E. Kravtsov, R. Brucas, B. Hjörvarsson, A. Hoser, G. McIntyre, A. Nefedov, F. Radu, A. Remhof, H. Zabel, J. Mag. Magnet. Mater. **286** 425 (2005).
[4] E. Kravtsov, A. Nefedov, F. Radu, A. Remhof, H. Zabel, A. Liebig, B. Hjörvarsson, A. Hoser, G. J. McIntyre, in preparation.
[5] B. Hjörvarsson, J. A. Dura, P. Isberg, T. Watanabe, T. J. Udovic, G. Andersson, C. F. Majkrzak, Phys. Rev. Lett. **79**, 901 (1997)
[6] V. Leiner, K. Westerholt, A. M. Blixt, H. Zabel, B. Hjörvarsson, Phys. Rev. Lett. **91**, 037202 (2003).

High Resolution Backscattering Spectrometer (BSS)



Instrument Parameters

Beam tube:	NLI, cold neutrons, straight guide, 10 cm (height) × 7 cm (width)
Beam size at sample:	3.5 cm × 3.5 cm
Neutron flux at sample:	10^4 n/cm^{2}s
Background:	≈ 8 counts/h
Monochromators:	Si(111), $Si_{0.9}Ge_{0.1}$(111)
Analyser:	Si(111)
Detectors:	nine ^{3}He counters, one ^{3}He monitor
Incident energy:	2.08 meV Si(111), 2.07 meV $Si_{0.9}Ge_{0.1}$ (111)
Incident wavelength:	6.271 Å Si(111), 6.30 Å $Si_{0.9}Ge_{0.1}$ (111)
Energy transfer range:	–15 ... 15 µeV Si(111), –29 ... 1 µeV $Si_{0.9}Ge_{0.1}$ (111)
Energy resolution (FWHM):	1.2 ... 2.4 µeV Si(111), ≈ 2 µeV $Si_{0.9}Ge_{0.1}$ (111)
Elastic Q-range:	0.2 ... 1.9 Å^{-1}
Q-resolution:	0.05 Å^{-1} ... 0.25 Å^{-1}
Sample environment	orange cryostat 2 ... 300 K; closed cycle cryostat 12 ... 350 K; cryofurnace 80 ... 750 K; furnace 300 ... 1900 K

Instrument Responsible:

Dr. Andreas Wischnewski Tel. +49-(0)-2461-61-4714 Email: a.wischnewski@fz-juelich.de
Dr. Michaela Zamponi Tel. +49-(0)-2461-61-4775 Email: m.zamponi@fz-juelich.de

Institut für Festkörperforschung
Forschungszentrum Jülich GmbH
D-52425 Jülich

Experimental Report of Neutron Scattering Experiments at the FRJ-2 Reactor

Proposal number:	BSS-04-016, BSS-05-020		
Experiment title:	Rotational dynamics of methyl groups in the chloranilic acid plus tetramethylpyrazine complex: the influence of deuteration of the H-bond		
Dates of experiment:	02.09.2005, 1 day	Date of report:	25.02.2006
Experimental team: Names	Addresses		
A. Pawlukojc M. Prager	Institute of Nuclear Chemistry and Technology, Warsaw, Poland Forschungszentrum Jülich, Institut für Festkörperforschung		
Local Contact:	H. Grimm		

Experimental report text body

The charge transfer/hydrogen bond system chloranilic acid (CLA) plus tetramethylpyrazine (TMP) was successfully studied in a previous experiment [1]. The present work intends to investigate the effect of deuteration of the hydrogen bond linking the two molecular constituents. Due to the central role of such hydrogen bonds for the properties of charge transfer materials we expect characteristic changes from the interplay of lattice contraction, molecular reorientation and charge redistribution.

While the fully protonated material was investigated with the SiGe offset monochromator of the instrument in the energy range $-33<\Delta E[\mu eV]<+3$ at an energy resolution $\delta E=1.9\mu eV$ [1] the deuterated compound is investigated at exactly the same configuration of the instrument (fig. 2) and with improved energy resolution $\delta E=1.1\mu eV$ in a symmetric energy range $-18<\Delta E[\mu eV]<+18$ using the Si[111] monochromator. Such spectra contain only the inner tunnelling lines Fig. 1). Fig. 2 shows that the band at 29μeV is almost unaffected from deuteration while the band at 19μeV is clearly shifted to lower energies, cf ref. 2. The shift of the 29μeV band follows an Arrhenius dependency with activation energy of about 8.6meV which is very similar to that of the protonated material. The Fig.1 shows a comparison of the inner tunnelling lines of the protonated (xxx) and deuterated (ooo) material. Instead of one strong tunneling band at 3.3μeV in TMP:h-CLA we observe a doublet with one transition at slightly higher, the other at clearly lower energy. A very rough estimate on the corresponding potential barriers based on a pure $\cos(3\phi)$ potential leads to changes of -1.5% and +6.8%, respectively.

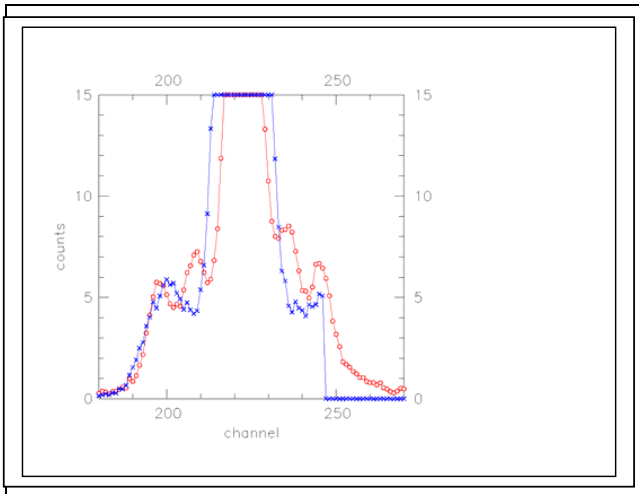


Fig. 1 Tunnel spectra of TMP:h-CLA (xxx) and TMP:d-CLA. for TMP:h-CLA the accessible energy range ends at -3μeV.

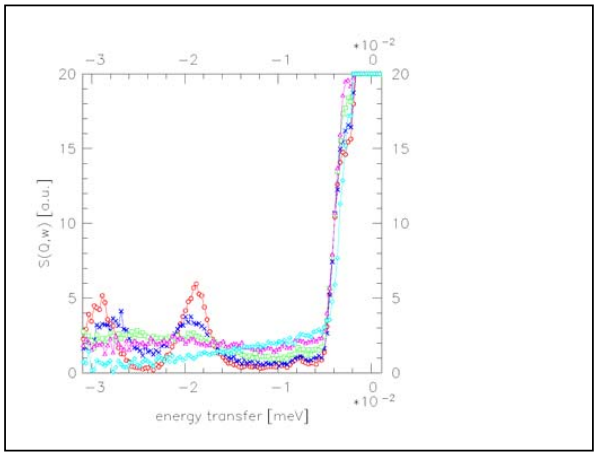


Fig. 2 Temperature dependence of the high energy tunnelling Bands inTMP:CLA-d2. T=4.5K (red) to 31K(cyan).

The comparison with the pure donor compound TMP has shown [1] that the methyl rotational potential is significantly weaker in the TMP-CLA complex. This means that intermolecular interaction strongly contributes to the rotational potential. The dominance of steric effects is supported by an opposite change of the hindering barrier observed in 2,6-DMP-CLA [2]. Deuteration of the hydrogen bond on the other hand is not expected to change the geometry of the environment significantly. Therefore the observed change is not unlikely to be due to effects of charge redistribution.

A comprehensive analysis of all spectra is under way. As in earlier cases it shall be based on a full quantum mechanical treatment of the lattice dynamics in three dimensions [3].

[1] M Prager, A Pawlukojc, L Sobczyk, E Grech, H Grimm, J. Phys.: Condens. Matter 17,5725(2005)
[2] Experimental report FRJ2 2005, BSS-05-028
[3] M.R. Johnson, M. Prager, H. Grimm, M.A. Neumann, .J. Kearley, C.C. Wilson, Chem. Phys. 244,49(1999)

Institut für Festkörperforschung
Forschungszentrum Jülich GmbH
D-52425 Jülich

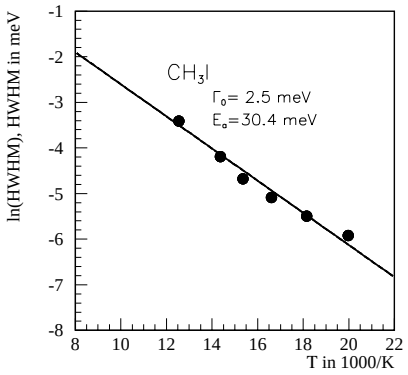
Experimental Report of Neutron Scattering Experiments at the FRJ-2 Reactor

Proposal number:	BSS-04-017		
Experiment title:	Quasi-elastic neutron scattering of methyl iodide		
Dates of experiment:	09. - 15.05.2005	Date of report:	03.03.2006
Experimental team: Names:	Addresses:		
Oliver Kirstein Michael Prager Hans Grimm	Bragg Institute, ANSTO, Menai, NSW 2234, Australia Institut für Festkörperforschung, FZJ, D-52428 Jülich, Germany Institut für Festkörperforschung, FZJ, D-52428 Jülich, Germany		
Local contact:	Hans Grimm		

Usually, the dynamics of the majority of rotating groups in molecular crystals can be described by a mean-field model known as the Single Particle Model (SPM) [1]. An analysis of experimental results which goes beyond a phenomenological use of the SPM must be able to explain the rotational potential, which determines the dynamics of the rotating group, based on the crystal structure and the fundamental interatomic and intermolecular interactions. There are different ways of modeling the dynamics of molecules by using e.g. ab-initio, DFT, force-field and quantum chemistry or transferable pair-potential calculations. The latter method was used to describe the lattice and rotational dynamics of the methyl halides by using pair potentials based on Universal Force Fields (UFF) [2]. Values that characterize the potential, which determines the dynamics of the rotating group such as the tunneling frequency and transition to the first librational state were calculated and compared to the earlier experimental results already mentioned [3]. In order to complete the experiments done so far quasi-elastic neutron scattering experiment on methyl iodide was performed in order to obtain values for the activation energies. The results will be used for comparison with calculations and to refine or determine potential parameters. The sample is available from commercial suppliers such as Aldrich with a chemical purity $\geq$99.55% and was used in the experiments without any further purification. The scattering probability of the sample was approximately 25%. The experimental data obtained using the backscattering spectrometer BSJ in its standard configuration (i.e. Si(111) monochromator, incident energy 2.08 meV, energy transfer $\pm$ 17 μeV) were transformed into $S(Q,\omega)$ using standard programs in order to derive the relevant physical parameters in this case the width of the quasi-elastic Lorentzian contribution to the spectrum.

The evaluation involved the following steps

- Subtraction of the background
- Determination of the resolution function
- Convolution of the theoretical spectrum with the resolution function
- Fit of the convoluted spectra to the measured data



The temperature dependent linewidth of the Lorentzian is shown in the figure above in which the logarithm of the HWHM is plotted versus 1000/T (HWHM in meV, T im K). By applying a least squares fit to the data we obtain an attempt frequency of $\Gamma_0 = 2.5(\pm 0.8)$ meV. This value is in agreement with attempt frequencies of other compounds containing CH_3 groups. The activation energy, which is the difference between the height of the rotational potential and the ground state is $E_a = 30.4(\pm 2.3)$ meV. Taking the previously measured tunneling and the librational transitions of 2.44 μeV and 14.57 meV, respectively, we obtain for the three- and sixfold terms of the Fourier-expansion of the rotational potential the following combination (V_3, V_6)=(41.4 meV, 1.6 meV). This combination allows to calculate an activation energy of $E_a = 33.5$ meV. There is good agreement between the theoretical SPM model and the experiment indicating that the dynamics can be well described by applying the SPM approach.

References

[1]W. Press, Single Particle Rotations in Molecular Crystals, Springer Tracts in Modern Physics (Springer, Berlin 1981), Vol. 81

[2]A. K. Rapp, C. J. Casewitt, K. S. Colwell, W. A. Goddard III, W. M. Skiff, J. Am. Chem. Soc., Vol 114, No. 25, 1992

[3]O. Kirstein, M. Prager, J. Chem. Phys., Vol. 120, No. 11, 5199 (2004)

Institut für Festkörperforschung
Forschungszentrum Jülich GmbH
D-52425 Jülich

Experimental Report
of Neutron Scattering Experiments
at the FRJ-2 Reactor

Proposal number:	BSS-04-019		
Experiment title:	Dynamic Miscibility Effects in a Blend of Polymers with Very Different Tg		
Dates of experiment:	17/01/2005-01/02/2005	Date of report: 08/02/2005	
Experimental team: Names	Addresses		
Caroline Genix Juan Colmenero Arantxa Arbe Dieter Richter	Donostia International Physics Center, Apdo. 1072, 20080 San Sebastian, SPAIN Dpto. de Física de Materiales, UPV/EHU, , “ , “ , “ Unidad de Física de Materiales, CSIC-UPV/EHU, “ , “ , “ IFF, FZJ, Jülich, Germany		
Local Contact:	Andreas Wischnewski		

Experimental report text body

The aim of this experiment was to investigate the effect of blending on the dynamical behaviour of a polymer. The system chosen was poly(ethylene oxide) / poly(methyl methacrylate) (PEO/PMMA), which has the advantage to show very different glass transition temperatures T_g for each of the pure components (PEO: T_g=213K; PMMA: T_g=400K). By backscattering we wanted to follow the scattering dominated by the incoherent contribution of the hydrogens of the protonated component in the blend, where the other component is deuterated, and compare these results with those obtained for the pure homopolymers.

The BSS measurements have been performed on the following samples: pure PEO (fully protonated) at 4, 300, 350, 375 and 400K, and two blends of PEO/PMMA (25%/75%), where one of the two components was protonated (h) and the other deuterated (d). For hPEO-dPMMA we investigated 4, 300, 325, 350, 375, 400, 425, 450 and 500K, and for dPEO-hPMMA 4, 350, 400 and 450K. This corresponds to the region well above the glass transition for PEO but close or below to that of PMMA.

The samples were placed in Aluminum flat containers at 45º with respect to the incident beam. The thicknesses were such that a transmission of ≈ 0.9 was calculated. With λ=6.27Å a Q-range of 0.16 … 1.87Å^{-1} was accessed and an energy window of ±17μeV was explored. Reasonable statistics was achieved with measuring times of about 18 hours. Vanadium and empty cell measurements were also carried out to correct the spectra.

For Q=0.56Å^{-1} Fig. 1 shows the spectra corresponding to PEO pure and in the blend at 350 and 400K. A clear slowing down in the dynamics of PEO is observed as effect of blending. A quantitative analysis of the spectra in terms of stretched exponential functions is currently being performed.

On the other hand, the dynamical behaviour of the PMMA component at temperatures close to the glass transition of the pure PMMA seems to be dominated by the rotation of its α-methyl group. This is shown in Fig. 2, where we have described the scattering curves by assuming that the main chain and ester methyl groups contributions are just elastic (that for the ester methyl group is modulated by the EISF, since its rotation is very fast at these temperatures [1]).

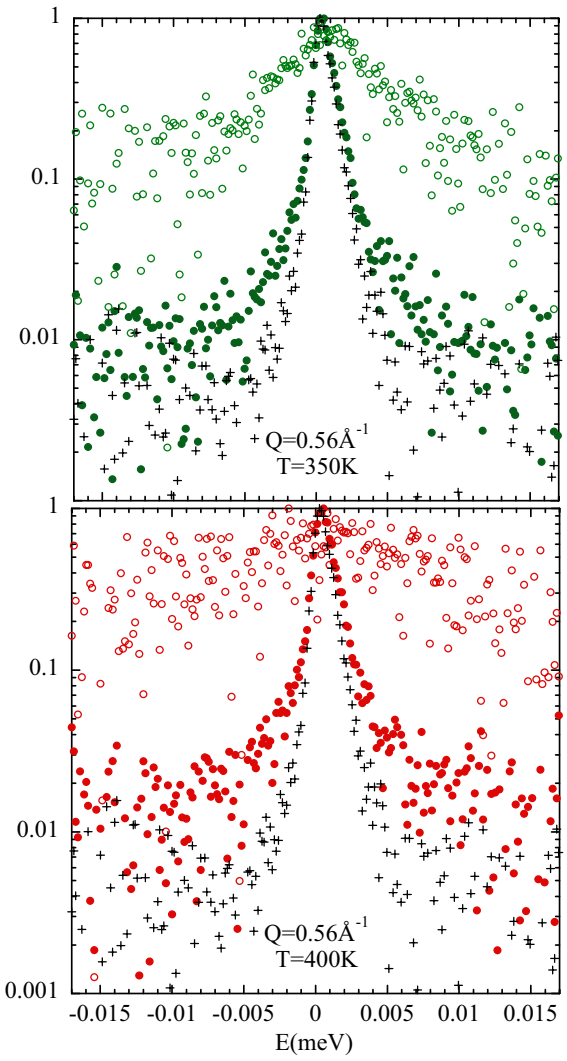


Fig. 1: Scattering function measured at 0.56 Å^{-1} for pure PEO (protonated) (empty symbols) and the blend containing 25% of protonated PEO in a deuterated PMMA matrix (full symbols): 350K (upper) and 400K (lower). The functions are normalized to their maximum intensities. The resolution function is displayed by the crosses.

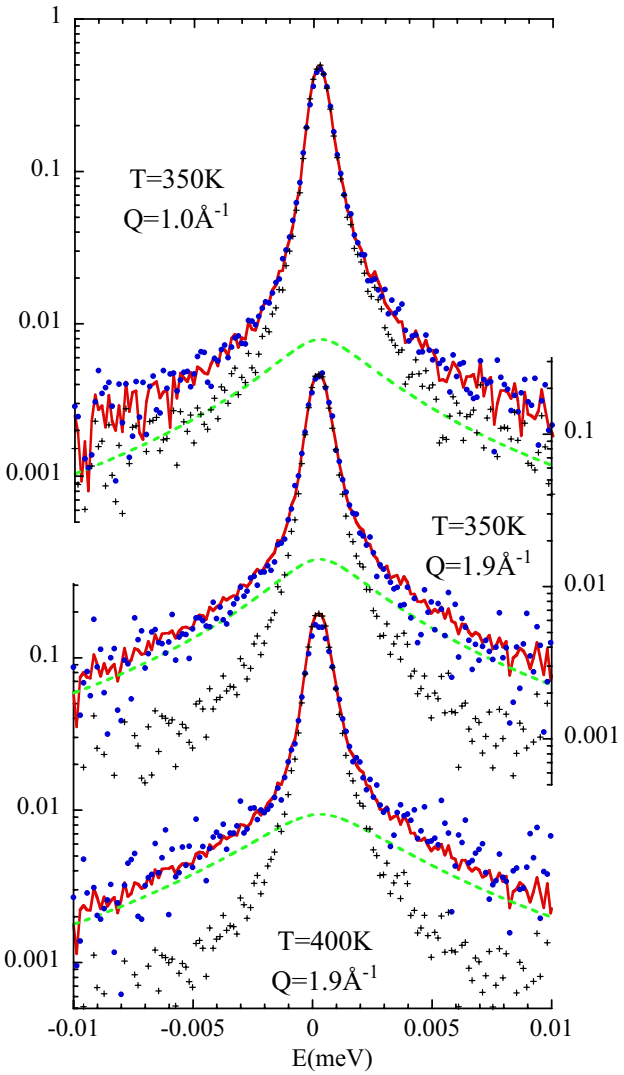


Fig. 2: Spectra obtained from a sample containing 75% of protonated PMMA and 25% of deuterated PEO at the Q-values and temperatures indicated. Solid lines: descriptions assuming the rotation of the α-methyl groups in PMMA as the only origin of the quasielastic broadening. Dotted lines: quasielastic contributions. Crosses: resolution.

References:

[1] A. J. Moreno, A. Alegría, J. Colmenero, B. Frick, Macromolecules **34**, 4886 (2001)

Institut für Festkörperforschung
Forschungszentrum Jülich GmbH
D-52425 Jülich

Experimental Report
of Neutron Scattering Experiments
at the FRJ-2 Reactor

Proposal number:	BSS-04-023		
Experiment title:	**Superparamagnetism in hematite nanoparticles**		
Dates of experiment:	14.-23. 4. 2005	Date of report:	29. 05. 2005
Experimental team: Names	Addresses		
Christian R. H. Bahl Kim Lefmann	Materials Research Department, AFM-228 Risø National Laboratory Frederiksborgvej 399 DK-4000 Roskilde Denmark		
Local Contact:	Andreas Wischnewski		

Experimental report text body

The finite size of magnetic nanoparticles ensures that they are single domain particles, and will introduce spin dynamics, which are absent in bulk materials. The magnetisation direction may reverse spontaneously when the thermal energy is near the energy barrier given by the easy-axis anisotropy, so-called superparamagnetism (SPM). It is also possible to induce collective magnetic excitations, where the spins oscillate coherently around the easy-axis in quantised energy levels. The spacing between these gives rise to inelastic resonance peaks. Usually, the superparamagnetic relaxation is much slower than the collective magnetic excitation precessions. However, at elevated temperature when the two time scales become comparable a new relaxation regime is predicted to occur: isotropic relaxation of the spins. This should be observed as a dramatic reduction in the neutron scattering signal from the magnetic Bragg reflections. However, despite this extreme dynamic spin relaxation coherent magnetic order is still maintained in the nanoparticle, due to the strong exchange coupling within it.

We have studied two samples of 8 nm canted antiferromagnetic hematite (α-Fe_2O_3). One that was prepared by drying an aqueous suspension of particles, and one prepared by coating the nanoparticles with a layer of phosphate before drying, to minimize the (exchange) interactions between the individual particles.

The characteristic time between the spontaneous flipping of the spins is given by an Arrhenius-type equation. This flipping time results in a broadening of the quasi-elastic peak at the antiferromagnetic scattering vectors with a Lorentzian line shape. This broadening we have previously measured by neutron scattering at Rita2 (Paul Scherrer Institute, Switzerland). But due to poor resolution and overlap from the collective magnetic excitation signals at ±0.2meV, the width of the peak has been difficult to measure.

The high resolution of the BSS and positions of the collective magnetic excitation signals far beyond the limits of the BSS energy scale, have now enabled us to measure the width of the quasi-elastic peak more confidently.

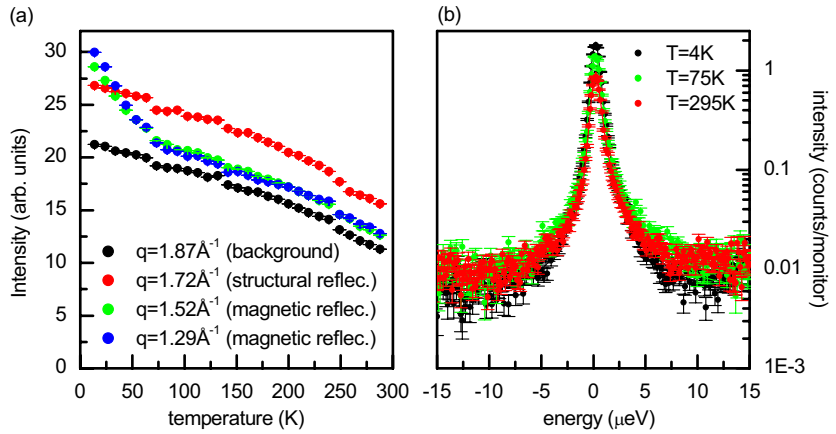


Figure 1. Measurements acquired for the sample of weakly interacting hematite nanoparticles: (a) Elastic temperature scans at two antiferromagnetic reflections at q =1.29 Å^{-1} (1.37 Å^{-1}) and 1.52 Å^{-1} (1.51 Å^{-1}) and a structural at 1.72 Å^{-1} (the q-values in () indicate the positions of the Bragg reflections). Clearly, the BSS setup is ideal for measuring hematite. (b) Inelastic energy scans at q =1.29 Å^{-1}, T=4, 75, 295K. Fits to the data are represented by the full lines.

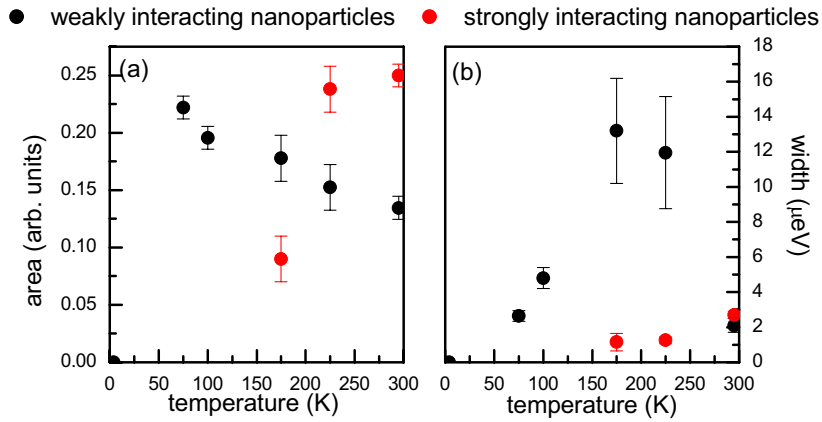


Figure 2. Integrated area and width of the quasi-elastic signal as a function of temperature as determined from the fits.

The preliminary analysis of the inelastic neutron scattering data shows the expected decrease of the integrated area of the quasi-elastic signal with temperature (Fig. 2(a)). However, the important detail documenting the change into the isotropic relaxation regime is shown by the width of the quasi-elastic peak as a function of temperature (Fig. 2(b)). The width increases up to T~175K as expected for superparamagnetic relaxation (thermally induced), but then it dramatically decreases for T>175K. We have performed a few measurements on the sample of strongly interacting hematite nanoparticles (the interactions are known to block the magnetic relaxations), these indeed show that the SPM-isotropic relaxation crossover sets in at a higher temperature than for the weakly interacting nanoparticles.
Further data analysis and more experimental investigations are needed to determine the details of the SPM-isotropic relaxation mechanisms, the effect of inter-particle interactions and nanoparticle size, and thereby allowing us to experimentally prove the existence of isotropic spin relaxation in magnetic nanoparticles.

Institut für Festkörperforschung
Forschungszentrum Jülich GmbH
D-52425 Jülich

Experimental Report
of Neutron Scattering Experiments
at the FRJ-2 Reactor

Proposal number:	BSS-04-025		
Experiment title:	**Dynamic miscibility in miscible polymer blends**		
Dates of experiment:	27 – 31 January 2005	Date of report:	5 December 2005
Experimental team: Names	Addresses		
Juan Colmenero Arantxa Arbe Roberto Pérez Aparicio Dieter Richter	Dpto. de Física de Materiales, UPV/EHU, Apdo. 1072, 20080 San Sebastian, SPAIN Unidad de Física de Materiales, CSIC-UPV/EHU, “ , “ , “ Dpto. de Física de Materiales, UPV/EHU, Apdo. 1072, 20080 San Sebastian, SPAIN IFF, FZJ, Jülich, Germany		
Local Contact:	HANS GRIMM		

Experimental report text body

Motivated by the question of the dynamic miscibility in polymer blends (see, e.g., [1-3]), the main goal of our general project was to investigate the effect of blending on the dynamical processes in the polymer blend head-to-head polypropylene / poly(ethylene propylene) (HHPP/PEP) (T_g(HHPP)=248K, T_g(PEP)=213K). Taking advantage of isotopic labeling, the dynamics of both components in the blend could be isolated by means of quasielastic neutron scattering. A first set of measurements were performed at the backscattering spectrometer IN16 (ILL, Grenoble). There, both homopolymers and a 50%/50% blend where the PEP component was fully deuterated (h-HHPP/d-PEP) were investigated. In this way we characterized the dynamical processes for the two pure systems and the effect of blending on HHPP (the high-T_g component). We established that, while the methyl group rotations observed in the glassy state are not affected by blending, the subdiffusive atomic motions in the segmental relaxation regime become faster in the presence of PEP chains. Unfortunately, synthesis problems with deuterated HHPP prevented the experimental isolation of the PEP component in the blend. Nevertheless, with the information on the dynamical behavior of HHPP in the blend provided by the IN16 experiments at hand, we could in principle deduce the dynamics of PEP in the blend from measurements on the fully protonated sample. This was the aim of this experiment.

We thus investigated the 50%/50% HHPP/PEP blend, where both components were fully protonated, by means of BSS with λ=6.271Å in the Q-range $0.16 \leq Q \leq 1.87$ Å^{-1}. Measuring times were of about 19 hours per T. The thickness of the sample was such that a transmission of 0.9 was calculated (0.2 mm). The temperatures investigated were 300, 325, 350, 375 and 400 K (all of them above the glass transition of the blend, Tg≈228K). The instrumental resolution of the spectrometer was determined from the sample at 4K. Measurements of background and Vanadium were performed in order to correct the data.

The spectra obtained for the fully protonated blend (see an example in Fig. 1) reflect the dynamics of hydrogen atoms from both blend components. A first global description of the spectra delivered timescales in between those determined for HHPP in the blend and pure PEP (see Fig. 2), indicating a very fast dynamics for PEP in the blend. A further analysis of the data considering the information of HHPP dynamics in the blend leads to the timescales shown in Fig. 2 as empty squares for the PEP component in the blend. It seems that PEP dynamics is hardly affected by blending. Figure 1 shows the both components of the blend after the analysis performed.

The extremely weak influence of blending on the low-T_g component dynamics of this system was not expected (see, e.g., [1]). Therefore, further analyses and/or new measurements are necessary in order to establish well these results.

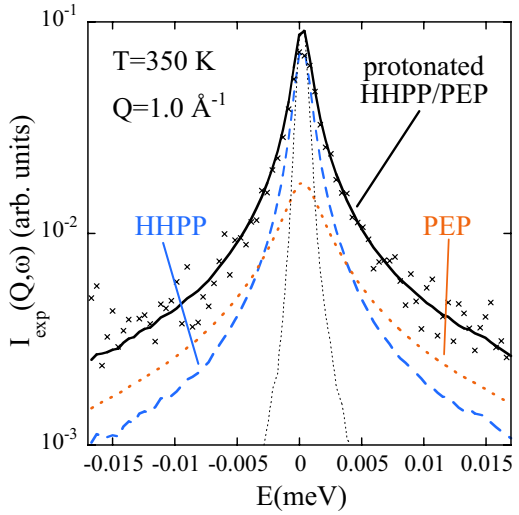


Fig. 1: Scattering function in logarithmic scale for the fully protonated HHPP/PEP blend at Q= 1.0 Å^{-1} and 350K. The solid line is a fitting curve. Dashed line depicts the HHPP contribution imposed from previous IN16 results and dashed-dotted the PEP contribution deduced. The dotted line shows the instrumental resolution.

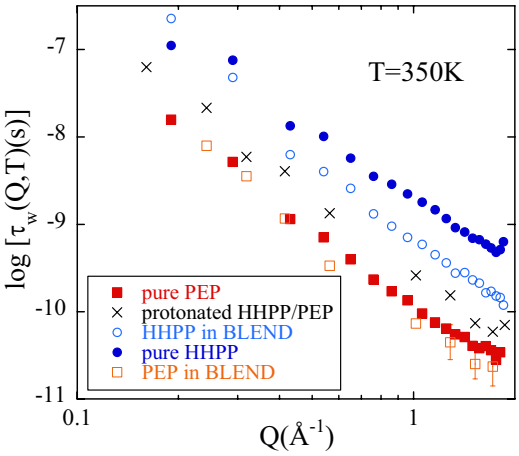


Fig. 2: Momentum-transfer dependence of the characteristic times for segmental dynamics obtained at 350 K for HHPP hydrogens in the homopolymer (full circles, IN16) and in the blend h-HHPP/d-PEP (empty circles, IN16), and for PEP hydrogens in the homopolymer (full squares, IN16) and in the blend with HHPP (empty squares, BSS). The crosses show the global timescale obtained when the BSS HHPP/PEP (fully protonated) spectra are described by a single stretched exponential.

REFERENCES

[1] T. P. Lodge and T. C. B. McLeish, Macromolecules **32**, 5278 (2000).

[2] I. Cendoya, A. Alegría, J. M. Alberdi, J. Colmenero, H. Grimm, D. Richter, B. Frick, Macromolecules **32**, 4065 (1999).

[3] S. Hoffmann, L. Willner, D. Richter, A. Arbe, J. Colmenero, B. Farago, PRL **85**, 772 (2000).

[4] W. W. Graessely et al., Macromolecules **28**, 1260 (1995).

[5] The partial structure factors of hhPP and PEP have already been investigated by us at FRJ-2 Reactor in Exp. Rep. DNS-04-008 (2004).

Institut für Festkörperforschung
Forschungszentrum Jülich GmbH
D-52425 Jülich

Experimental Report
of Neutron Scattering Experiments
at the FRJ-2 Reactor

Proposal number:	BSS-04-027		
Experiment title:	Neutron backscattering on nanoconfined poly(methyl phenyl siloxane)		
Dates of experiment:	16.02.–15.03.2005	Date of report: 24.03.2006	
Experimental team: Names	Addresses		
Dr. Schönhals, A. Dr. Zorn, R. Mayorova, M.	Bundesanstalt für Materialforschung und –prüfung, Unter den Eichen 87, 12205 Berlin Forschungszentrum Jülich, Institut für Festkörperphysik Forschungszentrum Jülich, Institut für Festkörperphysik		
Local Contact:	M. Zamponi, A. Wischnewski		

Experimental report text body

The influence of a spatial nano-confinement on both the methyl group rotation and the microscopic dynamics of the glass-forming polymer poly(methyl phenyl siloxane) (PMPS) (glass transition temperature $T_g = 213$ K) was investigated. Dielectric spectroscopy shows that the segmental dynamics of PMPS is accelerated close to T_g compared to the bulk (confinement effect). Moreover a transition from a Vogel-Fulcher-Tammann-like temperature dependence of the relaxation time to an Arrhenius type is found for a pore size of 5 nm indicating a change in the dynamics. This also supported by DSC experiments. Incoherent inelastic neutron scattering (NS) was carried out on PMPS confined to Sol/Gel-glasses (pore sizes: 7.5, 5.0, 2.5 nm) and on a bulk sample as reference.

The glasses were treated in vacuum to remove impurities. The polymer was injected into the vacuum chamber and the pores were filled by capillary wetting. The experiments were done on the back scattering spectrometer (BSS) (wave length of λ=6.271 Å, energy resolution of 1 μeV; energy transfer range of 17 μeV). To have a broader time range additional experiments were carried out on the Time-of-Flight spectrometer IN6 and on the backscattering instrument IN16 at the Institut Laue Langevin (ILL, Grenoble France). The spectra were corrected with data obtained for an unfilled nanoporous glass (5 nm) sealed under a He atmosphere.

Fig. 1 depicts the incoherent intermediate scattering function $S_{Inc}(Q,t)$ for confined PDMS at T = 120 K. The points between 0.5 ps and 20 ps originate from the Fourier transform of IN6 data; those at t > 150 from BSS/Jülich. The data are analysed by fitting the KWW-function to the data where A(Q) is the Elastic Incoherent Structure Factor (EISF) for the methyl group dynamics and DWF is the Debye-Waller

factor: $S_{Inc}(Q,t) = DWF \cdot ((1 - A(Q))\exp(-t/\tau)^{\beta} + A(Q))$. For decreasing pore size the EISF increases due to an increasing amount of immobilized CH_3 groups probably located in a boundary layer at the pore walls. Fig. 2 compares the relative amount of the immobilized CH_3 groups in confinement versus inverse pore size for PMPS and poly(dimethyl siloxane) (PDMS). For both polymers approximately the same pore size dependence is obtained. Therefore it is concluded that both polymers forming a boundary layer of similar thickness inside the pores.

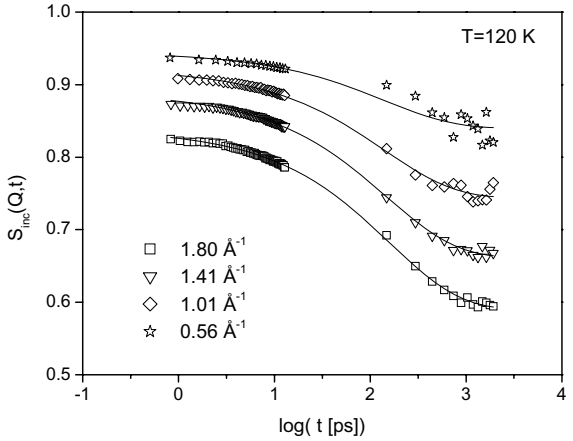


Fig. 1: $S_{Inc}(Q,t)$ for PMPS confined to pores of 7.5 nm. Lines are described in the text.

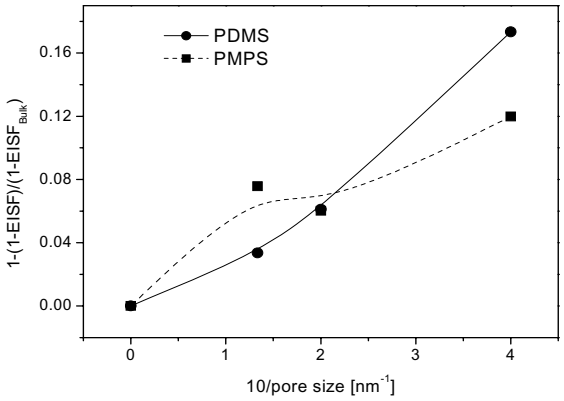


Fig. 2: Relative amount of the immobilized CH_3 groups versus inverse pore size.

Above T_g the decrease in $S_{Inc}(Q,t)$ is due to different processes which include vibrational contributions, methyl group reorientations and the segmental dynamics.

The ansatz $S_{Inc}(Q,t) = DWF \cdot ((1-A)\exp(-(t/\tau_{CH_3})^{\beta_{CH_3}}) + A\exp(-(t/\tau_{Seg})^{\beta_{Seg}}))$ is used to analyze the data. The shape parameters β_{CH3} and β_{Seg} are taken from an analysis of the CH_3 group rotation and from dielectric spectroscopy, respectively. Mean relaxation times are calculated by $\tau = \tau_{KWW}\Gamma(1/\beta)/\beta$. The relaxation times obtained by NS agree in both their absolute values and in their temperature dependence with those measured by dielectric and thermal spectroscopy. For the bulk and PMPS confined to 7.5 nm pores the temperature dependence of the relaxation times obeys the VFT-equation but the relation $\tau_{Seg}(T)$ for PMPS imbedded in pores crosses that of the bulk. This points to the fact that the thermodynamic state of the confined polymer is different from that of the bulk. For smaller pores sizes than 7.5 nm the temperature dependence of the relaxation time changes from a VFT to an Arrhenius-like behaviour. It is concluded that the character of the underlying fluctuations is dramatically changed and that an intrinsic length scale is relevant for glassy dynamics to appear in PMPS.

Institut für Festkörperforschung
Forschungszentrum Jülich GmbH
D-52425 Jülich

Experimental Report
of Neutron Scattering Experiments
at the FRJ-2 Reactor

Proposal number:	BSS-05-001		
Experiment title:	Methyl rotational dynamics in acetone-D_2O clathrate		
Dates of experiment:	2.4.2005, 7 days	Date of report:	25.2.2006
Experimental team: Names	Addresses		
M. Prager	Institut für Festkörperforschung, Forschungszentrum Jülich		
Local Contact:	H. Grimm		

Experimental report text body

Due to the weakness of interaction with its environment acetone in acetone-water clathrate is expected to represent a guest molecule with a methyl rotational potential and methyl-methyl coupling predominantly caused by intramolecular interaction [1,2,3]. Therefore the system can be modelled as a single particle problem and is in this form accessible to a simple mathematical treatment.
The actual experiment is a continuation of the experiment BSS-04-014. The formation of the clathrate structure after a dedicated annealing procedure could be proven by a modified vibrational density of states which was measured at the TOF spectrometer SV29. Such controlled samples were transferred to the BSS instrument and introduced cold into its cryostat. The samples do not show inelastic intensity in the energy regime $18<\Delta E[\mu eV]<18$ of the instrument. Additional annealing procedures led to no changes. This must mean that the internal barrier in the isolated acetone molecule is such strong that no tunnel splitting is observable. Gaussian98 calculations shall confirm this conclusion.

[1] C. Gutt, W. Press, A. Hüller, J. Tse, H. Casalta, J. Chem. Phys. **114**,4160(2001)
[2] M. Prager, J. Pieper, A. Buchsteiner, A. Desmedt, J. Phys. Condens. Matter **16**,7045(2004)
[3] M. Prager, J. Baumert, W. Press, M. Plazanet, J.S. Tse, D.D. Klug, PCCP **7**,1228(2005)

Institut für Festkörperforschung
Forschungszentrum Jülich GmbH
D-52425 Jülich

Experimental Report
of Neutron Scattering Experiments
at the FRJ-2 Reactor

Proposal number:	BSS-05-005		
Experiment title:	In vivo characterisation of selectively hydrogenated nucleic acids in deuterated Escherichia coli cells		
Dates of experiment:	19.06. – 25.06.2005	Date of report:	07/06/2006
Experimental team: Names	Addresses		
Joseph Zaccai Jasnin, Marion Tehei, Moeava	Institut Laue Langevin, Grenoble Cedex 9, France Institut de Biologie Structurale, Laboratoire de Biophysique Moléculaire, Grenoble, France CNR-INFM, Institut Laue Langevin, Grenoble Cedex 9, France		
Local Contact:	Zamponi, M.		

Abstract

A very slow cell water of *Haloarcula marismortui*, an extremely halophilic organism, was discovered on the backscattering spectrometer IN16 at ILL (Grenoble – France). In distinction to *E. coli* organism, K+ was retained within the cells of *Haloarcula marismortui* even in the absence of metabolism. Therefore, it was hypothesized that the slow mobility of cell water in *Haloarcula marismortui* indicates a water structure responsible for the large and specific amounts of K+ bound within these cells. In order to reinforce this hypothesis, we did the experiments on *E. coli* using the spectrometer BSS (FRJ-2, Jülich), which have about the same resolution then IN16. Data from BSS experiments on *E. coli* cells revealed that this extremely slow cell water do not exist in this organism.

Background

Water dynamics has been studied extensively by neutron scattering from the early days of the method [1]. In recent years the study has been extended to the water associated with proteins by using fully deuterated phycocyanin [2]. Diffusion in general and the dynamics of water inside cells are of considerable interest because crowding creates a local environment that is very far from the dilute conditions usually studied in biochemical and biophysical experiments. Many important questions have to be addressed. For example, is the crowding and association of water with intra-cellular structures different in different cell types? To what extent will additional 4M salt have an additional impact in the cytoplasm as it occurs in extremely halophilic archaeal cells? *Haloarcula marismortui (Hm)*, an Archaeal species isolated from the Dead Sea, attracted our attention some years ago because of its high selectivity for K^+ (selectivity coefficient K^+_{in}:Na^+_{in} / K^+_{out}: Na^+_{out}, ~ 20,000) and because of the high permeability of the outer membrane. In distinction to the non-halophile cells *E. coli*, K^+ was retained within the cell even in the absence of metabolism. As the Na^+ has a half-time of exchange with the outside medium of less than 1 min while the K^+ has a time of exchange of over 24 h [3], it followed that the cell K^+ must be bound in some way or other. At the time, the only systems known with a very high binding selectivity were antibiotics such as nonactin and valinomycin. The structure responsible for their specificity is a «cage» of 6 – 8 carbonyl oxygen atoms arranged in space according to a definite pattern. If the same principle were to be responsible for K^+ binding in *H. marismortui*, 24 – 32 moles oxygen per litre of cell water would be required, enormous amounts of oxygen atoms that cannot be supplied exclusively by the organic components of the cell.

It is therefore suggested that the oxygen atoms required might be furnished by the ordering of water molecules forming a tertiary system of water, KCl and cell proteins.
Neutron scattering experiments were designed to examine intra-cellular water diffusion, following on previous work by Ginzburg and collaborators, using a variety of methods, on the cytosolic environments in the extreme halophile *Haloarcula marismortui* (*Hm*). The results revealed an extremely slow water component in *Hm*. Quasielastic Neutron Scattering (QENS) experiments were performed on the IN16 neutron spectrometer at ILL, on samples of fully deuterated *Hm* [3]. The BSS neutron spectrometer at FRJ-2 has about the same resolution then IN16. This spectrometer is therefore well adapted to examine whether this extremely slow water exists in *E. coli.*

Methods and results

Deuterated *E. coli* cell samples were prepared in collaboration with the Deuteration Laboratory of the Institut Laue Langevin and resuspended in H2O or D2O solutions. The two cell samples were named D-cells H2O and D-cells D2O, respectively. Sample holders were made of aluminum and measured 4 x 3 cm with a depth of 0.2mm. The quasielastic experiments were performed at 285K on the BSS backscattering spectrometer using an incident wavelength of 6.27 Å. The elastic energy resolution (FWHM) is 1.2 μeV corresponding to time scales of about 1 ns. The scattering was measured over a wave-vector range of 0.2 < Q < 1.9 Å-1. All samples, including the vanadium calibration sample and empty aluminum can, were oriented at 45° with respect to the incident neutron beam direction. The vanadium sample (a purely elastic scatterer) was measured in order to define the instrument resolution and to correct for detector efficiency. The measured spectra were corrected, normalized, grouped, and transformed into energy transfer spectra. The spectra of the D-cells H2O and D-cells D2O samples are identical in all the Q range (Figure 1), demonstrating that the extremely slow cell structured water do not exist in *E. coli* cells. Thus, our data reinforce our hypothesis. The existence of the very slow water component in *H. marismortui* suggests a specific water structure, which would also be responsible for the large amounts of K^+ ions found to be bound within these cells.

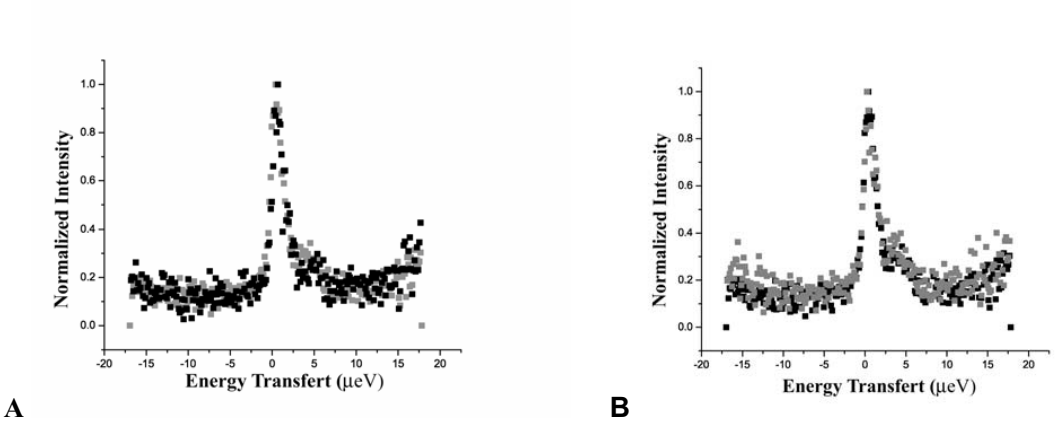


Figure1: Normalized quasielastic spectrum of D-cells H_2O (gray) and D-cells D_2O (black) at Q = 0.31 A^{-1} (A) and Q = 1.86 A^{-1} (B).

References

(1) Egelstaff P.A. (1965) Thermal Neutron Scattering. Academic Press. London and New York.
(2) Bellissent-Funel M. C., Teixeira J., Chen S. H., Dorner B., Middendorf H. D., Crespi H. L. (1989). Low-frequency collective modes in dry and hydrated proteins. Biophys. J. 56, 713-716.
(3) Ginzburg, M., Sachs, L. & Ginzburg, B. Z. (1970) *J. Gen. Physiol.* **55,** 187-207.
(4) Tehei M., Franzetti B., Wood K., Gabel F., Fabiani E., Jasnin M., Zamponi M.Oesterhelt D., Zaccai1 G., Ginzburg M., Ginzburg B.Z. (2006) Neutron scattering reveals extremely slow water in a Dead Sea organism. In revision for PNAS.

Institut für Festkörperforschung
Forschungszentrum Jülich GmbH
D-52425 Jülich

Experimental Report
of Neutron Scattering Experiments
at the FRJ-2 Reactor

Proposal number:	BSS-05-006		
Experiment title:	Self motions of PMMA close and above the glass transition		
Dates of experiment:	16/05/2005-25/05/2005	Date of report: 11/10/2005	
Experimental team: Names	Addresses		
Caroline Genix Juan Colmenero Arantxa Arbe Dieter Richter	Donostia International Physics Center, Apdo. 1072, 20080 San Sebastian, SPAIN Dpto. de Física de Materiales, UPV/EHU, , “ , “ , “ Unidad de Física de Materiales, CSIC-UPV/EHU, “ , “ , “ IFF, FZJ, Jülich, Germany		
Local Contact:	Andreas Wischnewski		

Experimental report text body

The aim of this experiment was to investigate the segmental relaxation in syndiotactic poly(methyl methacrylate) (PMMA) (T_g=400K) through the hydrogen motions. The sample studied was PMMA with deuterated ester-methyl group (PMMAd3). In this way the spectra revealed the dynamics of the main-chain and α-methyl group hydrogens (see scheme), while the ester-methyl hydrogens were "hidden" for neutrons. The reason to avoid contributions from such atoms was that in a recent MD-simulations study the dynamics of the ester side group has been found to be significantly faster than that associated to the main chain [1].

The BSS measurements have been performed at 4, 300, 350, and each 25K between 400K and 525K.

The sample was placed in an Aluminum flat container at 45º with respect to the incident beam. The thicknesses were such that a transmission of ≈ 0.9 was calculated. With λ=6.27Å a Q-range of 0.16 … 1.87Å^{-1} was accessed and an energy window of ±17μeV was explored. Measuring times of about 20 hours were employed to achieve reasonable statistics, as can be appreciated in Fig. 1 (at 300K measurement we counted only for 7 hours). Vanadium and empty cell measurements were also carried out to correct the spectra.

From our last results obtained by BSS and MD-simulations on PMMA in a PEO/PMMA blend [1], we expected that below 400K the quasielastic broadening of the PMMAd3 spectra could only relate to the α-methyl group rotation in the BSS window. The quantitative analysis of the spectra at 300K, 350K and 400K by using this approach delivers a good description of the experimental data and allows determining the characteristic timescale for this rotation. The results [see Fig. 2(a)] are in good agreement with those obtained in [1] for PMMA in the blend, corroborating the hypothesis that blending does not affect such localized motions.

Above 400K, additional broadening is observed that should be attributed to the segmental relaxation. We described such contribution by the Fourier transform of a stretched exponential function, $\exp[-(t/\tau)^{\beta}]$. In the fitting procedure, the values of the β parameter were fixed to those obtained from dielectric spectroscopy experiments on PMMA (β = 0.3 for 425K, 0.5 for 450K and 0.56 for higher temperatures). The α-methyl group rotation was taken into account by construction of an "effective resolution" including the quasielastic broadening expected from this motion properly weighed by the relative abundance of such atoms and the appropriated EISF. Assuming statistically independent rotation and segmental relaxation, the global dynamics is described by the convolution of both functions. Very satisfactory fits are achieved, as can be seen in Fig. 1. Moreover, the characteristic times obtained at Q = 1 $Å^{-1}$ for segmental dynamics of PMMA are in a good agreement with dielectric spectroscopy results [see Fig. 2(a)]. Finally, Fig. 2(b) shows the Q-dependence of the characteristic times obtained for the α-relaxation. Weaker dependences with respect to that expected in the Gaussian approximation [$\propto Q^{-2/\beta}$] are found. This might be a consequence of the heterogeneous dynamics developed by the different hydrogens in the sample.

References:

[1] A.-C. Genix, A. Arbe, F. Alvarez, J. Colmenero, L. Willner, D. Richter, PRE **72**, 31808 (2005)

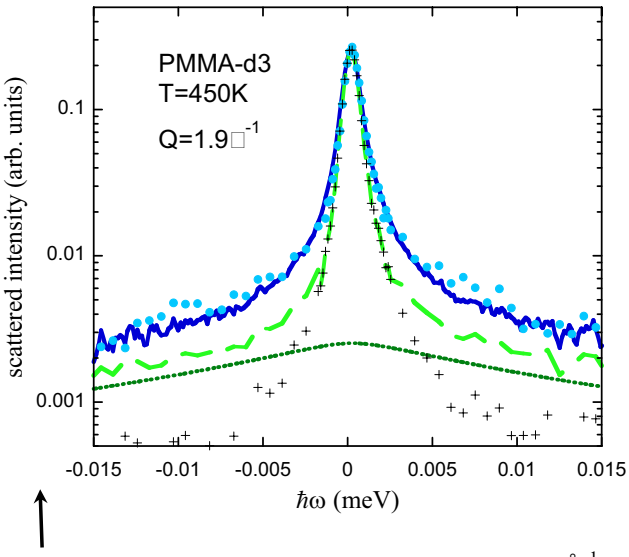
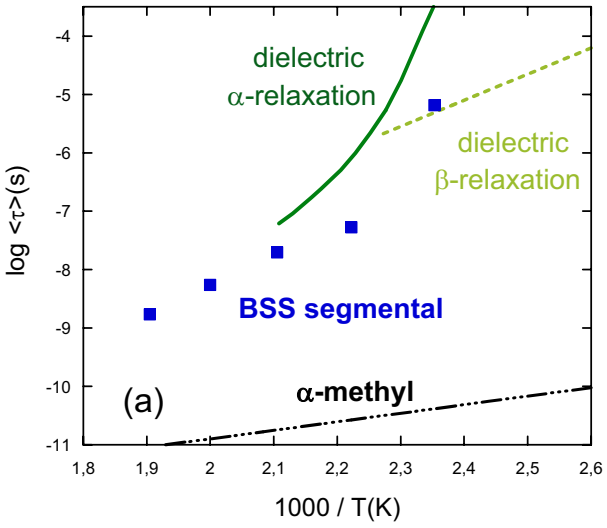


Fig. 1: Scattering function measured at Q =1.9 $Å^{-1}$ and 450 K for PMMAd3. The solid line is a fitting curve consisting of a KWW function to describe the overall segmental dynamics convoluted with an effective resolution (dashed line) giving account for the α-methyl group rotations. The quasielastic component of the α-methyl group rotations is depicted by the dotted line. The resolution function is shown by the crosses.



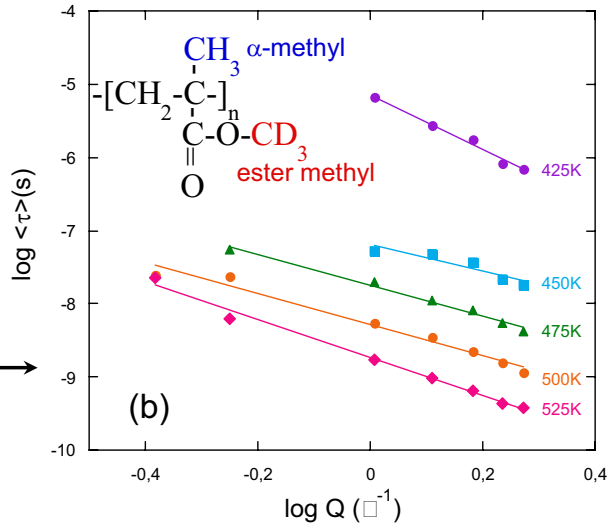


Fig. 2: Characteristic times for segmental motion of PMMA. (a) Temperature dependence for Q = 1 $Å^{-1}$; (b) Momentum transfer dependence for the temperatures investigated

Institut für Festkörperforschung
Forschungszentrum Jülich GmbH
D-52425 Jülich

Experimental Report
of Neutron Scattering Experiments
at the FRJ-2 Reactor

Proposal number:	BSS-05-007		
Experiment title:	Elastic fixed window scan of glass-forming propyleneglycol		
Dates of experiment:	11.–13.04.2005	Date of report:	19.05.2005
Experimental team: Names	 Addresses		
Maria Mayorova Andreas Wischnewski Reiner Zorn	IFF, FZ Jülich IFF, FZ Jülich IFF, FZ Jülich		
Local Contact:	Andreas Wischnewski		

Experimental report text body

This is a preparatory experiment for future inelastic neutron scattering experiments on a microemulsion containing propyleneglycol (PG) as nanoscopic droplets. Details of the system are described in ref. 1. The special interest for this microemulsion arises from the fact that one can observe the glass transition of the inner microphase (PG) separately and thus study the confinement effect on the glass transition.

Here we performed an elastic fixed window scan on the *bulk* reference. Previous work has shown that this is often not a trivial task because of the tendency of low-molecular liquids to crystallise. The experiment was done using a hollow cylindrical aluminium sample holder with anodised surfaces. The sample was quenched in liquid nitrogen and an up-scan from 2 K to 325 K was done. If crystallisation would have occurred this could be clearly seen from an abrupt increase of elastic intensity. Experiments on IN16 with its diffraction detector in parallel have shown that, surprisingly, this criterion is even clearer than the occurrence of Bragg peaks (in predominantly incoherently scattering samples).

Subtraction of the empty container and corrections for self-shielding were done by the ILL program SQWel adapted to the Jülich BSS data format.

As Fig. 1 shows the elastic scans do not show any such signature of crystallisation. Instead, the intensity decreases monotonously with temperature. This proves that the given construction of the sample holder can be used in future experiments over the whole temperature region without taking the risk of crystallisation during the measuring time.

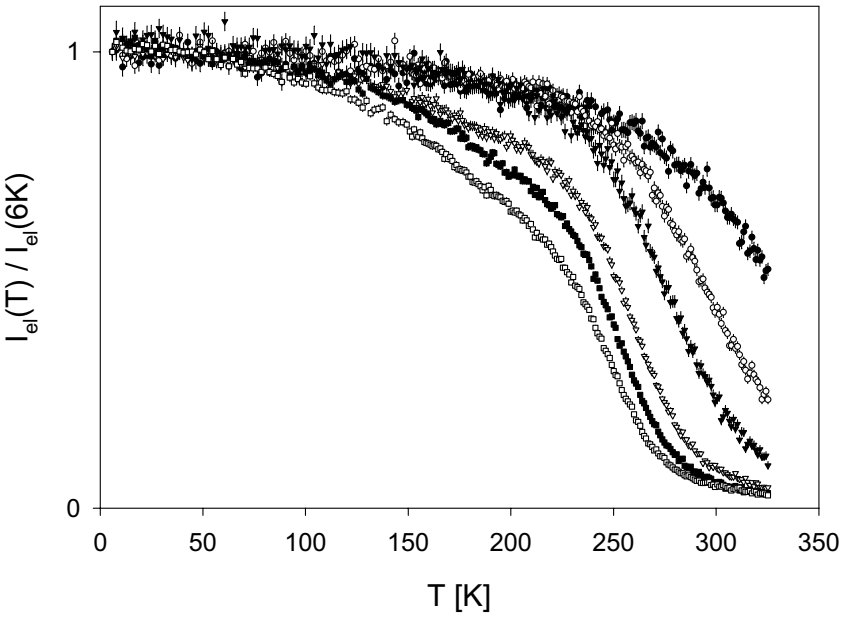


Fig. 1: Elastic scans of propyleneglycol: intensities normalised to 5.9 K. Q values: ● 0.20 Å^{-1}, ○ 0.37 Å^{-1}, ▼ 0.56 Å^{-1}, ▽ 1.02 Å^{-1}, ■ 1.41 Å^{-1}, □ 1.80 Å^{-1}.

From the elastic scans mean-square displacements $\langle u^2 \rangle$ of the scatterers (predominantly protons) were calculated using the cumulant expression

$$I_{\mathrm{el}}(Q) \propto \exp\left(-\frac{\langle u^2 \rangle}{3} Q^2 + \frac{A \langle u^2 \rangle^2}{72} Q^4 \right).$$

Fig. 2 shows the result. (The non-Gaussianity parameter A was not extracted because it contains also the multiple scattering effects.) The mean-square displacement shows the characteristic behaviour for glass-forming materials. At low temperatures it is roughly proportional to temperature, at intermediate temperatures it increases more strongly due to fast processes, and above T_g = 167 K a strong increase due to the α relaxation sets in. What is remarkable is that the methyl group rotation is not visible. From measurements on polymers containing methyl groups it is expected to show up as a step in the mean-square displacement at about 120 K with an amplitude $\frac{3}{8}\langle u^2 \rangle_{\mathrm{CH_3}} = 0.38$ Å^2. If at all it takes place at a higher temperature indicating that the barrier height for methyl-group rotation is larger than in other substances.

[1] Lin-Min Wang, Fang He, R. Richert, *Phys. Rev. Lett.* **92**, 095701 (2004)

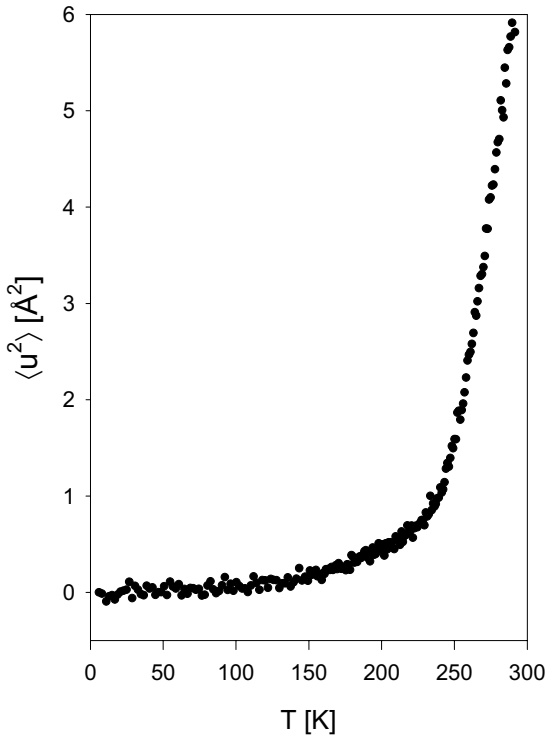


Fig. 2: Mean-square displacement of protons in popyleneglycol at the characteristic time corresponding to the resolution of the Jülich BSS spectrometer (≈ 2 ns)

Institut für Festkörperforschung
Forschungszentrum Jülich GmbH
D-52425 Jülich

Experimental Report
of Neutron Scattering Experiments
at the FRJ-2 Reactor

Proposal number:	BSS-05-008		
Experiment title:	**Concentration dependence of PEO dynamics in a blend of PEO/PMMA**		
Dates of experiment:	25.05 – 29.05.2005 06.06 – 07.06.2005 15.06 – 21.06.2005	Date of report:	28.11.2005
Experimental team: Names	Addresses		
Katarzyna Niedzwiedz Dr. Andreas Wischnewski Dr. Michael Monkenbusch Prof. Dr. Dieter Richter	IFF, Forschungszentrum Jülich, 52425 Jülich IFF, Forschungszentrum Jülich, 52425 Jülich IFF, Forschungszentrum Jülich, 52425 Jülich IFF, Forschungszentrum Jülich, 52425 Jülich		
Local Contact:	Dr. Andreas Wischnewski Dr. Michaela Zamponi		

Experimental report text body

Although it is well known for a long time that the dynamics of each component of a binary polymer mixture is affected by blending, the dynamic miscibility and in particular the question whether or not there exists a corresponding length scale is still matter of strong controversy [1]. The unsolved problem of how local friction arises in chemically heterogeneous environments makes it impossible to predict the properties of a blend system on basis of what is known about the behaviour of each component of the mixture.
Of particular interest are blends where the dynamics of the pure components are well separated in time, i.e. with a very different glass transition temperature T_g of the components. In this case the slow (high T_g) ingredient forms a stiff network within the faster (low T_g) component.

In this experiment we investigated the miscible PEO / PMMA blend ($T_g^{PEO} \approx 210$ K, $T_g^{PMMA} \approx 400$ K) with two different compositions: 35 % PEO / 65 % PMMA and 50 % PEO / 50% PMMA.

Since we were interested in the motion of the faster component (PEO) blends with protonated PEO and deuterated PMMA were measured. The data were corrected for background (the intensity coming from an empty cell was measured separately) and the instrument resolution was determined by measuring the blend sample at T=4 K.

Preliminary treating of the data shows changes in the PEO dynamics for the different samples. Figures 1 –3 illustrate the dynamic structure factor for the different compositions of the PEO / PMMA blend. One can see that with increasing PEO concentration the intensity decreases and the spectra become broader, i.e. the quasielastic scattering is more pronounced as it is found for increasing Q-values or temperatures.

A full evaluation of the data is still going on. For a quantitative description one in particular needs to account for the elastic contribution to the signal from coherent scattering.

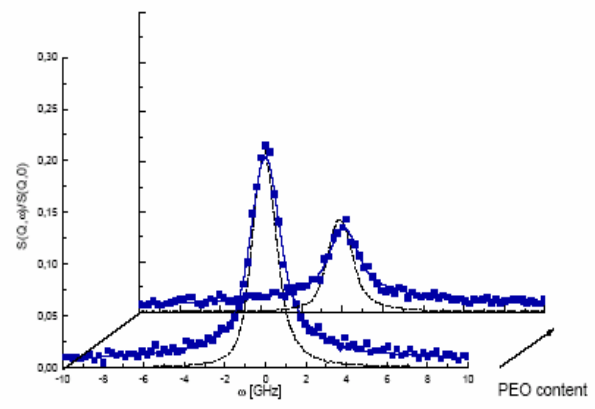


Fig. 1 Neutron scattering spectra of a PEO/PMMA blend with different concentrations: 35%PEO / 65%PMMA and 50% PEO / 50% PMMA at T = 375 K and Q = 1.017 Å^{-1}. The dashed lines show the instrument resolution (blend at T = 4 K), the solid lines represent fits with the Kohlrausch-Williams-Watts (KWW) function for a stretching parameter β = 0.5.

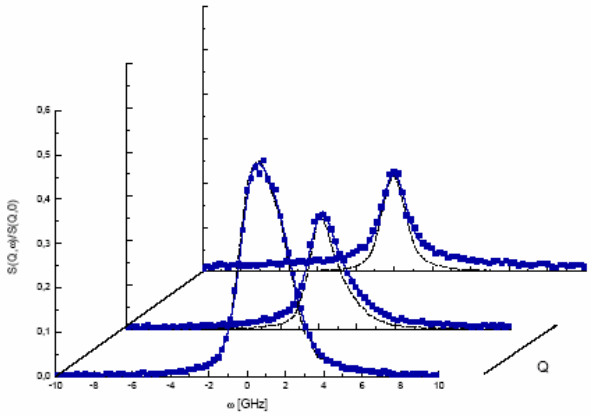


Fig. 2 Neutron scattering spectra of a blend with 35% PEO and 65% PMMA at T = 350 K and different Q values: 1.287, 0.564 and 0.242 Å^{-1}. The dashed lines shows the instrument resolution, the solid lines represent fits with the KWW function for β = 0.5.

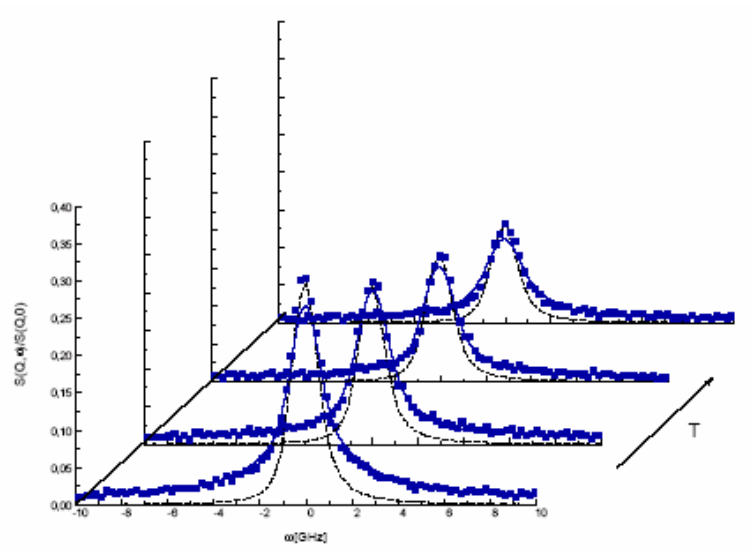


Fig. 3 Neutron scattering spectra for a blend with 35% PEO and 65% PMMA in a temperature range between 350 K and 425 K in steps of 25 K at Q = 1.017 Å^{-1}. The dashed lines show the instrument resolution, the solid lines represent fits with the KWW function for β = 0.5.

[1] S. Hoffman et al., Physical Review Letters 85, 772 (2000)

Institut für Festkörperforschung
Forschungszentrum Jülich GmbH
D-52425 Jülich

Experimental Report
of Neutron Scattering Experiments
at the FRJ-2 Reactor

Proposal number:	BSS-05-009		
Experiment title:	**Elastic fixed window scan of a glass forming microemulsion**		
Dates of experiment:	07–15.06.2005	Date of report:	06.06.2006
Experimental team: Names	Addresses		
Zorn, Reiner Mayorova, Maria	Institut für Festkörperforschung, Forschungszentrum Juelich Instititut für Festkörperforschung, Forschungszentrum Juelich		
Local Contact:	Andreas Wischnewski, Michaela Zamponi		

Experimental report text body

The effect of the soft confinement (microemulsion) on the microscopic dynamics of the glass-forming liquid Propylene Glycol (PG) with T_g=167 K was investigated. For this purpose a three component microemulsion was chosen: propylene glycol as investigated material which was enclosed within the inversed micelles, AOT – ionic surfactant for system stabilization, decalin as oil phase (T_g=135K). In such a system investigated the glass-forming liquid is surrounded with a more fluid environment near its T_g. Dielectric spectroscopy revealed an acceleration of PG dynamics close to T_g compared to the bulk (confinement effect) and 7K shift of its T_g to lower value [1]. The incoherent neutron elastic spectra measurements were done with the PI spectrometer (wave length of λ=6,30 Å) on PG confined in reversed micelles (averaged radius about 8,5 Å) and pure PG. To extract information concerning confined PG data obtained for a completely deuterated microemulsion were subtracted from data for a microemulsion with protonated PG and deuterated other components.

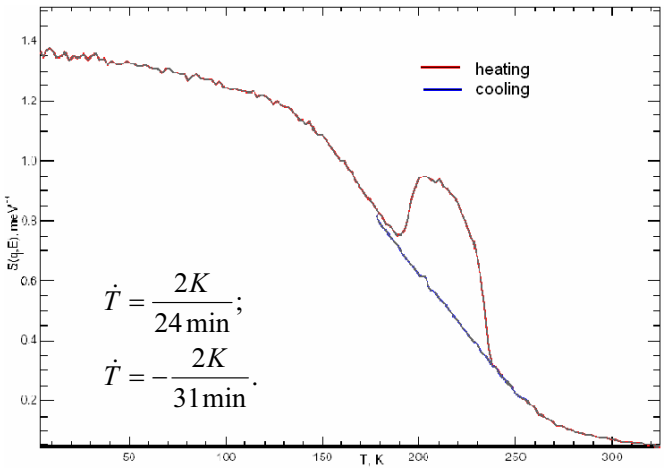


Fig.1. Confined PG elastic spectra.

As one can conclude from Fig.1 there is temperature range of crystallization of confined PG for the heating branch which was previously not detected because this temperature range was not studied (Fig. 1). So to avoid this crystallization cooling branch should be chosen.

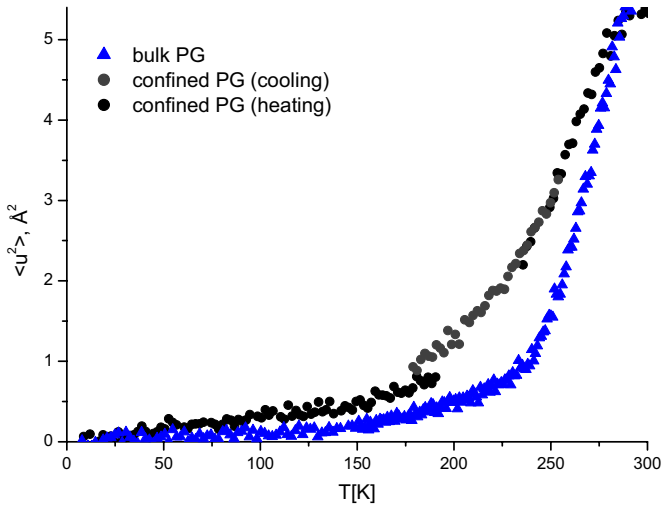


Fig. 2. Mean square displacement.

The information about mean squire displacement was extracted from a cumulant expansion of the incoherent scattering function. From comparison results for bulk and confined PG it can be concluded that there is shift of glass transition temperature to lower temperature range (Fig. 2).

Institut für Festkörperforschung
Forschungszentrum Jülich GmbH
D-52425 Jülich

Experimental Report
of Neutron Scattering Experiments
at the FRJ-2 Reactor

Proposal number:	BSS-05-010		
Experiment title:	Influence of the matrix on the confinement effect in polymer blends close to the glass transition		
Dates of experiment:	24/10/2005-06/11/2005	Date of report:	29/05/2006
Experimental team: Names	Addresses		
Anne-Caroline Genix Arantxa Arbe Juan Colmenero Andreas Wischnewski Dieter Richter	Donostia International Physics Center, Apdo. 1072, 20080 San Sebastián, SPAIN Unidad de Física de Materiales, CSIC-UPV/EHU, “ , “ , “ Dpto. de Física de Materiales, UPV/EHU, , “ , “ , “ IFF, FZJ, Jülich, GERMANY IFF, FZJ, Jülich, GERMANY		
Local Contact:	Andreas Wischnewski (BSS), Werner Schweika (DNS)		

Experimental report text body

Currently, a big deal of activity in polymer research is focused on the question of the dynamic miscibility, i.e., how the dynamics of each component in a miscible blend are affected by blending. Particularly interesting are blends of components with very different glass-transition temperature, T_g, as poly(ethylene oxide) / poly(methyl methacrylate) (PEO/PMMA) [PEO: T_g=214K, PMMA: T_g=400K]. In a very recent backscattering experiment [1], the space/time resolution and selectivity (H/D) of neutron scattering allowed us to directly observe the confined and heterogeneous nature of the molecular motions of PEO in the blend. It lead to the following scenario: at temperatures close to the blend T_g, the presence of the hardly moving PMMA matrix leads to the creation of little pockets of mobility where PEO can move [1]. However, this confinement effect - consequence of a non-equilibrium situation - still deserves a deep scrutiny. In this experiment we have chosen to focus on the influence of the matrix on the confinement effect.

The system investigated was poly(ethylene oxide) / polyethersulfone (PEO/PESF), where the difference between the T_g's for each of the pure components is of the order of 260K (PESF: T_g=476K). By backscattering we wanted to follow the scattering dominated by the incoherent contribution of the hydrogens of the protonated (h) PEO component in the blend, where the other component is deuterated (d), and compare these results with those previously obtained for the PEO in a blend with PMMA [1] and in a blend with poly(vinyl acetate) (PVAc) [2]. The BSS measurements have been performed on the following samples: pure PESF (deuterated) at 4, 250, and 400K, and a blend of hPEO/dPESF (25%/75%) at 4, 250, 270, 290, 350, 375 and 400K. This corresponds to the region well above the glass transition for PEO but close to or below that of PESF. The samples were placed in Aluminum flat containers at 45º with respect to the incident beam. The

thicknesses were such that a transmission of ≈ 0.9 was calculated. With λ=6.27Å a Q-range of 0.16 … 1.87Å^{-1} was accessed and an energy window of ±17μeV was explored. Reasonable statistics was achieved with measuring times of about 30 hours. Vanadium and empty cell measurements were carried out to correct the spectra. For Q=1Å^{-1}, Fig. 1 shows the spectra corresponding to PEO pure [1] and in the blend at 350 K. A clear slowing down in the dynamics of PEO is observed as effect of blending.

In addition, we used the diffuse scattering spectrometer (DNS) in its diffraction mode, in order to determine the Q-dependence of the relative amount of the coherent contribution to scattering of the samples. λ was set to 3.3Å enabling a Q-range up to 3.36Å^{-1}. The samples were placed into a hollow cylinder and in Aluminum flat container, for the blend and the pure PESF, respectively. The blend was measured at the same temperatures investigated by BSS (with exception of the measurement at 20K) and the pure PESF at room temperature only. Measuring times of one hour were employed. Measurements of NiCr, Vanadium and both empty sample-holders were also carried out to correct the experimental data. We realized from these diffraction measurements (see Fig. 2) that the deuteration level of the PESF sample was not as high as expected. This implies that incoherent contributions coming from the PESF component in the blend will have to be also taken into account. A quantitative analysis of the BSS spectra in terms of a log-normal distribution of relaxation times is currently being performed.

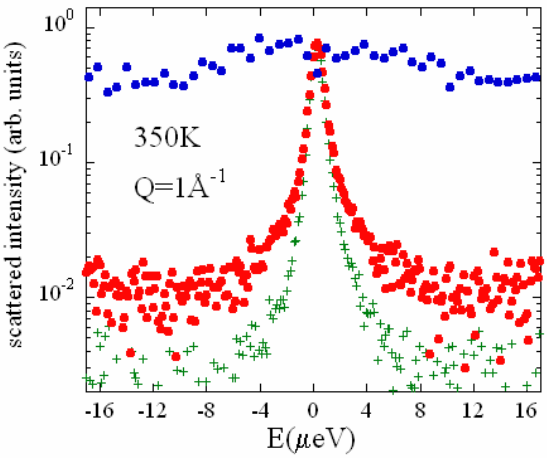


Fig. 1: Scattering function measured at 1 Å^{-1} and 350 K for pure PEO (protonated) (blue circles) [1] and the blend containing 25% of protonated PEO in a deuterated PESF matrix (red circles symbols). The functions are normalized to their maximum intensities. The resolution function is displayed by the crosses.

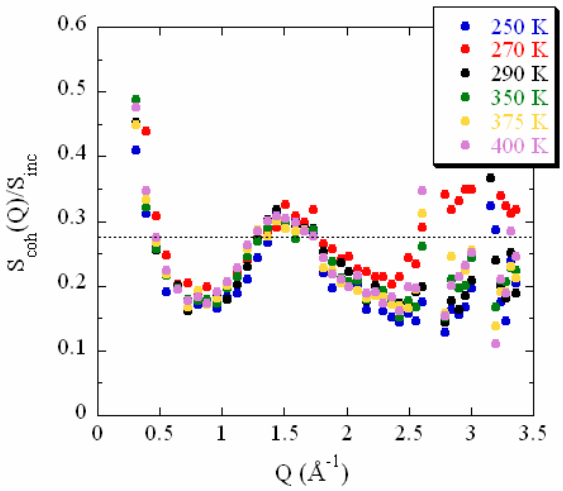


Fig. 2: Ratio between the coherent and incoherent scattering intensities measured by means of DNS at several temperatures for the blend hPEO/dPESF (25%/75%). The dotted line indicates the expected level for the same blend but with fully deuterated PESF component.

References:

[1] C. Genix et al., Experimental Report FZJ: BSS-04-019; A.-C. Genix et al., Phys. Rev. E 2005, *72*, 031808.

[2] M. Tyagi et al., Macromolecules 2006, *39*, 3007.

Institut für Festkörperforschung
Forschungszentrum Jülich GmbH
D-52425 Jülich

Experimental Report
of Neutron Scattering Experiments
at the FRJ-2 Reactor

Proposal number:	BSS-05-011		
Experiment title:	Rotational dynamics of methyl groups in di-amino-durene		
Dates of experiment:	2.7.2005 – 9.7.2005	Date of report:	25.2.2006
Experimental team: Names	Addresses		
A. Pawlukojc M. Prager	Institute of Nuclear Chemistry and Technology, Warsaw, Poland Institut für Festkörperforschung, Forschungszentrum Jülich GmbH		
Local Contact:	H. Grimm		

Experimental report text body

A study of charge transfer complex diaminodurene(DAD):tetracyanoquinodimethane (TCNQ) with the methylated benzene derivative DAD (Fig.1) as electron donor and TCNQ as acceptor molecule is complemented by a study of the pure donor compound to get a starting point for the discussion of steric and charge changes in the molecular complex. While the methyl groups of DAD in TCNQ show no tunnelling, pure DAD does. An improved energy resolution of the backscattering spectrometer BSS1 is obtained in the present experiment compared to the previous one [1] by using the standard centered setup with the unpolished Si[111] monochromator: δE=1.1μeV. This allows to resolve the previously observed inelastic bands.

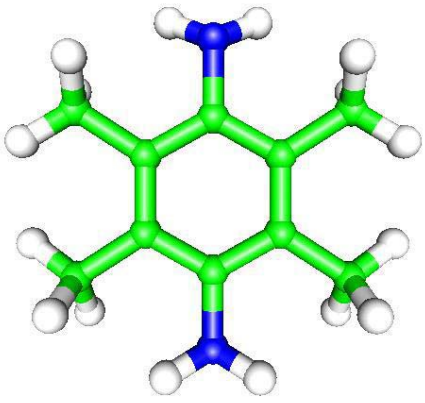


Fig.1 Schematic view of diaminodurene molecule.

The figure 2 compares the spectrum of DAD taken at a sample temperature T=4.5K with the resolution function of the spectrometer. The presence of 3 tunneling transitions is visible and confirmed by a fit procedure. The three tunnelling transitions at energies 1.5, 4.0 and 6.5μeV show relative intensities are 2:1:1 compared to an elastic intensity of 35. The inner line was not seen in the previous experiment. The band intensities can be interpreted with respect to structural properties. If we assume that all tunnel splittings are resolved and allow for some spurious elastic intensity from Bragg reflections etc we can conclude that the unit cell of DAD contains a single type of molecules at a site of no symmetry.

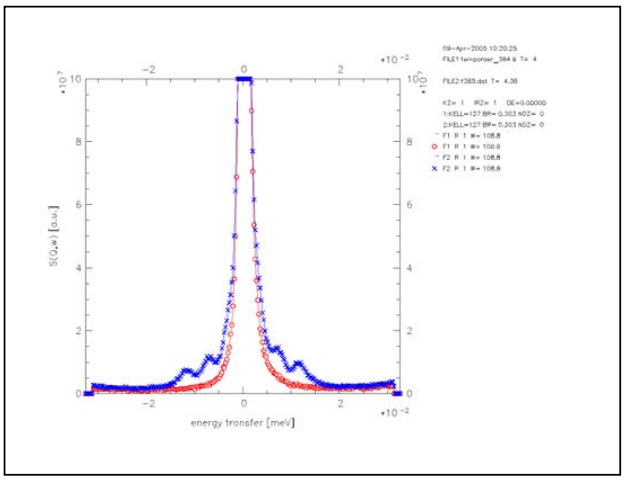


Fig.2 Spectrum of diaminodurene (xxx) in the μeV range. Sample temperature T=4.5K. Resolution function (ooo) for comparison

[1] Experimental reports FRJ2 2004, BSS-04-003

Institut für Festkörperforschung
Forschungszentrum Jülich GmbH
D-52425 Jülich

Experimental Report
of Neutron Scattering Experiments
at the FRJ-2 Reactor

Proposal number:	BSS-05-012		
Experiment title:	Effect of solvents on dynamics of a β-lactoglobulin protein		
Dates of experiment:	18-29, August, 2005	Date of report:	1 March, 2006
Experimental team: Names	Addresses		
BELLISSENT-FUNEL, Marie-Claire YOSHIDA, Koji	Laboratoire Léon Brillouin (CEA-CNRS), CEA-Saclay 91191 Gif-sur-Yvette cedex, FRANCE Laboratoire Léon Brillouin (CEA-CNRS), CEA-Saclay 91191 Gif-sur-Yvette cedex, FRANCE		
Local Contact:	Dr. Andreas Wischnewski		

Experimental report text body

Solvent plays an important role in the protein folding. Alcohol, which is one of them, has the capability to increase the content of secondary structure (α-helix) in proteins and to denaturate the protein. In the present experiment, in order to observe the solvent effect on protein dynamics, inelastic neutron scattering of β-LG (BLG) with adsorbed H_2O, D_2O, ethanol, and deuterated ethanol (4 samples) were measured with High Resolution Backscattering Spectrometer (BSS). Amount of adsorbed solvents for all samples is 0.5 g per g of dry protein. The Q values for each sample are ranging from 1.6 to 18.2 nm^{-1}. Temperatures measured are 280 K and 298 K. Measuring time was 24 hours per spectrum. In addition, we measured an enpty can and a vanadium plate for resolution measurement. (The energy resolution is 1.3 ~ 1.8 μeV.)

Figure 1 shows some typical dynamical structure factors at Q= 9.7 nm^{-1}. The peak intensities of samples were normalized to that of vanadium spectra. The quasielastic peaks of both H_2O-BLG and ethanol-h-BLG are clearly shown in the Figure 1 (a). These spectra contain both contributions from surface water (or ethanol) molecules and protein. Although some features of hydrated protein dynamics from sub-picosecond to nanosecond were previously revealed by elastic, quasielastic, and inelastic incoherent neutron-scattering measurements [1], the present results revealed that such a slow dynamics of protein exists in ethanol as well as in water. The relaxation of surface water molecule and protein in H_2O-BLG is faster than that of ethanol molecule and protein in ethanol-h-BLG. Previously, we measured water and ethanol adsorbed BLG with the zero-field spin echo spectrometer located at reactor Orphée of LLB and investigated the intermediate incoherent scattering functions $I(Q,t)$ at Q = 8 - 18 nm^{-1}. A relatively slow relaxation was found, implying the

existence of a slow dynamics of both protein and surface solvents. The present results look in agreement with the NSE results. From the difference between the quasielastic spectra shown in Fig.1 (b), we will deduce the dynamic properties of surface water [2]. The same information can be obtained for surface ethanol from Fig. 1 (c). Fig 1 (d) exhibits some tiny differences between dynamics of BLG respectively in D_2O and ethanol-d. There is same tendency for dynamics of BLG protein in D_2O to be faster than in ethanol-d. It is consistent with MD simulation results that a small peptide (melittin) in pure water takes more various conformations than in alcohol-water mixture [3].

The present results will allow us to access the local site dynamics of the protein depending on the solvents. This dynamic information will give us important hints to understand the role and underlying mechanism of solvents such as water and alcohols in protein folding. The further analysis is in progress.

References

[1] F. Gabel, D. Bicout, U. Lehnert, M. Tehei, M. Weik, G. Zaccai, *Quart. Rev. Biophys*. **35**, 327 (2002).

[2] S. Dellerue, M.-C. Bellissent-Funel, *Chem. Phys.* **258**, 315 (2000).

[3] M. Fioroni, K. Burger, A. E. Mark, D. Roccatano, *J. Phys. Chem. B* **105**, 10967 (2001).

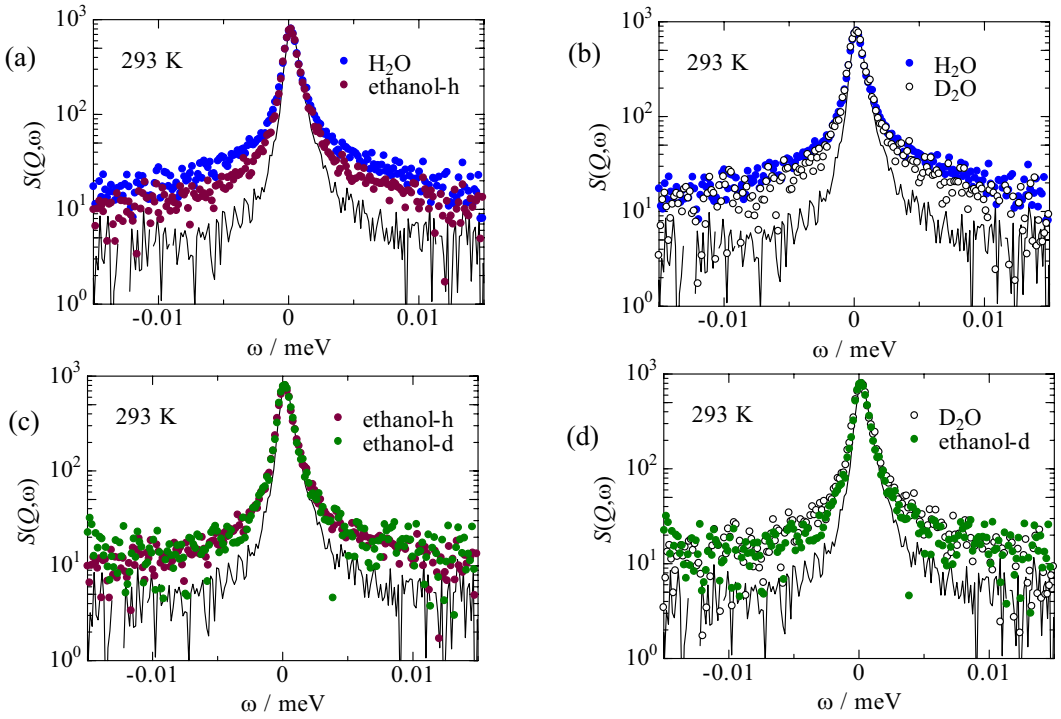


Fig.1. Dynamical structure factors of water and ethanol adsorbed BLG powder at Q = 9.7 nm^{-1}. The solid lines indicate the resolution function. The peak intensities of samples are normalized to that of vanadium spectra. (a) H_2O-BLG and ethanol-h-BLG at 293 K, (b) H_2O-BLG and D_2O-BLG at 293 K, (c) ethanol-h-BLG and ethanol-d-BLG at 293 K, and (d) D_2O-BLG and ethanol-d-BLG at 293 K.

Institut für Festkörperforschung
Forschungszentrum Jülich GmbH
D-52425 Jülich

Experimental Report
of Neutron Scattering Experiments
at the FRJ-2 Reactor

Proposal number:	BSS-05-016		
Experiment title:	**Extraction of radial and longitudinal dynamics of nano-alumina confined polymer electrolytes.**		
Dates of experiment:	12/12/2005 to 19/12/2005	Date of report:	13/01/2006
Experimental team: Names	Addresses		
Karine Lagrené Jean-Marc Zanotti	Laboratoire Léon Brillouin (CEA-CNRS) C.E.A Saclay 91191 Gif-sur-Yvette Cedex France		
Local Contact:	Dr. Michaela Zamponi		

Experimental report text body

Introduction

Porous alumina membranes (AAO) are macroscopically highly ordered nano-confining systems made of oriented parallel cylindrical channels. The "average out" of dynamical information occurring in isotropic confining systems can be then overcome by proper relative orientation of the AAO pore axes relative to the beam. The objective of the experiment was to extract the radial and longitudinal dynamical effect of confinement on hydrogenated PEO.

Experimental

The PEO used in the present study was hydrogenated PEO (molecular weight = 600,000 g/mol, Aldrich). A 0.2 ± 0.05 mm thickness PEO film was prepared by melting under vacuum at 95°C the needed amount of PEO directly into the neutron measuring cell (total polymer mass 430 mg).

Porous alumina membranes (AAO) are macroscopically highly ordered nano-confining systems made of oriented -tens of microm long- parallel cylindrical channels. MEB image of such a LLB custom made AA0 membrane show that the average pore radius is 20 nm. A single membrane is a 1 cm^2 single plate.

Confined samples were prepared by melting, under vacuum at 95°C, onto porous alumina membranes AAO membranes hydrogenated PEO 600000 g/mol. height such membranes filled with polymer were prepared. We estimate the total mass in the beam to be about 40 mg.

A quick test SANS experiment has been performed on the KWS-1 spectrometer (courtesy Dr. Pyckhout-Hinsen) on empty and full AAO membranes. Based on a contrast argument we are confident that the membranes pores were filled by the polymer.

Using BSS, an elastic scan has been performed on both the bulk and confined samples. As seen from figures 2 and 3, the melting temperature of the confined polymer is reduced by 10 degree compared to the bulk. These results are in agreement with previous DSC measurement (Figure 4), confirming a striking confinement effect.

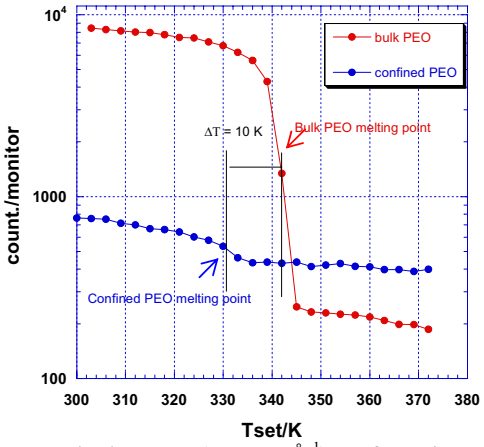


Figure 1: Elastic scans (Q=1.28 Å^{-1}) performed on bulk PEO and confined PEO from 300 K to 373 K.

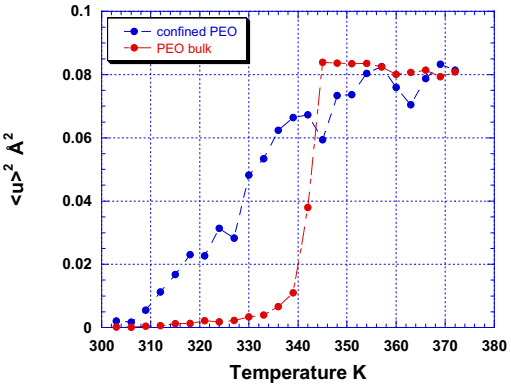


Figure 2: Temperature dependence of the mean square displacement <u>^{2} for the bulk and confined PEO.

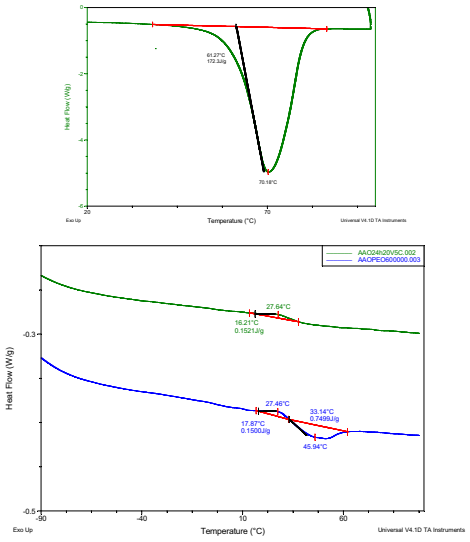


Figure 3: DSC measurement for bulk (top) and confined PEO (blue curve bottom plot, empty AA0 membrane is the green curve).

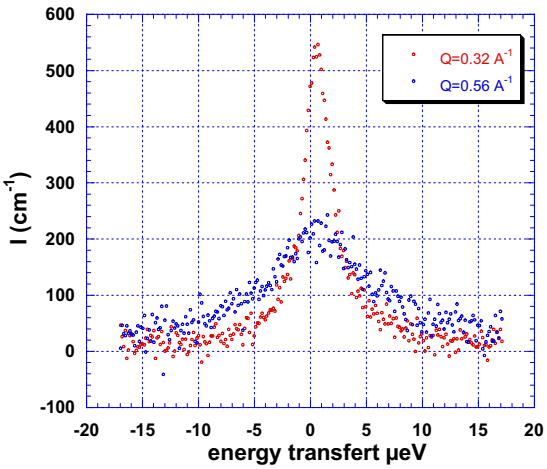


Figure 4: Bulk PEO S(Q,ω) at T = 373 K.

Scattering was nevertheless too weak to perform inelastic scans on the confined polymer above the melting point (see relative intensities Fig.1). We have therefore performed a full inelastic measurement on the bulk sample (Figure 4).

To obtain excellent statistics, this measurement has been performed at a single temperature (373 K) so as to test a new model (describing bulk PEO dynamics) under development in our team.

Institut für Festkörperforschung
Forschungszentrum Jülich GmbH
D-52425 Jülich

Experimental Report
of Neutron Scattering Experiments
at the FRJ-2 Reactor

Proposal number:	BSS-05-017		
Experiment title:	**Isotropic spin relaxation in hematite (α-Fe_2O_3) nanoparticles**		
Dates of experiment:	28.09. - 07.10. 2005	Date of report:	17. 10. 2005
Experimental team: Names	Addresses		
Christian R. H. Bahl Luise Theil Kuhn (Dr.) Hjalte Sylvest Jacobsen	Materials Research Department, AFM-228 Risø National Laboratory Frederiksborgvej 399 DK-4000 Roskilde Denmark		
Local Contact:	Andreas Wischnewski		

Experimental report text body

The present experiment is a continuation of experiment number BSS-04-023. Here the spontaneous reversal of the magnetisation due to thermal effects, so-called superparamagnetism, was studied in hematite nanoparticles. To samples of 8 nm nanoparticles of the canted antiferromagnet hematite (α-Fe_2O_3) were studied, one as-prepared, where there is a strong interparticle (exchange) interaction, and one where the particles have been individually coated with phosphate thus reducing these interactions significantly. In the present work the study of these two samples was continued. The aim was to study the phenomenon of isotropic relaxation of the spins, which is predicted to occur when the time scale of superparamagnetism and collective magnetic excitations becomes similar. Collective magnetic excitations are coherent precessions of the spins around the easy axis of magnetisation.

Isotropic relaxation is predicted to be observed as a large reduction in the scattering signal from a magnetic Bragg reflection. Elastic temperature scans of the sample of the strongly interacting particles are presented in Figure 1. As can be seen, the intensity decreases in all of the detector channels, probably due to water bound to the surface of the particles. However, the signal in the channels recording magnetic Bragg peaks (q=1.52Å^{-1} and q=1.28, Bragg peaks at q=1.51 Å^{-1} and 1.37Å^{-1}) decreases fastest. Normalising these signals by the signal from the structural reflection (q=1.72Å^{-1}, Bragg peak at q=1.70Å^{-1}) gives the data in Figure 2. The solid green line is from data recorded previously on the weakly interacting sample. This displays a very rapid decrease of intensity around 50 K. The data from the sample of strongly interacting particles has a gradual decrease at low temperatures, becoming more rapid at higher temperatures, as illustrated by the two black line segments as guides to the eye. The initial slow decrease can be ascribed to the decrease in the average magnitude of the spins caused by the increasing opening angles of the collective precessions with temperature. The Neél temperature is at around 950 K, so there is no significant decrease in the magnetisation due to temperature.

The later onset of isotropic relaxation and less dramatic decrease was expected in the sample of strongly interacting particles, as the interactions will lead to a broad distribution of timescales for the spin dynamics.

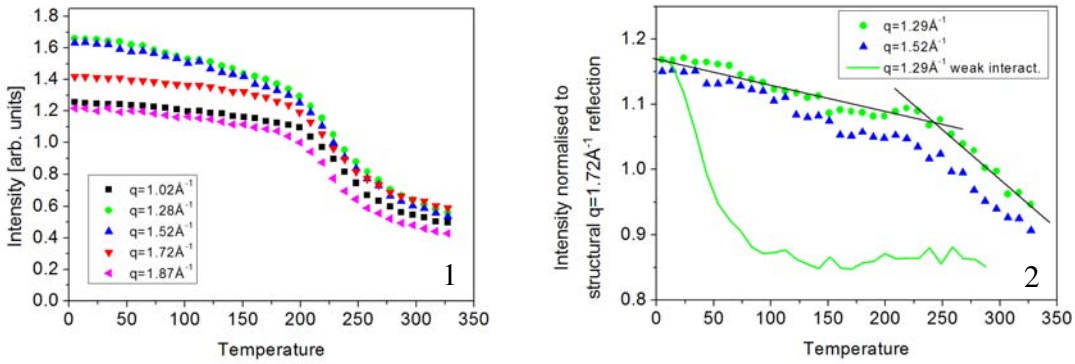


Figure 1: Elastic intensity from five of the detector channels. The detectors centred around q=1.28 Å^{-1} and q=1.52 Å^{-1} record antiferromagnetic reflections at q=1.37 Å^{-1} and q=1.51 Å^{-1} and the detector centred at q=1.72 Å^{-1} records the structural reflection at q=1.71 Å^{-1}. The detectors centred at q=1.02 Å^{-1} and q=1.87 Å^{-1} measure background q- values. The decrease of the magnetic reflections with temperature is seen, but it is difficult to quantify it, as the intensity in all the channels drops.

Figure 2: Comparison of the elastic signals for the strongly interacting particles (▲ and ●) and the weakly interacting particles (solid line), normalised to the signal from the structural reflection at q=1.72 Å^{-1}. The line segments are guides to the eye, illustrating the two rates of decrease.

The areas and widths of the quasi-elastic peaks from the superparamagnetic signals are fitted with a Lorentzian line shape. As this Lorentzian signal is quite weak, great care should be taken when fitting. Some preliminary parameters of the fitted Lorentzian are presented in Figure 3 as solid symbols. The open symbols are the fitted parameters from the previous experiment. It is clearly seen how the width and area of the quasi-elastic Lorentzian grow exponentially in the sample of weakly interacting particles, before gradually decreasing. In the sample of strongly interacting particles, the increase is slower and the area only saturates, but does not decrease at the measured temperatures.

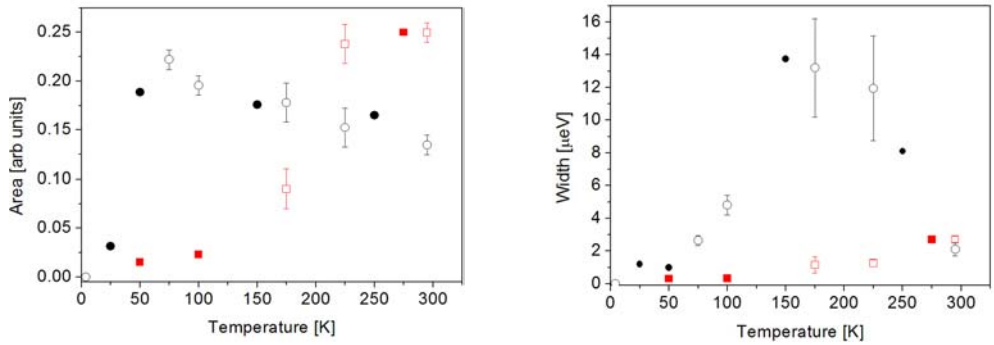


Figure 3: The width and area of the quasielastic Lorentzian, due to superparamagnetism. The graphs show the data from the sample of weakly interacting particles (● and ○) and data from the sample of strongly interacting particles (■ and □). The closed symbols are preliminary fits to the data from the present experiment, while the open symbols display the data from the previous experiment.

In conclusion, we have shown that the relaxation of spins in hematite nanoparticles changes from a regime of superparamagnetism, to one of isotropic spin relaxation. In the strongly interacting particles, the onset of this transition is delayed, due to a larger and broader energy barrier. The interacting particles effectively act as one large particle.

Institut für Festkörperforschung
Forschungszentrum Jülich GmbH
D-52425 Jülich

Experimental Report
of Neutron Scattering Experiments
at the FRJ-2 Reactor

Proposal number:	BSS-05-018		
Experiment title:	**Effect on poly(ethylene oxide) dynamics of intercalation in sheet silicate**		
Dates of experiment:	15.08 – 17.08.2005 29.08 – 02.09.2005 16.09 – 19.09.2005	Date of report:	02.03.2006
Experimental team: Names	Addresses		
Dr. Helen Hermes Dr. Henrich Frielinghaus Dr. Wim Pyckhout-Hintzen Dr. Andreas Wischnewski Prof. Dr. Dieter Richter	IFF, Forschungszentrum Jülich, 52425 Jülich IFF, Forschungszentrum Jülich, 52425 Jülich IFF, Forschungszentrum Jülich, 52425 Jülich IFF, Forschungszentrum Jülich, 52425 Jülich IFF, Forschungszentrum Jülich, 52425 Jülich		
Local Contact:	Dr. Andreas Wischnewski		

Experimental report text body

Polymer-clay nanocomposites have been found to exhibit enhanced mechanical and fire-retardant properties. Often, the clay must be organically "modified" to facilitate mixing with apolar polymers. To minimise the number of variables, we concentrate on a system in which the polymer interacts favourably with the clay without the need for such modification, i.e. the polyethylene oxide-montmorillonite system. Montmorillonite (MMT) is a naturally occurring layered silicate clay. In the dry state the individual platelet-like clay sheets which are about 1nm thick are stacked. A sandwich structure is formed if polymer intercalates between these platelets. To date, studies of polymer-clay composites and clay dispersions have been mainly limited to structural studies using small angle x-ray scattering. It is expected that studying the effect of confinement on the polymer chains and relating this to the enhanced mechanical properties observed will lead to an understanding of the behaviour of nanocomposites in general.

We have recently used solution intercalation to prepare composites of poly(ethylene oxide) (PEO) and sodium montmorillonite. Initial small angle neutron scattering experiments have been performed and the data described successfully[1]. X-ray scattering and differential scanning calorimetry measurements have confirmed that using this sample preparation method and a suitable composition, it is possible for all the PEO to be intercalated between the silicate layers. The thickness of the intercalated PEO layers is 0.815 nm and extremely constant. Thus, this system is ideal for investigating the effect of extreme confinement on the dynamics (and conformation) of PEO polymer chains.

In the literature, nuclear magnetic resonance has been used to investigate similar samples on the local scale[2]. Molecular dynamic simulations over the temperature range 273-423 K have been compared with these results and suggest that contrary to what might be expected, the confined polymer chains are less well ordered than in the bulk[3].

This BSS experiment on a system with 20% PEO (fully protonated) / 80 % MMT was a feasibility study to test whether the segmental dynamics of these two-dimensional PEO chains are accessible by backscattering.

Fig. 1 compares spectra at T=375 K and T=425 K with the resolution (sample at T= 4 K). A temperature dependent broadening is clearly visible. This illustrates that the dynamics are within the energy window of the BSS spectrometer. An extensive quantitative evaluation of the data is on-going.

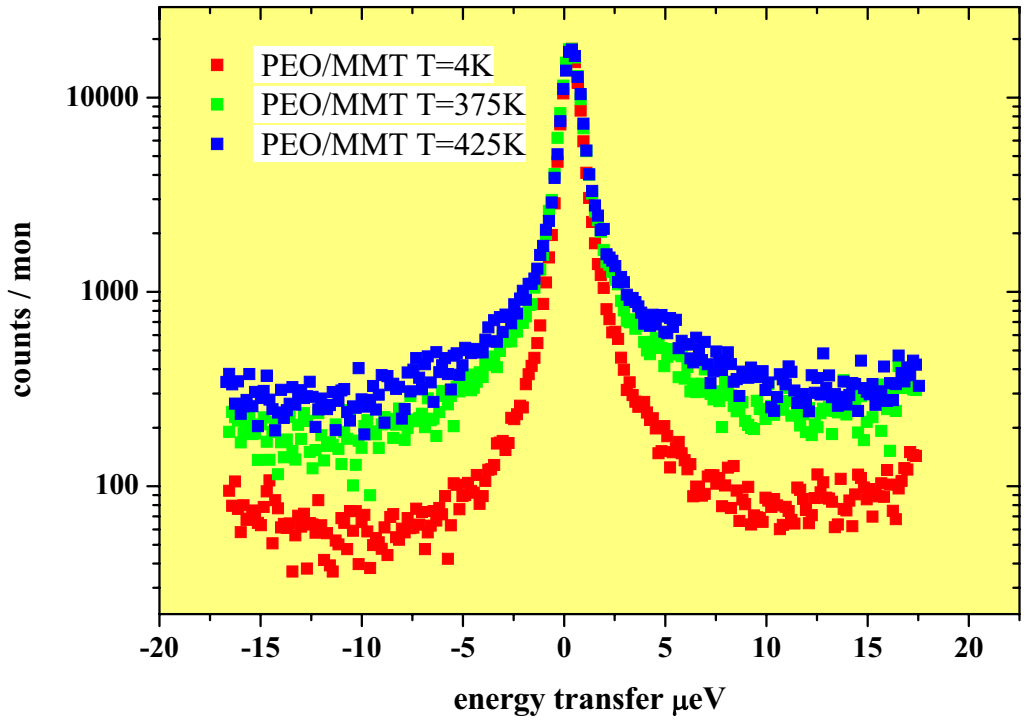


Fig.1: BSS spectra of 20% protonated PEO in MMT for T = 4K (resolution), 375 K and 425 K for Q = 1.7 Å^{-1}. The data are normalized to the same peak height.

References

1. H.E. Hermes, H. Frielinghaus, W. Pyckhout-Hintzen, D. Richter, Experimental report kw1-04-025
2. see for example: S. Wong, R.A. Vaia, E.P. Giannelis, D.B. Zax, *Solid State Ionics*, **86-88**, 547-557 (1996)
3. V. Kuppa, E. Manias, *J. Chem. Phys*., **118**, 3421-3429 (2003)

Institut für Festkörperforschung
Forschungszentrum Jülich GmbH
D-52425 Jülich

Experimental Report
of Neutron Scattering Experiments
at the FRJ-2 Reactor

Proposal number:	BSS-05-021		
Experiment title:	Isomerism and methyl rotational potentials of xanthines containing two methyl groups		
Dates of experiment:	1.12.2005, 4 days	Date of report:	25.2.2006
Experimental team: Names	Addresses		
A. Pawlukojc M. Prager	Institute of Nuclear Chemistry and Technology, Warsaw, Poland Forschungszentrum Jülich		
Local Contact:	M. Prager		

Experimental report text body

The methylxanthines represent a biologically most important class of molecules. These rather simple double ring molecules include the natural drugs caffeine, theobromine and theophylline which are used in daily live and medical application.

Caffeine is an alkaloid found in such foods as coffeefruit, tea etc. Its main pharmacological properties are a stimulant action on the central nervous system with psychotropic effects and stimulation of respiration, a stimulation of the heart rate. By oxidative demethylation caffeine is metabolized in the liver to the dimethylxanthines theobromine, theophylline and paraxanthine. In a second step demethylation leads to monomethylxanthines. Other metabolic steps follow. Theobromine is an alkaloid found in cocoa and chocolate. Theobromine has an antitussive effect superior to codeine by suppressing vagus nerve activity. Theophylline is a drug, a phosphodiesterase inhibitor, that is widely used in therapy for respiratory diseases. It is naturally found in black tea and green tea. The main actions of theophylline are relaxation of bronchial smooth muscle, positive inotropic (increases heart muscle contractility and efficiency) and positive chronotropic (increases heart rate) impact. It lowers blood pressure and has some anti-inflammatory effect. While caffeine, theobromine and theophylline are biologically active paraxanthin, interestingly, is inactive and therefore also non toxic.

Theobromine, theophylline and 1,7-dimethylxanthin (paraxanthin) are isomeric molecules. While the first two alkaloids are contained in natural fruits the last material represents an artificially made analogue. The molecules differ by the positions of the 2 methyl groups on the double ring. The figure shows theophylline as an example

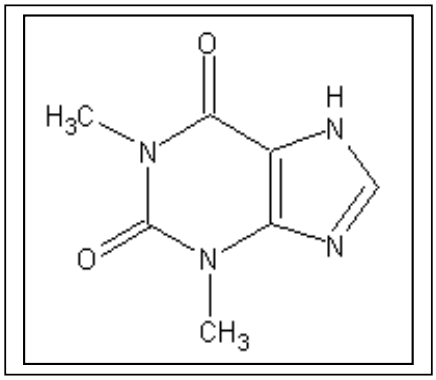


Fig. 1 Molecular structure of theophylline

In theobromine the methyl group between the two oxygens is moved to the upper nitrogen on the 5-ring. In 1,7-dimethylxanthin the bottom CH_3 is moved to this position. In caffeine with its third methyl group all three nitrogen sites on the double ring with single bonds bind a methyl group. This structure allows no isomeric form. The question ois whether the similarity of molecular structure is found in a similarity of methyl dynamical behaviour. It is well known from the halomesitylenes and their derivatives that the hindering potential can strongly and often unexpectedly change with the methyl group position and neighborhood in the ring [1].

This experiment complements the investigation of lattice modes [2]. Two techniques were used to characterize the methyl rotational dynamics: the fixed window technique (FW) and real spectroscopy. The figures 2 shows a spectrum comparing theophylline with a tunneling band at about 16μeV and 1,7-dimethyl-xanthine without. Fig 3 reproduces the FW scan of theophylline. The intensity step at low temperature is a sign beginning stochastic reorientation. The corresponding soft rotational potential is consistent with the observed large tunnel splitting. The decay looks even to be a superposition of two dynamic processes. A similar two step behaviour is observed for theobromine. Caffeine and 1,7-dimethyl-xanthine show the corresponding decays at higher temperatures and as theobromine no tunnel transition. Further studies are planned.

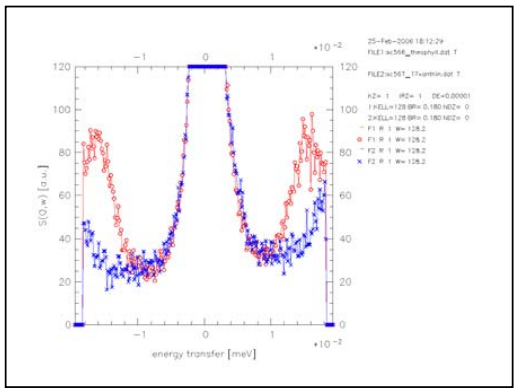


Fig. 2 spectra of theophylline (ooo) and 1,7-dimethyl-xanthine

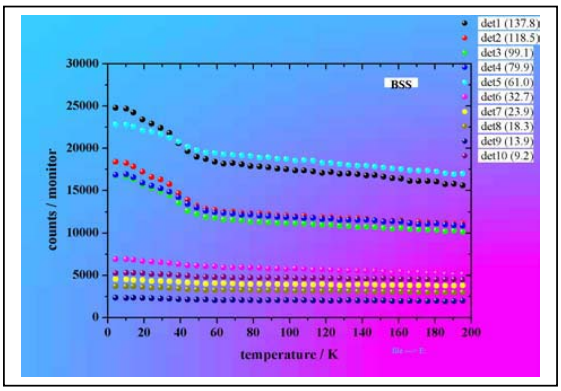


Fig. 3 Fixed-window scan of theophylline.

Despite of close structural similarities of the molecules there are clear differences in the spectra. The data analysis is in progress and will be based on DFT and lattice dynamical calculations.

[1] A. del Rio, A. Boucekkine, J. Meinnel, J. Comp. Chem. 24,2093(2003)
[2] Experimental Reports FRJ2 2005, this volume, Report S29-05-006

Institut für Festkörperforschung
Forschungszentrum Jülich GmbH
D-52425 Jülich

Experimental Report
of Neutron Scattering Experiments
at the FRJ-2 Reactor

Proposal number:	BSS-05-023		
Experiment title:	Hydrogen dynamics in doped and undoped sodium alanate		
Dates of experiment:	25.01.-29.01.2006 and 17.02.-26.02.2006	Date of report:	02.06.2006
Experimental team: Names	Addresses		
Shi, Qing Jacobsen, Hjalte S. Lefmann, Kim Vegge, Tejs	Materials Research Department Risø National Laboratory, Building 229 Frederiksborgvej 399, P.O. Box 49 DK-4000 Roskilde, Denmark		
Local Contact:	Michaela Zamponi		

Experimental report text body

Introduction

In 1997 Bogdanovic and Schwickardi [1] discovered that transition metal doped sodium alanate, $NaAlH_4$, reversibly ab- and desorbs hydrogen at near ambient conditions. Since then the so-called complex hydrides have dominated the international research in solid-state hydrogen storage. The theoretical hydrogen storage capacity in complex hydrides is very high; upwards of 20 weight percent. However, little information is available about the catalytic effect of titanium on cyclic hydrogen ab- and desorption. Apart from the addition of Ti-based compounds, in particular $TiCl_3$, the hydrogen kinetics can also be improved by decreasing grain size [2]. Although a number of experiments aimed at investigating the hydrogen dynamics in $NaAlH_4$ and Na_3AlH_6 have been performed [3], no conclusive knowledge about the possible catalytic effect on local hydrogen motion, rotation and long-range diffusion has been obtained at present. Quasielastic neutron scattering (QENS) was proposed for providing information of these types of processes.

Experimental

The QENS measurements of undoped $NaAlH_4$ and Na_3AlH_6, and similar samples doped with 4 mol% $TiCl_3$, were performed at the BSS instrument of FRJ-2, Jülich. All four sample powders were prepared by high energy ball milling which was used to disperse the catalyst and lower relaxation times. All materials handling was performed in an argon-filled glove box and a 0.1 mm Al sandwich sample container was employed to minimize multiple scattering. First, inelastic temperature scans in a large temperature range were performed to reveal the presence of temperature dependent structural and dynamic effects. The neutron backscattering measurements were preformed continuously on the same geometry to obtain the quasielastic spectra.

Results

The results of the elastic temperature scan on Na_3AlH_6 are shown in Figure 1. No substantial temperature drops are observed at low temperatures, but a slow drop is observed at high temperatures.

Figure 2 shows the QENS spectra of undoped Na_3AlH_6 at different temperatures, where only the highest temperatures display a quasielastic broadening. Due to safety considerations we were unfortunately unable to go to higher temperatures

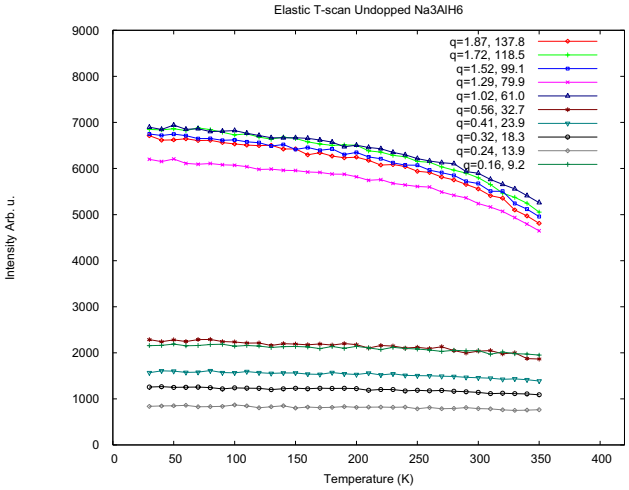


Figure 1

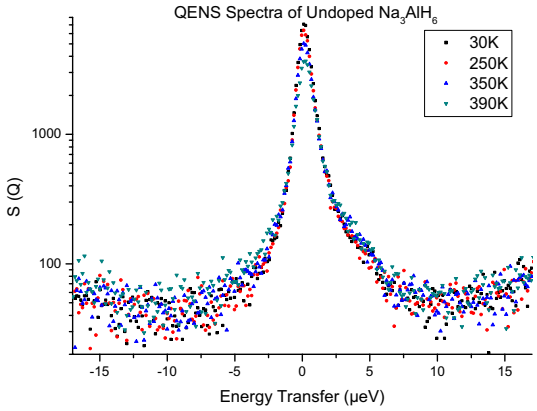


Figure 2

For each sample, QENS spectra were obtained at three-four different temperatures, and the data were processed by standard procedures. The instrumental resolution function was determined from the measured QENS spectra of each sample at low temperature (30K), and a quasielastic broadening of the signal was observed at temperature above 290K. The Lorenzian halfwidth of the quasielastic component is proportional to the hydrogen hopping rate and the diffusion constant. Using the Chudley-Elliot model [4] to describe the scattering vector dependence of the quasielastic Lorenzian halfwidth as a function of scattering vector can describe hydrogen jump diffusion in solids.

The long range hydrogen diffusion is found to be minimal, even when the materials are doped with $TiCl_3$, and the primary effect of the dopants can therefore be concluded not to be increased hydrogen diffusion in sodium alanate. The analysis of the processed data is currently being finalized and compared to values from density functional theory (DFT) calculations [5].

[1] B. Bogdanovic and M. Schwickardi, *J. Alloys Compds* **253**, 1 (1997).
[2] A. Andreasen, T. Vegge, and A.S. Pedersen, *J. Solid State Chem.* **178**, 3672-3678 (2005).
[3] O. Palumbo, R. Cantelli, A. Paolone, C.M. Jensen, S.S. Srinivasan, *J. Phys. Chem. B* **109**, 1168 (2005).
[4] C.T. Chudley and R.J. Elliot, *Proc. Phys. Soc.* **77**, 353 (1961).
[5] J. Voss, Q. Shi, H.S. Jacobsen and T. Vegge (to be published).

Institut für Festkörperforschung
Forschungszentrum Jülich GmbH
D-52425 Jülich

Experimental Report
of Neutron Scattering Experiments
at the FRJ-2 Reactor

Proposal number:	**BSS-05-024**		
Experiment title:	**Nature of Ag+ motion in silver iodide close to the superionic transition**		
Dates of experiment:	Feb 6th to Feb 12th 2006	Date of report:	May 17th 2006
Experimental team: León, Carlos	GFMC, Dpto. Fisica Aplicada III, Universidad Complutense Madrid Madrid 28040, SPAIN		
González, Miguel Angel [2]	Instituto de Ciencia de Materiales de Aragón & Institut Laue-Langevin 6 rue Jules Horowitz B.P. 156, 38042 Grenoble Cedex 9 (France)		
Local Contact:	Michaela Zamponi		

Experimental report text body

Objectives:
It is well known that AgI undergoes a superionic transition at 420 K in which the ionic conductivity increases about four orders of magnitude. We have previously performed Admittance Spectroscopy measurements that show that this dramatic increase of ionic conductivity is preceded by a continuous and smooth change in the dynamics of silver ions. In order to confirm the validity of our interpretation of the ionic conductivity measurements using an independent technique we performed a neutron scattering experiment aimed to probe directly the dynamics of the silver ions.
Results:
Before starting with the inelastic scans, and in order to choose the appropriate temperatures for them, we performed several (30 minute long) elastic scans in the temperature range 300 - 420 K looking for any changes in intensity due to silver ion hopping. However, the elastic peak intensity was always rather low, and did not show any step or change in slope with increasing temperature. Then we decided to start with an inelastic scan at room temperature for 24 hours. The scattering signal observed was quite poor in all detectors, except in two of them due to bragg reflections at the corresponding Q ranges. When correcting for resolution and background, the signal was indistinguisable from noise. We tried then to see any difference at a higher temperature, 417 K, close to the superionic transition from the beta to the alpha phase. But again the signal was indistinguisable from noise.
Unfortunately, it seems that the energy range explored in a backscattering experiment does not allow to investigate silver ion hopping dynamics in the beta phase, even at the highest temperatures close to superionic transition. The smaller energies / longer time scales accessible by a neutron spin-echo experiment may be more appropriate for it. We can not discard, however, that the low intensity of the inelastic scattering signal was just a consequence of the high absorption in this material.

Institut für Festkörperforschung
Forschungszentrum Jülich GmbH
D-52425 Jülich

Experimental Report
of Neutron Scattering Experiments
at the FRJ-2 Reactor

Proposal number:	BSS-05-026		
Experiment title:	Side-group motions of PMMA close and above the glass transition		
Dates of experiment:	09.01.-15.01.2006	Date of report:	22.06.2006
Experimental team: Names	Addresses		
Anne-Caroline Genix Arantxa Arbe Juan Colmenero Dieter Richter	Donostia International Physics Center, Apdo. 1072, 20080 San Sebastian, SPAIN Unidad de Física de Materiales, CSIC-UPV/EHU, “ , “ , “ Dpto. de Física de Materiales, UPV/EHU, , “ , “ , “ IFF, FZJ, Jülich, Germany		
Local Contact:	Andreas Wischnewski		

Experimental report text body

The aim of this experiment was to investigate the side-group dynamics in syndiotactic poly(methyl methacrylate) (PMMA) (T_g=400K) through the hydrogen motions. The dynamics of the side group is believed to play an essential role in the β-relaxation of this polymer. Large amplitude motions involving 180º flips around the C-C bond connecting the main chain and the ester group have been found from NMR studies close to the glass transition [1]. Jumps of even larger amplitude have recently been observed by us for the ester-group hydrogens from fully atomistic MD-simulations [2].

The sample studied was PMMA-d5 with both the main chain and the α-methyl group deuterated (see inset in Fig.1). In this way, the scattering is dominated by the incoherent contribution of the hydrogens of the ester methyl group. The BSS measurements have been performed at 6 temperatures: 4K, each 25K between 425K and 500K, and 520K. The sample was placed in an Aluminum flat container at 45º with respect to the incident beam. The thickness was such that a transmission of ≈ 0.9 was calculated. With λ=6.27Å a Q-range of 0.16 … 1.87$Å^{-1}$ was accessed and an energy window of ± 17μeV was explored. Measuring times of about 20 hours were employed to achieve reasonable statistics, as can be appreciated in Fig. 1. Vanadium and empty cell measurements were also carried out to correct the spectra.

From our last results obtained by DNS measurements [3] at 300K on the same sample, we know that the measured spectra contain a coherent contribution which will be non-negligible close to the first maximum of the corresponding static structure factor (Q_{max} ≈ 0.8 $Å^{-1}$). The Q-dependence of the characteristic times for the collective motions can be determined from our MD-simulations on PMMA at 580K and 540K. In Refs [2, 3],

it has been shown, that the structural and dynamical properties of PMMA are well reproduced by our MD-simulations allowing a 65K temperature shift. Thus, for the quantitative analysis of the BSS spectra at 520K and 475K, we described the coherent contribution by the Fourier transform of a stretched exponential function, $\exp[-(t/\tau)^{\beta}]$, with τ and β fixed from the MD-results at 580K and 540K, respectively. As a first approach, the contribution related to the incoherent scattering in the sample was also described by the Fourier transform of a stretched exponential function with β fixed to 0.5. The global side group dynamics is described by the sum of both functions where the respective proportions to the total scattering are given by the DNS data [3]. As can be seen in Fig.1, this fitting procedure delivers a reasonable description of the experimental data and allows determining the characteristic timescales for incoherent scattering. The results are displayed in Fig. 2 where they are compared to i) the timescales issued from the MD-simulations for the self motions of the ester hydrogens and ii) the data previously obtained by us from BSS measurements on PMMA-d3 [4]. In the PMMA-d3 sample, only the ester methyl group was deuteraded, which allowed accessing the dynamics of the main-chain and α-methyl group hydrogens [2, 4]. In Fig. 2, the characteristic times of self motions of the side groups in PMMA are significantly faster than those related to the main chain and α-methyl group, in good agreement with the MD-simulations results. However, the difference in the experimental timescales for main chain and ester side group seems to be more important in the high-Q range, whereas the MD-results suggest an increasing difference when moving towards lower-Q values. Further analysis is now needed to get deeper insight in the complex dynamics of the side groups in PMMA.

References:

[1] K. Schmidt-Rohr et al, Macromolecules 27, 4733 (1994)

[2] A.-C. Genix, A. Arbe, F. Alvarez, J. Colmenero, B. Farago, A. Wischnewski, D. Richter, submitted to Macromolecules

[3] A.-C. Genix, A. Arbe, F. Alvarez, J. Colmenero, W. Schweika, D. Richter, Macromolecules 39, 3947 (2006)

[4] A.-C. Genix et al, Experimental Report BSS-05-006

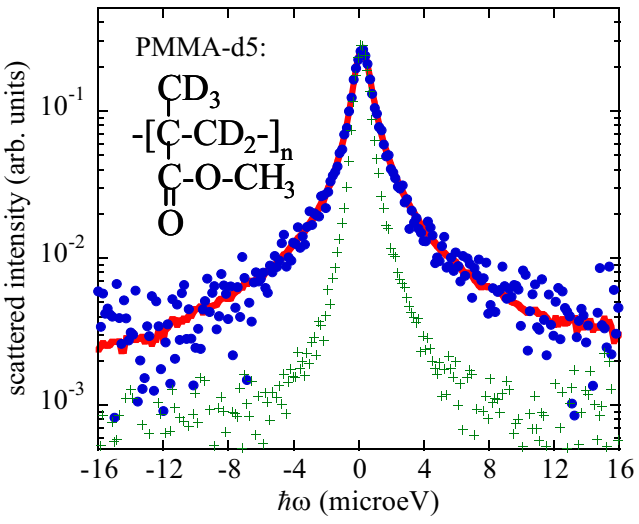


Fig. 1: Scattering function measured at Q =1.02 Å^{-1} for PMMA-d5 at 520K. The solid line is a fitting curve by means of the procedure described in the text to describe the overall dynamics of the side groups. The resolution function (PMMA-d3 at 4K) is shown by the crosses.

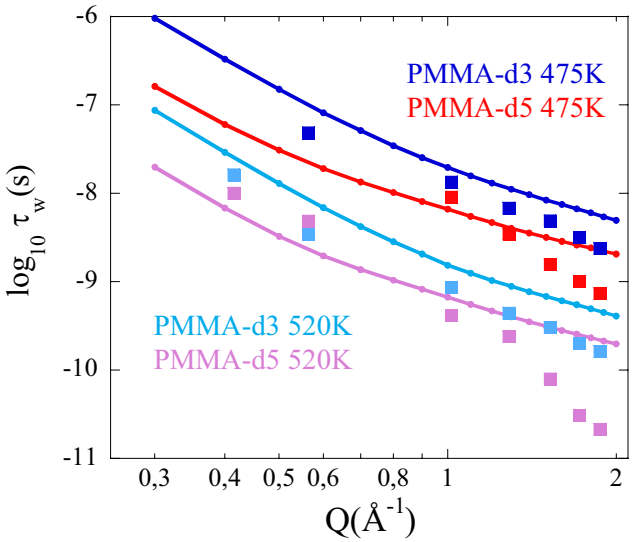


Fig. 2: Momentum transfer dependence in PMMA-d3 (blue) and PMMA-d5 (red) at 520K (light) and 475K (dark). Experimental results are represented by points and the corresponding MD-results by lines.

Institut für Festkörperforschung
Forschungszentrum Jülich GmbH
D-52425 Jülich

Experimental Report
of Neutron Scattering Experiments
at the FRJ-2 Reactor

Proposal number:	BSS-05-027		
Experiment title:	Backbone dynamics in poly(ethyl methacrylate): a neutron scattering characterization of the process leading to randomization of the chain		
Dates of experiment:	16.01.-24.01.2006	Date of report:	22.06.2006
Experimental team: Names	Addresses		
Anne-Caroline Genix Arantxa Arbe Juan Colmenero Dieter Richter	Donostia International Physics Center, Apdo. 1072, 20080 San Sebastian, SPAIN Unidad de Física de Materiales, CSIC-UPV/EHU, “ , “ , “ Dpto. de Física de Materiales, UPV/EHU, , “ , “ , “ IFF, FZJ, Jülich, Germany		
Local Contact:	Andreas Wischnewski, Werner Schweika		

Experimental report text body

The aim of this experiment was to investigate the segmental relaxation in poly(ethyl methacrylate) (PEMA) (T_g=338K) through the hydrogen motions. The sample studied was PEMA with deuterated alkyl side group. In this way, the spectra revealed the dynamics of the main-chain and α-methyl group hydrogens (see scheme), while the side-group contributions (CD_2-CD_3) were "hidden" for neutrons.

The BSS measurements have been performed at 9 temperatures: 4K, 250K, 285K, 325K, 400K, 425K, 454K, 487K and 520K. The sample was placed in an Aluminum flat container at 45º with respect to the incident beam. The thickness was such that a transmission of ≈ 0.9 was calculated. With λ=6.27Å a Q-range of 0.16 … 1.87$Å^{-1}$ was accessed and an energy window of ± 17μeV was explored. Measuring times of about 21 hours were employed to achieve reasonable statistics, as can be appreciated in Fig. 1. Vanadium and empty cell measurements were also carried out to correct the spectra. In addition, we performed DNS measurements on the same sample at 20K, 300K, 319K, 344K, 370K, 400K, 438K, 442K, by using the same container as for BSS. We used a wavelength of 3.3Å and measuring times of one hour were employed. Measurements of NiCr, Vanadium and empty cell were also carried out to correct the experimental data. DNS results are crucial for the proper dynamic (BSS) data correction and analysis. Results obtained at 300K are presented in Fig. 2 where two clearly distinguishable peaks can be observed at about 0.6 and 1.3$Å^{-1}$, in good agreement with a recent WAXS study [1] on this sample.

From our last results obtained by BSS and MD-simulations on PMMA [2, 3], we expected that, also for PEMA, the quasielastic broadening of the BSS spectra below T_g would only relate to the α-methyl group rotation. The

quantitative analysis of the spectra at 250K, 285K and 325K in terms of methyl group rotation delivers a very good description of the experimental data when using the parameters previously obtained by us in PMMA for the α-methyl group rotation (see Fig. 1). As expected, the increase of the side chain length from PMMA to PEMA does not seem to affect such localized motion. Above 338K, additional broadening is observed that should be attributed to the segmental relaxation. In a first approach, we will assume statistically independent rotation of the α-methyl group and segmental relaxation. Then, the global dynamics can be described by the convolution of both functions. In this framework, the α-methyl group rotation can be taken into account by construction of an "effective resolution" including the quasielastic broadening expected from this motion properly weighed by the relative abundance of such atoms and the appropriated EISF [3]. The segmental dynamics contribution will be described by the Fourier transform of a stretched exponential function, $\exp[-(t/\tau)^{\beta}]$.

The strongly heterogeneous and anisotropic motions proposed from recent NMR studies [4] should give rise to severe deviations from Gaussian behavior of the H-segmental dynamics. Therefore, the determination of the Q-dependence of the timescales characteristic for segmental motions is crucial to check the NMR results on this polymer.

References:

[1] M. Wind et al., J. Chem. Phys. **112**, 014906 (2005),

[2] A.-C. Genix, A. Arbe, F. Alvarez, J. Colmenero, L. Willner, D. Richter, PRE **72**, 31808 (2005)

[3] A.-C. Genix, A. Arbe, F. Alvarez, J. Colmenero, B. Farago, A. Wischnewski, D. Richter, submitted to Macromolecules

[4] M. Wind et al., PRL **91**, 155702 (2003); M. Wind et al., Macromol. Chem. Phys. **206**, 142 (2005).

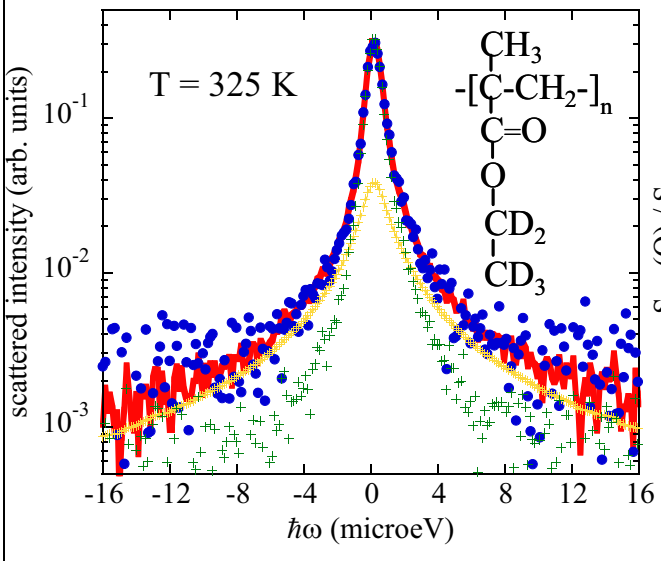


Fig. 1: Scattering function measured at Q=1.9Å^{-1} and 325 K for PEMA with deuterated alkyl groups. The red solid line is a fit by means of methyl group rotation. The yellow line shows the quasielastic component corresponding to methyl-group dynamics. The resolution function is shown by the crosses.

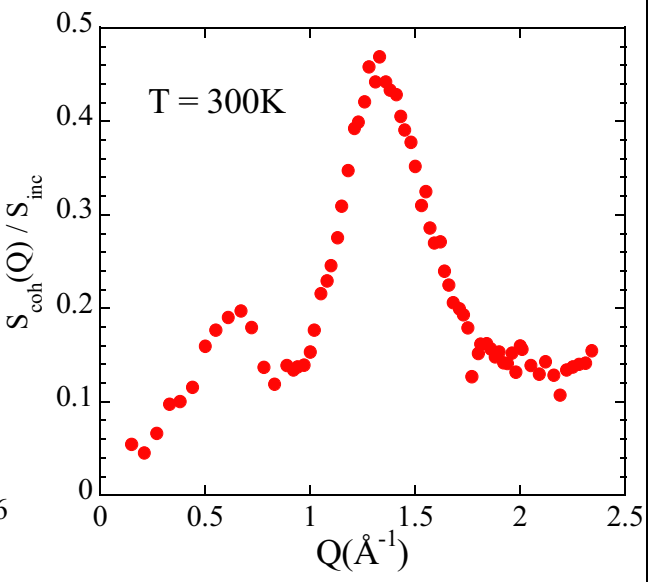


Fig. 2: Ratio between the coherent and incoherent scattering intensities measured by means of DNS at 300K in PEMA with the alkyl side group deuterated.

Institut für Festkörperforschung
Forschungszentrum Jülich GmbH
D-52425 Jülich

Experimental Report of Neutron Scattering Experiments at the FRJ-2 Reactor

Proposal number:	BSS-05-028		
Experiment title:	Rotational dynamics of methyl groups in the chloranilic acid plus 2,6-dimethylpyrazine complex		
Dates of experiment:	2.9.2005, 6 days	Date of report:	25.2.2006
Experimental team: Names	 Addresses		
A. Pawlukojc M. Prager	Institute of Nuclear Chemistry and Technology, Warsaw, Poland Forschungszentrum Jülich		
Local Contact:	H. Grimm		

Experimental report text body

The study of charge transfer/H-bond complexes using methyl rotational potentials as sensitive local probes is extended from the first investigated complex tetramethylpyrazin:chloranilic acid (TMP:CLA) [1] towards new systems. The actual compound, 2,6-dimethylpyrazin(DMP):CLA, was chosen since on the one hand the pure 2,6-DMP is already carefully studied with respect to structure [2] and dynamics [3] and since on the other hand the crystal structure of the complex is also known [4]. In pure 2,6-DMP the methyl groups feel a weak potential resulting in large tunnel splittings [3]. Therefore the influence of an electron acceptor neighbour on the lattice dynamics and methyl rotation in the molecular alloys of the charge-transfer type is expected to be accessible to spectroscopy.

The backscattering spectrometer was used in its centered configuration. A tunnel transition in the protonated DMP:CLA complex was observed at 3.30μeV (fig. 1, ooo). It shows an intensity of about 6.4% of the elastic intensity. If one calculates this ratio for the mean momentum transfer $Q=1.6A^{-1}$ theoretically for the case of one resolved and one unresolved (=elastic) tunnel band at the presence of the 2 protons of the chloranilic acid one gets a value 8.3%. Keeping in mind that there are other sources of elastic scattering this is a good confirmation that the crystal structure determined at T=100K is unchanged down to the T=4.5K, the sample temperature in the present experiment.

The tunneling tranition was investigated as a function of temperature. The line is to near to the elastic line to allow the more interesting line broadening to be reliably quantified. The temperature evolution of the position could be evaluated, however, and is shown in an Arrhenius presentation in fig. 2. The solid line represents a fit and gives an activation energy $E_S=16meV$ what is not to different from the observed energy of the methyl librational mode.

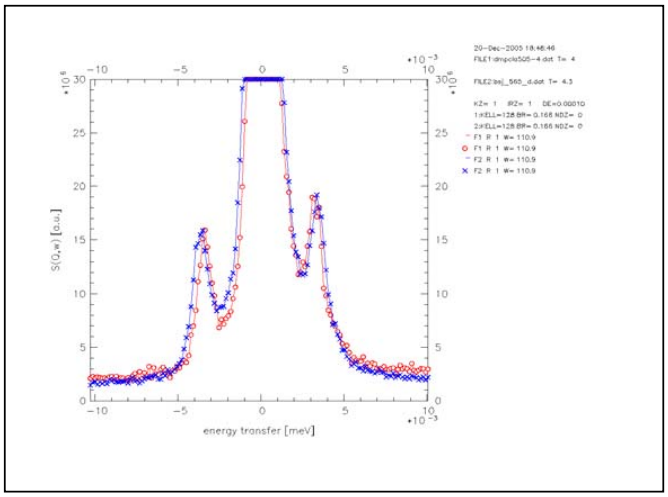


Fig. 1: Spectra of 2,6-DMP:h-CLA (ooo) and 2,6-DMP:d-CLA (xxx). Sa,mple temperature T=4.5K.

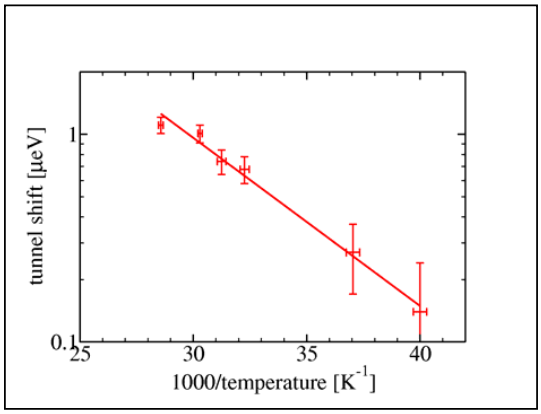


Fig. 2: Shift of the tunnel peak of 2,6-DMP:h-CLA with temperature. Arrhenius-plot.

Finally, the influence of deuteration of the cloranilic acid, i.e. the hydrogen bond, is searched for. Fig. 1, xxx, shows the spectrum of 2,6-DMP:d-CLA. The tunnelling band is unexpectedly found at weakly higher energy than in the protonated material. Usually the opposite effect is observed: the better localisation of deuterons causes a hardening of the material.

The methyl rotational potential in the 2,6-DMP:CLA complex is stronger as in pure 2,6-DMP. This means that intermolecular interaction strongly contributes to the rotational potential. The dominance of steric effect is supported by the opposite change of the hindering barrier observed in TMP:CLA [1]. An effect of charge transfer from the donor to the acceptor species of a complex is expected to cause changes of similar sign. Our data show that - if such an effect exists – it is largely hidden by the overwhelming dominance of structural changes.

A final data evaluation is in progress.

[1] M Prager, A Pawlukojc, L Sobczyk, E Grech, H Grimm, J. Phys.: Condens. Matter 17,5725(2005)
[2] E. KaiserMorris, A. Cousson, W. Paulus, F. Fillaux, Acta Cryst. E57,o1116(200)
[3] B. Nicolai, E. Kaiser, F. Fillaux, G.J. Kearley, A. Cousson, W. Paulus, Chem. Phys. 226,1(1998);
[4] W Sawka-Dobrowolska, G Bator, L Sobczyk, E Grech, J Nowicka-Scheibe, A Pawlukojc, Struct. Chem., in press;

Institut für Festkörperforschung
Forschungszentrum Jülich GmbH
D-52425 Jülich

Experimental Report
of Neutron Scattering Experiments
at the FRJ-2 Reactor

Proposal number:	BSS-05-029		
Experiment title:	**Supplementary backscattering experiments on a glass-forming microemulsion**		
Dates of experiment:	28.11.–06.12.2005	Date of report:	06.06.2006
Experimental team: Names	Addresses		
Mayorova Maria Zorn Reiner	Institut für Festkörperforschung, Forschungszentrum Juelich Institut für Festkörperforschung, Forschungszentrum Juelich		
Local Contact:	Michaela Zamponi		

Experimental report text body

The increasing demand of materials which are required to perform on spatial scales as small as several nanometers challenges our understanding of how geometrical confinement and interfacial situations change the properties of condensed matter. In the present work dynamics of viscous PG near its glass transition is to be explored for the case of soft confinement. Soft confinement is realized by a microemulsion as described below. For this purpose a three component system using PG as polar phase, decalin as nonpolar phase, and ionic surfactant AOT was chosen. The glass transition temperatures of the bulk PG and decalin are Tg=167 K and Tg=135 K, respectively. This microemulsion with reverse micelles is stable and optically clear**.** The sample has the composition (by weight of undeuterated compounds): PG 10,2%, AOT 36,1%, Decalin 53,7%.

To get information about slow dynamics, incoherent inelastic spectra have been obtained with back scattering spectrometer PI and then after Fourier transformation have been combined with time-of-flight data from NEAT (HMI, Berlin). To extract information concerning confined PG, data obtained for the completely deuterated microemulsion were subtracted from data for microemulsion with protonated PG and deuterated other components. Measurements were performed for two temperatures (230K and 270K). Unfortunately, the sample crystallized at 230 K so that the spectra taken at that temperature could not be evaluated. This happened completely unexpected because the temperature was reached by cooling the sample and in previous experiments (e.g. BSS-05-009) this was sufficient to avoid crystallization.

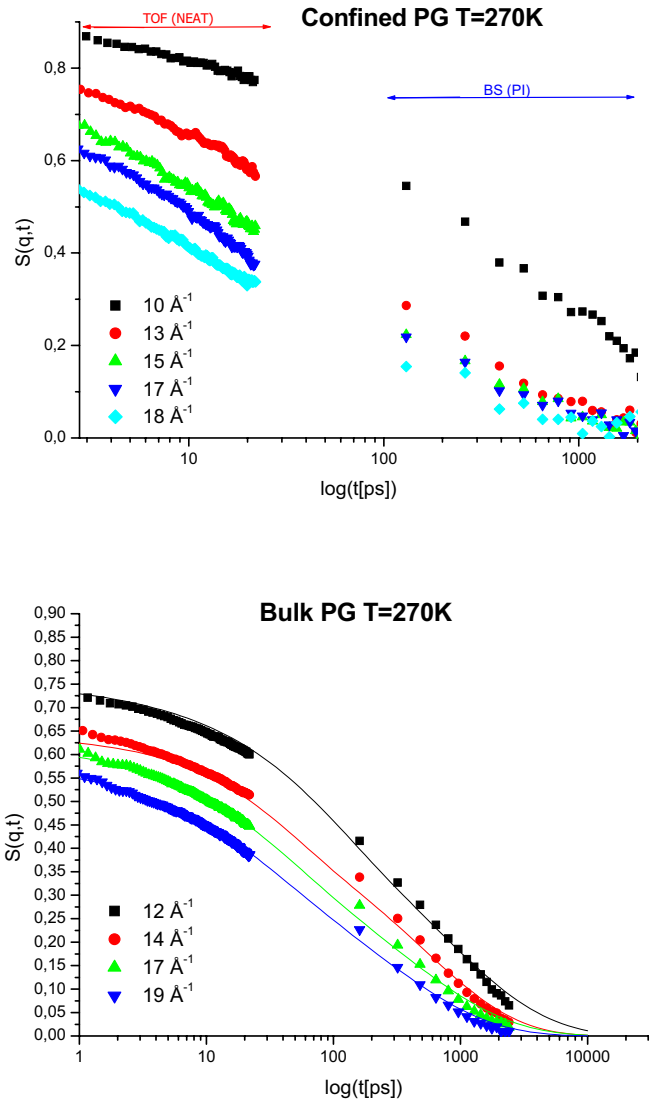


Fig. 1 Comparison of the intermediate scattering function S(Q,t) of PG confined in the microemulsion with bulk PG.

The comparison of the scattering function behavior for bulk and confined PG (Fig.1) provides information that in the case of confined PG the α relaxation is more stretched. This is a quite common behavior for this type of relaxation in confined glass forming liquids as the α relaxation is related to the cooperative group motion. The interaction between interfacial liquid layer and the static wall (hard confinement) or fluid environment (soft confinement) leads to existence of molecular groups with dynamics affected by the host material, which in turn results in stretching of α relaxation.

Institut für Festkörperforschung
Forschungszentrum Jülich GmbH
D-52425 Jülich

Experimental Report
of Neutron Scattering Experiments
at the FRJ-2 Reactor

Proposal number:	BSS-05-030		
Experiment title:	**Temperature dependence of hemoglobin dynamics in intact erythrocytes: A neutron scattering study**		
Dates of experiment:	16.-17.02.2006	Date of report:	05.06.2006
Experimental team: Names	Addresses		
A. Stadler J. Zaccai G. Artmann	ILL, 6 rue Jules Horowitz, BP 156, 38042 Grenoble, France ILL, 6 rue Jules Horowitz, BP 156, 38042 Grenoble, France FH Aachen, Ginsterweg 1, 52428 Jülich, Germany		
Local Contact:	Michaela Zamponi		

Experimental report text body

Incoherent elastic neutron scattering of red blood cells (RBC) has been measured with the spectrometer BSS. The glycocalix matrix of RBC has been removed by neuramidase treatment, intracellular hemoglobin has been stabilized by decarbolyxation with CO. A rather dilute concentration of RBC in H_2O has been measured to prevent the cells from destruction and to ensure the possibility of comparison with existing micropipette aspiration data [1], as a consequence only rather low intensity was measured at high q^2-values.

A diffusion model [2] could be fitted to the measured intensity according to

$$S(q^2) = \frac{C}{1 + \frac{D}{\Gamma} \cdot q^2}, \qquad (1)$$

the diffusion coefficient is named by D, Γ has got the value of $7.6*10^{-8}cm^2/s$ in the case of BSS and the coefficient C was introduced to take into account the temperature dependent loss of intensity.
The fit of equ. (1) is shown in Fig. 1 for the minimal and maximal measured temperatures. The coefficient C was determined by extrapolating $S(q^2)$ to $0Å^{-2}$, the temperature behaviour of C is shown in Fig. 2. The breakpoint at around 312K can be interpreted with the onset of large-range motions which are out of the time-space window of the instrument BSS.
The determined diffusion coefficient increases rather linearly with temperature and is shown in Fig. 3.

A more detailed data analysis is in the way. Additional neutron scattering experiments to study the thermal motions of intracellular hemoglobin of RBC are in preparation.

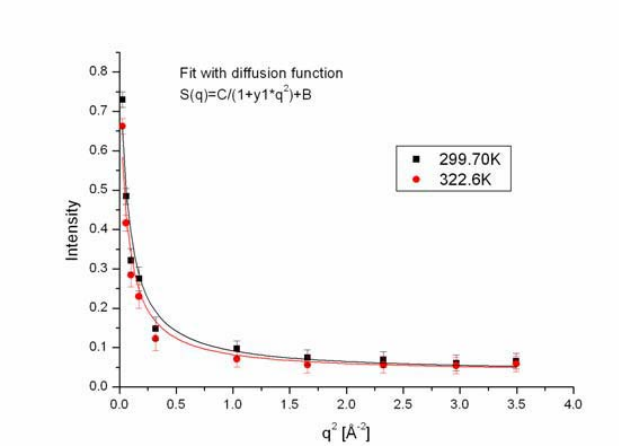


Fig. 1 Fit of model of free diffusion to the measured intensity S(q2) at two different temperatures.

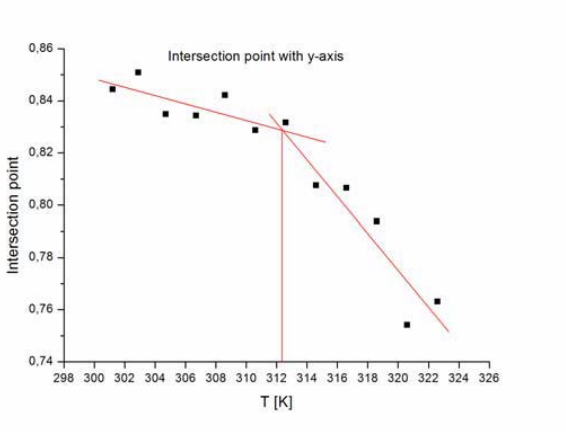


Fig. 2 At T≈312K the sharp drop of S(q2→0Å-2) indicates the onset of long-range motions which are out of the time-space window of the neutron spectrometer.

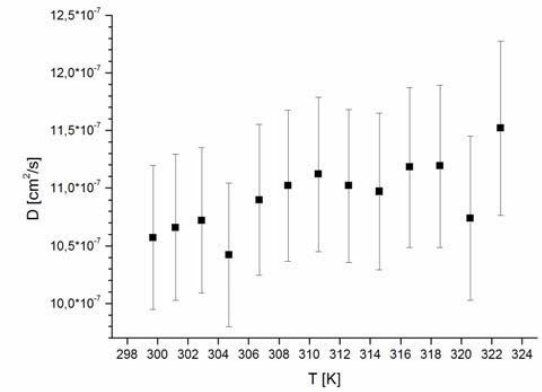


Fig. 3 The determined diffusion coefficient increases with temperature.

[1] Artmann G.M., Kelemen C., Porst D., Büldt G., Chien S. (1998)Temperature transitions of protein properties in human red blood cells. Biophys. J., 75: 3179-3183

[2] Gabel F. (2005) Protein dynamics in solution and powder measured by incoherent elastic neutron scattering: the influence of Q-range and energy solution. Eur. Biophys. J., 34:1-12

Institut für Festkörperforschung
Forschungszentrum Jülich GmbH
D-52425 Jülich

Experimental Report
of Neutron Scattering Experiments
at the FRJ-2 Reactor

Proposal number:	BSS-06-001		
Experiment title:	**Dynamics of syndiotactic polypropylene**		
Dates of experiment:	12.02.-14 .02.2006	Date of report:	23.05.2006
Experimental team: Names	Addresses		
M.Zamponi A.Wischnewski	Institut für Festkörperforschung, Forschungszentrum Jülich		
Local Contact:	M. Zamponi		

Experimental report text body

The topological confinement in polymer melts can be explored by mechanical (rheology) and microscopic (neutron spin echo (NSE) spectroscopy) experiments. For the so far investigated polymers (polyethylene (PE), polyethylpropylene (PEP)) the value for the confinement length obtained by NSE is considerable higher than the rheological value, however the ratio is about the same. To clarify if the observed discrepancies stem only from the different experimental techniques or from two different length scales in the polymer melt, the dynamical behaviour of a polymer with different properties shall be explored. If the deviations are only an experimental 'artefact' they should be comparable for all the polymers, independent on the properties. On the other hand if the two methods explore two different length scales (longitudinal and transversal confinement length) the ratio for a very stiff polymer should be different than for PE and PEP. Syndiotactic polypropylene (s-PP) is an ideal candidate since the stiffness parameter (C_∞) is significantly larger than for the other polymers but at the same time the segmental friction is expected to be low.

As a preparatory study for a proposed neutron spin echo experiment, neutron back scattering on a fully protonated s-PP sample has been performed. Inelastic scans at two temperatures (463K and 483K) have been done (fig.1). The obtained spectra show a clear quasi-elastic broadening, the observed temperature dependence is only weak. The quasi-elastic broadening can be described by a stretched exponential function with $\beta=0.5$ (Rouse expectation). The characteristic relaxation time is then $\tau=9\pi/(Wl^4)*q^{-4}$, where the Rouse rate $W=3kT/\xi l^2$ is determined by the segmental friction ξ. For each q-value the relaxation time has been fitted. Then from the resulting q-dependence of the time scale the Rouse parameter Wl^4 can be estimated (fig.2). From the fit Wl^4 has been calculated to be about 20000Å^{4}ns^{-1} at a temperature of 483K (13500Å^{4}ns^{-1} at 463K). Using this value in the reptation model the dynamic structure factor can be calculated, showing that the segmental motion is in the right time and q-range to be observed with the high resolution of NSE.

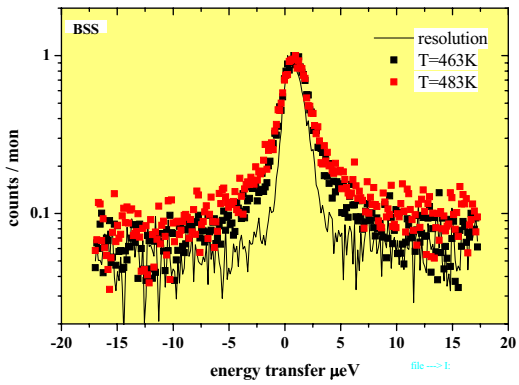


Fig.1: Neutron backscattering spectra of s-PP at two different temperatures in comparison to the resolution (line) for q=0.24Å^{-1}.

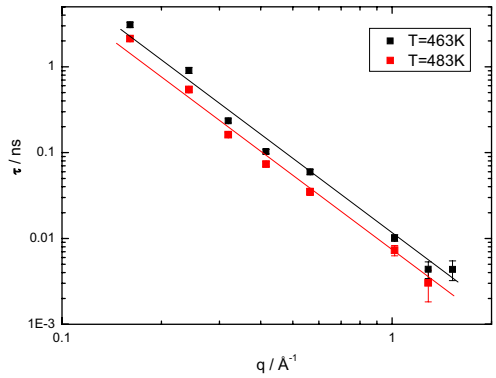


Fig.2: Characteristic relaxation time in dependence of q obtained from the BSS spectra. Lines: expected q-dependence $\tau=a*q^{-4}$.

Institut für Festkörperforschung
Forschungszentrum Jülich GmbH
D-52425 Jülich

Experimental Report
of Neutron Scattering Experiments
at the FRJ-2 Reactor

Proposal number:	BSS-06-002, BSS-06-003		
Experiment title:	**Dynamics of intercalated PEO in an PEO-MMT-nanocomposite**		
Dates of experiment:	15.3.2006 - 21.3.2006 21.4.2006 - 1.5.2006	Date of report:	9.5.2006
Experimental team: Names	Addresses		
Tobias Zacherle Dr. Andreas Wischnewski Prof. Dr. Dieter Richter	IFF, Forschungszentrum Jülich, 52425 Jülich IFF, Forschungszentrum Jülich, 52425 Jülich IFF, Forschungszentrum Jülich, 52425 Jülich		
Local Contact:	Dr. Andreas Wischnewski Dr. Michaela Zamponi		

Experimental report text body

In these experiments we investigated the dynamics of PEO (Poly-ethylene-oxide) intercalated between silicate sheets in the PEO-MMT-nanocomposite. In recent years research in the field of nanocomposites has increased dramatically, focussing both on the favourable properties of these materials [1] and the fact, that they represent model-systems for 2-d confinement for polymers [2]. One is interested in possible differences that may occur in comparison to the behaviour of bulk-polymer.
As the sample-preparation is somewhat difficult, we compared in previous SANS-measurements different preparation methods, in particular:

1. The method of freeze-drying. In this procedure one dries the MMT-PEO-solution by freezing it first and then sublimating the solvent. One obtains a fluffy material which needs to be pressed afterwards and dried in the vacuum.
2. The method of distillation under low pressure (film-method). Here the solution is dried by slowly reducing the pressure and vapourising the solvent. A gelous kind of material is obtained, depending on the time of distillation and this gel is further dried in the air on the sample-container and then in the vacuum.

As the film-method proved to be the better choice, we decided to stick to this procedure for our BSS-samples. Nevertheless we prepared two different kinds of samples for the two BSS-experiments. For the first one, we used water (H_2O) as a solvent, for the second one heavy water (D_2O). The second samples were believed to yield better results due to the lower incoherent scattering of deuterated water.

In both cases significant broadening of the peaks could be observed, i.e. the dynamics is within the energy window of the spectrometer. In addition the curves show the expected behaviour that the peaks broaden with increasing temperature. In the first plot, the results for the samples prepared with water are shown:

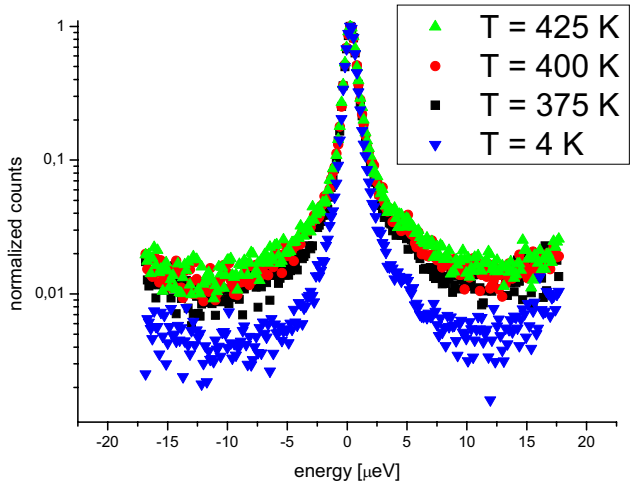
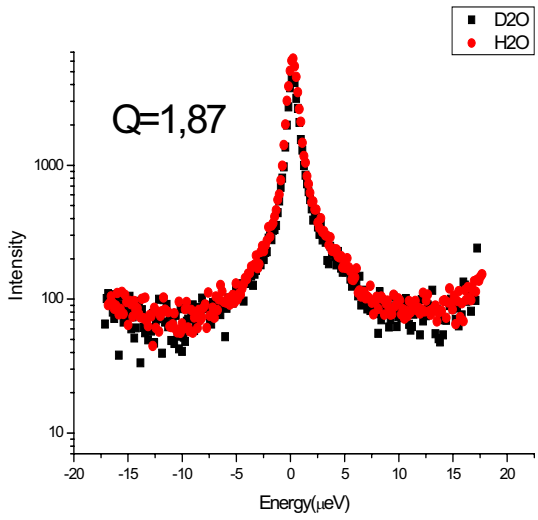
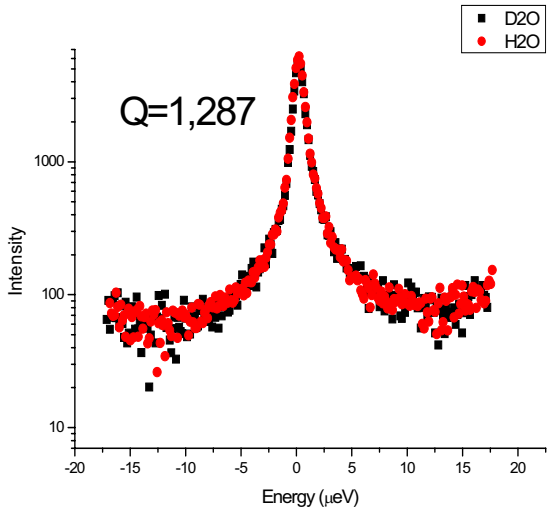


Fig1:
One sees clearly the broadening of the peaks with higher temperature. The slowest dynamics is obtained for the 4K resolution-curve, the fastest dynamics for the 425K measurement.

We were able to extract the corresponding relaxation-times τ, but a detailed analysis of the data is still ongoing.

In the second experiment – as already mentioned – we measured a sample for which D_2O was used as a solvent in the preparation-process. We did expect to see a rather big difference in the peaks, but it turned out that the two samples did behave very similar. Thus it can be concluded that the use of water or heavy water doesn´t play a major role during the preparation for the drying in the vacuum seems to be very efficient in both cases. So there isn´t any significant quantity of the solvent left in the sample.





On the two plots above, we show the results for the two experiments for two different Q-values. One sees, that the peaks are the same.

[1] S.S. Ray, M. Okamoto; Polymer/layered silicate nanocomposites: a review from preparation to processing; *Prog. Polym. Sci.* **2003**, *28*, 1539-1641
[2] R. Krishnamoorti et al.; Structure and Dynamics of Polymer-Layered Silicate Nanocomposites; *Chem. Mater.* **1996**, *8*, 1728-1734

Institut für Festkörperforschung
Forschungszentrum Jülich GmbH
D-52425 Jülich

Experimental Report
of Neutron Scattering Experiments
at the FRJ-2 Reactor

Proposal number:	BSS-06-004		
Experiment title:	**Multiple scattering of PEO/PMMA**		
Dates of experiment:	08.04.2006 –17.04.2006	Date of report:	22.05.2006
Experimental team: Names	Addresses		
Katarzyna Niedzwiedz Dr. Andreas Wischnewski Dr. Michael Monkenbusch Prof. Dr. Dieter Richter	IFF, Forschungszentrum Jülich, 52425 Jülich IFF, Forschungszentrum Jülich, 52425 Jülich IFF, Forschungszentrum Jülich, 52425 Jülich IFF, Forschungszentrum Jülich, 52425 Jülich		
Local Contact:	Dr. Andreas Wischnewski		

Experimental report text body

It is well known for blend systems that the behaviour of each component is influenced by the presence of the second one. However, up to now, it is impossible to predict the properties of a blend based on what is known about the behaviour of the pure components [1].

In particular interesting are blends of components with very different glass transition temperatures T_g, i.e. the dynamics of the pure components is well separated in time.
A good candidate for a systematic study of this topic by neutron scattering is the miscible PEO / PMMA blend, a system with widely separated glass transitions ($T_g^{PEO} \approx 210$ K, $T_g^{PMMA} \approx 400$ K).

Our first investigations on this system (35% h-PEO / 65 % d-PMMA and 50 % h-PEO / 50 % d-PMMA) shows that the PEO component is very mobile, but the dynamics seems to be restricted to small length scales. Moreover, we found that the low Q data ($Q < 1$ Å^{-1}) strongly deviate from the Debye-Waller-Factor (DWF), Eq. (1), which we found for the high Q data, see Fig. [1].

$$I = DWF = \exp\left(-\frac{Q^2\langle u^2\rangle}{3}\right) \qquad (1)$$

Here, $\langle u^2 \rangle$ is the mean square displacement determined by the fast processes.

An explanation for this deviation may multiple scattering. Therefore, to estimate the multiple scattering effect, we measured the 35% h-PEO / 65% d-PMMA blend system with a different thickness of the samples: d = 0.3mm, 0.5mm and 3mm. The measurements were done at three temperatures T = 375 K, 400 K and 425 K. For the proper data correction we determined the resolution of the instrument by measuring all samples at T= 4 K and the background by measuring the empty cell.

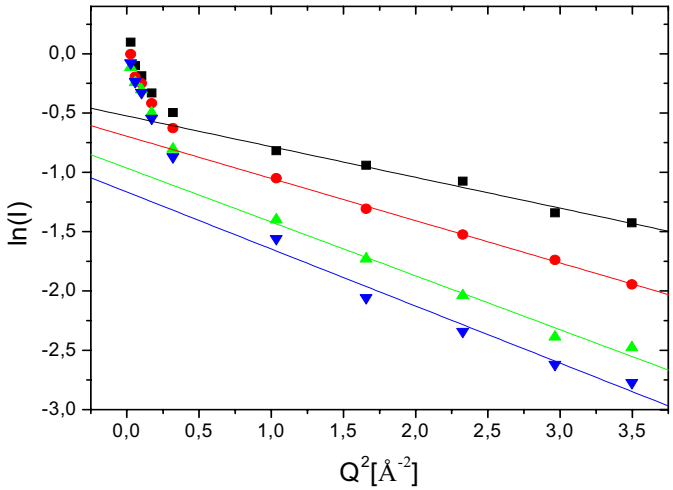


Fig. 1 Scattering intensity as a function of Q for the blend sample 35% h-PEO / 65% d-PMMA of 1mm thickness at different temperatures (black squares – 350 K, red circles – 375 K, green triangles up – 400 K, blue triangles down – 425 K). Solid lines represent fits with the DWF.

To have a good comparison of the scattering intensity we applied the identical fitting procedure to all data sets. The distribution function of relaxation times for the fast component PEO was fitted with the Kohlrausch-Williams-Watts (KWW) function. For the slow component PMMA we assume that it is stiff at the measured temperatures, so it contributes only to the elastic scattering. Thus the only fitted parameters were the total intensity I and the relaxation time τ of PEO, see Eq. [2]

$$I(Q,\omega) = DWF * FT\left\{\left[f * \exp(-(t/\tau)^{0.5}) + (1-f)\right] * resolution\right\} \quad (2)$$

Here, f is the relative amount of quasielastic scattering coming from PEO in the blend system, this value is known from an earlier DNS measurement.

Comparing the results obtained for the total intensity (Fig. [2], data for the sample with d=1mm coming from a previous BSS measurement, BSS-05-008), we observe that with increasing thickness of the sample up to 1mm, the scattering intensity decreases. Moreover, the deviation from the DWF for small Q seems to be systematic and is observed even for 0.3 mm thick sample. Clear evidence of multiple scattering is visible only for the 3 mm thick sample.

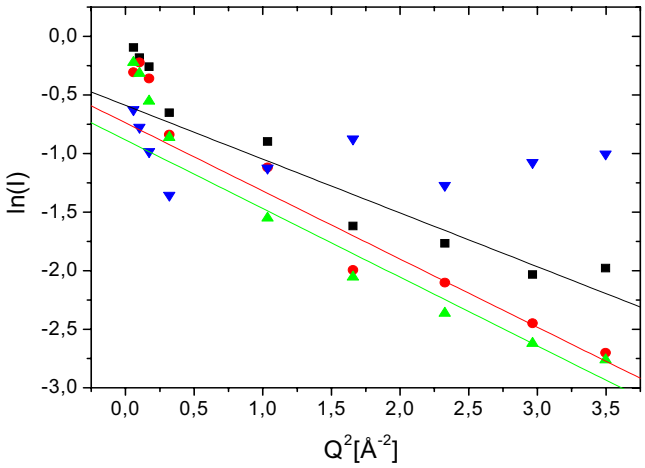
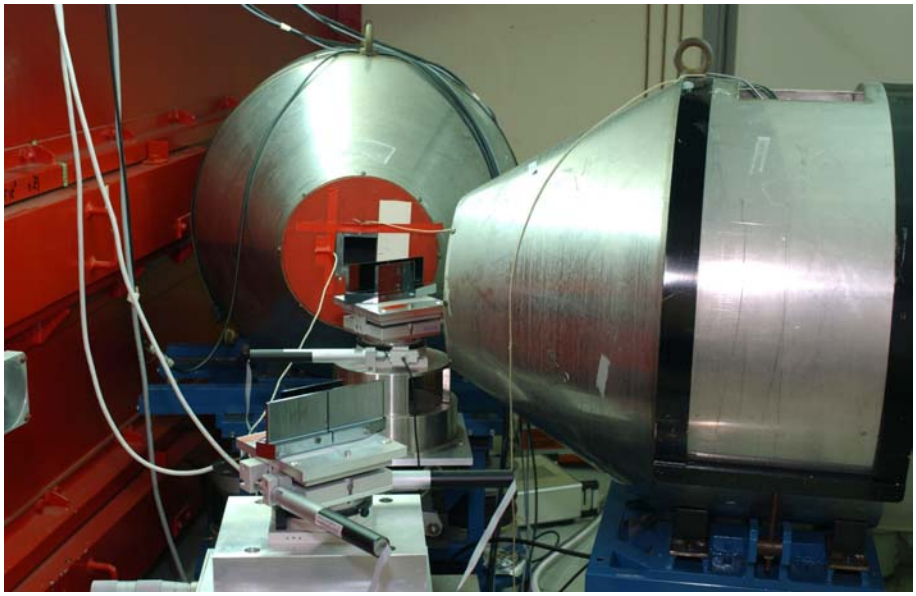


Fig.2 Scattering intensity of the blend sample 35% h-PEO / 65% d-PMMA as a function of Q at T=425 K for different samples thickness (black squares – 0.3mm, red circles – 0.5mm, green triangles up – 1mm, blue triangles down – 3mm). Solid lines represent fits with the DWF.

[1] S. Hoffman et al., Physical Review Letters 85, 772 (2000)

Double Crystal Diffractometer (DKD)



Instrument Parameters

Beam tube:	NLIIA straight guide cross section of guide 4.5 cm (height) × 3 cm (width)
Monochromator:	Si-crystal with coherent SiO_2 precipitates or graphite
Incoming beam ***- Cross section:*** ***- Sample size:***	 ≈ 10 cm^2 3 × 3 cm (max.)
Neutron flux at sample:	> 10^4 n/s (with graphite monochromator)
Momentum transfer range:	2×10^{-5} $Å^{-1} \leq Q \leq 10^{-3}$ $Å^{-1}$
Ancillary equipment:	heater device and pressure cell as for KWS1

Instrument Responsible

Dr. Dietmar Schwahn Tel. +49-(0)2461-61-6661 Email: d.schwahn@fz-juelich.de

Institut für Festkörperforschung
Forschungszentrum Jülich GmbH
D-52425 Jülich

Experimental Report
of Neutron Scattering Experiments
at the FRJ-2 Reactor

Proposal number:	DKD-04-005, KW3-04-016		
Experiment title:	The large-scale structures and morphologies formed by the co-crystallization of PEB-n random copolymers and paraffin waxes (5)		
Dates of experiment:	09.09.04 – 24.09.04 11.03.05 – 15.03.05 19.04.05 – 22.04.05 19.05.05 – 23.05.05	Date of report:	29.05.06
Experimental team: Names	Addresses		
Aurel Radulescu, Emmanuel Kentzinger, Jörg Stellbrink, Dietmar Schwahn, Manfred Heiderich	Forschungszentrum Jülich Institut für Festkörperforschung D-52425 Jülich Germany		
Local Contact:	Dr. E.Kentzinger, Dr.D.Schwahn		

Experimental report text body

As conventional SANS revealed [1,2] the PEB-n random copolymers form in solution needle-like aggregates in decreasing temperature. When paraffin wax is added to the polymer solution the scattering patterns collected under different contrast conditions and revealing the conformation of the polymer or wax within the common aggregates change strongly in comparison with the case of single polymer or paraffin wax solutions. When the copolymer self-assembles at temperatures higher than the wax crystallization point a complex shish-kebab-like morphology seems to occur [2]. Formation and structural evolution of such morphology was only partially understood by analysing the conventional SANS data. These allowed only an incomplete characterization of the common polymer-wax aggregates which seem to extend rather vastly in size surpassing the length scale covered by the conventional SANS method. Therefore new structural investigations were performed by involving the focusing-SANS (F-SANS) and the ultra- SANS (U-SANS) instruments set-up at the FRJ-2 reactor in Jülich. Combining the conventional-, focusing- and ultra-small angle neutron scattering methods the multilevel structures showing characteristic sizes from 10 μm to 1 nm and formed upon cooling in common solutions of semi-crystalline PEB-7.5 copolymers and waxes could be fully characterized. The conformation of the polymer and wax molecules within the common aggregates was analysed separately by using the contrast matching. The structural and density parameters of the aggregates have been evaluated using models. The experimental data collected in a slit-geometry at the U-SANS double-diffractometer were transformed into the pin-hole geometry according to a procedure described in [3]. An example of the scattering data collected over a very wide Q-range is given in Fig.1 where the scattering patterns under wax contrast are present at two temperatures within the wax-copolymer common aggregation regime for a mixed solution of 0.6% low M_W PEB-7.5 copolymer and 4% C_{24} wax in decane. The Q^{-2} power law behaviour at intermediate Q and the peak at around $Q^*=0.025$ $Å^{-1}$ shown at 0°C (also by the polymer scattering patterns not presented here) reveal a co-crystallization of polymer and wax into thin, very large platelets forming a correlated arrangement.

The lateral size of these platelets can be evaluated by analysing the Guinier regime identified at low Q. The model analysis of this morphology in terms of the paracrystalline structure factor applied to an ensemble of finite size discs, each disc being made by a wax and a polymer embedded layers is presented as solid line. The wax scattering pattern at -10°C reveals that the wax massively crystallizes and grows from thin platelets into large objects with sharp interfaces (Q^{-4} power law at higher Q). From an inspection of the low Q data measured by FSANS (10^{-4} to $2x10^{-3}$ Å^{-1}) and USANS (below 10^{-4} Å^{-1}) a coexistence of two structures showing different characteristic sizes can be identified (the vertical arrows indicate the observed Guinier regimes). The smaller shows a 2-dimensional morphology that is revealed by the Q^{-2} power law regime identified within the Q range covered by FSANS. The unified Beaucage equation [4] for multiple structural levels and scattering data extending over many decades describes well the F-SANS data and prove the existence of thick plates (d=0.23μm) which must result by the filling of the space between the thin correlated platelets identified at 0°C with continuously growing wax crystallites. The additional scattering at low Q indicates the formation of much larger aggregates whose characterization is difficult. This is done by analysing scattering data where the Guinier regime is absent. A 1-dimensional morphology can be tentatively attributed to these aggregates via the assignment of Q^{-1} for low Q. The neutron scattering findings for this later aggregation stage were complimented by the microscopy observations shown in Fig.2. Different copolymer-wax combinations and wax amounts investigated for the case of the copolymer self-assembling event occurring well-before the wax crystallization point revealed basically the same common crystallization features as those described above and thus, the formation and evolution of a hierarchical morphology showing multilevel structures. First, the polymer 1-dimensional morphology showing density modulations occurs [1]. Then, wax crystals are formed and nucleated by the crystalline nuclei of the polymer needles. The wax grows laterally in large platelets also involving further polymers still in solution. The primordial polymeric structure serves to template the lateral platelets in a correlated shish-kebab-like arrangement. Late aggregation leads to a massive crystallization of the wax surplus and formation of large compact 1-dimensional structure.

References: [1] H.S.Asbaugh et al., Macromolecules 35, 7044, 2002; [2] A.Radulescu et al., J.Pol.Sci. B 42, 3113, 2004; [3] D.Schwahn, and M.H.Yoo, *Springer Proceedings in Physics* vol.10, Springer Verlag: Berlin, Heidelberg, New York, Tokyo, 1986, p 83; [4] G.Beaucage, J.Appl.Cryst. 29, 134, 1996.

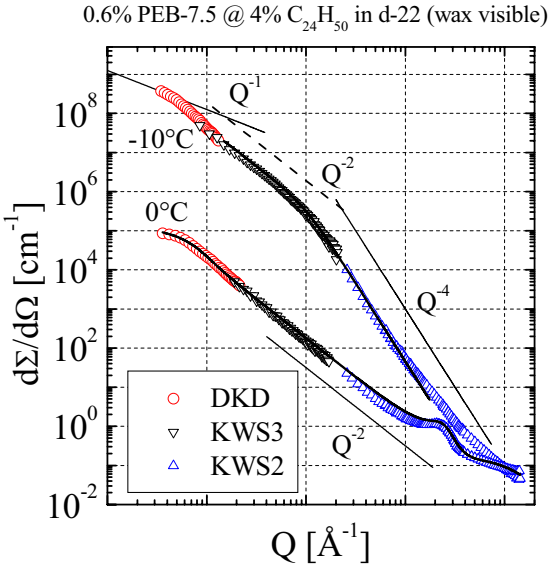


Fig.1 - Scattering patterns under wax contrast from a mixed solution of 0.6% low M_W PEB-7.5 copolymer and 4% C_{24} wax in decane.

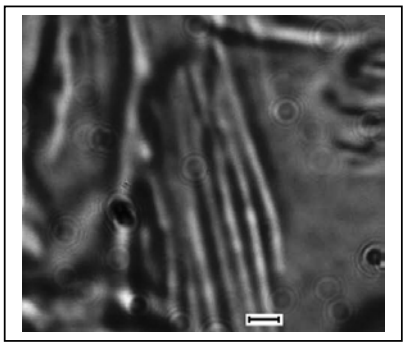


Fig.2 – A micrograph of the aggregates formed in the same solution at -10°C (scale bar 10μm).

Institut für Festkörperforschung
Forschungszentrum Jülich GmbH
D-52425 Jülich

Experimental Report
of Neutron Scattering Experiments
at the FRJ-2 Reactor

Proposal number:	DKD-04-006		
Experiment title:	Determination of the main size of cley mesocopic/macroscopic structures in archaeological and reference samples		
Dates of experiment:	20 days March/April 2005 09.11. – 10.11.2005	Date of report:	01-06-2006
Experimental team: Names	Addresses		
A. Botti	Univ. Roma TRE,Dip. Fisica “E. Amaldi”,via della vasca navale 84,00146 Roma(IT)		
Local Contact:	D. Schwahn, M. Heiderich		

Experimental report text body

A series of 18 reference pottery samples has been measured on DKD diffractometer: They differ from each other in terms of maximum firing temperature, heating rate and composition.
This experiment represents, in chronological order, last attempt at determining the main size of the grains which constitute the pottery bulk. Previous experiments on KWS2/PAXE and KWS3 failed because of the limitations in the minimum Q achievable, which made the determination of the grains Rg not reliable.
The data, collected in slit geometry, have been converted in pinhole geometry.
Multiple scattering effects have been minimized by drawing a tiny amount of pottery powder and depositing it on the surface of a scotch tape.

A selection of the data, which include a series of samples with fixed heating rate and composition but different temperatures, are shown in Figure 1 in a ln(I) vs Q^2 plot. By linear fitting the low Q range it is possible to estimate the main size of the structures which give rise to the scattering signal.
These values are represented in Figure 2 for different maximum firing temperature. Although slightly scattered a decreasing trend is clear.

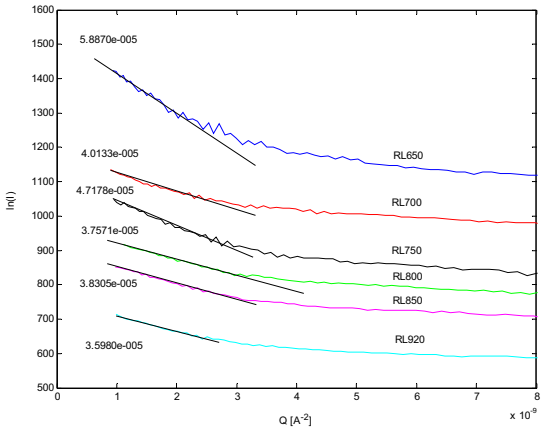


Figure 1: ln(I) vs Q^2 for samples with a reddish clay material, fired at slow heating rate at different maximum firing temperature. Lines are the best linear fits.

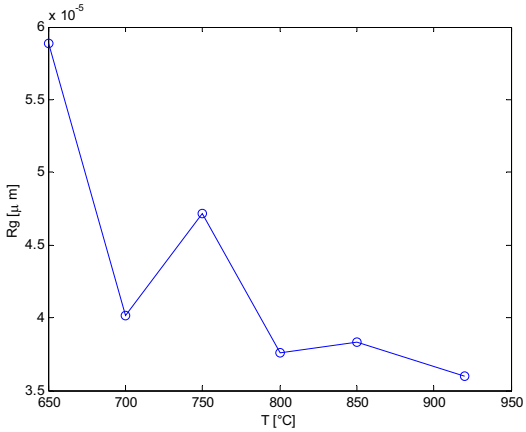


Figure 2: Dependence of the grain Rg on the maximum firing temperature. The samples are the same of Figure 1.

The results of previous experiments (not shown) on the SANS and USANS instruments were compatible with two scenarios: the grains have a rough surface which is quantified by a power law exponent (*d*) and a typical main size, Rg, (or distribution of sizes) and these two parameters are not correlated one with the other [1]; Or the firing process can be described by a growing process. According to the latter scenario firing process, and in particular the maximum firing temperature, changes the grain distribution: the small grains melt in the bigger ones. This process lowers the intensity at high Q and increases the intensity at low Q and thus giving an increasing *d* exponent; as it has been seen in SANS measurements [1]. Such process should, at the same time, shift the Rg parameter to higher values and push the bending point in the measured intesity to lower Q values.
According to the present results of the DKD experiment the growing mechanism has to be rejected: the grains, as shown in Figure 2 diminish their average sizes while temperature increases. This is an evidence that excludes an effect of the change of the grains size distribution on the value of the power law exponent.
The average size of the clay grains falls in the micrometer range.

[1] A. Botti, M.A. Ricci, A. Sodo, G. De Rossi, W. Kockelmann, J. Archaeological Science 33 307 (2006).

Institut für Festkörperforschung
Forschungszentrum Jülich GmbH
D-52425 Jülich

Experimental Report
of Neutron Scattering Experiments
at the FRJ-2 Reactor

Proposal number:	DKD-06-001, KW3-06-003		
Experiment title:	Large scale size morphology of alternating copolymers in solution (parts 1 and 2)		
Dates of experiment:	11.03.06-15.03.06	Date of report:	29.05.06
Experimental team: Names	Addresses		
Aurel Radulescu	Forschungszentrum Jülich Institut für Festkörperforschung D-52425 Jülich Germany		
Local Contact:	Dr.E.Kentzinger, Dr.D.Schwahn		

Experimental report text body

Recently, SANS studies have revealed that in dilute solution upon cooling the random copolymers PEB-*n* (where *n* represents the number of ethyl side branches per 100 backbone carbon) form 1-dimensional aggregates which, depending on the crystalline degree of the copolymer tuned by *n*, are either open objects (like for PEB-11) or present a longitudinal alternation of crystalline and amorphous sequences (like for PEB-7.5) [1,2]. A similar behaviour is shown by the PE-PEP crystalline amorphous star polymers with the crystallisable PE blocks in the star center [1] and by the alternating isotactic-atactic polypropylene (iPP-aPP) copolymers [3]. Thus, the general morphology of self-assembling materials with multiple alternating crystalline and amorphous blocks appears to be rodlike instead of 2-dimensional which is favoured by the crystalline-amorphous diblock architecture. Focusing SANS (f-SANS) and ultra SANS (u-SANS) investigations complimented by microscopy observations have shown that the PEB-n random copolymers form multilevel morphologies and, besides the 1D aggregates form additionally large structures with sizes within the micrometer length scale. Stimulated by these conclusions and also by the microscopy observations of some large scale soft aggregates formed by the alternating iPP-aPP copolymers in dodecane solution (Fig.1) we performed new f-SANS and u-SANS investigations of the self-assembling behaviour of these materials in solutions. Structural measurements involving the KWS-3 and DKD instruments have been performed on 1% polymer solution in dodecane at room temperature. The data collected at the DKD instrument in slit-geometry have been transformed into pin-hole geometry using the procedure described in [4]. Then, the scattering patterns from the iPP-aPP aggregates in solution have been analysed over the whole Q range covered by combining the conventional-, focusing- and ultra-SANS instruments at FRJ-2 reactor, namely $3x10^{-5} \div 0.2Å^{-1}$. These results are presented din Fig.2 and reveal a multilevel organization of the polymers: at a lower length-scale the polymers aggregate by yielding 1D objects whose characteristic scattering exhibits a Q^{-1} power law behaviour. The thickness and the density of these aggregates have been evaluated elsewhere [3]. At a larger length-scale (larger than $2\pi/Q^*$, where Q^* is

marked in the figure) a second kind of aggregates occurs and gives rise to the scattering revealed at low Q by f-SANS and u-SANS. These must be the spherulitic-like soft aggregates revealed by the micrographs. We may conclude that a hierarchy of structures appears in this case, the formation of large-scale aggregates being a result of the association of many 1D thin aggregates. The Q^{-4} behavior of the scattering from the soft large scale aggregates is not yet understood as long as such behavior is typical for the scattering of compact structures showing sharp interfaces with the environment. The analysis and interpretation of the experimental data is in progress.

References: [1] D.Schwahn et al., Macromolecules 35, 861, 2002; [2] A.Radulescu et al. J.Pol.Sci. B Pol.Phys. 42, 3113, 2004; [3] A.Radulescu et al. Macromolecules 37, 6962, 2004; [4] D.Schwahn, and M.H.Yoo, *Springer Proceedings in Physics* vol.10, Springer Verlag: Berlin, Heidelberg, New York, Tokyo, 1986, p 83

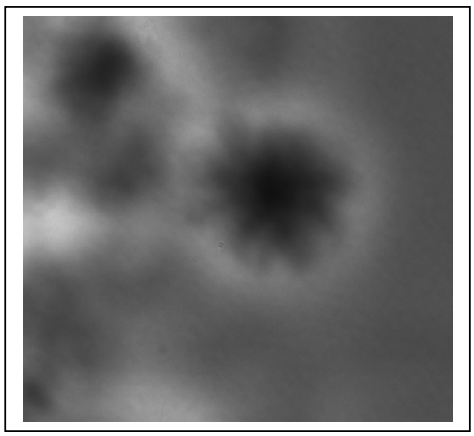


Fig.1 – Micrograph of the aggregates formed by the iPP-aPP alternating copolymers in dodecane at room temperature; the size of the spherulitic-like soft aggregate is about 4 μm.

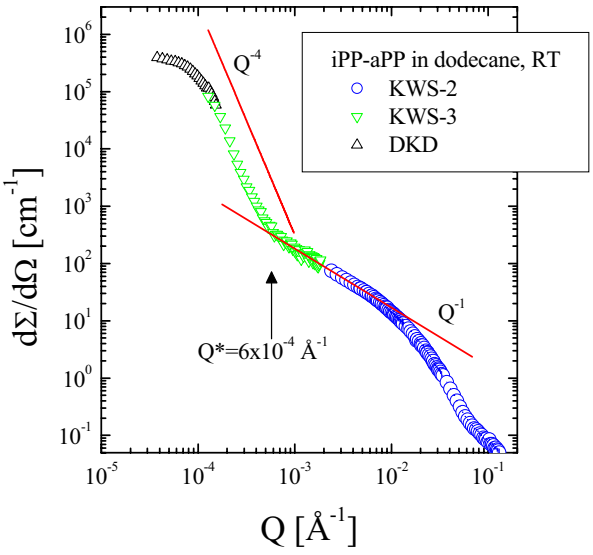


Fig.2 – Wide-Q scattering pattern from aggregates of iPP-aPP copolymers in dodecane collected at room temperature by combining conventional-, focusing- and ultra-SANS.

Time-of-flight Spectrometer for Diffuse Neutron Scattering (DNS)



Instrument Parameters

Beam tube:	NL-1, straight neutron guide, 10 cm (height) × 7 cm (width)
Monochromator:	double focusing graphite, 6 crystals, each 5 × 4 × 0.2 cm^3
Wavelength:	3.3 Å < λ < 5.5 Å
Energy:	7.4 meV > $E_{initial}$ > 2.7 meV
Energy resolution:	0.9 meV > ΔE > 0.15 meV (FWHM, elastic)
Momentum transfer:	< 3.5 $Å^{-1}$ (elastic)
Vertical:	< 0.5 $Å^{-1}$ (elastic)
Polarizer:	focusing supermirror FeCoV/Ti:N
Transmission:	30 % to 50 % for correct spin
Sample position ***- Neutron flux:*** ***- Beam size:*** ***- Special sample*** ***- Environments:***	 (10^7... 3 × 10^6) n/cm^2s max. 6 cm (height) × 2 cm (width) split-coil magnet 5 tesla with dedicated cryostat, T > 2 K furnace T < 1600 °C, sample rotation inside
Detectors:	52(+12) ^{3}He-detectors (4 bar), solid angle: 0.3 srad
Angular range:	0° < 2Θ < 135°
Vertical:	2Θ < 15°
Distance to sample:	80 cm
Options for analysis ***- Time-of-flight:*** ***- Bragg:*** ***- Polarization:***	 disk chopper, duty cycle 0.05 104 graphite analyzers for E_{final} = 7.4 meV 12 detector unit with polarisation analysis; focusing, supermirrors FeCoV/Ti:N

Instrument Responsible

Dr. Werner Schweika Tel. +49-(0)-2461-61-6650 Email: w.schweika@fz-juelich.de
Dr. Yixi Su Tel. +49-(0)-2461-61-4786 Email: y.su@fz-juelich.de

Institut für Festkörperforschung
Forschungszentrum Jülich GmbH
D-52425 Jülich

Experimental Report
of Neutron Scattering Experiments
at the FRJ-2 Reactor

Proposal number:	DNS-02-009		
Experiment title:	**Investigation of Magnetic and Structural Correlations in the diluted semiconductor $Ga_{1-x}Mn_xAs$ (x=0.05)**		
Dates of experiment:	Dec. 2004	Date of report:	May 2005
Experimental team: Names	Addresses		
K.-U. Neumann	Dept. of Physics, Loughborough University, Loughborough LE11 3TU **UK**		
Local Contact:	W. Schweika		

Experimental report text body

The magnetism of MnAs shows evidence for a strong coupling of magnetic and lattice degrees of freedom. The transition from a ferromagnetic to a paramagnetic phase proceeds via a 1st order phase transition in which the crystallographic structure changes discontinuously from a hexagonal space group at low temperatures to an orthorhombic one at higher temperatures. The change in the size of the magnetic moment is significant. Just below the transition the ordered magnetic moment is ~70% of the ground state moment. After the crystallographic transformation the substance is paramagnetic with strong ferromagnetic short range order correlations.

For diluted compounds, in which MnAs is substituted into a matrix of GaAs, also shows magnetism and ferromagnetic ordering. The amount of MnAs which can be dissolved in the matrix is limited to a few percent. The amount of MnAs can be increased for thin film samples, while bulk material is limited to approximately 5% maximum. Despite the high degree of dilution in a non-magnetic matrix the transition temperatures are surprisingly high, exceeding 100K for optimally prepared thin film samples.

In order to investigate the formation of a macroscopic ferromagnetic state for a diluted MnAs sample a neutron scattering experiment has been carried out in order to determine the nuclear and magnetic scattering as a function of temperature.

The scattering at high temperatures (300K) and at low temperatures (10K) are shown in figures 1 and 2.

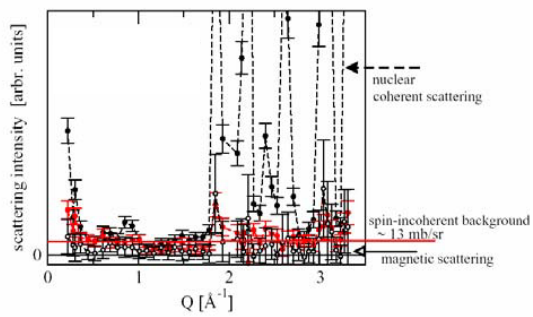


Figure 1: scattering of $Mn_xGa_{1-x}As$ at T=300K.

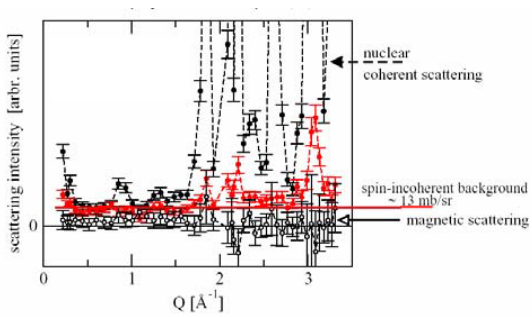


Figure 2: Scattering of $Mn_xGa_{1-x}As$ at 10K

A particular problem with the investigation of these samples is phase separation and the segregation of a ferromagnetic MnAs phase. This results in ferromagnetic inclusions at low temperatures which prevent spin polarized neutrons from being used to probe magnetic correlations. As figures 1 and 2 demonstrate spin polarized neutrons can be used to probe diluted $Mn_xGa_{1-x}As$ samples, if sufficient care is exercised in the preparation of these samples. However, due to the low concentration of magnetic scatters the measurement time for each sample has to be much longer.

The experiment has looked at several samples differing in the concentration of Mn. For samples with a high concentration the problem of depolarization of the neutron beam arises. For samples with a low concentration and with the appropriate heat treatment, suitable samples for bulk measurements are available for neutron scattering experiments. A substantial proportion of the experimental time was used to establish and verify the optimal experimental conditions. The resulting magnetic correlations, however, have been obtained only with a large error bar such that on the basis of the initial measurements no definite statements can be made as to the temperature dependence of magnetic correlations.

In conclusion the experiment confirms the feasibility of measuring magnetic correlations in diluted ferromagnets such as $Mn_xGa_{1-x}As$. However, longer measurements are needed in order to establish details of the magnetic correlation functions and their temperature dependence.

Institut für Festkörperforschung
Forschungszentrum Jülich GmbH
D-52425 Jülich

Experimental Report
of Neutron Scattering Experiments
at the FRJ-2 Reactor

Proposal number:	DNS-04-011		
Experiment title:	Low-frequency dynamics of spin and orbital polarons in ferromagnetic insulating manganites		
Dates of experiment:	21-04-06 to 02-05-06	Date of report:	06-06-06
Experimental team: Names	Addresses		
Dr. Y. Su	Institut für Festkörperforschung, Forschungszentrum Juelich		
Local Contact:	Dr. W. Schweika		

Experimental report text body

"1/8"-doped $La_{1-x}Sr_xMnO_3$ ($x \approx 1/8$) is among the most fascinating in a large class of highly correlated transition-metal oxides, where the interplay between charge, spin, orbital and lattice degrees of freedom plays a key role in determining their highly unusual properties. When a small amount of holes are introduced into A-type anti-ferromagnetic $LaMnO_3$ via chemical substitutions, a ferromagnetic insulator (FMI) emerges at low temperatures. While the experimental evidences strongly suggest the existence of complex charge/orbital ordering (CO/OO) in the FMI regime [1], the exact nature of CO/OO is yet to be fully established. The fingerprints of possible CO/OO can also be reflected from the nature of magnetic correlations. For example, a change of the anisotropy of exchange coupling (J_{ij}) is expected at the OO transition [2]. In addition, the doping induced holes often have a strong tendency to be segregated into hole-rich or hole poor regions to minimize Coulomb interaction and magnetic frustration, so that the corresponding exchange coupling may also be dramatically altered. One famous example is the occurrence of intriguing spin fluctuations due to the stripe order in high-T_C superconducting copper oxides [3]. The magnetic exchange constants can usually be obtained via measuring spin-waves excitations in a magnetically ordered phase below the Curie temperature (T_C). In the paramagnetic phase above T_C, it is also possible to extract exchange constants from a quantitative fitting to a diffuse magnetic scattering pattern [4].

Comprehensive investigations of magnetic correlations of this peculiar compound have been undertaken on a large single crystal at time-of-flight spectrometer DNS. Both diffuse magnetic scattering and spin-wave excitation were obtained with the neutron wavelength of 4.8 Å over a large temperature range. As shown in Fig.1, in the ferromagnetic metallic regime (155 K < T < 190 K), the diffuse magnetic scattering is found to show a prominent *rod*-like feature extended along the $[100]_C$ direction in the reciprocal space of a pseudo-cubic setting. Due to the presence of severe twining in this perovskite compound, e.g. (110)/(001) twining in the

orthorhombic setting, the observation of this *rod*-like diffuse scattering strongly suggests the presence of a significant anisotropy of magnetic correlations in this compound, i.e., strong exchange coupling in the orthorhombic ***a-b*** plane (J_{ab}) and weak inter-plane coupling (J_c). In addition, the low-energy spin-wave excitation was also measured. In contrast to the results obtained in several recent investigations via triple-axis spectrometer [5-6], no splitting in the spin-wave branch can be observed up to 10 meV, as shown in Fig.2. Complete data treatment is in progress.

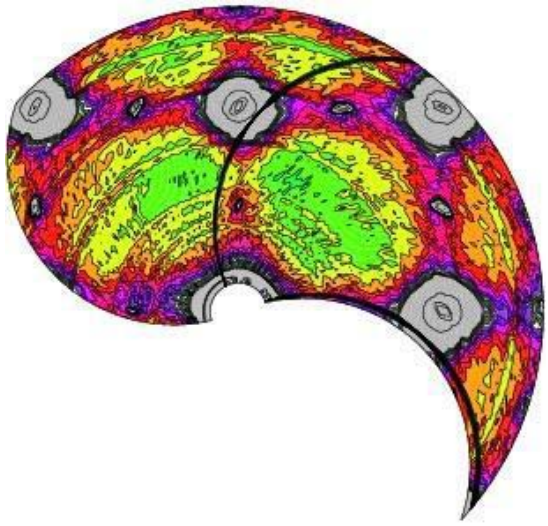


Fig.1 Diffuse magnetic scattering measured at 170 K. (Data shown is the integration over the time channels of all elastic lines.)

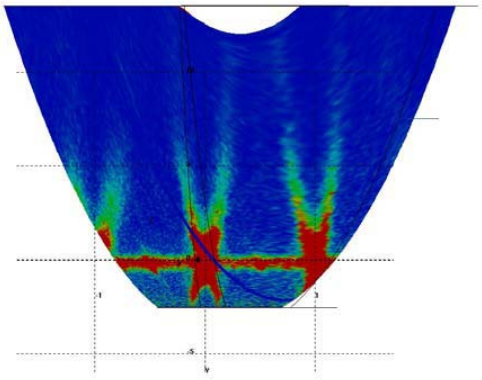


Fig.2 Spin-wave braches measured at 120 K. The horizontal axis is ***Q***, the vertical one is *E* (mev).

[1] J. Geck, *et al.*, Phys. Rev. Lett. **95**, 236401 (2005)
[2] Y. Endoh, *et al.*, Phys. Rev. Lett. **94**, 017206 (2005)
[3] J.M. Tranquada, *et al.*, Nature, **429**, 534 (2004)
[4] T. Chatterji, *et al.*, Phys. Rev. B **65**, 134440 (2002)
[5] M. Hennion, *et al.*, Phys. Rev. B **73**, 104453 (2006)
[6] Y. Su, *et al.*, unpublished

Institut für Festkörperforschung
Forschungszentrum Jülich GmbH
D-52425 Jülich

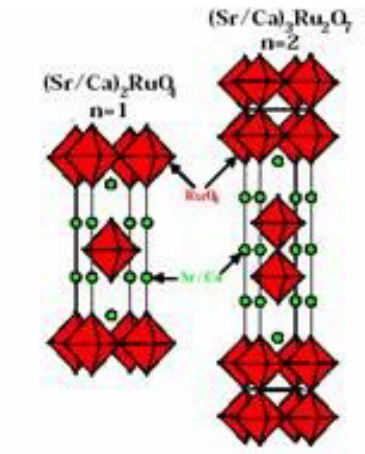
Experimental Report
of Neutron Scattering Experiments
at the FRJ-2 Reactor

Proposal number:	DNS-04-065		
Experiment title:	**P re cuus o rf s tahf ropl tt acf i rots e nrhutR rDRl o rtal f octchf orcf r El $_x$ms b dml f e rEl $_{y-s}$l a$_{2-s}$ms b $_d$**		
Dates of experiment:	. arch 60th-20th 2005	Date of report:	. arch 86st 200A
Experimental team: Names	d 11resses		
Hermann RaphaLlA Gran1Cean Fernan1eA Rong1ing JinA Egami , akeshi	j niKersitV1e é iège è Dept. 1e Ph1si–ue è . 5 è . 4000 é iège è . elgium j niKersitV1e é iège è Dept. 1e Ph1si–ue è . 5 è . 4000 é iège è . elgium y ak Ri1ge National é aborator1Ay ak Ri1geA, NAj Sd j niKersit1 of , ennesseeADept . aterial Science an1 EngineeringAq noxKilleA, NAj Sd		
é ocal Bontact:	Dr. T . SchCeika		

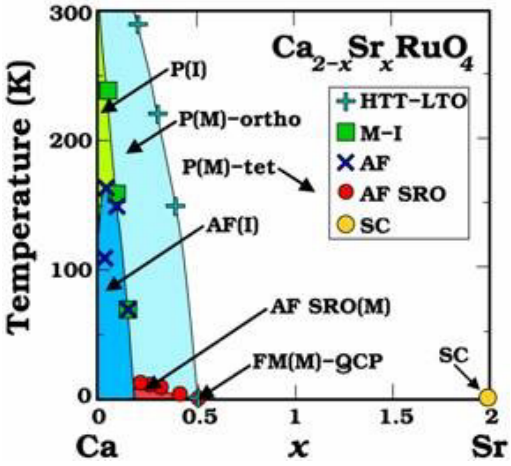
x 3D ac9 f tl 5a Dhatrt 3tr0he n
S

, he 1iscoKer1 of exotic supercon1uctiKit1 in Sr_2Ruy_4 ". aenoA6""4] an1 its structural similarit1 to é a_2Buy_4Aa parent compoun1 for the high-temperature supercon1uctorsAhas generate1 much interest in the Ru11les1en-Popper vRP[series of ruthenium oxi1esAvSr]Ba[$_{I1\ u}$Ru$_t$y $_{sI1\ u}$ "NakatsuCA6""""A2000A2006WFrie1tA2006WGalKinA2006Aé eeA2002]. , he similarities betCeen Sr_2Ruy_4 an1 high-temperature supercon1uctors are best emphasize1 b1 consi1eration of the famil1 of compoun1sABa$_{2-t}$Sr$_t$Ruy $_4$AChose cr1stal structure is shoCn in Figure 6. , he experimentall1 obserKe1 behaKior for these compoun1s as a function of 1opingAshoCn in Figure 2Ahas remarkable similarities Cith the first obserKe1 high-temperature supercon1uctorA é $a_{2-t}Sr_tBuy_4$. . oth sets of compoun1s haKe an insulating antiferromagnetic wdF. [groun1 state wdFwf[in Fig. 2[Aa structural phase transition separating high temperature tetragonal wH, , [an1 loC-temperature orthorhombic wé, y [phases wH, , -é, y in Fig. 2[Aa paramagnetic metallic phase at larger Kalues of*t* wPw [-tet in fig. 2[Aan1 a supercon1ucting phase wSB in fig. 2[. In a11ition to proKi1ing a neC s1stem Chere the eKolution from antiferromagnetism to supercon1uctiKit1 can be explore1Athe phase 1iagram of Ba$_{2-t}$Sr$_t$Ruy $_4$ contains rich an1 exotic behaKior attribute1 to structural an1 magnetic instabilities.

, he first obCectiKe of this proCect is to obtain the magnitu1e of the magnetic moments in Ba_2Ruy_4 an1 $Ba_{6.5}Sr_{0.5}Ruy_4$ an1AfurtherAto obtain real-space spin-spin correlation function from the Fourier-transform of the magnetic structure factor. , he secon1 obCectiKe is to un1erstan1 the tetragonal to orthorhombic structural phase transition associate1 to the rotation of the Ruy $_A$ octahe1ra aroun1 the z-axis in $Ba_{6.5}Sr_{0.5}Ruy_4$Athrough scattering on a single cr1stal. , he origin of this lattice 1eformation is not un1erstoo1Aan1 a 1iffuse scattering stu11 is expecte1 to 1iel1 insight into the mechanism of this phase transition.

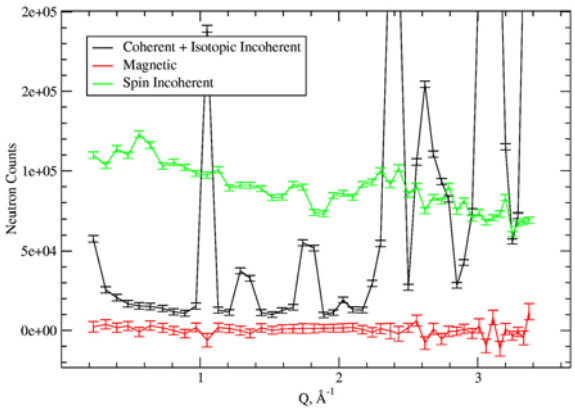


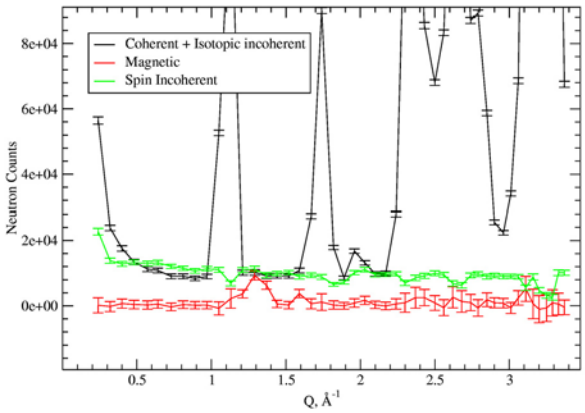
7 di 4y: Schematic cr1stal of the*n1* Y6 an1*n1* Y2 Ru11les1en Popper ruthenates.



7 di 4x6 Phase 1iagram of the*n1* Y 6 $Ba_{2-t}Sr_tRuy_4$ s1stem

, he magnitu1e of the magnetic scattering in $Ba_{6.5}Sr_{0.5}Ruy_4$ has proKen too small to obtain an1 information on the spin correlation in that material. In Ba_2Ruy_4 the onl1 significant magnetic scattering obserKe1 has been obserKe1 at + Y 6.88 * -6 an1 , Y 600 q Asee Figure 8Aan1 this peak is absent at 200 q . During this series of measurements it has appeare1 that the magnitu1e of the spin incoherent scattering in both compoun1s is extremel1 1ifferentAsuggesting that the amount of humi1it1 that these compoun1s trap is much larger than preKious11 belieKe1.
, he secon1 part of the measurements 1i1n8 1iel1 the expecte1 result because the –ualit1 of the single cr1stal Casn8 sufficientAso that Ce coul1n8 collect a usable inelastic signal from the phonon scattering at loC temperature.





7 di 4366r; he scattering b1 $Ba_{6.5}Sr_{0.5}Ruy_4$ at 6.(q AleftAthe scattering b1 Ba_2Ruy_4 at 600 q Aright.

R **u a f p o6**
y . Frie1tA . . ra1enAG. d n1reAP. d 1elmannAS. NakatsuGan1 9 . . aneoAv2006[A*a i on rl : [rP r***63**A6) 4482.
é .. . GalKinAR.S. Perr1Ad .T . , 1lerAd .P. . ackenzieAS. NakatsuGAan1 9 . . aneoAv2006[A*a i on rl : [rP* **63**A 6A6602.
9 . . aenoAH. HashimotoAq . 9 oshi1aAS. NishizakiA, . FuGtaAJ.G. . e1norzAan1 F. é ichtenbergG*2x6*””4[*A4 HZ] -: r* **37x**A582.
J.S. é eeA9 .S. é eeA, .T . NohAS.-J. y hAJaeGin 9 uAS. NakatsuGAH. FukazaCaAan1 9 . . aenoAv2002[*a i on rl : [rg: 22r***89**A25) 402.
S. NakatsuGan1 9 . . aneoAv2000[*A a i on rl : [rg: 22- rn***8d**A2AAA
S. NakatsuGan1 9 . . aneoAv2000[*A a i on rl : [rP r***6x**AA45(.

Institut für Festkörperforschung
Forschungszentrum Jülich GmbH
D-52425 Jülich

Experimental Report
of Neutron Scattering Experiments
at the FRJ-2 Reactor

Proposal number:	DNS-04-06.		
Experiment title:	**P re cuus o nf s tahf ropl tt acf i rots e nrhutR roDsf Fi xl oorDRl o rhutR rps Dal t or ml hdEy4Saby41 s 2 hx4rh3985r0ryr0r3904**		
Dates of experiment:	8 aA24th d June 61th 2005	Date of report:	8 arch L6st 200.
Experimental team: Names	ACCresses		
Hermann Rapha1l, GranCjean FernanCe, Egami Kakeshi, Stercel Ferenc	VniUersité Ce Liège d Dept–Ce PhAsi. ue d y 5 d y 4000 Liège d y elgium VniUersité Ce Liège d Dept–Ce PhAsi. ue d y 5 d y 4000 Liège d y elgium VniUersitAof Kennessee, Dept 8 aterial Science anC Engineering, q noxUille, KN, VSA VniUersitAof Kennessee, Dept 8 aterial Science anC Engineering, q noxUille, KN, VSA		
Local Bontact:	Dr–T –SchCeika		

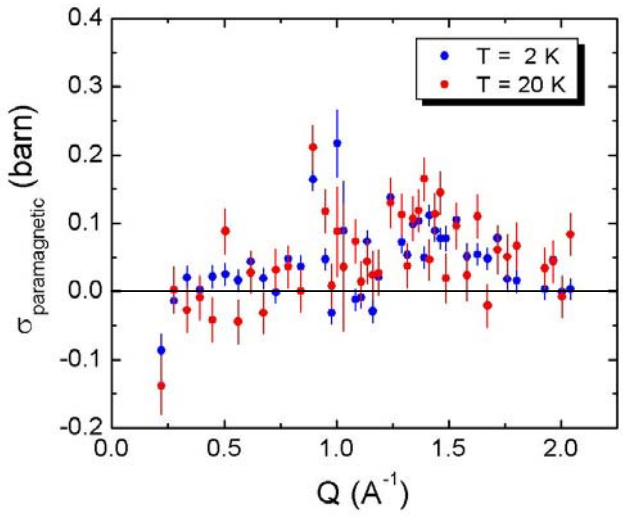
7yD ac6 f tl xra Dhatrt ytr3he n

In the cuprate superconCuctor sAstem $La_{6-x}Sr_xBu"_4$ antiferromagnetic long-range orCer Cisappears at x ” 0-02, anC superconCuctiUitA appears aboUe x ” 0-0. –At loC temperatures the region in-betCeen, 0-02] x] 0-0. is calleC the wspin-glass phase[–HoCeUer, the real nature of this phase is not Cell unCerstooC–Furthermore spin-glass-like sloC CAnamic spin correlation is suspecteC to persist up to high temperatures anC high Coping concentrations oUer the so-calleC pseuCo-gap region, but again its real nature is poorlA unCerstooC–Khe most important . uestion is hoC the spins confine the CopeC charges WoleYanC make the sAstem insulating, or poorlA conCucting– It is generallA belieUeC that the charges are confineC in the stripe state in this concentration range +6*, just as in the NC-CopeC $x \sim$ 0-625 samples +2*–HoCeUer, the eUiCence is onlA. uite inCirect anC confusing–Khe purpose of this measurement is to Cetermine the true spin configuration in this composition range anC Cetermine hoC spins are confining charges–

Khe objectiUe of this project is to Cetermine the spin correlation in LaW-xYSrWYBu" WYW-02] x] 0-6Yas a function of temperature anC Coping, x, anC hoC the spin correlation Ceteriorates Cith increasing temperature– Khis measurement is expecteC to giUe information on the spin-glass phase that is suspecteC to exist near the superconCucting phase in the LSB" phase Ciagram–

In the so-calleC pseuCo-gap phase unCer inUestigation it has been proposeC that there exists a mixture of nano-scale AF8 clusters anC possiblA paireC holes, but this conjecture is baseC upon the macroscopic measurements of spin susceptibilitAanC the N8 R spin-lattice relaxation time W1oC fre. uencA spin susceptibilitAY–Here Ce intenC to conCuct Cirect measurements–

Diffuse magnetic scattering has been obserUeC in $La_{6-14}Sr_{0-0.}Bu"_{4}$, likelA inCicating the presence of a spin-glass phase in this compounC at 2 q anC 20 q , see Figure 6–GiUen the small magnituCe of the magnetic scattering Cith respect to both the nuclear isotopic incoherent anC nuclear spin incoherent scattering, the analAsis of the Cata re. uires extremelA gooC Cetermination of all ancillarA parameters, such a backgrounC, flipping-ratios, anC absolute scattering–In orCer to assure both reproCucibilitAanC statistical UiabilitA of the Cata, Ce haUe preferreC to focus on onlA three samples, namelA $La_{2-x}Sr_{x}Bu"_{4}$ Cith x~ 0, 0-0. , anC 0-6– Khe first series of measurements has been conCucteC at L-L Å, in orCer to inUestigate the largest range of scattering Uectors possible–HoCeUer, the presence of manA strong DebAe-Scherrer rings at larger 8 spoils anA possibilitA to obtain a gooC separation of the magnetic anC incoherent scattering–Further these DebAe-Scherrer rings AielC strong multiple scattering that taints the Cata– Hence, for the most interesting sample, x ~ 0-0. , the results haUe been reproCuceC at a larger CaUelength of 4-(Å– Khis measurement has the aCUantage of both enhancing the resolution anC of reCucing the multiple scattering anC has shoCn the presence of the spin-glass phase–



6 d i 9d7 Paramagnetic scattering in $La_{6-14}Sr_{0-0.}Bu"_{4}$–Khe noise just beloC 6 9 $^{-6}$ is cause bA a DebAe-Scherrer ring–

R **u a f p o7**

6– ; –AnCo, q –SegaCa, S–q omiAa anC A–N–LaUroU, *Phys. Rev. Lett*–**88**, 6L7005 W2002Y–
2– J–8 –Kran. uaCa, y –J–Sternlieb, J–D–Axe, ; –Nakamura anC S–VchiCa, *Nature* **975**, 5. 6 W6115Y–

Institut für Festkörperforschung
Forschungszentrum Jülich GmbH
D-52425 Jülich

Experimental Report
of Neutron Scattering Experiments
at the FRJ-2 Reactor

Proposal number:	DNS-04-017		
Experiment title:	**A diffuse neutron scattering study of phase transitions in $Na_{0.75}CoO_2$**		
Dates of experiment:	February 28th- March 9th 2005	Date of report:	March 31st 2006
Experimental team: Names	Addresses		
Hermann Raphaël, Grandjean Fernande, Keppens Veerle, Mandrus David	Université de Liège – Dept. de Physique – B5 – B4000 Liège – Belgium Université de Liège – Dept. de Physique – B5 – B4000 Liège – Belgium University of Tennessee, Dept Material Science and Engineering, Knoxville, TN, USA Oak Ridge National Laboratory, Oak Ridge, TN, USA		
Local Contact:	Dr. W. Schweika		

Experimental report text body

The layered transition metal oxides, Na_xCoO_2, have been of considerable interest to the scientific community for the past few years. This family of materials has been known for some time[1] but the report by Terasaki et al.[2] concerning possible thermoelectric applications has rekindled interest in these compounds[3] It is very unusual for an oxide to have a relatively high thermopower yet a low metallic resistivity[4]. This result alone suggests interesting electronic correlations. The subsequent discovery of superconductivity at 5 K by Takada et al.[5] in a hydrated version of this material ($Na_{0.35}CoO_2$•1.3 H_2O) caused even greater excitement. Although the superconducting transition temperature is too low for applications, the structural and chemical similarities between Na_xCoO_2 compounds and cuprate superconductors provide hope of additional insight into the physics of superconductivity in layered transition metal oxides. The basic structure of Na_xCoO_2 ($0.3 < x < 0.9$) consists of planes of edge-sharing CoO_6 octahedra alternating with layers of Na. The are two crystallographically distinct Na sites, both of which are only partially occupied. In Na_xCoO_2, the Co ions in each plane form a triangular lattice rather that the square lattice found in the cuprates. A S=1/2 triangular lattice is of great interest to theorists because of the inherent geometrical frustration of antiferromagnetic order and since Anderson's original RVB model for superconductivity[6] was calculated for a triangular lattice. This experiment is focussed on single crystals and powder with $x \approx 0.75$. Crystals with this composition undergo an unusual magnetic spin-density-wave transition near 22 K, an order-disorder transition near 340 K and several subtle transitions at intermediate and lower temperatures that have recently be mapped by us using resonant ultrasound spectroscopy.

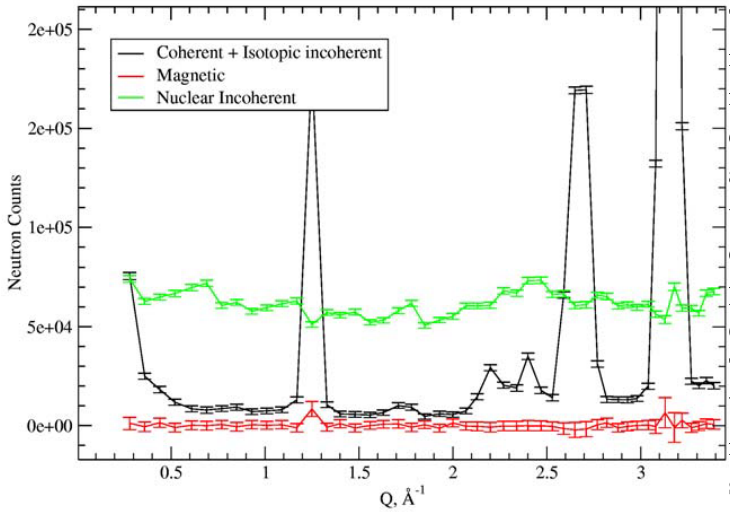


Fig. 1: Scattering by $Na_{0.75}CoO_2$ powder at 1.8 K.

The first goal of this project is to determine the real-space spin-spin correlation function in the novel complex metal oxide $Na_{0.75}CoO_2$ via a determination of the magnetic diffuse scattering across the antiferromagnetic phase transition, using polarization analysis. The second goal is to determine the spin excitation spectrum, and possible the magnetic exchange constants via an energy spectrum using time-of-flight analysis. The polarization analysis of the neutron scattering by $Na_{0.75}CoO_2$ powder at low temperature has not revealed any significant magnetic contribution, see Fig. 1. This permits one to set a limit on the maximum magnitude of the Co moments, but doesn't give any information on the magnetic correlations in the material. Given this result, it was decided that an investigation of the excitation spectrum was not feasible under these condition.

Instead it was preferred to measure the scattering by a $Na_{0.75}CoO_2$ single crystal at different temperatures. Unfortunately, this experiment suffered from the poor crystal quality. However, we observed weak incommensurate peaks at low Q, see Fig. 2, which are not of magnetic origin, as we checked by measuring the temperature dependence. The peaks are present at 10 K and remained visible at least up to 35 K. We tentatively attribute this type of Bragg reflection to a superstructure in the sodium layers.

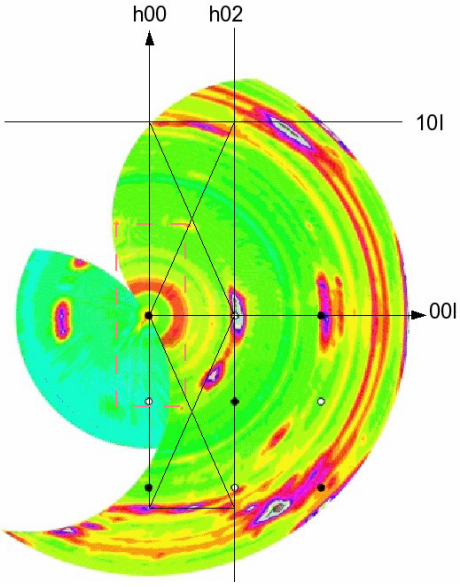


Fig. 2: Scattering by a $Na_{0.75}CoO_2$ single crystal at 10 K.

References:

1. C. Fouassier, G. Matejka, J.-M. Reau, and P. Hagenmuller, J. Solid State Chem. **6**, 532 (1973).
2. I. Terasaki, Y. Sasago, and K. Uchinokura, Phys. Rev. **B56**, R12685 (1997).
3. W. Koshibae, K. Tsutsui, and S. Maekawa, Phys. Rev. **B62**, 6869 (2000).
4. G. D. Mahan, B. C. Sales, and J. W. Sharp, Phys. Today **50**, 42 (1997).
5. K. Takada, H. Sakurai, E. Takayama-Muromachi, F. Izumi, R. A. Dilanian, and T. Sasaki, Nature **422**, 53 (2003).
6. P. W. Anderson, Mat. Res. Bull. **8**, 153 (1973).

Institut für Festkörperforschung
Forschungszentrum Jülich GmbH
D-52425 Jülich

Experimental Report
of Neutron Scattering Experiments
at the FRJ-2 Reactor

Proposal number:	DNS-04-018		
Experiment title:	A novel approach to the structure of ^{1}H-containing liquids: the case of liquid water		
Dates of experiment:	18-22 April, 2005	Date of report:	23 March 2006
Experimental team: Names	Addresses		
PUSZTAI, László SCHWEIKA, Werner	Research Institute for Solid State Physics and Optics, Hungarian Academy of Sciences, P.O. Box 49, Budapest, H-1525, Hungary (e-mail: lp@szfki.hu) FZ Jülich		
Local Contact:	W. Schweika		

Experimental report text body

Precise knowledge of the microscopic structure of liquid water is of utmost importance for most chemists and molecular biologists - the reason, quite simply, is that life on Earth is based on water and takes place in aqueous solutions. For this reason, water has been the subject of a huge number of diffraction studies. Despite this fact, liquid water is considered to be one of the most notorious cases: for instance, there is an uncertainty of about 0.15 Å even in terms of the *position* of the first intermolecular O-H distance (which characterize hydrogen bonding - so the knowledge of this distance is crucial!) [1]. The reason for this is, to cut the long story short, *hydrogen*.

Neutron diffraction with H/D substitution seems to be the only feasible way of deriving detailed information on the microscopic structure of hydrogenous (i.e., containing ^{1}H) systems. However, the exceptionally high level of spin-incoherency of ^{1}H renders more than 95 % of the measured diffraction signal from pure H_2O nearly useless ('background') from the structural point of view (see, e.g., [2]).

Neutron diffraction with H/D isotopic substitution poses great but many times, impassable difficulties during data analyses. Strangely enough, the beneficial potential of polarised neutron scattering has not really been exploited so far in this respect (maybe because traditional areas for polarised neutrons are quite far from chemistry and biology). Among very few instruments, the DNS instrument at FZ Jülich offers the possiblity polarized neutron diffraction for the wide-angle scattering of liquids.

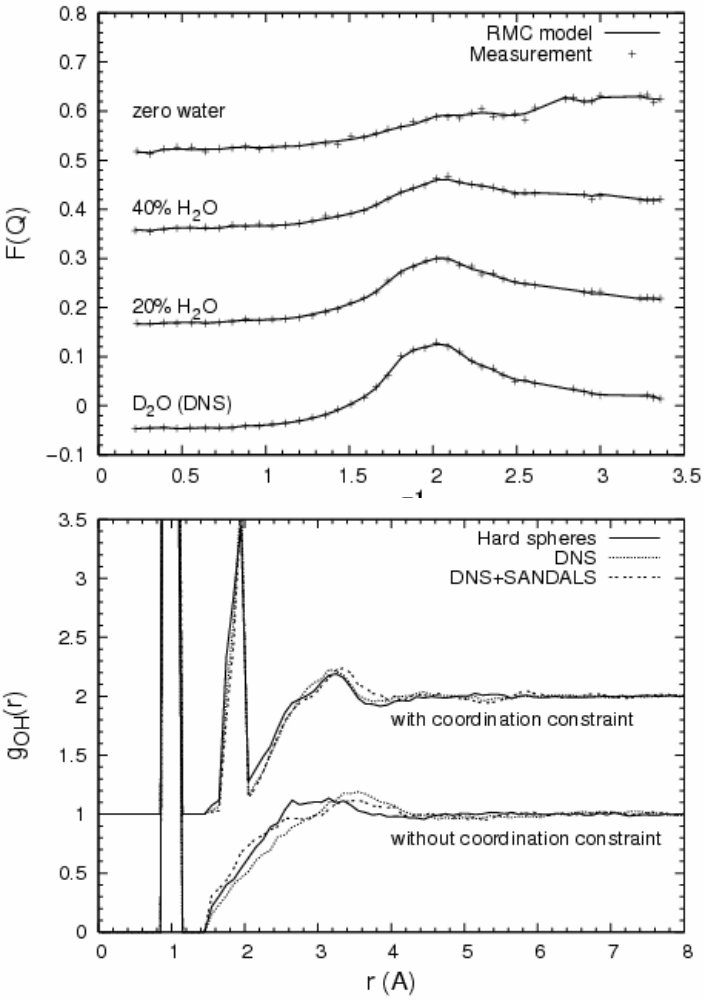
Polarized neutron diffraction measurements have been carried out on liquid water samples containing different amounts of light and heavy water (H_2O and D_2O, respectively). For each sample, temperature scans (under atmospheric pressure) were performed, within the normal liquid range of the samples. At each temperature, both the 'spin-flip' and 'non-spin-flip' scattering were determined, so that the coherent and the

incoherent contributions to the total scattering could be separated. The coherent total structure factors were then subjected to Reverse Monte Carlo (RMC) modeling [3] studies. In the RMC calculations, thousands of flexible water molecules were applied, so that the behavior of the bulk could be mimicked.

In the Figure to the right, coherent total scattering functions are shown for 4 different H/D isotopic compositions (symbols; 'zero water' contains about 65 % of H_2O and 35 % D_2O) at room temperature. The solid curves represent the corresponding Reverse Monte Carlo structural models, which were obtained by modeling all the 4 measured functions simultaneously. As it is obvious, the models are fully consistent with results of the DNS experiments within the uncertainties of the experiments.

From the particle co-ordinates in the model, several characteristics of the structure could be determined. For instance, the partial radial distributions functions (prdf) can easily be calculated directly from the co-ordinates, so that the (in many cases, rather cumbersome) process of traditional separation (using inversion of the coefficient matrix) may be avoided.

In the Figure to the right, the most important of the real space partial radial distribution functions, the O-H prdf is displayed, for various models of the structure. For reference, hard sphere Monte Carlo calculations have also been carried out; in this Figure, results from these simulations are also shown. It is obvious that for a meaningful description of hydrogen bonding, co-ordination constraints (on the non-bonding O…H atom pairs) had to be implemented, in addition to the constraints already imposed by the experimental data (see upper part of the Figure). Note that all but the hard sphere O-H prdf's are consistent with DNS data, measured between 0.2 and 3.4 $Å^{-1}$. Addition of D_2O data measured over a much wider Q-range [4] to the set of data modeled has not changed the prdf's; contrary, the new results from DNS impose a significant further confinement of the configurational space for the modeling procedure.



In summary, it has been demonstrated that the combination of polarized neutron diffraction and RMC modeling does present a feasible way for the determination of the microscopic structure of hydrogenous materials (including our example here, water). Extending the Q-range of the measurements, however, would be rather desirable; the new DNS instrument at FRM-II (Munich) will provide us with the possibility of measuring the signal beyond 5 $Å^{-1}$.

References

[1] L Pusztai, Phys. Rev. B 60, 11851 (1999)
[2] WE Thiessen and AH Narten, J.Chem. Phys.77, 2656 (1982)
[3] RL McGreevy and L Pusztai, Molec. Simul. 1, 359 (1988); for a recent review, see G Evrard and L Pusztai, J. Phys. Cond. Matt. 17, S1 (2005)
[4] AK Soper, F Bruni, MA Ricci, J.Chem. Phys. 106, 247 (1997)

Institut für Festkörperforschung
Forschungszentrum Jülich GmbH
D-52425 Jülich

Experimental Report
of Neutron Scattering Experiments
at the FRJ-2 Reactor

Proposal number:	DNS-05-004		
Experiment title:	**Spin excitations in frustrated triangular antiferromagnet $YMnO_3$**		
Dates of experiment:	29.9.05 – 7.10.05	Date of report:	December 14, 2005
Experimental team: Names	Addresses		
Tapan Chatterji W. Schweika	Institut Laue-Langevin, BP 156, 38042 Grenoble Cedex, France IFF, FZ Juelich		
Local Contact:	W. Schweika		

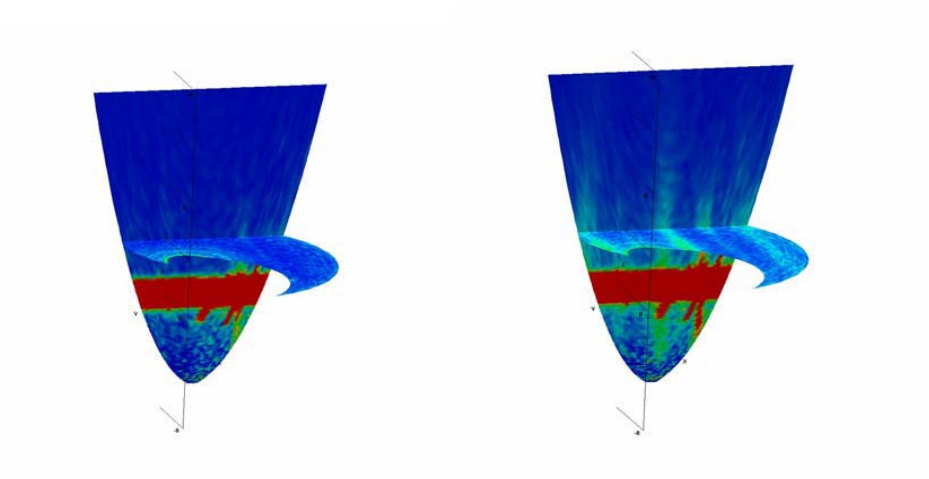
Experimental report text body

The hexagonal manganites $RMnO_3$ (R = Y, Ho, Er, Tm, Yb) are both ferroelectric and antiferromagnetic [1-6] and the corresponding order parameters couple to each other although the ferroelectric transition temperature is as high as T_C = 900 K whereas the Néel temperature is T_N = 90 K. This coupling between ferroelectric and magnetic order parameters yields the possibility of controlling electrical properties through magnetic field and vice versa and therefore hexagonal manganites may have potential applications in electronics. Due to the quasi-two dimensional triangular lattice, the magnetic system is geometrically frustrated, which is evidenced by the large ratio of Weiss-to-Néel temperature. We mapped the spin wave dispersion of $YMnO_3$ on the thermal triple-axis spectrometer IN3 of the Institute Laue-Langevin, Grenoble, using a multi-analyzer detector at two temperatures below and above T_N. This investigation suggested the existence of persistent spin wave above the ordering temperature. Due to the lack of beam time we confined our investigations in the (hol) scattering plane. In the present investigation on the DNS spectrometer we wished to extend the measurements in the (hhl) plane

We have measured spin dynamics of $YMnO_3$ in the (hhl) scattering plane on DNS of FZ-Jülich at T = 12, 40 and 75 K. This scattering plane was chosen because we previously investigated the spin dynamics on the thermal triple-axis spectrometer IN3. We knew that most of the inelastic scattering appears in (h0l) plane but wished to investigate the (hhl) plane that was not investigated before. At T = 12 and 40 K we observed practically no magnetic signal but only scattering intensity which we attributed to the phonon scattering. At T = 75 K which is 5 K above T_C we however observed paramagnetic scattering along Q = (1/2, 1/2, l). Fig. 1 and 2 gives the diffuse scattering at different temperatures.

References:

1. T. Katsufujii et al., Phys. Rev. B **64**,104419 (2001).
2. Th. Jolicouer and J.C. Le Guillou, Phys. Rev. B **40**, 2727 (1989).
3. T.J. Sato et al., Phys. Rev. B **68**, 014432 (2003).
4. J. Park et al., Phys. Rev. B **68**, 104426 (2003).
5. P.J. Brown, T. Chatterji and Th. Lonkai, to be published.
6. 6. J.M. Kosterlitz and D.J. Thouless, J. Phys. C **6**, 1181 (1973); J.M. Kosterlitz, J. Phys. C **7**, 1047 (1974)



T = 40 K T = 75 K

Fig. 1 – Diffuse scattering from $YMnO_3$ at T = 40 K and T = 75 K.

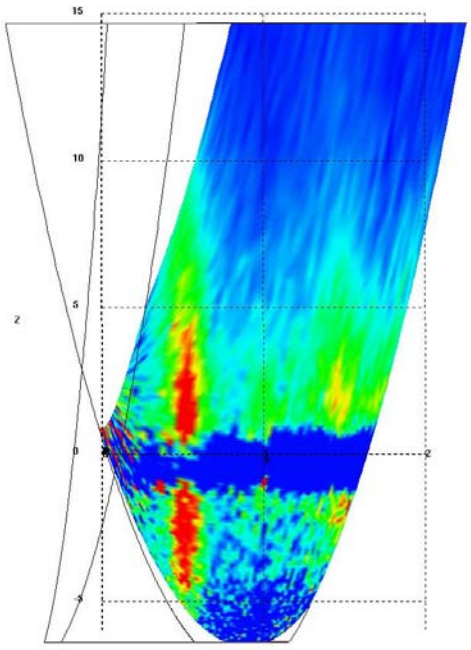


Fig. 2 – Magnetic scattering from $YMnO_3$ determined at T = 75 K after subtracting the background scattering measured at T = 12 K.

Institut für Festkörperforschung
Forschungszentrum Jülich GmbH
D-52425 Jülich

Experimental Report
of Neutron Scattering Experiments
at the FRJ-2 Reactor

Proposal number:	DNS-05-005		
Experiment title:	Magnetic Critical Scattering of MnO in Confined Geometry		
Dates of experiment:	10.05.05 – 21.05.05	Date of report:	31.05.06
Experimental team: Names	Addresses		
Mikhail Feygenson Dr. Werner Schweika Dr. Alexander Ioffe Prof. Thomas Brückel	Forschungszentrum Jülich GmbH Institut Für Festkörperforschung(IFF-STM) D-52425 Jülich Germany		
Local Contact:	Dr. Werner Schweika		

Experimental report text body

The aim of the experiment was to study the magnetic phase transition of MnO embedded in a porous glass. It has been claimed previously [1] that the discontinuous first order transition in the bulk becomes continuous in confined geometry. However, it is difficult to study the critical behavior because of a strong background from nuclear scattering in the glass. Therefore, we used XYZ polarization analysis at the DNS spectrometer that allow us to suppress this background by a few orders of magnitude and thus to observe a weak magnetic scattering.
The temperature dependence of the magnetic (½ ½ ½) Bragg peak was investigated for the wavelength of 5.24 Å within the temperature range from 2 K up to 130 K. Angular resolution was improved by a proper collimation of incident beam. As the reference, the MnO powder was investigated between 11K and 140K with the same setup. The temperature dependence of the magnetic (½ ½ ½) Bragg peak is shown in Fig.1. The measuring time is significantly increased comparing to the MnO powder due to the low content of MnO inside the glass. The normalized intensity for both samples obtained from the observed peaks is shown as a function of temperature in Fig.2.
It is seen that transition temperature for MnO glass is slightly increased compared to those for the MnO powder T_N = 118 K [2], however, the order parameter is lower for the MnO glass for most of the temperatures. The magnetic transition is second order as previously observed by Golosovsky et. al.[1]. There is a relation between pressure and ordering temperature [1,3]. According to the phase diagram given in [3] the transition temperature of MnO increases with increasing pressure. The frustration due to broken bonds at the interface can lead to the surface induced disorder as discussed in Ref.[4] and may explains why the order parameter of the MnO glass is lower compared to the bulk behavior and resembles a continuous phase transition.

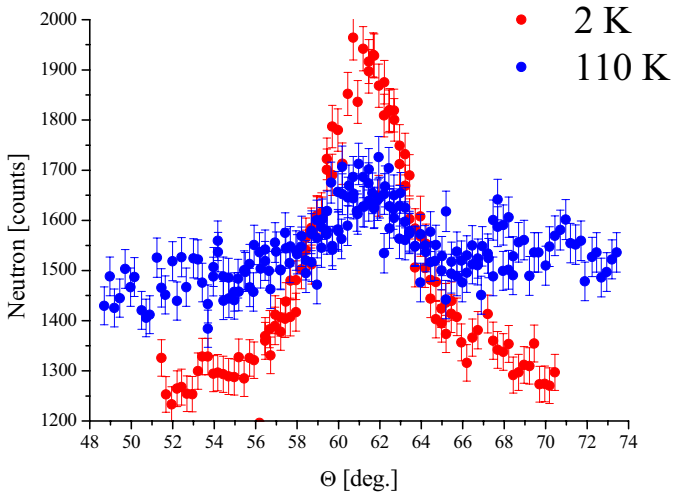


Fig.1. Magnetic (½ ½ ½) Bragg peak of MnO embedded in glass at 2 K and 110 K. The peak is observed in the spin flip channel and contains incoherent and magnetic scattering.

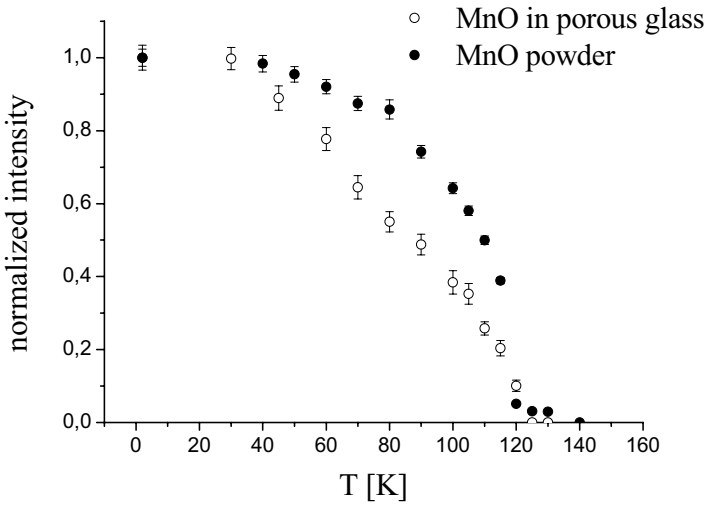


Fig.2. Normalized intensity as a function of temperature for the MnO powder embedded in a porous glass and for the MnO powder.

References:

[1] Golosovsky et. al., PRL 86 (2001).
[2] Lines et. al., PR. 139, 4A (1965)
[3] Yoo et. al., PRL 94 115502 (2005)
[4] Schweika et. al., PRB 53, 8937 (1996)

Institut für Festkörperforschung
Forschungszentrum Jülich GmbH
D-52425 Jülich

Experimental Report
of Neutron Scattering Experiments
at the FRJ-2 Reactor

Proposal number:	DNS-05-006		
Experiment title:	**Q-dependence of the coherent contribution to the scattering in a PEO-PMMA blend**		
Dates of experiment:	27.10.2005	Date of report:	25.11.2005
Experimental team: Names	Addresses		
Katarzyna Niedzwiedz Dr. Andreas Wischnewski Dr. Michael Monkenbusch Prof. Dr. Dieter Richter	IFF, Forschungszentrum Jülich, 52425 Jülich IFF, Forschungszentrum Jülich, 52425 Jülich IFF, Forschungszentrum Jülich, 52425 Jülich IFF, Forschungszentrum Jülich, 52425 Jülich		
Local Contact:	Dr. Werner Schweika		

Experimental report text body

The experiment was performed to determine the ratio of coherent and incoherent scattering intensities for a polymer blend with protonated PEO and deuterated PMMA.

To investigate the dynamics of the PEO chains in the blend, backscattering measurements on a mixture of protonated PEO and deuterated PMMA have been performed (proposal BSS-05-008). For a quantitative evaluation of the data one has to know how strong the incoherent (from protonated PEO) and coherent (from the deuterated PMMA and the single chain structure factor at low Q) contribution to the full scattering intensity is (see for example [1]).
For this purpose in this experiment we used the polarization analysis of the DNS spectrometer.

We have measured the ratio of coherent and incoherent scattering as a function of the momentum transfer. The wavelength of the incoming neutrons was 3.3 Å. The measurement was performed for the two different PEO / PMMA compositions as measured in the BSS-05-008 proposal: 35 % h-PEO / 65 % d-PMMA and 50 % h-PEO / 50 % d-PMMA (fig. 1).
Furthermore for the 35% h-PEO / 65% d-PMMA sample several temperatures were studied (fig. 2).

The information extracted from this experiment is an indispensable input for the data evaluation of the backscattering data.

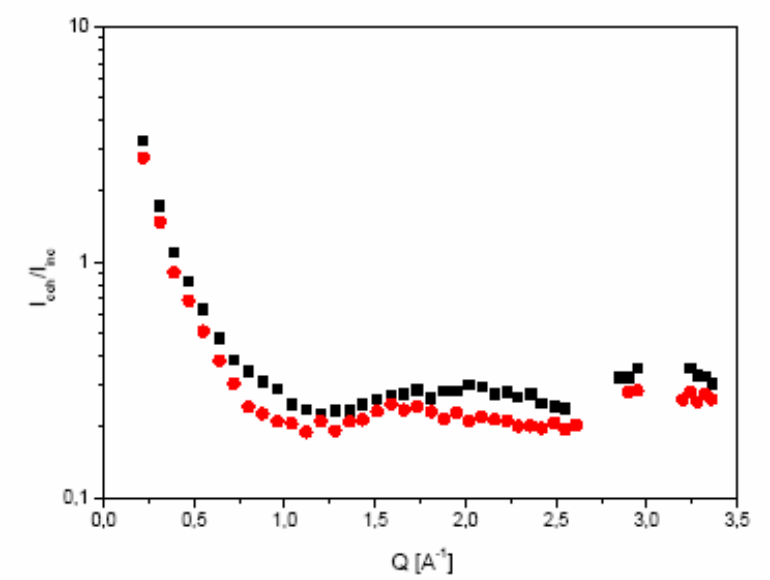


Fig. 1: Ratio between coherent and incoherent scattering intensities as a function of momentum transfer obtained for the h-PEO/d-PMMA polymer blend systems at T = 375 K. Black squares correspond to the 35% hPEO / 65% dPMMA sample and red circles to the 50% hPEO / 50% dPMMA sample.

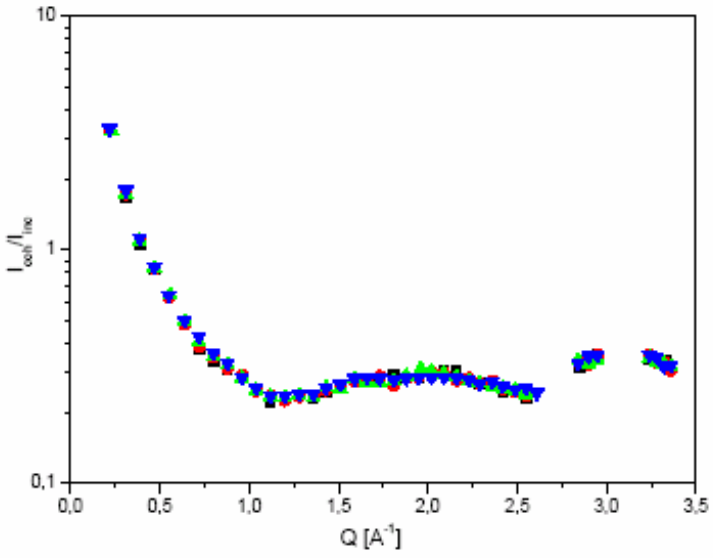


Fig. 2: Ratio between coherent and incoherent scattering intensities as a function of momentum transfer obtained for the 35% h-PEO / 65% d-PMMA polymer blend system at different temperatures: black symbols T=350K, red symbols T= 375K, green symbols T=400 K and blue symbols T=425 K.

[1] A.-C. Genix et al., Physical Review E 72, 031808 (2005)

Institut für Festkörperforschung
Forschungszentrum Jülich GmbH
D-52425 Jülich

Experimental Report
of Neutron Scattering Experiments
at the FRJ-2 Reactor

Proposal number:	DNS-05-010		
Experiment title:	Characterisation of a glass-forming microemulsion in the intermediate Q range		
Dates of experiment:	08.12. – 14.12.2005	Date of report:	31.05.2006
Experimental team: Names	Addresses		
M. Mayorova R. Zorn	Institut für Festkörperforschung, Forschungszentrum Jülich Institut für Festkörperforschung, Forschungszentrum Jülich		
Local Contact:	W. Schweika		

Experimental report text body

To investigate the glass transition dynamics of propylene glycol (PG) confined to reverse micelles of nanometre size three component system was chosen: propylene glycol as investigated material which was enclosed within the inversed micelles, AOT – ionic surfactant for system stabilization, decalin as oil phase (T_g=135K).
The composition of the microemulsion used was h-PG: 10.2% / d-AOT: 36.1% / d-decahydronaphthalene (d-decalin): 53.7% (equivalent wt% of undeuterated compounds).
An earlier SANS experiment with h-PG/h-AOT/d-decaline isotopic composition showed that no aggregation of droplets takes place. The size of the droplets could not be determined unambiguously as observed data provide information only about low q range.
To complete obtained on SANS with higher *q* values measurements on DNS were performed. This allows one to separate coherent and incoherent scattering so one doesn't need to make additional mesuarements of the ddd microemulsion for subtraction.
Table I

T, °C	Ra, E	Rhs, E	p
-24	8,621	9,875	0,22
3,6	8,610	9,220	0,1859
48,9	8,548	8,581	0,1299

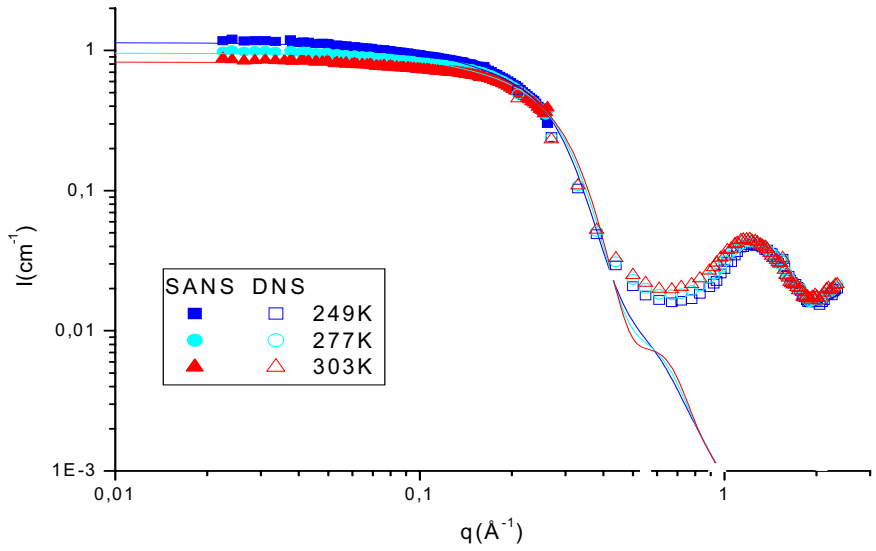


Fig. 1: SANS and DNS patterns of the h-PG/d-AOT/d-decalin microemulsion for temperatures – 24.0±1 °C, +3.6±1 °C, and +48.9±1 °C. The continuous lines show a fit with the model described below.

The SANS and DNS data were combined and fitted by a model based on the following assumptions: polydispersity is small, structure function has Percus-Yevick function form (characterized by an equivalent hard-sphere radius R_{hs}) and Schultz distribution (characterized by an average radius R_a and a polydispersity p) is suitable.

As a result of this fit it was found that there is an extremely small confinement with characteristic averaged radius of PG core about 0,86 nm. It is three times lower than it was predicted from a simple geometrical assumption (the volume fractions of AOT and PG and the thickness of the AOT layer from literature [1,2]). The fit parameters shown in Table I indicate that the average radius of particles stays roughly constant while there is a slight increase in polydispersity towards low temperatures. Comparison of experimental data and fit displays that there is considerable deviation between them only at high q range where a contribution of the PG molecule structure factor, which is not included in fit, plays the main role.

Inelastic spectra for hdd at 100K and 2 K and ddd at 100K samples were also obtained on DNS. They will be combined with data from Focus spectrometer to get the vibration density of states function which contains information about Boson peak, a deviation from linear behavior of density of states function due to an excess of states connected to the existence of localized soft modes.

[1] Lin-Min Wang, Fang He, R. Richert, *Phys. Rev. Lett.* **92**, 095701 (2004)
[2] M. Kotlarchyk, S.-H. Chen, J. S. Huang, M. W. Kim, *Phys. Rev. Lett.* **53**, 941 (1984)

Institut für Festkörperforschung
Forschungszentrum Jülich GmbH
D-52425 Jülich

Experimental Report
of Neutron Scattering Experiments
at the FRJ-2 Reactor

Proposal number:	DNS-05-012		
Experiment title:	Magnetic disorder and transitions in the chemical system (Y,Ca)$BaCo_4O_7$		
Dates of experiment:	7-13.11.2005	Date of report:	24.3.2006
Experimental team: Names	Addresses		
Martin Valldor Peter Lemmens Werner Schweika	Institut für Physik der Kondensierten Materie, TU-Braunschweig, Mendelssohnstrasse 3, D-38106 Braunschweig, Germany Institut für Physik der Kondensierten Materie, TU-Braunschweig, Mendelssohnstrasse 3, D-38106 Braunschweig, Germany Institut für Streumethoden, IFF, Forschungszentrum Jülich, D-52425 Jülich, Germany		
Local Contact:	Werner Schweika		

Experimental report text body

The two samples $YBaCo_4O_7$ and $Y_{0.5}Ca_{0.5}BaCo_4O_7$ were investigated using polarised neutrons to separate magnetic from nuclear scattering and data was collected at several different temperatures between 1.2 and 440 K. For $YBaCo_4O_7$, a magnetic order is seen below the postulated transition temperature (65 K) [1] as a sharp magnetic intensity (at 30 K) close to one of the nuclear Bragg-planes (101 ~ 1.3 $Å^{-1}$) (Fig.1). The sharpness of the magnetic peak indicates long-ranged order, but there is also a broad magnetic intensity with its maximum about 1.6 $Å^{-1}$, suggesting that parts of the spins still are disordered or fluctuating. At higher temperatures (100 K), the magnetic scattering is smeared out, but is not completely gone, indicating fluctuating short-range magnetic order. This is a further proof of extremely strong magnetic frustration, which was already seen in the magnetic susceptibility as a Curie-Weiss constant of about -1000 K [1]. At 300 K, The spins are fully decoupled and little structure is seen in the magnetic scattering apart from the average scattering factor of Co.

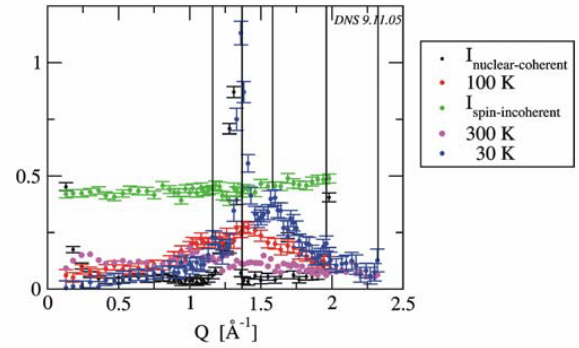


Fig.1 Neutron nuclear and magnetic scattering on $YBaCo_4O_7$ at three different temperatures.

$Y_{0.5}Ca_{0.5}BaCo_4O_7$ exhibits a totally different scattering behaviour although the only difference is that half of the Y has been substituted for Ca. This Ca substitution results in an increase in Co valence with drastic consequences for the magnetic coupling between the Co ions: no long-ranged order can be detected down to 1.2 K, but a broad intensity is observed with its maximum close to 1.33 $Å^{-1}$ (Fig.2). The lack of sharp magnetic peaks can only be explained by the fact that the chemical doping by Ca has cancelled the magnetic order, leaving a strongly frustrated magnetic lattice.

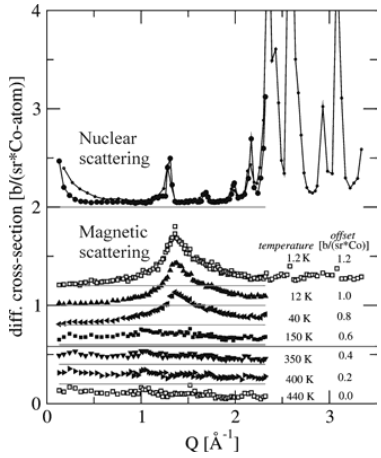


Fig.2 Neutron nuclear and magnetic scattering on $Y_{0.5}Ca_{0.5}BaCo_4O_7$ at several different temperatures; the magnetic scattering is drawn versus Q below the nuclear scattering; temperatures are indicated to the right of the data. The data have been shifted with an offset for comparisons.

The asymmetric peak shape indicates two-dimensional (2D) antiferromagnetic (AF) spin correlations, which are well described by theoretical predictions of Reimers and Berlinsky[2] for the 2D kagome AF with only nearest neighbor interactions. The spin correlations resemble the so-called $\sqrt{3}\times\sqrt{3}$ spin structure (Fig.3) for the Co atoms on the kagome layers in $Y_{0.5}Ca_{0.5}BaCo_4O_7$. The absence of an AF long range ordered state, in accordance with the Mermin-Wagner theorem, confirms the lack of any noticeable interlayer coupling as found in the un-doped material. When lowering the temperature, a peak of the magnetic diffuse intensity evolves at 1.33 $Å^{-1}$, which perfectly agrees with the ordering wave vector of the $\sqrt{3}\times\sqrt{3}$ spin structure for the cell parameter of a=6.3 Å of $Y_{0.5}Ca_{0.5}BaCo_4O_7$ (Fig.2). Further studies on similar systems, also with polarised neutrons, are on the way.

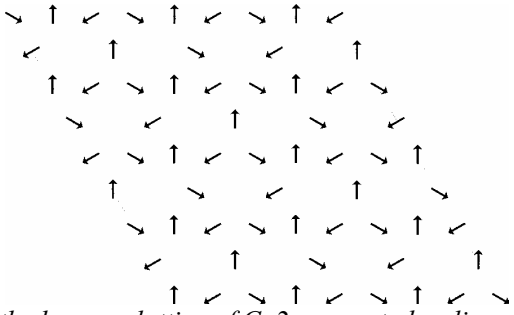


Fig.3 The in-plane spin motif on the kagome lattice of Co2, presented as lines where the crossing points are the sites for Co2. This spin structure is called $\sqrt{3}\times\sqrt{3}$ [2].

[1] Valldor, M. & Andersson. M. The structure of the new compound $YBaCo_4O_7$ with a magnetic feature. *Solid State Sci.* **4**, 923-931 (2002)
[2] Reimers, J.N. & Berlinsky, A.J. Order by disorder in the classical Heisenberg kagomé antiferromagnet. *Phys. Rev. B* **48**, 9539-9554 (1993).

Institut für Festkörperforschung
Forschungszentrum Jülich GmbH
D-52425 Jülich

Experimental Report
of Neutron Scattering Experiments
at the FRJ-2 Reactor

Proposal number:	DNS-05-013		
Experiment title:	High Spin – Low Spin transition in per deuterated Fe(NCS)2 (brt)2.D2O. The magnetic inelastic response as determined by xyz-PNA.		
Dates of experiment:	17.02. – 22. 02.2006	Date of report:	29.06.2006
Experimental team: Names	Addresses		
D.Visser W.Schweika	NWO-Physics, CCLRC ISIS Facility, Chilton Didcot, OX11 0QX, UK Institut für Festkörperforschung, Forschungszentrum Jülich GmbH D-52425 Jülich, Germany		
Local Contact:	Dr Werner Schweika		

Experimental report text body

Spin-crossover solids are materials which are studied for future applications of optical memories or numerical displays. These materials are also good examples of photo excitable materials. Optical switching at low-temperatures, below the high spin - low spin transition (T (hs-ls)) is achieved by the so-called direct or inverse LIESTT effect (Light Induced Excited spin State Trapping) [1, 2].

The structurally quasi two-dimensional molecular magnet $\{Fe(NCS)_2(brt)_2\}.H_2O(D_2O)$ was the first material reported to exhibit a high spin (HS) to low spin transition (LS) around the T↓ (hs-ls) = 124K with a hysteresis effect as wide as 20K on increasing the temperature: T↑ (hs-ls) = 144K. Since the Fe ions are co-ordinated via bi-triazole bridges, the effect of HS - LS transition is dramatic. The high temperature paramagnetic behaviour changes abruptly to a low temperature diamagnetic one at T (HS - LS) via a first-order structural phase transition. This transition is also accompanied with a colour change from transparent to purple. This transition has been observed by magnetisation, specific heat, Mössbauer and optical spectroscopy [3]. Recently we studied this transition with muon spin resonance [4]. In the diamagnetic phase one would have expected a silence in the muon relaxation behaviour. However, a complex relaxation behaviour is observed which was tentatively attributed to muonium formation but no hard evidence was obtained for a non-magnetic ground state in the low-temperature phase.

To obtain further information about the magnetic character of the$\{Fe(NCS)_2(brt)_2\}(D_2O)$, we determined the inelastic response using xyz-polarisation analysis at T = 160 K (high spin state) and T= 190 K (low spin state) using the high resolution set up on the DNS polarised neutron diffractometer. We performed TOF measurements on a powder sample of fresh fully deuterated $\{Fe(NCS)_2(brt)_2\}.(D_2O)$ sample. At T = 190 K , we observe two excitation levels in the energy loss side of the inelastic neutron response: 0.8 meV (as a shoulder near the elastic line) and 1.6 meV, see fig.1. These excitations are absent in the 90 K data, see fig.2 The difference spectrum of both data sets show both excitations clearly. Independently the magnetic signal can be observed in

the difference spectrum from the I y,*sf* - I y,*nsf* signal., see fig 3.

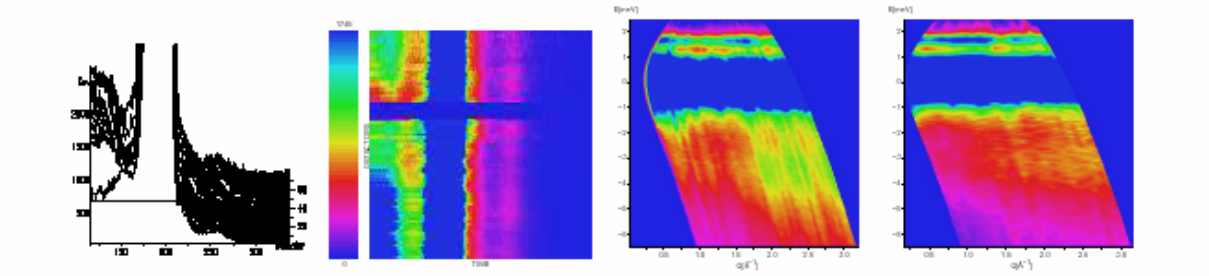


FIG. 1: T=160K, sum of all data, background corrected

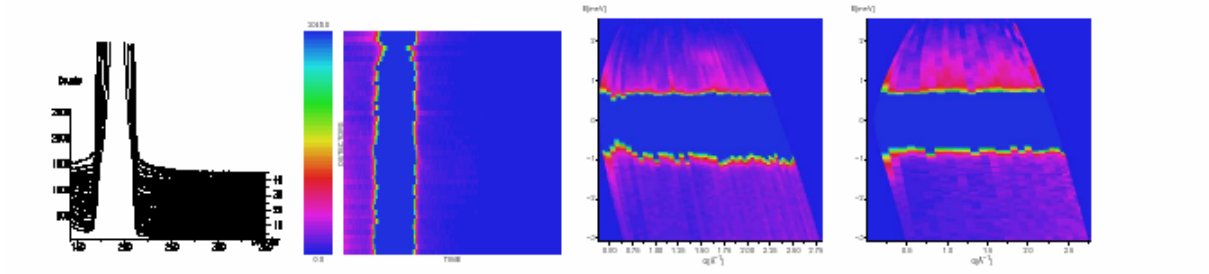


FIG. 2: T=90K, sum of all data, background corrected

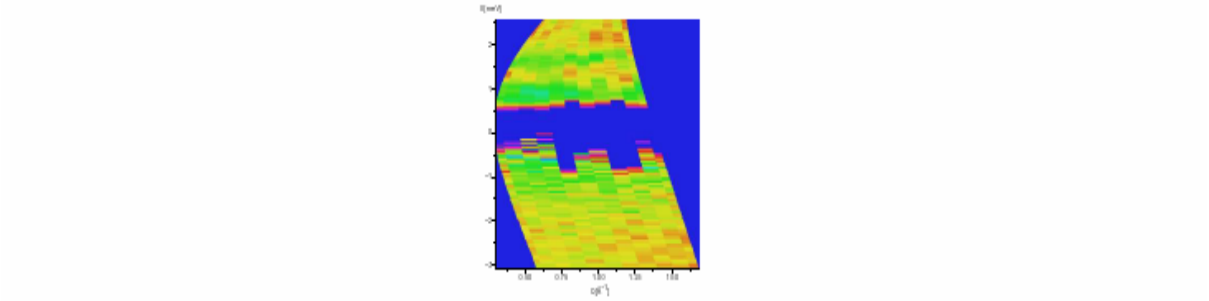


FIG. 4: T=160K. I_y, sf - I_y, nsf.A proof of the magnetic nature of these excitations is in principle possible using the xyz-method. However, the statistical quality if poor for such differences. An indication for the magnetic nature is found by taking differences [x_sf - x_nsf perp Q almost no signal and z_sf - z_nsf $\perp Q$ almost no signal]
but for y_sf - y_nsf $\| Q$, there is a signal, see figure above.

The magnetic excitations are dispersionless. This indicates that we are looking at crystal field levels instead of spinwave like excitations. Further analysis has to show if the intensity of the excitations are Q-dependent, which would mean that they would not be a single spin excitations. we have shown that the ground state of $\{Fe(NCS)_2(brt)_2\}(D_2O)$ is non-magnetic.

References:

[1] A. Desaix et al. Eur. Phys. J. B6 (1998) 183.
[2] O.Kahn et al. Science 279 (1998) 44.
[3] W. Vreugdenhil et al. Polyhedron 9 (1990) 2971.
[4] O.Roubeau et al. Chem Phys. Lett.395 (2004) 177.

Institut für Festkörperforschung
Forschungszentrum Jülich GmbH
D-52425 Jülich

Experimental Report
of Neutron Scattering Experiments
at the FRJ-2 Reactor

Proposal number:	DNS-05-014		
Experiment title:	The correlations between the ferroelectric and magnetic transitions in $REMn_2O_5$		
Dates of experiment:	01.12.2005	Date of report:	01.06.2006
Experimental team: Names	Addresses		
Lieh-Jeng Chang	Nuclear Science and Technology Development Center National Tsing Hwa University 101, Sec. 2, Kuang-Fu Road HsinChu, 30013, Taiwan		
Local Contact:	Dr. Yixi Su		

Experimental report text body

Introduction

There is currently a great interest in the materials that exhibit interplay between lattice distortions and electrical and magnetic ordering. Among these materials, magnetoelectrics, in which magnetism and ferroelectricity coexist and are mutually coupled, are being investigated extensively. These materials display phenomena such as the control of electrical polarization by the application of an external magnetic field, providing an additional degree of freedom for the design of new devices.[1] However; compounds showing large magnetoelectric effects are extremely rare. The magnetoelectric $TbMn_2O_5$ exhibits a profound interplay between electrical polarization and the applied magnetic field. This is demonstrated by two discoveries: the highly reversible switching of electrical polarization using relatively low magnetic fields of 0-2T; and the combined application of electric and magnetic field, which leaves a permanent imprint in the polarization.[2]

$TbMn_2O_5$ is an insulator and consist of linked $Mn^{4+}O_6$ octahedra and $Mn^{3+}O_5$ pyramids adopting space group *Pbam*. The octahedral share edges to form ribbons parallel to the c axis, adjacent ribbons being linked by pairs of corner-sharing pyramids.[1] The structure at room temperature is orthorhombic[3]. The reported neutron diffraction measurements on $TbMn_2O_5$ as a function of temperature and applied field which show unambiguous correlations between dielectric anomalies and changes in the periodicity of the spin structure. First, the onset of ferroelectricity at 38 K is associated with the appearance of incommensurate antiferromagnetic ordering $T_1 = 43$ K. At $T_2 = 33$ K, just above the maximum in spontaneous polarization **P**, propagation vector **k** locks into a commensurate value (1/2, 0, 1/4). Remarkably, at $T_3 = 24$ K, where the dielectric constant **ε** has an upward "jump", **k** becomes suddenly incommensurate again, a rare example of such a transition on cooling. The low temperature transition ($T_4 = 10$ K) coincides with a major increase of the Tb ordered moment. The 43 and 24 K transitions are accompanied by clear anomalies in the lattice parameters, particularly along the *b* "polar" axis, and in the atomic displacement parameters.[4]

Experiments

8 grams of $TbMn_2O_5$ polycrystalline sample have been prepared through conventional solid-state reaction method and characterized by powder x-ray diffraction and magnetization. All the observable peaks on the powder x-ray pattern can be well indexed for showing the sample to be single phase. A broad peak has been observed on the magnetic susceptibility from 50 to 20 K corresponding to the series of transitions mentioned above. Experiments were performed at DNS in an orange cryostat for temperatures between 1.2 K and 250 K. Neutron wavelength 4.8 Å was selected for the elastic scattering experiments. Neutron polarization analysis was also performed to separate the nuclear and magnetic scatterings.

Results

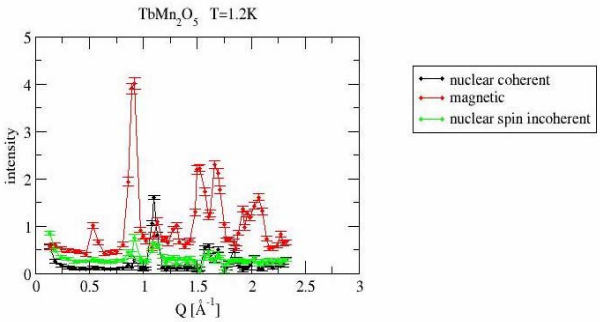


Fig. 1 Elastic scattering from DNS using neutron wavelength 4.8 Å at temperature 1.2 K with neutron polarization analysis. The nuclear spin incoherent peak at Q ~ 0.8 $Å^{-1}$ is thought not from nuclear but of magnetic origin due to insufficient separation. This may be due to either not perfect corrections for flipping ratio background and multiple scattering and / or it may have a cause also in the complex non-collinear structure.

Fig. 1 shows the elastic spectra using the neutron wavelength 4.8 Å taken at 1.2 K with neutron polarization analysis. The nuclear spin incoherent peak at Q ~ 0.8 $Å^{-1}$ is thought not from nuclear but of magnetic origin due to insufficient separation. This may be due to either not perfect corrections for flipping ratio background and multiple scattering and / or it may have a cause also in the complex non-collinear structure. The high magnetic background reveals that the magnetic moments have not ordered completely even down to 1.2 K.

Fig. 2 shows Magnetic peaks observed at different temperatures. Long-range ordered magnetic peaks are observed from ~ 39 K. This is consistent to the published results that the antiferromagnetic order occurs at 43 K.[4] The background at 250 K is lower than that of 48 K and 60 K is that at high T the width of the paramagnetic scattering will be about 250 K ~ 21.5 meV. This means that the transmission of the polarisation analysers, which are less efficient for faster neutrons, have to take into account This also means that only 60 to 50 % of the total paramagnetic scattering at high T have been observed. To clarify it, time-of-flight measurements and a more detailed analysis will be useful to quantify the whole contribution.

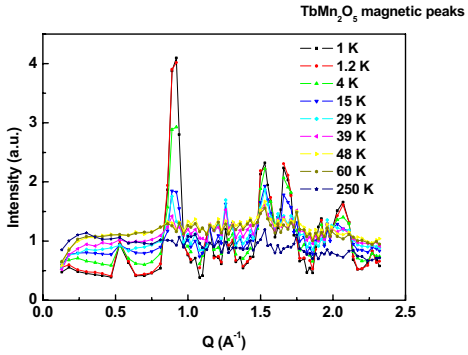


Fig. Magnetic peaks observed at different temperatures. Long-range ordered magnetic peaks are observed from ~ 39 K. This is consistent to the published results that the antiferromagnetic order occurs at 43 K.[4]

References:

1. G.R. Blake, et al., Phys. Rev. B **71**, 214402 (1995).
2. N. Hur, et al., Nature (London) **429**, 392 (2004).
3. D. Higashiyama and S. Miyasaka, Phys. Rev. B **72**, 064421 (2005).
4. L.C. Chapon et al., Phys. Rev. Lett **93**, 177402 (2004).

Institut für Festkörperforschung
Forschungszentrum Jülich GmbH
D-52425 Jülich

Experimental Report
of Neutron Scattering Experiments
at the FRJ-2 Reactor

Proposal number:	DNS-05-015		
Experiment title:	**Q - dependence of the coherent / incoherent contribution to the scattering of 20 % PEO- 80% Montmorillonite**		
Dates of experiment:	29.11.2005	Date of report:	09.03.2006
Experimental team: Names	Addresses		
Dr. Andreas Wischnewski Katarzyna Niedzwiedz Dr. Helen Hermes Dr. Michaela Zamponi Dr. Michael Monkenbusch Prof. Dr. Dieter Richter	IFF, Forschungszentrum Jülich, 52425 Jülich IFF, Forschungszentrum Jülich, 52425 Jülich IFF, Forschungszentrum Jülich, 52425 Jülich IFF, Forschungszentrum Jülich, 52425 Jülich IFF, Forschungszentrum Jülich, 52425 Jülich IFF, Forschungszentrum Jülich, 52425 Jülich		
Local Contact:	Dr. Werner Schweika		

Experimental report text body

The experiment was performed to determine the ratio of coherent and incoherent scattering intensities for a mixture of 20% protonated PEO in 80% montmorillonite.

We have recently used solution intercalation to prepare composites of poly(ethylene oxide) (PEO) and sodium montmorillonite (MMT). Initial small angle neutron scattering experiments have been performed and the data described successfully[1]. X-ray scattering and differential scanning calorimetry measurements have confirmed that using this sample preparation method and a suitable composition, it is possible for all the PEO to be intercalated between the silicate layers. The thickness of the intercalated PEO layers is 0.815 nm and extremely constant. Thus, this system is ideal for investigating the effect of extreme confinement on the dynamics and conformation of PEO polymer chains.

In a BSS experiment we have examined the same sample with 80% PEO content at temperatures between 375 and 425 K (proposal BSS-05-018). We found that the PEO – dynamics is in the BSS energy window and first indications of the effect of confinement in montmorillonite on the PEO dynamics have been seen. These results are promising, however, for a proper correction of the backscattering data of this system the information about the Q-dependence of the coherent / incoherent contribution to the structure factor is of utmost importance.

For this purpose the polarization analysis provided by the DNS spectrometer has been used.
We have measured the ratio of coherent and incoherent scattering as a function of the momentum transfer. The wavelength of the incoming neutrons was 3.3 Å.

The information extracted from this experiment is an indispensable input for the data evaluation of the above mentioned backscattering experiment.

References

1. H.E. Hermes, H. Frielinghaus, W. Pyckhout-Hintzen, D. Richter, Experimental report kw1-04-025

Institut für Festkörperforschung
Forschungszentrum Jülich GmbH
D-52425 Jülich

Experimental Report
of Neutron Scattering Experiments
at the FRJ-2 Reactor

Proposal number:	DNS-05-016		
Experiment title:	Magnetic correlations in the Kagomé system (Y,Ca)$BaCo_3(Al,Zn)O_7$		
Dates of experiment:	12.01. – 22.01.2006	Date of report:	06.06.2006
Experimental team: Names	Addresses		
Martin Valldor Yvonne Sanders Werner Schweika	Institut für Physik der Kondensierten Materie, TU-Braunschweig, Mendelssohnstrasse 3, D-38106 Braunschweig, Germany Institut für Streumethoden, IFF, Forschungszentrum Jülich, D-52425 Jülich, Germany Institut für Streumethoden, IFF, Forschungszentrum Jülich, D-52425 Jülich, Germany		
Local Contact:	Werner Schweika		

Experimental report text body

We studied the diffuse magnetic scattering from $CaBaCo_3AlO_7$, $YBaCo_3ZnO_7$, and $CaBaCo_3ZnO_7$ at several temperatures between 1.2 K and 300 K using the DNS instrument with polarised neutrons and xyz-polarisation analysis to separate magnetic from nuclear scattering.
A first results is that $CaBaCo_3AlO_7$ is not isostructural with the other compounds as previously reported [1], although the earlier data were based on single crystal X-ray diffractometry. Instead of the hexagonal unit cell, an orthorhombic has to be used to explain the nuclear scattering pattern from $CaBaCo_3AlO_7$, as can be seen in Fig.1. The orthorhombic cell is realised as the C-centring is broken and, since this is only obvious in neutron scattering data, the symmetry breaking is caused by changes in the oxygen substructure. However, due to low resolution in the obtained data, refinement of the more correct atomic structure of $CaBaCo_3AlO_7$ was not tried, but is planned for future investigations.

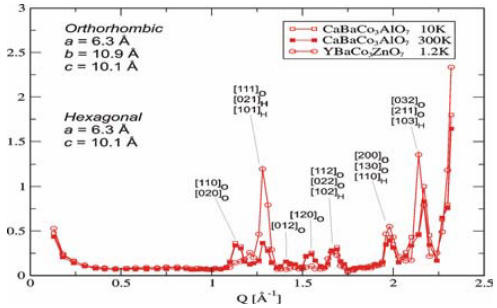


Fig.1 Comparison between nuclear scattering from the orthorhombic $CaBaCo_3AlO_7$ and the hexagonal $YBaCo_3ZnO_7$ as function of Q. Approximate unit cell parameters and indexed peaks are presented in the graph. The measuring temperatures are samples are indicated with different markers.

We do not observe any magnetic ordering transition for $CaBaCo_3AlO_7$ and $CaBaCo_3ZnO_7$ $CaBaCo_3ZnO_7$ down to a temperature of 1.2 K. This is surprising in view of the strong AF-coupling expected from the high negative Curie-Weiss constants (in between -500 and -1000 K)[2], and can be taken as a sign of highly frustrated spins and/or low dimensional spin systems. Indeed, the shape of the diffuse scattering is dominated by antiferro spin correlations. A broad diffuse peak evolves in the magnetic scattering of $CaBaCo_3AlO_7$ near 1.3 $Å^{-1}$ as shown in Fig.2a, while a more pronounced diffuse peak is found for $CaBaCo_3ZnO_7$, see Fig.2b.

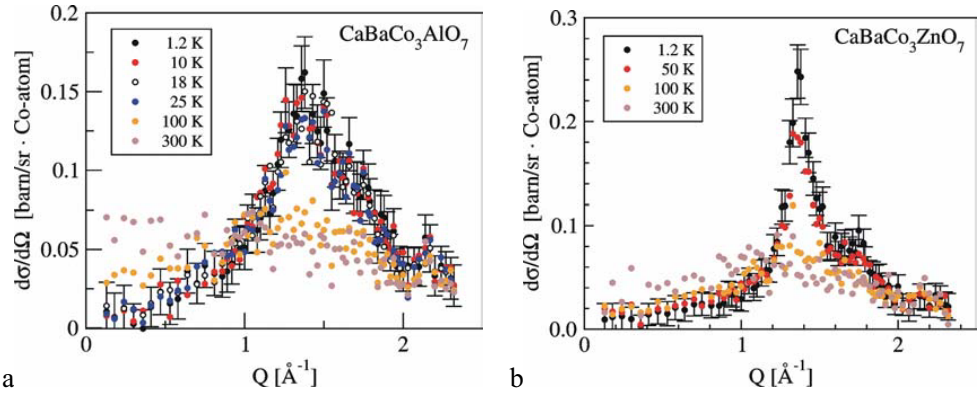


Fig.2 Magnetic scattering on $CaBaCo_3AlO_7$ (left) and $CaBaCo_3ZnO_7$ (right) at different temperatures as function of Q.

With respect to the atomic structure, the Co-sublattice can be viewed as kagomé layers which are weakly linked via another (trigonal) Co-layer. Therefore, one may expect in both compounds 2D AF spin correlations of Heisenberg spins, which would also explain the lack of Néel order down to 1.2 K. For the 2D kagomé AF with only nearest neighbor interactions, Reimers and Berlinsky[3] predicted an ordered ground state with staggered chirality, the so called $\sqrt{3}\times\sqrt{3}$ structure (Fig.3). The simulated short-range spin correlations at low but finite temperatures resemble our scattering data, with a diffuse peak close to 1.35 $Å^{-1}$. In $CaBaCo_3AlO_7$, it is easy to explain the lack of inter-planar coupling: Al sits between the kagomé layers and hinders any magnetic coupling. The Zn substituted compound has randomly distributed Zn ions in the kagomé layers and the magnetic diffraction contains more structure: a shoulder is visible on the high Q side of the maximum diffuse scattering. The spin dilution in the kagomé layers due to Zn and possible coupling between the kagomé layers leads to a more complex situation, which has to be analysed in more detail in future.

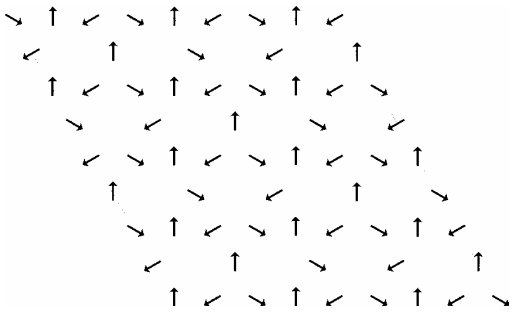


Fig.3 The in-plane spin motif on the kagome lattice of Co2, presented as lines where the crossing points are the sites for Co2. This spin structure is called the $\sqrt{3}\times\sqrt{3}$ structure[3].

[1] Valldor M., *Solid State Sciences* 6 (2004) 251-266
[2] Valldor M., *J. Phys. Chem. Solids* 66 (2005) 1025-1033
[3] Reimers, J.N. & Berlinsky, A.J. *Phys. Rev. B* **48**, 9539-9554 (1993).

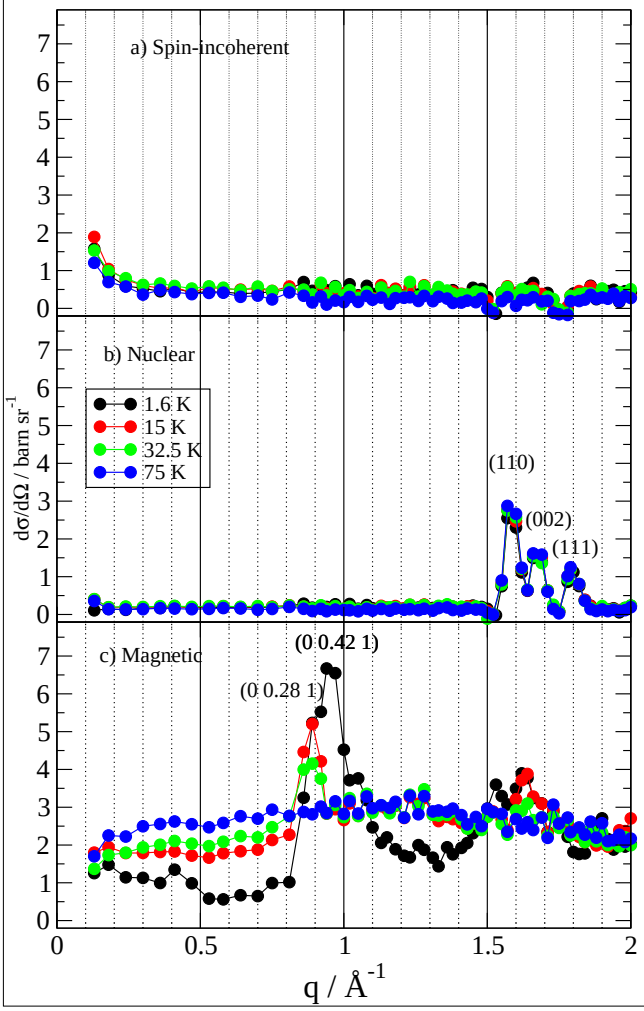
Institut für Festkörperforschung
Forschungszentrum Jülich GmbH
D-52425 Jülich

Experimental Report of Neutron Scattering Experiments at the FRJ-2 Reactor

Proposal number:	DNS-05-017		
Experiment title:	Polarised neutron diffraction from multiferroic $TbMnO_3$		
Dates of experiment:	9.1.06-12.1.06	Date of report:	23.5.06
Experimental team: Names:	Addresses:		
J. Voigt	Forschungszentrum Jülich		
Local contact:	W. Schweika		

We have studied the powder diffraction from $TbMnO_3$ with XYZ polarization analysis. The compound has attracted considerable interest because it exhibits multiferroic behaviour. Antiferromagnetic order and the ferroelectric polarization are intimately connected as evidenced by the polarization flop from the c-direction to the b-direction in an applied magnetic field of several Tesla [1]. The formation of the ferroelectric polarization at $T_c = 28$ K seems to be coupled to a magnetic reorientation transition from a collinear incommensurate (IC) magnetic structure to a non-collinear. This transitions involves also a long range ordering of the Tb^{3+} ions according to a recent neutron diffraction study [2]. The transition temperature is significantly higher than temperature $T_{N,Tb} = 8$ K, at which the Tb moments order with a different propagation vector as compared to the ordering of the Mn subsystem.
To resolve the magnetic structure, polarised neutron scattering give the full information about the vectors of the magnetic moments. A recent study of $TbMn_2O_5$ has raised the question, whether it is possible to distinguish collinear from non collinear magnetic structures. Supposedely the separation of nuclear, magnetic and spin-incoherent scattering breaks down, if the magnetic structure becomes non-collinear.
The 3.6 g of $TbMnO_3$ powder were mounted on DNS in a LH cryostat. Using the polarization setup, the scattering was recorded at 4 temperatures (1.6 K, 15 K, 35 K, 75 K) in the different phases identified in earlier studies, e.g [1]. For each temperature the spin-flip and non-spin-flip was collected, preparing the spin X,Y and Z direction respectively. The wavelength during the entire experiment was 4.75 Å. The different contributions shown in Fig. 1 were separated using the formulas given in [3] and calibrated by scattering from Vanadium.

Except for the small angle region and close to the structural Bragg reflections between 1.5 and 2 $Å^{-1}$, the separation works well at all temperatures. Close to the Bragg reflection and in forward direction the separation is not perfect. The forward direction can be explained by the fact, that the neutron beam is larger than the sample.
The different contributions of the Tb IC structure ($\vec{Q}$ =(0 0.42 1)) and the Mn IC ($\vec{Q}$ =(0 0.28 1)) structure overlap at $T = 1.6$ K. They agree with the results from [2]. The paramagnetic scattering is also significantly weaker at this temperature.
With increasing temperature, the IC Tb structure vanishes. The transition into the paraelectric state does not lead to a significant change in any of the different contributions. The paramagnetic scattering at small momentum transfer is increased, while the magnetic peak intensity decreases. In the paramagnetic state finally the magnetic intensity is fairly broad.
Even at T=1.6K there is still a significant degree of magnetic disorder. The slight increase towards small q indicates short-range ferro-type correlations within the AF-IC structure. There are no indications of long-range ferromagnetic correlations neither from magnetic scattering at a nuclear Bragg peaks nor from any loss in polarisation of the scattered beam.



References

[1] T. Kimura *et al.*, PHYSICAL REVIEW B **71**, 224425 (2005).

[2] M. Kenzelmann *et al.*, PHYSICAL REVIEW LETTERS **95**, 087206 (2005).

[3] W. Schweika, in *Polarized Neutron scattering*, edited by Th. Brückel and W. Schweika (Forschungszentrum Jülich, Jülich, 2002), Chap. 1, pp. 5–29.

Fig 1: Spin-incoherent, nuclear and magnetic scattering separated by XYZ polarization analysis at different temperatures.

Neutron Reflectometer with Polarization Analysis (HADAS)



Instrument Parameters

Monochromator:	(002) pyrolytic graphite double monochromator
Wavelength:	2 Å < λ < 6.5 Å, λ = 4.52 Å for reflectometry
Wavelength resolution:	1 %
Collimation:	0.1 mrad < ΔΘ < 10 mrad (unpolarized beam), 0.1 mrad < ΔΘ < 1.5 mrad (polarized beam)
Polarization analysis:	Stack of 30 double sided polarizing supermirrors (top m = 2.5, bottom m = 1.8) set up as divergent collimator
Detector:	2D position-sensitive scintillation detector, 80 mm diameter, resolution < 1.5 mm, at 1.6 m distance from the sample
Neutron flux at sample:	10^5 unpolarized neutrons /cm^{2}s with a collimation of ΔΘ = 2 mrad, 2×10^4 polarized neutrons /cm^{2}s with a collimation of ΔΘ = 1 mrad
Maximal beam size at sample:	50 mm × 10 mm (unpolarized), 20 mm × 10 mm (polarized with polarisation analysis)
Special sample environment:	Electromagnet 0.3 mT < $\mu_0 H$ < 1 T ; He flow cryostat 10 K < T < 300 K

Instrument Responsible

Dr. Ulrich Rücker Tel. +49-(0)-2461-61-6896 Email: u.ruecker@fz-juelich.de
Dr. Emmanuel Kentzinger Tel. +49-(0)-2461-61-3139 Email: e.kentzinger@fz-juelich.de

Institut für Festkörperforschung
Forschungszentrum Jülich GmbH
D-52425 Jülich

Experimental Report of Neutron Scattering Experiments at the FRJ-2 Reactor

Proposal number:	HAD-04-007		
Experiment title:	Magnetization reversal and depth profiling of exchange biased Co/CoO multilayers by polarized neutron reflectivity		
Dates of experiment:	17.06.04	Date of report:	February 21, 2006
Experimental team: Names:	Amitesh Paul, Ulrich Ruecker, Emmanuel Kentzinger, Thomas Brueckel		
Address:	Institut fr Festkrperforschung Forschungszentrum Jlich GmbH D-52425 Jlich, Germany Deutschland		
Local contact:	Amitesh Paul		

A reduction of the H_{EB} is seen in most thin-film systems after the first cycle of hysteresis loop for the subsequent reversal of FM magnetization [1]. Usually along with decrease in H_{EB} values a decrease in the coercivity is also noticed. A rearrangement of the AF domain structure has been suggested to be connected with the loss of magnetization in the AF and thereby the magnitude of H_{EB}. A connection of training effects to the microstructure is predicted [2] which was supported by Nowak *et al* [3] in their domain state model with nonmagnetic defects. However, presence [4]/absence [5] of training effect in some epitaxial systems with uniaxial/biaxial magnetic anisotropy rule out the connection of training effect with microstructure. Hoffmann [6] had shown by numerical simulations that the symmetry of magnetic anisotropy in antiferromagnet is crucial to understand training effects. An imbalance between two AF sublattice magnetization could easily explain the training effect in uniaxial as well as biaxial systems. Therefore it also supported the observed presence of training effects in polycrystalline samples which are expected to be more common with multiple equivalent easy magnetization axis. Polycrystallinity on the other hand limits the long range order in the AF layer which is restricted by the presence of grain boundaries and favors domain formation.
In the present report, we investigate the layer-by-layer evolution of the magnetization configuration of the same CoO/Co polycrystalline ML along a full magnetization loop by specular and off-specular Polarized Neutron Reflectometry (PNR) for a trained state and compare it with that of the untrained one. The field cooling axis and the reflectometer axis were the same. The reversal proceeds for both loop branches in a nonuniform mode for both cycles of measurements. All four specular reflectivity channels are measured at 15 different H_a, six of which are shown in Figure 1, together with least-square fits based on an extension of the Parratt formalism to magnetic MLs.

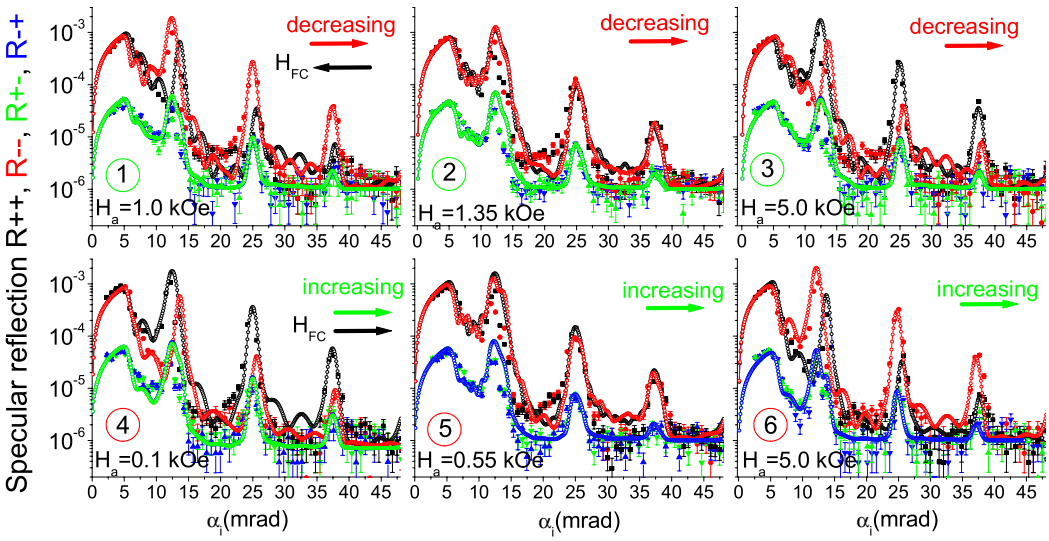


Figure 1. Measured and fitted NSF (R_{++} and R_{--}) and SF (R_{+-} and R_{-+}) reflectivity patterns of *continuous* SiO_2/Co(11.0 nm)/CoO(7.0 nm)]$_{\times 20}$/*Au*(50.0 *nm*) ML in the *trained state* at different applied fields H_a along increasing and decreasing fields where H_{FC}=-4.0 kOe.

This result indicates that the FM layer domains are always parallel or antiparallel to the applied field direction whether they are in the first or subsequent field cycles. Such stable configuration of the FM magnetization is achieved possibly due to the existence of multiple AF-FM interfaces in our ML which therefore satisfies the conditions for perpendicular configuration of the AF sublattices. However, under such a condition, the system is not expected to show any training effect either, as this would indicate the absence of rearrangements of AF magnetization after the first cycle. Our ML on the contrary, do show the existence of training effect as it clearly shows the decrease in H_c value. In case of a broken perpendicular arrangement, we would have expected the FM magnetization reversal only by rotation following the predictions of Hoffmann [6]. Thus we can say that in-spite of the initial magnetization rearrangements after the first cycle, the system retained the perpendicular arrangement in the second cycle. Alternatively, we can say that broken perpendicular arrangement has not been instrumental in deciding over the magnetization reversal mechanism in subsequent cycles.

References

[1] J. Keller *et al.*, Phys. Rev. B **66**, 14431 (2002).

[2] J. Nogues *et al.*, J. Magn. Magn. Mater. B **192**, 203 (1999).

[3] U. Nowak *et al.*, Phys. Rev. B **66**, 14430 (2002).

[4] L. Malkiniski *et al.*, Journ. Appl. Phys **93**, 6835 (2003).

[5] M. R. Fitzsimmons *et al.*, Phys. Rev. Lett. **84**, 3986 (2000).

[6] A. Hoffmann, Phys. Rev. Lett. **93**, 97203 (2004).

Institut für Festkörperforschung
Forschungszentrum Jülich GmbH
D-52425 Jülich

Experimental Report of Neutron Scattering Experiments at the FRJ-2 Reactor

Proposal number:	HAD-04-010		
Experiment title:	Investigating magnetization reversal in polycrystalline IrMn/CoFe multilayer w.rt. field cooling and measuring field directions		
Dates of experiment:	12.10.04	Date of report:	February 21, 2006
Experimental team: Names:	Amitesh Paul, Ulrich Ruecker, Emmanuel Kentzinger, Thomas Brueckel		
Address:	Institut fr Festkrperforschung Forschungszentrum Jlich GmbH D-52425 Jlich, Germany Deutschland		
Local contact:	Amitesh Paul		

The shift in hysteresis loop is given by an exchange bias field which is crucial for designing thin film magnetic sensors. The magnetization reversal in such systems is complex and are subject to recent studies. Asymmetric hysteresis loops due to different magnetization reversal process in different branches of the hysteresis loop are common [1, 2, 3, 4]. Theoretically the interpretation of the magnetization reversal was discussed in Ref. [5]. This is governed by an effective field H_{eff} arising from the anisotropy of the FM, the exchange bias field of the AF, and the applied field H_a. H_{eff} and the torque it exerts on the FM magnetization depend on the angle θ between H_a and the AF anisotropy axis or the field cooling axis H_{FC}. Beckmann *et. al* showed that depending on θ the reversal mode is either by coherent rotation (uniform reversal mode) for both loop branches or asymmetric with a nonuniform reversal for the increasing branch. Here nonuniform refer to the reversal of magnetization with no component perpendicular to the H_a direction which is essentially reversal by domain wall motion.
In the present report, we investigate the same polycrystalline IrMn/CoFe sample for different angles, θ =15°, 45° and 90°. We measure specular and off-specular Polarized Neutron Scattering from the specimen along each full magnetization loop: increasing (negative to positive) and decreasing (positive to negative) field sweeping direction of the H_a for the hysteresis loop with respect to the direction of H_{FC}. For θ=15° , we observe a crossover from sudden flipping of each layer magnetization to coherently rotating layers along the stack for both loop branches as we perform this layer-by-layer magnetometry. However, for θ =45° and 90° the reversal proceeds symmetrically and coherently in an uniform mode. The reversal is accompanied by fluctuations of the in-plane magnetization component perpendicular to H_a as observed earlier [6] irrespective of θ.

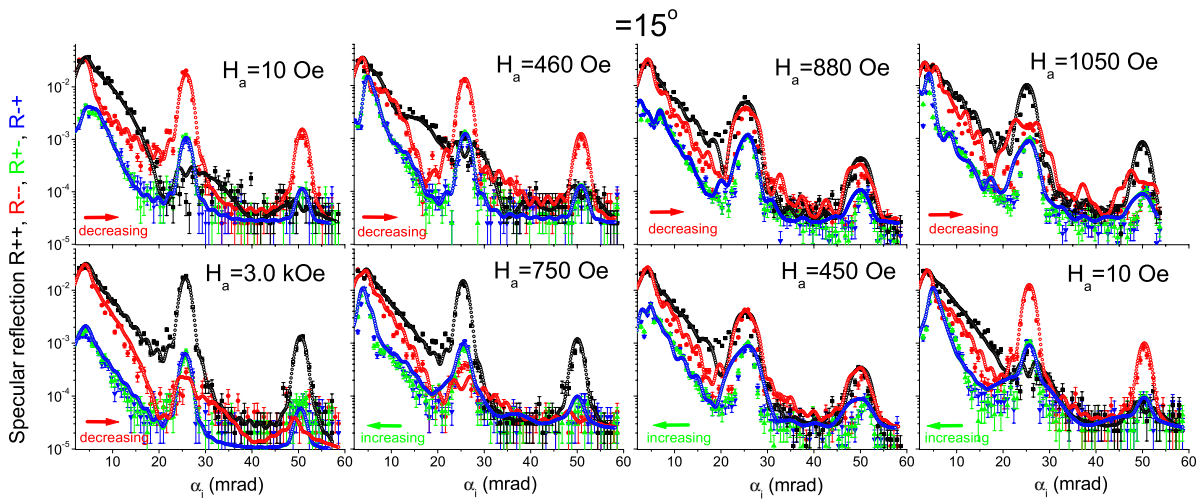


Figure 1. NSF and SF specular reflectivity patterns (solid symbols) along with their fits (open circle) for $[Ir_{20}Mn_{80}(6.0\ nm)/Co_{80}Fe_{20}(3.0\ nm)]_{10}$ ML with θ=15° along increasing and decreasing fields.

The details of the fitting procedure have been described earlier [6]. For θ=15°, each layer rotates or flips independently and *sequentially* with field strength, fanning around in different directions in a certain field which shows the layer resolved magnetization direction with respect to the H_a direction. On the deceasing field branch: the bottom layers start flipping first followed by the top layers as we increase the field strength. On the increasing branch: the top layers rotate in different directions while the bottom layers flip back. The flipping and rotation of layers are seen by the presence/absence of SF signals of different intensities as we sweep the field strength on both branches of the loop.
These observations are understood in general terms of the torque exerted on the system due to different effective field strengths and the corresponding angles with the magnetization axis. We systematically varied the relative strengths of the exchange and uniaxial anisotropies in a single multilayered system which is particularly possible due to *sequential* switching of layers with increasing N. All reversal modes are accompanied by small scale fluctuations of the perpendicular component of the in-plane magnetization on a length scale comparable to the grain size thus indicating the domain to domain fluctuations in the system. Our measurements show a gradual crossover from layer flipping (domain wall motion) for low torque regimes to coherent rotation for high torque regimes. Our experimental findings finally unravel the mysteries of magnetization reversal of exchange coupled systems and explain earlier observations of asymmetric and symmetric hysteresis loops.

References

[1] W.-T. Lee *et al.*, Phys. Rev. B **65**, 224417 (2002).

[2] M. R. Fitzsimmons *et al.*, Phys. Rev. Lett. **84**, 3986 (2000).

[3] M. Gierlings *et al.*, Phys. Rev. B **65**, 92407 (2002).

[4] F. Radu *et al.*, Phys. Rev. B **67**, 134409 (2003).

[5] B. Beckmann *et al.*, Phys. Rev. Lett. **91**, 187201 (2003).

[6] A. Paul *et al.*, Journ. Magn. Magn. Mater. **268**, 216, (2005); Phys. Rev. B **70**, 224410 (2004).

Institut für Festkörperforschung
Forschungszentrum Jülich GmbH
D-52425 Jülich

Experimental Report of Neutron Scattering Experiments at the FRJ-2 Reactor

Proposal number:	HAD-04-014		
Experiment title:	Magnetization reversal of a combination of narrow and wide magnetic stripes		
Dates of experiment:	17.-24.11.2004 10.-14.03.2005	Date of report:	19.06.2006
Experimental team: Names	Addresses		
Katharina Theis-Bröhl Dorothee Meyer	Ruhr-Universität Bochum Institut für Experimentalphysik IV 44780 Bochum Ruhr-Universität Bochum Institut für Experimentalphysik IV 44780 Bochum		
Local Contact:	Ulrich Rücker		

Experimental report text body

We performed polarized neutron reflectivity measurements on a periodic array consisting of alternating wide and narrow Fe bar. The bars have a width of 0.9 and 1.9 µm, a length of 30 µm and a height of 90 nm. They are arranged in lines as can be see in Fig. 1. The distance between the lines of bars is 10 µm and the distance between adjacent bars is 1.6 µm.

Longitudinal MOKE hysteresis loops (Fig. 2) were performed at different angles of sample rotation with respect to the applied field. Measurements at easy axis (field applied along the ridge of the bars) and at 45° represent stepped hysteresis loops respective of two different coercive fields of the wide and narrow stripes. We performed PNR measurements at the instrument ADAM (ILL) in the easy axis configuration using a pencil detector and a PSD. Measurements with a sample rotation of 45° were only performed with a pencil detector. The aim pf the present experiment was to repeat these measurements by using a PSD. In Fig. 3 we show a scan performed along the total reflection edge with a varying angle of incidence α_i and a constant exit angle α_f. In this scan reflections from both lateral periods can be observed: at small angles α_i the period of about 40 µm with respect to the array of lines of bars and at higher angles α_i the period of the unit cell of the wide and narrow bars of 6 µm

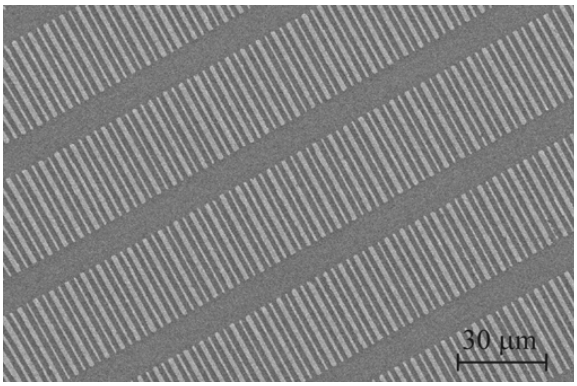


Fig. 1: Scanning electron microscopy image of the two dimensional array of lines of alternating wide and narrow Fe bars.

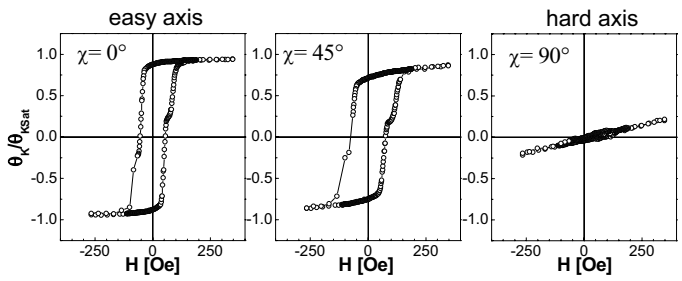


Fig: 2 MOKE hysteresis loops performed at different angles of sample rotation with respect to the applied field.

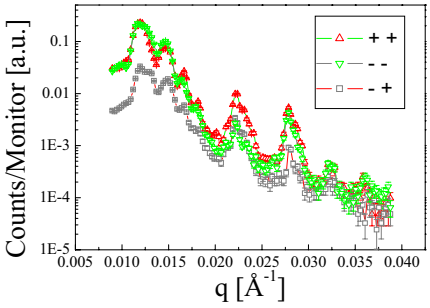


Fig. 3: Polarized neutron reflectivity measurement performed along the total reflection edge at α_f=const.

In the HADAS experiment we planned to measure polarized intensity maps at different magnetic fields in the 45° configuration. In Fig. 4 measurements performed at two different fields are presented. The measurements at 49.5 Oe (left maps) are performed at a field below the coercive fields of both types of stripes. It shows specular reflectivity, off-specular Bragg diffraction from the lateral period and some off-specular diffuse scattering. The second-order Bragg reflections have a higher intensity than the first order one. This is due to structure factor reasons. The measurements at 94 Oe (right maps) are performed in the antiparallel state of both types of stripes. In this case antiparallel alignment changes the magnetic structure factor resulting in higher intensity at the first-order Bragg reflections. Additionally; Bragg diffraction from the large period of the lines of bars of 40 μm can be observed close to the specular line. There can also be observed some changes with changing field.

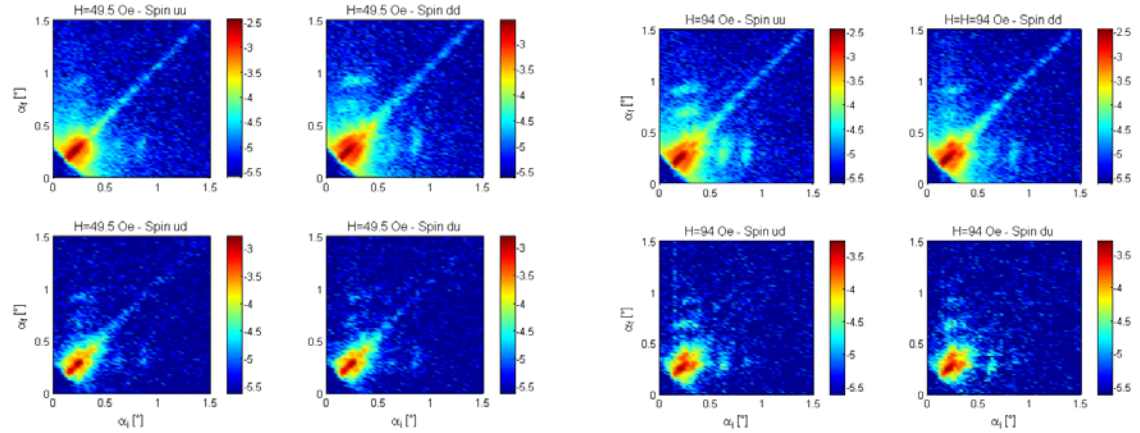


Fig.4: PNR maps performed at two different magnetic fields.

Unfortunately, we had to stop our experiment after measuring at 94 Oe because of enhanced background due to another experiment. This enhanced background already can be seen in the Spin up-down map taken at 94 Oe. Unfortunately, also the measurements performed in March 2005 were we got some additional days were not successful.

Institut für Festkörperforschung
Forschungszentrum Jülich GmbH
D-52425 Jülich

Experimental Report
of Neutron Scattering Experiments
at the FRJ-2 Reactor

Proposal number:	HAD-04-017		
Experiment title:	Polarized neutron reflectometry on discontinuous metal insulator multilayers		
Dates of experiment:	24.01.2005 to 07.02.2005	Date of report:	06.06.2006
Experimental team: Names	Addresses		
Prof. Dr. W. Kleemann S. Bedanta, M.Sc. Dr. O. Petracic	Angewandte Physik, Universität Duisburg-Essen, 47048 Duisburg Angewandte Physik, Universität Duisburg-Essen, 47048 Duisburg Angewandte Physik, Universität Duisburg-Essen, 47048 Duisburg		
Local Contact:	Dr. E. Kentzinger, Dr. A. Paul, Dr. U. Rücker		

Experimental report text body

Introduction :

Polarized neutron reflectivity (PNR) studies have been performed on granular multilayers $[Co_{80}Fe_{20}(t_n)/Al_2O_3(3nm)]_9$ for two different nominal thicknesses t_n = 1.7 nm and 1.8 nm (percolating ferromagnet). The measurements were done at several temperatures, T = 150, 300 and 350 K with the new cryostat in the field range of $0.47 \leq \mu_0 H \leq 12$ mT.

Motivation :

Interacting ferromagnetic nanoparticle systems $[Co_{80}Fe_{20}(t_n)/Al_2O_3(3nm)]_m$ where m represents the number of bilayers, show different kinds of collective behavior depending on the nominal thickness of CoFe layers t_n . For $t_n < 1$ nm one finds superspin glass (SSG) behavior [1], while at higher coverages (1 nm $< t_n <$ 1.5 nm) the interactions between the superspins give rise to a "superferromagnetic" (SFM) state with magnetic percolation, but particulate structure [2,3]. Above t_n = 1.4 nm percolation occurs, and the system behaves like a bulk ferromagnet (FM). The samples have an in-plane uniaxial anisotropy induced by the preparation method. The magneto-optic Kerr effect in polar geometry reveals absence of the polar component of magnetization in the sample, *i.e.* the sample magnetization lies in the film plane. SQUID measurements performed on samples with t_n = 1.7 nm and 1.8 nm show steps in the hysteresis. The possibility of layer-by-layer magnetization reversal in this sample is studied by PNR on these two samples.

Results and Discussions :

In this report we will discuss the results obtained from the *percolating ferromagnetic sample with* t_n = 1.8 nm. Fig. 1 (a) shows PNR data taken at positive saturation (12 mT). The FM state of the sample can be recognized by the splitting of the reflectivity edges where R^{++} (θ), is shifted to higher angles in comparison to $R^{--}(\theta)$ [3]. The first order structural superlattice Bragg peak at $2\theta = 4.6°$ is dominant in the R^{--} channel. Its position corresponds to a bilayer thickness $d \approx 5.6$ nm in agreement with X-ray results (data not shown here). The presence of a weak signal in the two SF channels R^{+-} and R^{-+} is primarily due to the finite flipping ratio of 18 corresponding to the limited efficiency of 94 % for the polarization analysis. The oscillatory behavior (Kiessig fringes) of R^{++} and R^{--} is due to the multilayer structure of the sample. The PNR data shown in Fig. 1(c) were taken at the weak guiding field (0.47 mT) of the neutrons after negatively saturating the sample. They closely refer to the negative remanence as indicated by the low angle data close to the plateau of total

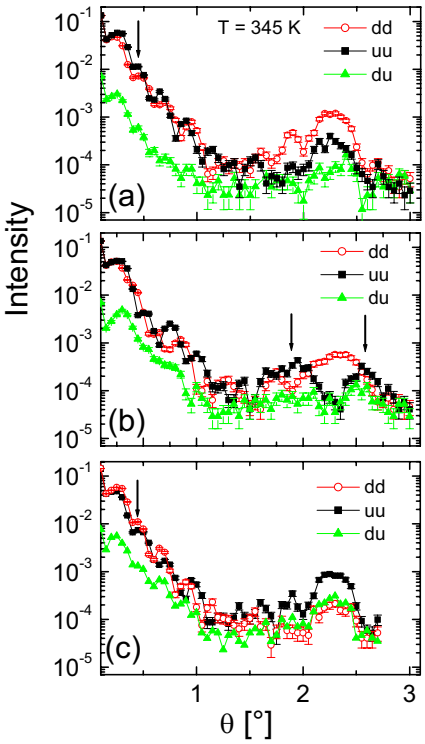


Fig.1. Spin-polarized neutron reflectivities R^{++} in red (dark gray), R^{--} in black and R^{+-} in green (light gray) *vs*. angle of incidence, θ, measured at T = 350 K and $\mu_0 H$ =12 mT (saturation) (a), close to the coercive field $\mu_0 H$ = 1.95 mT (b), and close to remanence in the guiding field of the neutrons, $\mu_0 H$ = 0.47 mT, after negative saturation (c) of *ferromagnetic* $[Co_{80}Fe_{20}(1.8nm)/Al_2O_3(3nm)]_9$.

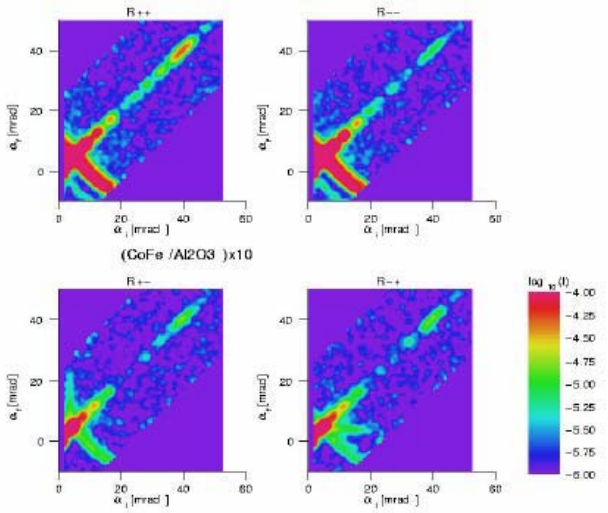


Fig.2. Off-specular scattering of polarized neutrons measured at the remanence of $\mu_0 H$ = 0.47 mT, after negative saturation of a *ferromagnetic* $[Co_{80}Fe_{20}(1.8nm)/Al_2O_3(3nm)]_9$ sample.

Interestingly measuring the neutron reflectivity at the coercive field the sample exhibits two enhanced satellites (arrows) near the 1st Bragg peak (θ = 2.3°) as shown in Fig. 1 (b). Analysing this specular reflectivity we found that this is probably due to an oscillating magnetization from FeCo layer to FeCo layer with a period of eight bilayers along the multilayer stack [5]. Presence of weak spin-flip intensity hints a transverse component of magnetization in the sample which may arise from the domain walls or from a transverse component of the net magnetization in the sample. We also observed off-specular scattering from this sample arising due to domains as shown in Fig. 2. Further analysis of the diffuse scattering will reveal the mean domain size in the sample. It has been found by the help of micromagnetic simulations that competition between long and short-ranged dipolar interactions apparently gives rise to this modulated magetization depth profile in magnetic multilayers. [6]

Similar results were obtained for the DMIM sample with t_n = 1.7 nm. The data analysis is in progress.

Conclusions and acknowledgements :

In the ferromagnetic samples an oscillatory magnetization depth profile is found. Off-specular scattering was observed from which one can calculate the mean domain size in the sample.

We thank Dr. A. Paul, Dr. Emmanuel Kentzinger and Dr. Ulrich Rücker for their support at HADAS and we gratefully acknowledge Forschungszentrum Jülich for the financial support for the work at Jülich.

Reference:

1. X. Chen et al., Phys. Rev. B **72** (2005) 214436.
2. W. Kleemann et al., Phys. Rev. B **63** (2001) 134423
3. S. Bedanta et al., Phys. Rev. B **72** (2005) 024419.
4. S. Bedanta et al. Phys. Stat. Sol (c) **1** (2004) 3288.
5. S. Bedanta et al. (to be published).
6. S. Bedanta et al. Phys. Rev. B (in press).

Institut für Festkörperforschung
Forschungszentrum Jülich GmbH
D-52425 Jülich

Experimental Report of Neutron Scattering Experiments at the FRJ-2 Reactor

Proposal number:	HAD-04-018, HAD-04-019		
Experiment title:	Test of a transmission polarizer device for KWS-2 – Part I and Part II		
Dates of experiment:	26.11. – 28.11.04 21.01. – 24.01.05	Date of report:	12.06.2006
Experimental team: Names	Addresses		
E. Kentzinger A. Ioffe U. Rücker	Institut für Festkörperforschung, Forschungszentrum Jülich		
Local Contact:	E. Kentzinger		

Experimental report text body

This experiment was entering in the project of equipping KWS-2 with polarized neutrons until its move to FRM-II.

A first try has been performed, using the spin down neutrons transmitted by the polarizer of NSE that is sharing the same neutron guide as KWS-2. This experiment was rather unsuccessful: a flipping ratio of only 2-to-3 was obtained at the KWS-2 sample position. We explain this by the bending of the KWS-2 guide and by the fact that the NSE-polarizer does not polarize the whole incoming divergence of the neutron guide.

A second idea that we had was to build a polarizer device based on transmission polarizers already tested on HADAS (see report HAD-03-005). Those transmission polarizers do not produce any small angle scattering in the -- and spin flip channels if they lie in a strong enough field ($\mu_0 H > 0.4$ Tesla). However, some ++ small angle scattering, due to interfacial roughness, is still present (see Fig. 1a).

In order to remove this small angle scattering, we have installed, 0.5 mm behind this polarizer, an identical transmission polarizer that would reflect this ++ scattering and bring it above the horizon. This idea has been tested and the measurement performed on such a device is shown in Fig. 1b. We see a strong reduction of the ++ small angle scattering around $\alpha_I = 5$ mrad and around the primary beam. Some small angle scattering intensity is still seen around $\alpha_F = 5$ mrad. We explain this by the fact that, due to the limited space at sample position on the HADAS instrument, we were not able to install a long enough 'analyzer' supermirror and that those small angle scattered neutrons therefore did not meet it.

Practically, the polarized SANS and GISANS measurements on KWS-2 were performed using only one single polarizing supermirror. As a matter of fact, the tests on KWS-2 surprisingly revealed that, in that case, the level of GISANS was smaller than using a two supermirrors set-up..

a) b)

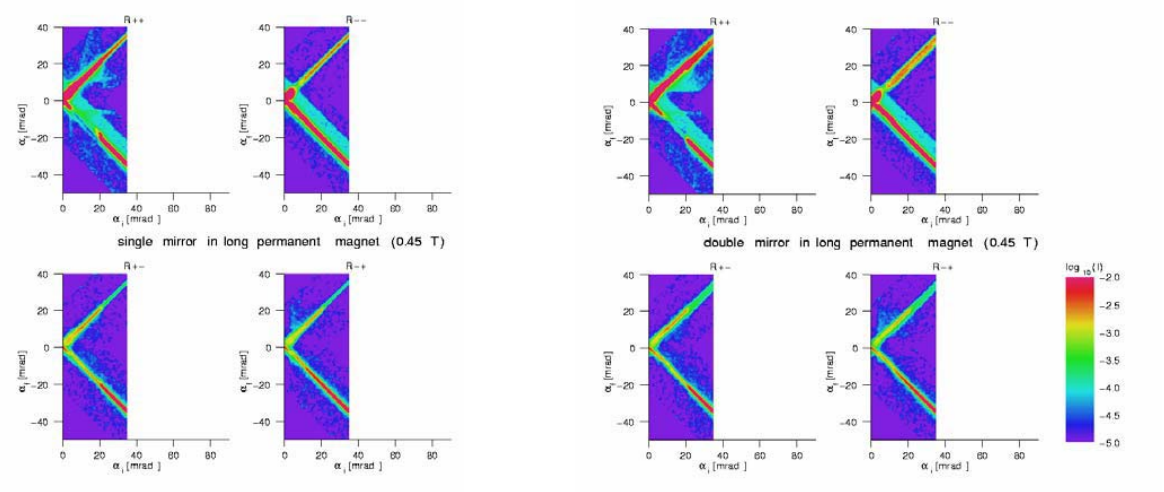


Fig.1: a) Reflectivity ($\alpha_F=\alpha_I$), off-specular scattering ($\alpha_F>0$), transmission ($\alpha_F=-\alpha_I$) and small angle scattering ($\alpha_F<0$) measured on a single transmission polarizer at an applied field of 0.45 Tesla. α_I and α_F are respectively the angles of incidence and exit of the neutrons with respect to the sample surface. The large background intensity just above the primary beam does not come from our sample but from diffuse scattering from the HADAS polarizer.
b) Same as before but with a second 'analyzing' supermirror placed 0.5 mm behind the first polarizer. (s1=s2=0.3 mm).

Institut für Festkörperforschung
Forschungszentrum Jülich GmbH
D-52425 Jülich

Experimental Report of Neutron Scattering Experiments at the FRJ-2 Reactor

Proposal number:	HAD-05-001		
Experiment title:	Magnetic field distribution in $YBa_2Cu_3O_7$ / $La_{2/3}Ca_{1/3}MnO_3$ multilayers		
Dates of experiment:	5.4. - 14.4.2005	Date of report:	June 1, 2005
Experimental team: Names:	Addresses:		
Hoppler Justin Murat Ay	Laboratory for Neutron Scattering, 5232 Villigen PSI, Switzerland Laboratory for Neutron Scattering, 5232 Villigen PSI, Switzerland		
Local contact:	Kentzinger Emmanuel		

Temperature dependent neutron reflectivity measurements showed an unexpected behaviour of the magnetic field distribution of superlattices consisting of $YBa_2Cu_3O_7$ and $La_{2/3}Ca_{1/3}MnO_3$ [1]. To get a better insight in this field distribution, measurements at different temperatures with polarized neutrons with spin analysis were performed on HADAS.
The sample was first cooled to 5 K in an applied magnetic field of 100 Oe. By keeping the applied magnetic field constant, off-specular measurements of all spin channels were performed at 5 K, 90 K, 130 K, 160 K, 200 K and 300 K.
At 5 K, which is well below the transition temperature of the superconductor ($T_c \approx 80$ K), a Bragg sheet at the first Bragg peak was found in the $(--)$ channel. In the same channel Yoneda-like wings with weak intensity at the first Bragg peak were also observed (Fig. 1) [2]. While the Bragg sheet indicates a correlation vertical to the layers, the Yoneda-like wings indicate a correlation in the plane of the layers. The Yoneda-like wings were found to be more pronounced in the two spin flip channels (Fig. 1). This means, those wings are caused by a magnetic correlation in the plane of the layers with some magnetic moments pointing out of the direction of the applied magnetic field.
When heating the sample to 90 K, both features remain with only slight changes.
At 130 K, the Bragg sheet in the $(--)$ channel becomes slightly smaller and the Yoneda-like wings decrease in the spin flip channels while they increase in the $(--)$ channel. One part of this transition between 90 K and 130 K may be induced by a structural phase transition of the substrate $SrTiO_3$ at $\sim$ 108 K. However there is clear evidence for a change in the magnetic field distribution, as the intensity of the Yoneda-like wings in the spin flip channel decreases.

The most significant change in the coherence, however, occures between 90 K and 130 K. The length of the Bragg sheet in the (−−) channel and the Yoneda-like wings in the spin flip channel decrease significantly. At 200 K, the Bragg sheet and the Yoneda-like wings dissappeare in all channels. As there is no Bragg sheet and there are no Yoneda-like wings visible at roomtemperature (which is above the ferromagnetic transition temperature $T_{Curie} \approx 240\,\mathrm{K}$), all correlations found must be of magnetic origin. Due to the magnetic correlation vertical to the layers, it seems that the ferromagnetic layers somehow couple at low temperatures.
This correlation remains to temperatures much higher than the superconducting transition temperature. Therefore it is not sure, whether this interaction is caused by superconductivity or not.

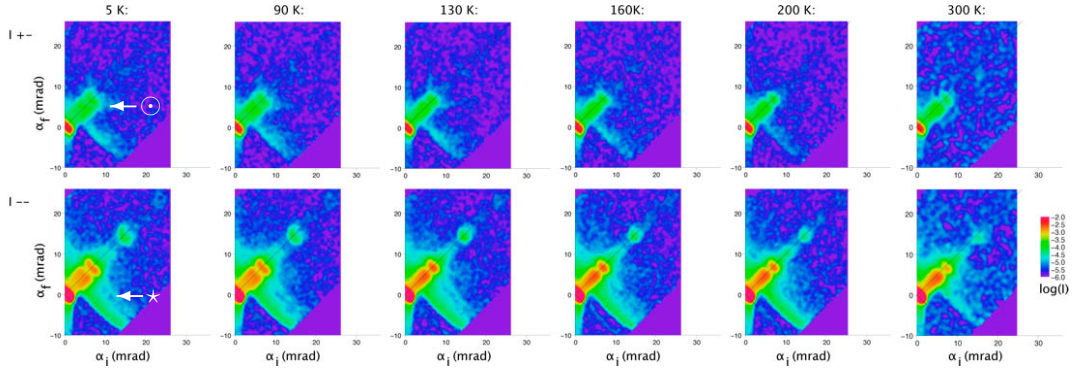


Figure 1: Off-specular and specular reflectivities of the spin flip channel (+−) and the non spin flip channel (−−) in an applied magnetic field of 100 Oe at 5 K, 90 K, 130 K, 160 K, 200 K and 300 K. The Bragg sheet (⋆) at the first Bragg peak in the (−−) channel and the Yoneda-like wings (⊙) at the first Bragg peak in the spin flip channel decrease the most between 130 K and 160 K.

To study out the influence of the applied magnetic field on this correlations, the sample was cooled from roomtemperature to 5 K in applied magnetic fields of 11 Oe, 100 Oe and of 4000 Oe (Fig. 2). We found that an applied field of 100 Oe results in a good alignement of the magnetic moments. Only then a magnetic correlation is obtained. In a magnetic field of 4000 Oe the magnetic correlation is different compared to in a field of 100 Oe. The vertical correlation length is increased and the Yoneda-like wings at the first Bragg peak are only visible in the (−−) channel, which means that the magnetic moments of the ferromagnet are aligned exactly along the applied field.

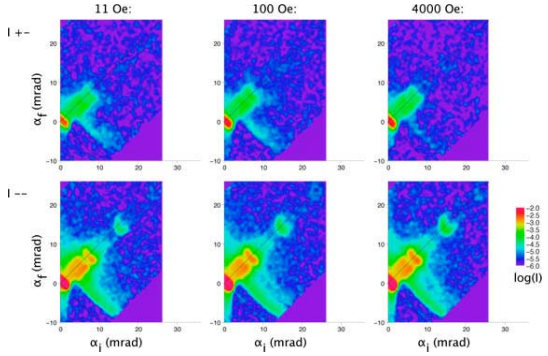


Figure 2: Off-specular and specular reflectivities of the spin flip channel (+−) and the non spin flip channel (−−) at 5 K in an applied magnetic field of 11 Oe, 100 Oe and 4000 Oe.

References:
[1]: J. Stahn et al., Phys. Rev. B, 71, 140509(R) (2005)
[2]: U. Pietsch et al., High-Resolution X-Ray Scattering, Springer (2004)

Forschungszentrum Jülich GmbH
D-52425 Jülich

Experimental Report of Neutron Scattering Experiments at the FRJ-2 Reactor

Proposal number:	HAD-05-002		
Experiment title:	Off-specular scattering from magnetic neutron wave-guides structures		
Dates of experiment:	24.05.2005-28.05.2005	Date of report:	31.03.2006
Experimental team: Names	Addresses		
Sergey KOZHEVNIKOV	Laboratoire Léon Brillouin UMR12, CEA/Saclay, bât. 563 91191 Gif-sur-Yvette Cedex, France Tel: +33 (0)1 69 08 96 51, FAX : +33 (0)1 69 08 82 61 e-mail: kozhevni@dsm-mail.saclay.cea.fr		
Frédéric OTT	Laboratoire Léon Brillouin UMR12, CEA/Saclay, bât. 563 91191 Gif-sur-Yvette Cedex, France Tel: +33 (0)1 69 08 61 21, FAX : +33 (0)1 69 08 82 61 e-mail: fott@cea.fr		
Local Contact:	Amitesh PAUL		

Experimental report text body

This investigation is the part of the project on development of neutron wave-guides (NWG). A NWG consists of a thin film of low optical index (Ti or Al) with thickness of 10-100 nm sandwiched between 2 layers of high optical index. The neutron wave can channel inside the guiding layer with low optical potential. The practical application of NWG is producing of highly collimated narrow (nm) beam which goes out from the edge of a sample while keeping a significant neutron flux. In such structures the interaction of the neutron beam is strongly enhanced when resonant states (or guided states) are created in the neutron wave-guide [1]. Several experiments have already been performed with non-magnetic neutron wave-guides [2-5]. Magnetic materials (permalloy, Fe, Ni) can be used for changing of an upper layer transparency and increasing of neutron beam intensity on the exit of a neutron wave-guide.

On reflectometer HADAS (neutron wavelength is ς=0.47 nm) we have investigated magnetic neutron waveguides Py10(20nm)/Ti70(10nm)/Py(50nm)/glass. On Fig. 1 a,b calculation of neutron wave function of spin states up and down inside the wave-guide Py20nm/Ti70/Py50/glass is shown. For each incidence conditions corresponding to a propagation mode in the wave-guide, there is an enhanced scattering in the wave-guide at the interfaces and this leads to dips in the total reflection region (Fig. 2). Another contribution in dips at the total reflection is wave-guiding effect which can be considered as additional absorption. Simultaneously, for each of the resonance conditions, the scattering by the interfaces is strongly enhanced and a significant off-specular scattering is observed (Fig. 3 a,b). Thus even small interfacial roughness effects are easily observed. For our study these “roughness” effects are parasitic effects. In magnetized state in 100 Oe magnetic field there is only non spin-flip off-specular reflection due to structural lateral roughness correlations.

In low magnetic field 2 Oe demagnetized state of wave-guide structure PyTiPy has been investigated. Additional spin-flip off-specular reflection due to magnetic domains in lateral direction has been observed.

This work has been done under contract Polarized Neutron Technology EUR 634505925-08 A-LABNA-01-06-08. This experiment has been supported by NMI3 program for users.

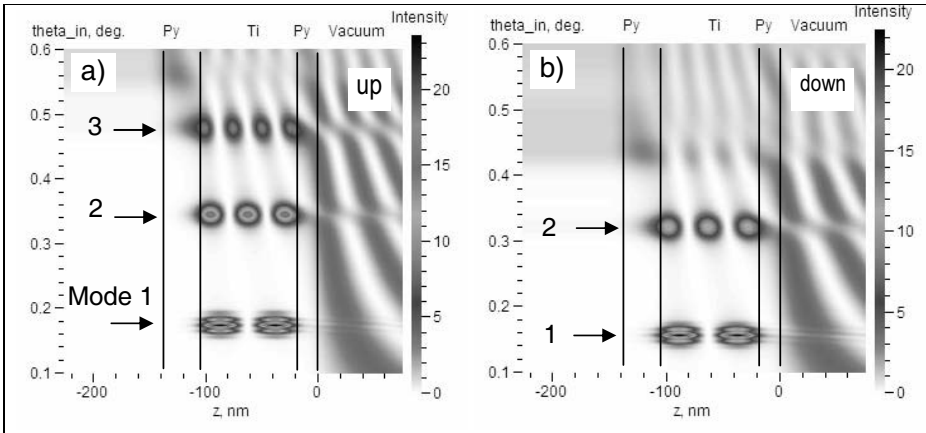


Fig. 1. Calculation of neutron wave-function $|..|^2$ for spin up (a) and down (b) inside wave-guide structure PyO4nm/Py17/Ti82/Py48/glass.

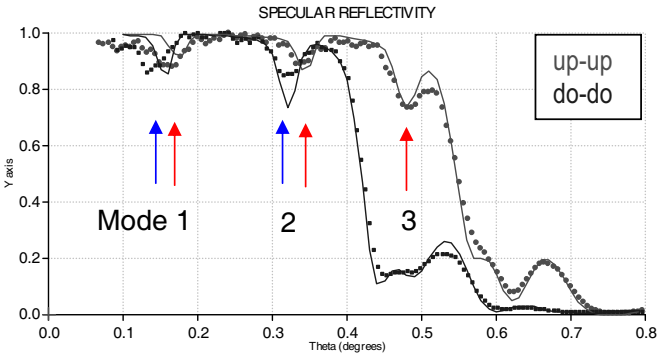


Fig. 2. Specular reflectivities up-up (red) and down-down (bleu) from structure Py20nm/Ti70/Py50/glass.

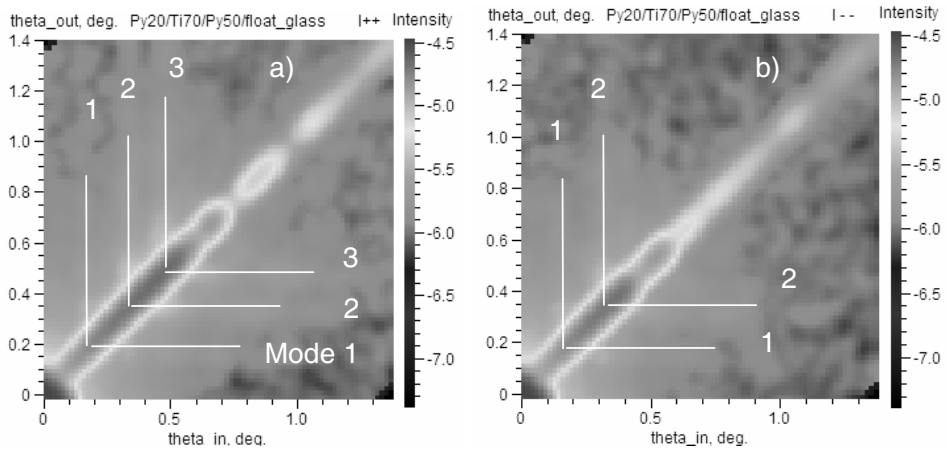


Fig. 3. Off-specular reflection from magnetized structure PyTiPy in 100 Oe for spin up-up (a) and down-down (b).

1. E. Kentzinger et al., Physica B **335** (2003) 89-94.
2. S.P. Pogossian et al., J. Mag. Mag. Mat. 237 (2001) 302-308.
3. S.P. Pogossian et al., J. of Physics D – Applied Physics 34 (2001) 1872-1877.
4. V.L. Aksenov et al., ILL experimental report, 2000, reflectometer ADAM.
5. F. Pfeiffer et al., Phys. Rev. Lett. 88 (2002) 055507-1.

Institut für Festkörperforschung
Forschungszentrum Jülich GmbH
D-52425 Jülich

Experimental Report of Neutron Scattering Experiments at the FRJ-2 Reactor

Proposal number:	HAD-05-003		
Experiment title:	Test of a 2D-CASCADE detector with high efficiency with reflectometry experiments		
Dates of experiment:	20.04. - 24.04.05	Date of report:	24.05.06
Experimental team: Names	 Addresses		
Dr. Werner Hinderer Dr. Martin Klein Dr. Christian Schmidt	Universität Heidelberg Physikalisches Institut Philosophenweg 12 69120 Heidelberg Tel.: +49-6221-549376		
Local Contact:	U. Rücker, E. Kentzinger		

Experimental report text body

The aim of this test session was to continue the evaluation of the CASCADE detector technology and to gain references by performing reflectometry with a glass plate covered with Nickel.

The first prototype of a 2D-CASCADE detector was successfully tested during the operation of the FRJ-2 reactor at the experimental test site EKN in November 2004. For this experiment, an extended and improved version of the 2D-CASCADE detector was characterized and used for reflectometry.

In figure 1 the reflection profile of a Nickel metallic film coated on glass is shown. The data points show the measured specular reflected neutron intensity (normalized to the incident neutron intensity). They were acquired with the scintillation detector of the HADAS instrument. From this profile one can determine the thickness of the metallic film. The fit (red curve) yields a thickness of (830 ±1) Å.

With the same setup, the measurement was repeated with the 2D-CASCADE detector.
The operation of the HADAS reflectometer by our group and the integration of the CASCADE detector into the HADAS environment took more time as expected. Thus there was not enough time to measure the reflection profile at larger angles as we did with the scintillation detector. The result is shown in figure 2. For the Nickel film one gets a thickness of (855 ±4) Å. A matching result for the two thickness determinations may be expected if more periodic oscillations would have been measured.

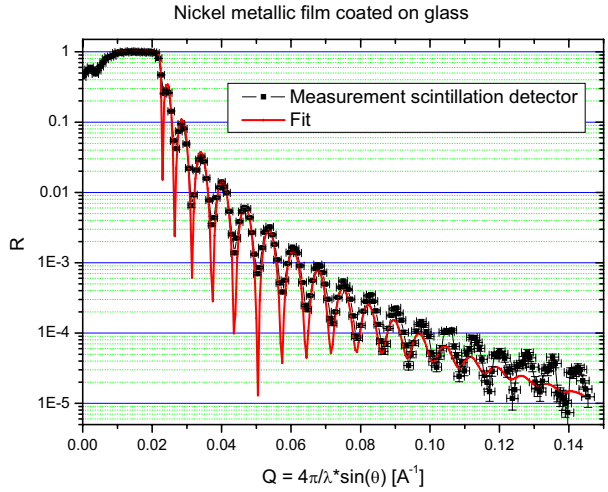


Figure 1: Curve of reflection from a Nickel surface measured with the scintillation detector at the HADAS instrument.

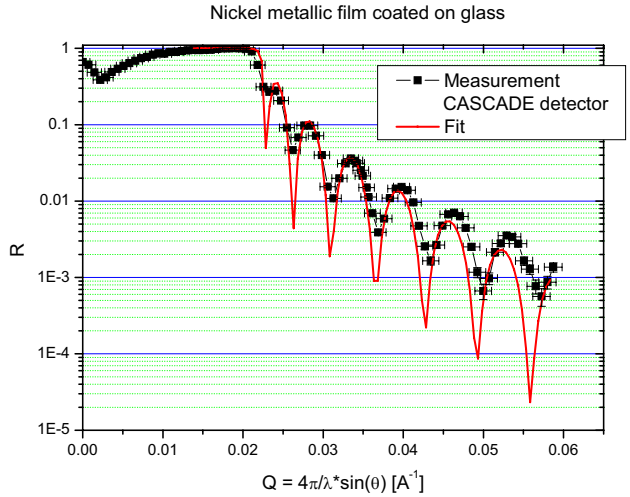


Figure 2: Curve of reflection from a Nickel surface measured with the 2D-CASCADE detector.

This beamtime showed that the 2D-CASCADE detector can be integrated into existing neutron instruments. The comparison between the 2D-CASCADE detector and the scintillation detector of the HADAS instrument demonstrates the correct working of the 2D-CASCADE detector.

Institut für Festkörperforschung
Forschungszentrum Jülich GmbH
D-52425 Jülich

Experimental Report of Neutron Scattering Experiments at the FRJ-2 Reactor

Proposal number:	HAD-05-004		
Experiment title:	Investigating structural evolution in Co/Cu multilayers with number of bilayers		
Dates of experiment:	14.04.05	Date of report:	February 22, 2006
Experimental team: Names:	Amitesh Paul, Ulrich Ruecker, Emmanuel Kentzinger, Thomas Brueckel		
Address:	Institut fr Festkrperforschung Forschungszentrum Jlich GmbH D-52425 Jlich, Germany Deutschland		
Local contact:	Amitesh Paul		

Physical properties of magnetic multilayer (MLs) such as interlayer coupling [1] and giant magnetoresistance (GMR) [2] are not only closely related to the structure of the multilayers, *i.e.* interface roughness and/or the evolution of the roughness along the ML stack,[3] but depend also on the details of the magnetic domain structure.[4] Recent investigations by Langridge *et al.*[4] and Paul *et al.*[5] have demonstrated the usefulness of neutron techniques in determining the field dependence of the antiferromagnetically (AF) coupled domain structure.
Recently, Borchers *et al.*[6] have shown the dependence of GMR on the vertical correlation of domains in a coupled ML at the coercive field. The loss of GMR was attributed to the vanishing of the vertical correlation. On the other hand, vertical correlation of domains was shown to exist at the coercive field for a coupled system.[4] However, though the variation of the domain size with applied field was addressed for weakly as well as strongly coupled systems, there is so far no investigation of the evolution of the domain characteristics along the growth direction of the ML. In previous work, we have observed that the strength of the AF coupling and the GMR values correlate with the structural evolution for increasing number of bilayers (N) of a ML.[3] In the present work, we report on the domain structure evolution in AF-coupled Co/Cu ML stacks as observed from neutron scattering measurements. These MLs show a high degree of morphological vertical correlation and small lateral correlation of the interface roughness.[3] We observe the domain structure of the Co layers to evolve from large to small vertically correlated domains along the stack. The larger ones remain AF aligned beyond the apparent saturation field, while the antiparallel alignment for the smaller breaks up at lower external fields.

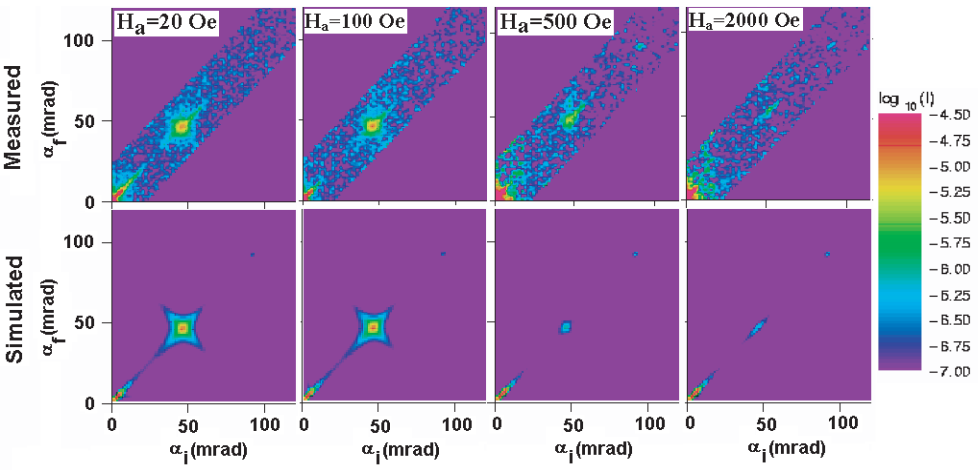


Figure 1. SF intensity maps (measured and simulated) at different fields for $[\mathrm{Co/Cu}]_{N=40}$ sample.

Details of the preparation and characterization of similar SiO_2/Co(1.45 nm)/[Cu(1.02 nm)/Co(1.45 nm)]$_{N=10\ or\ 40}$ structures as used here have been described [3]. The SF intensities near 46 mrad for $H_a = 500$ Oe are larger than the NSF intensities due to diffuse scattering and indicates the presence of lateral inhomogeneities caused by domains. This is best seen in the SF intensity maps shown in Fig. 1 for different H_a. The $\frac{1}{2}$-order Bragg peak at ∼46.5 mrad is broad along $Q_\parallel$ as well as along $Q_\perp$. Its intensity rapidly shrinks with distance from the specular line and also decreases with increasing H_a. Although all four channels are fitted within the single domain approximation, we note that the widths of the $\frac{1}{2}$-order Bragg peak of the SF intensities could not be reproduced because these peaks are diffuse in nature. Conventional magnetometry (MOKE and SQUID) yields a smaller value of the saturation field than the value determined from off-specular polarized neutron scattering. Thus, PNR reveals the magnetic state in more detail. Smaller domains most likely at the top of the ML with a size of 0.5-1.5 μm are saturated at a lower field of $\approx$ 500 Oe, whereas the larger domains ($\geq l_\parallel \approx 20$ μm) beneath remain AF-coupled beyond apparent saturation at $\approx$ 1.5 kOe.

References

[1] P. Grünberg, R. Schreiber, Y. Pang, M. B. Brodsky, and H. Sowers, Phys. Rev. Lett. **57**, 2442 (1986).

[2] M. N. Baibich, J. M. Broto, A. Fert, F. Nguyen van Dau, F. Petroff, P. Etienne, G. Creuzet, A. Friedrich, and J. Chazelas, Phys. Rev. Lett. **61**, 2472 (1988).

[3] A. Paul, T. Damm, D. E. Bürgler, S. Stein, H. Kohlstedt, and P. Grünberg, J. Phys.: Condes. Matter **15**, 2471 (2003).

[4] S. Langridge, J. Schmalian, C. H. Marrows, D. T. Dekadjevi, and B. J. Hickey, Phys. Rev. Lett. **85**, 4964 (2000).

[5] A. Paul, E. Kentzinger, U. Rücker, D. E. Bürgler, and P. Grünberg, Physica B **356**, 31 (2004).

[6] J. A. Borchers, J. A. Dura, J. Unguris, D. Tulchinsky, M. H. Kelley, C. F. Majkrzak, S. Y. Hsu, R. Loloee, W. P. Pratt, Jr., and J. Bass, Phys. Rev. Lett. **82**, 2796 (1999).

Institut für Festkörperforschung
Forschungszentrum Jülich GmbH
D-52425 Jülich

Experimental Report
of Neutron Scattering Experiments
at the FRJ-2 Reactor

Proposal number:	HAD-05-006, HAD-05-017		
Experiment title:	**Confinement Effects of Diblock Copolymers in Lamellar Micro-emulsions I, II**		
Dates of experiment:	**9.5., 27.5., 13.6., 18.8. - 20.8., 29.8., 26.9. - 29.9., 3.11.2005**	Date of report:	17.03.2006
Experimental team: Names	Addresses		
Simona Maccarrone Henrich Frielinghaus	Forschungszentrum Jülich GmbH, Institut für Festkörperforschung, D-52425 Jülich Forschungszentrum Jülich GmbH, Institut für Festkörperforschung, D-52425 Jülich		
Local Contact:	Ulrich Rücker		

Experimental report text body

The current work (PhD thesis) of Simona Maccarrone considers amphiphilic diblock copolymers in micro-emulsions. The domain size of the oil and water domains is changed by the selection of the oil chain length. Thus, the ratio between the domain size and the polymer size is varied. Confinement takes place when both sizes are similar. While a large part of the work focuses on bicontinuous microemulsions, which are characterized by phase diagram measurements and SANS experiments, the study should be extended to lamellar microemulsion with confined polymers. The quasi-Bragg peak is very sharp, and therefore conventional SANS experiments should be combined with SANS measurements at HADAS. HADAS allows to measure with a very high resolution in one direction ($\Delta Q_x/Q_x \approx 1\%$, in this direction the sample is aligned), while the resolution is relaxed in the other direction. The analysis of the bicontinuous microemulsions involves a theoretical apparatus, which neglects the pressure that one domain exerts on the surfactant film (more precise the osmotic pressure of the membrane). This pressure is included in the Caillé theory, which describes lamellar microemulsions. At higher confinement the pressure of the polymer on the membrane should be non-negligible, and therefore the consideration of lamellar microemulsions should be included in the work.
Compared to the bicontinuous microemulsions the lamellar microemulsion contains higher amounts of surfactant. Therefore the domain size is quite small. Especially due to the lack of a temperature control, the temperature window of the lamellar microemulsion was rendered quite large (typically ~18°C..32°C), and therefore high surfactant contents of 25%..30% were chosen. Initially the widely used $C_{10}E_4$ surfactant was selected, but to extend the range to lower confinement another $C_{14}E_5$ surfactant was involved. Four samples contained too few surfactant (20%) and coexistance of a bicontinuous and a lamellar microemulsion was obtained. Eigth samples were measured successfully with varying polymer size and constant surfactant amount. A reference sample without any polymer allowed to measure the change of the bending rigidity and the osmotic pressure according to the added polymer. All experiments are conducted at film contrast.

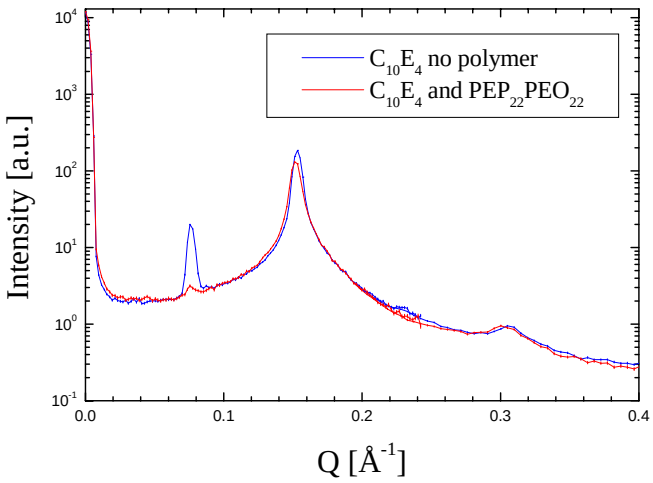


Figure 1: Logarithmic intensity as a function of the scattering vector Q (SANS-plot). On the left the primary beam is measured. At Q=0.15Å^{-1} the lamellar structure of the surfactant film is reflected (film-contrast). The superstructure of the domains appears at Q=0.08Å^{-1} due to the imperfect contrast matching. The second order peak is visible as well. Changes in the peak width are tiny.

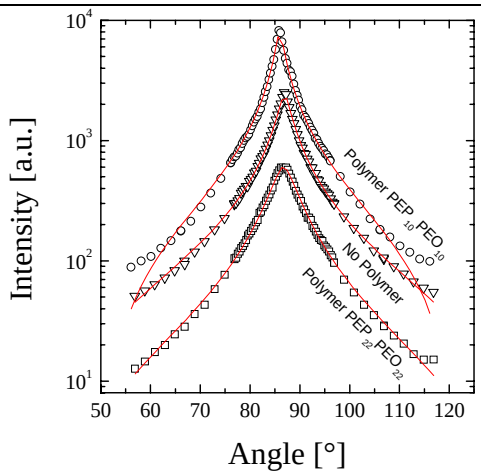


Figure 2: Rocking curves of three samples. The zero angle is at 90°. Intensities of the upper two samples are shifted by a factor of 3 and 10. Fit curves were used to describe the divergence phenomenologically. The highest curve is the sharpest, the lowest one is the broadest.

The measured curves (SANS and rocking) are evaluated in the following manner. The normal SANS scan shows several properties (Fig 1), namely (a) the primary beam at small scattering angles, (b) the quasi Bragg peak is observed at Q=0.15 Å^{-1}, (c) the superstructure of the domains is found at Q=0.08Å^{-1} due to imperfection in the contrast match, and (d) a second order peak is observed at Q=0.3Å^{-1}. Furthermore at low enough scattering angles (before the upturn of the primary beam) the scattering intensity can be extrapolated to the forward scattering S(0). Using the integral intensity of the primary beam, this S(0) can be calculated on an absolute scale, and therefore S(0) can be connected to the osmotic pressure. The quasi Bragg peak and the second order peak and intensities around (but not the superstructure peak) can be described by the Caillé theory. The detailed numerical handling has been described by Monkenbusch [1], only an additional integral due to the relaxed resolution in the perpendicular direction was necessary. The intensities were well described with an arbitrary amplitude factor, but the resulting bending rigidity κ and the osmotic compressibility B do not meet the expectations. The obtained κ was around $200k_BT$ while from SANS experiments one would expect 0.5 to 1 k_BT. A similar discrepancy was obtained between B and S(0). Furthermore, the changes in the peak sharpness are not extremely high, since the divergence is predicted to have an exponent $-(2-\eta)$. More promising are the rocking curves (Fig 2). Here the divergence has an exponent $-2(2-\eta)$. The sharpness of the peaks can be read off already visually.

All attempts to extract values for the bending rigidity had the following problem. With respect to the reference sample (no polymer), the obtained changes $\Delta\kappa$ had varying signs independent of the selected confinement. So the tendency increased / decreased bending rigidity was not observed within the accuracy of the experiment. The precision of this experiments is not high enough. While describing the SANS curves with the Caillé theory lead to unphysically high κ values, the determination of η by a phenomenological fit of the rocking curves lead to reasonable absolute values of κ. Nonetheless the changes of κ were not *systematically*.

The quality of the alignment was checked by conventional SANS measurements where the Bragg peaks were sharp in all directions. Anyhow the present understanding of the malfunction of this experiment is the imperfect aligning. All samples were heated up to ~50°C prior the cooling down to room temperature. At high temperatures the sample was one phase, then, at intermediate temperatures, there was a 2-phase region with coexisting lamellar and microemulsion phases, and finally the sample arrived at the 1-phase lamellar state. The intermediate 2-phase region might be the reason for individual perfection of alignment of each sample.

[1] K. D. Göcking, M. Monkenbusch, *Europhys. Lett.* **43**, 135 (1998)

,Institut für Festkörperforschung
Forschungszentrum Jülich GmbH
D-52425 Jülich

Experimental Report
of Neutron Scattering Experiments
at the FRJ-2 Reactor

Proposal number:	HAD-05-007		
Experiment title:	Stability of domain structure in exchange bias system CoFe/MnIr		
Dates of experiment:	11.05.-19.05.2005	Date of report:	14.06.2006
Experimental team: Names	Addresses		
Katharina Theis-Bröhl Boris Toperverg	Ruhr-Universität Bochum Institut für Experimentalphysik IV 44780 Bochum Ruhr-Universität Bochum Institut für Experimentalphysik IV 44780 Bochum		
Local Contact:	Ulrich Rücker		

Experimental report text body

We performed polarized neutron reflectometry studies on the instrument HADAS on an exchange bias (EB) system with imprinted magnetic microstripes. The sample studied is a $Co_{70}Fe_{30}$ (28 nm)/$Mn_{83}Ir_{17}$ (15 nm) ferromagnetic/ antiferromagnetic bilayer with buffer layers Cu(28 nm)/SiO_2 (50 nm) on Si(111) and a TaO-Ta(9 nm) top layer prepared by magnetron sputtering. The initial EB direction was set by field cooling in a magnetic in-plane field of 1 kOe after annealing at 275°C which is above the blocking temperature. Subsequently the film was covered by photoresist, which was patterned into equally spaced stripes with a width of 2.5 µm and a periodicity of 5 µm. Then the sample was bombarded with He^+ ions with a fluency of $1\cdot 10^{15}$ ions/cm^2 at 10 keV. During bombardment a magnetic field of 1 kOe aligned opposite to the initial EB direction was applied. This resulted in a stripe-like pattern with alternate sign of the unidirectional anisotropy, and hence the sign of the EB in neighboring stripes.
In previous measurements performed at the reflectometers HADAS and ADAM (ILL) we studied the easy axis behavior. [1] We found that the remagnetization within the different areas occurs at different magnetic fields, resulting in a field range with antiparallel orientation of magnetization. With the PNR measurements including quantitative data treatment using DWBA we were able to quantitatively determine the angle of magnetization. Instead of 180° (antiparallel alignment) we found that the magnetization is tilted and the angle between the magnetization in the two different areas is only 120° resulting in a net transverse orientation of magnetization. We explained this behavior with a model using energy contributions due to exchange between ferromagnetic layers, exchange between ferromagnetic and antiferromagnetic layers and anisotropy. In the intensity maps we found three different features of intensity: specular reflectivity, off-specular Bragg diffraction lines from the magnetic period and off-specular diffuse scattering from domains smaller than the coherence length. We observed Bragg reflections for n= ± 1, whereas for n= ± 2 they are suppressed. This is caused by the structure factor, resulting from the equal width of adjacent magnetic stripes in a unit cell.

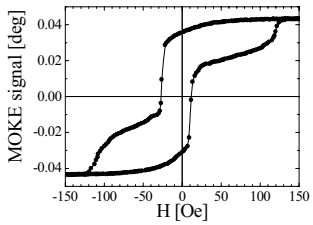


Fig. 1: Longitudinal MOKE hysteresis loop performed on the sample studied in the PNR experiment.

In the present experiment we rotated the sample by 45° and performed PNR measurements at different magnetic fields along the hysteresis loop shown in Fig. 1. The field values for which intensity maps were collected are: 3.5 Oe, 8 Oe, 17 Oe, 35 Oe, 53 Oe, 67 Oe,71 Oe (after negative saturation), 3.5 kOe (saturation), and 31 Oe (after positive saturation). In Fig. 2 several intensity maps are presented. We measured two non-spin-flip (NSF) and two spin-flip (SF) maps for each field value, but presented in Fig.2 are only the I^{++} and the I^{+-} maps. For comparison we show in Fig. 3 Kerr microscopy measurements taken also at 45° sample rotation with respect to the applied field and taken at different fields along the hysteresis loop.

In saturation at 3500 Oe only NSF specular reflectivity is visible because the magnetization of the film is completely oriented along the field orientation. The measurement at 3 Oe was performed just before the first reversal. Off-specular Bragg diffraction, however, can already be observed with a rather strong intensity. Obviously, rotational processes and formation of domains (concluded from off-specular spin-flip scattering) are different in the two magnetic stripe regions which leads to a rather strong magnetic contrast as can also be seen from a Kerr microscopy image in Fig. 3. Increasing the field to 22 Oe leads to less off-specular diffuse scattering and stronger Bragg-diffraction lines. This comes from the fact that now the magnetization of one part of the stripes is reversed and that small domains have disappeared. Further increase of the field results in a beginning reversal of the second part. Due to the canting of the stripe orientation with respect to the field the reversal is quite different compared to the easy axis behavior (field applied along the stripes). In case of the easy axis magnetization the stripes reverse one after the next. In the 45° case the width of the reversed magnetic stripes increases on the expense of the width of the stripes which are not yet reversed. This can clearly be seen in Fig. 3 in the Kerr microscopy image taken at 70 Oe. In the PNR measurement we observe this effect by the fact that second order Bragg diffraction lines occur, observed already at 35 Oe. The effect is even stronger at 67 Oe. Furthermore, again off-specular diffuse scattering is present, resulting from small domains which hardly can be seen from the Kerr microscopy image in Fig. 3. The maps taken at 31 Oe after saturation in a positive magnetic field do not show off-specular Bragg diffraction lines but strong off-specular diffuse scattering. Again this observation is in very good agreement with the Kerr microscopy image taken at 38 Oe where ripple domains clearly can be observed but not the magnetic stripe structure.

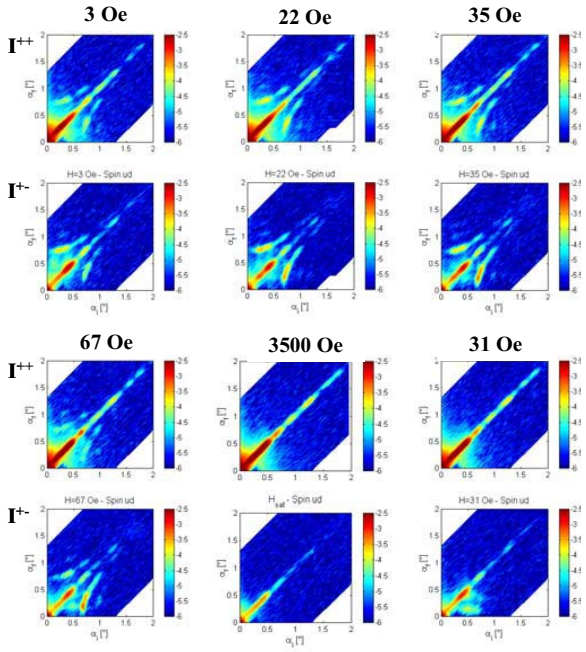


Fig. 2 Polarized intensity maps taken at different magnetic fields.

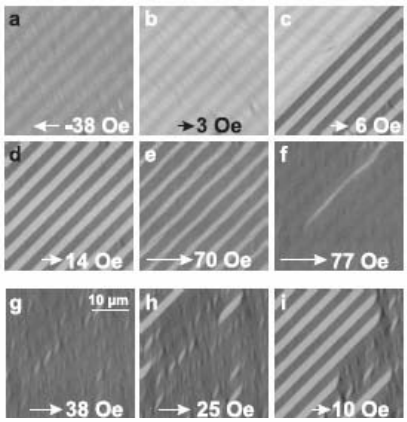


Fig. 3: Kerr microscopy measurements performed with an angle of 45° between sample and applied field.

This work was supported by DFG through SFB491.

References

[1] K. Theis-Bröhl, M. Wolff, A. Westphalen, H. Zabel, J. McCord, V. Höink, J. Schmalhorst, G. Reiss, T. Weis, D. Engel, A. Ehresmann, U. Rücker, B. P. Toperverg, Phys. Rev. B: 73 174408 (2006).

Institut für Festkörperforschung
Forschungszentrum Jülich GmbH
D-52425 Jülich

Experimental Report
of Neutron Scattering Experiments
at the FRJ-2 Reactor

Proposal number:	HAD-05-008		
Experiment title:	Multiply bound polymer brushes: understanding loops from triblock copolymers		
Dates of experiment:	14.06. – 21.06.2005	Date of report:	22.06.2006
Experimental team: Names	Addresses		
Mark Dadmun J. Kevin Rice	Chemistry Dept., University of Tennessee, Knoxville, TN 37996 Chemistry Dept., University of Tennessee, Knoxville, TN 37996		
Local Contact:	U. Ruecker		

Experimental report text body

Reactive compatibilization schemes, to produce copolymer interfacial modifiers, appear to be the most industrially applicable means to efficiently produce useful polymer blends from normally immiscible polymer systems. Blocky type copolymers have been shown to be the best interfacial modifiers, as the loops that are formed across the interface, which allow for physical entanglements across the interface, are critical to strengthening the inherently weak interfaces in immiscible polymer blend systems. We want to better understand the reactions of telechelic polymers, in terms of the relationship between kinetics, interfacial morphology, reactivity, and molecular weight, in order to optimize loop formation at soft polymeric interfaces.

To this end, we have undertaken a neutron reflectivity study to elucidate the optimal parameters involved in forming molecular loops through the reaction of telechelic polymers at soft polymeric interfaces. We began investigating the reaction of telechelic polymers at a soft polymeric interface using a model bilayer system consisting of polystyrene and poly(methyl methacrylate), and corresponding telechelics containing various end group functionalities capable of in situ coupling, and monitored the reaction of the deuterated polystyrene telechelics at the interface with neutron reflectivity. Through the use of this model system, the relationships between telechelic molecular weight, functional group reactivity, and reaction time versus reaction rate and extent of reaction were elucidated.

Three reactive pairs were studied: epoxy-carboxylic acid, anhydride-amine, and epoxy-amine. The effect of telechelic molecular weight was also investigated through the use of several different telechelic molecular weights for each reactive pair investigated. Samples were annealed at 150° C under vacuum for 15 minutes, 4 hours, 24 hours, 72 hours, and 108 hours, and reflectivity measurements were taken on the initial as cast films and after each successive annealing step. A representative plot of the evolution of the scattering length density profile with annealing time for the 20K molecular weight telechelic in the epoxy-carboxy system can be seen in Figure 1. It was found that the reactivity of the various functional groups played a significant

role in the kinetics of the in situ copolymer formation process. The anhydride-amine system showed maximum reaction within 0.25 hours, while the carboxy-epoxy and epoxy-amine systems required greater than 24 hours for complete reaction to occur. It is also speculated that different interfacial morphologies result from the reaction of differing functional groups to form copolymer at the immiscible interfaces although the same relationship seems to exist between telechelic molecular weight and total interfacial width, regardless of the end group functionality.

The experiments carried out here have shown that the in situ reaction of telechelics at soft, immiscible polymer/polymer interfaces to form copolymer surfactant molecules, contrary to most theoretical treatments of the process, is not a diffusion-controlled process. While no current theory of the reaction process fits well with our data, we have elucidated several parameters, including telechelic molecular weight and the magnitude of the reduction in interfacial tension, that appear to play a role in the kinetics of the interfacial reaction process. We have shown that copolymers formed from smaller molecular weight telechelics produce a higher reduction in interfacial tension, as evidenced by the larger interfacial widths, at modified interfaces, as opposed to higher molecular weight telechelics. The interfacial excesses measured at the longest annealing time for the smaller molecular weight copolymer samples (<80K molecular weight telechelic) are all above the theoretical value at which the interfacial tension should be zero. This leads us to believe that the triblock copolymers formed from lower molecular weight telechelics are able to pack more tightly at the interface and that these interfaces modified with low molecular weight telechelics are more susceptible to thermal fluctuations, leading to more copolymer formation and a greater reduction in the interfacial tension.

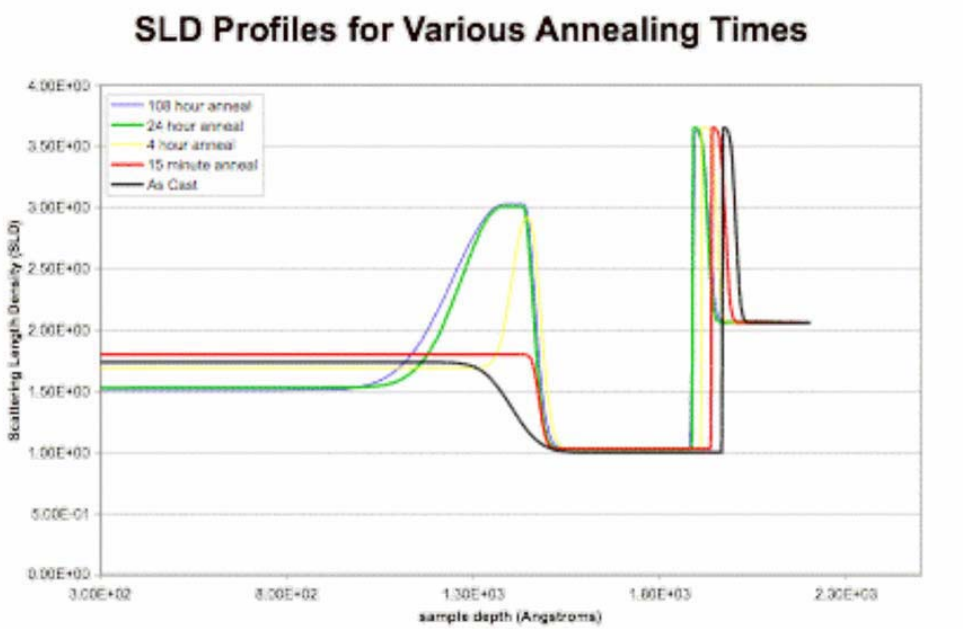


Figure 1. Evolution of the scattering length density profile with annealing time for the 20K molecular weight telechelic sample.

Institut für Festkörperforschung
Forschungszentrum Jülich GmbH
D-52425 Jülich

Experimental Report
of Neutron Scattering Experiments
at the FRJ-2 Reactor

Proposal number:	HAD-05-009		
Experiment title:	Understanding the structure of brushes and formed from imbedded functionalities		
Dates of experiment:	21.06. – 27.06.2005	Date of report:	22.06.2006
Experimental team: Names	Addresses		
Mark Dadmun J. Kevin Rice Ken Carter	Chemistry Dept., University of Tennessee, Knoxville, TN 37996 Chemistry Dept., University of Tennessee, Knoxville, TN 37996 Polymer Science Dept., University of Massachusetts, Amherst, MA 01003		
Local Contact:	U. Ruecker		

Experimental report text body

These reflectivity experiments were completed to elucidate the structure and properties of polymer brushes that are created from these imbedded functionalities and compare them to other polymer brushes. The experiments were completed on three polymer brush systems, which consist of deuterated polystyrene brushes that are approximately 50 nm long. The goal of the experiment is to determine the correlation between the ability of an initiator to grow a polymer brush to its depth in the initial film. The results from the three samples examined demonstrate that the three samples exhibit very different profiles for the deuterated polymer brush.

In the resultant density profiles, the first two clearly have significant amount of brush that grows from the initiator layer away from the interface, as the interface between the deuterated brush and protonated film is very broad. However, the third sample grows almost all chains from the protonated layer surface, as evidenced by the sharp interface between the layers. Clearly there exist fundamental differences in these films, however, they were synthesized to be very similar. We are currently working with our collaborators attempting to elucidate the cause for this observed variation in the brush structure. Clearly the results indicate that initiator may grow polymer chains from any depth, however, we must determine what parameters are important in controlling this behavior. Further experiments are planned to elucidate these factors.

Institut für Festkörperforschung
Forschungszentrum Jülich GmbH
D-52425 Jülich

Experimental Report of Neutron Scattering Experiments at the FRJ-2 Reactor

Proposal number:	HAD-05-010		
Experiment title:	Magnetic field distribution in $YBa_2Cu_3O_7$ / $La_{2/3}Ca_{1/3}MnO_3$ multilayers		
Dates of experiment:	22.8. - 29.8.2005	Date of report:	December 9, 2005
Experimental team: Names:	Addresses:		
Hoppler Justin Christian Schanzer	Laboratory for Neutron Scattering, 5232 Villigen PSI, Switzerland Laboratory for Neutron Scattering, 5232 Villigen PSI, Switzerland		
Local contact:	Kentzinger Emmanuel		

Temperature dependent neutron reflectivity measurements showed an unexpected behaviour of the magnetic field distribution in superlattices consisting of $YBa_2Cu_3O_7$ (YBCO) and $La_{2/3}Ca_{1/3}MnO_3$ (LCMO) [1]. To get a better insight in this field distribution, measurements at different temperatures with polarized neutrons and spin analysis were performed on HADAS.
The sample consisted of eight double layers YBCO / LCMO on a $SrTiO_3$ substrate with layer thicknesses of 252 Å and 260 Å, respectively. It was first cooled to 5 K in an in-plane applied magnetic field of $H = 100$ Oe. A strong correlation of the magnetic roughness was observed out-of-plane and a weaker one in-plane of the layers. This correlations disappeared when heating the sample to $T > 130$ K (proposal number HAD-05-001).
The correlation of the magnetic roughness disappeared at a temperature $T' \approx 140$ K well separated from the transition temperature of the ferromagnet ($T_{\mathrm{Curie}} \approx 240$ K) and the transition temperature of the superconductor ($T_c \approx 80$ K). Therefore the question arose whether T' represents a third phase transition in the superlattice or an effect induced by superconductivity at $T < T_{\mathrm{c}}$, but preserved as particular magnetic ordering up to much higher temperatures than T_{c}.
In order to determine the temperature at which the magnetic correlations set in during cooling, further measurements on HADAS were performed: The same sample was subsequently cooled in an applied magnetic field of $H = 100$ Oe from room temperature to 160 K, 130 K, 90 K, 60 K and 5 K.
No vertical correlation of the magnetic roughness was found as it was when heating, but the lateral correlation was found to increase independent of the temperature history at $T < T'$ (*Yoneda-like wings* in the $(+-)$-channel) (Figure 1).

There are two possible explanations for the missing of the vertical correlation in the second experiment:
Either the *Bragg sheet* observed in the first experiment has been an artefact, or the lateral coherence length of the neutrons has been too small in the second experiment. The latter explanation is more likely, because the *Bragg sheet* has reproducible been observed during the first experiment and because the diaphragm in front of the sample has been closer to the sample in the second experiment than in the first one. The decrease of the coherence length of the neutrons due to the shifted second diaphragm could be sufficient to oversee the vertical correlation. This would mean that the vertical correlation length is of the order of 25 μm.
At $T > 90\,\mathrm{K}$ *Yoneda wings* were observed in the (++)-channel. This means, that the upper LCMO-layer is not fully magnetized at higher temperatures, leading to an uncorrelated magnetic roughness at the surface. This effect occures only when cooling.
Due to the smaller coherence length of the neutrons no vertical correlation was observed when cooling. To prove or disprove the independence of the history of temperature, this experiment should be repeated with a lateral coherence length of neutrons of more than 30 μm at the position of the second bragg reflex.

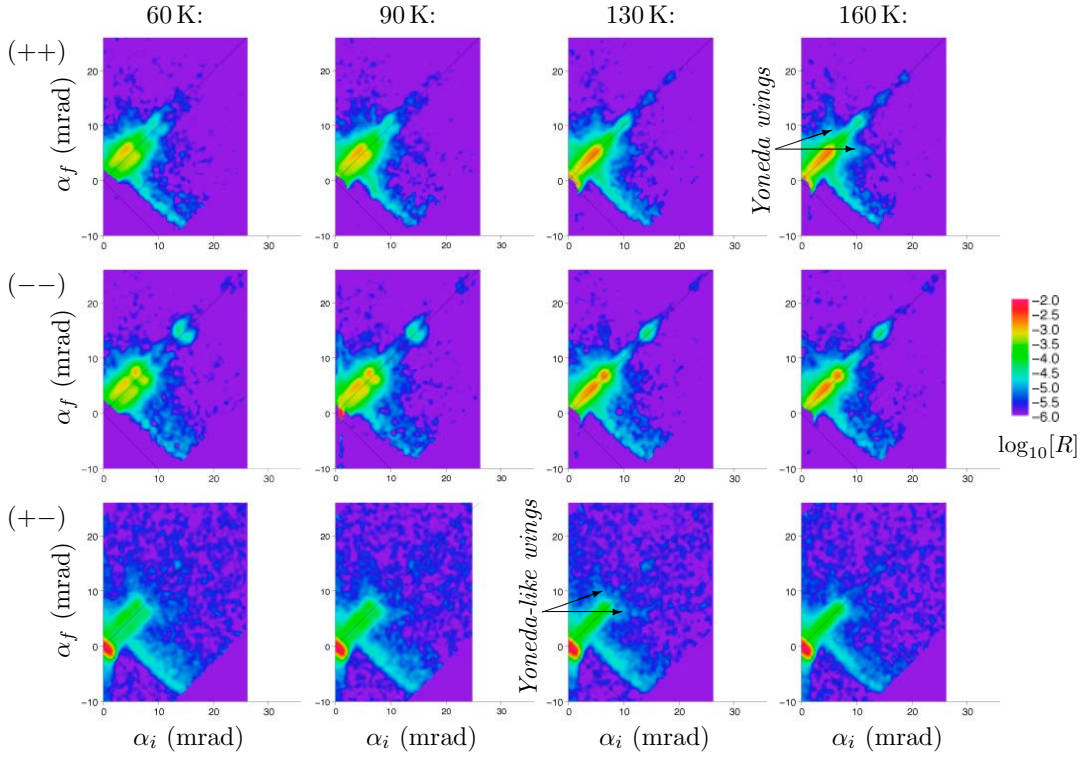


Figure 1: Reflectivity of a [YBCO (252 Å) / LCMO (260 Å)]$_8$ multilayer in an applied magnetic field of $H = 100\,\mathrm{Oe}$ at different temperatures when cooling from room temperature. The two non-spinflip channels are shown with background subtracted, while the spinflip channel (+−) is shown without background subtraction.

References:
[1]: J. Stahn *et al.*, Phys. Rev. **B**, 71, 140509(R) (2005)

Institut für Festkörperforschung
Forschungszentrum Jülich GmbH
D-52425 Jülich

Experimental Report of Neutron Scattering Experiments at the FRJ-2 Reactor

Proposal number:	HAD-05-015		
Experiment title:	Polarized neutron reflectometry on discontinuous metal insulator multilayers		
Dates of experiment:	30.09.2005 to 06.10.2005	Date of report:	06.06.2006
Experimental team: Names	Addresses		
Prof. Dr. W. Kleemann S. Bedanta, M.Sc.	Angewandte Physik, Universität Duisburg-Essen, 47048 Duisburg Angewandte Physik, Universität Duisburg-Essen, 47048 Duisburg		
Local Contact:	Dr. A. Paul, Dr. E. Kentzinger, Dr. U. Rücker		

Experimental report text body

Introduction :
Polarized neutron reflectivity (PNR) studies have been performed on granular multilayers $[Co_{80}Fe_{20}(t_n)/Al_2O_3(3nm)]_{10}$ for the nominal thicknesses t_n = 1.5 nm (percolating ferromagnet). Most of the measurements were done at T = 150 K with a new cryostat and in the field range $0.47 \leq \mu_0 H \leq 12$ mT.

Motivation :
Several types of interlayer coupling have been studied theoretically and experimentally (*e.g.* [1]). In magnetic multilayer systems with insulating spacer layers and flat interfaces, dipolar interactions are dominant. They favor antiparallel orientation of the intra-planar magnetization between adjacent layers. For rough interfaces the so-called Néel or orange peel interlayer coupling has to be considered [2,3]. In 1962, Néel [2] pointed out that there should be ferromagnetic coupling between adjacent films due to magnetic dipoles at the interface induced by a correlated morphological corrugation. Competition between these dipolar interactions and Néel coupling may lead to an unusually modulated magnetization depth profile in a magnetic multilayer system.
Recently we have reported of such a magnetization depth profile in metal-insulator multilayers of $[Co_{80}Fe_{20}(t_n)/Al_2O_3(3nm)]_9$ with t_n = 1.6, 1.7 and 1.8 nm [4,5]. Here we report on a study of the effect of the number (odd or even) of bilayers on the modulated magnetization depth profile in a magnetic multilayer system. To this purpose, we have studied a DMIM sample with t_n = 1.5 nm comprising an even number (10) bilayers.

Results and Discussions :
Fig. 1 (a) shows PNR data taken at positive saturation (12 mT). The FM state of the sample can be recognized by the splitting of the reflectivity edges where $R^{++}(\theta)$, is shifted to higher angles in comparison to $R^{--}(\theta)$. The first order structural superlattice Bragg peak at 2θ = 4.9° is dominant in the R^{--}-channel. Its position corresponds to a bilayer thickness $d \approx 5.3$ nm in agreement with X-ray results (data not shown here). The presence of a weak signal in the two SF channels R^{+-} and R^{-+} is primarily due to the finite flipping ratio of 18 corresponding to the limited polarization efficiency of 94 %. The oscillatory behavior (Kiessig fringes) of R^{++} and R^{--} is due to the multilayer structure of the sample. The PNR data shown in Fig. 1(c) were taken at the weak guiding field (0.47 mT) of the neutrons after negatively saturating the sample. They are compatible with the negative remanence as indicated by the low angle data close to the plateau of total reflection, *e. g.* at 2θ = 0.8° (arrow), where $R^{--} > R^{++}$. The presence of a weak signal in the two spin-flip channels is primarily due to the limited efficiencies (94%) of both the polarizer and analyzer. As there is no significant spin-flip scattering, there is obviously no magnetization component perpendicular to the applied field.

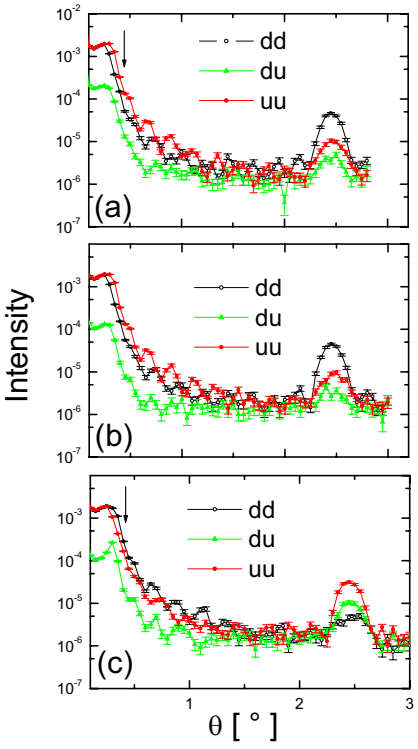


Figure 1: Spin-polarized neutron reflectivities R^{++} in red (dark gray), R^{--} in black and R^{+-} in green (light gray) *vs*. angle of incidence, θ, measured at T = 150 K and $\mu_0 H$ =12 mT (saturation) (a), close to the coercive field $\mu_0 H$ = 5.2 mT (b), and close to remanence in the guiding field of the neutrons, $\mu_0 H$ = 0.47 mT, after negative saturation (c) of *ferromagnetic* $[Co_{80}Fe_{20}(1.5nm)/Al_2O_3(3nm)]_{10}$.

Since this sample exhibited a sharp hysteresis, it was very difficult to measure at the coercive field. Fig. 1(b) shows a PNR measurement at a magnetic field a little higher than the coercive field. But as can be seen the field was sufficient to switch the magnetization to positive saturation. Therefore we were unfortunately not able to measure at the coercive field to observe the modulated magnetization depth profile as previously observed in other samples, which exhibit satellite peaks around the first Bragg peak. However, further attempts will be made on similar samples with even number of bilayers and rounded hysteresis such that it will be possible to measure at the coercive field.

Conclusions and acknowledgements :

Lack of spin-flip scattering suggests that magnetization reversal occurs via domain wall motion in this ferromagnetic sample. Unfortunately we did not observe any off-specular scattering from which one can calculate the mean domain size in the sample. This might be due to the resolution limit of the neutron beam, which cannot resolve domains being larger than $\xi \approx 30$ μm or the limited intensity available. Further attempts will be made on similar sample with even number of bilayers to check the effect of number of layers on the magnetization depth profile.

We thank Dr. A. Paul, Dr. Emmanuel Kentzinger and Dr. Ulrich Rücker for their support at HADAS and we gratefully acknowledge Forschungszentrum Jülich for the financial support for the work at Jülich.

References:

1. P. Bruno, Phys. Rev. B **52**, 411 (1995).
2. L. Néel, C. R. Acad. Sci. **255**, 1676 (1962).
3. B. D. Schrag *et al.*, Appl. Phys. Lett. **77**, 2373 (2000); S. Tegen *et al.*, J. Appl. Phys. **89**, 8169 (2001).
4. S. Bedanta et al. Phys. Rev. B (in press).
5. S. Bedanta et al. (to be published).

Institut für Festkörperforschung
Forschungszentrum Jülich GmbH
D-52425 Jülich

Experimental Report
of Neutron Scattering Experiments
at the FRJ-2 Reactor

Proposal number:	HAD-05-016		
Experiment title:	**Test of neutron optical devices for TREFF@FRM-II**		
Dates of experiment:	21.09.2005, 8.11.2005	Date of report:	28.06.2006
Experimental team: Names	Addresses		
Ulrich Rücker Stefan Mattauch	IFF, FZ Jülich JCNS-FRM II, FZ Jülich		
Local Contact:	Ulrich Rücker		

Experimental report text body

Due to the shutdown of the FRJ-2 reactor, major parts of HADAS will be used to build the TREFF reflectometer at the FRM-II reactor in Garching as a test and characterization beamline for neutron optical devices. For setting up this instrument and being able to characterize it and to compare it with HADAS, we need to check some neutron optical devices before using them to build TREFF.

Fig. 1 and 2 show in comparison the polarized neutron reflectivity from a standard NiTi m=2 supermirror and a nonmagnetic m=2 supermirror, where Ni is replaced by a nonmagnetic Ni-V-alloy. Both mirrors have been obtained from S-DH GmbH, Heidelberg.

The intense spinflip signal (see Fig. 2) clearly shows that the standard supermirror strongly depolarizes the beam. Therefore, this kind of neutron mirrors is not suitable to transport a polarized beam in the instrument. In contrast to that, the spinflip signal in Fig. 1 is completely due to the imperfect polarization of the beam in HADAS. No depolarization is caused by the nonmagnetic supermirror. The reflectivity is well comparable with a standard supermirror.

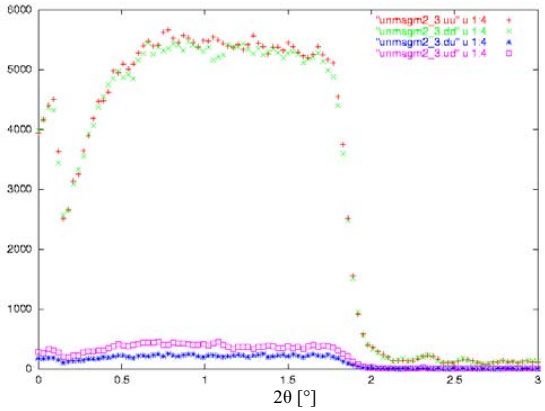


Fig. 1: PNR from a nonmagnetic $Ni_{1-x}V_x$ / Ti supermirror

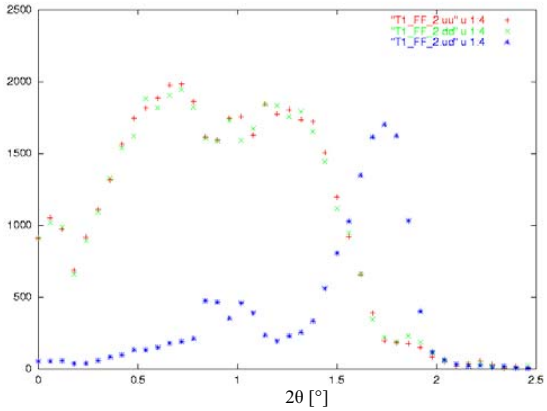


Fig. 2: PNR from a standard NiTi supermirror

Fig. 3 shows the reflectivity of unpolarized neutrons from a Ni coated glass plate, which is well bigger than the beam. It can be seen, that with an angular resolution of $\Delta\theta$=0.4 mrad, HADAS offers 5 orders of magnitude between total reflection and background. This experiment will serve as a reference for the characterization of TREFF.

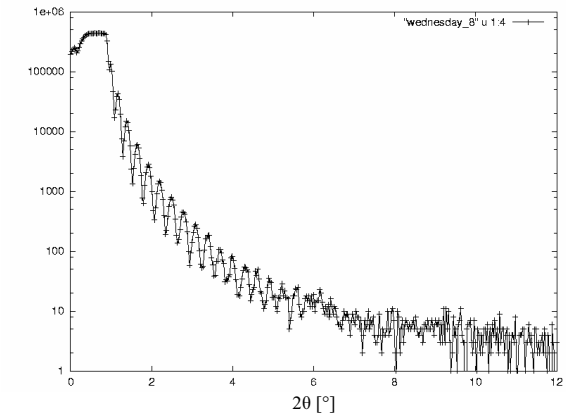
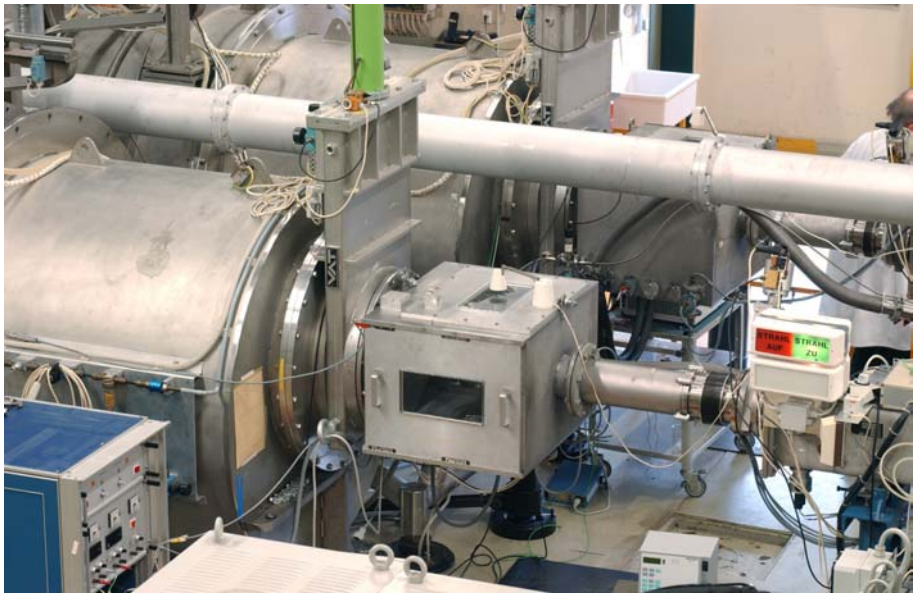


Fig.3: Reflectivity from a 80 nm thick Ni film on a glass substrate

In addition, several graphite crystals, a magnetic reference sample of 1 cm² size, and a polarizing supermirror which shows strong off-specular scattering were characterized to be able to compare TREFF's capabilities in different setups with HADAS.

Small Angle Neutron Scattering Instrument (KWS1)



Instrument Parameters

Beam tube:	NLIIA straight guide; cross section: 4.5 cm (height) × 3 cm (width)
Monochromator:	velocity selector (DORNIER); $\Delta\lambda/\lambda = 0.2$
Incoming beam ***- Entrance aperture:*** ***- Sample aperture:***	 variable; suggested: 3 cm × 3 cm variable; suggested: 1 cm × 1 cm
Collimation:	length variable from 1 m to 20 m
Detector ***- Active area:*** ***- Scintillator:*** ***- Space resolution:*** ***- Max. pulse rate:*** ***- Detection probability:*** ***- γ-sensitivity:***	 60×60 cm^2 in 128×128 channels ^{6}Li-glass, 1 mm thickness 0.5×0.5 cm^2 ca. 1 MHz (τ_{dead} = 3 μsec) 95 % for $\lambda = 7$ Å 2×10^{-4} (1 MeV)
Neutron flux at sample:	2×10^5 ... 2×10^7 n/cm^2 s depending on collimation $\lambda = 7$ Å wavelength and entrance aperture 3×3 cm^2
Wavelength:	4.5 Å < λ < 15 Å
Momentum transfer range:	10^{-3} Å^{-1} < Q< 0.2 Å^{-1} optional $Q_{max} \cong 1$ Å^{-1}
Ancillary equipment:	automatic sample holder in vacuum and air; heating devices: –40 to 200°C; pressure cell: $p = 1$ ... 2000 bar / $T \approx -30$ to 200°C; strain rigs and temperature control unit for quenched-elongational studies of melts (liquid N_2)

Instrument Responsible

Dr. Dietmar Schwahn Tel. +49-(0)-2461-61-6661 Email: d.schwahn@fz-juelich.de
Dr. Wim Pyckhout-Hintzen Tel. +49-(0)-2461-61-4681 Email: w.pyckhout@fz-juelich.de

Institut für Festkörperforschung
Forschungszentrum Jülich GmbH
D-52425 Jülich

Experimental Report of Neutron Scattering Experiments at the FRJ-2 Reactor

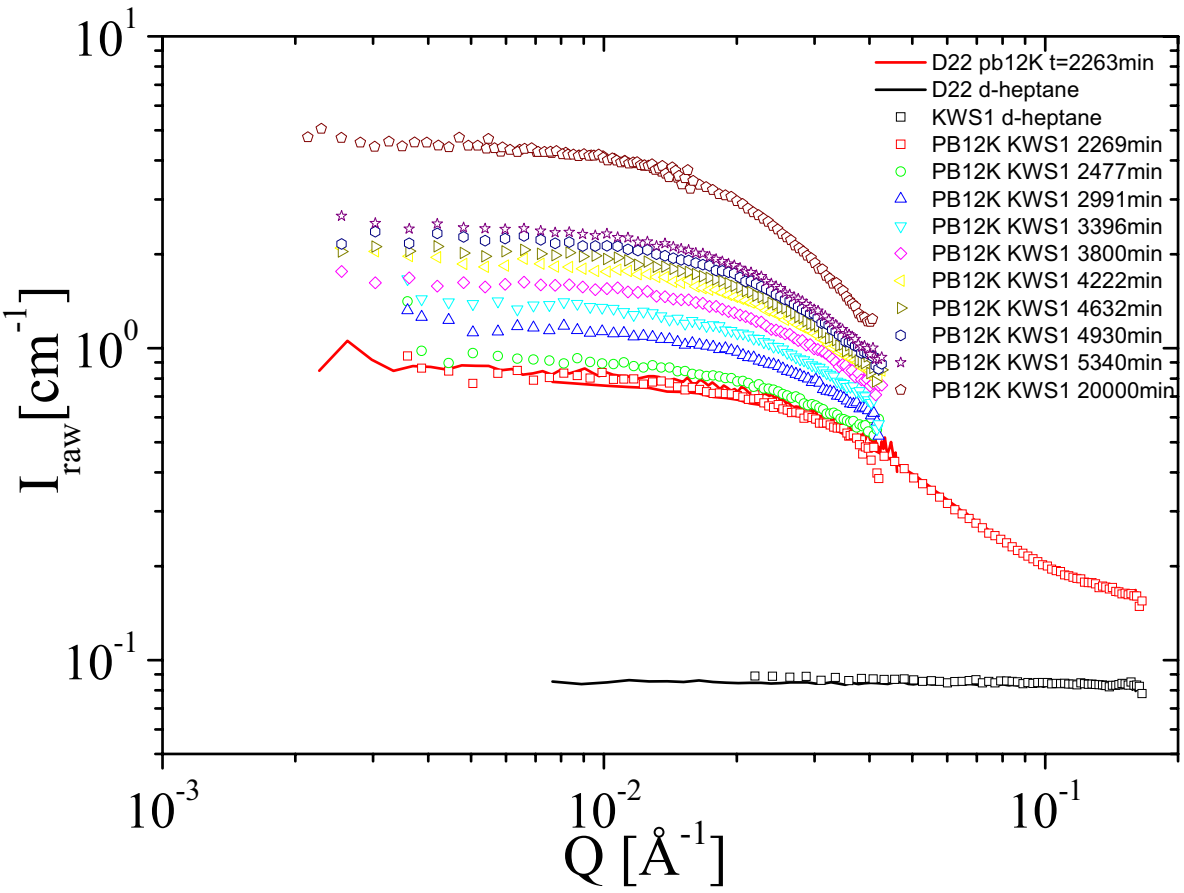
Proposal number:	KW1-04-036, KW1-04-084		
Experiment title:	Final stages of living anionic polymerisation		
Dates of experiment:	17.01.-20. 01. 2005 25.01.2005, 04.02.2005	Date of report:	06.06.2006
Experimental team: Names	Addresses		
J. Stellbrink A. Niu	IFF, FZ Jülich, D-52425 Jülich, Germany IFF, FZ Jülich, D-52425 Jülich, Germany		
Local Contact:	J. Stellbrink		

Experimental report text body

Anionic polymerisation is one of the key polymerisation techniques yielding well defined polymers both with respect to molecular weight distribution as well as architecture[1)]. In recent experiments we were able to relate in detail monomer conversion and initiation processes of "living" anionic polymerisation with structural details combining in-situ high resolution 1H-NMR and in-situ small angle neutron scattering (SANS). The combination of NMR and SANS opens a new realm of research into polymerisation processes, which appear to reveal completely new aspects of this polymerisation mechanism.

This proposal will be a continuation of an experiment recently started using D22 (ILL). There we followed by insitu SANS the structure formation in the initiation period of "living" anionic polymerisation. However, due to the limited beam time at ILL we were only able to follow the polymerisation for 1 ½ days. After the experiment all samples were quenched to -78°C and stored at this temperature, since we have shown that the polymerisation no longer progresses under these circumstances.

In this experiment we used KWS1 to follow the final stages of the anionic polymerisation after warming up the D22 samples again to 8°C, see fig. 1. Here the raw data, i.e. scattering intensity in absolute units [cm^{-1}],



from the last run at D22, at reaction time t=2263 minutes, are compared to the runs performed at KWS1 starting with t=2269 minutes. Also shown are data for the pure solvent d-heptane which show first of all the reproducibility and quality of absolute calibration (≤3%). The data sets from the polymerizing sample nearly fall on top of each other, which proofs the ability to quenching the polymerisation at T=-8°C.

References:

[1] M. Szwarc, M van Beylen, Ionic Polymerization and Living Polymers, Chapman&Hall: N.Y./London (1993)

[2] A. Z. Niu, J. Stellbrink, J. Allgaier, L. Willner, A. Radulescu, D. Richter, B. W. König, R. P. May, L. J. Fetters, J. Chem. Phys., **122**, 134906, (2005)

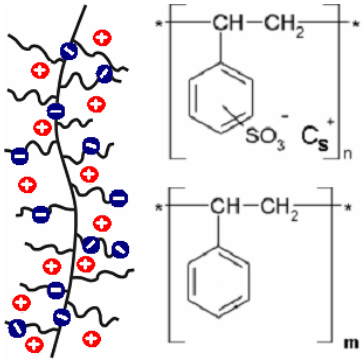
Institut für Festkörperforschung
Forschungszentrum Jülich GmbH
D-52425 Jülich

Experimental Report of Neutron Scattering Experiments at the FRJ-2 Reactor

Proposal number:	KW1-04-040		
Experiment title:	Small Angle Neutron Scattering of Polystyrene Sulfonate Combs		
Dates of experiment:	13/11/04-15/11/04 & 5/3/05-6/3/05	Date of report:	12/12/05
Experimental team: Names	Addresses		
A. Papagiannopoulos	School of Physics and Astronomy University of Leeds Woodhouse Lane LS2 9JT Leeds UK		
Local Contact:	Aurel Radulescu		

Experimental report text body

We performed a small angle neutron scattering study on dilute solutions of polystyrene sulfonate combs of 5 different architectures **(figure 1)**. Both main-chain and side-chains consist of highly charged polystyrene sulfonate with Cs as the counterion. Solutions were prepared in D_2O at a concentration of 0.1 mg/ml and were studied with and without added salt. The experiments were run at 3 different camera lengths (2m, 8m and 20m). The form factors of the PSS combs were succesfully measured at the full scattering vector (q) provided by KWS-1 (0.002 to 0.2 $Å^{-1}$) and the data was put together **(figure 2)** with complementary measurements from static light scattering in order to extend the q-range to even lower values (0.0008 Å-1).



Comb	*number of main-chain monomers*	*number of side-chain monomers*	*number of branches*
11	952	286	24
12	952	329	9
13	1905	673	30
14	1876	324	14
16	1905	286	≥150

Figure 1: Polystyrene sulfonate comb with the negatively charged monomers and positive counterions. The structure of the monomers is presented which is styrene sulfonate (top) and styrene (bottom) with n / (n+m) = 85%. On the right a table with the characteristics of the different comb architectures is presented.

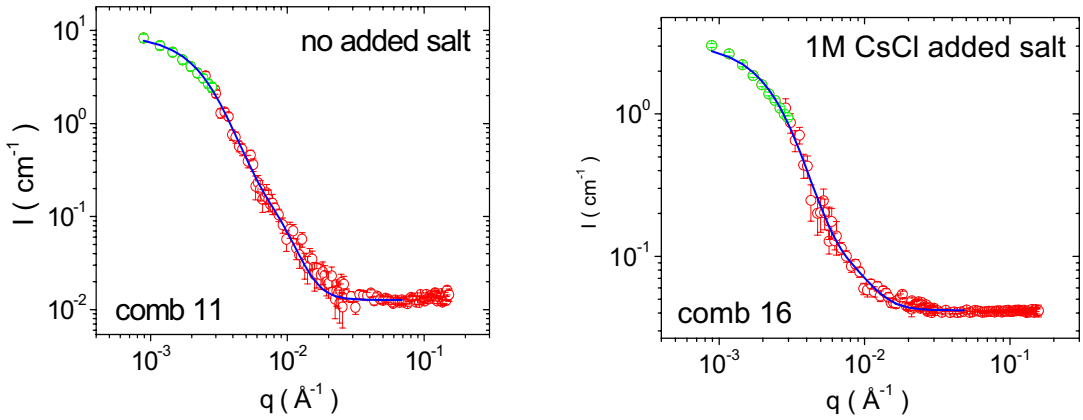


Figure 2: Combined small angle neutron scattering intensity (red) and static light scattering (green) from polystyrene sulfonate combs. The best fits with form factors of cylindrical shapes are shown with continous lines **[1]**. Static light scattering profiles have been shifted along the y-axis since the two techiniques do not agree in absolute scale.

The cylindrical form factors gave very good fits for all the combs in both cases with or without added salt **(figure 2)**. Attempts to fit with other geometries i.e. spheres and ellipsoids did not provide satisfactory fits to the experimentally measured form factors. The dimensions of the cylinders are consistent with linear polyelectrolyte chains that retain their dilute-solution conformation unperturbed, when they are placed on a comb structure. An estimation of the length of the cylindrical comb is $L \approx L_{main} + 2L_{side}$ **(figure 3)**, where L_{main} and L_{side} is the length of the main-chain and side-chain respectivelly, if these chains were free in solution and not attached on a comb. The length of the comb consists of the length of the unperturbed main-chain increased by the length of the unperturbed side-chains, that tilt parallel to the cylinder axis and outwards so that they minimise the repuslive interaction with other side-chains. The radius of the cylinders has been shown to agree with the size of an unperturbed side-chain **[1]**.

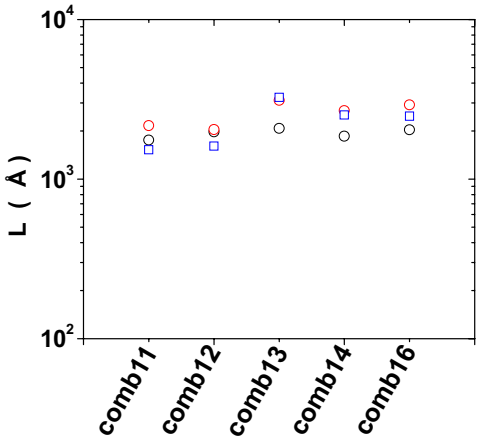


Figure 3: The length of the cylindrical polyelectrolyte combs. The circles are the experimentally observed values for no added (red) and added (black) salt The error bars are smaller than the size of the data points. The squares are theoretical predictions under the assumption of unperturbed main and side-chains.

The size of a flexible linear polyelectrolyte chain in dilute solution with no added salt can be calculated **[2]** by the expression, $L_{linear} \approx \frac{n\,b}{B}$, where n is the number of monomers of the chain, b the monomer length and B the expansion parameter. For polystyrene sulfonate the values $b \approx 3$ Å and $B \approx 3$ where used as they are confirmed to describe the structure of this polyelectrolyte **[1,2]**.

It is also shown **(figure 3)** that the combs decrease in size upon addition of salt, but not significantly, i.e. the size is still comparable with the theoretical prediction for the case of no added salt.

The dimensions of the comb molecules from this study were in agreement with independent measurements of the hydrodynamic radii by dynamic light scattering **[1]**.

References:

[1] A. Papagiannopoulos, PhD Thesis, University of Leeds **2005**.
[2] A.V. Dobrynin et al., Macromolecules **28**, 1859 **1995**.

Institut für Festkörperforschung
Forschungszentrum Jülich GmbH
D-52425 Jülich

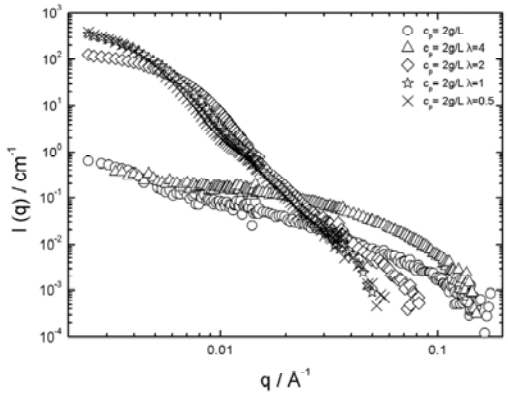
Experimental Report of Neutron Scattering Experiments at the FRJ-2 Reactor

Proposal number:	KW1-04-062		
Experiment title:	Electrostatic self-assembly of hydrophilic block copolymers		
Dates of experiment:	31.01.05-02.02.05	Date of report:	10.03.06
Experimental team: Names:	Addresses:		
Frank Reinhold	MPI für Polymerforschung, Ackermannweg 10, 55128 Mainz		
Local contact:	Wim Pyckhout-Hintzen		

Small angle neutron scattering on complexes of PEO-b-MAA and PAMAM dendrimers

Electrostatic interaction of polyelectrolytes with oppositely charged molecules leads to complex nano-sized structures which can be used as drug delivering systems, templates for crystallisation or for colloid formation of inorganic materials. Therefore many systems have been investigated in that field of research. But polyelectrolyte complexes precipitate if their charges are saturated by the counterions. Therefore it is not possible to build a large variety of structures of these polyelectrolyte complexes in solution. Double hydrophilic block copolymers which are composed of a charged and an uncharged but still hydrophilic block can be used to increase the solubility of polyelectrolyte complexes, because the uncharged block will keep the aggregated structure in solution.
We investigate the complexation behaviour of polyethylene oxide-b-methacrylic acid with NH_2-terminated PAMAM dendrimers, i.e. large counterions with a size of 1 nm to 15 nm.
Small angle neutron scattering was performed to obtain information about the radii of gyration and the shape of complexes formed by polyethylene oxide-b-methacrylic acid and polyamidoamine dendrimers of generation 4. Samples with an concentration of 2 g/L and different charge ratios λ in deuterated buffer soultions at $pH = 6$ and $pH = 7$. It was measured at detector distances at 20m, 8m, 2m and 1.25m. The calibration was performed with B_4C and plexiglass.

Figure 1 shows the scattering curves at different charge ratios in pH7 buffer solution. One can clearly observe the differences in scattering of aggregated and not aggregated particles. The radii of gyration, calculated by extrapolation of the linear Guinier plots, show a continuous increase in both buffer solutions starting at the radius of the copolymer. Pair distance distribution functions obtained from this measurement by indirect Fourier transformation (figure 2) can reveal information about density and shape of the particles. The comparison with different models shows that the tailing cannot be described by a sphere model, even a polydisperse one. An ellipsoidal shape seems to be the best explanation. The intersection of the function with the x-axis gives the maximum particle dimension (geometrical diameter). It shows the same trend as the hydrodynamic radius from dynamic light scattering data and by calculating the ratio R_G/R one receives again information about the shape of the particles. For a homogenous sphere $R_G = 0.775R$ that means the value 0.65 obtained from the experiment indicates approximately a spherelike structure. This is slightly different to the results of the indirect Fourier transformation, which gives the more detailed information.



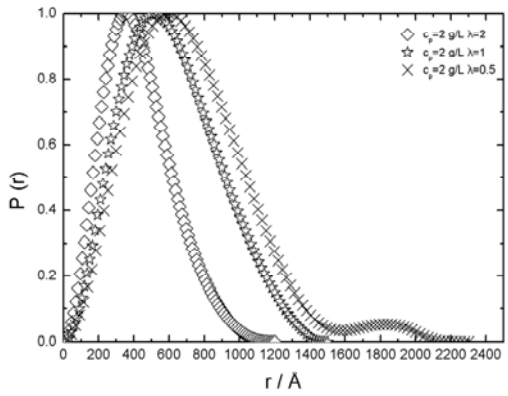


Fig.1 (left side): Scattering curves of PEO-b-MAA and PAMAM-dendrimer G4 in pH7 buffer solution.
Fig.2 (right side): Pair distance distribution functions of complexes formed by PEO-b-MAA and PAMAM-dendrimers in pH7 buffer solution.

Institut für Festkörperforschung
Forschungszentrum Jülich GmbH
D-52425 Jülich

Experimental Report
of Neutron Scattering Experiments
at the FRJ-2 Reactor

Proposal number:	KW1-04-065		
Experiment title:	**Conformation of the cytoplasmic part of the trasducer**		
Dates of experiment:	26.08.2005	Date of report:	28.03.2006
Experimental team: Names	Addresses		
Ivan Budyak Vitaliy Pipich Georg Büldt Judith Klein-Seetharaman	Forschungszentrum Jülich, IBI-2 Forschungszentrum Jülich, IFF Forschungszentrum Jülich, IBI-2 Forschungszentrum Jülich, IBI-2; University of Pittsburgh, USA		
Local Contact:	Dr. D. Schwahn, Dr. V. Pipich		

Experimental report text body

The SANS measurements were done at the KWS-I instrument at the FRJ-2 research reactor (Research Center Jülich, Germany). A neutron wavelength of λ=7 Å with sample-to-detector distances of 2 and 4 m were used to get a range in scattering vector $Q=2\pi/\lambda$ values of 0.01 to 0.2 $Å^{-1}$. Protein samples containing 2 and 7.5 mg/ml pHtrII-cyt in dPBS and 5 mg/ml pHtrII-cyt in dPBS + 4M KCl were analyzed at room temperature in quartz cells with 1-mm path lengths. The data were corrected for the detector efficiency, the scattering from the empty cell and solvent, and then radially averaged and calibrated in absolute units by a plexiglas secondary standard. Scattering curves were fitted using the approximation proposed by Beaucage (Beaucage, *J.Appl. Cryst.,* 1996) which combines both the Guinier regime (Guinier and Fournet, *Small Angle Scattering of X-rays.* 1955) and the fractal regime:

$$I(Q) = G\exp(-R_g^2Q^2/3) + P[erf(R_gQ/\sqrt{6})]^3/Q \quad (1)$$

where R_g is the radius of gyration, G is the Guinier prefactor

$$G = \Phi(1-\Phi)V\Delta\rho^2 \quad (2)$$

and P is the amplitude of the fractal part

$$P = \Phi(1-\Phi)\pi^2r^2V\Delta\rho^2. \quad (3)$$

Using this equation, the following features can be derived from the curve: (i) the zero Q intercept gives the particle volume if the concentration is known, (ii) the slope of the Guinier region is equal to $-R_g^2/3$ and therefore gives the particle size, (iii) the slope of the mass fractal dimension indicates the shape, (iv) and the Porod region gives the surface area and surface fractal dimension (Beaucage, *J.Appl. Cryst.,* 1996).

We used SANS to complement our observations from analytical gel-filtration and crosslinking experiments, that the cytoplasmic part of the transducer II from *Natronobacterium pharaonis* (pHtrII-cyt) is predominantly monomeric in PBS (Dulbecco and Vogt, *J.Exp.Med.*, 1954) and dimeric in PBS + 4 M KCl. All measurements were carried out in buffers prepared in D_2O to improve the signal:noise ratio.

The concentration-normalized experimental data are plotted in Fig.1 for pHtrII-cyt in dPBS as open circles (○) and in dPBS + 4M KCl as open squares (□). In both cases, the scattering intensity I(Q) follows the scaling law Q^{-1} over a wide Q range of 0.03 to 0.2 $Å^{-1}$ (Fig. 1, dashed line). The observation of a $I(Q) \sim Q^{-1}$ dependence is consistent with an elongated (rod-like) shape of pHtrII, both in dPBS and in dPBS + 4M KCl and can be approximated with a cylinder.

The volume fraction of protein Φ was calculated from the ratio between the pHtrII-cyt concentration and the protein density in H_2O, $\Phi = c/d_p$; the volume of the cylinder was assumed to be equal to the molecular volume of protein $V = M/N_a/d_p$. From Eq. 2 and 3, the length and the radius of the protein molecules can be calculated according to:

$$L = \pi G/P \quad (4)$$

$$r = \sqrt{(V/\pi/L)} \quad (5)$$

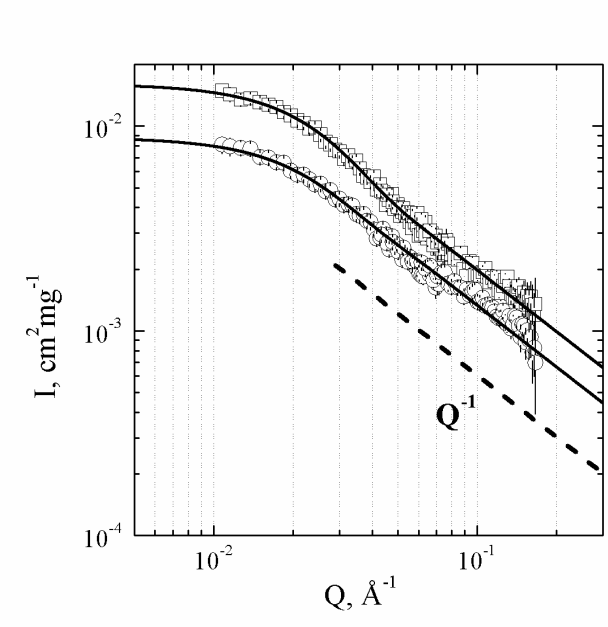
The values for the length and radius obtained for the pHtrII-cyt molecules in dPBS buffer were L_{PBS}=202±5 Å and r_{PBS}=7.2±0.3 Å, respectively. From these values, the radius of gyration R_g was calculated based on the cylinder model. For a cylinder of length L, radius r and unifrom mass distribution, R_g is given by:

$$R_g^2 = L^2/12 + H^2/2 \quad (6)$$

For pHtrII-cyt, this gives a radius of gyration of R_g = 58.5 Å. This value is similar to the radius of gyration value obtained directly from Eq. 1, which was 50.8±0.8 Å. The overall shape of the SANS spectrum measured in dPBS + 4M KCl was essentially identical to that observed in dPBS buffer alone. In contrast, the reduced zero intensity G:

$$G/c = 1/d_p V \Delta\rho^2 \quad (7)$$

in the presence of 4 M KCl in dPBS buffer was 1.8 higher than the zero intensity G observed in dPBS buffer alone. This increase can either result from a change in the particle volume V and/or the square of the scattering contrast. If we assumed a constant volume ($V_{SALT}=V_{PBS}$), the scattering length density of HtrII-cyt in D_2O would be $\rho_p = 2.3*10^{10}$ cm^{-2}. This value would be much lower than expected for proteins in D_2O and could only be accounted for if the protein would bind hundreds of K^+ ions. On the other hand, if we assumed a constant scattering length density ($\rho_p^{SALT}=\rho_p^{PBS}$), the particle volume would increase by a factor of 12. Thus, the result indicates that the increase in zero intensity must result from a combined increase in particle volume and change in scattering contrast. In particular, if we assume $V_{SALT}=2V_{PBS}$, the scattering length density of pHtrII-cyt in dPBS + 4 M KCl becomes $\rho_p = 3.22*10^{10}$ cm^{-2}. This value is very close to the value typically observed for proteins in D_2O. The decrease of the scattering length density from $4.37*10^{10}$ cm^{-2} in dPBS to $3.22*10^{10}$ cm^{-2} in the presence of 4 M salt suggests exclusion of D_2O from the protein's interior, either by "tightening" of the structure and/or by binding of K^+ ions.



The volumes and scattering length densities from the above calcuations were used to approximate the experimental scattering curve by using Eq. 1. The resulting curve is shown in Fig. 1. The molecule length and radius were calculated according to Eq. 4 and 5. The length and radius increased from L_{PBS}=202±5 Å and r_{PBS}=7.2±0.3 Å to L_{SALT}=248±7 Å and radius r_{SALT}=9.1±0.4 Å. When calculating the radii of gyration using these values and comparing them to the direct calculation using Eq. 1, a significant difference between R_g=56±1 Å (obtained from Eq. 1) and R_g=72 Å (calculated from Eq. 6) was observed. Since the experimental value is less than the theoretical value, the mass is either concentrated at the center of the cylinder or the cylinder is not ideal, i.e. the diameter at the center is larger than that on the edges. Thus, there is non-homogeneous mass distribution within the pHtrII-cyt dimer molecule in the presence of 4 M KCl in contrast to the pHtrII-cyt monomer in dPBS alone, which displayed uniform mass distribution.

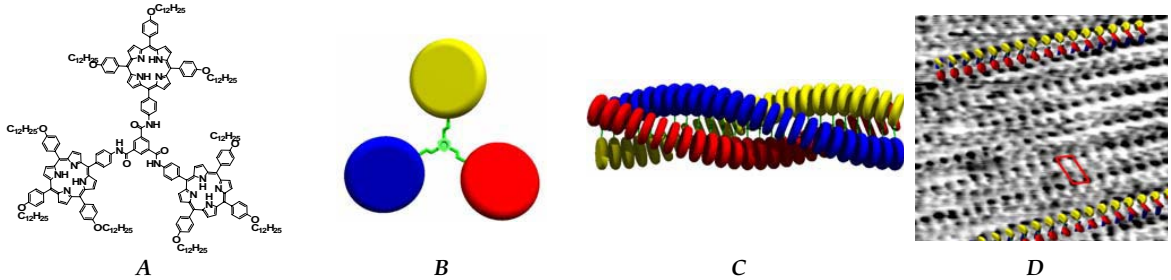
Institut für Festkörperforschung
Forschungszentrum Jülich GmbH
D-52425 Jülich

Experimental Report
of Neutron Scattering Experiments
at the FRJ-2 Reactor

Proposal number:	KW1-04-069		
Experiment title:	**Aggregation behaviour of disk-like porphyrin trimers.**		
Dates of experiment:	11-13 March 2005	Date of report:	6 October 2005
Experimental team: Names	Addresses		
Van Hameren, Richard Feiters, Martin Elemans, Hans Rowan, Alan Nolte, Roeland	Institute for Molecules and Materials Radboud Universiteit Nijmegen Toernooiveld 1 6525 ED Nijmegen The Netherlands		
Local Contact:	Dr. Wim Pyckhout-Hintzen		

Experimental report text body

Our group has recently demonstrated that porphyrin hexamers and dodecamers can form ring-shaped aggregates at the solid-liquid interface. [1-3] Previous SANS measurements have demonstrated that the porphyrin hexamers self-assemble into cylindrical-shaped aggregates in deuterated chloroform ($CDCl_3$). [4] We have designed and synthesized a disk-shaped porphyrin trimer (TAP, Figure 1A), which upon dissolution in $CDCl_3$ aggregates into columnar stacks, as established by NMR. The aggregation is governed by π–π stacking of aromatic surfaces of the porphyrins in combination with the formation of an intermolecular hydrogen bonding network between the amide functions of neighbouring molecules. Finally, the molecule is appended with long alkyl tails which enhance the solubility.



A ***B*** ***C*** ***D***

Figure 1*. Chemical structure* ***(A)*** *and schematic representation* ***(B)*** *of TAP, which self-assembles into columnar stacks* ***(C)****. At the solid-liquid interface, the columnar stacking of TAP was confirmed by STM* ***(D)****: scan size = 21 x 24 nm², V_{bias} = - 369 mV, I_{set} = 1.0 pA.*

The performed SANS measurements clearly demonstrated that in both $CDCl_3$ and deuterated toluene (toluene-d8), TAP self-assembles into cylindrical-shaped particles (Figure 2). It must be stated that TAP gelates the $CDCl_3$ at the applied concentrations and therefore the long alkyl tails are expected to be (almost) fully stretched. Taking this into account, the diameter of the cylindrical particles corresponds in both solvent systems to the diameter of one molecule. The different stacking behaviour can also be seen in the average length of a stack; the obtained length in $CDCl_3$ (47 nm) is 9 times longer than the length in toluene-d8 (5.3 nm). This can be explained by the interference of the aromatic toluene-d8 solvent molecules with the π–π stacking of TAP, which decreases the supramolecular interactions, resulting in smaller stacks.

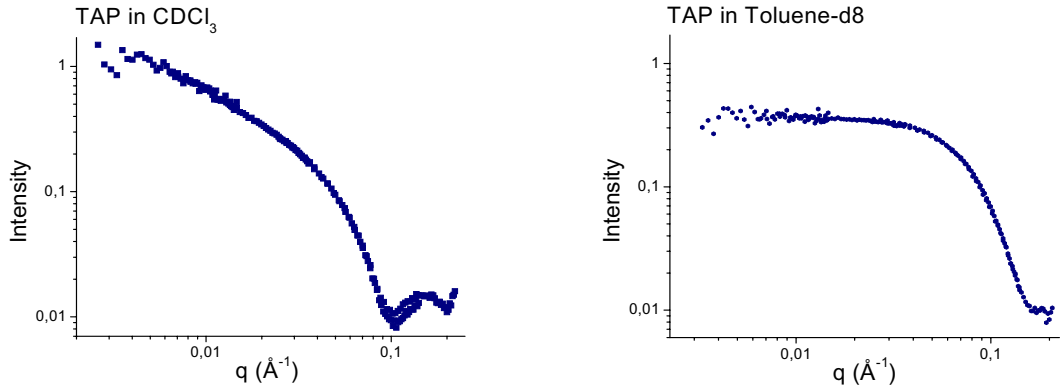


Figure 2. *SANS measurements in $CDCl_3$ and toluene-d8 at 293 K, at concentrations of 15,0 g/l and 15,3 g/l respectively. Both demonstrate the presence of cylindrical aggregates, however, the difference in length of the stacks is substantial.*

Secondly, the influence of the temperature and the concentration on the length of the self-assembled stacks was investigated. The SANS experiments in $CDCl_3$ showed that the length of the aggregates decreases with temperature and increases with concentration.

The SANS measurements in toluene-d8 demonstrated less predictable phenomena. Increasing the temperature from 293 to 343 K did not significantly change the average length of the aggregates (Figure 3). Remarkably, an increase in concentration decreases the average length slightly. On the contrary, the diameter slightly increases at a higher concentration, resulting in an almost constant volume of an average stack and thus the number of molecules in one stack remains constant. Apparently, increasing the concentration in toluene-d8 leads only to an increase in the number of stacks, but not to an increase in the average length of the aggregates of TAP.

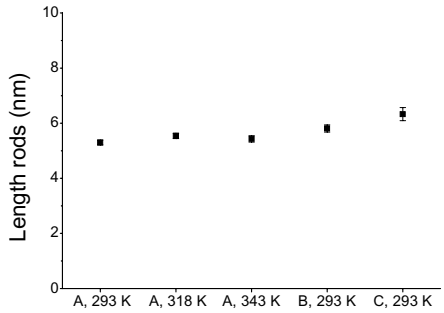


Figure 3. *The average length of a columnar stack of concentration (A: = 15,0 g/l; B: = 7,4 g/l; C = 3,7g/) and temperature (Kelvin).*

The change in the length-diameter ratio might be a property of the stack, but might also be an artefact as a result of experimental and fitting errors. Therefore, no conclusions can be drawn concerning this observation.

[1] J. A. A. W. Elemans, et al. *Adv. Mater.*, **2003**, 15, 2070.
[2] M. C. Lensen et al. *Chem. Commun.*, **2004**, 762.
[3] M.C. Lensen et al. *Chem-Eur. J.*, **2004**, 10, 831.
[4] M. C. Lensen et al. *Experimental reports 2004, Forschungszentrum Jülich GmbH,* **2005**, 280.

Institut für Festkörperforschung
Forschungszentrum Jülich GmbH
D-52425 Jülich

Experimental Report of Neutron Scattering Experiments at the FRJ-2 Reactor

Proposal number:	KW1-04-070		
Experiment title:	Change of heterogeneities with deformation: focus on low deformation		
Dates of experiment:	01/2006	Date of report:	31/05/06
Experimental team: Names	Addresses		
CASAS Frédéric ABA-SIMIONESCO Christiane MONTES Hélène LEQUEUX François	Laboratoire de Chimie Physique bat 349 Université Paris Sud 91405 Orsay cedex Laboratoire de Chimie Physique bat 349 Université Paris Sud 91405 Orsay cedex ESPCI, UMR 7615, 10 Rue Vauquelin 75005 PARIS ESPCI, UMR 7615, 10 Rue Vauquelin 75005 PARIS		
Local Contact:	Henrich Frielinghauss		

Experimental report text body

A polymer can be stretched and several studies have shown that heterogeneities are created during stretching [1-3]. Since a glassy polymer is an out-of–equilibrium thermo-dynamical state in which disorder or intern stress can be trapped, many works explain that the disorder increases as it undergoes an inelastic deformation; for instance, Oleinik speaks about micro-domains which are created and grow [1]. On one hand, a cold drawn polymer is considered as strongly heterogeneous at all scales involved at the different stages of the deformation. First strong density fluctuations are observed at local scales (A-B Fig 1). Beyond the yield point (B), conformation changes of the polymer chains appear leading to orientation fluctuations (B-C figure 1)[3](10 nm).

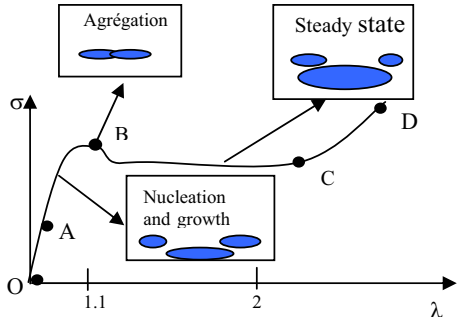


Figure 1 : Representation of creation of heterogeneities during deformation process. This process was proposed by Oleinik[1].

The aim is to observe the influence of different deformations on low deformations. We want to study particularly the influence of lambda because, as shown in Figure 1, for small λ, PMMA must be heterogeneous and when the deformation become larger, we reach the plastic domain where it is possible that the sample has reached a homogeneous state with aggregated defects. So, we performed SANS measurements on glassy PMMA samples stretched at different deformation on a q range from 0.002 $Å^{-1}$ and 0.15 $Å^{-1}$ (KWS1). Measurements were done on samples composed of 90% of crosslinked protonated PMMA chains. We compare the structure of the PMMA stretched chains. This experiment is the continuity of a precedent proposal (KW3-04-002).

A part of the results of our experiment are represented in the figures 2a, 2b and 3a, 3b for PMMA stretched at 94°C and V=0.002mm/s for two deformations; λ=1.15 and λ=1.4. The results show no particular length scale appears for small deformation (λ=1.15). For higher deformation (λ=1.4), we observed a non affine deformation which occurs in the plastic domain and which was observed in for deformation of λ=2. So, no lengths are characteristic of the disorder associated to low deformation in the q range of the experiment. This experiment need to be completed by more experiments at higher q range because the disorder occurs at smaller length scale.

[1] E.F. Oleinik et al. Polym. Sci **35** 11 (1993) 1819 ; [2] R. Quinson et al. J. Mat. Sci **31** (1996) 4387 ;[3] Hasan O et al J. polym. Sci., PartB, 1993,31,185

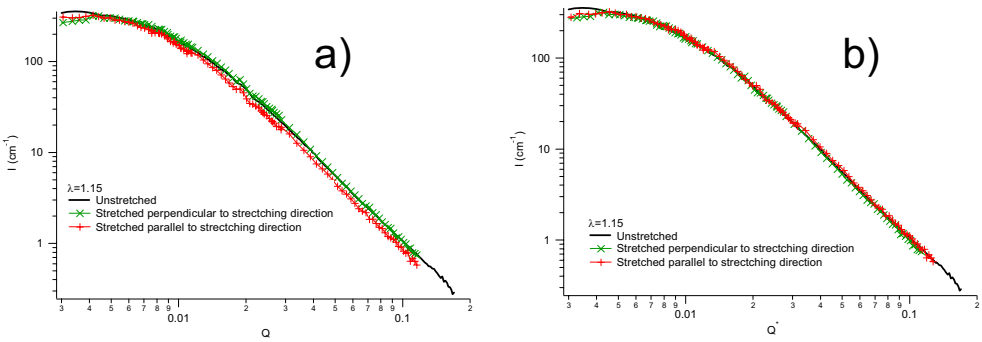


Figure 2 : a) SANS measurement of PMMA stretched at 94°C, V=0.002mm/s and λ=1.15. b) Same sample where data were plotted versus the reduced variable q* that takes into account the affine deformation of chains : perpendicular to the stretching direction $q^*=q/\sqrt{\lambda}$, parallel to the stretching direction $q^*=q\times\lambda$.

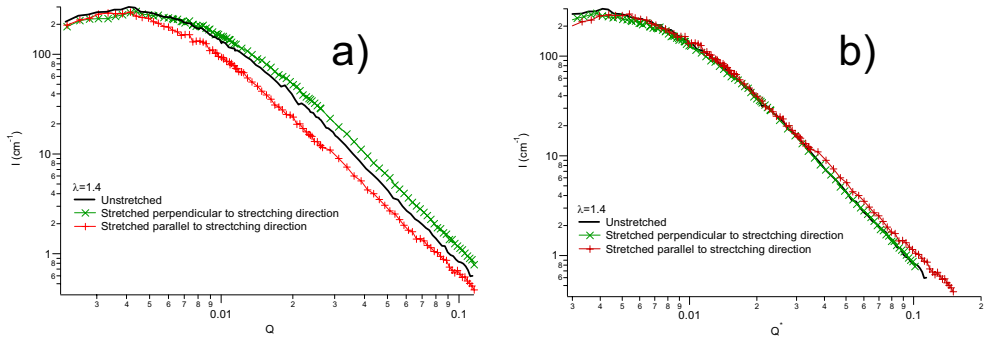


Figure 3 : a) SANS measurement of PMMA stretched at 94°C, V=0.002mm/s and λ=1.4. b) Same sample where data were plotted versus the reduced variable q* that takes into account the affine deformation of chains : perpendicular to the stretching direction $q^*=q/\sqrt{\lambda}$, parallel to the stretching direction $q^*=q\times\lambda$.

Institut für Festkörperforschung
Forschungszentrum Jülich GmbH
D-52425 Jülich

Experimental Report
of Neutron Scattering Experiments
at the FRJ-2 Reactor

Proposal number:	KW1-04-071		
Experiment title:	Effects of different salts on aggregation features of β-lactoglobulin		
Dates of experiment:	18.05. – 22.05.2006	Date of report:	09.06.2006
Experimental team: Names	Addresses		
Raffaele Sinibaldi Maria Grazia Ortore Francesco Spinozzi Paolo Mariani Flavio Carsughi	Dipartimento di Scienze Applicate ai Sistemi Complessi, Università Politecnica delle Marche, Via Brecce Bianche, 60131 Ancona, Italy Forschungszentrum Jülich, D-52425 Jülich		
Local Contact:	Dr. Wim Pyckhout-Hintzen		

Experimental report text body

ß-lactoglobulin (ßLG) is the major whey protein found in the milk of bovine and other ruminants. It is an acidic stable protein which exists at the normal pH of bovine milk as a dimer consisting of two monomeric subunits with a molecular weight of 18350 Da (162 residues). ßLG assumes a monomeric native structure at pH 2.3 in the absence of salt, and the dimeric structure is stabilized increasing the ionic strength of the solution.
We have already studied the structural properties of ßLG in acidic solutions (pH 2.3), evidencing the presence of a monomer-dimer equilibrium affected by the ionic strength, obtained with NaCl [3].
In order to derive the factors which control the BLG stability and interactions, we have compared the effects of NaCl to other different salts, which will be chosen according to the Hoffmeister series. In particular, at acidic pH in aqueous solutions containing NaH_2PO_4 , $NaClO_4$ and NaSCN (i.e., from stabilizing cosmotropes to disruptive chaotropes). Literature data show that the mechanism of the anions binding is dependent by their chaotropic effects [5]: sedimentation equilibrium analysis of ßLG in the presence of various concentration of different kind of salts has confirmed that the order of the effectiveness of various anions follows the electroselectivity series. In particular, multivalent anions have been demonstrated to be more effective than monovalent ones, and among them chaotropic anions more effective than kosmotropic ones. Such differences cannot be simply explained, first of all because the Debye-Huckel screening effect of salts is independent of anion species. In BLG, we observed that when the NaCl raises the surface free energy of the protein, protein-protein attraction increases, leading to a process of dimerization [4]. However, on lysozyme and ovalbumin [6] it has been shown that if the surface chemistry of proteins is altered by binding of a specific ion, salting-in is observed when the interactions between (kosmotrope) ion-protein complexes are more repulsive than those between the uncomplexed proteins, while salting-out is observed when interactions between (chaotrope) ion-protein complexes are more attractive than those of the uncomplexed proteins.

Moreover, the thermodynamic characterisation of the process of ßLG dimerization in different salts confirmed the dominant role of the hydrophobic effects [5], revealing at different temperature small differences from the kind of salt present in solution. We have performed SANS experiments on ßLG dilute solution (8 mg/ml) in water with different salts and in fully deuterated conditions. The experimental landscape (Fig.1 and Fig. 2) clearly confirms the order of the effectiveness of different anions following the Hoffmeister series.

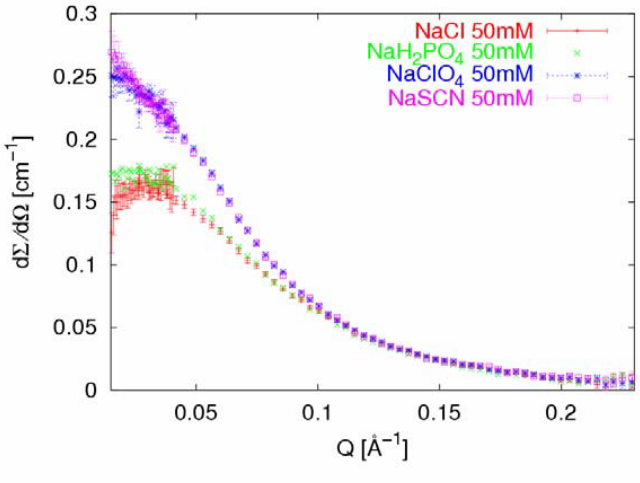


Fig.1 Differential Cross Sections relative to ßLG solutions containing the same ionic strength (50mM) obtained with different salts.

More precisely, data concerning ßLG dissolved at the ionic strength of 50mM show that the dimerization process has been induced by chaotropic anions in a more efficiently way. The ßLG monomer fraction increases from 67% (NaCl) to 98% (NaSCN), as resulting from the fitting procedure.
The same trend has been reproduced at the highest ionic strength (100mM): in this condition the chaotropic anions induce the formation of bigger aggregates, whose contribution in the form factor hides structure factor modifications. The experimental landscape confirm literature's suggestion about the different anion effectiveness on ßLG monomer-dimer equilibria.

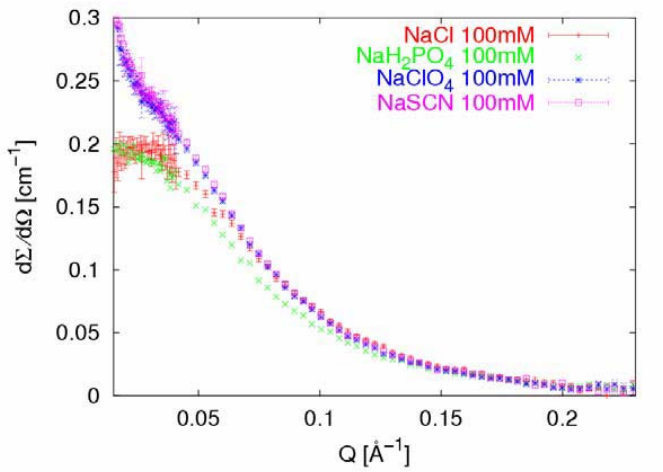


Fig.2 Differential Cross Sections relative to ßLG solutions containing the same ionic strength (100mM) obtained with different salts.

[1] Jasminka Godovac-Zimmermann. 1988. The structural motif of ß-lactoglobulin and retinol-binding protein: a basic framework for binding and transport of small hydrophobic molecules. Trends in Biochemical Sciences, Volume 13, Issue 2:64-66
[2] A. C. T. North. 1989.Three-dimensional arrangement of conserved amino acid residues in a superfamily of specific ligand-binding proteins. International Journal of Biological Macromolecules, Vol. 11, Issue 1: 56-58
[3] Baldini G, Beretta, S. G. Chirico, E. Maccioni, F. Spinozzi, P. Mariani, H. Franz. 1999. Salt-Induced Association Of Beta-Lactoglobulin By Light And X-Ray Scattering. Macromolecules, 32:6128-6138
[4] Spinozzi, F., D. Gazzillo, A. Giacometti, P. Mariani and F. Carsughi. 2002. Interaction of proteins in solution from small angle scattering: a perturbative approach. Biophys. J., 82:2165–2175
[5] Sakurai K., Oobatake M. and Goto Y. 2001. Salt-dependent monomer-dimer equilibrium of bovine ß-lactoglobulin at pH 3. Protein Science, 10: 2325:2335
[6] Curtis R.A., Ulrich J., Montaser A. et al. Hofmeister-Series Effects. Protein-protein interactions in concentrated electrolyte solutions. Biotechnology and Bioengineering, 79, 4:367:380.

Institut für Festkörperforschung
Forschungszentrum Jülich GmbH
D-52425 Jülich

Experimental Report
of Neutron Scattering Experiments
at the FRJ-2 Reactor

Proposal number:	KW1-04-072		
Experiment title:	Heterogeneous polymer micelles and their interactions with proteins		
Dates of experiment:	1.3-4.3/2005 at KW1 4.3-8.3/2005 at KW3	Date of report:	25.12.05
Experimental team: Names	Addresses		
BIANCO-PELED, Havazelet	Department of Chemical Engineering, Technion, Haifa, ISRAEL 32000		
SHAMAI,Keren	Department of Chemical Engineering, Technion, Haifa, ISRAEL 32000		
BITTON,Ronit	Department of Chemical Engineering, Technion, Haifa, ISRAEL 32000		
Local Contact:	Dr. Aurel Radulescu		

Experimental report text body

Background

The use of polymer brushes as surface modifiers has been recently shown to be a very promising way of manipulating the interaction of surfaces with proteins[1]. For example, hydrophilic polymer brush has been shown to be the most effective method to prevent adsorption of proteins. Contrary, other polymers are known to be attractive to proteins. In the preformed experiments we examined whether it is possible to control the adsorption of proteins to a colloid particle by using a "heterogeneous polymer brushes" (HPB). To the best of our knowledge, no one has experimentally attended that question yet.

Objectives

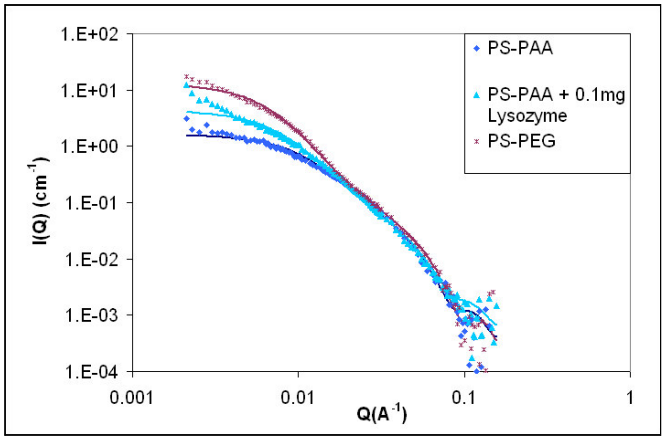
The objectives of this project are to study the HPB created *via* self-assembly of a mixture of neutral (polystyrene-b-Polyethylene glycol) (PS_{34}-PEG_{377}) and charged (polystyrene-b-polyacrylic acid) (PS_{32}-PAA_{277}) diblock copolymers. And to examine the relations between the composition of the micelles and their protein binding properties using Lysozyme (a ~2nm negatively charged protein) as a model.

Experimental

Since PS-PAA is not soluble in aqueous media, the block copolymers were first dissolved in Tetrahydrofuran (THF) which is a common solvent for both the hydrophobic (PS) and hydrophilic (PEG, PAA) blocks. Then, addition of water, a selective precipitant of the PS block, induces micelles formation. Homogeneous brushes were constructed for each block copolymer at different concentrations (1mg/ml, 3mg/ml) and heterogeneous brushes were constructed from 3mg/ml binary mixtures at different compositions (S1-10%, S2-25%, S3-50%, S4-75%, S5-90% PS-PAA). Scattering curves were measured on the KWS1 instrument with and without addition of proteins. Few of the samples were measured on the KWS3 as well.

Results

Our first experiments involved 1mg/ml PS-PAA micelles and 1mg/ml PS-PEG micelles (fig 1). The scattering curves were fitted to theoretical model of micelles with a spherical core (R) and Gaussian polymer chains (Rg) attached to the surface, where Nc is the number of chains in each micelle [2].



	R (Å)	Rg (Å)	N_c
PS-PAA	50	101	23
PS-PAA + 0.1 mg lysozyme	50	139	23
PS-PEG	45	154	62

Fig 1: Scattering curves for ◊) 1mg/ml PS-PAA micelles Δ) 1mg/ml PS-PAA micelles with 0.1 mg/ml of Lysozyme x) 1mg/ml PS-PAA micelles. The solid lines represent the curves fit to theoretical model of spherical block copolymer micelles (1).

As can be seen after addition of protein to the PS-PAA sample there is an increase in the shell dimension Rg, which may suggest protein adsorption on the micelles. Aditionaly, a 60% increase in the shell electron density was observed. The "excess" scattering at the low angles might be due to the presence of a second population of larger objects.The scattering from PS-PEG micelles with added lysozyme was not measured since PEG is commonly used polymer for prevention of protein adsorption on biomaterials surfaces [3].

In the second part of our experiment, we measured the scattering from the homogeneous and the heterogeneous micelles at 3mg/ml before and after the protein addition (fig 2). The two disticted slopes, observed in all scattering curves, suggest a bimodal size distribution. Using Gunier approximation and the position of the maxima at about 0.02 A^{-1}, values of Rg~3000Å and Rg~300Å were calculated for the large and the small particles. The size of the larger particles was obtained from further measurements at the KWS-3 instrument. A simple mathematical analysis have shown that the scattering curves of the heterogeneous micelles is not a superposotion of its two homogeneous curves. Therfore we concluded that mixed micelles were obtained. A comparison between the scattering curves before and after the protein addition revealed changes in the peak position. These differences are believed to result from protein adsorption and seems much more significant at 50% and 75% of PS-PAA block. A higher percentage of PS-PAA does not increase the protein adsorption. This may be due to an optimal composition for protein adsorption.

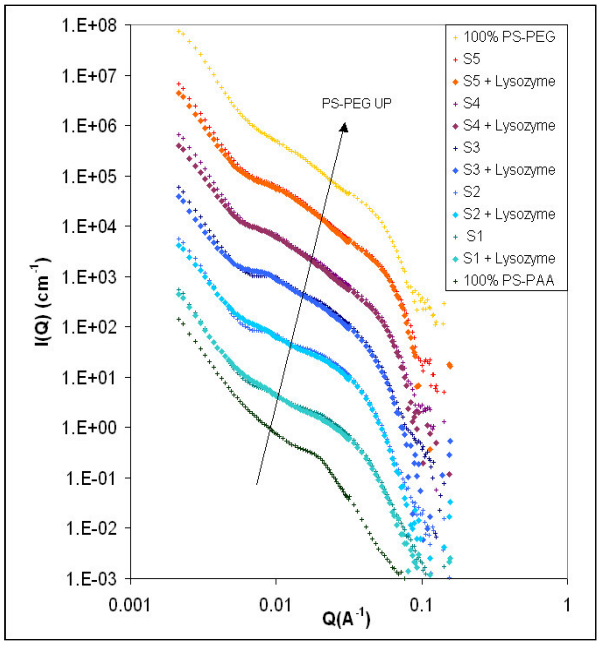


Fig 2: Scattering curves from homogeneous and heterogeneous micelles 3mg/ml before (+) and after (♦) Lysozyme addition.

1. Zhao, B. and Brittain, W. J. Polymer brushes: surface-immobilized macromolecules. *Progress in Polymer Science*, (2000), Vol. **25**(5), p. 677-710.
2. Pedersen, Jan Skov; Gerstenberg, Michael C. Scattering Form Factor of Block Copolymer Micelles. *Macromolecules* (1996), 29(4), 1363-5.
3. Gref, R., Domb, A., Quellec, P., Blunk, T., Mueller, R. H., Verbavatz, J. M. and Langer, R. The controlled intravenous delivery of drugs using PEG-coated sterically stabilized nanospheres. *Advanced Drug Delivery Reviews*, (1995), Vol. **16**(2,3), p. 215-33.

Institut für Festkörperforschung
Forschungszentrum Jülich GmbH
D-52425 Jülich

Experimental Report of Neutron Scattering Experiments at the FRJ-2 Reactor

Proposal number:	KW1-04-073		
Experiment title:	Complex Coacervate Core Janus Micelles		
Dates of experiment:	11-13 April 2005	Date of report:	21 December 2005
Experimental team: Names	Addresses		
Hellweg, Thomas Barneveld, Peter Voets, Ilja Hofs, Bas	TU Berlin STRANSKI LABORATORIUM Sekr. ER1 Strasse des 17.Juni 112 10623 BERLIN, Germany Laboratory of Physical Chemistry and Colloid Science Wageningen University P.O. Box 8038 6700 EK Wageningen, Netherlands		
Local Contact:	Dietmar Schwahn		

Experimental report text body

Janus micelles (micelles with a micro-phase separated corona) have generated substantial research interest in modern polymer and colloid science. So far, the existence of reversible Janus micelles has not been reported. This research work aims to study the coronal structure of reversible complex coacervate core micelles (figure 1), spontaneously formed through a combination of associative and segregative micro phase separation, simply by mixing two aqueous diblock copolymer solutions.

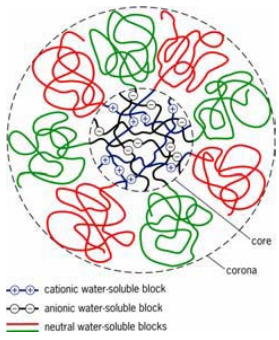


Figure 1: Schematic representation of a Complex Coacervate Core Janus Micelle, indicating the complex coacervate core formed by the polyelectrolyte blocks and the micro-phase separated corona.

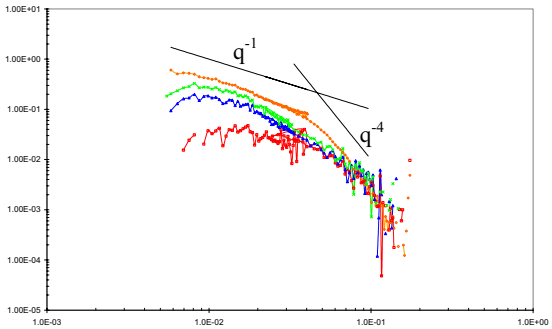


Figure 2: Contrast series for micelles consisting of PAA^{42}-$PAAm^{417}$ and P_2MVP^{44}-$dPEO^{300}$ (10g/l, 1mM $NaNO_3$, pH=5.5, 25ºC) for 29% (green), 36% (blue), 54% (red) and 100% D_2O (orange).

We have applied contrast variation as a tool to study corona structure and we have investigated the effect of temperature as a switch between Janus and non-Janus type.

As the scattering curves at different temperatures up to 80ºC in pure D_2O superimpose onto one single master curve, we conclude that temperature is not substantially changing the (corona) structure of the micelles.

A typical contrast series for the highest concentration is presented in figure 2. Interpretation of these series in terms of coronal structure (through contrast calculations and form factor/R_g fits for various micellar morphologies and coronal structure) is in progress.

Institut für Festkörperforschung
Forschungszentrum Jülich GmbH
D-52425 Jülich

Experimental Report
of Neutron Scattering Experiments
at the FRJ-2 Reactor

Proposal number:	KW1-04-076		
Experiment title:	Investigation of the gel structures from mixtures of chitosan and fibrinogen		
Dates of experiment:	7 to 9-March-2005	Date of report:	15-Feb-2006
Experimental team: Names	Addresses:		
Yuan Wang Dong Qiu Terence Cosgrove	School of Chemistry University of Bristol Cantock's Close Bristol BS8 1TS UK		
Local Contact:	Dr. Wim Pyckhout-Hintzen		

Experimental report text body

(Please use 12 pt letters here !)

Chitosan is the N-deacetylated derivative of chitin, a naturally abundant polysaccharide found in the exoskeleton of shellfish like shrimps or crabs. [1] Gelatin is another natural polymer, which is obtained by thermal denaturation or physical and chemical degradation of collagen. [2] Due to their biocompatibility, low toxicity, biodegradability and adhesiveness, the blends of chitosan and gelatin have been largely studied for potential uses in pharmaceutical fields [3], tissue engineering and wound dressing [4]. In this project, we studied the structure of the composite solution of chitosan, gelatin and a polyelectrolyte, polystyrene sulfonate sodium (PSSNa).

Macromolecules may form structures on different length scales in solution [5]. De Gennes [6] predicted that the pair correlation function for a polymer in a good solvent follows the Ornstein-Zernike law, which has a Lorentzian form in Q-space

$$I(Q) = \frac{I(0)}{1 + Q^2 \xi^2} \quad (1)$$

where ξ is the average correlation length and *I(0)* is the fitted scattering intensity at zero Q. For large scale inhomogeneity, an adaptation [7] of the Debye-Bueche equation [8] was used which is given by

$$I(Q) = \frac{I(0)}{(1 + Q^2 a^2)^2} \quad (2)$$

where *a* is the average inhomogeneity length. Therefore, we can see that at different Q-ranges, scattering from different length scale structure dominate. The results are summarized in Table 1. The concentration of PSSNa is fixed in this study.

It is shown that these polymers can be mixed evenly. The correlation length decreases with the increase of gelatin content, however, when no chitosan in present, the correlation length increases again, which suggests a complex interaction between polystyrene sulfonate and gelatin and the important role played chitosan. The large scale structure size decreases monotonically with the gelatin content, which is in good agreement with the rheological measurements. This suggests that the rheological behavior is mainly determined by the large scale inhomogeneity length. A detailed analysis is in progress.

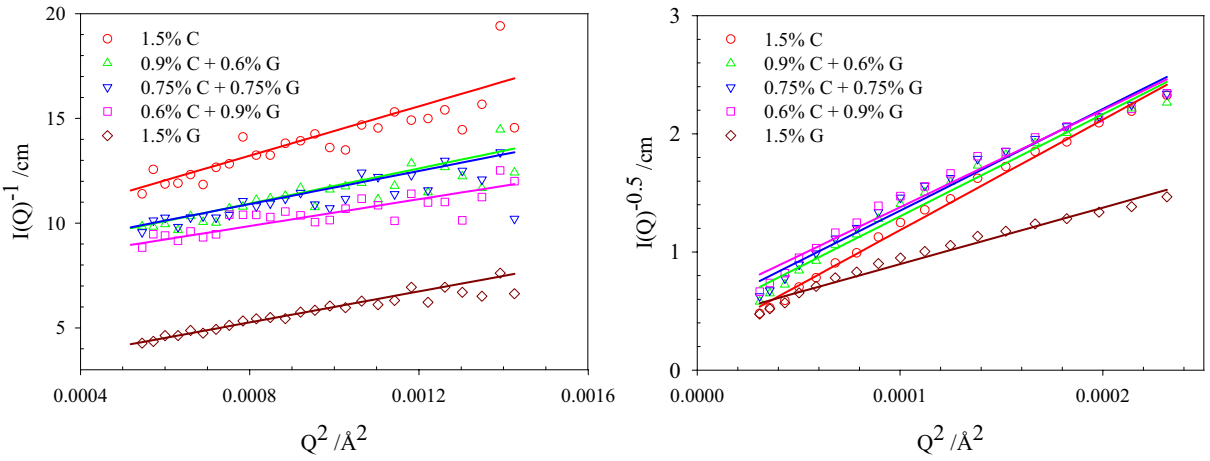


Figure 1. Fits of scattering from mixtures of chitosan, gelatin to the Lorentzian model (left) and Debye-Bueche model (right).

Table 1. Parameters obtained from the fits in Figure 1.

Chitosan Weight Fraction	1	0.6	0.5	0.4	0
Inhomogenity Length (Å)	193.7	140.6	132.7	121.7	106.8
Correlation Length (Å)	26.3	23.5	22.6	20.9	40.1

References:

[1] Majeti, N.V.; Ravi, K. *Reactive & Functional Polymers* **2000**, *46*, 1.

[2] Bigi, A.; Bracci, B.; Cojazzi, G.; Panzavolta, S.; Roveri, N. *Biomaterials* **1998** *19*, 2335.

[3] Yao, K. D.; Yin, Y.J.; Xu, M. X.; Wang, Y. F. *Polymer International* **1995** *38*, 77.

[4] Cheng, M. Y.; Deng, J. U.; Yang, F.; Gong, Y. D.; Zhao, N. M.; Zhang, X. F. *Biomaterials* **2003**, *24*, 2871.

[5] Pezron, I.; Djabourov, M.; Leblond, J. *Polymer* **1991**, *32*, 3201.

[6] de Gennes, P. G. *Scaling Concepts in Polymer Physics;* Cornell University Press: Ithaca, New York, **1979**.

[7] Kobersterin, J. T.; Picot, C.; Benoit, H. C. *Polymer* **1985**, *26*, 641.

[8] Debye, P.; Bueche, A. M. *J. Appl. Phys.* **1949**, *20*, 518.

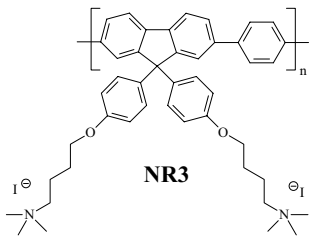
Institut für Festkörperforschung
Forschungszentrum Jülich GmbH
D-52425 Jülich

Experimental Report of Neutron Scattering Experiments at the FRJ-2 Reactor

Proposal number:	KW1-04-077		
Experiment title:	Structural studies on aggregates formed between nonionic surfactants and water soluble fluorene copolymers		
Dates of experiment:	6-7 April and 13-14 June 2005	Date of report:	3/12/05
Experimental team: Names	Addresses		
Hugh D. Burrows Matti Knaapila	Departamento de Química, Universidade de Coimbra, 3004-535 Coimbra, Portugal OEM Research Group, Departmenty of Physics, University of Durham, South Road, Durham DH1 3LE, UK		
Local Contact:	Dr Wim Pyckhout-Hintzen		

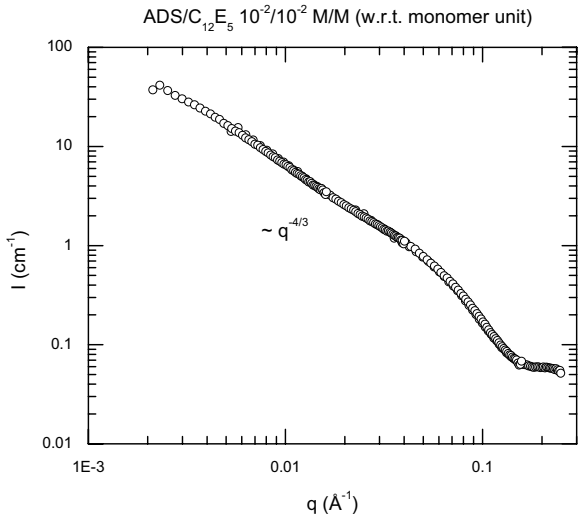
Experimental report text body

Conjugated polyelectrolytes are finding increasing applications as sensors for chemical and biological systems.[1,2] However, they tend to aggregate and have low solubility in aqueous solutions, such that organic cosolvents are normally needed to dissolve them, limiting their application in the sensing of biological systems such as nucleic acids. We have recently suggested, based on the results of fluorescence measurements, that nonionic surfactants, such as pentaethyleneglycol monododecyl ether ($C_{12}E_5$), can break up these aggregates and incorporate these polymers in long, cylindrical micelles.[2] However, proof of this was missing The objective of these small angle neutron scattering (SANS) measurements was to obtain structural information on the species formed with the cationic conjugated polyelectrolytes poly{9,9-bis[6-(N,N-dimethylamino)hexyl]fluorine-co-1,4-phenylene} iodide (NR3), and a commercial equivalent (ADS181), in the presence of $C_{12}E_5$ in aqueous (D_2O) solutions. The structure of NR3 is given below.



NR3

SANS studies were carried out on $C_{12}E_5$ solutions in D_2O (1 – 10 mM) alone, and with varying concentrations of either NR3 or ADS181 (up to 10 mM in terms of monomer units). These were corrected for transmission, background, sample cell, and detector efficiency. Typical data as a log-log plot for 10 mM ADS181 in $C_{12}E_5$ (10 mM) / D_2O solution is shown below.



Control SANS experiments were made with the polymer NR3 in perdeuterobenzene and D_2O solutions. The SANS results support the idea that the surfactant breaks up aggregates of the conjugated polyelectrolytes, and indicate that in the presence of $C_{12}E_5$, NR3 or ADS181 are present in similar wormlike micelles to those observed with the pure surfactant. The results are in agreement with NMR studies on these systems. However, the SANS data suggest that the fairly rigid polymers induece more ordered segments into the surfactant aggregates. Detailed analysis and modelling of the data is in progress, and is being combined with dynamic light scattering studies.

References

1. L. Chen, D.W. McBranch, H.-L. Wang, R. Helgerson, F. Wudl, D.G. Whitten, *Proc.Natl.Acad.Sci.*, 1999, **96**, 12287.
2. B.S. Gaylord, A.J. Heeger, G.C. Bazan, *Proc.Natl.Acad.Sci.*. 2002, **99**, 10954.
3. H.D. Burrows, V.M.M. Lobo, J. Pina, M.L. Ramos, J. Seixas de Melo, A.J.M. Valente, M.J. Tapia, S. Pradhan, U. Scherf, *Macromolecules*, 2004, **37**, 7425.

Institut für Festkörperforschung
Forschungszentrum Jülich GmbH
D-52425 Jülich

Experimental Report
of Neutron Scattering Experiments
at the FRJ-2 Reactor

Proposal number:	KW1-04-078		
Experiment title:	Quantitative relationship between non linear mechanical properties and particle arrangement in model filled elastomers.		
Dates of experiment:	February 2005 (2 days)	Date of report:	March 2006
Experimental team: Names	Addresses		
Thomas Chaussée Hélène Montes	PPMD-ESPCI Esc H 10, rue Vauquelin 75005 PARIS		
Local Contact:	Henrich Frielinghaus		

Experimental report text body

Filled elastomers are widely used for their interesting mechanical properties that can be adapt to the use. But we do not understand how the surface interaction between the particle surface and the elastomeric matrix influences the mechanical behavior of so-filled elastomer. Therefore we decided to produce some model silica-filled elastomers using different grafts in order to modulate the surface interaction. Grafts studied are: n-Octyltriethoxysilane (C8TES) in order to perform a weak inter action and Methacryloxypropyltrimethoxysilane (TPM) for the covalent bonding.

The so-filled elastomers were prepared using Ford method[1], consisting in grafting the particle directly and trandfer it to the monomer using dialysis. Suspensions were then adjusted to the write concentration by diluting the initially concentrated suspension, and a polymerizing initiator as well as a cross linker is added and polymerization is performed by alternative UV lighting. The so obtained elastomers are then characterized by SANS in order to identify the dispersion state of the particle in the poly(ethyl acrylate) matrix.

We have characterized for each graft three different sizes of silica particles: from 30 nm to 100 nm, using three typical concentration of 0.09, 0.13 and 0.16 in volume fraction.

The results showed that for strong interacting particles (TPM graft), all size and concentration leads to very well dispersed states (fig. 1).

Whereas for weaker interaction only the SANS measurements leads to the aggregation of the particles whatever the size or the concentration of the particles (fig. 2). Measurements done on the initial suspension of C8TES-grafted silica show that the particles are very well dispersed in the monomer media. This let us think that aggregation occurs during the polymerization step and can be due to depletion.

Therefore we decided to work on the polymerization step, we think that using temperature can have some effect on the final dispersion. Heating the sample during polymerization may bring enough energy to thepaticles to deaggregate them, whereas cooling down the system to 0°C or -20°C may freeze the system in a good

dispersion state. We also wanted to modify the interaction between the silica particle and the poly(ethyl acrylate) matrix using graft such as: Acetoxyethyldimethylchlorosilane (MCSNC) to perform some hydrogen bonding and Hexamethyldisilazane (HMDS) to get some weak interaction.

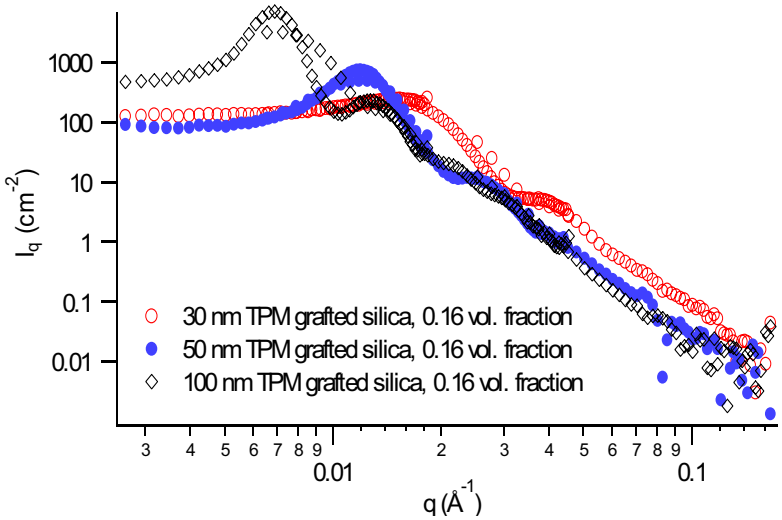


Fig.1 TPM grafted silica particles, 30 nm (red), 50 nm(blue) and 100 nm (red)

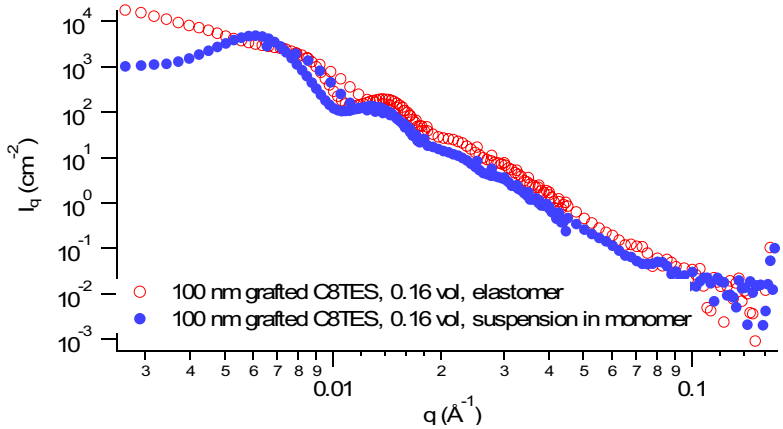


Fig.2 100 nm grafted silica particles, dispersion in poly(ethyl acrylate) matrix in red, and ethylacrylate monomer in blue

Institut für Festkörperforschung
Forschungszentrum Jülich GmbH
D-52425 Jülich

Experimental Report
of Neutron Scattering Experiments
at the FRJ-2 Reactor

Proposal number:	KW1-04-081		
Experiment title:	Hierarchical structure of silica and Carbon Black 1		
Dates of experiment:	29.01. – 30.01.2005	Date of report:	01.06.2006
Experimental team: Names	Addresses		
G. J. Schneider V. Vollnhals D. Göritz W. Pyckhout-Hintzen	Institut für Physik Universität Regensburg 93040 Regensburg Gerald.schneider@physik.uni-regensburg.de Institut für Festkörperforschung, Forschungszentrum Jülich		
Local Contact:	Dr. W. Pyckhout-Hintzen		

Experimental report text body

1. Abstract
Carbon Blacks are important fillers used for improving many of the properties of elastomeric materials. The characteristics obtained depend on the structure of the filler and its specific surface, and therefore on its bonding with the rubbery matrix. However the reinforcement mechanism is still not understood to any great extent. Therefore the structure of different commercially produced carbon black samples shall be investigated by means of small angle neutron scattering. By measuring the scattered intensity as a function of scattering length the size and the surface roughness of the aggregates and its spatial arrangement can be determined.

2. Introduction
Dispersing carbon black in rubber improves mechanical properties such as the elastic modulus, tensile strength and abrasion resistance. The effects due to different active fillers are influenced both by the specific inner surface and by the hierarchical structure of the filler. Due to these facts the commercially produced carbon blacks are classified by an industrial norm [1]. Each code starts with a letter describing the processing technique. Concerning the present work carbon-black samples produced with furnace method will be investigated, i.e. the starting letter is N. Afterwards, a number of the form XYZ, describing the structure of carbon black with regard to the reinforcement properties, follows. X is a measurement of the mean diameter of the aggregates and YZ reflects its spatial arrangement. Although not classified by the norm, Maier showed the dependence of the mechanical properties of carbon black filled rubber from the adsorption of polymer chains at the surface of the aggregates [2]. In addition Niedermeier et. al demonstrated the linkage to the surface roughness of the aggregates by computer simulations [3]. By measuring the scattered intensity as a function of scattering length q ($q = 4\pi/\lambda \sin(\theta/2)$), and plotting the result in a log-log-plot, the slope is a function of the roughness of the aggregates, or to be more precise the surface fractal dimension.

Additionally with the same experiment the size of the aggregates and its spatial distribution can be determined. In the present work the series N 110 up to N 990 will be investigated. According to the norm the mean diameter of these carbon black samples vary from 10 nm to 250 nm [1]. These structure sizes can be easily covered by using KWS 1.

3. Results

Figure 1 shows scattering diagrams, i.e. the intensity as a function of the scattering length, for the different samples. For the purpose of a better comparison the intensity values are normalized, therefore the intensity is in arbitrary units. Considering first the q-values larger than 0.2 nm^{-1} the almost identical slopes are evident. For values smaller than q = 0.2 nm^{-1} each curve shows a crossover to a second slope. As can be shown the crossover reflects the diameter of the aggregates and the slope at small length scales its spatial distribution. From N 110 to N 990 the crossovers shift to a lower scattering length, i.e. to a higher length scale. The slope at small length scales increases starting from N 110 to N 990.

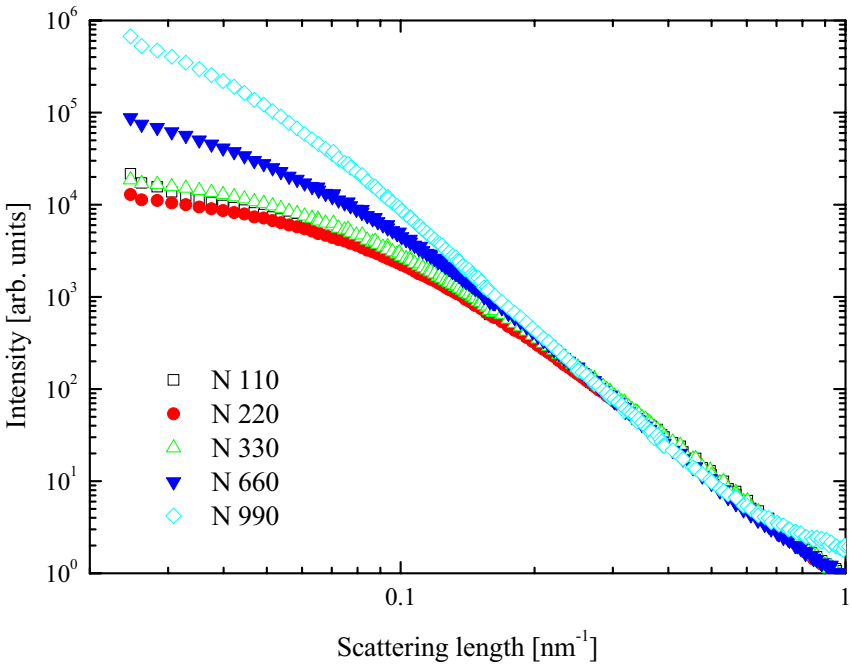


Figure 1: Intensity as a function of scattering length for different carbon black samples.

4. Discussion

The results should only be discussed qualitatively. The shifting of the crossover is in concordance with the norm, but the slopes at small length scales do not reflect the norm. However closest attention should be paid to the surface roughness. Since the slopes are almost identical no change in the surface roughness is expected for the different samples. Therefore the adsorption behavior should not change for the different fillers, and therefore the mechanical properties should not differ.

4. Conclusion

The use of KWS 1 to investigate the structure of carbon black samples was shown. Especially the surface roughness of different samples was shown to be equal.

[1] R. H. Schuster, Verstärkung von Elastomeren durch Ruß, Teil 1, Beiträge zur Technologie des Kautschuks und verwandter Stoffe, hrsg. Vom Wirtschaftsverband der deutschen Kautschukindustrie (WdK) (1989)
[2] P. Maier, D. Göritz, Kautsch. Gummi Kunstst. 49, 18 (1996)
[3] W. Niedermeier, H. Raab, J. Stiersdorfer, S. Kreitmeier, D. Göritz, Kautsch. Gummi Kunstst. 47, 799 (1994)

Institut für Festkörperforschung
Forschungszentrum Jülich GmbH
D-52425 Jülich

Experimental Report
of Neutron Scattering Experiments
at the FRJ-2 Reactor

Proposal number:	KW1-04-082		
Experiment title:	Solution properties of inorganic diblock-copolymer micelle complexes for nanodot arrays		
Dates of experiment:	26.01.05-29.01.05	Date of report:	24.03.06
Experimental team: Names	Addresses		
Karthäuser, Silvia Rathgeber, Silke Kronholz, Stephan	Forschungszentrum Jülich GmbH IFF; Elektronische Materialien Forschungszentrum Jülich GmbH IFF Forschungszentrum Jülich GmbH IFF, Elektronische Materialien		
Local Contact:			

Experimental report text body

An A-B diblock copolymer consists of two chemically different, covalently bonded macromolecular chains. If these exhibit different solubilities, micelles are formed in appropriately chosen solvents. In a non polar solvent for example the non polar chain segment is dissolved while the polar chain segment is insoluble and tends to form the core of a micelle. According to the chemical and physical interactions characterizing the monomer units, the micelles can bind other components, for example leading to complexation or binding of a transition metal compound. In our case the micelle cores are loaded with a transition metal salt ($HAuCl_4$) which can be reduced to metal nanoparticles.

Dilute solutions of loaded micelles can be used to prepare a thin self-assembled film on a flat substrate. The film is created by dipping the substrate into the micellar solution and pulling it out again at a controlled velocity. If the conditions are chosen appropriately a micellar monofilm is built after evaporation of the solvent. Subsequent plasma treatment can be used to remove the polymer, which means that only small metal nano-particles are left on the substrate. The location and order of the particles corresponds to the quasi-hexagonal pattern of the closely packed micelles in the original film. This rather regular pattern can serve as template for the building up of nanodot arrays instead of using e-beam lithographic methods with the advantage of easy achievable nanometer sizes with low costs. Our aim was to investigate the correlation between the micellar structure in solution and the resulting arrangement on the substrate after deposition.

In our SANS experiment we wanted to complete our measurements including experiments on the solution properties of the unloaded micellar solutions built from the two different blockcopolymers, (Poly2) and the more asymmetric diblock-copolymer (Poly1). Furthermore our aim was to complete our data set on Poly1 for the same amounts of gold load as measured for Poly2.

In the SANS experiment we have measured the solution properties of unloaded micelles with both fixed block length ratios (Poly1 and Poly2) and micelles built up by Poly1 with varying amounts of gold load. Concentrations have been varied between those relevant for film preparation down to dilute solutions to obtain the form factor yielding information about the structure of a single micelle. The form factors of gold loaded micelles (L=0.2 and L=0.5) built up from Poly2 are shown in figure 1. As a reference the data obtained for the unloaded micelles (L=0) are also included. From these form factors the density profiles for the PVP core, the PS shell and the Au distribution were calculated by a simultaneous core-shell model fit. Figure 2 shows a comparison between Poly1 and Poly2 with the same gold load.

We compared the micelle dimensions and the average inter-micelle spacing in solutions with those obtained from dried monofilms. Obviously the inter-micelle spacing in the dried film is much smaller than the micelle dimension in solution and approaches the dimension of a fully collapsed micelle in case the dipping process is performed slow enough. Currently a publication containing these results is ready to be submitted.

References:

[1] J. Spatz, M. Möller and P. Ziemann, Phys. Blätter **55**, 49 (1999).
[2] J. Spatz, S. Mössmer, C. Hartmann and M. Möller, Langmuir **16**, 407 (2000).
[3] O. Glatter, J. Appl. Chryst. **10**, 415 (1977); J. Appl. Chryst. **14**, 101 (1981).

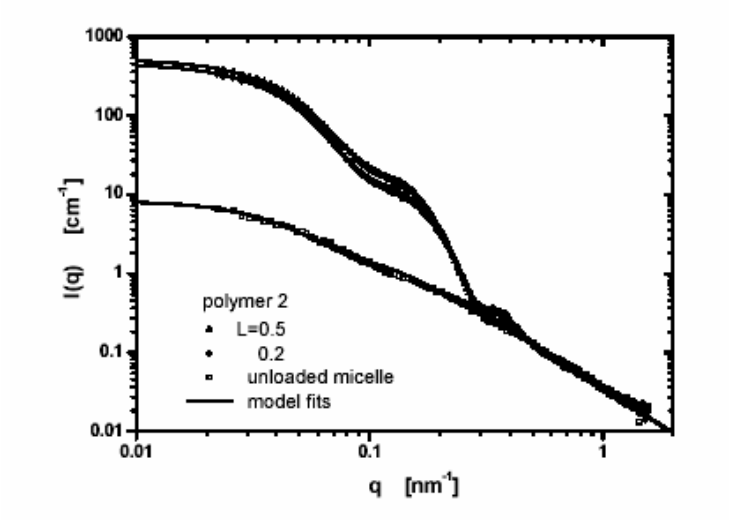


Figure 1:
Form factors obtained for gold loaded micelles (Poly2) with different amounts of Au including the unloaded micelle. The solid lines show the results of the model fit.

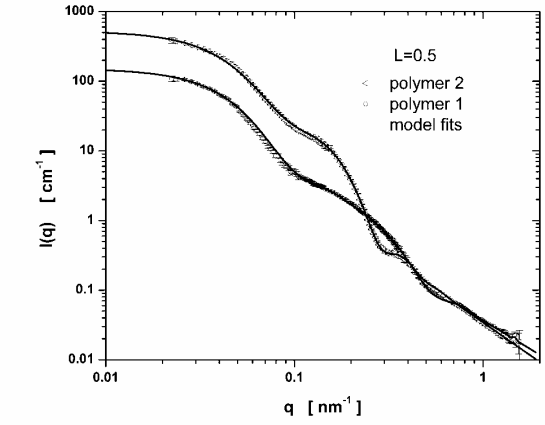


Figure 2:
Form factors for loaded micelles with different block length but same gold load (L=0.5). The solid lines show the results of the model fit.

Institut für Festkörperforschung
Forschungszentrum Jülich GmbH
D-52425 Jülich

Experimental Report
of Neutron Scattering Experiments
at the FRJ-2 Reactor

Proposal number:	KW1-04-085		
Experiment title:	Micellar properties of PB-PS-PB triblock copolymers in alkanes		
Dates of experiment:	31.01. – 02.02.2005	Date of report:	30/05/2006
Experimental team: Names			
Reidar Lund Lutz Willner Dieter Richter	DIPC, University of Basque Country, Spain Institut für Festkörperforschung, FZJ, Jülich, Germany Institut für Festkörperforschung, FZJ, Jülich, Germany		
Local Contact:	Wim Pychout-Hintzen		

Experimental report text body

In this experimental session, we have investigated the mesoscopic structure of micelles formed by poly(butadiene)-poly(styrene)-poly(butadiene) (PB20-PS20-PB10, the numbers indicate the molecular weight in kg/mole) triblock copolymers immersed in n-hexadecane. The aim was to characterise the micellar properties (aggregation number, core radius etc) with the particular aim to compare the data with previous results obtained on diblock analogue PS10-PB10. The concentration was varied between 0.25- 1 vol.%. No concentration dependent micellization behaviour was found, but the effective forward scattering was observed to decrease with increasing concentration signaturing a repulsive interaction between the micelles.
In order to obtain detailed structural information, the micelles were measured using under three contrast conditions; core contrast (purely deuterated hexadecane), shell contrast (nearly purely hydrogenated hexadecane) and in a average contrast where the interference scattering between the PS and PB parts is visible. The partial form factors including a fit to the core-shell model[1] is shown in figure 1.

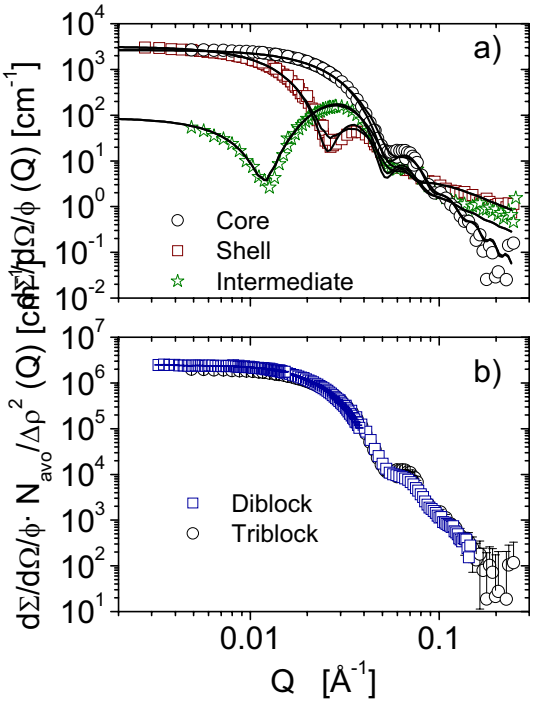


Figure 1. a) Partial form factors of PB10-PS20-PB10 micelles in hexadecane at 20 ªC. The solid lines display fit to a core-shell model. b) Comparison between the core scattering of the triblock micelles and the corresponding under core contrast. .

ehler! Textmarke nicht definiert.

The data have been fitted with a core-shell model revealing that both the core and the corona can be best fitted with a compact, constant density profile. The aggregation number, P, was found to be approximately 53 chains per micelles which almost perfectly corresponds to the half of the P of the diblock PS10-PB10 micelles which is rather intuitively reasonable as the triblock chain exhibit the double volume compared to the diblock This is seen directly in the in figure 2 b) where the normalized scattering curves of the cores of both the diblock and triblock micelles are plotted together. Both the forward scattering as well as the minimum coincide very well indicating the same micellar volume and core radius. This is a very important input for the kinetic measurements where we aim to understand the role of chain topology on the exchange kinetics. As both micellar systems has the same size of the core, the kinetic results can bed directly compared.

References:

1. R. Lund, L. Willner, J. Stellbrink, A. Radulescu, and D. Richter, Macromolecules **37**, 9984 (2004).

Institut für Festkörperforschung
Forschungszentrum Jülich GmbH
D-52425 Jülich

Experimental Report of Neutron Scattering Experiments at the FRJ-2 Reactor

Proposal number:	KW1-04-086		
Experiment title:	Study of the formation of silica filler particles obtained from a sol-gel transition inside a rubber.		
Dates of experiment:	24-25/09/2005	Date of report:	28/03/2006
Experimental team: Names	 Addresses		
Heinrich Martine Pyckhout-Hintzen Wim	IFF Forschungszentrum Jülich		
Local Contact:	Heinrich Martine		

Experimental report text body

This proposal is a part of a study concerning the formation of single, non-agglomerated spherical silica particles from a sol-gel interaction inside a crosslinked network: a PI network swollen in tetraethoxysilan (TEOS, $(C_2H_5O)_4Si$) is immersed in a 2% (w) aqueous solution of ethylamine (EA). The TEOS trapped in the network reacts with the water to produce silica, following the reaction: $(C_2H_5O)_4Si + 2\ H_2O \rightarrow SiO_2 + 4\ C_2H_5OH$ [1-3]. This method has been used commercially and showed to yield considerably reinforced networks without having to rely on the mixing or processing of both filler particles and polymer chains. This effectively reduces degradation of chains or also the inefficient incorporation of silica in the rubber. The kinetics of the reaction of ortho-silicate with water was not studied in real-time. This SANS investigation should reveal structural details of the process.

In the first part of the study, we have investigated the formation of silica particles in a PI-network (M_w = 200 kg.mol^{-1}, M_c = 8 kg.mol^{-1}) directly in the neutron beam, on the q-range 0.01 < q (Å^{-1}) < 0.08 during the 2 first days of the precipitation reaction. The particles radius R obtained in this q-range from Guinier approximations showed that after the 1st hour of reaction and till the 8th hour, particles are progressively growing to reach a size corresponding to R = 40 Å, remaining constant till the end of the experiment (= 2 days of reaction). More details are given in experimental report 2004, KW1-04-057.

Knowing the important times of the reaction from this first set of experiments, we have investigated in details the silica formation and aggregation processes in this proposal. For this purpose, we have prepared samples made of PI networks (M_w = 200 kg.mol^{-1}, M_c = 100 kg.mol^{-1}) swollen in TEOS, allowed to react with an aqueous solution of EA for limited specific times between 1/2 hour and 1 day. The use of these “quenched”

samples has the advantage that SANS experiments can be performed on the full q-range ($0.002 < q\ (Å^{-1}) < 0.2$) to obtain information at all the available length scales and at different stages of the reaction.

The obtained structure functions S(q) are given on Figure 1, together with the corresponding predictions from the empirical approach for polymeric mass fractals of Beaucage [4]. A 2-level structure is observed with respective radii Rcore and Rcluster and power law exponents Ps and Pclu. The radii as a function of the reaction time are plotted on Figure 2, and the fits parameters are summarized in Table 1.

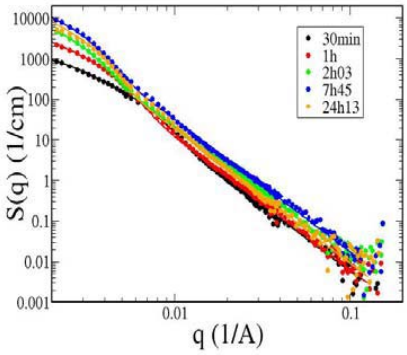


Fig 1: Structure functions for the different reaction times (points for experiment, lines for theory [4]).

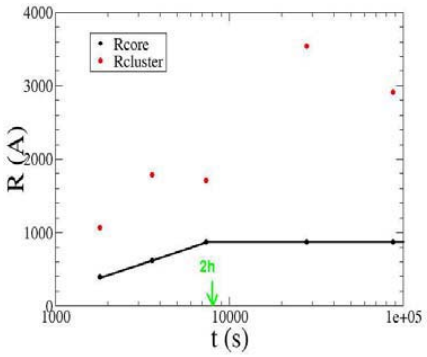


Fig 2: Radii of the 2 structures of the Beaucage model as a function of the reaction time.

Figure 2 and Table 1 show that the radius of the 1st level structure (Rcore) is increasing during the first 2 hours of the precipitation reaction and afterwards remains constant to a value of about 870 Å. At the same time, the radius of the 2nd level structure (Rcluster) seems always to increase. The exponent Pclu indicates that different aggregation processes are involved during the reaction (a value of 2.5 is a sign for a diffusion-limited-aggregation process and 1.8 a sign for cluster-cluster aggregation process).

Time	Rcore (Å)	Ps	Rcluster (Å)	Pclu
30 min	397	3.3	1071	2.4
1 h	619	3.3	1789	2.2
2 h 03	868	3.3	1710	1.8
7 h 45	868	3.3	3540	1.8
24 h 13	868	3.3	2912	2.9

Table 1: Radii of the 2 structures (Rcore and Rcluster) and power law exponents Ps and Pclu.

The preliminary results given here show that SANS is a powerful technique to follow the processes of silica precipitation and aggregation which occur at different times and length scales.
But further experiments and data evaluations are necessary to understand the silica formation process as a function of the obtainment conditions especially how the value of M_c is influencing the primary particle size.

[1] J.E. Mark et al, Polymer Bulletin, **12,**413(1984)
[2] Y. Ning et al., Polymer Bulletin, **13**,155(1985)
[3] C. Jiang et al., Makromol. Chem, **115**, 2609(1984)
[4] G. Beaucage, J.Appl.Crystallography **28,** 717 (1995) ; G. Beaucage, J.Appl.Crystallography **29,** 134 (1996)

Institut für Festkörperforschung
Forschungszentrum Jülich GmbH
D-52425 Jülich

Experimental Report
of Neutron Scattering Experiments
at the FRJ-2 Reactor

Proposal number:	KW1-05-001		
Experiment title:	**Study of the mechanism of formation of poly(vinylalcohol) hydrogels by freeze/thaw techniques**		
Dates of experiment:	16-21 May 2005	Date of report:	5 June 2006
Experimental team: Names	Addresses:		
Finizia Auriemma, Roberto Triolo Rosa Ricciardi.	Dipartimento di Chimica, Università di Napoli Federico II, Complesso Monte Sant' Angelo, via Cintia, 80126 Napoli (Italy) Università degli Studi di Palermo, Dipartimento di Chimica Fisica, Viale delle Scienze, Parco d'Orleans II, 90128 Palermo (Italy) Dipartimento di Chimica, Università di Napoli Federico II, Complesso Monte Sant' Angelo, via Cintia, 80126 Napoli (Italy)		
Local Contact:	Vitaly Pipich		

Experimental report text body

The kinetics of sol-gel transition of homogeneous aqueous poly(vinyl alcohol) (PVA) solutions during freezing and thawing cycles has been investigated by SANS experiments. SANS measurements of PVA solutions in heavy water at different polymer concentrations have been performed during consecutive freezing (-13°C) and thawing (20°C) steps, as a function of time (Figure 1).

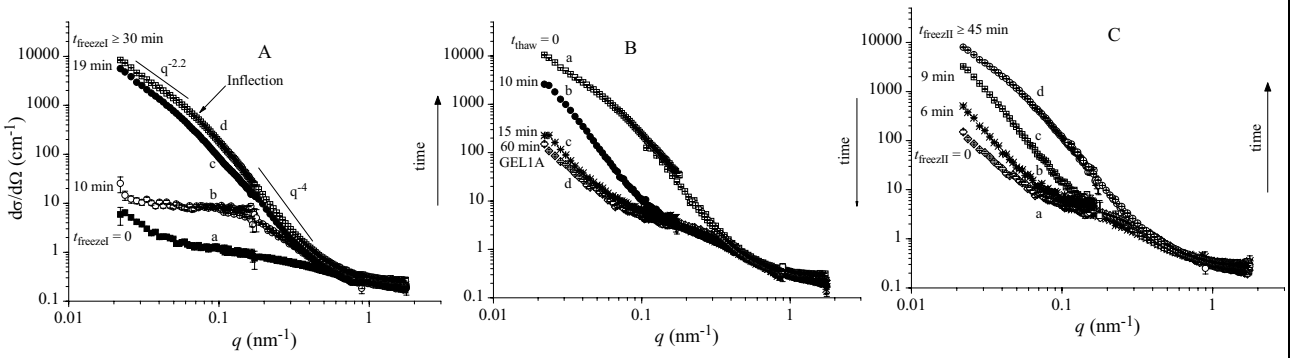


Figure 1. SANS curves from the solution with volume fraction of PVA equal to 0.086 during three consecutive steps made up of a first freezing at -13°C (A), thawing at 20°C (B), and II freezing at -13°C (C). The elapsed time (min) after each quenching is indicated.

During the freezing of the initially homogeneous solutions, the crystallization of the solvent is not complete, but an unfrozen liquid microphase having eutectic composition is also formed as indicated by curve d of Figure 1A that presents an inflection point at $q = 0.07$ nm^{-1} and two power law dependence in q in the two regions separated by the inflection point. This process is fast, and is accompanied by the confined crystallization of PVA inside the unfrozen microphase (Figure 2). Crystallization of PVA, in turn, is slowed down by vitrification.

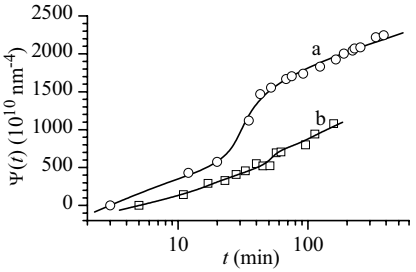


Figure 2. Crystallization of PVA in the unfrozen liquid microphase is indicated by increase of the scattering invariant ($\Psi(t)$) of PVA solutions at different concentrations evaluated from the SANS data collected in the q range 0.1 – 1 nm^{-1}. (a) Solution with volume fraction of PVA equal to 0.086; (b) Solution with volume fraction of PVA equal to 0.042.

Upon thawing (Figure 1B), ice crystals melt, obtaining a transparent gel that becomes opaque in ~200 min, due to a slow and progressive increase of the size of micro-heterogeneities (dilute and dense regions) imprinted during the fast freezing by the crystallization of water.

The present study shows conclusive evidences that the physical cross-links responsible for the formation of the microgel fraction acting as building blocks for the development of the macroscopic gel network in these systems are crystallites, that form already in the early 60 min of fast freezing. The crystallization of PVA in confined environment of eutectic composition is general, but the formation of a macroscopic gel occurs only for solutions with PVA concentration higher than a critical value, via the clustering association of the droplets of the microgel fraction. This is indicated by significant differences between the SANS curves from frozen solutions more concentrated in PVA (curves a and b of Figure 3) that form a gel upon thawing and that of a less concentrated PVA solution (curve c of Figure 3) that does not form a gel even for prolonged time at –13°C.

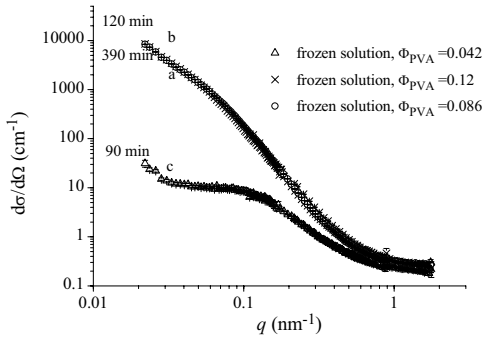


Figure 3. Comparison of the SANS curves recorded at –13 °C from the frozen solution with volume fraction of PVA equal to 0.086 at the end of I freezing (curve a, 390 min freezing) with those from frozen solutions with volume fraction of PVA equal to 0.042 and 0.12 after ≈ 90and ≈120 min freezing at this temperature, respectively (curve b and c, respectively) (B).

For solutions with PVA concentration below a critical value, indeed, the droplets of unfrozen liquid microphase remain isolated entities in the ice matrix (curve c of Figure 3).

Institut für Festkörperforschung
Forschungszentrum Jülich GmbH
D-52425 Jülich

Experimental Report
of Neutron Scattering Experiments
at the FRJ-2 Reactor

Proposal number:	KW1-05-002		
Experiment title:	Interaction of phenol with PNIPA gels		
Dates of experiment:	23-25/05/2005	Date of report:	09/01/2006
Experimental team: Names	Addresses		
E. Geissler K. László	Laboratoire de Spectrométrie Physique, Université J. Fourier de Grenoble, 38402 St Martin d'Hères cedex, France Department of Physical Chemistry, Budapest University of Technology and Economics, H-1511 Budapest, Hungary		
Local Contact:	Vitali Pipich		

Experimental report text body

SANS measurements were performed on a series of PNIPA gels swollen either in pure D_2O or in the contrast matched condition 82%H_2O/18%D_2O, with varying amounts of deuterated phenol. Three sample-detector distances were used, and in the case of the contrast matched samples, counting times at the longest distance amounted to 6 hours to ensure reasonable statistics. Figure 1 shows the results for unfunctionalized PNIPA gels. The strong signal from the gel in D_2O consists of a power law behaviour at low q together with a scaling law of the form $a/(1+(q\xi)^2)^{d/2}$, where the value of the fractal dimension was $d\approx1.6$, which is consistent with that predicted by scaling theory. If all the phenol molecules were attached to the polymer chains, then they would exhibit the same structure factor $S(q)$ as the gel in pure D_2O. On the basis of this $S(q)$ and armed with a knowledge of the relative contrast factors of PNIPA in D_2O and deuterated phenol in the contrast matched solvent, as well of their corresponding concentrations, an estimate could be made of the fraction of phenol molecules in the sample that are in contact with the polymer. For the sample containing 44 mM phenol, the result, (5±1)%, is consistent with macroscopic measurements of the uptake of phenol in this system. For the sample containing 20 mM phenol, on the other hand, the observed fraction was (0±1)%, i.e. zero within experimental error. The precision of these results is a considerable improvement on that of dynamic light scattering [1], which detected no adsorbed phenol in either case. An account of these measurements will appear in the NATO ASI series of a workshop in Kiev in November 2005 [2].

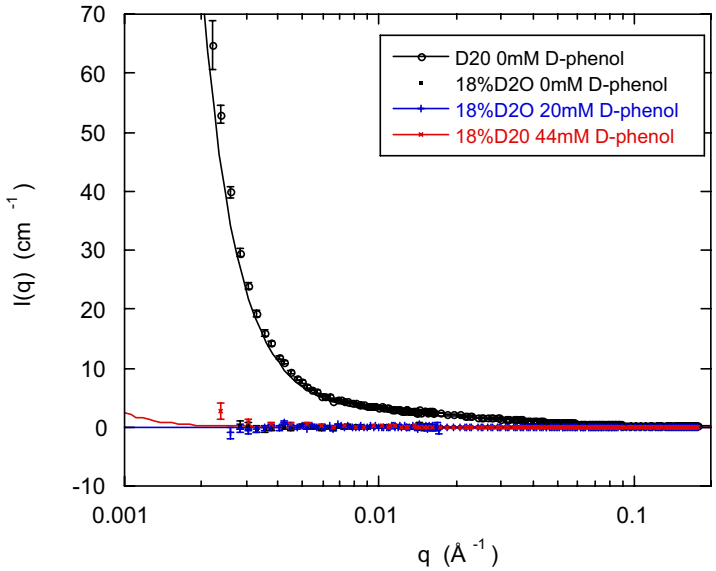


Figure 1. SANS curves from PNIPA in fully deuterated water and in contrast matches water at 18%D_2O. The continuous curves shown are proportional to the empirical fitting relation for the pure D_2O data,

$$I(q) = bq^{-3.2} + a/\left[1+\left(q\xi\right)^2\right]^{0.8}$$

where ξ=41 Å, b=2.7 10^{-7}, a=3.4 cm^{-1}.

Reference

[1] K. László, K. Kosik, C. Rochas, E. Geissler *Macromolecules* **36**, 7771-7776 (2003).
[2] K. László, K. Kosik, E. Wilk, E.Geissler:Interaction of Phenolic Pollutants with PNIPA Hydrogels, NATO ARW "Pure and Applied Surface Chemistry and Nanomaterials for Human, Life and Environmental Protection, NATO ASI Series, in press

Institut für Festkörperforschung
Forschungszentrum Jülich GmbH
D-52425 Jülich

Experimental Report of Neutron Scattering Experiments at the FRJ-2 Reactor

Proposal number:	KW1-05-006		
Experiment title:	Determination of the stability range of a microemulsion		
Dates of experiment:	17.02.05	Date of report:	09.05.05
Experimental team: Names	 Addresses		
Reiner Zorn Maria Mayorova Wim Pyckhout-Hintzen	IFF, FZ Jülich		
Local Contact:	Wim Pyckhout-Hintzen		

Experimental report text body

The droplet microemulsion to be studied here has the peculiar property that the hydrophilic and hydrophobic components undergo glass transitions well separated in their dynamics. It is thus possible to study the glass transition dynamics of propyleneglycol (PG) confined to spheres of about 5 nm. These kind of investigations have been of increasing interest during the last years. For the materials here, dielectric experiments were already done [1] and experiments using inelastic neutron scattering at ILL Grenoble and FZ Jülich are planned.

Before starting the dynamical experiments it is necessary to check whether the microemulsion preserves its structure in the temperature range where those experiments are planned. SANS data on a similar system (D_2O/AOT/decane) [2] indicate that at about room temperature an aggregation of droplets takes place (Fig. 1). This would restrict the temperature range for the dynamic experiments in the worst case making the latter unfeasible.

We therefore performed SANS on a microemulsion which – apart from the fact that we use normal AOT instead of deuterated which is too precious for this test – is identical to that to be studied by inelastic neutron scattering. The temperature range chosen was that which is spanned by the inelastic experiments in the 'worst case', i.e. –20 … +73.5°C.

The composition of the microemulsion used was h-PG: 10.2% / h-AOT: 36.1% / d-decahydronaphthalene (d-decalin): 53.7% (equivalent wt% of undeuterated compounds). To take care of the background, pure d-decalin was subtracted. Its scattering was about 1/30 of that of the microemulsion so that the resulting correction was only minor.

Fig. 1 shows SANS data from the lowest, highest, and one intermediate temperature exemplarily. It can be seen that except for a change in intensity the scattering due to thermal expansion does not change. If at all, a slight but continuous change of the droplet dimension takes place. In any case a drastic change of the scattering pattern due to aggregation (as observed in [2]) can be excluded. This means that microemulsions of this type can be used for studies of the dynamics over a wide temperature range.

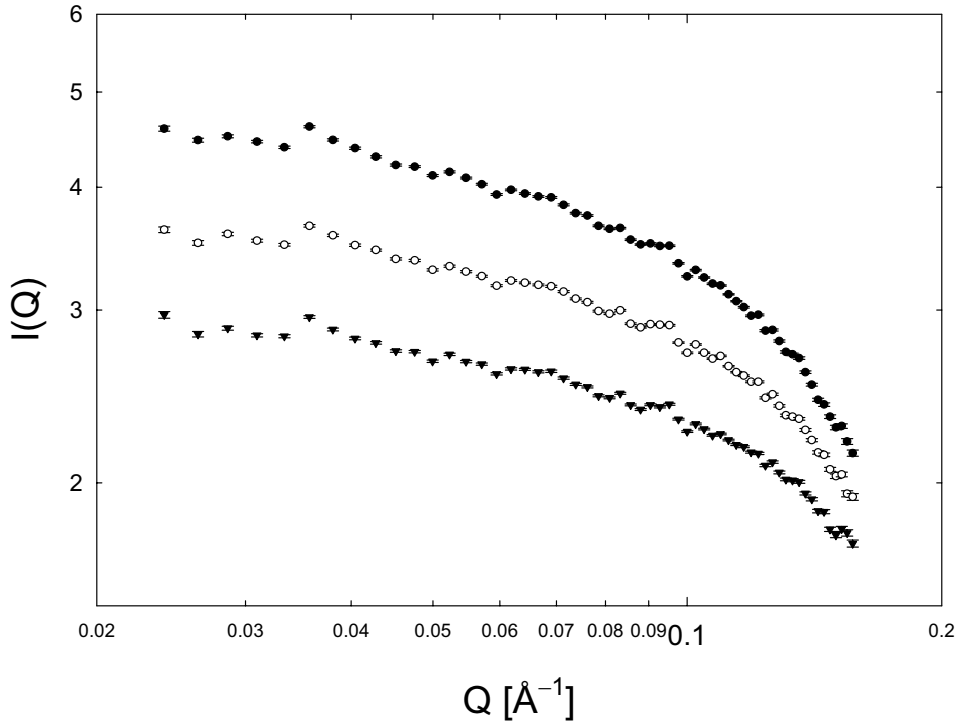


Fig.1: SANS patterns of the h-PG/h-AOT/d-decalin microemulsion for temperatures –20±1 °C, +17±1 °C, and +73.5±1 °C

The secondary objective of the experiment, the determination of the droplet size, could not be fulfilled. The naïvely calculated radius of gyration, 0.9…1.0 nm is far too small to be compatible with the estimate from the composition, 2.7 nm. The probable reason for this is that the microemulsion is rather concentrated. This means that the structure factor has to be taken into account: $I(Q)=P(Q)S(Q)$. Since $S(Q)$ increases at low Q this leads to a reduction of the slope of the Guinier plot, i.e. a reduction of the apparent R_g.

Because the calculation from composition shows that the droplet diameter is already close to the droplet distance (for the contrast here which includes the AOT shell in the "droplet") we refrain from fitting this data with a model. Rather we will propose to repeat the experiment with a contrast showing the PG core selectively.

[1] Lin-Min Wang, Fang He, R. Richert, *Phys. Rev. Lett.* **92**, 095701 (2004)
[2] L. Arleth; J. S. Pedersen, *Phys. Rev. E.* **63**, 061406 (2001)

Institut für Festkörperforschung
Forschungszentrum Jülich GmbH
D-52425 Jülich

Experimental Report
of Neutron Scattering Experiments
at the FRJ-2 Reactor

Proposal number:	KW1-05-007		
Experiment title:	Investigating the decomposition of MAO by contrast variation		
Dates of experiment:	15.06. – 16.06.2005	Date of report:	28.06.2006
Experimental team: Names	Addresses		
Aizhen, Niu Jörg, Stellbrink Jörgen, Allgaier	Institut für Festkörperforschung, Forschungszentrum Juelich Institut für Festkörperforschung, Forschungszentrum Juelich Institut für Festkörperforschung, Forschungszentrum Juelich		
Local Contact:	Pyckhout-Hintzen, Wim		

Experimental report text body

Coates et al. [1] reported a new stereoselective titanium complex for olefin polymerization. Upon treatment with methylaluminoxane (MAO), this complex was found to be active for the polymerization of propylene at 0°C in toluene. Unexpectedly the obtained polymer exhibited a narrow molecular weight distribution (M_w/M_n~1.1). The amazing point is that the first synthesis of high molar mass syndio-polypropylene-block-poly(ethylene-co-propylene) diblock copolymer (M_n= 145 100, M_w/M_n=1.12) was achieved, when a slight overpressure of ethylene was added to the reactor after formation of the living syndiotactic polypropylene. The living nature of the catalyst allows the synthesis of block copolymers previously unavailable from Ziegler-Natta catalysts. However, the kinetics and mechanism of living olefin polymerization is still poorly understood. On the basis of research experience and knowledge of living anionic polymerization of dienes and styrene, we plan to develop the combined time resolved NMR and SANS technique to the field of living olefin polymerization, discover the fundamental mechanism and kinetics of the living olefin polymerization.

Although MAO, AlCH3-O, is a well established compound in olefin polymerization, nearly nothing is known about its structure. Only from pfg-^{1}H-NMR experiments a dynamic radius of approximately 10-15Å was estimated.

In a first experiment we investigated the aggregation behaviour of the h-MAO in d-toluene by SANS. We found two species of particles contributing to the scattering intensity. The first is the primary aggregate of MAO, which forms a Gaussian chain-like structure with an approximate size of ~50Å. The second species has a characteristic size beyond the spatial resolution capability of SANS and is visible only as a power law decay, ~Q^{-4}, in the low-Q regime. Since the low-Q scattering shows a profound time-dependence, it can probably be attributed to decomposition products of the relatively instable MAO, which mainly contain

intermediate species with an atomic composition of approximately $Al_2O_{2.5}CH_3$, which finally forms amorphous Aluminiumoxide, Al_2O_3.

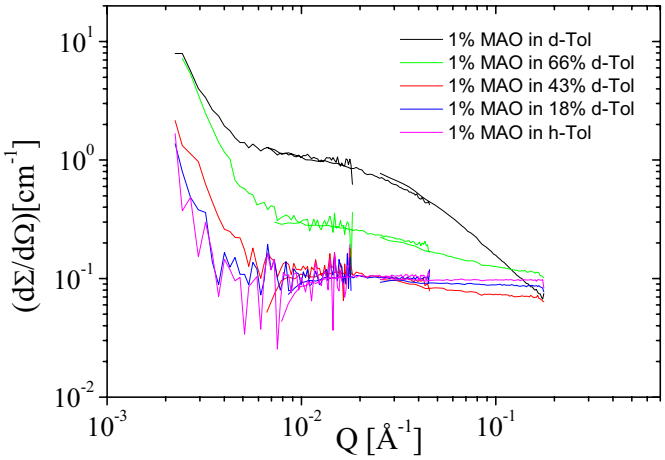


Figure 1 SANS profiles of contrasts variation of untreated 1% MAO solutions.

Now systematic investigations were performed: determine the composition of the decomposition products by contrast variation. Here 5 different were investigated for the untreated MAO, with scattering length densities adjusted to match either $Al_2O_{2.5}CH_3$, $\rho=1.79\times10^{10}cm^2 \approx 18$ vol.-% d-toluene and Al_2O_3, $\rho=4.09\times10^{10}cm^2 \approx 66$ vol.-% h-toluene, plus both full contrast and one intermediate contrast, see Fig. 1. The SANS results show that the main decomposition products are not Al_2O_3. The further data analysis and experiments on element analysis are in progress.

[1] J. Tian, P. D. Hustad, G. W. Coates, J. Am. Chem. Soc. 2001, 123, 5134.

Institut für Festkörperforschung
Forschungszentrum Jülich GmbH
D-52425 Jülich

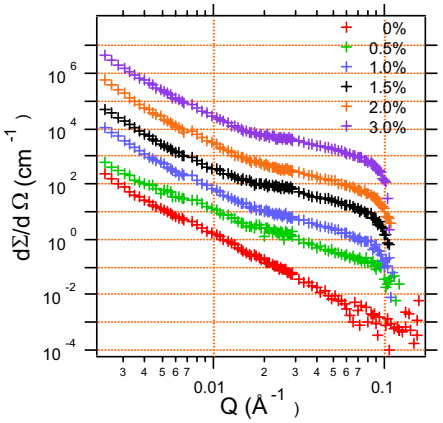
Experimental Report
of Neutron Scattering Experiments
at the FRJ-2 Reactor

Proposal number:	KW1-05-008		
Experiment title:	Small Angle Neutron Scattering on Blends of Poly (Styrene-ran-Vinyl Phenol) with Liquid Crystalline Polyurethane		
Dates of experiment:	18.04. – 22.04.2005	Date of report:	22.06.2006
Experimental team: Names	Addresses		
Mark Dadmun Rujul Mehta	Chemistry Dept., University of Tennessee, Knoxville, TN 37996 Chemistry Dept., University of Tennessee, Knoxville, TN 37996		
Local Contact:	D. Schwahn		

Experimental report text body

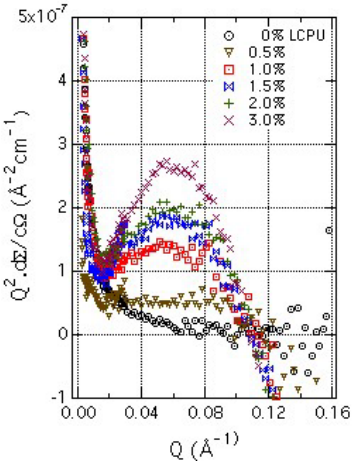
As result of our previous work [1], liquid crystalline polyurethanes (LCPU) are found to be miscible with a random copolymer of vinyl phenol (VPh) and styrene (dPS-VPh); with optimum hydrogen bonding between the -COOH groups of the LCPU and the -OH present in the styrenic matrix. Availability of a truly miscible molecular composite presents a unique opportunity of studying the conformation of polymer chains containing rigid-rods that are uniformly dispersed in a flexible coil matrix.

The LCPU (Mw 31700, PDI 1.64) and d8PS-VPh copolymer (12% VPh, M w 55700, PDI 1.42) were synthesized. Blends of LCPU and d8PS-VPh were prepared having compositions, 0.5-5%, (wt% LCPU). The SANS measurements were performed using the instrument KWS1 (Q range 0.02 to 1.6 nm-1). Scattering curves of neat copolymer and the blends show a remarkable upturn in the scattering at low Q (Fig. 1). It is evident that VPh segments (not deuterated) in the random copolymer form a large-scale dynamically cross-linked structure, facilitated by the presence of hydrogen bonding within the VPh segments. Scattering curve for neat dPS-VPh fits reasonably well to the Debye-Bueche model in the low Q (<0.26 nm-1). The correlation length of 27.3 nm obtained from this fit, represents the size of VPh aggregates that form the network.



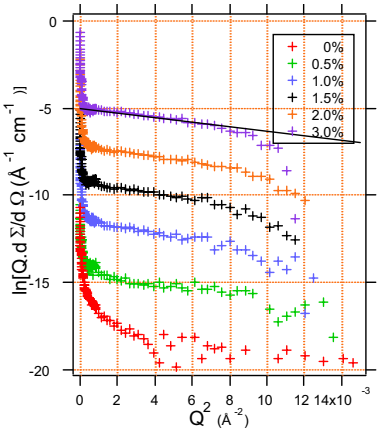
At higher Q (>0.26 nm-1), the scattering curve obeys the scattering equation given by Benoit et al [2], which describes cross-linked polymers with a characteristic negative intercept in the Zimm representation and yields the size of the vinyl phenol linkages, which form the network as 13.3 nm.

Addition of small amounts of LCPU in the scattering media resulted in a measurable change in the character of the scattering. A substantial reduction in the scattering is observed, within the low Q range (curve due to 0.5%); indicating that LCPU molecules act to disrupt the hydrogen bonded ensemble. Thus, we infer that the presence of a large scale structure in the copolymer is due to intra-species hydrogen bonding within the VPh segments of the copolymer; an arrangement that is measurably disrupted by addition of small amounts of LCPU, with a reduced correlation length of 22.5 nm.



What is interesting to observe in these curves is the additional scattering that occurs in the blends in the mid to high Q regime (>0.16 nm-1), which is clearly seen in the Kratky representation [3]. In the case of neat copolymer, scattering from copolymer chain segments that are forming the network result in a plateau approached from above. Interestingly, the scattering data from copolymer-LCP blends show a clear deviation from the plateau (Fig. 2). This additional scattering contains the information regarding the conformation of the LCP molecules.

The excess scattering not present in the data from the pure copolymer was fitted to the Kratky-Porod worm-like chain (KPWC) model. KPWC model describes scattering arising from a thin needle and is applied to systems containing rigid rods. Figure 3 shows the linear fit of the scattering data to the KPWC model providing a clear evidence of presence of rod-like structures within the blend. The cross-sectional radius of gyration obtained from this fit ranges from 26 nm to 15 nm, and serves as an indication of the cross-sectional size of the LCP rigid rods. The mid-high Q data was also fitted to a Zimm plot, providing a molecular weight of the rigid rods as 32985. This is in agreement with the Mw of the LCPU measured by GPC (31700). The length of the rigid rods obtained from KPWC fit ranged from 72.5 to 180.1 nm.



1. Macrom. Rapid Comm. 2001, 22, 779; Polymer 2000, 42, 1591; Macrom. 2002, 35, 5049; Macrom. 2003, 36, 3196
2. Macrom. 1993, 26, 579
3. Macrom. 1991, 24, 1269

Institut für Festkörperforschung
Forschungszentrum Jülich GmbH
D-52425 Jülich

Experimental Report
of Neutron Scattering Experiments
at the FRJ-2 Reactor

Proposal number:	KW1-05-009		
Experiment title:	**β-cyclodextrin in hydrophobically modified alginate solutions**		
Dates of experiment:	31.08.2005 – 05.09.2005	Date of report:	15/02/2006
Experimental team: Names	Addresses		
Céline Galant Kenneth D. Knudsen Anna-Lena Kjøniksen Bo Nyström Reidar Lund	Department of Physics, Institute for Energy Technology, P. O. Box 40, N-2027 Kjeller, Norway Department of Chemistry, University of Oslo, P. O. Box 1033, Blindern, N-0315 Oslo, Norway IFF-Neutronenstreuung, Forschungszentrum Jülich, D-52425 Jülich, Germany		
Local Contact:	W. Pyckhout-Hintzen, D. Schwahn		

Experimental report text body

We proposed to study the properties of new supramolecular structures obtained by mixing in water a hydrophobically modified biopolymer (HM-alginate) and a branched polymer of beta-cyclodextrin (poly(β-CD)). It was expected that the formation of inclusion complexes between the hydrophobic segments of HM-alginate and the β-CD cavities of poly(β-CD) results in a system with i) thickening properties because of the aggregation between both polymers, and ii) specific inclusion properties related to the presence of β-CD units available for the complexation of additional molecules (i.e. hydrophobic drugs, for example). Combination of properties i) and ii) makes the HM-alginate/poly(β-CD) system a potential candidate for biomedical applications such as controlled drug delivery.

SANS spectra from HM-alginate (1.0 wt.%)/poly(β-CD) mixtures in D_2O, have been collected with varying concentrations of poly(β-CD), at T = 25°C (Figure 1). Data collected for separated solutions of each of the polymers have also been collected and serve as reference in the process of evaluating the effect of mixing the two components.
Analysis of the SANS data shows that the clustering strength (1) of the mixtures rises with increasing poly(β-CD) concentration in the HM-alginate solution. The formation of aggregates with increasing size is characterized by an enhancement of the low q scattering as the poly(β-CD) concentration is increased. Because both components are protonated, it was not possible to use the contrast matching method. However, the scattering intensity of HM-alginate appeared very weak compared to that of poly(β-CD). Consequently, it has been assumed that the scattering from the poly(β-CD) in the mixtures is the dominating contribution to the total scattering intensity.

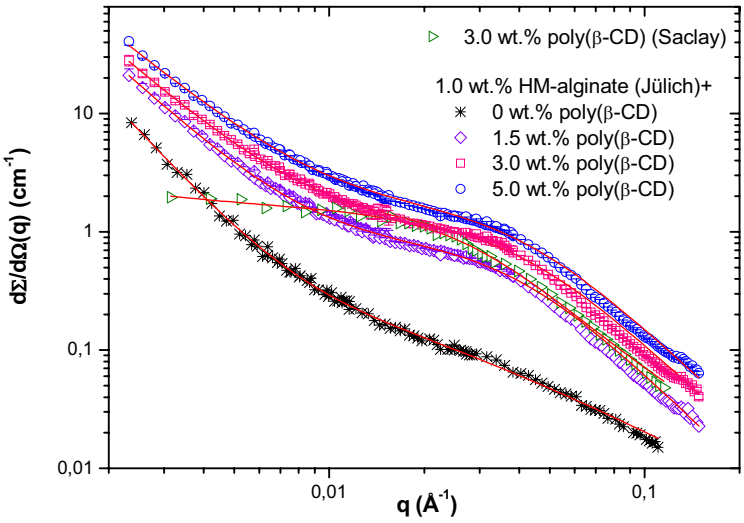


Figure 1. Influence of the poly(β-CD) concentration on SANS from HM-alginate (1.0 wt.%)/poly(β-CD) mixtures in D_2O, at T = 25°C. The green triangles (▷) refer to the scattering from a poly(β-CD) solution (3.0 wt.%) in D_2O, measured at Saclay.

Based on the power law behavior of the scattering, a picture of the clusters structure has been proposed, where the HM-alginate chain interacts with the branched and compact architecture of poly(β-CD) only at the surface of the latter via inclusion complex formation between the HM-alginate hydrophobic segments and the β-CD cavities, thus making the inner structure of the poly(β-CD) unaffected (Figure 2).

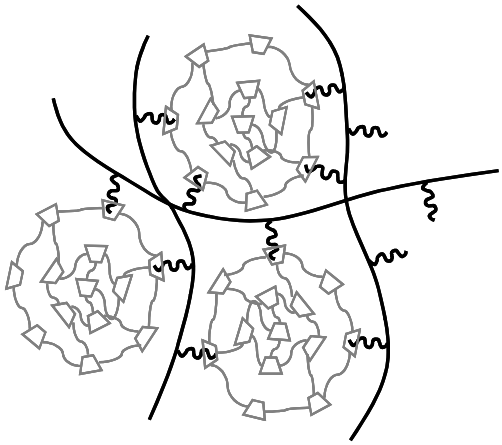


Figure 2. Scheme of the structure of a cluster resulting from inclusion interactions between the HM-alginate (represented in dark) and the poly(β-CD) chains (represented in grey).

(1) Hammouda, B.; Ho, D. L.; Kline, S. Macromolecules 2004, 37, 6932.

Institut für Festkörperforschung
Forschungszentrum Jülich GmbH
D-52425 Jülich

Experimental Report
of Neutron Scattering Experiments
at the FRJ-2 Reactor

Proposal number:	KW1-05-011		
Experiment title:	**Structural Investigation of inorganic salt nanoparticles confined in reversed micelles**		
Dates of experiment:	10-12 June 2005	Date of report:	25.03.06
Experimental team: Names	Addresses		
Prof. M.Gradzielski	Technische Universität Berlin, Stranski-Laboratorium für Physikalische Chemie und Theoretische Chemie, Sekretariat TC 7, Strasse des 17.Juni 124, D-10623 Berlin (Germany)		
Dr. Cristina Giordano	Università degli Studi di Palermo, Dipartimento di Chimica Fisica "F. Accascina" Viale delle Scienze, Parco d'Orleans II, Dipartimento di Chimica - Edificio 17 I-90128 Palermo (Italy)		
Local Contact:	Dr. W. Pyckhout-Hintzen		

Experimental report text body

The preparation and characterization of nanoparticles of inorganic salts is a highly active topic of current scientific research due to its large potential for applications [1, 2]. Among the various physical and chemical methods employed to obtain such nanoparticles, an interesting and promising route is based on the use of solutions of nearly dry reversed micelles as confining media since they easily allow both the entrapment and the stabilisation of very small nanoparticles of water-soluble salts within the hydrophilic core of reversed micelles or surfactant liquid crystals [3, 4]. The procedure allowing the preparation of such systems has been described in previous reports [5,6].

The formation of inorganic salts nanoparticles in the liquid samples was ascertained by SAXS [5, 6] and for the solid salt/surfactant composites, by WAXS and transmission electron microscopy (TEM). A typical TEM micrograph of a composite is shown in fig. 1. It can be noted that during the solvent evaporation an initial crystallization process takes place that leads to larger nanoparticles in the solid composites [5].

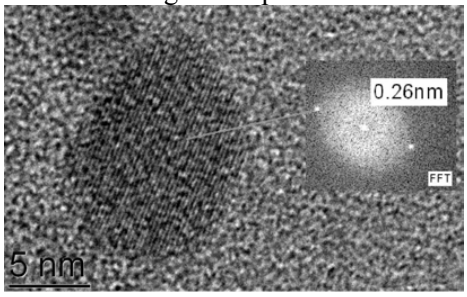


Fig. 1: TEM micrograph of a $CoCl_2$ nanoparticle in AOT matrix clearly showing the crystalline layering of 2.6 Å.

However, for a more detailed structural picture, especially for very small nanoparticles of 1-4 nm size we performed these SANS measurements. The SANS technique, by means of external contrast variation, allows for a simultaneous determination of the size of the inorganic nanoparticles in liquid phase and their surrounding surfactant shell by choosing properly the contrast of the oil phase. In particular, we have investigated various inorganic salts (Cobalt (II) chloride and Yttrium (III), Copper (II), Barium (II) and Ytterbium nitrate) entrapped within the core of AOT reversed micelles dispersed both in D-Octane and H-Octane. Results showed that the entrapment of ionic clusters involves an increase of the micelle radius which is correlated with the salt/surfactant molar ratio (R_s). For each salt investigated, indeed, experiments were performed using two R_s values in order to study the effect of this parameter on the micellar size.
Figure 2 shows SANS scattering profiles of Yb(III) nanoparticles-containing in AOT reversed micelles dispersed in an organic solvent using a contrast variation, for an independent determination of the scattering from the core and from the shell

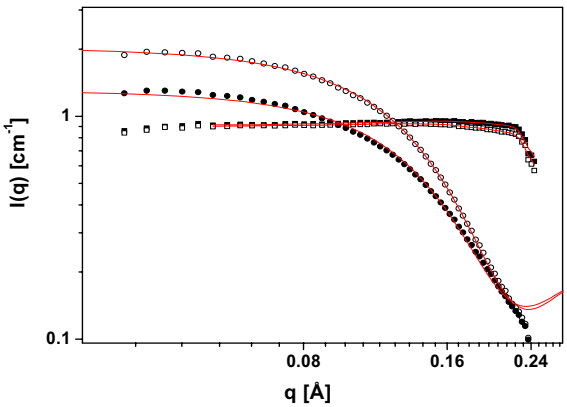


Fig 2: *SANS curves of Yb(III) nanoparticles-containing in AOT reversed micelles, at two different salt/AOT molar ratio (R_s), dispersed in D-Octane (circles) and H-Octane (squares), respectively. Yb(III)/AOT/D-Octane at R_s=0.04 (●, R: 16.3 Å) and R_s=0.085 (○, R: 17.3 Å) and Yb(III)/AOT/H-Octane at R_s=0.04 (■, R: 4.7 Å) and R_s=0.085 (□, R: 5.7 Å). It can be noted that by increasing R_s an increase of the micellar core radius is observed.*

Taking into account that the mean radius of bare AOT reversed micelles in D-hydrocarbon is around 15.0 Å [7], depending on W (the |water|/|surfactant| molar ratio), the present experimental data emphasize that salt is confined in form of very small nanoparticles (nanoparticle core radius around 5 Å). Results are in good agreement with SAXS results (R:10.8 Å, R_s=0.05 and R:11.1 Å, R_s=0.11), considering that SAXS is due to the contrast between regions with different electron densities and considering the reversed micelle structure, so that R must be interpreted as the mean radius of the hydrophilic micellar core (salt+head groups).
However, it was not yet possible to establish detailed and general relationship between R_s and R, and accordingly more detailed experiments still have to be done, in which the composition of the samples that is governed by R_s and also the type of salt contained have to be varied systematically, as also the type of salt employed appears to play a decisive role.

References

[1] Nanoparticles. From Theory to Application, G. Schmidt (Ed.), Wiley-VCH, Weinheim, 2004
[2] P. Ball, L. Garwin, *Nature*, 355, 761 (1992)
[3] J.H. Fendler, *Chem Rev* 87, 877 (1987)
[4] V. Turco Liveri, In: Rosoff M (ed) Nano-surface chemistry, vol 1. Dekker, New York, pp 473-504 (2002)
[5] C. Giordano, A. Longo, V. Turco Liveri, A.M. Venezia, *Coll. Polym. Sci.* 281, 229 (2003)
[6] C. Giordano, A. Longo, A. Ruggirello, V. Turco Liveri, A.M. Venezia, *Coll. Polym. Sci*. 283, 265 (2004)
[7] Gorski, Ostanevich, *J.l Phys.* IV 3, 149 (1993)

Institut für Festkörperforschung
Forschungszentrum Jülich GmbH
D-52425 Jülich

Experimental Report of Neutron Scattering Experiments at the FRJ-2 Reactor

Proposal number:	KW1-05-012		
Experiment title:	*In vivo* characterisation of crowding in Escherichia coli cells		
Dates of experiment:	07/06/2005	Date of report:	8/12/2005
Experimental team: Names	Addresses		
Marion Jasnin	IBS 41 rue Jules Horowitz 38027 Grenoble Cedex 1 France		
Joseph Zaccai, Kathleen Wood	ILL 6 rue Jules Horowitz BP 156 38042 Grenoble Cedex 9 France		
Local Contact:	Martine Heinrich		

Experimental report text body

E.coli is a rod-shaped bacterium of 0.8µm×2µm, surrounded by a membrane of about 300 Å thick. In a simple description, the cell is made up of three types of macromolecules: lipids, proteins and RNA, which represent 87% of the *E.coli* total dry weight. The cytoplasmic membrane consists in a lipid bilayer with membrane proteins (60% w/w). Inside the cell, RNA is mainly localised inside ribosomes, large macromolecular machines that contain both proteins (40%) and RNA (60%) and represent 25% of the macromolecular dry weight. The cell cytoplasm also contains cytoplasmic proteins. In the present work, we used small angle scattering and the solvent contrast variation technique on whole *E.coli*, to match successively lipids, proteins and RNA, and investigate the molecular crowding *in vivo*. Lipids are matched out at 11% D_2O, proteins at 41% D_2O and RNA at 68% D_2O. Membrane is also matched out at 20% D_2O and ribosomes at 56% D_2O.

Two types of sample were examined on KWS-1: high concentrated cell sample (*E.coli* paste) and diluted *E.coli* (10 mg/ml cell paste, dilution 1:20). For each of these two samples, cells were observed in buffer containing 0, 12, 22, 41, 54, 68, 80 and 100% D_2O. SANS experiments were performed with a wavelength of 7 Å at KWS-1. Three sample-to-detector distances (2, 8 and 20 m) were employed to cover a Q-range of 0.002-0.2 $Å^{-1}$. 2-D data were corrected pixel wise for instrumental background and detector efficiency, and radial averaged over the full detector. In parallel, two solvent conditions (0 and 100% D_2O) for paste samples were examined on KWS-3, to acquire a wide range of scattering vector for extreme solvent conditions (from 10^{-4} to 10^{-3} $Å^{-1}$ on KWS-3 and from 10^{-3} to 10^{-1} $Å^{-1}$ on KWS-1).

The experiments revealed an anisotropic distribution of the intensity for the paste samples, which became isotropic after dilution. Another important feature, already observed during the precedent experiment, is the presence of a main peak around Q equals 0.02$Å^{-1}$ for both types of sample. We reported in Fig 1.a the Q-dependence of the scattering cross-sections for the paste samples, radial averaged over the full detector that gives an acceptable approximation for the anisotropic spectra. The anisotropy for the intensity results in a shifting in Q of the peak position, depending on the sample. Since the anisotropy disappears after dilution, we attributed the anisotropy to the cell paste preparation, in particular to the ordered stacking of the bacteria during centrifugation.

The peak reveals the presence of a structure which repeats itself inside the sample. We previously thought about the periodical stacking of planar objects, separated by about 330 Å, as given by the Q-value of the peak. (The real position of the peak is given by the diluted curves. Only the scattering intensity of the 100% D_2O diluted sample was sufficiently high to reveal a clear peak, at Q equals 0.019 $Å^{-1}$ (Fig.1.b)).

This hypothesis was checked by the contrast variation technique. The contribution of the different component inside the cell was extracted, using their various compensation points. We looked at the influence of the contrast on the peak intensity (without taking into account the precise position of the peak). Fig. 2 represents the intensities at each contrast and Fig. 3 the corresponding Guinier plots, both between Q equals 0.01 and 0.05 $Å^{-1}$ that corresponds to the Q-range of macromolecules. It reveals a very large peak at high contrasts: 68% D_2O (match point of the RNA), 80% and 100% D_2O. At 41% D_2O, compensation point of the proteins, the peak becomes smaller and it disappears at 22% D_2O (match point of the membrane) and 12% D_2O (match point of the lipids). At 0% D_2O, a small peak appears. All the scattering curves confirm that the peak arises from the membrane. Membrane is made up of lipids (40% w/w) and proteins. Obviously, the peak is matched out when membrane and lipids are matched out. At 41%, the peak is not as intense as at high contrasts (such as 68%) where the contribution due to the lipids and proteins dominates, which is in good agreement with the matching of membrane proteins.

Moreover, a radius of gyration was extracted from the Guinier plot at 22% D_2O and found to be 65 Å, which corresponds to the radius of gyration of the ribosome, only visible when the membrane is matched out.

Moreover, it becomes clear that the anisotropy distribution for the paste sample intensity must be due to the ordered stacking of the membrane during centrifugation.

This experiment is of fundamental importance because it put into light that it is possible to isolate the contribution of different part of the cell under molecular crowding conditions. Non dynamical mapping of the cell is possible *in vivo,* using the contrast variation technique. It opens the way to new amazing experiments that could enrich in a very unique way the knowledge about whole cell.

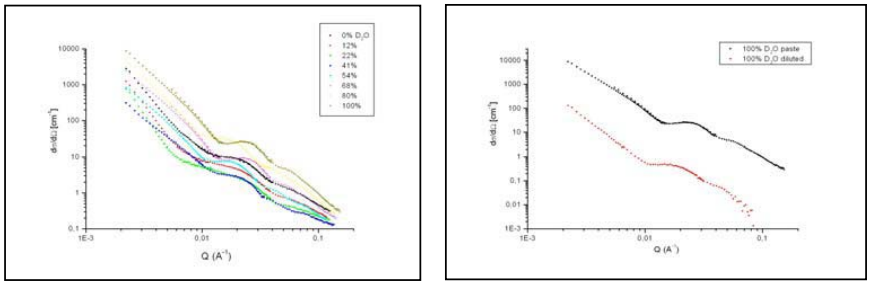


Fig1.a Q-dependence of the scattering cross-sections for the paste samples, radial averaged over the full detector. 1b. 100% D_2O paste and diluted samples.

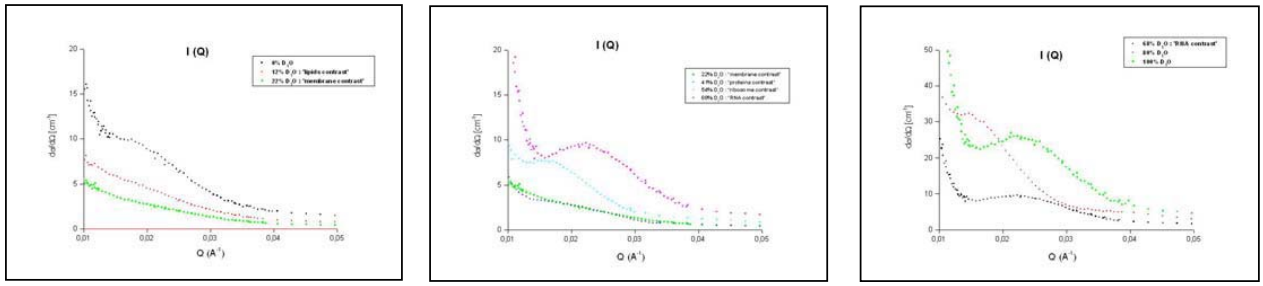


Fig2. Q-dependence of the scattering cross-sections for the paste samples (linear scale)

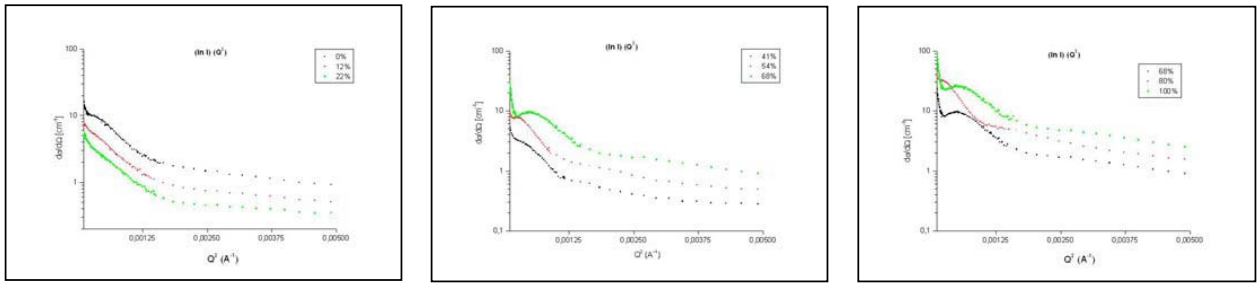


Fig3. Guinier plots for the paste samples.

Institut für Festkörperforschung
Forschungszentrum Jülich GmbH
D-52425 Jülich

Experimental Report
of Neutron Scattering Experiments
at the FRJ-2 Reactor

Proposal number:	KW1-05-014		
Experiment title:	Micellar properties of PB-PS-PB triblock copolymers in alkanes: Kinetics of chain exchange.		
Dates of experiment:	22.04. – 25.04.2005	Date of report:	14.6.2006
Experimental team: Names	Addresses		
Reidar Lund Lutz Willner Hermis Iatrou	Institut für Festkörperforschung, Forschungszentrum Jülich Institut für Festkörperforschung, Forschungszentrum Jülich University of Athens		
Local Contact:	Wim Pyckhout-Hintzen		

Experimental report text body

Recently, we have studied the equilibrium chain exchange kinetics in diblock copolymer micelles by time resolved small angle neutron scattering (TR-SANS). The principles of this novel technique have already been published /1/. Three structurally different systems have been investigated: i) a starlike micelle prepared from an asymmetric poly(ethylene-*alt*-propylene) – poly(ethylene oxide) (PEP-PEO) diblock copolymer in water/dimethylform - amide (DMF) as selective solvent mixture for PEO, ii) a compact micelle obtained from a symmetric polystyrene-polybutadiene (PS-PB) diblock in DMF as selective solvent for PS, and iii) the inverted analogue formed by the same PS-PB diblock in n-alkanes (C_{10} – C_{16}) which are all selective for PB. The latter micelles contain 35 - 50% solvent in the core. The observed exchange kinetics in each of these micellar structures reveals as a general characteristic behaviour a very broad distribution of relaxation rates which in fact follows a logarithmic time decay. This clearly deviates from a single exponential predicted by the theory of Halperin and Alexander /2/. This theory describes the exchange by a simple insertion/expulsion mechanism of single unimers based on the classical Aniansson and Wall mechanism derived for low molecular surfactant micelles.
The observed logarithmic time dependence can neither be explained by the polydispersity of the block copolymers and/or by different micellar sizes nor by parallel existing exchange scenarios like fusion and fission or isotope effects. Instead the observed time dependence is associated with “hierarchical constrained dynamics”, i.e. dynamics which involves a sequence of correlated processes characterized with an increasing characteristic time. We have attributed these processes to strong coupling of the chain dynamics induced by the confinement and topological interactions in the core /3,4/.
In the present study we have investigated the effect of polymer chain architecture on the exchange kinetics. A change in polymer architecture drastically changes the topological situation inside the micellar core. Therefore this experiment will elucidate the role of chain topology and core dynamics on the expulsion kinetics in

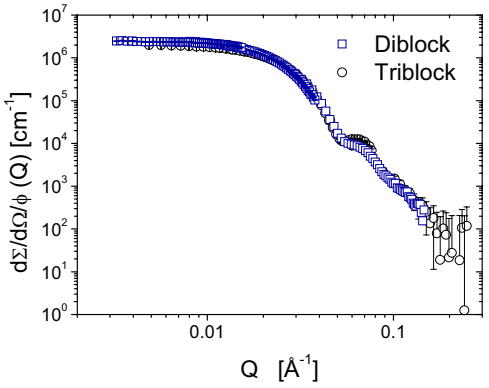
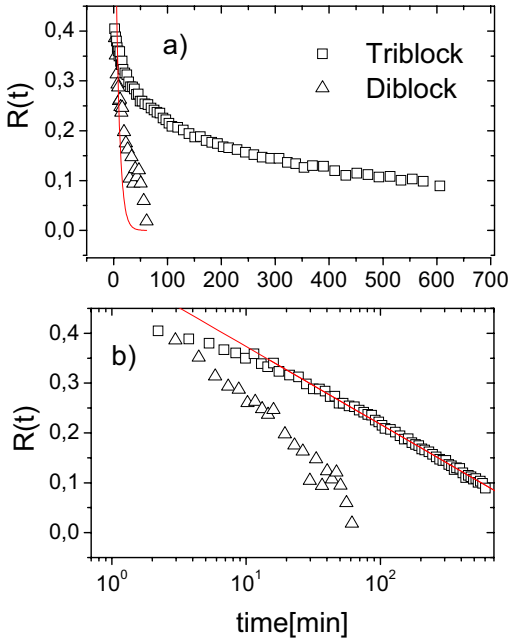


Figure 1 Core contrast measurements of d-PB10-h-PS10 diblock and d-PB10-h-PS20-d-PB10 triblock copolymers in hexadecane revealing identical PS-core size.



polymeric micelles. As a model system we have chosen PB-PS-PB triblock copolymer micelles in n-alkanes as selective solvents. An ideal comparison is possible in case both polymers form micelles with the same core size. This can be expected from double diblocks: $(PB10\text{-}PS10)_2$ = PB10-PS20-PB10.

Three triblock copolymers have been prepared for the present study: h-PB10-h-PS20-h-PB10, d-PB10-d-PS20-d-PB10 and d-PB10-h-PS20-d-PB10 with almost identical polymer characteristics. The partly labelled triblock copolymer, d-PB10-h-PS20-d-PB10, has been used to determine the structural details of the micelles by SANS/contrast variation experiments. An example is shown in Figure 1 which shows the core contrast measurements of the d-PB10-h-PS20-d-PB10 in comparison with the diblock analogue in hexadecane. These results show that the micelles have exactly the same structural characteristics since both curves lie on top of each other. In particular the amount of solvent in the core is seen to be identical. Thus the kinetics of the two micelles can be directly compared and a direct study of the influence of chain architecture can be made.

The two fully labeled triblock copolymers have been used for the TR-SANS study. Figure 2a) shows the corresponding relaxation curve in comparison with the one of the diblock. We have chosen a situation where the micelles contain a large amount of solvent, approximately 45%, therefore geometrical correlations in the core should disappear. This is observed for the diblock copolymer which gives a Halperin-Alexander like single exponential indicating that no chain correlations are present.

On the other hand compared to the diblock the kinetics of the triblock is drastically slower and again approaches the log time dependence for longer times as shown in Fig. 2b. Hence the topological constraints in the triblock are significantly affecting the kinetics and gives rise to a similar coupling between the chains as observed for the diblocks

Figure 2a) Relaxation curves of the PS-PB diblock and triblock copolymers in dodecane. Solid line indicates a single exponential predicted by theory. b) lin-log representation of the same data. Solid line reflects the log time dependence.

with more dense cores. We explain this by increased chain correlations in the core due to “knots” present in the triblock copolymer system. This directly confirms the importance of chain topological interactions on the exchange kinetics in polymeric micelles. We plan to model this in more detail in the future.

/1/ Willner, L.; Poppe, A.; Allgaier, J.; Monkenbusch, M.; Richter, D. *Europhys. Lett.* 55 (2001), 667.
/2/ Halperin, A.; Alexander, S. *Macromolecules* 22 (1989), 2403.
/3/ Lund, R.; Willner, L.; Stellbrink, J.; Richter, D. *Phys. Rev. Lett* **96**, 068302 (2006).
/4/ Lund, R.; Willner, L.; Richter, D.; Dormidontova, E.E. *Macromolecules* accepted.

Institut für Festkörperforschung
Forschungszentrum Jülich GmbH
D-52425 Jülich

Experimental Report of Neutron Scattering Experiments at the FRJ-2 Reactor

Proposal number:	KW1-05-017		
Experiment title:	Nanoparticles of calcium phosphate, functionalised with DNA		
Dates of experiment:	14.04.2006	Date of report:	17.05.2006
Experimental team: Names	Addresses		
Viktoriya Sokolova Oleg Prymak Matthias Epple	Institut für Anorganische Chemie Universität Duisburg-Essen Universitätsstraße 5-7 D-45117 Essen, Germany		
Vitaliy Pipich Dietmar Schwahn	Institut für Festkörperforschung Forschungszentrum Jülich D-52425 Jülich / Germany		
Local Contact:	Vitaliy Pipich		

Experimental report text body

In principle, a shell structure of a DNA/mineral complex can be proven with SANS by using the contrast matching technique. However, this technique only works when mineral and DNA have different scattering length densities. The scattering length density of crystalline calcium phosphate can be calculated (ρ=4.4x10^{10}cm^{-2}), whereas ρ for DNA has to determined experimentally. So, we first carried out measurements on five 7.5mg/ml DNA aqueous solutions of varying light and heavy water content; the scattering profiles are shown in Figure 1. In Figure 2 the square root of the scattering intensities at the peak maximum are plotted as function of the D_2O content. The intersection of the red and black (dashed) lines give the matching

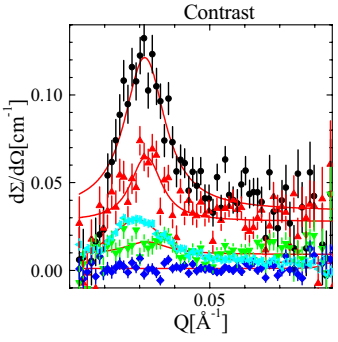


Figure 1. Scattering profiles from DNA in D_2O/H_2O mixtures

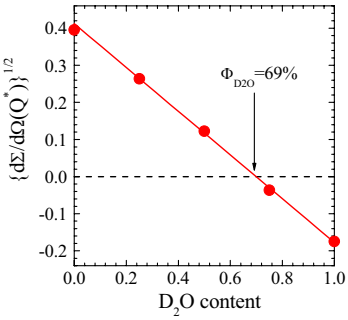


Figure 2. Scattering Contrast: DNA

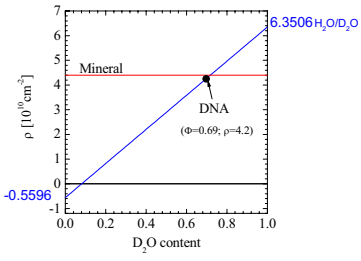


Figure 3. Matching points of DNA and calcium phosphate in D2O/H2O mixture

concentration of D_2O, namely Φ_{D2O}=0.69 giving ρ=4.23x10^{10}cm^{-2}. In Figure 3 the black circle corresponds to the matched scattering length density of DNA in H_2O/D_2O. The matching point of the mineral is defined by the intersection of the blue and red lines. We concluded from these measurements that the scattering length density of both components is very similar which does not allow a distinction of both components. Therefore we investigated DNA/mineral complex only in D_2O solution.

The DNA/mineral complexes were prepared as follow: (1C) 0.5ml of freshly mineralised calcium phosphate (0.0X M) was mixed with 0.5ml of 1mg/ml heavy water solution of DNA, stabilizing mineral growth by localization at the surface; (2C) two-shell particles were expected by addition of 0.5ml freshly mineralised calcium phosphate to 1ml of 1C-solution; (3C) 2C + 0.5ml of DNA mixture; (4C) 3C + 0.5ml of calcium phosphate mixture.

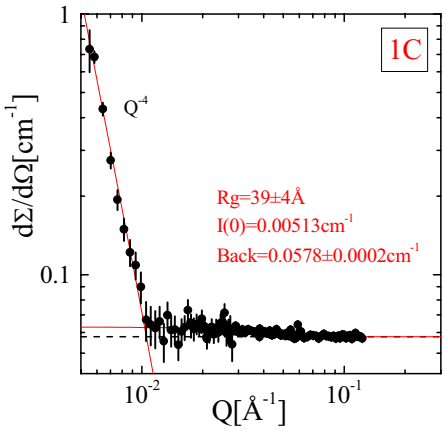


Fig. 4 Scattering curve for 1C-sample

In Figure 4 a representative scattering curve is depicted. As the mineral/DNA complex are larger than 2000Å only the Q^{-4} tail of the form-factor is detected within the available Q-range. Scattering of unbound DNA can be easily separated in the Q-range above 10^{-2}Å^{-1}. So, the scattering signal $d\Sigma/d\Omega(Q)$ was fitted assuming an incoherent superposition of the signals from the mineral/DNA complex, unbound DNA and background according to

$$d\Sigma/d\Omega(Q) = P_4/Q^4 + I(0)\exp(-R_g^2Q^2/3) + I_{BACK} \qquad (1)$$

The amplitude P_4 is proportional to the total surface of the mineral/DNA complex; I(0) the prefactor of the Guinier law and proportional to the concentration of unbound DNA; R_g the radius of gyration of unbound DNA; I_{BACK} the background scattering of D_2O.

Assuming a constant number of the mineral/DNA particles, the normalized scaling amplitude P_4 should continuously increase for the 1C to 4C samples. But from the experiment a continuous decrease is obtained (Figure 5). This means aggregation of the DNA/mineral complexes.

In Figure 6 the "step" dependence of the radius gyration of unbound chains calculated from high-Q range; the average value is R_g=34Å. In Figure 7 the "step" dependence of the forward scattering normalized to the volume of added DNA-mixture shows a dramatically decrease of the relative unbound chain number after the second step.

In conclusion, the growth of shells following the step-by-step addition DNA and mineral appears not the right model for the present samples. The DNA/mineral complexes showed a strong tendency of aggregation.

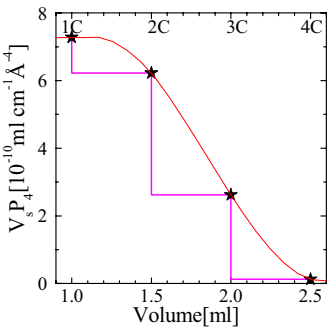


Figure 5 Surface of particles

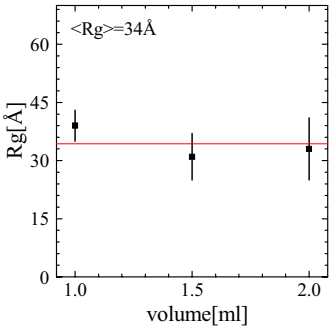


Fig. 6 Scattering from unbound DNA: Rg

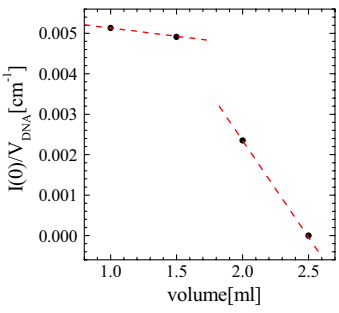


Fig.7. Scattering from unbound DNA:I(0)

Institut für Festkörperforschung
Forschungszentrum Jülich GmbH
D-52425 Jülich

Experimental Report
of Neutron Scattering Experiments
at the FRJ-2 Reactor

Proposal number:	KW1-05-018		
Experiment title:	Scattering length density of h-PEO and d/h-PEO in H2O/D2O mixtures		
Dates of experiment:	21.-23. Feb. 2005	Date of report:	31. May 2006
Experimental team: Names	Addresses		
G. Rother[1] J. Stellbrink D. Richter	Institut fuer Neutronenstreuung, Institut fuer Festkoerperforschung, Forschungszentrum Juelich, D-52425 Juelich		
Local Contact:	D. Schwahn		

Experimental report text body

The experiment aimed to study the scattering length density of poly- ethylene oxide in different mixtures of H2O and D2O. This experiment was stimulated by unexplained results for the small angle neutron scattering from PEP-PEO micelles. During the analysis it turned out that the description of the scattering data is not possible by using the nominal values of the scattering length densities of PEP and PEO. One possible explanation for this discrepancy is the preferential adsorption of one species from H2O/D2O mixtures to the PEO, which would virtually change the scattering length density of PEO. For that reason we preformed a contrast-variation experiment with h-PEO homopolymer dissolved in different mixtures of H2O and D2O. The data indicate some isotope effect. The results are still being examined.

Institut für Festkörperforschung
Forschungszentrum Jülich GmbH
D-52425 Jülich

Experimental Report
of Neutron Scattering Experiments
at the FRJ-2 Reactor

Proposal number:	KW1-05-019		
Experiment title:	Form factor of silica aggregates in reinforced latex films		
Dates of experiment:	14.05. – 16.05.2005	Date of report:	23. 05. 2006
Experimental team: Names	Addresses		
Wim Pyckhout-Hintzen Julian Oberdisse	Institut für Festkörperforschung, Forschungszentrum Jülich GmbH LCVN, Université Montpellier II, 34095 Montpellier Cedex, France		
Local Contact:	Wim Pyckhout-Hintzen		

Experimental report text body

ABSTRACT:

Elastomers filled with hard and small particles are of great importance to the rubber industry. A former SANS study of our model systems, colloidal silica in PMMA/PBuA latexes, has dealt with the structure determination at fairly high volume fractions of filler. Therefore, modelling was somewhat hampered by the unknown shape of aggregates in the samples. This proposal aims primarily at the form factor of dilute silica aggregates in latex films to allow the higher concentration samples to be analyzed completely. We also planned to do a preparatory experiment, where we wanted to look at the deformation of the aggregates under uniaxial strain ($\lambda = L/L_o = 1.5$, 2., 2.5, 3. …), but this could not be done due to lack of time and problems with the sample stretching.

CONTEXT:

In the past, we have investigated the structure and the rheological properties of silica aggregates embedded in a polymeric matrix made by coalescence and fusion of latex nanoparticles. Concerning the silica structure, the main findings are [1-4]:

(i) A strongly pH (between 4 and 10, before solvent evaporation) and weakly silica concentration (between 3% and 15%v) dependent aggregation, higher pH yielding smaller aggregates (N_{agg} between a few beads and several thousand).

(ii) A strong interaction peak between aggregates making the disentanglement of inter-aggregate structure and aggregate shape difficult.

The **aim of the present proposal** was to measure a first set of new samples at much lower silica concentration (between 0.5 and 2.5%v).

PRELIMINARY RESULTS:

In Figure 1a, the scattered intensity of a series of samples (fixed solution pH 7.5, varying silica volume fraction Φ in final nanocomposite) is shown in a I(q)/Φ presentation. The data overlaps nicely in the intermediate and large-q range. The overlap at high q means of course that the primary particle is the same. In the intermediate q-range, the overlap corresponds to an identical intra-aggregate organization. In this specific case, a power law $I(q) \propto q^{-2.7}$ reproduces the intermediate scattering quite nicely (this is also shown in Figure 1b). At small angles, a systematic deviation is observed: higher concentrations give lower reduced intensity. This means that the average aggregation number is lower at higher concentrations.

A similar evolution is observed at pH 7, where three more samples were measured at approximately identical silica volume fractions. In Figure 1b, we compare one of these intensities to the scattering of the individual bead, the form factor of which was measured at low concentration in heavy water. The high-q scattering was adjusted manually. The difference in small angle scattering gives the average aggregation number of the aggregates, approximately 100 in this case. The results for all samples are given in the tables below. It is found as expected that the aggregation number is higher at lower pH. More surprisingly, it depends rather strongly on the volume fraction. Additional experiments will be needed to see if this behaviour is reproducible.

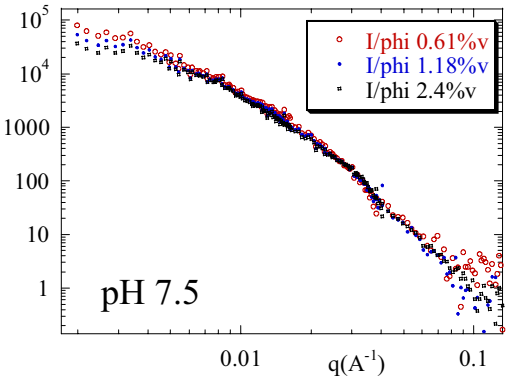


Figure 1a

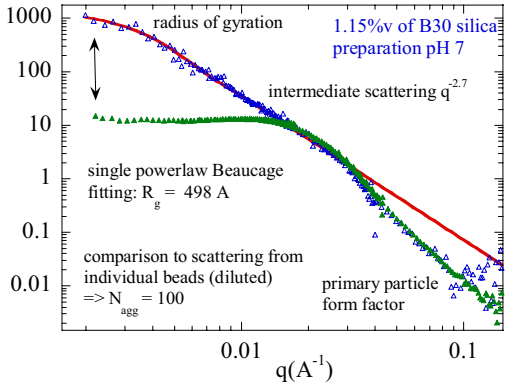


Figure 1b

A simple analysis of the data can be done in terms of a simple fractal law relating aggregate size and aggregation number: $N_{agg} = (R/a)^d$. Here R is the measured radius of gyration, a the primary particle radius, and d the fractal dimension (d = 2.7). The results are compared to the data in the tables below, assuming a = 92 Å. This number was chosen as an illustration because it reproduced nicely the behaviour for pH 7.5. In any event, it is of the right order of magnitude, the R_g of particles being approximately 100 Å. More elaborate analyses using Reverse Monte Carlo methods are currently undertaken.

Φ (pH 7.5)	R_g (Å)	I_o (cm^{-1})	N_{agg}	N_{agg}(mod.)
0.61%	485	588	90	90
1.18%	420	701	60	60
2.4%	348	930	36	36

Φ (pH 7)	R_g (Å)	I_o (cm^{-1})	N_{agg}	N_{agg} (mod.)
0.58%	564	1166	180	134
1.15%	498	1434	100	95
2.3%	458	2353	91	76

REFERENCES:

[1] Structure of Latex-Silica Nanocomposite Films: A Small Angle Neutron Scattering Study, J. Oberdisse, B. Demé, *Macromolecules*, **35**, 4397-4405, 2002

[2] Structure and Rheological Properties of Latex-Silica Nanocomposite Films: Stress-Strain Isotherms, J. Oberdisse, *Macromolecules* 2002, **35**, 9441-9450

[3] Structure and rheological properties of soft-hard nanocomposites: Influence of aggregation and interfacial modification, J. Oberdisse, A. El Harrak, G. Carrot, J. Jestin, F. Boué, *Polymer*, 2005**, 46**, 6695-6705

[4] Aggregation of colloidal nanoparticles in polymer matrices, J. Oberdisse, *Soft Matter* 2006, **2**, 29-36

Institut für Festkörperforschung
Forschungszentrum Jülich GmbH
D-52425 Jülich

Experimental Report
of Neutron Scattering Experiments
at the FRJ-2 Reactor

Proposal number:	KW1-05-020		
Experiment title:	Characterization of polyhexadiene polymers from living olefin polymerization		
Dates of experiment:	2005-05-16,17,18	Date of report:	2006-05-31
Experimental team: Names	Addresses		
Aizhen, Niu Jörg, Stellbrink Jörgen, Allgaier	Institut für Festkörperforschung, Forschungszentrum Juelich Institut für Festkörperforschung, Forschungszentrum Juelich Institut für Festkörperforschung, Forschungszentrum Juelich		
Local Contact:	Pyckhout-Hintzen, Wim		

Experimental report text body

Polymeric materials are currently more indispensable to modern society than at any other point in history. Polyolefins are by far the most important commercial class of synthetic polymers. Several ground-breaking reports have appeared in the recent literature concerning living olefin polymerization. The importance of these living olefin polymerization catalysts is laegely proportional to their ability to form block copolymers with high glass or melting transition blocks from common commercial monomers such as ethylene and propylene, as these materials have applications as compatibilizers and elastomers. In the last 5 years, there was a renaissance in living olefin polymerization, building rapidly on the foundation set solidly by Doi and coworkers over two decades ago. However, the kinetics and mechanism of living olefin polymerization is still poorly understood and there is no any scattering work has been done on this field. Coates et al. reported a new stereoselective titanium complex for olefin polymerization. Upon treatment with methylaluminoxane (MAO), this complex was found to be active for the polymerization of propylene at 0°C in toluene. Unexpectedly the obtained polymer exhibited a narrow molecular weight distribution (M_w/M_n~1.1). The amazing point is that the first synthesis of high molar mass syndio-polypropylene-block-poly(ethylene-co-propylene) diblock copolymer (M_n= 145 100, M_w/M_n=1.12) was achieved, when a slight overpressure of ethylene was added to the reactor after formation of the living syndiotactic polypropylene. The living nature of the catalyst allows the synthesis of block copolymers previously unavailable from Ziegler-Natta catalysts. On the basis of research experience and knowledge of living anionic polymerization of dienes and styrene, we plan to develop the combined time resolved NMR and SANS technique to the field of living olefin polymerization, discover the fundamental mechanism and kinetics of the living olefin polymerization.

In order to study the real living olefin polymerisation system efficiently, the investigations of activator-MAO, catalyst, mixture of MAO/catalyst and polymers solutions should be done in advance to get significant knowledge on the living olefin polymerisation system. Nice beam-time supports were offered for the MAO, Catalyst and mixture of MAO/catalyst characterization from KWS1 and KWS2.

Now a set of 4 polyhexadiene polymers with M_w of 10K-100K were prepared by Coates' group in Cornell University. The characterization of these polymers has been done in 4 concentrations for each polymer.

Institut für Festkörperforschung
Forschungszentrum Jülich GmbH
D-52425 Jülich

Experimental Report of Neutron Scattering Experiments at the FRJ-2 Reactor

Proposal number:	KW1-05-021, KW1-05-043, KW1-05-038		
Experiment title:	Biomineralization in the presence of the protein Ovalbumin: Freezing stop technique - contrast variation.		
Dates of experiment:	13.05. – 14.05.2006 04.10. – 07.10.2006 22.08. – 24.08.2006	Date of report:	31.05.2006
Experimental team: Names	Addresses		
V. Pipich D. Schwahn	Institut für Festkörperforschung Forschungszentrum Jülich D-52425 Jülich Germany		
Local Contact:	V. Pipich		

Experimental report text body

Controlled formation of nanostructures with predicted properties is a global aim of biomineralization. The initial stage of mineralization is a crucial period in the formation of minerals as to large extend it determines the morphology of the final nanoparticles. Therefore, monitoring the early stages is an important topic. Small angle neutron scattering technique is a powerful tool for in vitro controlling the size and morphology of the growth of particles in the mineralization process. However, it is a rather slow technique as the accumulation time usually needs minutes whereas the crucial time of the initial time of mineralization are usually seconds or even less.

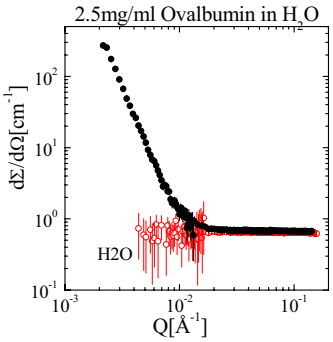


Fig.1. Scattering curves: ice and protein/ ice complex

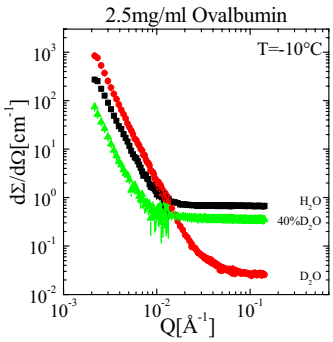


Fig.2. Scattering curves of protein/ice complex in: H_2O, D_2O and 40% D_2O.

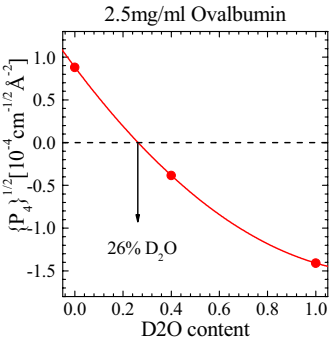


Fig.3. $\{P_4\}^{1/2}$ versus D_2O content.

Therefore, we tried to slow down the process of mineralization in two ways: (a) by freezing the sample in liquid nitrogen at the different stages; (b) by increase the viscosity of the solvent.

In Figure 1 the scattering profiles after quenching pure water (red circles) and 2.5 mg/ml protein Ovalbumin in water (black circles) in liquid nitrogen were measured at –10°C. The scattering signal from pure water contains only constant background, whereas the protein solution contains a signal from individual chains at high Q-range and scattering from aggregated proteins within the low Q-range. In order to check the reason for low Q-range scattering we carried out additional measurements with the proteins in D_2O and D_2O/H_2O mixtures. In Figure 2 the scattering curves of 2.5mg/ml protein Ovalbumin in H_2O, D_2O and 40% D_2O/ H_2O mixture are collected. Even though the 40% D_2O content represents the matching condition for proteins the strong scattering signal is still present. The scattering signal follows Q^{-4} power law with the amplitude P_4. In Figure 3 the square root of P_4 as function of D_2O content shows the matching point of the aggregate at 26%. Aggregation of proteins at freezing in liquid nitrogen induces inhomogeneous crystallization of water or formation of amorphous ice within the protein aggregates. Therefore, it is difficult to follow the mineralization process by freezing technique.

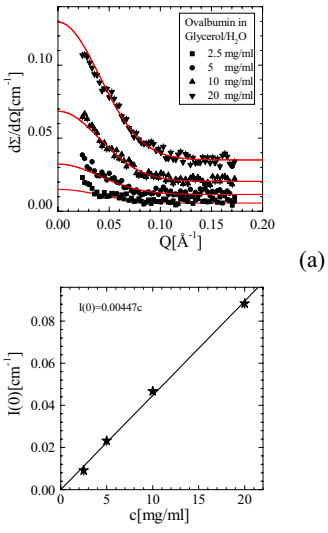


Fig.4. (a) Scattering curves: 2.5, 5, 10 and 20 mg/ml Ovalbumin in 67% glycerol mixture; (b) forward intensity of corresponding scattering curves.

The second method of slowing down mineralization is the increase of the solvent viscosity. A glycerol/water mixture was selected as the biomineralization media. The crystallization temperature of pure glycerol(G) and water(W) is 20°C and 0°C, respectively, but their mixture with 67% glycerol content has a freezing temperature of –60°C. Therefore, by the variation of glycerol content we can vary the viscosity of the media over a broad range. Another advantage of this mixture is its widespread use as an agent for keeping of biomaterials in refrigerator.

In a first step we measured the conformation of the protein Ovalbumin in G/W mixture with 67% glycerol content. The scattering profiles of several concentrations of the proteins are presented in Fig.4(a). The simultaneous fit of SANS data by is Guinier law is shown by red lines. The radius of gyration is obtained Rg=30±0.5Å. The forward scattering as function of the protein content shows linear dependence as demonstrated in Fig.4(b).

The mineralization reaction was carried out in G/W mixture with 67% glycerol content and neutral pH=7. Solutions of 0.1M calcium chloride and sodium carbonated were mixed directly in the Helma-cell, and then the scattering signal was measured at 20m sample-to-detector position every 10 minutes, during 12 hours. In Figure 5(a) the typical scattering curve from samples with and without protein. Within the measured Q-range the scattering curves follow a power law with the fractal exponent of 2.6 in both cases. Such kind of fractal dimension is characteristic for diffusion-limited aggregation.

The time evolution of the amplitude of the power law $Q^{-2.6}$ of the scattering curves with and without proteins is plotted in Figure 5(b). The shape of the time dependences of $P_{2.6}$ looks similar, but in the presence of proteins the scattering intensity is approximately 10% higher.

In conclusion, two methods of slowing down the mineralization process were tested by SANS. In the G/W mixture the aggregation of calcium carbonate particles occured in a fractal structure. The size of the initially nucleated particles was limited by the high viscosity (R<200Å), which afterwards formed fractal-like aggregates.

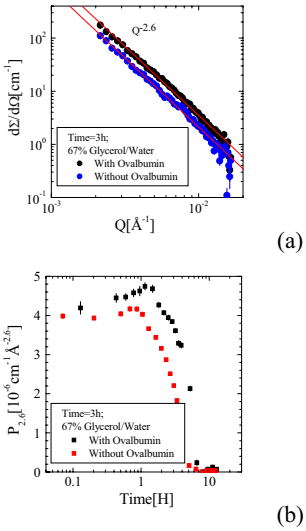


Fig.5. (a) Scattering profiles of mineral particles in 67% glycerol mixture with and without Ovalbumin; (b) scaling amplitude versus time

Institut für Festkörperforschung
Forschungszentrum Jülich GmbH
D-52425 Jülich

Experimental Report
of Neutron Scattering Experiments
at the FRJ-2 Reactor

Proposal number:	KW1-05-022		
Experiment title:	Characterisation of a glass-forming microemulsion		
Dates of experiment:	20.06.05	Date of report:	30.09.05
Experimental team: Names	 Addresses		
Reiner Zorn Maria Mayorova Wim Pyckhout-Hintzen	IFF, FZ Jülich		
Local Contact:	Wim Pyckhout-Hintzen		

Experimental report text body

The droplet microemulsion to be studied here has the peculiar property that the hydrophilic and hydrophobic components undergo glass transitions well separated in their dynamics. It is thus possible to study the glass transition dynamics of propyleneglycol (PG) confined to spheres of of nanometer size. These kind of investigations have been of increasing interest during the last years. For the material here, a propyleneglycol/AOT/decaline microemulsion, dielectric experiments were already done [1] and experiments using inelastic neutron scattering at ILL Grenoble and FZ Jülich are planned.

Before starting the dynamical experiments we wanted to determine the droplet size by SANS. An earlier SANS experiment (KW1-05-006) with h-PG/h-AOT/d-decaline isotopic composition showed that no aggregation of droplets takes place. The size of the droplets could not be determined unambiguously but the results already indicated that the droplet size would be much smaller than expected, about 1 nm.

Therefore, we now performed SANS on a microemulsion with hdd isotopic composition. We used detector distances of 1.25 m and 2 m yielding a Q range from 0.023 $Å^{-1}$ to 0.25 $Å^{-1}$.

The composition of the microemulsion used was h-PG: 10.2% / d-AOT: 36.1% / d-decahydronaphthalene (d-decalin): 53.7% (equivalent wt% of undeuterated compounds). To take care of the background, pure d-decalin was subtracted. Its scattering was about 1/13 of that of the microemulsion so that the resulting correction was only minor.

Fig. 1 shows SANS data from the lowest, highest, and one intermediate temperature exemplarily.

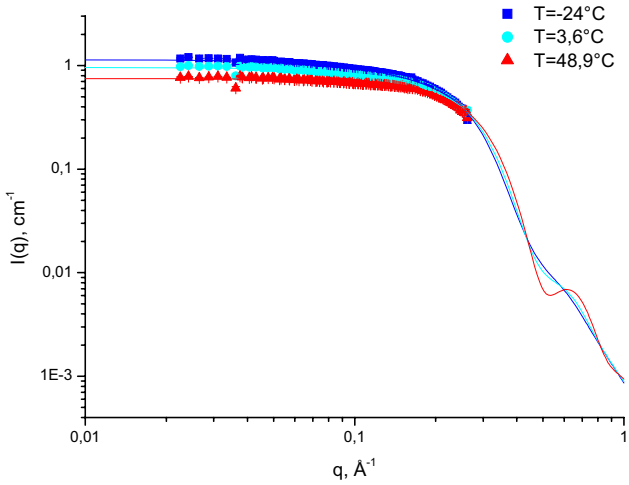


Fig. 1: SANS patterns of the h-PG/d-AOT/d-decalin microemulsion for temperatures –24.0±1 °C, +3.6±1 °C, and +48.9±1 °C. The continuous lines show a fit with the model described below.

The SANS data were fitted by a model combining a Schultz distribution of spheres (characterized by an average radius R_a and a polydispersity p) with a Percus-Yevick type structure factor (characterized by an equivalent hard-sphere radius R_{hs}). The fit parameters shown in Table I indicate that the average radius of particles stays roughly constant while there is a slight increase in polydispersity towards low temperatures.

T, °C	Ra, Å	Rhs, Å	p
-24	8,621	9,875	0,22
3,6	8,610	9,220	0,1859
48,9	8,548	8,581	0,1299

Table I: Structural parameters of the microemulsion at three temperatures.

It can be seen that the preliminary result of an extremely small droplet radius could be corroborated. Indeed, the radius is much smaller than estimated in ref. 1, 23 Å. But there, the radius was not measured but concluded from geometrical values, the volume fractions of AOT and PG and the thickness of the AOT layer from literature [2]. The weakness of that approach is obviously that this thickness is not constant when the droplet size is decreased. Rather, the area per AOT headgroup is a constant. While both extrapolations yield the same asymptotic behaviour for large droplets they differ considerably for such small droplets as here.

In retrospect, from the SANS data and the fits the choice of instrument was inappropriate. While the resolution was better than enough, the Q range of 0.25 $Å^{-1}$ was not sufficient to see the characteristic features of the scattering law. We therefore will apply for an experiment involving higher Q values.

[1] Lin-Min Wang, Fang He, R. Richert, *Phys. Rev. Lett.* **92**, 095701 (2004)
[2] M. Kotlarchyk, S.-H. Chen, J. S. Huang, M. W. Kim, *Phys. Rev. Lett.* **53**, 941 (1984)

Institut für Festkörperforschung
Forschungszentrum Jülich GmbH
D-52425 Jülich

Experimental Report of Neutron Scattering Experiments at the FRJ-2 Reactor

Proposal number:	KW1-05-023		
Experiment title:	Kontrast Variation an Fetuin-A/Ahsg - Mineral Aggregaten		
Dates of experiment:	07.04-12.04.2006	Dates of report:	02.06.06
Experimental team: Names	Addresses		
Dr. Wolf-Alexander Heiß Dr. Dietmar Schwahn	IZKF BioMAT Universitätsklinikum Pauwelsstraße 30 D-52074 Aachen IFF, FZ-Jülich, D-52425 Jülich		
Local Contact:	Dr. Dietmar Schwahn		

Experimental report text body

Without potent inhibitors, a mineral solid would form in a solution that is supersaturated with regard to calcium and phosphate ions. The plasma protein fetuin-A is capable to buffer a high ion load by formation of colloidal protein-mineral aggregates, denoted as calciprotein particles (CPP). Price et. al. reported a two-step ripening of the CPPs [1], however the underlying structural transformations remained unclear. In order to understand the structural aspects of inhibition, we studied the CPP growth employing contrast variation.

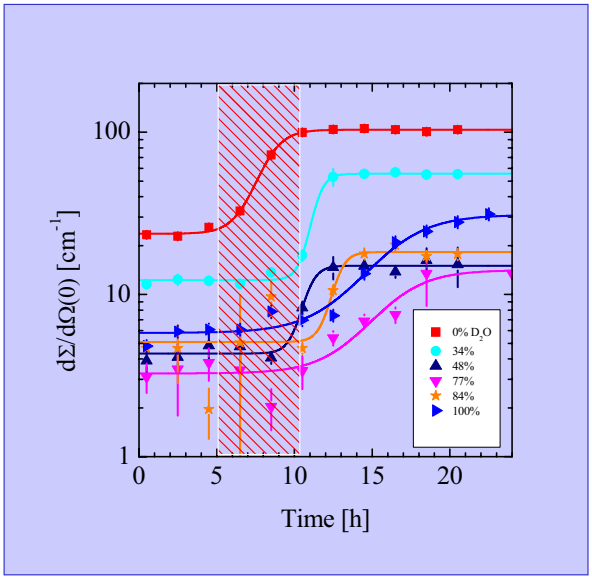
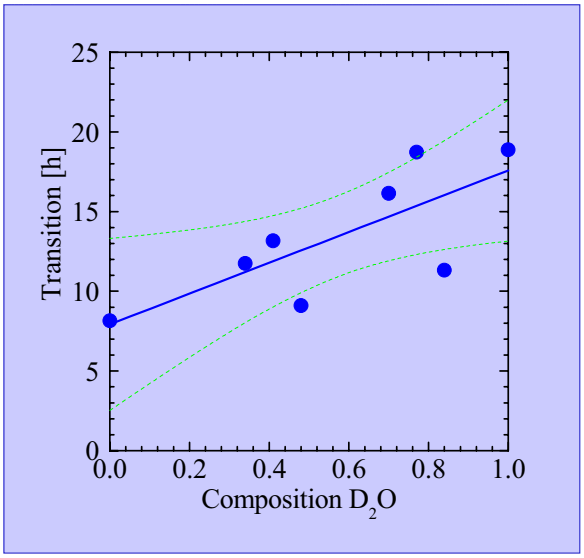


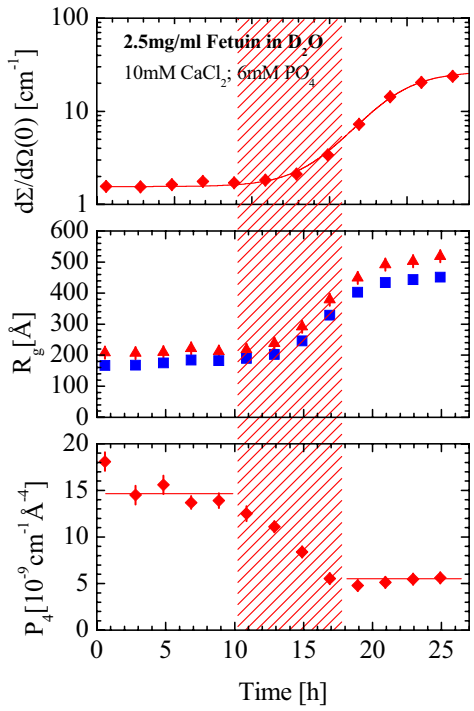
Figure 1 shows the individual time dependent scattering intensities for each contrast. We observed a transformation process from about 5 to 10 hours of incubation indicated by an increase in scattering intensity. At 41% the protein is matched and consequently only the mineral contributes to the total scattering intensity. At 77% the mineral is matched and only the protein is visible.



Interestingly, a linear correlation between the D_2O content and the transformation rate exists (Figure 2, blue line). Despite the variance of this transformation (green lines), a clear trend is visible.

Figure 3 top shows the scattering intensity of a sample containing 2.5 mg/ml bovine fetuin-A, 10 mM $CaCl_2$ and 6 mM PO_4 in 100% D_2O. In this case the increase in scattering intensity indicating the transformation started after 10 h and ended roughly after 20 h, evidencing again a D_2O caused delay concerning the onset and duration of transformation.

Before the transformation the CPPs have a radius of gyration of 170-200 Å. During transformation their size increases to ~500 Å (figure 3, middle). P_4 is an indicator of the surface extension (figure 3, bottom). We observed a decrease in surface during transformation which is expected from a coarsening mechanisn.



Institut für Festkörperforschung
Forschungszentrum Jülich GmbH
D-52425 Jülich

Experimental Report
of Neutron Scattering Experiments
at the FRJ-2 Reactor

Proposal number:	KW1-05-024		
Experiment title:	**Influence of shear on asphaltene orientation in crude oils**		
Dates of experiment:	21.09. - 24.09. 2005	Date of report:	06.06.2006
Experimental team: Names	Addresses		
J. Stellbrink U. Scheven	IFF, FZ Jülich, D-52425 Jülich, Germany Schlumberger Cambridge Research, Cambridge, CB3 0EL, U.K.		
Local Contact:	J. Stellbrink		

Experimental report text body

Asphaltenes are a class of large hydrocarbon molecules comprised of fused poly-aromatic ring cores adorned with short aliphatic chains. In heavy oils they exist as stable colloidal suspensions of micellar structures. Recently Porte et. al. [1] have surveyed the many established experimental results on asphaltene solubility in apolar solvents, and the implications of these results for the mechanisms driving the aggregation processes.

In this experiment we investigated the asphaltene aggregation as a function of temperature and external shear in different types of crude oils using Rheo-SANS. I.e. a Niobium-Couette-cell coupled to a strain controlled Rheowis-Fluid rheometer as sample cell (d=2x0.5mm) in radial and tangential geometry. Figure 1 shows the scattering profile without external shear, indicating the existence of two types of aggregates. The primary micelle with an R_g of approximately 30Å and the secondary aggregate with a characteristic length of several thousand Angstroms. One has to keep in mind, that the contrast results only from differences in proton content and density of the different compounds of the crude oil, since all material is protonated. So the overall scattering intensity is, at least a larger Q-vectors, relatively low. In addition the high incoherent background in this Q-regime complicates data analysis.

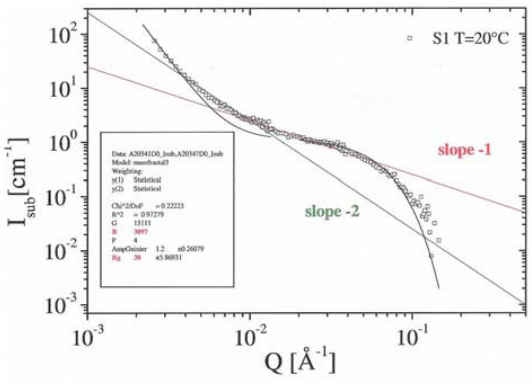


Figure 1: SANS intensity in absolute units versus scattering vector Q for a crude oil without shear.

This incoherent background was estimated from the intensity a the highest Q-vector and finally subtracted from all data sets. Moreover, in tangential geometry the required small sample aperture of 0.5x20mm, which has to fit to the gap size, finally gives that poor data statistics, that we here present only data obtained in radial geometry.

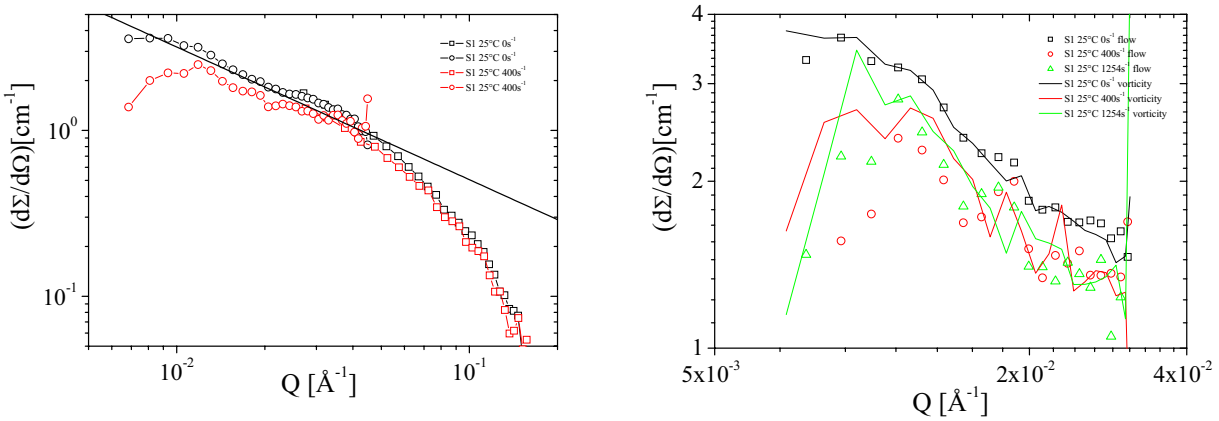


Figure 2: SANS intensity in absolute units for different external shear rates obtained in radial geometry. Left hand side: radial averaged data. Right hand side: Data re-grouped along the flow and the vorticity direction, respectively.

Figure 2 compares data with and without shear. On the left hand side of figure 2 radial averaged data are shown, where only a small effect of external shear is observed. A slightly decreasing scattering intensity at small Q is found, whereas the slope remains constant ≈0.8. On the right hand side we compare data, which were either obtained in flow or vorticity direction. Within experimental error no difference between flow and vorticity direction is observed for all applied shear rates. Also the direct 2D detector images show no indications of anisotropy. In summary, Rheo-SANS [2] is an excellent tool to investigate crude oils, but for a more sophisticated data analysis data of much higher quality are prerequisite, which can only be obtained by considerably longer measurement times.

References:

[1] G. Porte et al., *Langmuir*, **19**, 40-47, (2003)
[2] T.G. Mason, M.Y. Lin, *J. Chem. Phys.*, **119**, 565, (2003)

Institut für Festkörperforschung
Forschungszentrum Jülich GmbH
D-52425 Jülich

Experimental Report
of Neutron Scattering Experiments
at the FRJ-2 Reactor

Proposal number:	**KW1-05-025**		
Experiment title:	**SWELLING OF DENSE MICROGEL SYSTEMS**		
Dates of experiment:	07.11. – 14.11.2005	Date of report:	23/03/06
Experimental team: Names	Addresses		
ANTONIO FERNANDEZ BARBERO	DEPARTAMENTO DE FISICA APLICADA UNIVERSIDAD DE ALMERIA 04120-ALMERIA SPAIN		
ALBERTO FERNANDEZ DE LAS NIEVES	DEPARTAMENTO DE FISICA APLICADA UNIVERSIDAD DE ALMERIA 04120-ALMERIA SPAIN		
ENRIQUE LÓPEZ CABARCOS	DEPARTAMENTO DE FISICO QUIMICA FARMACEUTICA FACULTAD DE FARMACIA UNIVERSIDAD COMPLUTENSE DE MADRID 28040-MADRID SPAIN		
Local Contact:	MARTINE HEINRICH		

Experimental report text body

Microgels are three-dimensional cross-linked polymer networks immerse in a fluid with dimensions in the colloidal range. In previous works we studied different aspects of thermosensitive, cross-linked poly(N-isopropylacrylamide) [poly(NIPAM)] microgels in D2O. They present a continuous volume transition from swollen to deswollen states at 34ºC. The process is thermoreversible without any kind of hysteresis. We investigated the internal structure of the microgel particles, finding inhomogeneous core-shell structures. The interaction between core and shell was then followed during the volume phase transition [1]. Molecular motions of poly(NIPAM) microgels were investigated in the swollen and collapsed states and during the volume phase transition. More applicated experiments concerning microgel-based biosensors were also investigated using neutron scattering [2].

Ionized VP microgel were also invetigated. When particles are collapsed, phase coexistence and finally a pure crystal phase become apparent, following the expected behaviour for hard spheres. However, ***for swollen particles***, the behaviour is fairly different. Even for concentrations higher than the 100% in volume, which means that the swollen microgels have to de-swell due to the external interaction with the rest of the particles, we know by visual inspection that these dense microgels never crystallize. From light scattering experiments we observed structure peaks in the colloidal range shifting towards higher Q values, following a power law $q_{max} \sim \varphi^{1/3}$, which corresponds to neighbouring particles (Figures 1 and 2).

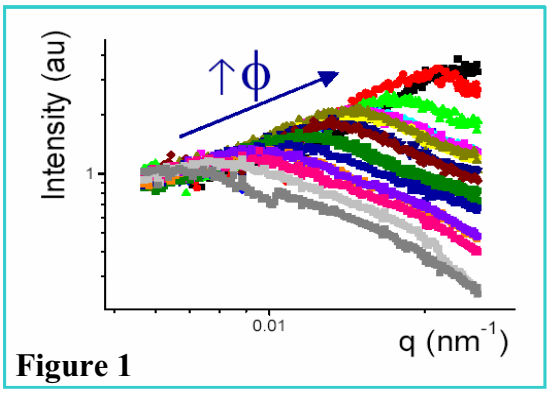


Figure 1

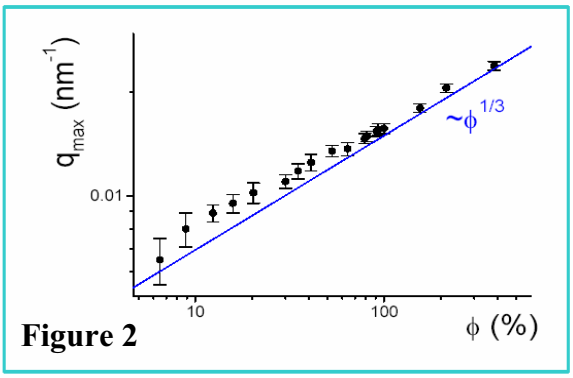


Figure 2

The SANS experiments we are reporting here were designed to monitore the deformation of swollen microgel particles at high particle concentration. 8 different samples were measured at the USANS instrument KWS3 and SANS-KWS1. We measured I(Q) for a swollen VP microgel 0.25% cross-linked with DVB, at different particle concentrations. Figure 3 shows rescaled SANS curves for increasing particle concentration, overlaped on the light scattering curves. A high-Q peak, shown in Figure 4, becomes apparent.

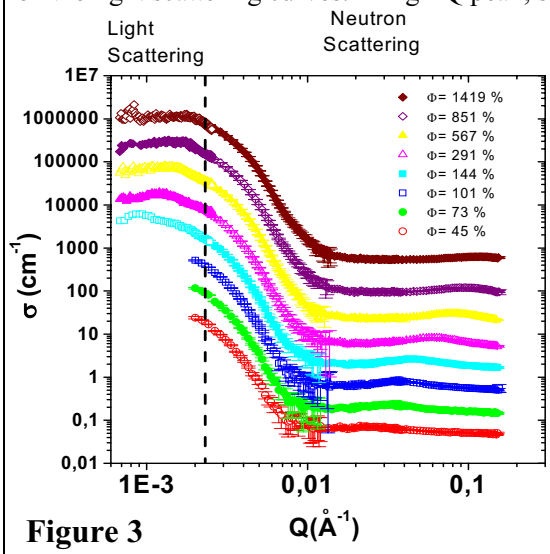


Figure 3

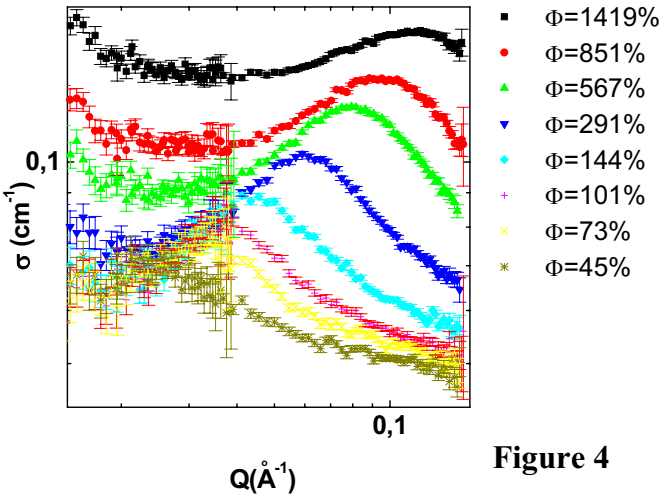


Figure 4

The peak shifts to higher Q values as the particle concentration raises. This indicates an internal structure reducing in size. The nature of this structure has not been identified yet. New experimets are in process using particles with different cross-linker concentrations to estimate if the structure factor change is due to internal particle restructuring or to particle deformation. Additionally, new proposals have been submitted for SANS experiements using dense temperature-sensitive microgels to conclude if the observed structure is charge-induced. The polymer dymamics has been investigated with NMR.

1.- A. Fernández-Barbero, A. Fernández Nieves, I.Grillo, E. López Cabarcos,
Physical Review E, 66 , 051803 (2002).

2.- E. López Cabarcos, B. J. Rubio Retama, B. López Ruiz, M. Heinrich, A. Fernández-Barbero,
Physica A, 344, 417- 423, (2004).

Institut für Festkörperforschung
Forschungszentrum Jülich GmbH
D-52425 Jülich

Experimental Report
of Neutron Scattering Experiments
at the FRJ-2 Reactor

Proposal number:	KW1-05-028		
Experiment title:	Exploring the RNA World: adenine-dependent ribozymes		
Dates of experiment:	15.08. – 19.08.2005	Date of report:	08.06.2006
Experimental team: Names	Addresses		
Joseph ZACCAI Yan-Li LI	ILL, Grenoble, France Institut Jacques Monod, Paris, France		
Local Contact:	Dietmar Schwahn		

Experimental report text body

The "RNA World" hypothesis was formulated in the context of the search for the molecular ancestor of living organisms. The central role of RNA in contemporary metabolism includes both informational and catalytic properties, and DNA can be considered as a modified form of RNA, which is more stable in order to conserve and pass on genetic information more efficiently. Despite a number of associated difficulties, the RNA World hypothesis has powerful advantages in its favour. Contemporary transfer RNA contains a rich collection of functionalised bases created by post-transcriptional modification. RNA can thus gain functionality by using catalytic building blocks such as imidazole, thiol, amino, carboxylate groups etc. as cofactors. Nucleotides can acquire, by chemical modification, all the functional groups of amino acids (Maurel and Ninio, 1987). Moreover, primeval nucleotides were not necessarily restricted to the standard ones, as we know them today. Many coenzymes are nucleotide analogues, making it not unlikely that such modified nucleotides played an essential role in prebiotic catalysis.

By using *in vitro* selection, we have recently discovered new hairpin-ribozymes strictly dependent on adenine, *i.e.* RNA enzymes capable of handling adenine as a cofactor for the reversible self-cleavage of an oligo-nucleotide target. Such studies have evolutionary implications since cofactor assisted ribozymes could be considered as remnants of RNA World ribozymes, handling exogenous prebiotic reactive ligands as cofactors.

Two adenine-dependent hairpin ribozymes (ADHR1, ADHR2) were isolated by *in vitro* selection from a degenerated hairpin ribozyme population (Meli et al., 2003). We characterised the cleavage reaction patterns and kinetics under various conditions and found that both aptamers have Mg^{2+} requirements for adenine-assisted cleavage similar to the wild-type hairpin ribozyme.

The aim of the SANS experiments was to obtain a structural description for the ADHR1 and ADHR2 molecules (each of molar mass 29200 g/mole, containing 85 bases), and their conformational changes upon adenine binding under different conditions. As has been shown previously (Li et al., 1983, Zaccai and Xian, 1988) SANS is a very well-suited method for such low resolution structural studies because of the polyelectrolyte nature of the RNA, and the sensitivity of the scattering patterns to salt conditions and macromolecular hydration.

The following results were obtained during a few days of experiment on KWS-1 spread over 2005 and 2006:

- The RNA samples were aggregated in D_2O solvents and the data could not be exploited.

- Good, reproducible data were obtained for both ADHR1 and ADHR2, and two mutants in H_2O buffered solvent with 100mM NaCl. An analysis of the forward scattering on an absolute scale and of the radius of gyration in the Guinier approximation as well as the general tendency of the $I(Q)$ dependence indicated the RNA molecules, in both cases, are in the form of elongated dimers compatible with two-hairpin confirmations arranged in a parallel or antiparallel configuration.

- A time course experiment was designed following the slow kinetics of adenine-dependent cleavage, observed by gel chromatography. For both ADHR1 and ADHR2, the scattering curve did not change after addition of adenine over a 24h period. This indicated that the dimer structure was unaltered, and that under non-denaturing conditions the cleaved RNA products remained in association.

The analysis of the scattering curves is now continuing, by using model fitting SAS programs in order to obtain a more refined view of the three-dimensional structure of the RNA dimer in solution, and correlating the results with biochemical data from various mutants. A publication is in preparation for *Nucleic Acids Research.*

References

Li Z.Q., Giegé R., Jacrot B., Oberthür R., Thierry J.C., Zaccai G. (1983). Structure of phenylalanine-accepting transfer ribonucleic acid and of its environment in aqueous solvents with different salts. *Biochemistry.* 22:4380-4388.

Maurel, M-C and Ninio, J. 1987, Catalysis by a prebiotic nucleotide analog of histidine. Biochimie, 69, 551-553.

Meli, M., Vergne, J. and Maurel, M-C.
"In vitro selection of adenine-dependent hairpin ribozymes" *J. Biol. Chem.*, (2003), 278, 11, 9835-9842.

Zaccai G., Xian S.Y. (1988). Structure of phenylalanine-accepting transfer ribonucleic acid and of its environment in aqueous solvents with different salts.II *Biochemistry.* 27:1316-1320.

Institut für Festkörperforschung
Forschungszentrum Jülich GmbH
D-52425 Jülich

Experimental Report
of Neutron Scattering Experiments
at the FRJ-2 Reactor

Proposal number:	KW1-05-031		
Experiment title:	Structural study of a novel class of contrast agents for using in Magnetic Resonance Imaging techniques		
Dates of experiment:	07th-10th November 2005	**Date of report:**	07st December 2005
Experimental team: Names	**Addresses**		
Prof. Luigi Paduano	Università degli Studi di Napoli "Federico II", Dipartimento di Chimica, Complesso universitario di M.S. Angelo, Via Cinthia, 80126 Napoli, Italy		
Dr Gaetano Mangiapia	Università degli Studi di Napoli "Federico II", Dipartimento di Chimica, Complesso universitario di M.S. Angelo, Via Cinthia, 80126 Napoli, Italy		
Mauro Vaccaro	Università degli Studi di Napoli "Federico II", Dipartimento di Chimica, Complesso universitario di M.S. Angelo, Via Cinthia, 80126 Napoli, Italy		
Local Contact:	Dr. Aurel Radulescu		

Experimental report text body

The purpose of this research project has been the development of peptide containing supramolecular amphiphilic aggregates as selective nanocarriers for high-relaxivity Magnetic Resonance Imaging (MRI) contrast agent. Our aggregates were formed by the bioactive peptide CCK8 (the bio-specific probe) able to target the aggregates on cholecystokinin receptors that are known to be overexpressed by many tumours, and a chelate molecule (DTPAGlu) able to carry a large number of Gd ions (contrast agent) to highlight the presence of such tissues; both the moieties were bound to a hydrofobic double-tail (18 carbon atoms). All the molecules have been synthesized at University of Naples, "Federico II" – Interuniversitary Center for Bioactive Peptides and are named as $(C18)_2$DTPAGlu and $(C18)_2$CCK8. These surfactant molecules are capable of forming aggregates of different size and shape, such as micelles and vesicles, in aqueous solution by varying the method of preparation and the environmental conditions in solution such as pH, ionic strength and temperature. We have realized a detailed study of structural evolution of the aggregates by varying pH since the increasing interest in current clinical diagnostic for pH responsive MRI contrast agents.
Figure 1 shows some of the SANS data obtained for the systems $(C18)_2$DTPAGlu–D_2O and $(C18)_2$DTPAGlu–$(C18)_2$CCK8-D_2O at different pH values. Correspondent systems containing Gd^{3+} have also been analyzed. The figure shows clearly the evolution of supramolecular aggregates with the pH from micelles to vesicles or bilayer aggregates. At pH 7.4 the scattering intensity shows at low q values a q^{-2} decay typically of the double layer scattering, but the scattering profile also shows the presence of a rising peak in the intermediate q range ($0.02 < q < 0.06$ Å^{-1}) that are originated by the presence of micelles. At lower pH values, as pH 3, the cross-scattering section shows a clear q^{-2} decay in whole the q range analyzed, indicating the presence of only bilayer structures in the system.By decreasing pH the carboxylic groups present in the DTPAGlu moiety are protoned and the formation of low curvature and large aggregates such as vesicles or in general bilayer is advantaged.In order to extract quantitative parameters from SANS data we have expressed the scattering cross section as a sum of a term expressing the scattering of sheets and a term proper of the scattering of cylinders,

neglecting the interference term between the two kinds of aggregates

$$\frac{d\sigma}{d\Omega}(q)=\left[\int_0^{\pi/2}\frac{\sin^2\left(ql\cos\phi/2\right)}{\left(ql\cos\phi/2\right)^2}\frac{9\left[j_1(qR\sin\phi)\right]^2}{(qR\sin\phi)^2}\sin\phi\,d\phi\right]\left(\rho_{cyl}-\rho_0\right)^2\pi Rl+2\pi\left(\rho_{ves}-\rho_0\right)^2 S\tau^2\frac{1}{q^2}\frac{\sin^2\left(\frac{q\tau}{2}\right)}{\left(\frac{q\tau}{2}\right)^2}+\left(\frac{d\sigma}{d\Omega}\right)_{inch}$$

where R and l are respectively the radius and the height of cylinders, while S is the area of sheet per unit volume of sample. Table 1 shows the results obtained through the fitting of previous equation to the experimental data. Assembled molecules form cylinders with a quite large aggregation number (~ 100). The surfactants composing our micelles are disposed with their alkylic tails parallel to cylinder radius and this latter has been evaluated to be nearly the same to the length of molecule.

SANS measurements have also allowed getting the value of the vesicular thickness that ranges between 50 Å and 70 Å depending pH value. Revealing the formation of more compact aggregates as the pH is decreased.

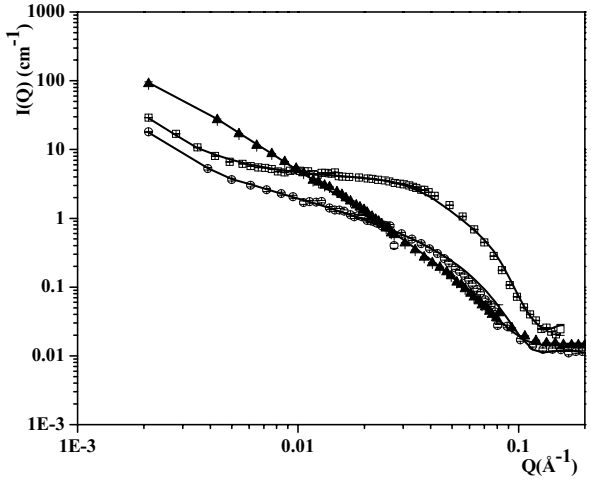


Figure 1. – SANS data obtained at 25°C for the following systems:

∀ $(C18)_2$DTPAGlu (0.00079 mol kg^{-1})- $(C18)_2$L5CCK8 (0.00038 mol kg^{-1}) – D_2O at pH 7.4

– $(C18)_2$DTPAGlu (0.00063 mol kg^{-1})- $(C18)_2$L5CCK8 (0.00037 mol kg^{-1}) – D_2O at pH 4.5

7$(C18)_2$DTPAGlu (0.00063 mol kg^{-1})- $(C18)_2$L5CCK8 (0.00038 mol kg^{-1}) – D_2O at pH 3

Curves presented have been obtained from the fitting of the model described in the text to the experimental scattering cross sections.

Systems	pH	Nagg	R(Å)	h(Å)	τ(Å)
$(C18)_2$DTPAGlu (0.00079 mol kg^{-1})- $(C18)_2$L5CCK8 (0.00038 mol kg^{-1})- D_2O	7.4	125±15	39±3	198±39	70±5
$(C18)_2$DTPAGlu (0.00081 mol kg^{-1})- $(C18)_2$L5CCK8 (0.00036 mol kg^{-1})- D_2O (not extruded)	7.4	102±10	38±4	108±23	71±4
$(C18)_2$DTPAGlu (0.00063 mol kg^{-1})- $(C18)_2$L5CCK8 (0.00037 mol kg^{-1})- D_2O	4.5	771±80	36±2	710±60	58±3
$(C18)_2$DTPAGlu (0.00063 mol kg^{-1}) – $(C18)_2$L5CCK8 (0.00038 mol kg^{-1})- D_2O	3				47±5
$(C18)_2$DTPAGlu(Gd) (0.00079 mol kg^{-1})- $(C18)_2$L5CCK8 (0.00037 mol kg^{-1}) - D_2O	7.4	110±17	35±3	203±33	72±5
$(C18)_2$DTPAGlu(Gd) (0.00063 mol kg^{-1})- $(C18)_2$L5CCK8 (0.00039 mol kg^{-1})- D_2O	4.5	723±65	34±2	741±82	63±10
$(C18)_2$DTPAGlu(Gd) (0.00063 mol kg^{-1})- $(C18)_2$L5CCK8 (0.00032 mol kg^{-1})- D_2O	3				51±6

Table 1. Structural values obtained for micelle aggregates and vesicles, gotten through the fitting of the model described in the text to the experimental data. The symbols presented are:

N_{agg}	Aggregation number of cylindrical micelles.	l	Height of the cylinders
R	Radius of the cylinders	τ	Vesicular thickness

Institut für Festkörperforschung
Forschungszentrum Jülich GmbH
D-52425 Jülich

Experimental Report
of Neutron Scattering Experiments
at the FRJ-2 Reactor

Proposal number:	KW1-05-032		
Experiment title:	Structure of gels formed by pH-responsive core-shell-corona aqueous micelles		
Dates of experiment:	29.09.2005 – 03.10.2005	Date of report:	25.03.2006
Experimental team: Names	Addresses		
Bernard Leyh Nicolas Willet Jean-François Gohy Robert Jérôme	Laboratoire de Dynamique Moléculaire, Département de Chimie, Université de Liège, B-4000 SART-TILMAN C.E.R.M., Département de Chimie, Université de Liège, B-4000 SART-TILMAN CMAT, Université Catholique de Louvain, B-1348 LOUVAIN-LA-NEUVE C.E.R.M., Département de Chimie, Université de Liège, B-4000 SART-TILMAN		
Local Contact:	Dr. Martine Heinrich		

Experimental report text body

The self-assembling of triblock copolymers leads to novel micellar architectures that can be sensitive to external stimuli.[1-7] Their behaviour in selective solvents still needs to be studied in detail. In this project, self-assembling of triblock copolymers of polystyrene$_{200}$-*b*-poly(2-vinylpyridine)$_{140}$-*b*-poly(ethylene oxide)$_{590}$ has been further investigated. This copolymer self-assembles into pH-responsive core-shell-corona micelles in aqueous solution.[4-5] It also leads to the formation of a gel at 8 w/w% in a DMF/water mixture. A soft-to-hard gel transition is observed upon acidification.

Due to time limitations and to the low scattering signal of our systems, we have focused on the analysis of the structure factor in the vicinity of the overlap concentration, c*, at neutral and acidic pH. Microscopy experiments,[4,5] as well as our previous SANS experiments,[8] show that the poly(2-vinylpyridine) shell thickness increases approximately by a factor of two when the initially neutral pH is decreased to a value of about 5. This also induces a swelling of the external PEO corona as proven by both dynamic light scattering and SANS.[8] As a result, the overlap concentration is observed to decrease upon decreasing pH, from about 3 w/w % in neutral solution to 0.6 w/w % under acidic conditions. We performed a systematic study of the evolution of the structure factor as a function of the copolymer concentration and as a function of pH. The analysis of the results should provide us with information on the intermicellar interactions.

The following experiments have been performed: (i) measurement of the scattering cross section for neutral aqueous solutions of polystyrene$_{200}$-*b*-poly(2-vinylpyridine)$_{140}$-*b*-poly(ethylene oxide)$_{590}$ at increasing copolymer concentrations in the 2.0 – 4.0 w/w % range; (ii) similar measurements in acidic solutions corresponding to the complete protonation of the poly(2-vinylpyridine) block; the investigated copolymer concentrations were in the 0.4 – 0.8 w/w % range.

The macroscopic scattering cross section at increasing copolymer concentrations under neutral conditions could be well described using the Percus-Yevick (PY) hard sphere model,[9] as shown in Figure 1. The total scattering intensity is assumed to be proportional to the product of the form factor and of the PY static structure factor. The fitted parameters are displayed in Table 1.

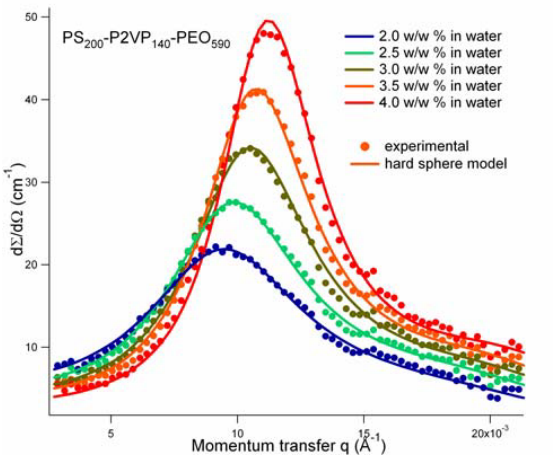


Figure 1 Scattering cross sections under neutral pH conditions

[PS-*b*-P2VP-*b*-PEO] (w/w %)	Volume fraction Φ	Sphere diameter σ (Å)	Radius of gyration R_g (Å)
2.0	0.19	590	115
2.5	0.23	590	110
3.0	0.27	570	110
3.5	0.30	570	110
4.0	0.34	560	108

Table 1 Fitted parameters from the experimental data of figure 1 and the Percus-Yevick hard sphere model

When the copolymer concentration is raised, the first peak of the structure factor becomes progressively larger and narrower, indicating a tendency to a longer range ordering of the micellar solution. A moderate decrease of σ takes place indicating that one is approaching the overlap concentration. The product of the copolymer concentration by σ^3/Φ remains constant within experimental errors.

A similar data handling has been applied to the cross sections recorded at lower pH. In agreement with our previous SANS analysis of the form factor,[8] the global sphere diameter is increased by a factor of approximately 2 and is now in the 1000-1200 Å range. A significant steady decrease of σ is observed when the copolymer concentration is raised, as a result of the overlap between micelles. To reach a more realistic picture of the interactions between charged micelles in acidic solution, we are now performing an analysis based on the rescaled mean spherical approximation.[10]

[1] Riess, G. *Prog. Polym. Sci.* **2003**, *28*, 1107
[2] (a) Goldacker, T.; Abetz, V.; Stadler, R.; Erukhimovich, I.; Leibler, L. *Nature* **1999**, *398*, 137. (b) Stupp, S. I.; LeBonheur, V.; Walker, K.; Li, L.S.; Huggins, K. E.; Keser, M.; Amstutz, A. *Science* **1997**, *276*, 384.
[3] Erhardt, R.; Böker, A.;Zettl, H.; Kaya, H.; Pyckout-Hintzen, W.; Krausch, G.; Abetz, V.; Müller, A. H. E. *Macromolecules* **2001**, *34*, 1069.
[4] Gohy, J.-F.; Willet, N.; Varshney, S.; Zhang, J.X.; Jérôme, R. *Angew. Chem. Int. Ed.* **2001**, *40*, 3214
[5] Gohy, J.-F.; Willet, N.; Varshney, S.; Zhang, J.X.; Jérôme, R. *e-Polymers* **2002**, 35
[6] Lei, L.C.; Gohy, J.F.; Willet, N.; Zhang, J.X.; Varshney, S.; Jérôme, R. *Macromolecules*, **2004**, *37*, 1089
[7] Lei, L.C.; Gohy, J.F.; Willet, N.; Zhang, J.X.; Varshney, S.; Jérôme, R. *Polymer*, **2004**, *45*, 4375
[8] Leyh, B.; Willet, N.; Lei, L; Heinrich, M.; Gohy, J.-F.; Jérôme, R. *Neutron Scattering at FRJ-2. Experimental Reports 2003*, Brückel, Th; Richter, D. Tietze-Jaensch, Zorn, R., Editors, pp. 174-175
[9] Percus, J. K.; Yevick, G. J. *Phys. Rev.* **1958**, *110*, 1
[10] Hansen, J.-P.; Hayter, J. B. *Mol. Phys.*, **1982**, *46*, 651

Institut für Festkörperforschung
Forschungszentrum Jülich GmbH
D-52425 Jülich

Experimental Report
of Neutron Scattering Experiments
at the FRJ-2 Reactor

Proposal number:	KW1-05-033		
Experiment title:	Drug-induced variations of the microviscosity, shape and size of lipid bilayers: interaction of cholesterol and methyl-β-cyclodextrins with DMPC and DPPC liposomes		
Dates of experiment:	28.10.2005 – 31.10.2005	Date of report:	26.03.2006
Experimental team: Names	Addresses		
Mohamed Ali Bahri Angeliki Grammenos Maryse Hoebeke	Laboratoire de Physique Biomédicale, Département de Physique, Université de Liège, B-4000 SART-TILMAN		
Jean-Pierre Gaspard	Laboratoire de Physique de la Matière Condensée, Département de Physique, Université de Liège, B-4000 SART-TILMAN		
Bernard Leyh	Laboratoire de Dynamique Moléculaire, Département de Chimie, Université de Liège, B-4000 SART-TILMAN		
Local Contact:	Dr. Martine Heinrich		

Experimental report text body

Liposomes resulting from the self-assembling of phospholipids are important models of biological membranes because their spherical bilayer structure separates two aqueous media, like the cell plasmic membrane.[1,2] Unilamellar vesicles are particularly relevant, also because they can be used as drug delivery agents.

The aim of this project is to investigate the interaction between liposomes, resulting from the self-assembling of amphiphilic dimyristoylphosphatidylcholine (DMPC) or dipalmitoylphosphatidyl-choline (DPPC) chains, and molecules like cholesterol and cyclodextrins. The addition of drugs can affect the membrane microviscosity and the structural parameters of the liposomes, both effects being possibly linked. A better understanding of the drug action mechanism requires therefore quantifying these two key-observables. Our strategy consists in combining two experimental approaches: SANS to derive the size parameters of the liposomes and ESR (Electron Spin Resonance) to probe the microviscosity.

The effect of cholesterol, at various concentrations, on the DMPC liposomes has been studied quantitatively by ESR at room temperature. The membrane saturation in cholesterol is made progressively from the head group to the centre of the bilayer. The mechanism by which the microviscosity is increased involves the association of cholesterol with fatty acid side chains, reducing their rotational mobility. Cyclodextrins are cyclic oligosaccharides with a hydrophilic outer surface and a lipophilic central cavity. Some cyclodextrins extract cholesterol from biological membranes.[3] They have also been observed to release some liposome-encapsulated drugs without disrupting the vesicles.[4] In the present work, we consider the interaction between randomly methylated β-cyclodextrins, denoted Rameb, and cholesterol-containing DMPC or DPPC liposomes. One essential question is whether the cholesterol extraction by Rameb is accompanied or not by the disruption of the liposomes.

The following experiments have been performed: (i) measurement of the form factors of the DMPC liposomes in D_2O with increasing concentrations of Rameb (0 – 0.03 mol/L range) and at two temperatures (14°C and 34°C), i.e., below and above the gel-liquid transition temperature; (ii) measurement of the form factors of cholesterol-containing (30%) DMPC liposomes, in the same Rameb concentration range and at 14°C and 34°C; (iii) measurement of the form factor of cholesterol-containing DPPC liposomes without and with Rameb (0.03 mol/L). Typical data are displayed in Figure 1. They illustrate the effect of cholesterol insertion followed by its extraction by the Rameb cyclodextrin.

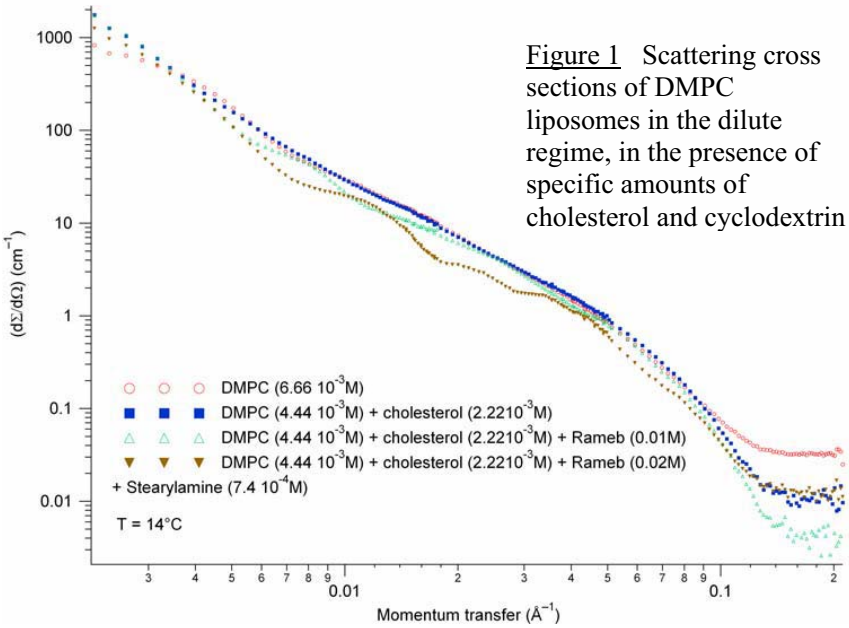


Figure 1 Scattering cross sections of DMPC liposomes in the dilute regime, in the presence of specific amounts of cholesterol and cyclodextrin

These data show that the liposomes survive the cholesterol extraction by the Rameb cyclodextrin. An analysis of the radii of gyration (R_g) leads to the following conclusions.

(i) Progressive addition of Rameb in the absence of cholesterol leads to an increase of R_g, starting from 460 Å, followed by a rapid levelling off (around 550 Å) which is reached already at a Rameb concentration between 0.005 mol/L and 0.01 mol/L. This confirms that the cyclodextrin molecules get adsorbed, possibly under dynamic equilibrium conditions, onto the liposome external layer.

(ii) This increase is somewhat larger below the transition temperature.

(iii) The insertion of cholesterol into the lipidic part of the double-layer leads logically to a substantial increase of R_g, which then reaches 700 Å. Addition of increasing amounts of Rameb at 14°C to the cholesterol-containing liposome solution leads first to a further increase of R_g and then to a decrease without reaching the values observed in the absence of cholesterol. A possible mechanism is that Rameb gets first adsorbed, thus increasing R_g, then extracts cholesterol before being desorbed and replaced by free cyclodextrin molecules, so that R_g decreases. The fact that the radius of gyration remains larger than without cholesterol is an indication that cholesterol extraction is not complete under our concentration conditions.

This analysis will be completed by fitting the experimental scattering cross sections to a model taking into account the different contrasts associated with the internal structure of the liposomes with and without cholesterol and Rameb.[5-7] This will provide us with the relevant structural parameters.

[1] M. Hoebeke, X. Damoiseau, H.J. Schuitmaker and A. Van de Vorst, *Biochem. Biophys. Acta*, **1420** (1999) 73-85

[2] S. Svenson, *Current Opinion in Colloid & Interface Science*, **9** (2004) 201-212

[3] E.P.C. Kilsdonk, W.J. Johnson, G.H. Rothblat and F.W. Bangerter, *Atherosclerosis*, **115** (1995) S100

[4] L. Boulmedarat, G. Piel, A. Bochot, S. Lesieur, L. Delattre and E. Fattal, *Pharmaceutical Research*, **22** (2005) (in press)

[5] M. Hoebeke, M. Bahri, J.-P. Gaspard and B. Leyh, *Neutron Scattering at FRJ-2. Experimental Reports 2004, Forschungszentrum Jülich*, pp 286-287

[6] M.A. Kiselev, P. Lesieur, A.M. Kisselev, D. Lombardo, V.L. Aksenov, *J. Appl. Phys. A* **74** (2002) S1654-S1656

[7] M.A. Kiselev, E.V. Zemlyanaya, V.K. Aswal, *Los Alamos National Laboratory Preprint Archives*, Physics (2004), pp. 1-10

Institut für Festkörperforschung
Forschungszentrum Jülich GmbH
D-52425 Jülich

Experimental Report
of Neutron Scattering Experiments
at the FRJ-2 Reactor

Proposal number:	KW1-05-034		
Experiment title:	Firing technology for medieval ceramic production in the Salento region (Italy)		
Dates of experiment:	05-11-2006	Date of report:	02-03-2006
Experimental team: Names	Addresses		
Alberto Botti Armida Sodo Maria Antonietta Ricci	Univ. Roma TRE, Dip. di Fisica "E. Amaldi", via della vasca navale 84, 00146 Roma (Italy)		
Marco Leo Imperiale Paul Arthur	Univ. Lecce (Italy)		
Local Contact:	Wim Pyckhout-Hintzen		

Experimental report text body

The early medieval production of the Byzantine kiln of "Cantiere Mitello" by Otranto, a small harbour on the Apulian Adriatic see, has been investigated through SANS measurements.
We have collected the small angle scattering patterns of 41 samples which belong to five different groups: namely three types of amphorae with different shapes, a typology of painted amphorae and a series of tableware. All the sherds are coeval and dated back to the VII-VIII century AD.
The samples did not undergo a specific preparation beside a micro-destructive drawing of a tiny amount of ceramic powder. This has been set down of a tape film in manner to form a thin layer. The tape film has been measured separately and subtracted as sample holder.
The small thickness of the samples avoided distortion of the curves caused by multiple scattering processes. Moreover the data have been collected on a Q range from 2e-3 to 1.6e-1, well below the upper cut off of the fractal behaviour (from DKD and KWS3 measurements estimated to be ~ 1-10 μm) [1]. The high Q tail shows indeed on a double logarithmic scale a linear behaviour (see Figure 1), and the data can be fitted with a simple function of the type

$$I(Q) = I_O Q^{-d} + BG$$

Where Io is a prefactor, BG is the level of the incoherent scattering and d is the fractal dimension of the aggregates of the ceramic.

The results of the fitting procedure are plotted in Figure 2 as bars of different colour. In the x axis is reported the fractal dimension, while on the y axis only a dummy value, always the same for all the samples. This graph shows the possible gathering of the d values around a specific value for different typology of objects.
Following the procedure described in Ref 2, the aim of this study was to asses whether the production of "Cantiere Mitello", one of the few examples of Byzantine kilns in Italy [3], adopted different firing strategies according to the final product. A further question concerned the differences between the technologies used by the coeval potters of the west coast, settled in Campania in Miseno and Cuma and more connected to Rome, and that one used on the east cost and facing the Easter Empire: they had distinct customers and end markets.

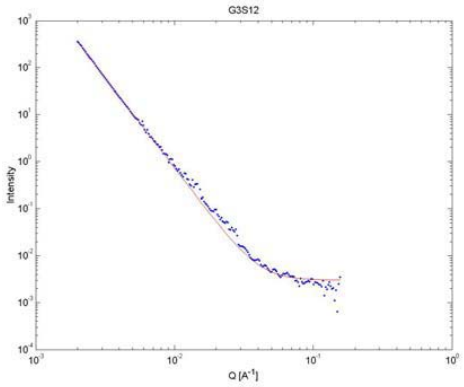


Figure 1

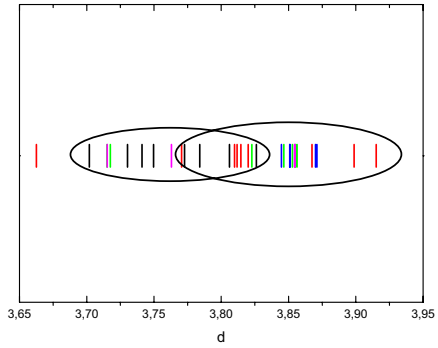


Figure 2

From previous experiments it has been established that once the mineralogical composition has been fixed, *d* linearly depends on the maximum firing temperature and it is independent on heating rate. [2]
From Figure 2, this implies that the tableware (black bars) have been fired at lower temperature compared to the amphorae (coloured bars).
Moreover, all the samples from Otranto have been fired at a temperature higher than that used in the kiln of Miseno and Cuma. At this stage, the latter conclusion must be considered only as an hypothesis, because of the correlation of the absolute value of *d* with the phase content of the sherds. This hinders, as long as the mineralogical composition of the Otranto samples is not known (TOF-ND measurements are scheduled for June 2006), a straightforward comparison of the two productions.

[1] A. Botti, Experimental Report of Neutron Scattering Experiments at the FRJ-2 Reactor, p. 343 (2004).
[2] A. Botti, M. A. Ricci, G. De Rossi, W. Kockelmann, A. Sodo, J. Archaeological Science, **33** 307 (2006).
[3] M. Leo Imperiale, Proceedings of: III Congresso Nazionale di Archeologia Medievale (Salerno 2-5 October 2003)

Institut für Festkörperforschung
Forschungszentrum Jülich GmbH
D-52425 Jülich

Experimental Report
of Neutron Scattering Experiments
at the FRJ-2 Reactor

Proposal number:	KW1-05-035		
Experiment title:	**Conformation of the cytoplasmic part of the trasducer**		
Dates of experiment:	26.08.2005	Date of report:	28.03.2006
Experimental team: Names	Addresses		
Ivan Budyak Vitaliy Pipich Georg Büldt Judith Klein-Seetharaman	Forschungszentrum Jülich, IBI-2 Forschungszentrum Jülich, IFF Forschungszentrum Jülich, IBI-2 Forschungszentrum Jülich, IBI-2; University of Pittsburgh, USA		
Local Contact:	Dr. D. Schwahn, Dr. V. Pipich		

Experimental report text body

The SANS measurements were done at the KWS-I instrument at the FRJ-2 research reactor (Research Center Jülich, Germany). A neutron wavelength of λ=7 Å with sample-to-detector distances of 2 and 4 m were used to get a range in scattering vector $Q=2\pi/\lambda$ values of 0.01 to 0.2 $Å^{-1}$. Protein samples containing 2 and 7.5 mg/ml pHtrII-cyt in dPBS and 5 mg/ml pHtrII-cyt in dPBS + 4M KCl were analyzed at room temperature in quartz cells with 1-mm path lengths. The data were corrected for the detector efficiency, the scattering from the empty cell and solvent, and then radially averaged and calibrated in absolute units by a plexiglas secondary standard. Scattering curves were fitted using the approximation proposed by Beaucage (Beaucage, *J.Appl. Cryst.,* 1996) which combines both the Guinier regime (Guinier and Fournet, *Small Angle Scattering of X-rays.* 1955) and the fractal regime:

$$I(Q) = G\exp(-R_g^2Q^2/3) + P[erf(R_gQ/\sqrt{6})]^3/Q \quad (1)$$

where R_g is the radius of gyration, G is the Guinier prefactor

$$G = \Phi(1-\Phi)V\Delta\rho^2 \quad (2)$$

and P is the amplitude of the fractal part

$$P = \Phi(1-\Phi)\pi^2r^2V\Delta\rho^2. \quad (3)$$

Using this equation, the following features can be derived from the curve: (i) the zero Q intercept gives the particle volume if the concentration is known, (ii) the slope of the Guinier region is equal to $-R_g^2/3$ and therefore gives the particle size, (iii) the slope of the mass fractal dimension indicates the shape, (iv) and the Porod region gives the surface area and surface fractal dimension (Beaucage, *J.Appl. Cryst.,* 1996).

We used SANS to complement our observations from analytical gel-filtration and crosslinking experiments, that the cytoplasmic part of the transducer II from *Natronobacterium pharaonis* (pHtrII-cyt) is predominantly monomeric in PBS (Dulbecco and Vogt, *J.Exp.Med.*, 1954) and dimeric in PBS + 4 M KCl. All measurements were carried out in buffers prepared in D_2O to improve the signal:noise ratio.

The concentration-normalized experimental data are plotted in Fig.1 for pHtrII-cyt in dPBS as open circles (○) and in dPBS + 4M KCl as open squares (□). In both cases, the scattering intensity I(Q) follows the scaling law Q^{-1} over a wide Q range of 0.03 to 0.2 $Å^{-1}$ (Fig. 1, dashed line). The observation of a $I(Q) \sim Q^{-1}$ dependence is consistent with an elongated (rod-like) shape of pHtrII, both in dPBS and in dPBS + 4M KCl and can be approximated with a cylinder.

The volume fraction of protein Φ was calculated from the ratio between the pHtrII-cyt concentration and the protein density in H_2O, $\Phi = c/d_p$; the volume of the cylinder was assumed to be equal to the molecular volume of protein $V = M/N_a/d_p$. From Eq. 2 and 3, the length and the radius of the protein molecules can be calculated according to:

$$L = \pi G/P \quad (4)$$

$$r = \sqrt{(V/\pi/L)} \quad (5)$$

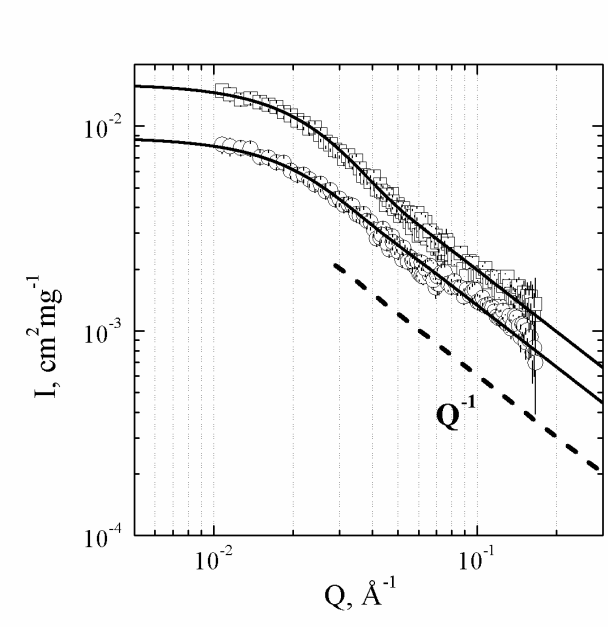
The values for the length and radius obtained for the pHtrII-cyt molecules in dPBS buffer were L_{PBS}=202±5 Å and r_{PBS}=7.2±0.3 Å, respectively. From these values, the radius of gyration R_g was calculated based on the cylinder model. For a cylinder of length L, radius r and unifrom mass distribution, R_g is given by:

$$R_g^2 = L^2/12 + H^2/2 \quad (6)$$

For pHtrII-cyt, this gives a radius of gyration of R_g = 58.5 Å. This value is similar to the radius of gyration value obtained directly from Eq. 1, which was 50.8±0.8 Å. The overall shape of the SANS spectrum measured in dPBS + 4M KCl was essentially identical to that observed in dPBS buffer alone. In contrast, the reduced zero intensity G:

$$G/c = 1/d_p V \Delta\rho^2 \quad (7)$$

in the presence of 4 M KCl in dPBS buffer was 1.8 higher than the zero intensity G observed in dPBS buffer alone. This increase can either result from a change in the particle volume V and/or the square of the scattering contrast. If we assumed a constant volume ($V_{SALT}=V_{PBS}$), the scattering length density of HtrII-cyt in D_2O would be $\rho_p = 2.3*10^{10}$ cm^{-2}. This value would be much lower than expected for proteins in D_2O and could only be accounted for if the protein would bind hundreds of K^+ ions. On the other hand, if we assumed a constant scattering length density ($\rho_p^{SALT}=\rho_p^{PBS}$), the particle volume would increase by a factor of 12. Thus, the result indicates that the increase in zero intensity must result from a combined increase in particle volume and change in scattering contrast. In particular, if we assume $V_{SALT}=2V_{PBS}$, the scattering length density of pHtrII-cyt in dPBS + 4 M KCl becomes $\rho_p = 3.22*10^{10}$ cm^{-2}. This value is very close to the value typically observed for proteins in D_2O. The decrease of the scattering length density from $4.37*10^{10}$ cm^{-2} in dPBS to $3.22*10^{10}$ cm^{-2} in the presence of 4 M salt suggests exclusion of D_2O from the protein's interior, either by "tightening" of the structure and/or by binding of K^+ ions.



The volumes and scattering length densities from the above calcuations were used to approximate the experimental scattering curve by using Eq. 1. The resulting curve is shown in Fig. 1. The molecule length and radius were calculated according to Eq. 4 and 5. The length and radius increased from L_{PBS}=202±5 Å and r_{PBS}=7.2±0.3 Å to L_{SALT}=248±7 Å and radius r_{SALT}=9.1±0.4 Å. When calculating the radii of gyration using these values and comparing them to the direct calculation using Eq. 1, a significant difference between R_g=56±1 Å (obtained from Eq. 1) and R_g=72 Å (calculated from Eq. 6) was observed. Since the experimental value is less than the theoretical value, the mass is either concentrated at the center of the cylinder or the cylinder is not ideal, i.e. the diameter at the center is larger than that on the edges. Thus, there is non-homogeneous mass distribution within the pHtrII-cyt dimer molecule in the presence of 4 M KCl in contrast to the pHtrII-cyt monomer in dPBS alone, which displayed uniform mass distribution.

Institut für Festkörperforschung
Forschungszentrum Jülich GmbH
D-52425 Jülich

Experimental Report
of Neutron Scattering Experiments
at the FRJ-2 Reactor

Proposal number:	KW1-05-036		
Experiment title:	Kinetics and dimensions of polymeric stabilised zirconia sols. Sol synthesis for microporous zirconia membranes with power plant gas separation as application		
Dates of experiment:	15.08.2005 11.12.2005	Date of report:	13.03.2006
Experimental team: Names	Addresses		
G.J.W. van der Donk Dr. Tim Van Gestel Dr. Wim Pyckhout-Hintzen	Forschungszentrum Jülich, IWV1 Forschungszentrum Jülich, IWV1 Forschungszentrum Jülich, IFF		
Local Contact:	Dr. Wim Pyckhout-Hintzen		

Experimental report text body

Due to the Kyoto protocol, increasing intensive research is in progress to separate CO_2 from the power plant exhaust. This can be performed at the 'End of Pipe' (post combustion) or with new concepts such as pre combustion (H_2/CO_2) or oxy-fuel (N_2/O_2) processes. Inorganic microporous membranes benefits from the mechanical, thermal and chemical stability above carbon based polymers. Present inorganic microporous membranes with high permeation are based 30 nm thin layers of silica with particles less than 10 nm [1]. Silica microporous membranes lack the stability in humid conditions at high temperate. Zirconia is known for its thermal stability. These microporous membranes with pore size smaller than 1 nm can be applied in gas separation applications.
However, the polymeric zirconia or titania synthesis is more complex than the polymeric silica sol due to the fast kinetics of the hydrolysation process. The zirconia sol is a polymer, fractionated, and therefore the sol can be idealised as a sphere. Zirconia sols have been analysed with dynamic light scattering resulting in estimated/calculated particle size diameter of 3-10 nm. However, neither SAXS or DLS could give us accurate information on the mass and surface fractal.
Van Gestel has prepared three different polymeric sols, one titania based sol and two zirconia based sols. One of the zirconia sols has been synthesised with a bimodular particle size distribution (Figure 1). The cluster structure (shape) of these sols can only be studied with small angle diffraction. 0.5 wt% diluted zirconium and titanium sols have been prepared in propanol. These sols are diluted for good coating behaviours and fulfil the Guinier approximation requirement of diluted particles. The sol is based on a polymer chain of a metal ion with acetylacetone and propyl groups. The presence of propyl groups and propanol as solvent resulted in a calculated low contrast, which can result in significant noise in the scattering intensity. Deuterated ethanol (EtOH-d6) was added in a 50/50% weight ratio to increase the contrast. Standard SANS procedure was followed for measuring the three samples including a solvent (propanol- EtOH-d6) and empty quartz cells.

The scattering intensities of both zirconium and titanium sols with average sol size (DLS) of 5 nm were rather low and resulted in a high noise/signal ratio. The log-log plot intensity and scattering vector, the Porod plot, of the bi-modular zirconium sol resulted in high noise at relative large scattering vector. (Figure 2). But, a clear trend could be observed in the small scattering vector region. This indicates a mass fractal dimen-si-onal of about 1.3 when we assume that the particles are monodispersed. It is assumed that the dimensional fractal is stable due to the diffusion limitation of the cluster-cluster aggregation[2]. The dimensional fractal can be dependent on the water and acid content in the sol. This behaviour is not studied for these samples, yet. There-fore, the value of dimensional frac-tal can only indicate a sparser appearance of the polymer structure. The log intensity – log Q^2 plot presented the Guinier region where the sol size could be determined (Figure 3 and Figure 4). The bi-modular zirconium sol size distri-bution is confirmed with SANS. Clearly, two slopes could be identi-fied resulting in a particle size of 12(3) and 35 (5) nm. The curve is a combination of both slopes. It is hard to distinguish both slopes, the error is estimated. DLS suggest peaks at 6 and 60 nm (Figure 1).
A second SANS beam time was approved. Sols with higher concentration will be syn-thesised to increase the intensity. Four sols have been prepared with a higher concentration ~15wt% to obtain a higher contrast. The new samples are not diluted with EtOH-d6 to maintain high concentrated samples. A zirconia and titania sols have been prepared with caprionic acid as catalyser and another zirconia and titania have been prepared with diethyl-amine as cata-lyser. Unfortuneately, only the last sample resulted in an acceptable result to obtain the particle size of 4 nm.

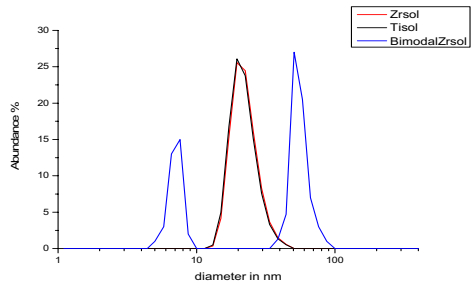


Figure 1 Sol size distribution of zirconia and titania based sols.

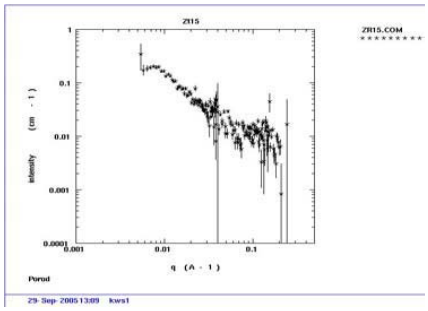


Figure 2 Porod plot of zirconium sol #Zr15

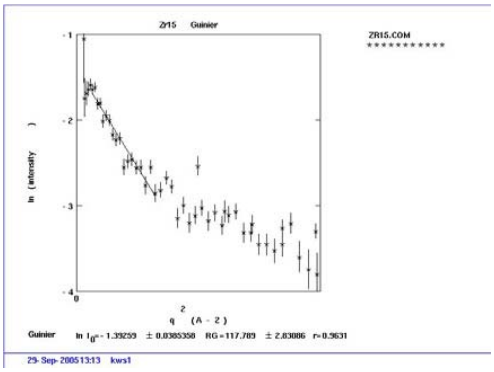


Figure 3 Guinier plot of zirconium sol #Zr15 with steep slope

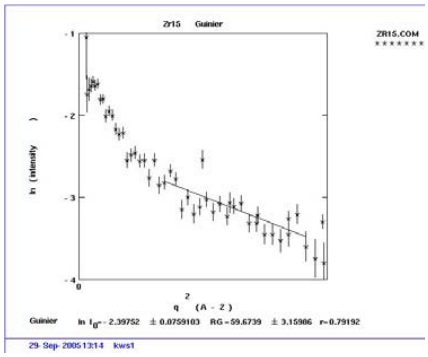


Figure 4 Guinier plot of zirconium sol #Zr15 with flat slope

SANS measurements confirms the bimodular particle size of the zirconia sample #Zr15 and the particle size of the second titania polymeric sol. Unfortunately, the intensity of all the samples is rather low and therefore could not enhance the accurate results of the DLS measurements.

1. de Vos, R. M. in *Inorganic material science* (University of Twente, Enschede, 1998).
2. Maene, N., Nair, B. N., D'Hooghe, P., Nakao, S. I. & Keizer, K. Silica-polymers for processing gas separation membranes: High temperature growth of fractal structure. *Journal of Sol-Gel Science and Technology* **12**, 117-134 (1998).

Institut für Festkörperforschung
Forschungszentrum Jülich GmbH
D-52425 Jülich

Experimental Report
of Neutron Scattering Experiments
at the FRJ-2 Reactor

Proposal number:	KW1-05-037		
Experiment title:	Conformation of cyclic polystyrene in entangled state: characterization of single chain in theta solvent and melt state		
Dates of experiment:	21.09. – 23.09.2005	Date of report:	27.03.2006
Experimental team: Names	 Addresses		
Michael Kapnistos Dimitris Vlassopoulos Wim Pyckhout-Hintzen	Forth, Crete Forth, Crete FZJ		
Local Contact:	Wim Pyckhout-Hintzen		

Experimental report text body

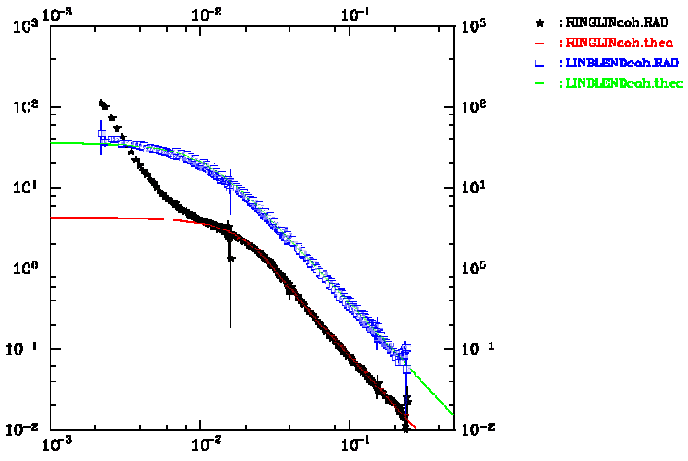


Fig: comparison of the main 'actors' in the melt state

The conformation of ring polymers has been theoretically and experimentally investigated in the past but several problems with samples, sample quality with respect to the ring architecture and others had been reported. In this experiment we use a well characterized ring which had been synthesized by Jacques Roovers and which had been analysed by several techniques before. We were interested also in the blending of this particular ring with a linear chains. Chains of this particular architecture exhibit new interesting properties which are related to the architectural build-up of the components. To sustain the mixing rheology of ring PS with linear the conformation of the ring polystyrene was measured in both theta and melt state.

The ring polymer in solvent exhibited the expected structural details which were tested against several approaches now available for the ring-type architecture. These approaches are semi-empirical in nature but are valuable as simple exponents which relate again to the intrinsic viscosity of the ring solutions are parameters. The chain conformation data: (see Bensafi et al. Polymer International, 49:175-183(2000)) are described by $Rg \sim N^{\nu} l$ and $\nu \sim 0.6$ in good solvent for both linear and cyclic polymer. For theta conditions all values between 0.4 and 0.45 are possible according to this publication. In linear chains the exponent increases even to 0.5. Within the assumption of Gaussian statistics this leads to the expression for every internal distance as: $\langle r_{ij}^2 \rangle = l^2|i-j|(1-|i-j|/N)$ which leads to $Rg^2 = Nl^2/12$ for rings in melt.

This changes by excluded volume interactions in different ways. As an assumption: Rg^2(good solvent limit)= Rg^2(theta) α^3 and α being the Flory swelling. 3 models have been proposed in literature which is very fast summarized as

1. Bloomfield-Zimm
   $\langle r_n^2 \rangle = l^2 n^{1+e}(N-n)^{1+e}/(n^{1+e}+(N-n)^{1+e}$
2. Yu-Fujita
   $\langle r_n^2 \rangle = l^2 n^{1+e}[(1-(n/N)^{1+e}]$
3. Maschke (empirical)
   $\langle r_n^2 \rangle = l^2 n^{1+e}[1-(n/N)]^{1+e}$

For the formfactor in the Gaussian approximation this leads :
$Pc(q) = 2\ \mathrm{int}(0,1)\ dx(1-x)\ \exp(-q^2\langle r_n^2 \rangle/6)$ with
$x = n/N$ and $Pc(q=0)=1$.
The new formfactors can be introduced easily by $\mu = q^2 N^{1+e} l^2/6$ (e=0 for theta, e~0.1-0.3 for good solvent) and numerical integration using mathematical library software.
In order to evaluate without restriction the formfactor of the ring in the blend with linear chains, the linear chain itself was characterized in the melt state and parameters determined. For the RPA equation for ring with linear all linear parameters could be fixed therefore. The results is shown in the upper figure: the pure linear blend behaves perfectly and the ring-linear combination scatters similar to the theta-solution in low angles. The upturn at $q<0.01$ is NOT due to demixing in the melt as also the solutions without linear chains showed the same feature. In the theta solvent the upturn is shown, in the good solvent limit this is only recognizable which tells us that the 'aggregate' of rings is swollen heavily as well and disappears in the beamstop. From absolute intensities its contribution is of the order of 10%. Both plots show the comparison with the linear chain in log-log and kratky representation. The small peak in the 2-moment of the intensity is typical for the ring structure although it is only shallow. At high q the scattering is again gaussianlike. The critical lengthscale at which pollution of the formfactor of the rings appear is sufficiently separated to allow the simple dimension to be analzed with high accuracy. These experiments were the base for upcoming deformed structural analysis.

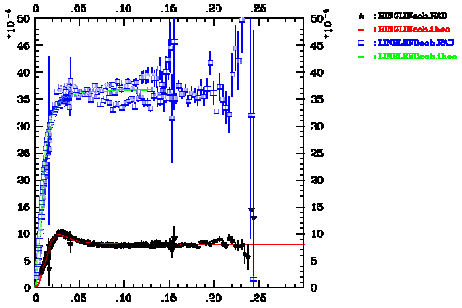


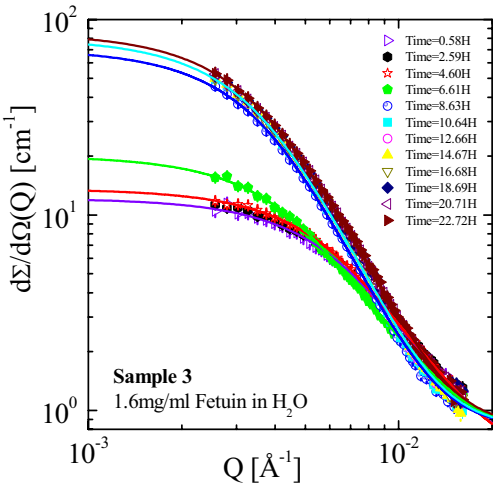
Fig: kratky-representation of ring and ring/lin blend

Institut für Festkörperforschung
Forschungszentrum Jülich GmbH
D-52425 Jülich

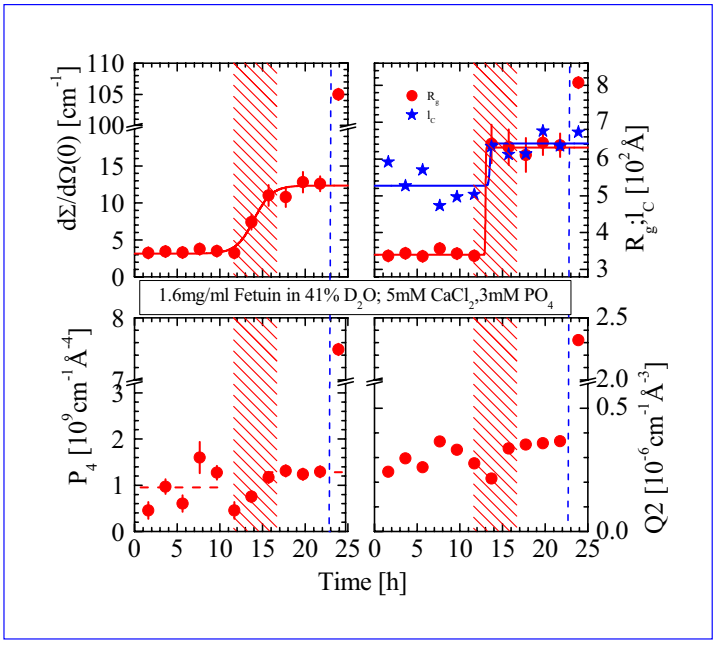
Experimental Report of Neutron Scattering Experiments at the FRJ-2 Reactor

Proposal number:	KW1-05-039		
Experiment title:	SANS Untersuchung colloidaler Protein-Mineral Aggregate bei geringeren Konzentrationen		
Dates of experiment:	16.09. – 19.09.2005	Dates of report:	02.06.2006
Experimental team: Names	Addresses		
Dr. Wolf-Alexander, Heiß	IZKF BioMAT Universitätsklinikum Pauwelsstraße 30 D-52074 Aachen		
Dr. Dietmar Schwahn Dr. Hitoshi Endo	IFF, FZ-Jülich, D-52425 Jülich		
Local Contact:	Dr. Dietmar Schwahn		

Experimental report text body



After having studied the fetuin-A mediated inhibition of calcium phosphate precipitation at a concentration of 2.5 mg/ml fetuin-A, 10 mM $CaCl_2$, 6 mM PO_4 we decreased the fetuin-A and ion concentrations (1.6 mg/ml bovine fetuin-A, 5 mM $CaCl_2$, 3 mM PO_4) for this series of experiments. Figure 1 shows the time dependent increase in scattering intensity. Similar to our previous experiments, we observed a two stage ripening. The transformation starts after 5 hours and is finished within eight hours of incubation at room temperature.



At a 41% D_2O the scattering length density of the protein is matched. Hence only the mineral contributes to the total scattering intensity. The concentrations for this experiment were: 1.6 mg/ml bovine fetuin-A, 5 mM $CaCl_2$, 3 mM PO_4. During the transition from the first to the second stage we observed again an increase in the scattering intensity and the radius of gyration (from 350 to 560 Å). Simultaneously the surface extension dropped but then slowly increased again. The course of the second moment Q2 also shows a discontinuous but inverse behavior. Q2 slowly decreases during transformation but suddenly jumps up towards the end of this process.

Institut für Festkörperforschung
Forschungszentrum Jülich GmbH
D-52425 Jülich

Experimental Report
of Neutron Scattering Experiments
at the FRJ-2 Reactor

Proposal number:	KW1-05-041, KW1-05-047, KW1-06-018		
Experiment title:	Chain conformation in novel, natural-synthetic hybrid block copolymers		
Dates of experiment:	26-28/9/05, 11-13/11/05, 24-27/5/06	Date of report:	6th June 2006
Experimental team: Names	Addresses		
Dr. L.J.R. Foster [1,2] Dr. D. Schwahn [2] Dr. V. Pippich [2]	[1] Bio/polymers Research Group, School of Biotechnology and Biomolecular Sciences, University of New South Wales, Sydney NSW 2052, Australia. [2] Institut für Festkörperforschung, Forschungszentrum Jülich GmbH, 52425 Jülich, Germany		
Local Contact:	Dr. D. Schwahn		

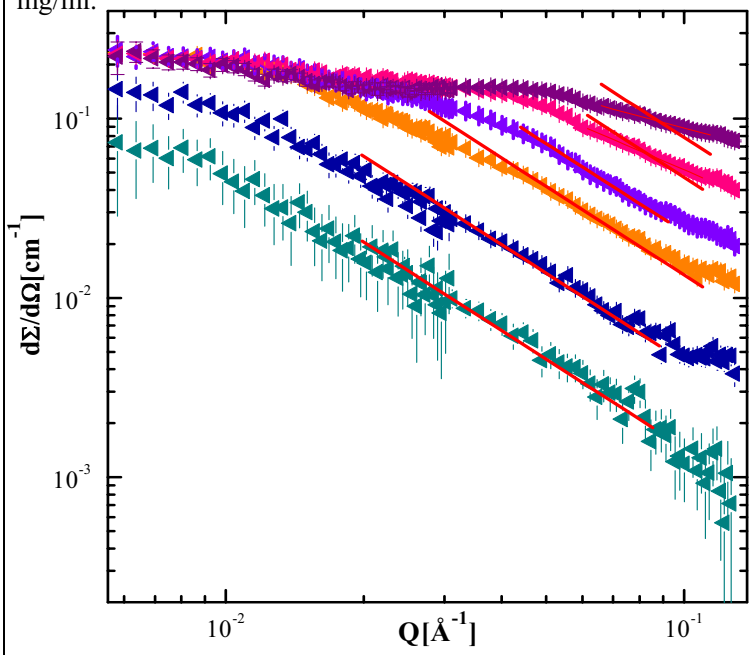
Experimental report text body

Introduction Polyhydroxyalkanoates (PHAs) are a family of biopolyesters synthesized by a wide range of microorganisms. The most common of these biopolymers is Polyhydroxybutyrate (PHB), which has received considerable interest as an environmentally friendly bioplastic and as a biomaterial for biocompatible medical implantation devices. PHB however, is just one member of a family of biopolymers possessing in excess of 105 different monomeric components. These novel biopolymers have material properties ranging from the rigid and highly crystalline to flexible, rather amorphous and elastomeric *[1]*. Another member of interest is Polyhydroxyoctanoate (PHO). PHB and PHO are representative members of PHAs possessing short and medium chain length substituents in the side chain (*scl*PHA and *mcl*PHAs).

We have recently synthesised natural-synthetic hybrids of PHB and PHO by 'end-capping' hydrophobic PHA chains with hydrophilic diethylene glycol (PHB-DEG and PHO-DEG respectively) *[2]*. The family of PEGs has a wide range of members varying in molecular mass and structure. A number of biocompatible members have important biomedical functions such as organ and tissue preservation *[3]*. Material surfaces modified by covalent attachment of PEG chains are resistant to cell and protein adsorption *[4]*. During solvent casting PHA-PEG hybrids self-assembled into ordered microporous arrays *[5]*. These microporous films, by virtue of their biocompatible composition and morphology, have the potential to serve a range of biomedical and biotechnological applications.

The objective of this research is to elucidate the influence of the relatively small hydrophilic group in these hybrids on polymer chain conformation, with a particular reference to their ability to form microporous films. In this regard, a synthetic block copolymer: Polystyrene-*b*-polydimethylacrylate which forms highly ordered microporous films is used as a positive control. Thus, based on electron microscopy studies, the degree of organisation in microporous films increases in the following sequence: PS-PDMA > PHB-DEG > PHO-DEG.

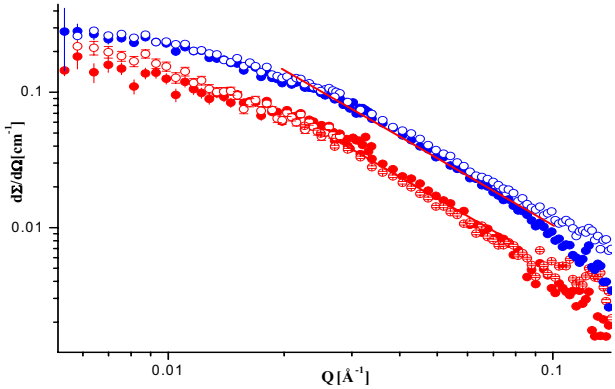
Experimental A series of SANS experiments have been carried out to analyse the conformation of the following polymer chains *(a)* Polyhydroxyoctanoate (PHO), *(b)* Polyhydroxybutyrate (PHB), *(c)* Poly(hydroxybutyrate-*co*-hydroxyvalerate 8%) (P(HB-*co*-8HV), *(d)* PHO-Diethylene Glycol (PHO-DEG), *(e)* PHB-Diethylene Glycol (PHB-DEG), *(f)* Deuterated PHO-hydrogenated DEG (dPHO-DEG) and *(g)* Polystyrene-*b*-polydimethylacrylate (PS-PDMA). – SANS experiments were performed with biopolymers in solutions using deuterated chloroform and deuterated methylene chloride at a concentration range of 3-100 mg/ml.



Results & Discussion Chloroform is a standard solvent for this family of biopolymers but solvent can play an important role in final device morphology in the processing of these biomaterials *[6]*. Figure 1 illustrates the change in scattering for PHO in solution with deuterated chloroform at a variety of concentrations. The best visual fit for the slope of the scattering data (1.5 mg/ml) was 1.64, confirming chloroform as a 'good solvent'. Above about 36 mg/ml the scattering shows the influence of the 'structure factor'.

Figure 1: Scattering data for solutions of biopolymer PHO in deuterated chloroform with variations in concentration (mg ml^{-1}): (◀) 1.36, (◀) 3.15, (◀) 9.68, (◀) 18.28, (◀).81, (◀) 72.19.

A Zimm plot of scattering data suggests a PHO chain radius of gyration of approximately 130 ±5 Å which is maintained until approximately 4 mg ml^{-1}, after which it decreases exponentially, suggesting an overlap concentration between 4 and 9.7 mg ml^{-1}. A linear inverse relationship also exists for the correlation lengths derived from this decrease in apparent Rg.



The patterns of scattering data for the hybridised PHA samples in solution with deuterated solvents were similar to their non-hybridised counterpart (Figure 2). Hybridisation of the PHA chain appeared to have no significant influence on the slope with best estimates at $Q^{-1.64}$. Thus, our preliminary analysis suggests that end-capping the hydrophobic PHA chains with relatively small groups of hydrophilic DEG apparently had no effect on the chain conformation when in solution in chloroform.

Figure 2: Scattering data for solutions of biopolymer PHO and its natural-synthetic hybrid of PHO-DEG in deuterated chloroform with variations in concentration (mg ml^{-1}): (➢) PHO-DEG (4.89) compared to (➢) PHO (3.96) and (➢) PHO-DEG (9.79) compared to (➢)PHO (10.59).

[1] Steinbüchel, A. In: Rehm H-J, Reed G, editors. Biotechnology. Weinheim, Germany: John Wiley & Sons, **1996**.
[2] Sanguanchaipaiwong, V; Gabelish, CL; Hook, J; Scholz, C. & Foster LJR. *Biomacromolecules* **2004**;5(2):643.
[3] Harris JM. Poly(ethylene glycol) chemistry: biotechnical and biomedical applications. New York, USA: Plenum **1992**.
[4] Inada Y, Matsushima A, Kodera Y, Nishimura H. *J. Bioact Compat Polym.* **1990**;5:343.
[5] Foster, LJR; Sanguanchaipaiwong, V; Gabelish, C. & Hook, J. *Polymer* **2005** 46(17):6587-6594.
[6] Foster, LJR; Davies, SM. & Tighe, BJ. *J. Biomater. Sci. Polymer Edn.* **2001** 12(3), 317-336.

Institut für Festkörperforschung
Forschungszentrum Jülich GmbH
D-52425 Jülich

Experimental Report
of Neutron Scattering Experiments
at the FRJ-2 Reactor

Proposal number:	KW1-05-045, KW1-06-008		
Experiment title:	Temperature dependence of conformational and association states in hyperthermophile ICDH		
Dates of experiment:	23.01. – 26.01.2006 20.03. – 22.03.2006	Date of report:	12.06.2006
Experimental team: Names	Addresses		
Marion Jasnin Dominique Madern Joseph Zaccai	IBS 41 rue Jules Horowitz 38027 Grenoble Cedex 01 France ILL 6 rue Jules Horowitz, BP 156 38042 Grenoble Cedex 9 France		
Local Contact:	Martine Heinrich		

Experimental report text body

Isocitrate dehydrogenases (ICDH) are a broadly distributed group of metal-dependent decarboxylating enzymes, involved in cellular energy metabolism. Relations between structure and function of the ICDH and phylogenetic studies have established that this enzyme family is split into three main groups [1]. Group I contains Archaeal and Bacterial $NAD(P)^+$-dependent ICDH. Group II is made up of Eukaryotic NAD^+-dependent ICDH. Group III, which has been identified recently, is made up of Archaeal and Bacterial $NAD(P)^+$-dependent enzymes, whose sequences group together at a long evolutionary distance from both groups I and II.

Crystallographic and solution studies have demonstrated that ICDH from groups I and II are dimeric [1-3]. In our laboratories in Norway and France, we are studying the ICDH (III) from the hyperthermophile bacterium *Thermotoga maritima* (Tm), which lives at 80°C, with the aim of achieving a molecular understanding of the group III enzymes. Using analytical centrifugation (AUC) we explored the oligomeric state of Tm ICDH (III) at 20°C, in parallel with enzymes from groups I and II. Compared to all ICDH described to date that are dimeric, Tm ICDH (III) exists also as a tetramer. Experimental sedimentation profiles were well fitted by a mixture of tetramer and dimer.

Recently, crystallisation trials for the ICDH (III) dimer have been successful. X-ray diffraction data have been collected and the structure of the dimer was published few weeks ago (Karlstrom et al., paper in press). In parallel, solutions of the ICDH (III) dimer and of the ICDH (III) tetramer have been successfully prepared, allowing small angle neutron scattering measurements on each of these oligomeric species.

One sample of the ICDH (III) dimer, in 50mM Tris-HCl pH8 containing 0.1M NaCl, and another of the tetramer in the same conditions (for which both oligomeric species exist), were examined on KWS1. Considering the hyperthermophile nature of the enzyme, a significant question relates to the conformational state of Tm ICDH as a function of temperature, and, in particular, to the conformational state of the ICDH enzyme at physiological temperature. Hence, measurements were performed for 2 temperatures, 20°C and 70°C, using the wide range of scattering vectors of KWS1. Three other solvent conditions were also investigated for the dimer (ammonium sulphate, betain and trehalose), in order to see if there was a change in the conformational state of the enzyme due to high hydrophobic interactions. The experiments were performed with a wavelength of 7 Å. Three sample-to-detector distances (2, 4 and 8 m) were employed to cover a Q-range of 0.01-0.2 $Å^{-1}$. 2-D data were corrected pixel wise for instrumental background and detector efficiency, and radial averaged over the full detector.

Results

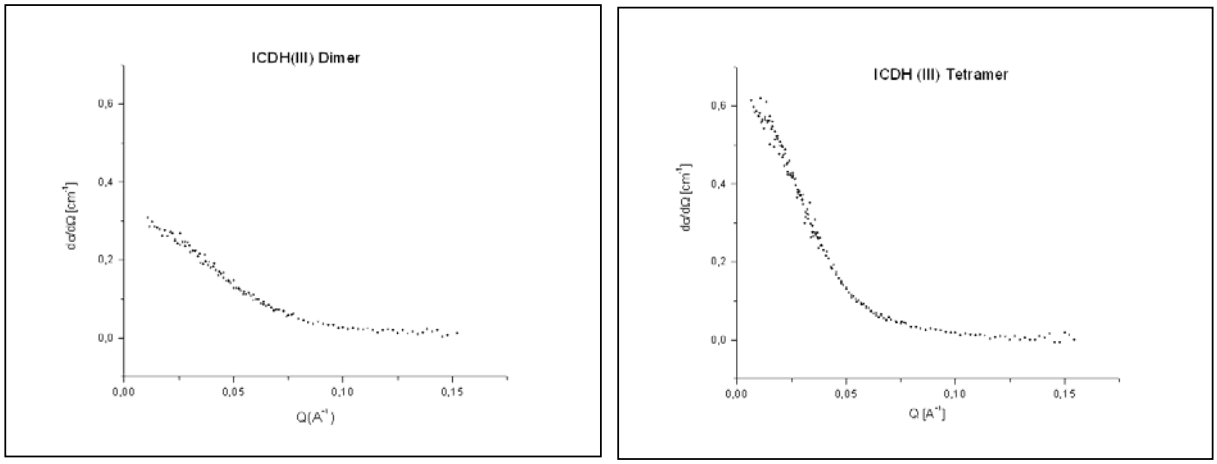


Figure 1. Q-dependence of the scattering cross-sections for the ICDH (III) dimeric (left) and tetrameric (right) states, in 50mM Tris-HCl pH8.

We reported in Figure 1 the Q-dependence of the scattering cross-sections for the Tm ICDH (III) dimer and tetramer, at 20°C. The radius of gyration for both oligomeric species was extracted from the small angle region: 30 Å for the dimer and 45 Å for the tetramer, which is in good agreement with the expected values calculated with the molecular weight.
No change in the conformational state appeared neither at the physiological temperature of the enzyme, nor when the dimeric enzyme was investigated in the other solvent conditions.

Currently, we are using the Svergun's suite of programs and the large angle scattering curves to model the tetramer conformation in terms of the dimer crystal structure.
From the large angle scattering curve of the tetramer, we obtained an average low resolution model for the tetrameric state. This experimental model is compared with the model calculated from both the dimer crystal structure and the large angle scattering curve of the tetramer.

References

[1] Steen IH, Madern D, Karlstrom M, Lien T, Ladenstein R, Birkeland NK. (2001) Comparison of isocitrate dehydrogenase from three hyperthermophiles reveals differences in thermostability, cofactor specificity, oligomeric state, and phylogenetic affiliation. *J Biol Chem.* 76(47):43924-31.
[2] Singh SK, Matsuno K, LaPorte DC, Banaszak LJ. (2001) Crystal structure of Bacillus subtilis isocitrate dehydrogenase at 1.55 A. Insights into the nature of substrate specificity exhibited by Escherichia coli isocitrate dehydrogenase kinase/phosphatase. *J Biol Chem.* 276(28):26154-63.
[3] Karlstrom M, Stokke R, Steen IH, Birkeland NK, Ladenstein R. (2005) Isocitrate dehydrogenase from the hyperthermophile Aeropyrum pernix: X-ray structure analysis of a ternary enzyme-substrate complex and thermal stability. *J Mol Biol.* 45(3):559-77.

Institut für Festkörperforschung
Forschungszentrum Jülich GmbH
D-52425 Jülich

Experimental Report
of Neutron Scattering Experiments
at the FRJ-2 Reactor

Proposal number:	KW1-05-046		
Experiment title:	Quaternary structure of a protein-RNA complex involved in nuclear export		
Dates of experiment:	11/12/2005-15/12/2005	Date of report:	20/03/2006
Experimental team: Names	Addresses		
Frank Gabel	European Molecular Biology Laboratory Meyerhofstrasse 1 D – 69117 Heidelberg Germany		
Local Contact:	Vitaliy Pipich		

Experimental report text body

Introduction:
In the experiment conducted at FRJ2 at the FZJ in December 2005, we proposed to record SANS data from a protein-RNA complex named "TAP-CTE" that is involved in the export of viral RNA from the cell nucleus to the cytoplasm [1]. Combined with SANS data of its individual components (isolated TAP and isolated CTE) and with NMR data, we are able to propose a low resolution model of the complex in solution (see Fig. 4 below).
The following samples were measured by SANS experiments on KWS1 at the C2D2 and the C4D4 detector-collimator configurations: Isolated CTE (in 100%H2O at a concentration of 5 mg/ml), isolated TAP (100% H2O, 10 mg/ml), TAP-CTE (0%, 42%, 70% and 100% D2O at 10 mg/ml). All samples were screened for aggregation at the C8D8 configuration. The normalized data sets (against plexiglas) were subtracted for the background scattering determined by the respective buffer runs using the raw data program PRIMUS [2]. The thus processed data sets were then evaluated further using the programs GNOM [3] and DAMMIN [4] in order to determine low-resolution envelopes of the components and the complex as a whole.

Results:
Figure 1 shows the logarithm of the normalized and buffer-subtracted scattering intensities of TAP-CTE at 100% H2O (in red) and TAP-CTE at 42 % D2O (in blue) as a function of the scattering vector s (in inverse nm). Figure 2 represents the low resolution model of the CTE (in red), obtained at the matching point of the protein (42% D2O) with DAMMIN. Superposed is a computer-generated atomic model in blue, based on the CTE base-pair sequence and homology models. The agreement is very good. The experimentally determined molecular weight of 21 kDa is in good agreement with the theoretically predicted one of 20 kDa. The radius of gyration of 23 Angstrom is also very reasonable.

Figure 3 shows a low-resolution model of the whole complex obtained at 100% H2O with DAMMIN from the experimental data. Its radius of gyration of 27 Angstrom and the molecular weight of 48 kDa (theoretical 50 kDa) are reasonable. Unfortunately, the experimental data at the protein matching point (70% D2O) did not provide a convincing low-resolution shape of TAP inside the complex, the radius of gyration and molecular weight being too large. A possible explanation may be the high D2O content in the buffer that is known to favor aggregation.

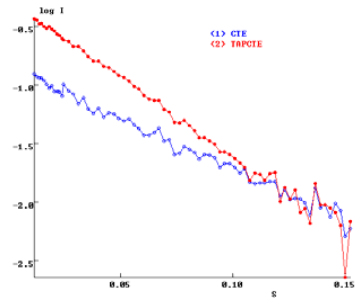


Figure 1

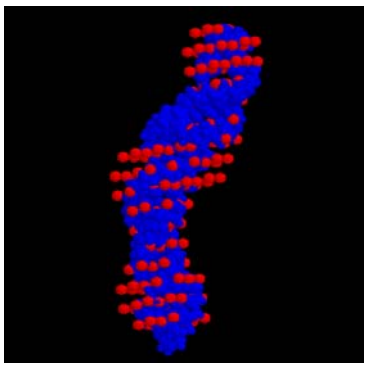


Figure 2



Figure 3

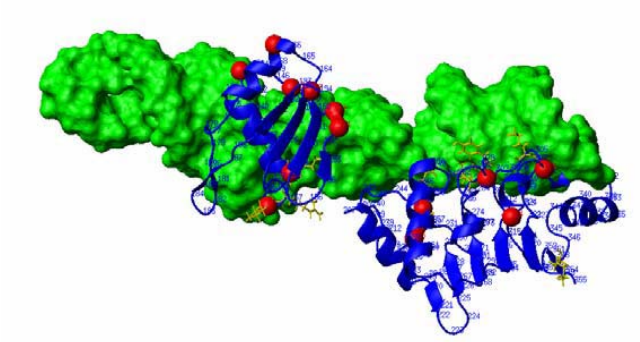


Figure 4

Figure 4 shows a model of the TAP-CTE complex based on the CTE model and the TAP crystal structure [1], optimized against the SANS data. In this model, NMR chemical shift perturbations, residual dipolar couplings and mutational data were equally taken into account. At the moment, we are optimizing the information provided by NMR.

References:

[1] Liker et al. (2000) *EMBO J.* **19**(21): 5587-5598.
[2] Konarev et al. (2003) *J Appl Cryst* **36**: 1277-1282.
[3] Svergun D (1992) *J Appl Cryst* **25**: 495-503.
[4] Svergun D (1999) *Biophys J* **76**: 2879-2886.

Institut für Festkörperforschung
Forschungszentrum Jülich GmbH
D-52425 Jülich

Experimental Report of Neutron Scattering Experiments at the FRJ-2 Reactor

Proposal number:	KW1-05-047, KW1-05-063, KW1-06-011, KW1-06-018		
Experiment title:	Chain conformation in novel, natural-synthetic hybrid block copolymers		
Dates of experiment:	11-13/11/05, 26-28/1/06, 15-16/4/06, 24-27/5/06	Date of report:	6th June 2006
Experimental team: Names	Addresses		
Dr. L.J.R. Foster [1,2] Dr. D. Schwahn [2] Dr. V. Pippich [2]	[1] Bio/polymers Research Group, School of Biotechnology and Biomolecular Sciences, University of New South Wales, Sydney NSW 2052, Australia. [2] Institut für Festkörperforschung, Forschungszentrum Jülich GmbH, 524425 Jülich, Germany		
Local Contact:	Dr. D. Schwahn		

Experimental report text body

Introduction Polyhydroxyalkanoates (PHAs) are a family of biopolyesters synthesized by a wide range of microorganisms. The most common of these biopolymers is Polyhydroxybutyrate (PHB), which has received considerable interest as an environmentally friendly bioplastic and as a biomaterial for biocompatible medical implantation devices. PHB however, is just one member of a family of biopolymers possessing in excess of 105 different monomeric components. These novel biopolymers have material properties ranging from the rigid and highly crystalline to flexible, rather amorphous and elastomeric *[1]*. Another member of interest is Polyhydroxyoctanoate (PHO). PHB and PHO are representative members of PHAs possessing short and medium chain length substituents in the side chain (*scl*PHA and *mcl*PHAs).

We have recently synthesised natural-synthetic hybrids of PHB and PHO by 'end-capping' hydrophobic PHA chains with hydrophilic diethylene glycol (PHB-DEG and PHO-DEG respectively) *[2]*. The family of PEGs has a wide range of members varying in molecular mass and structure. A number of biocompatible members have important biomedical functions such as organ and tissue preservation *[3]*. Material surfaces modified by covalent attachment of PEG chains are resistant to cell and protein adsorption *[4]*. During solvent casting PHA-PEG hybrids self-assembled into ordered microporous arrays *[5]*. These microporous films, by virtue of their biocompatible composition and morphology, have the potential to serve a range of biomedical and biotechnological applications.

The objective of this research is to elucidate the influence of the relatively small hydrophilic group in these hybrids on polymer chain conformation, with a particular reference to their ability to form microporous films. In this regard, a synthetic block copolymer: Polystyrene-*b*-polydimethylacrylate which forms highly ordered microporous films is used as a positive control. Thus, based on electron microscopy studies, the degree of organisation in microporous films increases in the following sequence: PS-PDMA > PHB-DEG > PHO-DEG.

Experimental We have applied SANS to investigate the conformation of polymer chains in solution with the purpose of investigating their ability, or lack thereof to self-assemble into microporous films. Complementing our studies of these polymers in solution we have also applied SANS to their melt-pressed and solution cast films. In the former we have also investigated the affects of temperature through the melt-phase (25-80°C).

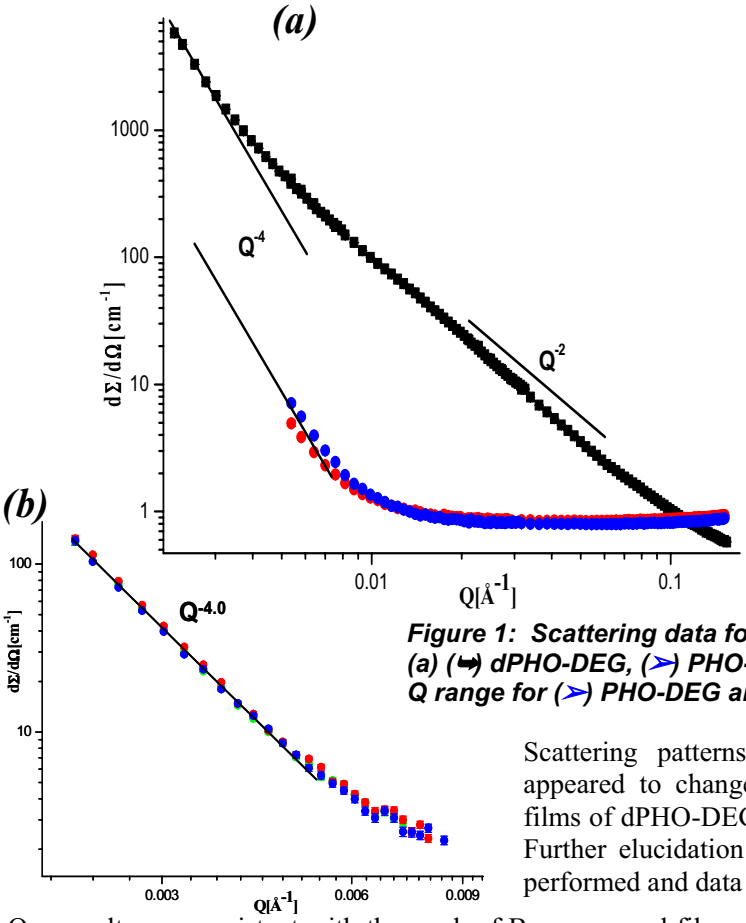


Figure 1: Scattering data for melt-pressed films at room temperature (a) (➥) dPHO-DEG, (➢) PHO-DEG and (➢) PHO. (b) enlargement of Low Q range for (➢) PHO-DEG and (➢) PHO.

Results & Discussion SANS analysis of melt-pressed films of PHO, PHO-DEG and dPHO-DEG were performed to determine incoherent background scattering and to investigate the possibility of any local organisation. Figure 1b reveals the scattering at low Q (Q^{-4}) which maybe associated with the chain organisation during processing such as lamellae. In contrast, the scattering pattern for dPHO-DEG, which consists of 80% deuterated PHO end-capped with protonated DEG, changed from Q^{-2} (Gaussian coils) at high Q to Q^{-4} in the low Q range. We can theorise that during the melt preparation process the DEG segments orientate themselves to form non-ordered thin 'platelet-like' structures (Figure 1).

Scattering patterns of PHO films generated during melting appeared to change little, however changes were apparent for films of dPHO-DEG over its melting point between 50 and 60°C. Further elucidation using a blend of PHO and dPHO has been performed and data is currently under analysis.

Our results are consistent with the work of Beaucage and films of PHB which also showed a power law of -2 *[6]*. Across the Q range examined, rather than a discrete transition regime between power law -2 and power law -4 scaling, the polymer displayed a gradual transition.

Thus, our results suggest end-capping of the hydrophobic PHA chains with a small synthetic hydrophilic group has an influence on polymer chain conformation during melt and solvent processing of the polymer into bioplastic films.

[1] Steinbüchel, A. In: Rehm H-J, Reed G, editors. Biotechnology. Weinheim, Germany: John Wiley & Sons, **1996**.
[2] Sanguanchaipaiwong, V; Gabelish, CL; Hook, J; Scholz, C. & Foster LJR. *Biomacromolecules* **2004**;5(2):643.
[3] Harris JM. Poly(ethylene glycol) chemistry: biotechnical and biomedical applications. New York, USA: Plenum **1992**.
[4] Inada Y, Matsushima A, Kodera Y, Nishimura H. *J. Bioact Compat Polym.* **1990**;5:343.
[5] Foster, LJR; Sanguanchaipaiwong, V; Gabelish, C. & Hook, J. *Polymer* **2005** 46(17):6587-6594.
[6] Beaucage, G; Rane, R; Sukumaran, S; Satkowski, MM; Schehtman, LA. & Doi, Y. *Macromolecules* **1997** 30:4158-4162.

Institut für Festkörperforschung
Forschungszentrum Jülich GmbH
D-52425 Jülich

Experimental Report of Neutron Scattering Experiments at the FRJ-2 Reactor

Proposal number:	KW1-05-048		
Experiment title:	SANS investigations of the amorphous layer on aragonite nacre platelets		
Dates of experiment:	31.10. – 03.11.2005	Date of report:	21.06.2006
Experimental team: Names	Addresses		
Helmut Cölfen	Max-Planck-Institute of Colloids and Interfaces Colloid Chemistry Am Mühlenberg 1 14476 Golm Germany		
Vitaliy Pipich Dietmar Schwahn	Institut für Festkörperforschung Forschungszentrum Jülich D-52425 Jülich / Germany		
Local Contact:	Vitaliy Pipich		

Experimental report text body

The aim of the present research was to understand the internal structure of aragonite plates extracted from nacre of the seashell *HaliotisLaevigata*. By HRTEM and solid state ^{1}H & ^{13}C-NMR, an amorphous layer of the calcium carbonate was observed. By SANS we measured a cleaned powder of the nacre in D_2O/H_2O mixtures of different D_2O-content and in air.

The scattering from the proteins inside the mineral is almost contrast-independent; the volume fraction, volume and mineral/protein contrast are constant. The radius and volume fraction of the bound proteins are 53Å and near 6%, respectively. The latter value is in agreement with 5% protein content from thermogravimetry. Blue and green lines are the preventative fitting curves of data by the Guinier law to highlight the bimodal distribution in system.

In Figure 2 the first ($Qd\Sigma/d\Omega(Q)$) and second ($Q^2d\Sigma/d\Omega(Q)$) moments of the scattering curve from Figure 1 are depicted showing clearly a bimodal distribution. The area under second moment is proportional to the volume fraction Φ and the scattering contrast $\Delta\rho^2$: $Q_2 = \int_0^\infty Q^2 d\Sigma/d\Omega(Q)dQ = 2\pi^2\Phi(1-\Phi)\Delta\rho^2$. The red lines represent a Gaussian fit of the first and second moment of the scattering within the intermediate Q-range (II); the green lines represent a lognormal distribution of the "bound" proteins. The ratio between first and second moment gives a chord-size $l_c = \pi Q_1/Q_2$.

In conclusion, we might have observed scattering from an amorphous layer of the aragonite calcium carbonate surface. From the ratio between first and second moment a dimension of the amorphous discs was calculated near 700Å.

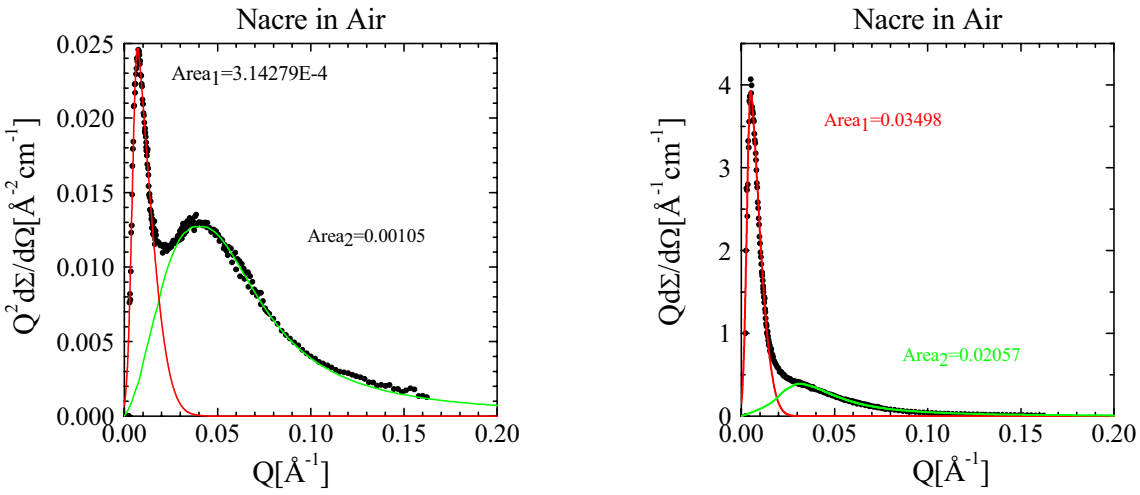


Figure 2. The second and first moment of the scattering curve of the nacre powder in Fig. 1.

Institut für Festkörperforschung
Forschungszentrum Jülich GmbH
D-52425 Jülich

Experimental Report
of Neutron Scattering Experiments
at the FRJ-2 Reactor

Proposal number:	KW1-05-049		
Experiment title:	New Zirconium based catalysts for living olefin polymerization		
Dates of experiment:	2005-11-03	Date of report:	2006-06-05
Experimental team: Names	 Addresses		
Aizhen Niu Jörg Stellbrink Jürgen Allgaier	Institut für Festkörperforschung, Forschungszentrum Jülich Institut für Festkörperforschung, Forschungszentrum Jülich Institut für Festkörperforschung, Forschungszentrum Jülich		
Local Contact:	Wim Pyckhout-Hintzen		

Experimental report text body

Coates et al. [1] reported a new stereoselective titanium complex for olefin polymerization. Upon treatment with methylaluminoxane (MAO), this complex was found to be active for the polymerization of propylene at 0°C in toluene. Unexpectedly the obtained polymer exhibited a narrow molecular weight distribution (M_w/M_n~1.1). The amazing point is that the first synthesis of high molar mass syndio-polypropylene-block-poly(ethylene-co-propylene) diblock copolymer (M_n= 145 100, M_w/M_n=1.12) was achieved, when a slight overpressure of ethylene was added to the reactor after formation of the living syndiotactic polypropylene. The living nature of the catalyst allows the synthesis of block copolymers previously unavailable from Ziegler-Natta catalysts. However, the kinetics and mechanism of living olefin polymerization is still poorly understood. On the basis of research experience and knowledge of living anionic polymerization of dienes and styrene, we plan to develop the combined time resolved NMR and SANS technique to the field of living olefin polymerization, discover the fundamental mechanism and kinetics of the living olefin polymerization.

In recent SANS experiments we investigated the living polymerisation of poly(hexadienes) using a Titanium catalyst/MAO activator. We found that this system shows some unexpected precipitation after mixing of the individual compounds at low temperatures. I.e. rigorous stirring is required for keeping the catalyst/co-catalyst complex in solution, which is a prerequisite for successful polymerisation. Unfortunately this is not possible in the SANS cell and in particular not in the NMR cell, so that an absolute calibration in terms of sample concentration was not achievable.

Therefore we used another catalyst system to avoid this solubility problem. The new catalyst system contains a Hafnium complex as catalyst and low molecular weight Boron hydride compounds as activator. In this experiment, catalyst, cocatalyst and monomer mixture was stored at -80˚C after sealed off in chemistry lab. Then it was warm up to 20˚C for the in-situ SANS measurement. Figure 1 shows that the polymerization is very fast at the beginning of the polymerization and the whole conversion of the monomer is only 40% after the polymerization finished.

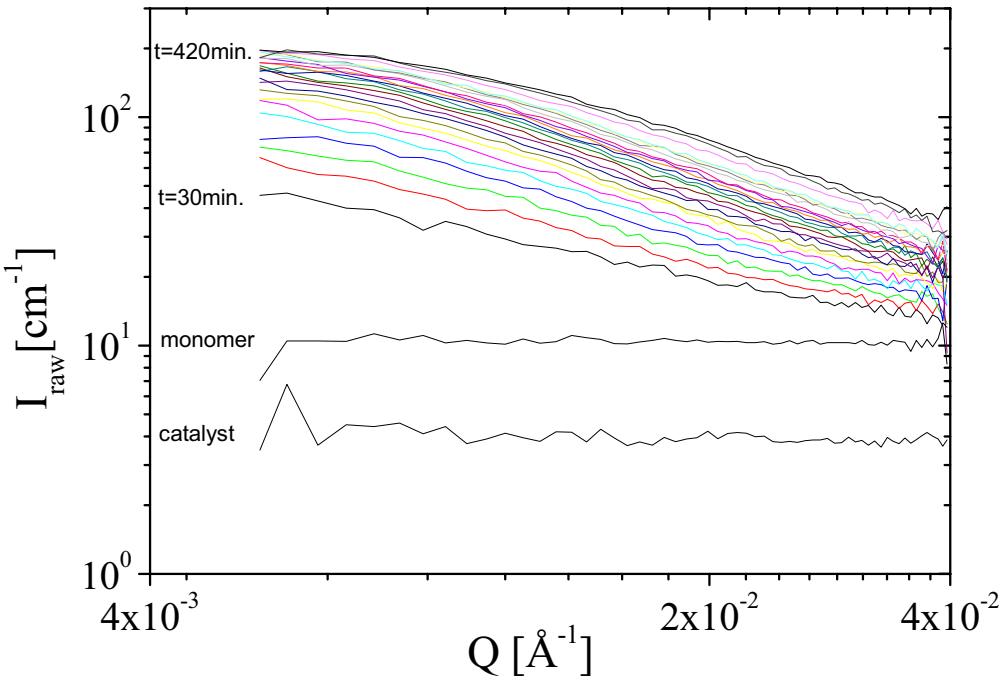


Figure 1: Metallocene catalysed Polymerisation of octene followed by real time SANS experiments at 20°C.

[1] J. Tian, P. D. Hustad, G. W. Coates, J. Am. Chem. Soc. 2001, 123, 5134.

Institut für Festkörperforschung
Forschungszentrum Jülich GmbH
D-52425 Jülich

Experimental Report
of Neutron Scattering Experiments
at the FRJ-2 Reactor

Proposal number:	KW1-05-050		
Experiment title:	**Highly turbid, highly efficient microemulsions with sticker polymers**		
Dates of experiment:	28.10.2005	Date of report:	21.03.2006
Experimental team: Names	Addresses		
Henrich Frielinghaus, Christian Frank, Simona Maccarrone, Martin Brodeck, Gaetano Mangiapia	Forschungszentrum Jülich GmbH, Institut für Festkörperforschung, D-52425 Jülich Forschungszentrum Jülich GmbH, Institut für Festkörperforschung, D-52425 Jülich Forschungszentrum Jülich GmbH, Institut für Festkörperforschung, D-52425 Jülich Forschungszentrum Jülich GmbH, Institut für Festkörperforschung, D-52425 Jülich Forschungszentrum Jülich GmbH, Institut für Festkörperforschung, D-52425 Jülich		
Local Contact:	Henrich Frielinghaus		

Experimental report text body

The initial inspection of microemulsions is done by phase diagram measurements. Usually the visual inspection of the turbidity and of birefringence allows the identification of basically all known phases. Especially the one-phase bicontinuous microemulsion is easily to determine in the neighborhood of two-phase regions. If the surfactant becomes more and more efficient – this can also be obtained by the addition of polymers – the bicontinuous microemulsion scatters light very strongly, and the strongly scattering one-phase state cannot be distinguished anymore from the two-phase state. The idea of this measurement was determination of the minimal surfactant content for efficiency boosted microemulsions by small angle neutron scattering (SANS). The efficiency of the non-ionic $C_{10}E_4$ surfactant was increased by a $C_{10}E_{100}$ sticker polymer with amounts of more than 10% relative to the total amphiphile. Sticker polymers with a short hydrophobic sticker and a normally long hydrophilic block have been approved to boost the efficiency of surfactants equally well compared with amphiphilic diblock copolymers. The initial idea of the SANS experiments was the direct observation of the Porod scattering of the demixing domains. The actual results gave us an indirect conclusion for some of the samples.

Two example measurements are shown in figure 1. At the lower temperature a for bicontinuous microemulsions typical correlation peak is observed at $Q = 0.005Å^{-1}$. This is not the case for the higher temperature. Since the temperature is the only change between the measurements, the sample formed a bicontinuous microemulsion at the lower temperature, and the sample was demixed at the higher temperature for the following reason: The amount of surfactant does not change and, therefore, allows to form domains of only one length scale. This length scale has been observed at the lower temperature.

The initially expected Porod behavior at lower scattering angles ($Q < 0.005Å^{-1}$) was not observed at the higher temperature since the Q-range was limited. This Porod behaviour of the macro-domains is to be distinguished from the Porod scattering of the micro-domains. The presence of surfactant always allows to form micro-

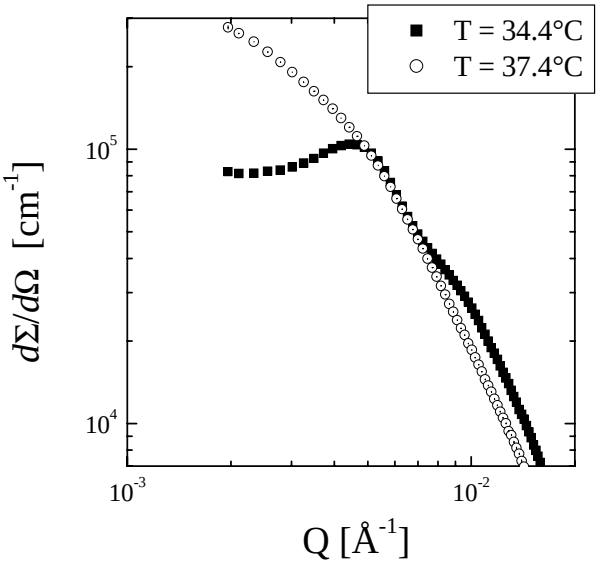


Figure 1: Macroscopic cross section as a function of the scattering vector Q of a turbid microemulsion at two different temperatures. At the lower temperature a correlation peak is found, which indicates a one-phase microemulsion. At the higher temperature the correlation peak is lost, and the microemulsion forms two phases. It should be mentioned that the transmission is 7%, and multiple scattering is an issue. For instance the shoulder at Q = 0.01Å^{-1} (34.4°C) is due to multiple scattering.

domains within macro-domains with enough surfactant. An extension to lower Q values was tried by the reduction of the wavelength to 9Å and 11Å for the lower temperature. Unfortunately, the correlation peak was strongly diminished due to the multiple scattering, and the whole measurement did not contain any useful information anymore. Already the in figure 1 presented measurements contain multiple scattering effects. The transmission was 7%, and a clear shoulder at Q = 0.01Å^{-1} was observed. Since no lamellar phase is expected, the double scattering of the correlation peak is the right explanation for the shoulder.

The remaining samples contained even less surfactant and therefore a correlation peak at even lower Q was expected. Due to multiple scattering at these even larger structures (the transmission was 2%) the correlation peak was not observable. Only a Porod behavior from the micro-domains was observed. At the higher temperature a similar scattering pattern as in figure 1 was obtained. For these other samples the indications of the bicontinuous microemulsion state and the two phase state are weaker as for the first sample. In a repetition of this experiment a much thinner sample (0.1mm) or a much lower contrast (D_2O/H_2O mixtures) would be desired in order to avoid multiple scattering and to allow measurements at even lower Q with longer wavelengths. At present we did not follow this suggestion since the extremely high polymer contents were not essential for the actual research. Nonetheless, the obtained technical knowledge will be used for applications in the future where polymers will allow an extremely high efficiency boosting. Then visual inspections will not yield the desired results, and only neutron scattering experiments with the right contrast or sample thickness can distinguish the different phases.

Institut für Festkörperforschung
Forschungszentrum Jülich GmbH
D-52425 Jülich

Experimental Report of Neutron Scattering Experiments at the FRJ-2 Reactor

Proposal number:	KW1-05-051		
Experiment title:	SANS investigation on the origin of the dynamic heterogeneity in poly(vinyl acetate).		
Dates of experiment:	10-01-2006 to 13-01-2006	Date of report:	05-06-2006
Experimental team: Names	Addresses		
1. Madhusudan Tyagi 2. Angel Alegria	Donostia International Physics Center, 20018, San Sebastián, SPAIN Física de Materiales, Facultad de química, Apdo. 1072, 20080 San Sebastián, SPAIN		
Local Contact:	M. Heinrich		

Experimental report text body

Poly(vinyl acetate) (PVAc) is a well known amorphous polymer which presents a series of curious experimental peculiarities[1]. We recently studied[2] PVAc using quasi-elastic neutron scattering (QENS), dielectric relaxation spectroscopy (DRS) and ^{13}C NMR. The characteristic times observed by QENS showed an anomalous dependence of momentum transfer, indicating the possible existence of heterogeneities in the system even at high temperatures. In addition, spin lattice relaxation times T_1 were found to be decoupled from dielectric characteristic times. Interestingly, all the carbon atoms (including in methyl group and carbonyl group) showed same temperature dependence of T_1 times indicating homogeneity at monomer level. Based on these results it was concluded that the dynamics of PVAc shows anomalous behaviour because of the heterogeneous dynamics even far above glass transition temperature. In order to go deeper into the problem recently, we made measurements on small molecule analog of poly(vinyl acetate) (trimer of vinyl acetate) using neutron spin echo[3], DRS and ^{13}C NMR. The decoupling of characteristic times between DRS and ^{13}C spin-lattice relaxation time reduced greatly because one does not expect heterogeneities to be present at high temperatures in small molecule glass formers. The purpose of this experiment was to look for any signs of corresponding structural heterogeneities in PVAc by measuring the static structure factor S(Q) and form factor P(Q) of PVAc in low-Q range. The static structure factor of PVAc was measured at three different temperatures viz. 336K, 377K and 413K. The form factor of PVAc in 90dPVAc/10hPVAc blend was also measured at the same temperatures. For this purpose, the detector positions were set at three distances, namely 2m, 8m and 20m to cover the Q range roughly between 0.003 and 0.16$Å^{-1}$. In addition, measurements were made with empty beam, with plexi glass and boron carbide for background and sensitivity of the detectors.

The corrected experimental data is shown in Figs.1 and 2. The abnormality in the data can be seen from the presence of so-called porod regime at low Q-values which might be a consequence of some air bubbles of micrometer size in the samples. Nevertheless, the actual data for the samples could be separated as porod regime has a well defined set of characteristics. The refined data does not show a clear peak in the structure factor (open symbols Fig.1). However, it shows a continuous increase in the low-Q regime which might be an indication of domains whose sizes are bigger than the spatial scales explored by SANS. However, the presence of porod regime makes it difficult to conclude anything conclusive from these measurements. On the other hand, the form factor of PVAc could be fitted to modified Debye form:

$$P(Q) = \frac{2}{(U+1)x^2}\left[(1+Ux)^{-1/U} - 1 + x\right]$$

where $U=(M_W/M_n)-1$ and $x=<R^2>Q^2/1+2U;$ when modified to polydispersity (M_W/M_n=2.5) of the sample. The resulting radius of gyration R_g changes from 91 to 96Å between the measured temperatures 336K and 413.

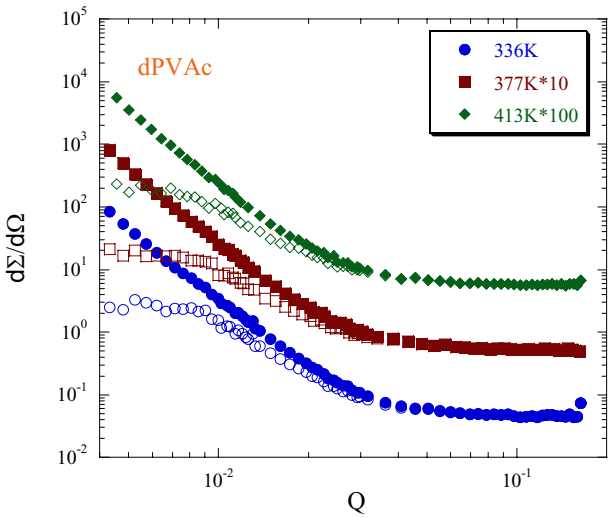


Fig.1: The scattering cross sections for dPVAc at measured temperatures. For the sake of clarity, actual data has been multiplied by 10 and 100 in case of 377K and 413K, respectively. The corresponding empty symbols show the data after making corrections for porod regime at low-Q values.

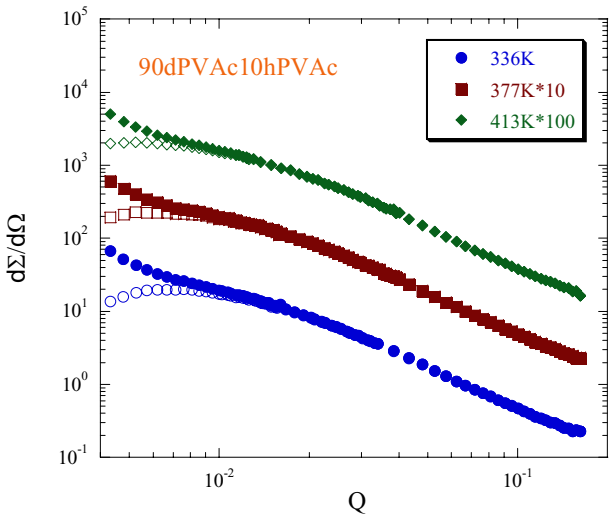


Fig.2: Scattering cross sections for 90dPVAc10hPVAc at different temperatures. For the sake of clarity, actual data has been multiplied by 10 and 100 in case of 377K and 413K, respectively. The corresponding empty symbols show the data after making corrections for porod regime at low-Q values.

References:

1. *1. F. Alvarez, A. Alegria, J. M. Alberdi and J. Colmenero, in Trends in Non-crystalline Solids, edited by A. Conde, C. F. Conde, and M. Millan (World Scientific, Singapore, 1991).*
2. *M. Tyagi, A. Alegria and J. Colmenero, Journal of Chemical Physics, Vol. 122, 244909 (2005).*
3. *A. Alegria, M. Tyagi and J. Colmenero, Dynamics of low molecular weight glass former in low-Q range by NSE. Report submitted to FRJ Juelich (proposal No. NSE-05-001).*

Institut für Festkörperforschung
Forschungszentrum Jülich GmbH
D-52425 Jülich

Experimental Report of Neutron Scattering Experiments at the FRJ-2 Reactor

Proposal number:	KW1-05-052		
Experiment title:	Aggregation behaviour of disk-shaped porphyrin catalysts		
Dates of experiment:	21-22 Jan. 2006	Date of report:	22-May-2006
Experimental team: Names	Addresses		
Van Hameren, Richard Feiters, Martin Elemans, Hans Rowan, Alan Nolte, Roeland	Institute for Molecules and Materials Radboud Universiteit Nijmegen Toernooiveld 1 6525 ED Nijmegen The Netherlands		
Local Contact:	Dr. Wim Pyckhout-Hintzen		

In Nature, porphyrins are abundantly applied, both as catalysts and chromophores. For example, manganese porphyrins are known to be able to catalyse epoxidation reactions. In this type of reactions, an oxygen atom is incorporated into the double bond of an alkene, yielding an epoxide (Figure 1)[1].

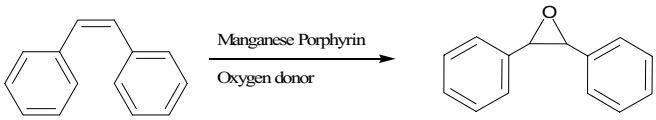


*Figure 1. Schematic representation of the epoxidation of cis-stilbene, catalysed by **1**.*

Recently, we have synthesised manganese porphyrin trimer **1** (Figure 2). In CD_2Cl_2 solution this molecule is expected to self-assemble in small columnar stacks[2]. Catalysis experiments involving the epoxidation of cis-stilbene by **1** have demonstrated that the addition of bidentate axial ligands, such as pyrazine and DABCO, to this catalyst during the reaction, changes the turnover frequency compared to the situation when they are absent. Surprisingly, we found that when the amount of DABCO or pyrazine was increased (0 → 3 eq. vs. **1**), an initial decrease in turnover number and an optimum at 2.5 equivalents of axial ligand were observed. We attribute this behaviour to a complicated interplay between the activation and related to that the reactivity of the catalyst, as well as changes in the stacking behaviour of the catalyst molecules. From literature it is known that the presence of nitrogen-based ligands can increase the catalytic reactivity,[1,3] and in addition, it is expected that upon their binding to the catalyst the stacking of **1** is either disfavoured or enhanced.
By means of SANS, we have investigated the stacking behaviour of **1** in CD_2Cl_2 as a function of the amount of axial ligand present (pyrazine or DABCO). In addition, we have investigated the influence of other chemicals used for the catalysis, e.g. mesitylene (internal standard) and *cis*-stilbene (substrate), on the stacking behaviour.

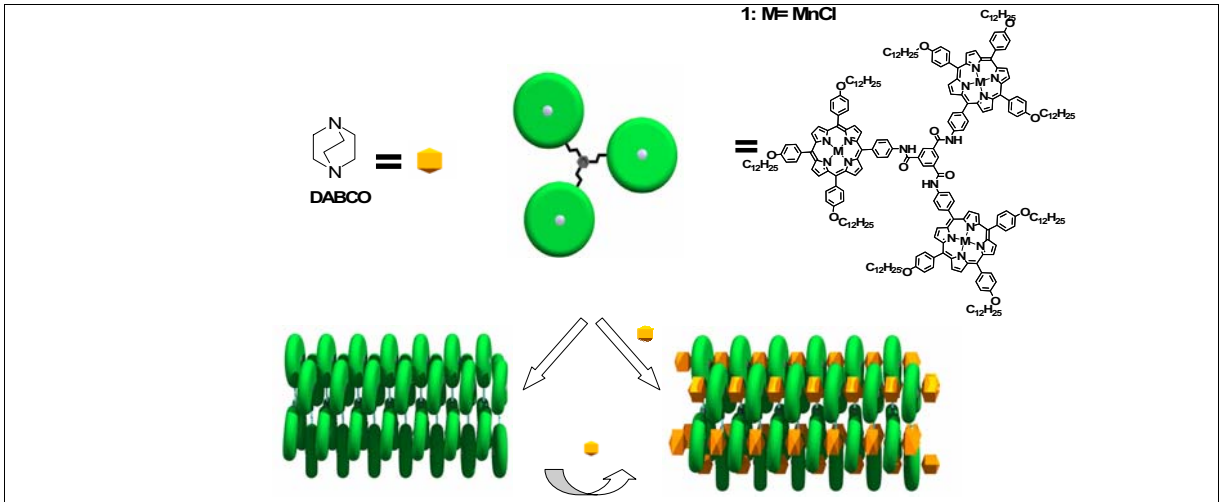


*Figure 2. Schematic representation of the formation of a supramolecular polymer stacks by **1** and the binding of DABCO within these stacks.*

The SANS measurements unambiguously demonstrated the presence of cylindrical particles in a solution of pure **1** in CD_2Cl_2 ([**1**] = 6.6μM), with a diameter of 2.3 nm, which is in excellent agreement with the diameter of the aromatic part of the molecule. The average length of the cylinders was 7.1 ± 0.1 nm, corresponding to approximately 14 molecules of **1**, assuming a distance between two molecules of 0.5 nm (molecular mechanics modelling, force field: MMFF94). Upon gradual addition of either pyrazine or DABCO to the solution, the diameter of the cylinder remains constant within experimental error, while the average length of the stack decreases (Figures 3A&B). Apparently, the binding of axial ligands competes with the stacking process, resulting in the formation of smaller stacks of **1**. The effect is somewhat more pronounced for the DABCO ligands, which might be related to a slightly smaller N-N distance in this compound as compared to pyrazine (N-N distance DABCO = 0.256 nm, pyrazine = 0.278 nm (Semi-Empirical calculations, parameters: PM3)).

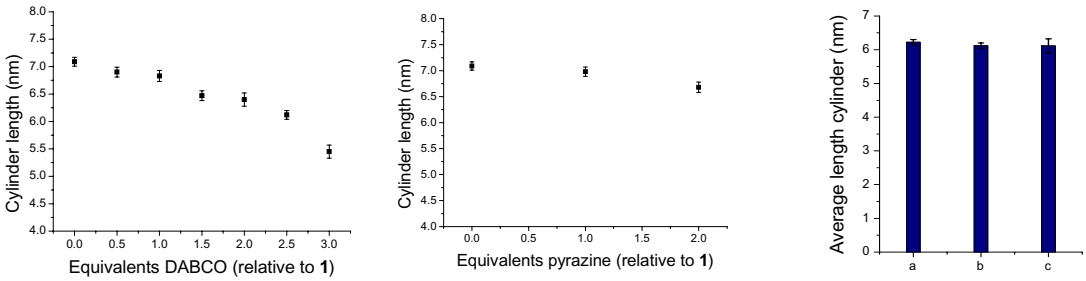


*Figure 3. Overview of the SANS-measurements. The average length of the stack decreases with both an increasing amount of DABCO (A) and pyrazine (B) and does neither change in presence of the mesitylene and cis-stilbene nor substitution of CH_2Cl_2 by toluene-D8 (C legend: a = toluene-D8, b = CD_2Cl_2, c = b + mesitylene + cis-stilbene) ([**1**] = 6.7 μM, 2.5 equivalents of DABCO).*

In addition, the SANS measurements demonstrated that neither a change in solvent from CD_2Cl_2 to toluene-D8, nor the presence of chemicals used for catalysis lead to a substantial change in stacking behaviour (Figure 3C).

1. A) A.N. de Sousa, M.E.M.D. de Carvalho, Y.M. Idemori, *J. Mol. Catal. A-Chem.*, **2001**, 1; B) A. W. van der Made, R. J. M. Nolte, W. Drenth, *Recl. Trav. Chim. Pays-Bas* **1990**, *109*, 537
2. M. C. Lensen, S. J. T. Van Dingenen, J. A. A. W. Elemans, H. P. Dijkstra, G. P. M. van Klink, G. van Koten, J. W. Gerritsen, S. Speller, R. J. M. Nolte, and A. E. Rowan, *Chem. Commun*., **2004**, 762.
3. Q. Z. Ren, J. W. Huang, X.B. Peng, L. N. Ji, *J. Mol. Catal. A-Chem.*, **1999**, 9.

Institut für Festkörperforschung
Forschungszentrum Jülich GmbH
D-52425 Jülich

Experimental Report
of Neutron Scattering Experiments
at the FRJ-2 Reactor

Proposal number:	KW1-05-054		
Experiment title:	The interaction of polypeptides with carbon nanotubes		
Dates of experiment:	07.03.-11.03.2006	Date of report:	05.06.2006
Experimental team: Names	Addresses		
COHEN, Yachin GRANITE, Merav	Department of Chemical Engineering, Technion, Haifa, ISRAEL 32000 Department of Chemical Engineering, Technion, Haifa, ISRAEL 32000		
Local Contact:	Dr. Wim Pyckhout-Hintzen		

Experimental report text body

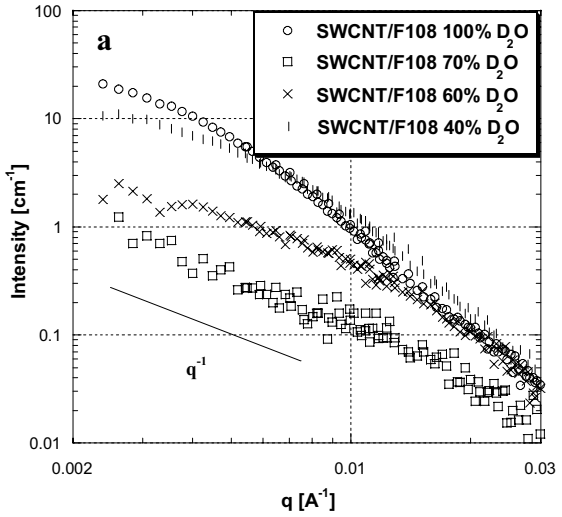
Background
Carbon nanotubes are known by their remarkable unique mechanical, optical, thermal and electronic properties. In production they tend to form bundles with different diameters and chirality, which results in diminishing of their unique properties. Many efforts have been made in order to separate bundles and form stable dispersions. Significant recent developments have been in the use of synthetic polypeptides ("un-natural proteins") for dispersing single-walled carbon nanotubes (SWCNTs) in water.

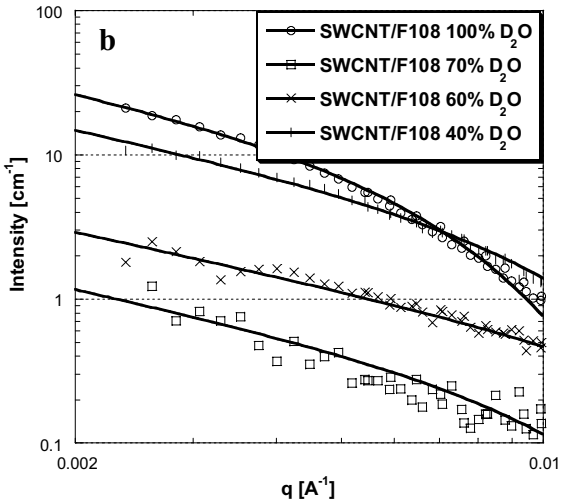
Objectives
The objective of this study is to understand the way polypeptides and block copolymers interact with the surface of SWCNTs and to elucidate the conformation of the polymer interacting with the nanotubes. Weather it is the "polymer wrapping" model, where the polymer is tightly wrapped about the nanotube surface or a rather loose adsorption so that the polymer coil surrounding the tubes form steric hindrance to re-aggregation.

Experiments
SANS measurements were conducted at KWS1 and due to the elongated feature of the carbon nanotube and the polymers around it the 20m sample-detector distance was required. Measurements of the bare polymer solutions, in different D_2O/H_2O mixtures, were conducted to ascertain the bare polymer conformation and scattering length density, they were followed by SANS measurements of the nanotube dispersions with contrast variation to evaluate the polymer conformation in the adsorbed state. Four polymers were studied: synthetic block copolymer of styrene (~5kDa) and sodium acrylate (~30kDa) (PSSA), a di-block copolymer of ethylene oxide and propylene oxide (Pluronic F-108), a synthetic oligo-peptide: poly (FFDD) [single letter notation: F=phenyl alanine, D = aspartic acid] with about 30 amino-acid units and Lysozyme.

Results

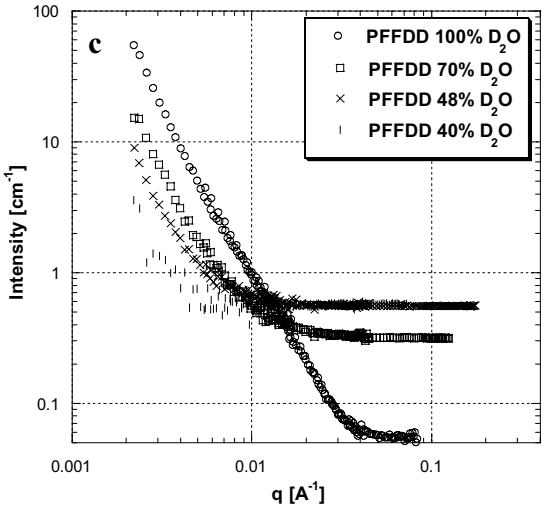
The scattering results of SWCNT/F-108 dispersions containing 0.5% (w/w) SWCNT and 5% Pluronic F-108 in four different D_2O/H_2O mixtures after subtractions are shown in figure (a) below. Figure (b) and the table below show the Guinier approximation for cylinder, $I(q) \sim q^{-1}\exp(-1/2\, r_c^2 q^2)$, and the cross-section radius of gyration (r_c) for different contrasts. The SANS pattern of SWCNT/F-108 in 60/40 D_2O/H_2O shows nearly a q^{-1} power law of I(q) as well as the smallest gyration radius, which may indicate a significant tight binding of the hydrophobic blocks to the nanotubes.

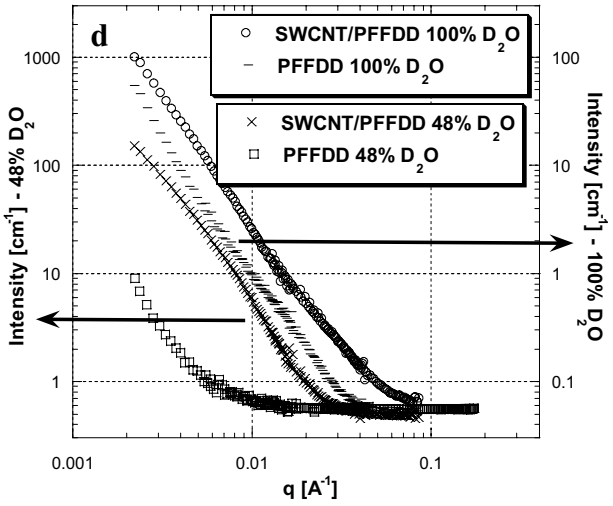




Guinier Cylinder Approximation					
% D_2O	Gyration radius (r_c)	% D_2O	Gyration radius (r_c)	% D_2O	Gyration radius (r_c)
100	200	80	205	60	67
90	189	70	120	40	125

The scattering patterns of the polypeptide (FFDD) containing 1% (w/w) in four different D_2O/H_2O mixtures and the results of SWCNT/poly (FFDD) dispersions containing 0.2% (w/w) SWCNT and 1% poly (FFDD) in two different D_2O/H_2O mixtures are both shown below in figures (c) and (d) respectively. It is very clear that the small amount of nanotubes increases the intensity at the low q range and presents an overlapping of intensity patterns at large q range. The bare polymer at 40% D_2O shows almost constant scattering which may indicate an almost matched contrast.





Institut für Festkörperforschung
Forschungszentrum Jülich GmbH
D-52425 Jülich

Experimental Report
of Neutron Scattering Experiments
at the FRJ-2 Reactor

Proposal number:	KW1-05-056		
Experiment title:	Microstructure Investigation of Porous Doped Graphites using Small-Angle Neutron Scattering		
Dates of experiment:	07.02.06 to 08.02.06	Date of report:	13.06.2006
Experimental team: Names	Addresses		
K. Mergia, K. Stefanopoulos	National Centre for Scientific Research "Demokritos" 15310 Aghia Paraskevi Attikis Greece		
Local Contact:	Martine Heinrich		

Experimental report text body

The aim of the project was to measure the pore microstructure in samples of doped and undoped graphites using the small-angle neutron scattering (SANS) technique. The samples have a porosity that varies from to totally closed to totally open. Closed porosity cannot be determined with the conventional methods and SANS is a powerful tool for determining the size distribution and volume fraction of porosity in nanoporous materials.

Carbon and graphite are attractive materials for high-temperature applications due to their high thermal conductivity, low electrical resistivity, high strength, high modulus, excellent thermal shock resistance and light weight. They are widely used as engineering materials, such as heaters, electrical contacts, high-temperature heat exchangers, rocket nozzles, plasma facing materials in fusion devices and leading edges of aircraft wings, etc. [1–3]. A main drawback of carbon-based materials is their chemical erosion under hydrogen bombardment which for plasma facing applications has to be avoided [4]. Doping of carbon with small amounts of certain elements is known to reduce chemical erosion. In addition, other properties such as high thermal conductivity and high thermal shock resistance can be also improved by doping of carbon. Some dopants show a catalytic degree on the graphitization, leading to a higher degree of graphitization.

For fabricating the doped graphite samples a self-sintering powder of mesophase carbon based on petroleum residues was used. The powder was jet-milled down to a mean particle size of the order of 1 μm. As dopants metallic carbides showing catalytic effect on the graphitization were used i.e. TiC and ZrC. The carbides were added to the carbon powder up to a metal concentration of ~4 at% [5]. The graphitization temperature employed was 2700 and 2750°C with a dwell time of 1 hour. After the graphitization process the doped materials were subjected to an additional hot isostatic pressing (HIP) step to obtain a higher densification.

Five samples of undoped and doped graphites were measured at room temperature using Small Angle Neutron Scattering. The existence of dopants influence the type and the extent of the porosity present in the samples during the fabrication process. As dopants TiC and ZrC were used.

The contrast matching technique was used in order to distinguish open from closed porosity using the adequate ratios of H20/D2O. All the samples were measured dry and wet.

In fig. 1 is shown the cross section versus the scattering vector of undoped graphite with 12.3% total porosity and 6.9% open porosity, measured dry (open circles) and wet (open squares). As it is expected the scattering is lower for the wet samples since in this case the scattering from the open pores is matched out with that of the matrix and only the scattering from the closed pores is revealed. In fig. 2 the cross section versus the scattering vector of TiC doped graphite with 10.5 % total porosity and no open porosity, measured dry (open circles) and wet (open squares). In this case the scattering from the wet and dry samples is almost identical as it would be expected since the sample has only closed porosity.

The treatment of the data is underway for the evaluation of the results.

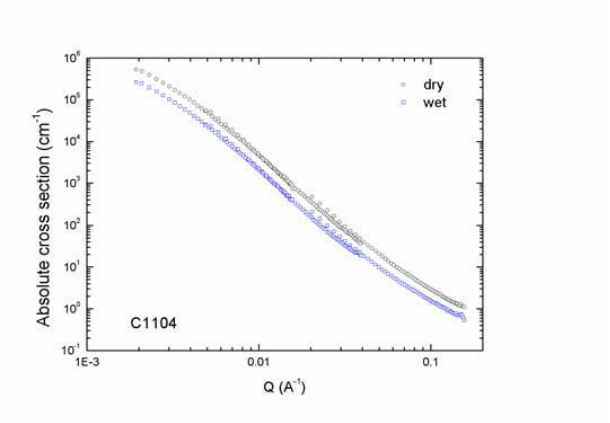


Fig. 1 Absolute cross versus scattering vector of undoped graphite with 12.3% total porosity and 6.9% open porosity, measured dry (open circles) and wet (open squares).

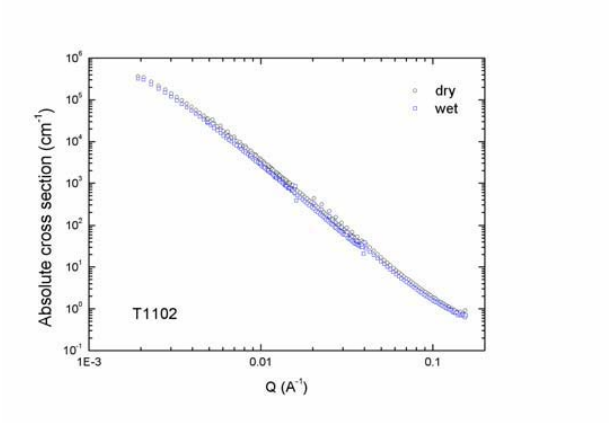


Fig. 2 Absolute cross versus scattering vector of TiC doped graphite with 10.5 % total porosity and no open porosity, measured dry (open circles) and wet (open squares).

References

[1] Fitzer E., Carbon 25 (1987) 163.
[2] Blazewicz S, Blocki J, Chlopek J, Godlewski J, Mickalowski J, Pakonski K, *et al*., Carbon 34 (1996) 1393.
[3] Qian JP, Liu X, Li PY., J Nucl Mater 191-194 (1992) 340.
[4] Federici G, *et al*., Nucl. Fusion 41 (2001) 1967.
[5] C. Garcia-Rosales, N. Ordas, E. Oyarzabal, J. Echeberria, M. Balden, S. Lindig, R. Behrish, J. Nucl. Mater. 307-311 (2002) 1282.

Institut für Festkörperforschung
Forschungszentrum Jülich GmbH
D-52425 Jülich

Experimental Report
of Neutron Scattering Experiments
at the FRJ-2 Reactor

Proposal number:	KW1-05-057		
Experiment title:	**Neutron scattering study of IKK kinase complex**		
Dates of experiment:	December 10 – 15, 2005	Date of report:	20.02.2006
Experimental team: Names	Addresses		
Xavier Lee [1], **Joseph DiDonato [1]** **Guiseppe Zaccai [2]**	1 Department of Cancer Biology, Cleveland Clinic Foundation, 9500 Euclid Avenue, Cleveland, Oh USA 44195 2 Institut de Laue-Langevin, Avenue de Martyrs, 38042, Grenoble, France		
Local Contact:	Dr. Dietmar Schwahn		

Experimental report text body

Results

IKK kinase complex is an important unity in signal transfer in living cells. IKK complex is consisted of three components, for IKKα, IKKβ and IKKγ. During the experiment in Juelich we tried to study the three components separately. Based on the results we obtained in July 2005 at ILL, Grenoble, IKKγ forms a trimer in solution. The structure is extremely compact with a Rg of 28 Å for a molecular weight (M.W.) of 150 Kda compared with hemoglobin with a Rg of 26 Å for a M.W. of 62 Kda. Hemoglobin is considered as a regular protein molecule in terms of its folding. Biochemical evidence indicates the trimer formation is not due to the concentration effect but natural phenomena. To further study the monomer structure and the regulatory role of the IKKγ we have expressed the IKKγ in two parts. The 'front part' (FE) is consisted of two third of the molecule and the 'back part' (BE) of one third of the molecule. With the scattering curves of these two parts of IKKγ we obtained the models of the FE and BE of the molecule. They both formed dimmers in solution. However, if we put them together they formed a monomer with a distinct structure obtained based on the scattering curve. During our experiment at ILL we experienced a serious technical problem for IKKα as well as for IKKβ. They aggregated in solution. We tried using various additives such as high salt, detergents and even IKKγ, still we failed to break down the aggregates. In Juelich we found a way to break down the aggregates through the use of 1M of urea. This concentration of urea keeps the biological activity of these two components intact. This new finding helped us to obtain a preliminary model of IKKβ which is consistent with biochemical evidences. All this information is very interesting because so far there is no any structural information on this complex. The results are also quite exciting because they are complimentary to what we had known before in terms of the biological activities. The neutron scattering experiment opens up a horizon for further structural studies of the complex. At this stage for such a huge complex only neutron scattering can offer us useful information on the relationship between structure and function.

Problems

During our December 2005 experiment in Juelich we encountered the following problems:

1) The samples of FE and BE of IKKγ had contamination of higher molecular weight aggregates. Therefore, the Rg calculated based on the final model was more than twenty percent lower than the Rg based on the Guinier approximation.
2) The samples of IKKα and IKKβ formed aggregation which could not be broken up using high salt, detergents and other biochemical reagents except for 1 M urea. The sample still kept its activity in 1 M urea. During the experiment we had used almost twenty percent of the beam time to find out this phenomenon which we did not know before the experiment.
3) We know based on the biochemical evidence that front end of IKKγ interacts with IKKα and IKKβ. This is considered as the key interaction for the regulatory role of IKKγ. Because of time limit we could only confirm that the interaction existed in our last experiment but we did not have time to collect data for the modeling.
4) The concentration of our sample IKKα and IKKβ were too low (around 1mg/ml) for the data collection. Therefore the model we obtained needed to be confirmed using higher concentration of the same protein.

Future Prospect

Based on these problems we need to continue our efforts trying to deal with all these problems so that we can obtain precise results and more accurate models of the complex.

Acknowledgement

We would like to thank the Forschungszentrum in Juelich for the success of our experiment. As usual the Forschungszentrum offers us the excellence of instrumentation, experienced and efficient local contacts as well as friendly atmosphere for our experimental success.

Institut für Festkörperforschung
Forschungszentrum Jülich GmbH
D-52425 Jülich

Experimental Report of Neutron Scattering Experiments at the FRJ-2 Reactor

Proposal number:	KW1-05-058, KW1-06-012, KW1-06-022		
Experiment title:	Thermal composition fluctuation in the PEO/PMMA blend		
Dates of experiment:	05.12. – 07.12.2005 11.03. – 13.03.2006 27.04. – 01.05.2006	Date of report:	31.05.2006
Experimental team: Names	Addresses		
K. Niedzwiedz, A. Wischnewski, D. Richter D. Schwahn, V. Pipich	Institut für Festkörperforschung Forschungszentrum Jülich D-52425 Jülich Germany		
Local Contact:	V. Pipich		

Experimental report text body

Thermal composition fluctuations in the binary PEO/PMMA blend were investigated for five different compositions of PEO homopolymer Φ_{PEO}=0.1, 0.25, 0.35, 0.5 and 0.75. The scattering signal was measured heating from room temperature to 160°C and afterwards cooling down with temperature steps of 5K. A hysteresis effect was observed only for the sample with 0.35 PEO content, where the glass transition and crystallization temperature are close. Below the crystallization temperatures the scattering intensity increases by more than two orders of magnitude. In the phase diagram (Figure1) the crystallization temperatures are depicted by black triangles.
Scattering curves for three concentrations (cooling down) are plotted in Figure 2 by filled squares. The scattering cross-section $d\Sigma/d\Omega(Q)$ was analyzed by the random phase approximation (RPA)

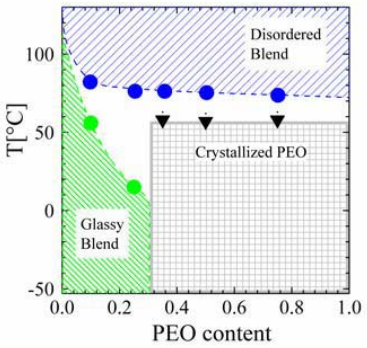


Figure 1. Phase diagram.

$$\frac{1}{d\Sigma/d\Omega(Q)} = \frac{N_a}{\Delta\rho^2}\left\{\frac{1}{\Phi_{PEO}V_{PEO}P_{PEO}(QR_g^{PEO})} + \frac{1}{\Phi_{PMMA}V_{PMMA}P_{PMMA}(QR_g^{PMMA})} - 2\frac{\chi}{V_0}\right\} \quad (1)$$

with Φ volume fraction, V molecular volume, P(Q) Debye function, Rg the radius of gyration, $V_0 = \sqrt{V_{PEO}V_{PMMA}}$ the reference molecular volume, and χ the interaction parameter. In Figure 2 red lines correspond to the fits of the experimental data by Eq. (1) with χ and R_g^{PEO} as adjustable parameters.

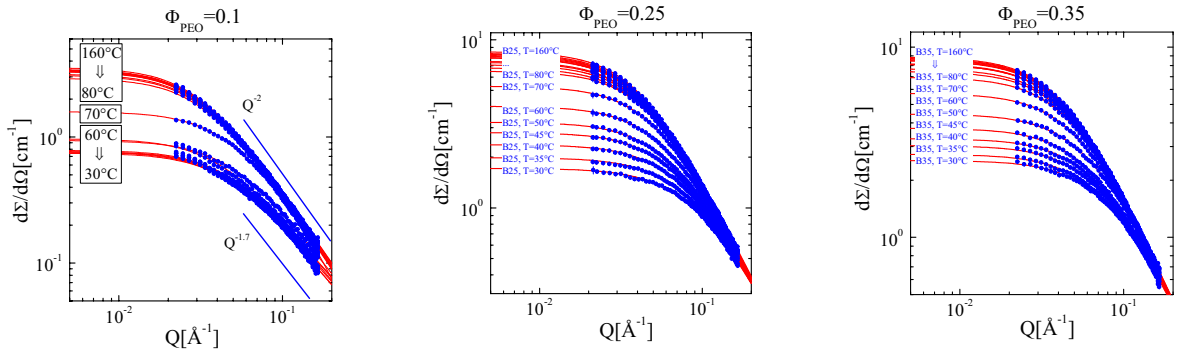


Figure 2. Scattering profiles of Φ_{PEO}=0.1, 0.25 and 0.35.

In Figure 3 the interaction parameter is plotted as a function of the inverse temperature for three characteristic compositions. Below Φ_{PEO} =0.3 no crystallization was observed; but the temperature dependence of χ shows three characteristic temperature regimes: (a) "real" disorder (T>85°C), where χ is a weak function of temperature (lower critical separation temperature is above 600K); (b) "real" glassy blend (T<56°C), where composition fluctuations are completely frozen; (c) intermediate temperature range (85°C<T<56°C), where interaction parameter becomes "strongly" negative. A strong suppression of the interaction parameter (forward scattering) was observed for all samples. On the phase diagram (Figure 1), temperatures, where the χ-parameter changes behavior, are plotted by blue circles.

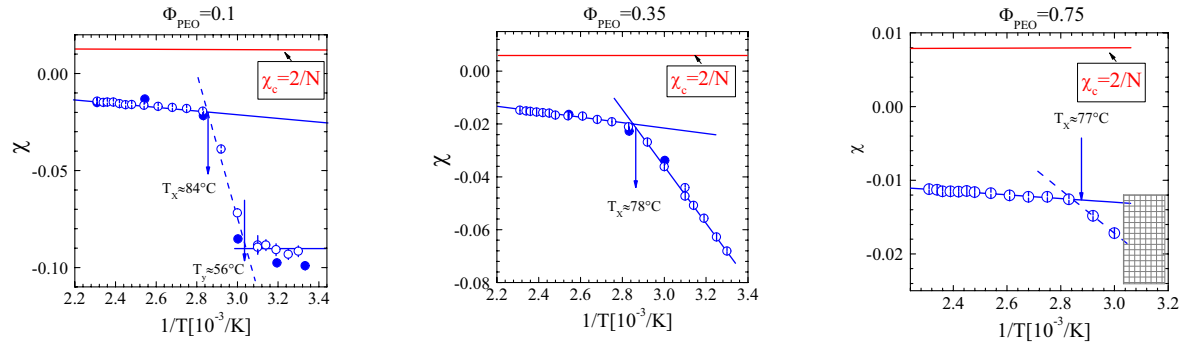


Figure 3. Interaction parameter χ as function of the inverse temperature: Φ_{PEO}=0.1, 0.25 and 0.75

The blue circles in Figure 4 represent the PEO-PMMA interaction parameter as a function of PEO-content at T=90°C. The χ-parameter is negative for all concentrations. A negative sign of the χ-parameter means that PMMA-PEO interactions are preferred with respect to the PMMA-PMMA and PEO-PEO ones. The huge difference between χ and the critical interaction parameter χ_c (red circles) confirms the remoteness of the critical separation temperature.

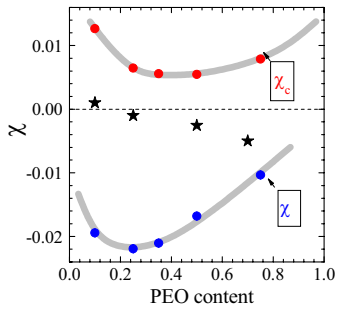


Figure 4. Interaction parameter χ vs. PEO content.

In conclusion, during these proposal periods we obtained the phase diagram of the binary polymer blend PEO/PMMA by SANS: crystalline and glassy boundaries were guided; temperature and concentration dependences of the interaction parameter and radius of gyration of PEO-chain were obtained by RPA analysis of SANS data.

Institut für Festkörperforschung
Forschungszentrum Jülich GmbH
D-52425 Jülich

Experimental Report
of Neutron Scattering Experiments
at the FRJ-2 Reactor

Proposal number:	KW1-05-059		
Experiment title:	New Hafnium based catalysts for living olefin polymerisation – Characterisation of final products		
Dates of experiment:	2005-12-1,2,3	Date of report:	2006-06-04
Experimental team: Names	Addresses		
Aizhen Niu Jörg Stellbrink Jürgen Allgaier	Institut für Festkörperforschung, Forschungszentrum Jülich Institut für Festkörperforschung, Forschungszentrum Jülich Institut für Festkörperforschung, Forschungszentrum Jülich		
Local Contact:	Wim Pyckhout-Hintzen		

Experimental report text body

Coates et al. [1] reported a new stereoselective titanium complex for olefin polymerization. Upon treatment with methylaluminoxane (MAO), this complex was found to be active for the polymerization of propylene at 0°C in toluene. Unexpectedly the obtained polymer exhibited a narrow molecular weight distribution (M_w/M_n~1.1). The amazing point is that the first synthesis of high molar mass syndio-polypropylene-block-poly(ethylene-co-propylene) diblock copolymer (M_n= 145 100, M_w/M_n=1.12) was achieved, when a slight overpressure of ethylene was added to the reactor after formation of the living syndiotactic polypropylene. The living nature of the catalyst allows the synthesis of block copolymers previously unavailable from Ziegler-Natta catalysts. However, the kinetics and mechanism of living olefin polymerization is still poorly understood. On the basis of research experience and knowledge of living anionic polymerization of dienes and styrene, we plan to develop the combined time resolved NMR and SANS technique to the field of living olefin polymerization, discover the fundamental mechanism and kinetics of the living olefin polymerization.

In recent SANS experiments we investigated the living polymerisation of poly(hexadienes) using a Titanium catalyst/MAO activator. We found that this system shows some unexpected precipitation after mixing of the individual compounds at low temperatures. I.e. rigorous stirring is required for keeping the catalyst/co-catalyst complex in solution, which is a prerequisite for successful polymerisation. Unfortunately this is not possible in the SANS cell and in particular not in the NMR cell, so that an absolute calibration in terms of sample concentration was not achievable.

Therefore we used another catalyst system to avoid this solubility problem. The new catalyst system contains a Hafnium complex as catalyst and low molecular weight Boron hydride compounds as activator. In the reactor period 2005/08 we performed first test experiments on that system and were able to follow a polymerisation in real-time by insitu-SANS.
Meanwhile we have terminated the polymerisation, cleaned and dried the resulting polymer and characterised it by standard techniques (GPC, NMR). Now the polymer has to be characterised by SANS too, in particular in terms of its radius of gyration, R_g, to allow a quantitative interpretation of the previously performed insitu experiments. Therefore we need to investigate a concentration series in dilute solution (4 concentrations $\leq$ 0.5 Vol.- %, Zimm-analysis). The molecular weight of the final polymer is approximately 100 000 g/mole.

[1] J. Tian, P. D. Hustad, G. W. Coates, J. Am. Chem. Soc. 2001, 123, 5134.

Institut für Festkörperforschung
Forschungszentrum Jülich GmbH
D-52425 Jülich

Experimental Report
of Neutron Scattering Experiments
at the FRJ-2 Reactor

Proposal number:	KW1-05-061		
Experiment title:	Conformation of a cyclic polystyrene within a linear blend in entangled state: characterization of strain dependence		
Dates of experiment:	18.01. – 19.01.2006	Date of report:	17.05.06
Experimental team: Names	Addresses		
Michael Kapnistos Wim Pyckhout-Hintzen	Forth, Crete FZJ		
Local Contact:	Wim Pyckhout-Hintzen		

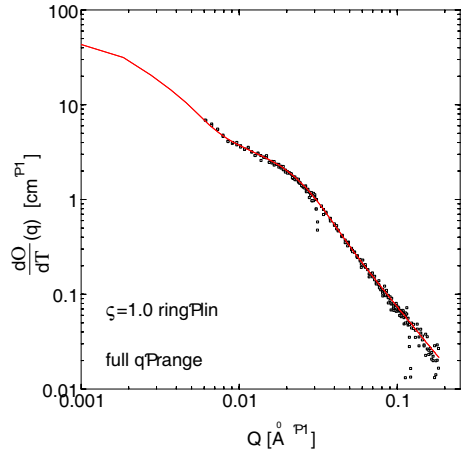
Experimental report text body

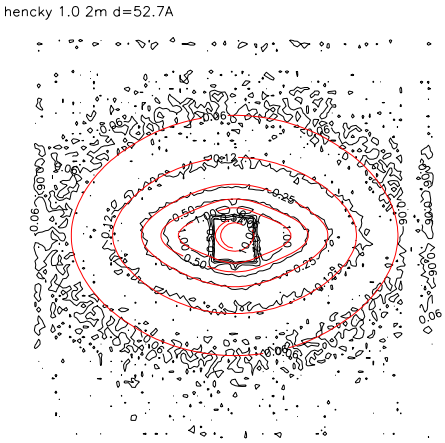
SANS studies on a blend of linear polystyrene with a ring-architecture polystyrene were started and in a first stage the deformation behaviour of the ring was studied. The results are to be compared with pure linear blends and linked to the un-usual rheology of ring-linear blends. Samples were stretched in a filament stretching rheometer to hencky strains up to 2 i.e. 700% of deformation. The scattering of a deformed ring with tube confinement was described as for simple linear polymers but modified for the architecture – deformed tube axes with segmental fluctuations – and fits of the full 2d detector could be obtained with only 1 single structural parameter, i.e. the tube diameter. The tube diameter is about 78A for 170% strain (λ = final_length/initial_length=2.7) (compare to d(rheology)= 90A) and decreases to 54 and 50A for deformation ratios λ of 4.5 and 7.4. The tube diameter does not seem to be deformed as in the case of polyisoprene. As the ring is 1% in linear, we see the single ring characteristics.

The anisotropic patterns can be calculated in terms of the components along the principal strain axes and the direction cosines e.g. if the strain is parallel to the x-axis, and ϕ is the angle between the strain axis (x) and a direction of the scattering vector q such that qx= q cos ϕ and qy= q sin ϕ. A linear tube-constrained structure factor ,

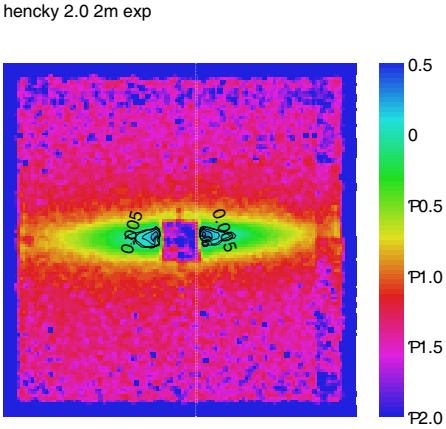
$$S(q,\lambda) = 2\int_0^1 d\eta \int_0^{\eta} \prod_{x,y,z} \exp(-(qR_g\lambda)^2(\eta-\eta') - (qR_g)^2(1-\lambda^2)\{\frac{d^2}{2\sqrt{6}R_g^2}(1-\exp(-\frac{(\eta-\eta')}{\frac{d^2}{2\sqrt{6}R_g^2}}))\}$$

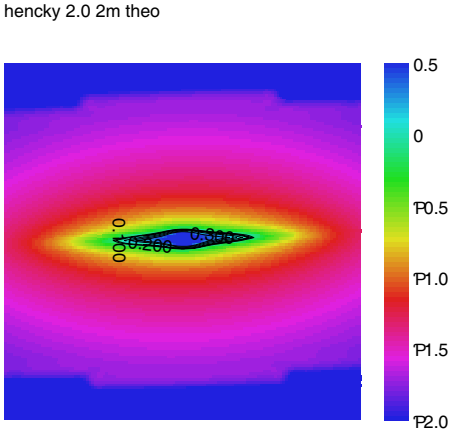
can be generalized for the case of a ring.





left: isotropic ring scattering + parasitic low scattering. right: deformed ring to lambda=2.7 with full 2d-fit, stretching direction is along vertical direction





left: experimental scattering at lambda=7.4 effect of 2d-resolution become clear.

right: best fit. The anisotropy is perfectly matched and

The scattering at low q is due to impurities which are well separated from the ring scattering and allow a perfect determination of the necessary parameters. The modelling of this parasitic scattering was done using a Beaucage powerlaw approach for 2d anisotropic data and it was tested whether the choice of this modelling would lead to different parameters of the ring structure or are identical if the lowest q data are left out.
It showed that the same results are retrieved and therefore the situation is of well separated character. This is the first examination of ring segmental parameters at all and a correlation with rheological data could be started.

Institut für Festkörperforschung
Forschungszentrum Jülich GmbH
D-52425 Jülich

Experimental Report
of Neutron Scattering Experiments
at the FRJ-2 Reactor

Proposal number:	KW1-05-062		
Experiment title:	Structural studies on the polymer coil relaxation of (linear polystyrene) after exposure to elongational flow		
Dates of experiment:	17.01. – 18.01.2006	Date of report:	14.05.2006
Experimental team: Names	Addresses		
Nielsen, Jens Pyckhout-Hintzen, W	Univ. Copenhagen and Risoe, DK Institut für Festkörperforschung, Forschungszentrum Jülich		
Local Contact:	W. Pyckhout-Hintzen		

Experimental report text body

At Riso an elongational flow rheometer was designed, that allows for a controlled elongational flow of constant elongation rate up to a total macroscopic stretch factor $\lambda = \exp(\dot{\varepsilon}t) \approx 40$ where t is the time of flow. The possibility to attain of such high stretch factors for well nearly monodisperse linear polymer melts is new and the measurements of stress alone have had a number of important consequences for our theoretical understanding of polymer dynamics. Moreover preliminary SANS experiments have revealed that the coil stretching under such conditions are more than 50% of the fully extended tube when exposed to elongation rate of $\dot{\varepsilon}$=0.1 s^{-1} .

A recent modification to our rheometer allows us to stop the flow abruptly within the centre of the sample, dynamically controlling the sample diameter in a electronic feed-back loop. Using the time-temperature superposition this gives access to controlled pseudo-real-time relaxation studies with high resolution within time ranges from well below the Rouse time to far beyond the reptation time. Preliminary stress-relaxation function has already been measured in such experiments, and will be measured as well for all the samples used in the SANS experiments.

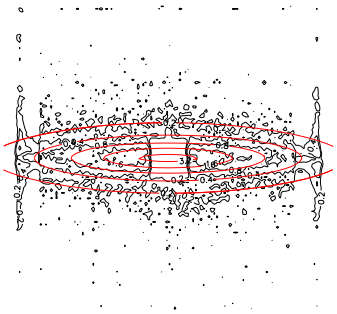
For the SANS studies the polystyrene samples are quenched well below the glass temperature within time scales much lower than the Rouse time. To eliminate possibly fast relaxation near the chain ends, only the centre part of the polymer chains are deuterium labelled which gives us further a length scale more easily accommodated by the SANS facility.

The results are expected to provide new information on the relaxation of linear polymer chains from a well defined but highly stretched initial state. In particular the results enable the testing of the classic separation of relaxation into a fast mode of relaxation of stretch along a primitive path (by Rouse dynamics) and a slow relaxation of orientation of effective tube elements (by reptation) as was seen recently by Blanchard et al in a polyisoprene system.

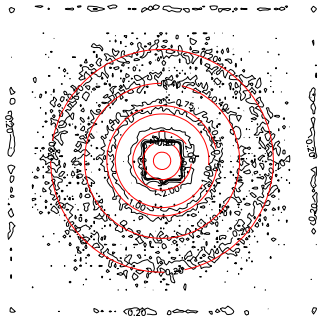
Experimentally, the investigation was very difficult as the resulting samples after stretching in the rheometer were very thin and needle-like centrally where the beam is placed. Special diaphragms were made of 8mm slit length and width of 0.5mm to cover the whole sample. Counting rates were as low as 20cps at low q and never reached more than 500 cps at high q. Therefore, it puts an enormous strain on the machine in that all additional corrections from backgrounds and collimation must be known accurately. It proved that the smallest q's were not fittable and only high q are available of average quality.

The purpose of the experiment – to analyze the radius of gyration in the highly non-linear state and the tube diameter of the chain – was not completely reached as the high q data both are sensitive to the strain of the chain as well as primarily the segmental fluctuations. It would have been fruitful to obtain former strain dependence from small q fittings and keep it constant for the determination of the diameter which itself could be strain dependent by the way. The evolution of the anisotropy is clear, however, and more external information e.g. for the microscopic strain are needed to yield the full parameter set.
More-over, the scattering on the deformed pure triblocks in order to gain intensity and to take profit from the sensitivity of a correlation hole effect to strain were also not ideal as the expected peaks did not show up due to several possible reasons: polydispersity in the blocks, degradation due to the very stringent conditions of preparation to give mixtures of labelled components.

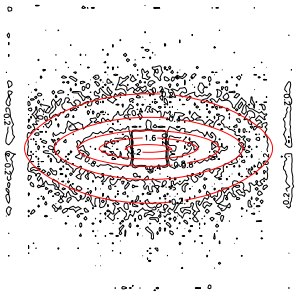
Therefore a final evaluation of the data is not yet possible and awaits combination with other techniques.
Some preliminary data fittings are shown here: on the left, the 0s data (virtually no relaxation) are described using the Warner-Edwards model with tube diameter 26A which is much lower than the isotropic one from the plateaumodulus. On the right, the relaxed sample with t=350s shows increased isotropy and is fairly well described by roughly a double diameter, i.e. 72A. Compared in the middle is a 2D fitting of the isotropic set with a Debye curve from which the reference Rg was extracted.



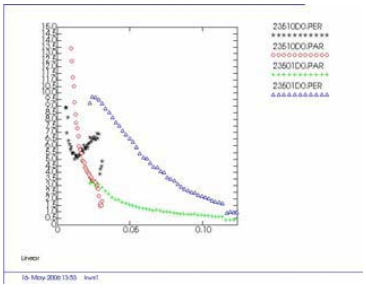
0 s



iso



350 s



Pure triblock peaks: besides resolution effects, an unexpected upturn at q~0.01 is visible which is a signature of impurities or degradation..

Institut für Festkörperforschung
Forschungszentrum Jülich GmbH
D-52425 Jülich

Experimental Report
of Neutron Scattering Experiments
at the FRJ-2 Reactor

Proposal number:	KW1-05-064		
Experiment title:	Hierarchical structure of silica and Carbon Black 2		
Dates of experiment:	15.01. – 17.01.2006	Date of report:	01.06.2006
Experimental team: Names	Addresses		
G. J. Schneider V. Vollnhals D. Göritz	Institut für Physik Universität Regensburg 93040 Regensburg Gerald.schneider@physik.uni-regensburg.de		
W. Pyckhout-Hintzen	Institut für Festkörperforschung, Forschungszentrum Jülich		
Local Contact:	Dr. W. Pyckhout-Hintzen		

Experimental report text body

1. Abstract

Carbon Black is the most important filler in tire industry. However the correlation between structure and mechanical properties of the filled elastomers has not been understood up to now. The purpose of this report is to show discrepancies between the results of neutron scattering experiments and the structural parameters described by industrial norms.

2. Introduction

Carbon Black is the filler of choice to improve the properties of elastomers. Nowadays different Carbon Blacks are distinguished by industrial norms (ASTM classification). For the purpose of a short overview tab.1 summarizes some characteristics for the Carbon Blacks N 326, N 330, N 339 and N 375. For efficient development of fillers for rubbers the linkage from structure, described by the norms, to the improvement of mechanical properties is of large interest. The purpose of this report is to show the difference between the parameters listed in tab. 1 and the structure of the Carbon Blacks determined by neutron scattering experiments.

4. Experiment and Theory

By measuring the scattered intensity as a function of scattering length q ($q = 4\pi/\lambda \sin(\theta/2)$), and plotting the result in a log-log-plot, typically a curve with different slopes can be observed. Whereas the structure size can be extracted from the position of the crossover between two regions with different slopes, the slope itself gives

	CTAB surface area [m^2/g]	DBP absorption [ml/(100 g)]	Compressed DBP absorption [ml/(100 g)]
N 326	**83**	**72**	**68**
N 330	**82**	**102**	**85**
N 339	**92**	**120**	**104**
N 375	**96**	**114**	**96**

Tab. 1: Characteristics of the investigated Carbon Blacks. CTAB surface area according to ASTM D 3765. DBP absorption according to ASTM 2414; Compressed DBP absorption according to ASTM D 3493-90.

information about the structure or to be more exact, the mass fractal dimension or the surface roughness, i. e. the surface fractal dimension, depending on the length scales considered.

3. Results

Figure 1 shows the scattered intensity as a function of the scattering length, for different Carbon Black samples. For the purpose of a better comparison the intensity values are normalized, therefore the intensity is in arbitrary units. Considering first the q-values larger than 0.2 nm^{-1} the almost identical slopes are evident. For values smaller than q = 0.2 nm^{-1} each curve shows a crossover to a second slope. For the regime q < 0.06 nm^{-1} the scattering diagram reflects the mass fractal dimension. The change of the slope in this regime should reflect the dependence of the values for the different Carbon Blacks listed in tab. 1. However, as one can see in fig. 1, there is no systematic dependence.

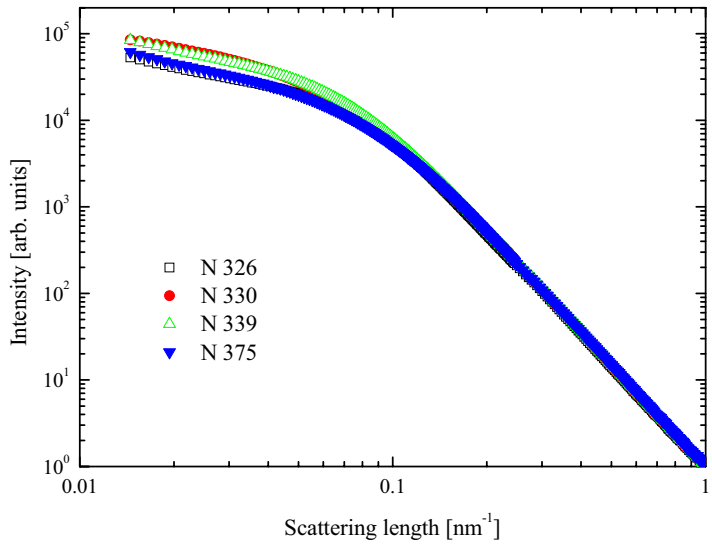


Figure 1: Intensity as a function of scattering length for different Carbon Black samples.

4. Conclusion

It was shown that the dependence of the structure from the type of Carbon Black found by means of scattering experiments disagrees with the characteristics defined by the norms. Since Carbon Black determines the mechanical properties of elastomers to a great extent, this result is important for future developments of high performance rubbers used in industry.

Institut für Festkörperforschung
Forschungszentrum Jülich GmbH
D-52425 Jülich

Experimental Report
of Neutron Scattering Experiments
at the FRJ-2 Reactor

Proposal number:	KW1-05-065		
Experiment title:	Final stages of "living" anionic polymerisation investigated by contrast variation SANS		
Dates of experiment:	13.01. – 15.012.2006	Date of report:	03.06.2006
Experimental team: Names	Addresses		
Aizhen, Niu Jörg, Stellbrink Jürgen, Allgaier	Institut für Festkörperforschung, Forschungszentrum Jülich Institut für Festkörperforschung, Forschungszentrum Jülich Institut für Festkörperforschung, Forschungszentrum Jülich		
Local Contact:	Pyckhout-Hintzen, Wim		

Experimental report text body

Anionic polymerisation is one of the key polymerisation techniques yielding well defined polymers both with respect to molecular weight distribution as well as architecture[1)]. In recent experiments we were able to relate in detail monomer conversion and initiation processes of "living" anionic polymerisation with structural details combining in-situ high resolution 1H-NMR and in-situ small angle neutron scattering (SANS). The combination of NMR and SANS opens a new realm of research into polymerisation processes, which appear to reveal completely new aspects of this polymerisation mechanism. With this proposal we ask for 3 days beam time at KWS-1 in order to determine by means of contrast variation the time dependent composition of intermediate species present in the initiation period. These "cross aggregates", mixed aggregates of growing polymer chains and unreacted initiator molecules, seem to crucially determine the active centre reactivities in the early stages of these living anionic polymerisations. Clear evidence for the existence of cross aggregates can be obtained by performing time-resolved SANS experiments under different contrast conditions. Matching either the initiator or the growing polymer chain by selective use of protonated/deuterated compounds will resolve all the structural details and composition of intermediate species present in the initiation period. It is essential to do the experiments with different butyllithium concentrations, that means different molecular weights to understand the increasing reactivity of butyl lithium with increasing concentration.

This experiment is a continuation of an experiment recently started using D22 (ILL). There we followed by insitu SANS the structure formation in the initiation period of "living" anionic polymerisation using contrast variation. However, due to the limited beam time we were only able to follow the polymerisation for 1 ½ days. After the experiment all samples were quenched to -78°C and stored at this temperature. We have shown that the polymerisation no longer progresses under these circumstances.

In detail the following time-resolved experiments should be performed: For in total 6 different samples, i.e. 3 initiator concentrations at 3 contrasts (full, polymer and butyllithium contrast) the scattering profiles were followed in real-time for two days, see Fig. 1.

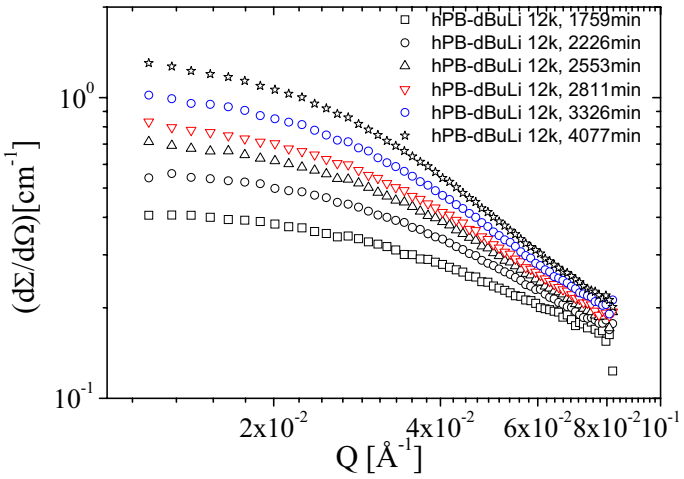


Fig. 1 Scattering profiles obtained by real time SANS from KWS-1, the later stages of living anionic polymerization of butadiene in d-heptane at 8°C using d-tert-butyllithium as initiator. The scattering contribution of solvent was not subtracted.

References:

1. M. Szwarc, M van Beylen, Ionic Polymerization and Living Polymers, Chapman&Hall: N.Y./London (1993)
2. A. Z. Niu, J. Stellbrink, J. Allgaier, L. Willner, A. Radulescu, D. Richter, B. W. König, R. P. May, L. J. Fetters, J. Chem. Phys., **122**, 134906, (2005)

Institut für Festkörperforschung
Forschungszentrum Jülich GmbH
D-52425 Jülich

Experimental Report
of Neutron Scattering Experiments
at the FRJ-2 Reactor

Proposal number:	KW1-06-001, KW1-05-041, KW1-05-047		
Experiment title:	Chain conformation in novel, natural-synthetic hybrid block copolymers		
Dates of experiment:	26.09. - 28.09.2005 11.11. -13.11.2005 16.02. -18.02.2006	Date of report:	06.06.2006
Experimental team: Names	Addresses		
Dr. L.J.R. Foster [1,2] Dr. D. Schwahn [2] Dr. V. Pippich [2]	[1] Bio/polymers Research Group, School of Biotechnology and Biomolecular Sciences, University of New South Wales, Sydney NSW 2052, Australia. [2] Institut für Festkörperforschung, Forschungszentrum Jülich GmbH, 524425 Jülich, Germany		
Local Contact:	Dr. D. Schwahn		

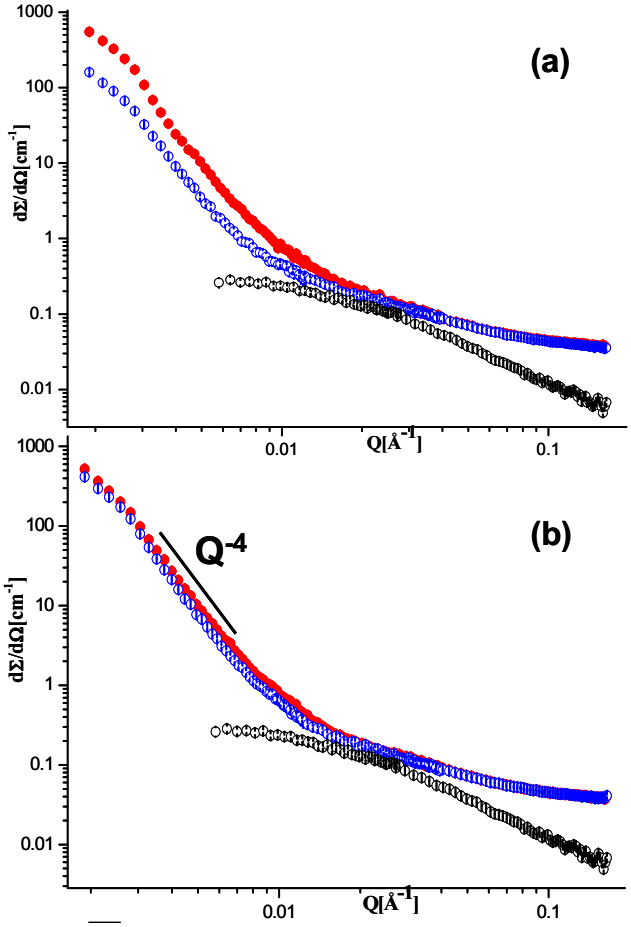
Experimental report text body

Introduction Polyhydroxyalkanoates (PHAs) are a family of biopolyesters synthesized by a wide range of microorganisms. The most common of these biopolymers is Polyhydroxybutyrate (PHB), which has received considerable interest as an environmentally friendly bioplastic and as a biomaterial for biocompatible medical implantation devices. PHB however, is just one member of a family of biopolymers possessing in excess of 105 different monomeric components. These novel biopolymers have material properties ranging from the rigid and highly crystalline to flexible, rather amorphous and elastomeric *[1]*. Another member of interest is Polyhydroxyoctanoate (PHO). PHB and PHO are representative members of PHAs possessing short and medium chain length substituents in the side chain (*scl*PHA and *mcl*PHAs).

We have recently synthesised natural-synthetic hybrids of PHB and PHO by 'end-capping' hydrophobic PHA chains with hydrophilic diethylene glycol (PHB-DEG and PHO-DEG respectively) *[2]*. The family of PEGs has a wide range of members varying in molecular mass and structure. A number of biocompatible members have important biomedical functions such as organ and tissue preservation *[3]*. Material surfaces modified by covalent attachment of PEG chains are resistant to cell and protein adsorption *[4]*. During solvent casting PHA-PEG hybrids self-assembled into ordered microporous arrays *[5]*. These microporous films, by virtue of their biocompatible composition and morphology, have the potential to serve a range of biomedical and biotechnological applications.

The objective of this research is to elucidate the influence of the relatively small hydrophilic group in these hybrids on polymer chain conformation, with a particular reference to their ability to form microporous films. In this regard, a synthetic block copolymer: Polystyrene-*b*-polydimethylacrylate which forms highly ordered microporous films is used as a positive control. Thus, based on electron microscopy studies, the degree of organisation in microporous films increases in the following sequence: PS-PDMA > PHB-DEG > PHO-DEG.

Experimental A series of SANS experiments were carried out to investigate the conformation of natural and hybridised PHA chains in the presence of micro-quantities of water (1% v/v). Deionised water was added to quartz cuvettes and vigorously mixed prior to placing in the neutron beam – SANS experiments were performed with biopolymers in solutions using deuterated chloroform and deuterated methylene chloride at concentrations range of 10 and 40 mg/ml. Scattering data was collected upon mixing and after standing for 10-12 hours. Samples were then remixed and low Q scattering collected every 20 minutes for 10 hours.



Results & Discussion Previous results showed an apparent failure of the DEG groups to influence chain conformation in solution. This is unsurprising given the difference in molecular mass between the natural and synthetic groups (approximately 600:1). However, the introduction of micro-quantities of water (1% v/v) followed by vigorous mixing, had noticeable visual effects. For example, while the chloroform solutions of PHO rapidly partitioned into two phases, the solutions of PHO-DEG appeared to form a stable microemulsion.

Figure 1: Scattering data for solutions of PHO and PHO-DEG in deuterated chloroform (10mg ml^{-1}) after addition of 1% (v/v) water and vigorous mixing, (a) PHO and (b) PHO-DEG, (➢) data from 1st and (➢)10th hour of scattering and (➢)PHO/PHO-DEG in absence of H_2O.

As an example of the experimental data acquired, Figure 1 illustrates the change in scattering patterns of the PHO and PHO-DEG biopolymer solutions with the addition of water, which can be readily observed at low Q with a best visual estimate of -4. At 10 mg ml^{-1} this low Q scattering of PHO decreased significantly with time, suggesting the gradual partitioning of water from the PHO solution (Figure 1a). In contrast, PHO-DEG solution at a similar concentration showed little change in scattering after standing for 10 hours (Figure 1b). Increasing the PHO-DEG concentration to 40mg ml^{-1} apparently facilitated this 'microemulsion' effect, with the scattering increasing with standing.

Thus, our results suggest the incorporation of water into the PHO-DEG solution and its long term stability, while in a solution of PHO it gradually partitions. Thus, the small hydrophilic DEG may facilitate some degree of self-assembly and suggest that key factors in microporous film formation may be chain conformation and mobility.

[1] Steinbüchel, A. In: Rehm H-J, Reed G, editors. Biotechnology. Weinheim, Germany: John Wiley & Sons, **1996**.
[2] Sanguanchaipaiwong, V; Gabelish, CL; Hook, J; Scholz, C. & Foster LJR. *Biomacromolecules* **2004**;5(2):643.
[3] Harris JM. Poly(ethylene glycol) chemistry: biotechnical and biomedical applications. New York, USA: Plenum **1992**.
[4] Inada Y, Matsushima A, Kodera Y, Nishimura H. *J. Bioact Compat Polym.* **1990**;5:343.
[5] Foster, LJR; Sanguanchaipaiwong, V; Gabelish, C. & Hook, J. *Polymer* **2005** 46(17):6587-6594.

Institut für Festkörperforschung
Forschungszentrum Jülich GmbH
D-52425 Jülich

Experimental Report
of Neutron Scattering Experiments
at the FRJ-2 Reactor

Proposal number:	KW1-06-002		
Experiment title:	Final stages of "living" anionic polymerisation investigated by contrast variation SANS		
Dates of experiment:	22.02. – 24.02.2006	Date of report:	02.06.2006
Experimental team: Names	Addresses		
Aizhen, Niu Jörg, Stellbrink Jörgen, Allgaier	Institut für Festkörperforschung, Forschungszentrum Juelich Institut für Festkörperforschung, Forschungszentrum Juelich Institut für Festkörperforschung, Forschungszentrum Juelich		
Local Contact:	Pyckhout-Hintzen, Wim		

Experimental report text body

Anionic polymerisation is one of the key polymerisation techniques yielding well defined polymers both with respect to molecular weight distribution as well as architecture[1)]. In recent experiments we were able to relate in detail monomer conversion and initiation processes of "living" anionic polymerisation with structural details combining in-situ high resolution 1H-NMR and in-situ small angle neutron scattering (SANS). The combination of NMR and SANS opens a new realm of research into polymerisation processes, which appear to reveal completely new aspects of this polymerisation mechanism.

The "cross aggregates", mixed aggregates of growing polymer chains and unreacted initiator molecules, seem to crucially determine the active centre reactivities in the early stages of these living anionic polymerisations. Clear evidence for the existence of cross aggregates can be obtained by performing time-resolved SANS experiments under different contrast conditions. Matching either the initiator or the growing polymer chain by selective use of protonated/deuterated compounds will resolve all the structural details and composition of intermediate species present in the initiation period. It is essential to do the experiments with different butyllithium concentrations, that means different molecular weights to understand the increasing reactivity of butyl lithium with increasing concentration.

With this proposal we ask for 2 days beam time at KWS-1 in order to characterize the final living and the terminated stages of anionic polymerisation by means of contrast variation.

This work is a continuation of experiments recently started using D22 (ILL) and KWS-1. In D22, we followed by insitu SANS the structure formation in the initiation period of "living" anionic polymerisation using contrast variation. After the experiment all samples were quenched to -78°C and stored at this temperature. We have shown that the polymerisation no longer progresses under these circumstances. In the last experiment performed at KWS-1, the later polymerization stages were monitored at 8°C from reaction time 2000 min to 15000 min.

In detail , for in total 6 different samples, i.e. 3 initiator concentrations at 3 contrasts (full, polymer and butyllithium contrast), the final living and the terminated stages were measured with sets up D20C20, D8C8 and D4C4, see Fig. 1.

References:

1. M. Szwarc, M van Beylen, Ionic Polymerization and Living Polymers, Chapman&Hall: N.Y./London (1993)
A. Z. Niu, J. Stellbrink, J. Allgaier, L. Willner, A. Radulescu, D. Richter, B. W. König, R. P. May, L. J. Fetters, J. Chem. Phys., **122**, 134906, (2005)

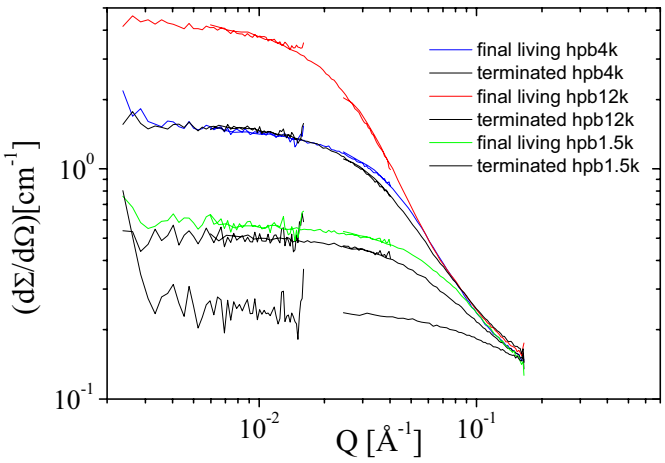


Fig. 1 SANS profiles of final living and terminated chains of polybutadiene with d-tert-butyllithium as initiator.

Institut für Festkörperforschung
Forschungszentrum Jülich GmbH
D-52425 Jülich

Experimental Report
of Neutron Scattering Experiments
at the FRJ-2 Reactor

Proposal number:	KW1-06-003		
Experiment title:	**Chain conformation of syndiotactic polypropylene**		
Dates of experiment:	25.-26.02.2006	Date of report:	01.06.2006
Experimental team: Names	Addresses		
V. Pipich M.Zamponi	Institut für Festkörperforschung, Forschungszentrum Jülich		
Local Contact:	V.Pipich		

Experimental report text body

Syndiotactic polypropylene (s-PP) is a very interesting polymer for dynamical investigations since it is a very stiff polymer but at the same time has a low segmental friction (see also BSS_06_001). As a preparatory experiment the stiffness parameter (C_∞) and its temperature dependence shall be determined by static measurements.

The static structure factor for 3 different temperatures in the range of the dynamical experiments (463K, 473K, 483K) and three different concentration of a few percent (1%, 2%, 3%) deuterated s-PP in a protonated s-PP matrix have been measured (molecular weights 158 kg/mol resp. 136 kg/mol). The experiments have been performed in vacuum at a neutron wavelength of 7Å covering a q-range of about 0.002-0.2 $Å^{-1}$.

For all the samples no temperature dependence of the static structure factor in the limited temperature range have been observed (fig.1). At low q-values all samples displayed a stronger scattering intensity then expected (fig.2). This scattering pattern follows a q-dependence ~ q^{-4}, indicating that it probably stems from scattering on small bubbles within the samples.

The concentration dependent scattering intensity can be accounted for by subtracting the incoherent background level and dividing the resulting data by the volume fraction $\phi(1-\phi)$ for each sample. All data then agree, except for the excess forward scattering at low q. Therefore the radius of gyration is concentration independent and can be fitted for all three samples simultaneous.

The data are well described by a sum of a Debye function with background and a function $A*q^{-4}$ to describe the forward scattering. The constants for background and forward scattering and the radius of gyration are fitted (lines in fig.2). The resulting radius of gyration is R_g=165 Å, giving a segment length of l=7Å, which is close to the literature values of about 7.6 Å (Jones et al., Macromolecules 2002). With the relation $l^2 = C_\infty n l_0^2$, n the average number of main-chain bonds per monomer (2) and l_0 the average bond length (1.54 Å), C_∞ is estimated to be 10.5 (literature value 9.12).

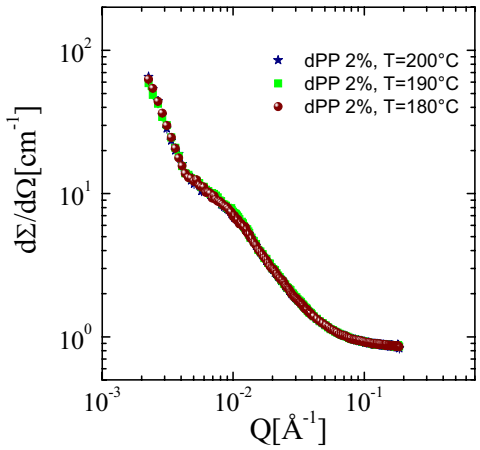


Fig.1: Temperature dependent scattering intensity for one sample.

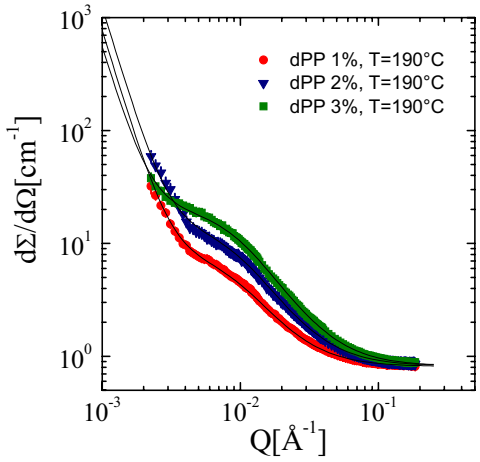


Fig.2: Concentration dependent scattering intensity for one temperature. Lines are a simultaneous fit of the different concentrations.

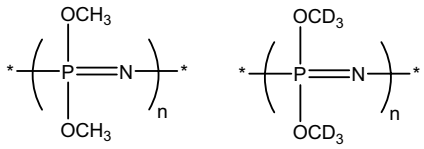
Institut für Festkörperforschung
Forschungszentrum Jülich GmbH
D-52425 Jülich

Experimental Report of Neutron Scattering Experiments at the FRJ-2 Reactor

Proposal number:	KW1-06-004		
Experiment title:	Investigation of chain dynamics in poly(bismethoxyphosphazene)		
Dates of experiment:	09.02.2006 – 11.02.2006	Date of report:	25.05.2006
Experimental team: Names	Addresses		
Yunus Karatas Prof. Dr. Hans-Dieter Wiemhöfer	Institut für Anorganische und Analytische Chemie Westf. Wilhelms-Universität, Corrensstr. 30 48149 Münster		
Local Contact:	W. Pyckhout-Hintzen, R. Zorn		

Experimental report text body

Polyphosphazenes which contain phosphor and nitrogen atoms joined by formally unsaturated bonds represent one of the largest classes of inorganic polymers, because a wide variety of side chains can be used to modify and fine tune both the chemical and physical properties of these polymers. One of the possible future applications of these inorganic polymers is as solid polymer electrolytes in lithium batteries, where these materials serve as solvents for salts acting as ionic conductors.



Many techniques have been applied to the characterization of polyphosphazenes up to now, however neutron scattering is not yet known for them. Therefore, first neutron scattering experiment have been performed with the model polymers (left) in order to understand solution and melt properties of the polyphosphazenes. The next step of the experiment was to look for the influence of salt on the melt conformation of the polymers.

SANS experiments were performed with the KWS1 spectrometer at the FRJ-2 Dido reactor in Jülich, Germany. The reactor runs at 20 MW and has a D20 moderator. Data were collected at distances sample-to-detector of 2, 8 and 20m which lead to an equivalent scattering vector range q between 0.002 and 0.2A^{-1} approximately using a neutron wavelength λ= 7 A with a wavelength spread $\Delta\lambda/\lambda$=0.20.

Polymer Solutions in DMF-d6: Dilute solutions were characterized using the Zimm extrapolation method (Figure 1). The radius of gyration and second virial coefficient values were extracted from double extrapolation of the Zimm's plot. These results (Rg = 144.7 and Mw = 95000 g/mol) were comparable to the results found by GPC in our lab. The A_2 value found for the polymers in DMF at room temperature (8.6E-4) is typical for polymers in a good solvent. The slope of 2 and 8 m data as shown in Figure 2 is 1.647 which is in exact agreement with the expected excluded volume exponent predicted by Flory's theory.

Polymer and salt-in-polymer in molten state: Polymer melts were prepared by mixing 5 vol-% of the deuterated polyphosphazene with 95 vol-% of non-deuterated one. 5 and 10 wt-% $LiSO_3CF_3$ containing salt-in-polymer systems were investigated additionally using the same polymer composition of the melt. The

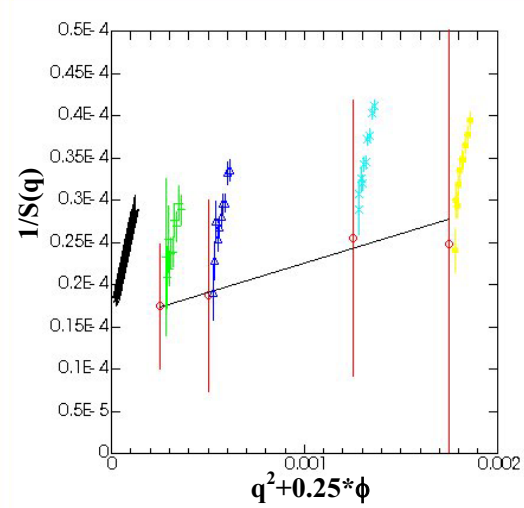


Figure 1. Zimm plot for polymer dissolved in DMF-d6

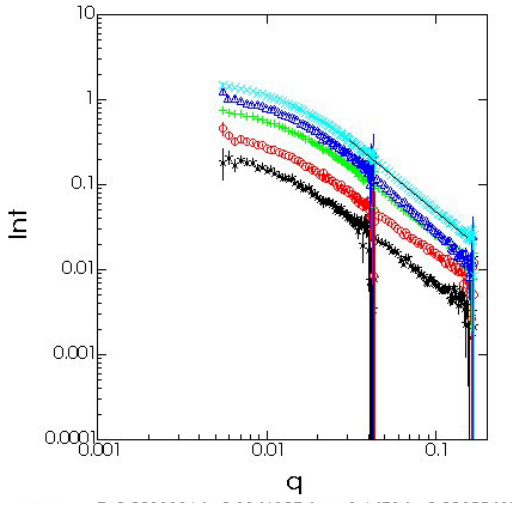


Figure 2. Scattering intensity of polymer solution as a function of wave factor

scattering at low q in the blends is from the polymer. It can be excluded from the observed q-dependence that it is a 'simple' mixing effect or Flory-Huggins interaction term between the deuterated and non-deuterated polymer. The data show a typical levelling-off in the same way as the solutions (usable data: q > 0.007 A^{-1}), below this it goes up.

Summary: R_g values were calculated using both the Guinier fitting and Schultz-Zimm-Flory distribution. R_g goes down a little from 85 to 83 if T is increased from 12.5 to 60.6°C polymer melt, which is virtually constant for salt-in-polymer systems (Table 1). These results show that the salt added to the melt has no effect on the conformation of the polymer. Increasing the temperature didn't change the behaviour. That means diffusive transport of the ions is dominating for this particular polyphosphazene system.

Table 1. Schultz-Zimm-Flory distribution

Name	T	Phi	Rg	Rg_n	Bgr	Epsilon
Polymer melt	12.5	0.89	85	61.9	0.903	1.01
Polymer melt	36.6	0.84	83.6	60.1	0.931	1.02
Polymer melt	60.6	0.85	83.2	61.9	0.925	1.01
5 wt-% salt-in-polymer	12.5	0.78	84.5	62.0	0.86	1.01
5 wt-% salt-in-polymer	36.6	0.73	84.4	59.4	0.89	1.02
5 wt-% salt-in-polymer	60.6	0.73	85.1	60.6	0.90	1.02
10 wt-% salt-in-polymer	12.5	0.69	83.1	62.0	0.85	1.00
10 wt-% salt-in-polymer	36.6	0.65	84.2	60.5	0.87	1.02
10 wt-% salt-in-polymer	60.6	0.66	84.4	62.5	0.87	1.01
						<1.01>

Institut für Festkörperforschung
Forschungszentrum Jülich GmbH
D-52425 Jülich

Experimental Report
of Neutron Scattering Experiments
at the FRJ-2 Reactor

Proposal number:	KW1-06-005		
Experiment title:	**A characterization of Fe3O4 particles in solution**		
Dates of experiment:	11.02. – 13.02.2006	Date of report:	15.05.2006
Experimental team: Names	Addresses		
Pyckhout-Hintzen,W	FZJ		
Local Contact:	Wim Pyckhout-Hintzen		

Experimental report text body

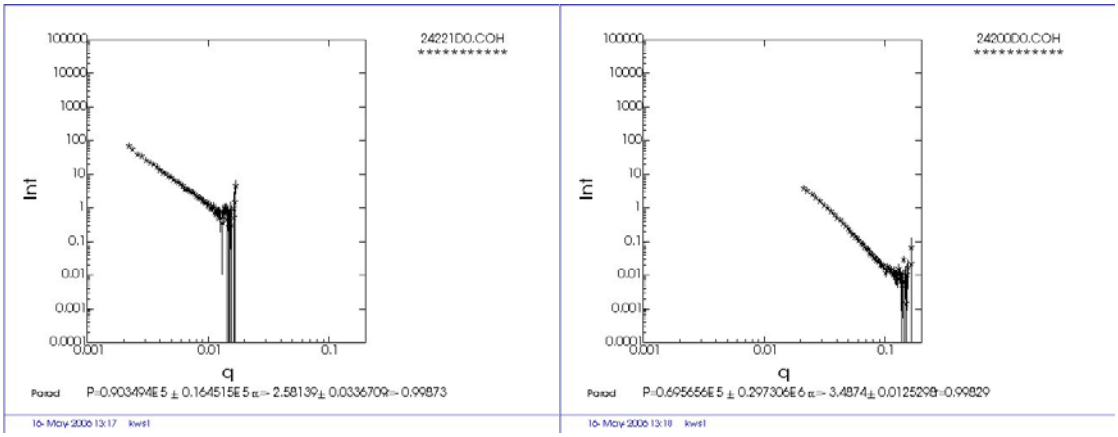
Smart materials have seen increased interest lately. In the following experiment we wanted to characterize a commercial Fe3O4 sample, which was dispersed in water and which could be modified afterwards to be blended with homopolymers if the structure is suitable. Therefore the emphasis is on the clustering behaviour and sizes of the primary nanoparticles and the aggregated structures.

Before any blending with a polymer can be tried, a prior characterization of the particle is required. According to the company who synthesized and sells chemically-modified nanoparticles for all kinds of purposes (Micromod Rostock,D) the diameter is about 200nm for the aggregate with size-polydispersity <1.1. SANS measurements of the solution should reveal all necessary structural details of the particle, its fractal structure as well as the structure factor in the case of more concentrated solutions.

The choice fell on this preparate due to the density: as it is 5g/ml this should not be visible in the nanometer scale. Data were obtained from diluting the original solution of concentration 25mg/ml of Fe3O4 down to 1/20 of the stock solution in order to isolate eventually the structure factor. It shows experimentally that there is no measurable contribution of S(q) whatsoever and perfect scaling with volume fraction of magnetite is reached.

An evaluation of the log-log intensities yields following preliminary parameters of the system: clearly clusters with mass fractal dimension of about 2.5-2.6 are found as is typical for precipated silica fillers e.g. or carbon black. The surface fractal exponent is also very similar and is found to be 6-3.5=2.5 where the q-dependence is q^(-3.5). If ones assumes the particles to be flat and not fractally, i.e. the surface scattering is described is q(-4) then the radius of the primary particles which is extracted is about 27.5nm or diameter about 60nm.

This is in fair agreement with the size of Fe3O4 crystallites which could be the building blocks. This is according to the company of the order of 15-20nm. Further descriptions have not yet been performed nor could a blending with polymer be tried in the lacxk of time.



Left: Mass fractal of the clusters is 2.6.

Right: surface fractal dimension is 2.5 roughly.

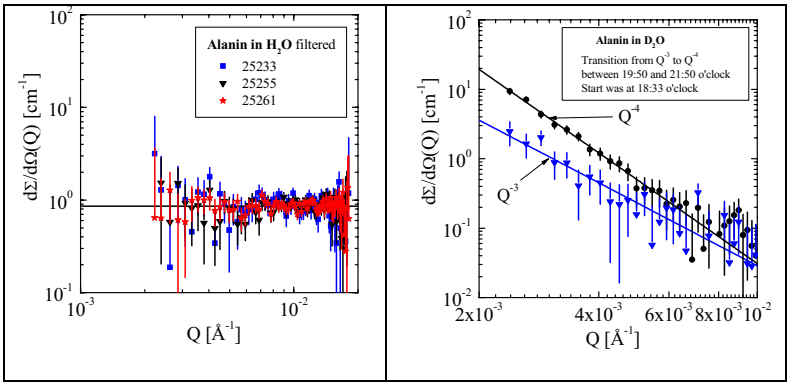
Institut für Festkörperforschung
Forschungszentrum Jülich GmbH
D-52425 Jülich

Experimental Report of Neutron Scattering Experiments at the FRJ-2 Reactor

Proposal number:	KW1-06-009		
Experiment title:	DL-Alanine Mesocrystal formation		
Dates of experiment:	13.03. - 15.03. 2006	Date of report:	18.05.06
Experimental team: Names	Addresses		
	PD Dr. habil. Helmut Cölfen Max-Planck-Institute of Colloids and Interfaces Colloid Chemistry Am Mühlenberg 1 14476 Golm Germany Tel: --49 331 567-9513 Fax: --49 331 567-9502		
Local Contact:	Dietmar Schwahn		

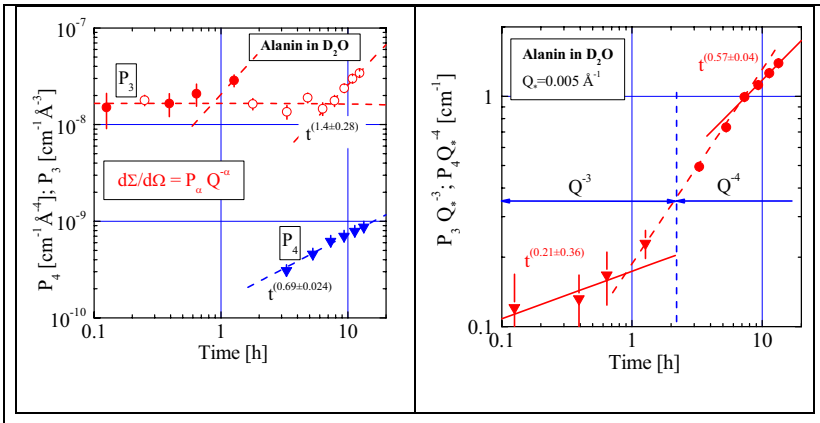
Experimental report text body

DL-alanin was found to form so called mesocrystals, which are superstructures of nanoparticles in crystallographic register. It is unclear how these highly aligned structures form and also, the inner structure of the well facetted mesocrystals is largely unknown. Therefore, a SANS experiment was carried out and performed on different scattering contrasts.



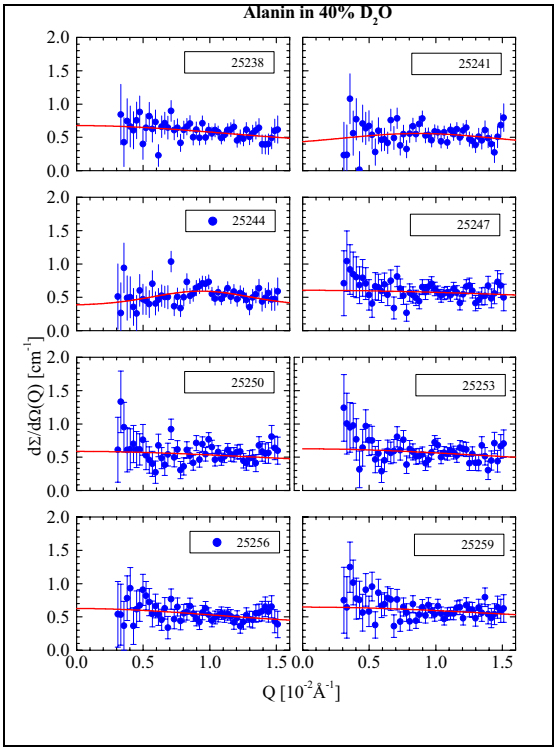
No coherent scattering from alanin was visible in H_2O, probably the incoherent scattering from H_2O was too large. On the other hand in D_2O coherent scattering was visible, showing large particles of at least µm particle size, whose large Q tails showed Q^{-3} power law behavior in the beginning and later a transition to Q^{-4} behavior characteristic for compact particles. This transition took place two hours after starting the reaction.

This observation is consistent with DLS and electron microscopy results, which show small precursor particles in solution particles of ca. 70 nm size and large particles > 10 µm. The latter are the nanoparticle superstructures, which are seen in SANS. The SANS result indicates that the µm-sized mesocrystals have an inner structure composed of nanoparticles, which fuse together to finally form compact Alanin single crystals.



The time reproducibility of the measurements was not so good. As Alanin was always found on the surface of the scattering cell, heterogeneous nucleation of the superstructures from nanocrystal building units can be assumed. These nanoparticles are only seen in DLS but not in SANS where the scattering from the large particles dominates. Despite the insufficient time reproducibility, the scaling behaviour is found constant (left figure, open and closed circles) so that it can be considered to be reproducible. An increase in the amplitude of the surface is indicated by the increase in P_4 in the left plot and the marked increase in P_3 shows the growth of the µm particles – most likely from the ca. 70 nm precursor particles detected in solution by DLS. The fusion of the nanoparticles inside a micrometer sized crystal to a compact single crystal without inner structure could be followed with a relatively sharp transition from Q^{-3} to Q^{-4} behaviour around 2h. (right figure).

In 40% D_2O aqueous solution which is the matching condition for alanin no scattering should be visible. Scattering from heterogeneities of radius of gyration of about 110 Å is found nearly independent of time. This value is smaller than the hydrodynamic radius variation of 35 nm of the 70 nm primary particle building units detected in DLS. The reason for this discrepancy is still unknown.



Summarizing, the SANS experiments showed clearly, that mesocrystals have an inner structure. This structure compacts with time to a large crystal without inner structure (a single crystal). Although the primary nanoparticle building units could not be detected in solution, as their concentration was too low and/or was hidden behind the scattering from the large units to be detected, the SANS experiments give clear evidence, that the detected large (> 1 micrometer) crystals are composed of subunits, which later became a compact structure. A time evolution of this process could be evidenced. This is an important finding, as it underlines an alternative crystallization pathway – the formation of a single crystal from nanoparticle building units via a mesocrystal intermediate rather than the textbook view, which considers single crystal formation via growth by attachment of single molecules to a critical crystal nucleus.

Institut für Festkörperforschung
Forschungszentrum Jülich GmbH
D-52425 Jülich

Experimental Report
of Neutron Scattering Experiments
at the FRJ-2 Reactor

Proposal number:	KW1-06-013		
Experiment title:	**Micellar re-structuring after interfacial tension jump**		
Dates of experiment:	24.3. 2006 18.-19.4. 2006	Date of report:	06.06.2006
Experimental team: Names	Addresses		
J. Stellbrink	IFF, FZ Jülich, D-52425 Jülich, Germany		
Local Contact:	J. Stellbrink		

Experimental report text body

Recently we investigated the self assembly of the amphiphilic block copolymer poly(ethylenepropylene)-poly(ethyleneoxide), $M_{w,PEP}$= 1000 g/mol, $M_{w,PEO}$= 20000 g/mol (PEP1-PEO20), in different water/dimethylformamide mixtures by small angle neutron scattering (SANS) [1]. The solvent composition could be used to precisely adjust the functionality of these star-like micelles, but also the intermicellar exchange kinetics [2]. In aqueous solution no exchange of individual block copolymers between different micelles could be observed, even at elevated temperatures, i.e. all micelles are completely kinetically frozen. On the other hand, in water/DMF mixtures with a mole fraction $x_{dmf} \geq 0.25$ the exchange of individual block copolymers is in the minute range and follows a logarithmic time dependence [2].
In addition we used star-like PEP-PEO micelles as an analogue of regular star polymers (*ultra-soft* colloids) to compare the experimental equilibrium phase diagram in the packing fraction (η) / functionality (f) representation to theoretical predictions for regular star polymers [2]. Still under discussion is the competition between vitrification and crystallization at higher concentrations/packing fractions. For star-like micelles no crystal formation was observed at higher functionalities, $f \geq 70$, as predicted by theory. Here an amorphous gel or glass phase was found for concentrations above the overlap packing fraction η^*. At smaller functionalities, i.e. $f \leq 70$, on the other hand, the predicted bcc-structure was found experimentally. This is in contradiction to experimental observations for regular star polymer solutions, where for all f only amorphous phases were found.
We now want to relate the existence of crystalline phases in the phase diagram of star-like micelles to its exchange kinetics. It might be that the observed crystal formation is due to a structural re-arrangement of the individual micelles, which is of cause prohibited for regular star polymers due to its covalent cross-linking phase.

To shed some light onto this topic, we need as a first step star-like micelles with low enough *f* to form a crystalline phase, but nevertheless frozen exchange kinetics. Such micelles might be formed by an "interfacial quench/jump", i.e. by rapid changes of solvent composition. Therefore we investigated micellar re-structuring by time-resolved SANS experiments after such an "interfacial quench/jump". Fig. 1 show the obtained SANS scattering intensities for two samples, which were independently prepared starting from the same initial solution with a mole fraction of $x_{m,d\text{-}DMF}$=0.3 and a initial polymer concentration $\Phi_{initial}$=3.0%. One millilitre of this initial solution was rapidly poured under continuous stirring into 2ml of pure D_2O, resulting in a final solvent composition of $x_{m,d\text{-}DMF}$=0.06, and Φ_{final}=1.0%. Whereas the first sample was already prepared 9 days before the SANS beam time, the second one was mixed directly at the experiment, Δt=5 minutes for D8C8 (Δt=1 hour for the complete Q-range). As fig. 1 clearly shows, there is no difference visible. This would mean, that there is either a very fast exchange, t≤5minutes, or no exchange at all. Fig. 1 also compares two samples directly prepared in either the initial or final solvent, now at a smaller volume fraction Φ=0.5% to get rid of the

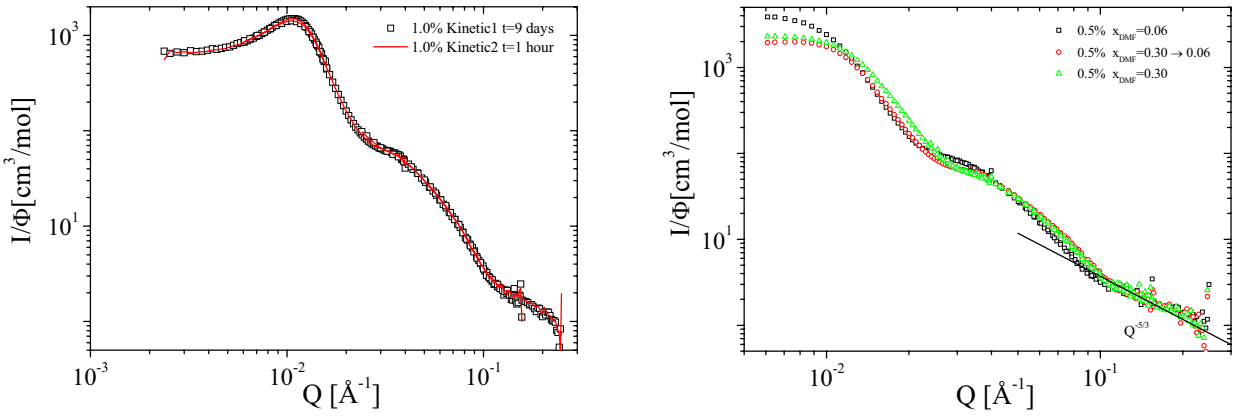


Figure 1: I(Q) in absolute units vs. scattering vector Q obtained by SANS. Left hand side: Two samples after "interfacial quench/jump". Right hand side: Samples at different solvent composition, see text

structure factor effects. Here one sees that the sample directly prepared at $x_{m,d\text{-}DMF}$=0.06 shows a bigger intensity at Q=0 indicating a higher functionality, whereas the forward scattering for the other two samples is more or less the same. This shows that the functionality of $x_{m,d\text{-}DMF}$=0.3 is transferred into the $x_{m,d\text{-}DMF}$=0.06 solution and that therefore the micellar exchange kinetics are still completely frozen.

References:

[1] R. Lund, L. Willner, J. Stellbrink, A. Radulescu and D. Richter, *Macromolecules*, **37**, 9984, 2004.
[2] R. Lund, L. Willner, J. Stellbrink, P. Lindner, and D. Richter, *Phys. Rev. Letters,* **96**, 068302, 2006.
[3] M. Laurati, J. Stellbrink, R. Lund, L. Willner, D. Richter, and E. Zaccarelli, *Phys. Rev. Letters*, **94**, 195504, 2005.

Institut für Festkörperforschung
Forschungszentrum Jülich GmbH
D-52425 Jülich

Experimental Report
of Neutron Scattering Experiments
at the FRJ-2 Reactor

Proposal number:	KW1-06-014		
Experiment title:	New Hafnium based catalysts for living olefin polymerisation III		
Dates of experiment:	24.-03. – 25.03.2006	Date of report:	31.05.2006
Experimental team: Names	Addresses		
Aizhen, Niu Jörg, Stellbrink Jörgen, Allgaier	Institut für Festkörperforschung, Forschungszentrum Juelich Institut für Festkörperforschung, Forschungszentrum Juelich Institut für Festkörperforschung, Forschungszentrum Juelich		
Local Contact:	Pyckhout-Hintzen, Wim		

Experimental report text body

Coates et al. [1] reported a new stereoselective titanium complex for olefin polymerization. Upon treatment with methylaluminoxane (MAO), this complex was found to be active for the polymerization of propylene at 0°C in toluene. Unexpectedly the obtained polymer exhibited a narrow molecular weight distribution (M_w/M_n~1.1). The amazing point is that the first synthesis of high molar mass syndio-polypropylene-block-poly(ethylene-co-propylene) diblock copolymer (M_n= 145 100, M_w/M_n=1.12) was achieved, when a slight overpressure of ethylene was added to the reactor after formation of the living syndiotactic polypropylene. The living nature of the catalyst allows the synthesis of block copolymers previously unavailable from Ziegler-Natta catalysts. However, the kinetics and mechanism of living olefin polymerization is still poorly understood. On the basis of research experience and knowledge of living anionic polymerization of dienes and styrene, we plan to develop the combined time resolved NMR and SANS technique to the field of living olefin polymerization, discover the fundamental mechanism and kinetics of the living olefin polymerization.

In recent SANS experiments we investigated the living polymerisation of poly(hexadienes) using a Titanium catalyst/MAO activator. We found that this system shows some unexpected precipitation after mixing of the individual compounds at low temperatures. I.e. rigorous stirring is required for keeping the catalyst/co-catalyst complex in solution, which is a prerequisite for successful polymerisation. Unfortunately this is not possible in the SANS cell and in particular not in the NMR cell, so that an absolute calibration in terms of sample concentration was not achievable.

Therefore we used another catalyst system to avoid this solubility problem. The new catalyst system contains a Hafnium complex as catalyst and low molecular weight Boron hydride compounds as activator. In the reactor period 2005/08 we performed first test experiments on that system and were able to follow a polymerisation in real-time by insitu-SANS. However, we discovered that the final product shows not the expected properties with respect to polydispersity and molecular weight, indicating some partially inactive catalyst/co-catalyst compounds. This would also explain the surprisingly high scattering intensity and slow kinetics observed in the scattering experiment. Meanwhile, after extensive test polymerisations, we were able to overcome these problems and follow the polymerisation under substantially improved conditions by insitu-SANS experiments.

[1] J. Tian, P. D. Hustad, G. W. Coates, J. Am. Chem. Soc. 2001, 123, 5134.

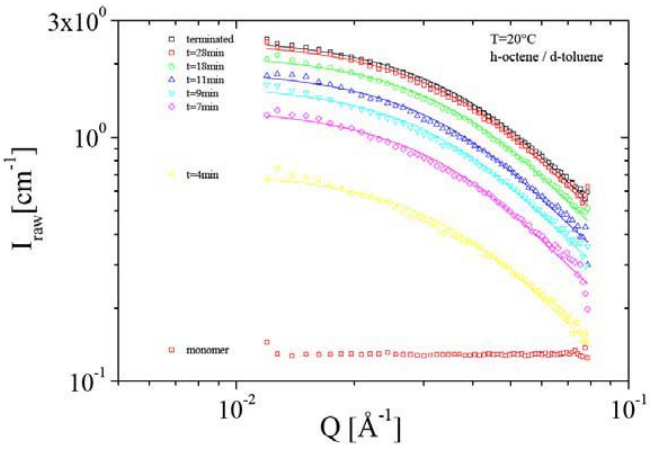


Figure 1: Living polymerisation of octene followed by real time SANS experiments at 20°C, the solid lines are fits to the Beaucage form factor.

Institut für Festkörperforschung
Forschungszentrum Jülich GmbH
D-52425 Jülich

Experimental Report
of Neutron Scattering Experiments
at the FRJ-2 Reactor

Proposal number:	KW1-06-015		
Experiment title:	**Exploratory study of montmorillonite nanocomposite sample preparation**		
Dates of experiment:	22.03.2006 – 23.03.2006	Date of report:	17.05.2006
Experimental team: Names	 Addresses		
Tobias Zacherle Dr. Wim Pyckhout-Hintzen Dr. Henrich Frielinghaus Prof. Dr. Dieter Richter	IFF, Forschungszentrum Jülich, 52425 Jülich IFF, Forschungszentrum Jülich, 52425 Jülich IFF, Forschungszentrum Jülich, 52425 Jülich IFF, Forschungszentrum Jülich, 52425 Jülich		
Local Contact:	Dr. Wim Pyckhout-Hintzen, Dr. Henrich Frielinghaus		

Experimental report text body

In the last few years there has been a dramatic increase of research in the field of nanocomposites [1]. In particular intercalated polymers in these composites are of vital interest since they are confined in two dimensions and therefore these systems can be seen as model-systems for the conformation and dynamics of polymers in two dimensions. In the present experiment PEO and MMT were used due to their favourable interaction properties like the good adsorption of the hydrophilic PEO on the silicate surface. As the sample-preparation is somewhat tricky, we first wanted to gain some experience in it and then – in a second experiment – focus on the conformation and structure of the PEO.

The aim of this first SANS-experiment was to investigate samples obtained by different preparation processes. In general we employed two techniques which lead to even optically quite distinct samples. The first method, was to solve the PEO and the MMT in water and then to dry this solution by freezing it with fluid nitrogen and then sublimating the solvent (freeze-drying). One does obtain a fluffy material afterwards which needs to pressed. The second method was to distillate the solution under low pressure and slowly vaporizing the solvent. This yields a gelous material which can be given onto the sample-container and further dried in the vacuum. The samples obtained by this method will be referred to as films. Four different kinds of samples were prepared:
(1) a freeze dried sample, pressed under atmospheric pressure
(2) a freeze dried sample, pressed under vacuum for several hours
(3) a film
(4) a film with oligomers added during preparation

We measured at different distances to the detector and at different temperatures T (room-temperature, 70°C, 85°C, and 100°C). We didn´t find any temperature-dependence of our results. But we did find a big difference between the film and the freeze-dried-sample:

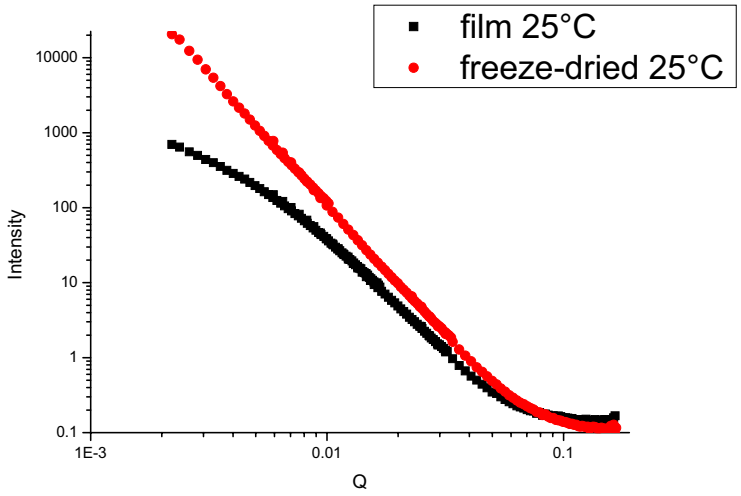


Fig1: Comparison between film and freeze-dried sample at T = 25°C.
One clearly sees less forward scattering in the film.

The film shows much less forward-scattering than the freeze-dried sample. This is believed to be due to a faulty stacking of the silicate-layers in the freeze-dried sample, which gave rise to big holes scattering at small angles because of their large sizes (with a q-dependence of q^{-4}). We didn't see any effect neither of the added oligomer nor of the different pressing procedures for the freeze-dried-sample.
The scattering-curve of the film could be fitted with the model of H. Frielinghaus [2]. In this model two Poisson-distributions of stack-sizes (tactoids) are assumed. The stacks are oriented randomly and one is able to explain the q^{-3} - dependence of the data of the film-sample.

As a conclusion one has to state, that the film-method is the best choice for the sample-preparation and we will stick to this method for upcoming experiments.

[1] R. Krishnamoorti et al.; Structure and Dynamics of Polymer-Layered Silicate Nanocomposites; *Chem. Mater.* **1996**, *8*, 1728-1734
[2] H. Hermes et al.; Quantitative analysis of small angle neutron scattering data from montmorillonite dispersions; to be published in *Polymer*

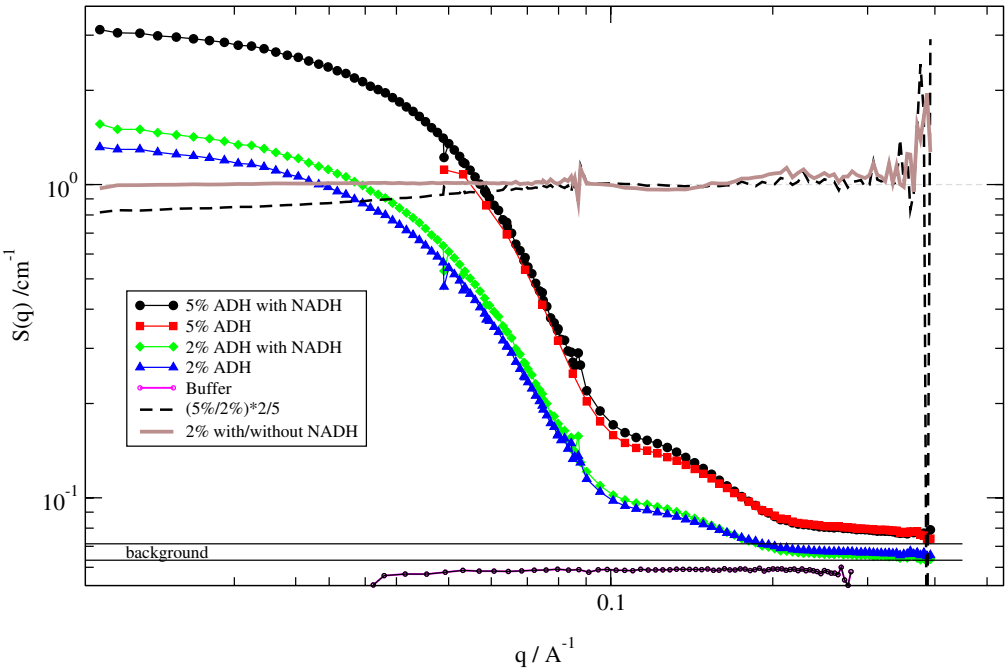
Institut für Festkörperforschung
Forschungszentrum Jülich GmbH
D-52425 Jülich

Experimental Report
of Neutron Scattering Experiments
at the FRJ-2 Reactor

Proposal number:	KW1-06-016		
Experiment title:	Internal dynamics and structure of protein alcohol dehydrogenase by binding of cofactor: Structure		
Dates of experiment:	Apr. 2006	Date of report:	Mai 2006
Experimental team: Names	 Addresses		
Ralf Biehl Bernd Hoffmann Michael Monkenbusch Rudolf Merkel Dieter Richter	FZJ/IFF FZJ/ISG FZJ/IFF FZJ/ISG FZJ/IFF		
Local Contact:	Wim Pyckhout-Hintzen		

Experimental report text body

Most proteins are characterized by a defined tertiary structure when analyzed by crystallographic experiments. Binding of other biomolecules or substrates changes the tertiary structure of these proteins in specific regions often by more than 1 Angstrom. Intermediate states of an enzymatic reaction often depend on structural modifications. For most enzymatic reactions only a very few of these structural states are know from crystallographic snap shots since these experiments freeze the structure in a defined state. Molecular dynamic simulations as well as experiments using thermophilic proteins additionally strongly suggest highly dynamic structural fluctuations even in the absence of any bound factor. Such fluctuations are best considered as an ensemble of structural states, only some of which are competent for substrate binding or catalysis. These structural states are absolutely essential for protein function and mainly take place in protein domains also structurally modified when bound to a binding partner. The intense dynamics of specific protein regions likely adapts the protein structure to the one of its binding partner enabling its binding that would be excluded in a rigid conformation. Our experiments are directed to visualize and characterize ground state structural dynamics within a protein as well as structural fluctuations when bound to a cofactor or inhibitor. The analysis of proteins either bound or unbound to additional factors will allow the detailed characterization of dynamic protein areas and may possibly open a new way in protein dynamic analysis. Up to now a direct experimental observation of such protein dynamics is still missing.
As model system we depend on a protein with known structural transformations upon substrate binding. These transformations may be on the large or small scale between protein domains of sufficient size. Here, the alcohol dehydrogenase (ADH) from yeast will be used as model system. In our Experiment we want to examine configurationally changes due to binding of the cofactor to assist our planned experiments by neutron spinecho spectroscopy.



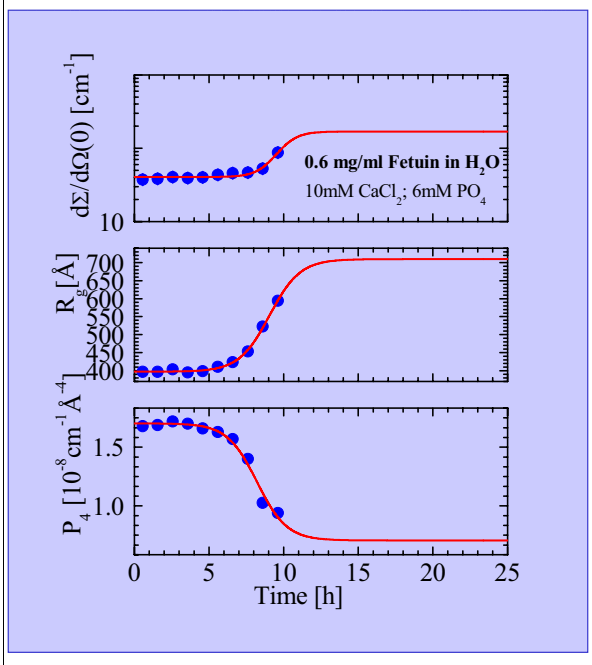
The graph shows the SANS date for concentrations of 2% and 5% with and without added NAD. The low q part of the 5% without NAD is missing due to a frozen sample. The shoulder above 0.1 A^{-1} is typical for the tetrameric flat structure (two dimmers parallel oriented) as it isn't found for the dimeric structure. the expected small peak at about 0.3 A^{-1} was not detected as it is smeared by the resolution of the instrument and results only in a small plateau. To compare the structural features we calculate, after subtracting the flat background, the ratio between the 2% curves and between the 2 concentrations with added NAD. For the 2% samples we observe over the full range of accessible scattering vectors a flat structure less curve. An additional constant factor of 0.86 acounts for the obvious loss of concentration between the two curves. Compared to the 5% sample we observe a decrease of intensity at low q. This is due to an increasing interaction between the proteins as they are closer at this higher concentration. We observe the influence of the structure factor.
From these data we can only conclude that the effect of a bound NAD is less than we can detect with these measurements.

Institut für Festkörperforschung
Forschungszentrum Jülich GmbH
D-52425 Jülich

Experimental Report of Neutron Scattering Experiments at the FRJ-2 Reactor

Proposal number:	KW1-06-017		
Experiment title:	SANS Untersuchung zur Stabilitätsgrenze kolloidaler Protein-Mineral Aggregate		
Dates of experiment:	07.04-12.04.2006	Dates of report:	02.06.2006
Experimental team: Names	Addresses		
Dr. Wolf-Alexander Heiß	IZKF BioMAT Universitätsklinikum Pauwelsstraße 30 D-52074 Aachen		
Dietmar Schwahn Hitoshi Endo	IFF, FZ-Jülich, D-52425 Jülich		
Local Contact:	Dietmar Schwahn		

Experimental report text body



Fetuin-A in a supersaturated solution with regard to calcium and phosphate produces colloidal protein – mineral particles, denoted as CPPs. Preliminary investigations with our biochemical precipitation assay concerning the limits of CPP stability evidenced that at least 0.6 mg/ml fetuin-A are necessary to stabilize a solution containing 10 mM $CaCl_2$ and 6mM PO_4 at pH 7.4.

In this series of experiments we observed an increase in scattering intensity after roughly 8h at room temperature. At the same time the radius of gyration increased starting from 400 Å while the total surface extension decreased.

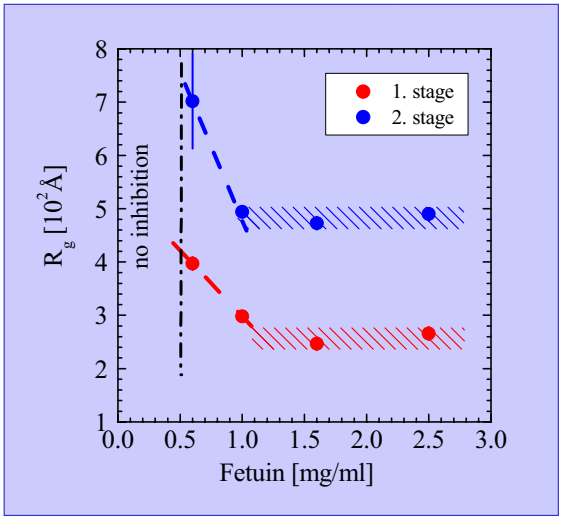


Figure 2 shows the relationship between the fetuin-A concentration and the radius of gyration at our standard supersaturation (10 mM $CaCl_2$, 6 mM PO_4). At high fetuin-A concentrations (>1.2 mg/ml) small CPPs with a radius of gyration of approximately 250 Å formed for the first ripening stage and of approximately 500 Å for the second, respectively. A reduction below that threshold of 1,2 mg/ml fetuin-A led to considerably larger CPPs with a radius of gyration of 300 – 400Å for the first stage and max 700 Å for the second, respectively. Moreover, these experiments confirmed our results obtained from our precipitation assay that 0.5 -0.6 mg/ml fetuin-A represent the lower limit of CPP stability.

Institut für Festkörperforschung
Forschungszentrum Jülich GmbH
D-52425 Jülich

Experimental Report
of Neutron Scattering Experiments
at the FRJ-2 Reactor

Proposal number:	KW1-06-019		
Experiment title:	New Hafnium based catalysts for living olefin polymerisation IV: Effect of reaction temperature.		
Dates of experiment:	20.04.2006	Date of report:	01.06.2006
Experimental team: Names	Addresses		
Aizhen, Niu Jörg, Stellbrink Jürgen, Allgaier	Institut für Festkörperforschung, Forschungszentrum Juelich Institut für Festkörperforschung, Forschungszentrum Juelich Institut für Festkörperforschung, Forschungszentrum Juelich		
Local Contact:	Pyckhout-Hintzen, Wim		

Experimental report text body

Coates et al. [1] reported a new stereoselective titanium complex for olefin polymerization. Upon treatment with methylaluminoxane (MAO), this complex was found to be active for the polymerization of propylene at 0°C in toluene. Unexpectedly the obtained polymer exhibited a narrow molecular weight distribution (M_w/M_n~1.1). The amazing point is that the first synthesis of high molar mass syndio-polypropylene-block-poly(ethylene-co-propylene) diblock copolymer (M_n= 145 100, M_w/M_n=1.12) was achieved, when a slight overpressure of ethylene was added to the reactor after formation of the living syndiotactic polypropylene. The living nature of the catalyst allows the synthesis of block copolymers previously unavailable from Ziegler-Natta catalysts. However, the kinetics and mechanism of living olefin polymerization is still poorly understood. On the basis of research experience and knowledge of living anionic polymerization of dienes and styrene, we plan to develop the combined time resolved NMR and SANS technique to the field of living olefin polymerization, discover the fundamental mechanism and kinetics of the living olefin polymerization. In recent SANS experiments we investigated the living polymerisation of poly(octene) using a new catalyst system contains a Hafnium complex as catalyst and low molecular weight Boron hydride compounds as activator. In the reactor period 2005/08 we performed first test experiments on that system and were able to follow a polymerisation in real-time by insitu-SANS. However, we discovered that the final product shows not the expected properties with respect to polydispersity and molecular weight, indicating some partially inactive catalyst/co-catalyst compounds. This would also explain the surprisingly high scattering intensity and slow kinetics observed in the scattering experiment. Meanwhile, after extensive test polymerisations, we were able to overcome these problems and followed the polymerisation under substantially improved conditions by insitu-SANS experiments. Now the expected molecular weigh is finally obtained and the polymerisation

could be followed although the kinetics are extremely fast (The polymerisation is already completed after approximately 30 minutes: Analysis of the forward scattering I(Q=0) as a function of time gives a characteristic time of only 8.3 minutes at 20°C). Another clear result is that the growing chain is not aggregated as we know for "living" anionic polymerisation [2-4], because the polymerizing chain at full conversion shows the same scattering profile as the terminated chain.
To follow the structural changes in more detail we planed to decrease temperature to about 0°C to slow down the polymerisation. Unfortunately, the catalyst of this reaction has only 50% activity, we have to wait for the preparing of a new catalyst. Therefore the final product from last experiment on KWS1 was characterized at different concentrations. Further data analysis and corresponding NMR measurements are in progress.

[1] J. Tian, P. D. Hustad, G. W. Coates, J. Am. Chem. Soc., **123**, 5134 (2001).
[2] A.Z. Niu, J. Stellbrink, J. Allgaier, L. Willner, A. Radulescu, D. Richter, B.W. König, R.P. May, L.J. Fetters, *J. Chem. Phys.*, **122,** 134906 (2005).
[3] J. Stellbrink, J. Allgaier, L. Willner, D. Richter, T. Slawecki, L.J. Fetters, *Polymer*, **43**, 7101, (2002)
[4] J. Stellbrink, L. Willner, O. Jucknischke, D. Richter, P. Lindner, L.J. Fetters, J.S. Huang, *Macromolecules*; **31**, 4189 (1998) and *Macromolecules,* **32**, 5321 (1999).

Institut für Festkörperforschung
Forschungszentrum Jülich GmbH
D-52425 Jülich

Experimental Report
of Neutron Scattering Experiments
at the FRJ-2 Reactor

Proposal number:	KW1-06-020		
Experiment title:	Comparison of stretched PS melts: influence of architecture		
Dates of experiment:	13.04. – 16.04.2006	Date of report:	14.05.06
Experimental team: Names	 Addresses		
Pyckhout-Hintzen,W. Jens Kroman Nielsen	FZJ DTK Copenhagen		
Local Contact:	Wim Pyckhout-Hintzen		

Experimental report text body

We had proposed to measure the strain and tube diameter in deformed polystyrene melts which are partially labelled and/or vary in the architecture.

Recent developments in the description of the scattering patterns of deformed melts have lead to new discussions. A major topic of this is the size of the tube diameter which comes out of small angle neutron scattering data, neutron spin echo spectroscopy and last but not least from linear rheology.
The previous success in describing the relaxation of a linear polyisoprene as a function of time after a step strain has opened the door to different architectures which, depending on the labelling, should be more or less active towards relaxation. 3 different blends which separately from each other have been evaluated at different times and with different prognostics about what is going to be the main parameter of determination for the anisotropy could reveal new information and sustain the former observations. A model-independent technique as e.g. neutronspin echo is still necessary, however.

The proposal has been combined with a former KW1 proposal on deformed rings (KW1-05-061) and deformed diluted PS-triblocks (KW1-05-62) and data from these will be just transferred. The new data concern mainly the linear homopolymer blend which was actually present in both former experiments.

S(q) can be written as

$$S(q) = \frac{1}{N^2} \sum_{i,j} \exp(-q^2 < r_{ij}^2 > / 6)$$

which can be written of course in its single components x, y and z. That means that the scattering law is only determined by the mean square distance between pairs of monomers.
The scattering now sees 2 things: first, there is a time-average which one can write as

$$r = \bar{r} + \delta r$$

and the ensemble average which then can be written as

$$< r^2 >=< \bar{r}^2 > + < (\delta r)^2 >$$

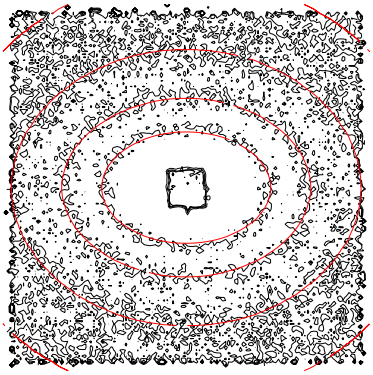
and δr is the instantaneous fluctuation away from a mean position.
The mean position of a polymer chain is of course determined by the environment which can be network or crosslinks or just the fact that there are other chains. The chain axis couples affinely to the macroscopic deformation and therefore we could write r→λr and

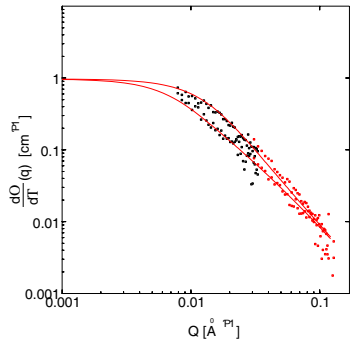
$$r = \lambda \bar{r} + \delta r$$

The fluctuations are treated as harmonic potentials and one can assume all kinds of deformation couplings to the strain. E.g. for networks it was found by several authors that the fluctuation width couples to the strain with $\sqrt{\lambda}$ whereas for uncross linked chains typically no deformation dependence could be found experimentally. We will stick to this last observation.
This means also inherently that the total deformation of a chain is always somewhat less than affine. Therefore the difference between the chain's deformation at the smallest angles and the deformation in a spatial range which corresponds to the fluctuation width is measurable with SANS.
This problem has been solved for a constrained cross linked linear chain inside a phantom network or melt and discussed by Warner and Edwards 1982. The scattering theory for a tube-constrained linear chain has been worked out by us (and afterwards confirmed by Read et al) and leads to the structure factor

$$S(q,\lambda) = 2\int_0^1 d\eta \int_0^\eta \prod_{x,y,z} \exp(-(qR_g\lambda)^2(\eta-\eta') - (qR_g)^2(1-\lambda^2)\{\frac{d^2}{2\sqrt{6}R_g^2}(1-\exp(-\frac{(\eta-\eta')}{\frac{d^2}{2\sqrt{6}R_g^2}}))\}$$

Fits to a deformed sample were successful and yield ideal values for Rg=147.5A which agrees with the estimate of Rg= 0.28 sqrt(Mw) and a tube radius of about (47.0+/- 5)A, i.e. (94 +/- 5)A tube diameter. This is in perfect agreement with data from the plateaumodulus and agrees also well with the segmental fluctuation range, i.e. about 80A of the PS rings at a comparable deformation. The tube radius is not deformed as was the case for linear poly-isoprene. Further comparison has still to be done.





Institut für Festkörperforschung
Forschungszentrum Jülich GmbH
D-52425 Jülich

Experimental Report
of Neutron Scattering Experiments
at the FRJ-2 Reactor

Proposal number:	KW1-06-021		
Experiment title:	**Study of montmorillonite nanocomposite structure and comparison to previous results**		
Dates of experiment:	13.04.2006 – 14.04.2006	Date of report:	17.05.2006
Experimental team: Names	Addresses		
Tobias Zacherle Dr. Wim Pyckhout-Hintzen Dr. Henrich Frielinghaus Prof. Dr. Dieter Richter	IFF, Forschungszentrum Jülich, 52425 Jülich IFF, Forschungszentrum Jülich, 52425 Jülich IFF, Forschungszentrum Jülich, 52425 Jülich IFF, Forschungszentrum Jülich, 52425 Jülich		
Local Contact:	Dr. Wim Pyckhout-Hintzen, Dr. Henrich Frielinghaus		

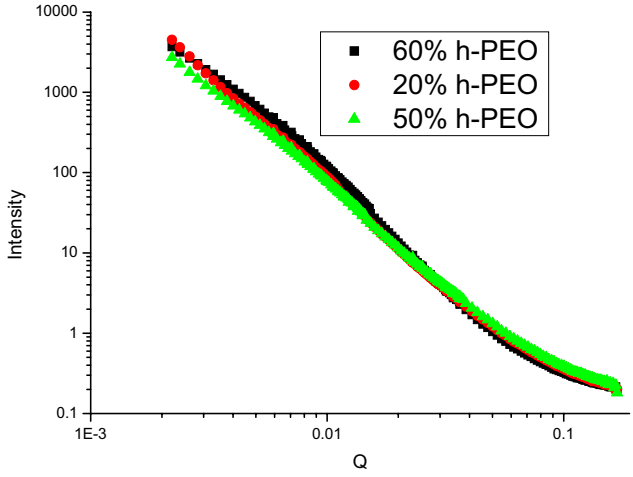
Experimental report text body

Polymer-clay-composites are of big interest due to the fact that they represent model-systems for polymers confined in two dimensions [1]. In addition to that there is a wide range of possible applications of these new materials [2]. The material under investigation in this experiment was a PEO-MMT-composite. Since we had compared the different kinds of preparation-methods in a previous experiment and had found the film-preparation to be the best choice, all the samples used in the experiment were films. Further on we used D_2O as solvent during preparation, because of its superior scattering properties compared to ordinary water.

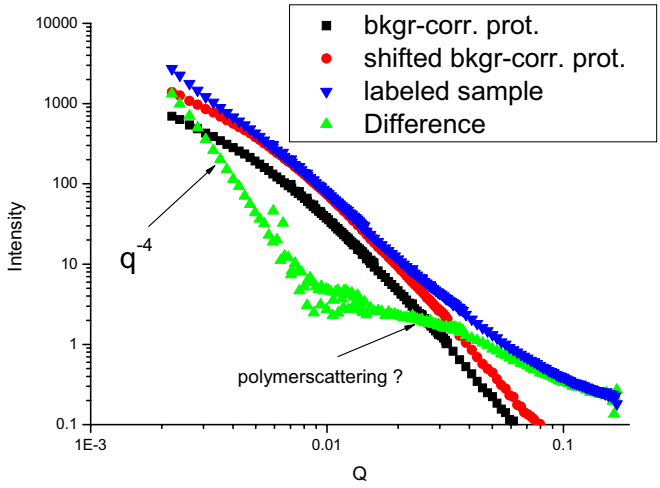
In the present experiment, we tried a contrast-match between the silicate layers and the PEO. Therefore we made a blend of deuterated and protonated PEO in order to match the average scattering length of the polymer with the one of the MMT. In this way we hoped to eliminate the scattering of the silicate stacks and to obtain a pure polymer-signal. By analyzing this signal one can conclude the radius of gyration of the polymer confined in between the silicate layers and thus see the conformation of the PEO in two dimensions.
We did prepare 3 samples with different relative content of deuterated-protonated PEO, whereas the total amount of PEO remained fixed: 20 weight-% PEO, 80weight-% MMT:
(1) 50 vol-% protonated PEO
(2) 20 vol-% protonated PEO
(3) 60 vol-% protonated PEO

The expected matching point was for 50 vol-% protonated PEO. Typical adsorption-times of the PEO in the literature are 24 h (although this is unknown), so the two polymers were added successively.

Our results are presented below:



One sees that „stack-scattering“ is still dominating, as there is no hint of a Guinier-plateau, which would be an indication of the wanted polymer-scattering. So we did not succeed with our contrast-match. Although the theoretical matching condition shows smaller excess-intensity and a more polymer-like q-dependence at low q.



A preliminary analysis under the assumption of additivity of scattering contributions of polymer and silicate reveals two features:
1) We might have had phase-separation of the deuterated and protonated PEO. This is indicated by the green line. The exponent of the q-dependence at low q can be explained by large regions having contrast in scattering-length, which would occur if the two kinds of PEO had not mixed.
2) We saw polymer-scattering in the form of a Debye-curve at higher q, but it cannot be excluded that this signal comes from PEO, which was not intercalated between the silicate platelets.

Possibly a preferential adsorption of one of the polymers due to the successive addition has hampered the contrast-match-conditions. Adsorption-time is apparently much shorter than 24 h.
For the experiments in the future we will improve our sample-preparation-process in order to avoid phase-separation and finally get the desired contrast-match.

[1] R. Krishnamoorti et al.; Structure and Dynamics of Polymer-Layered Silicate Nanocomposites; *Chem. Mater.* **1996**, *8*, 1728-1734
[2] S. S. Ray, M. Okamoto; Polymer/layered silicate nanocomposites: a review from preparation to processing; *Prog. Polm. Sci*. **2003**, *28*, 1539-1541

Small Angle Neutron Scattering Instrument (KWS2)



Instrument Parameters

Beam tube:	NLIIB bent guide, cross section: 4.5 cm (height) × 3 cm (width)
Monochromator:	velocity selector; $\Delta\lambda/\lambda$ = 10 %
Neutron flux at sample:	10^5 to 6×10^6 n/cm^2 s depending on collimation; for 20 MW reactor power λ = 7 Å wavelength and entrance aperture of 3 × 3 cm^2
Collimation:	variable apertures at 1 m, 2 m, 4 m, 8 m, 14 m, 18 m, 20 m distance from sample opening width variable 0.5 ... 4.5 cm vertical opening width variable 0.5 ... 3.0 cm horizontal
Beam size at sample:	typically 1 cm × 1 cm
Detector ***- Active area:*** ***- Scintillator:*** ***- Space resolution:*** ***- Max. pulse rate:*** ***- Detection probability:*** ***- γ-sensitivity:***	 60 × 60 cm^2 in 128×128 channels ^{6}Li-glass, 1 mm thickness 0.5 × 0.5 cm^2 ca. 1 MHz (τ_{dead} = 3 μsec) 95 % for λ = 7 Å 2×10^{-4} (1 MeV)
Elastic Q-range:	$10^{-3} \le Q/Å^{-1} \le 0.3$ (typically $2 \times 10^{-3} \le Q/Å^{-1} \le 0.2$)
Sample environment:	evacuated sample chamber / open beam line cryofurnace 200 ... 500 K; shear cell of Searle type

Instrument Responsible

Dr. Henrich Frielinghaus Tel. +49-(0)-2461-61-5093 Email: h.frielinghaus@fz-juelich.de
Dr. Aurel Radulescu Tel. +49-(0)-2461-61-4685 Email: a.radulescu@fz-juelich.de

Institut für Festkörperforschung
Forschungszentrum Jülich GmbH
D-52425 Jülich

Experimental Report
of Neutron Scattering Experiments
at the FRJ-2 Reactor

Proposal number:	KW2-04-007		
Experiment title:	Small-angle neutron scattering studies of block copolymers adsorbed on perfluorocarbon emulsions		
Dates of experiment:	21.01.2005 – 25.01.2005	Date of report:	03.03.2006
Experimental team: Names	Addresses		
Terence Cosgrove Melissa Sharp Steve King	School of Chemistry, University of Bristol, Cantock's Close, Bristol, BS8 1TS, UK School of Chemistry, University of Bristol, Cantock's Close, Bristol, BS8 1TS, UK CLRC Rutherford Appleton Laboratory, Chilton, Didcot, Oxfordshire, OX11 0QX, UK		
Local Contact:	Martine Heinrich		

Experimental report text body

The conformation of adsorbed polymer or surfactant molecules in colloidal systems is of both fundamental importance and relevant to a wide range of technical systems. Our interest, in the pharmaceutical sciences, lies in the use of colloidal materials as drug delivery and targeting systems for the treatment of diseases as diverse as AIDS and cancer, the ultimate objective of this work is to develop means of directing drugs to a particular organ or cellular site, thus increasing their efficacy and reducing side-effects. Much recent work has centred on the use of adsorbed polymers to control the in vivo fate of drug-loaded colloidal particles. For example, it has been proven possible to select polymers to maximise vascular residence, or to cause preferential targeting of colloids to the bone marrow or the lymphatic system[1]. Such targeting effects are primarily dependent on the nature of the surfactant, and are largely independent of the material from which the core of the particles is composed.

We have studied the interfacial layer structure of adsorbed polymers using light scattering, and have carried out some SANS experiments, in order to obtain greater detail. We use perfluorocarbon emulsions as the colloidal cores; these materials have the advantage that they can be contrast matched to their environment using approximately 72% D_2O in water. Perfluorocarbon emulsions can be made in a wide range of diameters from 80 – 1000 nm, of low polydispersity, with a wide range of adsorbed polymeric material. They are of pharmaceutical interest in their own right as oxygen transport media[2], and have been extensively studied as "artificial blood". The polymers that were used to stabilise the emulsions were Pluronics, which are block copolymers, consisting of propylene oxide (PO) and ethylene oxide (EO), of the form $(EO)_n(PO)_m(EO)_n$. The emulsions used in this set of experiments had diameters of 294 nm and 319 nm when stabilised by, respectively, Pluronic F68 and Pluronic F127.

The small-angle neutron scattering experiments were carried out on instrument KWS-2 using sample-detector distances of 2m and 8m and a neutron wavelength of 6Å. This led to an approximate Q-range of 0.007 - 0.2 $Å^{-1}$. The emulsion concentration used for the majority of the measurements was 5 v/v %. The emulsions were stabilised by either Pluronic F68 or Pluronic F127. The emulsions were studied either off-contrast or where the oil phase was contrast matched to the water phase. This required approximately 72% D_2O. In addition to this the effect of salt was measured, using 0.2M NaCl solution. The effect of the emulsion concentration was studied, using emulsion concentrations of 10, 15 and 20 v/v %. All of these experiments were carried out both on and off contrast. Finally, we attempted to carry out the measurements contrast matching the polymer. This required approximately 16% D_2O. All measurements were carried out at 25°C.

The results obtained had a good signal to noise ratio. However, the data obtained contained peaks as a result of either a detector or a software malfunction. These peaks were not a result of the samples studied. We are still looking for a good way of dealing with this problem, and the data has therefore yet to be fitted.

A typical example of the data is shown in Figure 1 below. The sample measured is 5% emulsion stabilised by Pluronic F68, with the oil phase contrast matched.

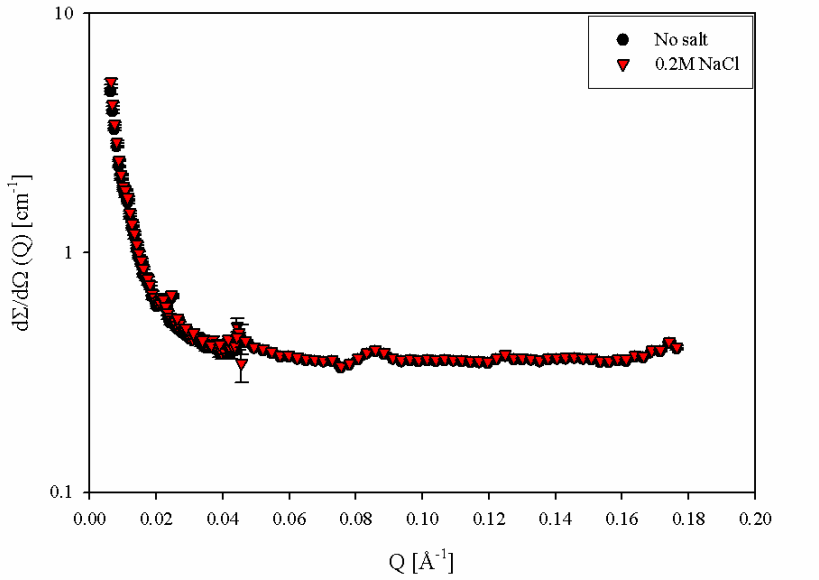


Figure 1

References

(1) Illum, L.; Davis, S. S.; Muller, R. H.; Mak, E.; West, P. *Life Sciences* **1987**, *40*, 367.
(2) Krafft, M. P. *Advanced Drug Delivery Reviews* **2001**, *47*, 209-228.

Institut für Festkörperforschung
Forschungszentrum Jülich GmbH
D-52425 Jülich

Experimental Report
of Neutron Scattering Experiments
at the FRJ-2 Reactor

Proposal number:	KW2-04-008		
Experiment title:	**Characterization of deformed and undeformed Al-alloys**		
Dates of experiment:	19.-20.01.2006	Date of report:	22.06.2006
Experimental team: Names	 Addresses		
Henrich Frielinghaus Andreas Ulbricht Frank Bergner	Institut für Festkörperforschung, Forschungszentrum Jülich GmbH Forschungszentrum Rossendorf e.V. Forschungszentrum Rossendorf e.V.		
Local Contact:	Henrich Frielinghaus		

Experimental report text body

Background

The evaluation of safety and integrity of mechanically loaded structures such as the fuselage of commercial aircraft is based on fracture and damage mechanics concepts. In damage mechanics a damage function as well as damage parameters are needed in order to predict the mechanical behaviour of the component. SANS measurements offer the possibility to detect microstructural changes (including damage and evolution of the dislocation network) on the nanometer size scale while probing volumes much larger than grain size. Crystal dislocations are believed to cause rather weak SAS contrast for both X rays and neutrons. It was therefore surprising to observe, in a preliminary investigation, a strong deformation-induced anisotropy of contrast in specimens of thin-sheet wrought Al-Mg-Si alloy AA6013T4 deformed in tension up to uniform elongation. The aim of the present experiment was to reproduce the effect of deformation using optimized experimental conditions for both the naturally aged alloy (T4) investigated before and an artificially aged condition (T6) of the same alloy. The comparison of the two aging conditions should enable us to contribute to the understanding of the mechanism of deformation-induced contrast.

Experimental setup

The SANS experiment was carried out with a beam diameter of 10 mm and a neutron wavelength of 0.53 nm. Three different sample detector distances (14 m, 4 m and 1.25 m) and corresponding collimation lengths were used to measure scattering intensities with a scattering vector, Q, approximately ranging from 0.02 to 1.2 nm^{-1}. In order to enhance statistics, a number of six segments of 1.6 mm thick tensile specimens were placed front to back to form one compound sample for each condition. The compound samples of both undeformed and uniformly stretched material of 6013T4 (uniform elongation 18.5%) and 6013T6 (uniform elongation 7.5%) were exposed to the same experimental conditions to ensure optimum comparability.

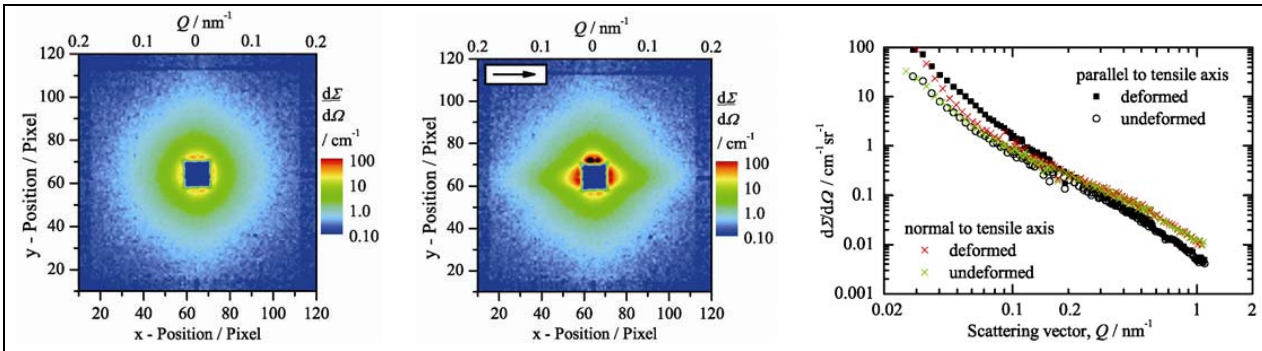


Fig. 1. SANS images of undeformed (left) and uniformly stretched Al alloy 6013T4 with the tensile direction indicated by an arrow (middle), scattering curves for Q vector parallel and normal to tensile axis (right).

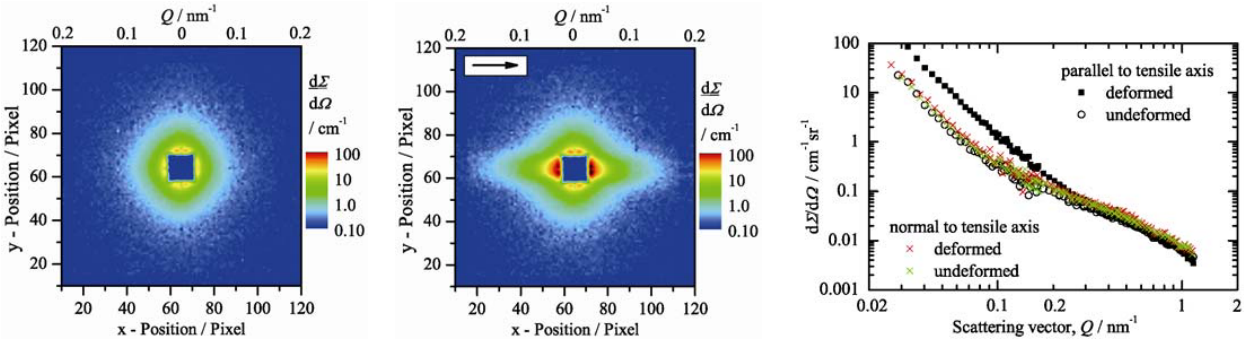


Fig. 2. SANS images of undeformed (left) and uniformly stretched Al alloy 6013T6 with the tensile direction indicated by an arrow (middle), scattering curves for Q vector parallel and normal to tensile axis (right).

Results

We are interested in the deformation-induced change of both scattered intensity and anisotropy. Two-dimensional patterns of the SANS intensities measured in the Q-range up to 0.2 nm^{-1} are shown in figures 1 and 2 for Al-alloy 6013T4 (aged at room temperature) and 6013T6 (aged at 190 °C), respectively. The same colour scaling is used for the intensity in both figures. Scattering curves corresponding to the horizontal (Q parallel to tensile axis) and vertical (Q perpendicular to tensile axis) sections through the centre of the patterns are placed on the right hand side of these figures.

The following findings can be extracted from the experimental results:

- The in-plane scattering anisotropy of the undeformed thin-sheet materials is weak for both conditions.
- For the naturally aged condition T4 there is a pronounced deformation-induced increase of anisotropy, which basically agrees with the result of the preliminary measurements mentioned above.
- The same type of anisotropy is even more pronounced for the artificially aged condition T6. This is surprising, because the uniform elongation applied to these specimens (7.5%) was much smaller than for condition T4 (18.5%).
- At increasing Q-values the scattering curves for the undeformed and the stretched material cross one another in the case of T4 and approach one another in the case of T6.

It is well known that the contrast caused by single dislocations strongly depends on the type and orientation of the dislocation relative to the neutron beam and to the Q-vector. We therefore assume that the deformation-induced increase of anisotropy is caused by the formation of special arrangements of dislocations. The effect of the initial microstructure on the evolution of the dislocation network has to be considered in order to explain the observations summarized above on a quantitative basis. In any case, 2D SANS patterns are an extremely sensitive means to detect effects of anisotropy in plastic deformation.

Institut für Festkörperforschung
Forschungszentrum Jülich GmbH
D-52425 Jülich

Experimental Report of Neutron Scattering Experiments at the FRJ-2 Reactor

Proposal number:	KW2-04-018		
Experiment title:	Performance of new Couette rheometer – Measurement of shear induced deformation of star-like micelles		
Dates of experiment:	28.01. – 01.02.2005	Date of report:	24.05.2006
Experimental team: Names	Addresses		
G. Rother, J. Stellbrink, L. Willner, D. Richter	Forschungszentrum Jülich, Institut für Festkörperforschung Forschungszentrum Jülich, Institut für Festkörperforschung Forschungszentrum Jülich, Institut für Festkörperforschung Forschungszentrum Jülich, Institut für Festkörperforschung		
Local Contact:	Dr. H. Frielinghaus		

Experimental report text body

The experiment aimed to test the installation and operation of the new Rheowis rheometer in the KWS environment.

The installation of the instrument on the standard sample table was possible using a special adapter plate. The rheometer is designed to operate at high rotational speed, we measured up to shear rates of 8000 Hz successfully. For the future even 10.000 Hz might be possible, but require some small improvements in the instrument. We studied the scattering from several diluted and concentrated samples of protonated and deuterated PEP1-PEO20 in water and water/DMF mixtures.

So far we measured the shear behaviour of the structure factor of h-PEP1-h-PEO20 at a volume fraction of 3% With increasing shear rate a shift of the peak position to lower Q has been observed. The origin of this effect is not fully understood yet. Secondly the shear behaviour of the form factor of PEP1-PEO under zero average contrast conditions has been studied. The results of this measurement are shown in Figure 2. We found a deacrease of the scattering intensity at low Q with increasing shear. Further evaluation of this complex system is necessary to obtain a comprehensive picture of the structural effects of shear appliance to that colloidal system. For the forthcoming experiments the electronic setup will be improved. The analysis of the data is underway.

Institut für Festkörperforschung
Forschungszentrum Jülich GmbH
D-52425 Jülich

Experimental Report of Neutron Scattering Experiments at the FRJ-2 Reactor

Proposal number:	KW2-04-020		
Experiment title:	Interactions in concentrated sterically stabilized colloidal dispersions		
Dates of experiment:	6 to 9-Mar-2005	Date of report:	2-Mar-2006
Experimental team: Names	Addresses:		
Dong Qiu Yuan Wang Terence Cosgrove	School of Chemistry University of Bristol Cantock's Close Bristol BS8 1TS UK		
Local Contact:	Dr. Wim Pyckhout-Hintzen		

Experimental report text body

(Please use 12 pt letters here !)

The stability of colloidal dispersions depends on the inter-particle interactions. Colloidal dispersions can be stabilized by electrostatically or sterically repulsion or both[1]. The steric repulsion can be imparted by both physically adsorbed and surface grafted polymer chains in good solvents. We have already studied the steric interaction by physically adsorbed polymer chains[2, 3]. In this study, we used the polystyrene latex with grafted PEO chains as a model system. The latex was synthesized by incorporating PEO macromonomer (PEO 1000 Mw) with styrene monomer during the emulsion polymerization process. Latex samples were dispersed in D_2O/H_2O mixture to make the PEO layers invisible. Therefore, a simple spherical form factor is applicable. 20 mM NaCl was present to screen the electrostatic repulsion caused by surface charges.

Figure 1 shows the scattering spectra. Surprisingly, no structure factors were found even for concentrated samples (0.13 volume fraction). All the data can be perfectly fitted by a hard-sphere form factor, the results are shown in Table 1. It can be seen that these latex particles are very monodisperse and they are very stable against electrolyte. They did not flocculate even in presence of 0.1 M NaCl.

The good stability of these colloidal particles against electrolyte implies the presence of an effective PEO layer on the particle surface. These layers seem to be very thin (no structure factor). However, they can provide a considerably high energy obstacle to keep the particles apart against van der Waals attraction. These latex particles can be a perfect model for studying hard-sphere behaviors. Regretably, we did not observed the steric interaction by SANS directly, but their behavior in ionic environment supports such an interaction. Considering the short length of the PEO chains, the steric interaction could be expected to be short range. A higher volume fraction or longer grafted polymer chains may be needed for such an effect. This is part of our ongoing work.

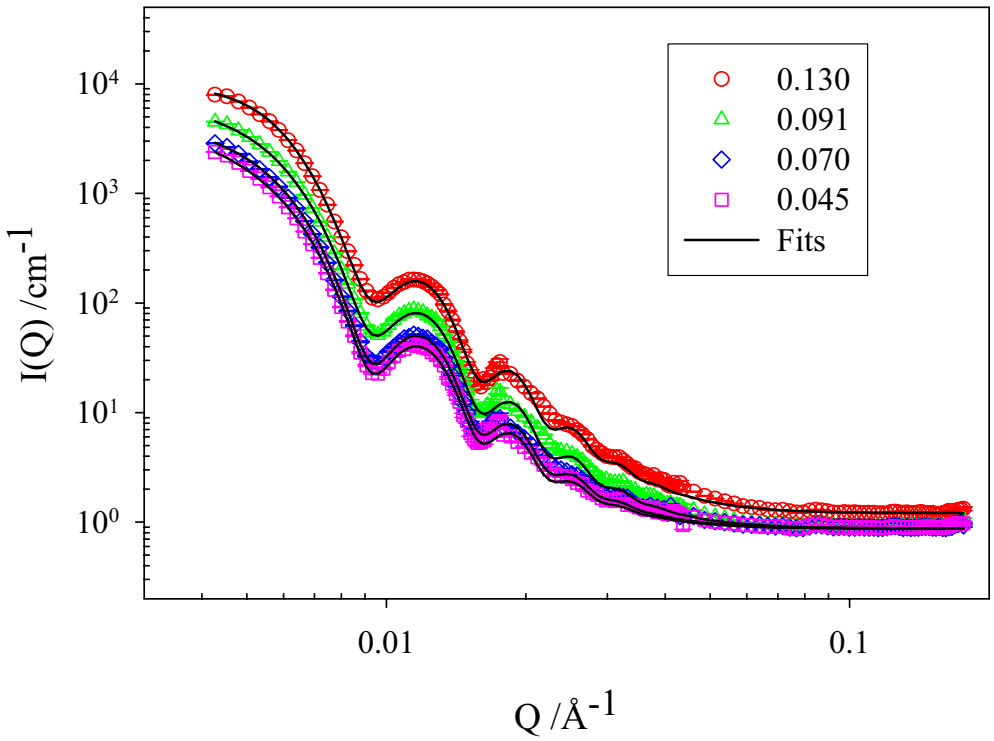


Figure 1. The SANS spectrums of polystyrene latex with grafted PEO at different volume fractions.

Table 1. Parameters used to fit the experimental data in Figure 1.

Volume Fraction	0.130	0.091	0.70	0.045
Particle Radius (Å)	480 ± 2	478 ± 2	477 ± 2	477 ± 2
Polydispersity	0.06	0.06	0.07	0.07

Reference:
1. Hunter, R. J., *Foundation of Colloid Science,* Clarendon Press: Oxford, **1987**; Vol. I.
2. Qiu, D.; Cosgrove, T. *Experimental report for* KW1-03-013，2005.
3. Qiu, D.; Dreiss, C.A.; Cosgrove, T.; Howe, A. M. *Langmuir*, **2005**, *21*, 9964..

Institut für Festkörperforschung
Forschungszentrum Jülich GmbH
D-52425 Jülich

Experimental Report of Neutron Scattering Experiments at the FRJ-2 Reactor

Proposal number:	KW2-04-021		
Experiment title:	Microstructure and magnetic interactions in FeAg granular thin films		
Dates of experiment:	10-14 May 05	Date of report:	1 Jun 06
Experimental team: Names:	Addresses:		
Ana García Prieto	Dpto. Electricidad y Electrónica, UPV-EHU, Apartado 644, 48080 Bilbao, Spain		
Gustavo Sarmiento	Dpto. Electricidad y Electrónica, UPV-EHU, Apartado 644, 48080 Bilbao, Spain		
Local contact:	Henrich Frielinghaus		

Small Angle Neutron Scattering (SANS) experiments were performed on Fe_xAg_{100-x} ($x = 6, 15, 25, 31, 49$) granular thin films. The films, of thicknesses ranging between 80 and 150 nm, were prepared by laser ablation and lay over a Si substrate of $\approx 250\mu$m thick.
SANS experiments on granular samples can provide evidence of the existence of very small Fe clusters that otherwise are very complex to detect by XRD or TEM due to their small size ($\approx$ 4 nm). Moreover, magnetic information can be obtained due to the magnetic character of the Fe clusters.
Previous magnetic and magnetotransport measurements on these samples show that for $x \leq 25$ the magnetic response is superparamagnetic-like, with no coercivity and remanence and not saturated hysteresis loops at 300 K. From Langevin fits of the hysteresis loops a cluster size of 4 nm has been estimated. As the Fe concentration increases ($x > 25$) the loops lose their superparamagnetic character: coercivity and remanence appear suggesting a new ferromagnetic-like regime with a prevalence of exchange coupling over the dipolar interactions [1, 2].
Regarding the magnetotransport response of the samples, all of them show Giant Magnetoresistance (GMR) when the magnetic field is in the sample plane and Extraordinary Hall Effect (EHE) when is perpendicular for $x \geq 25$, this anisotropic response being due to the planar shape of the Fe clusters.
The SANS experiments were made at room temperature in transmission configuration. Four different detector distances were used in order to cope with a suitable range in Q, from 0.003 to 0.34 Å^{-1} with $\lambda = 5.3$Å.

Results of the SANS measurements performed at KWS-2 are shown in Figure 1.

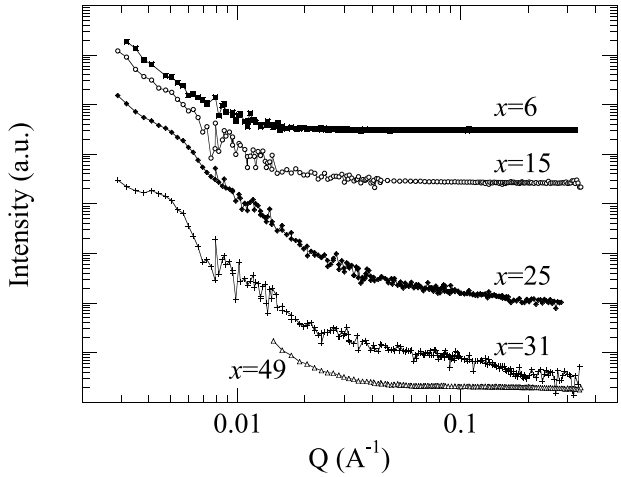


Figure 1: SANS measurements performed at KWS-2 for Fe_xAg_{100-x} ($x = 6, 15, 25, 31, 49$) thin films.

From a qualitative analysis of the curves, the samples with $x < 25$ show a similar shape, with a steep decrease of the intensity at low Q followed by a plateau. For $x > 25$ there is a shoulder at low Q and a slower decrease of the intensity up to the highest Q. This could be a fingerprint of the magnetic transition at $x = 25$ inferred from the analysis of the hysteresis loops.
From fittings of the curves at high Q (Porod region) we have found that the Fe-Ag interface is mainly not sharp, which suggests that there could be some atomic substitution between the two species. However, fittings of the low Q region to a Guinier law result in particle sizes inconsistent with the ones extracted from the magnetization loops. Further numerical studies are being performed by a complex analysis consisting on fitting the curves to a spherical form factor under the Perkus-Yevik approximation for hard spheres. From this procedure we expect to complete the information on the sizes, size-distribution and concentration of the magnetic nanoparticles as a function of Fe concentration.

References

[1] *Magnetic and magnetotransport behaviour of granular Fe_xAg_{100-x} thin films*, G. Sarmiento, M.L. Fdez-Gubieda, I. Orue, J. Magn. Magn. Mat., accepted

[2] *The role of the interface on the magnetic behaviour of granular $Fe_{50}Ag_{50}$ film*, M.L. Fdez-Gubieda, G. Sarmiento, L. Fernández-Barquín, I. Orue, J. Magn. Magn. Mat., accepted

Institut für Festkörperforschung
Forschungszentrum Jülich GmbH
D-52425 Jülich

Experimental Report
of Neutron Scattering Experiments
at the FRJ-2 Reactor

Proposal number:	KW2-04-022, KW2-05-032		
Experiment title:	**Test of a polarized neutron setup at KWS-2**		
Dates of experiment:	03.10. – 04.10.2005	Date of report:	13.06.2006
Experimental team: Names	Addresses		
E. Kentzinger H. Frielinghaus A. Ioffe M. Feygenson Th. Brückel	Institut für Festkörperforschung, Forschungszentrum Jülich Institut für Festkörperforschung, Forschungszentrum Jülich Institut für Festkörperforschung, Forschungszentrum Jülich Institut für Festkörperforschung, Forschungszentrum Jülich Institut für Festkörperforschung, Forschungszentrum Jülich		
Local Contact:	H. Frielinghaus		

Experimental report text body

The aim of this experiment was to check whether one could obtain a polarized beam at KWS-2 by installing a polarizer at sample position and whether this primary beam could be kept clean from any small angle scattering from this polarizing device.
The drawing and the picture of Fig.1 explains the set-up:

1) The polarized neutron beam was produced using a Fe/Si supermirror device working in transmission. In that way, the direction and the collimation properties of the beam were not affected. Previous measurements have shown that the small angle scattering of such a supermirror is relatively weak, provided that the supermirror is put in a large enough field (see report HAD-04-018).
2) The projection of the spin on the quantization axis was changed by using a radio-frequency spin flipper. The main advantages of the use of such a spin flipper at a SANS machine are that there is no material into the beam (therefore no scattering is produced by this device), and that it can flip neutrons over a relatively wide wavelength spectrum range. At the exit of the flipper, an absorber plate was installed (B_4C powder on Cd) in order to absorb the + neutrons specular reflected by the polarizer.
3) The polarization of the thus obtained neutron beam and the flipping ratio of the flipper were tested by studying the reflection of spin-up and spin-down neutrons by a FeCoV/TiN polarizing supermirror.

The results are shown in Fig.2 which shows measurements performed at C8-D3. A relatively clean empty beam was obtained. In following experiments, the intensity around the empty beam was better suppressed by replacing the absorber plate at the exit of the flipper by a slit.
The polarization efficiency was analyzed by installing a polarizing supermirror in a remanent state after the flipper. In that state, this device mainly reflects spin-down neutrons. From the bottom part of Fig.2, we can deduce a flipping ratio of the whole set-up equal to 35, big enough to perform polarized GISANS experiments.

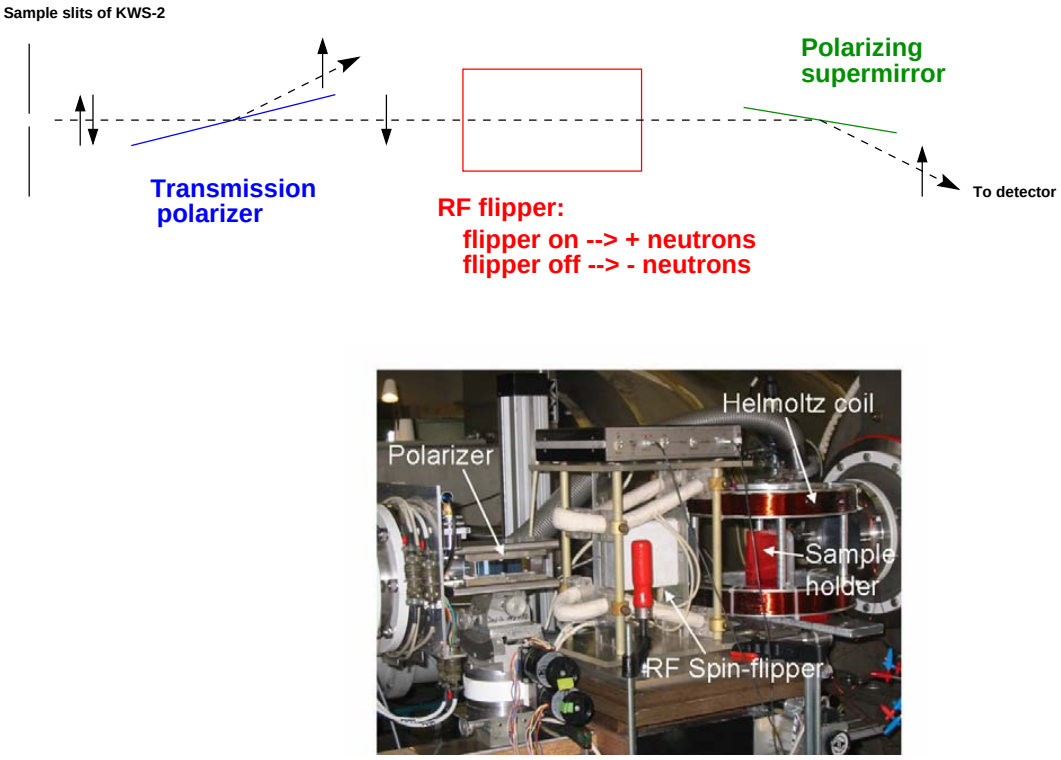


Fig. 1: Sketch and photo of the set-up used at KWS-2 to measure polarized GISANS from a polarizing supermirror.

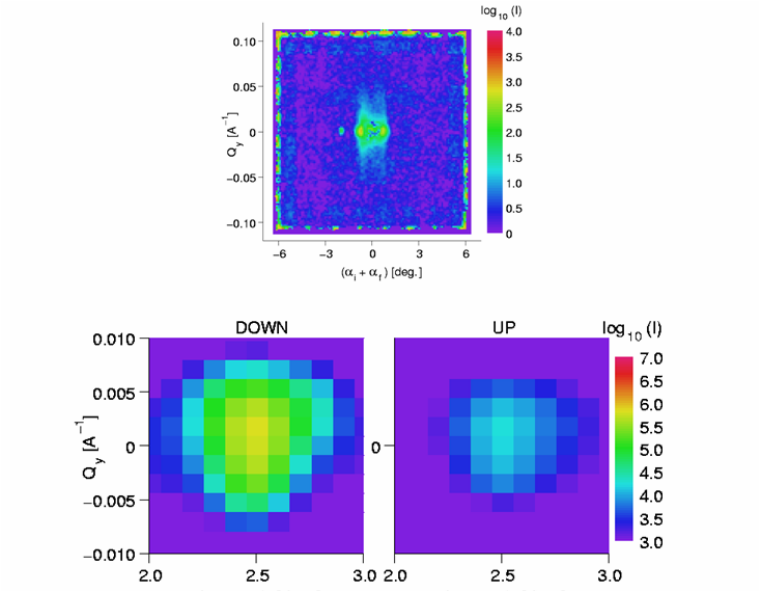


Fig. 2: Top: 'Empty beam' of the polarized neutron experiment. Bottom: Spin down and Spin down reflectivity of the supermirror in its remanent state at an angle of incidence set close below the effective angle of total reflection.

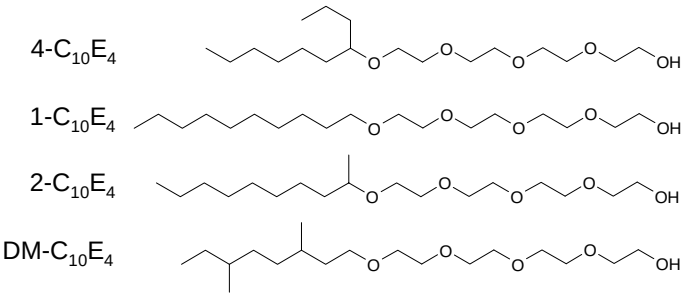
Institut für Festkörperforschung
Forschungszentrum Jülich GmbH
D-52425 Jülich

Experimental Report
of Neutron Scattering Experiments
at the FRJ-2 Reactor

Proposal number:	KW2-05-001		
Experiment title:	**Non-ionic surfactants with different alkyl-chains**		
Dates of experiment:	05.03.2005 – 06.03.2005 10.03.2005 – 11.03.2005 09.04.2005 – 11.04.2005	Date of report:	09.03.2006
Experimental team: Names	Addresses		
Henrich Frielinghaus Christian Frank Simona Maccarrone Jürgen Allgaier	Institut für Festkörperforschung, Forschungszentrum Jülich GmbH, D-52425 Jülich Institut für Festkörperforschung, Forschungszentrum Jülich GmbH, D-52425 Jülich Institut für Festkörperforschung, Forschungszentrum Jülich GmbH, D-52425 Jülich Institut für Festkörperforschung, Forschungszentrum Jülich GmbH, D-52425 Jülich		
Local Contact:	Henrich Frielinghaus		

Experimental report text body — Non-ionic surfactants with different alkyl-chains

Technical $C_{10}E_4$ surfactants have been synthesized by ethoxylysation of different decanols. The various isomers 4-decanol, 1-decanol, 2-decanol and di-methyl-octanol lead to a branched structure of the hydrophobic alkyl-block. These branched surfactants are very interesting in applications, but have never been investigated systematically. Here, we studied 4 microemulsions of D_2O, decane, and one of the $C_{10}E_4$ surfactants. Phase diagrams were determined and compared to the SANS measurements we present here.



Scheme 1: Chemical structures of the 4 surfactant molecules. They were synthesized from different decanols by ethoxylysation. The alcohols were 4-decane, 1-decane, 2-decane and an octanol with two methyl side groups.

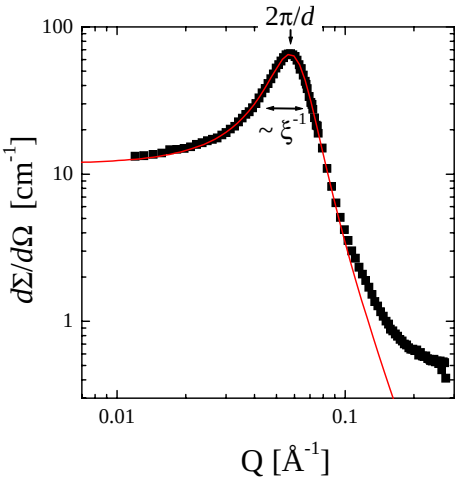


Figure 1: Typical SANS pattern of the surfactant 4-$C_{10}E_4$. Red curve is a fit to the Teubner-Strey theory. The obtained parameters are the domain size *d* and the correlation length ξ.

A typical SANS pattern is shown in figure 1. A correlation peak appears, the position of which is connected to the domain size *d*, and the width of which is inversely proportional to the correlation length ξ. A more refined description is achieved by a fit of the Teubner-Strey formula [1]. At larger scattering angles Q deviations occur due to (a) the lack of describing the true surface (true Porod constant is larger), and (b) due to the incoherent background which has not been subtracted so far.

The obtained parameters *d* and ξ are plotted as a function of the membrane volume content Ψ in figure 2. The domain size measures the average distance of two consecutive domains, and therefore is twice as large as the correlation length. The domain size can be described by a theory of Roux [2]. Roughly the domain size is inversely proportional to the membrane content, but in the refined model a logarithmic correction takes care of the membrane fluctuations which lead to a larger surface compared with the planar membrane. The theory describes the measured domain size well with a single parameter, the film thickness δ.

The so obtained film thickness δ is shown as a function of the surfactant molecule in figure 3. For the last three surfactants 1-$C_{10}E_4$, 2-$C_{10}E_4$, and DM-$C_{10}E_4$ the backbone length seems to have direct influence on the film thickness. The highly pure 1-$C_{10}E_4$ has a film thickness of 12.0Å. Our technical 1-$C_{10}E_4$ has a little longer ethylene oxide chain which explains the larger δ of 14.7Å. It is known that the surfactant molecules are strongly tilted by 66° relative to the normal axis of the membrane. The reduction of one backbone carbon therefore would lead to a reduced film thickness by 0.52Å. The regression line represents this slope well. Thus, the film thickness of the 3 surfactant molecules is not influenced by the branching. The branching influence is much higher for the 4-$C_{10}E_4$ surfactant since the branch is 3 carbons long. A change of the tilt angle might be an explanation.

The bending rigidity κ is obtained by the structural parameters by the Gaussian random field theory which predicts $\kappa \sim \xi/d$. Comparing the phase diagrams (not shown here) with the bending rigidity one finds: The lower the minimal surfactant concentration (fish tail point) is the larger the bending rigidity is. Obviously a more rigid membrane leads to larger structures with a better surface to volume ratio. The largest κ is obtained by the normal 1-$C_{10}E_4$. The next lower κ is obtained by DM-$C_{10}E_4$, which obviously has the smallest perturbation of the branching since the methyl groups have the largest distance to the hydrophilic head. The other two surfactants 2-$C_{10}E_4$ and 4-$C_{10}E_4$ have the branching directly connected at the hydrophilic head. The shorter side group leads to the next lower κ, while the relatively large side group leads to the lowest κ.

We therefore could explain the film thickness and the surfactant efficiency (and κ) by the molecule structure.

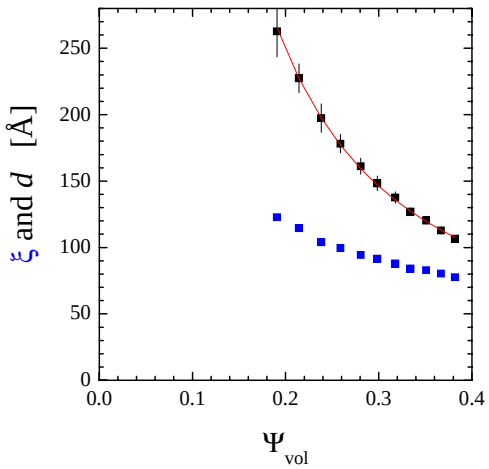


Figure 2: The domain size *d* and the correlation length ξ obtained by the Teubner-Strey fit to the SANS measurements as a function of the membrane content Ψ. The fitted line is due to the theory of Roux [2].

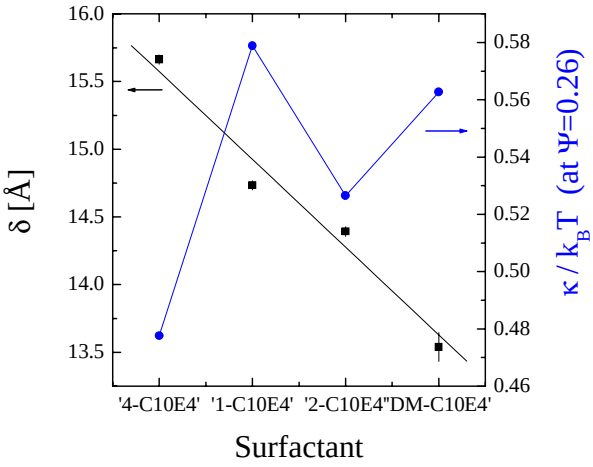


Figure 3: The film thickness δ obtained by the description of the domain size *d* by Roux's theory [2]. The bending rigidity κ is read off at a constant membrane content Ψ = 0.26.

References:

[1] M. Teubner, R. Strey, *J. Chem. Phys.* **87**, 3195 (1987)

[2] D. Roux, F. Nallet, E. Freyssingeas, G. Porte, P.Bassereau et al., *Europhys. Lett.* **17**, 575 (1992)

Institut für Festkörperforschung
Forschungszentrum Jülich GmbH
D-52425 Jülich

Experimental Report
of Neutron Scattering Experiments
at the FRJ-2 Reactor

Proposal number:	KW2-05-002, KW3-05-001		
Experiment title:	Self-assembling behavior of crystalline/amorphous random copolymers in dilute solutions: 3-segments PEB-6.5/8.9/10.1 and 4-segment PEB-2.6/6.0/10.9/13.2 in decane studied with SANS (parts 2 and 3)		
Dates of experiment:	12.04.05 – 15.04.05 17.05.05 – 23.05.05	Date of report:	29.05.06
Experimental team: Names	Addresses		
Aurel Radulescu, Emmanuel Kentzinger, Jörg Stellbrink,	Forschungszentrum Jülich Institut für Festkörperforschung D-52425 Jülich Germany		
Local Contact:	Dr.H.Frielinghaus, Dr.E.Kentzinger		

Experimental report text body

The self-assembly of poly(co-olefins) in dilute solution has been shown via SANS to yield either plate-like or needle-like micelles-like micelles [1,2]. The resultant supramolecular structures are dependent upon the copolymer architecture. The crystalline-amorphous diblock co-polymers yield self-assembled hairy plates while the corresponding random co-polymers yield one-dimensional needle shaped aggregates. Both kinds of polymers are able to modify the wax crystal structures in dilute solution. The diblock copolymers form a 2-d morphology consisting of a crystalline core surrounded by amorphous brushes. The core nucleates the wax crystals while the brush keeps them small and prevents their 3-d development. The PEB-*n* random copolymers (*n* - the number of ethyl sides per 100 backbone carbons) show selectivity in their wax crystal modification capacities depending on their crystallinity that is tuneable by *n*, i.e. the lower *n* the higher the crystallization tendency and the higher the temperature at which it initially occurs. By SANS and rheology [2] it was stated that efficient PEB-*n* additives for oil industry would contain graded ethylene content. Therefore, a SANS study of the self-assembling morphology in solution and wax crystal modification capacity of multi-segment random copolymers presenting graded ethylene content was initiated recently [3]. The study focused on two multi-segment copolymers, a triblock PEB-6.5/8.9/10.1 and a tetrablock PEB-2.6/6.0/10.9/13.2 and reported about the temperature behaviour of the self-assembling properties of these materials in decreasing temperature from the single coil regime (85°C) up to 0°C. The present experiments continued the structural study of the polymer aggregates formed at temperatures below 0°C and extended the investigation to a larger length scale by involving the focusing-SANS technique. In this way structures showing characteristic sizes from 1 µm to 1 nm formed upon cooling in solutions of multi-block random copolymers could be characterized. The conventional SANS investigations performed at -10°C and 0°C revealed that the scattering patterns do not change qualitatively in comparison with those collected at temperatures above 0°C and quantitatively show a continuous increase of the scattered intensity level. One can roughly conclude that the morphology of the

aggregates formed by multiblock random copolymers in solution does not change only their number increases in decreasing temperature. Fig.1 shows the scattering patterns from the structures formed by the two investigated multi-block copolymers at -20°C in decane. These present most likely a 1-dimensional morphology as it is revealed by the Q^{-1} power law behavior of the scattering at low Q. The 1D morphology must be formed by core-shell crystalline-amorphous substructures as long as the highly crystallizable PEB-2.6, PEB-6.0 and PEB-6.5 blocks should form compact crystalline objects. The focusing-SANS (F-SANS) investigations have been stimulated by the microscopy observations revealing large-scale aggregates with sizes in the range of micrometers formed by the multi-block copolymers in solution. Fig.2 presents the joined conventional-SANS and F-SANS scattering patterns: it seems that the 1D crystalline-amorphous objects associate and form soft spherulitic-like aggregates with radii ranging between 1.5 μm as in case of the tri-block material (Beaucage analysis of the F-SANS data for a power law of Q^{-4} [4]) and 5 μm as for the tetra-block material (revealed by the micrographs, Fig.3). The analysis of the structural and density parameters of these morphologies in terms of models and the elucidation of the contradictory Q^{-4} behavior of the scattering from soft structures as those revealed by microscopy is in progress.

References: [1] D.Richter et al., Macromolecules 30, 1053, 1997; [2] H.S.Ashbaugh et al., Macromolecules 35, 7044, 2002; [3] experimental report KW1-04-026 FRJ-2; [4] G.Beaucage, J.Appl.Cryst. 29, 134, 1996.

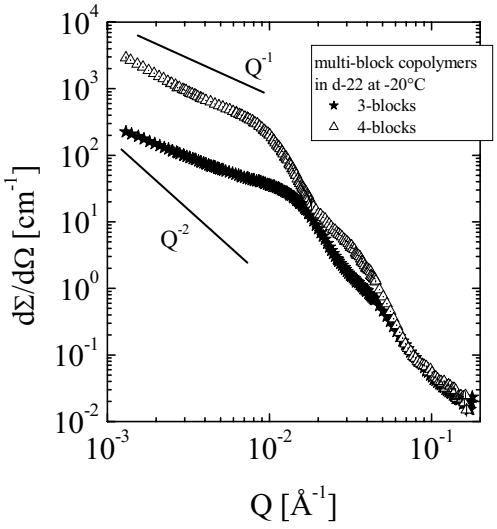


Fig.1 – Conventional SANS patterns from multi-block random copolymers. The Q^{-1} power-law behaviour of the scattering at low Q is obvious.

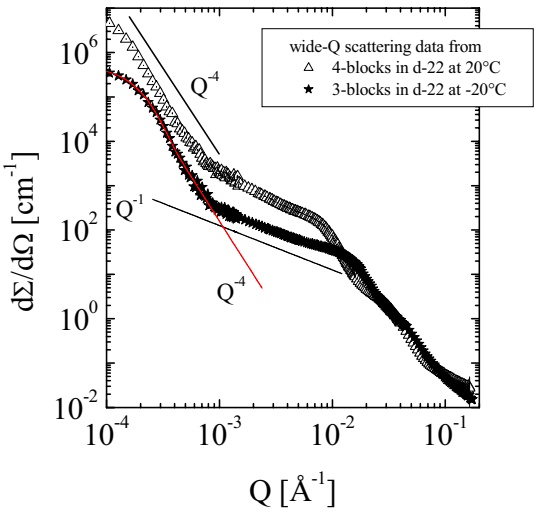


Fig.2 – Wide-Q scattering patterns from multi-block random copolymers. The Beaucage analysis of the scattering at low Q is depicted by the red curve.

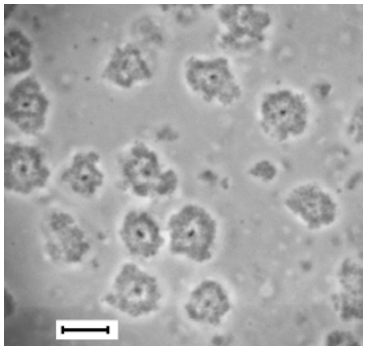


Fig.3 – Micrograph from a solution of tetra-block PEB-n copolymer in decane at 20°C; the scale bar represents 10 μm.

Institut für Festkörperforschung
Forschungszentrum Jülich GmbH
D-52425 Jülich

Experimental Report
of Neutron Scattering Experiments
at the FRJ-2 Reactor

Proposal number:	KW2-05-003, KW2-05-012, HAD-05-014		
Experiment title:	**Investigating the GISANS method on KWS-2 – Part I and Part II**		
Dates of experiment:	15.–20.04.2005 22.–28.06.2005	Date of report:	13.06.2006
Experimental team: Names	Addresses		
E. Kentzinger H. Frielinghaus U. Rücker Th. Brückel	Institut für Festkörperforschung, Forschungszentrum Jülich Institut für Festkörperforschung, Forschungszentrum Jülich Institut für Festkörperforschung, Forschungszentrum Jülich Institut für Festkörperforschung, Forschungszentrum Jülich		
Local Contact:	H. Frielinghaus		

Experimental report text body

The aim of this experiment was to learn the Grazing Incidence SANS (GISANS) method. GISANS enables to study the in-plane correlations in a thin film sample on the 1-to-100 nm length scales. It is complementary to off-specular scattering at a reflectometer, method that probes the correlations in the 1–to-10 µm range.

GISANS can be performed at a SANS machine equipped with a precise goniometer at sample position. It uses the fact that, at a SANS machine, the beam impinges on the sample with a beam that is collimated along the two perpendicular directions perpendicular to the incoming wave vector $\mathbf{k_i}$. At a reflectometer, the beam is collimated oly along one of those two directions and enables to resolve Q_x and Q_z as defined in Fig.1. At a SANS reflectometer, Q_y, the y-component of the scattering wave vector **Q**, can also be resolved, allowing to probe correlations at the nanometer length scale (Fig. 1).

We show here some of the results obtained on a remanent polarizing m=2.5 supermirror. A study of its remagnetization process had already been been performed on HADAS (c.f. report HAD-03-009). The aim was to obain more information of the interface roughness and magnetic lateral correlations. We therefore measured the GISANS signal on this sample, varying the angle of incidence of the neutrons from 0 to 2.5° (λ = 6.3 Å), and at several applied magnetic fields. Also, several sample-wrt-beam geometries and several collimation and sample-to-detetor distances have been probed.

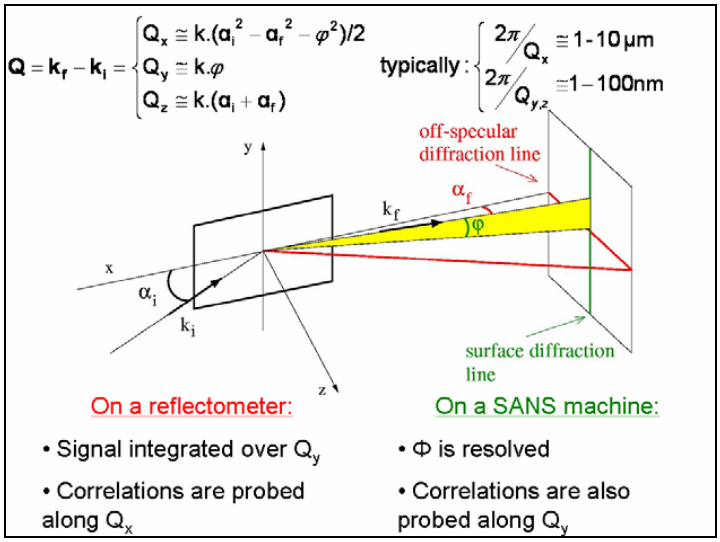


Fig.1: The GISANS geometry. Along Q_y, in-plane correlations can be probed in the 1-to-100 nm length scales.

We show in Fig.2 some of the results obtained with the applied field applied along the easy axis of magnetization and perpendicular to $\mathbf{k_i}$. Those data will be explained in the light of the polarized GISANS measurements presented in the report KW2-05-033.

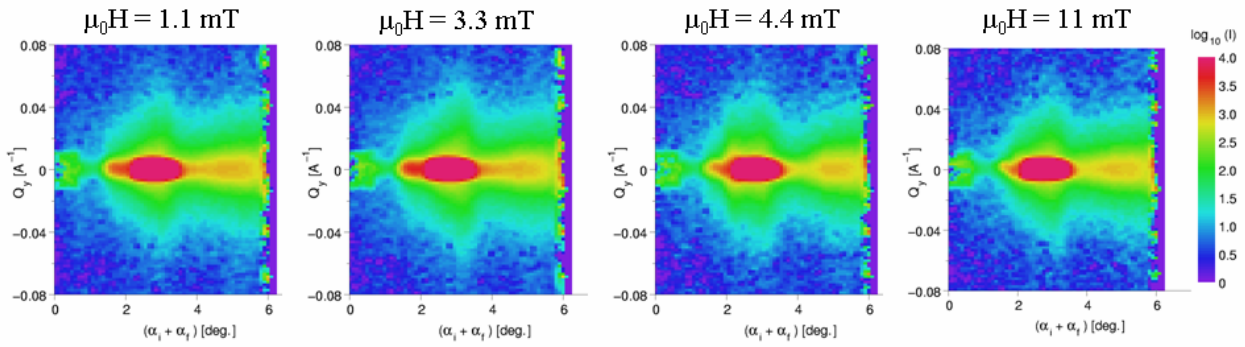


Fig.2: Field dependency of the GISANS signal measured on the supermirror at an angle of incidence α_i=1.5°, a collimation length of 8 m and a sample-to-detector distance of 3 m. Exposure time: 20 minutes per image.

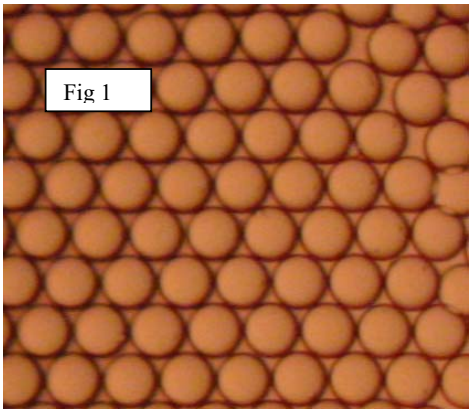
Institut für Festkörperforschung
Forschungszentrum Jülich GmbH
D-52425 Jülich

Experimental Report
of Neutron Scattering Experiments
at the FRJ-2 Reactor

Proposal number:	KW2-05-004		
Experiment title:	Interactions of polymer and surfactant at the oil/water interface of monodisperse emulsions.		
Dates of experiment:	12.03. – 18.03.2006	Date of report:	30.06.2006
Experimental team: Names	Addresses		
Terence Cosgrove Dong Qiu Andrew Woodward	School of Chemistry, University of Bristol, Cantock's Close, Bristol, BS8 1TS, U.K.		
Local Contact:	Jörg Stellbrink and Aurel Radulescu		

Experimental report text body

Oil in water emulsions will coalesce unless stabilised by an emulsifier. The most commonly used stabilisers are amphiphilic species such as surfactants and polymers. These chemical species reduce the interfacial tension between the oil and water phases. This is achieved by combining hydrophilic and hydrophobic moieties on one molecule. The molecules adsorb to the boundary between hydrophilic and hydrophobic phases, with the two moieties adsorbed into respective, favoured, phases.



Complex emulsion systems might contain more than one surface active species, in which case there will be competition for adsorption to the interface, and the formation of mixed micelles in solution. Our initial aim was to investigate the interaction between polymers and surfactants in emulsion systems.

We have formed monodisperse emulsions of poly-(dimethylsiloxane) in water. The emulsion were made using micro-fluidic chips that were designed based on those reported by Anna[1] and Xu[2]. Using monodisperse emulsions reduces the need for statistical particle size distribution functions when fitting models to the scattering data.

Figure 1 shows a mondisperse emulsion made from 50% deuterated PDMS [14K] and 50% hydrogenated PDMS [1K] with a size of approximately 40µm stabilized by H-SDS. This sample was contrast matched with a 44% D_2O 56% H_2O mixture. Unfortunately the samples were in very limited supply because of problems with the micro-fluidic device making it impossible to carry out the full range of experiments proposed.

Figure 2 shows a combined data set obtained form KWS-2 and KWS-3 for a sample of the PDMS emulsion in pure D_2O. There is a characteristic Q^{-4} decay from the emulsion/solution interface and the intensity at low Q is directly related to the surface/volume ratio in the sample. The minimum Q is 4.5 x 10^{-5} A^{-1} which sets a minimum size of approx 15 μm putting it outside of the range required for estimating the droplet size. It was our aim to make a smaller particle and to use data from DKD, but that data was unusable.

Figure 2 PDMS/SDS Emulsion in D_2O

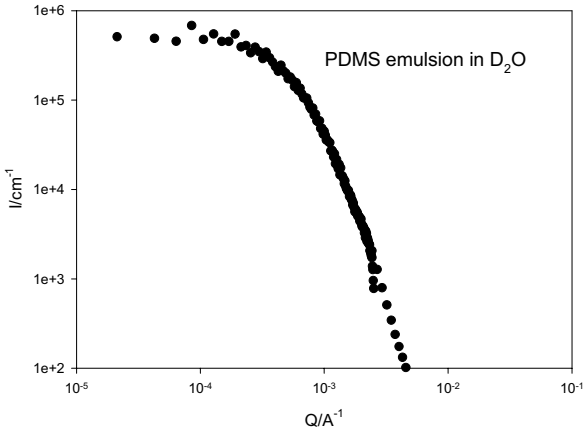


Figure PDMS/SDS in Contrast Matched D_2O/H_2O

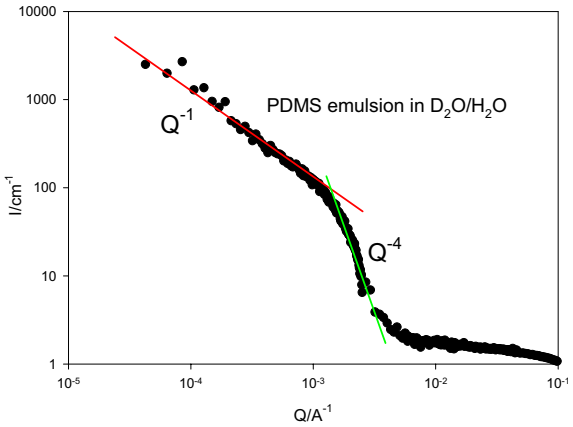


Figure 3 shows data with the emulsion contrast matched to a mixture of D_2O/H_2O. Under these circumstances the scattering from the emulsion is minimized. Unfortunately it proved impossible to make a pure D emulsion because of the high viscosity of the polymers available and a mixture of a high molecular weight D and a low molecular H were used. This meant that even under contrast match conditions there is some residual polymer scattering. The signal we were looking for was from H-SDS at the interface and it proved impossible to deconvolute these data. On a qualitative view the scattering showed three domains. At low Q a Q^{-1} which we believe originated from the polymer mixture. The Q^{-4} region may be a result of the emulsion not being fully contrasted. The high Q region may be attributable to the H-SDS.

Institut für Festkörperforschung
Forschungszentrum Jülich GmbH
D-52425 Jülich

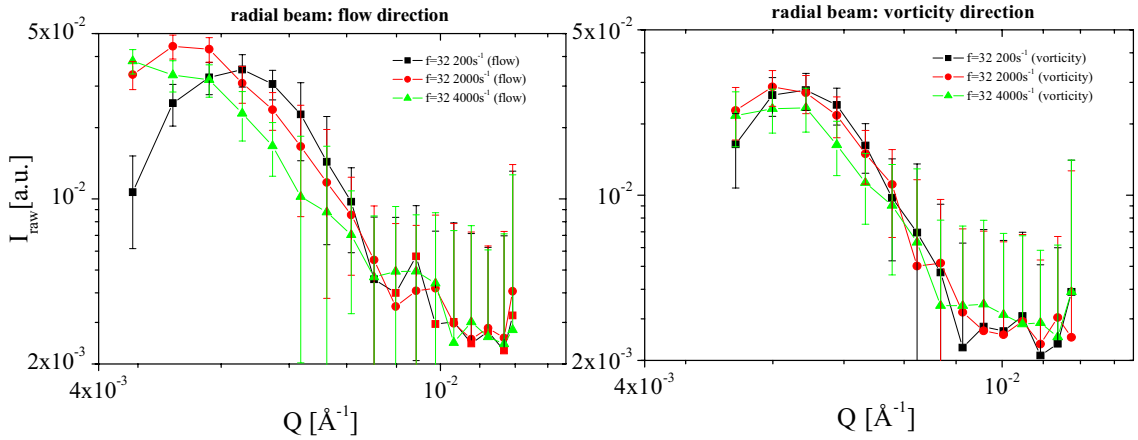
Experimental Report
of Neutron Scattering Experiments
at the FRJ-2 Reactor

Proposal number:	KW2-05-005, KW2-06-007		
Experiment title:	**Shear-induced deformation of low functionally star polymers**		
Dates of experiment:	28.11.-30. 11. 2005 10.04.-13. 04. 2006	Date of report:	06.06.2006
Experimental team: Names	Addresses		
J. Stellbrink G. Rother B. Lonetti	IFF, FZ Jülich, D-52425 Jülich, Germany IFF, FZ Jülich, D-52425 Jülich, Germany IFF, FZ Jülich, D-52425 Jülich, Germany		
Local Contact:	J. Stellbrink		

Experimental report text body

Ultra-soft colloids possess a soft shell and a hard core. They can by synthesized by, e.g., grafting flexible polymers to the surface of a sphere or by using block-copolymer micelles. The interesting feature of such systems is the possibility of a deformation of the soft shell in shear flow. In a recent theoretical work the structural and dynamical properties of ultra-soft colloids in shear flow was investigated [1]. The underlying model was based on a regular star polymer, i.e. f linear polymer chains with equal molecular weight M_w, tethered to a central microscopic core (the limiting ultra-soft colloids). Arm number f, arm length M_w, and shear rate $\dot{\gamma}$ was systematically varied. A strong deformation of the colloids in shear flow was observed. With increasing shear rate, the component of the radius-of-gyration tensor in the flow direction increases, whereas the other two components decrease. Thus, soft colloids with a larger number of arms are aligned to a less extent than those with a smaller number of arms. We expect that a system with a very large number of arms behaves essentially like a spherical object. Increasing the length of an arm from 10 monomers to 20 monomers yields a comparable behaviour. The slope of the curves is identical, merely the time scale is shifted, which corresponds to a different characteristic relaxation time. However, a crucial point in comparing theory with experiment for shear deformation of polymeric systems is the necessary minimum shear rate $\dot{\gamma}_{\min}$ to observe such a deformation. If the characteristic time of the experimental system, τ_c, is smaller than the inverse minimum shear rate, the systems relaxes before any shear deformation can be observed. Recently it was found, that $\dot{\gamma}_{\min}$ seems to scale with N^{-2}, where N is the degree of polymerization (number of repeat units). Therefore high molecular weight polymers would be the ideal experimental system for such a comparison.

In our first experiment we investigated therefore high molecular weight poly(butadiene) star polymers [2] with intermediate functionality f=6 and f=32 in d-cis-decalin by means of Rheo-SANS experiments in radial configuration. The preliminary results show some evidence for the theoretically expected effects of external shear, although the data statistics are rather poor, see fig 1. Whereas along the vorticity (= neutral) direction the intensity seems to be more or less independent of the applied shear rate, along the flow direction there is a systematic shift towards lower Q-values indicating some extension of the star polymer.



In our second experiment we investigated the same star polymers in a solvent of much higher viscosity, i.e. deuterated bis-(2-ethylhexyl)-phthalate (DOP). DOP has a nearly two orders of magnitude higher viscosity than the previously used d-cis-decalin (≈68cp instead of 3cp), which enhances the expected effect. Unfortunately it was not possible to keep the star polymers long enough dissolved to perform high quality SANS experiments. DOP is a marginal solvent for butadiene, so we had to compete with (partial) phase separation of the polymer, which crucially obstructs our experiment. Therefore we investigated in addition an 18-arm polyisoprene star polymer in DOP, which has a much lower M_w=7500g/mol, but here no effects of shear were observed.

References:

[1] M. Ripoll, R. G. Winkler, and G. Gompper, *Phys. Rev. Letters*, **96**, 188302, 2006.

[2] Stellbrink, J. Allgaier, D. Richter, A. Moussaid, A.B. Schofield, W.C.K. Poon, P.N. Pusey, P. Lindner, J. Dzubiella, C.N. Likos, H. Löwen, *Appl. Phys. A*, **74** [Suppl.], S355–S357, 2002.

f	M_w 10^{-6} [g/mol]	$D_{p,arm}$	R_g [Å]	B_w [g/mol]	$A_2 \cdot 10^4$ [cm^{3}mol/g^2]
2	0.57±0.04	14685	510±35	19.9±0.4	9.60±1.0
6	1.51±0.06	5093	521±6	19.9±0.5	7.00±0.24
16	3.45±0.27	3537	511±5	25.0±1.2	2.96±0.33
32	4.87±0.39	2944	514±5	22.0±1.6	1.06±0.28

Table 1: Molecular characteristics of the used poly(butadiene) star polymers obtained by SANS in perdeuterated cis-decaline [2]. M_w: molecular weight, $D_{p,arm}$: arm degree of polymerization, R_g: radius of gyration, B_w: blob molecular weight, A_2: Second virial coefficient.

Institut für Festkörperforschung
Forschungszentrum Jülich GmbH
D-52425 Jülich

Experimental Report of Neutron Scattering Experiments at the FRJ-2 Reactor

Proposal number:	KW2-05-006		
Experiment title:	Investigating lateral magnetization correlations in exchange biased IrMn/CoFe multilayers		
Dates of experiment:	15.04.05	Date of report:	May 17, 2006
Experimental team: Names:	Amitesh Paul, Emmanuel Kentzinger, Henrich Frielinghaus, Thomas Brueckel		
Address:	Institut fr Festkrperforschung Forschungszentrum Jlich GmbH D-52425 Jlich, Germany Deutschland		
Local contact:	Henrich Frielinghaus		

When a ferromagnet (FM)/antiferromagnetic (AF) bilayer is cooled below its blocking temperature in an external, a direct exchange coupling between FM and AF layers results in the shift of the hysteresis loop of the ferromagnetic layer (shift of the center from the zero field) along field axis which is termed as the exchange bias. Consequently, the hysteresis loop of the FM layer is usually shifted to negative fields.
The exchanged bias spin-valves studied in the present work are multilayer (ML) structures of $[Ir_{20}Mn_{80}(6.0nm)/Co_{80}Fe_{20}(3.0nm)]$x N prepared by dc magnetron sputtering, where N is the number of bilayers. The microstructure reveal a structural evolution of cluster sizes and shrinking of FM domains with N [1]. We found sequential switching of the layers that we relate to the microstructural evolution along the stack and no indication of coherent rotation of the magnetization was observed in our ML.
SF intensity maps for the specimen with N=10, when measured at HADAS show lateral magnetization fluctuations perpendicular to the applied field direction during the magnetization reversal. However, the length scales were much lower (200 Nm) than lateral coherence length of the neutron beam. A quantitative evaluation of the lateral length scale was beyond the scope of the present measurement geometry at HADAS. Thus in this work, therefore, we intended to measure the depth resolved length scales of such fluctuations perpendicular to the field direction which are originated from domains within the layers for the N=10 ML. We think GISANS technique is the unique way to explore such magnetization fluctuations which are directly linked to the magnetization reversal of exchange biased systems from vertically un-correlated magnetic domains.

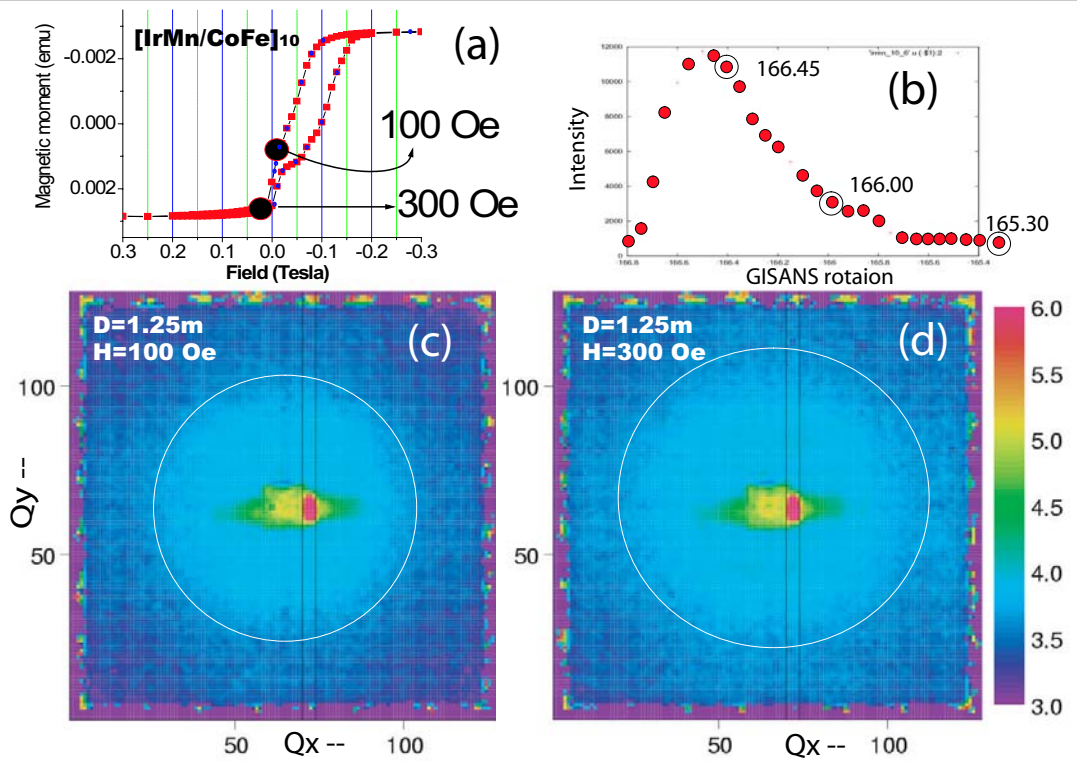


Figure 1. (a) SQUID hysteresis loop for $[Ir_{20}Mn_{80}(6.0\ nm)/Co_{80}Fe_{20}(3.0\ nm)]_{10}$ ML
(b) GISANS rotating motor position indicating the measurement angle corresponding to the critical angle θ_c and other higher angles.
(c) GISANS diffuse scattering spectra for two different applied fields (H) at a fixed D.

The measurements are done at two remanence fields for increasing [300 Oe] (Fig 1 (a)) and decreasing [100 Oe] fields with respect to the field cooling direction after saturating the specimen with + and - fields. We first determine the angles at which measurements are to be done. A specular scan of the intensity with increasing GISANS motor position give us the angles corresponding to three different regimes (Fig 1 (b)). In Fig 1 (c) and (d) are shown the intensity map for two different applied fields (H) at a foxed detector distance (D). Unfortunately, we can see only a halo of diffuse intensity around the specular beam (indicated in circle). These intensities at 100 Oe seems to grow to some extent at 300 Oe. This indicates, at least, the different size of the domains for the two remanence state of magnetization due to two opposite field history the sample undergoes. These diffusely scattered intensities are therefore supposedly arising from the domains within the layers of the ML stack. However, we could not observe the depth dependencies as expected even on varying with three detector distances. We find a possible problem in magnetizing the sample properly as there was no magnet available at the sample space which can induce a strong field of around 4.0 kOe to saturate the sample completely. The present results are nevertheless useful feedback for future measurements.

References

[1] A. Paul *et al.*, Journ. Magn. Magn. Mater. **268**, 216, (2005); Phys. Rev. B **70**, 224410 (2004).

Institut für Festkörperforschung
Forschungszentrum Jülich GmbH
D-52425 Jülich

Experimental Report
of Neutron Scattering Experiments
at the FRJ-2 Reactor

Proposal number:	KW2-05-007		
Experiment title:	CRITICAL FLUCTUATIONS AND ADSORPTION OF INDIVIDUAL FLUIDS CONFINED IN POROUS MEDIA: CONTINUATION		
Dates of experiment:	May 19. – May. 23, 2005	Date of report:	12-21-2005
Experimental team: Names	Addresses		
Y. B. Melnichenko G. D. Wignall D. R. Cole	Condensed Matter Sciences Division ORNL P.O.Box 2008 Oak Ridge, TN 37831-6393		
Local Contact:	Dr. H. Frielinghaus		

Experimental report text body

The adsorption of supercritical fluids in porous materials has been the subject of intense experimental and theoretical interest over the last decade. A supercritical fluid (SCF) is a substance at a pressure and temperature above its liquid-gas critical point where the coexisting (subcritical) liquid and gaseous phases become indistinguishable. At high pressure, the density of a SCF may become sufficient to provide substantial solvent power. At the same time, the diffusivity of solutes in SCFs is higher than in liquids due to a much lower viscosity, which facilitates mass transfer. The combination of tunable solvent power, practically unlimited miscibility with gases as well as advantageous mass transfer properties make SCFs an attractive alternative to subcritical (liquid) solvents for a variety of technological applications such as heterogeneous catalysis, adsorptive separations, regeneration of adsorbers and SCF chromatography [1]. Simplified theoretical considerations of heterogeneous processes are often based on an assumption that supercritical solvents in porous media can be treated as a continuum and thus the adsorption of the solvent molecules by the surface of solid porous adsorbents can be ignored. It is now being recognized however that when an adsorbate gas or supercritical fluid is in contact with a solid adsorbent, the attractive molecule-solid forces enhanced by strong micropore field effects can create a region near solid surface where the local adsorbate density is different from that in the homogeneous bulk phase [2]. The adsorbed phase is believed to extend to a distance of few molecular diameters from the surface far away from the critical point, and to become long ranged as the critical point is approached. An understanding of the structure and thermodynamic properties of the adsorbed phase at different conditions is fundamental to the successful development and optimization of reaction and separation processes involving SCF – solid interactions as well as to the fluid storage and carbon dioxide sequestration technologies [2].

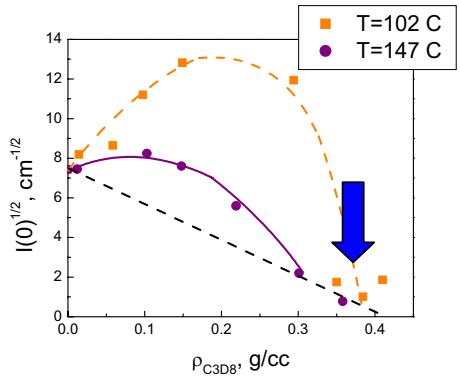


Fig.1. Variation of I(0) of d-propane in aerogel at two different temperatures shown in the inset. ZAC for this system is reached at ρC3D8=375 g/cc (shown by the arrow).

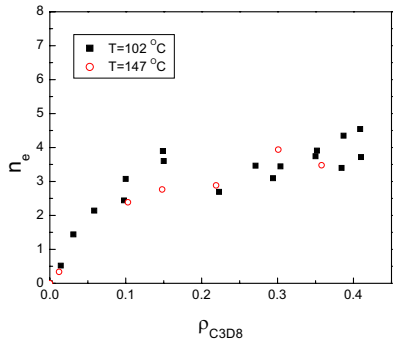


Fig.2. Variation of excess adsorption parameter for d-propane saturated aerogel with the fluid density at two temperatures shown in the inset.

During our recent experiments we were studying the adsorption behavior of deuterated propane in aerogels with the physical density of silica 0.1 g/cc which corresponds to the porosity of 96%. The aim of experiments was to compare the adsorption behavior of d-propane with that of supercritical carbon dioxide (SC CO_2) studied before at similar conditions [2]. From the point of view of SANS, the experimental condition for the two fluids in aerogel are very different as the zero average condition (ZAC) can not be reached for SC CO_2 which would require pressurizing the fluid to experimentally unachievable density of 1.27 g/cc [2]. At the same time, ZAC for d-propane in aerogel can be reached at ρ_{C3D8}=0.375 g/cc which lies within experimental window of the ORNL high pressure cell (see Fig. 1). This fact opens an interesting opportunity of extracting direct information about the density of adsorbed phase at ZAC condition.

Fig.2 shows the variation of excess adsorption of confined d-propane determined using a methodology described in [2]. The values of this parameter are an order of magnitude higher than excess adsorption of SCF in zeolites and superactivated carbons, although it is somewhat smaller than excess adsorption of CO_2 in similar aerogels. Another interesting difference between adsorption behavior of SC CO_2 and SC d-propane is the temperature invariance of excess adsorption of d-propane which indicates that the pores of the matrix are get filled with the adsorbed fluid already at temperatures exceeding the liquid-gas critical temperature (T_C=97 ^{O}C) by 50 degrees. The data processing of the pressure dependence of adsorption of d-propane in aerogels is now finished and a paper describing these effects is being written and will be submitted to JCP within few months. We hope to explore the variation of adsorption of d-propane with temperature during our next experimental session in February 2005.

1 Supercritical Fluids: Fundamentals for Applications (E. Kiran and J. M. H. Levelt-Sengers, eds), Kluwer Academic Publ., Dodrecht, Boston, London, 1993

2 Y. B. Melnichenko, G.D. Wignall, D. R. Cole, H. Frielinghaus, submitted to J. Chem. Phys.

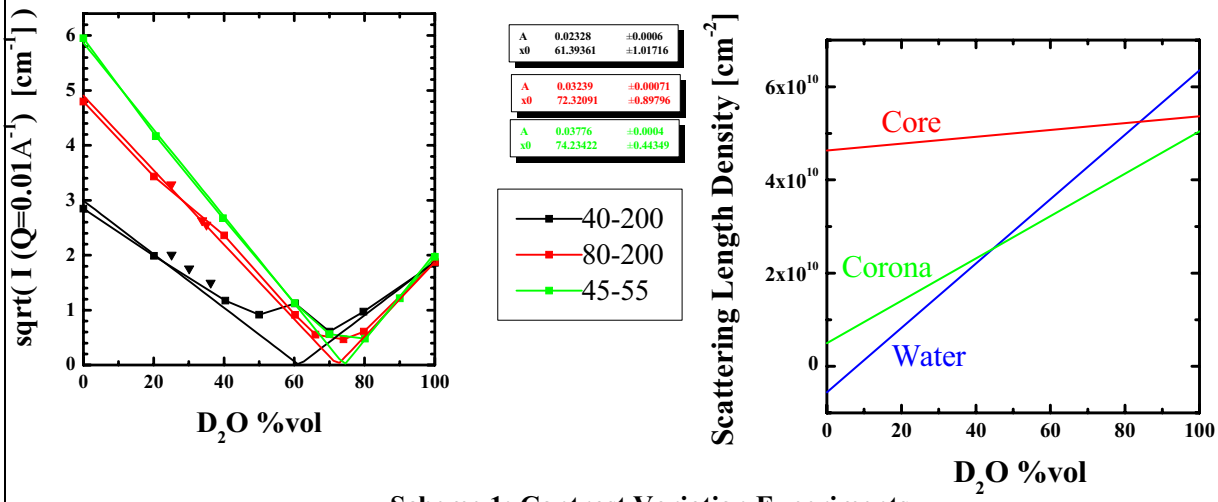
Institut für Festkörperforschung
Forschungszentrum Jülich GmbH
D-52425 Jülich

Experimental Report
of Neutron Scattering Experiments
at the FRJ-2 Reactor

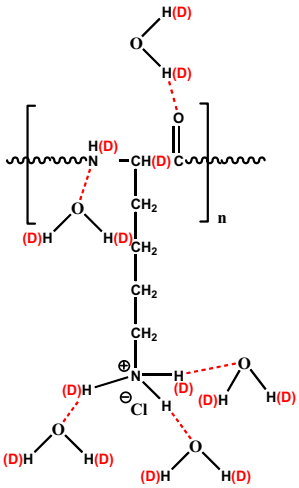
Proposal number:	KW2-05-008, KW2-05-042		
Experiment title:	Examination of the micellar behaviour of amphiphilic triblock copolypeptides of the ABA type, where A is polylysine and B is poly(r-benzyl-L-glutamate), in water by SANS		
Dates of experiment:	25.08.05-06.09.05 and 16.01.06-23.01.06	Date of report:	25.05.06
Experimental team: Names	Addresses		
Hermis Iatrou Henrich Frielinghaus	**University of Athens, Chemistry Department** **Institut für Festkörperforschung, Forschungszentrum Jülich GmbH, Germany**		
Local Contact:	Henrich Frielinghaus		

Experimental report text body

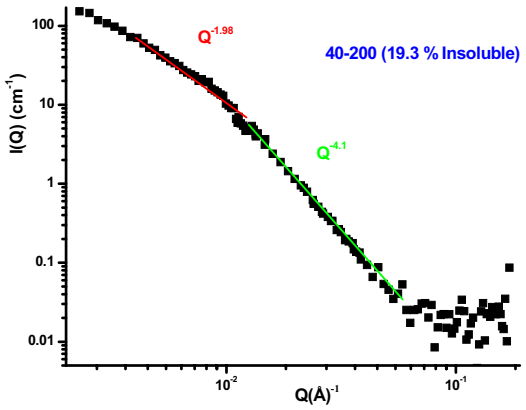
We have synthesized amphiphilic triblock copolypeptides of the ABA type, where A and B are poly-L-lysine and poly(γ-benzyl-L-glutamate), respectively. These copolypeptides are potential candidates for the formation of vesicles in water and conditions close to the one of the human body, very interesting for biomedical applications such as drug delivery systems. The synthesized triblock copolypeptides poly(-L-lysine)-b-poly(γ-benzyl-L-glutamate)-b-poly(-L-lysine) are amphiphilic copolypeptides, since the outer blocks are water soluble, whereas the middle block is insoluble. In order to distinguish where the insoluble and the soluble part exists within the aggregate, partially deuterated samples were synthesized, i.e. the benzyl groups of the poly(γ-benzyl-L-glutamate) part was partially deuterated. This gives enough contrast to mach exactly either the core or the corona of the micelles that will be formed. Three different triblock copolypeptides have been synthesized, with the same molecular weights but different compositions, the 40-200, 80-200 and 45-55. The investigation of the micellar behaviour of amphiphilic triblock copolypeptides was performed in this project in a pH 7-8, at room temperature. Initial experiments were be performed by LALLS in the University of Athens, which showed that the formed aggregates were large (about 100 nm radius) and spherical in shape. SANS was performed in KWS2, in order to find the molecular characteristics of the aggregates. First, we performed measurements of dilute solutions of the copolypeptides in mixtures of D2O and H2O, in order to calculate the scattering length density and the density of each part, i.e. the polylysine and PBLG parts. Then, measurements were performed in protonated and deuterated water in different concentrations. The contrast variation experiments gave a density of 1.13 g/ml for the polylysine part, and 1.32 for the PBLG part. Moreover, hydrogen bonding was assumed for the water soluble part of polylysine, where 5 molecules of water were linked to the polylysine molecule. Moreover, it was concluded that two of the hydrogens on the backbone of the aminoacids were exchanging with deuteriums, in order to match the experimental results (Scheme 2). The Scheme 1 shows the contrast variation experimental and fitted data.



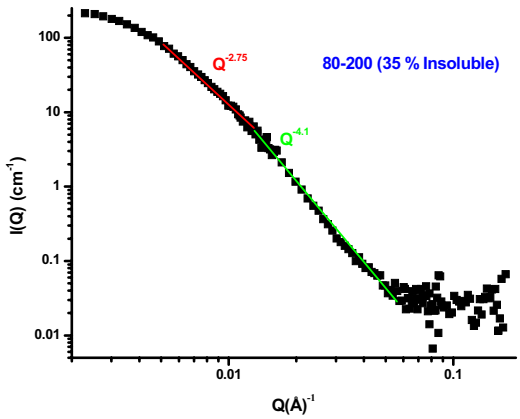
Scheme 1: Contrast Variation Experiments



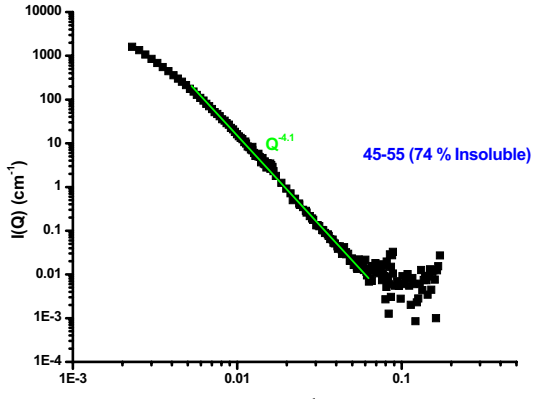
Scheme 2: Proposed form of the polylysine part



Scheme 3: I(Q)=f(Q) for the 40-200 sample



Scheme 4: I(Q)=f(Q) for the 80-200 sample



Scheme 5: I(Q)=f(Q) for the 45-55 sample

Institut für Festkörperforschung
Forschungszentrum Jülich GmbH
D-52425 Jülich

Experimental Report
of Neutron Scattering Experiments
at the FRJ-2 Reactor

Proposal number:	KW2-05-009		
Experiment title:	Quantitative relationship between non linear mechanical properties and particle arrangement in model filled elastomers.		
Dates of experiment:	May 2005	Date of report:	March 2006
Experimental team: Names	Addresses		
Thomas Chaussée Hélène Montes	PPMD-ESPCI Esc H 10, rue Vauquelin 75005 PARIS		
Local Contact:	Henrich Frielinghaus		

Experimental report text body

Filled elastomers are widely used for their interesting mechanical properties thatn can be adapt to the use. But we do not understand how the surface interaction between the particle surface and the elastomeric matrix influences the mechanical behavior of so-filled elastomer. Therefore we decided to produce some model silica-filled elastomers using different grafts in order to modulate the surface interaction. Grafts studied are: n-Octyltriethoxysilane (C_8TES) and Hexamethydisilazane (HMDS) in order to perform a weak interaction and Acetoxyethyldimethylchlorosilane (MCSNC) to perform some hydrogen bonding.
The samples were prepared using ford method using dialysis to get the silica suspension in the ethyl acrylate monomer. Suspensions were then adjusted to the write concentration by diluting the initially concentrated suspension, and a polymerizing initiator as well as a cross linker is added and polymerization is performed by alternative UV lighting. Before and during the polymerization step suspensions were cooled down to or 0°C in order to freeze the system, or heated to 50°C or 60°C in order to bring some energy to deaggregate the particles during polymerization. The so obtained elastomers are then characterize by SANS in order to identify the dispersion state of the particle in the poly(ethyl acrylate) matrix.
Figure 1 didn't exhibit any correlation peak around 0.01 $Å^{-1}$ q values, this means that there is no particular distance between two silica particles size. However it doesn't exhibit a strong increase in the low q region, it means that there shouldn't be any aggregates in the filled elastomers.
On figure 2 and 3 we are not able to see any difference on the Intensity curves whatever the size or the graft. It means that temperature has no influence on the dispersion state of the grafted silica particles.

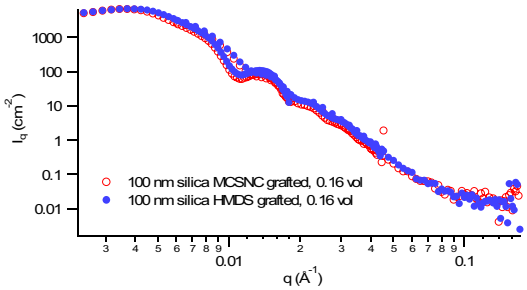


Fig. 1: 100 nm silica grafted HMDS or MCSNC synthetised at Room temperature

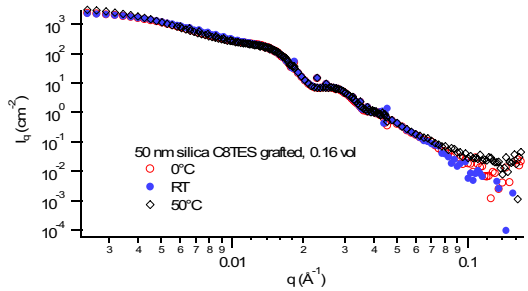


Fig. 2: 50 nm silica grafted C8TES synthetised at 0°C (red), RT (blue), 50°C (black)

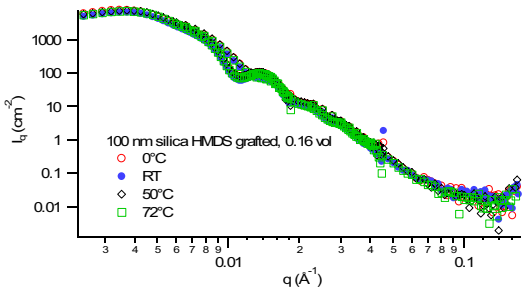


Fig. 3: 100 nm silica grafted HMDS synthetised at 0°C (red), RT (blue), 50°C (black) and 72°C (green)

Institut für Festkörperforschung
Forschungszentrum Jülich GmbH
D-52425 Jülich

Experimental Report
of Neutron Scattering Experiments
at the FRJ-2 Reactor

Proposal number:	KW2-05-010, KW2-05-018, KW2-05-035		
Experiment title:	**Confinement effects of diblock copolymers in bicontinuous microemulsions – part I, II, III**		
Dates of experiment:	16. – 17.05. 2005, 24. – 26.08. 2005, 25. – 26.10. 2005	Date of report:	21.03.2006
Experimental team: Names	Addresses		
Simona Maccarrone Henrich Frielinghaus	Forschungszentrum Jülich GmbH, Institut für Festkörperforschung, D-52425 Jülich Forschungszentrum Jülich GmbH, Institut für Festkörperforschung, D-52425 Jülich		
Local Contact:	Henrich Frielinghaus		

Experimental report text body

Amphiphilic diblock copolymers have approved to increase the efficiency of surfactants dramatically (polymer boosting effect). In the first studies [1] the domain size of oil or water domains was relatively large compared to the polymer size. Initial simulations by Auth [2] predicted deviations from the ideal behaviour with increasing confinement of the polymer. At intermediate confinement the efficiency boosting is even more dramatic. At high confinement a reversed behaviour is predicted. The current study investigates the sensitivity of the polymer boosting effect as a function of the degree of confinement.

Microemulsions consist of immiscible oil and water. The third component, the surfactant, mediates between oil and water. Domains of pure oil and water are formed, whose surfaces are covered by the amphiphile. For equal volumes of oil and water a minimum amount of surfactant is needed to form a one-phase bicontinuous microemulsion. This amount is a measure for the efficiency of the surfactant.

When adding amphiphilic diblock copolymers to the microemulsion, this macro surfactant molecule is anchored in the surfactant membrane, and the two different blocks are situated in their pleasant environment [1]. Furthermore, it was shown that the diblock copolymer increases the bending rigidity. This result explains the empirically found polymer boosting effect, which describes a drastic enhancement of the surfactant efficiency. Stiffer membranes allow the formation of larger domains with a better surface to volume ratio. Theories agree well with these first studies.

Several bicontinuous microemulsions were studied intensively in phase diagram measurements. A single relatively large diblock copolymer PEP_{22}-PEO_{22} was chosen. The domain spacing of the microemulsions was varied by the use of different oils (hexane, octane, decane, undecane, dodecane, tridecane, tetradecane) influencing the efficiency primarily. The polymer amount over the total amphiphile quantity that we could add changes significantly going from the shortest chain oils (4 %) up to the longest chain oils (0.025%) leaving the phase diagrams almost unchanged.

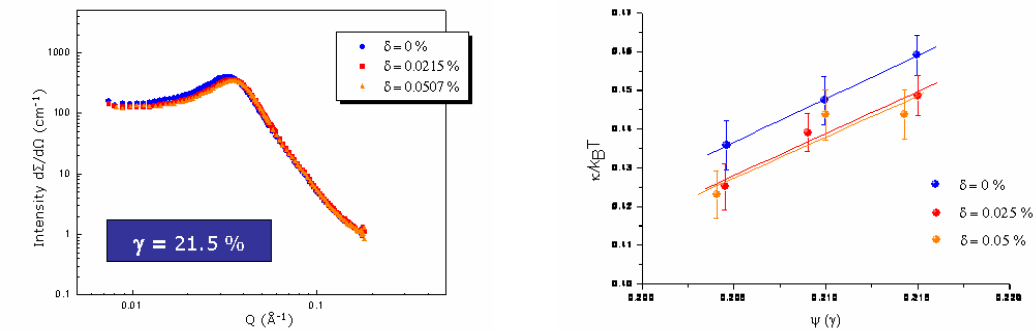


Figure 1. The plot on the left shows how, at fixed concentration, the addition of polymer doesn't affect visibly the peak width for tetradecane microemulsions. On the right, we have the decreasing of the bending rigidity κ as far as we add some polymer.

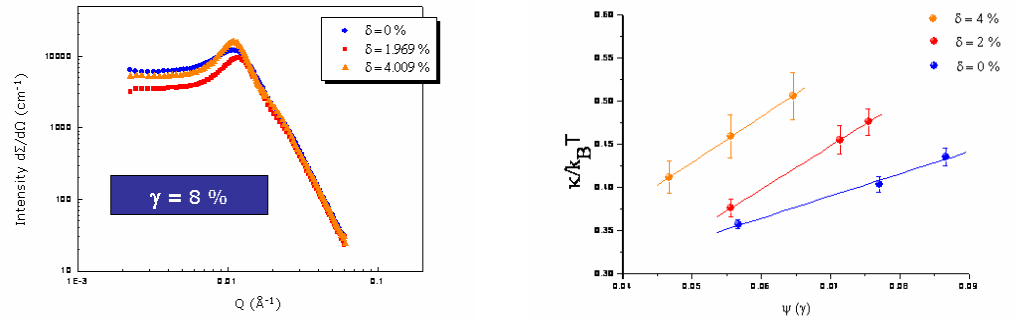


Figure 2. The plot on the left shows how, at fixed concentration, the addition of polymer for hexane systems can affect the peak width. On the right, we have the increasing of the bending rigidity κ with polymer addition.

By small angle neutron scattering (SANS) the structure of a microemulsion is studied, which can be characterized by the domain spacing *d* and the correlation length ξ. The Gaussian random field theory connects these two parameters with the bending rigidity κ.

As examples, we can see the behaviour of the 2 extreme cases: tetradecane and hexane systems. For the former, it seems to not have significant variations of the peak position as well as the width (fig.1 left). But performing the calculations of the bending rigidity we found a decreasing of κ with polymer addition (fig.1 right "antiboosting effect").

For the latter, it was found the reverse behaviour. As it is shown in the fig.2, the peak is affected by the polymer presence on the membrane, and becomes sharper that means an increasing of the correlations length. In this case, the bending rigidity increases because we have more polymer on the membrane surface, that becomes more rigid.

After collecting all these data, we are also able to draw the sensitivity rate Ξ of the variation of κ as a function of confinement expresses by the inverse of the ratio d/R_g where *d* is the domain size and R_g is the radius of gyration of our polymer. To cover a wider range of confinement we measured subsequently also hexane, eptane, octane and decane using a smaller polymer PEO_{10}-PEO_{10} in order to get more points in delimitiation of the curve. What we observed is a constant value of Ξ for the low confinement regime (more efficient microemulsions with short chain oils) that means that polymer is comfortable in the domains but with a lot of space that doesn't allow it to affect so much the membrane stiffness. Then the intermediate regime comes with a slight increasing around $d/R_g \sim 4$ and a strong decreasing after $d/R_g \sim 2$ for high confinement as a proof of the antibooster behaviour of the less efficient micromulsions with long chain oils. The whole measured behaviour agrees semi-quantitatively with the theoretical prediction (simulation by Auth [2]).

[1] B. Jakobs, T. Sottmann, R. Strey, J. Allgaier, L. Willner, D. Richter *Langmuir* **15**, 6707 (1999)
[2] PhD thesis: T. Auth, University Köln, 2003

Institut für Festkörperforschung
Forschungszentrum Jülich GmbH
D-52425 Jülich

Experimental Report
of Neutron Scattering Experiments
at the FRJ-2 Reactor

Proposal number:	KW2-05-011		
Experiment title:	Test measurements of Co nanoparticles in microemulsion		
Dates of experiment:	17.06 – 20.06.05	Date of report:	14.03.06
Experimental team: Names	Addresses		
Feygenson Mikhail, Pollmeier Klaus, Kentzinger Emmanuel Dr.,	Forschungszentrum Jülich GmbH Institut Für Festkörperforschung (IFF-STM) D-52425 Jülich Germany		
Sager Wiebke Dr.,	Forschungszentrum Jülich GmbH Institut Für Festkörperforschung (IFF-IWM) D-52425 Jülich Germany		
Local Contact:	Dr. Henrich Frielinghaus		

Experimental report text body

We have produced cobalt nanoparticles in a microemulsion following the recipe given by Pileni et. al., (1999). The microemulsion is of the so called water-in-oil type and consists of water droplets surrounded by surfactant molecules Igepal or $C_{12}E_5$. We used mixture of deuturated and protonated oil in order to reduce the incoherent scattering from hydrogen as well as to obtain different contrasts in the system. The particles obtained are small enough (typically 6 to 10 nm) to be mono-domain.
The aim was to measure the magnetic and the nuclear form factors of the cobalt nanoparticles, F_M and F_N, respectively and the structure factor in an external magnetic field.
The number of microemulsions containing Co nanoparticles were prepared and stabilized by both surfactants. We have found two appropriate contrasts for the samples. They contain such amount of protonated water and oil to have a reasonable level of the incoherent scattering. These are: “shell” contrast – when the scattering length density (SLD) of water matches the one for the oil and Co nanoparticles themselves. The second one is “core-shell” contrast with 100 % deuturated oil and water. The magnet with maximum field up to 0.4T and direction perpendicular to the incoming neutron beam was used.
The first measurements of Co nanoparticles in the “core-shell” contrast displayed the scattered intensity with two pronounced minima (Fig.1). The first minimum at Q = 0.1 $Å^{-1}$ was attributed to the scattering from water droplets and the second one at Q = 0.18 $Å^{-1}$ was recognized as the scattering form Co nanoparticles with sizes smaller then the size of the droplets. The scattering curve did not show any applied magnetic field dependence.
Then the measurements of deuturated hexane (Fig.2.) were carried out. Unexpectedly, the minimum shows up at Q = 0.18 $Å^{-1}$. It turned out that at the detector distance D = 1.25m the sample position was too far from the detector which leads to the artificial minimum at higher Q values. The problem was recognized and solved at the last day of the beam time. In Fig.2. the re-measured d-hexane with correct setup is shown.

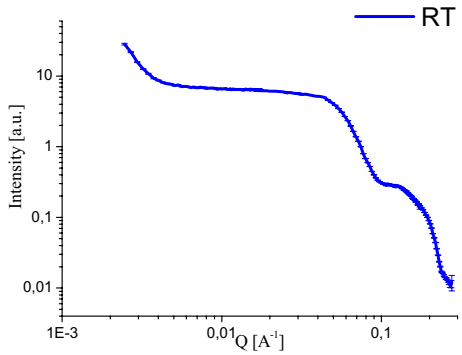


Fig.1. Co nanoparticles in microemulsion (core-shell contrast)

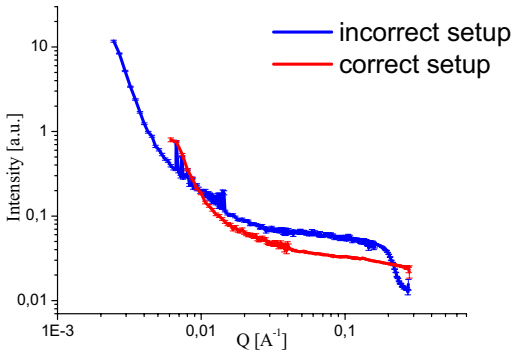


Fig.2. Scattering curve of d-hexane at two setups

From this figure we were able to distinguish between the real scattering from the sample and the artificial minimum at higher Q. Due to time constrains, the calibration measurements could not be done properly, which makes impossible to reduce the data to the absolute units.
Despite the technical problems the qualitative conclusions can be made.
Samples re-measured with correct setup did not show a minimum at higher Q which would characterize the Co nanoparticles. The scattering from the water droplets suppressed the scattering from the particles themselves due to the low content of cobalt in a microemulsion.
The next step will be to extract Co nanoparticles from microemulsions and re-disperse them into solution.

Institut für Festkörperforschung
Forschungszentrum Jülich GmbH
D-52425 Jülich

Experimental Report
of Neutron Scattering Experiments
at the FRJ-2 Reactor

Proposal number:	KW2-05-013; KW2-05-022; KW3-05-002		
Experiment title:	Paraffin crystallization in solution in the presence of multi-segment PEB-n random copolymers (parts 1, 2 and 3)		
Dates of experiment:	08.06.05-16.06.05 28.11.05-01.12.05	Date of report:	29.05.06
Experimental team: Names	Addresses		
Aurel Radulescu	Forschungszentrum Jülich Institut für Festkörperforschung D-52425 Jülich Germany		
Local Contact:	Dr.H.Frielinghaus, Dr.E.Kentzinger		

Experimental report text body

The self-assembly of poly(co-olefins) in dilute solution has been shown via SANS to yield either plate-like or needle-like micelles-like micelles [1,2]. The resultant supramolecular structures are dependent upon the copolymer architecture. The crystalline-amorphous diblock co-polymers yield self-assembled hairy plates while the corresponding random co-polymers yield one-dimensional needle shaped aggregates. The PEB-n random copolymers (n - the number of ethyl sides per 100 backbone carbons) show selectivity in their wax crystal modification capacities depending on the ethylene content of the backbone. This behavior relates to the graded ethylene content of PEB-n copolymers that leads to different self-assembling temperatures: the lower n, the higher the self-assembling temperature [2]. All PEB-n copolymers self-assemble in open 1-d structures. This conclusion has stimulated further structural studies of multiblock copolymers in solution where blocks represent poly(ethylene-butene) random copolymers (PEB-n) showing graded ethylene contents and thus, different crystallization degrees. Recently [3] conventional and focusing SANS studies of self-assembling in decane solution of a triblock and tetrablock PEB-n copolymers have been performed. The structural results complimented by microscopy observations concluded that these materials form in solution core-shell structures showing a 1D overall aspect which associate and give raise to occurrence of large scale spherulitic-like soft aggregates with sizes within the micrometric range. In the present study we investigated the wax crystal modification capacity of the triblock and tetrablock PEB-n copolymers by performing conventional and focusing SANS experiments on different wax-copolymer mixtures in decane and for different wax concentrations. Mainly three wax-copolymer combinations have been studied over a wide temperature range, between the single coil temperature (typical at 85°C) and the common aggregation regime, well below 0°C: the triblock PEB-6.5/8.9/10.1 was combined with 1% and 4% C24 tetracosane and with 1% C36 hexatriacontane while the tetrablock PEB-2.6/6.0/10.9/13.2 copolymer was combined with 0.5%, 1%, and 4%C36 hexatriacontane. The study aimed at first the modification of the wax crystals structure under the polymer

influence comparing with the pure wax solutions in decane. The conventional SANS investigations have shown that both waxes form in decreasing temperature under the influence of these multiblock copolymers 2-dimensional thin aggregates and do not grow anymore into big compact crystals with sizes of hundred of micrometers as in the case of pure wax solution. Examples of the wax scattering patterns for two wax-multiblock copolymer mixtures are presented in Fig.1 and 2. The Q^{-2} power law behaviour is indicative for scattering from 2D aggregates while the thickness of such aggregates can be evaluated from the Guinier regime observed towards high Q. The inset of Fig.1 present a 2D Guinier plot of the scattering pattern which allows a direct evaluation of the aggregate thickness and concludes that the wax form monolayers whose thickness is given by the length of the wax molecules, about 32Å and 45Å in the case of C_{24} and C_{36} waxes, respectively. At low Q and for low temperature conditions the scattering patterns show an increasing intensity which deviates from the Q^{-2} power law and proves that the wax is involved in some large scale aggregates. From this observation and taking into account that the multiblock copolymers yield large spherulitic-like soft aggregates showing a strong scattering at very low Q (focusing SANS range) we may conclude that the wax platelets formed under the polymer influence template to some extent the polymer morphology and show an association or agglomeration which gives raise to occurrence of large scale waxy structures too. However, the microscopy observation have shown that the mixed aggregates of waxes and multiblock copolymers present almost the same morphology like those formed by the polymer alone and have even a slightly smaller size than these ones. The focusing SANS experiments performed on the same samples under the wax contrast conditions provided unreliable results as long as the samples transmission was very low. Because the multiblock copolymers have been available only in protonated state in order to match them with the solvent and to have only the wax "visible" for the SANS investigations protonated solvent was required. In this way at KWS3 multiple scattering effects dominated and led to unsatisfactory data.

References: [1] D.Schwahn et al., Macromolecules 35, 861, 2002; [2] A.Radulescu et al. J.Pol.Sci. B Pol.Phys. 42, 3113, 2004; [3] experimental reports KW2-05-002;KW3-05-001 FRJ-2 Jülich.

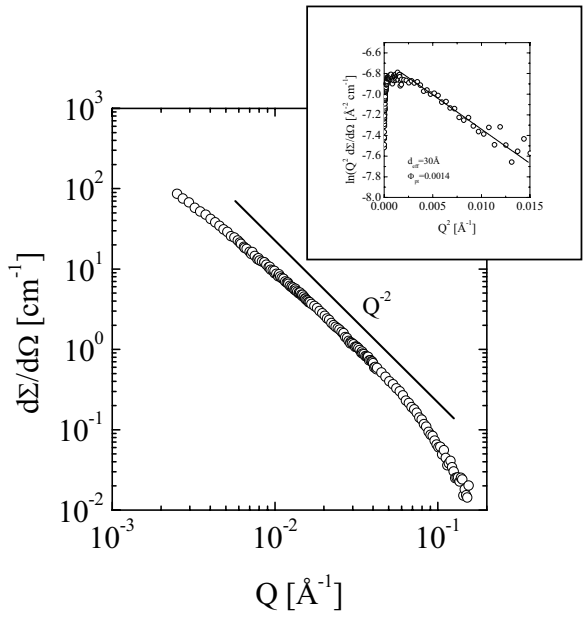


Fig.1 – The scattering pattern under the wax contrast form a mixture of 1% C24 and 1% triblock copolymer in decane at -20°C. The inset shows a 2D Guinier plot allowing the evaluation of the thickness of wax platelets.

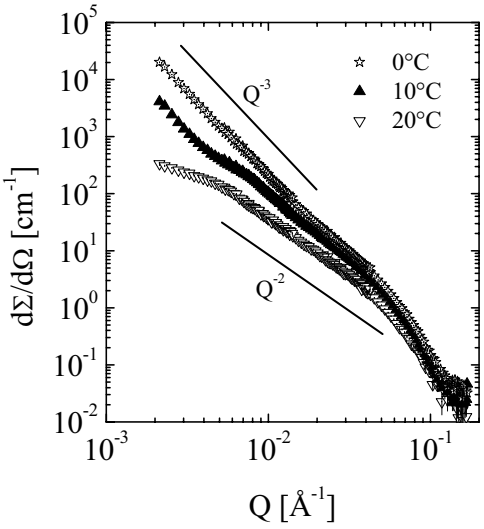


Fig.2 – The temperature evolution of the wax scattering pattern for a mixture of 1% C36 and 1% tetrablock copolymer in decane.

Institut für Festkörperforschung
Forschungszentrum Jülich GmbH
D-52425 Jülich

Experimental Report
of Neutron Scattering Experiments
at the FRJ-2 Reactor

Proposal number:	KW2-05-014, KW3-05-005		
Experiment title:	**T-induced jamming in dense solution of star-like micelles**		
Dates of experiment:	23.5.-25. 5. 2005 19.4.-24. 4. 2005 24.8.-26. 8. 2005	Date of report:	06.06.2006
Experimental team: Names	Addresses		
J. Stellbrink G. Rother	IFF, FZ Jülich, D-52425 Jülich, Germany IFF, FZ Jülich, D-52425 Jülich, Germany		
Local Contact:	J. Stellbrink		

Experimental report text body

Recently we investigated the phase behaviour of star-like micelles formed by the amphiphilic block copolymer poly(ethylenepropylene)-poly(ethyleneoxide), $M_{w,PEP}$= 1000 g/mol, $M_{w,PEO}$= 20000 g/mol, in different water/DMF mixtures by small angle neutron scattering (SANS) [1] and partly by light scattering and rheology. Changing the solvent composition changes the aggregation number (or functionality) of the micelles due to changes in the interfacial tension between the core-forming, hydrophobic PEP and the solvent. This enabled us to construct the equilibrium phase diagram in the packing fraction (η) / functionality (f) representation and compare it to theoretical predictions for regular star polymers [2]. Still under discussion is the competition between vitrification and crystallization. For star-like micelles no crystal formation was observed at $f \geq 70$ as predicted by theory. Here an amorphous gel or glass phase was found above the overlap packing fraction η*. At smaller functionalities, i.e. $f \leq 70$, on the other hand, the predicted bcc-structure was found experimentally. This is in contradiction to experimental observations for regular star polymer solutions, where for all f only amorphous phases were found.

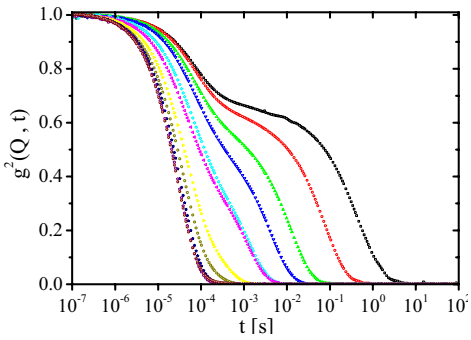


Figure 1: Intensity autocorrelation function $g^2(Q,t)$ observed in a dynamic light scattering experiment for a dense solution of star-like micelles, Φ=3%, T=80°C→4°C (from left to right).

By dynamic light scattering we found experimental evidence for a temperature induced glass transition resulting from a change in packing fraction, which originates from a temperature induced change in solvent quality, see fig.1. This phenomenon is similar to what has recently been observed for regular star polymers by Kapnistos et al. [3].

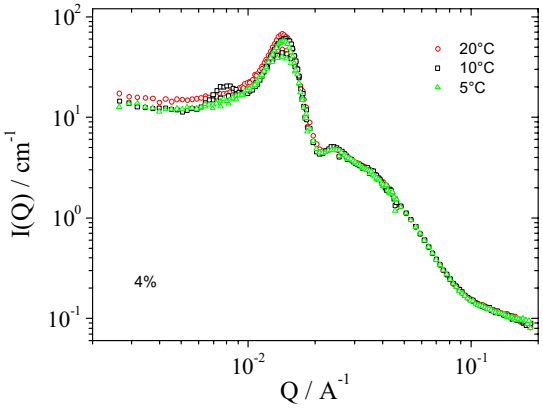


Figure 2: Temperature dependent SANS intensity for star-like PEP1-PEO20 micelles in D2O (full contrast), Φ=0.04.

In this experiment we followed the T-induced changes in the static structure factor S(Q) by small angle neutron scattering (SANS, KW1) and ultra-small angle neutron scattering (U-SANS, KW3) and observed some interesting changes in particular in the low-Q-regime, see fig. 2. Here the T-dependent occurrence of a pre-peak is clearly visible, which indicates some changes in the microscopic structure although macroscopically (rheology) the sample was found to be in the solid state for all temperatures shown. Liquid samples, on the other hand, just showed a T-dependent broadening of the main structure factor peak.

To extend the Q-range we also investigated some samples by U-SANS (KW3) to check for some T-induced clustering, but unfortunately the intensity of all samples was only slightly above the background, so that no data with reasonable statistics could be collected.

In summary, all these results show that star-like PEP-PEO micelles are an easy-to-establish, “tuneable” model system for regular star polymers (ultra-soft colloids)..

References:

[1] R. Lund, L. Willner, J. Stellbrink, A. Radulescu and D. Richter, *Macromolecules*, **37**, 9984, 2004.

[2] M. Laurati, J. Stellbrink, R. Lund, L. Willner, D. Richter, and E. Zaccarelli, *Phys. Rev. Letters*, **94**, 195504, 2005.

[3] M. Kapnistos *et al.*, Phys. Rev. Lett. **85**, 4072, 2000.

Institut für Festkörperforschung
Forschungszentrum Jülich GmbH
D-52425 Jülich

Experimental Report of Neutron Scattering Experiments at the FRJ-2 Reactor

Proposal number:	KW2-05-015		
Experiment title:	Transition from droplets to bicontinuous structures via cylindrical networks: experiment as support for theory		
Dates of experiment:	15.08.2006-19.08.2006	Date of report:	18.05.2006
Experimental team: Names	Addresses:		
Tobias Foster Thomas Sottmann	Institute for Physical Chemistry, Luxemburger Str. 116, 50939 Cologne, Germany		
Local Contact:	Henrich Frielinghaus		

Experimental report text body

One of the most difficult, fascinating and still unsolved problems in the fundamental research on microemulsion systems is the understanding of how a globular microemulsion (e.g. water droplets in a continuous oil phase) transforms into a disordered, bicontinuous structure. In the recent years theories were developed which predict this structural transition to occur via an intermediate, thermodynamically stable phase of cylinders that, near the bicontinuous region of the phase diagram, join up into a complex network structure [1].

The first evidence for this transition relies on experimental studies of microemulsion phase behaviour and viscosity, as well as on measurements of the electric conductivity of oil-rich microemulsions. Figure 1a shows a typical phase diagram for oil-rich microemulsions, here for the system D_2O – *n*-decane(d22) – $C_{10}E_4$. The microemulsion phase (1) is found for intermediate temperatures, with two-phase regions for higher- ($\overline{2}$) and lower (2) temperatures. Samples are characterized by surfactant/(oil+surfactant) mass fraction γ_b and the water mass fraction w_A. For nonionic water-in-oil microemulsions, the mentioned spherical or globular structures are found at temperatures just below of the *wefb* (Fig1a). As the temperature is decreased, the spontaneous curvature (negative by definition for w/o-droplets) of the amphiphilic film increases [2], and elongated, cylindrical structures are formed. These structures branch at temperatures sufficiently close to the lower phase boundary to form a system-spanning network of connected cylinders.

This transition from discrete- to connected structures can be monitored by measurements of the electric conductivity which increases by several orders of magnitude when the temperature is lowered starting from the *wefb*. This trend is shown in Figure 1b.) for an oil-rich microemulsion of the system H_2O/NaCl – *n*-decane(h22) – $C_{10}E_4$, whereby addition of NaCl (mass-fraction ε of NaCl/(water+NaCl)) assures sufficient conductivity of the water-phase.

This structural transition from globular- to bicontinuous microstructure can be monitored by systematic

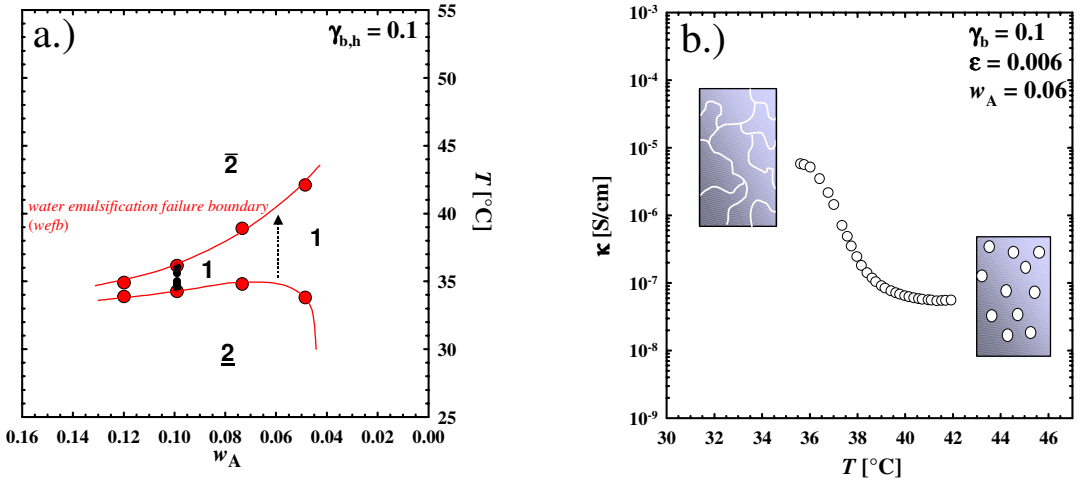


Figure 1: a.) Phase diagram of the oil-rich side in the system D_2O – *n*-decane(d22) – $C_{10}E_4$, with sample compositions characterized by the mass fractions γ_b and w_A (definitions and more details see text). b.) electric conductivity of a microemulsion sample in the system H_2O/NaCl – *n*-decane(h22) – $C_{10}E_4$ when the temperature is increased as indicated by the dotted arrow in a.).

temperature dependent neutron scattering measurements. The black points in Figure 1a.) indicate the temperatures studied for one given composition of the sample. Exemplary temperature dependent scattering curves are shown in Figure 2a.). With decreasing temperature, the forward scattering intensity

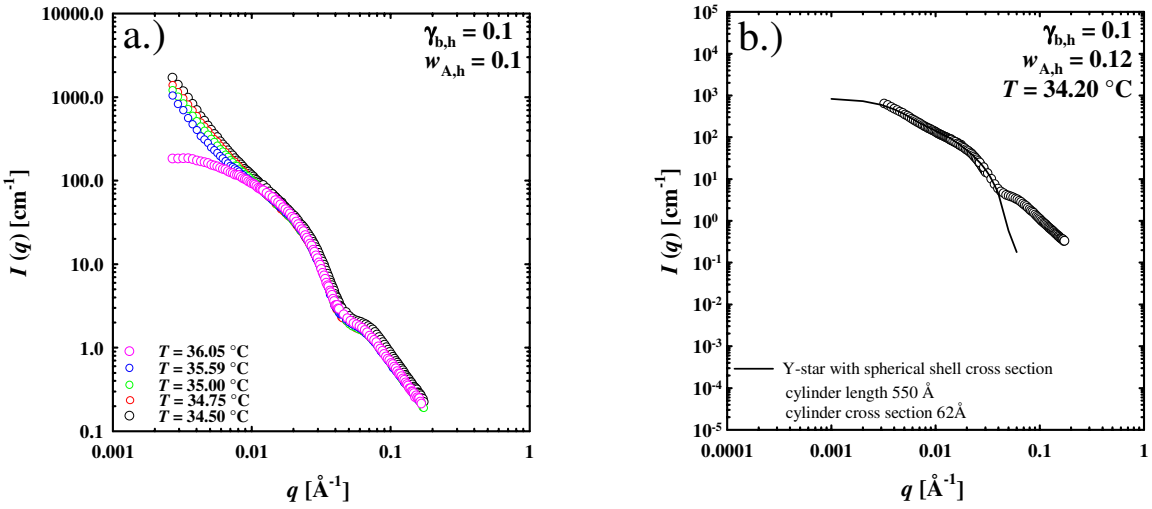


Figure 2: a.) Representative neutron scattering data for D_2O – *n*-decane(d22) – $C_{10}E_4$ microemulsions at various temperatures. b.) representative fit of the low-temperature SANS data with a model derived in collaboration with Sam Safran, Weizmann Institute of Science.

increases strongly, indicating the formation of large structures. Furthermore, the pronounced q^{-1}-decay for intermediate *q*-values indicates the presence of cylindrical structures. The data are currently analyzed using a novel form factor for the scattering from three long cylinders which are joined by network junctions. A typical result is shown in Figure 2b), yielding two length scales, namely the lengths of the cylinders and the radius of the cylinder cross section.

[1] T. Tlusty et al., *Phys.Rev.Letts.* **78**, 2616 (1997).
[2] R. Strey, *Colloid and Polymer Sci.* **272**, 1005 (1994).

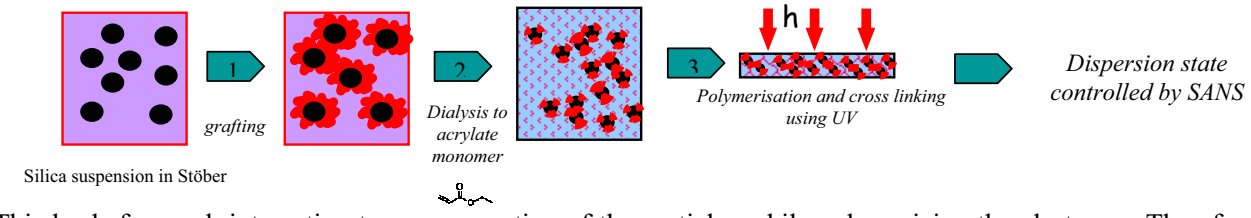
Institut für Festkörperforschung
Forschungszentrum Jülich GmbH
D-52425 Jülich

Experimental Report of Neutron Scattering Experiments at the FRJ-2 Reactor

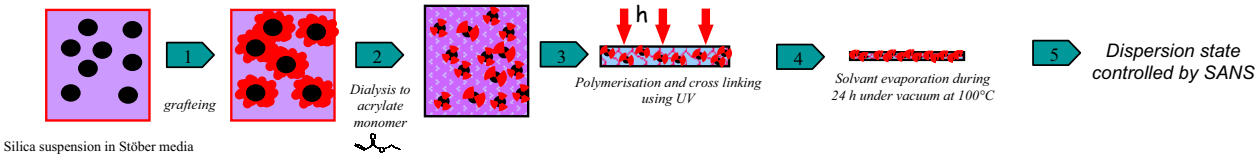
Proposal number:	KW2-05-016		
Experiment title:	Quantitative relationship between non linear mechanical properties and particle arrangement in model filled elastomers.		
Dates of experiment:	December 2005	Date of report:	March 2006
Experimental team: Names	Addresses		
Thomas Chaussée Hélène Montes	PPMD-ESPCI Esc H 10, rue Vauquelin 75005 PARIS		
Local Contact:	Henrich Frielinghaus		

Experimental report text body

Filled elastomers are widely used for their interesting mechanical properties that can be adapt to the use. But we do not understand how the interactions between the particle surface and the elastomeric matrix influences the mechanical behavior of so-filled elastomers. Therefore we decided to produce some model silica-filled elastomers using different grafts in order to modulate the surface interaction. Grafts studied are: n-Octyltriethoxysilane (C8TES) and Hexamethyldisilazane (HMDS) in order to perform a weak interaction and Acetoxyethyldimethylchlorosilane (MCSNC) to perform some hydrogen bonding.
In previous work we used Ford method to synthesize our elastomers. The protocol could be schematized as follow:



This leads for weak interaction to an aggregation of the particles while polymerizing the elastomer. Therefore we decided to modify the protocol as follow:



We think that the use of a co-solvent will help to avoid depletion phenomenon during the polymerization.
Results (fig. 1 to 3) show that the addition of ethanol leads to better dispersion states whatever the silica concentration, size or the graft. For example in fig. 1 we observe for 100 nm C8TES-grafted silica systems (synthetised in the presence of ethanol 1/1, w/w) a correlation peak at 0.08 Å-1 whereas the synthesis without solvent leads to increase at low q characteristic of the presence of big particle aggregates.

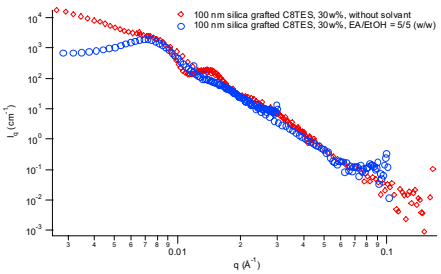


Fig. 2: 100 nm HC8TES-grafted silica, synthetised in the presence of ethanol (blue) or without any co-solvent (red)

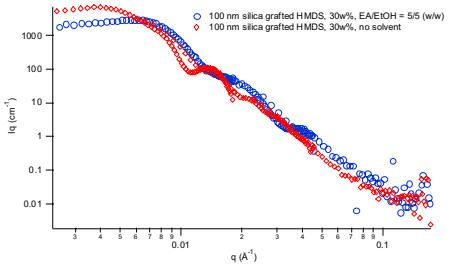


Fig. 2: 100 nm HMDS-grafted silica, synthetised in the presence of ethanol (blue) or without any co-solvent (red)

The presence of a co-solvent is the way to obtain well dispersed silica whatever the interaction between the matrix and the particle is.
We now need to work on the type of co-solvent used to improve the quality of the dispersion and to see in which condition (quantity of solvent, quantity of cross-linker and polymerization initiator) it is possible to obtain a polymer matrix having the required mechanical behavior.

Institut für Festkörperforschung
Forschungszentrum Jülich GmbH
D-52425 Jülich

Experimental Report
of Neutron Scattering Experiments
at the FRJ-2 Reactor

Proposal number:	KW2-05-017		
Experiment title:	**Self-assembly mechanism in octo-peptide gels**		
Dates of experiment:	24.10. – 28.10.2005	Date of report:	06.06.2006
Experimental team: Names	Addresses		
A. Saiani A. Mohammed A. Miller A. Konstantopoulos R. Zhang	School of Materials, The University of Manchester, Grosvenor Street, Manchester, M1 7HS, UK School of Chemical Engineering and Analytical Science, The University of Manchester, Sackville Street, Manchester, PO Box 88, M60 1QD, UK		
Local Contact:	Henrich Frielinghaus		

Experimental report text body

We have investigated the self-assembling and gelation properties of a set of octa-peptides based on the following amino acids: alanine (A), phenyalanine (F), lysine (K; charge +), arginine (R charge; +), glutamic acid (E; charge –) and aspartic acid (D; charge –). The amino acid sequence has been varied in order to create two types of octa-peptides one with alternating charges and one with charges located at the two end of the peptide. The overall peptide charge was kept neutral. The peptides investigated are summarized below:

AEAEAKAK	FEFEFKFK	FDFDFKFK	FDFDFRFR
AEAKAEAK	FEFKFEFK	FDFKFDFK	FDFRFDFR

Peptide solutions and gels were prepared by dissolving the desired amount of peptide in deuterated water at high temperature, 80ºC. The solutions were then cooled at room temperature and depending on the peptide sequence and the overall concentration gels were formed.

Except for the alanine based peptides it was found that the scattering profiles of our samples did not depend on the sequencing but on the type of amino acid used in the sequence. Very different scattering patterns were obtained as illustrated in figure 1 for the different octa-peptides.

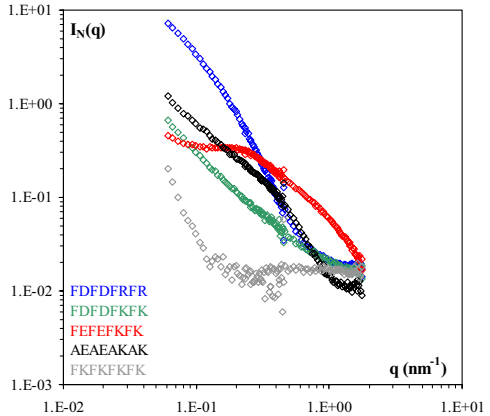


Figure 1: Intensity scattered by the different peptides samples (Conc. 20 mg ml^{-1}).

Figure 2 shows a Kratky plot ($q^2I(q)$ vs. q) of the intensities scattered by the AEAEAKAK solutions at 10 and 80 mg ml^{-1}. As can be seen characteristic curves of rod-like structures were obtained. The data could be fitted using a plain-rod model as described by equation 1.

$$q^2 I_A = 4\pi q C_D \mu_L \left[\frac{J_1(qr)}{qr}\right]^2 \qquad (1)$$

The agreement between the model and the experimental curves was found to be good. These results suggest that AEAEAKAK peptide does self-assemble and form rod-like structures i.e. fibers in solution. A diameter of ~ 6 nm was obtained for the fibers diameter for both samples. No gels were formed on cooling indicating that these fibers are not able to aggregate or entangle and form 3D networks and hydrogels at the investigated concentrations. For the AEAKAEAK peptide the scattering patterns do not suggest the presence of any structure. This seems to indicate that this peptide does not self assemble in solution at the concentrations investigated underlining the important role played by the amino acid sequence

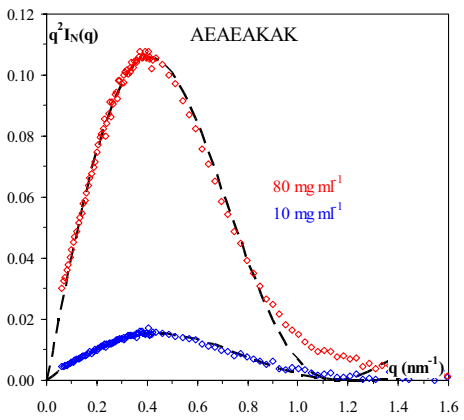


Figure 2: Intensity scattered by AEAEAKAK solutions.

When alanine is replaced by phenylalanine gels are formed readily. The scattering curves for FEFEFKFK samples are shown in figure 3. A clear scattering maxima is observed in the I(q) vs q curve when the samples form gels. The two lower concentrations 2 and 5 mg ml^{-1} do not form gels. Using the Bragg relation ($d = 2\pi/q^*$) an estimation of the mesh size of the gel can be obtained from the position of the maxima. In our case depending on the concentration 15 to 30 nm is obtained for the network mesh size. The position of the maxima was found to be sensitive to concentration and annealing time and temperature. The scattering curves of the low concentration solutions could again be fitted using a plain-rod model. A thickness of ~ 7 nm was found in this case. FEFEFKFK samples seems to form fiber of the same diameter as the AEAEAKAK samples but in this case the fibers are able to aggregate or entangle and form a 3D network resulting in the formation of an hydrogel. Similar results were obtained for the FEFKFEFK samples and when glutamic acid (E) is replaced by aspartic acid (D).

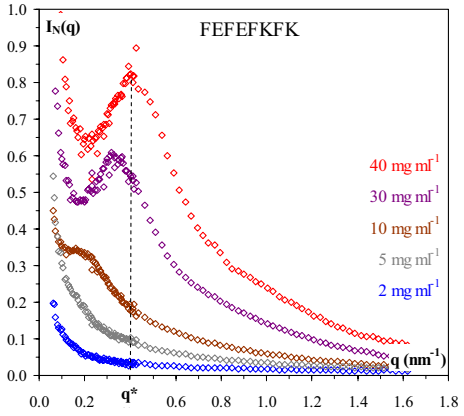


Figure 3: Intensity scattered by FEFEFKFK samples.

When arginine (R) is used to replace lysine (K) large differences are observed in the scattering patterns. As shown in figure 4 a maximum is observed in the Kratky representation for the FDFRFDFR sample at 30 mg ml^{-1}. This curve suggests the presence, as for the AEAEAKAK samples of rod-like structures but with a larger diameter. Fitting the curves has not been possible yet as the low q part of the scattering pattern is missing. At lower concentration no structure seems to form.

Conclusion

This work has shown the importance of peptide sequence and type on the self-assembling properties and hydrogel formation. Results are still being analyzed in order to extract additional information like the linear mass of the fibers. Additional experiments at low q are required for some of the peptide.

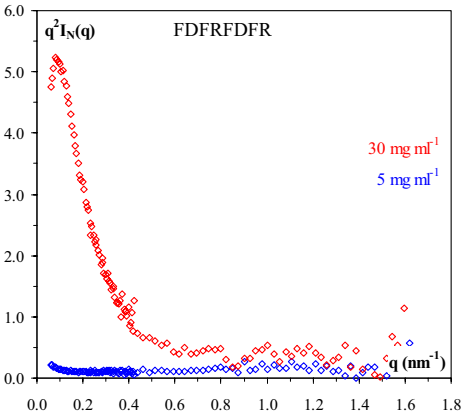


Figure 3: Intensity scattered by FEFEFKFK samples.

Institut für Festkörperforschung
Forschungszentrum Jülich GmbH
D-52425 Jülich

Experimental Report
of Neutron Scattering Experiments
at the FRJ-2 Reactor

Proposal number:	KW2-05-019		
Experiment title:	**SANS Investigation of bi-continous microemulsions in presence of sticker polymers**		
Dates of experiment:	27.08.2005	Date of report:	17.03.2006
Experimental team: Names	Addresses		
Henrich Frielinghaus Gaetano Mangiapia	Forschungszentrum Jülich GmbH, Institut für Festkörperforschung, D-52425 Jülich Forschungszentrum Jülich GmbH, Institut für Festkörperforschung, D-52425 Jülich, and Dipartimento di Chimica, University Napoli, 80126 Napoli, Italy		
Local Contact:	Henrich Frielinghaus		

Experimental report text body

Amphiphilic diblock copolymers were the first polymers found to increase the efficiency of surfactants in microemulsions dramatically (polymer boosting effect). The idea of amphiphilicity has been brought to an extreme by the new sticker polymers. Only a short hydrophobic C_{10} sticker is connected to the hydrophilic E_{100} block, a polymer of 100 ethylene oxide units. The questions arising for this new polymer are: (1) Is this unbalanced amphiphile still fully active at the membrane, i.e. does this polymer decorate the surfactant film as the diblock copolymer? (2) Does the polymer increase the efficiency equally well as the diblock copolymers (with respect to the polymer mass)? (3) Does the imbalance have any effect at all?
Prior to the neutron scattering experiments phase diagram measurements have been made. Here the one phase region of the bicontinuous microemulsion was determined. In a temperature vs. surfactant amount plot the one phase region looks like a fish tail, and the fish body is the 3-phase coexistence region. Both regions are connected in one point, the fish tail point, where the surfactant fails to dissolve the equal amounts of oil and water. The efficiency of a surfactant is measured by this minimum amount of surfactant γ_{ftp}. Plotting this γ_{ftp} as a function of the rescaled polymer amount $\sigma \cdot R_{ee}^2$, one obtains a measure for the sensitivity of the boosting effect, which can be compared to diblock copolymers. With respect to the total amount of polymer, the polymer boosting is comparable to diblock copolymers. This result agrees well with Lipowsky's theory [1].
The second measure is the temperature at the fish tail point. For symmetric diblock copolymers this temperature stayed constant within the accuracy due to the symmetry of the system. For the new sticker polymers this temperature increased with growing polymer amount. The imbalance of the polymer causes some spontaneous curvature which is balanced by the increased temperature. The sensitivity of this effect agrees well with Lipowsky's theory [1].
The macroscopically determined phase diagram is connected to microscopically defined parameters of the Helfrich model. The model assumes the elastic properties of the surfactant film to be dominant in the free ener-

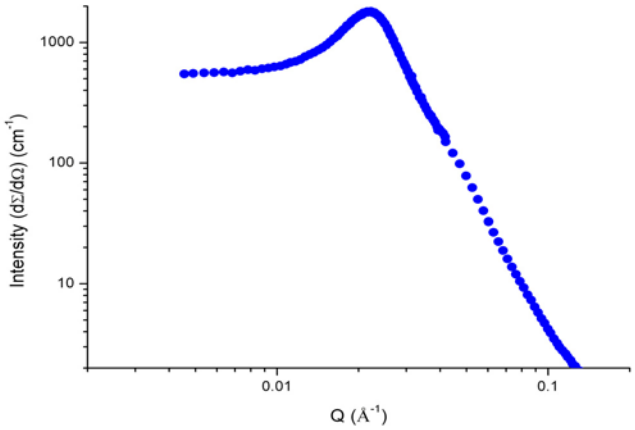


Figure 1: A typical SANS curve: Macroscopic cross section as a function of the scattering angle Q. The peak position ~2π/*d* is connected with the domain size *d*, while the peak width ~1/ξ is inversely proportional to the correlation length.

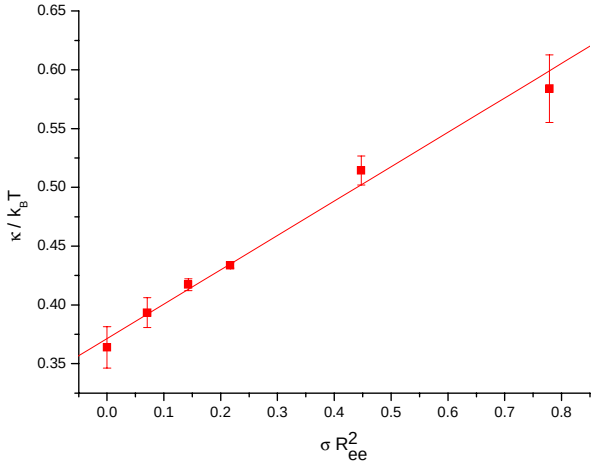


Figure 2: The obtained bending rigidity κ as a function of the scaled polymer amount. Using the Gaussian random field theory κ is related to the structural parameters according to $\kappa/k_BT = 0.85\ \xi/d$. The slope measures the sensitivity of the polymer effect, and is comparable to diblock copolymers.

gy of the microemulsion. The three important parameters are the spontaneous curvature c_0, and two elastic moduli, namely the bending rigidity κ and the saddle splay modulus $\bar{\kappa}$. The spontaneous curvature decreases with increasing temperature and increases with increasing sticker polymer amount. At the fish tail point the spontaneous curvature is zero, so the two contributions are balanced. The elastic moduli are spatially renormalized parameters with a logarithmic dependence on the surfactant amount. The absolute values of the elastic moduli increase with increasing polymer amount. At the fish tail point the saddle splay modulus is a negligible constant, and so the renormalization is balanced with the polymer term. This balance leads to an exponential dependence of the minimal surfactant amount with respect to the scaled polymer amount.

In theories the moduli κ and $\bar{\kappa}$ behave extremely similar, just the signs of the moduli are opposite ($\kappa>0$ and $\bar{\kappa}<0$). Thus a quantitative comparison of the macroscopically determined $\bar{\kappa}$ with κ is desired. Small angle neutron scattering experiments determine the domain structure if bulk contrast is chosen. A typical SANS pattern is shown in figure 1. One obtains the domain size *d* and the correlation length ξ, which are connected to the bending rigidity $\kappa/k_BT = 0.85\ \xi/d$ according to the Gaussian random field theory. Three different surfactant amounts were measured in the one phase region for each polymer amount. For each polymer amount an inter-/extrapolation of κ was made to a constant surfactant amount; thus, the spatial renormalization does not play a role anymore. The directly measured bending rigidity κ as a function of the polymer amount is depicted in figure 2.

The sensitivity of both moduli on the polymer amount agree quantitatively between the sticker polymer and the diblock copolymer. Thus, the used amount of polymer is dominant for the efficiency boosting. The cheaper and biodegradable sticker polymers would exchange the diblock copolymers in applications.

The detailed comparison of the sensitivities between the real measurements and theoretical predictions show a 1.5 (to 2) times more sensitive behavior of the experimental systems. This might be due to the structure of real polymers and also due to confinement effects. More interesting is the agreement between the sensitivity of both moduli as predicted by the theory. While these monofunctional sticker polymers have the same effect on κ and $\bar{\kappa}$, some starlike polymers with higher functionality might imbalance the sensitivity of the two moduli. Bifunctional polymers are already investigated (KW2-05-031, KW2-05-036, KW2-05-046, KW2-05-049), and higher functionalities remain an interesting subject for applications in the future.

References:

[1] C. Hiergeist, R. Lipowsky, *J. Phys. II France* **6**, 1465 (1996)

Institut für Festkörperforschung
Forschungszentrum Jülich GmbH
D-52425 Jülich

Experimental Report
of Neutron Scattering Experiments
at the FRJ-2 Reactor

Proposal number:	KW2-05-020		
Experiment title:	**Determination of the structure of chitosan and poly(vinylpyrrolidone) hydrogels in the presence of anionic surfactants**		
Dates of experiment:	28/08/2005	Date of report:	15/12/2005
Experimental team: Names	Addresses		
Gaetano Mangiapia	IFF – Neutronenstreuung, Forschungszentrum Jülich GmbH, D-52425 Jülich Tel. +49 2461 61 6048 (g.mangiapia@fz-juelich.de)		
Henrich Frielinghaus	IFF – Neutronenstreuung, Forschungszentrum Jülich GmbH, D-52425 Jülich Tel. +49 2461 61 5093 (h.frielinghaus@fz-juelich.de)		
Local Contact:	G. Mangiapia		

Experimental report text body

Chitosan [CHT] is a polycationic biopolymer obtainable from partial enzymatic or alkaline deacetylation of chitin, a natural and abundant polysaccharide occurring in crustaceous shells, insect exoskeletons and in associations with proteins and minerals. The good biocompatibility, natural availability, and the excellent physical, chemical and mechanical properties shown by CHT, make it a good candidate for using in medical field, as component in cosmetic products, agriculture and in water treatment. One of the most attractive features of CHT that has captured the attention of researchers from both academic and industrial areas, is the capability to form semirigid films and hydrogels with good swelling properties. This characteristic, together with its cationic nature, has allowed forming swellable pH-sensitive CHT gels used as stomach-targeted drug delivery systems, and CHT complexes useful in gene delivery applications.

In order to create new biomaterials with more helpful characteristics, CHT is often used as blend with other polymers and/or in combination with surfactants. The use of polymer blends allows, in principle, having new gels with properties which are different to those of single components, whereas polymer surfactant complexes, where present, can significantly modify the characteristics of solutions and hydrogels (for instance improved swelling properties), opening new possibilities of applications.

The purpose of this research project has been to perform a structural characterization of CHT and CHT/poly(vinylpyrrolidone) [PVP] hydrogels, obtained by means of SANS measurements. Furthermore, in order to create hydrophobic domains within the gel, that can in principle be used to dissolve lipophilic drugs, CHT and CHT/PVP gels have also been investigated in the presence of sodium decylsulfate [C10OS], one of the most widespread anionic surfactants.

Figure 1 reports scattering cross sections $d\Sigma/d\Omega$ for CHT and CHT/PVP hydrogels in D_2O. The scattering profile of both systems can be described in terms of the average distance between crosslinks (the mesh size ξ) arising from the thermal fluctuations of the polymer concentration, and in terms of the correlation distance ζ among polymer rich domains. With the hypothesis $\zeta >> \xi$, the scattering cross section can be expressed as a sum of a lorentzian function that takes into account of the thermal fluctations, and of an "excess term" describing the presence of inhomogeneities inside the hydrogel structure

$$\frac{d\Sigma}{d\Omega} = \frac{S_{OZ}}{1+q^2\xi^2} + \frac{S_{ex}}{\left(1+q^2\zeta^2\right)^2} + \left(\frac{d\Sigma}{d\Omega}\right)_{inc} \qquad (1)$$

where $(d\Sigma/d\Omega)_{inc}$ represents the incoherent contribution to the cross section measured. By fitting eq. (1) to the experimental data it has been possible to estimate both the parameters ξ and ζ (see table 1).

With the aim to investigate a possible interaction among polymeric chains forming the hydrogel structures and C10OS micelles or micelle-like aggregates, SANS measurements of CHT and CHT/PVP hydrogels have been performed in mixtures of H_2O/D_2O and in the presence of fully deuterated C10OS [DC10OS], in order to observe scattering arising only from the surfactant. Figure 2 reports scattering cross sections obtained for CHT and CHT/PVP hydrogels in the presence of DC10OS (0.1 mol kg^{-1}) in a mixture H_2O/D_2O such to make null the scattering contribution due to the hydrogels. For comparison it has also been reported $d\Sigma/d\Omega$ values for C10OS (0.1 mol kg^{-1}) in D_2O; furthermore, for a better comparison, data of figure 2 have been multiplied for a scale factor. Inspection of the figure reveals the presence of a single broad maximum, characteristic of micellar systems where significant correlations between micelles or micelle-like aggregates are present. Moreover, the position of the maximum in $d\Sigma/d\Omega$ occurs at the same value of the scattering vector modulus q (≈ 0.073 $Å^{-1}$), indicating that a similar correlation distance exists among all the aggregates, and suggesting a lack of interaction between micelles and polymeric chains. On those bases, in order to extract structural information about the aggregates, systems have been modeled as a collection of charged prolate ellipsoidal micellar aggregates. From the fitting it has been possible to extract the micellar aggregation number N_{agg}, the actual charge z, the major and minor semiaxis of the hydrophobic core a and b, and the thickness of the hydrophilic shell δ. Table 2 reports the values of these parameters for the systems investigated, and from its inspection it is possible to note similar values obtained for all the systems, except for the value of the charge z. Micellar actual charge of systems containing hydrogels is sensibly reduced, probably because of the presence of residual positive charges on chitosan backbone that should shield C10OS aggregates. According with these results micelles of decylsulfate are free to move inside the polymeric gel, and could be in principle used as carriers for lipophilic drugs.

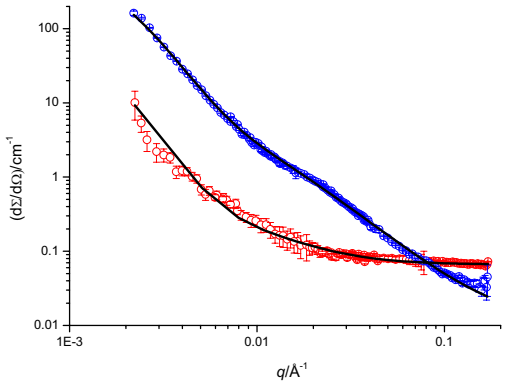


Figure 1 – Scattering cross sections obtained at 25°C for hydrogels of CHT (–) and CHT/PVP (–) in D_2O. Curves obtained from the fitting of the model described in the text are also reported.

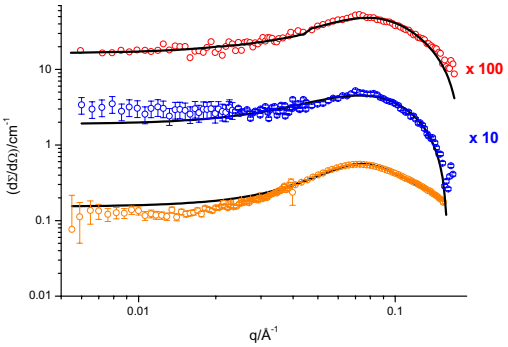


Figure 2 – Scattering cross sections obtained at 25°C for C10OS (–) in D_2O and for DC10OS in the presence of CHT (–) and CHT/PVP (–) hydrogels in mixtures H_2O/D_2O. In all the systems the concentration of surfactant is 0.1 mol kg^{-1}. Curves obtained from the fitting of the model described in the text are also reported.

	ξ/Å	ζ/Å
CHT	96 ± 2	548 ± 10
CHT/PVP	85 ± 9	850 ± 40

Table 1 – Mesh size ξ and inhomogeneity distance ζ for CHT and CHT/PVP hydrogels in D_2O obtained from the fitting of the model described in the text.

	N_{agg}	z	a/Å	b/Å	δ/Å
C10OS	46±2	-35±2	15.3±1.2	14.1±0.5	3.4±0.2
DC10OS/CHT	49±3	-8±1	16.2±0.9	14.1±0.5	3.5±0.1
DC10OS/CHT/PVP	44±2	-10±2	14.6±1.0	14.1±0.5	3.4±0.1

Table 2 – Micellar parameters obtained for C10OS in D_2O and for DC10OS in the presence of CHT and CHT/PVP hydrogels in contrast match mixtures H_2O/D_2O. In all the systems the concentration of surfactant is 0.1 mol kg^{-1}. The table reports the aggregation number N_{agg}, the actual charge z, the major and minor semiaxis of the hydrophobic core a and b respectively, and the hydrophilic shell thickness δ.

Institut für Festkörperforschung
Forschungszentrum Jülich GmbH
D-52425 Jülich

Experimental Report
of Neutron Scattering Experiments
at the FRJ-2 Reactor

Proposal number:	KW2-05-021		
Experiment title:	Effect of intercalation in sheet silicate on the conformation of poly(ethylene oxide)		
Dates of experiment:	19.08. – 20.08.2005	Date of report:	09.05.2006
Experimental team: Names	 Addresses		
Helen E. Hermes Henrich Frielinghaus	IFF, FZ-Jülich IFF, FZ-Jülich		
Local Contact:	Henrich Frielinghaus		

Experimental report text body

PEO-MMT interactions have been studied for many years[1]. Interest has intensified recently due to the model nature of the system for studying confined chains, and hopes that it may be a suitable candidate for solid-state batteries[2]. The indirect techniques IR and NMR have been used to examine the chain conformation of the intercalated PEO. X-ray scattering has also been widely used. From the results from these techniques and theoretical calculations, no consensus as to the conformation of PEO has been reached. The aim of these experiments was to determine using SANS the conformation of highly confined PEO chains.

We used solution intercalation to prepare composites of poly(ethylene oxide) (PEO) and sodium montmorillonite. X-ray scattering and differential scanning calorimetry measurements confirmed that using this sample preparation method and a suitable composition, it is possible for all the PEO to be intercalated between the silicate layers. The thickness of the intercalated PEO layers is 0.815 nm and extremely constant.

In this initial experiment we investigated a series of 6 samples with fixed montmorillonite content and fixed polymer molecular weight plus a reference h-d PEO blend. In the montmorillonite-PEO mixtures, the relative amounts of h-PEO and d-PEO were varied such that the average scattering length density of the polymer phase was varied around the scattering length density of the montmorillonite.

Figure 1 illustrates the data obtained from these SANS measurements at 20m detector distance. At these lowest Q values the contrast change must have the largest effect, but obviously no considerable trends are observed. Theoretically we expect the contrast match at ~50% deuterated content. Since all samples remain white after the freeze drying and pressing, still there must be a lot of air bubbles. Thus, the scattering from the air is dominating the obtained spectra independent of the selected contrast.

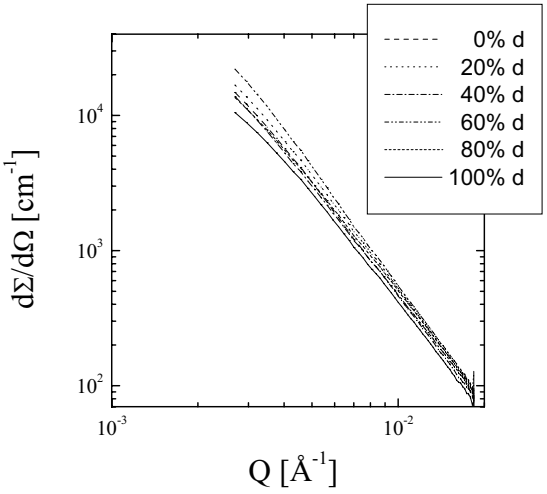


Figure 1: Scattering intensities of a contrast variation experiment on a PEO/MMT nanocomposite. The content of deuterated PEO was varied between 0 and 100%. Theoretically at ~50% the system should be contrast matched, and the chain scattering should be visible. Practically, no considerable change of the intensity is observed. All samples are white after the preparation, and so many air bubbles must be responsible for the observed scattering pattern independent of the selected contrast.

In latest experiments we changed the sample preparation from freeze drying to slowly drying (solvent casting), and first experiments looked more promising. T. Zacherle will obtain in the near future the full information about the scattering of confined PEO chains in montmorillonite clay sheets.

References

1. B.K.G. Theng, "Formation and properties of clay-polymer complexes", Elsevier Scientific, Oxford, 1979

2. P. Aranda, E. Ruiz-Hitzky, *Chem. Mater*. **4**, 1395-1403 (1992)

3. Experimental report KW1-04-025

Institut für Festkörperforschung
Forschungszentrum Jülich GmbH
D-52425 Jülich

Experimental Report
of Neutron Scattering Experiments
at the FRJ-2 Reactor

Proposal number:	KW2-05-023		
Experiment title:	Influence of temperature and solvent on the phase behaviour of $Co(AOT)_2$ –containing nonionic microemulsions		
Dates of experiment:	1.09 – 4.09.05	Date of report:	14.03.06
Experimental team: Names	Addresses		
Feygenson Mikhail, Pollmeier Klaus, Kentzinger Emmanuel Dr.,	Forschungszentrum Jülich GmbH Institut Für Festkörperforschung (IFF-STM) D-52425 Jülich Germany		
Sager Wiebke Dr.	Forschungszentrum Jülich GmbH Institut Für Festkörperforschung (IFF-IWM) D-52425 Jülich Germany		
Local Contact:	Dr. Henrich Frielinghaus		

Experimental report text body

For the synthesis of the Co nanoparticles we employed the interior of water-in-oil (w/o) microemulsions as nanoreactors, as originally proposed by Pileni et.al.(1999). In their early paper Pileni and coworkers used w/o microemulsions that were stabilized by NaAOT (sodium 2- diethylhexylsulfosuccinate), whereby the Co^{2+}-delivering microemulsion contained additionally $Co(AOT)_2$ and water and the second miroemulsion that delivered the reducing agent $NaBH_4$ contained only NaAOT and the aqueous $NaBH_4$-solution. In this way, particle size and polydispersity could be adjusted by the water-to-surfactant ratio (w/s) and the molar ratio between Co^{2+} and $NaBH_4$. The major problem of this approach, was the low yield of Co nanoparticles. In recent papers Pileni et al. used, therefore, a microemulsions stabilized by $Co(AOT)_2$ only to which they injected the aqueous $NaBH_4$- solution. However, this synthesis route is less defined since the microemulsions phase separate upon addition of the $NaBH_4$-solution.
In order to circumvent both the low yield of Co nanoparticles and undefined particle formation conditions due to phase separation, we explored a synthesis route in which we employed w/o microemulsions that are stabilized by the nonionic surfactants of the ethoxylated alkyl- or arylether series such as $C_{12}E_5$ and Igepal CO520 and contain the $NaBH_4$-solution. Co nanoparticle formation is then induced by injecting a solution of $Co(AOT)_2$ in hexane. In order to characterize the morphology of the microemulsions employed before and after addition of $Co(AOT)_2$, we performed SANS measured of the microemulsions in shell contrast at KWS-2 in August 2005. As can be seen from Fig. 1 the $C_{12}E_5$ stabilized microemulsions consist mainly of spherical droplets at high temperatures and transform only partially into cylinders at low temperatures within the one-phase region. However, Igepal stabilized microemulsions display a substantial cylinder fraction already at high temperatures and show the characteristic scattering from long cylinders at low temperatures (Fig.2). To mimic the 1 M $NaBH_4$-containing microemulsions we used 1.2 M NaCl-solutions as aqueous phase (Fig.3). Addition of $Co(AOT)_2$ lead similar to NaAOT to a cylinder-to-sphere transition.

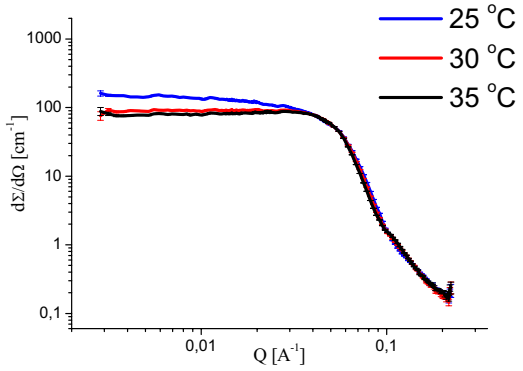


Fig 1: 13.6% $C_{12}E_5$, w/s=0.5, 1.2 M NaCl

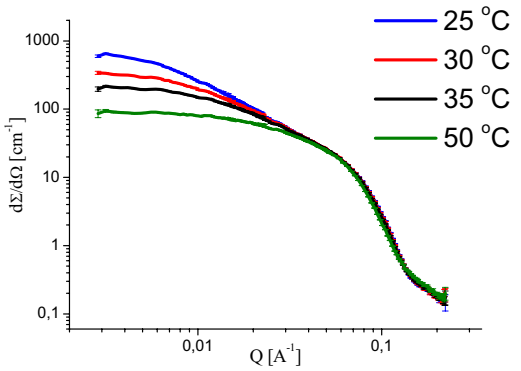


Fig 2: 13.6% Igepal, w/s=0.2, 1.2 M NaCl

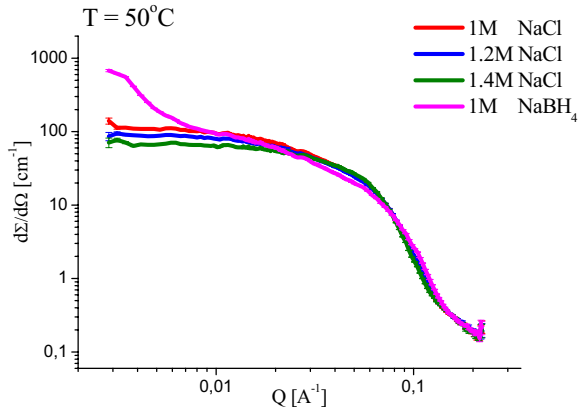


Fig 3: 13.6% Igepal, w/s=0.2

We also measured the temperature dependence of the Igepal and $C_{12}E_5$ stabilized microemulsions at different water-to-surfactant ratio.

Institut für Festkörperforschung
Forschungszentrum Jülich GmbH
D-52425 Jülich

Experimental Report
of Neutron Scattering Experiments
at the FRJ-2 Reactor

Proposal number:	KW2-05-025		
Experiment title:	**Critical fluctuations and absorption of individual fluids confined in porous media: continuation**		
Dates of experiment:	21.-25. Feb. 2006	Date of report:	31. May 2006
Experimental team: Names	Addresses		
G. Rother[1] Y. Melnichenko[1] G.D. Wignall[1]	[1] Center for Neutron Scattering, Oak Ridge National Laboratory, 1 Bethel Valley Rd, Oak Ridge, TN 37830, USA		
Local Contact:	H. Frielinghaus		

Experimental report text body

The experiment aimed to study the adsorption from supercritical and sub critical d-propane to silica aerogel. Measurements have been performed at the KWS2 instrument using a home-built pressure cell. First we studied the bulk properties of d-propane in the vicinity of the critical point. By performing pressure scans at different temperatures we determined the critical temperature of d-propane at $T_c = 91.0$°C, thus being shifted by 6.6 K towards lower temperatures with respect to h-propane. The critical pressure of bulk d-propane is at $p_c = 616$ psi, being the same as found in h-propane. After filling the pressure cell with silica aerogel (porosity 96%) pressure scans have been performed at temperatures of 50°C, 88°C, 91°C, 96°C, 102°C and 150°C. Small Angle Scattering data have been collected in the Q-range 0.01 Å-1 ≤ Q ≥ 0.18 Å-1 with a typical measurement time of 2 – 10 min (simultaneous measurement of Transmission data). We found strong alterations in the SANS and Transmission data with variation of pressure. Figure 1 shows the results of a pressure scan at the (bulk) critical temperature. These actual data are viewed in comparison to the calculated data for a two-phase system, in which we assume that the pores are evenly filled with nonadsorbed fluid of the respective density. We find strong deviations of our experimental data from the two-phase model in both small angle scattering and transmission. In our adsorbed phase model we assign all of these deviations to the existence of an adsorbed phase that comprises the third phase besides the silica aerogel and nonadsorbed fluid. The three-phase model of Wu (Polymer 1982) is employed to relate the invariant obtained from SANS data to volume fractions and scattering length densities of the three phases. Using a formalism that combines small angle scattering and transmission results we can readily calculate the volume fraction and density of this adsorbed phase without further model assumptions. The results of this calculation for the critical temperature are shown in figure 2.

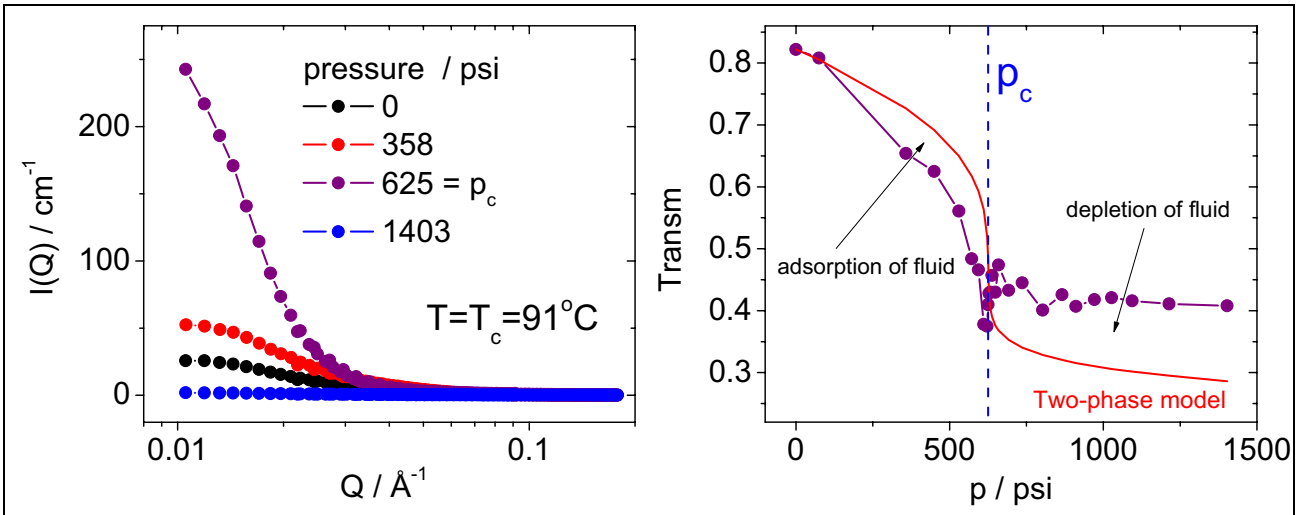


Figure 1: Results from a pressure scan at the critical temperature; left figure: SANS data, right figure: Transm.

The results give a detailed picture of the physical state of the pore liquid. We find the formation of a densified adsorbed layer at low densities, which reaches a maximum density of about 0.7 g/ml, being the density of liquid d-propane. The adsorbed layer fills the entire pore space at low and high densities. In the regime of medium densities our model suggests the breakdown of the adsorbed layer. At high densities we find depletion of fluid from the pore space. The third phase is now a low-density phase with a high volume fraction. Our findings are in general agreement with earlier findings of Findenegg and others, which found negative values of excess adsorption of fluids at high densities. In the future we plan to study the transition from the high-density adsorbed layer to the low density depletion layer in more detail.

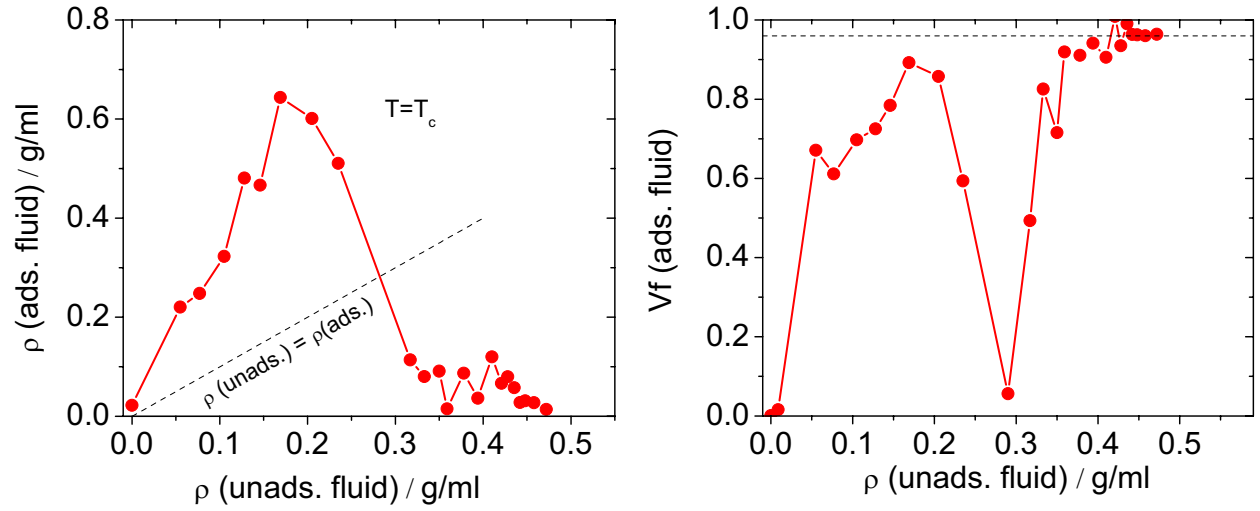


Figure 2: Physical properties of the adsorbed phase as a function of the density of unadsorbed fluid, shown for the critical temperature; left figure: density of adsorbed fluid, right figure: volume fraction of adsorbed fluid.

Institut für Festkörperforschung
Forschungszentrum Jülich GmbH
D-52425 Jülich

Experimental Report
of Neutron Scattering Experiments
at the FRJ-2 Reactor

Proposal number:	KW2-05-026		
Experiment title:	Struktur des denaturierten Proteins Rnase A		
Dates of experiment:	Sep. 2005	Date of report:	Mai 2006
Experimental team: Names	 Addresses		
Ralf Biehl Bernd Hoffmann Michael Monkenbusch Rudolf Merkel Dieter Richter	FZJ/IFF FZJ/ISG FZJ/IFF FZJ/ISG FZJ/IFF		
Local Contact:	Aurel Radulescu		

Experimental report text body

The protein folding and function is strongly coupled to the structure and the thermal equilibrium fluctuations. In view of the macromolecule energy landscape the protein folding follows a path from the unfolded state at high energy to the low energy state at the final configuration with intermediate states in between. Thereby the secondary and ternary structure is determined. Catalytic activities or transport mechanisms follow transitions between intermediate states in the energy landscape. All involve configurational changes on length scales from single amino acids to sizes of complete a helices or b sheets and the total size of the protein. Timescales reach from picoseconds to microseconds. A way to explore the energy landscape at equilibrium is to observe thermal fluctuations of the protein. By changing environmental parameters e.g. temperature the level of energy is changed.

Here as a starting point for our dynamical experiments we want to determine the structural changes of the protein during unfolding by temperature increase. The protein was examined under conditions providing the possibility of refolding to the natural state.

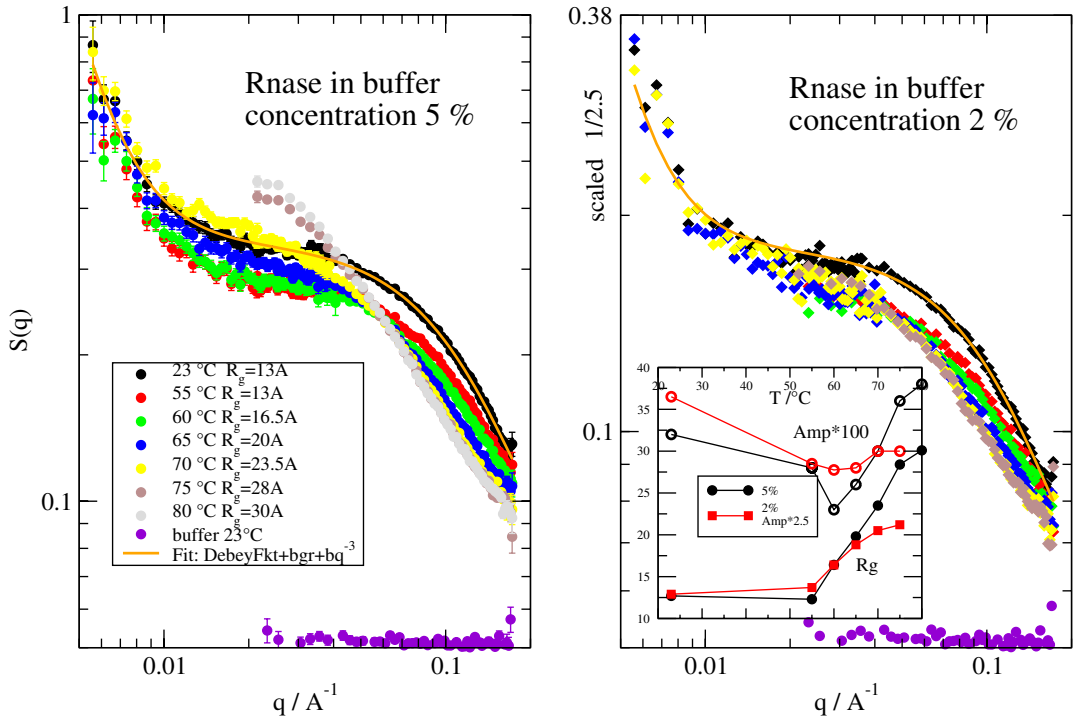


Figure 1: Sans Scattering data for different temperatures. Left: concentration of 5%, right: concentration of 2%. The inset in the right graph shows the radius of gyration and the intensity of a fit according to the debey formula including background and a power law q^{-3}.

Figure 1 shows the result of our measurements. Both concentrations show the same main features. At low q we observe an increasing intensity due to aggregates or dirt. We modeled this in our fits by a power law ~q^{-3}. At higher q we observe the typical plateau with decreasing intensity to highest q. As we expect the protein to unfold from its globular shape with increasing temperature, we have chosen a Debey function to model this even for the unfolded state. The Debey function

$$S(q)=2*(\exp(-q^2R_g^2)-1+q^2R_g^2)/\ q^4R_g^4 \qquad 1$$

is commonly used to describe a Gaussian distribution of point scatterers (eg. a free Gaussian chain) and is used here only to have a consistent model to evaluate the radius of gyration. To include the significant amount of aggregates and/or dirt inside the sample we add a power law q^{-3}. Also a constant background is assumed to account for the solvent scattering. As the orange curve in both plots shows this model describes our data well and gives similar results for both concentrations.

The inset in figure 1 shows the parameters of the resulting fits. From room temperature to 55 °C the we observe no significant change in R_g . Above the protein unfolds from R_g =13A to R_g=22A. At a concentration of 5% the increase at temperatures above 65°C is much higher. Comparison of the original data in the left graph show a significant increase and a change of the overall shape which we cannot observe for a concentration of 2%. We conclude that the increase of the scattering intensity is due to gel formation at highest temperature and concentration.

The 2% sample data will be compared to to NSE and DLS data measured on the same protein .

We will restrict our further experiments to Temperatures without gel formation.

Institut für Festkörperforschung
Forschungszentrum Jülich GmbH
D-52425 Jülich

Experimental Report of Neutron Scattering Experiments at the FRJ-2 Reactor

Proposal number:	KW2-05-027		
Experiment title:	Shear-induced structural changes of HM-alginate in the presence of poly-ß-cyclodextrin -an *in situ* Rheology and SANS study		
Dates of experiment:	26/09/2005	Date of report:	27/05/2006
Experimental team: Names	 Adresses		
Reidar Lund Bo Nyström Anna-Lena Kjøniksen	DIPC, University of Basque Country, Spain Dep. of Chemistry, University of Oslo, Norway. Dep. of Chemistry, University of Oslo, Norway		
Local Contact:	Henrich Frielinghaus		

Experimental report text body

β-cyclodextrins (β-CD) is a cyclic polysaccharide, it is cone-shaped consisting of a hydrophobic core that can encapsulate hydrophobic groups, and a hydrophilic external surface. In mixtures of hydrophobically modified polymers (e.g. HM-alginate) and β-CD the deactivation of the hydrophobic moieties will result in a weaker tendency to form association complexes. In this case we will not observe any shear-induced effects. However, if we instead of β-CD add to the solution of HM-alginate poly-β-cyclodextrin (poly-β-CD) formation of bridges may occur. In this case a viscosification takes place and complex shear dependence is observed. A striking and novel feature here is that the shear thickening behaviour is observed at a fairly high shear rate (10 s^{-1}). The magnitude of this effect is strongly temperature dependent (see Figure 1). One conjecture is that by applying a shear flow, the alginates and/or poly β-CD are extended and this effect facilitates the development of bridges. This gives rise to the viscosity maximum observed in the shear rate curve. At higher shear rates this structure is disrupted, and a shear thinning behaviour appears.

In order to understand the rheological behavior we wanted to investigate structural changes induced under shear. For this purpose we employed a shear cell apparatus in the neutron beam and measured the structure factor over the whole Q-range accessible as a function of three different shear-rates, 2, 10, 50 s^{-1}. The scattering was initially detected continuously with some minutes interval (typically 10 min) by performing continuous scans at intermediate Q (8 m detector distance) while the shear was being applied. However, no time dependent features were found. Representative results showing the scattering curves over the whole Q-range (20, 8 and 2m detector distance) are given in Figure 2.

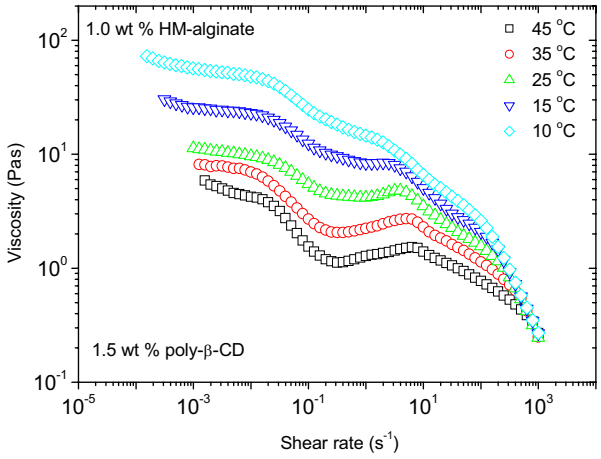


Figure 1. Shear rate dependence of the viscosity of a sample containing 1.0 wt % HM-alginate and 1.5 wt % poly-β-CD at different temperatures.

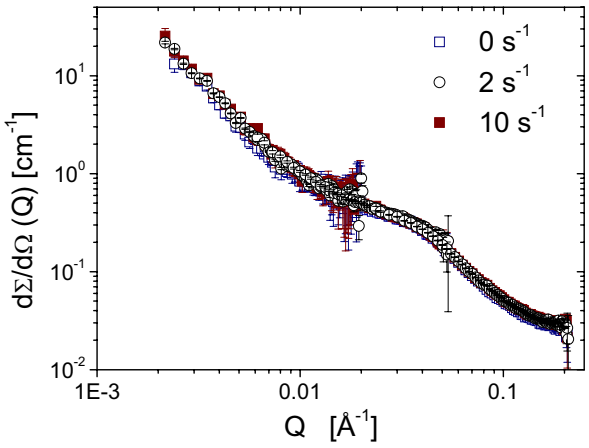


Figure 2. In situ Rheo-SANS results of the same HM-Alginate/poly-β-dextrin) mixture at different shear rates. 25 °C

As seen in the figure we observe no effect of shear on the overall scattering from the sample. This is rather intriguing as shearing of the sample has dramatic effects on the rheology. Indeed comparing with figure 1 we observe strong shear dependence and even a significant shear-thickening at relatively high shear rates (around 10 s^{-1}). Hence the results likely demonstrate that the structural changes occur on length scales much larger than the mesoscopic length scales covered by SANS (here approximately 300 – 3 nm). Similar findings have also been found for jammed soft star-like colloids of different arm numbers, where the rheology shows a rather rich behavior being undetected by SANS [1]. The main results of this experiment are part of an article published in Biomacromolecules [2].

REFERENCE:

1. Barbara Lonetti and Joerg Stellbrink *Private communication*
2. Virginie Burckbuchler, Anna-Lena Kjøniksen, Céline Galant, Reidar Lund, Catherine Amiel, Kenneth D. Knudsen and Bo Nyström *Biomacromolecules,* ***in press***

Institut für Festkörperforschung
Forschungszentrum Jülich GmbH
D-52425 Jülich

Experimental Report of Neutron Scattering Experiments at the FRJ-2 Reactor

Proposal number:	KW2-05-028, KW2-05-051		
Experiment title:	Characterization of star-like micelles by contrast variation		
Dates of experiment:	12.11. - 14. 11.2005 15.02.2006	Date of report:	06.06.2006
Experimental team: Names	Addresses		
J. Stellbrink B. Lonetti	IFF, FZ Jülich, D-52425 Jülich, Germany IFF, FZ Jülich, D-52425 Jülich, Germany		
Local Contact:	J. Stellbrink		

Experimental report text body

We investigated the phase behaviour of star-like micelles formed by the amphilic block copolymer poly(ethylenepropylene)-poly(ethyleneoxide), $M_{w,PEP}$= 1000 g/mol, $M_{w,PEO}$= 20000 g/mol, in different water/dimethylformamide mixtures by small angle neutron scattering (SANS) [1] and partly by light scattering and rheology. Changing the solvent composition changes the aggregation number (or functionality), f, of the micelles due to changes in the interfacial tension between the core-forming, hydrophobic PEP and the solvent. This enabled us to construct the experimental equilibrium phase diagram in the packing fraction (η) / functionality (f) representation and compare it to theoretical predictions for regular star polymers, see fig.1. In particular the location of the fluid/solid phase boundary and the glass line was derived. Recently we synthesized a new PEP-PEO block copolymer with same molecular weight and block composition, but different H/D-labelling, i.e. protonated PEP and partially deuterated PEO. Moreover, this polymer has been prepared in larger amounts to be able to perform rheological and Rheo-SANS experiments also at higher volume fractions. As a first step we had to characterize the corresponding micelles with respect to their functionality f, radius of the hydrophilic shell, R_{shell}, and radius of the hydrophobic core, R_{core}. Prerequisite for such a characterisation is an exact determination of the experimental matching points by SANS contrast variation experiments.

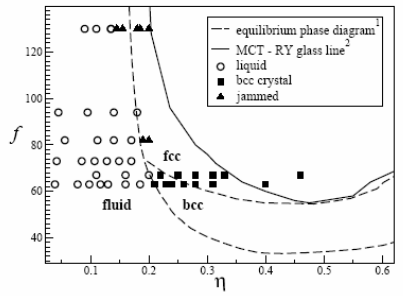
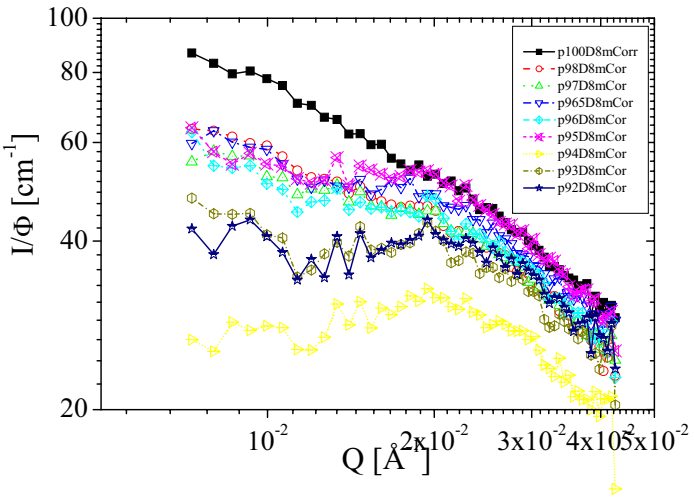


Figure 1: Experimental phase diagram of star-like micelles compared to theory.

In this experiment we investigated (very) dilute micellar solutions, Φ=0.25%, in different H_2O/D_2O mixtures. Besides the two pure isotopic solvents ("full contrast") and an intermediate contrast with Φ_{D2O}=50%, a detailed series of contrasts around the nominal core contrast, Φ_{D2O}=96% was investigated. Figure 1 shows the corresponding SANS curves obtained at KWS2. One has to keep in mind that the experiment is pushing the SANS instrument to its limits due to the low concentration and the small changes in contrast, but already by visual inspection one sees that the (expected) forward scattering resulting from the PEO corona shows a minimum for a solvent mixture with Φ_{D2O}=95%. This is further confirmed by a more sophisticated data analysis using a core-shell form factor and taking into account all experimental uncertainties with respect to synthesis and characterisation of the used partially labelled diblock copolymer. Still under investigation is the question of preferred hydration/deuteration of the PEO corona in the H_2O-rich contrasts investigated.



References:

[1] M. Laurati, J. Stellbrink, R. Lund, L. Willner, D. Richter, and E. Zaccarelli, *Phys. Rev. Letters*, **94**, 195504, 2005.

Institut für Festkörperforschung
Forschungszentrum Jülich GmbH
D-52425 Jülich

Experimental Report
of Neutron Scattering Experiments
at the FRJ-2 Reactor

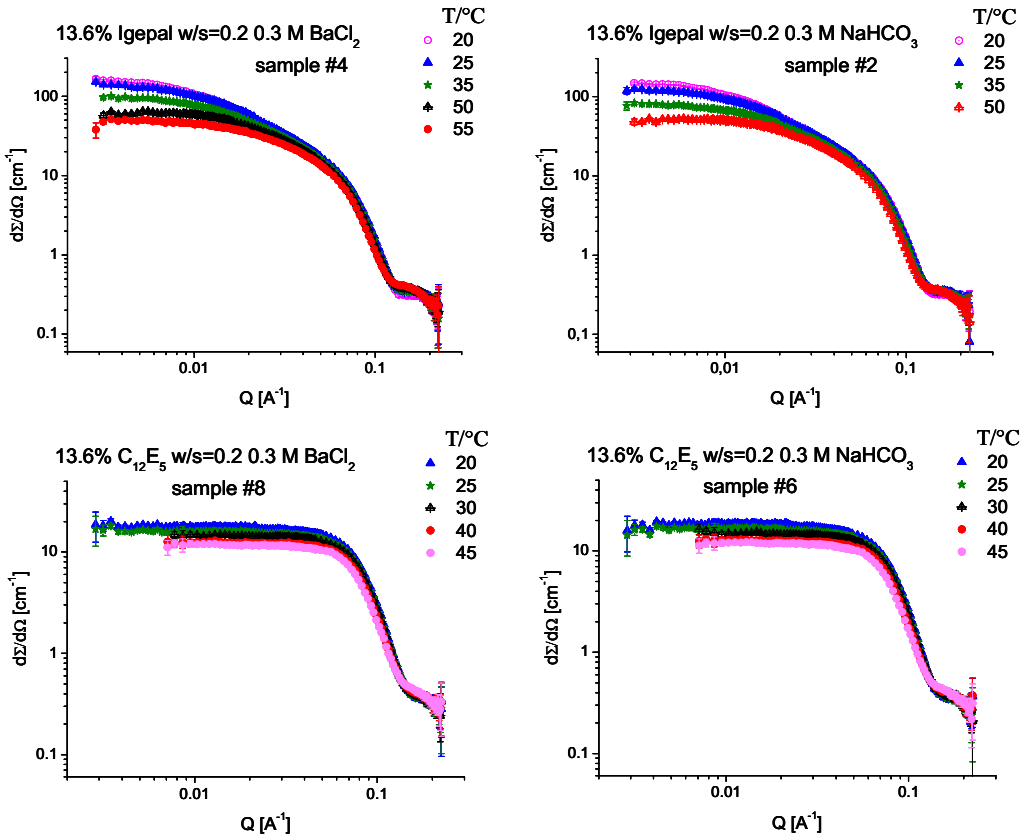
Proposal number:	KW2-05-030		
Experiment title:	Characterization of nonionic w/o microemulsions as precipitation media for the synthesis of $BaCO_3$ nanoparticles.		
Dates of experiment:	September 19-20, 2005 November 1-2, 2005 December 2-3, 2005	Date of report:	Dec. 15, 05
Experimental team: Names	Addresses		
W.F.C. Sager M. Feygenson	IFF-Soft Matter, FZ-Jülich P.O. Box 1913, 52425 Jülich IFF-8: Scattering Methods, FZ-Jülich P.O. Box 1913, 52425 Jülich		
Local Contact:	A. Radulescu		

Experimental report text body

In order to gain more insight into the "templating" role of the microemulsion, we studied in detail by transmission electron microscopy the formation of $BaCO_3$ nanocrystals within the one-phase region of different nonionic w/o microemulsions stabilized either by Igepal CO520 or $C_{12}E_5$. Inducing the precipitation of $BaCO_3$ by mixing two microemulsions, that differ only in the type of salt solubilised, allowed us to investigate, for the first time, the formation of nanoparticles within a large parameter space that comprises variations of the microemulsion composition, salt concentrations and temperature. A variety of nanostructures with well-defined morphology emerges ranging from (stacked) platelets, (self-assembling) rhombohedral nanocrystals, nano-needles, (ordered) hexagonal nanorods to nano-fibres and -bundles. Varying the conditions of the precursor microemulsions, therefore, permits to examine the transitions between the different nanostructures, e.g., transitions between needles and (hexagonal) nanorods, polygonal crystals and elongated rhombohedral crystals, systematically and to finally gain insight into the mechanisms of their formation. For the latter it is a prerequisite to know the morphology of the precursor microemulsions and to explore how changes in the morphology of the microemulsions are reflected in the nanostructures formed.

During our KWS2-beamtime in September and November we focused on characterising the microstructure of the microemulsions formed by either Igepal CO520 or $C_{12}E_5$ as a function of temperature and salt concentration (0.1-0.3 M) within the aqueous phase for a water-to-surfactant ratio of w/s=0.2. Fig. 1 shows the temperature series of the measured scattering curves for 0.3 M $BaCl_2$ and 0.3 M $NaHCO_3$, respectively. As can clearly be seen, microemulsion droplets stabilized by $C_{12}E_5$ are within the one-phase region much more stable against aggregation and cylinder formation upon lowering the temperature than for the Igepal stabilized microemulsions. By a first analysis of our data with the 2-component model for spheres and cylinders, developed earlier for the analysis of scattering curves of AOT stabilized microemulsions [1], we found that for the $C_{12}E_5$ system the volume fractions of spheres decrease from about 80% to 50% between 50 °C and 20 °C, almost independent of the salt concentration. Albeit more effort is still necessary on the improvement of our model it is already clear that the cylinders shorten drastically at salt concentrations above 0.3 M.

Fig. 1

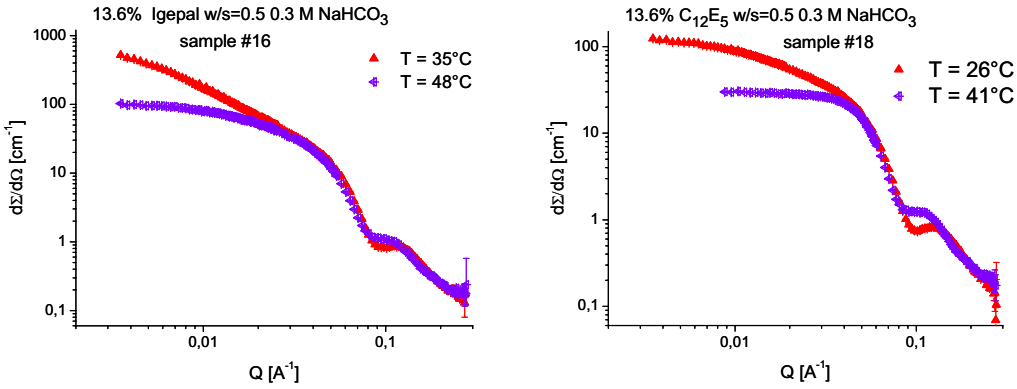


In the Igepal microemulsions, cylinders are already present in volume fractions of 40-60% even at the highest temperatures measured and reach volume fractions of 100% (far) above the lower phase boundary. An increase in the salt concentration has here only little effect on the cylinder length but reduces the number of cylinders significantly.

In December we started to extend our SANS study to higher w/s values and to also investigate microemulsions stabilized by mixtures of Igepal CO520 and $C_{12}E_5$. Fig. 2 shows scattering curves obtained just below the upper and just above the lower phase boundary for Igepal and $C_{12}E_5$ microemulsions at w/s=0.5 for 0.3 M $NaHCO_3$. At this water-to-surfactant ratio the cylinder fraction and cylinder length increases also for $C_{12}E_5$ microemulsions strongly upon lowering the temperature.

[1] D.I. Svergun, P.V. Konarev, V.V. Volkov, M.H.J. Koch, W.F.C. Sager, J. Smeets, and E.M. Blokhuis, J. Chem. Phys. 113, 1651 (2000).

Fig. 2



Institut für Festkörperforschung
Forschungszentrum Jülich GmbH
D-52425 Jülich

Experimental Report
of Neutron Scattering Experiments
at the FRJ-2 Reactor

Proposal number:	KW2-05-031, KW2-05-036, KW2-05-046, KW2-05-049		
Experiment title:	**Bi-continuous microemulsions in presence of bifunctional sticker polymers – part I, II, III, IV**		
Dates of experiment:	27. – 28.09., 27.10., 06. – 07.12.2005, 26.01.2006	Date of report:	21.03.2006
Experimental team: Names	Addresses		
Martin Brodeck Henrich Frielinghaus	Forschungszentrum Jülich GmbH, Institut für Festkörperforschung, D-52425 Jülich Forschungszentrum Jülich GmbH, Institut für Festkörperforschung, D-52425 Jülich		
Local Contact:	Henrich Frielinghaus		

Experimental report text body

After successfully introducing monofunctional sticker polymers (KW2-05-019), the bifunctional sticker polymers were investigated to complete the picture of multi-arm sticker polymers. A theory of T. Auth and G. Gompper [1] predicted a 10% higher sensitivity with respect to the total number of anchored arms. Higher functionalities increase the sensitivity even further. The aim of the present study is an experimental check of the predictions of this theory. Two bifunctional sticker polymers with different sticker lengths were synthesized, namely a $C_{12}(E_{100})_2$ and a $C_{16}(E_{100})_2$. The full information of phase diagram and SANS measurements was collected and compared amongst each other, with the monofunctional sticker and with theory.

Prior to the neutron scattering experiments phase diagram measurements have been made. Here the one phase region of the bicontinuous microemulsion was determined. In a temperature vs. surfactant amount plot the one phase region looks like a fish tail, and the fish body is the 3-phase coexistence region. Both regions are connected in one point, the fish tail point, where the surfactant fails to dissolve the equal amounts of oil and water. The efficiency of a surfactant is measured by this minimum amount of surfactant γ_{ftp}. Taking the oil solubility of the surfactant into account one obtains the membrane content $\Psi \approx \gamma_{ftp}$–0.01. Figure 1 shows the membrane content as a function of the scaled polymer content $\sigma \cdot R_{ee}^2$. The slope is measure for the strength of the polymer boosting effect. The monofunctional sticker polymer is an equally good booster as the diblock copolymer. The bifunctional sticker $C_{12}(E_{100})_2$ has the lowest effect. Three phase coexistence measurements yielded a high water solubility of this sticker – the $C_{12}(E_{100})_2$ is not fully active at the surfactant membrane. The $C_{16}(E_{100})_2$ on the other hand is almost not found in the water phase in agreement with the better boosting ability. Nonetheless, the $C_{16}(E_{100})_2$ is a worse booster as the monofunctional sticker.

The second measure is the temperature at the fish tail point. The imbalance of the unsymmetric polymers causes some spontaneous curvature which is balanced by the increased temperature. A similar picture is obtained as for the sensitivity of the membrane content Ψ. The details are not discussed in the present paper.

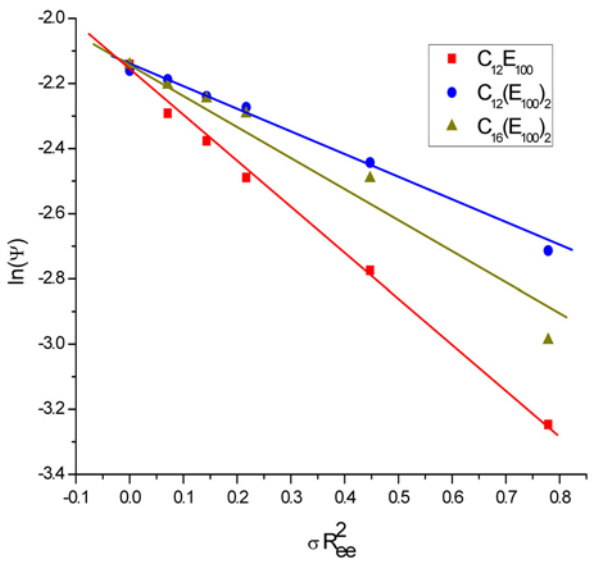


Figure 1: The minimum amount Ψ of surfactant needed to solubilize equal amounts of water and oil as a function of the scaled polymer amount. The monofunctional $C_{12}E_{100}$ sticker has a comparable boosting to the diblock copolymer, whereas the bifunctional sticker polymers are considerably weaker.

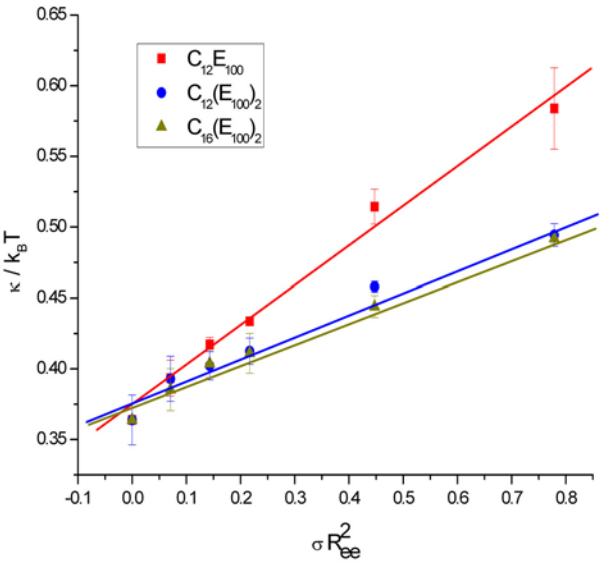


Figure 2: The by SANS measured bending rigidity κ as a function of the scaled polymer amount. The monofunctional sticker has a comparable sensitivity as a diblock copolymer. Both bifunctional sticker polymers have a considerably weaker sensitivity. This result in comparison with the theory remains an open question.

The macroscopically determined phase diagram is connected to microscopically defined parameters of the Helfrich model. The model assumes the elastic properties of the surfactant film to be dominant in the free energy of the microemulsion. The three important parameters are the spontaneous curvature c_0, and two elastic moduli, namely the bending rigidity κ and the saddle splay modulus $\bar{\kappa}$. The spontaneous curvature decreases with increasing temperature and increases with increasing sticker polymer amount. At the fish tail point the spontaneous curvature is zero, so the two contributions are balanced. The elastic moduli are spatially renormalized parameters with a logarithmic dependence on the surfactant amount. The absolute values of the elastic moduli increase with increasing polymer amount. At the fish tail point the saddle splay modulus is a negligible constant, and so the renormalization is balanced with the polymer term. This balance leads to an exponential dependence of the minimal surfactant amount with respect to the scaled polymer amount.

In theories the moduli κ and $\bar{\kappa}$ behave extremely similar, just the signs of the moduli are opposite ($\kappa>0$ and $\bar{\kappa}<0$). Thus a quantitative comparison of the macroscopically determined $\bar{\kappa}$ with κ is desired. Small angle neutron scattering experiments determine the domain structure if bulk contrast is chosen. One obtains the domain size *d* and the correlation length ξ, which are connected with the bending rigidity $\kappa/k_BT = 0.85\ \xi/d$ according to the Gaussian random field theory. Three different surfactant amounts were measured in the one phase region for each polymer amount. For each polymer amount an inter-/extrapolation of κ was made to a constant surfactant amount; thus, the spatial renormalization does not play a role anymore. The directly measured bending rigidity κ as a function of the polymer amount is depicted in figure 2. Again, the two bifunctional sticker polymers are much weaker than the monofunctional sticker. The monofunctional sticker polymer has a comparable sensitivity as the diblock copolymer.

The general picture about sensitivities of κ and $\bar{\kappa}$ is consistent within the measurements. The monofunctional sticker works equally well as efficiency booster compared to the diblock copolymer. The bifunctional sticker polymers do not work as effectively as the simple sticker. Measuring the activity of the polymer in the three phase coexistence states that the $C_{12}(E_{100})_2$ is not fully active, while the $C_{16}(E_{100})_2$ is supposedly strongly active. After the theory the bifunctional sticker polymers should be 10% stronger efficiency boosters. So the remaining question is if the theory is wrong, or if the activity measurements are interpreted wrongly, since this method is indirect.

[1] T. Auth, G. Gompper, *Phys. Rev. E* **68**, 051801 (2003)

Institut für Festkörperforschung
Forschungszentrum Jülich GmbH
D-52425 Jülich

Experimental Report
of Neutron Scattering Experiments
at the FRJ-2 Reactor

Proposal number:	KW2-05-033, KW2-05-038		
Experiment title:	**Investigating the polarized GISANS method at KWS-2 – Part I and Part II**		
Dates of experiment:	05.10. – 07.10.2005 04.11. - 06.11.2005	Date of report:	13.06.2006
Experimental team: Names	Addresses		
E. Kentzinger H. Frielinghaus Th. Brückel	Institut für Festkörperforschung, Forschungszentrum Jülich Institut für Festkörperforschung, Forschungszentrum Jülich Institut für Festkörperforschung, Forschungszentrum Jülich		
Local Contact:	H. Frielinghaus		

Experimental report text body

In order to investigate the polarized GISANS method, we measured polarized GISANS signal from a remanent polarizing supermirror, a system already studied by off-specular scattering on HADAS. The aim of this investigation was to have access to the correlation length of the structural and magnetic correlations, all smaller than the ones that can be probed on a reflectometer like HADAS. An un-polarized GISANS measurement was performed before on the same system (report KW2-05-003).

For this measurement, we used the set-up depicted in Fig.1 of report KW2-05-032. Some of the results obtained are depicted in Fig.1. In that picture, we show the GISANS signal measured at fixed angle of incidence and for different positive values of the applied magnetic field after the sample was saturated in the minus direction. Each state is measured first with spin-down incoming neutrons (flipper off), then with spin-up incoming neutrons (flipper on). As the applied magnetic field is increased, the diffuse signal is progressively transferred from the spin-down channel to the spin-up one.

The measured signals can be explained by comparing them with the off-specular scattering measured on the same sample on HADAS. In Fig.2 we show such measurements performed at $\mu_0 H$=3.1 mT, a field close to the 3.3 mT in Fig.1. In Fig.2 the positive α_f values spanned by the GISANS measurements are marked by red lines. The diffuse scattering at ($\alpha_i + \alpha_f$) values below, around and above the specular $\alpha_i + \alpha_f = 3°$ value in the spin-down and around the specular in the spin-up channel is scattering from the interfacial roughness correlations, as can be seen respectively in the I— and the I++ channels of Fig.2. The strong intensity around $\alpha_i + \alpha_f = 2°$ in the spin-down channel is scattering by the magnetic correlations, as can be seen in the I-+ channel of Fig.2. In this experiment, those correlations were not resolved, due to the too small collimation and sample-to-detector lengths. A tentative to resolve those long-range correlations is reported in the report KW2-06-005.

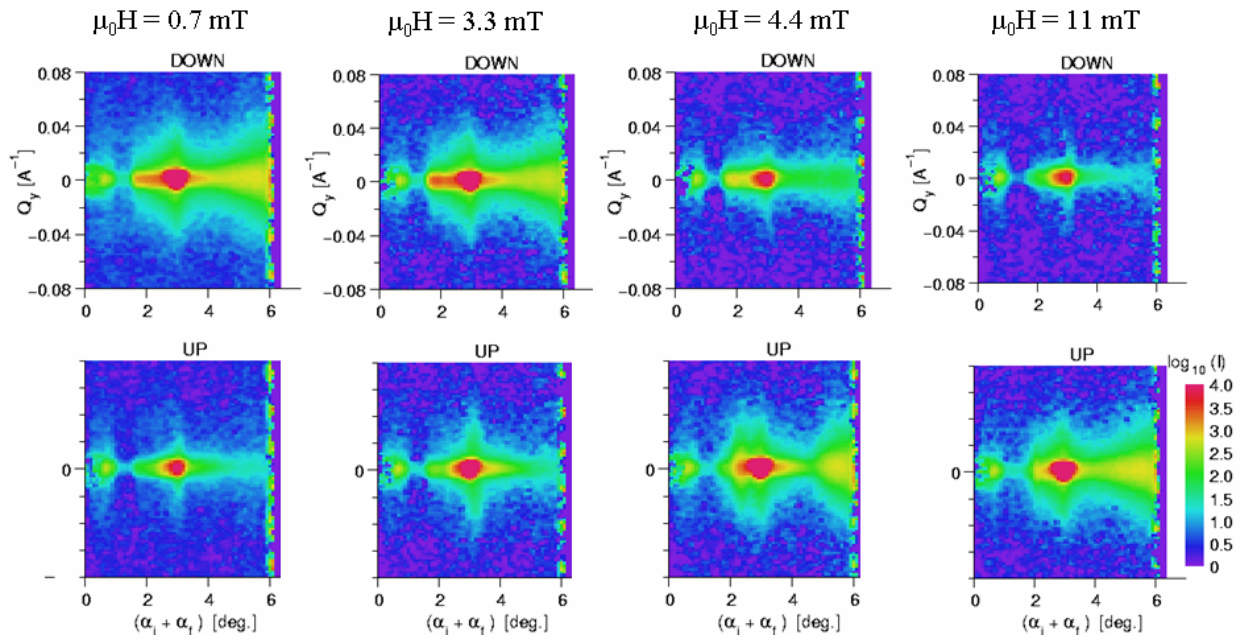


Fig.1: Polarized GISANS measured at αi=1.5° on a remanent polarizing supermirror at different applied fields $\mu_0 H$. In each case, the same state was measured with incoming spin-down and spin-up neutrons. Exposure time: 13 minutes per field and polarization. Those data can be compared with their unpolarized counterparts (Fig.2 of report KW2-05-003).

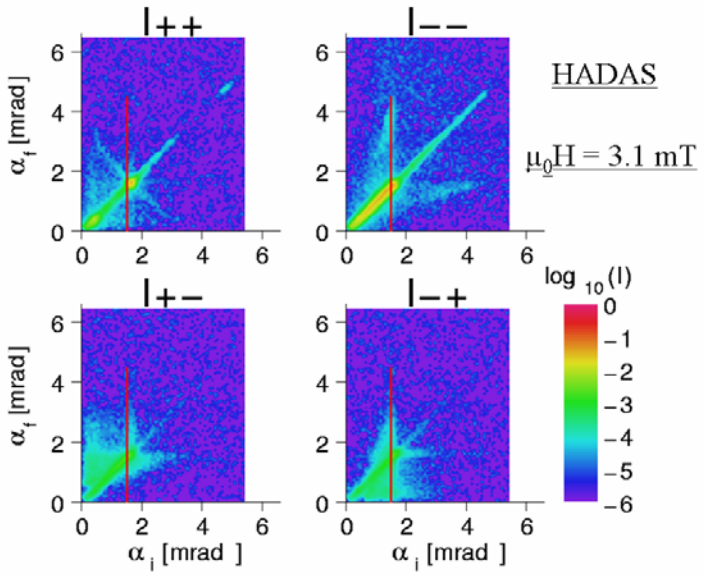


Fig.2: Reflectivity and off-specular scattering from the remanent polarizing supermirror measured on HADAS. This picture is shown in order to explain the GISANS signal measured at $\mu_0 H$=3.3 mT in Fig.1.

Institut für Festkörperforschung
Forschungszentrum Jülich GmbH
D-52425 Jülich

Experimental Report of Neutron Scattering Experiments at the FRJ-2 Reactor

Proposal number:	KW2-05-034		
Experiment title:	Self assembly Mechanism of Lysozyme Protein Hydrogels		
Dates of experiment:	10.03-13.03.2006 18.04.2006	Date of report:	04.06.2006
Experimental team: Names			
Dr Aline F.Miller Hui Yan Dr Alberto Saiani Amran Mohammad	School of Chemical Engineering and Analytical Science The University of Manchester Sackville Street, PO Box 88, Manchester M60 1QD, UK School of Materials The University of Manchester Grosvenor Street, Manchester M1 7HS, UK		
Local Contact:	Dr H. Frielinghaus		

Experimental report text body

Proteins have recently attracted considerable attention for their use as building blocks in the construction of novel materials. Many proteins are capable of self-assembling into β-sheet rich fibrils under appropriate conditions via intramolecular or intermolecular hydrogen bonding[1]. Such fibrils can further self-organise to form a three-dimensional fibrillar network, i.e. a protein hydrogel, which is able to retain up to 97% water or biological fluid[2]. By varying the amino acid sequence in addition to manipulating environmental conditions, such as sample concentration, pH or ionic strength, novel protein-based materials with desirable properties are beginning to be engineered[3].

In order to gain an insight into fibril formation and the gelation mechanism, hen egg white lysozyme (HEWL) has been used as a model protein. Phase diagrams have been mapped out and thermal and mechanical behavior of these systems has been under investigation using micro-differential scanning calorimetry (microDSC) and rheology respectively. Here we focussed on elucidating the structure of lysozyme hydrogels formed under reductive conditions (breaking di-sulphide bridges) as a function of protein and reductant concentration and temperature using SANS. Samples were prepared by dissolving the desired quantity of protein in D_2O, adding 20 or 50 mM of the reductant dithiothreitol (DTT) and heating the system to 90 °C. Above the critical gel concentration of 5 mg ml^{-1} thermo reversible, transparent hydrogels formed upon cooling.

Typical scattering curves for four different protein concentrations (10, 14.3, 42.9 and 57.2 mg ml^{-1}) with 20 mM DTT at 25 °C are shown in Figure 1. A maximum in scattering was obtained for each sample and its position shifted to higher q values with increasing concentration. An estimated value of the average mesh size, d, was obtained from the position of the peak maximum, q^*, through the Bragg relation: $d = 2\pi/q^*$.

The values obtained decrease as shown in Figure 2 with increasing protein concentration i.e. a denser network is formed. The narrow shape of the maxima observed also suggests the presence of a regular network with a relatively uniform mesh size. These results are in good agreement with those observed with cryo-SEM.

Scattering curves for all concentrations at 90 °C have also been recorded (results not shown). For the low concentration samples (10 and 14.3 mg ml^{-1}) the maximum in scattering disappeared, suggesting the gel network had melted. The peak remained, however, for the two higher concentrations. Such results are in good agreement with micro DSC measurements, which indicate the gels at high concentration had not melted completely at 90 °C. Samples were also diluted to see if we could observe scattering from individual fibrils. A typical Kratky plot is given in Figure 3 and by fitting the curve with a rod model we obtained an average fibril diameter of ~ 6nm.

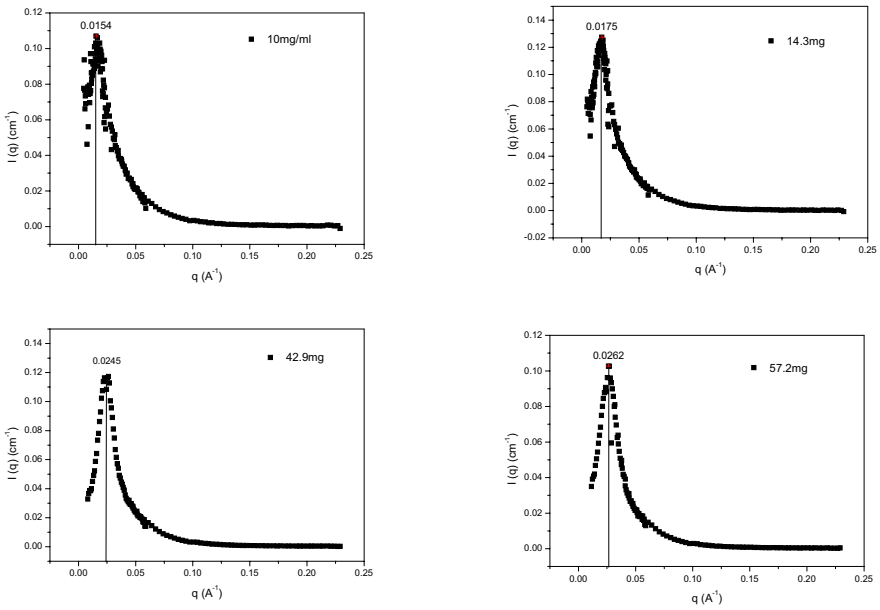


Fig. 1 Scattering curves of HEWL gels at various concentrations measured at 25 ºC.

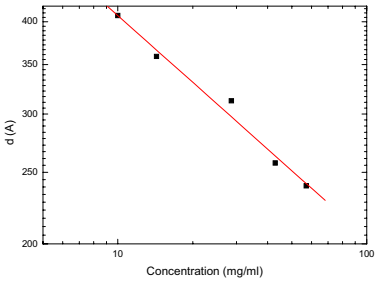


Fig. 2. Estimated mesh size, *d*, as a function of protein concentration.

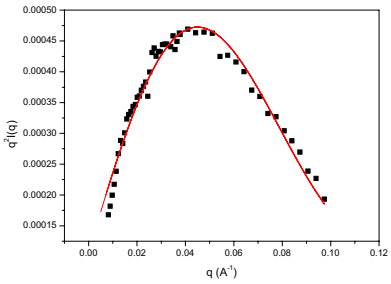


Fig.3 Kratky plot of a diluted gel sample at 25 ºC.

The results from our SANS experiments provide evidence of the fibrillar nature of our hydrogel as well as quantitative data on fibril dimension and hydrogel mesh size. We have also been able to identify the key role played by both concentration and temperature.

References

1. Fandrich, M., Fletcher, M.A. and Dobson, C.M. *Nature* **2001** *410*(6825), 165-166.
2. Miller, A.F**.** *Macromolecular Symposia,* **2005**, *220,* 109-114.
3. Aggeli, A., Bell,M., N. Boden, N., et al. *Nature*, **1997**. *386*(6622), 259-262.

Institut für Festkörperforschung
Forschungszentrum Jülich GmbH
D-52425 Jülich

Experimental Report
of Neutron Scattering Experiments
at the FRJ-2 Reactor

Proposal number:	KW2-05-037		
Experiment title:	**Structural study of supramolecular aggregates formed by a novel class of contrast agents potentially usuable in magnetic resonance imaging techniques**		
Dates of experiment:	07/11/2005	Date of report:	15/12/2005
Experimental team: Names	Addresses		
Gaetano Mangiapia	IFF – Neutronenstreuung, Forschungszentrum Jülich GmbH, D-52425 Jülich Tel. +49 2461 61 6048 (g.mangiapia@fz-juelich.de)		
Henrich Frielinghaus	IFF – Neutronenstreuung, Forschungszentrum Jülich GmbH, D-52425 Jülich Tel. +49 2461 61 5093 (h.frielinghaus@fz-juelich.de)		
Local Contact:	H. Frielinghaus		

Experimental report text body

Magnetic Resonance Imaging (MRI) is one of the most widely imaging technique used as diagnostic tool in clinical field. Its main advantage is that it allows rapid in vivo acquisition of images, and, under specific conditions, it makes possible imaging at cell resolution. The technique has proven very valuable for the diagnosis of a broad range of pathologic conditions in all parts of the body. Currently, stable Gd^{3+} poly(aminocarboxylate) complexes are widely used as contrast agents in MRI. These agents reduce the relaxation time of water protons present in the tissues, allowing to produce a higher quality (higher contrast) image. Although MRI gives very resolved images, it needs a relatively elevate concentration of contrast agent (10^{-4} mol dm^{-3}), due to its low sensitivity. To reach the required local concentration, many carriers have been developed such as micelles and vesicles, derivatized with a high number of metallic complexes.

The aim of this research project has been to characterize supramolecular aggregates formed by a new potential blood pool contrast agent $(C_{18}H_{37})_2CONHLys(DTPAGlu)CONH_2^{5-}$, in the following indicated as $(C18)_2DTPAGlu^{5-}$. This molecule, synthesized at the Interuniversitary Center for Bioactive Peptides (CIRPeB, Naples) and sketched in figure 1, contains the DTPAGlu chelating agent covalently bound to two C_{18} alkylic chains. The DTPAGlu is considered a very good chelating agent for paramagnetic metal ions (Gd^{3+}) used for applications in magnetic resonance imaging (MRI).

Through SANS measurements performed on both the systems containing $(C18)_2DTPAGlu^{5-}$ and its gadolinium(III) complex $[(C18)_2DTPAGlu(Gd)]^{2-}$, it has been possible to infer the capability of this contrast agents to form micellar and vesicular aggregates, depending on pH and ionic strength conditions.

Figure 2 shows scattering cross sections $d\Sigma/d\Omega$ obtained for binary solutions of $(C18)_2DTPAGlu^{5-}$ ($6.0\cdot10^{-4}$ mol kg^{-1}) at pH=3.0 and pH =4.5. Data obtained show the presence of scattering aggregates in both the systems, although they have very different characteristics.

In fact, $d\Sigma/d\Omega$ values at pH=3 show a power law dependence $d\Sigma/d\Omega \propto q^{-2}$ typical of the presence of bilayers; actually cryo-TEM measurements performed on this system have shown the existence of unilamellar vesicles that, due to the their dimension, may be regarded, in the q range spanned by SANS measurements performed, as randomly oriented infinite planar sheets. If τ represents the thickness of the sheets, in the region where $q\tau << 1$ scattering cross sections can be represented in a form analogous to the Guinier equation used to get radius of gyration

$$\ln\left(\frac{d\Sigma}{d\Omega}q^2\right) \cong \ln\left[2\pi S(\Delta\rho)^2\tau^2\right] - \frac{q^2\tau^2}{12} \qquad (1)$$

where S is the area of sheet per unit volume of sample, whereas $\Delta\rho$ is the scattering length density difference

between the sheet and the solvent. Thus, by reporting $\ln\left(q^2\,\mathrm{d}\Sigma/\mathrm{d}\Omega\right)$ vs. q^2 a straight plot with a slope $\tau^2/12$ should be obtained, allowing to determine the thickness of the vesicular double layer.
On the other hand, the pH growth from 3.0 to 4.5 leads to the destruction of the vesicular structure; in this case the power law found in SANS spectra, $\mathrm{d}\Sigma/\mathrm{d}\Omega \propto q^{-1}$, is characteristic of cylindrical aggregates. The presence of such transition can probably be attributed to the repulsion among the polar heads of DTPAGlu units: when pH is increased, carboxylic groups of DTPAGlu heads are deprotonated and repulsions start to become strong. This picture agrees with SANS measurements executed on $[(C18)_2DTPAGlu(Gd)]^{2-}$ solutions: such measurements have shown the presence of vesicles at pH=3.0 that still exist if pH is increased at 4.5. Gd-complexed DTPAGlu units have a smaller charge (–2); as result of that, the repulsions among polar heads are smaller if compared to those of DTPAGlu units. Effect of ionic strength has also been analyzed: the presence of NaCl in the system partially shields repulsions among polar heads. Indeed aqueous solutions of $[(C18)_2DTPAGlu(Gd)]^{2-}$ in the presence of NaCl, show vesicular aggregates even at physiological pH values (7.4).
Table 1 reports the values of τ obtained through eq. (1) for the systems analyzed, and the values of the radius R of cylindrical aggregates obtained by using the Guinier approximation of a cylinder form factor

$$\ln\left(\frac{\mathrm{d}\Sigma}{\mathrm{d}\Omega}q\right) \cong \ln\left[(\Delta\rho)^2\,\phi_{cyl}\left(1-\phi_{cyl}\right)\pi^2R^2\right] - q^2\frac{R^2}{4} \qquad (2)$$

where ϕ_{cyl} is the volume fraction of cylindrical aggregates. Actually the length of the cylinders cannot be extracted from the scattering data in the accessible range of the scattering vector q as indicated by the missing of the Guinier region at small q.

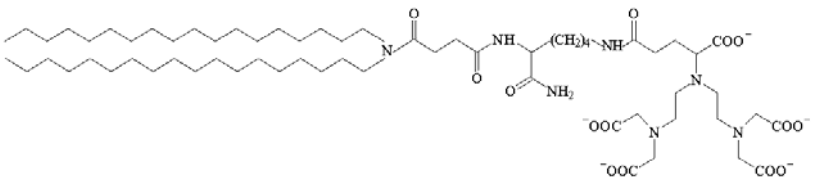


Figure 1 – Molecular structure of the $(C18)_2DTPAGlu^{5-}$ unimer.

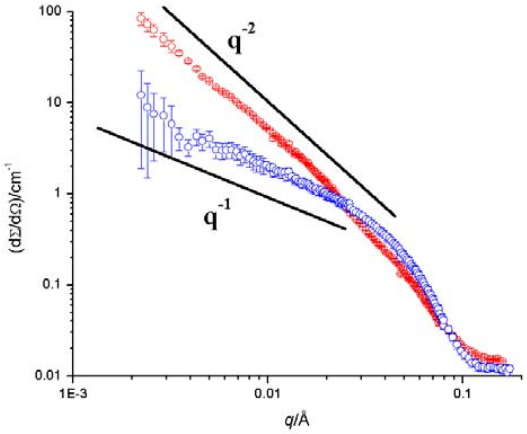


Figure 2 – Scattering cross sections obtained at 25°C for $(C18)2DTPAGlu^{5-}$ ($6.0\cdot10^{-4}$ mol kg^{-1}) at pH 3.0 (–) and 4.5 (–) in D_2O.

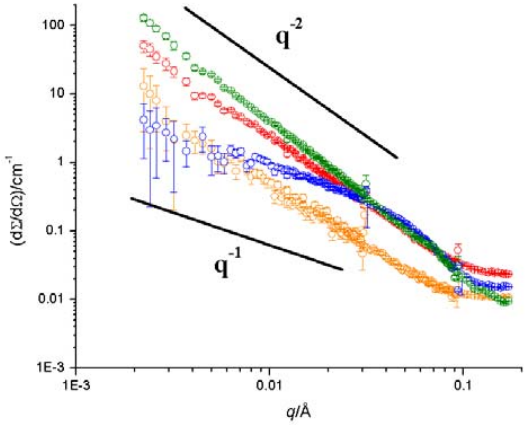


Figure 3 – Scattering cross sections obtained at 25°C for $[(C18)2DTPAGlu(Gd)]^{2-}$ ($4.1\cdot10^{-4}$ mol kg^{-1}) at pH 3.0 (–), 4.5 (–), and 7.4 (–) in D_2O, and at pH 7.4 (–) in NaCl 0.9% and D_2O.

	$(C18)_2DTPAGlu^{5-}$		$[(C18)_2DTPAGlu(Gd)]^{2-}$			
	pH 3.0	pH 4.5	pH 3.0	pH 4.5	pH 7.4	pH 7.4 + NaCl
τ/Å	47±5	—	51±6	53±8	—	53±4
R/Å	—	38±4	—	—	35±3	—

Table 1 – Values obtained from SANS data relative to the vesicular double layer thickness and the cylindrical radius of micelles.

Institut für Festkörperforschung
Forschungszentrum Jülich GmbH
D-52425 Jülich

Experimental Report
of Neutron Scattering Experiments
at the FRJ-2 Reactor

Proposal number:	KW2-05-039		
Experiment title:	**Test of the small detector**		
Dates of experiment:	14.12.2005	Date of report:	07.03.2006
Experimental team: Names	Addresses		
Henrich Frielinghaus	Institut für Festkörperforschung, Forschungszentrum Jülich GmbH, D-52425 Jülich		
Local Contact:	Henrich Frielinghaus		

Experimental report text body **Test of the small detector**

The new small detector is mounted at the KWS-2 for testing purposes. It is freely movable in front of the large area detector, but with a much higher resolution (0.5x0.5mm^2) in order to resolve much tinier structures than the large detector does (5x5mm^2). Finally in Munich, the new small detector will be operative at KWS-1 (and KWS-2) in order to obtain the following options: (a) In the center, close to the primary beam, one obtains much smaller scattering vectors which will be comparable to those of KWS-3 ($Q \approx 10^{-4}$Å). Here, a small collimation aperture is chosen. Lenses will improve the intensity and resolution. (b) Off the center, the peak width of sharp Bragg peaks can be resolved. A small collimation aperture is needed and neutron lenses are helpful. Additionally, a very good wavelength resolution (~1%) is needed, which will be obtained in a time-of-flight mode with a chopper. (c) In the grazing incidence (GI) SANS mode the scattered intensity is to be observed as well. Close to the specular reflex the wavelength resolution can be relaxed (~10%), whereas at larger scattering vectors the wavelength must be defined more precisely (~1%). For the GISANS mode lenses might help to increase the intensity, but the gain is due to only one dimension, which is certainly less than for the conventional SANS mode.

Two tests were performed in the conventional SANS geometry (as described by a and b). The first test of the small detector aimed at the primary beam, in order to get an idea about the minimal scattering vector possible. The second test was done with a diblock copolymer in a lamellar, ordered state. Due to the random orientation of the crystallites the powder-like sample showed a Debye-Scherrer ring. This ring was measured with the large detector and the small detector.

The collimation aperture at 20m distance was opened to 3x3mm^2. The sample aperture was 1x1mm^2. At a detector distance of 20m, the primary beam was measured by the small detector. The primary beam had a FWHM size of 8x8 pixels. Therefore the minimal possible scattering vector is 4 pixels x 0.5mm / 20000mm = 1x10^{-4}Å^{-1}. Since the primary beam simply looks tiny no figures are depicted.

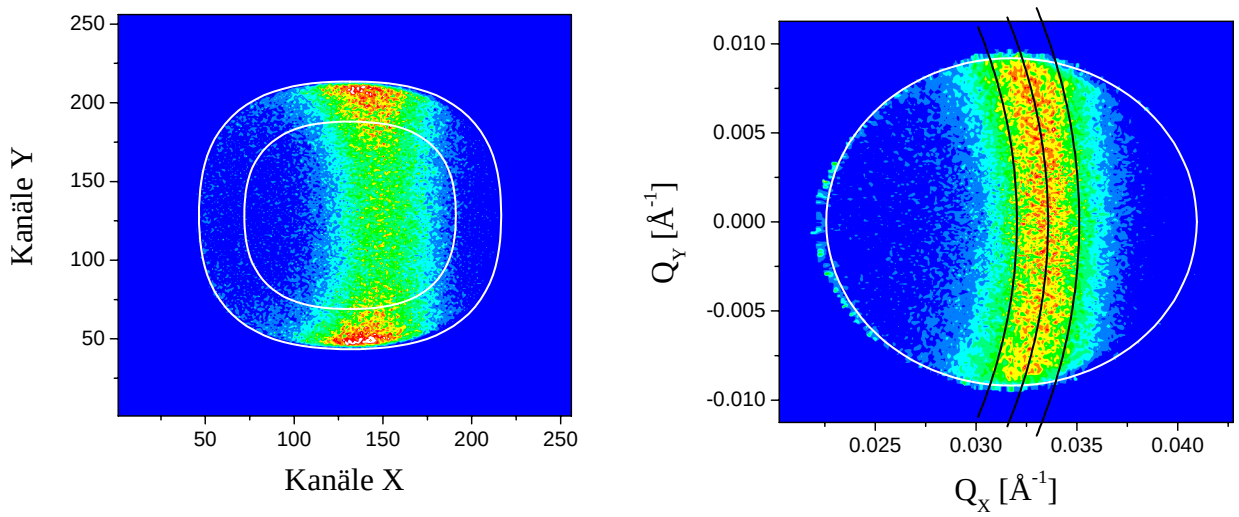


Figure 1: Section of a Debye-Scherrer ring measured with the new small detector. On the left side, the rawdata as obtained is shown. The detector has some square shaped distortions and furthermore the outer regions are compressed to a smaller area in the pixel memory. Therefore, more counts are obtained in the outer regions compared to the centre. The pixels can be mapped quite well on a non-distorted pixel-space as shown on the right hand side. Furthermore, the intensities are corrected by a sensitivity measurement. The final picture shows a section of a Debye-Scherrer ring with a reasonable intensity distribution.

The second test was made with the Debye-Scherrer ring of a diblock copolymer. The small detector was positioned on the right center of the ring as visualized by Figure 1. The obtained rawdata shows two defects of the small detector: (i) The pixels are mapped in a distorted way. Circles appear square like, and the outer regions of the detector are compressed to less pixels than the inner part. (ii) The measured intensity in the compressed outer part appears higher due to this mapping.

The intensity can be corrected by a sensitivity measurement. An incoherent Plexiglas sample scatters homogenously in all directions. The recorded intensity reflects all imperfections intensity-wise. The mapping of the pixels was followed by measuring a tiny primary beam. By moving the primary beam from the center to the outer parts (horizontally, vertically, and diagonally) the distortions of the mapping can be measured. A harmonic distortion with 4 maxima (octopole) was assumed to describe the real distortion. As observed by the corrected Debye-Scherrer ring the corrections seem to work very well. A refined measurement with a pinhole grid is about to show more details.

When comparing the intensity in the azimutally averaged form between the large detector and the small detector, the small detector yields a 10 times higher density of data points. Unfortunately, the resolution of both measured curves is exactly the same. For finite scattering vectors (Q = 0.033Å^{-1}) the resolution is strongly dependent on the wavelength distribution (10%), which could not be varied. Only by a chopper, a time of flight mode would allow to reduce the wavelength distribution to 1%. For the newly upgraded instruments in Munich this chopper is highly desirable.

Thus the new small, high resolution detector is successfully tested. In the ultra small angle mode lowest scattering vectors of 1x10^{-4}Å^{-1} are expected. In the high resolution mode at finite scattering angles a better wavelength resolution is required. The corrections of the distortions of the detector electronics seem to be promising. Thus, the full area of the small detector will be useful to collect as much data as possible. This correction can be transferred to other instruments using the same detector, namely KWS-3, MARIA and TREFF.

Institut für Festkörperforschung
Forschungszentrum Jülich GmbH
D-52425 Jülich

Experimental Report
of Neutron Scattering Experiments
at the FRJ-2 Reactor

Proposal number:	KW2-05-040, KW2-05-050, KW2-06-001, KW2-06-006, KW2-06-013		
Experiment title:	**Confinement Effects of Triblock Copolymers in Bicontinuous Microemulsions – Part I, II, III, IV, V**		
Dates of experiment:	04 - 05.12.2005 28 - 29.01.2006 18 - 20.02.2006 23 - 25.03.2006 08 - 09.04.2006 30.04.2006	Date of report:	10.05.2006
Experimental team: Names	Addresses		
Simona Maccarrone Henrich Frielinghaus	Forschungszentrum Jülich GmbH, Institut für Festkörperforschung, D-52425 Jülich Forschungszentrum Jülich GmbH, Institut für Festkörperforschung, D-52425 Jülich		
Local Contact:	Henrich Frielinghaus		

Experimental report text body

Microemulsions are thermodynamically stable and macroscopically homogeneous mixtures of two otherwise non-miscible components like oil and water, which are mediated by a third component, the surfactant. Microscopically oil and water form domains, the surfaces of which are covered by the amphiphile. For equal volumes of oil and water a minimum amount of surfactant is needed to form a one-phase bicontinuous microemulsion. This amount is a measure for the efficiency of the surfactant.
When adding amphiphilic diblock copolymers to the microemulsion, this macro surfactant molecule is anchored in the surfactant membrane, and the two different blocks are situated in their pleasant environment (Endo). Furthermore, the bending rigidity of the surfactant membrane is increased. This result explains the empirically found polymer boosting effect, which describes a drastic enhancement of the surfactant efficiency. Stiffer membranes allow the formation of larger domains with a better surface to volume ratio. Theories (Lipowsky) agree well with these first studies.
In our latest studies we studied diblock copolymers in microemulsions rendering the domain size d comparable to the polymer size (R_g). At relatively large d/R_g the confinement is weak, and the sensitivity of the polymer boosting effect is unchanged. With increasing confinement (d/R_g closer to 1) the sensitivity is only slightly enhanced, and finally a strongly reversed behaviour (anti-boosting) is observed. The behaviour at medium confinement shows a much lower sensitivity compared with the theory of Auth. This enhancement would have been very interesting for applications, while the reversed behaviour could be an explanation how red blood particles could sneak into small vessels.
The new polymer we studied is an amphiphilic triblock copolymer. This polymer has a hydrophilic mid-block of poly-ethylene oxide and two hydrophobic ends of relatively low molar mass. This polymer is able to anchor

at two points in the membrane (bridging). Choosing different domain d sizes compared to the polymer size (R_g) the bridging should change from connecting neighboured points (quite high d/R_g) to connecting also opposite membrane points (medium d/R_g). At medium confinement an enhanced boosting should be visible. At high confinement (low d/R_g) the anchoring should not play any role anymore and an anti-boosting should be observed.
The domain size was practically changed by the use of different oils (tetradecane, dodecane, decane, octane, hexane) as well as different surfactants were used to span a very wide range of confinement. Three polymer compositions δ were combined with three surfactant compositions γ around the critical point.
The strategy of the experiments was to combine macroscopic observations of the phase behaviour with microscopic measurements of the structure by small angle neutron scattering (SANS). Then both results will be compared on the basis of a common theoretical background. The Helfrich theory describes the elastic properties of the surfactant membrane to be dominating. The bending rigidity κ is the modulus of the mean curvature while the saddle splay modulus $\bar{\kappa}$ is connected with the Gaussian curvature. By SANS the structure of a microemulsion is studied, which can be characterized by the domain spacing d and the correlation length ξ. The Gaussian random field theory connects these two parameters with the bending rigidity κ. The phase diagram measurements can be connected with the modulus $\bar{\kappa}$. At the emulsification failure point (fish tail point, FTP) the spatially renormalized modulus $\bar{\kappa}_R$ is approximately zero, and changes of the surfactant content at the FTP give insight about relative changes of $\bar{\kappa}$ with changing polymer content. Thus two types of measurements can be compared on the basis of the theoretical concept of Helfrich.

Experimentally, we have found three configurational transitions as expected at $d/R_g \approx 2$, 5 and 8 (see figure 1). At high confinement ($d/R_g<2$) from the diblocks already observed reversed behaviour is found. Then at intermediate confinement ($2<d/R_g<5$) an enhanced polymer boosting effect is found. In the next region ($5<d/R_g<8$) the chances of bridging slowly fades away, and finally at very low confinement ($d/R_g>8$) the state is reached where only neighbouring points of the membrane are connected by the polymer. The observed regions are accompanied by other signals of the sensitivity of $\bar{\kappa}$ (not shown here).

All in all, the transition from medium confinement with enhanced boosting to low confinement with an anti-boosting might be very useful in applications. In processes the enhanced emulsification ability might be used in concert with high concentrations, while a separation of oil and water might be of interest after the cleaning process. So here we have found an intelligent polymer additive which reacts on the environment or process stage.

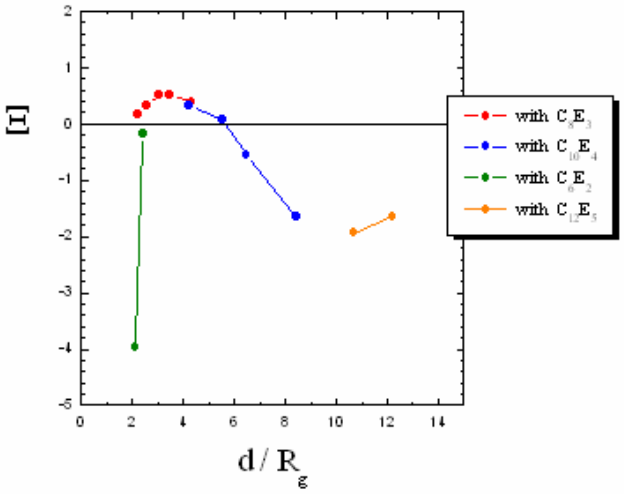


Figure 1: The sensitivity Ξ of the triblock copolymer effect on the bending rigidity as a function of the reciprocal confinement (d/R_g). The different coloured points are obtained by SANS measurements sorted by surfactants used.

Institut für Festkörperforschung
Forschungszentrum Jülich GmbH
D-52425 Jülich

Experimental Report
of Neutron Scattering Experiments
at the FRJ-2 Reactor

Proposal number:	KW2-05-041		
Experiment title:	Polarized neutron measurements of Co nanoparticles in solution		
Dates of experiment:	16.12.2005 - 18.12.2005	Date of report:	20.01.2006
Experimental team: Names	Addresses		
Feygenson Mikhail Pollmeier Klaus Emmanuel Kentzinger Sager Wiebke	IFF-8: Scattering Methods, FZ-Jülich P.O. Box 1913, 52425 Jülich IFF-Soft Matter, FZ-Jülich P.O. Box 1913, 52425 Jülich		
Local Contact:	A. Radulescu		

Experimental report text body

This experiment was the first part of the long–time proposal "Polarized neutron measurements of Co nanoparticles in solution" (KW2-05-041). We performed *non-polarized* small-angle neutron scattering on dodecanethiol-stabilized cobalt nanoparticles in d_8-toluene as preliminary experiment in order to be successfully able to consequently carry out polarized neutrons experiment.

The aim of the experiment was twofold: First, to obtain the scattering cross-section of Co nanoparticles in absolute units to thus be able to estimate the time needed to perform the polarized neutrons measurements. The second aim was to completely characterize the samples prepared. The Co-nanoparticles are originally synthesized by reducing Co^{2+} in a microemulsion medium. To stabilize the particles formed against instantaneous oxidation it is necessary to add dodecanethiol ($C_{12}H_{26}S$) to the microemulsion -as ligand that binds on the particle surface- prior to particle separation. Afterwards the Co-nanoparticles are precipitated by addition of a non-solvent (for the thiol-chain) to the microemulsion followed by centrifugation/filtration and re-dispersion steps to wash the particles free of any microemulsion residues. Finally toluol, which is used as good solvent for the thiol-chains, is evaporated and replaced by d_8-toluene. In this way dissolved thiol might additionally be present in the Co-nanoparticle dispersions and it is difficult to determine the accurate particle concentration. Therefore, we wanted to determine particle size and polydispersity as well as concentration.

To explore the possible concentration range, we investigated two samples (S60 and S61), whereby S61 was approximately 3 times more concentrated than S60 and also of higher purity. All measurements were performed at ambient conditions at a wavelength of 4.5Å. During our beam time, we were only able to measure S60 and S61 within a Q-range of $0.02Å^{-1}$ – $0.15Å^{-1}$ (corresponding to detector distances 2m and 8m, respectively) and S60 in the Q-range of $0.006Å^{-1}$ –$0.05Å^{-1}$. Additionally planed experiments could not be performed, because of a velocity selector problem occurring at the third day. Using a collimation distance of 4m at a detector distance of 2m increased significantly the number of incoming neutrons and thus decreased the measuring time by a factor of about 3. Quartz cells of 1mm were used as sample containers.

The measured scattering curve of sample S60 is presented in Fig.1 together with a simulation in absolute units. The particles display in a shell contrast due to the bound thiol (mono)layer (see inset). We attribute the upper part of the scattering curve to the scattering from Co nanoparticles which interferes at high Q with the scattering

from smaller particles, which might stem from aggregates of protonated dodecanethiol molecules in d_8-tolune. These aggregates are significantly smaller (form factor minimum not seen up to Q=0.15 $Å^{-1}$) than the Co-nanoparticles, but display a better contrast due to the larger difference in scattering length density between protonated dodecanethiol and d_8-toluene compared to cobalt and d_8-toluene. Therefore only small amounts of thiol aggregates can contribute already significantly to the scattering curve. The blue curve is simulated for spherical Co nanoparticles in d_8-toluene in core – shell contrast with a mean size of 9nm and polydispersity of 30%. The green curve shows the simulated contribution form small particles of pronated dodecanethiol with a mean size of 3nm and polydispersity of 14%. The model assumes tabulated values for scattering length densities of all materials in the sample.

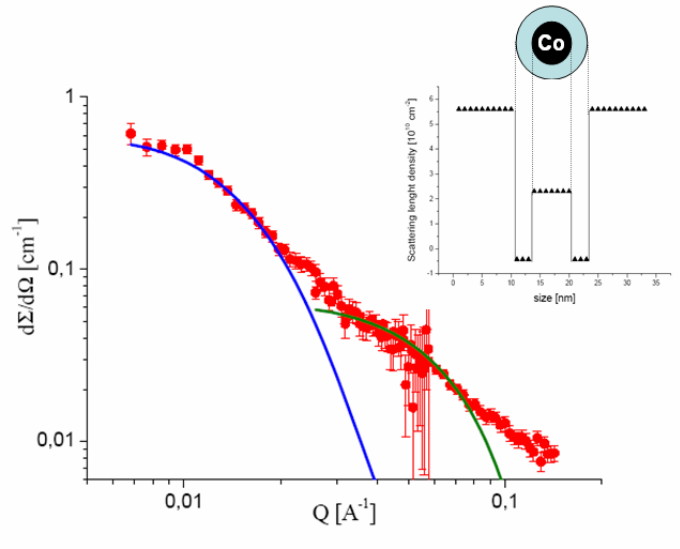


Fig.1.: Cobalt nanoparticles dissolved in d_8–toluene data and simulation. Inset: scattering length density profile of these particles assumed in simulation (blue curve).

In order to determine the increase in scattering intensity by using polarized neutrons the following simulation was performed: Due to the magnetic properties of cobalt the scattering length density increases under saturation conditions for neutrons polarized along the magnetic moments of cobalt (so-called "spin up" state of neutrons). This leads to an increase of the scattering intensity by a factor of 100 (compared with non – polarized neutron scattering) as shown in Fig.2.

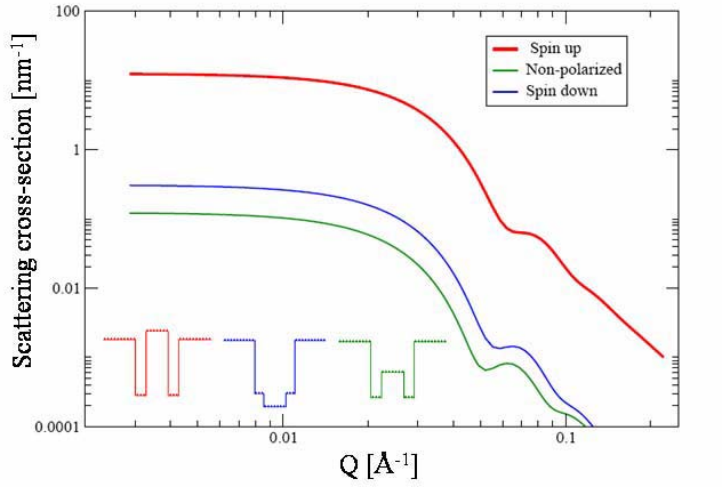


Fig.2.: Simulations of polarized small angle neutron scattering from Co nanoparticles in d_8-toluene. Inset: scattering density profile for spin up polarization, spin down and for unpolarized neutrons.

Based on the polarized neutron simulations and results form earlier reported SQUID measurements, we intend to use a polarized neutron setup for our next beam time at KWS-2. The measurements will be performed at room temperature within a permanent magnetic field of 0.5 T. To additionally increase the scattering intensity we would like to use 2mm quartz cells and to also measure an as high as possible concentrated particle dispersion.

Institut für Festkörperforschung
Forschungszentrum Jülich GmbH
D-52425 Jülich

Experimental Report
of Neutron Scattering Experiments
at the FRJ-2 Reactor

Proposal number:	KW2-05-043		
Experiment title:	**Small-angle neutron scattering of $Co_2Cr_{0.6}Fe_{0.4}Al$ Heusler films**		
Dates of experiment:	6.12.2005-9.12.2005	Date of report:	16.12.2005
Experimental team: Names	Addresses		
Dr. Diana Rata Dr. Emmanuel Kentzinger Dr. Aurel Radulescu Dr. Daniel Buergler	IFF/FZJ IFF/FZJ IFF/FZJ IFF/FZJ		
Local Contact:	Dr. Henrich Frielinghaus, Dr. Aurel Radulescu		

Experimental report text body

We performed small-angle neutron scattering experiments on KWS-2 in order to investigate the magnetic structure, in particular the magnetic domains, of $Co_2Cr_{0.6}Fe_{0.4}Al$ Heusler alloys thin films.

Previous experiments, *e.g.* magnetization *versus* temperature and x-ray magnetic circular dichroism, revealed a reduced magnetic moment compared to the theoretical bulk value. This could be due to atomic disorder (*i.e.* random distribution of Fe, Cr, and Al atoms in the cubic unit cell), which is an intrinsic characteristic of the Heusler compounds. A random distribution (fluctuations) of small magnetic domains could also give a strong decrease of the magnetic moments and of the spin polarization compared to the expected values. Neutron scattering is therefore a method of choice to get access to the domain structure throughout the volume of the Heusler films.

First test measurements were done on a 300 nm thick $Co_2Cr_{0.6}Fe_{0.4}Al$ film grown by magnetron sputtering on SiO_2 substrate. The Heusler films are ferromagnetic with Curie temperatures up to 600 K and magnetically very soft. Therefore, we measured at room temperature and small magnetic fields with unpolarized neutrons. We performed SANS and GISANS measurements at three different sample-to-detector distances, *e.g.* D2, D8, D20, in order to cover the whole Q range accessible with a neutron wavelength of 6 Å.

The most striking feature is the scattering at high Q values, which is characteristic for scattering from ~5 nm diameter clusters in a homogeneous matrix. In Fig. 1, we show the data obtained at C4-D2 for two different magnetic fields: saturating (11 mT) and coercive (6 mT) fields, respectively. This result is encouraging for further investigation.

In order to check whether this scattering is of magnetic origin, we would like to perform scattering of polarized neutrons. If the contrast between clusters and matrix is due to different net magnetizations, different intensities should be observed for + and – neutrons.

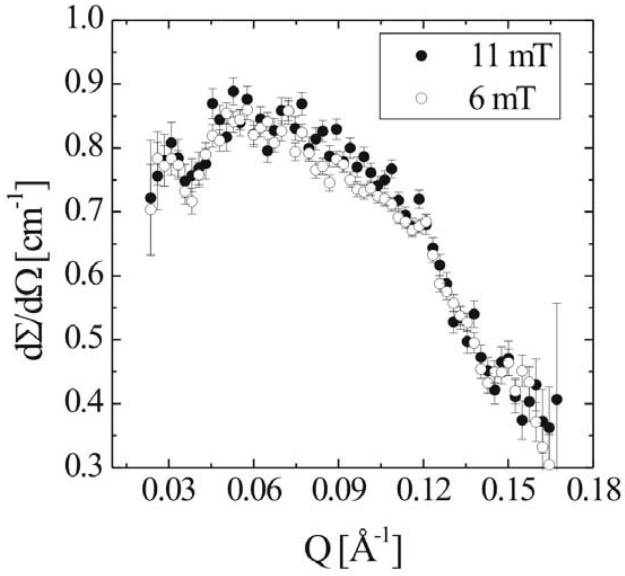


Figure 1. *SANS scattering from a 300 nm thick CCFA film at C4-D2 for 2 different fields.*

Institut für Festkörperforschung
Forschungszentrum Jülich GmbH
D-52425 Jülich

Experimental Report
of Neutron Scattering Experiments
at the FRJ-2 Reactor

Proposal number:	KW2-05-044		
Experiment title:	Structure modification of the multi-segment PEB-n random copolymer aggregates in solution induced by paraffin waxes		
Dates of experiment:	30.11.05-02.12.05	Date of report:	06.06.2006
Experimental team: Names	Addresses		
Aurel Radulescu	Forschungszentrum Jülich Institut für Festkörperforschung D-52425 Jülich Germany		
Local Contact:	Dr.H.Frielinghaus		

Experimental report text body

The self-assembly of poly(co-olefins) in dilute solution has been shown via SANS to yield either plate-like or needle-like micelles-like micelles [1,2]. The resultant supramolecular structures are dependent upon the copolymer architecture. The crystalline-amorphous diblock co-polymers yield self-assembled hairy plates while the corresponding random co-polymers yield one-dimensional needle shaped aggregates. The PEB-n random copolymers (n - the number of ethyl sides per 100 backbone carbons) show selectivity in their wax crystal modification capacities depending on the ethylene content of the backbone. This behavior relates to the graded ethylene content of PEB-n copolymers that leads to different self-assembling temperatures: the lower n, the higher the self-assembling temperature [2]. All PEB-n copolymers self-assemble in open 1-d structures. This conclusion has stimulated further structural studies of multiblock copolymers in solution where blocks represent poly(ethylene-butene) random copolymers (PEB-n) showing graded ethylene contents and thus, different crystallization degrees. Recently [3] conventional and focusing SANS studies of self-assembling in decane solution of a triblock and tetrablock PEB-n copolymers have been performed. The structural results complimented by microscopy observations concluded that these materials form in solution core-shell structures showing a 1D overall aspect which associate and give raise to occurrence of large scale spherulitic-like soft aggregates with sizes within the micrometric range. The conventional SANS investigations have shown that these multiblock copolymers modify the wax crystals morphology from big compact crystals with sizes of hundreds of micrometers as in the case of pure wax solution into 2-dimensional thin aggregates. In the present study we investigated the influence of the wax addition to the structure of the polymer aggregates. We performed at KWS2 instrument systematic SANS measurement of different combinations of waxes and multiblock copolymers for the contrast condition allowing the polymer visible. The solutions have been scanned over a very wide temperature range between the single coil regime and the aggregation regime, at temperatures well below 0°C. The influence of the wax addition to the structure of the polymer aggregates

could be noticed at temperatures below the wax crystallization point, the lower the low wax concentration is. Fig.1 and 2 show the scattering patterns of the two multibock copolymers investigated, the triblock PEB-6.5/8.9/10.1 and the tetrablock PEB-2.6/6.0/10.9/13.2 copolymers in parallel for the polymers alone in solution and mixed with C24 or C36 waxes in common solutions. The modifications of the scattering patterns when waxes are added are obvious. The overall morphology of the polymer aggregates which is characterized by the scattering at low Q does not change and seems to be that of 1-dimensional objects. Nevertheless, at low Q the level of the scattered intensity increases strongly when the wax is added which may lead to a conclusion that changes in either the contrast or the size of aggregates take place. The most evident qualitative changes occur at intermediate and high Q and prove that modification of the intimate structure of the 1D aggregates appear when wax starts to crystallize and interacts with the already formed polymer objects. We may conclude that a modification of the proposed core-shell morphology of the 1D aggregates takes place. A model interpretation of the experimental data is in progress.

References: [1] D.Schwahn et al., Macromolecules 35, 861, 2002; [2] A.Radulescu et al. J.Pol.Sci. B Pol.Phys. 42, 3113, 2004; [3] experimental reports KW2-05-002;KW3-05-001 FRJ-2 Jülich.

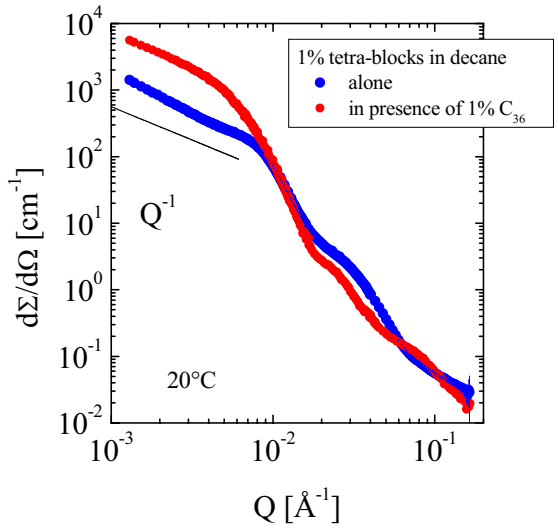


Fig.1 – The tetra-block copolymer scattering patterns when is alone and mixed with the C36 wax in decane.

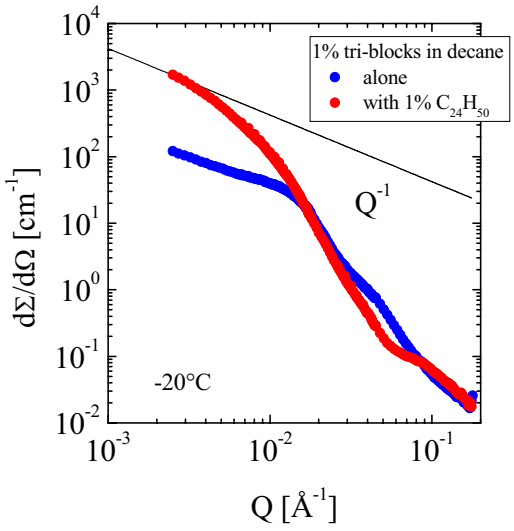


Fig.2 – The tri-block copolymer scattering patterns when is alone and mixed with the C24 wax in decane.

Institut für Festkörperforschung
Forschungszentrum Jülich GmbH
D-52425 Jülich

Experimental Report
of Neutron Scattering Experiments
at the FRJ-2 Reactor

Proposal number:	KW2-05-045		
Experiment title:	**Study of solutions of chitosan and poly(vinyl pyrolidone) in the presence of anionic surfactants**		
Dates of experiment:	08/12/2005	Date of report:	15/12/2005
Experimental team: Names	Addresses		
Gaetano Mangiapia	IFF – Neutronenstreuung, Forschungszentrum Jülich GmbH, D-52425 Jülich Tel. +49 2461 61 6048 (g.mangiapia@fz-juelich.de)		
Local Contact:	H. Frielinghaus		

Experimental report text body

Chitosan [CHT] is a polymer that is currently receiving a great deal of interest for medical and pharmaceutical applications, because of its non-toxicity, the high biodegradability and the capability to form hydrogels potentially usable as carrier for drug delivery applications. Furthermore this substance can be obtained in large quantities and in a very cheaply way, through the deacetylation of an alkaline solution of chitin, a natural compound extractable from crab shell.
The addition of hydrophilic polymers such as poly(vinyl pyrrolydone) [PVP], allow obtaining gels with better features compared to CHT alone. These include reduced irritation, improved film quality, improved flexibility, and enhanced drug dissolution. Blends of CHT with different hydrophilic polymers could thus be promising candidates for formulation in oral mucosal delivery systems.
Our research program is currently devoted to explore the possibility to use CHT/PVP hydrogels as drug delivery systems. The addition of a surfactant, through micelles formation, should allow creating hydrophobic domains whose extension could be modulated at will, useful for embedding lipophilic molecules. Previous SANS investigations on chemical hydrogels formed by CHT in the presence and absence of PVP have been performed (proposal nr. KW2-05-020). Effect of sodium decylsulfate [C10OS] in the gel matrix has also been analyzed, and in all cases no or weak interaction has been observed between the surfactant and the polymer matrix.
In order to get information on eventual interactions occurring among CHT, PVP and C10OS in solution, SANS measurements on the relative systems have been performed. Actually CHT is not soluble in water because of the neutral pH value of H_2O; by increasing the acidity of the system, aminic groups are protonated, and the solubility of the polymer grows up. SANS measurements of PVP in D_2O, in the presence and absence of C10OS have thus been performed.
Figure 1 reports scattering cross sections for PVA (1% wt) in D_2O in the absence and the presence of fully deuterated C10OS [DC10OS]. The inspection of the figure reveals a quite different conformation of PVP, depending on the presence of the surfactant. In the absence of C10OS, PVP can be described in terms of a Gaussian coil conformation, and the Debye equation can be fit to the experimental scattering cross sections $d\Sigma/d\Omega$, obtaining the gyration radius of the polymer R_g (see table 1)

$$\frac{d\Sigma}{d\Omega}(q) \propto \frac{\exp\left(-q^2R_g^2\right)+q^2R_g^2-1}{q^4R_g^4} \qquad (1)$$

On the other hand, conformation of PVP changes in the presence of C10OS. For this system, reported in figure 1, deuterated C10OS in heavy water was used in order to make very small the contrast between the solvent and the surfactant. Finally, to gain structural information on the system, measurements on PVP – C10OS – D_2O

ternary solutions have been performed. In figure 2 is reported one of the spectra obtained; for comparison scattering data collected for the system C10OS–D_2O at the same concentration of the surfactant are also reported. As it is possible to infer from the figure, the existence of a single broad maximum indicates the presence of aggregates with significant intercorrelations. The position of the maximum in $d\Sigma/d\Omega$ occurs at different values of the scattering vector modulus q, indicating different correlation distances in the two systems, i.e. the presence of micellar clusters in the ternary system bound onto the polymeric chains.

All data shown in figure 2 have also been analyzed quantitatively. Table 1 reports values obtained for C10OS micelles in D_2O: micelles have been modeled as charged prolate ellipsoids. From the fitting it has been possible to extract the micellar aggregation number N_{agg}, the actual charge z, the major and minor semiaxis of the hydrophobic core a and b, and the thickness of the hydrophilic shell δ. By neglecting scattering from PVP chains, it has also been possible to have information on the clusters, reported in table 1; in the analysis clusters have been treated as charged spherical objects ($a = b$), and the volume fraction of the polymer penetrated inside the micellar hydrophilic shell ϕ_{PVP} has been evaluated.

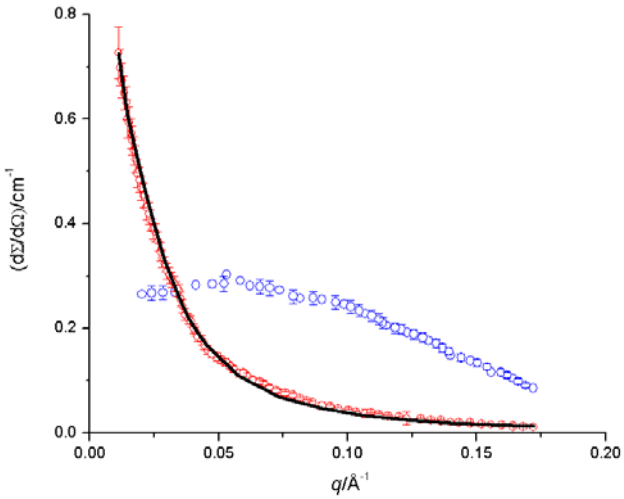


Figure 1 – Scattering cross sections obtained at 25°C for PVP (1%) in the absence (–) and in the presence (–) of DC10OS (0.08 mol kg^{-1}) in D_2O. For the first system, curve obtained from the fitting of the model described in the text is also reported.

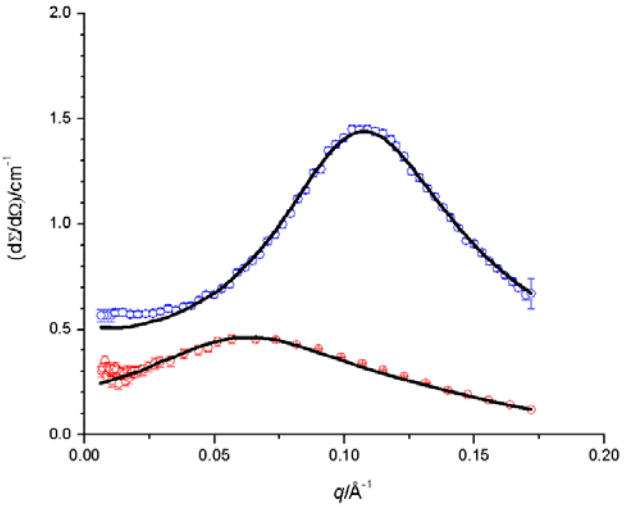


Figure 2 – Scattering cross sections obtained at 25°C for C10OS (0.08 mol kg^{-1}) in the absence (–) and in the presence (–) of PVP (1%) in D_2O. Curves obtained from the fitting of the model described in the text are also reported.

	R_g/Å	N_{agg}	z	a/Å	b/Å	δ/Å	ϕ_{PVP}
PVP	62±3	–	–	–	–	–	–
C10OS	–	50±4	-25±3	17.1±0.4	14.1±0.5	4.5±0.9	–
PVP – C10OS	–	30±2	-20±2	12.5±0.5	12.5±0.5	3.7±0.4	0.25±0.06

Table 1 – Structural parameters obtained for PVP, C10OS, and PVP/C10OS solutions in D_2O. In all the systems containing C10OS, the concentration of surfactant is 0.08 mol kg^{-1}.

Institut für Festkörperforschung
Forschungszentrum Jülich GmbH
D-52425 Jülich

Experimental Report
of Neutron Scattering Experiments
at the FRJ-2 Reactor

Proposal number:	KW2-05-048		
Experiment title:	**Small-angle neutron scattering of $Co_2Cr_{0.6}Fe_{0.4}Al$ Heusler films**		
Dates of experiment:	15.03.2006 – 17.03.2006	Date of report:	31.05.2006
Experimental team: Names	Addresses		
Dr. Diana Rata Dr. Emmanuel Kentzinger Dr. Aurel Radulescu Dr. Daniel Buergler	Institut für Festkörperforschung, Forschungszentrum Jülich Institut für Festkörperforschung, Forschungszentrum Jülich Institut für Festkörperforschung, Forschungszentrum Jülich Institut für Festkörperforschung, Forschungszentrum Jülich		
Local Contact:	Dr. Henrich Frielinghaus, Dr. Aurel Radulescu		

Experimental report text body

We performed small-angle neutron scattering experiments on KWS-2 in order to investigate the magnetic structure, in particular the magnetic domains, of $Co_2Cr_{0.6}Fe_{0.4}Al$ Heusler alloys thin films.

Previous experiments, *e.g.* magnetization *versus* temperature and x-ray magnetic circular dichroism, revealed a reduced magnetic moment compared to the theoretical bulk value. This could be due to atomic disorder (*i.e.* random distribution of Fe, Cr, and Al atoms in the cubic unit cell), which is an intrinsic characteristic of the Heusler compounds. A random distribution (fluctuations) of small magnetic domains could also contribute to the reduction of the magnetic moment and of the spin polarization, which is predicted to be 100% [1]. Neutron scattering is therefore the method of choice to get access to the domain structure throughout the volume of the Heusler films.

Small-angle neutron scattering experiments were done on 300 nm thick $Co_2Cr_{0.6}Fe_{0.4}Al$ films grown by magnetron sputtering on SiO_2 substrate at room temperature. The Heusler films are ferromagnetic with Curie temperatures up to 600 K and magnetically very soft [2]. Therefore, we measured at room temperature and small magnetic fields with unpolarized neutrons. We performed SANS measurements at two different sample-to-detector distances, *e.g.* D2 and D4, in order to cover the whole Q range accessible with a neutron wavelength of 4.5 Å.

Two interesting effects were observed in this experiment. Firstly, a clear magnetic field dependence of the scattering intensity was detected. In Figure 1, we show the data obtained at C8-D2 for three different magnetic fields: saturating (11 mT), coercive (6 mT) fields and zero field, respectively.

Secondly, a striking feature is the scattering at high Q values, which is characteristic for scattering from approximately 6 nm diameter clusters in a homogeneous matrix. Further investigation, using polarized neutrons, is needed in order to explain the origin of these effects. Small magnetic domains having a different net magnetization than the host matrix should give different intensities for + and – neutrons.

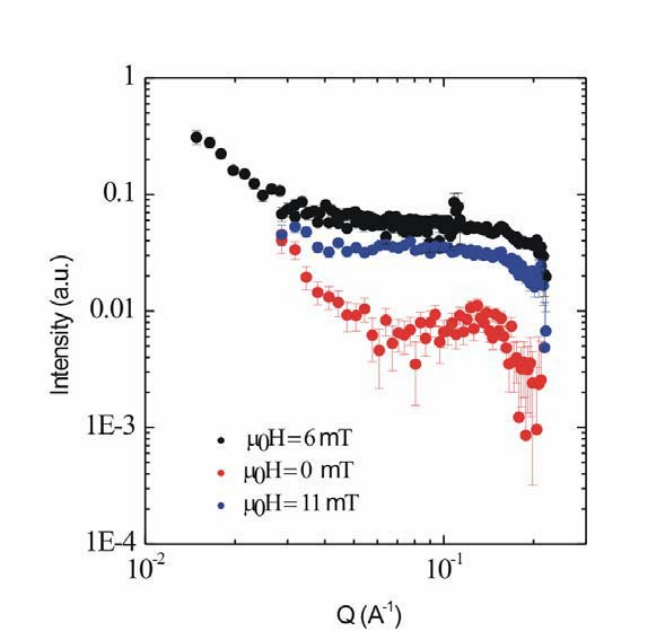


Figure 1. *SANS scattering from a 300 nm thick CCFA film at C8-D2 for 3 different fields.*

References:

[1] I. Galanakis, P. H. Dederichs, and N. Papanikolaou, Phys. Rev. B **66,** 174429 (2002).
[2] A.D. Rata, H. Braak, D.E. Bürgler, S. Cramm, and C.M. Schneider, cond-mat/0603649.

Institut für Festkörperforschung
Forschungszentrum Jülich GmbH
D-52425 Jülich

Experimental Report of Neutron Scattering Experiments at the FRJ-2 Reactor

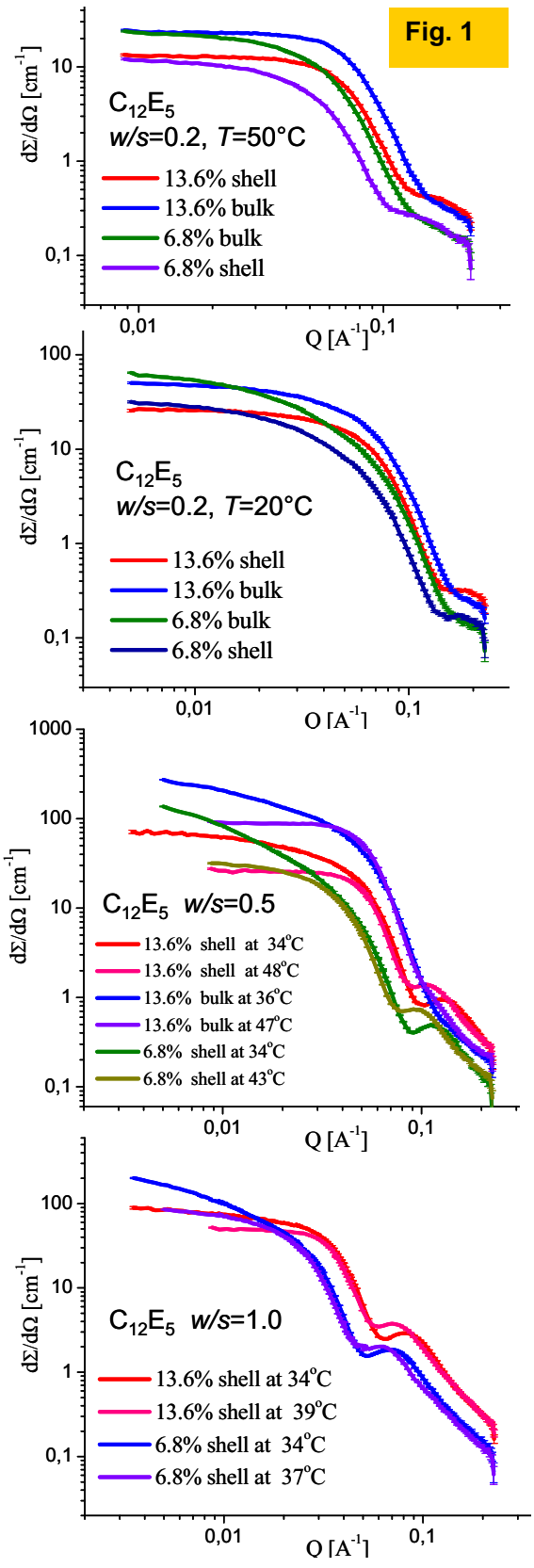
Proposal number:	KW2-05-052		
Experiment title:	Characterization of nonionic w/o microemulsions stabilised by nonionic (and ionic) surfactants as precipitation media for the synthesis of $BaCO_3$ nanoparticles.		
Dates of experiment:	16.01. – 17.01.2006 25.02. – 26.02.2006 08.03. – 09.03.2006	Date of report:	19.06.2006
Experimental team: Names	Addresses		
W.F.C. Sager M. Feygenson	IFF-Soft Matter, FZ-Jülich P.O. Box 1913, 52425 Jülich IFF-8: Scattering Methods, FZ-Jülich P.O. Box 1913, 52425 Jülich		
Local Contact:	A. Radulescu		

Experimental report text body

In 2003 we started an extended study on understanding crystallization processes of $BaCO_3$ nanoparticles in water-in-oil (w/o) microemulsions stabilized by nonionic surfactants only or mixtures of nonionic and ionic surfactants. Emphasis was first laid on investigating how far adjusting the compositions and precipitation conditions of the parental microemulsion precursors can be utilized to control the crystal structure, to tune particle morphology and to regulate particles aggregation processes. To be able to gain consistent ideas about the formation of the $BaCO_3$ nanoparticles in microemulsions of different structure and exchange kinetics, we want to map the $BaCO_3$ nanocrystals of different morphology onto a more generalized microemulsion structure landscape. For this we have to characterize both the nanoparticles formed by transmission electron microscopy (TEM) as well as the parental microemulsions by small angle scattering (SAS).

Since we found that using the two nonionic surfactants Igepal and $C_{12}E_5$, a large variety of different nanostructures with well-defined morphologies can be obtained ranging from amorphous filaments, cube and disc shaped meta-stable nanocrystals to witherite type rhombohedral nanocrystals, nanoplatelets, nanoneedles and (ordered) hexagonal nanorods as well as to nanofibres and bundles, it is of special interest to analyse the relationship between microemulsion morphology and particle formation kinetics for the microemulsions employed as precipitation medium.

During our allocated 3 beam times at KWS2 from January to March, 2006, we completed the temperature series started in 2005 for the Igepal and $C_{12}E_5$ stabilised microemulsions as function of salt concentration (0.1-0.3M salt) and water-to-surfactant ratio ($0.1 \leq w/s \leq 1$). For nonionic surfactants one expects a microemulsion droplet-to-cylinder transition within the one-phase microemulsion region with decreasing temperature and increasing w/s value. To analyse the data recorded we need to adapt the 2-component model for spheres and cylinders, developed earlier for the analysis of scattering curves of AOT stabilized microemulsions [1]. In the case of the nonionic microemulsions, the monomer solubility of the surfactant depends strongly on temperature, which leads to an increase in the droplet radius with increasing temperature. Furthermore we found that the cylinder length depends significantly on the temperature and that especially at $w/s > 0.2$ the low Q part of the



scattering curves is dominated by the structure factor. To obtain the missing information we measured the salt free microemulsions for $C_{12}E_5$ and Igepal at different contrast (bulk and shell) and at lower surfactant concentration and thus lower concentration of the dispersed phase (water and surfactant). These measurements were performed to obtain the necessary information about the thickness of the surfactant layer surrounding the water pools and a better insight into droplet-droplet and droplet-cylinder interactions.

Fig. 1 displays the scattering curves measured for the $C_{12}E_5$ system at *w/s* values of 0.2, 0.5 and 1.0 with only water as aqueous phase at surfactant concentrations of 6.8% and 13.6%. For the shell contrast measurements a mixture of D_20 and H_2O possessing the same scattering length density as the deuterated oil (continuous phase) was used, while for the bulk contrast measurements the scattering length density of the water phase was matched to the one of $C_{12}E_5$. Since the phase boundaries of the one-phase region depend on the kind and amount of deuterated compound used and the amount of surfactant, *Fig. 1* shows the scattering curves for the highest and lowest possible temperature within the one-phase region for each microemulsion measured. It can clearly be seen that the structure factor becomes important at the *w/s*≥0.5 and that significant amounts of longer cylinders are only formed at the higher *w/s*. At *w/s*=0.2 the dominant contribution to the scattering curves comes from spherical droplets. All *w/s* values studied show a shift of the scattering curves to smaller *Q* for the lower surfactant concentration. Since the monomer surfactant concentration depends only on the temperature, less surfactant is available at lower total surfactant concentration that is situated at the interface between the water and oil domains and thus the radii of droplets and/or cylinders become larger. At *w/s*=1.0 the 1/*Q*-dependence of the cylinder form factor is strongly depressed by the structure factor.

Besides the pure nonionic systems, we also started to study microemulsions stabilized by mixtures of one of the two nonionic surfactants and the ionic AOT (sodium di(2-ethyl hexyl)sulfosuccinate. For salt concentrations of 0.3 M we found that upon addding AOT to Igepal stabilized microemulsions by keeping the total amount of surfactant constant the sphere↔cylinder coexistence shifts to the sphere side. While for the pure Igepal microemulsion only long cylinders are observed at low temperature, 50% of AOT is sufficient to transform all cylinders into spherical droplets.

[1] D.I. Svergun, P.V. Konarev, V.V. Volkov, M.H.J. Koch, W.F.C. Sager, J. Smeets, and E.M. Blokhuis, J. Chem. Phys. 113, 1651 (2000).

Institut für Festkörperforschung
Forschungszentrum Jülich GmbH
D-52425 Jülich

Experimental Report
of Neutron Scattering Experiments
at the FRJ-2 Reactor

Proposal number:	KW2-06-002		
Experiment title:	**Relating rheology and structural changes using Rheo-SANS**		
Dates of experiment:	14.02. - 18.02. 2006	Date of report:	06.06.2006
Experimental team: Names	Addresses		
J. Stellbrink B. Lonetti	IFF, FZ Jülich, D-52425 Jülich, Germany IFF, FZ Jülich, D-52425 Jülich, Germany		
Local Contact:	J. Stellbrink		

Experimental report text body

We investigated the phase behaviour of star-like micelles formed by the amphilic block copolymer poly(ethylenepropylene)-poly(ethyleneoxide), $M_{w,PEP}$= 1000 g/mol, $M_{w,PEO}$= 20000 g/mol, in different water/dimethylformamide mixtures by small angle neutron scattering (SANS) [1, 2] and partly by light scattering and rheology. Changing the solvent composition changes the aggregation number (or functionality), f, of the micelles due to changes in the interfacial tension between the core-forming, hydrophobic PEP and the solvent. This enabled us to construct the experimental equilibrium phase diagram in the packing fraction (η) / functionality (f) representation and compare it to theoretical predictions for regular star polymers. One important feature of the star polymer phase diagram is a re-entrant melting, i.e. a fluid-crystal-fluid transition, which should occur in a limited region of functionalities. This transition is predicted by theory, but until now only little experimental evidence was found.

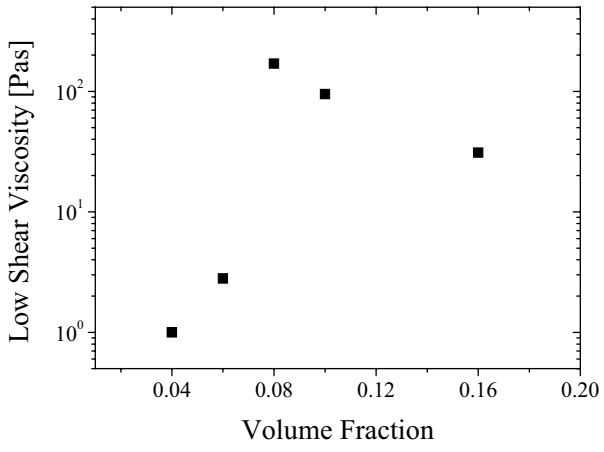


Figure 1: Concentration dependence of the low shear viscosity for star-like micelles.

In our recent rheology experiments on concentrated micellar solutions we observed an anomalous concentration dependence of the viscosity indicating a fluid-solid-fluid transition, see fig. 1. Additional SANS experiments in the same concentration range corroborated this phenomenon with respect to the anomalous concentration dependence of the structure factor peak. We interpret this as an indication for the predicted re-entrant melting and tried to further elaborate these results by supplementary Rheo-SANS experiments to relate in-situ viscosity to microscopic structure.

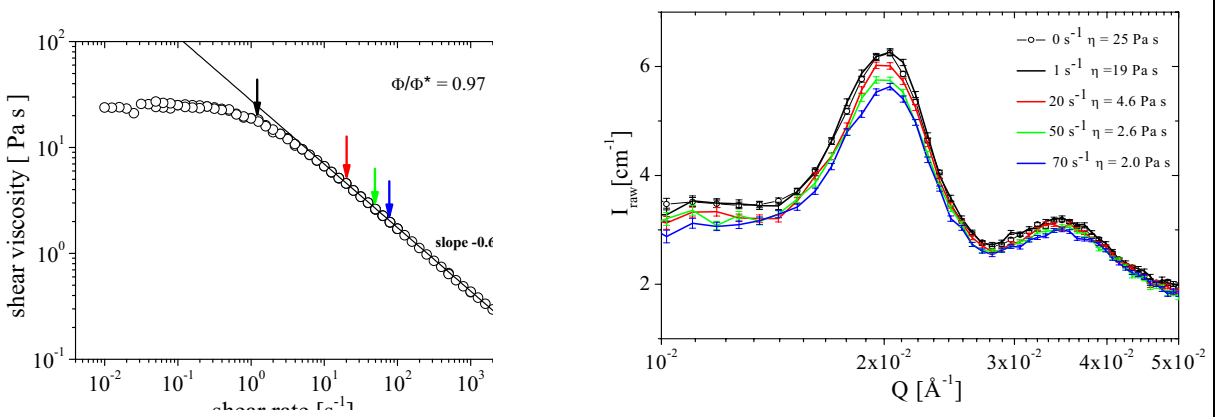


Figure 2: Flow curve (left) and SANS intensity (right) for a micellar solution of volume fraction Φ=0.08 (corresponding to 0.97c*).

Figure 2 compares the structure factor S(Q) obtained by Rheo-SANS to the corresponding the flow curve for a micellar solution at a volume fraction Φ=0.08 (corresponding to 0.97 Φ^*, with Φ^* the overlap concentration). The flow curve, i.e. the dependence of the shear viscosity η on shear rate $\dot{\gamma}$, shows a strong decrease of η with increasing $\dot{\gamma}$ (approximately 2 orders of magnitude). This gives a limiting power law $\eta \sim \dot{\gamma}^{-0.6}$ in the high shear rate regime. In the microscopic SANS level, on the other hand, only minor changes are observed. In the Rheo-SANS experiments performed in steady shear, the height of the main structure factor peak decreases only slightly with increasing $\dot{\gamma}$. This indicates a loss of local order, but the peak position, i.e. the characteristic particle distance, remains nearly unchanged. Also in oscillatory shear (amplitude sweep) no effects were visible in the SANS data. Therefore a decoupling of the microscopic structure of the sample from its macroscopic flow properties is observed.

References:

1. R. Lund, L. Willner, J. Stellbrink, A. Radulescu and D. Richter, *Macromolecules*, **37**, 9984, 2004.
2. M. Laurati, J. Stellbrink, R. Lund, L. Willner, D. Richter, and E. Zaccarelli, *Phys. Rev. Letters*, **94**, 195504, 2005.

Institut für Festkörperforschung
Forschungszentrum Jülich GmbH
D-52425 Jülich

Experimental Report
of Neutron Scattering Experiments
at the FRJ-2 Reactor

Proposal number:	KW2-06-003		
Experiment title:	**Test of the small detector – 2nd part.**		
Dates of experiment:	13.02.2006	Date of report:	09.05.2006
Experimental team: Names	Addresses		
Henrich Frielinghaus	Forschungszentrum Jülich GmbH, IFF, D-52425 Jülich, Germany		
Local Contact:	Henrich Frielinghaus		

Experimental report text body

In this following work to the first proposal KW2-05-039 now a grid is measured in front of the homogenously irradiated detector. This measurement displays the distortions of the detector best, and thus is a hardcore test for the corrections developed for this kind of detector.

As visualized in Figure 1 the irradiated area of the detector appears almost squared although the real area is a circle. The grid points close to the corners appear distorted most when compared to the ideal theoretical grid (indicated in black). The effect of the corrections is displayed in Figure 2. The area of the detector appears bigger and is much closer to a circular shape. All grid points lie much closer on the ideal grid. Nonetheless, some distortions remain, and individual lines of the grid randomly deviate from the theoretical lines. These remaining distortions cannot be treated by a simple mathematical formula. If such distortions shall be corrected in the future one has to triangulate the detector area, and force the originally measured grid on the ideal theoretical grid. The stability of such fine-tuning has to be tested.

All in all, a large step has been done towards the full adoption of the new, small, high resolution detector at the two SANS instruments in Munich.

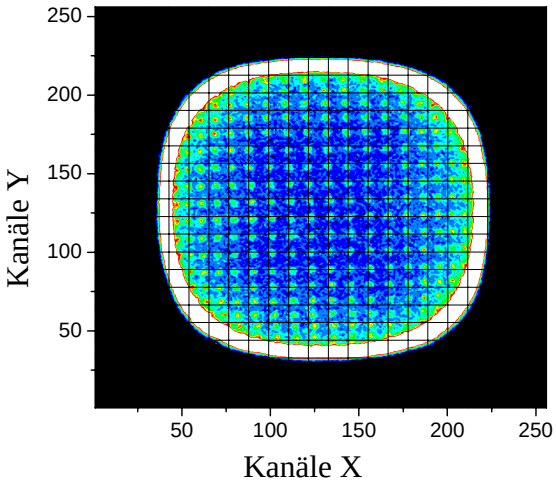


Figure 1: The untreated measurement of a grid in front of the small detector. The grid was homogenously illuminated. One can see the distortions especially at the corners of the irradiated area.

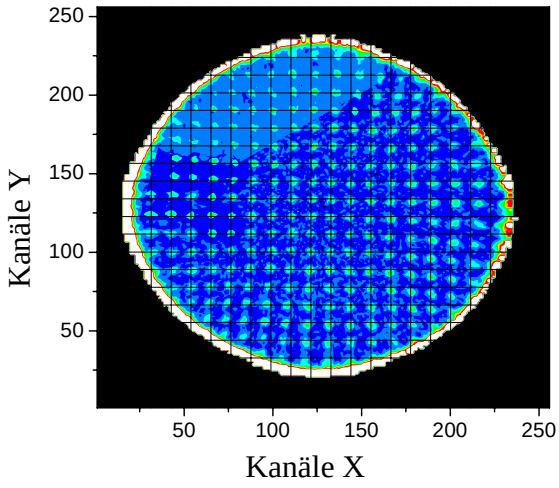


Figure 2: The corrected measurement of a grid. The grid holes are much more regular compared to the theoretical grid in black. Nonetheless some distortions remain, which might be corrected in the future.

Institut für Festkörperforschung
Forschungszentrum Jülich GmbH
D-52425 Jülich

Experimental Report
of Neutron Scattering Experiments
at the FRJ-2 Reactor

Proposal number:	KW2-06-004		
Experiment title:	Self-assembling in solution of alternating copolymers of vynil-tetramethylene (VTM) and methylenecyclopentane (MCP)		
Dates of experiment:	13.02.06 – 16.02.06	Date of report:	29.05.06
Experimental team: Names	Addresses		
Aurel Radulescu	Forschungszentrum Jülich Institut für Festkörperforschung D-52425 Jülich Germany		
Lewis J.Fetters	School of Chemical Engineering, Cornell University, Ithaca, NY 14853 USA		
Local Contact:	Dr.H.Frielinghaus		

Experimental report text body

Cycloolefin copolymers represent a class of thermoplastic materials of growing interest, with mechanical and physical properties ranging from those of amorphous glasses to those of thermoplastic elastomers. One of the problems of poly(cyclic olefins) is their high melting point T_m and glass transition temperature T_g, which are close to the decomposition temperatures of the polymers. Recent advances in catalyst systems for living olefin polymerization have made possible to synthesize polyolefin-based block copolymers with precisely controlled molecular weight, molecular weight distribution and tacticity. Recently [1], the interest in preparing polyolefin-based materials with an improved thermal properties led to the synthesis of a random copolymer with 1,3-ethylenecyclopentene (MCP) and 3-vyniltetramethylene (VTM) units by polymerization of 1,5-hexadiene. Two such materials generically called RTM4-34 and RTM4-80 were for the first time investigated in solution by SANS in order to obtain information about the radius of gyration R_G of the polymer coils, the molecular weight M_W and the virial coefficient A_2. For this purpose we investigated different polymer concentrations in dodecane at 30°C by using the KWS2 instrument. Fig.1 presents the scattering cross sections of RTM-34. From the analysis of the scattering cross-sections in terms of the Zimm approximation [2]

$$S(Q)^{-1} = \left[\frac{d\Sigma}{d\Omega}(Q)K\right]^{-1} = \frac{1}{V_w\Phi} + 2A_2 + LQ^2$$

the R_g and the forward scattering *S(0)* have been evaluated. Further analysis of the inverse forward scattering as a function of the inverse polymer concentration $1/\Phi$ provided the molar volume V_w and the virial coefficient A_2. Fig.2 presents the Zimm plot of the scattering cross sections and in the inset the evaluation of the V_W and A_2. The experimental scattering patterns have been well described by the Beaucage form factor [3] using the parameters evaluated by Zimm analysis as is revealed by the fits in Fig.1 (red curves).

The radii of gyration R_G were roughly about 160Å and 155Å while the evaluated molecular weight M_W was about 70K and 33K for RTM4-34 and RTM4-80, respectively.

References: [1] R.T.Mathers and G.W.Coates, Chem.Commun. 422, 2004; [2] A.Radulescu et al., J.Pol.Sci. B 42, 3113, 2004; [3] G.Beaucage, J.Appl.Cryst. 29, 134, 1996.

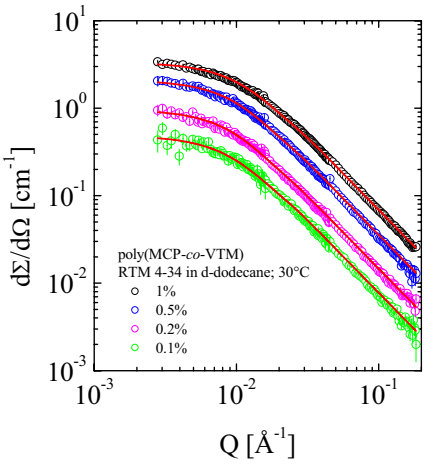


Fig.1 – The scattering cross sections of the RTM4-34 material in dodecane for different polymer concentrations. The red curves represent fits of the experimental data in terms of the Beaucage form-factor.

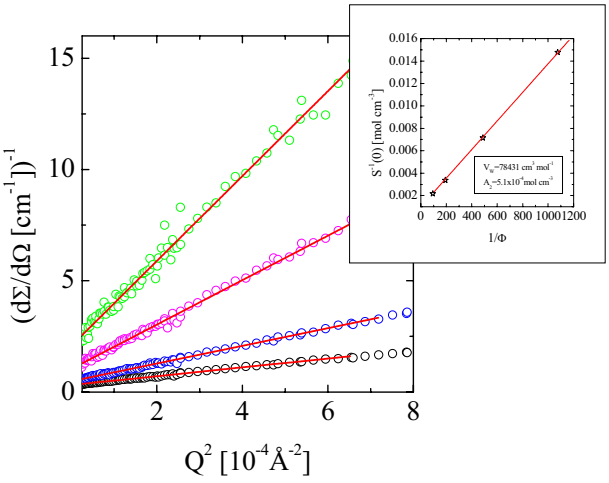


Fig.2 – Zimm plot of the data from Fig.1 and the analysis of the forvard scattering providing the molar volume V_W and virial coefficient A_2.

Institut für Festkörperforschung
Forschungszentrum Jülich GmbH
D-52425 Jülich

Experimental Report
of Neutron Scattering Experiments
at the FRJ-2 Reactor

Proposal number:	KW2-06-005		
Experiment title:	**High resolution polarized GISANS on a polarizing supermirror**		
Dates of experiment:	07.02.-12.02.2006	Date of report:	14.06.2006
Experimental team: Names	 Addresses		
E. Kentzinger H. Frielinghaus Th. Brückel	Institut für Festkörperforschung, Forschungszentrum Jülich Institut für Festkörperforschung, Forschungszentrum Jülich Institut für Festkörperforschung, Forschungszentrum Jülich		
Local Contact:	H. Frielinghaus		

Experimental report text body

As mentioned in report KW2-05-033, polarized GISANS was measured on a remanent polarizing supermirror at C8-D3. The GISANS signal from roughness correlations was well resolved. However, the GISANS signal from magnetic correlations was not well resolved from the Q resolution along the y direction. We present here a tentative to study the magnetic correlations using a longer collimation length and a longer sample-to-detector distance than before, namely C14-D14.

The measurements were performed using the same set-up as the one presented in report KW2-05-032. In Fig.1 we show an example of such a measurement, performed in a field of +5.5 mT after having saturated the sample in a negative magnetic field and at an angle of incidence of the neutrons $\alpha_i = 0.2°$. In both spin channels one observes at $\alpha_i + \alpha_f = 0.4°$ the specular reflection peak In the spin-up channel, a peak, well resolved from the Qy resolution, is observed at $\alpha_i + \alpha_f = 0.85°$ (i.e. at $\alpha_f = 0.65°$). It can be correlated with the enhancement of the off-specular scattering measured in the spin flip I+- channel at HADAS at $\alpha_i = 0.2°$ and around $\alpha_f = 0.65°$ (see Fig.2). This peak then originates from the scattering by magnetic correlations. From the width of the peak, much bigger the width of the Q_y resolution function (given by the Q_y width of the specular reflection), we deduce a lateral correlation length of the magnetic correlations equal to 300 nm.

In Fig.2 the range of positive α_f values that can be reached at the chosen sample-to-detector distance is depicted by red vertical lines. As can be seen it does not cover the whole range of α_f values where magnetic off-specular scattering is observed. Moreover, this range gets smaller as the angle of incidence α_i is increased. It therefore does not allow figuring out whether a depth dependency of the magnetic correlation length exits.

This issue is a quite general one at a SANS machine: when one wants to measure with a good resolution in wave vector transfer Q, the detector has to be brought far away from the sample, limiting therefore the range of accessible Q-values. At FRM-II, in order to measure high resolution GISANS at relatively high Q_z values, two ways will be probed:

1) Install a high resolution detector (HADAS-type) and reduce the wavelength resolution $\Delta\lambda/\lambda$ (by installing a chopper) on KWS-1.
2) Perform GISANS on KWS-3, using a good resolution along Q_y and a relaxed resolution along Q_z (entrance aperture small along the horizontal direction, large along the vertical one).

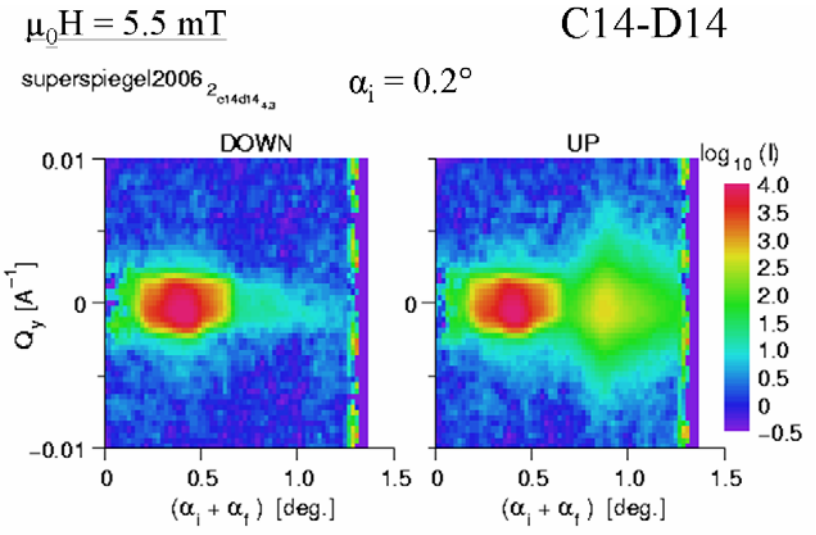


Fig.1: Polarized GISANS signal measured at C14-D14 on a remanent polarizing supermirror. Counting time: 23 minutes per spin channel.

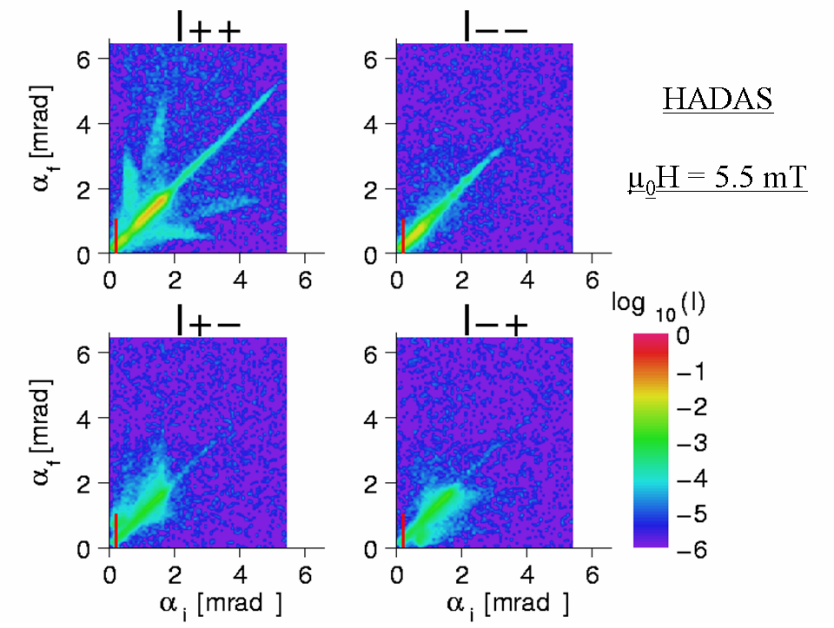


Fig.2: Off-specular scattering of polarized neutrons with polarization analysis measured at HADAS on the same supermirror as above and at the same applied magnetic field $\mu_0 H$.

Institut für Festkörperforschung
Forschungszentrum Jülich GmbH
D-52425 Jülich

Experimental Report
of Neutron Scattering Experiments
at the FRJ-2 Reactor

Proposal number:	KW2-06-008, KW2-06-014		
Experiment title:	**Bicontinuous microemulsions in presence of a sticker polymer with an ionic end group – part I, II**		
Dates of experiment:	20.03.2006 – 22.03.2006 7.4.2006	Date of report:	11.05.2006
Experimental team: Names	Addresses		
Martin Brodeck Henrich Frielinghaus	Forschungszentrum Jülich GmbH, Institut für Festkörperforschung, D-52425 Jülich Forschungszentrum Jülich GmbH, Institut für Festkörperforschung, D-52425 Jülich		
Local Contact:	Henrich Frielinghaus		

Experimental report text body

Monofunctional sticker polymers have successfully been investigated in earlier measurements (KWS2-05-019). A strong efficiency boosting was found . These sticker polymers consisted of an oil-soluble sticker (several carbon atoms) and a water-soluble polymeric chain. The question is wether a sticker polymer with a water-soluble sticker and an oil-soluble polymeric chain shows the same behaviour regarding the influence on the bending rigidity κ. Two different polymers with an ionic sticker have been investigated. The first of the two, COOH(t-butylacrylte), has an inonic sticker with approximately 50 water-soluble monomers. The second one, monocarboxy terminated polybutadiene, is made up of about 185 monomers. Carboxylic acid forms the sticker of the polymer. Therefore to anchor the sticker to the water-phase NaOH has to be added to the system. The carboxylic acid will dissociate in an alkaline environment. Three different allocations of NaOH and four different polymer concentrations (δ=0%, 3%, 6%, 10%) have been investigated for the first polymer. For the second polymer with the longer chain only one concentration of NaOH has been studied. Changing the concentration of NaOH will influence the amount of polymers that are able to attach to the interface.
To prepare the neutron scattering experiments phase diagram studies have been conducted on both polymers. In these measurements the phase behaviour is determined depending on the amount of surfactant and the temperature of the system. The minimum amount of surfactant needed to emulsify the system, γ_{ftp}, can then be extracted from the temperature vs. surfactant plot. This point, the so-called fish tail point, describes the efficiency of the polymer. Increasing the amount of polymer will decrease the minimum amount of surfactant needed to dissolve all available oil and water. The first of the two investigated polymers shows a relatively small boosting effect, which is probably due to the too short polymer chain. Therefore the second polymer with a longer water-soluble chain has been investigated. This polymer showed a stronger boosting effect, comparable to the efficiency of the polymer with oil-soluble sticker investigated earlier ($C_{12}E_{100}$).

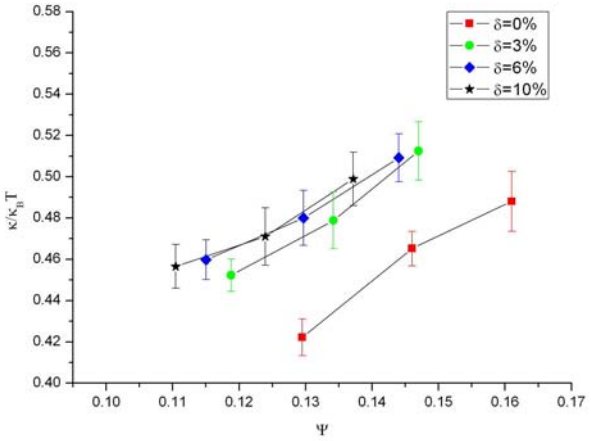


Figure 1: At pH 11.2 there are just enough Na^+-ions to anchor a polymer amount of δ=3% to the interface. Adding more polymer has almost no effect on the bending rigidity κ.

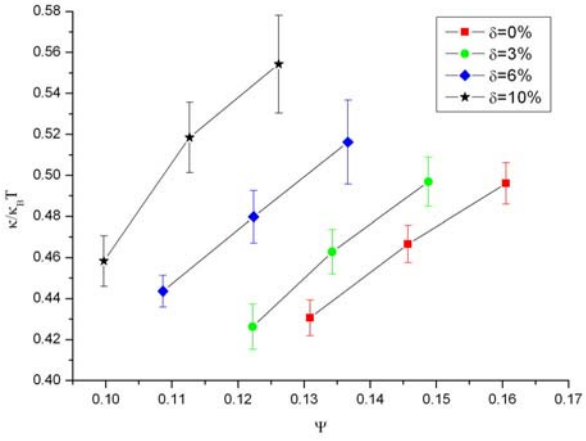


Figure 2: After an increase of the NaOH particles in the system the bending rigidity responses to an increased polymer amount of up to δ=10%.

The second information extracted from the phase diagram is the change of the spontaneous curvature c_0. Due to the unsymmetric polymer the change of the spontaneous curvature is balanced by a change of the temperature of the fish tail point. Both polymers behaved as expected with a decreased temperature.

The macroscopically determined phase diagram is connected to microscopically defined parameters of the Helfrich model. The model assumes the elastic properties of the surfactant film to be dominant in the free energy of the microemulsion. The three important parameters are the spontaneous curvature c_0, and two elastic moduli, namely the bending rigidity κ and the saddle splay modulus $\bar{\kappa}$. The spontaneous curvature decreases with increasing temperature and increases with increasing sticker polymer amount. At the fish tail point the spontaneous curvature is zero, so the two contributions are balanced. The elastic moduli are spatially renormalized parameters with a logarithmic dependence on the surfactant amount. The absolute values of the elastic moduli increase with increasing polymer amount. At the fish tail point the saddle splay modulus is a negligible constant, and so the renormalization is balanced with the polymer term. This balance leads to an exponential dependence of the minimal surfactant amount with respect to the scaled polymer amount.

To obtain the bending rigidity κ with small angle neutron scattering the bulk constrast has been chosen. With the Teubner-Strey-formula the domain size *d* and correlation length ξ can be extracted from the scattering patterns. The Gaussian random field theory is used to obtain the bending rigidity from these structural parameters. Figures 1 and 2 show the dependence of the bending rigidity on the surfactant amount ψ. Three surfactant amounts in the one phase region have been measured for every polymer concentration. This makes it possible to extract the bending rigidity for one surfactant concentration by extrapolating the data.

For the lowest concentration of NaOH (pH 11.2) only δ=3% of the polymer had the possibility to anchor to the interface. Further increasing the amount of polymer to δ=6% and δ=10% does not influence the bending rigidity κ any more. The polymer floats in the oil phases and the sample looks dim. Figure 1 shows the results of these measurements. Increasing the amount of NaOH to a pH of 12 will allow more of the polymers to stick to the membrane. In this case the bending rigidity is further increased by adding polymer, as can be seen in Figure 2. Even for δ=10% enough Na^+ is available. A further increase of the pH value to 13 (ten times the amount of NaOH) will decrease the sensitivity of κ. A polymer amount of δ=10% will increase the bending rigidity half as much as the same amount in a pH 12 solution.

The second polymer with longer chain was investigated at pH13. The phase diagram showed a higher efficiency. The neutron scattering experiments have shown that the sensitivity of the bending rigidity has also been increased by the longer polymer chain.

We have shown that the concept of the sticker polymers can be reversed from hydrophobic stickers to hydrophilic stickers. A comparable sensitivity of the efficiency was obtained. Thus, for application a larger set of polymers is accessible.

Institut für Festkörperforschung
Forschungszentrum Jülich GmbH
D-52425 Jülich

Experimental Report
of Neutron Scattering Experiments
at the FRJ-2 Reactor

Proposal number:	KW2-06-009		
Experiment title:	Influence of concentration and ligands on the behavior of Co-Nanoparticles in microemulsions and solutions		
Dates of experiment:	06.03. – 07.03.2006	Date of report:	06.06.2006
Experimental team: Names	Addresses		
Feygenson Mikhail Pollmeier Klaus Sager Wiebke Dr.	IFF-8: Scattering Methods, FZ-Jülich P.O. Box 1913, 52425 Jülich IFF-Soft Matter, FZ-Jülich P.O. Box 1913, 52425 Jülich		
Local Contact:	A. Radulescu		

Experimental report text body

Since our final goal aims at measuring magnetic and nuclear form factors of magnetic nanoparticles in solution and to thus determine the average magnetization density within single particles, we have been working from May 2005 onward on developing microemulsion- or micelle-based synthesis routes for magnetic cobalt nanoparticles with well-defined size distribution and tunable size as well as particle interaction.

In literature, there are basically two major routes described to synthesize magnetic Co-nanoparticles. The first route is based on the thermal decomposition of cobalt carbonyl compounds in a suitable surfactant/ligand environment (see, e.g. [1]), and requires high temperatures and/or high pressures and toxic starting compounds. The second route, originally proposed by Pileni et al. [2,3], employs water-in-oil (w/o) microemulsions as nanostructured reduction medium. Pileni and coworkers used as surfactant the double tailed Na*AOT* (sodium *di(2-ethylhexyl) sulfosuccinate*) in which the sodium ions were either partially or completely exchanged by cobalt ions. Co-nanoparticles were obtained by adding the reducing agent $NaBH_4$ solubilized in a Na*AOT* stabilized w/o microemulsion or directly as aqueous solution. Since we encountered, using the Pileni routes, low yields [2] or phase separation problems [3] that led to undefined reduction and particle formation, we started in 2005 to investigate the incorporation of nonionic microemulsions in the synthesis route. This allowed us to study the formation of Co-nanoparticles over a wider concentration and temperature range and to thus access a larger parameter space for particle morphological fine-tuning.

The Co-nanoparticles were prepared by employing w/o microemulsions that were stabilized by nonionic surfactants of the ethoxylated alkyl- or arylether series such as $C_{12}E_5$ and Igepal CO520 and contained $NaBH_4$ of different concentration in the aqueous cores. To these microemulsions different amounts of a reversed micellar solution of $Co(AOT)_2$ in a toluene/hexane solvent mixture can than easily be added in a controlled manner without leading to phase separation and undefined preparation conditions.

In order to (i) understand the Co-nanoparticle formation process within the w/o microemulsions used, to (ii) analyze the main factors that determine particle size and polydispersity and to (iii) study the role of the micro-

Fig. 1

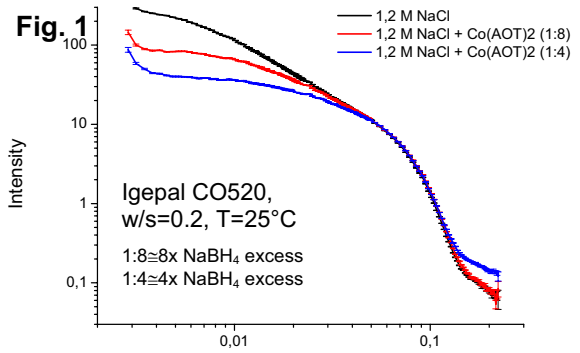


Fig. 2

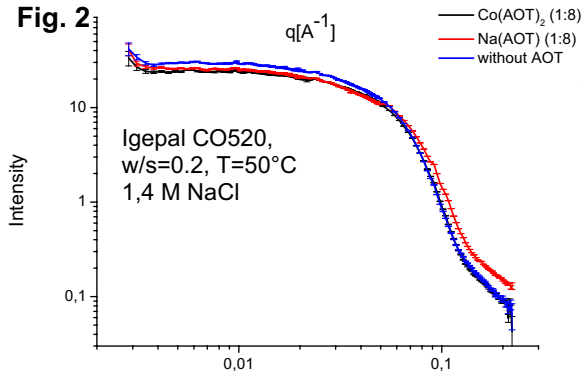


Fig. 3

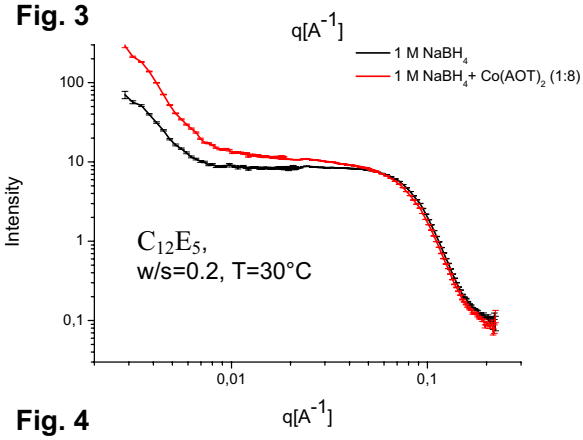
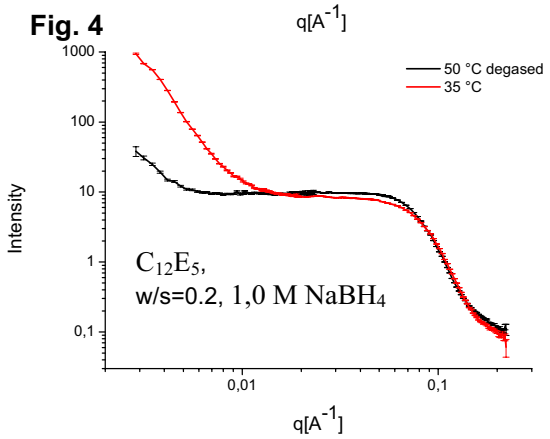


Fig. 4



[1] V.F. Puntes, K.M. Krishnan, A.P. Alivisatos, Science **2001**, *291*, 2115

[2] C. Petit, A. Taleb, M.P. Pileni, J. Phys. Chem. B **1999**, *103*, 1805

[3] I. Lisiecki and M.P. Pileni, Langmuir **2003**, *19*, 9486

emulsion during particle formation, we need to characterize the morphology of the microemulsions as function of salt content, water-to-surfactant ratio (*w/s*) and temperature before and after addition of Co(*AOT*)$_2$ and to record changes occurring during the Co-particle formation process.

For the nonionic w/o microemulsions we expect within the one-phase region spherical microemulsion droplets just below the upper phase boundary (solubilization limit), above which the w/o microemulsion expels (excess) water. With decreasing temperature the droplets transform gradually into cylinders, whereby volume fraction and cylinder length depend strongly on the surfactant used. Generally the $C_{12}E_5$ stabilized microemulsions appear to be more stable against the droplet-to-cylinder transition than the Igepal stabilized ones. In order to study changes of the microemulsion morphology occurring upon the addition of different amounts of Co(*AOT*)$_2$, we first had to find out how we can mimic the $NaBH_4$ solutions with NaCl in order to prevent particle formation and thus be able to study the Co(*AOT*)$_2$ influence independently from the changes occurring during nanoparticle formation.

In August 2005 we, therefore, started our SANS-investigation at KWS2 on characterizing the morphology of the microemulsions involved in the Co-nanoparticle synthesis by finding the NaCl concentration which displays the same dependence of the scattering curves with temperature and thus the same microstructural response as a 1.0M $NaBH_4$ containing microemulsion. We found that for Igepal as well as $C_{12}E_5$ stabilized microemulsions at two different *w/s* values of 0.2 and 0.5 a 1.2M NaCl solution can quite well be employed for mimicking.

In March 2006 we looked at the influence of AOT addition on the structure of the nonionic microemulsion and on reactions leading to Co-nanoparticle formation. Fig.1 displays the scattering curves for an Igepal stabilized microemulsion at *w/s*=0.2 and T=20°C. It clearly shows that the addition of Co(*AOT*)$_2$ shifts the sphere-cylinder equilibrium to the sphere side which would correspond to an increase in temperature. At high temperature the changes upon *AOT* addition are less pronounced and there is only little difference between adding Co(*AOT*)$_2$ or Na*AOT* at constant *AOT* concentration (see Fig.2). Fig.3 shows a reaction induced in a $C_{12}E_5$ stabilized microemulsion containing 1M $NaBH_4$ at w/s=0.2 and T=30°C by adding $Co(AOT)_2$ in a molar ratio of Co^{2+}:BH_4^- of 1:8. Differences before and after performing the reaction show up only at very low *q* and can be associated to H_2 bubble formation which also occurs when $NaBH_4$ reacts with water only. In this case bubble formation is significantly reduced after degassing (see Fig 4).

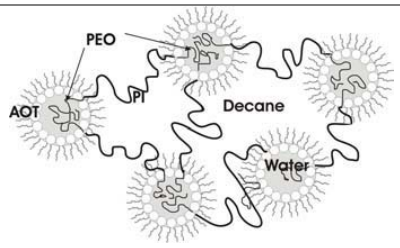
Institut für Festkörperforschung
Forschungszentrum Jülich GmbH
D-52425 Jülich

Experimental Report
of Neutron Scattering Experiments
at the FRJ-2 Reactor

Proposal number:	KW2-06-010		
Experiment title:	**Conformation of Network-Forming Triblock-Copolymers in Water-In-Oil Microemulsions**		
Dates of experiment:	22.04 – 23.04.2006 (reactor shutdown 22.04)	Date of report:	02.06.2006
Experimental team: Names	Addresses		
Tinka Spehr	Technische Universität Darmstadt Institut fuer Festkörperforschung Hochschulstrasse 8, 64293 Darmstadt	Institut Laue-Langevin 6, rue J.Horowitz F-38024 Grenoble F-38024 Grenoble	
Thomas Blochowicz	Technische Universität Darmstadt Institut fuer Festkörperforschung Hochschulstrasse 8, 64293 Darmstadt		
Local Contact:	Henrich Frielinghaus		

Experimental report :

The ternary microemulsion composed of the anionic surfactant AOT, water and decane as oil forms a droplet phase that is stable over a wide range of compositions in the vicinity of room temperature [Kot]. As the radius depends on a first approximation linearly on the ratio of water to surfactant [Dij], size and density of the droplets are independently tunable.
The addition of the amphiphilic triblock-copolymer PEO–(polyethyleneoxide, hydrophilic) –PI (Polyisoprene, hydrophobic) – PEO is assumed to lead to a transiently linked network (see sketch to the right).
The following experiments were planned:



(1) measurement of the scattering of **pure microemulsion** with shell contrast to determine the droplet form factor
(2) measurement of the scattering of **PI-homopolymers in d-decane** for comparision with the scattering of network forming polymers
(3) matching of the scattering length densities of water/heavy water, decane/d-decane to those of PEO and AOT to measure the scattering of the PI-middleblocks (**triblock-copolymer in microemulsion**)

Due to a shutdown of the reactor the main objectives of the experiment could not be achieved. Only some of the prepared samples have been measured. Because of the reduced time only empty beam was measured for background subtraction.

RESULTS:

1. pure microemulsion

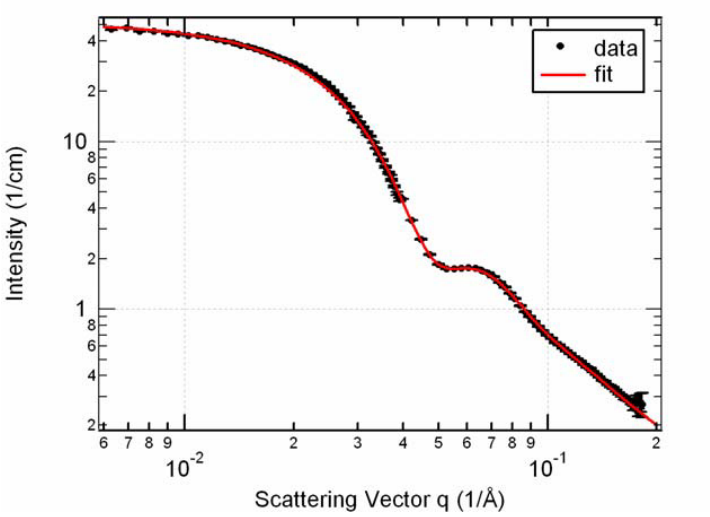


Fig. 1: Scattering from microemulsion droplets in shell contrast, fit of core-shell form factor taking into account polydispersity in size and structure factor for hard sphere potential

parameter	fitted value
$radius_{(watercore)}$	56.4 Å
$shell\ thickness_{(AOT)}$	5.9 Å
total radius	62.3 Å
polydispersity	24.1 %

The pure microemulsion (water to surfactant ratio ω = 40, droplet volume fraction Φ = 0.14) under shell contrast was measured at 288 K. Data has been acquired under the following instrumental settings: C8D8, 30 min and C4D2, 10 min.
The obtained structural information (see table) completes earlier results obtained by small angle X-ray scattering measurements.

2. PI homopolymer in d-decane

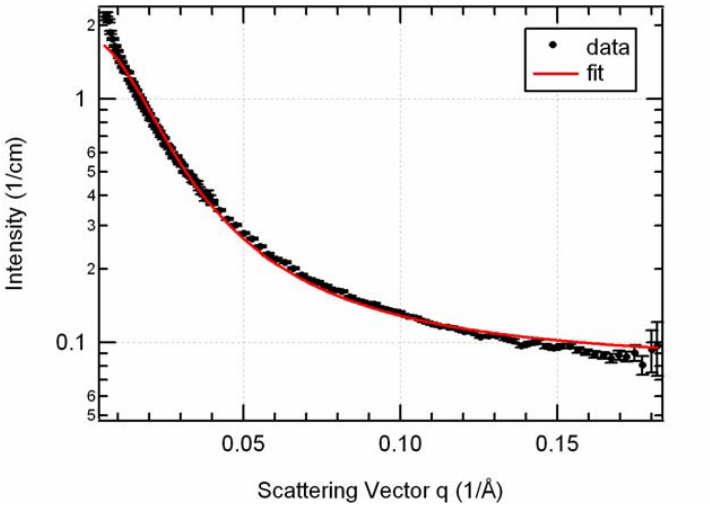


Fig.2: Scattering from PI homopolymers dissolved in deuterated decane, Debye fit

parameter	fitted value
radius of gyration	86 Å

The Polyisoprene (PI) homopolymer (43400 g/mol) was dissolved in d-decane.
Data has been acquired under the following instrumental settings: C8D8, 190 min and C4D2, 15 min.
Due to missing background measurements only preliminary data analysis is possible.
The disagreement of data and fit for small q-vectors might indicate that parts of the PI are cross-linked.

3. PEO-PI-PEO triblock-copolymer in microemulsion

No results have been obtained. Weak contrast between the PI-chains and the matched microemulsion requires longer measurements and accurate background subtraction. The matching of water cores and decane matrix to the AOT shell was possible. This information will help for future experiments on this system

[Dij] M. v. Dijk, M. v. Struis, J. Joosten, Y. Levine (1989), *J. Phys. Chem.* **93**, 2506
[Kot] M. Kotlarchyk, S. Chen, J. Rouch, P. Tartaglia (1984), *Phys. Rev. Lett.* **53**, 941

Institut für Festkörperforschung
Forschungszentrum Jülich GmbH
D-52425 Jülich

Experimental Report
of Neutron Scattering Experiments
at the FRJ-2 Reactor

Proposal number:	KW2-06-011		
Experiment title:	**Study of self-assembling peptides**		
Dates of experiment:	20.04.2006	Date of report:	06.06.2006
Experimental team: Names	Addresses,		
Dr. Paduano Luigi,	Chemistry Department University of Naples "Federico II" Naples, Italy		
Local Contact:	Dr. Aurel Radulescu		

Experimental report text body

Bio-molecule self assembling is a functional (sometimes pathological) property.
Proteins, peptides and all bio molecules interact and self-organize to form well-defined structures able to display specific functions. In the recent years the study of the basic principles underlying the biological processes of self-assembly has largely increased. The sequence named EAK16,1 (Ala-Glu-Ala-Glu-Ala-Lys-Ala-Lys)2, has shown a strong propensity to adopt a beta-sheet structure and to spontaneously form, in presence of salts, membranes completely non toxic and resistant to proteolytic digestion. A proposed model for membrane produced by molecules such as EAK16 stays on layers of parallel (or antiparallel) β-sheets held together on one side by hydrophobic bonding and on the other side by ionic bond between charged residues. Here we focus on a series of EAK-16 analogues (16- (Ala-Glu-Ala-Glu-Ala-Lys-Ala-Lys)^2 and 8-mer (Ala-Glu-Ala-Glu-Ala-Lys-Ala-Lys) peptides) designed to decode the role of charge and hydrophobic factors in modulating the self-assembling properties.2 NMR and CD analyses of a suite of a 16-mer and 8-mer self-assembling peptides were undertaken in order to correlate conformational properties and self-assembling propensity of the monomers. NMR measurements reveal, in particular, that some of the 16-mer peptides form aggregates insoluble or too large to contribute to the NMR spectra (high nuclear relaxation rates) while the 8-mer peptides appear to be free in solution even though able to adopt, in some amount, β/extended structures. For the 8-mer peptides with the highest hydrophobic character in the series, the β- structure is definitively evidenced by the relative intensities of NOE contacts.
In this context, SANS test measurements have allowed obtaining some information on the aggregates formed by the two samples (16- and 8-mer peptides). As shown in Figure 1a at the concentration explored there is a low presence of aggregates. The scattering intensity is quite flat except for a slight probably increase at low q.

At the same concentration (see Figure 1b) the 16-mer sample shows a cooperative tendency of the molecule to self assembles. I(q) shows a q^{-1} decay typically of cylindrical structure whose length is above 900 Å. This suggests that 16-mer peptides probably stick one on top of the other forming supramolecular aggregates whose shape is geometrically similar to rod.
Further measurements at different concentration and environmental condition should allow gaining detailed information of their structure.

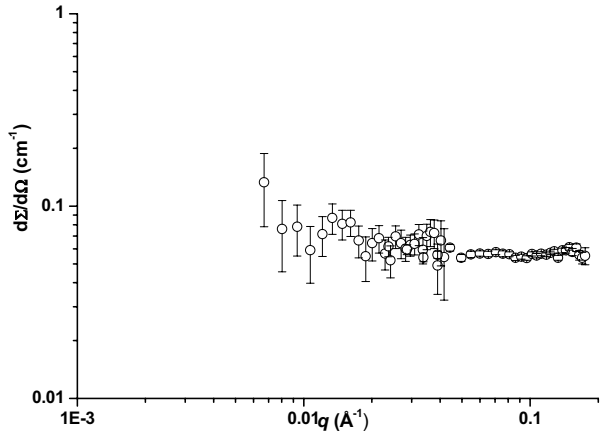


Figure 1a – Scattering cross sections measured at 25°C for the sample 8-mer

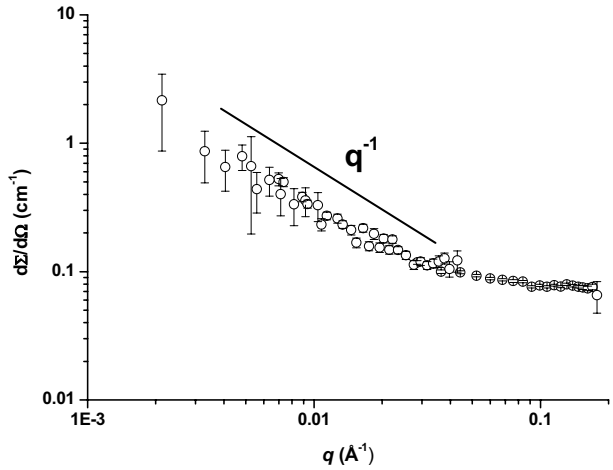


Figure 1b – Scattering cross sections measured at 25°C for the sample 16-mer

Institut für Festkörperforschung
Forschungszentrum Jülich GmbH
D-52425 Jülich

Experimental Report of Neutron Scattering Experiments at the FRJ-2 Reactor

Proposal number:	KW2-06-012		
Experiment title:	Benchmarking test on KWS-2 prior to move to Munich		
Dates of experiment:	01-02.05.06	Date of report:	06.06.2006
Experimental team: Names	 Addresses		
Henrich Frielinghaus Wim Pyckhout-Hintzen Aurel Radulescu	Forschungszentrum Jülich Institut für Festkörperforschung D-52425 Jülich Germany		
Local Contact:	Dr.H.Frielinghaus		

Experimental report text body

Several test investigations on benchmarking materials and materials of interest for instrumentation development have been performed at KWS-2 instrument prior to its movement to Garching at FRM-2 reactor.

1. The absolute scattering of X-ray machines is not often exploited. Therefore some practical samples are sought which scatter well enough and rather peaked so that the long time sampling of data can be avoided. A fluorinated commercial film is tried which was calibrated in SANS. The contrast is given by amorphous and crystalline regions and a typical polydisperse spherical form factor with small contributions form a hard-sphere interaction can be noticed (Fig.1). The neglect of the structure factor amounts up only to 5% in the peak and the sample can be readily applied in the accessible Q-range of the X-ray machine. From the maximum intensity a relation can be extracted from which SAXS intensities can be derived absolutely. This will depend on the power and current of the generated X-ray beam.

2. Of an extreme importance in designing a neutron scattering instruments are the entrance and end-of-guide windows which, in order to optimize the flux of the instrument, must remove as less as possible neutrons from the transported, transmitted or scattered beams. Two potential materials for neutron windows have been tested from the point of view of efficiency in the transmission of neutrons: Zr foil and Sapphire plate. Several thicknesses of both materials have been investigated at KWS2 instrument with regards to scattering and transmission as a function of the neutron wavelength. One could conclude that both materials reveal for a proper thickness of technical interest a very good transmission (higher than 97%). Sapphire shows a very weak scattering and transmits most of the beam while the Zr foils show a strong small angle scattering (Fig.2) which comes from the scattering on grains, the material

being polycrystalline

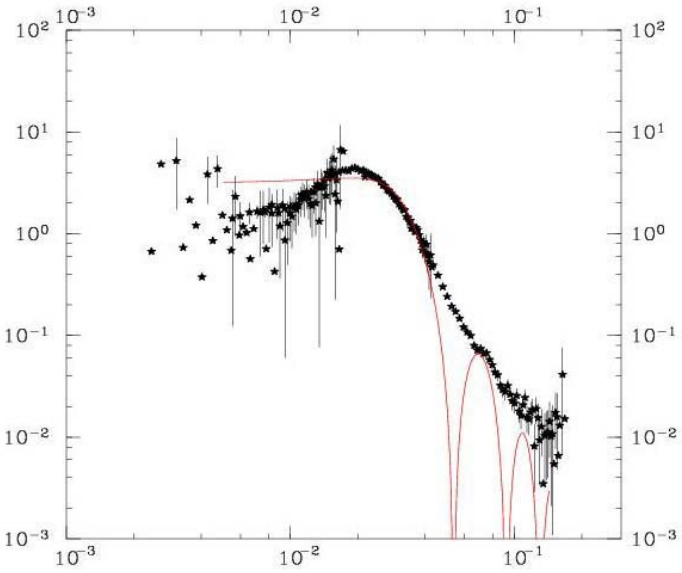


Fig.1 – Scattering cross section of fluorinated commercial film

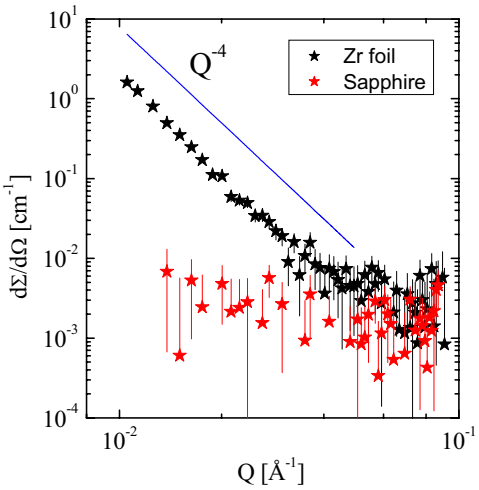


Fig.2 – Scattering cross sections of sapphire and polycrystalline Zr.

Institut für Festkörperforschung
Forschungszentrum Jülich GmbH
D-52425 Jülich

Experimental Report
of Neutron Scattering Experiments
at the FRJ-2 Reactor

Proposal number:	KW2-06-015		
Experiment title:	**Bicontinuous microemulsions in presence of polyelectrolytes**		
Dates of experiment:	27. – 29.04.2006	Date of report:	11.05.2006
Experimental team: Names	Addresses		
Martin Brodeck Henrich Frielinghaus	Forschungszentrum Jülich GmbH, Institut für Festkörperforschung, D-52425 Jülich Forschungszentrum Jülich GmbH, Institut für Festkörperforschung, D-52425 Jülich		
Local Contact:	Henrich Frielinghaus		

Experimental report text body

After measuring polymers with an ionic sticker (KWS2-06-008 and KWS2-06-014) a further step was taken by investigating polyelectrolytes. The analysed polyelectrolyte consists of a regular (non-ionic) hydrophobic chain (PB – polybutylene) and a hydrophilic chain (PAA – polyacrylic acid). Adding NaOH to the system will influence the behaviour of the polyacrylic acid. Different pH values were investigated, ranging from a 30% allocation of acryl acid molecules (in this case there was only one Na^+ particle for about 3 COOH groups) up to a 800% allocation. We expected a flexible to semi-flexible chain for the low allocation and a rod-like behaviour for a roughly 100% allocation due to the repelling charges. Further increasing the NaOH amount should result in a screening-effect of the negative oxygen-atoms at the chain and therefore a flexible to semi-flexible chain behaviour should be retained. Four different polyelectrolyte concentrations have been investigated (δ=0%, 1%, 2% and 3%) and the choice of the different pH values made it possible to compare different polyelectrolyte concentrations at constant allocation.

Prior to the neutron scattering experiments phase diagram measurements have been performed. They worked well for allocations of about 100% and above, lower concentrations of NaOH and therefore lower occupation resulted in abnormal behaviour of the phase boundaries. A one phase region was found for these allocations even for surfactant concentrations of down to 4%, but the typical fish-like shape was not retrieved. Instead, the upper phase boundary changed rapidly with the amount of surfactant, even increasing with lower concentration. It was particulary interesting to investigate the influence of the polyelectrolytes with these low allocations on the bending rigidity κ.

The bending rigidity κ can directly be measured with small angle neutron scattering. Therefore the bulk contrast is chosen by using deuterated water. The Teubner-Strey-formula can then be fitted to the scattering-curve (Figure 1) and two structural paramters, the domain size d and the correlation length ξ , are obtained from this fit. According to the Gaussian random field theory the bending rigidity κ is connected to these two structural parameters by $\kappa/k_BT = 0.85\ \xi/d$.

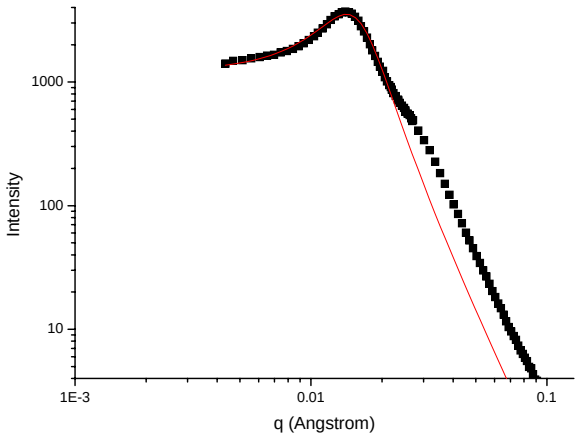


Figure 1: At typical scattering curve. By fitting the Teubner-Strey-formula the two structural parameters d and ξ can be extracted. The bending rigidity κ can then be calculated with the Gaussian random field theory.

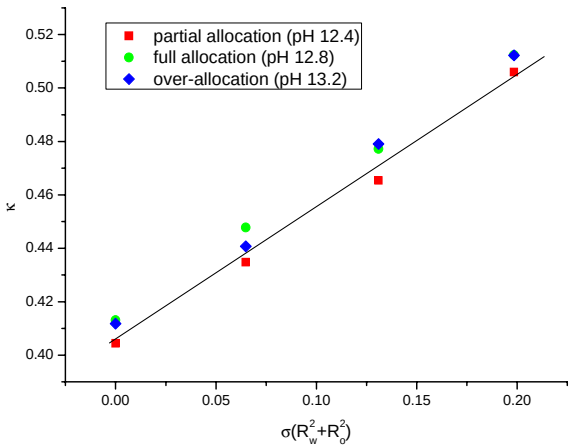


Figure 2: The bending rigidity κ depending on the scaled polymer amount. R_w and R_o are the end-to-end distances of the water-soluble and oil-soluble part of the polymer estimated for ideal chains (no charge effect).

36 samples have been prepared and measured, varying in polymer concentration δ, allocation (influenced by the pH value) and surfactant concentration. For the four different polymer concentrations δ three pH values have been examined: pH 12.4, pH 12.8 and pH 13.2. Changing the polymer concentration at a constant pH value also changes the allocation of the polyelectrolyte.

It was expected to find a lower sensitivity for the full allocation of the chain compared to lower and higher allocations. In this case roughly all COOH groups should have dissociated in the alkaline environment. The repelling charges would then stiffen the polymer and decrease its effect on the interface and the bending rigidity. Against these expectations the bending rigidity does not seem to be majorly influenced by the pH value of the solution. All three NaOH concentrations show similar behaviour (Figure 2). The bending riditiy was extracted for a constant surfactant concentration of 12%. This result is particularly interesting since the phase diagram studies have shown different behaviour depending on the allocation.

A possible explanation could be the limited domain size. The end-to-end distance of these polymers in the mushroom-regime is roughly 60 Å. A stretched polymer, which is significantly larger, would not fit into the domains the size of which ranges from 250 to 500 Å.

The sensitivity of the polyelectrolytes can be extracted from the slope of the SANS measured bending rigidity (Figure 2). We have seen a strong boosting for small polymer amounts. These first impressions have been confirmed by the SANS measurements. The sensitivity of the bending rigidity is about 50% stronger than for regular diblock copolymers.

The SANS experiments have revealed that, against the expectations, the ion allocation of the chains does not influence the bending rigidity. This result considers just the polymer amount to be dominating and neglects changes of the actual size of the polymer as really described by the theory. The consideration of the real size of the polymers is not possible at the present stage, since we simply did not measure the corresponding homopolymer size in a water/NaOH solution. It is furthermore astonishing, that (a) the polymer boosting effect is about 50% stronger for the polyelectrolyte compared to non-ionic polymers (based on a constant size assumption) and that (b) for low charge allocations the phase diagrams seem to open up and resemble to temperature insensitive phase diagrams as obtained for sugar based surfactants or ionic/non-ionic surfactant mixtures. Especially the last example (ionic/non-ionic surfactant mixtures) might have something in common with the polyelectrolyte containing microemulsions. Future work and thinking will shed more light on the current interesting results obtained so far.

Institut für Festkörperforschung
Forschungszentrum Jülich GmbH
D-52425 Jülich

Experimental Report
of Neutron Scattering Experiments
at the FRJ-2 Reactor

Proposal number:	KW2-06-016		
Experiment title:	**Investigation of dPS-PB diblock copolymer cylindrical phase with GISANS**		
Dates of experiment:	20.04.-21.04.2006	Date of report:	06.06.2006
Experimental team: Names	Addresses		
D. Korolkov E. Kentzinger L. Willner	Institut für Festkörperforschung, Forschungszentrum Jülich Institut für Festkörperforschung, Forschungszentrum Jülich Institut für Festkörperforschung, Forschungszentrum Jülich		
Local Contact:	Denis Korolkov		

Experimental report text body

Nanosized components hold considerable promise as forming the platform for an entirely new type of hardware technology. In such a future technology quantum effects in the nanoobjects might give rise to new functionalities. Sample preparation represents a major challenge.
Two fundamentally different methods are possible: the top-down approach of electron-beam- or interference-lithography or the bottom-up approach of using self-organised soft matter templates.
In our work we used self-organization as the most interesting and fast method for nanostructure fabrication. It allows us to produce nanostructures with a periodicity smaller then 50 nm on a large surface area. Selforganization of a diblock-copolymer with one deuterated component was used: dPS (deuterated polystyrene)-PB (polybutadiene). The ratio of the molecular weights of the two chains was chosen to be 20%/80%. After spin-coating on the Si substrate with native oxide layer and annealing in argon atmosphere samples self-organized into a cylindrical phase. Varying the thickness of the sample with different concentration of solutions and spin-coating speed it is possible to obtain two kind of alignment of the nano-structure: parallel to the surface and perpendicular. In Figure 1 one can see AFM images which don't give any information about bulk. But it is well known that in the case of cylindrical phase there is a thin layer of PS which covers Si wafer.

To explore the possible multilayer structure and the average period between cylinders parallel and perpendicular to the surface, we investigated two samples with different alignment of cylinders, whereby a sample with perpendicular cylinders was obtained from 0.5% solution and had thickness of about 20 nm. All measurements were performed at a wavelength of 6.3 Å.



Figure 1. AFM images of dPS-PB diblock copolymer after annealing. (left) Cylinders are perpendicular to the substrate. (right) Cylinders parallel to the substrate.

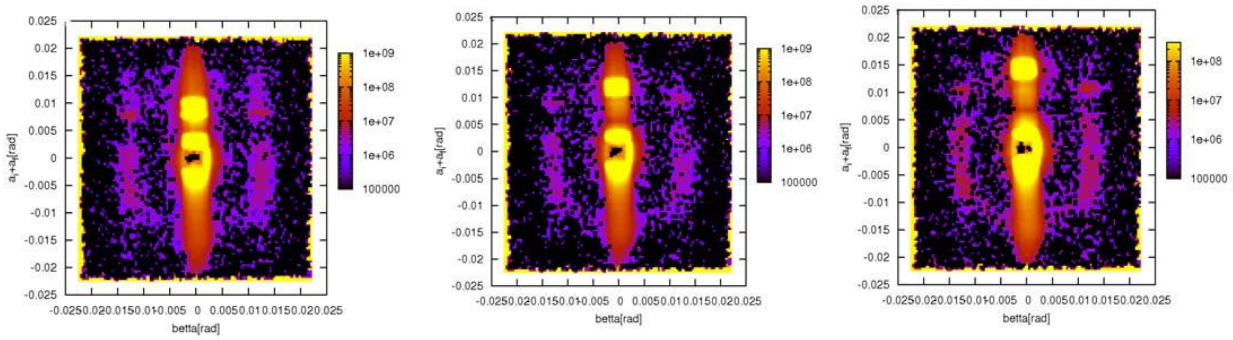


Figure 2. GISANS data of parallel cylinders, measured at different incident angles (from left to right: 0.35, 0.45, 0.55 deg.) for two hours each. Collimation and detector distances are 8m and 11 m respectively.

During our beam time we were only able to perform experiment at collimation distance of 8m and detector distance of 11m. Other distances could not be measured due to a KWS-2 computer problem. The measured GISANS data at different incident angles is presented in Fig.2. It is clear that diffuse peaks on both sides of a specular peak correspond to the lateral structure (parallel cylinders). Diffuse peaks are additionally modulated by reflectivity at low incident angle, because reflectivity terms for both incoming and outgoing wave have maximum near the angle of total reflection. Increasing an incident angle one can see that this modulation becomes less intensive, which is found to be in good agreement with theory. Additionally at an incident angle of 0.55^{o} one can see that Yoneda peak below specular reflection appears. This fact allows to define exactly the intensive part of diffuse peaks as Yoneda peaks too, because they have the same position on Q_z axis.

Unfortunately perpendicular cylinders at the same detector distance didn't give any suitable result due to a very thin layer and have to be investigated additionally. Also we were not able to get any multilayer information due to a very low Q_z range. Nevertheless GISANS is still the best method for obtaining average lateral structure information and we are going to use it further in the future.

Institut für Festkörperforschung
Forschungszentrum Jülich GmbH
D-52425 Jülich

Experimental Report of Neutron Scattering Experiments at the FRJ-2 Reactor

Proposal number:	KW2-06-017		
Experiment title:	Characterization of nonionic w/o microemulsions stabilised by nonionic (and ionic) surfactants as precipitation media for the synthesis of $BaCO_3$ nanoparticles.		
Dates of experiment:	24.04. – 26.04.2006	Date of report:	19.06.2006
Experimental team: Names	Addresses		
W.F.C. Sager	IFF-Soft Matter, FZ-Jülich P.O. Box 1913, 52425 Jülich		
M. Feygenson K. Pollmeier	IFF-8: Scattering Methods, FZ-Jülich P.O. Box 1913, 52425 Jülich		
Local Contact:	A. Radulescu		

Experimental report text body

In order to gain more insight into the "templating" role of microemulsions, we started in 2003 to study in detail by transmission electron microscopy (TEM) the formation of $BaCO_3$ nanocrystals within the one-phase region of different nonionic water-in-oil (w/o) microemulsions stabilized by nonionic surfactants. Adjusting the compositions and precipitation conditions of the parental precursor microemulsions allowed us for the first time to prepare a variety of different nanostructures with well-defined morphology ranging from (stacked) platelets, (self-assembling) rhombohedral nanocrystals, nano-needles, (ordered) hexagonal nanorods to nano-fibres and -bundles. Since we are interested in analysing the key parameters that determine the crystal size and shape and to investigate the underlying mechanisms of particle nucleation, growth and (orientational) coalescence, it is a prerequisite to determine the microstructure of the microemulsion before and during the reactions performed. This will finally provide a better basis for the theoretical description of crystallization process performed in confined but highly dynamic media.

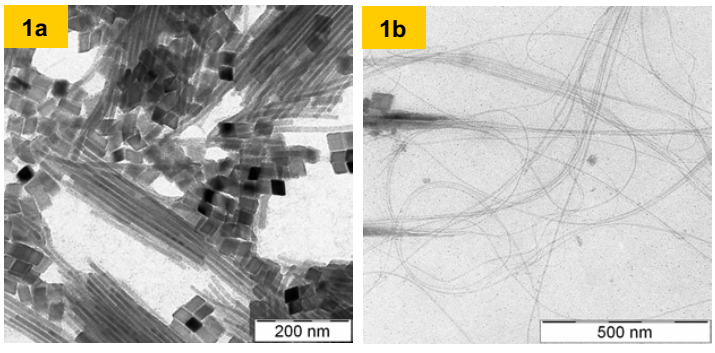


Fig.1: Nanoparticles formed after 5 min at 50 (a) and 23ºC (b) in microemulsions stabilised by $C_{12}E_5$ containing 0.1M salt.

In April 2006 we investigated the microstructure of the parental microemulsions before and after mixing by SANS for microemulsions stabilized by Igepal CO520 or $C_{12}E_5$ containing 0.1-0.3M salt at high (just below the upper phase boundary of the one-phase microemulsion region) and low temperatures (just above the upper phase boundary of the one-phase microemulsion region).

Fig. 2 displays SANS curves recorded during the reactions for the system $C_{12}E_5$, w/s=0.1 and 0.1M salts at 50 (2a) and at 23°C (2c) together with the curves of the two parental

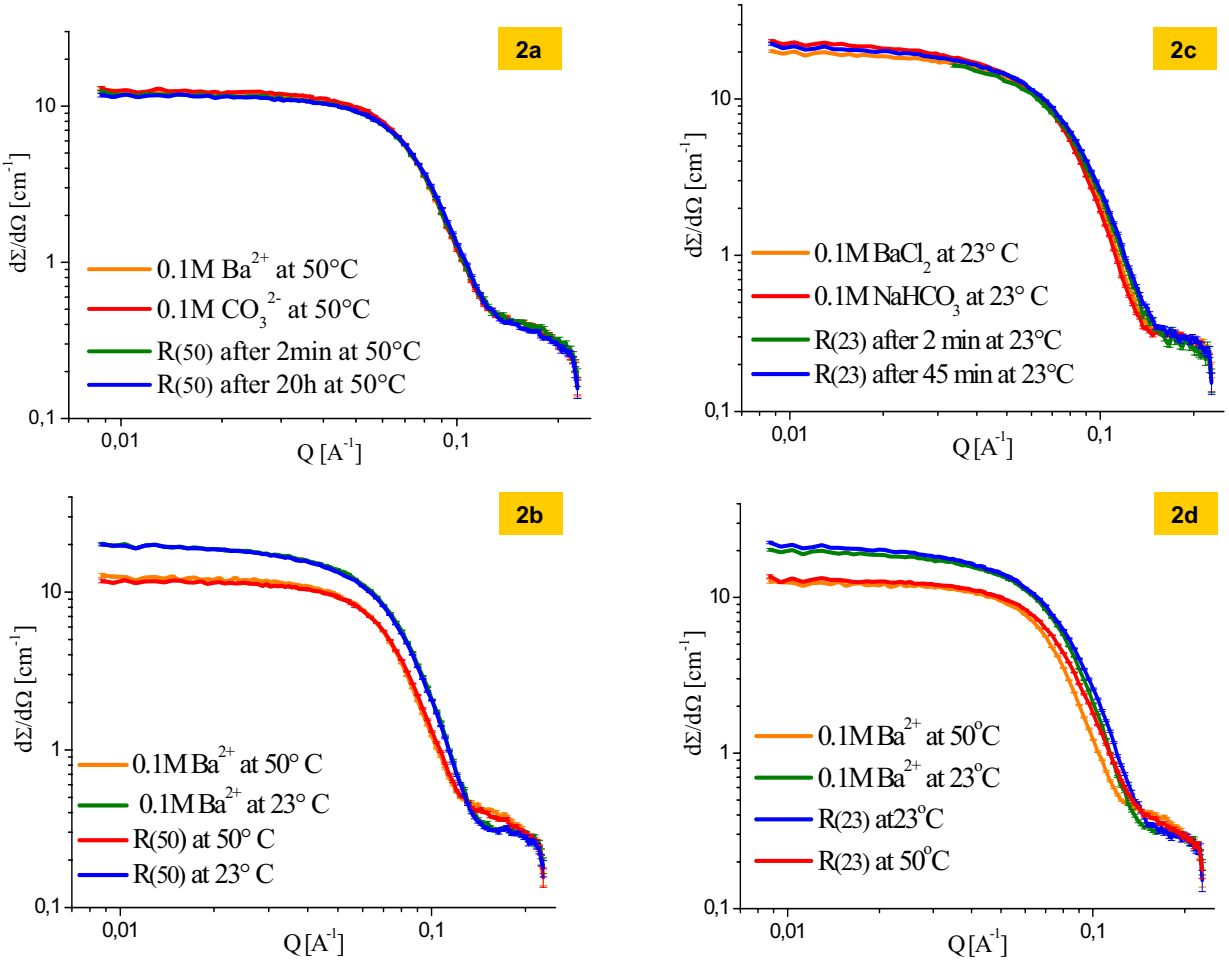


Fig. 2: SANS curves recorded for Ba^{2+} and CO_3^{2-}-containing microemulsions before and after mixing. SANS data of the reacting microemulsions were recorded form 2 seconds up to 1 day. The microemulsions were stabilized by $C_{12}E_5$, possessed a water-to-surfactant ratio w/s=0.2 and were made with 0.1M salt solutions.

precursor microemulsions. At 50 as well as 23°C the scattering curves obtained for the parental microemulsions overlap completely, indicating that changes observed during the reaction can only be caused by compositional and/or structural changes of the microemulsion occurring during the $BaCO_3$ crystallization. At 50°C the scattering curves of the parental microemulsions overlap at low and high wave vector Q with the ones obtained for the reaction after mixing (2min delay) and after 20h (2a). As can be seen from Fig.1a, the nanoparticles formed within the microemulsion (nanocubes and fine nanorods) are immediately of crystalline nature. With time the cubes dissolve and only fairly monodisperse rods are formed. To additionally proof that no changes occurred, we changed the temperature of the $BaCO_3$ containing microemulsion at later stages. The microemulsion in which the reaction has been performed at 50°C responds to temperature changes in the same way as the parental microemulsion (2b). At 23°C changes in the SANS curves between the parental and the reacting microemulsions show up directly after mixing (with 2min delay), but no further changes occur with time (2c). The shift in the minimum to higher Q indicates that the microemulsions lost water, which might be incorporated in the amorphous structures (1b). At 23°C first amorphous filaments form, that transform only slowly with time into larger needles. If the temperature is changed at later stages to 50°C the difference is even more pronounced (2d).

Institut für Festkörperforschung
Forschungszentrum Jülich GmbH
D-52425 Jülich

Experimental Report of Neutron Scattering Experiments at the FRJ-2 Reactor

Proposal number:	KW2-06-018		
Experiment title:	Time-resolved SANS for the crystallization from solution of *Syndiotactic*-polypropylene		
Dates of experiment:	16.04.06-18.04.06	Date of report:	29.05.06
Experimental team: Names	Addresses		
Aurel Radulescu	Forschungszentrum Jülich Institut für Festkörperforschung D-52425 Jülich Germany		
Local Contact:	Dr.H.Frielinghaus		

Experimental report text body

Crystallization from solution of syndiotactic polypropylene has been investigated by SANS over a wide temperature range [1]. Several solutions prepared for different molecular weights (M_W=3K, 8K, 43.4K, 61.4K and 85K) and different polymer volume fractions (Φ_{pol}=0.5% and 1%) have been measured. The polymer form multilevel large scale aggregates. The complex morphology of these aggregates was resolved by combined conventional SANS and ultra-SANS investigations. At lower length scale (nanometer order) 2-dimensional objects have been identified from the clear Q^{-2} behavior of the scattered intensity. For the high M_W materials almost all polymers were involved in a rapid crystallization event even once it started, just above 40°C. Since at low Q no deviation from the Q^{-2} slope was observed (a so-called Guinier regime) we concluded that very large platelets (of sizes much larger than 1000Å) are formed. At larger length scale the platelets form a spherulitic-like morphology. On the other way, the low M_W materials have shown a gradual crystallization from solution in decreasing temperature [2]. Nevertheless, they form similar platelets of almost the same thickness which associate also in spherulites, but these have sizes much smaller than those formed in the case of high M_W materials. Tthe lower the molecular weight, the lower the melting point of the polymer thus, temperatures around ambient represent a smaller undercooling from the melting point and consequently, the driving force for crystallization is smaller. This is the reason only part of polymers crystallize at ambient temperatures. In order to obtain new information about the kinetics of crystallization of lower MW sPP polymers from solution new SANS investigations of a 8K material in decane have been performed at the KWS-2 instrument. The study involved an investigation of the time-resolved crystallization of polymers at different crystallization temperatures. Short time (5 minutes) measurements have been performed at a shorter distance sample-to-detector distance (4m) and the evolution of the scattering pattern was monitorized over several hours for every temperature of interest. The crystallization temperatures investigated were 55, 47, 38 and 20°C. Before reaching the temperature of interest the sample was heated up to 95°C where the single coil regime was observed

(all polymers were in a single-coil conformation) and then cooled down rapidly up to the crystallization temperature of interest. An example of the time evolution of the scattering patterns collected at a crystallization temperature of 55°C is presented in Fig.1. The time evolution of the scattering intensity at the lowest Q value reached in the experiment is presented in the inset of Fig.1 for all crystallization temperatures investigated. The behaviour of this evolution is rather complex and an analysis in terms of possible models of crystallization kinetics is in progress.

References: [1] A.Radulescu et al. Macromolecules 37, 6962, 2004; [2] experimental report KW1-04-061 FRJ2.

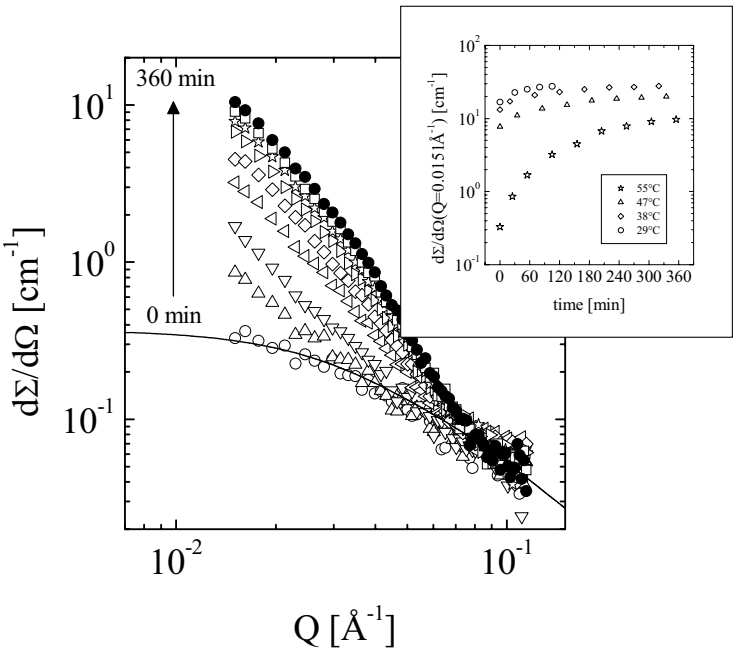


Fig.1 – Time evolution of the scattering pattern from 0.5% sPP 8K crystallizing in decane at 55°C; the solid curve represents the single coil form factor;
The inset shows the time evolution of the scattering intensity at the lowest Q value reached in the experiment for the polymer crystallizing at different temperatures

Focusing-Mirror High-Resolution Small Angle Scattering Instrument and Reflectometer (KWS-3)



Instrument Parameters

Wavelength:	$\lambda = (12.7 \pm 0.6)$ Å (9% FWHM)
Entrance aperture:	r_E = 1 to 10 mm
Wave vector resolution given by the opening of the entrance aperture:	$\Delta Q = k\, r_E / L \qquad (k = 2\pi/\lambda)$
Scattering wave vector range:	$10^{-4} \leq Q \leq 2 \times 10^{-3}$ Å^{-1} $10^{-4} \leq Q_z \leq 0.08$ Å^{-1} in reflectometry mode
Neutron intensity at sample position is proportional to the surface of the entrance aperture:	I = 180 n/s per mm^2 entrance aperture; for a wave vector resolution of 10^{-4} Å^{-1} (2 × 2 mm^2 entrance slit aperture) the intensity is therefore 720 n/s
Cross section of beam at sample position:	10 cm wide, 2 cm high
Detector:	Position sensitive detector, 8 cm diameter, 1.5 × 1.5 mm resolution

Instrument Responsible

Dr. Emmanuel Kentzinger Tel. +49-(0)-2461-61-3139 Email: e.kentzinger@fz-juelich.de
Dr. Jörg Stellbrink Tel. +49-(0)-2461-61-6683 Email: j.stellbrink@fz-juelich.de

Institut für Festkörperforschung
Forschungszentrum Jülich GmbH
D-52425 Jülich

Experimental Report
of Neutron Scattering Experiments
at the FRJ-2 Reactor

Proposal number:	KW3-04-008, KW3-04-015		
Experiment title:	**Influence of solvent quality on the micellization behaviour of PEP-PEO**		
Dates of experiment:	6.-15. 10. 2004 24.-26. 8. 2005	Date of report:	06.06.2006
Experimental team: Names	Addresses		
J. Stellbrink	IFF, FZ Jülich, D-52425 Jülich, Germany		
Local Contact:	J. Stellbrink		

Experimental report text body

Very recently we started using giant, star-like micelles (PEP5-PEO120, the number denotes the molecular weight in kg/mol) [1] as "*tunable analoga*" of unimolecular, regular star polymers. Here we found, that the intensity profile obtained for a micellar solution in a solvent mixture with a mole fraction x_{DMF}=0.5 shows completely different features than those for other mixtures. Whereas for solvent compositions x_{DMF}=0, 0.1, 0.2, 0.3, and 1 we found an intensity profile typical for a concentrated solution of micelles, *i.e.* a strong structure factor peak followed by an extended power law decay due to the blob scattering of the corona, the scattering profile for x_{DMF}=0.5 is dominated over nearly the whole Q-range, including that of the U-SANS instrument KWS-3, by a sequence of power laws. This is probably a precursor of the demixing of the micellar solution at this DMF mole fraction, which is found to take place a T≈25°C (The solution gets turbid) [2,3]. We have to emphasize that at the investigated temperature, T=≈30°C, the micellar solution is macoscopically completely clear and homogeneous.

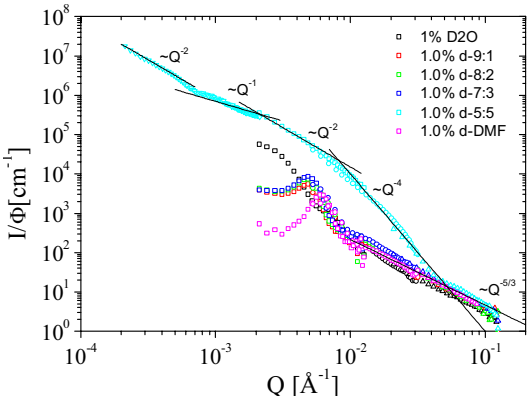


Figure 1: Intensitiy profile obtained by a combined U-SANS/SANS experiment vs. scattering vector Q for PEP5-PEO120 micelles in different mixtures of water and DMF.

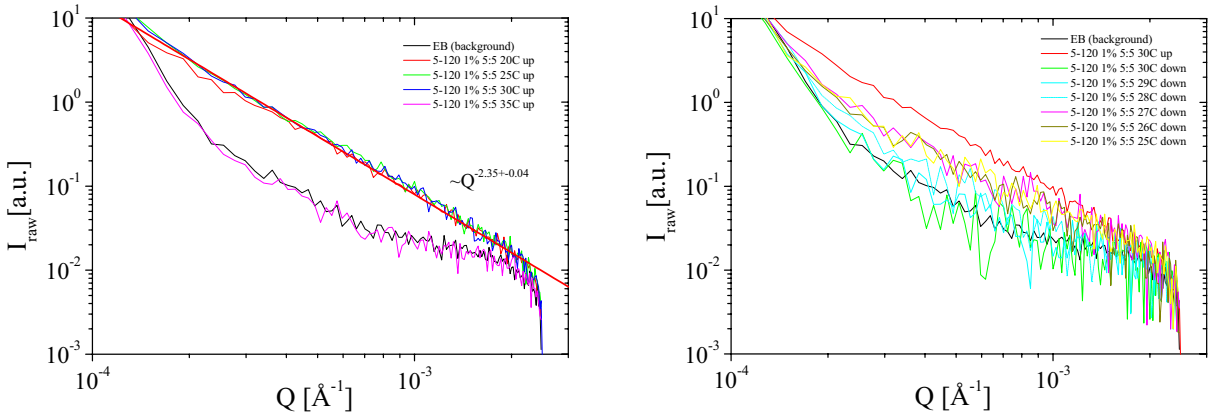


Figure 2: Intensity vs. scattering vector Q as a function of temperature upon heating (left) and cooling (right) for a micellar solution of PEP5-PEO120 in a water/DMF mixture with mole fraction $x_{m,dmf}$=0.5.

In this experiment we investigated in more detail the temperature effects in the U-SANS Q-range covered by KWS-3, i.e. $2x10^{-4} \leq Q \leq 2x10^{-4}$ Å. We found that the observed scattering curves depend crucially on thermal history of the sample, as can be seen in fig. 2. Here raw data for a temperature series upon heating (left) and cooling (right) are shown in comparison with the empty beam profile as background. Starting from the completely demixed state we slowly increased the temperature to 30°C and kept it constant for 12 hours, but still the typical power law $I \sim Q^{-2.35}$ of the demixed state is found. Only if the sample is heated further up to 35°C the intensity quickly decreases until it finally reaches the background level. Upon cooling down again to 30°C, the intensity is not increasing again, even if the sample is kept at 30°C for several hours. Only after further cooling down to 27-26°C the previously observed power law slowly appears again. This means that the phase separation kinetics are extremely slow, which might results from the special need to form micelles (upon heating) and to dissolve these micelles (upon cooling), respectively during this phase transition. A phenomenon which certainly needs further investigation.

References:

[1] L. Willner, A. Poppe, J. Allgaier, M. Monkenbusch, D. Richter, *Europhys. Lett.*, **55**, 667 (2001)
[2] R. Lund, L. Willner, J. Stellbrink, A. Radulescu and D. Richter, *Macromolecules*, **37**, 9984, 2004.
[3] M. Laurati, J. Stellbrink, R. Lund, L. Willner, D. Richter, and E. Zaccarelli, *Phys. Rev. Letters*, **94**, 195504, 2005.

Institut für Festkörperforschung
Forschungszentrum Jülich GmbH
D-52425 Jülich

Experimental Report
of Neutron Scattering Experiments
at the FRJ-2 Reactor

Proposal number:	KW3-04-014		
Experiment title:	Structure analysis of sintered tungsten wires by SANS		
Dates of experiment:	23.01. – 30.01.2005	Date of report:	24. 05. 2006
Experimental team: Names	Addresses		
Adél Len	Research Institute for Solid State Physics and Optics 1121 Budapest Konkoly Thege u., 29-33 Hungary		
Local Contact:	Dr. Jörg Stellbrink		

Experimental report text body

Tungsten wire is the most frequently used material for lighting, electronic devices, thermocouples, cathodes. The usual temperature range in most of such wire applications needs extremly good high-temperature mechanical properties, e.g. good creep-resistance, high tensile-strength, resistance to early deformation and vibration. The doped tungsten ful-fills these requirementes. During the sintering most impurities escape, except a part of potassium, which remains in bubbles during the following thermomechanical treatments and the whole life of the lamp. The presence of potassium filled bubbles with characteristic diameter of 100 nm is responsible for the quality of the wire. The structure of bubbles follows the macroscopic deformation of the wire. As a consequence of oriented macroscopic strain induced by wire drawing the bubbels are oriented parallel to the wire axis. To analyse the morphology of the wires in the whole volume of the sample, we used the method of neutron scattering. Previous SANS measurements on samples taken from different steps of annealing were made. To analyse the relative surface changes of different shaped potassium bubbles a simple way of data treatment was used. We have found that even at the highest studied annealing temperatures a substantial amount of elongated inclusions remain in the wires. The present USANS measurement objective was to obtain information in ultra-small q range. The measurements were carried out on the KWS-3 USANS instrument.
The measured samples were: unannealed; annealed at 1150°C; annealed at 1850°C; annealed at 2200°C. The sample - detector distance was 9.3 m; the wavelength: 12.7 Å. These samples were taken from the different steps of heat treatment. The 0.5 mm diameter tungsten wires were placed in 3 layers in the aluminium sample holder.

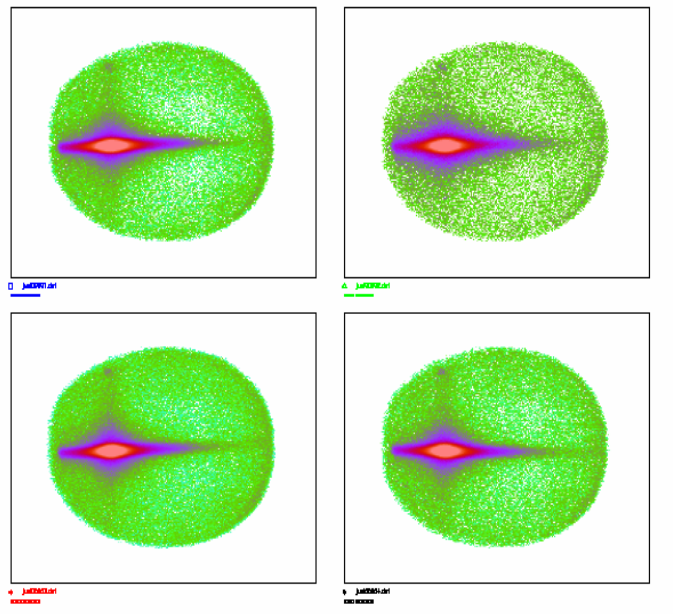


Fig.1. 2D scattering maps of the measured tungsten wires

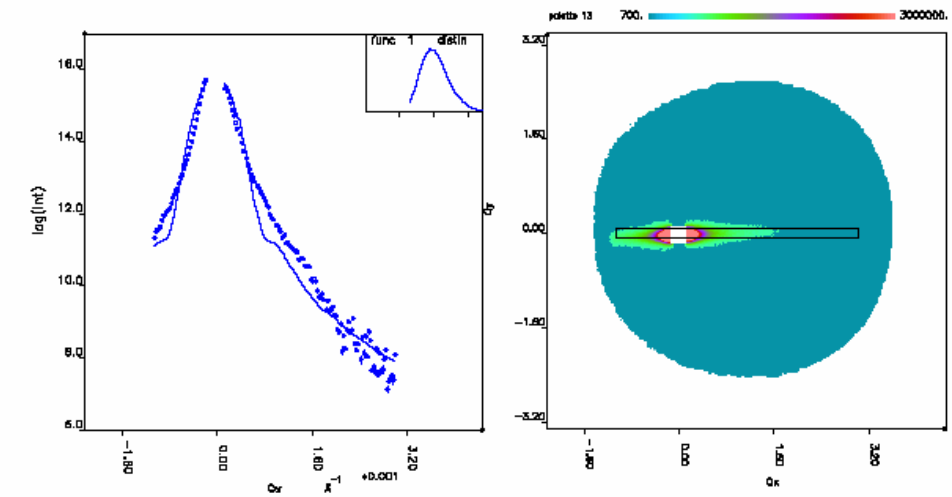


Fig.2. 2D fit of the unannealed tungsten sample

A rough two dimensional data treatment was made by using the cylinder model, which in comparison to the previously used model of ellipsoid proved to be a better approximation of the nano-scale structure of the tungsten wires. The low q range allowed us to obtain information about the size of the most elongated potassium filled bubbles.

Institut für Festkörperforschung
Forschungszentrum Jülich GmbH
D-52425 Jülich

Experimental Report
of Neutron Scattering Experiments
at the FRJ-2 Reactor

Proposal number:	KW3-04-016, DKD-04-005		
Experiment title:	The large-scale structures and morphologies formed by the co-crystallization of PEB-n random copolymers and paraffin waxes (5)		
Dates of experiment:	9.09.2004 – 24.09.2004 11.03.2005 – 15.03.2005 19.04.2005 – 22.04.2005 19.05.2005 – 23.05.2005	Date of report:	29.05.2006
Experimental team: Names	Addresses		
Aurel Radulescu, Emmanuel Kentzinger, Jörg Stellbrink, Dietmar Schwahn, Manfred Heiderich	Forschungszentrum Jülich Institut für Festkörperforschung D-52425 Jülich Germany		
Local Contact:	Dr. E.Kentzinger, Dr.D.Schwahn		

Experimental report text body

As conventional SANS revealed [1,2] the PEB-n random copolymers form in solution needle-like aggregates in decreasing temperature. When paraffin wax is added to the polymer solution the scattering patterns collected under different contrast conditions and revealing the conformation of the polymer or wax within the common aggregates change strongly in comparison with the case of single polymer or paraffin wax solutions. When the copolymer self-assembles at temperatures higher than the wax crystallization point a complex shish-kebab-like morphology seems to occur [2]. Formation and structural evolution of such morphology was only partially understood by analysing the conventional SANS data. These allowed only an incomplete characterization of the common polymer-wax aggregates which seem to extend rather vastly in size surpassing the length scale covered by the conventional SANS method. Therefore new structural investigations were performed by involving the focusing-SANS (F-SANS) and the ultra- SANS (U-SANS) instruments set-up at the FRJ-2 reactor in Jülich. Combining the conventional-, focusing- and ultra-small angle neutron scattering methods the multilevel structures showing characteristic sizes from 10 μm to 1 nm and formed upon cooling in common solutions of semi-crystalline PEB-7.5 copolymers and waxes could be fully characterized. The conformation of the polymer and wax molecules within the common aggregates was analysed separately by using the contrast matching. The structural and density parameters of the aggregates have been evaluated using models. The experimental data collected in a slit-geometry at the U-SANS double-diffractometer were transformed into the pin-hole geometry according to a procedure described in [3]. An example of the scattering data collected over a very wide Q-range is given in Fig.1 where the scattering patterns under wax contrast are present at two temperatures within the wax-copolymer common aggregation regime for a mixed solution of 0.6% low M_W PEB-7.5 copolymer and 4% C_{24} wax in decane. The Q^{-2} power law behaviour at intermediate Q and the peak at around $Q^*=0.025$ $Å^{-1}$ shown at 0°C (also by the polymer scattering patterns not presented here) reveal a co-crystallization of polymer and wax into thin, very large platelets forming a correlated arrangement.

The lateral size of these platelets can be evaluated by analysing the Guinier regime identified at low Q. The model analysis of this morphology in terms of the paracrystalline structure factor applied to an ensemble of finite size discs, each disc being made by a wax and a polymer embedded layers is presented as solid line. The wax scattering pattern at -10°C reveals that the wax massively crystallizes and grows from thin platelets into large objects with sharp interfaces (Q^{-4} power law at higher Q). From an inspection of the low Q data measured by FSANS (10^{-4} to $2x10^{-3}$ Å^{-1}) and USANS (below 10^{-4} Å^{-1}) a coexistence of two structures showing different characteristic sizes can be identified (the vertical arrows indicate the observed Guinier regimes). The smaller shows a 2-dimensional morphology that is revealed by the Q^{-2} power law regime identified within the Q range covered by FSANS. The unified Beaucage equation [4] for multiple structural levels and scattering data extending over many decades describes well the F-SANS data and prove the existence of thick plates (d=0.23μm) which must result by the filling of the space between the thin correlated platelets identified at 0°C with continuously growing wax crystallites. The additional scattering at low Q indicates the formation of much larger aggregates whose characterization is difficult. This is done by analysing scattering data where the Guinier regime is absent. A 1-dimensional morphology can be tentatively attributed to these aggregates via the assignment of Q^{-1} for low Q. The neutron scattering findings for this later aggregation stage were complimented by the microscopy observations shown in Fig.2. Different copolymer-wax combinations and wax amounts investigated for the case of the copolymer self-assembling event occurring well-before the wax crystallization point revealed basically the same common crystallization features as those described above and thus, the formation and evolution of a hierarchical morphology showing multilevel structures. First, the polymer 1-dimensional morphology showing density modulations occurs [1]. Then, wax crystals are formed and nucleated by the crystalline nuclei of the polymer needles. The wax grows laterally in large platelets also involving further polymers still in solution. The primordial polymeric structure serves to template the lateral platelets in a correlated shish-kebab-like arrangement. Late aggregation leads to a massive crystallization of the wax surplus and formation of large compact 1-dimensional structure.

References: [1] H.S.Asbaugh et al., Macromolecules 35, 7044, 2002; [2] A.Radulescu et al., J.Pol.Sci. B 42, 3113, 2004; [3] D.Schwahn, and M.H.Yoo, *Springer Proceedings in Physics* vol.10, Springer Verlag: Berlin, Heidelberg, New York, Tokyo, 1986, p 83; [4] G.Beaucage, J.Appl.Cryst. 29, 134, 1996.

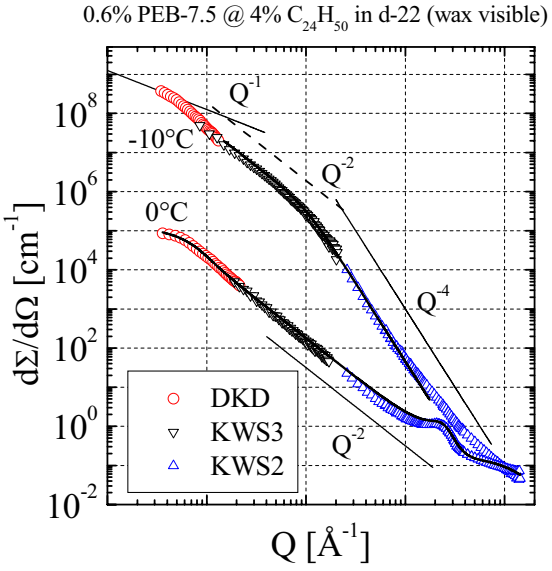


Fig.1 - Scattering patterns under wax contrast from a mixed solution of 0.6% low M_W PEB-7.5 copolymer and 4% C_{24} wax in decane.

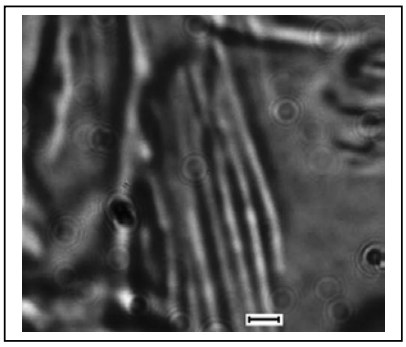


Fig.2 – A micrograph of the aggregates formed in the same solution at -10°C (scale bar 10μm).

Institut für Festkörperforschung
Forschungszentrum Jülich GmbH
D-52425 Jülich

Experimental Report of Neutron Scattering Experiments at the FRJ-2 Reactor

Proposal number:	KW3-05-004		
Experiment title:	Fractal geometry study on different polymerization stage of Ziegler-Natta $MgCl_2/TiCl_4$/polypropylene system by small angle neutron scattering		
Dates of experiment:	2005-9-29	Date of report:	2005-12-20
Experimental team: Names	Addresses		
Zhang, Li Han, Charles C. Chen, Dongfeng Dong, Jinyong	Beijing P. O. Box 275(30),Beijing,China,102413 State Key Laboratory of Polymer Physics and Chemistry, Institute of Chemistry, Chinese Academy of Sciences, Beijing, P. R. China,10080 Beijing P. O. Box 275(80),Beijing,China,102413 State Key Laboratory of Polymer Physics and Chemistry, Institute of Chemistry, Chinese Academy of Sciences, Beijing, P. R. China,10080		
Local Contact:	Wim Pyckhout-Hintzen, Jörg Stellbrink, Reiner Zorn，		

Experimental report text body

Since the Ziegler-Natta catalyst was discovered in the laboratories of K. Ziegler in the fall of 1953and G. Natta in spring of 1954 it is commercially very important and deserves the attention of the scientific and engineering community. So the growth of the polymer particle has aroused much interest in both academic and industrial laboratories [1-3]. This kind of molecules has been studied in the past years using a variety of techniques such as light microscopy, electron scanning microscopy, atomic force microscopy and optical tweezers yielding information on the shape, dynamics and mechanical properties [4]. However, these techniques require samples to be tethered to surfaces which could change the real shape of the polymer. The understanding and the full control achieved on the catalyst “replication” phenomenon have given a real “new dimension” by fractal geometry [5-7]. With the aid of concepts in fractal geometry, the relevant aspects of the structure of polypropylene based on Ziegler-Natta supported catalysts can be derived from small angle neutron scattering (SANS) experiments. The purpose of the SANS measurements performed on KWS-1 and KWS-3 was to get the fractal information on Ziegler-Natta $MgCl_2/TiCl_4$/polypropylene system.
In this experiment, we investigated the effects of polymerization time. To get different shape we choose two of them polymerized in high pressure and the last one polymerized in normal pressure. The polymerization time of the two samples polymerized in high pressure is half an hour and one and a half hour respectively, named as the medium sample and the big sample according to their sizes of the particles. The polymerization time of the last one polymerized in normal pressure is half an hour named the small sample. All the other conditions are the same among the three samples. One part of the experiment was carried out on KWS-1. for Q values ranging from 2.0×10^{-3} Å^{-1} to 1.5×10^{-1}Å^{-1}. The other part of the experiment was carried out on KWS-3. for Q values ranging from 2.2×10^{-5} Å^{-1} to 2.7×10^{-3}Å^{-1}. The data was gotten at room temperature with air in these three samples.

From Fig.1 we can see the scattering from the three samples shows a Q^{-4} power-law behavior which leads to the conclusion that from the scattering data we only can see a porous mass fractal due to the interaction between the particles and the air.

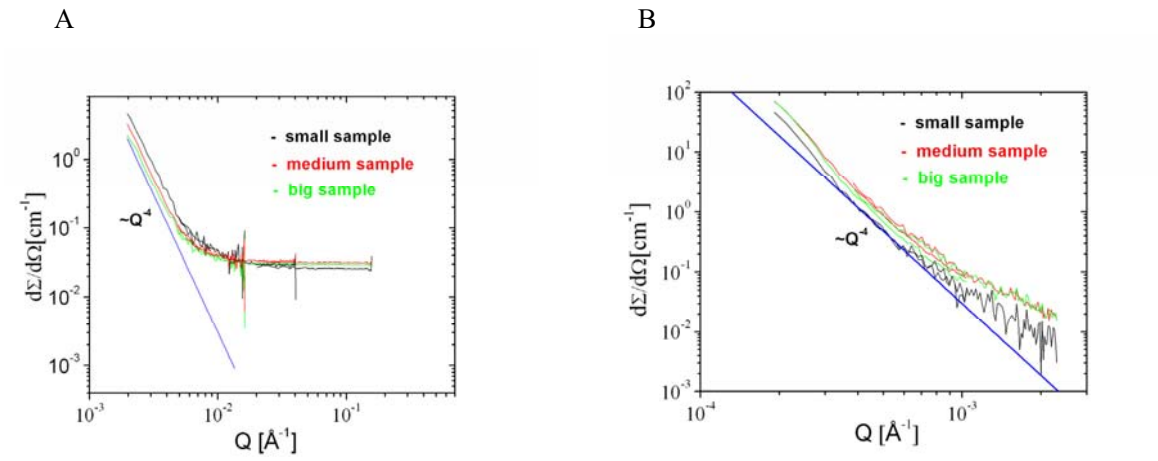


Fig. 1 Scattering pattern from PP measured at room temperature by using (A) KWS1 (B) KWS3 spectrometers in jülich. The power law regimes are indicated.

The interaction between the particles and the air is so strong that we can't get the other fractal information we really need from the experiments. So in future experiments we will measure with the sample solved in some kind of deuterated solvent in order to avoid this interaction to get the information of fractal geometry under consideration.

References

1. Ziegler, K., Angew. Chem., 1952, 64, 323.
2. Natta, G., Pasquon L., and Giachetti, E., Angew. Chem., 1957, 69, 213.
3. Natta, G., J. Polym. Sci., 1955, 16, 143.
4. John Boor, Jr., Ziegler-Natta Catalysts and Polymerizations, Academic Press, New York,1979
5. Mandelbrot, B. B., The Fractal Geometry of Nature, Freeman Press, San Francisco, 1982
6. Mccarthy, D. W., Mark, J. E., Schaefer, D. W., Journal of Polymer Science: Part B: Polymer Physics, 1998, 36,1167
7. Schaefer, D. W., Science, 1989, 243, 1023

Institut für Festkörperforschung
Forschungszentrum Jülich GmbH
D-52425 Jülich

Experimental Report
of Neutron Scattering Experiments
at the FRJ-2 Reactor

Proposal number:	KW3-06-001		
Experiment title:	Wax conformation within the large-scale morphologies in mixed solution of PEB-n copolymers and paraffin waxes		
Dates of experiment:	11.03.06-14.03.06	Date of report:	06.06.2006
Experimental team: Names	Addresses		
Aurel Radulescu	Forschungszentrum Jülich Institut für Festkörperforschung D-52425 Jülich Germany		
Local Contact:	Dr.E.Kentzinger		

Experimental report text body

The self-assembly of poly(co-olefins) in dilute solution has been shown via SANS to yield either plate-like or needle-like micelles-like micelles [1,2]. The resultant supramolecular structures are dependent upon the copolymer architecture. The crystalline-amorphous diblock co-polymers yield self-assembled hairy plates while the corresponding random co-polymers yield one-dimensional needle shaped aggregates. The PEB-n random copolymers (n - the number of ethyl sides per 100 backbone carbons) show selectivity in their wax crystal modification capacities depending on the ethylene content of the backbone. This behavior relates to the graded ethylene content of PEB-n copolymers that leads to different self-assembling temperatures: the lower n, the higher the self-assembling temperature [2]. All PEB-n copolymers self-assemble in open 1-d structures. This conclusion has stimulated further structural studies of multiblock copolymers in solution where blocks represent poly(ethylene-butene) random copolymers (PEB-n) showing graded ethylene contents and thus, different crystallization degrees. Recently [3] conventional and focusing SANS studies of self-assembling in decane solution of a triblock and tetrablock PEB-n copolymers have been performed. The structural results complimented by microscopy observations concluded that these materials form in solution core-shell structures showing a 1D overall aspect which associate and give raise to occurrence of large scale spherulitic-like soft aggregates with sizes within the micrometric range. The conventional SANS investigations have shown that these multiblock copolymers modify the wax crystals morphology from big compact crystals with sizes of hundreds of micrometers as in the case of pure wax solution into 2-dimensional thin aggregates. In the present study we investigated at the focusing SANS KWS3 instrument several mixed solutions of paraffin waxes and multiblock copolymers in order to obtain first information about the wax conformation at larger scale within the common wax-copolymer aggregates. An example of raw scattering patterns collected at room temperature from a mixed solution of C36 wax and tetrablock PEB-2.6/6.0/10.9/13.2 copolymer is shown in Fig.1. Unfortunately, the copolymers were available only in protonated state therefore, for allowing the wax visible we were forced

to use highly protonated solvent in order to match it with the polymer. This led to a strong multiple scattering effect which can be identified by the very low level of the samples forward scattering in comparison with that of the empty beam. Accordingly, the samples transmission is very low. Nevertheless, qualitative information about the wax morphology can be obtained which are expected to be useful for a more complete view of the structure and morphology of the common wax-copolymer aggregates in a combination with the conventional SANS data.

References: [1] D.Schwahn et al., Macromolecules 35, 861, 2002; [2] A.Radulescu et al. J.Pol.Sci. B Pol.Phys. 42, 3113, 2004; [3] experimental reports KW2-05-002; KW3-05-001 FRJ-2 Jülich.

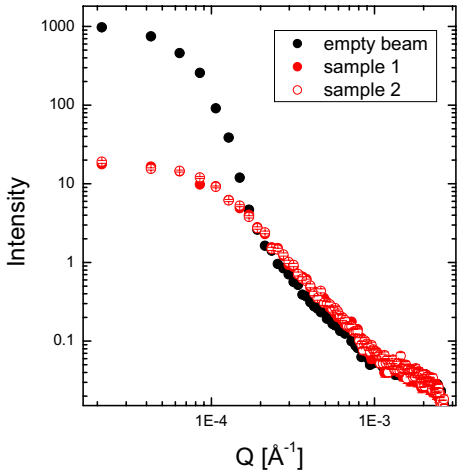


Fig.1 – The scattering intensities of two wax-copolymer mixed solutions in decane for C36 and PEB-2.6/6.0/10.9/13.2 tetrablock in parallel with the empty beam measurement.

Institut für Festkörperforschung
Forschungszentrum Jülich GmbH
D-52425 Jülich

Experimental Report
of Neutron Scattering Experiments
at the FRJ-2 Reactor

Proposal number:	KW3-06-002		
Experiment title:	**Measurement of two reference samples in the framework of the benchmarking of the SANS instruments of the HGF**		
Dates of experiment:	20.03. - 22.03.2006	Date of report:	12.06.2006
Experimental team: Names	Addresses		
E. Kentzinger	Institut für Festkörperforschung, Forschungszentrum Jülich		
Local Contact:	E. Kentzinger		

Experimental report text body

The purpose of this experiment was to measure two samples in the framework of the HGF SANS benchmarking. The two samples were:

1) A Polystyrene-block-Polyisoprene-block-Polystyrene (PS-PI-PS) Copolymer Thermoplastic
2) Silica spheres coated with stearyl alcohol in toluene

Those two samples were already measured on KWS-1 and KWS-2 by D. Schwahn. We report here on the results obtained on the PS-PI-PI sample.

The measurements were performed with entrance slit apertures of 2x2 mm^2 (i.e., a wave vector transfer resolution δQ of 10^{-4} $Å^{-1}$) and a beam size at sample position of 80x20 (width x height) mm2. The intensity at sample position was 300 n/s and the counting time 5 hours. After empty beam measurement, we deduced a transmission of 64 %. The radial average, subtracted from the empty beam, is depicted in Fig. 1.

We deduced a Q^{-4} dependency of the scattered intensity, in agreement with the KWS-1 and KWS-2 measurements performed at higher Q values (Top-right insert in Fig. 1).

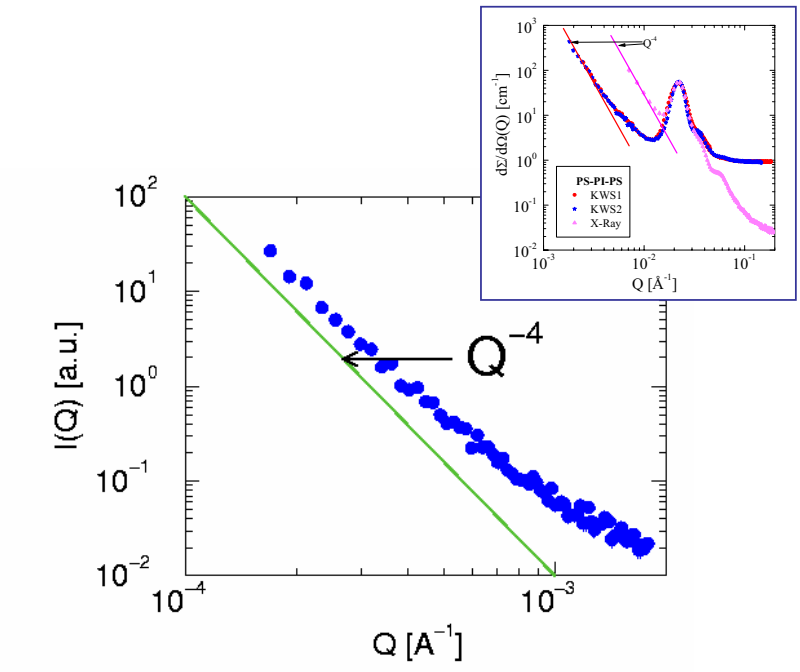
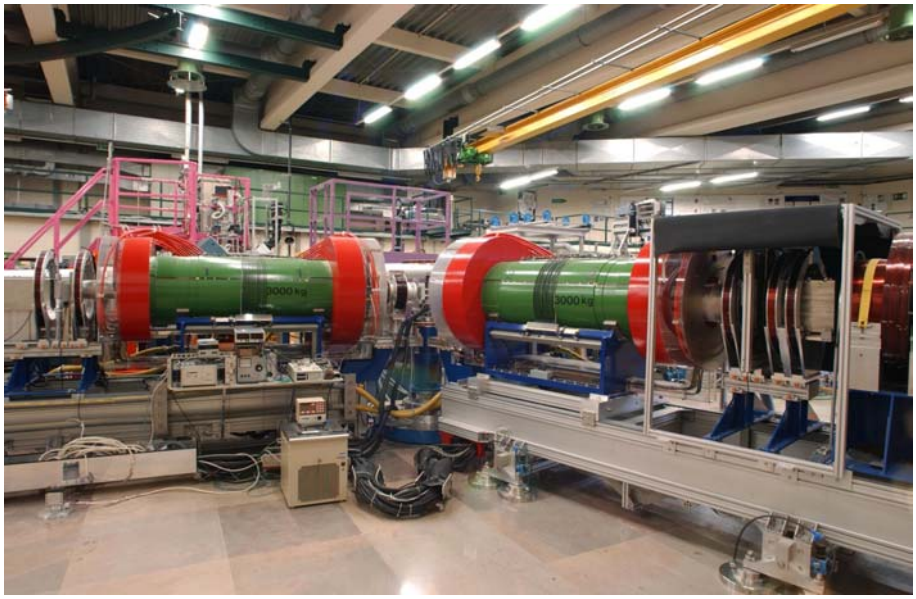


Fig. 1: Radial average of the very-small angle neutron scattering (V-SANS) measured at KWS-3 on a PS-PI-PS thermoplastic. Top-right: Radial averages obtained at KWS-1 and KWS-2

Neutron Spin Echo Spectrometer (NSE)



Instrument Parameters

Beam tube:	NLIIB curved guide
Monochromators:	polarizing multilayer mirror (FeGe) velocity selector (DORNIER) $\Delta\lambda/\lambda = 0.1$ (or 0.2)
Incoming beam ***- Cross section of guide:*** ***- Sample size:***	 4.5 cm (height) × 3 cm (width) 4 cm × 4 cm (max.)
Collimation:	by source and sample size or wire collimators 0.5° × 0.5°
Polarised neutron flux at sample (λ = 8 Å):	8×10^5 n/cm^2 s (natural collimation)
Wavelength range:	$\lambda = (8 \pm 2)$ Å, alternative mirror (6 ± 2) Å
Momentum transfer range:	0.01 ... 1.5 Å^{-1}
Fourier time range (in STD set-up):	0.04 ... 48 ns
Max. field integral:	0.5 Tm
Analyzer:	30 × 30 cm^2 CoTi supermirror Venetian blind
Detector:	32 × 32 1cm^2 cells ^{3}He multidetector

Instrument Responsible

Dr. Michael Monkenbusch Tel. +49-(0)-2461-61-4314 Email: m.monkenbusch@fz-juelich.de
Dr. Ralf Biehl Tel. +49-(0)-2461-61-4685 Email: ra.biehl@fz-juelich.de

Institut für Festkörperforschung
Forschungszentrum Jülich GmbH
D-52425 Jülich

Experimental Report
of Neutron Scattering Experiments
at the FRJ-2 Reactor

Proposal number:	NSE-04-004		
Experiment title:	Study of the charged groups dynamics in polystyrene based random ionomers		
Dates of experiment:	03.02. – 04.02.2005 13.05. – 17.05.2005 01.10. – 04.10.2005	Date of report:	18th May 2006
Experimental team: Names	Addresses		
Edoardo De Luca (Thomas Waigh – analysis)	Department of Chemistry, University of Durham, Durham, DH1 3LE, UK. (Biological Physics, Department of Physics and Astronomy, University of Manchester, Manchester, M60 1QD, UK.)		
Local Contact:	Ralf Biehl, Michael Monkenbusch		

Experimental report text body

The dynamics of phase separated micellar solutions of randomly sulphonated polystyrene ionomers in deuterated toluene were examined with neutron spin echo spectroscopy (NSE). The correlation functions demonstrated single exponential decays with a constant background offset. The relaxation rate (Γ) of the ionomer micelles in the q range 0.0268 to 0.131Å^{-1} were diffusive ($\Gamma \sim q^{-2}$) at small length scales with a hydrodynamic mesh size independent of molecular weight as expected for the collective diffusive mode of a cross-linked gel. At large length scales the scattering due to the phase separated network of micelles was stationary on time scales <20ns (**figure 1**). The results are in agreement with the model developed in previous small-angle neutron scattering experiments for concentrated solution of ionmeric micelles (**figure 2**) [1]. The NSE results for the associating ionomers are markedly different to the Zimm dynamics ($\Gamma \sim q^{-3}$) previously observed with semi-dilute and cross-linked polymers in a good solvent [2]. The ionomeric cross-links thus have a large impact on the chains dynamics at the nano second time scale. Increasing the temperature (T) of the samples causes the motion of the ionomer gel to increase in proportion to T/η (η is the viscosity, **figure 3**). No clear signature of the activated dynamics of the ionomeric stickers as a function of temperature was discernable.

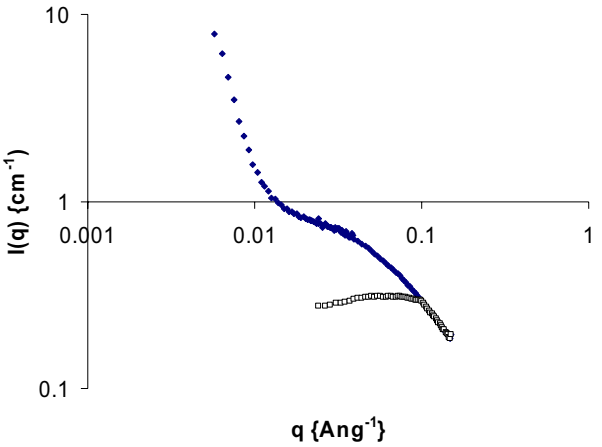


Figure 1. Small angle neutron scattering from 10%w/w random PSS ionomers (diamonds). The squares show the ergodic amplitude in the time window <20ns from NSE. These amplitudes are attributed to the motion of the internal gel dynamics of the ionomer micelles (**figure 2**).

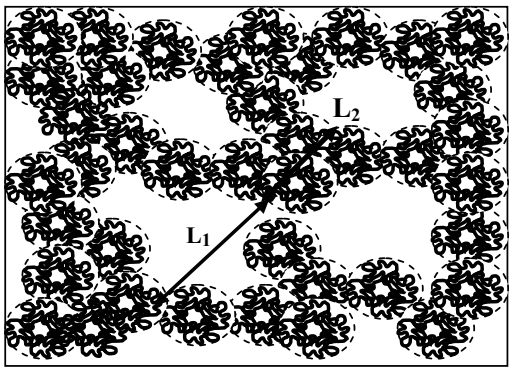


Figure 2. Morphology of random ionomer gels deduced from small angle neutron scattering. Two lengths scales are important; the average chord length (related to L_1 and L_2) of the microphase separated micellar structure and the average intrachain mesh size (ξ).

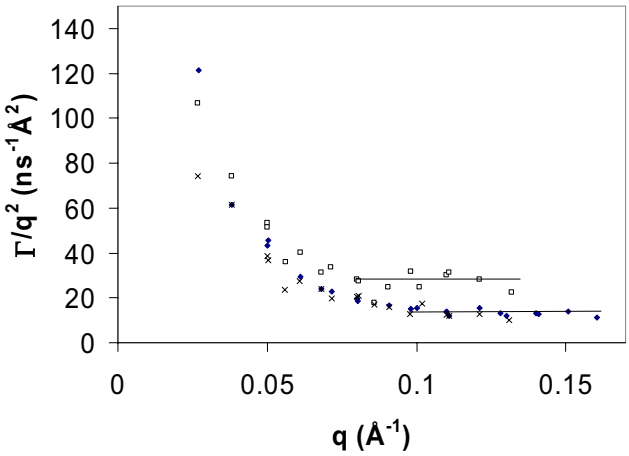


Figure 3. Relaxation rates for random PSS ionomers. Two different molecular weights (crosses and diamonds) are shown and samples at elevated temperatures (squares). The straight lines indicate the diffusive modes found at small length scales.

References

[1] E. de Luca, T.A.Waigh, J.S.Kim, W.Hintzen, 'Phase separation in randomly charged polystyrene sulphonate ionomers', *Polymer*, 46, 2005, 7109-7117.

[2] B.Ewen, D.Richter, B.Lehnen, 'Segmental diffusion of polymer molecules in solution as studied by means of quasi-elastic neutron scattering', *Macromolecules*, 12, 1980, 876-880.

Institut für Festkörperforschung
Forschungszentrum Jülich GmbH
D-52425 Jülich

Experimental Report
of Neutron Scattering Experiments
at the FRJ-2 Reactor

Proposal number:	NSE-04-007		
Experiment title:	Local dynamics and entanglements of hydrogen-bonded polymers		
Dates of experiment:	04.03. – 11.03.2005	Date of report:	05.06.2006
Experimental team: Names	Addresses		
Adrian S. Muresan Wim H. de Jeu	FOM-Institute for Atomic and Molecular Physics Kruislaan 407 1098 SJ Amsterdam Netherlands		
Local Contact:	Dr. Michael Monkenbusch		

Experimental report

In this project we studied the segmental dynamics of equilibrium polymers formed by strongly directional quadruple hydrogen-bonded dimmers. We observed a clear effect of friction heterogeneity along the backbone of the self-assembled chains. The friction heterogeneity has been attributed to the hydrogen-bonding connector groups, which in our case are quite bulky in comparison to the hydrocarbon spacers that link pairs of them in the basic molecular building blocks.

The system studied consisted of units of 30-60 covalently bonded THF monomers with quadruple hydrogen-bonding ureidopyrimidinone (UPy) groups attached at each end (see Figure 1). Two different types of labelling A and B were prepared, illustrated in Figure 2. In labelling A the elementary chains (≈ 74 monomers) were identical and had 15% hydrogenated monomers distributed at random in a matrix of deuterated monomers.. In labelling B we had a mixture of 15% hydrogenated elementary chains with ≈ 30 monomers and 85% deuterated elementary chains with ≈ 86 monomers. Due to the breaking and recombination of hydrogen bonds, the spatial distribution of the hydrogenated elementary chains was random. The two types of labelling A and B are qualitatively similar, the only difference being the size of the randomly placed hydrogenated unit: a single monomer in case A, a full elementary chain of ≈ 30 monomers in case B.

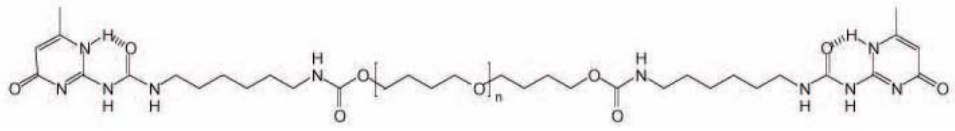


Figure 1. Chemical structure of the hydrogen-bonded polymer used. The two Upy groups at the ends of the single elementary chain pictured form four hydrogen bonds, giving rise to larger hydrogen-bonded polymers.

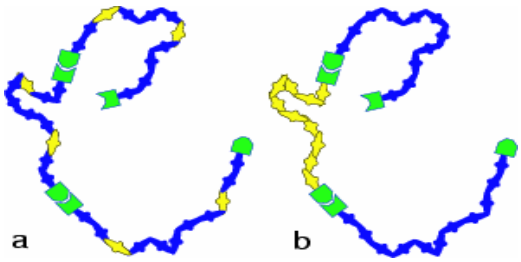


Figure 2. Schematic representation of the labeled polymeric systems A (a) and B (b). The deuterated blue and hydrogenated yellow monomers are covalently bonded while the green blocks represent the quadruple hydrogen bonding Upy groups.

The correlation functions for samples A and B as obtained by NSE at T = 353 K can at each q be well fitted by a function of the form $S(q, t) \sim \exp(-\alpha q^2\sqrt{t})$. The segmental friction coefficient ζ can be calculated from the coefficient of the exponential of decay $S(q^2\sqrt{t})$ from the relation $\zeta/l^2 = k_B T/(3\pi\alpha^2)$, in which l represents the rms size of a polymer segment. From the final results displayed in Figure 3 we obtain

$\zeta/l^2 = 0.84\times10^8$ Nsm^{-3} for labelling A;
$\zeta'/l'^2 = 2.55\times10^8$ Nsm^{-3} for labelling B.

The decay is slower for the system with labelling B as compared to labelling A. This is in conflict with the standard Rouse model for dynamically homogeneous chains, which predicts that because of dynamic scale invariance the two segmental friction coefficients should be the same.

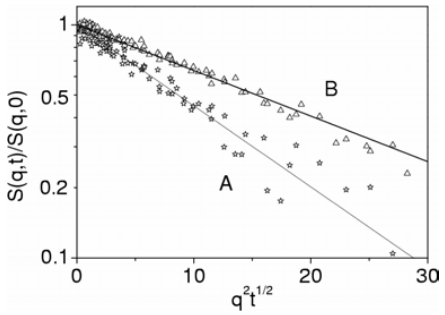


Figure 3. Logarithmic plot of the correlation function for the system with labelling A and B, respectively, at T = 353 K. The data is plotted as a function of $q^2\sqrt{t}$, with q represented in nm^{-1} and t in ns.

We attribute the observed slowing down for labelling B to dynamic heterogeneity of the system, which can be understood as follows. For labelling A, the labelled monomers are distributed along the elementary chain. Only small monomers close to the large connecting UPy groups will feel their effect and slow down. The dynamics of the majority of small monomers further way from the bulky groups will not be affected by this effect. In contrast, for the labelling B, due to the fact that the full elementary chain is labelled, the slowing-down effect by the bulky connectors cannot be avoided. Hence by incorporating the larger friction experienced by the bulky UPy groups into the Rouse model, the observed slower relaxation can be rationalized.

A.S. Muresan, J.L.A. Dubbeldam, H. Kautz, M. Monkenbusch, R.P. Sijbesma, P. van der Schoot, W.H. de Jeu: *Dynamic Heterogeneity in Hydrogen-Bonded Polymers*, Phys Rev. E (submitted).

Institut für Festkörperforschung
Forschungszentrum Jülich GmbH
D-52425 Jülich

Experimental Report
of Neutron Scattering Experiments
at the FRJ-2 Reactor

Proposal number:	NSE-04-008		
Experiment title:	Low energy spin dynamics in CMR perovskites		
Dates of experiment:	28.02. – 02.03.2005	Date of report:	19 May 2006
Experimental team: Names	Addresses		
F.J.Bermejo P. Romano	Dept. Electricity & Electronics, University of the Basque Country, Bilbao Rutherford Appleton Laboratory, Chilton, Didcot, UK		
Local Contact:	M. Monkenbusch		

Experimental report text body

The experiment was basically a feasibility test aiming to carry out NSE studies on the diffusive spin dynamics on $La_{0.7}Pb_{0.3}Mn_{1-x}Fe_xO_3$ ($0 < x < 0.3$) colossal magneto-resistive manganites. Previous data measured on a backscattering instrument (IN10 at ILL) evidenced the presence of diffusive spin dynamics for an iron-doped sample with x=0.2 which macroscopically behaves as an unconventional spin-glass.

Results measured on NSE are summarized in the accompanying graphs that depict the time and temperature dependence of the observed relaxation for the above mentioned sample.

Further measurements carried out using the IN11 spectrometer at the ILL gained from the previous experience using NSE and yielded a complete set of relaxation curves.

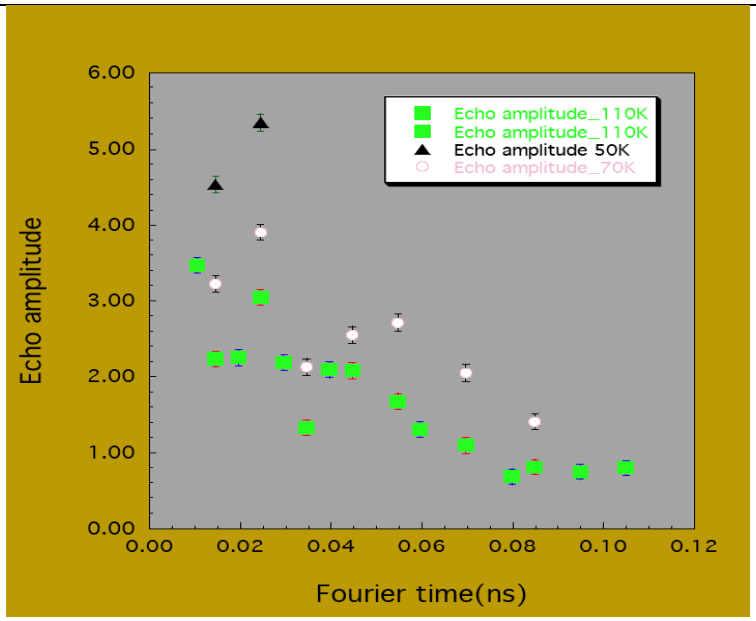


Fig.1 Echo amplitudes for the x=0.2 sample and some temperatures.

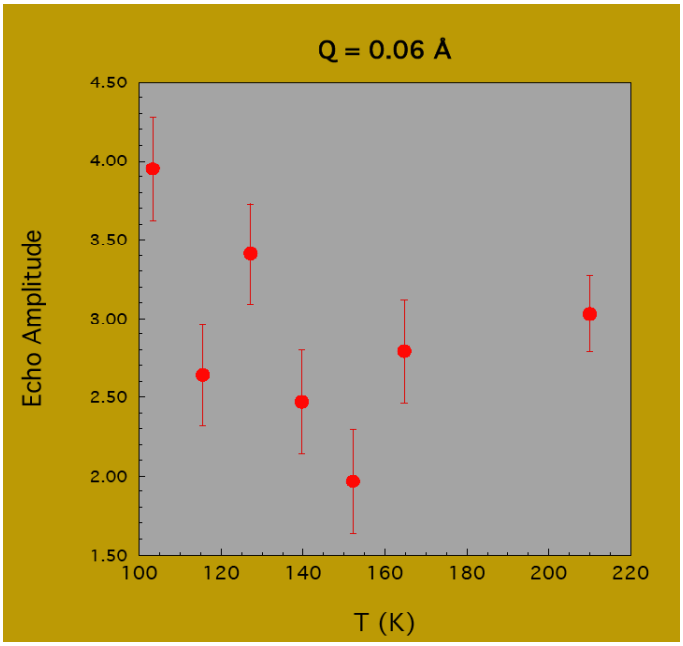


Fig.2 Temperature dependence of the echo amplitude for a fixed value of the momentum-transfer

Institut für Festkörperforschung
Forschungszentrum Jülich GmbH
D-52425 Jülich

Experimental Report
of Neutron Scattering Experiments
at the FRJ-2 Reactor

Proposal number:	NSE-04-018		
Experiment title:	**Diffusion of methylpentane in silicalite**		
Dates of experiment:	15/08-24/08/2004	Date of report:	22/02/2006
Experimental team: Names	Addresses		
H. Jobic	Institut de Recherches sur la Catalyse 2, avenue Albert Einstein 69626 Villeurbanne France		
Local Contact:	M. Monkenbusch		

Experimental report text body

MFI-type zeolites (ZSM-5 and its Al-free analogue silicalite) are amongst the most industrially important zeolites. For example, MFI-type zeolites are used to separate linear from branched alkanes (the branched alkanes are of higher value to increase the octane number of gasoline). In the real processes, there are usually mixtures of several linear and branched alkanes. Predictions are difficult since the reported diffusivities of each component vary in a wide range, despite extensive work. Whereas the diffusion of linear alkanes in silicalite has been studied by several techniques [1], there is much less work on the diffusion of branched alkanes in this zeolitic structure.

The diffusion of isobutane, the simplest branched alkane, has been recently measured by neutron spin-echo (report NSE-02-012). The diffusion of a slightly bulkier molecule: 2-methylpentane, one of compounds obtained from petroleum refining or catalytic cracking, could also be measured on the NSE spectrometer. Intermediate scattering functions were recorded at different Q values and temperatures (e.g. Figure 1). This is the first time that the diffusion of this alkane is characterized by a microscopic method (PFG NMR does not work for this system).

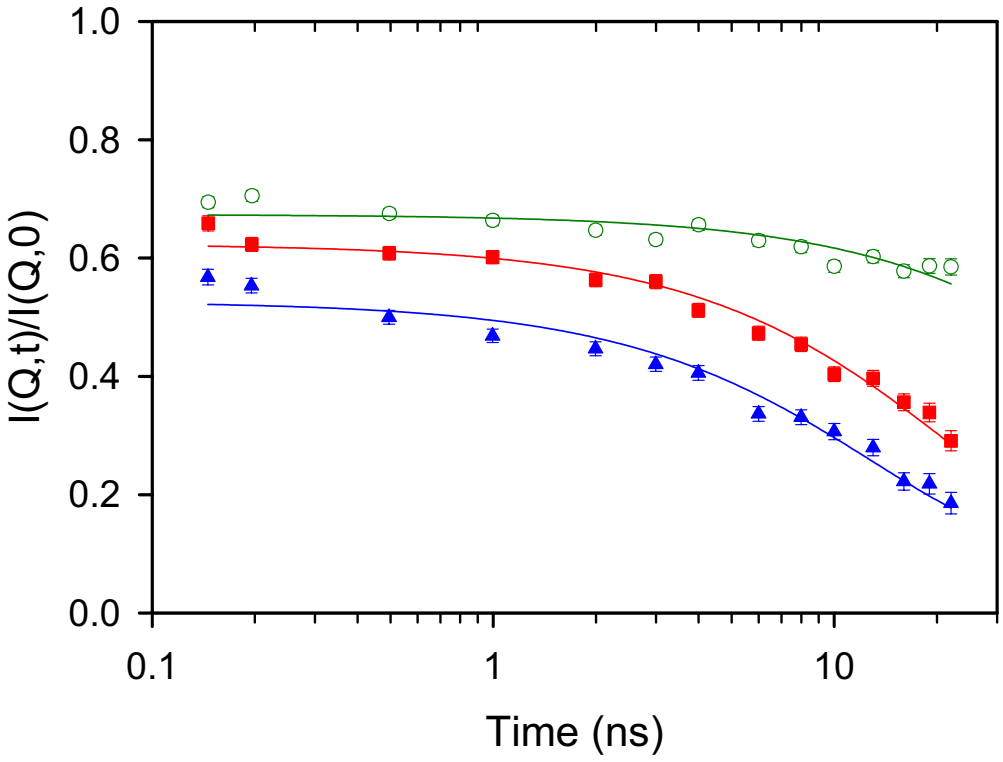


Figure 1. Normalised intermediate scattering functions obtained for 2-methylpentane at 580 K in silicalite, for different Q values: (○): 0.1, (■): 0.2, and (▲) 0.3 Å^{-1}.

Diffusion coefficients were extracted using a jump diffusion model. The value obtained at 490 K: 3.5 × 10^{-12} m^2s^{-1}, is noticeably lower than the diffusivity of isobutane at the same temperature: 2.1 × 10^{-12} m^2s^{-1} (ratios varying from 2 to 20 have been reported in the literature from macroscopic techniques). An activation energy for diffusion could also be estimated: 36 kJ/mol.

Reference

[1] H. Jobic, J. Mol. Catal. A 158 (2000) 135.

Institut für Festkörperforschung
Forschungszentrum Jülich GmbH
D-52425 Jülich

Experimental Report
of Neutron Scattering Experiments
at the FRJ-2 Reactor

Proposal number:	NSE-04-019		
Experiment title:	Single-time relaxation dynamics in molecular nanomagnets		
Dates of experiment:	03 March 2005	Date of report:	17/05/2006
Experimental team: Names	Addresses		
Flavio Carsughi	Dipartimento di Scienze Applicate ai Sistemi Complessi (SASC) Universita' Politecnica delle Marche, Via Brecce Bianche I-60131 Ancona Italy INSTITUT FUER FESTKOERPERFORSCHUNG Forschungszentrum Juelich Leo Brand Strasse D-52425 Juelich		
Roberto Caciuffo	Institute for Transuranium Elements Postfach 2340, D-76125 Karlsruhe		
Local Contact:	Michael Monkenbusch		

Experimental report text body

An exploratory experiment was performed to verify the possibility of measuring by neutron spin-echo spectroscopy the long-time decay of the intra-cluster spin-spin correlation functions in a molecular nanomagnet.

The investigated system was a ring-shaped octanuclear cluster, containing 7 Cr ions (s = 3/2) and one Mn ion (s = 5/2) with antiferromagnetic nearest-neighbor exchange coupling and a spin ground state S = 1. Three grams of polycrystalline, partially deuterated material (90% D atoms per cluster) have been used in a standard cryostat.

The NSE spectrometer has been used in its standard mode of operation at fixed Fourier times, between 0.01 and 10 ns. In spite of the high degree of deuteration, hydrogen spin-incoherent scattering was still very high, comparable in magnitude to the nuclear coherent scattering and about a factor 50 more intense than the magnetic signal. Data have been collected with the π flipper removed for a value of the momentum transfer Q= 0.8 $Å^{-1}$ corresponding to minima in the elastic coherent scattering distribution (away from Bragg peaks).

Measurements have been performed at T= 19 K, while scanning the Fourier time by varying the precession field in the accessible range. Polarization analysis to normalize the echo amplitude has been performed removing the $\pi/2$ flippers. The results were disappointing. The experiment suffered by low counting rate and bad signal to noise ratio. Although some decay of the spin-spin temporal correlation function has been observed, the quality of the data is such that no substantial conclusions can be reached. The physics addressed is, however, quite interesting and further efforts seems justified. Further experiments should be performed on fully deuterated samples, for Q values where the S(Q) function is not contaminated by Bragg peaks. Furthermore, the echo group should be measured for an extended range of the symmetry coil current to better define the amplitude and the phase of the signal.

Institut für Festkörperforschung
Forschungszentrum Jülich GmbH
D-52425 Jülich

Experimental Report
of Neutron Scattering Experiments
at the FRJ-2 Reactor

Proposal number:	NSE-04-022		
Experiment title:	Tuning the structural α-relaxation in Poly(methyl methacrylate) (PMMA) by neutron spin echo		
Dates of experiment:	26/01/2005-02/02/2005	Date of report: 08/02/2005	
Experimental team: Names	Addresses		
Caroline Genix Juan Colmenero Arantxa Arbe Dieter Richter	Donostia International Physics Center, Apdo. 1072, 20080 San Sebastian, SPAIN Dpto. de Física de Materiales, UPV/EHU, , “ , “ , “ Unidad de Física de Materiales, CSIC-UPV/EHU, “ , “ , “ IFF, FZJ, Jülich, Germany		
Local Contact:	Michael Monkenbusch		

Experimental report text body

With these NSE experiments on fully deuterated poly(methyl methacrylate) (PMMA-d8) we wanted to investigate the temperature dependence of the dynamic structure factor at its first maximum ($Q_{max} \approx 0.8 Å^{-1}$). With increasing temperature, this first peak in the structure factor S(Q) shows an increase of intensity and shifts towards lower Q-values, suggesting that it mainly reflects interchain correlations. In this way, we would isolate the α-relaxation in a polymer showing a very important contribution of the secondary relaxation as studied by other techniques [1].

With a wavelength of 8Å and by using the furnace we have investigated a temperature range between the glass transition temperature T_g (T_g =400K) and ≈500K. TiZi was used to determine the resolution function at the same Q-value. As can be seen in Fig. 1, a decay of the dynamic structure factor is observed for all temperatures investigated, even at the glass transition; there, however, the dynamics of the α- or structural relaxation should be too slow to lead to a decay of the interchain correlations in the NSE dynamic window. For this reason a further measurement on the sample was performed at 300K. Even at such low temperature, clearly in the glassy state, a non negligible decay was observed (see Fig. 1).

The relaxation times have been obtained from a fit of the NSE data by Kohlrausch-Williams-Watts (KWW) functions $S(Q,t) \propto \exp-[t/\tau(T)]^{\beta}\}$ with a stretching exponent β of 0.5. The descriptions delivered can be seen in Fig. 1. Figure 2 shows the temperature dependence of the so obtained time scales τ(T). Well above T_g the times follow the behaviour expected for the α-relaxation as observed from spectroscopic techniques (DS) [1]. Below 450K, strong deviations with respect to such temperature dependence become evident.

This phenomenon reminds the decoupling of timescales reported for 1,4-polybutadiene at the first minimum of S(Q) [2], that was later interpreted in terms of the merging of the α- and β-relaxations in that polymer [3]. However, such a scenario would not explain our NSE results on PMMA, since they have been obtained at the first peak, where the contributions from secondary relaxations should be strongly suppressed [3].

These astonishing results suggest that either the resolution function of the NSE instrument changes from the PMMA-d8 to the TiZi measurements (e.g. due to a small change in the sample size) or that indeed a relaxational process different from the α-process –a secondary relaxation- leads to the decay of the correlations at the first peak in this polymer. It is of utmost importance to clarify this question by checking the results on the low temperature measurements with an independent experiment.

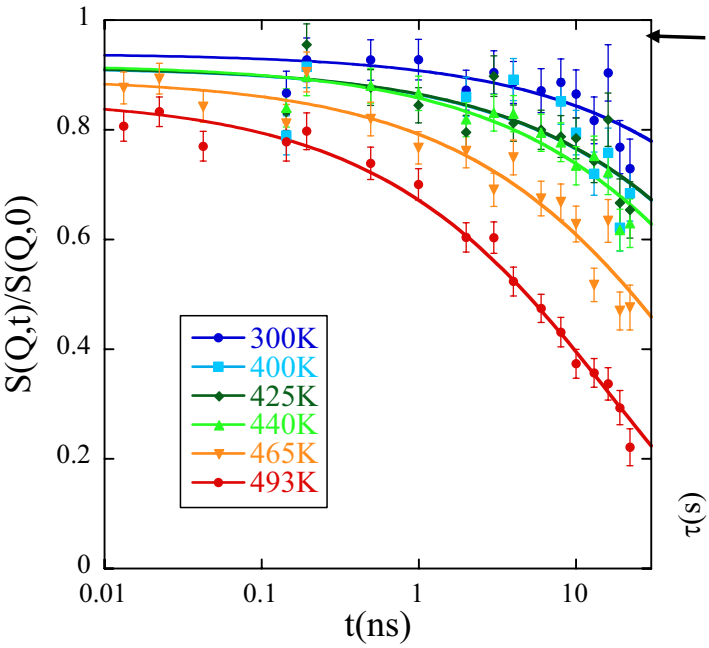


Figure 1: Dynamic structure factor measured by NSE on a fully deuterated PMMA sample at the first maximum ($0.8Å^{-1}$) and the temperatures indicated. The solid lines are fits with KWW functions with β=0.5.

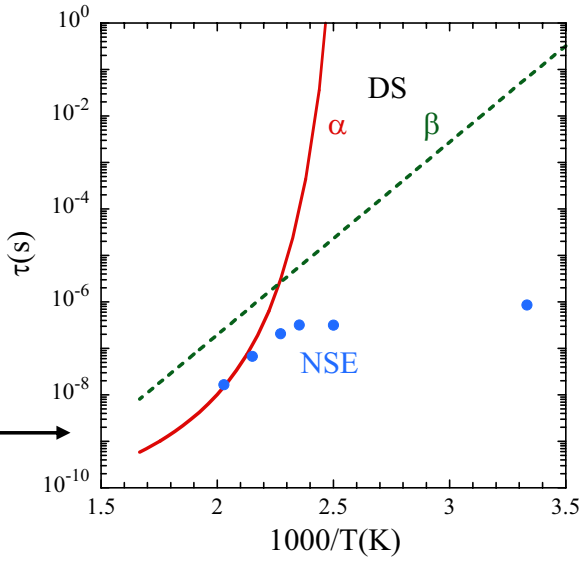


Figure 2: Arrhenius plot of the relaxation times obtained from these NSE measurements (circles) and those by dielectric spectroscopy for the α- (solid line) and β-relaxations (dotted line) [1].

References

[1] R. Bergman, F. Alvarez, A. Alegría and J. Colmenero, J. Chem. Phys. **109**, 7546 (1998)

[2] D. Richter, R. Zorn, B. Farago, B. Frick and L. J. Fetters, Phys. Rev. Lett. **68**, 71 (1992)

[3] A. Arbe, D. Richter, J. Colmenero, B. Farago, Phys. Rev. E **54**, 3853 (1996)

Institut für Festkörperforschung
Forschungszentrum Jülich GmbH
D-52425 Jülich

Experimental Report
of Neutron Scattering Experiments
at the FRJ-2 Reactor

Proposal number:	NSE-04-024		
Experiment title:	**Chain dynamics of a short 1.5kg/mol PE chain in a long matrix**		
Dates of experiment:	May 2005	Date of report:	15.5.2006
Experimental team: Names	 Addresses		
M. Monkenbusch M.Zamponi A.Wischnewski	IFF, FZ Juelich		
Local Contact:	M. Monkenbusch		

Experimental report text body

In the reptation model for long chain polymer melts the topological constraints due to entanglements are described by a virtual tube which follows the primitive path of the observed test chain. However, this definition means, that a test chain with a length in the order of one entanglement distance can not be captured in a tube. This conclusion does not depend on the matrix properties and holds even if the matrix chains are much longer than the test chain.

For a short chain with a length in the order of one entanglement length (M_e) in a long matrix therefore free Rouse behaviour is expected. A previous measurement (NSE_04_015) of labeled 2.5kg/mol polyethylene (PE) chains in a long chain (36kg/mol) PE matrix revealed deviations from the expected Rouse behaviour. The chain length was slightly above the entanglement length (M_e=2kg/mol for PE). Therefore now the dynamic structure factor of a 1.5kg/mol PE chain in the same long matrix has been measured.
The experiments have been performed at a temperature of 509K (as before), covering a momentum transfer range from 0.5nm^{-1} to 0.96nm^{-1}. The data were corrected for resolution and background, latter estimated from a fully deuterated sample of the matrix chains.

In comparison to the 2.5kg/mol chain the dynamic of the 1.5kg/mol chain is considerably faster but still do not follow the expected Rouse behaviour (fig.1). Comparing the data to the Rouse function with known Rouse rate (solid lines), a strong slowing down of the dynamic is observed. Also by fitting the Rouse rate the data cannot be described. If the fit is limited to times below the entanglement time (7ns) the short time range agree with the Rouse model (dashed lines) but at longer times the dynamic is significantly slower. Although the chain is below the entanglement length and therefore should not be object of topological constraints the deviation of the dynamic structure factor indicates that the short chain is captured in the tube built by the long chain matrix.

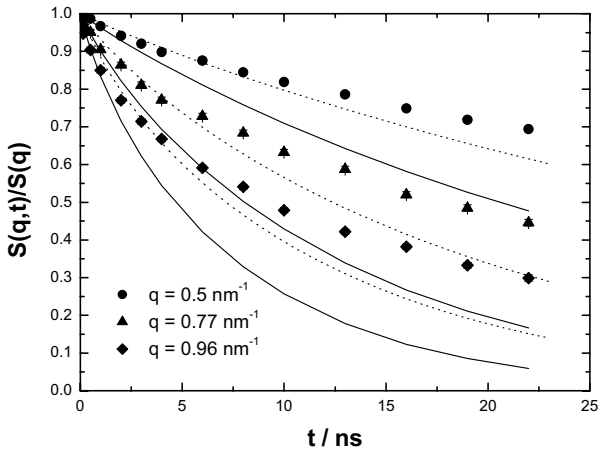


Fig.1: Dynamic structure factor of a h-1.5kg/mol chain in d-36kg/mol matrix. Q-values as indicated in the plot. Lines: solid Rouse expectation, dashed Rouse fit.

For the lowest q-value the center of mass diffusion dominates and internal modes are negligible so that the center of mass mean squared displacement can be extracted (fig.2). For a free Rouse diffusion a linear time dependence of the mean squared displacement is expected, whereas the data show a clear subdiffusive motion ($<r^2>\sim t^{0.7}$). This again points to the surprising result that the short chains, although they are below M_e, can not move freely.

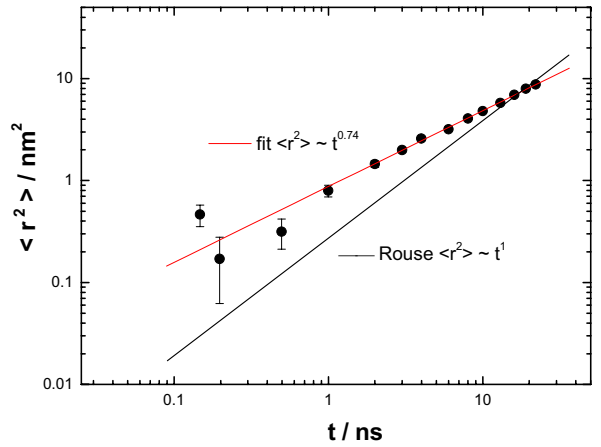


Fig.2: Center of mass mean squared displacement for $q=0.5nm^{-1}$ for the h-1.5kg/mol chain in the long chain matrix. The black line shows the Rouse expectation of normal diffusion, the red line is a fit of the data.

Institut für Festkörperforschung
Forschungszentrum Jülich GmbH
D-52425 Jülich

Experimental Report
of Neutron Scattering Experiments
at the FRJ-2 Reactor

Proposal number:	NSE-05-001		
Experiment title:	**Dynamics of glass forming liquids in the low-Q range. A direct comparison between a low molecular mass glass former and the polymer counterpart.**		
Dates of experiment:	16-05-05 to 29-05-05 and 06-06-05 to 13-06-05	Date of report: 03-10-2005	
Experimental team: Names	Addresses		
1.Ángel Alegría 2. Madhusudan Tyagi 3. Arantxa Arbe	Física de Materiales, Facultad de química, Apdo. 1072, 20080 San Sebastián, SPAIN Donostia International Physics Center, 20018, San Sebastián, SPAIN Unidad Física de Materiales (CSIC-UPV/EHU), Apartado 1072, 20080 San Sebastián SPAIN		
Local Contact:	M. Monkenbusch		

Experimental report text body

This work was carried out to examine the dynamics of trimer of vinyl acetate (3VA) which is a short chain counterpart of poly(vinyl acetate). The dynamics of polymeric systems and low molecular weight glass formers (GFL) share some universal features and have been paid lot of attention recently[1-3]. Typically, in GFL and polymeric systems one observes so-called anomalous sub-linear diffusive regime below Q=1Å^{-1} which is revealed in time dependence of intermediate scattering function S(Q,t) as ~$t^{-\beta}$. This is also reflected in Q-dependence of characteristic times as $\tau \sim Q^{-2/\beta}$. This anomalous diffusive regime continues down to very low Q values where finally, one expects the dynamics of GFL is to be dominated by center of mass diffusion of entire molecule which should be reflected in a simple exponential time decay of S(Q,t). In this simple diffusive regime momentum transfer dependence of characteristic times also becomes weaker and is given by $\tau \sim Q^{-2}$. On the contrary, one expects a crossover to Rouse dynamics in polymeric systems at low Q-values because of their chain connectivity. Our measurements on 3VA were made keeping this objective in mind.

The experiments were carried out on a fully protonated 3VA sample at 350K in order to get characteristic time scales in the window of NSE. The scattering functions were measured at 4 different Q-values viz. 0.08, 0.14, 0.20 and 0.28Å^{-1}. The wavelength of the incoming neutron beam was set to 8Å. As NSE signal strength in incoherent samples is weak because 2/3rd of the sample intensity is converted to background, each Q value was measured over a period of two days for 10 Fourier times to get good statistics. The sample was taken in a rectangular aluminium container of 5cm by 5cm size. As multiple scattering effects are efficiently suppressed, sample thickness was chosen to be 0.5mm which resulted in a transmission of close to 50% and increased very much needed intensity. In addition, empty container was measured at all the Q-values under identical conditions. The resolution of the instrument was also measured at different Fourier times using carbon powder.

Fig.1 represents all incoherent intermediate scattering functions measured at different Q values. The good quality of experimental points can be seen from low error bars in this figure. The scattering functions are fitted to stretched exponential function, $S(Q,t) \sim \exp\{-(t/\tau)^{\beta}\}$, where τ is the characteristic time. The characteristic times so obtained are shown in Fig.2 where in double logarithmic plot relaxation times are plotted against Q. The presence of anomalous diffusive regime at higher Q values is apparent through stretched exponential behaviour of S(Q,t). It can also be seen that all the three higher Q values can be described coherently with the same stretching parameter (which is deduced from the master curve of these Q-values). The characteristic time scales at the higher Q values follows a power law in momentum transfer dependence in the form of $\tau=\tau_0 Q^{-2/\beta}$ which is typically the case for a glass former as mentioned above.

However, a clear single exponential time decay of scattering function can be seen at lowest Q value measured in our experiments which is also shown in Fig.1 along with all other Q-values. Interestingly, a clear deviation of characteristic time from the trend followed by higher Q-values can be seen in Fig.2 Simple exponential behaviour of S(Q,t) followed by weaker momentum transfer dependence of characteristic time clearly shows that a crossover to simple diffusive-like mechanism takes place in our sample somewhere between 0.14 and 0.08$Å^{-1}$.

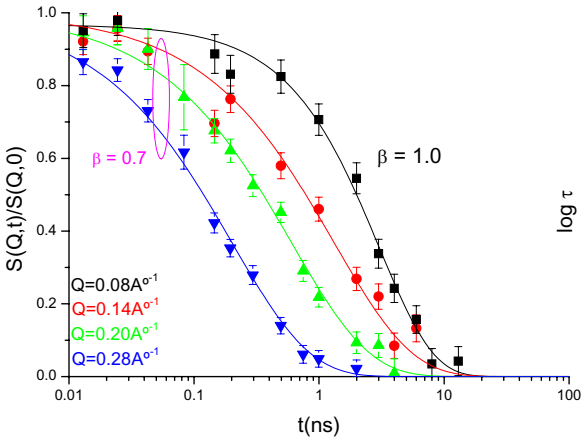


Fig.1: Incoherent intermediate scattering functions at different Q values. The solid lines are fits to stretched exponential function with β values shown in figure.

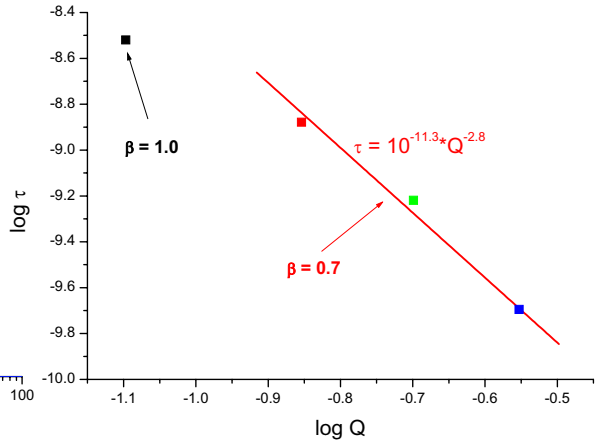


Fig.2: A double logarithmic plot of characteristic times derived from fitting of scattering function against momentum transfer Q.

References:

[1] Wayne L. et al. Macromolecules **37** (2004) 4711
[2] Yifu Ding, et al Macromolecules **37** (2004) 9264
[3] L. Goitiandia, A. Alegría, Journal of Chemical Physics **121** (2004) 1636

Institut für Festkörperforschung
Forschungszentrum Jülich GmbH
D-52425 Jülich

Experimental Report
of Neutron Scattering Experiments
at the FRJ-2 Reactor

Proposal number:	NSE-05-004		
Experiment title:	Tuning the structural α-relaxation in Poly(methyl methacrylate) (PMMA) by neutron spin echo – Checking low T-contributions		
Dates of experiment:	24/04/2005-26/04/2005	Date of report:	28/11/2005
Experimental team: Names	Addresses		
Caroline Genix Arantxa Arbe Juan Colmenero Dieter Richter	Donostia International Physics Center, Apdo. 1072, 20080 San Sebastian, SPAIN Unidad de Física de Materiales, CSIC-UPV/EHU, “ , “ , “ Dpto. de Física de Materiales, UPV/EHU, , “ , “ , “ IFF, FZJ, Jülich, Germany		
Local Contact:	Michael Monkenbusch		

Experimental report text body

The aim of this experiment was to clarify previous NSE results obtained by us on fully deuterated poly(methyl methacrylate) (PMMA-d8) ($T_g \approx 400K$) [1]. In that work [1], we had measured the dynamic structure factor S(Q,t) at its first maximum ($Q_{max} \approx 0.8Å^{-1}$) in the temperature range between room temperature (RT) and 500K. TiZr was used to determine the resolution function at the same Q-value. Our goal was to tune the α-relaxation of PMMA and to investigate whether or not it follows the general trend observed in more simple polymers like polyisoprene or polybutadiene. As can be seen in Fig. 1, a decay of $S(Q_{max},t)$ was observed for all the temperatures investigated and, surprisingly, even at 300K, which corresponds to the glassy state in PMMA. There, however, it is clear that the α-relaxation can not be responsible for any decay of the correlations in the dynamic window of NSE. Then they are only two possibilities: i) the resolution function changes from the PMMA-d8 to the TiZr measurements or ii) a relaxational process different from the α-relaxation (like maybe the β-relaxation) leads to the decay of the intermolecular correlations in this polymer (note that it would be quite an unexpected behavior).

That’s why, in order to understand this intriguing question, we have measured the same sample at RT and 50K in the cryostat. Both spectra were indistinguishable within the experimental uncertainties. Since at 50K, the scattering of the sample should be completely elastic (note that the tunneling of the ester methyl group does not lead to quasi-elastic broadening in the coherent case), we can conclude that the observed decay is due to our first hypothesis and the resolution function determined by the TiZr sample is inappropriate to correct our previous results [1].

References:

[1] C. Genix et al., Experimental Report NSE-04-022

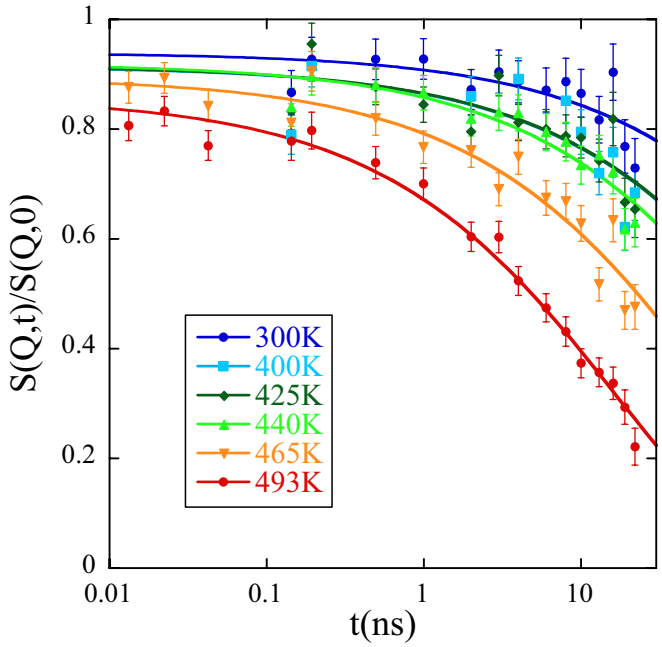


Figure 1: Dynamic structure factor measured by NSE [1] on a fully deuterated PMMA sample at the first maximum ($0.8Å^{-1}$) and the temperatures indicated. The solid lines are fits with KWW functions with β=0.5. The results of the present experiment show that these data have to be recorrected, since no decay of the structure factor is really observed at 300K.

Institut für Festkörperforschung
Forschungszentrum Jülich GmbH
D-52425 Jülich

Experimental Report
of Neutron Scattering Experiments
at the FRJ-2 Reactor

Proposal number:	NSE-05-005		
Experiment title:	**PEO chain dynamics in a PEO-PMMA blend**		
Dates of experiment:	04.04-20.04.2005	Date of report:	29.11.2005
Experimental team: Names	Addresses		
Katarzyna Niedzwiedz Dr. Andreas Wischnewski Prof. Dr. Dieter Richter Dr. Michael Monkenbusch	IFF, Forschungszentrum Jülich, 52425 Jülich IFF, Forschungszentrum Jülich, 52425 Jülich IFF, Forschungszentrum Jülich, 52425 Jülich IFF, Forschungszentrum Jülich, 52425 Jülich		
Local Contact:	Dr. Michael Monkenbusch Dr. Ralf Biehl		

Experimental report text body

Dynamics in polymer blends is a very attractive field of research. The unsolved problem of how local friction arises in chemically heterogeneous environments makes it impossible to predict the properties of a blend system on basis of what is known about the behaviour of each component of the mixture. Of particular interest are blends where the dynamics of the pure components are well separated in time, i.e. with a very different glass transition temperature T_g of the components. In this case the slow (high T_g) ingredient forms a stiff network within the faster (low T_g) component.

This work was motivated by unexpected NMR results reported by Lutz et al. [1] on a miscible PMMA/PEO blend, a system with widely separated glass transitions ($T_g^{PEO} \approx 210$ K, $T_g^{PMMA} \approx 400$ K). Lutz found that the PEO dynamics appears to be completely decoupled from the PMMA motions, e.g. at the glass transition of PMMA the PEO motion in terms of the rotational autocorrelation function is 12 orders of magnitude faster than that of PMMA. Apparently, the PEO chain can relax locally as if it was embedded in a PEO melt rather than a solid PMMA matrix.

We have investigated two samples with 25% PEO in a matrix of 75% deuterated PMMA. In the first case, for a fully protonated PEO component, the measurement was performed at T = 375 K for Q-values of 0.05, 0.08, 0.10, 0.14, 0.17 and 0.20 $Å^{-1}$. This sample has contrast only between the protonated PEO chains and the deuterated PMMA matrix, which is stiff at this temperature. Therefore we see no dynamic signal of the sample, the NSE response is purely elastic (fig. 1).

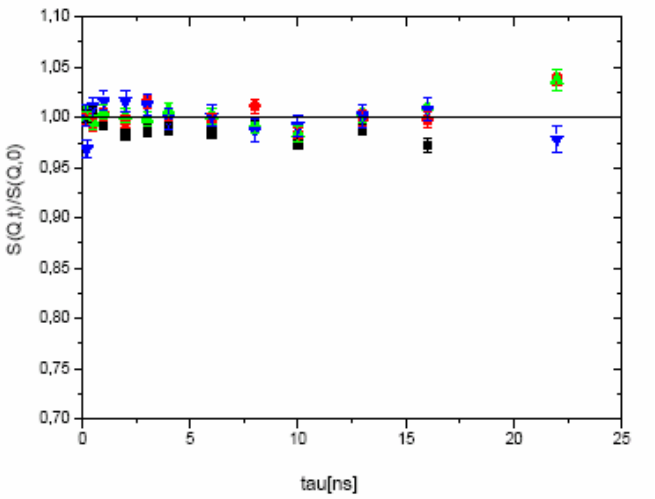


Fig. 1 The intermediate scattering function S(Q,t)/S(Q,0) obtained for a PEO/PMMA blend system (25% h-PEO and 75% d-PMMA) at T = 375 K and for different Q-values: Q = 0. 05 $Å^{-1}$ (squares), Q = 0. 08 $Å^{-1}$ (circles), Q = 0.10 $Å^{-1}$ (triangle up), Q = 0.14 $Å^{-1}$ (triangle down). The solid line at S(Q,t)/S(Q,0) = 1 is a guide for the eye.

The second sample was composed of 12.5 % h-PEO and 12.5 % d-PEO in the deuterated PMMA matrix. Here, the protonated PEO chains have a dynamic contrast to the deuterated PEO chains, the PEO dynamics becomes visible by NSE. Measurements were done at three different temperatures (T = 370 K, 400 K and 430 K) at Q = 0.20 $Å^{-1}$, Q = 0.28 $Å^{-1}$ and Q = 0.36 $Å^{-1}$. Moreover at T = 400 K also lower Q-values (Q = 0.08 $Å^{-1}$, Q = 0.14 $Å^{-1}$ and Q = 0.17 $Å^{-1}$) have been measured. The results for T = 400 K are compared to the scattering function of pure PEO at the same temperature in fig. 2. The dynamics for PEO in the blend is significantly slower than for the pure PEO system.

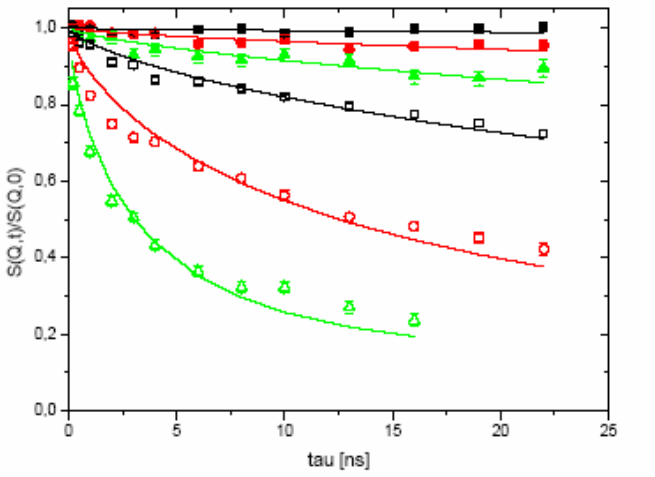


Fig. 2 Neutron spin echo data obtained for PEO (10% h-PEO in a d-PEO matrix, open symbols) compared to PEO in the blend (12.5% h-PEO, 12,5% d-PEO and 75% d-PMMA, full symbols) at T = 400 K. Squares correspond to data at Q = 0.10 $Å^{-1}$, circles to Q = 0. 15 $Å^{-1}$ and triangles to Q = 0.20 $Å^{-1}$. Solid lines are guides for the eye.

[1] T.R. Lutz et al., Macromolecules, 36, 1724 (2003)

Institut für Festkörperforschung
Forschungszentrum Jülich GmbH
D-52425 Jülich

Experimental Report
of Neutron Scattering Experiments
at the FRJ-2 Reactor

Proposal number:	NSE-05-007		
Experiment title:	**Confinement effects of diblock copolymers in bicontinuous microemulsions – A dynamic study**		
Dates of experiment:	23.06.2005	Date of report:	28.06.2006
Experimental team: Names	Addresses		
Simona Maccarrone Henrich Frielinghaus	Forschungszentrum Jülich GmbH, Institut für Festkörperforschung, D-52425 Jülich Forschungszentrum Jülich GmbH, Institut für Festkörperforschung, D-52425 Jülich		
Local Contact:	Olaf Holderer		

Experimental report text body

Microemulsions are thermodynamically stable and macroscopically homogeneous mixtures of two non miscible components like oil and water mediated by surfactant molecules. Under certain conditions of temperature and surfactant concentration, oil and water result completely mixed (1 phase region) and the minimum quantity of surfactant requested to solubilize equal amounts of oil and water is a measure for its "efficiency". Recently, it was found out that the addition of amphiphilic diblock copolymer can increase enormously the efficiency of the emulsification capacity of non ionic surfactants (boosting effect). Microscopically we have the monolayer of surfactant separating domains of oil and water. From a previous work done by Endo it was shown that the polymer decorates the membrane increasing its stiffness.
The Helfrich theory describes the elastic properties of the surfactant membrane to be dominating. The bending rigidity κ is the modulus of the mean curvature and by the Gaussian random field theory we are able to get this energetical parameter from a relationship involving the domain spacing d and the correlation length ξ. These two structural parameters are easily obtained from small angle neutron scattering (SANS) measurements.
Computer simulations by Auth initially came up with the idea, that polymer confinement could play a role in microemulsions. The simulations focus on anchored diblock copolymers. For low confinement the theoretical values were confirmed. At intermediate confinement the sensitivity of the polymer effect is increased due to the higher presence of the polymer at the interface. At very high confinement the diblock copolymer effect could be reversed to anti-boosting since then the anchoring does not play a role anymore and the entropy of a flat polymer is highly unfavourable. Our task was to verify and quantify eventually the maximum polymer boosting.
Several bicontinuous microemulsions were studied intensively rendering the domain size d comparable to the polymer size (R_g). Two symmetric diblock copolymers PEP_{22}-PEO_{22} and PEO_{10}-PEO_{10} were chosen. The domain spacing of the microemulsions was varied by the use of different oils (hexane, octane, decane,

dodecane, tetradecane) influencing the efficiency primarily. Experimentally we found at relatively large d/R_g where the confinement is weak, the sensitivity of the polymer boosting effect unchanged. With increasing confinement (d/R_g closer to 1) the sensitivity is only slightly enhanced, and finally a strongly reversed behaviour (anti-boosting) is observed. The behaviour at medium confinement shows a much lower sensitivity compared with the theory of Auth. This enhancement would have been very interesting for applications, while the reversed behaviour could be an explanation how red blood particles could sneak into small vessels.

After the structure of such microemulsions has been determined by SANS, we performed neutron spin-echo (NSE) experiments that is a well-suited method for studying the dynamic properties of microemulsions, since the Fourier time range of this technique matches with the characteristic time range of the membrane dynamics. This technique allows the direct determination of the "bare" (not renormalized) bending rigidity and changes due to the confinement of the diblock copolymers.

In this case the membrane bending rigidity is obtained by numerically integrating S(q,t) from the Zilman-Granek theory. The bending modulus is the only free fitting parameter. Our intention was to compare finally this bare membrane bending modulus to the renormalized one as obtained from SANS.

The NSE experiments have been carried out on the length scales of the confinement, where the theoretical maximum occurred. We performed the experiments in film contrast, i. e. with deuterated decane and dodecane, deuterated water and protonated surfactant and polymer (PEP_{22}-PEO_{22}). For both oils we prepared samples with and without added diblock copolymer at the same surfactant concentration, thus giving a direct access to the changes induced by the diblock copolymers.

From preliminary observations the relaxation time of the polymer doped microemulsion is faster than for the equivalent pure microemulsion. For example, in the case of decane, plotting the ratio of the NSE spectra relative to the system with and without polymer, we can observe a first comparison (see fig. 1). The variation of decay in time is visible for medium and high q while nothing almost changes for low q-values. Moreover from preliminary fittings no variation for the bending rigidity in the case of C10 is found while a decrease is obtained for dodecane. Everything in agreement with the previous SANS experiments. Anyway further more precise analysis are in progress.

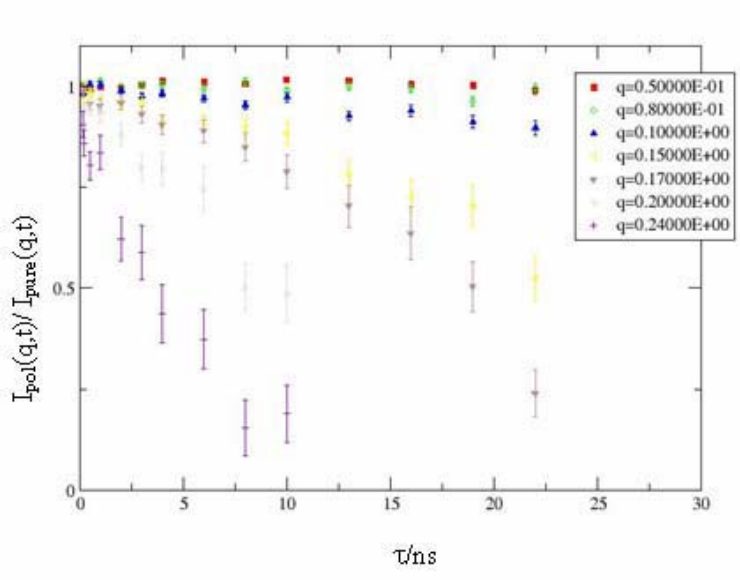


Figure 1. Ratio between NSE spectra for different q (nm^{-1}) values relative to decane-samples with and without polymer vs. time.

Institut für Festkörperforschung
Forschungszentrum Jülich GmbH
D-52425 Jülich

Experimental Report
of Neutron Scattering Experiments
at the FRJ-2 Reactor

Proposal number:	NSE-05-008		
Experiment title:	**High Q dynamic structure factor of PEO**		
Dates of experiment:	13.06-25.06.2005	Date of report:	29.11.2005
Experimental team: Names	 Addresses		
Katarzyna Niedzwiedz Dr. Andreas Wischnewski Dr. Michael Monkenbusch Prof. Dr. Dieter Richter	IFF, Forschungszentrum Jülich, 52425 Jülich IFF, Forschungszentrum Jülich, 52425 Jülich IFF, Forschungszentrum Jülich, 52425 Jülich IFF, Forschungszentrum Jülich, 52425 Jülich		
Local Contact:	Dr. Michael Monkenbusch Dr. Ralf Biehl		

Experimental report text body

Recent studies of a PEO / PMMA polymer blend by neutron spin echo spectroscopy (NSE-05-005) and backscattering (BSS-05-008) in Jülich revealed surprising results: At temperatures below and around the glass transition temperature T_g of the stiff PMMA matrix ($T_g \approx 400$ K) the dynamics of the low T_g component PEO ($T_g \approx 200$ K) is fast but restricted to small volumes of about 1 nm (confinement). Furthermore, the collective dynamics of PEO (as determined by NSE at lower Q) appears to be significantly slower compared to the self-motion as measured by BSS.

The observed behaviour resembles effects of a tube confinement in long entangled polymer melts, however, with unexpected (and probably unphysical) parameters for the reptation model.

The aim of this experiment was to compare the deviations of the PEO dynamics in a PEO/PMMA blend from the Rouse behaviour to the dynamics of the chains in the pure PEO system. Since the molecular weight is several times longer than the entanglement distance, it is expected that in the pure PEO system we will observe deviations from the Rouse model, which are due to entanglements and can be explained in the framework of the reptation model.

The investigated PEO chains had the same molecular weight as the one used in the PEO/PMMA blend (M_w = 24 kg/mol). To measure the coherent single chain dynamic structure factor a sample with 10% pratonated-PEO and 90% deuterated-PEO was used. The wavelength of the incoming neutrons was 8 Å, the temperatures were T= 350K, 375 K, 400 K, 430 K and the momentum transfer was 0.05 $Å^{-1}$ < Q < 0.30 $Å^{-1}$. The data were corrected for resolution (graphite) and background (fully deuterated PEO).

An example for the obtained intermediate scattering function S(Q,t)/S(Q,0) for PEO at T = 375 K is shown in fig. 1. The data were fitted with the Rouse model at short times up to 5 ns, with the friction coefficient as a free parameter. One clearly sees the deviations from the model at longer times as expected for long chain polymer melts.

However, to fully explore the reptation regime one has to perform this experiment with entirely entangled PEO chains (higher molecular weight) and at Fourier times up to at least 100 ns.

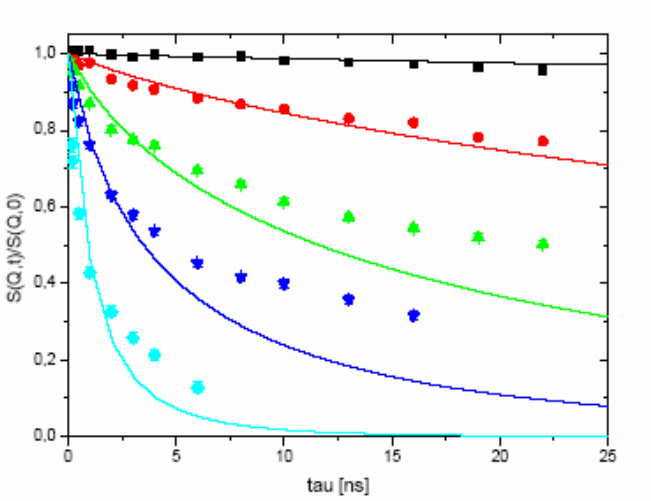


Fig. 1 Dynamic structure factor of PEO at T = 375 K, black squares corresponds to data at Q = 0.05 $Å^{-1}$, red circles - Q = 0.10 $Å^{-1}$, green triangles Q = 0.15 $Å^{-1}$, dark blue triangles Q = 0.20 $Å^{-1}$ and light blue diamonds Q = 0.30 $Å^{-1}$. Solid lines represent a fit with the Rouse model restricted to short times (from 0 to 5 ns).

Institut für Festkörperforschung
Forschungszentrum Jülich GmbH
D-52425 Jülich

Experimental Report
of Neutron Scattering Experiments
at the FRJ-2 Reactor

Proposal number:	NSE-05-009		
Experiment title:	**Cooperative dynamics in short chain polymers**		
Dates of experiment:	26.08.-31.08.2005	Date of report:	16.05.2006
Experimental team: Names	Addresses		
M.Zamponi R.Biehl A.Wischnewski	Institut für Festkörperforschung, Forschungszentrum Jülich GmbH Institut für Festkörperforschung, Forschungszentrum Jülich GmbH Institut für Festkörperforschung, Forschungszentrum Jülich GmbH		
Local Contact:	R.Biehl, M.Monkenbusch		

Experimental report text body

Recent experiments of short chains below the entanglement length in a long chain matrix revealed anomalous diffusion behaviour of the short chains (NSE-04-024). Although per definition the short chains should not be affected by the matrix chains and therefore should be able to diffuse freely, the center of mass mean squared displacement showed a clear subdiffusive regime. Apparently the short chains are subject to topological constraints or cooperative dynamics.

Diluting the matrix by adding a small number of oligomer it is expected that the anomalous diffusion of the short chains is influenced. Therefore the mixture as used before (10% labeled (protonated) 1.5kg/mol polyethylene (PE) chains in a deuterated 36kg/mol PE matrix) has been diluted by adding 20% oligomer (nonadecane). Unfortunately sample preparation turned out to be difficult since the oligomer did not precipitate. The solvent therefore had to be evaporated after mixing.

The dynamic structure factor has been measured under the same conditions as before: at a temperature of 509K for 3 different q-values, covering a momentum transfer range from 0.5nm^{-1} to 0.96nm^{-1}. The background correction was estimated from a fully deuterated sample of the matrix chains which was also diluted by 20% oligomer.

In fig.1 the dynamic structure factor of the diluted blend is shown in comparison to the undiluted sample. The observed difference is very small, the dynamics of the diluted sample tends to be somewhat faster, in agreement with the expectation. For the lowest q-value the center of mass mean squared displacement can be extracted from the dynamic structure factor, but apparently also the anomalous diffusion behaviour has not changed.

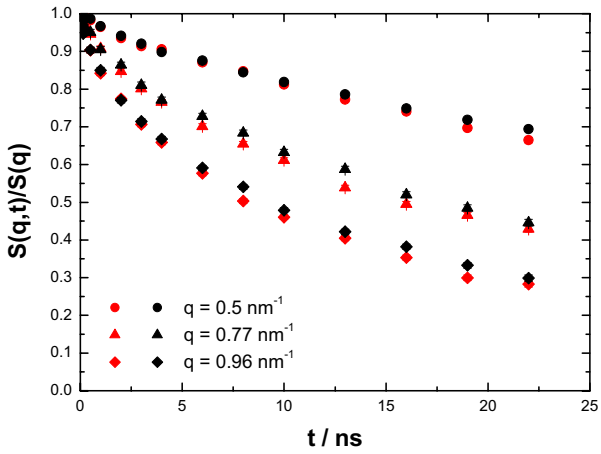


Fig.1: Dynamic structure factor of the diluted h-1.5kg/mol chain in d-36kg/mol matrix (red symbols) in comparison to the undiluted mixture (black symbols). Q-values as indicated in the plot.

A chemical analysis of the diluted sample after the measurement showed that not as much oligomer as expected was in the blend. Instead of the prepared 20% only about 5% oligomer was found. While heating under vacuum during the sample preparation also most of the oligomer must have evaporated. The small amount of remaining oligomer explains that there is only a small difference in the dynamic structure factor visible and that the dynamics is hardly influenced by the dilution.

Institut für Festkörperforschung
Forschungszentrum Jülich GmbH
D-52425 Jülich

Experimental Report
of Neutron Scattering Experiments
at the FRJ-2 Reactor

Proposal number:	NSE-05-010		
Experiment title:	**Anomalous diffusion in short chain polymer melts**		
Dates of experiment:	19.09-26.09.2005	Date of report:	22.05.2006
Experimental team: Names	Addresses		
M.Zamponi R.Biehl A.Wischnewski	Institut für Festkörperforschung, Forschungszentrum Jülich		
Local Contact:	R.Biehl, M.Monkenbusch		

Experimental report text body

Experiments of short chains in a long chain matrix have shown that although the short chains are below or about the entanglement length they are subject to topological constraints (NSE_04_024). The dynamic structure factor followed not the expected Rouse behaviour but was considerably slowed down. For such short chains the center of mass mean squared displacement can be extracted from the measured coherent dynamic structure factor at low wave vectors q. These didisperse blends show a clear subdiffusive regime at earlier times, again illustrating the influence of the topological confinement from the matrix chains.

A previous measurement of a short chain in a short matrix of the same molecular weight still showed deviations from the expected Rouse dynamics and a similar subdiffusive regime was found. The molecular weight (2.5kg/mol) was slightly above the entanglement length (M_e=2kg/mol), therefore in this experiment a short chain in a short matrix below M_e (1.5kg/mol) has been investigated by neutron spin echo spectroscopy. The sample consists of 10% protonated polyethylene (PE) chains with a molecular weight of 1.5kg/mol in a deuterated matrix of the same length. The experiments have been performed at a temperature of 509K at a wavelength of 8Å, covering a q-range of 0.5-1.0. nm^{-1}. The data have been corrected for resolution and background, latter estimated from a fully deuterated sample.

The resulting dynamic structure factor is displayed in fig.1. The data follows qualitatively Rouse dynamics (lines), but quantitativly the fitted Rouse rate deviates from the expectation. The apparent Rouse rate is much lower than the known literature value for PE. This is due to a significant slower diffusion than the Rouse expectation. If the diffusion is fitted separately for the lowest q-value, where internal Rouse modes are neglible, the value is nearly a factor 2 smaller. Fixing this diffusion constant and fitting the data again with the Rouse model for all q's, the right segmental friction, which determines the Rouse rate, is obtained.

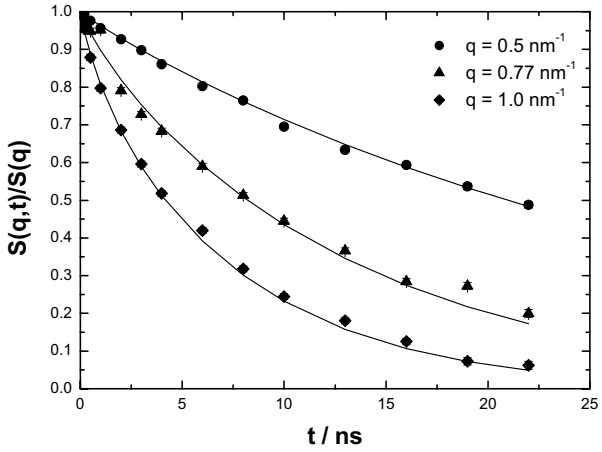


Fig.1: Dynamic structure factor of the 1.5kg/mol homopolymer melt,
q-values as indicated in the plot. Lines are a fit with the Rouse model.

For the lowest q-value the center of mass mean squared displacement can be extracted (fig.2). Only at very short times a slight deviation from the expected linear time dependence of normal diffusion is visible. Following the approach by Guenza (M. Guenza, Macromolecules **35**, 2714 (2002)) these deviations are due to intermolecular interactions and are expected to slow down the dynamics for times below the Rouse time of the chain. This is consistent with the experimental finding here. The Rouse time of the 1.5kg/mol chain is 4 ns, below this time the deviation from the Rouse expectation is evident.

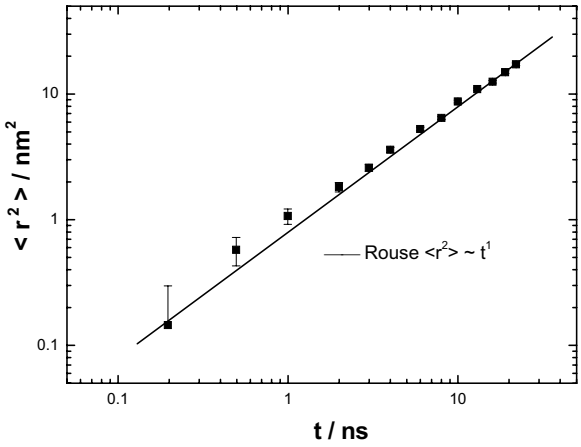
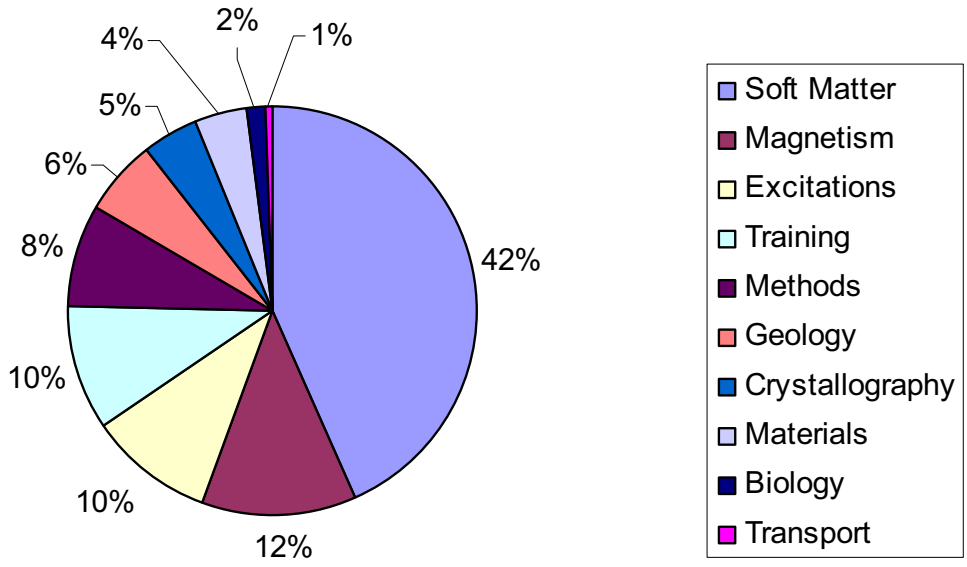


Fig. 2: Center of mass mean squared displacement for q=0.5 nm^{-1}.
The black line shows the Rouse expectation of normal diffusion.

Publications

In the following section publications of the years 2001 to now resulting from experiments at the Jülich research reactor FRJ-2 and neutron scattering instruments operated by FZ Jülich externally are listed. The list is based on the response of the users and therefore probably not complete. A total of 385 journal publications was reported to us, in addition to numerous invited talks, conference presentations, and theses. This is the highest number since the first issue of this report. We thank the experimenters for this great support!

The number of reported journal publications showed a significant increase from about 63 in the years 2000–2003, 79 in the year 2004, to 102 in the years 2005/6. This shows how the increasing user activity (especially due to the EU programme) beared fruit.



Distribution of topics of journal publications of the years 2001–now (without theses)

The figure above represents the breakdown of the journal publication number by topics. Clearly, soft matter research takes the largest share as it does for the experiments proposed. But also the hard matter activities divided into the categories magnetism, excitations, geology, crystallography, and materials make up for a considerable part of 37 %. Notable is the large fraction of methodological and educational publications which shows the significance of the FRJ-2 reactor for the development of new instruments and the training of new users.

Neutron Instruments and Methods

Publications

2005

Dohmen,L, Thelen,J, Alefeld,B
The Neutron Velocity Selector at the Focussing Small Angle Scattering Instrument in Jülich
J. Neutron Res. **13**, 275 (2005)

Kentzinger,E, Rücker,U, Paul,A, Brückel,Th
Layer resolved magnetization correlations in multilayers
Neutron News **16**, 26 (2005)

Paul,A, Kentzinger,E, Ruecker,U, Buergler,DE, Gruenberg,P
Polarized neutron scattering of exchaged-biased magnetic multilayers
Physica B **356**, 26 (2005)

Paul,A, Kentzinger,E, Ruecker,U, Buergler,DE, Gruenberg,P
Nonuniform and sequential magnetization reversal via domain structure formation for multilayered system with grain size induced enhanced exchange bias
European Physical Journal B **45**, 249 (2005)

Radulescu,A, Kentzinger,E, Stellbrink,J, Dohmen,L, Alefeld,B, Rücker,U, Heiderich,M, Schwahn,D, Brückel,T, Richter,D
KWS-3, the new (very) small-angle neutron scattering instrument based on focussing-mirror optics
Neutron News **16,** 18 (2005)

Schlapp,M, Ioffe,A, Conrad,H, Brückel,T, Fueß,H, vonSeggern,H
Novel materials and concepts for neutron image plates
Nucl. Instr. Meth. **A 551/1**, 46 (2005)

Schweika,W, Easton,S, Neumann,KU
Vector Polarization Analysis on DNS
Neutron News **16**, 14 (2005)

Tietze-Jaensch,H, Zorn,R, Brückel,T, Richter,D
Neutron Scattering at the Research Center Jülich
Neutron News **16**, 11 (2005)

2004

Ioffe, A.
Neutron speed echo add-on to TAS: an increase in resolution without the use of polarized neutrons
J. Magn. Magn. Mater. 272 (2004), 2136

Ioffe, A., Manoshin, S.
A neutron spin-echo spectrometer based upon thin magnetic film flippers: the simulation of performance
Physica B 345 (2004), 235

Kemmerling,G, Bünten,U, Clemens,U, Engels,R, Heiderich,M, Pyckhout-Hintzen,W, Rongen,H, Schelten,J, Schwahn,D, Zwoll,K
Performance Measurements of a new Large-Area Neutron Scintillation Detector System
IEEE Transactions on Nuclear Science **51**, 1098-1102 (2004)

Kentzinger,E, Dohmen,L, Alefeld,B, Rücker,U, Stellbrink,J, Ioffe,A, Richter,D, Brückel,Th
KWS-3, the new focusing-mirror ultra small-angle neutron scattering instrument and reflectometer at Jülich
Physica B **350**, e779-e781 (2004)

Schlapp,M, Conrad,H, vonSeggern,H
Pixelated neutron image plates
J. Phys. D: Appl. Phys. **37**, 2607-2612 (2004)

Schlapp,M, Hoelzel,M, Gilles,R, Ioffe,A, Brueckel,T, Fuess,H, von Seggern, H
Novel types of neutron image plates based on KCl^{2+}-LiF
Physica B **350**, e861-e864 (2004)

Schäfer,W, Kirfel,A, Phiesel,H, Skowronek,R
Construction and tests of a low-cost furnace for neutron powder diffractometry
Physica B **350**, e751-e754 (2004)

2003

Brückel, Th., Eccleston, R., Lauter, H., Maleyev, S., Rekveldt, Th., Schreyer, A., Schweizer, J., Toperverg, B.
Polarized neutron methods and instrumentation for pulsed sources
Physica B 335 (2003), 143 – 146

Kentzinger, E., Rücker, U., Toperverg, B.
Simulations of off-specular scattering of polarized neutrons from laterally patterned magnetic multilayers
Physica B **335** 82 (2003)

Monkenbusch, M.
NSE spectrometer of the next generation - where are the limits?
Neutron spin echo spectroscopy / ed.: F. Mezei ... - Berlin,2003. - (Lecture notes in physics , 601). - 3-540-44293-6. - S. 201 – 212

Mueller, R., Chang, L. J., Appelt, St., Haesing, W., Horriar-Esser, Ch., Ioffe, A., Brückel, Th.
Progress in the production of polarized 3He in Jülich
Physica B 335 (2003), 278 – 281

Schmidt, W., Ohl, M., Ruppert, H., Buchenau, U.
Instrumental setup for polarized neutron scattering experiments
Journal of applied physics,93 (2003),S. 7071 – 7073

Schweika, W.
Time-of-flight and Vector Polarization Analysis for Diffuse Neutron Scattering
Physica B 335 (1-4) (2003) pp.157-163

Schweika, W.
Time-of-flight and Vector Polarization Analysis for Diffuse Neutron Scattering
Proceedings of the 16th Meeting of the International Collaboration on Advanced Neutron Sources (2003), 199 - 206

Villa, M., Baron, M., Hainbuchner, M., Jericha, E., Leiner, V., Schwahn, D., Seidl, E., Stahn, J., Rauch, H.
Optimization of a Crystal Design for a Bonse-Hart Camera
J. Appl. Cryst **36**, 769 (2003)

2002

Ioffe, A., Conrad, H., Zeiske,T, Mueller,R, Küssel,E, Masalovich,S, Schlapp,M, Schmitz,B, Brückel, Th.
A new thermal neutron spectrometer/diffractometer for polarization analysis (SV30) at the research reactor FRJ-2
Applied Physics A **74**, 107 (2002)

Massalovitch,S, Ioffe, A., Küssel,E, Schlapp,M, Brückel, Th.
Development of Image Plate Based Neutron Detector International Workshop on Position-Sensitive Neutron Detectors - Status and Perspectives, ISSN 1433-559 **2**, 569 (2002)

Massalovitch,S, Ioffe, A., Küssel,E, Schlapp,M, vonSeggern,H, Brückel, Th.
Development of neutron image plate for low-flux measurements
Appl. Physics A [Suppl.] **74**, S118 (2002)

Schlapp,M, von Seggern,H, Massalovich,S, Ioffe, A., Conrad, H., Brückel, Th.
Materials for neutron image plates with low γ-sensitivity
Appl. Phys. A **74 [Suppl.]**, 109-111 (2002)

2001

Kemmerling,G, Engels,R, Bussmann,N, Clemens,U, Heiderich,M, Reinartz,R, Rongen H, Schelten J, Schwahn D, Zwoll K
A new two-dimensional scitillation detector system for small angle neutron scattering
Transactions on Nuclear Science **48**, 1114 (2001)

Rücker, U., Bergs,W, Alefeld,B, Kentzinger, E., Brückel, Th.
Polarization analysis for the 2D position-sensitive detector of the HADAS reflectometer
Physica B **297**, 140 (2001)

Schweika, W., Böni,P
The Instrument DNS: Polarization Analysis for Diffuse Neutron Scattering
Physica B **297**, 155-159 (2001)

Zeitelhack,K
Eurisys ^{3}He-proportional Counters squashed series
Internal Report 29-05-01, Technische Universität München (2001)

Invited Talks

2006

Frielinghaus,H
Polarisation analysis and grazing incidence SANS
JCNS Symposium and European User Meeting (Jülich) (2006)

PalaciosGómez,J, Walter,J, Jansen,E, Kirfel,A, Ennis,PJ, Kryshtab,T
Evidence of extinction in strong textured high purity copper
European Powder Diffraction Conference (EPDIC10) (Genf) (2006)

2005

Conrad,H
The triple axis spectrometer SV-30 at the Jülich research reactor FRJ-2
CIAE-Institutsseminar (Peking) (2005)

Kentzinger,E
Diffusion de neutrons en incidence rasante. Neutrons polarisés.
14èmes journées de la diffusion neutronique (Murol, France) (2005)

Kentzinger,E, Rücker,U, Toperverg,B, Frielinghaus,H, Ott,F, Brückel,Th
Depth-resolved investigations of lateral magnetic correlations in multilayers: from micrometer to nanometer length scales
International Workshop on Reflectometry, Off-specular scattering and GISANS (PSI, Villigen, Switzerland) (2005)

Monkenbusch,M
NSE and Soft-Matter
NSE2005, ILL-workshop (Grenoble) (2005)

Zorn, R
Neutron Scattering Facilities at the research reactor FRJ-2
CIAE-Institutsseminar (Peking) (2005)

2004

Schlapp,M
Materials for neutron image plates
E-MRS Fall Meeting (Warschau, Polen) (2004)

Schweika,W
Complete vector polarisation on time-of-flight instruments
Seminar (ISIS, Didcot, UK) (2004)

Schweika,W
Complete vector polarisation analysis on multi-detector and time-of-flight instruments
Deutsche Neutronenstreutagung (TU Dresden) (2004)

Schweika,W
Complete vector polarization analysis on multi-detector time-of-flight instruments
PNCMI 2004 (Washington) (2004)

2003

Ioffe, A.
Neutron Speed Echo add-on to TAS: an increase in resolution without the use of polarized neutrons
Seminar: TU München, FRM-II, 17.11.03

Schwahn, D.
First Neutron Experiments with "Bonse-Hart" Channel-Cut Crystals. Application of the USANS Technique at the FRJ-2 in Jülich
The first Workshop on the international Consortium of Ultra-Small-Angle-Scattering (IConUSAS) July 9.-10,2003,Oak Ridge,USA

Schweika, W.
Diffuse Streuung zur Untersuchung komplexer Festkörper
Seminar des Instituts für Theoretische und Angewandte Physik,Univ. Stuttgart,11.11.2003

Schweika, W.
Diffuse Scattering and Complete Polarization Analysis
Workshop on Single Crystal Diffuse Scattering at Pulsed Neutron Sources
Argonne 17.6.2003

Schweika, W.
Full Polarization Analysis on Time-of-Flight Instruments
ICANS-16, Düsseldorf-Neuss 15.5.2003

Schweika, W.
Ein neues thermisches Neutronen-Flugzeitspektrometer mit vollständiger vektorieller Polarisationsanalyse
TU München,Instrumentierungsausschuss,7.3.2003

2002

Kahle, S.
High Resolution Inelastic Neutron Scattering Spectroscopy
Joint ICTP-INFM School and Workshop on Spectroscopy Investigation of the Collect (Trieste) (2002)

Kentzinger, E.
KWS-3, the new Focusing Mirror SANS Instrument at Juelich
6th ESS- Scientific Advisory Commitee Meeting (Bochum, Germany) (2002)

Kentzinger, E.
First Experiments on the Focusing-Mirror USANS Diffractometer KWS-3
European Users Meeting Juelich Neutrons For Europe (Kerkrade, NL) (2002)

Prager, M.
Status and Experience with the time-focusing thermal TOF-spectrometer SV29 at Jülich
Paul-Scherrer-Institut (Villigen, CH) (2002)

Schweika, W.
Time-of-Flight and Polarization Analysis for Diffuse Neutron Scattering
Bad Honnef,ESS-Tage 15.-16.4.2002
Schweika, W.
Time of Flight and Polarization Analysis for Diffuse Neutron Scattering
Polarized Neutrons in Condensed Matter Investigations 2002 (Jülich) (2002)

Conference Presentations

2006

Conrad,H, Brückel,T, Bussmann,K, Küssel,E, Schmitz,B
A new thermal neutron spectrometer/diffractometer with polarization analysis at the research reactor FRJ-2
JCNS Symposium and European User Meeting (Jülich) Poster (2006)

Kentzinger,E
On the expected performance improvements of the focussing V-SANS instrument KWS-3
JCNS Symposium and European User Meeting (Jülich) Talk (2006)

Kentzinger,E, Rücker,U, Frielinghaus,H, Toperverg,B, Ott,F, Brückel,T
Depth-resolved investigation of structural and magnetic correlations in multilayers: From micrometer down to nanometer length scales
Heraeus Seminar: Nanoscale Magnets - Top down meets bottom up (Bad Honnef) Poster (2006)

Kentzinger,E, Rücker,U, Frielinghaus,H, Toperverg,B, Ott,F, Brückel,Th
Depth-resolved investigation of structural and magnetic correlations in multilayers: from micrometer down to nanometer length scales
JCNS Symposium and European User Meeting (Jülich) Poster (2006)

2005

Frielinghaus,H, Brückel,T, Richter,D
Upgrades of Neutron Scattering Instruments in Conjunction with the Relocation from Jülich to Munich
ICNS2005 (Sydney) Poster (2005)

Kentzinger,E
KWS-3
Benchmarking zur Kleinwinkelstreuung (in der HGF) (Akademie der Wissenschaften, Berlin) Talk (2005)

Kentzinger,E
Depth-resolved investigations of the magnetisation reversal process in micro- and nano-structured multilayers
2nd FRM-II Workshop on Neutron Scattering - Advanced Materials (Burg Rothenfleds am Main, Germany) Talk (2005)

Kentzinger,E
Depth resolved investigation of in-plane magnetic correlations in multilayers by scattering of polarised neutrons under grazing incidence
Institute Seminar (Walther-Meissner Institute, Garching, Germany) Talk (2005)

Kentzinger,E
Depth-resolved investigations of micro- and nano-structured magnetic multilayers by scattering of polarized neutrons under grazing incidence
Institute Seminar (PSI, Villigen, Switzerland) Talk (2005)

Kentzinger,E, Rücker,U, Toperverg,B, Ott,F, Brückel,Th
Depth-resolved investigation of the lateral magnetic correlations in polycristalline multilayers by reflectivity and off-specular scattering of polarised neutrons
Frühjahrstagung der Deutschen Physikalischen Gesellschaft (Berlin) Talk (2005)

Monkenbusch,M, Allgaier,J, Richter,D, Fetters,LJ, Mueller,K, Kreiling,S, Denicke K, Greiner A
Non-flexible polymer coils in solution-NSE investigation of alkyl substitued polynorbornenes in THF
NSE2005, ILL-workshop (Grenoble) Poster (2005)

2004

Conrad,H, Brückel,Th, Bussmann,K, Chang,LJ, Ioffe,A, Küssel,E, Mueller, R; Schmitz, B
A New Thermal Neutron Spectrometer / Diffractometer (SV-30) with Polarisation Analysis at the Research Reactor FRJ-2
Deutsche Neutronenstreutagung (TU Dresden) Poster (2004)

Conrad,H, Schäfer,W
A high intensity time-of-flight diffractometer for structure, texture and phase analyses of poly-crystalline matter
Deutsche Neutronenstreutagung (Dresden) Talk (2004)

Mattauch,S
Neutronen Einkristall-Diffraktometer (SV28) am FRJ-2
Gemeinsamme Jahrestagung DGK+DGKK (Jena) Talk (2004)

Stellbrink,J, Kentzinger,E, Dohmen,L, Alefeld,B, Rücker,U, Ioffe,A, Radulescu,A, Richter,D, Brückel,T
KWS-3, the New Focusing-Mirror USANS Instrument and Reflectometer at Julich
canSAS-IV (Rutherford Appleton Laboratory, Oxfordshire, UK) Poster (2004)

Walter,JM, Jansen,E, Skowronek,R, Kirfel,A, Froitzheim,N, Siemes,H, Köbler,U
Texture analysis and powder diffraction by neutrons: Different applications at SV7 in Jülich
Deutsche Neutronenstreutagung (Dresden) Poster (2004)

2003

Chang, L.-J., Mueller, R., Appelt, S., Häsing, F. W., Ioffe, A., Brückel, Th.
Progress of 3He spin-exchange for neutron polarization in Jülich
3rd European Conference on Neutron Scattering
Montpellier,France: 03.09.2003 - 06.09.2003 Poster

Ioffe, A., Monkenbusch,M, Ohl,M
Jülich progress in developments of Image Plate Detectors and correction elements for ultra-high resolution neutron spin-echo spectrometer
Annual TECHNI Meeting
Trieste,Italien: 08.10.2003 - 10.10.2003

Ioffe, A., Bussmann, K., Dohmen, L., Axelrod, L., Gordeev, G., Brückel, Th.
LAP-ND: a new neutron depolarization setup at FRJ-2
3rd European Conference on Neutron Scattering
Montpellier,France: 03.09.2003 - 06.09.2003 Poster

Ioffe, A.
Neutron Speed Echo add-on to TAS: an increase in energy resolution
ICM – International Conference on Magnetism
Rom, Italy, 27.07.-01.08.03

Ioffe, A.
Development of an Image Plate Detector in FZJ
Annual TECHNI Meeting, Coimbra, Portugal, 05.-06.05.03

Kentzinger, E., Dohmen,L, Alefeld,B, Rücker, U., Stellbrink,J, Ioffe, A., Richter, D., Brückel, Th..
KWS-3, Th.e new focusing-mirror small-angle neutron scattering instrument and neutron reflectometer at Jülich
3rd European Conference on Neutron Scattering
Montpellier,France: 03.09.2003 - 06.09.2003 Poster

Kentzinger, E., Dohmen,L, Alefeld,B, Rücker, U., Stellbrink,J, Richter, D., Brückel, Th..
KWS-3 : the new focusing mirror USANS instrument at Juelich
ICANS-XVI : 16th Meeting of the International Collaboration on Advanced Neutron Sources , Convention Center,Neuss
Neuss: 12.05.2003 - 15.05.2003 Poster

Massalovitch, S., Ioffe, A., Schlapp, M., von Seggern, H., Küssel, E., Brückel, Th.
Development of low g-sensitive neutron image plate detector at FZ Jülich (P)
3rd European Conference on Neutron Scattering
Montpellier,France: 03.09.2003 - 06.09.2003 Poster

Ohl,M, Monkenbusch,M
NSE correction devices
TECHNI Meeting
Coimbra,Portugal: 06.05.2003

Schäfer, W., Jansen, E., Kirfel, A.
Das Jülicher Texturdiffraktometer
Präsentation des Fachausschusses 'Texturen' im Rahmen des DGM-Tages 'Buisiness meets Students', 10.7.2003, Erlangen
Talk (Erlangen, 2003)

Schäfer, W., Kirfel,A, Phiesel,H, Skowronek,R
Construction and tests of a low-cost furnace for neutron powder diffractometry
European Neutron Scattering Conference 2003,Montpellier,F Poster

Schlapp,M, Hoelzel,M, Gilles,R, Ioffe,A, Brueckel,T, vonSeggern,H, Fuess, H
Neutron image plates with low g-sensitivity for SANS
ECNS (Montpellier, France) Poster (2003)

2002

Alefeld,B, Conrad, H., Dohmen,L, Ioffe, A., Kentzinger, E., Küssel,E, Prager, M., Rücker, U., Brückel, Th.
Instrument Modernisation Program at the FRJ-2 Reactor
ESS European Conference (Bonn) Poster (2002)

Dohmen,L, Alefeld,B, Kentzinger, E., Rücker, U., Stellbrink,J, Ioffe, A., Springer,T, Richter, D., Brückel, Th., Drochner,M, Engels,R, Kleines,H, Suxdorf,F, Zwoll,K
A High Resolution Small Angle Scattering Instrument and Reflectometer with Focusing Mirror (KWS3) at Juelich
Deutsche Neutronenstreutagung & ESS Meeting (Bonn) Poster (2002)

Massalovitch,S, Ioffe, A., Küssel,E, Brückel, Th., Schlapp,M, vonSeggern,H
The optimization of neutron image plate detector with low gamma-sensitivity
ESS-Konferenz (Bonn) Poster (2002)

Mueller,R, Chang,LJ, Appelt,St, Haesing,W, Horriar-Esser,Ch, Ioffe, A., Brückel, Th
Progress in the production of polarised ^{3}He in Jülich
Workshop on Polarised Neutrons in Condensed Matter Investigations (FZJ, Jülich) Poster (2002)

Schäfer, W., Jansen,E, Skowronek,R, Kirfel,A
Recent examples of scientific projects using the University of Bonn powder diffractometer SV7-a in Jülich
Deutsche Neutronenstreutagung 2002 and The European Spallation Source (Bonn) Poster (2002)

Schweika, W.
Diffuse Neutron Scattering -- time-of-flight and polarization analysis
ESS-Tage,15.4.2002,Bad Honnef

2001

Ioffe, A., Conrad, H., Zeiske, Th., Mueller,R, Küssel,E, Masalovich,S, Schlapp,M, Schmitz,B, Brückel, Th.
A New Thermal Neutron Spectrometer/Diffractometer for Polarization Analysis (SV30) at the research reactor FRJ-2
ICNS 2001 (München) Poster (2001)

Ioffe, A., Conrad, H., Zeiske, Th., Mueller,R, Küssel,E, Masalovich,S, Schlapp,M, Schmitz,B, Brückel, Th.
Spektrometer SV30 für Polarisationsanalyse mit thermischen Neutronen am Forschungsreaktor FRJ-2
Deutsche Neutronenstreutagung (Jülich) Poster (2001)

Kirfel,A, Schäfer, W.
Forschung mit Neutronen in den Außenstellen des Mineralogisch-Petrologischen Instituts der Universität Bonn in Jülich und England
BMBF-Veranstaltung Förderschwerpunkt Kondensierte Materie (Bonn) Talk (2001)

Mueller,R, Brückel, Th., Horriar-Esser,Ch
Entwicklung einer Anlage zur Herstellung von kernspin-polarisiertem ^{3}He am Forschungszentrum Jülich
Deutsche Neutronenstreutagung (FZJ, Jülich) Poster (2001)

Rücker, U., Bergs,W, Alefeld,B, Kentzinger, E., Brückel, Th.
The new neutron reflectometer with polarization analysis in Jülich
Deutsche Neutronenstreutagung (Jülich) Poster (2001)

Rücker, U., Bergs,W, Kentzinger, E., Brückel, Th.
Polarization Analysis for a neutron reflectometer with 2D position sensitive detector
European Neutron Polarization Initiative (Jülich) Talk (2001)

Rücker, U., Kentzinger, E., Bergs,W, Alefeld,B, Brückel, Th.
The new reflectometer with polarization analysis in Jülich
ICNS 2001 (Munich) Poster (2001)

Schlapp,M, vonSeggern,H, Massalovitch,S, Ioffe, A., Conrad, H., Brückel, Th.
Materials for neutron image plates with low gamma sensitivity
ICNS-Konferenz (München) Poster (2001)

Crystallography

Publications

2006

Bertold,C, Selke,R, Schäfer,W
Neutron and X-Ray diffraction study of a semi-randomly disordered chamosite-IIb
Clays and Clay Minerals (submitted June 2005) (2006)

Gatta,GD, Nastola,F, Bromiley,GD, Mattauch,S
The real topological configuration of the extra-framework content in alkali-poor beryl: a multi-methodological study
American Mineralogist **91**, 29-34 (2006)

Gatta,GD, Nestola,F, Bromiley,GD, Loose,A
New insight into crystal chemistry of topaz: a multi-methodological study
American Mineralogist **(in press)**, (2006)

Sreeraj,P, Wiemhöfer,H-D, Hoffmann,R-D, Skowronek,R, Kirfel,A, Pöttgen,R
Neutron Diffraction and Electrochemical Studies on $LiIrSn_4$
J. Solid State Chem. **179**, 355-361 (2006)

Sreeraj,P, Wiemhöfer,H-D, Hoffmann,R-D, Walter,J, Kirfel,A, Pöttgen,R
Neutron Diffraction and Electrochemical Studies on $LiAg_2Sn$
Solid State Sciences (in press, corrected proof, available online 26 May 2006) (2006)

2005

Iezzi,G, Gatta,GD, Kockelmann,W, DellaVentura,G, Rinaldi,R, Schäfer,W, Piccinini, M, Gaillard, F
LowT neutron powder diffraction and synchrotron-radiation IR study of synthetic amphibole $Na(NaMg)Mg_5 Si_8 O_{22} (OH)_2$
American Mineralogist **90**, 695-700 (2005)

2004

Kirfel,A, Zotov,N, Schäfer,W
Neutron diffraction study of KNO_3 at elevated temperatures
Physica B **350**, e387-e389 (2004)

2003

Caspary,D, Eckold,G, Elter,P, Gibhardt,H, Güthoff,F, Demmel,F, Hoser,A, Schmidt,W, Schweika, W.
The influence of demixing on the dynamics of ionic solids: inelastic neutron scattering from $Ag_xNa_{1-x}Cl$ single crystals
Journal of physics: condensed matter,15 (2003),S. 6415 – 6426

Le Toquin, R., Paulus, W., Cousson, A., Hernandez, O., Dhalenne, G., Revvcolevschi, A., Treutmann, W., Rheinstädter, M., Schmidt, W., Regnault, L.-P.
Structure, magnetism, and dynamics of $La_2CoO_{4+\delta}$
Proc. ECNS03, accepted for publication in Physica B

Neumann,M, Press,W, Nöldeke,C, Asmussen,B, Prager, M., Ibberson,RM
The crystal structure of methane phase III
Journal of chemical physics **119** (2003),S. 1586 – 1589

2002

Halevy,I, Salhov,S, Kimmel,G, Atzmony,U, Pereira,LCJ, Goncalves,AP, Schäfer, W.
High-pressure studies of a $ThMn_{12}$-type actinide compound: UFe_5Al_7
Journal of Physics: Condensed Matter **14**, 11189 (2002)

Prager, M., Press,W, Asmussen,B, Combet,J.
Phase III of methane: crystal structure and rotational tunneling
Applied physics A,74 (2002),S. 1360 – 1362

Schäfer, W., Kirfel,A
Neutron powder diffraction study on the thermal expansion of cuprite
Applied Physics A **74**, 1010 (2002)

Sosnowska,I, Schäfer, W., Kockelmann,W, Barbier,B, Andersen,KA, Troyanchuk,IO
Crystal structure and spiral magnetic ordering of $BiFeO_3$ doped with manganese
Applied Physics A **74**, 1040 (2002)

2001

Kockelmann,W, Schäfer, W., Kirfel,A, Klapper,H, Euler,H
Hydrogen positions in KCo-, CsCo-, CsNi-, and CsCu-Tutton's Salt type compounds determined by neutron powder diffraction
Materials Science Forum **378-381**, 274 (2001)

Schäfer, W., Halevy,I
Neutron powder diffraction on iron-rich rare earth-iron-aluminium intermetallics RFe_7Al_5 (R = Tb, Dy, Ho, Er)
Material Science Forum **378-381**, 414 (2001)

Sosnowska,I, Schäfer, W., Kockelmann,W, Troyanchuk,IO
Neutron diffraction studies of crystal and magnetic structure of $BiMn_xFe_{1-x}O_3$ solid solutions
Materials Science Forum **378-381**, 616 (2001)

Straessle, T., Furrer, A., Altorfer, F., Mattenberger, K., Boehm, M., Mutka, H.
HoAs: A model compound for the cooling by the barocaloric effect
J. Alloys and Compounds **323-324** (2001) 392-395

Invited Talks

2004

Bujak,M, Mattauch,S, Zaleski,J
Ferroelectric structure of $[(CD_3)_2ND_2]_3[Sb_2Cl_9]$ at 10 K
N2M2 Neutrons and Numerical Methods 2 (Grenoble, France) (2004)

2003

Brückel, Th.
Wechselspiel zwischen Spin-, Ladungs- und Orbital-ordnung in CMR-Manganaten
Seminar über Kristall- und Strukturchemie: RWTH Aachen, 11.07.03

Schweika, W.
Diffuse Streuung
Neutronenstreuung für Kristallographen,Univ. Köln, 08.10.2003

Conference Presentations

2005

Gatta,GD, Nestola,F, Petrelli,M
New insight into the crystal chemistry of alkali-poor beryl: The real topological configuration of the extra-framework content
National Congress of the Federazione Italiana di Scienze della Terra (Spoleto, September 2005) Poster (2005)

Oh,IH, Mattauch,S, Heger,G
Structural phase transitions with proton ordering in TlH_2PO_4
69.Jahrestagung der Deutschen Physikalischen Gesellschaft DPG (Berlin) Poster (2005)

Oh,IH, Mattauch,S, Heger,G
Structural phase transitions with proton ordering in TlH_2PO_4
13. Gemeinsame Jahrestagung der Deutschen Gesellschaft für Kristallographie (Köln) Poster (2005)

2004

Hu,C, Englert,U, Mattauch,S, Heger,G
Topological Study of Coordination Polymers Based on Halogen Bridged Octahedra
Gemeinsamme Jahrestagung DGK+DGKK 2004 (Jena) Poster (2004)

Hu,C, Englert,U, Mattauch,S, Heger,G
Hydrogen Bonds between Guanidinium and (Hydrogen)orthophosphate by X-ray and Neutron Methods
Gemeinsamme Jahrestagung DGK+DGKK 2004 (Jena) Poster (2004)

Mattauch,S
Single Crystal Diffraction Analysis on $[ND_2(CD_3)_2]_3Sb_2Cl_9$ (D-DMACA) in its Low Temperature Phase
11th International Seminar on Neutron Scattering Investigation in Condensed Matter (Poznan, Polen) Talk (2004)

Mattauch,S, Bujak,M, Zaleski,J
Single crystal diffraction analysis on $[ND_2(CD_3)_2]_3[Sb_2Cl_9]$ (D-DMACA) in its low temperature phase.
Deutsche Neutronenstreutagung 2004 (Dresden) Poster (2004)

2003

Holderna-Natkaniec,K, Ibberson,R M, Natkaniec,I, Prager, M.
Neutron-diffraction study of solid phases of 1,3,5-trimethylbenzene-d12
European Neutron Scattering Conference 2003,Montpellier,F Poster

Kirfel,A, Zotov,N, Schäfer, W.
Elevated temperature neutron diffraction study of the phase transitions in KNO_3
European Neutron Scattering Conference 2003,Montpellier,F Poster

Schäfer, W., Buschow, K. H. J.
Neutron diffraction on binary and pseudobinary RMg_3 intermetallics (R = La, Ce, Pr, Nd)
11. Jahrestagung der Deutschen Gesellschaft für Kristallographie, 10.-13.3.2003, Berlin, Poster (Berlin, 2003)

2002

Schäfer, W., Kirfel,A
Neutronenbeugung zum thermischen Verhalten von Cuprit
10. Jahrestagung der Deutschen Gesellschaft für Kristallographie (Kiel) Poster (2002)

Schäfer, W., Kirfel,A
On the unusual negative thermal expansion of cuprite
Deutsche Neutronenstreutagung 2002 and The European Spallation Source (Bonn) Poster (2002)

2001

Bieniok,A, Bertoldi,C, Schäfer, W., Heger,G, Amthauer,G
Strukturelle Untersuchungen an einem natürlichen Chamosit
79. Jahrestagung der Deutschen Mineralogischen Gesellschaft (Potsdam) Poster (2001)

Sauerwald,F, Wacker,K, Buck,P, Schäfer, W.
Neutronenbeugungsuntersuchungen (Rietveld) an Spinellmischkristallen $MnFe_2O_{4+\delta}$
9. Jahrestagung der Deutschen Gesellschaft für Kristallographie (Bayreuth) Talk (2001)

Schäfer, W., Kirfel,A
Neutron powder diffraction study on the thermal expansion of cuprite
ICNS 2001 (Munich) Poster (2001)

Schweika, W., Shramchenko,N, Caudron,R, Bellissent,R, Widom,M
Phason disorder in icosahedral AlPdMn quasicrystals
Deutsche Neutronenstreutagung (Jülich) Poster (2001)

Schweika, W., Shramchenko,N, Caudron,R, Bellissent,R, Widom,M
Phason disorder in icosahedral AlPdMn quasicrystals
International Conference on Neutron Scattering (München) Poster (2001)

Excitations

Publications

2006

Köbler,U, Hoser,A, Hoffmann,J-U, Thomas,C
One-dimensional bulk ferromagnets: $NdAl_2$ and hcp cobalt
Solid State Communications **6**, 301-305 (2006)

Köbler,U, Hoser,A
Effective spin description of crystal field effects in $NdAl_2$
Journal of Magnetism and Magnetic Materials **299**, 145-154 (2006)

Köbler,U, Hoser,A, Hoffmann,J-U
Crystal field effects in the 3d transition metal compounds
Physica B: Condensed Matter **382**, 98-104 (2006)

Vecchini,C, Moze,O, Hoser,A, Prager,M, Argyriou,D, Michels,A, J Weissmuller, C Lemier, R N Viswanath
A neutron scattering investigation of the magnetic structure and magnetic excitations in nanocrystalline Tb
Journal of Applied Physics **99**, 08F502 (2006)

2005

Elter,P, Eckold,G, Gibhardt,H, Schmidt,W, Hoser,A
Kinetics of decomposition in ionic solids: IV. Transition between nucleation and spinodal decomposition observed by time-resolved phonon spectroscopy
Journal of Physics-Condensed Matter **17 41**, 6559-6573 (2005)

Hermann,RP, Grandjean,F, Long,GJ
Einstein oscillartors that impede thermal transport
Am. J. Phys. **73**, 110-118 (2005)

Hermann,RP, Grandjean,F, Keppens,V, Schweika,W, Nolas,GS, Mandrus,DG, Sales BC, Christen HM, Bonville P, Long GJ
The Dynamics of the Guests in Filled Germanium Clathrates
Materials and Technologies for Direct Thermal-to-Electric Energy Conversion, Eds. J. Yang, T. P. Hogan, R. Runahashi, G. S. Nolas (Mater. Res. Soc. Symp. Proc. 886, Warrendale, PA, 2005) **886**, F10 (2005)

Hermann,RP, Schweika,W, Leupold,O, Rüffer,R, Nolas,GS, Grandjean,F, Long GJ
Neutron and Nuclear Inelastic Scattering Study of Einstein Oscillators in Ba-, Sr-, and Eu-filled germanium clathrates
Phys. Rev. B **72**, 174301 (2005)

Köbler,U, Hoser,A
Stable magnetic universality classes for T -> 0
Physica B **362**, 295-305 (2005)

Köbler,U, Hoser,A, Schäfer,W
On the temperature dependence of the magnetic excitations
Physica B **364**, 55-70 (2005)

Prager,M, Baumert,J, Press,W, Plazanet,M, Tse,JS, Klug,DD
Rotational tunneling of disordered methyl groups of CH_3F encaged in cubic I water clathrate
Phys. Chem. Chem. Phys. **7**, 1228 (2005)

Prager,M, Grimm,H, Natkaniecz,I
Rotational potentials of methyl groups and structures of low temperature phases of mesitylene: a neutron scattering study
Phys. Chem. Chem. Phys. **7**, 2587 (2005)

Prager,M, Pawlukojc,A, Sobczyk,L, Grech,E, Grimm,H
Inelastic neutron scattering study of tetramethylpyrazine in the complex with chloranilic acid
J. Phys. Condens. Matter **17**, 5725 (2005)

Sawka-Dobrowolska,W, Bator,G, Sobczyk,L, Pawlukojc,A, Ptasiewicz-Bak,H, Rundlöf,H, Krawczyk, Nowina-Konopka, Jagielski, Janik, Prager, Steinsvoll, Grech, Nowicka-Scheibe
Elastic, quasielastic and inelastic neutron scattering studies on the charge-transfer hexamethylbenzene-tetracyanoquinodimethane complex
J. Chem. Phys. **123**, 124305 (2005)

2004

Conrad,H, Kuhs,WF, Nuenighoff,K, Pohl,C, Prager,M, Schweika,W
Inelastic scattering and spectral measurements of advanced cold neutron moderator media
Physica B **340**, e647 (2004)

Eckold,G, Caspary,D, Elter,P, Güthoff,F, Hoser,A, Schmidt,W
Time-resolved phonons as a microscopic probe for demixing processes
Physica B **350**, 83 (2004)

Eckold,G, Caspary,D, Gibhardt,H, Schmidt,W, Hoser,A
Kinetics of Decomposition in Ionic Solids III: Time-evolution of phonon spectra during spinodal decomposition in AgCl-NaCl
J. Phys.: Condens.Matter **16**, 5945 (2004)

Hauer,B, Hempelmann,R, Udovic,TJ, Rush,JJ, Kockelmann,W, Schäfer,W, Jansen,E, Richter,D
Neutron scattering studies on vibrational excitations and the structure of ordered niobium hydrides
J. Phys. Cond. Mat. **16**, 5205 (2004)

Hense,K, Gratz,E, Nowotny,H, Hoser,A
Lattice dynamics and the interaction with the crystal electric field in $NdCu_2$
J. Phys. Cond. Mat. **16**, 5751 (2004)

Hense,K, Gratz,E, Nowotny,H, Loewenhaupt,M, Hoser,A
Crystal electric field-phonon interaction in $NdCu_2$
J. Magn. Magn. Mater. **272-276**, 368 (2004)

Kirstein,O, Prager,M
The lattice dynamics of the methyl halides described by pair potentials based on universal force fields
Journal of Chemical Physics **120**, 5199 (2004)

Prager,M, Pieper,J, Buchsteiner,A, Desmedt,A
Probing adsorption sites in a cubic II water clathrate cage by methyl group rotation of CH_3I guest molecules
J. Phys.: Condens. Matter **16**, 7045 (2004)

Prager,M, Pieper,J, Buchsteiner,A, Desmedt,A
Methyl rotational potentials as a probe of the cage potential surface in methyl iodide clathrate
Physica B **350**, e399 (2004)

2003

Caspary,D, Eckold,G, Elter,P
The influence of demixing on the dynamics of ionic solids: inelastic neutron scattering from Ag_xNa_{1-x} Cl single crystals
J. Phys. Cond. Mat **15**, 6415 (2003)

Conrad, H., Kuhs, W. F., Nünighoff, K., Pohl, C., Prager, M.
Inelastic neutron scattering and spectral measurements of advanced cold moderator materials
Proceedings of the 16th Meeting of the International Collaboration on Advanced Neutron Sources (2003), 921 - 929

Prager, M., Grimm,H, Desmedt,A, Lechner,RE
Methyl rotational potentials of trimethyl metal compounds studied by inelastic and quasielastic neutron scattering
Chemical physics **292** (2003),S. 161 - 169

2002

Elter,P, Eckold,G, Caspary,D, Güthoff,F, Hoser,A
Time-evolution of phonon spectra during decomposition in $Ag_xNa_{1-x}Br$ ionic crystals
Appl. Phys. A **74 [Suppl 1]**, 1169-1171 (2002)

Hoelzel,M, Danilkin,SA, Hoser,A, Ehrenberg,H, Wieder,T, Fuess,H
Phonon dispersion in austenitic stainless steel $Fe_{18}Cr_{12}Ni_2Mo$
Appl. Phys. A **74 [Suppl 1]**, 1013-1015 (2002)

Prager, M., Grimm,H, Parker,SF, Lechner,R, Desmedt,A, McGrady,S, Koglin,E
Methyl group rotation in trimethyl aluminum
J.Phys.: Cond. Matter **14**, 1833 (2002)

Prager, M., Schiebel,P, Combet,J
Rotational tunnelling and disorder in 4-iodo-toluene
Chem. Phys. **276**, 69 (2002)

Prager, M., Schiebel,P, Grimm,H
Dipolar interaction in $(NH_{3.6}D_{0.4})_2PtCl_6$
Appl. Phys. A **74 [Suppl.]**, 1363 (2002)

Prager, M., Schiebel,P, Grimm,H
Rotational Tunelling of NH_4 and NH_3D and dipolar interaction in $(NH_{3.6}D_{0.4})_2PtCl_6$
J. Chem. Phys. **116**, 10338 (2002)

Schweika, W., Maleyev,SV, Brückel, Th., Plakhty,VP, Regnault,L-P
Longitudinal spin fluctuations in the antiferromganet MnF_2 studied by polarized neutron scattering
Europhys. Lett. **60**, 446 (2002)

2001

Danilkin,SA, Fuess,H, Wieder,T, Hoser,A
Phonon dispersion and elastic constants in Fe-Cr-Mn-Ni austenitic steel
Journal of Materials Science **36 (4)**, 811-814 (2001)

Eckold,G
Kinetics of decomposition in ionic solids: neutron scattering study of the system AgBr-NaBr
Journal of Physics-Condensed Matter **13 (2)**, 217-240 (2001)

Kirstein,O, Prager, M., Combet,J, Johnson,MR
Ammonia group rotation in $Zn(NH_3)_4I_2$
Molecular Physics Report **31**, 47 (2001)

Köbler, U., Hoser,A, Englich,J, Snezhko,A, Kawakami,M, Beyss,M, Fischer, K
On the failure of the Bloch-Kubo-Dyson spin wave theory
Phys. Soc. Jpn. **70 (10)**, 3089-3097 (2001)

Köbler, U., Hoser,A, Kawakami,M, Abens,S
Observation of a spin wave exponent of 5/2 in the uniaxial antiferromagnet MnF_2
Physica B **307 (1-4)**, 175-183 (2001)

Invited Talks

2006

Hermann,RP
Localized vibrational modes in crystalline solids
JCNS Symposium and European User Meeting (Forschungszentrum Jülich, Germany) (2006)

Schweika,W, Herrmann,R
Soft local phonon modes in thermoelectric materials
DPG Frühjahrstagung (Dresden) (2006)

2005

Köbler,U
Experimentelle Untersuchungen von Magnetischen Materialien im Lichte der Renormierungsgruppentheorie
Mineralogisches Seminar (RWTH-Aachen Institut für Kristallographie) (2005)

Moze,O, Vecchini,C, Hoser,A, Prager,M, Roessli,B, Weissmüller,J
A neutron scattering investigation of the magnetic structure and magnetic excitations in nanocrystalline Tb
50th Annual Conference on Magnetism and Magnetic Materials (San Jose USA) (2005)

Prager,M, Press,W
The influence of molecular excitation on the lattice dynamics in methane clathrate
XIIIth International Workshop on ``Quantum atomic and molecular tunneling ... (Santiago de Compostella, Spain, 31 july) (2005)

2003

Prager, M.
Methyl rotational dynamics as probe of the water shell in methyl iodide clathrate
Janik's friends meeting 18 July 2003,Zakopane,Poland

2002

Prager, M.
Rotational potentials studied by spectroscopy and relaxation
6th International Conference on Quasielastic Neutron Scattering (Potsdam) (2002)

2001

Prager, M.
Rotational tunnelling: from simple to complex systems
HMI (Berlin) (2001)

Prager, M., Schiebel,P, Combet,J
Rotational tunnelling and disorder of 4-iodo-toluene
Quantum Atomic and Molecular Tunnelling 2001 (Nottingham UK) (2001)

Conference Presentations

2006

Hargreaves,J, Mitchell,PW, Balakrishnan,G, Hoser,A
Anharmonic Lattice Vibrations in Magnetite
Neutron and Muon Users Meeting (NMUM 2006) (Warwick (U.K.)) Poster (2006)

Köbler,U, Hoser,A
Effective spin description of crystal field effects in Cr_2O_3 and MnO
JCNS Symposium and European User Meeting (Jülich) Poster (2006)

Köbler,U, Hoser,A
The impact of renormalization group theory in magnetism
JCNS Symposium and european User Meeting (Jülich) Poster (2006)

Köbler,U, Hoser,A, Hoffmann,J-U
Relevant and non-relevant magnetic interactions
Frühjahrstagung der Deutschen Physikalischen Gessellschaft (Dresden) Poster (2006)

Köbler,U, Hoser,A, Schreiber,R, Thomas,C
Long range magnetic order in one and two dimensions
Structure meets magnetism (Bochum) Poster (2006)

2005

Danilkin,S, Hoser,A, Schweika,W, Bickulova,N
Diffuse scattering and low-energy phonons in Copper Selenide
International Conference on Neutron Scattering ICNS2005 (Sydney) Poster (2005)

Köbler,U, Hoser,A
Effective spin description of crystal field effects in $NdAl_2$
Frühjahrstagung der Deutschen Physikalischen Gesellschaft (Berlin) (2005)

Köbler,U, Hoser,A
Effective spin description of crystal field effects in Cr_2O_3 and MnO
International Conference on Neutron Scattering ICNS2005 (Sydney) Poster (2005)

Vecchini,C, Moze,O, Hoser,A, Roessli,B, Michels,K, Weissmüller,J
Magnetic excitations in nanocrystlline Terbium
International Conference on Neutron Scattering ICNS2005 (Sydney) Poster (2005)

2004

Hermann,RP, Grandjean,F, Bonville,P, Grimm,H, Schweika,W, Nolas,GS, Long, GJ
A neutron scattering study of the guest dynamics in filled germanium clathrates, Session J39–Fucus Session: Energy Harvesting: Materials & Phenomena, March Meeting of the APS (Montréal, 2004)

Hermann,RP, Grandjean,F, Bonville,P, Grimm,H, Schweika,W, Nolas,GS, Beekman,M, Long,GJ
Guest Tunnelling and Hopping in the Multiple Well Potential of Filled Clathrates
International Scientific Meeting of the Belgian Physical Society (Mons, Belgium) Talk (2004)

2003

Conrad, H., Kuhs,W, Nünighoff,K, Prager, M., Schweika, W.
Inelastic neutron scattering from CH4-clathrate, Th.F-clathrate and ice
ICANS-XVI : 16th Meeting of the International Collaboration on Advanced Neutron Sources , Convention Center,Neuss
Neuss: 12.05.2003 - 15.05.2003 (Poster)
Danilkin S.,Hoser A.,Schweika W.,Fuess H
Diffuse scattering and phonons in Cu2-xSe
European Conference on Neutron Scattering,Montpellier,3.-6.9.2003 (2003) Poster

Eckold,G, Caspary,D, Elter,P, Güthoff,F, Hoser,A, Schmidt,W
Time-Resolved Phonons as a Microscopic Probe for Demixing Processes
European Conference on Neutron Scattering, Montpellier,3.-6.9.2003 (2003) Poster

Hermann,RP, Schweika, W., Jin,R, Grandjean,F, Mandrus,D, Sales,BC, Long,GJ
Einstein Oscillator in Thallium Filled Antimony Skutterudites: Neutron Spectroscopy of Phonons in a Thermoelectric Material
DPG-Frühjahrstagung, Dresden, 24.-28.03.03

Hermann,RP, Long,GJ, Grandjean,F, Alp,EE, Sturhahn,W, Johnson,CE, Leupold O, Rüffer,R, Schweika,W
An Inelastic Nuclear Resonant and Inelastic Neutron Scattering Study of the Einstein Oscillators in Some Filled Antimony Skutterudites
International Conference on the Application of the Mössbauer Effect (Muscat, Sultanate of Oman) Talk (2003)

Meinnel, J., Grimm, H., Hernandez, O., Jansen, E.
Assignment of the three methyl tunneling lines in a trichloromesitylene (TCM) single crystal
3rdEuropean Conf. on Neutron Scattering, ECNS-2003, 03.-06.9.2003, Montpellier, France, Poster (Montpellier, 2003)

Prager, M., Desmedt,A, Pieper,J, Buchsteiner,A
Methyl rotational dynamics as probe of the water shell in methyl iodide clathrate
European Neutron Scattering Conference ECNS (2003),Montpellier,France Poster

2002

Caspary,D, Elter,P, Eckold,G, Schmidt,W
Time-evolution of phonon spectra during decomposition in ionic crystals
ESS Conference (Bonn) Poster (2002)

Danilkin,S, Skomorohov,A, Hoser,A, Fuess,H, Bickulova,NN, Rajevac,V
Lattice dynamics of superionic conductor $Cu_{2-\delta}Se$
ESS Conference (Bonn) Poster (2002)

Danilkin,SA, Skomorokhov,AN, Rajevac,V, Fuess,H, Hoser,A, Bickulova,NN
Crystal structure and lattice dynamics of superionic conductor $Cu_{2-x}Se$
5th International Conference Solid State Chemistry 2002 (Bratislava, Slovakia) Poster (2002)

Hense, K., Gratz,E, Lindbaum,A, Nowotny,H, Hoser,A, Güthoff,F, Klenke, J
Lattice Dynamics in YCu_2
ESS Conference (Bonn) Poster (2002)

2001

Caspary,D, Elter,P, Eckold,G
Zeitaufgelöste Phononen während der Entmischung in den Ionenkrsitallsystemen AgBr-NaBr und AgCl-NaCl
Deutsche Neutronenstreutagung (Jülich) Poster (2001)

Elter,P, Eckold,G, Caspary,D, Güthoff,F, Hoser,A
Time-evolution of phonon spectra during decomposition in $Ag_xNa_{1-x}Br$ ionic crystals
ICNS Conference (München) Poster (2001)
Hense, K., Gratz,E, Nowotny,H, Hoser,A, Güthoff,F
Lattice Dynamics in the orthorhomibic compound YCu_2
Deutsche Neutronenstreutagung (Jülich) Poster (2001)

Hoelzel,M, Danilkin,SA, Hoser,A, Ehrenberg,H, Wieder,T, Fuess,H
Phonon dispersion in austenitic stainless steel $Fe_{18}Cr_{12}Ni_2Mo$
ICNS Conference (München) Poster (2001)

Hölzel,M, Danilkin,S, Hoser,A, Wieder,T, Fuess,H
Phonon dispersion in nitrogen doped austenitic steels
Deutsche Neutronenstreutagung (Jülich) Poster (2001)

Magnetism

Publications

2006

Paul,A, Kentzinger,E, Rücker,U, Brückel,T
Symmetry and asymmetry during magnetization reversal in exchange biased multilayers and bilayers
Phys. Rev. B **73**, 092410 (2006)

Paul,A, Kentzinger,E, Rücker,U, Brückel,T
The angular dependence on the magnetization reversal in exchange biased multilayers
J. Phys: Cond. Mat. **18**, L149 (2006)

Paul,A, Kentzinger,E, Rücker,U, Bürgler,D, Brückel,T
Field-dependent magnetic domain structure in antiferromagnetically coupled multilayers by polarized neutron scattering
Phys. Rev. B **73**, 094441 (2006)

Theis-Bröhl,K, Wolff,M, Westphalen,A, Zabel,H, McCord,J, Höink,V, Schmalhorst,J, Reiss,G, Weis,T, Engel,D, Ehresmann,A, Rücker,U, Toperverg,B
Exchange-bias instability in a bi-layer with an ion beam imprinted stripe pattern of ferromagnetic/antiferromagnetic interfaces
Phys. Rev. B **73**, 174408 (2006)

Zabel,H
Neutron refectivity of spintronic materials
Materials today **9**, 42 (2006)

2005

Bedanta,S, Petracic,O, Kentzinger,E, Kleemann,W, Rücker,U, Paul,A, Brückel,T, Cardoso,S, Freitas,PP
Superferromagnetic domain state of a discontinuous metal insulator multilayer
Phys. Rev. B **72**, 024419 (2005)

Hecker,M, Schneider,CM, Mertins,HC, Rücker,U, Kentzinger,E
Magnetic order in Co/Cu multilayers studied by polarized soft X-rays and neutrons
J. Magn. Magn. Mater **286**, 416 (2005)

Kentzinger,E, Rücker,U, Paul,A, Brückel,Th
Layer resolved magnetisation correlations in multilayers
Neutron News **16**, 26 (2005)

Kravtsov,E, Brucas,R, Hjörvarsson,B, Hoser,A, McIntire,G, Remhof,A, Nefedov,A Radu,F, Zabel,H
Proximity effect of vanadium on strain and spin-density waves in thin Cr films
Journal of Magnetism and Magnetic Materials **286**, 425 (2005)

Kravtsov,E, Nefedov,A, Remhof,A, Radu,F, Zabel,H, Brucas,R, Hjörvarsson,B, Hoser,A, McIntyre,GJ
Reorientation of spin-density waves in Cr films induced by proximity effect of vanadium
Journal of Phyiscs: Condensed Matter **17**, 3143 (2005)

Köbler,U, Hoser,A, Bos,J, Schäfer,W, Pohlmann,L
Weak ferromagnets with integer and half-integer spin quantum numbers
Physica B **355**, 90-99 (2005)

Köbler,U, Hoser,A, Bos,J, Schäfer,W, Pohlmann,L
Weak ferromagnets with integer and half-integer spin quantum numbers
Physica B **355**, 90-99 (2005)

Köbler,U, Hoser,A, Schäfer,W
On the temperature dependence of the magnetic excitations
Physica B 364 **364**, 55-70 (2005)

Paul,A, Kentzinger,E, Rücke,U, Bürgler,D, Grünberg,P
Measurement and simulation of polarized neutron reflectivity and off-specular scatteirng from evolving magnetic domain structure in Co/Cu multilayers
Physica B **356**, 31 (2005)

Paul,A, Kentzinger,E, Rücker,U, Bürgler,D, Grünberg,P
Polarized neutron scattering from polycrystalline, exchange-biased magnetic multilayers
Physica B **356**, 26 (2005)

Paul,A, Kentzinger,E, Rücker,U, Bürgler,DE, Grünberg,P
Nonuniform and sequential magnetization reversal via domain structure formation for multilayers system with grain size enhanced exchange bias
EPJ B **45**, 249 (2005)

2004

Bedanta,S, Chen,X, Sahoo,S, Kleemann,W, Kentzinger,E, Nordblad,P, Cardoso S, Freitas PP,
Collective magnetic states of ferromagnetic nanoparticles in the superspin limit.
Phys. Stat. Sol. (c) **1**, 3288 (2004)

Endo,H, Schwahn,D, Colfen,H
An analysis of calcium carbonate / polymer hybrid crystals applying contrast variation
Physica B **350**, E943-E945 (2004)

Kravtsov,E, Nefedov,A, Radu,F, Remhof,A, Zabel,H, Brucas,R, Hjorvarsson,B, Hoser,A, Wilkins,SB
Proximity effect of vanadium on spin-density-wave magnetism in Cr films
Phys. Rev. B **70**, 4425 (2004)

Köbler,U, Hoser,A
Universal temperature dependence of the magnetic excitations
J. Magn. Magn. Mater **272-276**, 342 (2004)

Papathanassiou,GF, Yakinthos,JK, Schäfer,W
The antiferromagnetic structure of $ErPtGe_2$
J. Magn. Magn. Mat. **269**, 1 (2004)

Paul,A, Kentzinger,E, Rücker,U, Bürgler,DE, Grünberg,P
Sequence, symmetry and magnetic fluctuations of the magnetization reversal in exchange biased multilayers
Phys. Rev. B **70**, 224410 (2004)

Schäfer,W, Buschow,KHJ
Neutron Diffraction Study on Intermetallic Er_5Mg_{24} and Tm_5Mg_{24}
Mat. Sci. Forum **443-444**, 263 (2004)

Siouris,IM, Semitelou,IP, Yakinthos,JK, Schäfer,W
Presence of a spin glass state in antiferromagnetic Tb_2CuIn_3
Mat. Sci. Forum **443-444**, 391 (2004)

Tolinski,T, Schäfer,W, Kowalczyk,A, Andrzejewski,B, Hoser,A, Szlaferek,A
Magnetic properties of $TbNi_4Al$ and $DyNi_4Al$ compounds: investigation via neutron diffraction and magnetometry
Journal of Alloys and Compounds **385**, 28 (2004)

Voigt, J., Kentzinger, E., Rücker, U., Wermeille,D, Hupfeld,D, Schweika, W., Schmidt,W, Brückel, Th.
Direct observation of the interlayer exchange coupling mechanism in a magnetic [Er|Tb] multilayer
Europhysics Letters 65(4) (2004) 560-566 (2004)

2003

Kalvius,GM, Noakes,DR, Wäppling,R, Grosse,G, Schäfer, W., Kockelmann,W, Yakinthos,JK, Kotsanidis,PA
Spin dynamics and spin order in frustrated $TbCo_xNi_{1-x}C_2$
Physica B **326**, 465 (2003)

Kalvius,GM, Wagner,FE, Noakes,DR, Schreier,E, Wäppling,R, Zimmermann,U, Schäfer,W, Kockelmann,W ,Halevy,I ,Gal,J
Magnetic behaviour of YFe_xAl_{12-x}
Physica B **326**, 460 (2003)

Kentzinger, E., Rücker, U., Toperverg, B., Brueckel, Th.
Determination of the magnetic fluctuations in an Fe/Cr/Fe trilayer exhibiting a neutron resonance state
Physica B **335** 89 (2003)

Köbler, U., Englich, J., Hupe, O., Hesse, J.
Effective spin quantum numbers in Fe, Co and Ni
Physica B 339 (2003), 156 – 163

Köbler, U., Hoser, A., Hupfeld, D.
A complete description of the order parameter of Heisenberg-type magnets for $0 < T < Tc$
Physica B 328 (2003), 276 – 282

Lauter,HJ, Lauter-Pasyuk,V, Toperverg, B.P, Rücker, U., Milyaev,M, Romashev,L, Krinitsyna,T, Ustinov,V
Layer magnetization evolution in an Fe / Cr multilayer with uniaxial anisotropy
Physica B **335** 59 (2003)

Loewenhaupt,M, Schäfer, W., Niazi,A, Sampathkumaran,E V
Evidence for the coexistence of low-dimensional magnetism and long-range order in Ca_3CoRhO_6
Europhysics Letters **63** (2003) 374-380

Tolinski,T, Schäfer, W., Chelkowska,G, Kockelmann,W, Hoser,A, Andrzejewski,B, Szlaferek A, Kowalczyk A
Comparative studies of structural,magnetic and electronic properties of $NdNi_4Al$ and $NdNi_4B$ compounds
Mol. Phys. Rep. 38 (2003) 138

Tolinski,T, Schäfer, W., Kockelmann,W, Kowalczyk,A, Hoser,A
Neutron diffraction,magnetic,and transport studies of $NdNi_4Al$
Phys. Rev. B 68 (2003) 144403

Ziegenhagen, N., Rücker, U., Kentzinger, E., Lehmann,R, vanderHart,A, Toperverg, B., Brückel, Th
Magnetic Properties of Laterally Structured Fe/Cr Multilayers
Physica B **335** 50 (2003)

2002

Brückel, Th., Schweika, W. (Ed.)
Polarised neutron scattering: lectures
Schriften des Forschungszentrums Jülich, Materie und Material, Vol. 12 (2002)

Köbler, U., Hoser,A, Fischer,K, Beyss,M
The impact of fourth-order exchange interactions on the thermal variation of the order parameter
Appl. Phys. A **74 [Suppl 1]**, s604 (2002)

Papathanasiou,GF, Kotsanidis,PA, Yakinthos,JK, Schäfer, W.
The two antiferromagnetic phases of $TbPtGe_2$
J. Alloys and Compounds **343**, 26 (2002)

Rücker, U., Kentzinger, E., Toperverg, B., Ott,F, Brückel, Th.
Layer-by-Layer magnetometry on polarizing supermirrors
Applied Physics A **74**, 607 (2002)

Schweika, W.
Polarized neutron scattering
Schriften des Forschungszentrums Jülich,Reihe Materie und Material **12**
ISBN 3-89336-314-9
T. Brückel und W. Schweika (Eds.) (2002)

Schweika, W, Maleyev,S V, Brückel, Th., Plakhty,V P, Regnault,L P
Longitudinal spin fluctuations in the antiferromagnet MnF2
studied by polarized neutron scattering
Europhys. Lett. **60** (2002) 446

Voigt, J., Kentzinger, E., Rücker, U., Hupfeld, D., Schmidt, W., Ohl, M., Brückel, Th.
Interlayer coupling in [Er|Tb] superlattices
Appl. Phys. A **74** (2002) S1517

Voigt, J., Rücker, U., Nerger,S, Kentzinger, E., Hupfeld,D, Schmidt,W, Brückel, Th.
Structural and magnetic properties of [Er/Tb] superlattices
Journal of Magnetism and Magnetic Materials **240**, 559 - 561 (2002)

2001

Kalvius,GM, Wagner,FE, Schreier,E, Wäppling,R, Noakes,DR, Zimmermann,U, Schäfer, W., Kockelmann,W, Halevy,I, Gal,J
The magnetism of frustrated RFe_6Al_6 compounds studied by μSR and Mössbauer
Hyperfine Interactions **136/137**, 269 (2001)

Plakhty,V P, Schweika, W., Brückel, Th., Kulda,J, Gavrilov,S V, Regnault,L P, Visser,D
Chiral criticality in helimagnet Ho studied by polarized neutron scattering
Phys. Rev. B **64** (2001) 100402(R),Rapid Comm.

Siouris,IM, Semitelou,IP, Yakinthos,JK, Arons,RR, Schäfer, W.
Competing ferro- and antiferromagnetism in R_2CuIn_3 (R=Tb, Ho, Er) intermetallics studied by neutron diffraction and magnetization measurements
J. Magn. Magn. Mater **226**, 1128 (2001)

Invited Talks

2006

Brückel,T
Magnetism in Nanostructures: The Basics of Spintronics
International Symposium on Neutron Scattering: Electron Correlations, Magnetism (Karlsruhe) (2006)

Brückel,T
Magnetismus in Nanostrukturen: Grundlagen der Spintronic
Fakultäts-Kolloquium (Tübingen) (2006)

Brückel,T
Probing lateral magnetic correlations in nanostructures
ADAM-Workshop (Bochum) (2006)

Theis-Bröhl,K
Lateral Nanostructures
ADAM-Workshop (Bochum) (2006)

2005

Brückel,T
Methods and Techniques: Experimental Techniques for the Study of Magnetism
School on Pulsed Neutrons (Trieste) (2005)

Brückel,T
Magnetic Nanostructures and Correlated Electron Systems studied with Neutron and X-Ray Vision
Chinese Academy of Science (Peking) (2005)

Brückel,T
Layer Resolved Magnetic Correlations in Nanostructures
ICNS (Sydney) (2005)

Brückel,T
A Deeper Look into Magnetic Nanostructures and Correlated Electron Systems using Neutron and X-Ray Vision
CIAE-Seminar (Peking) (2005)

Zabel,H
Magnetic thin films and superlattices
15th Hercules course (Grenoble) (2005)

Zabel,H, Radu,F, Theis-Bröhl,K, Wolff,M
Magnetic Nanostructures
DPG-Frühjahrstagung, Symposium Perspectives of research with neutrons (Berlin) (2005)

2004

Brückel,Th
A Look into Magnetic Nanostructures using Neutron and X-Ray Vision
Kolloquium (Universität Heidelberg) (2004)

Paul,A
Neutron and X-ray scattering from exchange biased multilayers
Department of Materials Science and Engineering, KTH (Stockholm) (2004)

Paul,A
Nano-layered magnetic structures
Department of Astronomy and Astrophysics, Tata Institute of Fundamental Research (Mumbai, India) (2004)

Paul,A
Neutron scattering from exchange bias multilayers
Department of Physics and Astronomy, Katholik University (Leuven, Belgium) (2004)

Paul,A, Kentzinger,E, Ruecker,U
Polarized neutron reflectivity and off-specular scattering showing sequential and symmetric magnetization reversal from exchange-biased multilayers
Deutsche Neutronenstreutagung (Dresden) (2004)

Theis-Bröhl,K, Westphalen,A, Wolff,M, Zabel,H, Rücker,U, Schmalhorst,J, Rott,K, Brückl,H, Toperverg,B
Laterale Strukturen mit antiparalleler Ausrichtung
Deutsche Neutronenstreutagung (Dresden) (2004)

2003

Brückel, Th.
Nautrons and X-rays: a closer look into magnetic nanostructures
International Workshop on Low Dimensional Magnetism as seen by Photons and Neutrons
Technologiezentrum Ruhr, Bochum, 22.-23.05.03

Kentzinger, E.
Depth-resolved investigations of lateral correlations in magnetic layers by Polarized Neutron Scattering at Grazing Incidence
Universität Duisburg-Essen,15.7.2003

Köbler U.,Hoser A.
A new concept in magnetism
International Conference on Magnetism,27.7.-1.8., Rome (2003)

Schweika, W.
Phasonenunordnung in Al-Pd-Mn Quasikristallen
Institut für Kristallographie,RWTH Aachen
11.2.2003

2002

Brückel, Th.
The Colorful Palette of Magnetism: Resonant Magnetic X-Ray Scattering
Kolloquium (Max-Planck-Institut, Stuttgart) (2002)

Brückel, Th.
Von korrelierten Elektronen zu komplexen Legierungen: Festkörperforschung am IFF
HGF-Workshop Kondensierte Materie (FZJ, Jülich) (2002)

Brückel, Th.
FZJ @ MuCAT: Examples for Research Activities
APS User Science Seminar (Argonne, USA) (2002)

Lauter,HJ, Lauter-Pasyuk,V, Toperverg, B., Rücker, U., Romashev,L, Milyaev,M, Ustinov,V
Spin-flop transition in Fe / Cr multilayers
Polarized Neutrons in Condensed Matter investigations (Jülich) (2002)

Toperverg, B.
Diffuse neutron scattering on multilayers
XXXVI PNPI Winter School Condensed State Physics (Gatchina (RU)) (2002)

Toperverg, B.
Lateral magnetic patterns in thin films and layered superstructures: polarized neutron off-specular scattering
Seminar Ruhr-Universität Bochum (Bochum) (2002)

Toperverg, B.
Neutron scattering at grazing incidence
Workshop RNIKS-2002 (Gatchina(RU)) (2002)

Toperverg, B.
Neutron scattering at grazing incidence
IPNS / SNS Seminar (Argonne) (2002)

Toperverg, B.
Supermatrix formalism to model off-specular neutron scattering
The 7th International Conference on Surface X-Ray and Neutron Scattering (Lake Tahoe, CA) (2002)

Toperverg, B.
Theoretical interpretation and quantitativ analysis of data on reflectometry and off-specular scattering
Workshop Neutron Reflection: Progress in the Study of Interfaces (Grenoble) (2002)

Toperverg, B.
Theoretical interpretation of off-specular polarized neutron scattering from nanocomposite films
International Workshop on Nanocomposites: Materials, Neutrons and Data Interpretation (Argonne) (2002)

Toperverg, B.
Polarized neutron reflection and off-specular scattering
GKSS-Seminar (Geesthacht) (2002)

Ziegenhagen, N., Rücker, U., Kentzinger, E., Toperverg, B., Brückel, Th., Lehmann,R, van der Hart,A
Magnetic Properties of Laterally structured Fe/Cr Multilayers
Polarized Neutrons for Condensed Matter Investigations (Jülich) (2002)

2001

Kentzinger, E.
Reflectivity and off-specular scattering of neutrons from magnetic thin films
Deutschen Neutronenstreutagung 2001 (Juelich) (2001)

Schweika, W.
Temperature dependence of phason disorder in Al-Pd-Mn quasicrystals
04.-07.12.2001
Duisburg,Workshop on Quasicrystals

Toperverg, B.
Grazing Incidence Scattering with Polarized Neutrons: Examples and Applications
ANL Seminar (Argonne) (2001)

Toperverg, B.
Off-specular polarized neutron scattering from magnetic fluctuations in thin films and multilayers
ICNS 2001 (Munich) (2001)

Toperverg, B.
Polarized Neutron Off-specular Scattering from Magnetic Fluctuations in Films and Multilayers
NIST Seminar (Gaithersburg) (2001)

Conference Presentations

2006

Bedanta,S, Chen,X, Kleemann,W, Petracic,O, Kentzinger,E, Eimüller,T, Cardoso,S, Freitas,PP
Interacting ferromagnetic nanoparticles in the superspin limit: from modified superparamagnetism to collective magnetic states
Nanoscale Magnets - Top down meets Bottom up (Bad Honnef) Poster (2006)

Bedanta,S, Petracic,O, Chen,X, Rhensius,J, Kleemann,W, Kentzinger,E, Rücker,U, Paul,A, Brückel,T, Eimüller,T, Cardoso,S, Freitas,PP
From modified superparamagnetism to collective magnetic states in granular metal insulator multilayers
Physics in Low Dimensions: Structure meets Magnetism (Bochum) Poster (2006)

Bedanta,S, Petracic,O, Chen,X, Rhensius,J, Kleemann,W, Kentzinger,E, Rücker,U, Paul,A, Brückel,T, Eimüller,T, Cardoso,S, Freitas,PP
From modified superparamagnetism to collective magnetic states in granular metal insulator multilayers
DPG Frühjahrstagung (Dresden) Poster (2006)

Feygenson,M, Pollmeier,K, Kentzinger,E, Sager,W, Brückel,T, Paul,A
Magnetic Co nanoparticles in solution
DPG Frühjahrstagung (Dresden) Poster (2006)

Li,HF, Su,Y, Perßon,J, Meuffels,P, Walter,J, Skowronek,R, Brückel,T
Investigation on structure and magnetic properties of $La_{1-x}Sr_xMnO_3$
DPG Frühjahrstagung (Dresden) Poster (2006)

Paul,A, Brückel,T, Kentzinger,E, Rücker,U
Magnetization Reversal in Trained Exchange Biased Multilayers
Physics in Low Dimensions: Structure meets Magnetism (Bochum) Poster (2006)

Paul,A, Brückel,T, Kentzinger,E, Rücker,U
Angular dependence of magnetization reversal in exchange biased multilayers
DPG Frühjahrstagung (Dresden) Poster (2006)

Westphalen,A, Remhof,A, Theis-Bröhl,K, Zabel,H
Magnetic reversal of microstructured patterns
Nanoscale Magnets - Top down meets Bottom up (Bad Honnef) Poster (2006)

2005

Mouallem-Bahout,,M, Walter,JM, Skowronek,R, Moure,C, Peña,O
Cation distribution and magnetic properties of $(Co,Mn,Ni)_3O_4$ spinel investigated by neutron powder diffraction
GDR - Nouveaux états électroniques des matériaux (Batz sur mer, France) Talk (2005)

Paul,A, Kentzinger,E, Rücker,U, Brückel,T
Magnetization reversal in exchange biased multilayers with field direction
DPG Frühjahrstagung (Berlin) Poster (2005)

Rücker,U, Toperverg,B, Ott,F, Brückel,T
Zeeman splitting revisited: polarized neutron reflectometry under high magnetic fields
2nd FRM-II Workshop on Neutron Scattering - Advanced Materials (Burg Rothenfels am Main) Talk (2005)

TheilKuhn,L, Lefmann,K, Bahl,CRH, Morup,S, Wischnewski,A
Ordered magnetic structures without Bragg reflections - isotropic spin relaxation in magnetic nanoparticles
ICNS 2005 (Sydney, Australia) Poster (2005)

Theis-Bröhl,K, Toperverg,BP, McCord,J, Rücker,U, Schmalhorst,J, Höink,V, Brückel,H, Weiss,T, Engel,D, Ehresmann,A, Zabel,H
Domain propagation in ion bombarded magnetic wires with opposite exchange bias
DPG Frühjahrstagung (Berlin) Talk (2005)

Kravtsov,E
Spin density waves magnetism in thin Cr films: synchrotron and neutron results
INTAS workshop "Hierarchy of scales in magnetic nanostructures" (St. Petersburg, Russia) Talk (2004)

2004

Bedanta,S, Petracic,O, Kleemann,W, Kentzinger,E, Rücker,U, Paul,A, Brückel,Th, Cardoso,S, Freitas,PP
Polarized Neutron Reflectivity Studies on Discontinuous Metal Insulator Multilayers
Deutsche Neutronenstreutagung (TU Dresden) Poster (2004)

Chang,LJ, Schäfer,W, Jansen,E, Prager,M, Emmanuelle,S, Monkenbusch,M, Schweika,W, Perßon,J, Brückel,Th
Neutron scattering studies on pyrochlore $Ho_2Ru_2O_7$
Deutsche Neutronenstreutagung (Dresden) Poster (2004)

Feygenson,M, Ziegenhagen,N, Rücker,U, Kentzinger,E, Toperverg,B, Brückel,Th
X-ray and neutron scattering investigation of a laterally structured magnetic multilayer
Deutsche Neutronenstreutagung (TU Dresden) Poster (2004)

Kentzinger,E, Rücker,U, Toperverg,B, Ott,F, Brückel,Th
Layer-by-layer Investigation of the Magnetic Fluctuations in Polarizing Supermirrors
Deutsche Neutronenstreutagung (TU Dresden) Poster (2004)

Kentzinger,E, Rücker,U, Toperverg,B, Ziegenhagen,N, Paul,A, Brückel,Th
Layer-by-layer investigation of the magnetisation reversal process in magnetic multilayers by scattering of polarised neutron under grazing incidence
321. WE-Heraeus-Seminar (Bad Honnef) Poster (2004)

Kravtsov,E, Brucas,R, Hjorvarsson,B, Hoser,A, McIntyre,G, Nefedov,A, Radu,F, Remhof,A, Zabel,H
Proximity effect of vanadium on spin-density waves in Cr films
Deutsche Neutronenstreutagung (Dresden) Poster (2004)

Kravtsov,E, Nefedov,A, Radu,F, Remhof,A, Zabel,H, Hjorvarsson,B, Hoser A
Proximity effect of vanadium on spin-density wave magnetism in thin Cr films
5 International Symposium on Metallic Multilayers (Boulder USA) Talk (2004)

Köbler,U, Hoser,A
Long range magnetic order in three dimensions, a difficult problem
BENSC User Meeting (Berlin) Poster (2004)

Köbler,U, Hoser,A, Schäfer,W, Stüßer,N
Universal magnetic behaviour for T->0 and T-> Tc
Deutsche Neutronenstreutagung (Dresden) Poster (2004)

Paul,A, Kentzinger,E, Ruecker,U
Polarized neutron reflectivity and off-specular scattering in quantifying evolving domain structure of polycrystalline Co/Cu multilayers
Deutsche Neutronenstreutagung (Dresden) Talk (2004)

Paul,A, Kentzinger,E, Rücker,U, Bürgler,DE, Grünberg,P
Measurement and Simulation of Polarized neutron Reflectivity and off-specular scattering from evolving magnetic domain structure in Co/Cu multilayers
PNCMI 2004 (Washington) Poster (2004)

Paul,A, Kentzinger,E, Rücker,U, Bürgler,DE, Grünberg,P
Polarized neutron scattering of exchange-biased magnetic multilayers
PNCMI (Washington) Poster (2004)

Rücker,U, Kentzinger,E, Korolkov,D, Willner,L, Frielinghaus,H, Ziegenhagen,N, Brückel, Th, Toperverg, B
Investigation of lateral magnetic structures using neutron reflection techniques
321. WE-Heraeus-Seminar (Bad Honnef) Poster (2004)

2003

Köbler U.,Hoser A.
Critical behaviour of the magnetic order parameter for T->0 and for T->Tc
European Conference on Neutron Scattering,Montpellier,3.-6.9.2003 (2003) Poster

Köbler, U., Hoser, A., Bos, J., Schäfer, W.
Why does the spin wave theory fail?
Intern. Conference on Magnetism, ICM2003, 27.7.-1.8.2003, Roma, Italy

Köbler, U., Hoser, A., Schäfer, W.
Universal magnetic behaviour for T→0 and T→T_C
3rd European Conf. on Neutron Scattering, ECNS-2003, 03.-06.9.2003, Montpellier, France
Poster (Montpellier, 2003)

Köbler U., Hoser A., Schäfer W., Müller R., Bos J., Fischer K.
Warum richten sich reale Magnete nicht nach der Spinwellentheorie ?
Frühjahrstagung der DPG,Dresden,(2003)

Lauter,H.,Lauter-Pasyuk,V, Toperverg, B., Rücker, U., Milyaev,M, Romashev,L, Krinitsyna,T, V. Ustinov,V.
Layer magnetization evolution with magnetic field in an uniaxial Fe/Cr multilayer PNSXM 2003 (Venedig),4.-6. 8. 2003 Poster

Rücker, U., Feygenson,M, Toperverg, B., Kentzinger, E., Dalgliesh,R, Brückel, Th.
Neutron quantum well states used to increase the sensitivity for magnetic disorder
ECNS 2003 (Montpellier),3.-6. 9. 2003

Schäfer, W., Buschow, K. H. J.
Structure and ferromagnetic order of Er_5Mg_{24} and Tm_5Mg_{24}
11. Jahrestagung der Deutschen Gesellschaft für Kristallographie, 10.-13.3.2003, Berlin
Poster (Berlin, 2003)

Schweika, W., Maleyev,S V, Brückel, Th., Plakhty,V, Regnault,L P
Longitudinal spin fluctuations in the antiferromagnet MnF2 studied by polarized
neutron scattering
DPG-Frühjahrtagung Dresden 26.3.2003

Su, Y., Schweika, W., Istomin, K., Wermeille, D., Hupfeld, D., Fattah, A., Foucart, P., Brückel, Th.
Investigations of lightly doped La1-xSrxMnO3 with polarized neutrons and synchrotron X-rays (Poster)
PNSXM, Polarised Neutrons and Synchrotron X-rays for Magnetism (Venedig, Italien) 2003

Ziegenhagen, N., Rücker, U., Kentzinger, E., Lehmann,R, van der Hart,A,
Magnetic domains in a laterally structured Fe / Cr multilayer
Toperverg, B., Brückel, Th.
ECNS 2003 (Montpellier),3.-6. 9. 2003 Poster

Ziegenhagen, N., Rücker, U., Kentzinger, E., Toperverg, B., Lehmann, R., van der Hart, A., Brückel, Th.
Determination of the Magnetic Properties of a Laterally Structured Fe/Cr multilayer
ECNS 2003 (Montpellier),3.-6. 9. 2003

2002

Kalvius,GM, Noakes,DR, Wäppling,R, Schäfer, W., Kockelmann,W, Yakinthos,JK, Kotsanidis,PA
Spin dynamics and spin disorder in frustrated $TbCo_xNi_{1-x}C_2$
9th Intern. Conference on Muon Spin Rotation/Relexation/Resonance (Williamsburg, Virginia) Talk (2002)

Kalvius,GM, Wagner,FE, Noakes,DR, Schreier,E, Wäppling,R, Zimmermann,U, Schäfer, W., Kockelmann,W, Halevy,I, Gal,J
Magnetic behavior of YFe_xAl_{12-x}
9th Intern. Conference on Muon Spin Rotation/Relexation/Resonance (Williamsburg, Virginia) Talk (2002)

Kentzinger, E., Rücker, U., Toperverg, B., Brückel, Th.
Determination of the magnetic fluctuations in an Fe/Cr/Fe trilayer exhibiting a neutron resonance state
Polarized Neutrons for Condensed Matter Investigations (Juelich) Poster (2002)

Kentzinger, E., Toperverg, B., Rücker, U., Brückel, Th.
Simulation of Reflectivity and Off-Specular Scattering of Polarised Neutrons from Laterally Patterned Magnetic Multilayers
Workshop on Polarised Neutrons in Condensed Matter Investigations (FZJ, Jülich) Poster (2002)

Köbler, U., Hoser,A, Bos,J, Schäfer, W., Mueller,R, Fischer,K
On the thermodynamic universality classes of Heisenberg type magnets
Deutsche Neutronenstreutagung 2002 and The European Spallation Source (Bonn) Poster (2002)

Lemmens,P, Choi,KY, Güntherodt,G, Kageyama,H, Hiroi,Z, Schäfer, W., Geibel,C, Brenig,W, Gros,C, Valentini,R, Millet,P, Törnroos,KW, Johnsson,M, Mila,F
From singlet to Néel State - a substitution study on the spin tetrahedra system $Cu_2Te_2O_5(Br_{1-x}Cl_x)_2$
DPG Frühjahrstagung (Regensburg) Talk (2002)

Rücker, U., Kentzinger, E., Toperverg, B., Ziegenhagen, N., Brückel, Th.
Off-specular scattering from magnetic structures measured with full polarization analysis using HADAS@DIDO, Jülich
REFILL-Workshop (Grenoble) Poster (2002)

Rücker, U., Toperverg, B., Kentzinger, E., Brückel, Th.
Resonant states in a ferromagnetic quantum well for neutrons
ESS-Konferenz (Bonn) Poster (2002)

Schäfer, W., Buschow,KHJ
Neutron diffraction on intermetallic Er_5Mg_{24} and Tm_5Mg_{24}
8th European Powder Diffraction Conference (Uppsala) Poster (2002)

Siouris,IM, Schäfer, W.
Coexistence of spin glass states in the antiferromagnetic $Tb_2(Ag,In)_3$ and $Tb_2(Cu,In)_3$ systems
Deutsche Neutronenstreutagung 2002 and The European Spallation Source (Bonn) Poster (2002)

Siouris,IM, Semitelou,IP, Yakinthos,JK, Schäfer, W.
Presence of a spinglass state in antiferromagnetic Tb_2CuIn_3
8th European Powder Diffraction Conference (Uppsala) Poster (2002)

Su,Y, Istomin,K, Schweika, W., Fattah,A, Foucart,P, Meuffels,P, Brueckel Th
Polarization analysis of diffuse neutron scattering in lightly doped $La_{1-x}Sr_xMnO_3$
European Conference ESS (Bonn, Germany) Poster (2002)

Su,Y, Schweika, W., Istomin,K, Fattah,A, Foucart,P, Brueckel, Th.
Investigation of lightly doped $La_{1-x}Sr_xMnO_3$ single crystals with polarized neutrons and synchrotron X-rays
Polarized Neutrons in Condensed Matter Investigations (PNCMI) (Juelich, Germany) Poster (2002)

Voigt, J., Kentzinger, E.
Untersuchung magnetischer Übergitter mit Neutronen und Synchrotronröntgenstrahlung
Workshop Magnetismus und Streumethoden (Jülich) Talk (2002)

Voigt, J., Kentzinger, E., Rücker, U., Schmidt, W., Schweika, W., Brückel, Th.
Magnetic Structures and Phase Transitions in [Er|Tb] Multilayers
German Neutron Scattering Meeting / ESS Meeting, Bonn (2002)

Voigt, J., Kentzinger, E., Rücker, U., Schweika, W., Brückel, Th.
Magnetic Structures and Phase Transitions in Er/Tb Superlattices
ESS-Konferenz (Bonn) Poster (2002)

Ziegenhagen, N., Rücker, U., Kentzinger, E., Lehmann,R, vanderHart,A, Toperverg, B., Brückel, Th
Magnetic Properties of Laterally Structured Fe/Cr Multilayers
ESS-Konferenz (Bonn) Poster (2002)

2001

Köbler, U., Hoser,A, Fischer,K, Beyss,M
The impact of fourth-order exchange interactions on the thermal variation of the order parameter
ICNS Conference (München) Poster (2001)

Köbler, U., Hoser,A, Kawakami,M
Beobachtung eines Bloch Exponent von 5/2 am Antiferromagneten MnF_2 mit S=5/2 and axialer Austauschanisotropie
Deutsche Neutronenstreutagung (Jülich) Poster (2001)

Massalovitch,S, Ioffe, A., Küssel,E, Schlapp,M, Brückel, Th.
Development of the large-area 2D neutron detector based on the imaging plate
Deutsche Neutronenstreutagung (FZJ, Jülich) Poster (2001)

Massalovitch,S, Ioffe, A., Küssel,E, Schlapp,M, vonSeggern,H, Brückel, Th.
Development of neutron image plate for low flux measurements
ICNS-Konferenz (München) Poster (2001)

Rücker, U.
Untersuchung lateral strukturierter magnetischer Vielfachschichten
Workshop Magnetismus und Streumethoden, HMI (Berlin) Talk (2001)

Rücker, U., Kentzinger, E., Brückel, Th.
Spin-split diffuse scattering under grazing incidence from polarizing supermirrors
Deutsche Neutronenstreutagung (Jülich) Poster (2001)

Rücker, U., Kentzinger, E., Toperverg, B., Ott,F, Brückel, Th.
Spindependent diffuse scattering from polarizing supermirrors
ICNS 2001 (Munich) Poster (2001)

Schweika, W., Shramchenko,N, Caudron,R, Bellissent,R, Widom,M
Phason disorder in icosahedral AlPdMn quasicrystals
Deutsche Neutronenstreutagung 2001,19-21.2.2001,Jülich and ICNS 2001,9-13.10.2001,Munich

Siouris,I, Semitelou,JP, Yakinthos,JK, Schäfer,W, Arons,RR
Structure and magnetic Structure states of the rare earth intermetallics R_2AgIn_3 and R_2CuIn_3
Deutsche Neutronenstreutagung (Jülich) Poster (2001)

Sosnowska,I, Kockelmann,W, Schäfer,W, Barbier,B, Troyanchuk,IO
Influence of Mn doping on the crystal structure and magnetic order of $BiFeO_3$ - preliminary powder diffraction results
9. Jahrestagung der Deutschen Gesellschaft für Kristallographie (Bayreuth) Poster (2001)

Sosnowska,I, Kockelmann,W, Schäfer, W., Troyanchuk,IO
Influence of Mn doping on the crystal structure and magnetic order of $BiFeO_3$
Deutsche Neutronenstreutagung (Jülich) Poster (2001)

Sosnowska,I, Schäfer, W., Kockelmann,W, Barbier,B, Andersen,KA, Troyanchuk,IO
Crystal structure and spiral magnetic ordering of $BiFeO_3$ doped with manganese
ICNS 2001 (Munich) Poster (2001)

Toperverg, B., Kentzinger, E., Rücker, U., Brückel, Th.
Specular reflection and off-specular scattering of polarized neutrons from magnetic multilayers
Deutsche Neutronenstreutagung (FZJ, Jülich) Poster (2001)

Voigt, J., Kentzinger, E., Rücker, U., Schweika, W., Brückel, Th., Schmidt,W, Ohl, M Hupfeld, D
Proximity effects in Er/Tb superlattices: How Neutrons and X-Rays complement each other
International Conference on Neutron Scattering (München) Poster (2001)

Voigt, J., Schmidt,W, Ohl,M, Brückel, Th.
Magnetische Ordnung in Erbium/Terbium-Schichtsystemen
Deutsche Neutronenstreutagung (FZJ, Jülich) Poster (2001)

Soft Condensed Matter, Liquids, Glasses

Publications

2006

Burckbuchler,V, Kjøniksen,A-L, Galant,C, Lund,R, Amiel,C, Knudsen,KD, Nyström, B
Rheological and Structural Characterization of the Interactions between Cyclodextrin Compounds and Hydrophobically Modified Alginate
Biomacromolecules **7**, in press (2006)

Hermes,HE, Frielinghaus,H, Pyckhout-Hintzen,W, Richter,D
Quantitative analysis of small angle neutron scattering data from montmorillonite dispersions
Polymer **47**, 2147 (2006)

László,K, Kosik,K, Wilk,E, Geissler,E
Interaction of Phenolic Pollutants with PNIPA Hydrogels
in: Pure and Applied Surface Chemistry and nanomaterials for Human Life and Environmental Protection, NATO ASI series (2006)

Svanberg,C, Pyckhout-Hintzen,W, Boerjesson,L
Network Structure of Poly(methyl methacrylate)-based Gelds and Gel Electrolytes
Electro Chimica Acta **51**, 4153 (2006)

Wischnewski,A, Richter,D
Polymer Dynamics in Melts
in: Soft Matter Vol.1, ed. G. Gompper, M. Schick, p. 17, Wiley-VCH (2006)

Zamponi,M, Wischnewski,A, Monkenbusch,M, Willner,L, Richter,D, Likhtman,AE, Kali G, Farago B
Molecular Observation of Constraint Release in Polymer Melts
Physical Review Letters **96**, 238302 (2006)

2005

Ashbaugh,HS, Guo,X, Schwahn,D, Prud'homme,RK, Richter,D, Fetters,LJ
Interaction of Paraffin Wax Gels with Ethylene/Vinyl Acetate Copolymers
Energy & Fuels **19** , 138-144 (2005)

DeLuca,E, Waigh,T, Kim,J, Pyckhout-Hintzen,W
Phase separation in randomly charged polystyrene sulphonate ionomer solutions
Polymer **46**, 7109 (2005)

Dror,Y, Pyckhout-Hintzen,W, Cohen,Y
The Conformation of Polymers Dispersing Single-Walled Carbon Nanotubes in Water: A Small Angle Neutron Scattering Study
Macromolecules **38**, 7828 (2005)

Dror,Y, Salalha,W, Pyckhout-Hintzen,W, Yarin,A, Zussman,E
From Carbon Nanotube Dispersion to Composite Nanofibers
Prog. Coll. Polym. Sci. **130**, 64 (2005)

Galant,C, Kjøniksen,A-L, Knudsen,KD, Helgesen,G, Lund,R, Laukkanen,A, Tenhu, H, and Nyström, B
Physical Properties of Aqueous Solutions of a Thermo-Responsive Neutral Copolymer and an Anionic Surfactant: Turbidity and Small-Angle Neutron Scattering Studies.
Langmuir **21**, 8010 (2005)

Genix,AC, Arbe,A, Alvarez,F, Colmenero,J, Willner,L, Richter,D
Dynamics of poly(ethylene oxide) in a blend with poly(methyl methacrylate): A quasielastic neutron scattering and molecular dynamics simulations study
Phys. Rev. E **72**, 031808 (2005)

Holderer,O, Frielinghaus,H, Byelov,D, Monkenbusch,M, Allgaier,J, Richter,D
Dynamic properties of microemulsions modified with homopolymers and diblock copolymers: The determination of bending moduli and renormalization effects
J. Chem. Phys. **122** , 094908 (2005)

Kanaya,T, Monkenbusch,M, Watanabe,H, Nagao,M, Richter,D
Dynamics of deuterated polystyrene-protonated butadiene diblock copolymer micelles by neutron spin-echo
J. Chem. Phys. **122**, 144905 (2005)

Laurati,M, Stellbrink,J, Lund,R, Willner,L, Richter,D, Zaccarelli,E
Star-Like Micelles with Star-Like Interactions: A quantitative evaluation of structure factors and phase diagram
Phys. Rev. Letters **94**, 195504 (2005)

Loppinet,B, Fytas,G, Vlassopoulos,D, Likos,CN, Meier,G, Liu,GJ
Dynamics of Dense Suspensions of Star-Like Micelles with Responsive Fixed Cores
Macromol. Chem. Phys. **206**, 163 (2005)

Moitzi,C, Freiberger,N, Glatter,O
Viscoelastic wormlike micellar solutions made from nonionic surfactants: Structural investigations by SANS and DLS
J. Phys. Chem. B **109 (33)**, 16161 (2005)

Monkenbusch,M, Holderer,O, Endo,H, Allgaier,J, Frielinghaus,H
Exploring microemulsions with small angle neutron scattering and neutron spin-echo spectroscopy
Neutron News **16, 2**, 22 (2005)

Monkenbusch,M, Holderer,O, Frielinghaus,H, Byelov,D, Allgaier,J, Richter,D
Bending moduli of microemulsions; comparison of results from small angle neutron scattering and neutron spin-echo spectroscopy
Journal of Physics: Condensed Matter **17**, s2903 (2005)

Narros,A, Arbe,A, Alvarez,F, Colmenero,J, Zorn,R, Schweika,W, Richter, D
Partial Structure Factors in 1,4-Polybutadiene. A Combined Neutron Scattering and Molecular Dynamics Study
Macromolecules **38**, 9847 (2005)

Niu,AZ, Stellbrink,J, Allgaier,J, Willner,L, Radulescu,A, Richter,D, Koenig BW, May RP, Fetters LJ
An in situ Study of the t-Butyllithium Initiated Polymerization of Butadiene in d-Heptane via Small Angle Neutron Scattering and 1H-NMR
J. Chem. Physics **122**, 134906 (2005)

Pipich,V, Schwahn,D, Willner,L
Ginzburg number of a homopolymer / diblock copolymer mixture covering 3d-Ising, isotropic Lifshitz and Brasovskií; class of critical universality
Phys. Rev. Letters **94**, 117801 (2005)

Ricciardi,R, Mangiapia,G, LoCelso,F, Paduano,L, Triolo,R, Auriemma,F, de Rosa,C, Laupretre,F
Structural Organization of Poly(vinyl alcohol) Hydrogels Obtained by Freezing and Thawing Techniques: A SANS Study
Chemistry of Materials **17 (5)**, 1183-1189 (2005)

Pipich,V, Schwahn,D, Willner,L
Ginzburg number of a homopolymer / diblock copolymer mixture covering 3d-Ising, isotropic Lifshitz and Brasovskií; class of critical universality
Phys. Rev. Letters **94**, 117801 (2005)

Ricciardi,R, Mangiapia,G, LoCelso,F, Paduano,L, Triolo,R, Auriemma,F, de Rosa,C, Laupretre,F
Structural Organization of Poly(vinyl alcohol) Hydrogels Obtained by Freezing and Thawing Techniques: A SANS Study
Chemistry of Materials **17 (5)**, 1183-1189 (2005)

2004

Abbas,B, Schwahn,D, Willner,L
Phase Behavior of the Polybutadiene / Polystyrene Diblock Copolymer with Additions of the non-selective Solvent Dichlorobencene in Temperature and Pressure Fields
Journal of Polymer Science Part B: Polymer Physics **42** , 3179-3190 (2004)

Accardo,A, Tesauro,D, Roscigno,P, Gianolio,E, Paduano,L, D'Errico,G, Pedone,C, Morelli,G
Physicochemical Properties of Mixed Micellar Aggregates Containing CCK Peptides and Gd Complexes Designed as Tumor-Specific Contrast Agents in MRI.
Journal of the American Chemical Society **126 (10)**, 3097-3107 (2004)

Arbe,A, Colmenero,J, Richter,D, Monkenbusch,M, Willner,L, Farago,B
Crossover from Rouse dynamics to the alpha-relaxation in poly(vinyl-ethylene)
Pramana - Journal of Physics **63**, 33-40 (2004)

Arbe,A, Moral,A, Alegria,A, Colmenero,J, Pyckhout-Hintzen,W, Richter,D, Farago, B; FrickB
Neutron scattering and dielectric study on the structural and dynamical peculiar properties of poly(vinyl-chloride)
AIP Conference Proceedings: Slow Dynamics in Complex Systems, 02.-09.11.2003 : 3rd International Symposium on Slow Dynamics in Complex Systems / ed.: M. Tokuyama, I. Oppenheim **708**, 594-597 (2004)

Asteriadi,A, Sigel,R, Vlassopoulos,D, Meier,G, Dorgan,JR, Knauss,DM
Molecular Control of th Viscosity of Dendrically Branched polystyrene Solutions: From Polymeric to Colloidal Behavior
Macromolecules **37**, 1016 (2004)

Biehl,R, Guo,X, Prud'homme,RK, Monkenbusch,M, Allgaier,J, Richter,D
Diffusion of compact macromolecules through polymer meshes: mesh dynamics and probe dynamics
Physica B: Condensed Matter **350**, 76-78 (2004)

Byelov,D, Frielinghaus,H, Allgaier,J, Gompper,G, Richter,D
SANS studies of polymer efficiency boosting in microemulsions - diblock copolymers versus homopolymers
Physica B: Condensed Matter **350**, e931-e933 (2004)

Byelov,D, Frielinghaus,H, Holderer,O, Allgaier,J, Richter,D
Microemulsion Efficiency Boosting and the Complementary Effect. 1. Structural Properties
Langmuir **20**, 10433 (2004)

Colmenero,J, Alvarez,F, Narros,A, Arbe,A, Monkenbusch,M, Richter,D, Farago, B
Self-atomic motions in glass-forming polymers: neutron scattering and molecular dynamics simulations results
AIP Conf. Proc: Slow Dynamics in Complex Systems, 02.-09.11.2003 : 3rd International Symposium on Slow Dynamics in Complex Systems / eds.: M. Tokuyama, I. Oppenheim **708**, 655-658 (2004)

Colmenero,J, Arbe,A, Alvarez,F, Narros,A, Richter,D, Monkenbusch,M, Farago,B
Hydrogen motions and the alpha-relaxation in glass-forming polymers: Molecular dynamics simulation and quasi-elastic neutron scattering results
Pramana - Journal of Physics **63**, 25-32 (2004)

DiCola,E, Plucktaveesak,N, Waigh,TA, Colby,RH, Tan,JS, Pyckhout-Hintzen,W, Heenan RK
Structure and Dynamics in Aqueous Solutions of Amphiphilic Sodium Maleate-Containing Alternating Copolymers
Macromolecules **37**, 8457-8465 (2004)

Endo,H, Schwahn,D, Cölfen,H
On the Role of Block Copolymer Additives for Calcium Carbonate Crystallization - Neutron Scattering Investigation by Applying Contrast Variation
J. Chem. Phys. **120** , 9410-9423 (2004)

Ewen,B, Götz,H, Maschke,U
Structural and dynamic single chain behaviour in a binary blend of low molecular mass poly(siloxanes) as studied by small angle neutron scattering and neutron spin echo spectroscopy
Colloid Polym Sci **282**, 782-792 (2004)

Frielinghaus,H, Byelov,D, Allgaier,J, Gompper,G, Richter,D
Efficiency boosting and optional viscosity tuning in microemulsions studied by SANS
Physica B **350**, 186 (2004)

Goad,M, Pyckhout-Hintzen,W, Kahle,S, Allgaier,J, Richter,D, Fetters,LJ
Rheological properties of 1,4-polyisoprene over a large molecular weight range
Macromolecules **37**, 8135-8144 (2004)

Guo,X, Biehl,R, Pacheco,CR, Monkenbusch,M, Richter,D, Fu,L, Prud´Homme RK
Diffusion of protein in polymer solutions: A comparison between neutron spin echo spectroscopy and nmr measurements
Polymer Preprint **45**, 788 (2004)

Heinrich,M, Pyckhout-Hintzen,W, Allgaier,J, Richter,D, Straube,E, McLeish,TCB, Wiedenmann,A;Blackwell, RJ;Read, DJ
Small-angle neutron scattering study of the relaxation of a melt of polybutadiene H-polymers following a large step strain
Macromolecules **37**, 5054-5064 (2004)

Hu,XS, Biehl,R, Prud'homme,RK, Monkenbusch,M, Lal,J
Fluctuations of bare membranes and their modification on incorporation of polymers having equally spaced anchors
Physica B **350**, 217-219 (2004)

Kawabata,J, Nagao,M, Seto,H, Komura,S, Taheda,T, Schwahn,D, Yamada N, Nobuto H
Temperature and pressure effects on the bending modulus of monolayers in a ternary
Phys. Rev. Letters **92** , 056103 (2004)

Keiper,JS, Simhan,R, DeSimone,JM, Lynn,GW, Wignall,GD, Melnichenko,YB, Frielinghaus, H
Self-assembly of phosphate fluorosurfactants in carbon dioxide
Langmuir **20**, 1065 (2004)

Koizumi,S, Monkenbusch,M, Richter,D, Schwahn,D, Farago,B
Concentration fluctuations in polymer gel investigated by neutron scattering: Static inhomogeneity in swollen gel
Journal of Chemical Physics **121**, 12721-12731 (2004)

Leyh,B, Vangeyte,P, Heinrich,M, Auvray,L, DeClercq,C, Jerome,R
Self-assembling of poly(e-caprolactone)-b-poly(ethylene oxide) diblock copolymers in aqueous solution and at the silica-water interface
Physica B **350**, E901-E904 (2004)

Lopez-Cabarcos,E, RubioRetama,BJ, LopezRuiz,B, Heinrich,M, FernandezBarbero,A
Small angle neutron scattering study of the structural modifications induced by the entrapped glucose oxidase in polyacrylamide microgels
Physica A **344**, 417-423 (2004)

Lund,R, Willner,L, Stellbrink,J, Radulescu,A, Richter,D
Tuning of structure and kinetics of chain exchange in star-like PEP-PEO block copolymer micelles
Physica B: Condensed Matter **350**, e909-e912 (2004)

Lund,R, Willner,L, Stellbrink,J, Radulescu,A, Richter,D
Role of interfacial tension for the structure of PEP-PEO polymeric micelles. A combined SANS and pendant drop tensiometry investigation
Macromolecules **37**, 9984-9993 (2004)

Mangiapia,G, Accardo,A, Locelso,F, Tesauro,D, Morelli,G, Radulescu,A, Paduano,L
Mixed micelles composed of peptides and gadolinium complexes as tumor-specific contrast agents in MRI: a SANS study.
Journal of Physical Chemistry B **108 (45)**, 17611-17617 (2004)

Melnichenko,YB, Wignall,GD, Cole,DR, Frielinghaus,H
Density fluctuations near the liquid-gas critical point of a confined fluid
Phys. Rev. E **69**, 057102 (2004)

Monkenbusch,M, Wischnewski,A, Willner,L, Richter,D
Direct observation of the transition from free to constrained single segment motion in entangled polymer melts
Physica B: Condensed Matter **350**, 214 (2004)

Narros,A, Alvarez,F, Arbe,A, Colmenero,J, Richter,D, Farago,B
Hydrogen motions in the alpha relaxation regime of poly(vinyl ethylene): A molecular dynamics simulation and neutron scattering study
Journal of Chemical Physics **121**, 3282-3294 (2004)

Niu,AZ, Stellbrink,J, Allgaier,J, Willner,L, Richter,D, Koenig,BW, Gondorf, M;Willbold,S;Fetters,LJ;May,RP
A New View of the Anionic Diene Polymerization Mechanism
Macromolecular Symposia **215**, 1-15 (2004)

Niu,AZ, Stellbrink,J, Allgaier,J, Willner,L, Richter,D, Radulescu,A, Koenig, B W; Gondorf, M; Willbold, S; Fetters, L J; May, R P
Real-time SANS and 1H-NMR studies during 'living' anionic polymerization of butadiene in hydrocarbon media
Physica B **350**, e921-e925 (2004)

Pipich,V, Schwahn,D, Willner,L
The Lifshitz line of the disordered and microemuslion phase in an A/B/A-B three component homopolymer/diblock copolymer mixture
Physica B **350** , E897-E900 (2004)

Radulescu,A, Mathers,RT, Coates,GW, Richter,D, Fetters,LJ
A SANS study of the self-assembly in solution of syndiotactic polypropylene homopolymers, syndiotactic polypropylene-block-poly(ethylene-co-propylene) diblock copolymers, and an alternating atactic-isotactic multisegment polypropylene
Macromolecules **37**, 6962 (2004)

Radulescu,A, Schwahn,D, Monkenbusch,M, Fetters,LJ, Richter,D
Structural study of the influence of partially crystalline poly(ethylene-butene) random copolymers on paraffin crystallization in dilute solutions
Journal of Polymer Science B - Polymer Physics **42**, 3113 (2004)

Radulescu,A, Schwahn,D, Monkenbusch,M, Richter,D, Fetters,LJ
The interaction mechanism of triacontane praffin with semi-crystalline poly(ethylene-butene) random copolymers in dilute solution studied with SANS
Physica B: Condensed Matter **350**, e927 (2004)

Richter, D.
Viscoelasticity and microscopic motion in dense polymer systems
Diffusion in Condensed Matter, 2. Auflage, Eds. P. Heitjans and J. Kärger (Springer, Berlin 2004)

Richter,D, Monkenbusch,M, Willner,L, Arbe,A, Colmenero,J
Direct observation of the crossover from glassy alpha-relaxation to Rouse dynamics in a polymer melt
Europhysics Letters **66**, 239-245 (2004)

Russina,O, Triolo,A, Aihara,Y, Telling,MTF, Grimm,H
Quasi-elastic neutron scattering investigation of dynamics in polymer electrolytes
Macromolecules **37**, 8653 (2004)

Schwahn,D, Balz,M, Tremel,W
Crystallization of the $CaCO_3$ mineral in the presence of the protein Ovalbumin
Physica B **350**, E947-E949 (2004)

Stellbrink,J, Rother,G, Laurati,M, Lund,R, Willner,L, Richter,D
Poly(ethylene-alt-propylene)-poly(ethylene oxide) diblock copolymer micelles: a colloidal model system with tunable softness
Journal of Physics: Condensed Matter **16**, s3821-s3834 (2004)

Triolo,A, Russina,O, Lanza,M, Grimm,H
Complex Dynamics in Polymer Electrolytes
Notiziario Neutroni e Luce di Sincrotrone **9**, 32 (2004)

Vangeyte,P, Leyh,B, Heinrich,M, Grandjean,J, Bourgaux,C, Jerome,R
Self-Assembly of Poly(ethylene oxide)-b-poly(e-caprolactone) copolymers in aqueous solution
Langmuir **20**, 8442-8451 (2004)

Wischnewski,A, Zamponi,M, Monkenbusch,M, Willner,L, Pyckhout-Hintzen,W, Richter,D, Likhtman,AE;McLeish,T, Farago,B
Molecular observation of contour length fluctuations in polymer melts
Physica B: Condensed Matter **350**, 193 (2004)

2003

Alvarez,F, Colmenero,J, Zorn, R., Willner,L, Richter, D..
Partial structure factors of polyisoprene : neutron scattering and molecular dynamics simulation
Macromolecules, **36** (2003),S. 238 – 248

Arbe,A, Colmenero,J, Alvarez,F, Monkenbusch,M, Richter, D., Farago,B, Frick,B
Experimental evidence by neutron scattering of a crossover from Gaussian to non-Gaussian behavior in the alpha-relaxation of polyisoprene
Physical review E,**67** (2003),S. 051802

Arbe,A, Colmenero,J, Farago,B, Monkenbusch,M, Buchenau,U, Richter, D.
Intermediate length scale dynamics in glass forming polymers: coherent and incoherent quasielastic neutron scattering results on polyisobutylene
Chemical physics,**292** (2003),S. 295 - 309

Arbe,A, Colmenero,J, Richter, D..
Polymer dynamics by dielectric spectroscopy and neutron scattering - a comparison
Broadband dielectric spectroscopy/ ed.: F. Kremer ... - Berlin,Springer,2003. - 3-540-43407-0. - S. 685 - 718

Berriot,J, Montes,H, Martin,F, Mauger,M, Pyckhout-Hintzen,W, Meier,G, Frielinghaus,H.
Reinforcement of model filled elastomers: synthesis and characterization of the dispersion state by SANS measurements
Polymer,**44** (2003),S. 4909 - 4919

Botti,A, Pyckhout-Hintzen,W, Urban,V, Kohlbrecher,J, Richter, D., Straube,E
Silica-filled elastomers: polymer chain and filler characterization by a SANS-SAXS approach
Polymer,**44** (2003),S. 7505 - 7512

Cailliaux,A, Alba-Simionesco,C, Frick,B, Willner,L, Goncharenko,I.
Local structure and glass transition of polybutadiene up to 4 GPa
Physical review E **67** (2003),S. 010802

Colmenero,J, Arbe,A, Alvarez,F, Monkenbusch,M, Richter, D., Farago,B, Frick,B.
Self-motion and the alpha-relaxation in glass-forming polymers : molecular dynamic simulation and quasielastic neutron scattering results in polyisoprene
Journal of physics: condensed matter **15** (2003),S. 1127 - 1138

Colmenero,J, Arbe,A, Richter, D., Farago,B, Monkenbusch,M.
Dynamics of glass forming polymers by neutron spin echo
Neutron spin echo spectroscopy / ed.: F. Mezei ... - Berlin,2003. - (Lecture notes in physics , 601). - 3-540-44293-6. - S. 268 - 279

Dhont,JKG, Lettinga,MP, Dogic,Z, Lenstra,TAJ, Wang,H, Rathgeber,S, Carletto P, Willner L, Frielinghaus H, Lindner P
Shear-banding and microstructures of colloids in shear flow
Faraday Discuss. **123**, 157 (2003)

Endo,H, Cölfen,H, Schwahn, D.
Analysis of Polymer Templates in Calcium Carbonate - SANS Investigation Applying Contrast Variation
J. Appl. Cryst. **36**, 568 (2003)

Frick,B, Alba-Simionesco,C, Andersen,K. H, Willner,L
Influence of density and temperature on the microscopic structure and the segmental relaxation of polybutadiene
Physical review E,67 (2003),S. 051801

Fuetterer,T, Hellweg,T, Findenegg,GH
Particle Characterization by Scattering Methods in Systems Containing Different Types of Aggregates
Eds: Case,F, Alexandridis,P.
ACS symposium series 861: Mesoscale Phenomena in Fluid Systems
Chapter 8
American Chemical Society (2003)

Götz,H, Ewen,B, Maschke,U, Monkenbusch,M, Meier,G
Chain expansion and chain localisation in the homogenous regime of blends of liquid low molecular mass polysiloxanes as revealed by neutron scattering investgations
e-Polymers no. 011 (2003)

Gompper,G, Dhont,J. K. G, Richter, D..
Eine Welt zwischen Fest und Flüssig
Physik in unserer Zeit,34 (2003),S. 19 - 25

Gompper,G, Dhont,J. K. G, Richter, D..
Was ist 'Weiche Materie'? Komplexe Materialien auf mesoskopischer Skala
Physik in unserer Zeit,34 (2003),S. 12 - 18

le Goualher,G, Ewen,B, Maschke,U, Monkenbusch,M, Meier,G
Chain expansion and chain localisation in the homogenous regime of blends of liquid low molar mass polysiloxanes as revealed by neutron scattering investigations
e-polymers,(2003),011

Lang,P, Willner,L, Pyckhout-Hintzen,W, Krastev,R
Isotropic to Nematic Transition in Solutions of Cylindrical PB-PEO Block Copolymer Micelles Close to Wall
Langmuir **19** 7597(2003)

Melnichenko,YB, Wignall,GD, Schwahn, D.
Universal Behavior of Polymers in Blends, Solutions and Supercritical Mixtures and Implications for the Validity of the random Phase Approximation
Fluid Phase Equilibria, **212** 209 (2003)

Mendes,O, Viale,S, Santin,O, Heinrich,M, Picken,SJ
A small-angle neutron scattering investigation of rigid polyelectrolytes under shear
J. Appl Cryst **36**, 1000 (2003)

Monkenbusch,M.
Soft matter and biology
Neutron spin echo spectroscopy / ed.: F. Mezei ... - Berlin,2003. - (Lecture notes in physics , 601). - 3-540-44293-6. - S. 246 - 267

Radulescu,A, Schwahn, D., Richter, D., Fetters,LJ
Co-crystallization of Poly(ethylene-butene) Copolymers and Paraffin Molecules in Decane Solution studied by SANS
J. Appl. Cryst. **36**, 995 (2003)

Richter, D.
Polymer dynamics from large to small scales
Journal of applied crystallography,36 (2003),S. 389 - 396

Schwahn, D.
Small Angle Neutron Scattering in Polymer Blends
Chapter 12 in „Polymer Characterization Techniques and their Applications to Blends“ edited by George P. Simon (Oxford University Press 2003)

Schwahn, D., Balz,M, Bartz,M, Fomenko,A, Tremel,W
Nucleation and Growth of $CaCO_3$ Minerals on Biomimetic Templates studied by Small Angle Neutron Scattering
J. Appl. Cryst. **36**, 583 (2003)

Wischnewski,A, Monkenbusch,M, Willner,L, Richter, D., Kali,G.
Direct observation of the transition from free to constrained single-segment motion in entangled polymer melts
Physical review letters,90 (2003),S. 058302

Yang,B.-S, Lal,J, Mihailescu,M, Monkenbusch,M, Richter, D., Huang,J.-S, Russel,W. B, Prud'homme,R. K.
Dynamics of hydrophobically modified polymer doped surfactant bilayers : a neutron spin echo study
Neutron spin echo spectroscopy / ed.: F. Mezei ... - Berlin,2003. - (Lecture notes in physics , 601). - 3-540-44293-6. - S. 312 – 324

2002

Arbe,A, Colmenero,J, Alvarez,F, Monkenbusch,M, Richter, D., Farago,B, Frick,B
On the Nature of the non-Gaussianity in the alpha-Relaxation of Glass Forming Polyisopren
Physical Review Letters **89**, 245701 (2002)

Arbe,A, Colmenero,J, Richter, D.
Polymer dynamics by dielectric spectroscopy and neutron scattering - a comparison
in Broadband Dielectric Spectroscopy, Eds. F. Kremer & A. Schönhals, ISBN 3-540-43407-0 (2002)

Arbe,A, Moral,A, Alegria,A, Colmenero,J, Pyckhout-Hintzen,W, Richter, D., Farago,B
Heterogeneous Structure of Poly(vinyl chloride) as the Origin of Anomalous Dynamical Behavior
Journal of Chemical Physics **117**, 1336 (2002)

Ashbaugh,HS, Radulescu,A, Prud'homme,RK, Schwahn, D., Richter, D., Fetters,LJ
Interaction of paraffin wax gels with random crystalline/amorphous hydrocarbon copolymers
Macromolecules **35**, 7044 (2002)

Botti,A, Pyckhout-Hintzen,W, Richter, D., Straube,E
Filled elastomers: polymer chain and filler characterization by a SANS-SAXS approach
Physica A **304**, 230-234 (2002)

Botti,A, Pyckhout-Hintzen,W, Richter, D., Straube,E
An in situ rheological and SANS investigation of the crosslinking reaction of polyisoprene and dicumyl peroxide
Acta Rheologica **41**, 475 (2002)

Endo,H, Allgaier,J, Mihailescu,M, Monkenbusch,M, Gompper,G, Richter, D., Jakobs,B, Sottmann,T, Strey,R
Amphiphilic block copolymers as efficiency boosters in microemulsions: A SANS investigation of the role of polymers
Appl. Phys. A **74**, 392-395 (2002)

Fytas,G,Nothofer,G,Scherf,U,Vlassopolous,D, Meier,G
Structure and Dynamics of Nondilute Polyfluorene Solutions
Macromolecules **35**, 481-488 (2002)

Farago,B, Arbe,A, Colmenero,J, Faust,R, Buchenau,U, Richter, D.
Intermediate Length Scale Dynamics of Polyisobutylene
Physical Review E **65**, 051803 (2002)

Fetters,LJ, Lohse,DJ, Garcia-Franco,C, Brant,P, Richter, D.
Prediction of melt state polyolefin rheological properties: the unsuspected role of the average molecular weight per backbone bond
Macromolecules **35**, 10096-10101 (2002)

Frielinghaus,H, Schwahn, D., Willner,L, Freed,KF
Small Angle Neutron Scattering Studies of a Polybutadiene/Polystyrene Blend with Small Additions of Ortho-di-Chlorine-Benzene for varying Temperatures and Pressures Fields, Part II: Phase Boundaries and Flory-Huggins Parameter
J. Chem. Phys. **116,** 2241 (2002)

Frielinghaus,H, Byelov,D, Allgaier,J, Richter, D., Jakobs,B, Sottmann,T, Strey R
Polymer boosting effect in the droplet phase studied by small-angle neutron scattering
Appl. Phys. A 74 (2002) 408

Gohr,K, Schaertl,W, Willner,L, Pyckhout-Hintzen,W
SANS investigatons of PS-PB block copolymer micelles in a short chain PB homopolymer matrix
Macromolecules **35**, 9110 (2002)

Hardy,C, Bates,FS, Kim,MH, Wignall,GD
Model ABC Triblock Copolymers and Blends Near the Order-Disorder Transition
Macromolecules **35**, 3189 (2002)

Heinrich,M, Pyckhout-Hintzen,W, Allgaier,A, Richter, D., Straube,E, Read,DJ, McLeish,TCB, Groves,D, Blackwell,RJ, Wiedenmann,A
Arm relaxation in deformed H-polymers in elongational flow by SANS
Macromolecules **35**, 6650-6664 (2002)

Heinrich,M, Pyckhout-Hintzen,W, Richter, D., Straube,E, Wiedenmann,A
Relaxation of entangled model H-shaped polymers: a SANS investigation
Applied Physics A **74,** S380-S382 (2002)

Iatrou,H, Hadjichristidis,N, Meier,G, Frielinghaus,H, Monkenbusch,M
Synthesis and Characterization of Model Cyclic Block Copolymers of Styrene and Butadiene. Comparison of the Aggregation Phenomena in Selective Solvents with Linear Diblock and Triblock Analogues
Macromolecules **35**, 5426 (2002)

Jeng,U, Lin,T-L, Hu,Y, Chang,T-S, Canteenwala,T, Chiang,L-Y, H Frielinghaus
Study on Aqueous Mixtures of Fullerene-Based Star Ionomers and Sodium Dodecyl Sulfate
J. Phys. Chem. A **106**, 12209-12213 (2002)

Kahle,S, Willner,L, Monkenbusch,M, Richter, D., Arbe,A, Colmenero,J, Frick,B
Neutron Scattering on Partially Deuterated Polybutadiene
Applied Physics A **74**, 371 (2002)

Kawabata,Y, Nagao,M, Seto,H, Komura,S, Takeda,T, Schwahn, D.
Neutron Spin Echo Studies on the Effects of Temperature and Pressure in a Ternary Microemulsion.
Applied Physics **74 [Suppl.]**, S534 (2002)

Keiper,JS, Simhan,R, DeSimone,JM, Wignall,GD, Melnichenko,YB, Frielinghaus,H
New Phosphate Fluorosurfactants for Carbon Dioxide
J. Am. Chem. Soc. **124**, 1834 (2002)

Koizumi,S, Monkenbusch,M, Richter, D., Schwahn, D., Farago,B, Annaka,M
Frozen Concentration Fluctuations in a Poly(N-isopropyl acrylamide) Gel Studied by Neutron Spin Echo and Neutron Small-angle Sacttering
Applied Physics A [Suppl.] **74**, S399 (2002)

Koizumi,S, Monkenbusch,M, Richter, D., Schwahn, D., Farago,B, Annaka,M
Observation of Concentration Fluctuations in Polymer Gels Performed by Neutron Spin Echo
Journal of Neutron Research **10**, 155 (2002)

Krishnamoorti,R, Graesseley,WW, Zirkel,A, Richter, D., Hadjichristidis,N, Fetters,LJ, Lohse,DJ
Melt state polymer chain dimensions as a function of temperature
J. Polymer Science **B40**, 1768-1776 (2002)

Melnichenko,YB, Wignall,GD, Schwahn, D.
Universal Aspects of Macromolecules in Polymer Blends, Solutions, and Supercritical Mixtures
Phys. Rev E **65**, 061802 (2002)

Menge,H, Pyckhout-Hintzen,W, Meier,G, Straube,E
Butadiene rubbers: Topological constraints and microscopic deformations by mechanical and small angle neutron scattering investigation
Polymer Bulletin **48**, 183 (2002)

Mihailescu,M, Monkenbusch,M, Allgaier,J, Frielinghaus,H, Richter, D., Jakobs,B, Sottmann,T
Neutron scattering study on the structure and dynamics of oriented lamellar phase microemulsions
Phys. Rev. E **66**, 041504-1 (2002)

Montes,H, Monkenbusch,M, Willner,L, Rathgeber,S, Richter, D., Fetters,LJ, Farago B
Direct observation of domain wall excitations in symmetric diblock copolymer melts at and above the order-disorder transition
Europhys. Lett. **58**, 389 (2002)

Moral,A, Arbe,A, Alegria,A, Colmenero,J, Pyckhout-Hintzen,W, Richter, D., Farago B, Frick B
Heterogenous structure of poly(vinylchloride) as the origin of anomalous dynamical behaviour
J. Chem Phys. **117**, 1336 (2002)

Pipich,V, Schwahn, D., Willner,L
Complex phase behaviour near the Lifshitz line in a ternary polymer blend
Applied Physics A **74**, S345 (2002)

Pyckhout-Hintzen,W, Botti,A, Heinrich,M, Westermann,S, Richter, D., Straube,E
The length-scale dependence of strain in networks by SANS
Appl. Phys. A **74**, S368 (2002)

Radulescu,A, Schwahn, D., Fetters,L, Richter, D.
Crystallization of paraffin in decane in the presence of PEB-7 ethylene-butene random copolymers
Applied Physics A **74**, S411 (2002)

Rathgeber,S, Monkenbusch,M, Kreitschmann,M, Urban,V, Brulet,A
Dynamics of Star-burst Dendrimers in Solution in Relation to their Structural Properties
J. Chem. Phys. **117**, 4047 (2002)

Richter, D., Monkenbusch,M, Willner,L, Wischnewski,A, Arbe,A, Colmenero,J
Experimental Aspects of Polymer Dynamics
Polymer International **51**, 1211 (2002)

Schmidt, W., Buchenau, U.
A microscopic picture of the fast process in a polymer melt
Appl. Phys. A **74** (2002) S537

Schwahn, D., Frielinghaus,H, Willner,L
Small Angle Neutron Scattering Studies of a Polybutadiene/Polystyrene Blend with small Additions of Ortho-di-Chlorine-Benzene for varying Temperatures and Pressures Fields, Part I: Mean Field to 3D-Ising Crossover Behavior.
J. Chem. Phys. **116,** 2229 (2002)

Schwahn, D., Richter, D., Lin,M, Fetters,LJ
The Co-crystallisation of a Poly(ethylene-butene) Random Copolymer with C_{24} in n-Decane
Macromolecules **35**, 3762 (2002)

Schwahn, D., Richter, D., Wright,PJ, Symon,C, Fetters,LJ
Self-Assembling Behavior in Decane Solution of Potential Wax Crystal Nucleators Based on Poly(co-olefins)
Macromolecules **35**, 861 (2002)

Schwahn, D., Willner,L
Phase behaviour of binary polybutadiene copolymer mixtures as an examle of weakly interacting polymers
Applied Physics A **74**, S358 (2002)

Schwahn, D., Willner,L
Phase Behavior and Flory-Huggins Parameter of Binary Polybutadiene Copolymer Mixture of different Vinyl Content and Molar Volume
Macromolecules **35,** 239 (2002)

Senapati,S, Keiper,JS, DeSimone,JM, Wignall,GD, Melnichenko,YB, Frielinghaus,H, Berkowitz, ML
Structure of Phosphate Fluorosurfactant Based Reverse Micelles in Supercritical Carbon Dioxide
Langmuir **18**, 7371 (2002)

Stellbrink,J, Allgaier,J, Monkenbusch,M, Richter,D, Ehlers,G, Schleger,P
Self and collective dynamics of ordered star polymer solutions,
Appl. Phys. A **74** [Suppl.], 361 (2002)

Stellbrink,J, Allgaier,J, Richter, D., Moussaid,A, Schofield,AB, Poon,WCK, Pusey,PN, Lindner,P, Dzubiella,J, Likos,CN, Löwen,H
Partial structure factors in star/polymer colloid mixtures
Appl. Phys. A **74** [Suppl], 355 (2002)

Stellbrink,J, Allgaier,J, Willner,L, Richter, D., Slawecki,T, Fetters,LJ
Real time SANS study on head group self-assembly for lithium based anionic polymerisations
Polymer **43**, 7101-7109 (2002)

Stiakakis,E, Vlassopoulos,D, Likos,CN, Roovers,J, Meier,G
Polymer-mediated melting in ultrasoft colloidal gels
Physical Review Letters **89**, 208-302 (2002)

Stiakakis,E, Vlassopoulos,D, Loppinet,B, Roovers,J, Meier,G
Kinetic arrest of crowded soft spheres in solvents of varying quality
Physical Review E **66**, 051804 (2002)

Vass,S, Haimer,K, Meier,G, Klapper,M, Borbely,S
Small-angle neutron scattering study of poly(methyl methacrylate-sodium acrylate-methyl methacrylate) triblock copolymers in aqeous solution
Colloid Polym Sci **280**, 245-253 (2002)

Volkmer,D, Bredenkötter,B, Tellenbröker,J, Kögerler,P, Kurt,DG, Lehmann,P, Schnablegger H, Schwahn D, Piepenbrink M, Krebs B
Structure and Properties of the Dendron-Encapsulated Polyoxometalate $(C_{52}H_{60}NO_{12})12[(Mn(H_2O))_3(SbW_9O_{33})_2]$, a First Generation Dendrozyme
J. Am.Chem. Soc. **124**, 10489 (2002)

Yang,BS, Lal,J, Mihailescu,M, Monkenbusch,M, Richter, D., Huang,JS, Kohn J,Russel WB, Prud'homme RK
Neutron spin-echo study of dynamics of hydrophobically modified polymer-doped surfactant bilayers
Langmuir **18**, 6 (2002)

2001

Dzubiella,J, Jusufi,A, Likos,CN, vonFerber,C, Löwen,H, Stellbrink,J, Allgaier,J, Richter, D., Schofield,AB, Smith,PA, Poon,WCK, Pusey,PN
Effect of amphiphilic block copolymers on the structure and phase behavior of oil–water-surfactant mixtures
Phys. Rev. E **64**, 010401-1 (2001)

Edelmann,K, Janich,M, Hoinkis,E, Pyckhout-Hintzen,W, Hoering,S
The aggregation behaviour of Poly(ethylene oxide)-Poly(methyl methacrylate) diblock copolymers in organic solvents
Macromol. Chem. Phys **202**, 1638 (2001)

Endo,H, Mihailescu,M, Monkenbusch,M, Allgaier,J, Gompper,G, Richter, D., Jakobs,B, Sottmann,T, Strey,R, Grillo,I
Effect of amphiphilic block copolymers on the structure and phase behavior of oil-water surfactant mixtures
J. Chem. Phys. **115**, 580 (2001)

Erhardt,R, Boeker,A, Zettl,H, Pyckhout-Hintzen,W, Kaya,H, Krausch,G, Abetz,V, Mueller,A
Janus Micelles
Macromolecules **34**, 1069 (2001)

Frielinghaus,H, Schwahn, D., Dudowicz,J, Foreman,JKW, Freed,K
Application of the LCT to describe the Temperature, Pressure, and Microstructure Dependent Small Angle Neutron Scattering Experiments on Polybutadiene/ Polystyrene Blends
J. Chem. Phys. **114**, 5016 (2001)

Frielinghaus,H, Schwahn, D., Willner,L
Blends of Polybutadiene with different Vinyl Contents and Polystyrene studied with Small Angle Neutron Scattering in varying Temperature and Pressure Fields
Macromolecules **34,** 1751 (2001)

Gompper,G, Endo,H, Mihailescu,M, Allgaier,J, Monkenbusch,M, Richter, D., Jakobs,B, Sottmann,T, Strey,R
Measuring bending rigidity and spatial renormalization in bicontinuous microemulsions
Europhys. Lett. **56**, 683 (2001)

Gompper,G, Richter, D., Strey,R
Amphiphilic block copolymers in oil-water-surfactant mixtures: Efficiency boosting, structure, phase behavior and mechanism
J. of Physics: Condensed Matter **13**, 9055 (2001)

Götz,H, Ewen,B, Maschke, U, Meier,G, Monkenbusch,M
Neutron Scattering Investigations on the Statics and Dynamics of Polydimethyl- and Polyethylmethylsiloxane Melts
Macromol.Chem.Phys. **202**, 3334-3341 (2001)

Koizumi,S, Monkenbusch,M, Richter, D., Schwahn, D., Annaka,M
Frozen Concentration Fluctuations of a Poly (N-isopropyl aclyamide) Gel Decomposed by Neutron Spin Echo
J. Phys. Soc. Jpn. **70 Suppl. A**, 320-322 (2001)

Kratz,K, Hellweg,T, Eimer,W
Structural changes in NIPA microgel particles as seen by SANS,DLS,and EM techniques
POLYMER 42 (2001) 6631

Moreno,AJ, Alegria,A., Colmenero,J, Prager, M., Grimm,H, Frick,B
Methyl group dynamics in glassy toluene: a neutron scattering study
Journal of Chemical Physics **115**, 8958 (2001)

Melnichenko,Y, Wignall,GD, Schwahn, D.
Universal Behavior of Polymer Molecules in Blends, Solutions, and Supercritical Fluids
Polymeric Materials **85** (2001)

Mihailescu,M, Monkenbusch,M, Endo,H, Allgaier,J, Gompper,G, Stellbrink,J, Richter D, Jakobs B, Sottmann T, Farago B
Dynamics of bicontinuous microemulsion phases with and without amphiphilic block-copolymers
J. Chem. Phys **115**, 9563 (2001)

Prabhu,VM, Muthukumar,M, Wignall,GD, Melnichenko,YB
Dimensions of Polyelectrolyte Chains and Concentration Fluctuations in Semidilute Solutions of Sodium-Polystyrene Sulphonate as Measured by Small Angle Neutron Scattering
Polymer **42**, 8935 (2001)

Richter, D.
Neutrons in soft condensed matter
Conf. Proceedings ILL Millennium Symposium & European User Meeting (2001)

Richter, D., Monkenbusch,M, Arbe,A, Colmenero,J, Kahle,S, Colmenero,J
Neutron Scattering and the Glass Transition in Polymers: Present Status and Future Opportunities
Journal of Non-Crystalline Solids **287**, 286-296 (2001)

Schwahn, D., Frielinghaus,H, Mortensen,K, Almdal,K
Abnormal Pressure Dependence of the Order-Disorder Phase Boundary in (PEE,PEP)-PDMS Binary Polymer Blends and Diblock Copolymers
Macromolecules **34,** 1694 (2001)

Schwahn, D., Willner,L
Phase Behavior of Binary Polybutadiene Copolymer Mixtures with different Vinyl Content as an Example of a Blend of Weak Interacting Polymers
Polymeric Materials **85** (2001)

Smith,GD, Paul,W, Monkenbusch,M, Richter, D.
On the non-Gaussianity of chain motion in unentangled polymer melts
J. Chem. Phys. **114**, 4285 (2001)

Westermann,S, Pyckhout-Hintzen,W, Richter, D., Straube,E, Egelhaaf,S, May,R
On the length scale dependence of microscopic strain by SANS
Macromolecules **34**, 2186 (2001)

Wignall,GD, Alamo,RG, Mandelkern,L, Schwahn, D.
SANS Studies of Liquid-Liquid Phase Separation in Heterogeneous and Metallocene-based Linear Low Density Polyethylenes
Macromolecules **34**, 8160 (2001)

Willner,L, Poppe,A, Allgaier,J, Monkenbusch,M, Richter, D.
Time-resolved SANS for the determination of unimer exchange kinetics in block copolymer micelles
Europhys. Lett. **55**, 667-673 (2001)

Invited Talks

2006

Burckbuchler,V, Kjøniksen,A-L, Galant,C, Lund,R, Amiel,C, Knudsen,KD, Nyström, B
Structural and Dynamical Features in Aqueous Solutions of Amphiphilic Polymers in the Presence of Cyclodextrin or Polycyclodextrin
3rd Scandinavian Workshop on Scattering from Soft Matter (Uppsala, Sweden) (2006)

Frielinghaus,H
Polymer Additives in Microemulsions
Seminar Neutron Scattering in Material Science (Naples) (2006)

Frielinghaus,H, Brodeck,M, Maccarrone,S, Mangiapia,G, Frank,C, Allgaier,J, Richter D
New sticker polymers as efficiency boosters in microemulsions
3rd Zsigmondy Colloquium (Berlin) (2006)

OberdisseJulian,JO
Structure of Silica Aggregates in a Soft Polymeric Matrix
ILL Millenium Symposium (Grenoble) (2006)

Paduano,L
Supramolecular aggregates of amphiphilic gadolinium complexes as blood pool MRI/MRA contrast agents
JCNS Symposium and European User Meeting (Jülich) (2006)

Pyckhout-Hintzen,W, Richter,D, Straube,E
Small angle scsttering from nanocomposites
NANOCOMPOSITES Workshop (Montpellier,F) (2006)

Wischnewski,A
Dynamics of a miscible polymer blend: A quasielastic neutron scattering study
CONFIT 3 (Grenoble, France) (2006)

2005

Endo,H
Study on Mineralization with Polymers by Means of Contrast Variation SANS
ICNS 2005 (Sydney) (2005)

Frielinghaus,H, Maccarrone,S, Byelov,D, Allgaier,J, Richter,D
SANS Studies of Confined Polymers in Microemulsions
ICNS2005 (Sydney) (2005)

Holderer,O, Frielinghaus,H, Byelov,D, Monkenbusch,M, Allgaier,J, Richter,D
Interface fluctuations, membrane elasticity and renormalization effects in microemulsions
Neutron Spin Echo Workshop 2005 (Grenoble) (2005)

Richter,D
Wax control by self-assembling polymers – a scientific approach
Workshop on Neutrons & Energy for the Future (Washington DC) (2005)

Urban,V, Pyckhout-Hintzen,W, Straube,E
SANS on polymer networks
ACS Rubber Division (San Antonio, TX, USA) (2005)

Wischnewski,A
Chain dynamics in linear polymer melts: A neutron spin echo study
76th Annual Meeting of the Society of Rheology (Lubbock, Texas) (2005)

Wischnewski,A
Unraveling motions in polymer melts
Juelich Soft Matter Days 2005 (Bonn, Germany) (2005)

Zorn, R
Experiments on the dynamics of glass-forming systems using inelastic neutron scattering and macroscopic relaxation methods
CIAE-Institutsseminar (Peking) (2005)

2004

Cohen,Y
Interaction Between Amphiphilic Polymers and Carbon Nanotubes
HPPC-III, High Performance Polymers and Polymer Composites (Lanzhou, China) (2004)

Frielinghaus,H
Modifikation von Mikroemulsionen durch Polymeradditive
Institutsseminar (Universität Darmstadt) (2004)

Monkenbusch,M, Holderer,O, Frielinghaus,H, Byelov,D, Allgaier,J, Richter,D
Bending moduli in microemulsions: comparison of results from small angle neutron scattering and neutron spin-echo spectroscopy
Conference on Physics of Soft Matter Complexes (Tokyo, Japan, 29.11.2004 - 02.12.2004) (2004)

Richter,D
Polymer dynamics from large to small scales
Colloquium (University of the Saarland) (2004)

Richter,D
Polymer dynamics from large to small scales
Colloquium (University of Erlangen) (2004)
Richter,D
Polymer dynamics from large to small scales
Whitby Lectures (University of Akron) (2004)

Richter,D
Neutrons in soft matter science
Colloquium (Cornell University) (2004)

Richter,D
Neutrons in soft matter science
Colloquium (University of Heidelberg) (2004)

Richter,D
Neutrons in soft condensed matter
Whitby Lectures (Universität Akron) (2004)

Wischnewski,A
Chain dynamics in linear polymer melts
International conference on quasi-elastic neutron scattering (QENS) (Arcachon, France) (2004)

2003

Allgaier,J, Niu,A, Stellbrink,J, Willner,L, Richer,D, König,B, Gondorf, M; Wilbold, S; May R; Fetters LJ
A new view of the anionic diene polymerization mechanisme
International symposium on ionic polymerization (Boston, USA) (2003)

Blanchard,A, Pyckhout-Hintzen,W, Straube,E, Richter, D..
Relaxation mechanisms in polymers under strain
5th SINQ User Meeting : PSI Villigen
Villigen,Switzerland: 16.01.2003

Frielinghaus,H
Efficiency boosting and viscosity tuning in microemulsions studied by small angle neutron scattering
Bayreuth Polymer Symposium BPS'03, Bayreuth, 30.09.2003

Frielinghaus,H, Byelov,D, Allgaier,J, Gompper,G, Richter, D.
Efficiency boosting and viscosity tuning in microemulsions studied by SANS
3rd European Conference on Neutron Scattering
Montpellier,France: 03.09.2003 - 06.09.2003

Richter, D.
Emulsification efficiency boosting in microemulsions: The effect of amphiphilic diblock copolymers
Kolloquiumsvortrag : Universität Kyoto
Kyoto,Japan: 24.10.2003

Richter, D.
Large scale dynamics of polymer melts from reptation to intrachain friction
CECAM Workshop on Mesoscopic Modelling of Polymer Dynamics
Lyon,France: 02.02.2003 - 05.02.2003

Richter, D.
Neutrons in soft matter science
Workshop on 'Physics meets Biology'
San Sebastian,Spanien: 26.06.2003 - 28.06.2003

Richter, D.
Neutrons in soft matter science
International Symposium on Pulsed Neutron Science and Instruments
Tsukuba,Japan: 27.10.2003 - 30.10.2003

Richter, D.
Polymerdynamik : von der gesamten Kette bis zur einzelnen Bindung
Universitätskolloquium : Technische Universität Ilmenau
Ilmenau: 07.01.2003

Richter, D., Monkenbusch,M, Willner,L, Wischnewski,A, Arbe,A, Colmenero,J, Farago,B.
Intermediate scale dynamics in polymers
The Third International Symposium on Slow Dynamics in Complex Systems
Sendai,Japan: 03.11.2003 - 08.11.2003

Richter, D., Monkenbusch,M, Willner,L, Wischnewski,A, Zamponi,M, Arbe,A, Colmenero,J, McLeish,T. C. B, Likhtman,A. E.
Polymer dynamics from large to small scales
APS March Meeting 2003
Austin,TX: 03.03.2003 - 07.03.2003

2002

Clarke,N
Self Assembled Polymer Composites
High Polymer Conference (Devon, UK) (2002)

Colmenero,J
Atomic self motions and the alpha-relaxation in glass forming polymers. MD-simulations and quasielastic neutron scattering results
Juelich Soft Matter Days (Kerkrade) (2002)

Colmenero,J
Self motion and the alpha-relaxation in glass-forming polymers. Neutron Scattering Results
American Conference on Neutron Scattering (Knoxville, USA) (2002)

Kahle,S
Untersuchung der lokalen Relaxation von Polymeren mittels Neutronenstreuung
6. Labortreffen Relaxationsdynamik (Halle) (2002)

Kahle,S
Segmental Dynamics in Polyisobutylene: Comparison between Neutron Scattering and Computer Simulations
7. Labortreffen Relaxationsdynamik (Rostock) (2002)

Kahle,S
Local Dynamics in Polymers
Joint ICTP-INFM School and Workshop on Spectroscopic Investigation of the Dynamics in Disordered Systems (Trieste) (2002)

Melnichenko,YB
SANS studies of isotopically labelled polymers
Gordon Conf. on Isotopes in Biological and Chemical Sci. (Ventura, California, USA) (2002)

Melnichenko,YB
Universal aspects of macromolecules in small molecule and polymeric solvents
Mid-Atlantic Conf. on Thermodynamics (College Park, Maryland, USA) (2002)

Melnichenko,YB, Wignall,GD, Schwahn, D.
On the validity of the random phase approximation in weakly and strongly interacting polymer blends
Int. Conf. on Small-Angle Neutron Scattering (Venice, Italy) (2002)

Melnichenko,YB, Wignall,GD, Schwahn, D.
Universal aspects of macromolecules in polymer blends, solutions and supercritical mixtures and implications for the validity of the random phase approximation
Europ. Conf. on Thermodynamic Properties (London, UK) (2002)

Monkenbusch,M, Mihailescu,M, Endo,H, Allgaier,J, Gompper,G, Stellbrink,J, Richter D, Jakobs B, Sottmann T, Farago B
Dynamics of Microemulsions from Neutron Spin-Echo Experiments
6th international Conference on Quasielastic Neutron Scattering QENS2002 (Potsdam) (2002)

Richter, D.
Neutrons in soft matter science
Seminar (Fa. ExxonMobil) (2002)

Richter, D.
Wax control by self-assembling polymers - a science approach
6th Int. Symp. on the Science and Technology of Polymer Assembly (Kyoto) (2002)

Richter, D.
Polymer dynamics from large to small scales
XII. International Conference on Small Angle Scattering (SAS) (Venice) (2002)

Richter, D.
Polymer dynamics from large to small scales
American Conference on Neutron Scattering (ACNS) (Knoxville) (2002)

Schwahn, D.
Methode der Kleinwinkelstreuung mit Neutronen zur Untersuchung nano- und mesoskopischer Strukturen
Institut für Anorganische und Analytische Chemie, Johannes-Gutenberg-Universität (Mainz) (2002)

Kanaya,T, Monkenbusch,M, Watanabe,H, Nagao,M, Richter, D., Kaji,K
Dynamics of Polymer Micelles Studied by Neutron Spin Echo Technique - Breathing Mode or Zimm Mode
International Symposium Organized by ICR, Kyoto University (Uji, Kyoto, Japan) (2002)

2001

Allgaier,J
Synthesis, neutron small angle scattering and rheology of branched model polymers
Universität Bayreuth (Bayreuth) (2001)

Allgaier,J
From nonionic surfactants to their polymer analogues. Materials and micellar properties
Unilever research and development center (Port Sunlight, UK) (2001)

Allgaier,J, Endo,H, Gompper,G, Mihailescu,M, Monkenbusch,M, Richter,D, Jakobs, B; Sottmann, T; Strey R
Amphiphilicity boosting in microemulsions: The effect of poly(ethylene oxide-b-(ethylene-alt-propylene)) dilock copolymers
International symposium on ionic polymerization (Heraklion, Greece) (2001)

Erhardt,R, Boeker,A, Zettl,H, Kaya,H, Pyckhout-Hintzen,W, Krausch,G, Abetz,V, Mueller,A
Superstructures of janus micelles
ACS 221:56-PMSE,Part2 (USA, 2001)

Frielinghaus,H, Byelov,D, Allgaier,J, Richter, D., Sottmann,T, Strey,R
Mikroemulsionen mit Polymerbeigaben untersucht mit Neutronenkleinwinkelstreuung
Kolloquium der physikalischen Chemie der Uni-Münster (Uni-Münster) (2001)

Frielinghaus,H, Byelov,D, Endo,H, Allgaier,J, Stellbrink,J, Richter, D., Jakobs B, Sottmann T, Strey R
Polymer boosting effect in the Droplet Phase Studied by Small Angle Neutron Scattering
Jülich Soft Matter Days (Kerkrade) (2001)

Kahle,S
Dynamic Neutron Scattering on Partially Deuterated Polybutadiene
4th Int. Discussion Meeting on Relaxations in Complex Systems (Heraklion) (2001)

Richter, D.
Soft condensed matter
OECD Workshop on Large Facilities for Studying the Structure and Dynamics of Matter (Kopenhagen) (2001)

Richter, D.
Neutrons in soft condensed matter
Colloquium (Univ. Bayreuth) (2001)

Richter, D.
Neutrons in soft condensed matter
ILL Millennium Symposium (ILL Grenoble) (2001)

Richter, D.
Wax crystal modification by Random copolymers of the PEB-n type
Seminar (Univ. of Princeton) (2001)

Richter, D.
Experimental aspects of polymer dynamics
Conf. on Polymers in the Third Millennium (Montpellier) (2001)

Schwahn, D.
Scattering Experiments Relevant for Polymer Research at the Neutron Guide Laboratory of the Jülich Research Center
222nd ACS National Meeting (Chicago) (2001)

Wischnewski,A
Kettendynamik in Polymerschmelzen: Grenzen des Reptationsmodells
Deutsche Neutronenstreutagung (Juelich, Germany) (2001)

Wischnewski,A, Monkenbusch,M, Willner,L, Richter, D., Farago,B, Ehlers,G, Schleger,P
NSE spectroscopy on reptating polymers
IDMRCS (Kreta) (2001)

Conference Presentations

2006

Brodeck,M, Frielinghaus,H, Allgaier,J, Richter,D
Microemulsions with sticker polymers as efficiency boosters investigated by SANS
JCNS Symposium and European User Meeting (Jülich) Poster (2006)

Brodeck,M, Frielinghaus,H, Allgaier,J, Richter,D
Microemulsions with sticker polymers as efficiency boosters
Frühjahrstagung der DPG (Dresden) Poster (2006)

Brodeck,M, Frielinghaus,H, Mangiapia,G, Frank,C, Allgaier,J, Richter,D
New Sticker Polymers as Efficiency Boosters in Microemulsions
SoftComp Network Area Meetings (Venice) Talk (2006)

Chaussee,T
Effect of the surface interaction is silica filled elastomers on their mechanical properties
JCNS Symposium and European User Meeting (Jülich) Poster (2006)

Dror,Y, Pyckhout-Hintzen,W, Cohen,Y
The Conformation of Polymers Dispersing Single-Walled Carbon Nanotubes in Water: A Small Angle Neutron Scattering Study
American Physical Society Meeting (Baltimore, MD, USA) Talk (2006)

Frielinghaus,H, Hermes,H, Pyckhout-Hintzen,W, Richter,D
SANS Experiments and Model on Clay Dispersions and Nanocomposites
JCNS Symposium and European User Meeting (Jülich) Poster (2006)

Frielinghaus,H, Hermes,H, Pyckhout-Hintzen,W, Richter,D
Clay Dispersions
Frühjahrstagung der DPG (Dresden) Poster (2006)

Holderer,O, Frielinghaus,H, Byelov,D, Monkenbusch,M, Allgaier,J, Richter,D
Interface fluctuations, membrane elasticity and renormalization effects in microemulsions
Frühjahrstagung der DPG (Dresden) Poster (2006)

Iatrou,E
Influence of the macromolecular architecture on the formation of vesicles from amphiphilic copolypeptides in water
JCNS Symposium and European User Meeting (Jülich) Poster (2006)

Korolkov,D, Willner,L, Schlachter,A, Kentzinger,E, Frielinghaus,H, Farle,M, Brückel T, Paul A
Nanostructure fabrication using diblock-copolymers
Heraeus Seminar: Nanoscale Magnets - Top down meets bottom up (Bad Honnef) Poster (2006)

Korolkov,D, Willner,L, Schlachter,A, Kentzinger,E, Frielinghaus,H, Farle,M, Brückel T, Paul A
Nanostructure Fabrication using Diblock-Copolymers
JCNS Symposium and European User Meeting (Jülich) Poster (2006)

László,K, Kosik,K, Wilk,E, Geissler,E
Interaction of phenols with PNIPA gels
American Chemical Society 231 National Meeting (Atlanta Georgia) Talk (2006)

Maccarrone,S, Frielinghaus,H, Allgaier,J, Richter,D
SANS Experiments on Confined Polymers in Microemulsions
SoftComp Network Area Meetings (Venice) Talk (2006)

Maccarrone,S, Frielinghaus,H, Allgaier,J, Richter,D
Confined Polymers in Microemulsions
JCNS Symposium and European User Meeting (Jülich) Poster (2006)

Maccarrone,S, Frielinghaus,H, Allgaier,J, Richter,D
Confined polymers in microemulsions
DPG Frühjahrstagung 2006 (Dresden, Germany) Poster (2006)

Maccarrone,S, Frielinghaus,H, Allgaier,J, Richter,D
SANS Experiments on Confined Polymers in Microemulsions
SoftComp Annual Meeting 2006 (Venice, Italy) Talk (2006)

Mayorova,M, Zorn,R, Richter,D, Frick,B
Dynamics of glass-forming liquids in soft confinement
DPG Frühjahrstagung 2006 (Dresden) Poster (2006)

Mayorova,M, Zorn,R, Richter,D, Frick,B
Effect of soft confinement on the dynamics of glass-forming liquids
Dynamics in Confinement (ILL, Grenoble, France) Poster (2006)

Niedzwiedz,K
Large scale dynamics in the miscible blend of PMMA and PEO - the random Rouse model
SoftComp (Venice) Talk (2006)

Niedzwiedz,K, Wischnewski,A, Monkenbusch,M, Willner,L, Richter,D, Genix,A-C, Arbe A, Colmenero J, Straube E
Dynamics of miscible polymer blend PEO/PMMA high resolution neutron scattering
DPG - Frühjahrstagung (Dresden) Poster (2006)

Tyagi,M, Alegria,A, Alvarez,F, Colmenero,J, Monkenbusch,M, Frick,B
On the Q-dependence of the Atomic Motions in the alpha-Relaxation range: A neutron scattering study of the short chian analog of poly(vinyl acetate)
Workshop on dynamics in viscous liquids (Mainz, Germany) Poster (2006)

Zacherle,T, Pyckhout-Hintzen,W, Frielinghaus,H, Allgaier,J, Wischnewski,A, Richter,D
PEO-clay composites. First SANS and BSS results
SoftComp Annual Meeting (Venice) Talk (2006)

Zamponi,M, Wischnewski,A, Monkenbusch,M, Willner,L, Farago,B, Richter,D
Anomalous diffusion in short chain polymer melts
DPG Frühjahrstagung (Dresden) Talk (2006)

Zamponi,M, Wischnewski,A, Monkenbusch,M, Willner,L, Richter,D, Farago,B
Anomalous diffusion of short chains in binary polymer melts
Annual European Rheology Conference (Hersonisos, Greece) Talk (2006)

Zamponi,M, Wischnewski,A, Monkenbusch,M, Willner,L, Richter,D, Farago,B
Anomalous diffusion in short chain polymer melts
Workshop on Dynamics in Viscous Liquids (Mainz) Talk (2006)

2005

Frielinghaus,H, Brodeck,M, Mangiapia,G, Frank,C, Allgaier,J, Richter,D
Small Angle Neutron Scattering Experiments on Polymer-Additives in Microemulsions
SoftComp Network Area Meetings (Bonn) Talk (2005)

Frielinghaus,H, Hermes,H, Pyckhout-Hintzen,W, Richter,D
Polymer clay nanocomposites
Jülich Soft Matter Days 2005 (Bonn) Poster (2005)

Frielinghaus,H, Maccarrone,S, Byelov,D, Allgaier,J, Richter,D
Confinement Effects of Polymers in Microemulsions
2nd FRM-II Workshop on Neutron Scattering (Burg Rothenfels) Talk (2005)

Frielinghaus,H, Maccarrone,S, Byelov,D, Allgaier,J, Richter,D, Auth,T
Polymer confinement effects in microemulsions
Bayreuther Polymer Symposium (Bayreuth) Poster (2005)

Hermes,H, Frielinghaus,H, Pyckhout-Hintzen,W, Richter,D
Polymer-Clay-Nanocomposites: A New Approach
SoftComp Network Area Meetings (Ancona) Talk (2005)

Holderer,O, Frielinghaus,H, Monkenbusch,M, Allgaier,J, Richter,D
Dynamic properties of microemulsions modified with homopolymers and diblock copolymers - the determination of bending moduli and renormalization effects
2nd FRM-II Workshop on Neutron Scattering (Burg Rothenfels) Talk (2005)

Maccarrone,S, Frielinghaus,H, Allgaier,J, Richter,D, Auth,T
Confined polymers in microemulsions
Jülich Soft Matter Days 2005 (Bonn) Poster (2005)

Mayorova,M, Zorn,R, Richter,D, Frick,B
Effect of soft confinement on the dynamics of glass-forming liquids
Jülich Soft Matter Days (Bonn) Poster (2005)

Monkenbusch,M, Holderer,O, Endo,H, Allgaier,J, Frielinghaus,H
Membranelastizität und Fluktuationen in Mikroemulsionen, SANS und NSE Untersuchungen
Seminar: Neutronen in Forschung und Industrie (München) Talk (2005)

Ramzi,A, vanNostrum,CF, Rijcken,CJF, Veldhuis,T, Hennink,WE
Transient Morphology of Degradable Polymeric Micelles Investigated by Light and Neutron Scattering
Dutch Polymer Days (Lunteren, Neteherlands) Talk (2005)

Tyagi,M, Alegria,A, Colmenero,J
On the Q-Dependence of the Atomic Motions in the alpha-relaxation Range. A Direct Comparison Between the Trimer of Vinyl Acetate and its Polymer Counterpart.
NSE-2005 (ILL, Grenoble) Poster (2005)

Stellbrink,J, Laurati,M, Lund,R, Rother,G, Willner,L, Richter,D, Zaccarelli,E
PEP-PEO Diblock Copolymer Micelles – A Colloidal Model System with tunable Softness
SoftComp Workshop: Colloids, Gels and Glasses (Leuven, Belgium) Talk (2005)

Zamponi,M, Wischnewski,A, Monkenbusch,M, Willner,L, Richter,D, Likhtman,A, Farago B, Kali G
The influence of constraint release on the reptation process: NSE study and comparison to simulation
DPG Frühjahrstagung (Berlin) Poster (2005)

2004

Frielinghaus,H
Der ‚Polymer-Boosting-Effekt' und der komplementäre Effekt in Mikroemulsionen untersucht mit Neutronenkleinwinkelstreuung
Deutsche Neutronenstreutagung (Dresden / D) Talk (2004)

Frielinghaus,H, Byelov,D, Holderer,O, Allgaier,J, Richter,D
Polymer boosting and the complementary effect -- microemulsions with polymer confinement effects
Jülich Soft Matter Days 2004 (Kerkrade / NL) Poster (2004)

Galant,C, Kjoniksen,A-L, Knudsen,KD, Laukkanen,A, Tenhu,H, Lund,R, Nystrom, B
Physical properties of aqueous solutions of a thermoresponsive PVCL-g-$C_1$1$EO_4$2 copolymer
MACRO 2004 (Paris) Poster (2004)

Guo,XH, Biehl,R, Pacheco,CR, Monkenbusch,M, Richter,D, Fu,L, Prud´homme RK
Diffusion of protein in polymer solutions: A comparison between neutron spin-echo spectroscopy and NMR measurements.
ABSTRACTS OF PAPERS OF THE AMERICAN CHEMICAL SOCIETY 228: U346-U346 145-POLY Par (USA) Poster (2004)

Hermes,HE, Frielinghaus,H, Pyckhout-Hintzen,W, Richter,D
Polymer-silicate nanocomposites: A small angle neutron scattering investigation
6th IPF Colloquium: Advanced heterogeneous polymer materials (Dresden, D) Poster (2004)

Hodrien,AJ, Voice,AM, Waigh,TA
Adsorption of DNA onto Charged Spheres
MRS Fall Meeting (Boston) Poster (2004)

Holderer,O, Byelov,D, Frielinghaus,H, Monkenbusch,M, Allgaier,J, Richter,D
Renormalization effects in bicontinuous microemulsions measured by SANS and NSE
Jülich Soft Matter Days 2004 (Rolduc, Kerkrade, Niederlande, 16.11.2004 - 19.11.2004) Poster (2004)

Holderer,O, Frielinghaus,H, Byelov,D, Monkenbusch,M, Allgaier,J, Richter,D
Dynamics of bicontinuous microemulsions modified by addition of homopolymers
7th International Conference on Quasi-Elastic Neutron Scattering (QENS 2004) (Arcachon, France, 01.09.2004 - 04.09.2004) Talk (2004)

Hu,XS, Biehl,R, Prud´homme,RK, Monkenbusch,M, Lal,J
Study of non-ionic surfactant lamellar phases on addition of charge
ABSTRACTS OF PAPERS OF THE AMERICAN CHEMICAL SOCIETY 227: U840-U840 230-COLL Par (USA) Poster (2004)

Korolkov,D, Willner,L, Kentzinger,E, Frielinghaus,H, Busch,P, Paul,A, Rücker, U; Brückel, Th
Grazing Incidence Small Angle Neutron Scattering from dPS-PB diblock copolymer films
Deutsche Neutronenstreutagung (TU Dresden) Poster (2004)

Mangiapia,G
A novel class of potential contrast agents for using in Magnetic Resonance
XXXIII Italian Congress of Physical Chemistry (Naples, 21-25 july) Talk (2004)

Melnichenko,YB, Wignall,GD, Cole,DR, Frielinghaus,H
Liquid-Gas Critical Phenomena Under Confinement: SANS Studies of CO2 in Aerogel
ACNS 2004 (College Park, Maryland, USA) Talk (2004)

Radulescu,A, Schwahn,D, Stellbrink,J, Kentzinger,E, Brückel,T, Richter,D, Mathers RT, Coates GW, Fetters LJ
Self-assembly in solution of partially crystalline polymers: multilevel structures investigated over four orders of magnitude in size scale by using the SANS instruments at the FRJ-2 reactor
Jülich Soft Matter Days 2004 (Kerkrade, The Netherlands) Poster (2004)

Stellbrink,J, Laurati,M, Lund,R, Rother,G, Willner,L, Richter,D, Zaccarelli E
PEP-PEO Diblock Copolymer Micelles - A Colloidal Model System with tunable Softness
From Hard to Ultra-soft Colloids (Koutulofari(Crete), Greece) Talk (2004)

Wischnewski,A, Zamponi,M, Monkenbusch,M, Willner,L, Richter, D., Likhtman,AE, McLeish,TCB, Farago,B, Kali,G
Molecular observation of mechanisms limiting the topological confinement in polymer melts: a neutron spin echo study
International Workshop on Dynamics in Viscous Liquids, Munich 17.03.04

Zamponi,M, Wischnewski,A, Monkenbusch,M, Willner,L, Richter,D, Farago,B, Likhtman
The influence of constraint release on the reptation process: NSE study and comparison to simulation
International Conference on Quasi-Elastic Neutron Scattering (Arcachon, France) Talk (2004)

2003

Biehl,R, Xuhong,G, Prud'homme,RK, Richter, D.
Diffusion of compact macromolecules through polymer meshes: mesh dynamics and probe dynamics
Workshop on 'Physics meets Biology'
San Sebastian: Poster 26.06.2003 - 28.06.2003

Blanchard,A, Pyckhout-Hintzen,W, Willner,L, Straube,E, Richter, D..
SANS study of non-linear relaxation mechanisms in an elongated polymer melt
DPG Frühjahrstagung
Dresden: 23.03.2003 - 28.03.2003 Poster

Byelov,D, Frielinghaus,H, Allgaier,J, Gompper,G, Richter, D.
SANS studies of polymer efficiency boosting in microemulsions - diblock copolymers versus homopolymers
3rd European Conference on Neutron Scattering
Montpellier,France: 03.09.2003 - 06.09.2003 Poster

Byelov,D, Frielinghaus,H, Allgaier,J, Richter, D.
Polymer efficiency boosting in microemulsions – diblock copolymers versus homopolymers
Jülich Soft Matter Days 2003, Kerkrade, NL, 19.11.2003 (Poster)

Frielinghaus,H, Byelov,D, Allgaier,J, Gompper,G, Richter, D.
SANS studies of microemulsions in the droplet phase with polymer as an efficiency booster
3rd European Conference on Neutron Scattering
Montpellier,France: 03.09.2003 - 06.09.2003 Poster

Frielinghaus,H, Byelov,D, Allgaier,J, Richter, D.
Microemulsions in the droplet phase with polymer as an efficiency booster
Jülich Soft Matter Days 2003, Kerkrade, NL, 20.11.2003 (Poster)

Heinrich,M, Pyckhout-Hintzen,W, Allgaier,J, Richter, D., Straube,E, Read,D. J, McLeish,T. C. B, Wiedenmann,A
Time evolution of strain relaxation in a model H-polymer
3rd European Conference on Neutron Scattering
Montpellier,France: 03.09.2003 - 06.09.2003 Poster

Heinrich,M, Pyckhout-Hintzen,W, Allgaier,J, Richter, D., Straube,E, Read,DJ, McLeish, TCB
Relaxation of deformed H-polymers in elongational flow
Jülich Soft Matter Days 2003, Kerkrade, NL, 20.11.2003 (Poster)

Heinrich,M, Pyckhout-Hintzen,W, Richter, D., Straube,E, Read,D, McLeish,TCB
Relaxation dynamics of entangled branched polymers investigated by SANS
DPG Frühjahrstagung
Dresden: 23.03.2003 - 28.03.2003

Hermes,HE, Frielinghaus,H, Pyckhout-Hintzen,W, Richter, D.
Polymer-silicate nanocomposites: A molecular level investigation
Jülich Soft Matter Days 2003
Kerkrade, Th.e Netherlands: 18.11.2003 - 21.11.2003 Poster

Holderer,O, Frielinghaus,H, Monkenbusch,M, Allgaier,J, Richter, D..
Influence of polymer addition on the dynamics of microemulsions
Jülich Soft Matter Days 2003
Kerkrade, Th.e Netherlands: 18.11.2003 - 21.11.2003 Poster

Lund,R, Willner,L, Stellbrink,J, Radulescu,A, Monkenbusch,M, Richter, D.
Kinetics and structure in block copolymer micelles studied by time resolved SANS
3rd European Conference on Neutron Scattering
Montpellier,France: 03.09.2003 - 06.09.2003 Poster

Lund,R, Willner,L, Stellbrink,J, Radulescu,A, Monkenbusch,M, Richter, D.
Tuning of exchange kinetics and structure of star-like polymeric micelles
International Workshop NATO Advanced Study Institute on 'Forces,Growth and Form in Soft Condensed Matter: At the Interface between Physics and Biology'
Geilo,Norway: 24.03.2003 - 03.04.2003 Poster

Lund,R, Willner,L, Stellbrink,J, Radulescu,A, Richter, D.
Chain exchange kinetics in block copolymer micelles: the system PS-PB in decane,hexadecane and DMF
Jülich Soft Matter Days 2003
Kerkrade, Th.e Netherlands: 18.11.2003 - 21.11.2003 Poster

Mihailescu,M, Monkenbusch,M, Allgaier,J, Frielinghaus,H, Richter, D., Jakobs,B, Sottmann,T
Dynamics of lamellar microemulsions – A neutron-spin-echo investigation
Workshop on 'Physics meets Biology'
San Sebastian: 26.06.2003 - 28.06.2003 Poster

Niu,A, Stellbrink,J, Allgaier,J, Willner,L, Richter, D., Fetters,L. J
Real-time SANS and 1H-NMR studies of self-assembly of living polymer chains in hydrocarbon media
DPG Frühjahrstagung
Dresden: 23.03.2003 - 28.03.2003 Poster

Niu,A, Stellbrink,J, Allgaier,J, Willner,L, Richter, D., König,B, Gondorf,M, Willbold,S, Fetters,L. J
A new view of the anionic diene polymerization mechanism
International Symposium on Ionic Polymerization (IUPAC)
Boston,Mass.: 30.06.2003 - 04.07.2003

Schwahn, D.
Thermal composition fluctuations and phase behaviour of an A/B/A-B homopolymer blend/diblock copolymer mixture
APS March Meeting
Austin,Texas: 06.03.2003

Willner,L, Lund,R, Radulescu,A, Stellbrink,J, Richter, D.
Tuning of chain exchange kinetics and structure in PEP-PEO block copolymer micelles
77th ACS Conference,Colloid and Surface Science Symposium
Atlanta/USA: 15.06.2003 - 18.06.2003

Wischnewski,A, Monkenbusch,M, Willner,L, Richter, D., Likhtman,A. E, McLeish,T. C. B, Farago,B
Constraints of motion in polymer melts: A coherent and incoherent neutron spin echo study
Workshop on 'Physics meets Biology'
San Sebastian: 26.06.2003 - 28.06.2003 Poster

Wischnewski,A, Zamponi,M, Monkenbusch,M, Willner,L, Pyckhout-Hintzen,W, Richter, D., Likhtman,A. E, McLeish,T. C. B, Farago,B
Molecular observation of contour-length fluctuations limiting topological confinement in polymer melts
3rd European Conference on Neutron Scattering
Montpellier,France: 03.09.2003 - 06.09.2003

Wischnewski,A, Zamponi,M, Monkenbusch,M, Willner,L, Pyckhout-Hintzen,W, Richter, D., Likhtman,A. E, McLeish,T. C. B, Farago,B
What limits reptation?
Wissenschaftliche Beiratssitzung
Jülich: 03.04.2003

Zamponi,M, Wischnewski,A, Monkenbusch,M, Willner,L, Richter, D., Farago,B.
Limiting effects in reptation dynamics: the onset of constraint release
Jülich Soft Matter Days 2003
Kerkrade, Th.e Netherlands: 18.11.2003 - 21.11.2003 Poster

Zamponi,M, Wischnewski,A, Monkenbusch,M, Willner,L, Richter, D., Likhtman,AE, McLeish,TCB
The influence of contour length fluctuations on the reptation process
DPG Frühjahrstagung
Dresden: 24.03.2003 - 28.03.2003

Zamponi,M, Wischnewski,A, Monkenbusch,M, Willner,L, Richter, D., Likhtman,A, McLeish,T, Farago,B
Proving the concept of contour length fluctuations in polymer melts
3rd European Conference on Neutron Scattering
Montpellier,France: 03.09.2003 - 06.09.2003 Poster

Zorn, R., Frick,B, Hartmann,L, Kremer,F, Schönhals,A, Richter, D.
Dynamics of confined glass-forming systems observed by neutron scattering
3rd European Conference on Neutron Scattering
Montpellier,France: 03.09.2003 - 06.09.2003 Poster

Zorn, R., Schönhals,A, Hartmann,L, Kremer,F, Frick,B, Richter, D.
Dynamics of confined glass-forming systems observed by inelastic/quasielastic neutron scattering
Jülich Soft Matter Days 2003
Kerkrade, Th.e Netherlands: 18.11.2003 - 21.11.2003 Poster

2002

Blanchard,A, Pyckhout-Hintzen,W, Heinrich,M, Straube,E, Willner,L, Richter, D.
Relaxation mechanisms in a streched linear polymer melt studied by SANS
Jülich Soft Matter Days (Kerkrade, NL) Poster (2002)

Byelov,D, Frielinghaus,H, Allgaier,J, Richter, D.
SANS studies of bicontinuous microemulsions with homopolymer and diblock copolymer additions
Jülich Soft Matter Days 2002 (Kerkrade) Poster (2002)

Byelov,D, Frielinghaus,H, Allgaier,J, Richter, D., Müller,S, Sottmann,T, Strey,R
SANS studies of bicontinuous microemulsions with homopolymer and diblock copolymer additions
ESS European Conference, Bonn, 15.5.2002 (Poster)

Frielinghaus,H, Byelov,D, Allgaier,J, Richter, D.
Small angle neutron scattering studies of microemulsions in the droplet phase with polymer as an efficiency booster
Jülich Soft Matter Days 2002 (Kerkrade) Poster (2002)

Frielinghaus,H, Byelov,D, Allgaier,J, Richter, D., Jakobs,B, Sottmann,T, Strey,R
Small angle neutron scattering studies of microemulsions in the droplet phase with polymer as an efficiency booster
XII international Conference on Small Angle Scattering, Venedig, IT, 26.8.2002

Frielinghaus,H, Byelov,D, Allgaier,J, Richter, D., Jakobs,B, Sottmann,T, Strey,R
Small angle neutron scattering studies of microemulsions in the droplet phase with polymer as an efficiency booster
ESS European Conference, Bonn, 15.5.2002 (Poster)

Heinrich,M, Pyckhout-Hintzen,W, Allgaier,J, Richter, D., Straube,E, Wiedenmann,A
Relaxation dynamics of entangled branched polymers investigated by SANS
Jülich Soft Matter Days 2002 (Kerkrade (NL)) Poster (2002)

Heinrich,M, Pyckhout-Hintzen,W, Richter, D., Straube,E, Wiedenmann,A
Time evolution of strain relaxation in a model-branched H-polymer by SANS
Deutsche Neutronenstreutagung 2002 (Bonn) Poster (2002)

Heinrich,M, Pyckhout-Hintzen,W, Richter, D., Straube,E, Wiedenmann,A
Time evolution of strain relaxation in a model-branched H-polymer by SANS
SAS2002 (Venezia (I)) Talk (2002)

Hermes,HE, Willner,L, Kreitschmann,M, Pyckhout-Hintzen,W, Richter,D
Small angle scattering investigation of linear and star trifluoroacetylated nylon-6
Juelich Soft Matter Days (Kerkrade, NL) Poster (2002)

Kahle,S, Monkenbusch,M, Richter, D., Ryckaert,JP, Koza,M
Local Dynamics in Polymers
ESS European Conference (Bonn) Poster (2002)

Kahle,S, Monkenbusch,M, Ryckaert,JP, Karatasos,K, Koza,M
Segmental Dynamics in Polyisobutylene: Comparison between Neutron Scattering and Computer Simulations
Juelich Soft Matter Days (Kerkrade) Poster (2002)

Lund,R, Willner,L, Monkenbusch,M, Radulescu,D, Richter,
Tuning of chain exchange kinetics and structure in PEP-PEO block copolymer micelles
Juelich Soft Matter Days (Kerkrade, The Netherlands) Poster (2002)

Lund,R, Willner,L, Radulescu,A, Richter, D.
Tuning of chain exchange kinetics and structure in PEP-PEO block copolymer micelles
International Meetings: ESS European Conference, The European Spallation Source- Satellite Meetings 16-17 May 2002 (Bonn, Germany) Poster (2002)

Monkenbusch,M
Segmental dynamics and confinement in polymer melts
Jülich Soft Matter Days 2002 (Kerkrade) Talk (2002)

Monkenbusch,M, Mihailescu,M, Allgaier,J, Richter, D., Jakobs,B, Sottmann,T, Yang BS, Prud'homme RK, Lal J
Neutron Spin Echo Study on the Modification of Surfactant Membrane Properties Due to Polymer Addition
American Conference on Neutron Scattering ACNS 23-27.6. 2002 (Knoxville) Talk (2002)

Niu,A, Stellbrink,J, Allgaier,J, Willner,L, Richter, D., Fetters,LJ
Real-time SANS and 1H-NMR studies during "living" anionic polymerisation of Butadiene in hydrocarbon media
ESS European Conference (Bonn, Germany) Poster (2002)

Niu,A, Stellbrink,J, Allgaier,J, Willner,L, Richter, D., Fetters,LJ
Real-time SANS and 1H-NMR studies during "living" anionic polymerisation of Butadiene in hydrocarbon media
Soft Matter Days 2002 (Kerkrade, Holland) Poster (2002)

Radulescu,A, Schwahn, D., Richter, D., Fetters,LJ
Co-crystallization of poly(ethylene-butene) copolymers and paraffin molecules in decane studied with SANS
Small Angle Scattering Conference SAS2002 (Venice, Italy) Poster (2002)

Rathgeber,S, Pakula,T, Wilk,A, Matyjaszewski,K
Regular branched Macromolecules: Structure of Bottlebrush Polymers in Solution
XII International Conference on Small-Angle Scattering (Venice, Italy) Talk (2002)

Wischnewski,A, Monkenbusch,M, Willner,L, Richter, D., Likhtman,AE, McLeish,TCB, Farago B
Constraints of Motion in Polymer Melts: A Coherent and Incoherent Neutron Spin Echo Study
Jülich Soft Matter Days 2001 (Kerkrade)

2001

Byelov,D, Frielinghaus,H, Endo,H, Allgaier,J, Richter, D.
Polymer anti boosting. A small angle neutron scattering study of the bicontinuous microemulsion.
Jülich Soft Matter Days 2001 (Kerkrade) Poster (2001)

Byelov,D, Frielinghaus,H, Endo,H, Allgaier,J, Richter, D.
Polymer anti boosting. A small angle neutron scattering study of the bicontinuous microemulsion
Int. Summerschool Fundamental Problems in Statistical Physics X (Odenthal-Altenberg) Poster (2001)

Frielinghaus,H, Endo,H, Allgaier,J, Richter, D., Jakobs,B, Sottmann,T, Strey R
Polymer boosting effect in der Tröpfchenphase - eine Studie mit Neutronenkleinwinkelstreuung
Würzburger Tagung Fortschritte für Wasch- und Reinigungsmittel (Würzburg) Poster (2001)

Frielinghaus,H, Byelov,D, Allgaier,J, Richter, D., Jakobs,B, Sottmann,T, Strey,R
Polymer boosting effect in the droplet phase studied by small-angle neutron scattering
International Conference on Neutron Scattering 2001, München, 11.09.2001 (Poster)

Heinrich,M, Pyckhout-Hintzen,W, Richter, D., Straube,E, Wiedenmann,A
Relaxation of entangled model H-shaped polymers: a SANS investigation
ICNS 2001 (München) Poster (2001)

Heinrich,M, Pyckhout-Hintzen,W, Richter, D., Straube,E, Wiedenmann,A
SANS investigations of relaxation dynamics of entangled model H-polymers
Deutsche Neutronenstreutagung 2001 (Jülich (D)) Poster (2001)

Kahle,S, Willner,L, Monkenbusch,M, Richter, D., Arbe,A, Colmenero,J, Frick,B
Dynamic Neutron Scattering on Partially Deuterated Polybutadiene
International Conference on Neutron Scattering (Muenchen) Poster (2001)

Kahle,S, Willner,L, Monkenbusch,M, Richter, D., Arbe,A, Colmenero,J, Frick,B
Dynamic Neutron Scattering on Partially Deuterated Polybutadiene
ILL Millennium Symposium (Grenoble) Poster (2001)

Kahle,S, Willner,L, Monkenbusch,M, Richter, D., Arbe,A, Colmenero,J, Frick,B
Dynamische Neutronenstreuung an partiell deuteriertem Polybutadien
Deutsche Neutronenstreutagung (Juelich) Poster (2001)

Melnichenko,YB, Wignall,GD, Schwahn, D.
Universal aspects of macromolecules in polymer blends, solutions, and supercritical mixtures, and implications for the validity of the RPA
222nd ACS National Meeting (Chicago, Illinois, USA) Talk (2001)

Mihailescu,M, Allgaier,J, Monkenbusch,M, Richter, D.
Dynamics of bicontinuous phase microemulsions with amphiphilic block-copolymer
Deutsche Neutronenstreutagung (Jülich) Poster (2001)

Mihailescu,M, Allgaier,J, Monkenbusch,M, Richter, D.
Structural and dynamical investigation of mixed amphiphilic membranes. A combined SANS-NSE study
ICNS (Munich) Poster (2001)

Monkenbusch,M, Mihailescu,M, Allgaier,J, Richter, D., Jakobs,B, Sottmann,T
Interface Dynamics in Bicontinuous Microemulsions Investigated by Neutron Spin Echo Spectroscopy
ACS Conference COLLOIDS2001 (Pittsburgh) Talk (2001)

Schmidt, W., Ohl, M., Buchenau, U., Koza, M.
Inelastic Neutron Scattering in Amorphous Systems at Low Momentum Transfer
Deutsche Neutronenstreutagung, Jülich (2001)

Schwahn, D.
Phase Behaviour of Binary Polybutadiene Copolymer Mixtures as an Example of Weakly Interacting Polymers
Jülich Soft Matter Days (Kerkrade (NL)) Talk (2001)

Schwahn, D.
Phase Behaviour of Binary Polybutadiene Copolymer Mixtures as an Example of Weakly Interacting Polymers
ICNS 2001 (Munich) Talk (2001)

Schwahn, D.
Phase Behaviour of weakly interacting binary Polybutadiene Copolymer mixtures with different Vinyl Content
222nd ACS National Meeting (Chicago) Talk (2001)

Wischnewski,A, Willner,L, Monkenbusch,M, Richter, D., Farago,B, Ehlers,G, Schleger,P
Constraints of motion in polymer melts: coherent and incoherent scattering analyzed by NSE
ICNS (Munich, Germany) Talk (2001)

Transport Processes

Publications

2002

Skripov,AV, Soloninin,AV, Sibirtsev,DS, Buzlukov,AL, Stepanov,AP, Balbach,JJ, Conradi M S, Barnes R G, Hempelmann R
^{45}Sc NMR and high-resolution quasielastic neutron scattering studies of localized H(D) motion in alpha-$ScH_x(D_x)$
Phys. Rev. B **66**, 054306 (2002)

2001

Dzheparov,F, Gul'ko,A, Heitjans,P, L'vov,D, Schirmer,A, Shestopal,V, Stepanov
Spin dynamics and beta-NMR after polarized neutrons capture
Physica B **297**, 288-292 (2001)

Biology

Publications

2006

Gabel,F, Wang,D, Madern,D, Sadler,A, Dayie,K, Daryoush,MZ, Schwahn D, Zaccai G, Lee X, Williams BRG
Dynamic Flexibility of Double-stranded RNA Activated PKR in Solution
Journal of Molecular Biology **Apr 06**, Epublished (2006)

2005

DiCola,E, Waigh,T, Trinick,J, Tskhovrebova,L, Houmeida,A, Pyckhout-Hintzen,W, Dewhurst C
Persistence length of titin from rabbit skeletal muscles measured with scattering and microrheology techniques
Biophysical Journal **88**, 4095 (2005)

Lebedev,DV, Filatov,MV, Kuklin,AI, Islamov,AKh, Kentzinger,E, Pantina,R, Toperverg,BP, Isaev-Ivanov,VV
Fractal nature of chromatin organization in interphase chicken erythrocyte nuclei: DNA structure exhibits biphasic fractal properties
FEBS Letters **579**, 1465-1468 (2005)

2002

Grimm,H, Sokolov,AP, Dianoux,AJ
Relaxation dynamics in dry and humid DNA
Applied Physics A **74**, S1248 (2002)

Sokolov,AP, Grimm,H, Kisliuk,A, Dianoux,AJ
Slow Relaxation Process in DNA
J.Biological Physics **27**, 313 (2002)

2001

Sokolov,AP, Grimm,H, Kisliuk,A, Dianoux,AJ
Slow relaxation process in DNA at different levels of hydration
J. Biol. Phys. **27**, 313 (2001)

Invited Talks

2005

Sinibaldi,R, Carsughi,F, Mariani,P, Ortore,MG, Spinozzi,F
Hydrophilicity of lysozyme in water/glycerol mixtures
FEBS Congress (Budapest) (2005)

2003

Grimm,H
Structure and external modes of DNA in wet-spun film
10th Int. Seminar on 'Neutron Scattering Investigation in Condensed Matter'
Poznan/Poland: 08.05.2003 - 10.05.2003

2002

Schwahn, D.
Grundlagen der Neutronenbeugung im Kleinwinkelbereich
Workshop Grundlegende Aspekte der Biomineralisation (Bochum) (2002)

Conference Presentations

2006

Budyak,IL, Pipich,V, Mironova,OS, Schlesinger,R, Büldt,G, Klein-Seetharaman,J
Conformational changes and oligomerization state of photophobic transducer, HtrII, from archaeon Natronobacterium pharaonis
JCNS Symposium and European User Meeting (Jülich, Germany) Poster (2006)

Konstantopoulos,A, Amran,M, Frielinghaus,H, Miller,A, Saiani,A
Self-assembly mechanism of model peptides
JCNS Symposium and European User Meeting (Jülich) Poster (2006)

2002

Schwahn, D.
Nucleation and Growth of $CaCO_3$ Minerals on Biomimetic Templates studied by SANS
XII International Conference on Small-Angle Scattering (Venice) Talk (2002)

Schwahn, D.
Untersuchungen zur Keimbildung und dem Kristallwachstum von $CaCO_3$ in wäßriger Lösung an biomimetisch strukturierten Grenzflächen
1. Bereichskolloquium Prinzipien der Biomineralisation (Bonn-Röttgen) Talk (2002)

Geology, Archaeology

Publications

2006

Gatta,GD, Nestola,F, Walter,JM
On the thermo-elastic behaviour of kyanite: a neutron powder diffraction study up to 1200°C
Mineralogical Magazine **(in press)**, (2006)

Pleuger,J, Roller,S, Froitzheim,,N, Walter,JM, Jansen,E
Structural evolution of the contact between two Penninic nappes (Zermatt-Saas zone and Combin zone, Western Alps) and implications for the exhumation mechanism and palaeogeography
International Journal of Earth Sciences (accepted May 2006) (2006)

Siemes,H, Klingenberg,B, Rybacki,E, Naumann,M, Schäfer,W, Jansen,E, Kunze, K
Glide systems of hematite single crystals in deformation experiments
Ore Geology Review (accepted March 2006) (2006)

2005

Pleuger,J, Froitzheim,N, Jansen,E
Folded continental and oceanic nappes on the southern side of Monte Rosa (western Alps, Italy): Anatomy of a double collision suture
Tectonics **24**, TC4013, doi: 10.1029 (2005)

Siouris,IM, Walter,JM
A neutron diffraction study of ancient Greek ceramics
Physica B (accepted November 2005) (2006)

2004

Iezzi,G, Gatta,GD, Kockelmann,W, Della Ventura,G, Rinaldi,R, Schäfer,W, Gaillard,F
A $P2_1/m$ amphibole at low temperature (8 K): a neutron powder diffraction study
Proc. 32nd International Geological Congress (2004)

Jansen,E, Schäfer,W, Kirfel,A
On the increasing use of the Jülich texture diffractometer for geological projects
Physica B **350**, e569 (2004)

Jansen,E, Schäfer,W, Kirfel,A
On the increasing use of the Jülich texture diffractometer for geological projects
Physica B **350**, e569 (2004)

Kahle,A, Winkler,B, Radulescu,A, Schreuer,J
Small-angle neutron scattering study of volcanic rocks
European Journal of Mineralogy 16 (2004), 407

Kurz,W, Jansen,E, Hundenborn,R, Pleuger,J, Unzog,W
Microstructures and preferred orientations of omphacite in Alpine eclogites: implications for the exhumation of (ultra-) high-pressure units
J. Geodynamics **37**, 1 (2004)

Prinz,DP, Pyckhout-Hintzen,W, Littke,R
Development of the meso- and macroporous structure of coals with rank as analyzed with small angle neutron scattering and adsorption experiments
Fuel 83 (2004) 547-556

Siemes,H, Klingenberg,B, Rybacki,E, Naumann,M, Schäfer,W, Kunze,K
Glide Systems of Hematite Single Crystals in Deformation Experiments
Applied Mineralogy: Developments in Science and Technology **2**, 947 (2004)

2003

Kockelmann,W, Kirfel,A, Jansen,E, Traum,R, Linke, R, Schreiner,M
Zerstörungsfreie Charakterisierung von Münzen mittels Neutronenbeugung
in Archäometrie und Denkmalpflege 2003 - Kurzberichte 2003 (ed. O. Hahn,Ch. Goedicke,R. Fuchs,I. Horn) S. 82-84

Linke,R, Kockelmann,W, Jansen,E, Kirfel,A, Schreiner,M, Traum,R, Denk,R
Neutron diffraction for non-destructive texture analysis of minted and cast "Taler" coins
Symposium Proceedings on „Numismatics & Technology: questions and answers"
Wien,25-26 April 2003,(2003) 113-123

Pleuger,J, Hundenborn,R, Kremer,K, Babinka,S, Jansen,E, Froitzheim,N
Structural evolution of the Adula nappe, Misox zone, and Tambo nappe in the San Bernardino area: Constraints for the exhumation of the Adula eclogites
Mitt. Österr. Geol. Ges. **94**, 99 (2003)

Siemes,H, Klingenberg,B, Rybacki,E, Naumann,M, Schäfer, W., Jansen,E, Rosière,CA
Texture, microstructure, and strength of hematite ores experimentally deformed in the temperature range 600° to 1100°C and at strain rates between 10^{-4} and 10^{-6} s^{-1}
J. Structural Geology **25**, 1371 (2003)

2002

Artioli,G, Kockelmann,W, Magerl,A, Mezei,F, Rinaldi,R, Schäfer, W., Schofield,PF, Zoppi,M
Cultural Heritage: Artefacts and Materials
in D. Richter (Ed.): The ESS-Project, New Science and Technology for the 21st Century, Vol.II, ESS Council, 6-47 (2002)

Pleuger,J, Jansen,E, Schäfer, W., Oesterling,N, Froitzheim,N
Neutron texture study of natural gneiss mylonites affected by two phases of deformation
Applied Physics A **74**, 1058 (2002)

Rinaldi,R, Artioli,G, Dove,MT, Schäfer, W., Schofield,PF, Winkler,B
Mineral Sciences, Earth Sciences, Environment and Cultural Heritage
in D. Richter (Ed.): The ESS-Project, New Science and Technology for the 21st Century, Vol. II, ESS Council, 4-89 (2002)

Schäfer, W.
Neutron diffraction applied to geological texture and residual stress analysis
European Journal of Mineralogy **14**, 263 (2002)

2001

Froitzheim,N, Pleuger,J, Hundenborn,R, Kremer,K, Babinka,S, Jansen,E
Constraints on the exhumation of the Adula nappe (Part 1): A top-north mega-shear zone in the roof of the nappe
Geol. Paläont. Mitt. Innsbruck **25**, 90 (2001)

Rinaldi,R, Artioli,G, Dove,MT, Schäfer, W., Schofield,PF, Winkler,B
Neutron Scattering in Mineral Science, Earth Science, and related fields with the European Spallation Source
in D. Richter (Ed.): Progress Report: ESS-SAC/ENSA Workshop on Scientific Trends in Condensed Matter, Engelberg, Schweiz, 91 (2001)

Siemes,H, Klingenberg,B, Jansen,E, Schäfer, W., Dresen,G, Rybacki,E, Naumann,M
Textures of experimentally deformed hematite ores with magnetite and wuestite
in: Electronic Proceedings (CD-ROM) of the 2001 Annual Conference of the International Association for Mathematical Geology, Cancun, Mexico, (2001)

Invited Talks

2005

Froitzheim,N, Pleuger,J
Tectonic studies of the European Alps using neutron texture goniometry
EGU General Assembly (Vienna) (2005)

2004

Pleuger,J, Froitzheim,N, Jansen,E
Folded oceanic sutures south of the Monte Rosa (Penninic Alps)
Réunion des sciences de la terre (Strasbourg) (2004)

2003

OliveiraJr,VT, Hackspacher,PC, Siemes,H, Schäfer,W
A textura do itabirito e suas iplicacoes cristalográficas e geológicas
IX. Simpósio Nacional de Estudos Tectônicos (Búzios, Brasil) (2003)

Siemes,H, Günther,A, Rosière,CA, Quade,H
Deformation partitioning and textures of banded iron ores
14th Conference on Deformation mechanisms, Rheology and Tectonics (DRT) (St. Malo, France) (2003)

Conference Presentations

2006

Pleuger,J, Froitzheim,N, Walter,JM
Deformation of the Monte Rosa nappe along the Stellihorn shear zone and the nappe's tail as revealed by neutron texture goniometry of mylonitic quartzites
EGU General Assembly (Vienna) Poster (2006)

Pleuger,J, Roller,S, Froitzheim,N, Walter,JM
Structural evolution of the contact between two Penninic nappes (Zermatt-Saas zone and Combin zone, Western Alps) and implications for exhumation mechanism
EGU General Assembly (Vienna) Poster (2006)

Pleuger,J, Roller,S, Walter,JM, Jansen,E, Froitzheim,N
Kinematik des Deckenkontaktes zwischen der Combinzone und der Zermatt-Saas-Zone (Penninische Decken, Westalpen) und deren Bedeutung für die Exhumierung der Zermatt-Saas-Zone
11. Symposium Tektonik, Struktur- und Kristallingeologie (Göttingen) Talk (2006)

Siemes,H, Klingenberg,B, Rybacki,E, Naumann,M, Walter,JM, Jansen,E, Kunze, K
Mikrostruktur und Textur nach Scherverformungsversuchen an Hämatit
11. Symposium Tektonik, Struktur und Kristallingeologie (Göttingen, Germany) Poster (2006)

2005

Pleuger,J, Froitzheim,N, Walter,JM
Internal deformation of the Monte Rosa nappe along the Stellihorn shear zone
7th Workshop on Alpine Geological Studies (Opatija) Poster (2005)

Siemes,H, Klingenberg,B, Rybacki,E, Naumann,M, Walter,JM, Jansen,E, Kunze, K
Microstructure and texture of hematite ore deformed to large strain in torsion
Jahrestagung der Deutschen Mineralogischen Gesellschaft (Aachen, Germany) Poster (2005)

Siemes,H, Rybacki,E, Schäfer,W, Kunze,K
Glide systems of hematite single crystals in deformation experiments
15th Conference on Deformation mechanisms, Rheology and Tectonics (DRT) (ETH Zürich, Switzerland) Poster (2005)

2004

Froitzheim,N, Pleuger,J, Roller,S, Jansen,E
The Matterhorn - really from Africa?
Réunion des sciences de la terre (Strasbourg) Poster (2004)

Froitzheim,N, Pleuger,J, Roller,S, Jansen,E
Das Matterhorn - wirklich aus Afrika?
10. Symposium Tektonik, Struktur- und Kristallingeologie (Aachen) Poster (2004)

Pleuger,J, Froitzheim,N, Jansen,E
Gefaltete ozeanische Suturen südlich des Monte Rosa (Penninische Alpen)
10. Symposium Tektonik, Struktur- und Kristallingeologie (Aachen) Poster (2004)

Siemes,H, Klingenberg,B, Rybacki,E, Naumann,M, Schäfer,W, Jansen,E, Kunze,K
Glide systems of hematite single crystals in deformation experiments
8. International Congress on Applied Mineralogy (Aguas de Lindoia (Brazil)) Poster (2004)

Siemes,H, Klingenberg,B, Rybacki,E, Naumann,M, Schäfer,W, Jansen,E, Kunze,K
Glide systems of hematite single crystals in deformation experiments
10. Symposium Tektonik, Struktur- und Kristallingeologie (Aachen) Poster (2004)

Siemes,H, Klingenberg,B, Rybacky,E, Nauman,M, Schäfer,W, Jansen,E, Kunze K
Glide Systems of Hematite Single Crystals in Deformation Experiments
ICAM (Sao Paulo) Talk (2004)

2003

E. Jansen, W. Kockelmann, A. Kirfel, R. Linke and M. Schreiner
Archaeometry by neutron diffraction: Test experiments for texture analysis of coins
11. Jahrestagung der Deutschen Gesellschaft für Kristallographie, 10.-13.3.2003, Berlin
Poster (Berlin, 2003)

E. Jansen, W. Kockelmann, A. Kirfel, R. Linke and M. Schreiner
Microstructure analysis of silver coins by means of time-of-flight neutron diffraction.
Conference on the Use of Ion Beams in Materials Science, Medicine and Archaeometry, 22.-24.5.2003, Namur, Belgium
Poster (Namur, 2003)

Jansen,E, Schäfer, W., Kirfel,A
On the increasing use of the Jülich texture diffractometer for geological projects
3rd European Conf. On Neutron Scattering ECNS 2003, 03.–06.09.03, Montpellier/France (Poster)

W. Kockelmann, A. Kirfel, E. Jansen, R. Linke, M. Schreiner, R. Traum and R. Denk
Non-destructive analysis of coins by neutron diffraction.
European Crystallographic Meeting ECM-21, 24.-30.8.2003, Durban, South Africa
Talk (Durban, 2003)

Kockelmann,W, Kirfel,A, Jansen,E,, Traum,R, Linke,R, Schreiner,M
Zerstörungsfreie Charakterisierung von Münzen mittels Neutronenbeugung
Jahrestagung des Arbeitskreises Archäometrie in der GdCh, Archäometrie und Denkmalpflege 2003, 12.–15.03.03, Berlin-Dahlem

J. Pleuger, N. Froitzheim, E. Jansen and W. Schäfer
Structural analysis of continental and oceanic rocks in the upper Sesia valley (Piemonte, northern Italy)
Meeting of the Swiss Tectonic Studies Group, November 2003, Basel, Swiss
Poster (Basel, 2003)

2005

Pleuger,J, Froitzheim,N, Walter,JM
Internal deformation of the Monte Rosa nappe along the Stellihorn shear zone
7th Workshop on Alpine Geological Studies (Opatija) Poster (2005)

Siemes,H, Klingenberg,B, Rybacki,E, Naumann,M, Walter,JM, Jansen,E, Kunze, K
Microstructure and texture of hematite ore deformed to large strain in torsion
Jahrestagung der Deutschen Mineralogischen Gesellschaft (Aachen, Germany) Poster (2005)

Siemes,H, Rybacki,E, Schäfer,W, Kunze,K
Glide systems of hematite single crystals in deformation experiments
15th Conference on Deformation mechanisms, Rheology and Tectonics (DRT) (ETH Zürich, Switzerland) Poster (2005)

2002

Froitzheim,N, Nagel, Th., Pleuger,J, Hundenborn,R, Jansen,E
Zwei Subduktionszonen und der Aufstieg der Adula-Eklogite
9. Symposium Tektonik - Strukturgeologie - Kristallingeologie (Erlangen) Talk (2002)

Kurz,W, Froitzheim,N, Jansen,E, Schäfer, W.
Neutron texture study of eclogite rocks from the Alps
ESS European Conference (Bonn) Poster (2002)

Rinaldi,R, Artioli,G, Kockelmann,W, Schäfer, W., Schofield,PF, Zoppi,M, Magerl,A
Cultural Heritage: Artefacts and Materials Scientific and Technological Challenges in the 21st Century (Dourdan (F)) Talk (2002)

Schäfer, W.
Rock textures studied by neutron diffraction at SV7-b
ESS-SAC-Workshop Earth Science (Cambridge (UK)) Talk (2002)

Schäfer, W., Jansen,E, Kirfel,A, Kurz,W, Froitzheim,N
Chances and challenges of rock texture investigations by neutron diffraction
XIX Congress and General Assembly of the International Union of Crystallography (Genf) Poster (2002)

Schäfer, W., Jansen,E, Skowronek,R, Kirfel,A
Rock texture investigations on the University of Bonn diffractometer SV7-b in Jülich
Deutsche Neutronenstreutagung 2002 and The European Spallation Source (Bonn) Poster (2002)

Siemes,H, Günther,A, Rosière,CA, Quade,H
Deformation partitioning and textures of banded iron ores
11th Quadrennial IAGOD Symposion and Geocongress (Windhoek, Namibia) Poster (2002)

2001

Froitzheim,N, Pleuger,J, Hundenborn,R, Kremer,K, Babinka,S, Jansen,E
Constraints on the exhumation of the Adula nappe (Part 1): A top-north mega-shear zone in the roof of the nappe
5th Workshop of Alpine Geological Studies (Obergurgl (A)) Talk (2001)

Pleuger,J, Jansen,E, Schäfer, W., Oesterling,N, Froitzheim,N
Neutron texture study of natural gneiss mylonites affected by two phases of deformation
ICNS 2001 (Munich) Poster (2001)

Rinaldi,R, Artioli,G, Dove,MT, Schäfer, W., Schofield,PF, Winkler,B
Comparative texture studies of complex systems, time evolution of rock texture, phase and texture analysis of archaeological materials
Scientific Trends in Condensed Matter Research and Instrumentation Opportunities (Engelberg (CH)) Talk (2001)

Rosière,CA, Siemes,H, Lagoeira,L, Quade,H, Schäfer,W, Jansen,E
Partial textures and deformations partitioning on itabirites
VIII. Simpósio National de Estudos Tectônicos 2001 (Recife (Pernambuco)) Poster (2001)

Siemes,H, Klingenberg,B, Jansen,E, Schäfer, W.
Texturuntersuchungen mit Neutronen an experimentell verformten Hämatiterzen mit Magnetit und Wüstit
9. Jahrestagung der Deutschen Gesellschaft für Kristallographie (Bayreuth) Poster (2001)

Siemes,H, Klingenberg,B, Jansen,E, Schäfer, W., Dresen,G, Rybacki,E, Naumann,M
Textures of experimentally deformed hematite ores with magnetite and wuestite
IAMG2001 (Cancun (Mexico)) Poster (2001)

Siemes,H, Klingenberg,B, Jansen,E, Schäfer, W., Dresen,G, Rybacki,E, Naumann,M
Texturen experimentell verformter Hämatiterze mit Magnetit und Wüstit
Deutsche Neutronenstreutagung (Jülich) Poster (2001)

Materials Science and Engineering

Publications

2006

Melnichenko,YB, Wignall,GD, Cole,DR, Frielinghaus,H
Adsorption of supercritical CO2 in aerogels as studied by SANS and neutron transmission techniques
J. Chem. Phys. **124**, 204711 (2006)

2005

Melnichenko,YB, Wignall,GD, Cole,DR, Frielinghaus,H
Liquid-gas critical phenomena underconfinement: SANS studies of CO2 in aerogel
J. Mol. Liquids **120**, 7 (2005)

Wignall,GD, Melnichenko,YB
Recent Applications of SANS in Strongly Interacting Soft Matter
Rep. Progr. Phys. **68**, 1761 (2005)

2004

Jansen,E, Schäfer,W, Kirfel,A, Palacios,J
On the Development of Copper Textures - Neutron Diffraction Control over a Period of 12 Years
Mat. Sci. Forum **443-444**, 239 (2004)

Raevac,V, Hoelzel,M, Danilkin,SA, Hoser,A, Fuess,H
Lattice dynamics in austenitic stainless steels $Fe_{18}Cr_{12}Ni_2Mo$ and $Fe_{18}Cr_{16}Ni_{10}Mn$
J. Phys.: Condens. Matter **16**, 2609 (2004)

2003

Danilkin,SA, Skomorokhov,AN, Hoser,A, Fuess,H, Rajevac,V, Bickulova,NN
Crystal structure and lattice dynamics of superionic copper selenide $Cu_{2-x}Se$
J. Alloys and Compounds **361**, 57 (2003)

Hermann,R P, Jin,R, Schweika, W., Grandjean,F, Mandrus,D, Sales,B C, Long,GJ
Einstein oscillators in thallium filled antimony skutterudites
Phys. Rev. Lett. 90(13) (2003) 135505
see also: Go-go Atoms give Heat the Shake (Arian Cho) Physical Review Focus,3 April 2003
and: Skittery Skutterudites
Nature Materials 2 (2003) 290

2002

Hoelzel,M, Danilkin,SA, Hoser,A, Ehrenberg,H, Wieder,T, Fuess,H
Phonon dispersion in austenitic stainless steel $Fe_{18}Cr_{12}Ni_2Mo$
Applied Physics **A74**, s1013 (2002)

Jansen,E, Kyek,A, Schäfer, W., Schwertmann,I
The structure of 6-line ferrihydrite
Applied Physics A **74**, 1004 (2002)

2001

Caspary,D, Eckold,G, Guethoff,F, Pyckhout-Hintzen,W
Kinetics of decomposition in ionic solids II: neutron scattering study of the system AgCl-NaCl
J. Phys.: Condens. Matter **13**, 11521 (2001)

Jansen,E, Schäfer, W., Kirfel,A, Neuroth,M
Neutron texture investigation on electrolytic $Li_2CO_3/KLiCO_3$ of a molten carbonate fuel cell
Materials Science Forum **378**, 718 (2001)

Maxelon,M, Pundt,A, Pyckhout-Hintzen,W
Small angle neutron scattering of hydrogen segregation at dislocations in palladium
Scripta Mater **44**, 817 (2001)

Maxelon,M, Pundt,A, Pyckhout-Hintzen,W, Barker,J, Kirchheim,R
Interactions of hydrogen and deuterium with dislocations in palladium as observed by small angle neutron scattering
Acta Materialia **49**, 2625 (2001)

Schäfer, W.
Texture in Materials and Earth Sciences
in Th. Brückel, G. Heger, D. Richter (Ed.): Neutron Scattering -Lectures-, Schriften des Forschungszentrums Jülich, Matter and Materials, Vol.9, p. 18.1 (2001)

Sosnowska,I, Przenioslo,R, Schäfer, W., Kockelmann,W, Hempelmann,R, Wysocki,K
Possible deuterium positions in the high temperature deuterated proton conductor $Ba_3Ca_{1+y}Nb_{2-y}O_{9-\delta}$ + x D_2O studied by neutron and X-ray powder diffraction
J. Alloys and Compunds **328**, 226 (2001)

Invited Talks

2004

Melnichenko,YB
Micron Pores in Vycor Porous Glass: Evidences from USANS
Annual National Meeting of the American Crystallographic Association (Chicago) (2004)

Conference Presentations

2006

PalaciosGómez,J, Walter,J, Jansen,E, Kirfel,A, Ennis,PJ, Kryshtab,T
Evidence of extinction in strong textured high purity copper
European Powder Diffraction Conference (EPDIC10) (Genova, Switzerland) Poster (2006)

Siemes,H, Klingenberg,B, Rybacki,E, Naumann,M, Walter,JM, Jansen,E, Kunze, K
Mikrostruktur und Textur bei Scherverformungsversuchen an Hämatiterzen
SNI2006 (Hamburg, Germany) Poster (2006)

2005

Holderer,O, Frielinghaus,H, Monkenbusch,M, Allgaier,J, Richter,D
Dynamics of supercritical water-in-carbon dioxide droplet microemulsions
Jülich Soft Matter Days 2005 (Bonn) Poster (2005)

2004

Melnichenko,YB, Wignall,GD, Cole,DR, Frielinghaus,H
Density Fluctuations Near the Liquid-Gas Critical Point of a Confined Fluid
APS Annual Meeting (Montreal, Canada) Talk (2004)

2003

Melnichenko,Y B, Wignall,G D, Cole,D R, Agamalian,M, Pozdnyakova,I, Schwahn, D., Frielinghaus,H, Radulescu,A, Kentzinger, E.
USANS and SANS Study of the Structure of Vycor Glass
The first Workshop on the international Consortium of Ultra-Small-Angle-Scattering (IConUSAS) July 9.-10,2003,Oak Ridge,USA
Rajevac V.,Hoelzel M.,Danilkin S.,Hoser A.,Fuess H
Lattice dynamics in austenitic stainless steels Fe-18Cr-12Ni-2Mo and Fe-18Cr-16Ni-10Mn
European Conference on Neutron Scattering,Montpellier,3.-6.9.2003 (2003)

2002

Jansen,E, Kyek,A, Schäfer, W., Schwertmann,U
Neutronenbeugung an nanokristallinem Ferrihydrit
10. Jahrestagung der Deutschen Gesellschaft für Kristallographie (Kiel) Poster (2002)

Jansen,E, Schäfer, W., Kirfel,A, Palacios,J
On the development of copper textures - neutron diffraction control over a period of 12 years
8th European Powder Diffraction Conference (Uppsala) Poster (2002)

Jansen,E, Schäfer, W., Kirfel,A, Palacios,J
Copper textures periodically monitored over twelve years
Deutsche Neutronenstreutagung 2002 and The European Spallation Source (Bonn) Poster (2002)

Zotov,N, Schäfer, W., Jansen,E, Kockelmann,W, Deleplane,R
Neutron diffraction studies of glasses in the Collaborative Research Project SFB 408 Bonn, Germany
Deutsche Neutronenstreutagung 2002 and The European Spallation Source (Bonn) Poster (2002)

2001

Jansen,E, Kyek,A, Schäfer, W., Schwertmann,U
The structure of 6-line ferrihydrite
ICNS 2001 (Munich) Poster (2001)

Schäfer, W., Jansen,E, Kirfel,A, Neuroth,M
Textur des $Li_2CO_3/KLiCO_3$-Elektrolytmaterials in Schmelzkarbonat-Brennstoffzellen
Deutsche Neutronenstreutagung (Jülich) Talk (2001)

Theses

2006

Casas,F
Structural heterogeneites of glass polymers after plastic deformation
PhD (physical chemistry), University Paris SUD XI (2006, *Soft condensed matter, Liquids, Glasses*)

2005

Ariane Blanchard
SANS study of the non-linear relaxation mechanisms in a step-strain elongated linear polymer melt
Dr. rer. nat. (Physical Chemistry), Mathematisch-Naturwissenschaftliche Fakultät, Westfälische Wilhelms-Universität Münster (2005*, Soft condensed matter, Liquids, Glasses*)

Dror,Y
Phase Equilibria and Structure Formation in Solutions of Carbon Nanotubes
Ph.D. (Chemical Engineering), Technion-Israel Institute of Technology (2005, *Soft condensed matter, Liquids, Glasses*)

Laurati,M
Phase behaviour and interactions of PEP-PEO star-like micelles
Dr. rer nat. (Physical Chemistry), Mathematisch-Naturwissenschaftliche Fakultät, Westfälische Wilhelms-Universität Münster (2005, *Soft condensed matter, Liquids, Glasses*)

Oh,IH
Strukturelle Phasenübergänge in TlH_2PO_4 und Kristallstrukturen von $Rb_{0.7}Tl_{0.3}H_2PO_4$ und $Rb_{0.5}Tl_{0.5}H_2PO_4$
Dr. rer. nat. (Crystallography), Institut für Kristallographie, RWTH Aachen (2005, *Crystallography*)

2004

Byelov, Dmytro
A SANS study of microemulsions with polymer additions
Dr. rer. nat. (Chemistry), Mathematisch-Naturwissenschaftliche Fakultät, Westfälische Wilhelms-Universität Münster (2004, *Soft condensed matter, Liquids, Glasses*)

Hermann,RP
A neutron scattering and Moessbauer spectral study of thermoelectric and magnetic materials
Dr. rer nat. (Physics), Universite de Liege - Belgium (2004, *Excitations*)

Lund,R
Chain exchange kinetics and structure of polymeric micelles - A comprehensive study of three model systems
Dr. rer nat. (Chemistry), Mathematisch-Naturwissenschaftliche Fakultät, Westfälische Wilhelms-Universität Münster (2004, *Soft condensed matter, Liquids, Glasses*)

Mangiapia,G
Structural study of supramolecular systems composed by synthetic polymers and surfactants involved in controlled release of biological substances
Ph D (Physical Chemistry), University of Naples Federico II, Chemistry Department (2004, *Soft condensed matter, Liquids, Glasses*)

Pipich, Vitaly
Ordering transition and critical phenomena in a three component polymer mixture at A/B homopolymer and a A-B diblockcopolymer
Dr. rer. nat. (Physical Chemistry), Mathematisch-Naturwissenschaftliche Fakultät, Westfälische Wilhelms-Universität Münster (2004, *Soft condensed matter, Liquids, Glasses*)

Zamponi,M
Polymerdynamik jenseits des Reptationsmodells
Dr. rer. nat. (Physics), Mathematisch-Naturwissenschaftliche Fakultät, Westfälische Wilhelms-Universität Münster (2004, *Soft condensed matter, Liquids, Glasses*)

2003

Elter,P
Untersuchung der Entmischungskinetik an Silber-Natriumbromid-Einkristallen mit zeitaufgelöster inelastischer Neutronenstreuung
Dr. rer. nat., Mathematisch-Naturwissenschaftliche Fakultät,Universität Göttingen (2003, *Crystallography*)

Kaya, Ugur Lehn Kaya
Mizellbildung amphiphiler Blockcopolymere in wässriger Lösung
Dr. rer. nat. (Physical Chemistry), Mathematisch-Naturwissenschaftliche Fakultät, Westfälische Wilhems-Universität Münster (2003, *Soft condensed matter, Liquids, Glasses*)

Schlapp, M
Entwicklung hocheffizienter, gamma-insensitiver Detektormaterialien und Bildplatten für Neutronen
Dissertation Materialwissenschaften, TU Darmstadt
Berichte des Forschungszentrums Jülich, 4076 (2003, *Neutron instruments and methods*)

Siouris, Y
Complex magnetic properties of R_2MIn_3 compounds – magnetic glasses, with R= rare Earth and M=Cu, Ag
PhD, Dept. of Electrical and Computer Engineering, Democritos University of Thrace, Greece (2003, *Magnetism*)

Voigt, J.
Magnetische Strukturen in [Er/Tb]-Schichtsystemen: Einfluß der magnetischen Nachbarschaft und konkurrierender Anisotropien
Dr. rer. nat (Physics), RWTH Aachen
Berichte des Forschungszentrums Jülich 4087 (2003, *Magnetism*)

2002

Caspary,D
Zeitaufgelöste inelastische Neutronenstreuung an entmischenden Silber-Natriumchlorid-Einkristallen
Dr. rer. nat. (Physical Chemistry), Physikalische Chemie, Universität Göttingen (2002, *Excitations*)

Elisbihani,K
Gammadiffraktometrie zur Untersuchung der ferroelektrischen Lock-In Phasenumwandlung in Rb_2ZnCl_4
Dr. rer. nat. (Physical Chemistry), Physikalische Chemie, Universität Göttingen (2002, *Excitations*)

Günther,A
Magnetische Anisotropie gebänderter Eisenerze und deren Beziehung zu kristallographischen Vorzugsorientierungen
Dr. rer. nat. (Geology), Mathematisch-Naturwissenschaftliche Fakultät, Technische Universität Clausthal (2002, *Geology, Archaeology*)

Hense, K.
CEF-Phonon interaction in the orhtorhombic compound $NdCu_2$
Dr. rer. nat. (Physics), TU Wien (2002, *Excitations*)

Hill,C
Curing and Morphology of Adhesives
M.Sc. (Polymer Science), Department of Chemistry, University of Durham (2002, *Soft condensed matter, Liquids, Glasses*)

Istomin,K
Interplay between Charge, Spin and Orbital Ordering in $La_{1-x}Sr_xMnO_3$ Manganites
Dr. rer. nat. (Physics), Fakultät für Mathematik, Informatik und Naturwissenschaften der RWTH Aachen (2002, *Magnetic structures*)

Kaya,H
Mizellbildung amphiphiler Blockcopolymere in wässriger Lösung
Dr. rer. nat. (Physics), Mathematisch-Naturwissenschaftliche Fakultät der Westfälischen Wilhelms-Universität Münster (2002, *Soft condensed matter, Liquids, Glasses*)

Mattauch,S
Untersuchung der strukturellen Phasenübergänge und Domänenbildung in den ferroischen Modellsubstanzen RbH_2PO_4 und RbD_2PO_4
Dr. rer nat. (Crystallography), Fakultät Bergbau, Hüttenwesen und Geowissenschaften,RWTH-Aachen (2002, *Neutron instruments and methods*)

Papathanassiou,G
Magnetic properties of $RPtGe_2$ compounds studied by neutron diffraction
Dr. (Physics), Department of Electrical and Computer Engineering, Democritos University of Thrace, Greece (2002, *Magnetic structures*)

Ziegenhagen, N.
Einfluss lateraler Oberflächenstrukturen auf die Eigenschaften von Fe/Cr-Schichtsystemen
Diploma (Physics), Fakultät für Mathematik, Informatik und Naturwissenschaften, RWTH Aachen (2002, *Magnetic structures*)

2001

Botti,A
Microscopic Deformations in Filled Networks
Dr. rer. nat. (Physical Chemistry), Mathematisch-Naturwissenschaftliche Fakultät der Westfälischen Wilhelms-Universität Münster (2001, *Soft condensed matter, Liquids, Glasses*)

Endo,H
Small Angle Neutron Scattering Investigation on the Emulsification Efficiency of Amphiphilic Block Copolymer in Microemulsions
Dr. rer. nat. (Chemistry), Mathematisch-Naturwissenschaftliche Fakultät der Westfälischen Wilhelms-Universität Münster (2001, *Soft condensed matter, Liquids, Glasses*)

Erhardt,R
Janus-Mizellen
Dr. rer. nat. (Chemistry), University of Bayreuth (2001, *Soft condensed matter, Liquids, Glasses*)

Hundenborn,R
Entstehung, Metamorphose und Deformation der basischen und ultrabasischen Gesteine in der Adula-Decke und der Misoxer-Zone, unter besonderer Berücksichtigung der Adula-Eklogite
Dipl.-Geol. (Geology), Geologisches Institut, Universität Bonn (2001, *Geology, Archaeology*)

Kowald,T
Jakobsit - Einfluss der Materialsynthese auf die elektrischen und magnetischen Eigenschaften
Dipl.-Mineraloge (Mineralogy), Fachbereich Geowissenschaften, Philipps-Universität Marburg (2001, *Crystallography*)

Meents,A
Kombinierte Strukturuntersuchungen der Tuttonsalze $(NH_4)_2(M \times 6H_2O)(SeO_4)_2$ (M = Mn,Co und Zn) mittels Röntgen- und Neutronenbeugung
Dipl. Min. (Mineralogy), Mineralogisch-Petrologisches Institut, Universität Bonn (2001, *Crystallography*)

Meven,M
Entwicklung eines hochauflösenden Röntgen-Einkristalldiffraktometers und Strukturuntersuchungen an $La_{2-x}Sr_xCuO_{4-}$ Einkristallen.
Dr. rer nat (Crystallography), Fakultät für Bergbau, Hüttenwesen und Geowissenschaften RWTH-Aachen (2001, *Crystallography*)

Mihailescu,M
A study of the structural and dynamical properties of microemulsions with amphiphilic block-copolymers
Dr. rer. nat. (Physical Chemistry), Mathematisch-Naturwissenschaftliche Fakultät der Westfälischen Wilhelms-Universität Münster (2001, *Soft condensed matter, Liquids, Glasses*)

Moreno,A
Estudio mediante tecnicas de dispersion de neutrones de la dinamica rotacional de grupos metilo en vidrios polimericos y de bajo peso molecular
Dr (Physics), Universidad del Pais Vasco (UPV/EHU) (2001, *Soft condensed matter, Liquids, Glasses*)

Pleuger,J
Strukturgeologische Untersuchungen in der Adula-Decke, Misoxer Zone und Tambodecke am Passo del San Bernardino
Dipl. Geol. (Geology), Geologisches Institut, Universität Bonn (2001, *Geology, Archaeology*)

Training

Publications

2005

Braden, M.
Inelastic Neutron Scattering: Phonons and Magnons (in: Laboratory Course Neutron Scattering) Schriften des Forschungszentrums Jülich, Reihe Materie und Material 28 (2005), 13-1 – 13-26

Brückel, Th., Heger,G, Richter, D., Zorn, R. (Hrsg.)
Neutron Scattering : lectures of the laboratory course held at the Forschungszentrum Jülich
New and rev. ed. from vol. 15,2003
Schriften des Forschungszentrumss Jülich,Reihe Materie und Material / Matter and Materials **15** (Jülich, Zentralbibliothek, 2005)

Brückel, Th.
Elastic Scattering from Many-Body Systems (in: Laboratory Course Neutron Scattering) Schriften des Forschungszentrums Jülich, Reihe Materie und Material 28 (2005), 3-1 – 3-28

Brückel, Th.
Magnetism (in: Laboratory Course Neutron Scattering) Schriften des Forschungszentrums Jülich, Reihe Materie und Material 28 (2005), 16-1 – 16-19

Conrad, H.
Neutron Sources (in: Laboratory Course Neutron Scattering) Schriften des Forschungszentrums Jülich, Reihe Materie und Material 28 (2005), 1-1 – 1-22

Conrad, H.
Spectroscopy: 1. The Triple-axis Spectrometer 2. The Back.scattering Spectrometer (in: Laboratory Course Neutron Scattering) Schriften des Forschungszentrums Jülich, Reihe Materie und Material 28 (2005), 9-1.1 – 9-2.7

Heger, G.
Symmetry in Crystals (in: Laboratory Course Neutron Scattering) Schriften des Forschungszentrums Jülich, Reihe Materie und Material 28 (2005), III-1 – III-15

Heger,G
Diffractometer (in: Laboratory Course Neutron Scattering) Schriften des Forschungszentrums Jülich, Reihe Materie und Material 15 (2003), 7-1 – 7-14

Heger,G
Structure Determination (in: Laboratory Course Neutron Scattering) Schriften des Forschungszentrums Jülich, Reihe Materie und Material 28 (2005), 12-1 – 12-17

Monkenbusch,M
Time-of-Flight Spectrometers (in: Laboratory Course Neutron Scattering) Schriften des Forschungszentrums Jülich, Reihe Materie und Material 28 (2005), 10-1 – 10-23

Monkenbusch,M, Zorn, R.
Neutron Spin-echo Spectrometer (in: Laboratory Course Neutron Scattering) Schriften des Forschungszentrums Jülich, Reihe Materie und Material 28 (2005), 11-1 – 11-19

Prager, M.
Translation and Rotation (in: Laboratory Course Neutron Scattering) Schriften des Forschungszentrums Jülich, Reihe Materie und Material 28 (2005), 17-1 – 17-20

Richter, D.
Basic Assumptions of Quantum Mechanics and the Born Approximation (in: Laboratory Course Neutron Scattering) Schriften des Forschungszentrums Jülich, Reihe Materie und Material 28 (2005), II-1 – II-32

Richter, D.
Properties of the Neutron, Elementary Scattering Processes (in: Laboratory Course Neutron Scattering) Schriften des Forschungszentrums Jülich, Reihe Materie und Material 28 (2005), 2-1 – 2-21

Richter, D.
Polymer Dynamics (in: Laboratory Course Neutron Scattering) Schriften des Forschungszentrums Jülich, Reihe Materie und Material 28 (2005), 15-1 – 15-29

Schwahn, D.
Small-angle Scattering and Reflectometry (in: Laboratory Course Neutron Scattering) Schriften des Forschungszentrums Jülich, Reihe Materie und Material 28 (2005), 8-1 – 8-16

Schwahn, D.
Soft Matter: Structure (in: Laboratory Course Neutron Scattering) Schriften des Forschungszentrums Jülich, Reihe Materie und Material 28 (2005), 14-1 – 14-18

Schweika, W.
Polarization Analysis (in: Laboratory Course Neutron Scattering) Schriften des Forschungszentrums Jülich, Reihe Materie und Material 28 (2005), 4-1 – 4-25

Seeck, O., Kentzinger, E.
Continuum Description: Grazing Incidence Neutron Scattering (in: Laboratory Course Neutron Scattering) Schriften des Forschungszentrums Jülich, Reihe Materie und Material 28 (2005), 6-1 – 6-26

Walter, J.M., Schäfer, W.
Texture in Materials and Earth Sciences (in: Laboratory Course Neutron Scattering) Schriften des Forschungszentrums Jülich, Reihe Materie und Material 28 (2005), 18-1 – 18-23

Zorn, R.
Fourier Transformation (in: Laboratory Course Neutron Scattering) Schriften des Forschungszentrums Jülich, Reihe Materie und Material 28 (2005), I-1 – I-28

Zorn, R., Richter, D.
Correlation Functions Measured by Scattering Experiments (in: Laboratory Course Neutron Scattering) Schriften des Forschungszentrums Jülich, Reihe Materie und Material 28 (2005), 5-1 – 5-24

2003

Güthoff,F, Grimm,H
Crystal Spectrometer: Triple-axis and Back-scattering Spectrometer (in: Laboratory Course Neutron Scattering) Schriften des Forschungszentrums Jülich, Reihe Materie und Material 15 (2003), 9-1 –9-17

Schäfer, W.
Texture in Materials and Earth Sciences (in: Laboratory Course Neutron Scattering) Schriften des Forschungszentrums Jülich, Reihe Materie und Material 15 (2003), 18-1 – 20

Seeck, O.
Continuum Description: Grazing Incidence Neutron Scattering (in: Laboratory Course Neutron Scattering) Schriften des Forschungszentrums Jülich, Reihe Materie und Material 15 (2003), 6-1 – 6-18

2002

Brown,PJ
Polarimetric Neutron Scattering III: Examples
Schriften des Forschungszentrums Jülich, Reihe Materie und Material 12 (2002), p. 169ff

Brückel, Th., Heger,G, Richter, D., Zorn, R. (Hrsg.)
Neutron Scattering : lectures of the laboratory course held at the Forschungszentrum Jülich
New and rev. ed. from vol. 9,2001
Schriften des Forschungszentrumss Jülich,Reihe Materie und Material / Matter and Materials **15**
(Jülich, Zentralbibliothek, 2002)

Brückel, Th., Schweika, W (Hrsg.)
Polarized Neutron Scattering
Schriften des Forschungszentrumss Jülich,Reihe Materie und Material / Matter and Materials **12**
(Jülich, Zentralbibliothek, 2002)

Brückel, Th.
Magnetic X-Ray and Polarised Neutron Scattering
Schriften des Forschungszentrums Jülich, Reihe Materie und Material 12 (2002), p. 323ff

Dorner,B
Inelastic Scattering of Polarized Neutrons from Magnetic Excitations
Schriften des Forschungszentrums Jülich, Reihe Materie und Material 12 (2002), p. 195ff

Maleyev, S
General Theory of Polarised Neutron Scattering in Magnetic Materials
Schriften des Forschungszentrums Jülich, Reihe Materie und Material 12 (2002), p. 99ff

Maleyev, S
Polarised Neutrons and Magnetism, Applications
Schriften des Forschungszentrums Jülich, Reihe Materie und Material 12 (2002), p. 121ff

Monkenbusch,M
Neutron Spin Echo Spectrometry
Schriften des Forschungszentrums Jülich, Reihe Materie und Material 12 (2002), p. 219ff

Schärpf,O
Polarization Elements
Schriften des Forschungszentrums Jülich, Reihe Materie und Material 12 (2002), p. 31ff

Schweika, W.
Introduction to Polarized Neutron Scattering
Schriften des Forschungszentrums Jülich, Reihe Materie und Material 12 (2002), p. 5ff

Schweizer,J
Magnetic Form Factors and Magnetization Densities Investigated by Polarized Neutron Diffraction
Schriften des Forschungszentrums Jülich, Reihe Materie und Material 12 (2002), p. 289ff

Toperverg, B.
Polarized Neutron Reflection and Off-Specular Scattering
Schriften des Forschungszentrums Jülich, Reihe Materie und Material 12 (2002), p. 247ff

Zorn, R
Inelastic Neutron Scattering: Dynamics of Polymers in „Neutrons, X-rays and Light: Scattering Methods Applied to Soft Condensed Matter“, Eds. P. Lindener, Th. Zemb, p. 221–258 (Elsevier, Amsterdam, 2002)

Lectures

2006

Braden, M.
Inelastic Neutron Scattering: Phonons and Magnons
Laboratory Course Neutron Scattering, Forschungszentrum Jülich, 13.-24.03.2006, Jülich (annually since 1997)

Brückel, Th.
Elastic Scattering from Many-Body Systems
Laboratory Course Neutron Scattering, Forschungszentrum Jülich, 13.-24.03.2006, Jülich (annually since 1997)

Brückel, Th.
Magnetism
Laboratory Course Neutron Scattering, Forschungszentrum Jülich, 13.-24.03.2006, Jülich (annually since 1997)

Brückel, Th.
Properties of the Neutron, Elementary Scattering Processes
Laboratory Course Neutron Scattering, Forschungszentrum Jülich, 13.-24.03.2006, Jülich (annually since 2003)

Conrad, H.
Neutron Sources
Laboratory Course Neutron Scattering, Forschungszentrum Jülich, 13.-24.03.2006, Jülich (annually since 1997)

Conrad, H.
Spectroscopy: 1. The Triple-axis Spectrometer 2. The Back-scattering Spectrometer
Laboratory Course Neutron Scattering, Forschungszentrum Jülich, 13.-24.03.2006, Jülich (annually since 2005)

Heger,G
Diffractometer
Laboratory Course Neutron Scattering, Forschungszentrum Jülich, 13.-24.03.2006, Jülich (annually since 1997)

Heger,G
Structure Determination
Laboratory Course Neutron Scattering, Forschungszentrum Jülich, 13.-24.03.2006, Jülich (annually since 1997)

Heger,G
Symmetry in Crystals
Laboratory Course Neutron Scattering, Forschungszentrum Jülich, 13.-24.03.2006, Jülich (annually since 2004)

Monkenbusch,M
Time-of-Flight Spectrometers
Laboratory Course Neutron Scattering, Forschungszentrum Jülich, 13.-24.03.2006, Jülich (annually since 1997)

Monkenbusch,M
Neutron Spin-echo Spectrometer
Laboratory Course Neutron Scattering, Forschungszentrum Jülich, 13.-24.03.2006, Jülich (annually since 1997)

Prager, M.
Translation and Rotation
Laboratory Course Neutron Scattering, Forschungszentrum Jülich, 13.-24.03.2006, Jülich (annually since 1997)

Richter, D.
Polymer Dynamics
Laboratory Course Neutron Scattering, Forschungszentrum Jülich, 13.-24.03.2006, Jülich (annually since 1997)

Richter, D.
Quantum Mechanics: Born Approximation
Laboratory Course Neutron Scattering,
Forschungszentrum Jülich, 13.-24.03.2006, Jülich
(annually since 2004)

Schwahn, D.
Small-angle Scattering and Reflectometry
Laboratory Course Neutron Scattering,
Forschungszentrum Jülich, 13.-24.03.2006, Jülich
(annually since 1997)

Schwahn, D.
Soft Matter: Structure
Laboratory Course Neutron Scattering,
Forschungszentrum Jülich, 13.-24.03.2006, Jülich
(annually since 1997)

Schweika, W.
Polarization Analysis
Laboratory Course Neutron Scattering,
Forschungszentrum Jülich, 13.-24.03.2006, Jülich
(annually since 1997)

Seeck, O.
Continuum Description: Grazing Incidence Neutron Scattering
Laboratory Course Neutron Scattering,
Forschungszentrum Jülich, 13.-24.03.2006, Jülich
(annually since 1997)

Walter, J.
Texture in Materials and Earth Sciences
Laboratory Course Neutron Scattering,
Forschungszentrum Jülich, 13.-24.03.2006, Jülich
(annually since 2004)

Zorn, R.
Correlation Functions Measured by Scattering Experiments
Laboratory Course Neutron Scattering,
Forschungszentrum Jülich, 13.-24.03.2006, Jülich
(annually since 1997)

Zorn, R.
Mathematical Methods: Fourier Transform
Laboratory Course Neutron Scattering,
Forschungszentrum Jülich, 13.-24.03.2006, Jülich
(annually since 2004)

Zorn, R.
Inelastic neutron scattering: dynamics of polymers
8th European School on Scattering methods applied to soft condensed matter, Bombannes/Frankreich (2002, biannually since 2000)

2004

Grimm,H
Crystal Spectrometer: Triple-axis and Back-scattering Spectrometer
Laboratory Course Neutron Scattering,
Forschungszentrum Jülich, 13.-24.03.2006, Jülich
(annually since 1997)

2003

Conrad, H.
Neutronen – Ein Geschenk der Natur
28. Fortbildungsveranstaltung für Physiklehrer:
Universität Bayreuth, 16.10.03

Schäfer, W.
Texture in Materials and Earth Sciences
Laboratory Course Neutron Scattering,
Forschungszentrum Jülich, 15.-26.09.2003, Jülich
(annually since 1997)

Zorn, R.
Polymer dynamics studied with neutron-spin echo
2nd PSI Summer School on Condensed Matter,
Zuoz/Schweiz (2003)

2002

Brown,PJ
Polarimetric Neutron Scattering III: Examples
Summer School Polarized Neutron Scattering,
Forschungszentrum Jülich 10.–14.09.02

Brückel, Th., Schweika, W (Hrsg.)
Polarized Neutron Scattering
Schriften des Forschungszentrumss Jülich,Reihe Materie und Material / Matter and Materials **12**
(Jülich, Zentralbibliothek, 2002)

Brückel, Th.
Magnetic X-Ray and Polarised Neutron Scattering
Summer School Polarized Neutron Scattering,
Forschungszentrum Jülich 10.–14.09.02

Dorner,B
Inelastic Scattering of Polarized Neutrons from Magnetic Excitations
Summer School Polarized Neutron Scattering,
Forschungszentrum Jülich 10.–14.09.02

Maleyev, S
General Theory of Polarised Neutron Scattering in Magnetic Materials
Summer School Polarized Neutron Scattering, Forschungszentrum Jülich 10.–14.09.02

Maleyev, S
Polarised Neutrons and Magnetism, Applications
Summer School Polarized Neutron Scattering, Forschungszentrum Jülich 10.–14.09.02

Monkenbusch,M
Neutron Spin Echo Spectrometry
Summer School Polarized Neutron Scattering, Forschungszentrum Jülich 10.–14.09.02

Richter, D.
Properties of the Neutron, Elementary Scattering Processes
Laboratory Course Neutron Scattering, Forschungszentrum Jülich, 16. - 27.9.2003, Jülich (annually since 1997)

Schärpf,O
Polarization Elements
Summer School Polarized Neutron Scattering, Forschungszentrum Jülich 10.–14.09.02

Schweika, W.
Introduction to Polarized Neutron Scattering
Summer School Polarized Neutron Scattering, Forschungszentrum Jülich 10.–14.09.02

Schweizer,J
Magnetic Form Factors and Magnetization Densities Investigated by Polarized Neutron Diffraction
Summer School Polarized Neutron Scattering, Forschungszentrum Jülich 10.–14.09.02

Toperverg, B.
Polarized Neutron Reflection and Off-Specular Scattering
Summer School Polarized Neutron Scattering, Forschungszentrum Jülich 10.–14.09.02